A Finite-Regulator Variational–Stochastic Programme: Geometry, Gauge Fields, Matter, and the Arrow of Time

By Shipei Hu

hexagon:2611.00711v1

Abstract

We develop a finite-regulator variational–stochastic programme organized by four principles: structured admissible change; compatible transport, dissipation and fluctuations; selection relative to a reference path law; and consistent observation across descriptions. The central question is which relationships between motion, statistics and response follow from shared dynamical data.

An exactly solved finite model shows how one transition operator gives thermal relaxation, growth-weighted population dynamics and Bayesian updating. Its unweighted occupancy, selected population endpoints and driven histories have distinct limiting distributions, all determined by the same specified rates. Equilibrium and kinetic inputs then predict a selection response. A martingale constraint gives a financial probability selection, while an underdamped oscillator connects Hamiltonian motion, thermal relaxation and fluctuation–response through one matched reservoir. These examples expose the common operations and the additional meanings supplied by each application.

For the regulated field law we derive Gibbs invariance, relative free-energy balance and a quadratic path-irreversibility rate under specified boundary, covariance and reversal conditions. Matched coframe and connection variations recover Einstein–higher-curvature and Yang–Mills equations; quantified remainders delimit their usual low-energy forms. Canonical Yang–Mills dynamics require constant kinetic coefficients. Stable-pole, stress Ward-identity and universal-coupling assumptions connect matter masses, WKB trajectories and tensor-sector inertial–gravitational mass equality. A boundary-dependent Schur criterion characterizes conditional Machian closure. Additive vacuum shifts show why equilibrium alone does not select the cosmological constant, and the declared 331 candidate is a realization rather than a unique group-selection theorem.

Coefficient-identification bounds and observation theorems determine which reduced quantities shared calibrated inputs fix. Exact Haar–Gaussian Gram bounds identify six lattice-action coefficients, including a volume-uniform normalized estimate on a periodic family; hidden states, sampling and operator choice delimit this identification. Finite fluid, quantum-noise and scalar-source models supply further balance and response relations. The matched finite-Galerkin fluid projection has injection, transfer and dissipation balances without establishing a continuum cascade. Bell-local, measurement-independent classical models obey CHSH, and shared noise parameters constrain coherence and repeated-readout correlations. For a specified metric common-weight scalar branch, a nonlinear conformal-slope bound, massive-fluid balance and coercive static-response estimate connect its coupling to a source-conditioned circular-radiation threshold. The trace-response illustration lies below three published binary-summary errors; it neither supplies nuclear sensitivities nor excludes arbitrary scalar theories.

The construction distinguishes a shared variational organization from a uniquely selected microscopic theory. Physical entropy production requires explicit reservoirs and local detailed balance; quantum completion requires positive physical states and measurement rules, with reflection positivity additionally needed for Euclidean reconstruction. Synthetic and retrospective calculations illustrate conditional predictions. Regulator-independent quantization, unique group–matter selection, independently fixed fundamental parameters, the Yang–Mills mass gap and continuum turbulence remain separate research problems.

2020 *Mathematics Subject Classification.* Primary 83C05, 81T13; Secondary 60H15, 82C31, 35Q30, 49L20, 76F55.

Keywords: variational–stochastic programme; Cartan geometry; gauge fields; path selection; stochastic thermodynamics; mutation–selection; information geometry; Einstein–Yang–Mills recovery; observation and reduction

Contents

1. Introduction 5
2. A common mechanism in representative finite models 12
3. The master configuration, action, and one path-space cost 23
4. Equilibrium, limits, and symmetry breaking 39
5. Geometric and gauge recovery from one Euler system 62
6. Group selection and the conditional (331) phase 107
7. Well-posedness, conditional recovery, and parameter matching 129
8. A concrete four-dimensional interacting regulator and its thermodynamic reduction 141
9. A discrete finite four-dimensional certification branch 147
10. Identifiable finite models, constrained motion, and positive quantum evolution 151
11. Equilibrium observables, sector separation, and falsifiability 209
12. Quantum completion, mass-gap boundary, entanglement, and Bell correlations 235
13. Nonequilibrium thermodynamics and regulated turbulence 263
14. A single mother equation for thermodynamics and hydrodynamic transport 307
15. Cross-sector response and independent validation 357
16. Joint recovery maps and quantitative defect certificates 411
17. A conditional kinetic interface and macroscopic conservation 421
18. Physical matching of additional interactions 424
19. Binary-pulsar constraints on a conditional scalar interaction 427
20. Stellar charges from common couplings and their observational transfer 434
21. Composite-matter response and identifiable stellar predictions 444
22. Common-weight response, stellar balance, and a conditional radiation envelope 455
23. Identifiability and eccentric-orbit radiation in the shared scalar branch 473
24. A frozen-parameter public-data holdout test 477
25. Physical-time evolution of the homogeneous constrained branch 484
26. Relativistic clock rates and gravitation without rest mass 486
27. Spatial correlation, inverse geometry, and an interacting mode limit 528
28. Physical reduction and quantum constraint tests 533
29. Equilibrium, evolution, and the calibration of time 535
30. A mother-parameter registry and a no-refit stellar transfer 537
31. Synthetic comparisons of uncertainty, memory and response 541
32. Conclusions and further directions 543

Appendix A. Variation of the master curvature 560
Appendix B. Proof of the Gibbs identity 561
Appendix C. Girsanov representation of the cost 562
Appendix D. Heat-kernel convention 563
Appendix E. Dimensions, normalization, and covariance under changes of units 564
Appendix F. Joint metrics, physical projections, and the meaning of unification 570
Appendix G. Finite-resolution dynamics, calibration, and identifiable predictions 573
Appendix H. Geometric response and independently distinguishing tests 578
Appendix I. Physical perturbations, angular power, and noise-calibrated tests 583
Appendix J. Selection, matching, and independent physical tests 593
Appendix K. Common-weight selection, radiative matching, and material observables 596
Appendix L. Microscopic inputs, effective restrictions, and identifiable predictions 605
Appendix M. Dynamic programming and adjoint selection for the common cost 609
Appendix N. Smooth stochastic symmetries and constrained physical realization 621
Appendix O. Coefficient restrictions and physically identified stochastic balances 627
Appendix P. Irreversible dynamics, convergence, and boundary symmetries 637
Appendix Q. What a fixed stochastic model determines 646
Appendix R. Geometric control, quantum reconstruction, and the gravitational limit 650
Appendix S. Einstein branches, a quantitative response bound, and a free gravitational limit 658
Appendix T. A complete four-dimensional classical interaction benchmark 674
Appendix U. Exact nonlinear feedback and a cross-channel response restriction 681
Appendix V. Generator conditions for the time arrow, attraction, and physical validation 687
Appendix W. Stochastic Noether balances: physical charges and Bellman contact symmetries 695

Appendix X. A common variational origin with a closed stochastic realization 699
Appendix Y. Endpoint measures, fluctuation identities, and three distinct arrows 707
Appendix Z. Scale consistency of the common variational architecture 710
Appendix AA. Quantum states, physical projections, and measurement selection 712
Appendix AB. Frozen quantum predictions and a spectral thought experiment 720
Appendix AC. Physical observation models and transfer between Bell runs 732
Appendix AD. Operational joint predictions and public coherence data 736
Appendix AE. Frequency-dependent phase noise and transfer between control sequences 746
Appendix AF. Cosmological fate: local equilibration and global non-extinction 756
Appendix AG. Assumptions connecting the finite and continuum branches 763
Appendix AH. Detailed connections with the sector constructions 764
References 784

1. **Introduction**

A common theory becomes informative when one choice of dynamical data restricts several observations at once. This requirement is familiar in physics: a model of matter should relate its motion, fluctuations and response through the same interactions. A related question arises in finance, where the prices of traded assets constrain the valuation of risks that cannot be replicated. In both settings, the central task is to identify what the stated dynamics and constraints determine, and what additional information an observation requires. The present programme uses this question to connect a geometric field construction with explicit models of relaxation and constrained probabilistic selection.

1.1. *Research question and physical motivation.* The four interactions conventionally described as gravitation, electromagnetism, the weak interaction, and the strong interaction are represented at presently accessible scales by theories with markedly different mathematical formulations. General relativity describes gravity through spacetime geometry, whereas the Standard Model describes the non-gravitational interactions through gauge fields and matter representations. The coexistence of these descriptions is experimentally successful over their respective domains, but their conceptual combination leaves a basic structural question: can the four sectors be regarded as different effective manifestations of one underlying dynamical principle rather than as theories placed side by side?

The question is addressed through a common variational and stochastic structure. Its guiding idea is that motion, fluctuation, relaxation and selection can be understood as connected operations on a specified space of possibilities. Geometry determines admissible changes; a reference law specifies their stochastic dynamics; constraints and observations determine how histories are selected or reweighted. The same questions also occur in communication, population evolution and decision-making, where the variables have different meanings. Their comparison can reveal common structures while making the additional physical, biological or economic conditions explicit.

For the physical realization, we fix a configuration space, geometric action, reference measure, mobility, noise law, objective and observation maps. The scientific question is which relationships these shared data impose between responses that would otherwise be specified separately. The following finite models explain this question constructively; the later geometric and stochastic developments supply its field realizations and effective limits.

To make the proposed connection testable rather than merely schematic, we also specify one finite four-dimensional interacting branch. Its link variables, regulated coframe coordinates, and order-parameter variables enter one positive

norm-square functional; the same frozen registry determines the finite generator, Gibbs reference, and entropy-production identity. This branch is the smallest representative on which the unified idea can be checked without silently importing a second action. A finite Euclidean regulator is a controlled theorem about that branch, whereas the Lorentzian constraint algebra, regulator-independent limit, and interacting quantum theory require separate proofs.

The physical motivation is more specific than a search for formal similarity. A unified description must explain how four ingredients cooperate: a variational principle selects admissible field changes, a reference measure gives those changes a probabilistic meaning, a positive response operator describes relaxation, and an observation map determines which part of the dynamics is measurable. These roles are often separated when gravity, gauge fields, matter, and nonequilibrium thermodynamics are written in different languages. The proposed framework tests whether they can be generated from one declared set of geometric and probabilistic data while preserving the distinctions that each sector requires.

The thermodynamic sector provides the decisive test of this proposal. The conservative Lorentzian branch describes field evolution through a generally indefinite action, whereas entropy production uses a positive quadratic form on dissipative directions. Consequently, the second law cannot be obtained by relabelling a Lorentzian action as a free energy. It must emerge after the field variables, reference measure, bath coupling, and physical projection have been specified. This is why the manuscript treats the finite-regulator construction as an explicit bridge: it makes the positivity, the Gibbs measure, the noise covariance, and the heat convention visible before any continuum or quantum claim is made.

The smallest representative of this idea is the four-dimensional interacting branch introduced later in the paper. Link variables, regulated coframe coordinates, and an order parameter enter one shared functional. Its finite generator has a unique Gibbs law and an exact Dirichlet dissipation identity. The branch therefore supplies an explicit finite test of the proposed architecture, whose physical interpretation still requires matching. It also clarifies the logical boundary of the result: a finite Euclidean theorem does not by itself establish the full Lorentzian constraint algebra, a regulator-independent field limit, or a positive interacting quantum Hilbert space. Those requirements are stated as subsequent tests, so that the physical motivation and the mathematical claims remain aligned.

Section 10 develops the finite construction further. It gives a response-based inverse map, an explicit energy-scale ambiguity, and a constrained nonlinear example. An alternative symmetric temporal regulator then gives a positive interacting quantum model at fixed spatial resolution. The distinction between

this model, physical gravitational constraints, and a spatial continuum limit determines the order of the remaining analysis.

The finite extensions also address how the common structure can be measured. A locally rotation-covariant logarithmic coframe model combines finite inverse moments with an explicit Gibbs generator (Section 10.12). Exact temporal endpoint normalization then distinguishes a removable row factor from the field-dependent physical inertia. At a fixed observation scale, determinant bounds quantify the probability of nearly singular averaged geometry. Finally, the retained gauge–scalar interaction gives an oscillatory backreaction and an explicit finite-time trajectory bound, illustrated with the same parameters in the coupled and frozen-scalar models (Section 10.16). These results connect symmetry, equilibrium, and response in calculable examples. Their model choices are stated so that finite constructions can be compared without identifying them with a common continuum theory by assumption.

1.2. *Four organizing principles.* The central proposal is to organize a theory by the possibilities for change, the law of its fluctuations, and the conditions that select or reweight its histories. Mechanical motion, relaxation, inference and selection then become different operations on specified dynamical data. This proposal is expressed by four principles.

Admissible change has a structure. Before assigning a cost, specify what can change and which relations must be preserved. In the field construction, a connection, its curvature, matter representations and constraints provide this structure. On a finite network, the corresponding data are states and allowed transition edges. An invariant pairing or a mobility determines how admissible changes are compared. These choices make symmetry and conservation part of the dynamics from the outset. They also explain why a displacement that is possible in one effective description may be forbidden in another.

Motion, fluctuations and relaxation use compatible data. A reference stochastic law assigns probabilities to histories. Its conservative drift can transport a state without lowering its energy; its dissipative drift and noise determine exchange with the environment. When a thermal realization is intended, the same reservoir scale and mobility must enter both damping and fluctuations. Equilibrium is then a stationary law, while a microscopic history continues to move. The conservative limit retains the transport law and removes damping and its matched noise together. This identifies the physical conditions under which reversible mechanics and irreversible relaxation belong to one description.

Selection compares histories relative to a reference. Boundary information, an observed signal, reproductive growth or an admissible control can change the weight assigned to a history. A relative-entropy cost expresses how far this new law departs from the reference law. With a declared dimensionless path score

G, the elementary variational problem is

$$\inf_{\mathbb{Q}\ll\mathbb{P}} \{D(\mathbb{Q}\|\mathbb{P}) - \mathbb{E}_{\mathbb{Q}} G\}. \tag{1}$$

Its minimizer is an exponentially reweighted path law. Section 2 derives this statement and shows how growth, Bayesian updating and a martingale constraint lead to different realizations. In the quadratic drift-control branch, the Girsanov identity supplies this relative-entropy geometry. The full joint residual objective retains its additional geometric and nonlinear terms. A mechanical action, in contrast, selects stationary trajectories through a first variation; its extremum can be a saddle. The common variational organization keeps these roles explicit.

A change of description must transport the law and its meaning. An observation or reduction maps the full state to a smaller description. The induced noise, memory, constraints and time scale must follow that map. A coarse observation can lose information and need not remain Markovian. Likewise, a distribution of present population types and a distribution along selected ancestral histories answer different questions even when one operator generates both. A common theory must specify these relations between descriptions, so that its parameters cannot be adjusted independently at each stage.

These principles shift the explanatory question. In addition to asking which equation fits each domain, we ask which parts of its motion, statistics, response and selection are fixed once the admissible changes and their reference law have been chosen. A shared mathematical structure can organize several disciplines without assigning identical physical meanings to their variables. A stronger physical unification arises when a specified microscopic realization also fixes the maps and common coefficients connecting its sectors.

1.3. *Representative models and contributions.* The argument begins with a finite model that can be solved completely. One transition generator gives a thermal relaxation law. Weighting its histories by reproductive growth gives a mutation–selection equation; weighting terminal states by an observation likelihood gives Bayesian updating. A financial example imposes a discounted-price martingale constraint and obtains a different probability law. An underdamped oscillator then exhibits conservative transport, matched noise and damping, and a fluctuation–response relation in one physical model. These examples establish the precise common operations before the field construction introduces its larger configuration space.

The contribution of this organization is a chain of explicit dependencies. For the finite example, an equilibrium fraction and one relaxation rate fix the transition generator; a separately specified growth difference then fixes the population equilibrium and a changed spectral rate. For the oscillator,

the same kinetic and reservoir parameters fix both response and fluctuations. The proofs identify which relations follow from shared inputs, which require a further constraint, and which are lost when an observation is changed. The underlying entropy, selection and change-of-measure methods have established precedents [48], [32], [90], [96], and [91]. Their role here is to give a transparent finite realization of the proposed organization and a concrete guide to its field-theoretic use.

The field construction asks a more specific question: which gravitational and internal equations follow from a common geometric action, and how closely do their selected solutions agree with established physics? The Cartan curvature contains the coframe, so its squared norm generates an Einstein term through a cross contraction. The internal variation generates a constitutive gauge equation whose canonical form depends on its kinetic coefficients. Section 5.8 puts these two mechanisms in one quantitative comparison. It derives the full coefficient-normalized gauge residual, separates equation consistency from solution stability, and demonstrates why resolving a mesh cannot remove a fixed physical correction. This turns the common variational origin into a sequence of explicit, testable requirements.

Quantitative consequences of shared inputs. Four calculations make the connection between a common structure and an observable more precise. Finite response measurements give an exact joint parameter set and a prediction bound that preserves their common calibration error (Section 10.2). An outgoing radial problem turns the prescribed source into a controlled surface response and radiated power (Section 22.5). An exactly solvable hidden-variable model measures the error caused by discarding memory and distinguishes two inequivalent short-memory scalings (Section V.6). Finally, an incomplete market shows how a declared reference law selects one price from the no-arbitrage interval and which changes of that reference remain unidentifiable (Section 2.5.1). The common contribution is a calculable dependence between inputs and outputs. The entropy projection, Gaussian dynamics and coercive variational estimates use established methods; the formulas specify their role and limits in the chosen realizations.

The remainder develops three connected results. First, one regulated geometric action, reference measure and mobility give coupled field equations and a stochastic law. Under the stated matching and low-energy conditions, these recover Einstein–Yang–Mills and matter equations; the thermal and fluid projections have their corresponding balance laws. Second, coefficient identification and target-observable theorems determine what calibrated shared inputs actually fix. Third, finite quantum, scalar-source and laboratory models expose relations that can be tested beyond the observations used for calibration. The quantum and continuum completions retain their separate hypotheses.

A geometric control construction sharpens this separation. Appendix R proves the correspondence between a quadratic ergodic control problem, a positive ground state and its reversible diffusion on a fixed regulated configuration space. It also constructs dynamics tangent to regular constraints, gives a quantitative local bound for an independently matched Einstein branch, and identifies a positive crossing-kernel condition for Euclidean reconstruction. A curved product-space example shows why the control equation alone cannot select the Einstein field equation. The finite gauge calculation tests the control mechanism. Appendix S then verifies an exact Einstein branch of the independent-connection Cartan sector, computes the quadratic response error from its specified coefficients, and constructs the spatial ultraviolet limit of free physical gravitational waves. Between these constructions, an exact nonlinear Einstein initial-data family permits arbitrary smooth spatial rotation of its shear. Its stochastic sampling requires explicit curvature-drift terms; tangent noise alone has a computable nonzero constraint defect. It also proves that the resummed four-derivative metric kernel fails physical-time reflection positivity. This identifies a concrete obstruction that an interacting completion must overcome.

Time supplies a further test of this organization. A probability law can describe relaxation without specifying a physical light cone, and an equilibrium distribution can remain unchanged when all transport rates are rescaled. Section 26.3 separates these questions through an exact clock-scaling identity and a quadratic hyperbolicity criterion. Section 26.4 then derives the common characteristic set of the matched scalar, gauge, Dirac and Einstein perturbation blocks. The calculation uses their physical kinetic terms and gauge constraints; it does not assume that the ungauged field determinants are nonzero. A synthetic wave-packet comparison distinguishes characteristic propagation from group delay, and an independent-lag experiment illustrates how dynamical calibration supports a prediction beyond an equilibrium histogram.

This development has applications wherever admissible dynamics, uncertainty and selection must be considered together: physical transport, communication through fluctuating environments, biological type selection and constrained financial decisions. Extending the same approach to social evolution requires explicit actors, transitions, resources and institutional feedback; a historical trend alone does not specify those quantities. The finite models below provide a construction for stated assumptions, rather than a universal social objective.

Section 2 gives the representative models, their proofs and a synthetic comparison. Section 3 introduces the master fields and objective. The subsequent sections develop equilibrium and effective field equations. The controlled

comparison in Section 5.8 then explains how their residuals and selected solutions are related. The matter sources lead into selection, physical matching, quantum structure and fluid transport. The conclusion returns to the common principles and the next physical questions. Appendix AH gives the detailed connections to the individual constructions, together with their assumption and notation tables.

The relation between equilibrium, geometry and time is sharpened by two explicit constructions below. A spatially correlated logarithmic coframe model has a nonlinear infinite-mode limit with uniform inverse moments (Section 27). A separate calibration result shows which additional transition measurement fixes the dynamical scale left undetermined by finite Gibbs populations (Section 29). Both constructions state their chosen reference laws and their relation to the full gravitational problem.

From shared principles to shared predictions. The eight companion studies follow different parts of one dependence chain. The particle construction fixes a representation and its matching rules; the fluid and second-law analyses identify the meaning of transport and heat; the quantum construction specifies the additional state and observable structure; and the cosmological and black-hole studies turn selected fields into source and detector responses. A coefficient can be transferred between these studies only after its field normalization, physical units, background and observation rule have been matched. This is where a common variational origin becomes more restrictive than a collection of separately calibrated models.

The scalar example makes that restriction concrete. Elementary coupling is only the first step: the material response and the exterior boundary determine the field produced by a body. Proposition 109 bounds this response even when the local restoring term vanishes or is weakly negative. It uses the energy required to continue the field into the exterior. The resulting residual bound separates an inaccurate numerical solution from a large physical response. This local advance supports the source calculation; the frequency-dependent response and the independently matched matter coefficients remain necessary for a binary-radiation prediction. Proposition 110 takes a further step by bounding an outgoing monopole response on a specified frequency band. Its scope is deliberately explicit: the binary dipole channel and the coupled matter response remain separate calculations.

The representative models now turn these principles into calculations. Their order follows the information needed for prediction: first a reference law, then a physical or economic constraint, and finally an observable that was not used to select the law. The financial example is expanded to an incomplete market so that the selection criterion has a visible role beyond the no-arbitrage equations themselves.

2. **A common mechanism in representative finite models**

A small model can reveal the organizing idea more clearly than a long list of applications. Consider finitely many states. The same transition law can describe a relaxing physical system, a changing population of types, or an unobserved environment in a communication channel. What changes between these interpretations is specified below: the observed quantity, the weight assigned to a history, or an additional constraint. The finite model realizes the stochastic and selection operations of the programme. Its states are not identified with a projection of the full gauge–gravity construction.

2.1. *A reference law and the direction of relaxation.* Let L be the row generator of an irreducible continuous-time Markov chain: $L_{ij} \geq 0$ for $i \neq j$ and $\sum_j L_{ij} = 0$. Column distributions obey $\dot{p} = L^{\mathsf{T}} p$. Assume detailed balance with a positive probability vector π:

$$a_{ij} := \pi_i L_{ij} = \pi_j L_{ji} \quad (i \neq j).$$

Write $u_i = p_i/\pi_i$. Then $\dot{p}_i = \sum_{j \neq i} a_{ij}(u_j - u_i)$. Consequently,

$$\frac{d}{dt} D(p\|\pi) = -\sum_{i<j} a_{ij}(u_i - u_j)(\log u_i - \log u_j) \leq 0. \tag{2}$$

Indeed, differentiation gives $\sum_i \dot{p}_i \log u_i$, because $\sum_i \dot{p}_i = 0$. Pairing the two orientations of every edge gives the displayed sum. Each summand is nonnegative because the logarithm is increasing. Positive initial probabilities suffice; irreducibility also makes the law positive at every strictly positive time for a general initial law.

The dissipation has a geometric form. Define the logarithmic mean $\Lambda(x, y) = (x - y)/(\log x - \log y)$, with $\Lambda(x, x) = x$, and let e_i be the coordinate vectors. The positive semidefinite operator

$$\mathsf{K}(p) = \sum_{i<j} a_{ij} \Lambda(u_i, u_j)(e_i - e_j)(e_i - e_j)^{\mathsf{T}}$$

satisfies $\dot{p} = -\mathsf{K}(p)\nabla_p D(p\|\pi)$. It acts in the simplex tangent space because $\mathsf{K}(p)\mathbf{1} = 0$. Thus the transition network and its conductances fix a relaxation geometry as well as a stationary distribution.

For a thermal interpretation with fixed energies E_i and $\theta = k_{\mathrm{B}} T > 0$, set $\pi_i = Z^{-1} e^{-E_i/\theta}$. Then $\theta D(p\|\pi) = \sum_i p_i E_i + \theta \sum_i p_i \log p_i + \theta \log Z$ is excess Helmholtz free energy. Equation (2) is its isothermal relaxation law. Temperature and reservoir matching supply this physical meaning; for an arbitrary transition network the same equation is a probability identity. The energy values fix π, whereas the conductances also fix the time scale.

2.2. *One variational identity for a reweighted law.* Let $\mathbb{P}$ be the reference path law on a finite horizon. For a bounded dimensionless path score G, put $Z_G = \mathbb{E}_{\mathbb{P}} e^G$ and define $d\mathbb{P}_G = e^G d\mathbb{P}/Z_G$. For any $\mathbb{Q} \ll \mathbb{P}$ with finite relative entropy,

$$D(\mathbb{Q}\|\mathbb{P}) - \mathbb{E}_{\mathbb{Q}} G = D(\mathbb{Q}\|\mathbb{P}_G) - \log Z_G. \tag{3}$$

This follows by substituting $\log(d\mathbb{P}_G/d\mathbb{P}) = G - \log Z_G$ in the definition of relative entropy. Nonnegativity of relative entropy proves that $\mathbb{P}_G$ is the unique minimizing law in (1). This standard variational identity underlies entropy projections and conditioned-process constructions [48] and [32].

For a state growth rate f_i and a positive terminal likelihood ℓ_i, choose

$$G = \int_0^T f_{J_t}\, dt + \log \ell_{J_T}, \qquad B = L + \operatorname{diag} f. \tag{4}$$

Rates L_{ij} and f_i have units of inverse time; ℓ_i is a dimensionless likelihood. The forward and backward equations are

$$n(t) = e^{B^{\mathsf{T}} t} p_0, \qquad h(t) = e^{B(T-t)}\ell, \qquad Z_G = n(t)^{\mathsf{T}} h(t).$$

The partition function is independent of the intermediate time because $\dot{n} = B^{\mathsf{T}} n$ and $\dot{h} = -Bh$. The marginal of the fixed-horizon reweighted law is

$$p_i^{G,T}(t) = \frac{n_i(t) h_i(t)}{Z_G}, \qquad L_{ij}^G(t) = L_{ij}\frac{h_j(t)}{h_i(t)} \quad (i \neq j). \tag{5}$$

To obtain the jump rate, condition on a transition $i \to j$ during a short interval: its reference weight is $L_{ij}\, dt$, and its remaining future weight changes from h_i to h_j. The diagonal is minus the sum of these off-diagonal rates. This is the finite-time Doob transform.

The initial law in this unrestricted variational problem is $p_{0i} h_i(0)/Z_G$. If the initial distribution must remain p_0, the minimization is instead performed separately conditional on $J_0 = i$. Its density is $e^G/h_{J_0}(0)$, its value is $-\sum_i p_{0i} \log h_i(0)$, and its jump rates still have the form in (5). The fixed-initial diffusion control problem uses this latter convention. This distinction preserves the initial condition when applying the path principle.

2.3. *Population selection and information updating.* Suppose types change with generator L and type i has a constant net reproductive rate f_i. In a continuous-time multitype branching realization, the expected counts satisfy $\dot{n} = L^{\mathsf{T}} n + \operatorname{diag}(f) n$. Normalizing these expected counts gives

$$p_i(t) = \frac{n_i(t)}{\sum_j n_j(t)}, \qquad \dot{p}_i = (L^{\mathsf{T}} p)_i + p_i(f_i - \bar{f}), \quad \bar{f} = \sum_j p_j f_j. \tag{6}$$

The subtraction of $\bar{f}$ follows by differentiating the normalization; no population-level foresight is needed. For a finite random population, a ratio of expected counts is not the expectation of the random fraction. A deterministic population

interpretation therefore uses an appropriate large-population limit or declares the expected-count normalization as the observable.

The selection part is $(\operatorname{diag} p - pp^{\mathsf{T}})f$. It is a gradient of $\bar{f}$ in the Fisher geometry on the interior simplex when f is fixed. Its squared gradient norm is $\operatorname{Var}_p(f)$. This established connection between selection and information geometry is discussed in [90] and [96]. Mutation adds a separate transport contribution. In particular,

$$\frac{d\bar{f}}{dt} = p^{\mathsf{T}}Lf + \operatorname{Var}_p(f), \qquad \frac{dD(p\|\pi)}{dt} = -\mathcal{D}_L(p) + \operatorname{Cov}_p(f, \log(p/\pi)), \tag{7}$$

where $\mathcal{D}_L$ is the nonnegative sum in (2). Neither full derivative has a fixed sign. The common framework therefore gives balance laws appropriate to each process, rather than imposing one increasing function on every evolution.

For an observed channel output y, let $\ell_i = P(y \mid J = i) > 0$. Setting $f = 0$ and weighting the terminal state gives

$$P(J_T = i \mid y) = \frac{\ell_i (e^{L^{\mathsf{T}}T} p_0)_i}{\sum_j \ell_j (e^{L^{\mathsf{T}}T} p_0)_j}.$$

This is Bayesian updating after prediction through the same channel environment. Relative likelihoods suffice; a common positive factor cancels. In a communication model, decoding, encoding and channel capacity require their specified input and output alphabets and constraints. The formula supplies the state-inference component.

For $\ell = \mathbf{1}$, the normalized population law in (6) equals the terminal marginal of the tilted law with horizon t. It is generally different from the intermediate marginal of a tilted law with a larger fixed horizon T, which contains the future factor $h(t)$. Thus endpoint selection and a selected history use the same operator but different observations.

2.4. *A two-state calculation with a common parameter set.* Take the transition and growth rates, in a chosen inverse-time unit,

$$\begin{aligned} L &= \begin{pmatrix} -1/5 & 1/5 \\ 4/5 & -4/5 \end{pmatrix}, \quad B = \begin{pmatrix} -1/5 & 1/5 \\ 4/5 & -1/5 \end{pmatrix}, \\ \pi &= (4/5, 1/5)^{\mathsf{T}}, \qquad f = (0, 3/5)^{\mathsf{T}}. \end{aligned} \tag{8}$$

The unweighted relaxation rate is one. A thermal realization has $E_2 - E_1 = \theta \log 4$. For $x = p_2$, the two evolutions are

$$\dot{x} = 1/5 - x, \qquad \dot{x} = 1/5 - (2/5)x - (3/5)x^2. \tag{9}$$

The first tends to $1/5$. In the second,

$$\frac{x(t) - 1/3}{x(t) + 1} = \frac{x(0) - 1/3}{x(0) + 1} e^{-4t/5},$$

so the selected fraction tends to $1/3$. Direct differentiation recovers the second equation and its initial value.

The matrix B has eigenvalues $1/5$ and $-3/5$, with positive right eigenvector $h = (1, 2)^{\mathsf{T}}$ for the first. The associated time-homogeneous driven generator is

$$\widehat{L} = \operatorname{diag}(h)^{-1}(B - \tfrac{1}{5}I)\operatorname{diag}(h) = \begin{pmatrix} -2/5 & 2/5 \\ 2/5 & -2/5 \end{pmatrix}.$$

Its stationary fraction is $1/2$. In a reversible reference model, the normalized population eigenvector is proportional to $\pi_i h_i$, whereas the driven stationary law is proportional to $\pi_i h_i^2$. Indeed, $\pi_i L_{ij} = \pi_j L_{ji}$ makes $\pi_i h_i^2 \widehat{L}_{ij} = \pi_j h_j^2 \widehat{L}_{ji}$. The three fractions $1/5, 1/3, 1/2$ consequently refer to unweighted occupancy, selected population endpoints, and occupancy along a driven history. Their difference is predicted by the same specified data.

The example also displays the competing terms in (7). At $x = 9/10$, the full mean fitness derivative is $-969/2500 < 0$, despite the nonnegative selection variance. Starting at $p = \pi$, the first derivative of $D(p\|\pi)$ is zero but its second derivative under selection is $36/625 > 0$. Mutation–selection therefore moves away from the bath equilibrium without contradicting the thermal relaxation identity for the unweighted process.

There is a direct parameter-transfer test. For arbitrary positive rates $a = L_{12}$, $b = L_{21}$, let $s = a + b$, $\varpi = a/s$, and use growth difference $\kappa = f_2 - f_1 > 0$, subtracting the common growth f_1. The equilibrium covariance of the state-2 indicator is $\varpi(1 - \varpi)e^{-st}$. Thus equilibrium fraction and correlation decay determine ϖ, s. With κ specified independently, the same operator gives

$$\Delta = \sqrt{s^2 + 2\kappa s(2\varpi - 1) + \kappa^2}, \qquad \lambda = (\kappa - s + \Delta)/2, \qquad x_* = \lambda/\kappa. \quad (10)$$

Here λ is the asymptotic expected-count growth rate and Δ is the driven relaxation rate. These formulas follow from the characteristic polynomial of B. The normalized population equation is $\dot{x} = s(\varpi - x) + \kappa x(1 - x)$, so $x_* \in (\varpi, 1)$. Its implicit derivatives are

$$\partial_\varpi x_* = s/\Delta > 0, \quad \partial_s x_* = (\varpi - x_*)/\Delta < 0, \quad \partial_\kappa x_* = x_*(1 - x_*)/\Delta > 0.$$

The same signs hold for λ, with $\partial_s \lambda < 0$. For $s \in [0.98, 1.02]$, $\varpi \in [0.195, 0.205]$ and $\kappa = 0.6$, corner evaluation gives, to the displayed precision, $\lambda \in [0.194277, 0.205778]$ and $x_* \in [0.323795, 0.342963]$. These are conditional propagated input ranges, not confidence intervals from observations.

2.5. *A martingale constraint and a financial law.* A financial model adds an economic constraint to probability selection. Let a stock have gross returns R_i, let the risk-free gross return be R_f, and let $p_i > 0$ be reference probabilities. Minimize $D(q\|p)$ subject to $\sum_i q_i = 1$ and $\sum_i q_i R_i = R_f$. For a nonconstant

return vector and R_f strictly between its minimum and maximum, the unique minimizer is

$$q_i = \frac{p_i e^{\zeta R_i}}{\sum_j p_j e^{\zeta R_j}}, \qquad \sum_i q_i R_i = R_f. \tag{11}$$

The derivative of the exponential-family mean with respect to ζ is $\mathrm{Var}_q(R) > 0$; its limiting means are the extreme returns. This proves existence and uniqueness of ζ, while the relative-entropy identity proves minimality.

For $p = (0.8, 0.2)$, returns $(0.9, 1.2)$, and $R_f = 1.02$, the constraint gives $q = (0.6, 0.4)$ and $\zeta = \log(8/3)/0.3$. A stock initially worth 100 has a one-period call payoff $(0, 20)$ at strike 100. In the frictionless two-state stock–bond market this payoff is replicable, and its price is $20(0.4)/1.02 = 400/51$. The martingale measure is already unique by completeness. In an incomplete market, minimizing entropy is an additional selection criterion among admissible martingale measures; no-arbitrage alone does not require that criterion [91]. The economic constraints supply the interpretation of the law. They do not follow from a thermal reservoir.

2.5.1. *Incomplete markets: what selects a price.* The two-state example separates the martingale constraint from a thermal interpretation, but completeness leaves no remaining probability to select. An incomplete market exposes the role of the variational principle more clearly. The information projection and martingale interpretation use established methods [48] and [91]. The economic question is how to value a payoff that cannot be replicated using the traded stock and bond. No-arbitrage restricts its price; a specified reference law and a selection rule supply additional information. This is the point at which the common variational structure has a substantive modeling role.

Consider a one-period frictionless market with a bond of initial value one and terminal value $R_f > 0$, and a stock with initial price $S_0 > 0$ and terminal values $s_1, \dots, s_n$. Every state has reference probability $p_i > 0$, with $\sum_i p_i = 1$. Put $\mu = R_f S_0$ and assume $\min_i s_i < \mu < \max_i s_i$. A strictly positive probability vector q satisfying $\sum_i q_i s_i = \mu$ is an equivalent martingale measure: the discounted stock has the same initial value and terminal expectation. For a terminal payoff $H = (H_1, \dots, H_n)$, it assigns the price $R_f^{-1} \sum_i q_i H_i$. Incomplete trading generally permits several such vectors and several prices for a nonreplicable payoff.

Proposition 1 (Entropy selection and its price sensitivity). *Let the terminal stock values be nonconstant and let the preceding strict interior and positivity assumptions hold. On the closed feasible simplex*

$$\mathcal{M}_\mu = \{q_i \geq 0 : \ \sum_i q_i = 1, \ \sum_i q_i s_i = \mu\},$$

the unique minimizer of $D(q\|p) = \sum_i q_i \log(q_i/p_i)$ *is*

$$q_i^\mu = \frac{p_i e^{\lambda(\mu) s_i}}{Z(\lambda(\mu))}, \qquad Z(\lambda) = \sum_i p_i e^{\lambda s_i}, \qquad \frac{Z'(\lambda(\mu))}{Z(\lambda(\mu))} = \mu. \tag{12}$$

The multiplier $\lambda(\mu)$ *is finite and unique, and every* q_i^μ *is positive. For every* $q \in \mathcal{M}_\mu$,

$$D(q\|p) = D(q\|q^\mu) + D(q^\mu\|p). \tag{13}$$

Hold p*, the terminal values* s_i*, the payoff* H_i*, and* R_f *fixed, and regard the target mean* μ *as the variable. The selected price* $C_H(\mu) = R_f^{-1} \sum_i q_i^\mu H_i$ *satisfies*

$$\frac{\mathrm{d}C_H}{\mathrm{d}\mu} = \frac{\mathrm{Cov}_{q^\mu}(H, S_1)}{R_f \,\mathrm{Var}_{q^\mu}(S_1)}. \tag{14}$$

For a call payoff $H_i = (s_i - K)_+$*, this derivative belongs to* $[0, R_f^{-1}]$.

Proof. Define $\psi(\lambda) = \log Z(\lambda)$. Differentiating the finite sum gives

$$\psi'(\lambda) = \sum_i q_i(\lambda) s_i, \qquad \psi''(\lambda) = \sum_i q_i(\lambda)[s_i - \psi'(\lambda)]^2 > 0. \tag{15}$$

Strict positivity follows because all tilted probabilities are positive and at least two stock values differ. As $\lambda \to -\infty$, terms with the smallest stock value dominate the finite sum, so $\psi'(\lambda) \to \min_i s_i$. As $\lambda \to +\infty$, the corresponding limit is $\max_i s_i$. The mean is continuous and strictly increasing; hence the intermediate value theorem gives exactly one finite multiplier with mean μ.

For this multiplier, $\log(q_i^\mu/p_i) = \lambda(\mu) s_i - \psi(\lambda(\mu))$. Therefore, for any feasible q, with $0 \log 0 = 0$,

$$D(q\|p) - D(q\|q^\mu) = \sum_i q_i \log \frac{q_i^\mu}{p_i} = \lambda(\mu)\mu - \psi(\lambda(\mu)) \tag{16}$$

$$= D(q^\mu\|p). \tag{17}$$

Relative entropy is nonnegative, with equality exactly when the two probability vectors coincide. This proves minimality and uniqueness on the entire feasible simplex, including its boundary.

Since $\psi'' > 0$, the inverse function theorem gives $\lambda'(\mu) = 1/\,\mathrm{Var}_{q^\mu}(S_1)$. Direct differentiation also gives $\partial_\lambda q_i = q_i(s_i - \mathbb{E}_q S_1)$, and thus $\partial_\lambda \mathbb{E}_q H = \mathrm{Cov}_q(H, S_1)$. Combining the two derivatives proves (14). Finally,

$$\mathrm{Cov}_q(H, S_1) = \frac{1}{2} \sum_{i,j} q_i q_j (H_i - H_j)(s_i - s_j), \tag{18}$$

$$\mathrm{Var}_q(S_1) = \frac{1}{2} \sum_{i,j} q_i q_j (s_i - s_j)^2. \tag{19}$$

The call function is increasing and one-Lipschitz, so every summand in the first line lies between zero and the corresponding summand in the second. Division by the positive variance proves the last assertion. □

This result supplies an exact measure of sensitivity within a declared model. The mean variation in (14) keeps terminal prices fixed. If $\mu = R_f S_0$ is varied through S_0 under these same conditions, the chain rule gives $\mathrm{d}C_H/\mathrm{d}S_0 = \mathrm{Cov}_q(H, S_1)/\mathrm{Var}_q(S_1)$. A model in which terminal stock values scale with S_0 has additional derivative terms and is a different comparison. Moreover, the multiplier has inverse-price units; equivalently one may use dimensionless returns and a dimensionless multiplier. A change of price units rescales the multiplier and leaves q^μ unchanged.

There is also an informative limit on what a selected price can identify. For any real c, replace the reference law by $\widetilde{p}_i = p_i e^{cs_i}/Z(c)$. The same selected law is obtained by replacing $\lambda(\mu)$ with $\lambda(\mu) - c$. Therefore all prices selected by this criterion remain unchanged under this family of reference-law transformations. A pricing law alone cannot determine the reference law in every direction.

The directions that do affect the price have an explicit formula. Let a_i be fixed and set $p_i(t) = p_i e^{ta_i}/\sum_j p_j e^{ta_j}$. Keep μ, the stock values, the payoff, and R_f fixed, and denote the corresponding selected law by $q(t)$. Differentiation at $t = 0$ gives

$$\left.\frac{\mathrm{d}C_H}{\mathrm{d}t}\right|_{t=0} = \frac{1}{R_f}\left[\mathrm{Cov}_{q^\mu}(H, a) - \frac{\mathrm{Cov}_{q^\mu}(H, S_1)\,\mathrm{Cov}_{q^\mu}(S_1, a)}{\mathrm{Var}_{q^\mu}(S_1)}\right]. \tag{20}$$

Indeed, the normalization in $p(t)$ cancels from the tilted law, so $q_i(t)$ is proportional to $p_i e^{ta_i + \lambda(t)s_i}$. Differentiating its mean constraint gives $0 = \mathrm{Cov}_q(S_1, a) + \lambda'(0)\,\mathrm{Var}_q(S_1)$, which determines $\lambda'(0)$. Differentiating the payoff mean then proves (20). The bracket is the covariance remaining after the stock direction has been removed. It vanishes when a_i is affine in s_i, consistently with the exact invariance above. Thus the reference law matters through changes that remain visible after the traded-price constraint has been imposed.

An explicit three-state comparison. Take the synthetic inputs

$$\begin{gathered} S_0 = 100, \quad R_f = 1.02, \quad (s_1, s_2, s_3) = (80, 100, 130), \\ p = (0.2, 0.5, 0.3), \qquad H = (0, 0, 30). \end{gathered} \tag{21}$$

Here $\mathbb{E}_p S_1 = 105$, whereas the martingale mean is 102. The reference law therefore cannot itself price the stock by discounted expectation. The entropy minimizer is its least relative-entropy adjustment subject to that pricing constraint.

Write $t = q_3$. Normalization and the mean constraint give

$$q_1 = \frac{3}{2}t - \frac{1}{10}, \qquad q_2 = \frac{11}{10} - \frac{5}{2}t, \qquad \frac{1}{15} < t < \frac{11}{25}. \tag{22}$$

The strict inequalities enforce equivalence to the positive reference law. Hence the call admits the open no-arbitrage price interval

$$\frac{100}{51} < C_H < \frac{220}{17}, \qquad 1.9607843 < C_H < 12.9411765. \tag{23}$$

The endpoints belong to the closure of this interval; at either endpoint an equivalent measure is lost. The payoff is not replicable, because its values at stock prices 80 and 100 force any affine stock–bond replicating payoff to vanish everywhere, contradicting the value 30 at stock price 130.

The selected point can be computed through a scalar polynomial. Put $x = e^{10\lambda} > 0$, cancel the common factor $e^{80\lambda}$, and obtain

$$(q_1, q_2, q_3) = \frac{(2, 5x^2, 3x^5)}{2 + 5x^2 + 3x^5}, \qquad 42x^5 - 5x^2 - 22 = 0. \tag{24}$$

The polynomial has exactly one positive root: its derivative is $10x(21x^3 - 1)$, so it first decreases from the negative value -22 and then increases strictly to infinity. Equivalently, uniqueness follows from the variance calculation above. The resulting values are

$$\lambda = -0.00948723241569055, \tag{25}$$

$$q^\mu = (0.2499157104069353, 0.5168071493217746, 0.2332771402712902), \tag{26}$$

$$C_H = 6.86109236092030, \qquad D(q^\mu \| p) = 0.0140872229460959, \tag{27}$$

$$\mathrm{Var}_{q^\mu}(S_1) = 305.9157104069353, \qquad \left.\frac{\mathrm{d}C_H}{\mathrm{d}\mu}\right|_{\mu=102} = 0.627985355345821. \tag{28}$$

These are model calculations, not observed option prices. The scalar polynomial permits exact rational bracketing of its root and of the selected call price, in addition to floating-point evaluation.

Figure 1 shows the selection on the feasible martingale line and the price response when the target mean changes. The second panel holds the terminal values, payoff, reference probabilities and bond return fixed; it implements precisely the comparison in (14).

The example also makes the economic assumption visible. If the reference probabilities are replaced by any strictly positive feasible vector, that vector becomes the entropy minimizer because its relative entropy with respect to itself is zero. Thus different admissible reference laws can select different prices within (23). The variational principle becomes empirically restrictive only after the reference law and its calibration are fixed independently of the target payoff price. It expresses a common constrained-selection operation; it supplies neither a thermal heat interpretation nor a unique market law without economic inputs.

This distinction leads naturally to the next model. Selection under a martingale constraint concerns the prices of traded risks, whereas a stationary

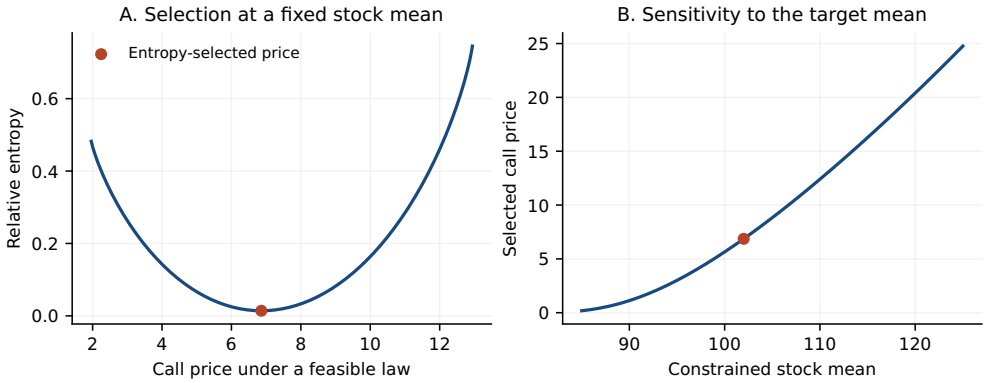


Figure 1. Synthetic incomplete-market calculation using (21). Left: relative entropy along the feasible martingale line, parameterized by the call price; the point marks the unique entropy minimizer. Right: the selected call price at 41 target stock means from 85 to 125, with the point marking the original mean 102. The reference law and terminal values are held fixed throughout the second comparison. These curves describe the stated model and do not use observed option prices.

process can also sustain probability currents. The cyclic example below explains why a fixed one-time distribution does not imply the absence of continuing change.

2.6. *Cyclic change and an institutional interpretation.* The same description also permits persistent cycles. On three states, give each clockwise transition rate 2 and each counterclockwise transition rate 1. The stationary law is uniform, yet the clockwise current on every edge is $1/3$. For even state variables, its stationary forward–reverse path relative-entropy rate is

$$\sum_{\{i,j\}} (\pi_i L_{ij} - \pi_j L_{ji}) \log \frac{\pi_i L_{ij}}{\pi_j L_{ji}} = \log 2$$

per chosen time unit. The sum has one orientation of each undirected edge. Stationarity therefore coexists with ongoing directed change. This model fits the path-selection principle but does not satisfy the detailed-balance assumption used in the thermal gradient calculation.

For an organizational application, the states may denote three institutional arrangements and the rates their empirically estimated replacement frequencies under fixed external conditions. A cyclic transition pattern is then described without assuming a global ranking of the arrangements. If resources, incentives or institutions alter the rates, they must be included as state variables or specified external inputs. The path entropy above quantifies statistical time

asymmetry; a heat or welfare interpretation requires further physical or social definitions. This provides a conditional model for social evolution within the common structure, with its own measurable transitions.

2.7. *Conservative motion and a matched reservoir.* The finite-state example describes probabilities and selection. A continuous physical realization also exhibits the transport part. For mass one, oscillator frequency ω, friction $\gamma \geq 0$, and reservoir energy $\theta > 0$, consider

$$dq = p\,dt, \qquad dp = (-\omega^2 q - \gamma p)\,dt + \sqrt{2\gamma\theta}\,dW_t, \qquad H = (p^2 + \omega^2 q^2)/2. \tag{29}$$

Units are fixed before setting the mass to one: q is displacement, p is momentum per unit mass, and H, θ are energies per unit mass. Time and displacement can then be expressed in chosen units. The equilibrium covariance is $\Sigma = \operatorname{diag}(\theta/\omega^2, \theta)$. Writing the drift matrix as $A = \left(\begin{smallmatrix} 0 & 1 \\ -\omega^2 & -\gamma \end{smallmatrix}\right)$, the identity $A\Sigma + \Sigma A^{\mathsf{T}} + \operatorname{diag}(0, 2\gamma\theta) = 0$ proves invariance of the Gaussian Gibbs law.

The Hamiltonian part $(p, -\omega^2 q)$ preserves energy and phase volume. Integration by parts for the damping and diffusion terms gives

$$\frac{d}{dt} D(\rho_t \| \pi) = -\gamma\theta \int \rho_t |\partial_p \log(\rho_t/\pi)|^2 \, dq\, dp,$$

for positive smooth densities with the stated boundary decay. Itô's formula also gives $d\mathbb{E}H/dt = -\gamma \mathbb{E}p^2 + \gamma\theta$. Thus the same γ governs damping and thermal injection. At $\gamma = 0$, both terms vanish and Hamilton's equations remain. This conservative recovery follows from the matched reservoir scaling, rather than from suppressing noise alone.

For a small force added to the momentum equation, the position impulse response is $\mathcal{R}_{qp}(t) = (e^{At})_{12}$. The equilibrium position covariance is $C_{qq}(t) = (e^{At}\Sigma)_{11}$. Since $A\Sigma$ has first column $(0, -\theta)^{\mathsf{T}}$,

$$\mathcal{R}_{qp}(t) = -\theta^{-1} \frac{d}{dt} C_{qq}(t), \qquad t > 0. \tag{30}$$

One parameter set therefore fixes mechanical response, equilibrium fluctuations and dissipation. The example makes the second organizing principle a measurable relation.

The scalar solution and matrix semigroup agree to 1.0×10^{-15} in the displayed two-state example. A separate numerical integration of its nonlinear equation agrees within 8.0×10^{-13}. Direct oscillator moment integration agrees with the matrix solution within 2.0×10^{-12}; the fluctuation–response identity differs by less than 4.5×10^{-16} in double precision. These checks concern the synthetic finite models. Their purpose is to make the common construction calculable before pursuing its field and empirical applications.

The examples establish a precise division of work for the larger programme. Geometry specifies admissible variables and constraints; the reference dynamics

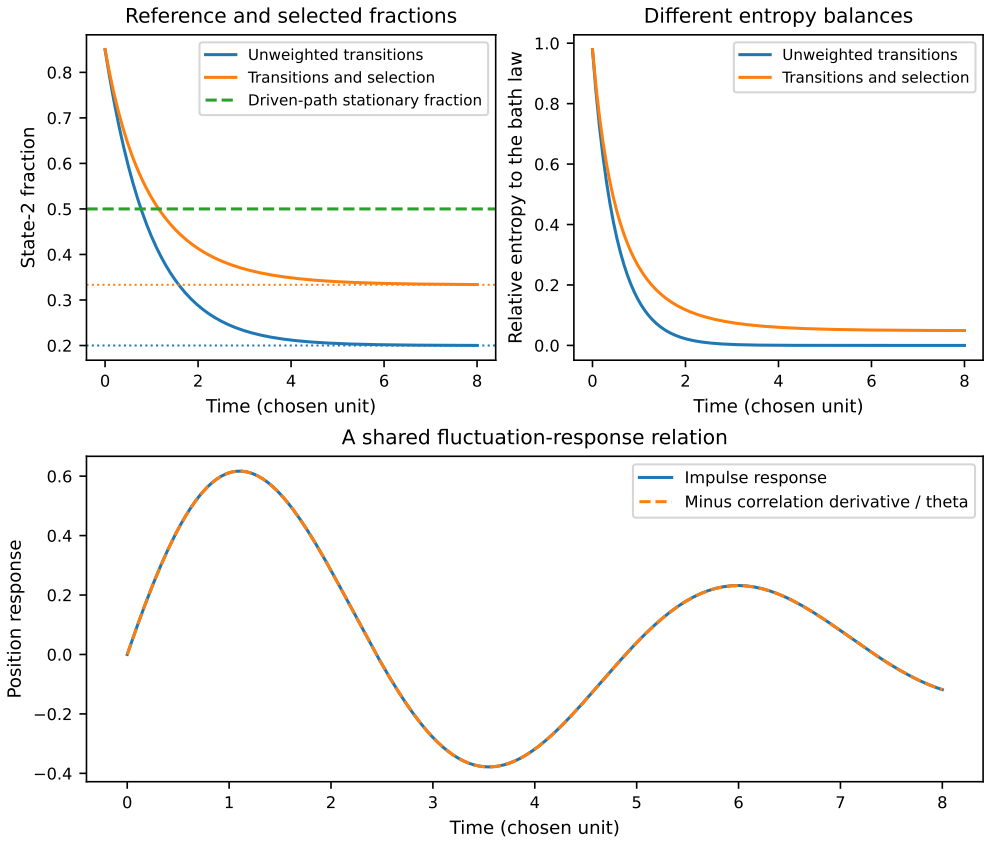


Figure 2. Synthetic representative models. Upper left: the two-state model with initial fraction 0.85 has different unweighted and selected population limits; the driven-history fraction is a third observable. Upper right: relative entropy to the bath law decreases for unweighted transitions, whereas selection permits a different balance. Below: the oscillator with $\omega = 1.3$, $\gamma = 0.4$ and $\theta = 0.8$ satisfies the fluctuation–response relation. Units are chosen consistently within each model; the panels do not identify biological rates with mechanical frequencies.

specifies transport and fluctuations; weighting and constraints specify selection; observation determines which law is being compared. The field construction now supplies the geometric data on which those operations act. A physical application gains explanatory force when these data fix several responses together.

3. The master configuration, action, and one path-space cost

3.1. *Master configuration space and unified geometry.* We now specify the objects on which the variational principle acts. Three spaces play different roles: the spacetime manifold carries the fields, the principal bundle describes their gauge transformations, and the configuration space carries the stochastic law. Keeping these spaces distinct is necessary for the later definitions of curvature, field-space gradients, and probability densities.

Definition 1 (Finite regulator). *A finite-regulator realization specifies a finite volume or compact domain, its boundary conditions, and finitely many retained field coordinates. A lattice spacing $a > 0$ can regulate ultraviolet wavelengths, while a spectral or Galerkin cutoff $N < \infty$ can regulate the number of modes; a given realization need not use both. Gauge variables can be retained on compact link groups, represented on a specified local gauge slice, or treated on a physical quotient. The choice must preserve the identities used in the corresponding result; a globally smooth gauge slice is not assumed. The coordinate state space, measure, operator domains, and all constrained directions are part of the regulator data. A numerical time step Δt is an additional approximation and is not the regulator a or N. Removing a, N, the finite volume, and Δt requires separate estimates, with an explicitly stated order of limits.*

In particular, a finite-dimensional Gibbs density is a classical probability law on the declared bosonic coordinates. It is not a probability density on Grassmann-valued fermion variables. Incorporating fermions into a positive Euclidean physical-state construction requires the additional steps described in Section 12.1.

3.2. *The microscopic configuration.* Let M be a smooth four-dimensional manifold used as the mathematical starting point. No physical spacetime metric is assumed as an independent microscopic field. A non-degenerate coframe contained in the Cartan connection will induce the Euclidean metric used by the geometric sector. In finite-dimensional or Galerkin calculations one may, before such a coframe is selected, introduce an auxiliary positive reference metric $\bar{g}$ and its volume form $\mathrm{vol}_{\bar{g}}$ to define Sobolev norms, regulators, and temporary analytic estimates. Every formula involving the physical curvature or the heat-kernel coefficients is to be read with the induced metric after the coframe exists; formulas proved on the regulator are statements about that regularized realization. A global physical Lorentzian completion, if it exists, must be obtained by a separately justified analytic continuation together with a proof of causality and unitarity. This global completion is stronger than the local continued Euler equations recovered below. We do not identify Euclidean stochastic time with physical time.

Let $\widetilde{G}$ be a Lie group with Lie algebra $\mathfrak{g}$, let $H \subset \widetilde{G}$ be a closed subgroup with Lie algebra $\mathfrak{h}$, and let $P_H \to M$ be a principal H-bundle. Because the translational generators are represented by a coframe, the master field is a Cartan connection $\mathbb{A} \in \Omega^1(P_H, \mathfrak{g})$, rather than an ordinary principal connection whose values are confined to $\mathfrak{h}$. Thus, in addition to H-equivariance and reproduction of fundamental vertical vector fields, a Cartan connection is a pointwise linear isomorphism $T_pP_H \to \mathfrak{g}$. These are the standard geometric requirements in gauge-geometric formulations of gravity [152], [118], and [122]. A concrete model must specify $(\widetilde{G}, H)$ and prove that the associated bundle exists globally; until then, the formulas below are local expressions. The master algebra is required to admit a representation in which spacetime translations, local rotations/boosts after continuation, and internal transformations occur as components of one algebraic structure. Explicitly, for $h \in H$ and $\xi \in \mathfrak{h}$, the Cartan axioms are

$$(R_h)^*\mathbb{A} = \mathrm{Ad}(h^{-1})\mathbb{A}, \qquad \mathbb{A}(\xi^{\#}) = \xi, \qquad \mathbb{A}_p : T_pP_H \longrightarrow \mathfrak{g} \text{ is an isomorphism.} \tag{31}$$

For a Cartan geometry of type $(\widetilde{G}, H)$, these axioms imply $\dim \mathfrak{g} = \dim P_H = \dim M + \dim H$ and identify $\mathfrak{g}/\mathfrak{h}$ with the tangent model of M. In the component notation used below we assume that the classes of the P_a form a basis of $\mathfrak{g}/\mathfrak{h}$, while the J_{ab} and T_A span the selected subalgebra $\mathfrak{h}$. If a reductive enlargement is used, it must be declared as the new isotropy algebra before taking the quotient; generators outside that declared isotropy algebra cannot be counted simultaneously as its basis elements. If a concrete model assigns any of these generators differently, the decomposition and all dimension counts must be changed accordingly. The Cartan-connection axioms used here are standard; see, for example, [145]. We now write the master algebra abstractly.

$$\mathfrak{g} = \mathrm{span}\{P_a, J_{ab}, T_A\}, \tag{32}$$

without assuming at this stage that the algebra is a direct sum. The brackets are

$$[P_a, P_b] = c_{ab}{}^{c}P_c + c_{ab}{}^{cd}J_{cd} + c_{ab}{}^{A}T_A, \tag{33}$$

$$[J_{ab}, P_c] = c_{ab,c}{}^{d}P_d, \qquad [T_A, P_b] = c_{Ab}{}^{c}P_c, \tag{34}$$

and similarly for the remaining generators. The coefficients are subject to the Jacobi identities. For a reductive splitting $\mathfrak{g} = \mathfrak{h} \oplus \mathfrak{m}$, the defining condition is $[\mathfrak{h}, \mathfrak{m}] \subseteq \mathfrak{m}$. It does not in general force $c_{ab}{}^{c} = 0$. The additional condition $[\mathfrak{m}, \mathfrak{m}] \subseteq \mathfrak{h}$ gives a symmetric reductive pair and does force that coefficient to vanish. Keeping $c_{ab}{}^{c}$ in the general curvature formula records the translational curvature term in a nonsymmetric reductive realization. In a nonreductive realization the chosen complement need not transform invariantly, and the corresponding local coframe splitting requires a separate formulation.

At least one nonzero mixed structure constant is a useful diagnostic of microscopic coupling, but it is neither necessary when the invariant pairing or field-space metric has cross-components nor sufficient for irreducibility. If we impose this diagnostic as a model-building requirement, it reads

at least one admissible mixed bracket in the master algebra is nonzero. (35)

Vanishing mixed brackets and an orthogonal invariant pairing imply factorization of these algebraic data, but not of the complete theory. A shared metric, scalar, reference measure, or mobility can still couple the factors. Reducibility requires factorization of the entire dynamical package in Definition 2.

After choosing a local section of P_H, the master connection is represented by

$$\boxed{\mathbb{A} = \ell^{-1} e^a P_a + \frac{1}{2}\omega^{ab} J_{ab} + A^A T_A,} \tag{36}$$

where $\ell > 0$ is a reference length, e^a is a coframe, $\omega^{ab} = -\omega^{ba}$ is a connection component, and A^A are internal components. Equation (36) is not yet a decomposition of four forces; it is the component expression of one connection in a chosen basis. All forms in the action and curvature formulas below are the pullbacks of these Cartan data to the base manifold through the chosen local section.

3.3. *Metric status and the meaning of the master geometry.* The metric used in the Euclidean action must be distinguished from the field-space metric used to define gradients and mobilities. On the non-degenerate coframe branch, the Cartan component e induces a spacetime metric by

$$g_e := \delta_{ab}\, e^a \otimes e^b, \qquad \mathrm{vol}_{g_e} := e^1 \wedge e^2 \wedge e^3 \wedge e^4. \tag{37}$$

Here an orientation and a Euclidean internal frame have been fixed. In the induced-metric realization the isotropy action on the coframe quotient is required to preserve the Euclidean form: if ρ_H denotes the action on $\mathfrak{g}/\mathfrak{h} \simeq \mathbb{R}^4$, then $\rho_H(h)^{\mathsf{T}}\rho_H(h) = I_4$ and $\det \rho_H(h) = 1$ for every admitted $h \in H$. Equivalently, for the connected component of H, in an infinitesimal basis one requires the symmetric part of each generator on the coframe indices to vanish. Without this condition the displayed metric depends on the choice of local isotropy frame and is not a gauge-invariant metric. A concrete model may replace this condition by an explicitly specified compensating field, but that field must then be included in the configuration and its variation. In the *induced-metric realization*, $g = g_e$ and the coframe is a component of $\mathbb{A}$ that is varied together with the other master variables. The non-degeneracy assumption means that $e_x : T_xM \to \mathbb{R}^4$ is an isomorphism on every point of the branch under consideration; it is not a consequence of the stochastic notation.

For a finite-dimensional regulator one may instead use a fixed reference metric g_0 in the Hodge operator and volume form. This is the *background-regularized realization*; in that case the action and all heat-kernel coefficients are defined relative to g_0, and no claim that the spacetime metric is generated by the master dynamics is made. Whenever the symbol g is used without a subscript below, the intended realization must therefore be stated: $g = g_e$ when the coframe is dynamical, and $g = g_0$ in a fixed-background calculation. In particular, Appendix A freezes e, g, and vol_g while deriving only the connection component of the Euler–Lagrange equation; the full induced-metric theory requires the additional coframe and volume variations. The notation $\mathbb{G}$ for the positive field-space metric is independent of the spacetime metric g, although a concrete realization may construct $\mathbb{G}$ from g after gauge fixing.

The phrase "master geometry" consequently refers to the tuple $(P_H, \mathbb{A}, e, \omega, g_e)$ on the induced branch, or to $(P_H, \mathbb{A}, g_0)$ in a background-regularized branch. These two realizations share the algebraic curvature formulas, but only the first can support a claim that the metric itself is part of the dynamical master configuration. A Lorentzian metric, if obtained by continuation, requires a separate choice of real form and a proof of the corresponding analytic, causal, and unitarity properties.

Choose a basis $\{T_I\} = \{P_a, J_{ab}, T_A\}$, write $\mathbb{A} = A^I T_I$, and denote the structure constants by $[T_I, T_J] = C_{IJ}{}^K T_K$. The master curvature is

$$\boxed{\mathbb{F} = \mathrm{d}\mathbb{A} + \mathbb{A} \wedge \mathbb{A}.} \tag{38}$$

In components,

$$\mathbb{F} = F^I T_I, \qquad F^K = \mathrm{d}A^K + \frac{1}{2} C_{IJ}{}^K A^I \wedge A^J. \tag{39}$$

This component identity is exact and includes every gravitational–internal mixed term through the same structure constants. In the adapted local notation of (36), one has, for example,

$$T^a = \ell \left(\mathrm{d}A^{P_a} + \frac{1}{2} C_{IJ}{}^{P_a} A^I \wedge A^J \right), \tag{40}$$

$$R^{cd} = 2 \left(\mathrm{d}A^{J_{cd}} + \frac{1}{2} C_{IJ}{}^{J_{cd}} A^I \wedge A^J \right), \tag{41}$$

$$\mathbb{F}^A = \mathrm{d}A^{T_A} + \frac{1}{2} C_{IJ}{}^{T_A} A^I \wedge A^J. \tag{42}$$

If the selected algebra has the usual Lorentz brackets, the first two lines contain $\mathrm{d}e^a + \omega^a{}_b \wedge e^b$ and $\mathrm{d}\omega^{cd} + \omega^c{}_e \wedge \omega^{ed}$; the remaining terms are not omitted but are exactly the corresponding $C_{IJ}{}^K$-contributions. In particular, the coefficient of the $e^a \wedge e^b$ term in R^{cd} is fixed by $C_{P_a P_b}{}^{J_{cd}} \ell^{-2}$ under the normalization in (39); it is present precisely when $[P_a, P_b]$ has the displayed J_{cd}-component.

3.4. *Matter, order parameter, and information as one state variable.* Let $E_\Psi \to M$ be the representation bundle for the complete matter multiplet Ψ, and let $E_H \to M$ be a representation bundle in which a possible scalar order parameter Φ_H takes values. Let $E_\chi \to M$ be the specified information-state bundle, possibly the trivial real line bundle, and let χ be a section of E_χ. Let $E_\sigma := M \times \mathbb{R}$ carry the dimensionless shared scalar coordinate σ used below; its covariant differential is simply $\mathrm{d}\sigma$. The scalar is a genuine configuration coordinate whenever the joint candidate is used, not a parameter silently added after variation. The information state is not assumed to be a new fundamental force. It is an auxiliary or potentially fundamental variable whose physical status must be determined by the selection problem. Its inclusion is motivated by the fact that probability, entropy, and state preparation enter the stochastic principle. The order parameter is written explicitly because its covariant derivative and its representation are needed in the conditional electroweak statement below; omitting it from the primitive configuration would make that statement ill-typed.

Define the field configuration

$$\boxed{\mathbb{X} = (\mathbb{A}, \Psi, \Phi_H, \sigma, \chi),} \tag{43}$$

The spacetime geometry is derived from the translational component of $\mathbb{A}$, rather than appended as a fifth independent interaction. The precise induced metric, the alternative fixed-background regularization, and the scope of the fixed-coframe variation are given in Subsection 3.3 and equation (37). This cross-reference is important: the regularized stochastic identities do not by themselves assert that a heat-kernel calculation creates a metric from no geometric data. Let $\mathfrak{X}$ denote the chosen configuration manifold (finite dimensional or rigorously regularized when analytic identities are used) containing these quintuples. We reserve μ_{info} for the information-state parameter entering $\mathfrak{I}$, while the evolving probability law of $\mathbb{X}_t$ is denoted by μ_t (or by its density p_t when a reference volume exists). Thus the probability law is not confused with a field coordinate, and $\mathfrak{X}$ contains the geometric and matter/order-parameter variables themselves. In particular, μ_t is not a variational component of $\mathbb{X}$ in the present formulation; it enters through the probability and free-energy layer. Identifying μ_t with a component of the primitive state would produce a McKean–Vlasov problem and would require a separate variational and Fokker–Planck analysis.

A master covariant derivative is defined by

$$\mathbb{D} = \mathrm{d} + \rho_{\mathrm{rep}}(\mathbb{A}), \tag{44}$$

where ρ_{rep} denotes the relevant representation. Since E is associated to the principal H-bundle, this notation presupposes either that the representation extends from H to the selected action of the full Cartan algebra $\mathfrak{g}$, or that $\mathbb{D}$

is explicitly understood to use only the $\mathfrak{h}$-component of $\mathbb{A}$. A concrete model must make this choice before the covariant derivatives below are defined. Thus

$$\mathbb{D}\Psi, \qquad \mathbb{D}\Phi_H, \qquad \mathbb{D}\chi \tag{45}$$

are components of one covariant differential rather than separately postulated kinetic terms. The representation used for E_H must be specified (or extended from H to $\mathfrak{g}$) before $\mathbb{D}\Phi_H$ is defined.

3.5. *The single master action.* The geometric construction supplies curvature and covariant derivatives, but a scalar action also requires pairings and normalizations. We state these data before forming the extended norm. Their positivity controls the Euclidean action; their gauge equivariance ensures that the value of the action is independent of the chosen local representative.

3.6. *Invariant pairing.* Let $\langle\cdot,\cdot\rangle_{\mathfrak{g}}$ be an invariant bilinear form on the master algebra:

$$\langle[X,Y],Z\rangle_{\mathfrak{g}} + \langle Y,[X,Z]\rangle_{\mathfrak{g}} = 0 \qquad \forall X,Y,Z \in \mathfrak{g}. \tag{46}$$

In the basis $\{T_I\}$, write $\langle T_I, T_J\rangle_{\mathfrak{g}} = h_{IJ}$. For a general master algebra, the invariant form may contain mixed blocks, but this is not automatic. Distinct simple ideals in a direct-product algebra are orthogonal for every invariant bilinear form, even when the ideals are isomorphic. Indeed, if $X = [U,V]$ belongs to one simple ideal and Y belongs to another, invariance gives $\langle[U,V],Y\rangle_{\mathfrak{g}} = -\langle V,[U,Y]\rangle_{\mathfrak{g}} = 0$; every element of a simple ideal is a sum of such commutators. The same argument makes every perfect ideal orthogonal to the centre. Mixed invariant pairings within an abelian centre remain possible. Consequently, for the explicit product candidate in Section 5.4, the gravitational–internal coupling is carried by the shared order parameter and the coupled field-space mobility, not by an assumed cross-pairing between the simple Lie-algebra factors. Whether the full extended pairing is block diagonal is determined by its representations and shared field dependence. Symmetry reduction can induce further block structure, but is not required for an invariant orthogonal decomposition already present microscopically. For a non-compact real form, an invariant form is generally indefinite; consequently, the positivity assumption used for the Euclidean stochastic theory entails a specified Euclidean/compact real slice (or another explicitly defined positive regularization) and cannot be transferred to the Lorentzian continuation without a separate argument.

Let $\mathbb{G}$ be the positive field-space metric on the bosonic variables, let $\mathbb{G}_H$ denote the positive pairing on the scalar order-parameter sector, and let $\mathbb{K}$ be the specified regularized fermionic pairing. Let $\mathscr{T}_{\mu_{\mathrm{info}}}$ be a μ_{info}-dependent Hilbert bundle over M, obtained from a specified realization of the tangent space to the probability-law manifold at μ_{info}. Let $\mathscr{E}_{H,0}$ be an optional algebraic auxiliary bundle. If a candidate is to generate a scalar potential from the

one-norm principle, it must supply a specified map $\mathfrak{U}_H : E_H \times \mathbb{R} \to \mathscr{E}_{H,0}$; if no such bundle and map are present, no scalar potential is claimed to follow from the master action. We then set

$$\begin{aligned}\mathscr{E}_{\mathrm{ext}} := (\Lambda^2 T^*M \otimes \mathfrak{g}_{P_H}) \oplus (T^*M \otimes E_\Psi) \oplus (T^*M \otimes E_H) \\ \oplus (T^*M \otimes E_\sigma) \oplus (T^*M \otimes E_\chi) \oplus \mathscr{E}_{H,0} \oplus \mathscr{T}_{\mu_{\mathrm{info}}},\end{aligned} \tag{47}$$

Here $\mathfrak{g}_{P_H} := P_H \times_{\mathrm{Ad}|_H} \mathfrak{g}$; the extended curvature is a section of this bundle. This distinguishes a bundle from its space of differential-form sections. The restrictions of $\mathbf{h}$ to the bosonic, scalar, and regularized fermionic sectors are built from $\mathbb{G}$, $\mathbb{G}_H$, and $\mathbb{K}$, respectively. The seven entries in this direct sum have different form degrees and fibre types; their addition below is therefore shorthand for the ordered tuple, not an untyped sum. We fix a continuous graded bilinear form $\mathbf{h}$ on $\mathscr{E}_{\mathrm{ext}}$, including the required Hodge maps and reference scales, and assume that it is non-degenerate and positive on the chosen Euclidean real slice. Without this assumption the expression is not a norm and neither boundedness below nor a Gibbs measure follows. For Grassmann-valued matter variables, this positivity statement refers to the associated regularized quadratic form after the fermionic integration; it is not a claim that a Grassmann algebra carries an ordinary pointwise norm. In particular, $\mathfrak{I}(\mu_{\mathrm{info}})$ is required to be represented as a section over M, not merely as an abstract functional derivative. At the abstract level used here, $\mathfrak{I}$ is an unspecified map from the admissible probability-law manifold into this section bundle; a concrete realization must define that map (for example, by specifying an information functional and its variational derivative). No particular information functional or gradient representation of $\mathfrak{I}$ is assumed here. The preceding section-valued requirement is part of the data, not a consequence of notation. Let $\mathcal{P}$ denote the chosen manifold of admissible probability laws on the regularized configuration space. More explicitly, a realization must provide an evaluation or pullback map

$$\mathcal{E}_{\mu_{\mathrm{info}}} : T_{\mu_{\mathrm{info}}}\mathcal{P} \longrightarrow \Gamma(M, \mathscr{T}_{\mu_{\mathrm{info}}}). \tag{48}$$

and $\mathfrak{I}$ denotes a specified map whose value is interpreted through $\mathcal{E}_{\mu_{\mathrm{info}}}$. Without such a map the last component is only a formal ordered entry and the master action is not yet a well-typed geometric functional.

We also require the pairing used in the action to be equivariant under every gauge transformation admitted by the chosen bundle. If R_g is its induced action on the extended bundle, the required condition is

$$\mathbf{h}(R_g U, R_g V) = \mathbf{h}(U, V) \qquad \text{for all admissible } g \text{ and } U, V \in \mathscr{E}_{\mathrm{ext}}. \tag{49}$$

Thus the Hodge operators, reference scales, and mixed blocks entering $\mathbf{h}$ must be H-equivariant (or equivariant under a declared extension of the action). The Lie-algebra identity (46) alone does not imply (49) for the full extended tuple.

The same requirement must be imposed on every map used to form that tuple. If R_h^H and R_h^0 denote the actions on E_H and $\mathscr{E}_{H,0}$, respectively, then

$$\mathfrak{U}_H(R_h^H\Phi,\sigma) = R_h^0\mathfrak{U}_H(\Phi,\sigma), \qquad h\in H. \tag{50}$$

Here σ is a gauge singlet, as specified in the configuration. The information source must either be gauge invariant, $R_h\mathfrak{I}(\mu_{\mathrm{info}}) = \mathfrak{I}(\mu_{\mathrm{info}})$, or transform as a declared spurion. If $\mathbf{h}$ depends on the field, its condition is the corresponding equivariance identity $\mathbf{h}_{h\cdot\mathbb{X}}(R_hU,R_hV) = \mathbf{h}_{\mathbb{X}}(U,V)$. These conditions are part of the definition of a gauge-covariant realization; they do not follow from positivity of the fibre pairing. We now define

$$\boxed{\begin{aligned}\mathbf{F}_{\mathrm{M}}^{\mathrm{ext}} := \Big(&\mathbb{F}, \ell_\Psi^{-1}\mathbb{D}\Psi, \ell_H^{-1}\mathbb{D}\Phi_H, \ell_\sigma^{-1}\mathrm{d}\sigma,\\ &\ell_\chi^{-1}\mathbb{D}\chi, \ell_V^{-2}\mathfrak{U}_H(\Phi_H,\sigma), \ell_\mu^{-1}\mathfrak{I}(\mu_{\mathrm{info}})\Big) \in \Gamma(M,\mathscr{E}_{\mathrm{ext}}).\end{aligned}} \tag{51}$$

where $\ell_\Psi, \ell_H, \ell_\sigma, \ell_\chi, \ell_V, \ell_\mu$ are reference scales introduced only to make the components dimensionally commensurate; ℓ_μ is associated with the fixed information parameter μ_{info}. The algebraic component $\mathfrak{U}_H(\Phi_H,\sigma)$ is the precise place at which a Higgs-type potential may enter the one-norm construction. For example, after a specified reduction of the $\mathscr{E}_{H,0}$ block, its diagonal contribution can define a function $V_H(\Phi_H)$; this is not an independently added scalar potential. If the candidate supplies no such map, the later Higgs discussion is only a target condition and no potential is derived. Because μ_{info} is fixed in the present formulation, the last entry is a prescribed source section rather than an independently stochastic coordinate. It can influence the drift only through the chosen pairing and its cross-blocks with the varied fields; if the pairing is block diagonal and the source is field-independent, its contribution is an additive constant and does not alter the field equations. A dynamical information law would require promoting μ_{info} to the configuration and rederiving the stochastic and equilibrium identities. The construction is formal until the Hilbert realization, the reference measure, and the pairing $\mathbf{h}$ are supplied. The stochastic and Gibbs arguments below are understood on a bosonic finite-dimensional or regularized realization (for example, after the fermionic variables have been integrated out); no Itô diffusion on a raw Grassmann algebra is asserted. The positive Euclidean norm of a component such as $\mathbb{D}\Psi$ produces only a quadratic second-order form of schematic type $\langle\mathbb{D}\Psi, \mathbb{K}\mathbb{D}\Psi\rangle$. It does not, without an additional construction, equal the first-order chiral Dirac functional $\int \overline{\Psi}\ \not{D}\,\Psi$. Obtaining the latter requires a specified Grassmann functional integral, a Dirac operator and its adjoint, a fermion measure, the determinant or Pfaffian phase, and a regulator for chiral and gauge anomalies. Thus any occurrence of $\overline{\Psi}\not{\mathscr{D}}\Psi$ in a matched effective target is a conditional fermionic interface, not a consequence of positivity of the bosonic master norm alone.

The master action is therefore the single norm-square

$$\boxed{\mathcal{S}_{\mathrm{M}}[\mathbb{X}] = \frac{1}{4}\int_M \left\langle \mathbf{F}_{\mathrm{M}}^{\mathrm{ext}}, \mathbf{F}_{\mathrm{M}}^{\mathrm{ext}} \right\rangle_{\mathbf{h}} \, \mathrm{vol}_g} \tag{52}$$

Here "one pairing" means the single graded pairing $\mathbf{h}$ on $\mathscr{E}_{\mathrm{ext}}$. The objects h_{IJ}, $\mathbb{G}$, $\mathbb{K}$, and the reduced κ_{AB} are its restrictions or induced blocks after the relevant geometric structures have been fixed; they are not independent action functionals. Any order-parameter potential is, by definition, included as a component of the extended curvature in $\mathscr{E}_{\mathrm{ext}}$; introducing an independent additive potential would violate the one-norm principle. Equation (52) is the fundamental definition used in the conceptual formulation. Appendix A derives the fixed-background connection variation; Section 5.1 treats the metric and Hodge dependence associated with a dynamical coframe. A complete Euler–Lagrange system also includes the matter and order-parameter variations and any field dependence of the pairing. The information-state parameter is fixed, so there is no probability-law Euler–Lagrange equation in this formulation. If the Hodge maps in $\mathbf{h}$ are built from the induced metric $g[\mathbb{X}]$, then $\mathbf{h}$ is field-dependent in the full problem; freezing it is an explicitly stated fixed-background slice. The primitive action is the squared norm of an extended master curvature. Its components and invariant pairing are part of the primitive data. After those data are fixed, expansion determines the displayed sector terms. This representation alone does not determine independently variable block weights or potentials: an arbitrary nonnegative sum can also be represented as a norm on a direct sum. A substantive unification claim therefore requires constraints on the primitive data, a nonfactorization result for the complete dynamics, and jointly compatible physical projections. The evolving probability law enters through the stochastic and free-energy layers below.

The extended-curvature formulation also imposes that the order-parameter potential be generated by the same master data. No independent sector-specific potential is introduced at the microscopic level. In a concrete realization, the scalar potential must arise from the internal components, algebraic constraints, or auxiliary directions of $\mathbf{F}_{\mathrm{M}}^{\mathrm{ext}}$. The observed masses and couplings must consequently arise through vacuum selection and matching.

In the stochastic and equilibrium sections, μ_{info} in $\mathfrak{I}(\mu_{\mathrm{info}})$ is held fixed as an information-state parameter, and its dependence is suppressed in the notation $\mathcal{S}_{\mathrm{M}}[\mathbb{X}]$. If μ_{info} is instead identified with the evolving law μ_t of $\mathbb{X}_t$, the model becomes a McKean–Vlasov system and the Markov Fokker–Planck and Gibbs statements below require a separate derivation; that nonlinear-law case is not asserted here.

3.7. *Factorization of the complete dynamics.* The distinction can be stated formally. Suppose the configuration manifold were a product

$$\mathfrak{X} = \mathfrak{X}_g \times \mathfrak{X}_i \tag{53}$$

and suppose both the invariant pairing and the action factorized:

$$h = h_g \oplus h_i, \qquad \mathcal{S}_{\mathrm{M}} = \mathcal{S}_g + \mathcal{S}_i. \tag{54}$$

If, in addition, the reference measure is a product and the mobility and all shared field dependence split into the same independent factors, the associated dynamics factorizes. A block decomposition of the action alone does not give that conclusion. The irreducibility requirement below therefore concerns the complete configuration, action, measure, and stochastic data.

Definition 2 (Microscopic irreducible unification). *A master model is called microscopically irreducible if its complete data package admits no nontrivial product decomposition into two independent configuration spaces, reference measures, actions, admissible density classes, and Markov generators. A decomposition of the Lie algebra into orthogonal invariant ideals is only a diagnostic for such a factorization; it is neither necessary nor sufficient. In particular, a simple master algebra can still be accompanied by an independent neutral field, while a direct-product algebra can remain coupled through a shared scalar, metric, measure, or mobility. The four low-energy sectors are said to be emergent if their decoupled effective actions are obtained only after a mathematically specified limiting or symmetry-breaking operation.*

This definition is intentionally stronger than simply writing a larger Lagrangian. For later reference, collect the microscopic data into the single object

$$\Gamma := \big(\widetilde{G}, H, P_H, \mathfrak{g}, \mathcal{R}, \mathbf{h}, \mathscr{E}_{\mathrm{ext}}, \mathfrak{U}_H, \mathfrak{I}, \mathfrak{X}_\Gamma, \nu_\Gamma, \mathbb{G}_\Gamma, \mathbb{M}_\Gamma, \mathfrak{m}_\Gamma, \mu_{\mathrm{info}}\big). \tag{55}$$

Here $\mathcal{R}$ denotes all representation data, including the matter and order-parameter representations; $\mathfrak{X}_\Gamma$ and ν_Γ are the candidate configuration space and reference-measure class; and $\mathfrak{m}_\Gamma$ records whether the metric is induced by the coframe or held fixed as a regulator. Across the abstract candidate class, the residual group, representation content, and coupling parameters may vary with Γ; they are not universal conclusions of the notation. In the worked candidate Γ_0, the internal group and the displayed matter representations are explicit inputs. They become predictions only if independent selection, anomaly, and matching arguments determine them from a previously fixed admissible class. The irreducibility requirement is a requirement on the entire package Γ, not on a Lie bracket alone: a nonzero mixed bracket is neither necessary nor sufficient if the pairing, representation maps, or mobility still split into independent blocks.

3.8. *The extended norm and its component expansion.* The distinction can be made algebraically. Let $\mathbf{F}_{\mathrm{M}}^{\mathrm{ext}}$ be a vector in an extended bundle $\mathscr{E}$ with invariant metric $\mathbf{h}$. The only primitive scalar is

$$\mathfrak{e}_{\mathrm{M}} = \frac{1}{4}\left\langle \mathbf{F}_{\mathrm{M}}^{\mathrm{ext}}, \mathbf{F}_{\mathrm{M}}^{\mathrm{ext}} \right\rangle_{\mathbf{h}}. \tag{56}$$

A decomposition $\mathscr{E} = E_1 \oplus \cdots \oplus E_k$ expands this contraction into its diagonal and permitted mixed terms. This coordinate expansion does not by itself establish either independence or coupling. Mixed components are allowed only when the representation and invariance conditions permit them; distinct simple ideals are already orthogonal for an invariant Lie-algebra pairing. Shared field dependence can nevertheless couple orthogonal blocks. Sector separation is an emergent property only when a specified limiting argument establishes the corresponding factorization of the effective dynamics. For example, on two compact simple ideals the positive invariant pairing can have the form

$$\mathbf{h}_{\mathrm{alg}} = \alpha(-B_{\mathfrak{su}(2)}) \oplus \beta(-B_{\mathfrak{su}(3)}), \qquad \alpha, \beta > 0, \tag{57}$$

where the B's are the Killing forms. After fixed generator normalizations, the ratio of the two curvature coefficients is α/β, which is unrestricted by positivity alone. A common multiplier $w(\sigma)$ cancels from that ratio. Accordingly, the extended norm provides a common variational formulation; relations among its independent weights require further microscopic constraints or a solved selection problem.

3.9. *The common path-space cost functional.* The action determines variational forces once a mobility and a reference measure have been chosen. A diffusion then adds fluctuations with a specified covariance. The control cost measures the additional forcing needed to change that diffusion's drift. This construction connects the geometric action to probability without differentiating Brownian sample paths.

The normalization in this stochastic realization must be stated separately from that of a Lorentzian mechanical action. If an unnormalized geometric functional $\mathcal{I}_{\mathrm{M}}$ has action units, choose an action unit $I_{\mathrm{ref}} > 0$ and an energy unit $E_{\mathrm{ref}} > 0$, and use

$$\overline{S}_{\mathrm{M}} := \mathcal{I}_{\mathrm{M}}/I_{\mathrm{ref}}, \qquad U_{\mathrm{M}} := E_{\mathrm{ref}}\overline{S}_{\mathrm{M}}, \qquad \mathcal{S}_{\mathrm{M}} \equiv U_{\mathrm{M}}, \qquad \theta = E_{\mathrm{ref}}\overline{\theta}. \tag{58}$$

Here $\mathcal{I}_{\mathrm{M}}$ has action units, $\overline{S}_{\mathrm{M}}$ and $\overline{\theta}$ are dimensionless, and U_{M}, $\mathcal{S}_{\mathrm{M}}$, and θ have energy units whenever dimensional stochastic variables are used. We retain $\mathcal{S}_{\mathrm{M}}$ in the existing variational identities as the energy-normalized notation. A dimensionless version is always obtained by dividing it by E_{ref}, not merely by setting $\hbar = c = 1$. Thus $\mathcal{S}_{\mathrm{M}}/\theta$ is dimensionless. The reference factors may be included in the pairing in (52); the subsequent stochastic equations use this energy-normalized functional. The ratio $I_{\mathrm{ref}}/E_{\mathrm{ref}}$ is a unit conversion, not a

derived material clock, and I_{ref} is not identified with Planck's constant without additional quantum matching. The physical Lorentzian action, whose stationary variation gives the mechanical equations, retains its own normalization. A residual control cost with energy units cannot be identified with it merely by using the same word *action*. Appendix E gives the component units, the conversion of the noise and generator, and the corresponding transformation of the path and terminal costs.

3.10. *Master mobility and stochastic dynamics.* All stochastic and equilibrium identities in this section and in Section 4.1 are understood on a fixed physical configuration slice $\mathfrak{X}_{\mathrm{phys}}$, or on the quotient by gauge orbits. In a gauge-fixed realization the reference measure includes the stated Faddeev–Popov (or equivalent BRST/BV) factor; on a quotient it is the corresponding quotient measure. The raw unreduced field space is used only as notation for the master variables. A probability construction requires a positive reference measure on that slice or quotient; a signed Faddeev–Popov determinant or a Grassmann-valued BRST integral is not by itself such a measure. Removing gauge zero modes is necessary in these realizations, but does not prove confinement, finiteness of the partition function, or invertibility on all remaining directions.

Let $\mathfrak{X}$ be a separable Hilbert realization of the configuration space, and let $\mathbb{M}(\mathbb{X}) : T^*\mathfrak{X} \to T\mathfrak{X}$ be a mobility operator with a specified domain. Assume that it is symmetric and nonnegative with respect to the field-space metric (strict positivity is imposed whenever an ordinary inverse is used). In the finite-dimensional or Galerkin realization used for the identities below, the stochastic equation is interpreted in the Itô sense. The variational derivative $\delta\mathcal{S}_{\mathrm{M}}/\delta\mathbb{X}$ is a cotangent vector. Whenever self-adjointness is invoked, the field-space metric supplies the cotangent–tangent identification; equivalently, if $\mathbb{G}$ is the field-space metric, the gradient is $\operatorname{grad}_{\mathbb{G}} \mathcal{S}_{\mathrm{M}} = \mathbb{G}^{-1}\delta\mathcal{S}_{\mathrm{M}}/\delta\mathbb{X}$. To keep the types explicit, write $\flat_{\mathbb{G}} : T\mathfrak{X} \to T^*\mathfrak{X}$ for this metric identification and define the induced tangent mobility

$$\widehat{\mathbb{M}} := \mathbb{M} \circ \flat_{\mathbb{G}} : T\mathfrak{X} \longrightarrow T\mathfrak{X}, \qquad \langle u, \widehat{\mathbb{M}} v\rangle_{\mathbb{G}} = \langle \widehat{\mathbb{M}} u, v\rangle_{\mathbb{G}}, \qquad \langle u, \widehat{\mathbb{M}} u\rangle_{\mathbb{G}} \geq 0. \tag{59}$$

Thus expressions containing a differential, such as $\mathbb{M}\,\mathrm{d}f$, use the cotangent-to-tangent map, whereas expressions containing a Riemannian gradient, such as $\widehat{\mathbb{M}}\,\nabla_{\mathbb{X}} f$, use the induced tangent operator. In coordinates the cotangent-to-tangent map has components M^{ij}, whereas the tangent endomorphism has components $\widehat{M}^i{}_j = M^{ik}G_{kj}$. Their matrices coincide only in an orthonormal affine chart. The displayed Itô equation below uses such a fixed Hilbert or finite-dimensional affine realization; on a curved configuration space the generator, rather than an uncorrected vector drift, specifies the intrinsic diffusion. To make the covariance convention independent of coordinates, let U be the noise

Hilbert space and choose a noise frame $\mathcal{E}_{\mathbb{X}} : U \to T_{\mathbb{X}}\mathfrak{X}$ satisfying, in a coordinate chart, $\mathcal{E}_{\mathbb{X}}\mathcal{E}_{\mathbb{X}}^{\mathsf{T}} = G^{-1}$. Let $\widehat{\mathbb{M}}_{\mathbb{G}}^{1/2}$ denote the positive square root with respect to $\langle\cdot,\cdot\rangle_{\mathbb{G}}$. We use $\sqrt{2\theta}\widehat{\mathbb{M}}_{\mathbb{G}}^{1/2}\mathcal{E}_{\mathbb{X}}$ as the noise coefficient. Its coordinate covariance is $2\theta M^{ij}$, while its field-space covariance is $2\theta\widehat{\mathbb{M}}$ when the adjoint is taken with respect to $\mathbb{G}$. In finite-dimensional coordinates, putting $R = \widehat{\mathbb{M}}_{\mathbb{G}}^{1/2}$ makes this verification explicit:

$$R^{\mathsf{T}}G = GR, \quad R^2 = MG, \quad \boldsymbol{\sigma}\boldsymbol{\sigma}^{\mathsf{T}} = 2\theta RG^{-1}R^{\mathsf{T}} = 2\theta R^2G^{-1} = 2\theta M. \tag{60}$$

The first equality expresses self-adjointness in the field-space metric. It explains why a coordinate-standard Wiener process cannot be multiplied by the matrix R alone in a nonorthonormal chart.

Write $\mathbb{B}$ for the complete reference drift. Its dependence on θ is suppressed except when a small-noise limit is taken. On the reversible coordinate realization relative to $\nu(\mathrm{d}x) = m_\nu(x)\mathrm{d}x$, it is

$$\mathbb{B}^i(x) = -M^{ij}(x)\partial_j\mathcal{S}_{\mathrm{M}}(x) + \theta\beta_\nu^i(x), \quad \beta_\nu^i(x) = \frac{1}{m_\nu(x)}\partial_j\big(m_\nu(x)M^{ij}(x)\big)\,. \tag{61}$$

Section 4.1 derives this correction from the forward equation. With constant mobility and a flat reference density the correction vanishes and the drift reduces to $-\mathbb{M}\,\delta\mathcal{S}_{\mathrm{M}}/\delta\mathbb{X}$. The general stochastic equation is

$$\boxed{\mathrm{d}\mathbb{X}_t = \mathbb{B}(\mathbb{X}_t)\,\mathrm{d}t + \sqrt{2\theta}\widehat{\mathbb{M}}_{\mathbb{G}}^{1/2}(\mathbb{X}_t)\mathcal{E}_{\mathbb{X}_t}\,\mathrm{d}W_t.} \tag{62}$$

where W_t is a cylindrical Wiener process on U and $\theta > 0$ is the fluctuation scale. An infinite-dimensional strong Itô equation with values in the state Hilbert space requires the displayed composite coefficient to be an admissible Hilbert–Schmidt, or more generally radonifying, noise coefficient. A mild equation may instead be driven by cylindrical noise when its linear evolution family supplies enough smoothing. For example, in the autonomous case with linear generator $-A$ and noise coefficient Σ, the stochastic convolution is state-space valued under the sufficient condition

$$\int_0^T \left\|e^{-sA}\Sigma\right\|_{\mathcal{L}_2(U,\mathcal{H})}^2 \mathrm{d}s < \infty \qquad \text{for every } T < \infty. \tag{63}$$

The nonlinear exponential realization in Section 10.22 uses this mild convention: its unsmoothed identity covariance is cylindrical, whereas its stochastic convolution is $\mathcal{H}$-valued. In either formulation the drift must be defined on its declared domain; these analytic properties are not consequences of the notation. The exact Gibbs and dissipation identities use the reversible generator associated with (61). In infinite dimension the coordinate divergence is replaced by a justified generator or Dirichlet-form construction relative to the specified reference measure.

Equation (62) specifies the stochastic law. Existence and uniqueness require the hypotheses in Section 7.5. In the induced-metric realization one must also prove that the nondegenerate coframe branch is invariant, or stop the process at its boundary and specify boundary conditions. This is a substantive analytic requirement: $e_t = e_0 + \sqrt{2\theta}W_t$, with $e_0 > 0$, hits zero almost surely in one dimension. Nondegeneracy at the initial time therefore cannot supply boundary nonattainment for an arbitrary coframe diffusion. Gravity and gauge fields receive projections of a common noise operator. Whether those projections are statistically correlated is determined by the corresponding covariance blocks, as examined in Section 11.7.

3.11. *Definition of the unified cost.* For an absolutely continuous skeleton path $x : [0,T] \to \mathfrak{X}$ in the fixed affine realization, define the deterministic skeleton control cost. The velocity and drift are compared in that realization. In a finite-dimensional or uniformly elliptic realization, $\widehat{\mathbb{M}}(x)^{-1}$ is the ordinary inverse; in a degenerate realization we write $\widehat{\mathbb{M}}(x)^{\dagger}$ for the Moore–Penrose inverse on the tangent range and impose

$$\dot{x}_t - \mathbb{B}(x_t) \in \operatorname{Ran} \widehat{\mathbb{M}}(x_t) \quad \text{for a.e. } t. \tag{64}$$

If this range constraint fails, the cost is defined to be $+\infty$. Here $\|v\|^2_{\widehat{\mathbb{M}}^{-1}}$ (respectively $\|v\|^2_{\widehat{\mathbb{M}}^{\dagger}}$) means $\langle v, \widehat{\mathbb{M}}^{-1}v\rangle_{g_{\mathfrak{X}}}$ (respectively $\langle v, \widehat{\mathbb{M}}^{\dagger}v\rangle_{g_{\mathfrak{X}}}$) in the tangent-space pairing. In every finite-dimensional realization used below, $g_{\mathfrak{X}}$ is the restriction of the field-space metric $\mathbb{G}$; it is not an additional independent metric. This convention avoids silently applying a cotangent operator to a tangent vector.

$$\boxed{\mathcal{J}_T[x] := \frac{1}{4\theta}\int_0^T \|\dot{x}_t - \mathbb{B}(x_t)\|^2_{\widehat{\mathbb{M}}(x_t)^{\dagger}}\, \mathrm{d}t.} \tag{65}$$

This formula defines the skeleton cost in finite dimension or on a closed noise range. In a uniformly elliptic realization the Moore–Penrose inverse is the ordinary inverse. In infinite dimension the correct finite-energy domain is generally larger than $\operatorname{Ran}\widehat{\mathbb{M}}$. For a bounded nonnegative covariance operator, define

$$\|v\|^2_{\widehat{\mathbb{M}}^{\dagger}} := \inf_{\widehat{\mathbb{M}}^{1/2}z = v} \|z\|^2 = \|\widehat{\mathbb{M}}^{\dagger/2}v\|^2, \qquad v \in \operatorname{Ran}\widehat{\mathbb{M}}^{1/2}. \tag{66}$$

The infimum over an empty set is $+\infty$. The right-hand side is a quadratic-form value, so it does not require v to lie in the operator domain of $\widehat{\mathbb{M}}^{\dagger}$. In this setting (64) is replaced by membership in $\operatorname{Ran}\widehat{\mathbb{M}}^{1/2}$, together with square integrability of the minimum-norm control. For example, on ℓ^2, if $\widehat{\mathbb{M}}e_n = n^{-2}e_n$ and $v_n = n^{-2}$, then $\sum_n n^2 v_n^2 < \infty$, whereas $\sum_n n^4 v_n^2 = \infty$. Thus v has finite control energy but does not belong to $\operatorname{Ran}\widehat{\mathbb{M}}$. Finite-dimensional range notation must therefore not be carried to the continuum without this distinction.

The functional uses the common master action and mobility, with the interaction sectors represented by components of x, $\mathbb{M}$, and $\mathcal{S}_{\mathrm{M}}$. Sharing this functional does not independently fix the relative coefficients or the physical projections of those components. The functional is defined on absolutely continuous skeletons. It does not require a derivative of a stochastic sample path: nondegenerate diffusion paths are not absolutely continuous, while degenerate realizations can include deterministic directions.

The zero-cost condition follows from positivity on the noise range:

$$\mathcal{J}_T[x] = 0 \quad \Longleftrightarrow \quad \dot{x}_t = \mathbb{B}(x_t) \quad \text{for a.e. } t, \tag{67}$$

provided the norm is strictly positive on the relevant tangent space; in the degenerate case this equivalence is understood within the range-constrained class specified above. Uniqueness of a zero-cost path additionally requires a fixed initial condition and uniqueness for the drift equation. Positivity of the cost identifies its zeros; it does not prove uniqueness for an ordinary differential equation with an irregular drift.

Thus the zero-cost dynamics follows the complete reference drift. It is a gradient flow when $\beta_\nu = 0$; at positive noise scale a general reversible coordinate drift also includes $\theta\beta_\nu$. Stationary points of the uncorrected gradient flow solve the Euler–Lagrange equations only when the mobility is injective on the physical variations. A degenerate mobility can annihilate a nonzero action differential, so that implication needs the stated injectivity or an appropriate restriction of the variation space. The stochastic time describes relaxation in configuration space; its relation to physical Lorentzian time is a separate construction.

At positive θ, the skeleton formula also requires its coordinate convention. For a smooth time-independent change $y = \Upsilon(x)$, the Itô transformation rule is

$$b_y^\alpha = \partial_i \Upsilon^\alpha b_x^i + \theta M^{ij} \partial_i \partial_j \Upsilon^\alpha, \quad \dot{y}^\alpha - b_y^\alpha = \partial_i \Upsilon^\alpha (\dot{x}^i - b_x^i) - \theta M^{ij} \partial_i \partial_j \Upsilon^\alpha. \tag{68}$$

The last term shows that the finite-noise residual obtained from the coordinate Itô drift is not a vector under a general nonlinear reparameterization. Equation (65) therefore refers to the fixed affine or declared chart realization, rather than to an unspecified coordinate-independent functional on smooth curves. For a concrete example, let $\mathrm{d}X_t = \sqrt{2\theta}\,\mathrm{d}W_t$ on $\mathbb{R}$, and set $Y_t = e^{X_t}$. Itô's formula gives $\mathrm{d}Y_t = \theta Y_t\,\mathrm{d}t + \sqrt{2\theta} Y_t\,\mathrm{d}W_t$. The constant paths $x_t = 0$ and $y_t = 1$ describe the same curve in the two coordinates, but their costs computed directly from the two Itô drifts are

$$\mathcal{J}_T^x[0] = 0, \qquad \mathcal{J}_T^y[1] = \frac{1}{4\theta} \int_0^T \frac{(0-\theta)^2}{1^2}\,\mathrm{d}t = \frac{\theta T}{4}. \tag{69}$$

The discrepancy vanishes at the leading small-noise scale but is nonzero at every fixed $\theta > 0$ and $T > 0$. The reference generator and the relative entropy

of diffusion path laws are intrinsic. In particular, the difference between controlled and reference drifts transforms as $v_y = D\Upsilon\, v_x$, because the common Itô correction cancels. This is the drift difference used in the Girsanov calculation below. A finite-noise geometric skeleton on a curved configuration manifold requires a further specified connection or equivalent stochastic convention; the leading small-noise rate in Section 4.5 is unaffected by this order-θ term.

3.12. *Relation to relative entropy.* Consider a controlled process

$$\mathrm{d}\mathbb{X}_t^u = \mathbb{B}(\mathbb{X}_t^u)\mathrm{d}t + \mathbb{B}_0(\mathbb{X}_t^u)u_t\mathrm{d}t + \boldsymbol{\sigma}(\mathbb{X}_t^u)\mathrm{d}W_t^u, \tag{70}$$

where $\mathbb{B}$ denotes the complete reference Itô drift. For constant mobility and a flat reference density, $\mathbb{B} = -\mathbb{M}\delta\mathcal{S}_{\mathrm{M}}/\delta\mathbb{X}$; for the general reversible realization use (61), derived again in (80). The residual in (65) therefore always uses the drift of the process being controlled. In either case, $\mathbb{B}_0$ is a prescribed control operator, and $\boldsymbol{\sigma}\boldsymbol{\sigma}^* = 2\theta\widehat{\mathbb{M}}$. Here W^u is Brownian under the controlled law $\mathbb{P}^u$, whereas W denotes the Brownian motion under the reference law $\mathbb{P}^0$. Assume that the two laws have the same initial distribution, that $v_t := \mathbb{B}_0(\mathbb{X}_t^u)u_t$ is a progressively measurable functional of the canonical state path in its own completed filtration under both laws, lies in the range of $\boldsymbol{\sigma}(\mathbb{X}_t^u)$, and yields an exponential martingale satisfying Novikov's condition. The process v_t, and hence $\boldsymbol{\sigma}^\dagger v_t$, must be defined on the canonical path space under both laws; evaluating it only on a controlled weak solution would not by itself define the Radon–Nikodym density under the reference law. In the finite-dimensional realization, or more generally when $\boldsymbol{\sigma}$ has closed range, let $\boldsymbol{\sigma}^\dagger$ denote the Moore–Penrose inverse on that range. The control coordinate u_t and the Brownian shift are not the same object: set $\widehat{u}_t := \boldsymbol{\sigma}^\dagger v_t$. If $\mathbb{B}_0$ has a kernel, different control coordinates can produce the same drift increment v_t; the relative entropy depends only on v_t and uses the minimum-norm shift $\widehat{u}_t$. Assume also uniqueness in law for the controlled martingale problem and $\mathbb{E}^u\int_0^T \|\widehat{u}_t\|^2\mathrm{d}t < \infty$. The first assumption identifies the tilted reference law with the proposed controlled law; the second justifies taking expectation of its log density. Because the drift increment is measurable in the state-path filtration, the density is itself a state-path functional, as shown in Appendix C. Girsanov's theorem (see [105]) then yields

$$\mathrm{KL}(\mathbb{P}^u\|\mathbb{P}^0) = \frac{1}{2}\mathbb{E}^u\int_0^T \left\|\boldsymbol{\sigma}^\dagger v_t\right\|^2 \mathrm{d}t. \tag{71}$$

Define the controlled-law cost by

$$\mathcal{C}_T(u) := \frac{1}{2}\mathbb{E}^u\int_0^T \left\|\boldsymbol{\sigma}^\dagger v_t\right\|^2 \mathrm{d}t. \tag{72}$$

If a deterministic absolutely continuous skeleton x satisfies $\dot{x}_t = \mathbb{B}(x_t) + v_t$, then the corresponding quadratic control energy is exactly the skeleton functional $\mathcal{J}_T[x]$ after using $\boldsymbol{\sigma}\boldsymbol{\sigma}^* = 2\theta\widehat{\mathbb{M}}$. For a genuinely random adapted control, $\mathcal{C}_T$ is

the expectation of that energy under $\mathbb{P}^u$. It is not legitimate to identify v_t with the derivative of a sample diffusion path.

$$\boxed{\mathrm{KL}(\mathbb{P}^u \| \mathbb{P}^0) = \mathcal{C}_T(u).} \tag{73}$$

Therefore relative entropy is not an additional physical cost in this formulation. It is a probabilistic representation of the same path-deviation cost under the reference stochastic dynamics; the finite-dimensional Radon–Nikodym calculation is given in Appendix C.

The equality concerns path-space relative entropy for the specified controlled dynamics. It does not identify this entropy with the state-space free energy introduced below: the two functionals have different domains. If controls use randomness not observable from the state path, projection from the enlarged probability space gives only the data-processing bound

$$\mathrm{KL}(\mathrm{Law}(X^u) \| \,\mathrm{Law}(X^0)) \le \frac{1}{2}\mathbb{E}^u \int_0^T \|\widehat{u}_t\|^2 \,\mathrm{d}t. \tag{74}$$

Equality requires measurability of the likelihood ratio in the retained state path. This condition specifies exactly when the control energy is a representation of path entropy.

4. **Equilibrium, limits, and symmetry breaking**

4.1. *Equilibrium generated by the same principle.* The path-space calculation compares controlled trajectories. Equilibrium instead concerns probability distributions at a fixed stochastic time. The link between them is the chosen reversible generator: it uses the same action and mobility, while its divergence correction depends on the reference measure. Deriving the forward equation makes that dependence explicit. Here "reversible generator" means self-adjointness in the equilibrium L^2-space, equivalently detailed balance for this overdamped branch. It does not mean that the diffusion coefficient vanishes. Later, $b_{\mathrm{rev}} = \mathbb{L}\nabla E$ denotes the conservative part of a parity-aware reversible–irreversible decomposition. These uses are consistent: the present overdamped generator has no conservative anti-self-adjoint part, while the later generator may have one whose sign is reversed by the time-reversal parity involution.

4.2. *Fokker–Planck equation.* Fix a finite-dimensional physical configuration manifold and a positive reference measure ν. In a chart write $\nu(\mathrm{d}x) = m_\nu(x)\,\mathrm{d}x$, where m_ν is smooth and positive. The density p_t is always taken with respect to ν; its density with respect to coordinate Lebesgue measure is $\rho_t = m_\nu p_t$. These two densities have different forward equations. For a vector field V, the reference divergence is

$$\mathrm{div}_\nu V := m_\nu^{-1}\partial_i(m_\nu V^i). \tag{75}$$

Here and below repeated coordinate indices are summed. For a scalar f, $\nabla_j f$ means $\partial_j f$, whereas $\nabla_{\mathbb{X}} f$ is the field-space metric gradient. The contravariant mobility M^{ij} acts on the covector $\mathrm{d}f$.

Consider the coordinate Itô equation $\mathrm{d}X^i = b^i\,\mathrm{d}t + \sigma^i_\alpha\,\mathrm{d}W^\alpha$, with $a^{ij} = \sum_\alpha \sigma^i_\alpha \sigma^j_\alpha = 2\theta M^{ij}$. Itô's formula gives

$$Lf = b^i \partial_i f + \theta M^{ij} \partial_i \partial_j f. \tag{76}$$

For a smooth compactly supported test function f, two integrations by parts against $\mathrm{d}x$, or the corresponding boundary conditions, give

$$\begin{aligned} \frac{\mathrm{d}}{\mathrm{d}t} \int f p_t m_\nu \,\mathrm{d}x &= \int (Lf) p_t m_\nu \,\mathrm{d}x \\ &= \int f \left\{ -\partial_i (b^i m_\nu p_t) + \theta \partial_i \partial_j (M^{ij} m_\nu p_t) \right\} \mathrm{d}x. \end{aligned} \tag{77}$$

Consequently the adjoint relative to ν is

$$\partial_t p_t = -\frac{1}{m_\nu} \partial_i (m_\nu b^i p_t) + \frac{\theta}{m_\nu} \partial_i \partial_j (m_\nu M^{ij} p_t). \tag{78}$$

For comparison, retaining only the gradient part of (61) gives the uncorrected coordinate drift $b^i = -M^{ij}\partial_j \mathcal{S}_{\mathrm{M}}$ and the forward equation

$$\partial_t p_t = \frac{1}{m_\nu} \partial_i (m_\nu p_t M^{ij} \partial_j \mathcal{S}_{\mathrm{M}}) \quad + \frac{\theta}{m_\nu} \partial_i \partial_j (m_\nu M^{ij} p_t). \tag{79}$$

The second term contains one factor m_ν inside the two coordinate derivatives. It cannot be replaced by iterating the vector divergence on the components of a rank-two tensor. Equation (78) is the density form of the usual forward equation [137].

Define in this chart

$$\begin{aligned} b^i_{\mathrm{rev}} &= -M^{ij}\partial_j \mathcal{S}_{\mathrm{M}} + \theta \beta^i_\nu, \\ \beta^i_\nu &:= \frac{1}{m_\nu} \partial_j (m_\nu M^{ij}) = \partial_j M^{ij} + M^{ij} \partial_j \log m_\nu. \end{aligned} \tag{80}$$

An Itô drift transforms with a second-derivative correction under changes of coordinates, so β^i_ν alone is not asserted to be a vector. The invariant object is the divergence-form generator

$$L_{\mathrm{rev}} f = \frac{\theta e^{\mathcal{S}_{\mathrm{M}}/\theta}}{m_\nu} \partial_i \left(m_\nu e^{-\mathcal{S}_{\mathrm{M}}/\theta} M^{ij} \partial_j f \right). \tag{81}$$

Expanding the derivative, and using $M^{ij} = M^{ji}$, recovers (76) with the drift in (80). This also specifies the equation on overlapping charts.

For clarity, the cancellation in the forward equation is

$$\begin{aligned} \partial_j (m_\nu M^{ij} p_t) &= p_t \partial_j (m_\nu M^{ij}) + m_\nu M^{ij} \partial_j p_t, \\ -m_\nu b^i_{\mathrm{rev}} p_t + \theta \partial_j (m_\nu M^{ij} p_t) &= m_\nu M^{ij} (p_t \partial_j \mathcal{S}_{\mathrm{M}} + \theta \partial_j p_t). \end{aligned} \tag{82}$$

Applying $m_\nu^{-1}\partial_i$ now yields

$$\partial_t p_t = \mathrm{div}_\nu \left[p_t \widehat{\mathbb{M}} \nabla_{\mathbb{X}} \mathcal{S}_{\mathrm{M}} + \theta \widehat{\mathbb{M}} \nabla_{\mathbb{X}} p_t \right]. \tag{83}$$

No constancy assumption on the mobility is needed for this identity. If the uncorrected coordinate drift is retained, this flux has the same generator only when $\beta_\nu = 0$ in the specified chart. A sufficient case is constant mobility and constant m_ν in affine coordinates. In that case,

$$\partial_t p_t = \mathrm{div}_\nu \left[\widehat{\mathbb{M}} (p_t \nabla_{\mathbb{X}} \mathcal{S}_{\mathrm{M}} + \theta \nabla_{\mathbb{X}} p_t) \right]. \tag{84}$$

Define the free energy relative to a fixed positive, sigma-finite reference measure ν. The units of this reference are fixed so that its densities have a dimensionless logarithm. This does not require ν to have finite mass: Lebesgue measure on a noncompact configuration space cannot be normalized by division by its total mass. Replacing ν by a nonconstant weighted measure changes the model unless the action is changed by the compensating logarithmic term. For comparison of different microscopic candidates, Section 6.1 imposes a common normalization separately. If gauge symmetries are present, ν must be a positive measure on a well-defined quotient or on a specified gauge-fixed domain with a nonnegative Jacobian. A formal signed Faddeev–Popov determinant does not define a probability reference measure. These choices do not themselves imply $0 < Z < \infty$. For normalized densities p, q with $p \ll q$, we use

$$\mathrm{KL}(p\|q) := \int_{\mathfrak{X}} p(\mathbb{X}) \log \frac{p(\mathbb{X})}{q(\mathbb{X})} \, \nu(\mathrm{d}\mathbb{X}). \tag{85}$$

$$\mathcal{F}[p] = \int_{\mathfrak{X}} p(\mathbb{X}) \mathcal{S}_{\mathrm{M}}(\mathbb{X}) \, \nu(\mathrm{d}\mathbb{X}) + \theta \int_{\mathfrak{X}} p \log p \, \nu(\mathrm{d}\mathbb{X}). \tag{86}$$

In this formulation, $\mathcal{F}$ is not a second cost added to $\mathcal{J}_T$. It is the Lyapunov functional induced by the same master action and the entropy of the probability state. As a sum of two ordinary integrals, (86) is defined here on densities satisfying $\int p|\mathcal{S}_{\mathrm{M}}| \, d\nu + \int p|\log p| \, d\nu < \infty$. If $0 < Z < \infty$, its relative extension is $\mathcal{F}_{\mathrm{rel}}[p] = -\theta \log Z + \theta \, \mathrm{KL}(p\|p_*)$. This agrees with the separate-integral definition on that domain but also applies when the individual terms cannot be separated. In particular, finite relative entropy alone does not justify subtracting two infinite energy or entropy terms.

4.3. *Dissipation identity.*

THEOREM 2 (Free-energy dissipation). *Suppose that $\mathfrak{X}$ is connected and the symmetric mobility is positive definite. Let the density solve* (83)*; this includes the uncorrected equation when $\beta_\nu = 0$. Assume that p_t is smooth, strictly positive, normalized, and has finite free energy and finite displayed dissipation. Assume also that differentiation under the integrals and the integration by parts used below are valid, with zero boundary flux and vanishing boundary*

pairings. These conditions hold, for example, for smooth positive solutions on a compact manifold without boundary, or with suitable decay and domination on a noncompact realization. Then

$$\frac{\mathrm{d}}{\mathrm{d}t}\mathcal{F}[p_t] = -\int_{\mathfrak{X}} p_t \left\langle \nabla_{\mathbb{X}} \left(\mathcal{S}_{\mathrm{M}} + \theta \log p_t\right), \widehat{\mathbb{M}} \nabla_{\mathbb{X}} \left(\mathcal{S}_{\mathrm{M}} + \theta \log p_t\right) \right\rangle \nu(\mathrm{d}\mathbb{X}) \leq 0. \quad (87)$$

Equality holds if and only if

$$\nabla_{\mathbb{X}} \left(\mathcal{S}_{\mathrm{M}} + \theta \log p_t\right) = 0 \quad (88)$$

where $p_t > 0$.

Proof. Differentiate (86) and use conservation of total probability. The term $\theta \int p_t \, \nu(\mathrm{d}\mathbb{X})$ contributes zero through the constant part of the first variation because $\int \partial_t p_t \, \nu(\mathrm{d}\mathbb{X}) = 0$. More explicitly, since

$$\frac{\delta \mathcal{F}}{\delta p} = \mathcal{S}_{\mathrm{M}} + \theta(1 + \log p), \quad (89)$$

we obtain

$$\frac{\mathrm{d}}{\mathrm{d}t}\mathcal{F}[p_t] = \int \left(\mathcal{S}_{\mathrm{M}} + \theta \log p_t\right) \partial_t p_t \, \nu(\mathrm{d}\mathbb{X}). \quad (90)$$

Set $H_t = \mathcal{S}_{\mathrm{M}} + \theta \log p_t$. Equation (83) is $\partial_t p_t = \mathrm{div}_\nu(p_t \widehat{\mathbb{M}} \nabla_{\mathbb{X}} H_t)$. The assumed boundary or decay condition gives the integration-by-parts identity $\int f \, \mathrm{div}_\nu V \, \nu(\mathrm{d}\mathbb{X}) = -\int \langle \nabla_{\mathbb{X}} f, V \rangle \, \nu(\mathrm{d}\mathbb{X})$. Applying it with $f = H_t$ and $V = p_t \widehat{\mathbb{M}} \nabla_{\mathbb{X}} H_t$ gives

$$\frac{\mathrm{d}}{\mathrm{d}t}\mathcal{F}[p_t] = -\int \left\langle \nabla_{\mathbb{X}}(\mathcal{S}_{\mathrm{M}} + \theta \log p_t), \widehat{\mathbb{M}} \nabla_{\mathbb{X}}(\mathcal{S}_{\mathrm{M}} + \theta \log p_t) \right\rangle p_t \, \nu(\mathrm{d}\mathbb{X}). \quad (91)$$

Positive definiteness of $\widehat{\mathbb{M}}$ proves the inequality. Equality is equivalent to vanishing of the quadratic form almost everywhere, which gives the stated condition. □

4.4. *Equilibrium measure.* For constant mobility satisfying the compatibility condition in the preceding theorem, or for the state-dependent Itô equation with the reversible divergence correction (80), the equilibrium density satisfies

$$\boxed{p_*(\mathbb{X}) = Z^{-1} \exp\left[-\frac{\mathcal{S}_{\mathrm{M}}(\mathbb{X})}{\theta}\right],} \quad (92)$$

provided the displayed integrals are well defined (or are interpreted through a common lower-semicontinuous extension), and

$$Z = \int_{\mathfrak{X}} \exp\left[-\frac{\mathcal{S}_{\mathrm{M}}(\mathbb{X})}{\theta}\right] \nu(\mathrm{d}\mathbb{X}) < \infty. \quad (93)$$

In addition, when $\mathcal{F}[p_*]$ is treated as a finite ordinary number, $\mathcal{S}_{\mathrm{M}}p_*$ and $p_* \log p_*$ are required to be integrable. Moreover,

$$\boxed{\mathcal{F}[p] - \mathcal{F}[p_*] = \theta\, \mathrm{KL}(p\|p_*).} \tag{94}$$

Equation (94) shows why entropy and action combine naturally at equilibrium, while the path cost remains a single object. Once the reference measure, action, fluctuation scale, and reversible generator have all been fixed, this identity determines the equilibrium density. The action alone does not determine the reference measure. The algebraic Gibbs identity is recorded in Appendix B.

THEOREM 3 (Equilibrium as the unique zero-dissipation state). *Assume $\mathfrak{X}$ is connected, $0 < Z < \infty$, the integrability conditions stated above hold, and the positive definite mobility and reversible dynamics satisfy the hypotheses of the preceding theorem. Assume also that the admissible probability densities are normalized, absolutely continuous with respect to the reference volume, and have finite relative entropy with respect to p_*. Then p_* is the unique minimizer of $\mathcal{F}$ up to equality almost everywhere, and $p_t = p_*$ is the unique zero-dissipation equilibrium among smooth positive admissible densities for which the dissipation identity applies. This assertion does not by itself exclude singular invariant measures or imply convergence to equilibrium.*

Proof. Let $r = p/p_*$, defined almost everywhere with respect to $\pi_*(\mathrm{d}x) = p_*(x)\nu(\mathrm{d}x)$. Both densities are normalized, so $\int r\, \mathrm{d}\pi_* = 1$. The scalar function $\varphi(r) = r \log r - r + 1$, extended by $\varphi(0) = 1$, is nonnegative and vanishes only at $r = 1$. Consequently,

$$\mathrm{KL}(p\|p_*) = \int \varphi(r)\, \mathrm{d}\pi_* \geq 0. \tag{95}$$

Together with (94), this proves the minimum and its uniqueness. For a smooth positive zero-dissipation density, positive definiteness of the mobility makes $\nabla_{\mathbb{X}}(\mathcal{S}_{\mathrm{M}} + \theta \log p) = 0$. Connectedness makes this scalar function a constant, say c, and hence $p = e^{c/\theta} e^{-\mathcal{S}_{\mathrm{M}}/\theta}$. Normalization gives $e^{c/\theta} = Z^{-1}$, so $p = p_*$. Conversely this density makes the flux vanish and therefore is stationary and has zero dissipation under the stated boundary conditions. □

4.5. *A stochastic meaning of minimum action.* The phrase "minimum action" requires care. The stochastic formulation does not identify every physical realization with a pointwise minimizer of the classical Euclidean action. The mathematically precise statement is that the stochastic path measure is centered on the master drift and the relative cost of a controlled path is the squared Cameron–Martin displacement from that drift. With a prescribed initial condition and no terminal constraint, the deterministic master trajectory is the unique zero-cost path among range-constrained admissible skeletons

whenever the drift equation is unique. If endpoints or other path constraints are imposed, the minimizer generally has positive cost and must solve a separate constrained variational problem.

Recall that $\mathbb{B}$ denotes the complete drift, including the reference correction in a reversible realization. Define its gradient part by

$$\mathbb{B}_{\mathrm{grad}}(\mathbb{X}) = -\mathbb{M}(\mathbb{X})\frac{\delta \mathcal{S}_{\mathrm{M}}}{\delta \mathbb{X}}. \tag{96}$$

For an absolutely continuous skeleton x and positive definite tangent mobility, the cost is

$$\mathcal{J}_T[x] = \frac{1}{4\theta}\int_0^T \|\dot{x}_t - \mathbb{B}(x_t)\|^2_{\widehat{\mathbb{M}}(x_t)^{-1}}\,\mathrm{d}t. \tag{97}$$

Its zero set consists of solutions of $\dot{x} = \mathbb{B}(x)$. This is a statement about paths with a fixed initial value. It does not say that every configuration visited by such a path is a stationary point of the Euclidean action.

The distinction matters even on a compact state space. On the circle, take $\mathcal{S}_{\mathrm{M}} = 0$, $m_\nu = 1$, and $M(x) = 2 + \sin x$. Then $\mathbb{B}_{\mathrm{grad}} = 0$, whereas the reversible drift is $\mathbb{B}(x) = \theta \cos x$. For the constant path $x_t = 0$,

$$\mathcal{J}_T[x] = \frac{1}{4\theta}\int_0^T \frac{\theta^2}{2}\,\mathrm{d}t = \frac{\theta T}{8}. \tag{98}$$

The cost would be zero for the different diffusion obtained by discarding the reference correction. The positive value therefore records a difference between two reference dynamics, rather than a failure of the Gibbs identity.

For a finite-dimensional approximation with orthonormal affine coordinates $x \in \mathbb{R}^n$, suppose that $\widehat{\mathbb{M}}(x)$ is uniformly positive definite on the region under consideration. The degenerate case requires the corresponding range constraint and a separate large-deviation theorem. To state the small-noise limit, write $b_\theta = b_0 + \theta\beta_\nu$, with $b_0 = \mathbb{B}_{\mathrm{grad}}$, and let $\mathcal{J}_T^\theta$ emphasize the noise-scale dependence of the cost. Under the regularity and exponential-tightness assumptions of the Freidlin–Wentzell principle, the limiting rate functional is

$$I_T[x] = \frac{1}{4}\int_0^T \left\langle \dot{x} - b_0(x), \widehat{\mathbb{M}}(x)^{-1}(\dot{x} - b_0(x))\right\rangle \mathrm{d}t. \tag{99}$$

For a path on which all the following integrals are finite, direct expansion of the square gives

$$\begin{aligned}\theta\mathcal{J}_T^\theta[x] = I_T[x] &- \frac{\theta}{2}\int_0^T \langle \dot{x} - b_0(x), \widehat{\mathbb{M}}(x)^{-1}\beta_\nu(x)\rangle\,\mathrm{d}t \\ &+ \frac{\theta^2}{4}\int_0^T \langle \beta_\nu(x), \widehat{\mathbb{M}}(x)^{-1}\beta_\nu(x)\rangle\,\mathrm{d}t.\end{aligned} \tag{100}$$

In particular, a vanishing reference correction gives the exact identity $I_T = \theta\mathcal{J}_T^\theta$. For an individual path the two correction integrals can also cancel even when

$\beta_\nu \neq 0$; no converse is asserted on that basis. In the general reversible case $\theta \mathcal{J}_T^\theta[x] \to I_T[x]$ on this fixed-path domain. This algebraic convergence alone does not prove a path-space large-deviation principle; tightness, coefficient control, and the initial-law hypotheses are also required. Under those hypotheses, probabilities have the logarithmic asymptotics $\mathbb{P}(X^\theta \approx x) \asymp \exp[-I_T[x]/\theta]$ [72]. Here the notation concerns sufficiently small path neighborhoods at logarithmic scale, not a pointwise density. The infinite-dimensional extension requires the appropriate Cameron–Martin geometry and its own compactness estimates.

4.6. *Macroscopic and microscopic limits of the same system.* The preceding rate functional concerns rare paths as the noise amplitude vanishes. Two other limits clarify how the same stochastic description can produce deterministic collective motion and local Gaussian fluctuations. They use different rescalings and should therefore be stated separately.

4.7. *Macroscopic deterministic limit.* The following equations are admissible reduced models of the master system, not automatic consequences of an abstract projection. To make the required relationship explicit, choose finite-dimensional embeddings $\iota_N : \mathfrak{X}_N \to \mathfrak{X}$ and projections $\Pi_N : T\mathfrak{X} \to T\mathfrak{X}_N$ with $\Pi_N \iota_{N*} = \mathrm{Id}$ on the retained modes. After a common nondimensionalization, assume

$$\Phi_N = \mathcal{S}_{\mathrm{M}} \circ \iota_N, \qquad M_Q^N(q) := \Pi_N \widehat{\mathbb{M}}(\iota_N q) \Pi_N^*, \qquad \boldsymbol{\sigma}_{Q,N} \boldsymbol{\sigma}_{Q,N}^* = \frac{2\theta}{N} M_Q^N. \tag{101}$$

The adjoint Π_N^* is the metric adjoint, with cotangent inputs identified through the previously specified Riesz maps. The last relation is the collective-averaging scaling hypothesis; it does not follow from projection alone. We assume that the state-dependent matrices M_Q^N converge locally uniformly to a limiting mobility M_Q on the common coordinate domain. In the convergence argument below, all collective coordinates are identified with one fixed finite-dimensional domain in $\mathbb{R}^d$, independently of N. This assumption concerns the retained collective variables; the dimension of the underlying microscopic regulator may still increase with N. For the tangent limit below, an analogous choice is $Q = \Pi_Q \mathbb{X}$, $b = \Pi_Q \mathbb{B}$, and $\boldsymbol{\sigma}_Q = \Pi_Q \boldsymbol{\sigma}$ on the retained subspace. If no maps satisfying these conditions are supplied by a concrete realization, the displayed reduced equations remain specified SDE examples rather than consequences of the master action. Even the restriction of the action and compression of the mobility do not, on their own, identify the reduced drift. An exact projection must also satisfy, on the retained branch,

$$\Pi_N \mathbb{B}(\iota_N q) = -M_Q^N(q) \nabla_Q \Phi_N(q) + r_N^{\mathrm{proj}}(q), \tag{102}$$

where the defect is zero for an exact closure and must vanish in the declared scaling for an asymptotic closure. Reference-drift corrections and the influence of discarded variables are included in this defect unless retained explicitly.

For example, take $\iota(q) = (q, 0)$, $\Pi(x_1, x_2) = x_1$, $\mathcal{S}(x_1, x_2) = (x_2 + 1)^2/2$, and

$$M = \begin{pmatrix} 1 & \zeta \\ \zeta & 1 \end{pmatrix}, \qquad |\zeta| < 1, \qquad \Phi(q) = \tfrac{1}{2}, \quad M_Q = 1. \tag{103}$$

The restricted-action drift is zero, whereas the projected master drift on $\iota(q)$ is $-\Pi M \nabla \mathcal{S} = -\zeta$. The off-diagonal mobility transmits a force from the discarded direction. Thus the reduced SDE below includes a closure assumption, not just a change of notation. Its convergence proof applies when that assumption holds, or when a vanishing projection defect is added to the drift residual controlled in (109).

Introduce a collective variable Q^N and consider

$$\mathrm{d}Q_t^N = -M_Q^N(Q_t^N)\nabla_Q \Phi_N(Q_t^N)\mathrm{d}t + \sqrt{\frac{2\theta}{N} M_Q^N(Q_t^N)}\mathrm{d}B_t. \tag{104}$$

Assume that every M_Q^N and its limit M_Q are symmetric nonnegative, so that the displayed square roots are their positive matrix square roots. Fix $T < \infty$. Assume that the paths Q^N and the solution Q of the limiting equation remain in one common compact set K on $[0, T]$, that $Q_0^N \to Q_0$ in probability, and that the mobilities, their square roots, and $\nabla \Phi_N$ converge locally uniformly on the common coordinate domain. Assume that the limiting equation is locally well posed with a unique solution. The uniform trace and Lipschitz bounds used below are also imposed on K. If compact containment is available only after localization, the following estimates first apply to stopped processes; removing the stopping times requires exit probabilities tending to zero uniformly in N. Then the martingale part obeys

$$\sup_{0 \le t \le T} \left\| \sqrt{\frac{2\theta}{N}} \int_0^t M_Q^N(Q_s^N)^{1/2}\, \mathrm{d}B_s \right\| \longrightarrow 0 \tag{105}$$

in probability, and every weakly convergent subsequence satisfies

$$\dot{Q}_t = -M_Q(Q_t)\nabla_Q \Phi(Q_t), \qquad Q(0) = Q_0. \tag{106}$$

Indeed, in integral form

$$\begin{aligned} Q_t^N &= Q_0^N - \int_0^t M_Q^N(Q_s^N)\nabla_Q \Phi_N(Q_s^N)\, \mathrm{d}s + Z_t^N, \\ Z_t^N &:= \sqrt{\frac{2\theta}{N}} \int_0^t M_Q^N(Q_s^N)^{1/2}\, \mathrm{d}B_s. \end{aligned} \tag{107}$$

If $\sup_N \operatorname{tr} M_Q^N \le C$ on the common compact region, the Burkholder–Davis–Gundy inequality gives

$$\mathbb{E}\sup_{t\le T}\|Z_t^N\|^2 \le \frac{8\theta}{N}\mathbb{E}\int_0^T \operatorname{tr} M_Q^N(Q_s^N)\,\mathrm{d}s \le \frac{8\theta CT}{N}. \tag{108}$$

Hence $Z^N \to 0$ in probability in the uniform topology. Local uniform convergence of the drifts and uniqueness of the limiting ordinary differential equation then imply, by the usual Gronwall estimate applied to (107), convergence of every tight subsequence to (106). For completeness, let $b_N(q) = -M_Q^N(q)\nabla_Q\Phi_N(q)$ and $b(q) = -M_Q(q)\nabla_Q\Phi(q)$. On the common compact region assume $\sup_N \operatorname{Lip}(b_N) \le L$ and $r_N := \sup_q \|b_N(q) - b(q)\| \to 0$. If Q solves (106), subtraction of the two mild equations gives

$$\sup_{s\le t}\|Q_s^N - Q_s\| \le \|Q_0^N - Q_0\| + \sup_{s\le t}\|Z_s^N\| + r_N t + L\int_0^t \sup_{u\le s}\|Q_u^N - Q_u\|\,\mathrm{d}s. \tag{109}$$

Gronwall's lemma consequently yields

$$\sup_{t\le T}\|Q_t^N - Q_t\| \le e^{LT}\left(\|Q_0^N - Q_0\| + \sup_{t\le T}\|Z_t^N\| + r_N T\right) \longrightarrow 0 \tag{110}$$

in probability. These explicit Lipschitz and drift-convergence hypotheses are one sufficient set of conditions behind the subsequence statement. Thus collective averaging removes the stochastic forcing. The limiting trajectory is deterministic when Q_0 is deterministic; for random Q_0, it is the deterministic ODE flow applied to that random initial state, and remains random only through its initial condition.

Proposition 4 (Conditional macroscopic equilibrium convergence). *Fix $\theta > 0$ and the undriven reversible branch* (83)*. Assume the connectedness, positive-definite mobility, boundary, and integrability hypotheses of* (87)*, and write $\pi_\theta(\mathrm{d}x) = p_*(x)\nu(\mathrm{d}x)$, with p_* given by* (92)*. For densities relative to ν, define*

$$\begin{aligned} \mathcal{F}_\theta(p) &:= \theta\,\mathrm{KL}(p\|p_*),\\ \mathcal{D}_\theta(p) &:= \theta^2\int p\,\left\langle \nabla\log(p/p_*), \widehat{\mathbb{M}}\nabla\log(p/p_*)\right\rangle\,\mathrm{d}\nu. \end{aligned} \tag{111}$$

Assume that the Fokker–Planck semigroup is continuous on the closure K of the forward density orbit in a declared metrizable topology, that K is compact and consists of smooth positive admissible densities, and that $\mathcal{F}_\theta$ and $\mathcal{D}_\theta$ are continuous on K. Require the integrated free-energy identity to hold for every orbit starting in K. Compact free-energy sublevels are one sufficient source of precompactness, but do not replace these continuity and admissibility requirements. Then

$$p_t \longrightarrow p_* \quad \text{in the declared topology as } t\to\infty. \tag{112}$$

In particular, this implies weak convergence of probability measures if the topology dominates weak convergence. Separately, suppose that the dissipation identity holds along the orbit and that a logarithmic Sobolev estimate is available with the convention $\mathcal{F}_\theta(p) \le C_{\mathrm{LS}}\mathcal{D}_\theta(p)$, where $0 < C_{\mathrm{LS}} < \infty$. This quantitative conclusion does not require the compact-orbit argument:

$$\mathcal{F}_\theta(p_t) \le e^{-t/C_{\mathrm{LS}}}\mathcal{F}_\theta(p_0). \tag{113}$$

Without these compactness, uniqueness, and coercive-dissipation hypotheses, Gibbs invariance or minimum cost alone does not imply attraction. The conclusion is therefore a conditional statement about convergence of the law, not a claim that every microscopic coordinate becomes static.

Proof. Equations (87) and (94) give $\dot{\mathcal{F}}_\theta = -\mathcal{D}_\theta \le 0$. The nonnegative free energy therefore has a limit L. Compactness of K gives an omega-limit point q: along some $t_n \to \infty$, $p_{t_n} \to q$. Continuity gives $\mathcal{F}_\theta(q) = L$. For any fixed $s \ge 0$, semigroup continuity gives $p_{t_n+s} \to P_s^* q$, and hence $\mathcal{F}_\theta(P_s^* q) = L$. Apply the integrated identity to this limiting orbit:

$$0 = \mathcal{F}_\theta(q) - \mathcal{F}_\theta(P_s^* q) = \int_0^s \mathcal{D}_\theta(P_r^* q)\,\mathrm{d}r.$$

Continuity and nonnegativity of the integrand imply $\mathcal{D}_\theta(q) = 0$. Positive definiteness and strict positivity of q give $\nabla \log(q/p_*) = 0$; connectedness and normalization give $q = p_*$. Thus every omega-limit point is p_*. If the orbit did not converge, a sequence staying outside a neighborhood of p_* would have a different limit point by compactness, a contradiction. This proves (112). For the quantitative assertion, the stated logarithmic Sobolev bound gives $\dot{\mathcal{F}}_\theta \le -\mathcal{F}_\theta/C_{\mathrm{LS}}$. Multiplying by $e^{t/C_{\mathrm{LS}}}$ and integrating proves (113). □

Here $\mathcal{D}_\theta$ is relative-free-energy dissipation for the specified undriven reversible branch. Its identification with physical entropy production requires reservoir calibration; it is not the stationary path entropy rate of an arbitrary driven diffusion. On a degenerate energy-conserving branch, connectedness, zero-set uniqueness, and coercivity must instead be established on the chosen invariant energy leaf. Neither statement implies global attraction across disconnected components.

Remark 5 (An explicit nonempty class of convergence hypotheses). *In a regulated affine chart, take $\nu = \mathrm{d}x$, $\mathcal{S}_{\mathrm{M}}(x) = k|x|^2/2$, and $\widehat{\mathbb{M}} = \mathfrak{m}I$, with $k, \mathfrak{m} > 0$. The process and its invariant covariance are*

$$\mathrm{d}X_t = -\gamma X_t\,\mathrm{d}t + \sqrt{2\theta\mathfrak{m}}\,\mathrm{d}W_t, \qquad \gamma = \mathfrak{m}k, \qquad C_* = (\theta/k)I. \tag{114}$$

The Gaussian logarithmic Sobolev inequality [85] *gives*

$$\mathrm{KL}(p\|p_*) \le \frac{\theta}{2k}\int p\,|\nabla \log(p/p_*)|^2\,\mathrm{d}x, \mathcal{F}_\theta(p) \le \frac{1}{2\gamma}\mathcal{D}_\theta(p). \tag{115}$$

For an initial Gaussian with mean a and covariance C_*, the mean is $e^{-\gamma t}a$, the covariance remains C_*, and direct integration yields

$$\mathcal{F}_\theta(p_t) = \frac{k|a|^2}{2}e^{-2\gamma t}, \qquad \mathcal{D}_\theta(p_t) = \mathfrak{m}k^2|a|^2e^{-2\gamma t} = 2\gamma\mathcal{F}_\theta(p_t). \tag{116}$$

Thus the rate in (113) *is attained with $C_{\mathrm{LS}} = 1/(2\gamma)$. Pinsker's inequality also gives $\|p_t - p_*\|_{L^1(\nu)} \le \sqrt{2\mathcal{F}_\theta(p_0)/\theta}\, e^{-\gamma t}$. This is a finite-regulator realization of probabilistic attraction, not a derivation of a Lorentzian particle mass or of gravitational collapse.*

4.8. *Microscopic tangent limit.* The opposite statement must be formulated carefully. It is not correct to say without qualification that the physical drift "becomes zero" microscopically. The correct statement concerns the rescaled tangent process. Let

$$Y_t^h = \frac{Q_{ht} - Q_0}{\sqrt{h}}. \tag{117}$$

Suppose Q_0 is deterministic and

$$\mathrm{d}Q_t = b(Q_t)\mathrm{d}t + \boldsymbol{\sigma}_Q(Q_t)\mathrm{d}W_t \tag{118}$$

and $b, \boldsymbol{\sigma}_Q$ are locally bounded and continuous at Q_0. Then

$$Y_t^h = \sqrt{h}\int_0^t b(Q_{hs})\mathrm{d}s + \frac{1}{\sqrt{h}}\int_0^{ht}\boldsymbol{\sigma}_Q(Q_s)\mathrm{d}W_s. \tag{119}$$

If $\sup_{s\le hT}\|b(Q_s)\| \le C_b$ on the localization event, then

$$\sup_{t\le T}\left\|\sqrt{h}\int_0^t b(Q_{hs})\,\mathrm{d}s\right\| \le C_bT\sqrt{h} \longrightarrow 0. \tag{120}$$

Thus the drift term vanishes in probability. The second term has quadratic variation

$$\left\langle \frac{1}{\sqrt{h}}\int_0^{h\cdot}\boldsymbol{\sigma}_Q(Q_s)\,\mathrm{d}W_s\right\rangle_t = \frac{1}{h}\int_0^{ht}\boldsymbol{\sigma}_Q(Q_s)\boldsymbol{\sigma}_Q(Q_s)^*\,\mathrm{d}s \longrightarrow t\,\boldsymbol{\sigma}_Q(Q_0)\boldsymbol{\sigma}_Q(Q_0)^* \tag{121}$$

and its jumps vanish because the martingale is continuous. Since continuity of Q at the deterministic initial point gives $\sup_{s\le hT}\|Q_s - Q_0\| \to 0$ in probability, the displayed quadratic-variation convergence holds in probability. The martingale functional central-limit theorem therefore gives the Gaussian limit

$$\boldsymbol{\sigma}_Q(Q_0)W_t. \tag{122}$$

Hence

$$Y^h \Rightarrow \boldsymbol{\sigma}_Q(Q_0)W \qquad (h \downarrow 0). \tag{123}$$

The drift disappears only after the microscopic tangent rescaling. This distinction is essential for mathematical correctness.

4.9. *Time reversal is a property of path laws, not of one coefficient.* The preceding limits separate a deterministic collective trajectory from a Gaussian tangent fluctuation. They do not, by themselves, classify either limit as reversible or irreversible. Four notions must be kept distinct:

(i) a complete ordinary differential equation may be solved both forward and backward, so its flow maps are invertible;
(ii) a deterministic equation is physically time-reversal covariant only after a parity involution on its variables has been specified;
(iii) a stationary stochastic process is statistically reversible when its entire path law is invariant under the corresponding reversal;
(iv) thermodynamic irreversibility is quantified by a positive forward-versus-reversed path-space relative entropy, or equivalently by an irreversible probability current under the hypotheses below.

These distinctions and their path-space formulations follow the standard stochastic-thermodynamic treatment of diffusion reversal and odd-parity variables [31], [146], and [144]. The first statement is a property of uniqueness for an ODE. It is not the same as the second statement. In particular, an invertible gradient-flow map can still select a preferred time direction through a strict Lyapunov function.

Let Θ be a smooth involution of the finite-regulator state space. Positions and scalar amplitudes are normally even, while momenta and magnetic variables may be odd. For a path $\omega \in C([0,T];\mathcal{X})$, define

$$(\mathcal{T}_T\omega)(t) := \Theta\omega(T-t), \qquad 0 \le t \le T. \tag{124}$$

If $\mathbb{P}_\pi^{[0,T]}$ is the stationary path law with invariant density π, its finite-time arrow is measured by

$$\mathscr{A}_T(\pi) := D_{\mathrm{KL}}\Big(\mathbb{P}_\pi^{[0,T]} \,\Big\|\, \mathbb{P}_\pi^{[0,T]} \circ \mathcal{T}_T^{-1}\Big) \ge 0. \tag{125}$$

This definition has an operational meaning: it is the information available for distinguishing a stationary movie from the same movie run backward with all odd variables parity reversed. Statistical reversibility is exactly $\mathscr{A}_T(\pi) = 0$ for every $T > 0$.

Proposition 6 (Coefficient limits do not determine time reversal). *Let*

$$\mathrm{d}X_t^\varepsilon = b_\varepsilon(X_t^\varepsilon)\,\mathrm{d}t + \sqrt{2D_\varepsilon(X_t^\varepsilon)}\,\mathrm{d}W_t \tag{126}$$

be a smooth, conservative diffusion on a torus, or on $\mathbb{R}^d$ with the decay and generator-domain conditions needed for the integrations by parts below. Assume that the stationary forward and reversed martingale problems are unique in law, their Girsanov density is a true martingale, and the expected drift-change quadratic energy is finite on each finite interval. These conditions hold for

smooth uniformly elliptic coefficients on a torus. A reflected-domain version additionally requires compatible forward and reversed boundary realizations; zero probability flux alone does not specify them. Suppose first that all variables are even, $D_\varepsilon = D_\varepsilon^{\mathsf{T}} \succ 0$*, and* $\pi_\varepsilon > 0$ *is a smooth invariant density. Define*

$$J_{\varepsilon,i}[\rho] := b_{\varepsilon,i}\rho - \partial_j(D_{\varepsilon,ij}\rho). \tag{127}$$

Then the drift of the stationary reversed process is

$$b^R_{\varepsilon,i} = -b_{\varepsilon,i} + 2\pi_\varepsilon^{-1}\partial_j(D_{\varepsilon,ij}\pi_\varepsilon), \qquad b_\varepsilon - b^R_\varepsilon = \frac{2J_\varepsilon[\pi_\varepsilon]}{\pi_\varepsilon}. \tag{128}$$

Consequently, the following conditions are equivalent:

$$\mathbb{P}^{[0,T]}_{\pi_\varepsilon} = \mathbb{P}^{[0,T]}_{\pi_\varepsilon} \circ \mathcal{T}_T^{-1} \text{ for every } T \quad \Longleftrightarrow \quad J_\varepsilon[\pi_\varepsilon] = 0 \quad \Longleftrightarrow \quad \mathcal{L}_\varepsilon = \mathcal{L}_\varepsilon^{\dagger,\pi_\varepsilon}. \tag{129}$$

Moreover, the stationary entropy-production rate is

$$\mathrm{epr}_\varepsilon := \lim_{T\to\infty} \frac{1}{T}\mathscr{A}_T(\pi_\varepsilon) = \int_{\mathcal{X}} \frac{J_\varepsilon[\pi_\varepsilon]^{\mathsf{T}} D_\varepsilon^{-1} J_\varepsilon[\pi_\varepsilon]}{\pi_\varepsilon}\,\mathrm{d}x \geq 0. \tag{130}$$

For a positive semidefinite diffusion matrix, the same identity holds with $D_\varepsilon^\dagger$ *only when the forward–reverse drift difference lies in* $\operatorname{Ran} D_\varepsilon$*, its pseudoinverse energy is finite, the relevant range is measurable with controlled rank, the Girsanov exponential is a true martingale, and the two martingale problems are unique in law. Otherwise the path laws need not be mutually absolutely continuous.*

If $D_\varepsilon \to 0$ *and* $b_\varepsilon \to b_0$*, the limiting ODE is time-reversal covariant under a smooth involution* Θ *only if*

$$\mathrm{d}\Theta_x\, b_0(x) = -b_0(\Theta x). \tag{131}$$

If instead $b_\varepsilon \to 0$ *and* $D_\varepsilon \to D_0$*, the limiting pure diffusion is reversible with respect to a positive density* π_0 *precisely when*

$$\partial_j(D_{0,ij}\pi_0) = 0. \tag{132}$$

Thus neither $D_\varepsilon \to 0$ *nor* $b_\varepsilon \to 0$*, considered alone, determines time-reversal symmetry.*

The limits in this proposition are singular at the level of path measures. For example, a nondegenerate diffusion law may be mutually singular with the law of its deterministic limit, so the finite-diffusion relative-entropy rate need not converge to the relative entropy of the limiting process. The criteria above are therefore applied before the singular limit, or together with a separately proved weak-convergence, large-deviation, or Γ-convergence statement. No continuity of the arrow functional in the diffusion parameter is assumed.

Proof. The stationary forward equation is $\partial_t \rho = -\partial_i J_{\varepsilon,i}[\rho]$. Integrating the generator by parts in $L^2(\pi_\varepsilon)$ gives the adjoint drift in (128). Hence the forward and reversed generators agree exactly when the stationary current vanishes, which proves (129). The two processes have the same covariance $2D_\varepsilon$. Girsanov's formula and (128) therefore give

$$\frac{1}{2}\int (b_\varepsilon - b_\varepsilon^R)^{\mathsf{T}}(2D_\varepsilon)^{-1}(b_\varepsilon - b_\varepsilon^R)\,\pi_\varepsilon\,\mathrm{d}x = \int \frac{J_\varepsilon[\pi_\varepsilon]^{\mathsf{T}} D_\varepsilon^{-1} J_\varepsilon[\pi_\varepsilon]}{\pi_\varepsilon}\,\mathrm{d}x.$$

Stationarity removes the endpoint relative-entropy contribution, proving (130). For the deterministic limit, if $x(t)$ solves $\dot{x} = b_0(x)$, differentiation of $y(t) = \Theta x(-t)$ shows that y solves the same equation exactly when (131) holds. Finally, setting $b_0 = 0$ in (127) proves (132). □

For odd variables, assume that Θ preserves the state domain and its boundary conditions, $\Theta_{\#}\pi = \pi$, the generator domains are mapped into each other, and the diffusion is parity covariant:

$$D(\Theta x) = \mathrm{d}\Theta_x\, D(x)\, \mathrm{d}\Theta_x^{\mathsf{T}}.$$

Let $U_\Theta f = f \circ \Theta$. The parity-corrected detailed-balance condition is

$$\mathcal{L}^{\dagger,\pi} = U_\Theta \mathcal{L} U_\Theta. \tag{133}$$

If

$$\mathcal{L} = \mathcal{A} + \mathcal{S}, \qquad \mathcal{A}^{\dagger,\pi} = -\mathcal{A}, \qquad \mathcal{S}^{\dagger,\pi} = \mathcal{S}, \tag{134}$$

and

$$U_\Theta \mathcal{A} U_\Theta = -\mathcal{A}, \qquad U_\Theta \mathcal{S} U_\Theta = \mathcal{S}, \tag{135}$$

then (133) follows. This operator identity reconciles two uses of the term reversible in this paper. The overdamped Gibbs generator (81) has $\mathcal{A} = 0$ and is itself self-adjoint. In the later reversible–irreversible decomposition, $\mathbb{L}\nabla E$ supplies the conservative anti-self-adjoint transport, whose sign is reversed by Θ, while the mobility and diffusion form the symmetric sector.

The irreversible-current formula can also be made explicit when odd variables are present. Its statement needs more than an algebraic split of the drift.

Proposition 7 (Entropy rate with linear time-reversal parity). *Consider a stationary, nonexplosive diffusion with generator $\mathcal{L}f = b \cdot \nabla f + D_{ij}\partial_i\partial_j f$ and smooth positive invariant coordinate density π. Its state space is $\mathbb{R}^d$ with sufficient decay for integration by parts, or a torus. Let $\Theta x = Px$, where P is an orthogonal involution preserving the domain and, on a torus, the period lattice. Assume*

$$P^2 = I, \qquad \pi(Px) = \pi(x), \qquad D(Px) = PD(x)P^{\mathsf{T}}, \qquad D(x) \succ 0. \tag{136}$$

Assume that the forward and reversed martingale problems are unique in law, the Girsanov density relating them is a true martingale, and its expected quadratic energy is finite on every finite interval. Define

$$\begin{gathered} c_i(x) := \pi(x)^{-1}\partial_j\big(D_{ij}(x)\pi(x)\big), \quad b_{\mathrm{irr}}(x) := \tfrac{1}{2}\big(b(x) + Pb(Px)\big), \\ J_{\mathrm{irr},i}(x) := \pi(x)b_{\mathrm{irr},i}(x) - \partial_j\big(D_{ij}(x)\pi(x)\big). \end{gathered} \tag{137}$$

The parity-reversed path law has drift

$$b^{R\Theta}(x) = -Pb(Px) + 2c(x), \qquad b(x) - b^{R\Theta}(x) = 2J_{\mathrm{irr}}(x)/\pi(x). \tag{138}$$

Consequently, for the path-law relative entropy $\mathscr{A}_T(\pi)$ in (125)*,*

$$\frac{\mathscr{A}_T(\pi)}{T} = \int_{\mathcal{X}} \frac{J_{\mathrm{irr}}^{\mathsf{T}} D^{-1} J_{\mathrm{irr}}}{\pi}\,\mathrm{d}x \geq 0. \tag{139}$$

The equality holds for every $T > 0$, not only asymptotically, under these stationary hypotheses.

Proof. The ordinary stationary reverse has drift $b^R = -b + 2c$, by (128). Parity covariance and invariance of π imply $c(Px) = Pc(x)$. Since P is linear, the pushforward drift is $Pb^R(Px)$, with no additional Itô Hessian term; this gives (138). The reversed law starts with $\Theta_{\#}\pi = \pi$, so there is no initial relative-entropy term. Both laws have covariance $2D$. Taking the controlled expectation of the log Girsanov density gives

$$\mathscr{A}_T(\pi) = \frac{1}{4}\mathbb{E}\int_0^T (b - b^{R\Theta})^{\mathsf{T}} D^{-1}(b - b^{R\Theta})(X_t)\,\mathrm{d}t = T\int_{\mathcal{X}} \frac{J_{\mathrm{irr}}^{\mathsf{T}} D^{-1} J_{\mathrm{irr}}}{\pi}\,\mathrm{d}x. \tag{140}$$

The first factor is $\frac{1}{2}(2D)^{-1}$; substitution of the drift difference cancels the factor $\frac{1}{4}$. Stationarity supplies the last equality. Positive definiteness of D gives nonnegativity. □

For degenerate D, replacement by $D^{\dagger}$ requires the range, measurability, finite-energy, and absolute-continuity conditions following (130). Zero probability flux alone does not specify a boundary diffusion: a reflected version additionally needs the same conormal reflection and compatible generator domains for both path laws. A nonlinear parity map would introduce an Itô Hessian correction and is not covered by Proposition 7.

For example, underdamped Langevin dynamics with constant particle mass $m_{\mathrm{p}} > 0$ is

$$\mathrm{d}q_t = p_t/m_{\mathrm{p}}\,\mathrm{d}t, \qquad \mathrm{d}p_t = -\nabla V(q_t)\,\mathrm{d}t - \gamma p_t\,\mathrm{d}t + \sqrt{2\gamma m_{\mathrm{p}}\theta}\,\mathrm{d}W_t. \tag{141}$$

Assume $\gamma, \theta > 0$, a normalizable Gibbs density, appropriate periodic or confining position data, and well-posed stationary dynamics. Then $\Theta(q,p) = (q,-p)$ and $\pi \propto \exp[-(p^2/(2m_{\mathrm{p}}) + V(q))/\theta]$. Its diffusion matrix is degenerate, but direct calculation gives $b_{\mathrm{irr}} = (0, -\gamma p) = c$. Thus $J_{\mathrm{irr}} = 0$ and the parity-corrected stationary entropy rate is zero, although the Hamiltonian transport current

$\pi(p/m_{\mathrm{p}}, -\nabla V)$ need not vanish. This example demonstrates why the total current cannot be substituted for the irreversible current in the presence of momenta.

The two limits above now have an exact interpretation. Along the macroscopic gradient-flow limit (106),

$$\frac{\mathrm{d}}{\mathrm{d}t}\Phi(Q_t) = -\left\langle \nabla_Q \Phi(Q_t), M_Q(Q_t)\nabla_Q \Phi(Q_t)\right\rangle \le 0. \tag{142}$$

For ordinary reversal, $\Theta = \mathrm{Id}$, condition (131) would require $b_0 = -b_0$. Except at a stationary point, the deterministic gradient flow is therefore dissipative even though its martingale term has disappeared. Noise suppression establishes determinism, not physical reversibility.

Conversely, periodize a constant version of the tangent diffusion (123) on a torus and put

$$D_0 := \tfrac{1}{2}\boldsymbol{\sigma}_Q(Q_0)\boldsymbol{\sigma}_Q(Q_0)^*.$$

Its uniform invariant density has zero current and its stationary path law is reversible. If it is prepared instead with a nonuniform density, then

$$\begin{aligned} J[\rho_t] &= -D_0\nabla\rho_t, \\ \frac{\mathrm{d}}{\mathrm{d}t}D_{\mathrm{KL}}(\rho_t\|\pi_{\mathrm{unif}}) &= -\int \rho_t \left\langle \nabla \log\frac{\rho_t}{\pi_{\mathrm{unif}}}, D_0\nabla\log\frac{\rho_t}{\pi_{\mathrm{unif}}}\right\rangle \mathrm{d}x \le 0. \end{aligned} \tag{143}$$

On a finite interval $[0,T]$, the drift of the process viewed backward is

$$b^R(s,x) = 2D_0\nabla\log\rho_{T-s}(x). \tag{144}$$

Thus a driftless forward equation can exhibit a transient arrow from a nonequilibrium initial law, while the same diffusion is exactly reversible at uniform equilibrium.

The intuitive statement that the macroscopic branch is reversible can be made correct only through a matched scaling. Consider

$$\mathrm{d}X_t^\alpha = [b_{\mathrm{cons}}(X_t^\alpha) + \alpha b_{\mathrm{diss}}(X_t^\alpha)]\,\mathrm{d}t + \sqrt{2\alpha D(X_t^\alpha)}\,\mathrm{d}W_t, \qquad \alpha \downarrow 0. \tag{145}$$

To justify the phrase fluctuation–dissipation partner, assume that a Θ-invariant density π satisfies

$$b_{\mathrm{diss},i}(x) = \pi(x)^{-1}\partial_j(D_{ij}(x)\pi(x))\,, \tag{146}$$

with the corresponding zero-flux or periodic boundary condition, and that $\nabla\cdot(b_{\mathrm{cons}}\pi) = 0$. The same factor then suppresses the dissipative response and its fluctuation partner. On every fixed finite time interval, under the usual tightness and coefficient-convergence hypotheses, the limit is $\dot{X} = b_{\mathrm{cons}}(X)$. It is Θ-reversible if b_{cons} satisfies (131) and the process is prepared in the Θ-invariant stationary law. By contrast, the collective scaling (104) suppresses only the noise unless an additional scaling is imposed on the gradient drift, so reversibility cannot be inferred from that limit alone.

The fixed-time qualification cannot be dropped. Even if the stationary entropy-production rate is $O(\alpha)$, observation on a time scale $T_\alpha = O(\alpha^{-1})$ can accumulate an order-one forward–reverse relative entropy. Hence the limits $\alpha \downarrow 0$ and $T \to \infty$ need not commute.

This is the precise sense in which the framework unifies the two temporal descriptions. The common generator contains a conservative transport sector, a fluctuation–dissipation sector, and any external drive. Changing scale can alter which sector is visible, but the arrow of time at that scale is always decided by parity, probability current, boundary and initial data, and the forward–reverse path law. The apparent conflict between microscopic and macroscopic time is therefore removed by separating distinct mathematical questions, not by assigning reversibility to the disappearance of one coefficient.

4.10. *Physical entropy production and a coarse-graining no-go result.* The path-space calculation acquires a thermodynamic meaning only after the forward protocol, reversed protocol, reservoirs, and physical time parameter have been specified. If their path laws are mutually absolutely continuous, define the trajectory-wise total entropy production by

$$\Delta s_{\mathrm{tot}}[\omega] := k_{\mathrm{B}} \log \frac{\mathrm{d}\mathbb{P}_{\mathrm{F}}}{\mathrm{d}(\mathbb{P}_{\mathrm{R}} \circ \mathcal{T}_T^{-1})}(\omega). \tag{147}$$

Normalization of the Radon–Nikodym derivative gives the integral fluctuation identity and its relative-entropy consequence [103], [47], and [144]:

$$\mathbb{E}_{\mathrm{F}} \exp\!\left(-\frac{\Delta s_{\mathrm{tot}}}{k_{\mathrm{B}}}\right) = 1, \qquad \mathbb{E}_{\mathrm{F}} \Delta s_{\mathrm{tot}} = k_{\mathrm{B}} D_{\mathrm{KL}}\big(\mathbb{P}_{\mathrm{F}} \,\big\|\, \mathbb{P}_{\mathrm{R}} \circ \mathcal{T}_T^{-1}\big) \geq 0. \tag{148}$$

The first equality is measure theoretic. Interpreting it as physical entropy production additionally requires local detailed balance and a declared heat, work, and reservoir bookkeeping convention. In particular, the auxiliary stochastic relaxation time used in a Euclidean sampler has not been proved equal to Lorentzian physical time.

The Crooks and Jarzynski work relations are a more specialized consequence, not synonyms for (148). Suppose the system is coupled to an isothermal reservoir at the physical energy scale $\theta = k_{\mathrm{B}} T_{\mathrm{bath}}$, satisfies local detailed balance, and is driven by an energy $E(x; \lambda_t)$. The forward process starts in canonical equilibrium at λ_0, and the reverse process starts in canonical equilibrium at λ_T with the reversed protocol and the correct parity of all external controls. In the absence of other work sources, use the work-on-system convention

$$W[\omega] := \int_0^T \partial_\lambda E(X_t; \lambda_t)\, \dot{\lambda}_t \, \mathrm{d}t, \qquad \Delta F_{\mathrm{eq}} := -\theta \log\big(Z(\lambda_T)/Z(\lambda_0)\big). \tag{149}$$

This F_{eq} is the canonical equilibrium free energy, not the relative-free-energy functional of an arbitrary evolving density. The first law $\Delta E = W - Q_{\mathrm{bath}}$,

together with the equilibrium endpoint densities, gives the path identity

$$\log \frac{\mathrm{d}\mathbb{P}_{\mathrm{F}}}{\mathrm{d}(\mathbb{P}_{\mathrm{R}} \circ \mathcal{T}_T^{-1})}(\omega) = \frac{W[\omega] - \Delta F_{\mathrm{eq}}}{\theta}. \tag{150}$$

Here the reservoir entropy change is $Q_{\mathrm{bath}}/T_{\mathrm{bath}}$. The endpoint system-entropy term cancels $\Delta E/\theta$, leaving the right-hand side. If forward and reversed work densities exist, marginalizing the path identity and using $W_R[\mathcal{T}_T\omega] = -W[\omega]$ gives

$$\frac{p_{\mathrm{F}}(w)}{p_{\mathrm{R}}(-w)} = \exp\!\left(\frac{w - \Delta F_{\mathrm{eq}}}{\theta}\right), \qquad \mathbb{E}_{\mathrm{F}} e^{-W/\theta} = e^{-\Delta F_{\mathrm{eq}}/\theta}. \tag{151}$$

The second equality follows directly by substituting (150) in (148); it does not require work densities. Noncanonical initial laws, multiple reservoirs, or a mismatch between stochastic and physical time require additional boundary or entropy terms. These work identities therefore apply only after the stated physical interface has been established [103], [47], and [144].

There is also a useful no-go theorem for emergence by exact filtering. Let Π be a measurable path projection that intertwines reversal, $\Pi \circ \mathcal{T}_T = \mathcal{T}_T^Q \circ \Pi$. Data processing gives

$$D_{\mathrm{KL}}\big(\mathbb{P}_{\mathrm{F}} \,\big\|\, \mathbb{P}_{\mathrm{R}} \circ \mathcal{T}_T^{-1}\big) \geq D_{\mathrm{KL}}\Big(\Pi_{\#}\mathbb{P}_{\mathrm{F}} \,\Big\|\, \Pi_{\#}\mathbb{P}_{\mathrm{R}} \circ (\mathcal{T}_T^Q)^{-1}\Big). \tag{152}$$

Consequently, if the complete stationary master path law is reversible, every exact reversal-compatible projection of it is also reversible. Coarse graining can hide entropy production; it cannot create fundamental positive path-space entropy production from an exactly reversible law. An irreversible macroscopic closure must therefore identify at least one additional source: a nonequilibrium low-entropy initial condition, external driving or reservoirs, unobserved odd variables, memory discarded by a Markov approximation, or a singular noncommutation of long-time and regulator limits. The forcing and dissipation assumed in the finite Navier–Stokes branch are such physical interface data; they do not follow from equilibrium Gibbs notation alone.

The same distinction survives quantization. For a closed state with unitary evolution,

$$S_{\mathrm{vN}}(U\rho U^\dagger) = S_{\mathrm{vN}}(\rho). \tag{153}$$

Growth of a reduced quantum entropy must come from entanglement with discarded degrees of freedom, an environment, measurement, coarse graining, or special boundary data. The framework therefore resolves the apparent conflict between reversible and irreversible descriptions by identifying their different path laws and information levels. It does not derive the cosmological low-entropy initial condition, often called the past hypothesis.

Remark 8 (Three distinct time reversals). *The involution Θ above is a classical kinematic parity map on the regulated state coordinates. In Lorentzian*

quantum theory, time reversal is represented antiunitarily, and the weak interaction permits fundamental CP and T violation while remaining compatible with CPT under its standard hypotheses. Fundamental T-odd couplings, violation of stochastic detailed balance, and thermodynamic entropy production are therefore different statements. When the microscopic dynamics is T-odd, the reversed experiment uses the conjugate time-reversed dynamics and reversed external protocol; it is not obtained by running the same coefficients backward. CKM or PMNS phases alone do not derive the second law or a low-entropy cosmological boundary condition.

4.11. *Four complementary meanings of a time arrow.* The distinction between reversible microscopic equations and irreversible macroscopic behavior becomes clearer when one specifies the object that is being reversed. An equation, a probability law, a Markov evolution, and a recorded history are different objects. The four descriptions below connect these objects without treating them as equivalent. We adapt the organization of the autonomous isothermal analysis in [100]; its information-theoretic arguments apply to the regulated process independently of a thermodynamic interpretation.

Fix a regulator and let P_t be its conservative Markov semigroup with invariant probability μ. Write

$$\nu_t = \nu_0 P_t, \qquad f_t = \frac{d\nu_t}{d\mu}, \qquad H_\mu(t) = D_{\mathrm{KL}}(\nu_t \| \mu). \tag{154}$$

The entropy is dimensionless. If the reference is a physically calibrated Gibbs equilibrium, with energy scale $\theta = k_{\mathrm{B}} T_{\mathrm{bath}}$, the excess free energy is θH_μ. Invariance alone does not make μ a thermal equilibrium: a driven stationary law can also be invariant.

4.11.1. *Generator structure and physical reversal.* Let Θ be the declared state-space parity involution and assume $\Theta_{\#}\mu = \mu$. Its action on observables is $U_\Theta h = h \circ \Theta$, so $U_\Theta^2 = I$. For fixed external parameters that are unchanged by physical reversal, generalized detailed balance takes the form

$$\mathcal{D}_\Theta := \mathcal{L}^{\dagger,\mu} - U_\Theta \mathcal{L} U_\Theta = 0. \tag{155}$$

The equality is understood on a common invariant core and extended to the semigroups under their well-posedness hypotheses. External magnetic fields or other time-odd parameters must instead be reversed in the comparison generator. For the underdamped equilibrium decomposition $\mathcal{L} = \mathcal{A} + \mathcal{S}$, one can have

$$\mathcal{A}^{\dagger,\mu} = -\mathcal{A}, U_\Theta \mathcal{A} U_\Theta = -\mathcal{A}, \qquad \mathcal{S}^{\dagger,\mu} = \mathcal{S}, U_\Theta \mathcal{S} U_\Theta = \mathcal{S}. \tag{156}$$

Then $\mathcal{L}^{\dagger,\mu} = \mathcal{S} - \mathcal{A} = U_\Theta \mathcal{L} U_\Theta$. Friction, noise, and Hamiltonian transport can therefore all be nonzero in a statistically reversible stationary process. Positivity

of the dissipative Dirichlet form and violation of stationary physical reversal are not the same assertion.

4.11.2. *Information loss and the absence of a Markov inverse.* For every invariant-measure-preserving Markov kernel, data processing gives

$$D_{\mathrm{KL}}(\nu P_t\|\mu) \le D_{\mathrm{KL}}(\nu\|\mu). \tag{157}$$

Suppose the inequality is strict for a specified ν with finite relative entropy. No Markov kernel Q can simultaneously satisfy

$$(\nu P_t)Q = \nu, \qquad \mu Q = \mu. \tag{158}$$

Indeed, data processing under Q would imply $D_{\mathrm{KL}}(\nu\|\mu) \le D_{\mathrm{KL}}(\nu P_t\|\mu)$, contradicting strictness. This is an obstruction to positive probability recovery with the same reference law. It does not forbid constructing a reversed diffusion, solving a backward equation on a smaller domain, or introducing a recovery operation that uses additional information or changes the reference law. The physical reverse of a diffusion is not generally its inverse semigroup.

4.11.3. *Ordering, convergence, and nonrecurrence of laws.* Contraction orders the evolving distributions by H_μ. To establish attraction to μ, rather than mere nonincrease, suppose that a diffusion entropy chain rule and a coercive estimate give

$$\frac{d}{dt}H_\mu(t) = -\mathcal{I}_\mu(f_t), \qquad \mathcal{I}_\mu(f) \ge 2\lambda H_\mu(f\mu), \quad \lambda > 0. \tag{159}$$

Here $H_\mu(f\mu) = D_{\mathrm{KL}}(f\mu\|\mu)$, and λ has inverse-time units in the declared clock. For instance, the second inequality follows from an appropriately normalized logarithmic Sobolev inequality. Integration yields

$$H_\mu(t) \le e^{-2\lambda(t-s)}H_\mu(s), \qquad t \ge s. \tag{160}$$

If $\nu_t = \nu_s$ for $t > s$ and $H_\mu(s) < \infty$, this inequality forces $H_\mu(s) = 0$ and hence $\nu_s = \mu$. Thus a nonequilibrium probability law cannot exactly recur under this strict contraction.

This statement does not exclude return of an individual trajectory to a previously visited region. Poincare recurrence concerns a measure-preserving transformation on a finite invariant measure space, not equality of an evolving nonequilibrium ensemble with its earlier law. Its hypotheses do not require finite dimensionality. Nor does a Gibbs minimizer by itself prove (160). In kinetic models, noise acts only in momentum directions; quantitative convergence may require hypocoercivity rather than an elliptic estimate. Convergence of laws also does not imply that fluctuating sample paths settle at a single deterministic field configuration.

4.11.4. *Distinguishability of paths and relaxation of histories.* For a finite window of duration T, retain the declared physical reverse experiment and its endpoint convention. Its law, pulled back by path reversal to the forward coordinates, is denoted by $\widehat{\mathbb{P}}_{\mathrm{R},T}$. Define

$$\Sigma_T = D_{\mathrm{KL}}(\mathbb{P}_{\mathrm{F},T} \| \widehat{\mathbb{P}}_{\mathrm{R},T}). \tag{161}$$

This measures the information distinguishing forward and reversed movies. At a stationary nonequilibrium law, $H_\mu(t) = 0$ when the system starts from μ, while Σ_T/T can be strictly positive. In particular, neither Σ_T nor its rate is generally the decrease of H_μ. Physical entropy units require multiplication by k_{B} and the local-detailed-balance interface of Section 4.10.

A history law introduces a third quantity. For a moving window $Y_t(s) = X_{t+s}$, $-h \le s \le 0$, let η_t be its law and η_{ss} a stationary history law. A history relaxation functional would be

$$H_{\mathrm{hist}}(t) = D_{\mathrm{KL}}(\eta_t \| \eta_{\mathrm{ss}}). \tag{162}$$

It must be analyzed with the actual shift-and-boundary-update dynamics of the window, or a valid augmented state when the projected process has memory. A symmetric sampler of a chosen path-space Gibbs density is not automatically that history process. A stationary circulating process has $\eta_t = \eta_{\mathrm{ss}}$ but can still have positive Σ_T/T. History relaxation and history reversal therefore remain different questions.

Object	What the corresponding assertion establishes
Generator and parity	Whether the stationary law has generalized physical detailed balance.
Positive Markov recovery	Whether a strictly contracting step can be undone without changing the invariant reference or adding information.
Evolving probability law	Whether a quantified decay estimate gives convergence and excludes exact nonequilibrium-law recurrence.
Forward and reversed paths	Whether recorded histories reveal a time direction, with physical entropy meaning after reservoir calibration.

Table 1. Four complementary descriptions of time direction. None is defined by the vanishing of a single drift or diffusion coefficient.

For the unified programme, these distinctions separate three uses of equilibrium: selecting a background, proving attraction of a regulated ensemble, and testing detailed balance of its stationary histories. The HJB value function selects an admissible feedback for a specified cost; it is not interchangeable with any of these entropy functionals. A sustained turbulent state belongs to the driven branch: stationary statistics need not eliminate injection, dissipation, or

path asymmetry. The detailed proofs, endpoint bookkeeping, and exactly solvable comparisons are developed in the thermodynamics companion paper. This classification does not determine a cosmological low-entropy initial condition or prove global convergence of gravitational collapse.

4.12. *A common fast–slow formulation.* A single equation can contain both regimes through a scale parameter ε. The following display is schematic until one specifies domains, boundary conditions, and a finite-dimensional or regularized realization in which M_Q and M_Z are positive self-adjoint mobility operators with sufficiently regular square roots. If either mobility depends on the state, the corresponding reference-volume divergence correction from (80) is also required:

$$\mathrm{d}Q_t^\varepsilon = -M_Q \nabla_Q \Phi(Q_t^\varepsilon, Z_t^\varepsilon)\mathrm{d}t + \sqrt{2\theta M_Q}\mathrm{d}B_t, \tag{163}$$

$$\mathrm{d}Z_t^\varepsilon = -\varepsilon^{-1} M_Z \nabla_Z C(Q_t^\varepsilon, Z_t^\varepsilon)\mathrm{d}t + \sqrt{2\theta\varepsilon^{-1} M_Z}\mathrm{d}W_t. \tag{164}$$

For these equations to use one potential, impose $\nabla_Z C = \nabla_Z \Phi$, equivalently $C(Q,Z) = \Phi(Q,Z) + c(Q)$ on each connected fast fiber. Otherwise the display describes two different potentials and need not have a joint reversible equilibrium. Under this compatibility condition, a finite conditional partition function gives

$$\begin{aligned} Z(Q) = \int e^{-\Phi(Q,z)/\theta}\, \nu_Z(\mathrm{d}z), \quad F_{\mathrm{slow}}(Q) = -\theta \log Z(Q), \\ \nabla_Q F_{\mathrm{slow}}(Q) = \int \nabla_Q \Phi(Q,z)\, \pi(\mathrm{d}z \mid Q). \end{aligned} \tag{165}$$

Here ν_Z is independent of Q, differentiation under the integral is assumed justified, and $\pi(\mathrm{d}z \mid Q) = Z(Q)^{-1} e^{-\Phi(Q,z)/\theta}\nu_Z(\mathrm{d}z)$. The last identity follows by differentiating $Z(Q)$ and dividing by $-Z(Q)/\theta$. For constant slow mobility, averaging thus produces the drift $-M_Q \nabla_Q F_{\mathrm{slow}}$; its slow noise remains $\sqrt{2\theta M_Q}\,\mathrm{d}B_t$. Taking $\varepsilon \to 0$ alone does not eliminate that noise. A deterministic macroscopic limit additionally uses the collective or small-noise scaling specified earlier. Convergence to the averaged equation requires uniform mixing of the fast dynamics, tightness, and a justified averaging theorem; time-scale separation alone does not supply these estimates.

4.13. *Symmetry breaking and the emergence of four sectors.*

4.14. *Residual symmetry.* Let φ_* denote a chosen vacuum value of the fields that break the local symmetry. In a local trivialization its stabilizer in the finite-dimensional isotropy group H is

$$H_{\varphi_*} := \{h \in H : \ h \cdot \varphi_* = \varphi_*\}. \tag{166}$$

The symbol φ_* is distinct from the real gauge-singlet scalar σ used in Section 5.4; that singlet alone cannot break the internal gauge group. Replacing φ_* by

another representative conjugates H_{φ_*}, so the residual subgroup is defined intrinsically up to conjugacy. Globally, a vacuum section of constant orbit type defines a reduction to this subgroup when such a reduction exists. The stabilizer of the whole section inside the gauge-transformation group $\mathfrak{G}$ is generally infinite dimensional; it must not be identified with the finite-dimensional fiber group H_{φ_*}. The low-energy gauge group is therefore not assumed to be fundamental. It is the stabilizer of a selected phase, provided the selection problem has a solution. In a gauge-invariant finite-volume measure, a local gauge-noninvariant expectation value is zero by Elitzur's theorem [64]. Accordingly, φ_* and the displayed brackets below denote either a representative on a declared gauge-fixed slice or an orbit-level order parameter. The physical statements are the stabilizer of the orbit, gauge-invariant composites such as $\varphi_*^\dagger\varphi_*$, and the covariant-derivative mass matrix. A literal local gauge-symmetry breaking expectation value requires a separately specified gauge fixing and, where relevant, an infinite-volume limit.

If the selected phase admits a reductive complement, the corresponding Lie algebra decomposition is

$$\mathfrak{h} = \mathfrak{h}_{\varphi_*} \oplus \mathfrak{h}_{\text{broken}}, \tag{167}$$

where $\mathfrak{h}_{\varphi_*} = \text{Lie}(H_{\varphi_*})$, and this decomposition is available only after the vacuum has been selected. The broken directions acquire masses or decouple only if the Hessian of the specified vacuum and kinetic terms has the required positive gap. The translational Cartan quotient $\mathfrak{g}/\mathfrak{h}$ supplies the coframe; it is not a list of massive internal gauge bosons.

4.15. *Candidate Standard-Model phase.* A candidate residual internal symmetry is

$$G_{\text{SM}} = SU(3)_c \times SU(2)_L \times U(1)_Y. \tag{168}$$

Equation (168) is a candidate output of the abstract selection problem and a prescribed input of the worked model in Section 5.4. A complete derivation would have to show that it solves the selection problem introduced below and that all competing admissible phases have larger master cost or fail consistency conditions.

After a scalar order parameter Φ_H is selected in a representation that, at low energy, is equivalent to the usual electroweak doublet, the residual breaking is

$$SU(2)_L \times U(1)_Y \longrightarrow U(1)_{\text{em}}. \tag{169}$$

With the conventional normalization,

$$Q = T_3 + Y. \tag{170}$$

Here Y is the Standard Model hypercharge convention used in (235) and in the anomaly sums below. A convention using $Y/2$ instead would require rescaling

every displayed hypercharge and the associated $U(1)$ coupling; no such rescaling is made in this paper. The representation and normalization must ultimately be derived from the master selection problem if the theory is to claim prediction rather than reconstruction.

5. Geometric and gauge recovery from one Euler system

5.1. *Gravity as a low-energy projection.* Before reducing the curvature blocks, write the connection component of the master Euler–Lagrange equation in constitutive form. Let $\iota_{\mathfrak{h}} : \mathfrak{h} \hookrightarrow \mathfrak{g}$ be the inclusion of the isotropy algebra and let $\iota_{\mathfrak{h}}^* : \mathfrak{g}^* \to \mathfrak{h}^*$ be its dual restriction. At fixed coframe an admissible connection variation has the form $\delta\mathbb{A} = \iota_{\mathfrak{h}}(\delta a)$, with $\delta a \in \Omega^1(M, \operatorname{ad} P_H)$; the translational component $\ell^{-1}\delta e$ is not varied in this calculation. If $\mathcal{L}_{\mathrm{M}}$ is the local master density, set the differential-form convention, at fixed coframe and fixed constitutive tensor,

$$\begin{aligned} \delta_a \mathcal{S}_{\mathrm{M}} = \int_M \langle \mathbb{P} \wedge \mathbb{D}_{\mathbb{A}} \iota_{\mathfrak{h}}(\delta a) \rangle + \int_M \langle \mathbb{J}_{\mathrm{ext}} \wedge \iota_{\mathfrak{h}}(\delta a) \rangle \,, \\ \mathbb{P} \in \Omega^2(M, \operatorname{ad}^* P), \qquad \mathbb{J}_{\mathrm{ext}} \in \Omega^3(M, \operatorname{ad}^* P). \end{aligned} \tag{171}$$

The brackets in this formula pair the adjoint and coadjoint bundles; no identification between them is assumed. The boundary term is assumed to vanish. Since $\deg \mathbb{P} = 2$, covariant integration by parts gives $\mathbb{P}\wedge\mathbb{D}_{\mathbb{A}}\delta\mathbb{A} = \mathbb{D}_{\mathbb{A}}(\mathbb{P}\wedge\delta\mathbb{A}) - \mathbb{D}_{\mathbb{A}}\mathbb{P}\wedge\delta\mathbb{A}$. Stationarity therefore fixes the sign convention below. When $\mathcal{L}_{\mathrm{M}}$ is written as a local four-form, the notation $\partial\mathcal{L}_{\mathrm{M}}/\partial\mathbb{F}$ means precisely this fiber derivative, including the Hodge and reference-density factors; it is not a derivative of a scalar with an untyped form degree. Thus

$$\mathbb{P} := \frac{\partial \mathcal{L}_{\mathrm{M}}}{\partial \mathbb{F}}, \qquad \iota_{\mathfrak{h}}^*(\mathbb{D}\mathbb{P} - \mathbb{J}_{\mathrm{ext}}) = 0. \tag{172}$$

Here $\mathbb{D}$ acts on coadjoint-valued forms. The second relation is exactly the fixed-coframe connection equation: testing only against δa determines only the restriction to $\mathfrak{h}^*$. It does not assert that the translational component of $\mathbb{D}\mathbb{P} - \mathbb{J}_{\mathrm{ext}}$ vanishes. The coframe equation also varies the Hodge operator, the volume form, and every other dependence on e; matter and order-parameter variations supply further equations. Let π_ω and π_{int} denote the projections from $\mathfrak{h}^*$ onto the rotational and residual internal dual blocks of a selected gauge-fixed splitting. If the reduced covariant derivative preserves these blocks and the residual constitutive pairing has no off-diagonal term, equation (172) gives

$$\pi_\omega \iota_{\mathfrak{h}}^*(\mathbb{D}\mathbb{P}) = \pi_\omega \iota_{\mathfrak{h}}^*(\mathbb{J}_{\mathrm{ext}}), \qquad \pi_{\mathrm{int}} \iota_{\mathfrak{h}}^*(\mathbb{D}\mathbb{P}) = \pi_{\mathrm{int}} \iota_{\mathfrak{h}}^*(\mathbb{J}_{\mathrm{ext}}). \tag{173}$$

These are two components of the same fixed-coframe variational equation, not two primitive actions. They must, however, be distinguished from the coframe

equation. Let the full variational derivative of the master action, including all matter and order-parameter terms, be denoted by

$$\mathcal{E}_{\mathrm{M}} := (\mathcal{E}_e, \mathcal{E}_\omega, \mathcal{E}_A, \mathcal{E}_\Phi, \mathcal{E}_\sigma, \mathcal{E}_\Psi, \mathcal{E}_\chi, \ldots) = 0, \qquad \begin{aligned} \mathcal{E}_e &:= \frac{\delta \mathcal{S}_{\mathrm{M}}}{\delta e}, \quad \mathcal{E}_\omega := \frac{\delta \mathcal{S}_{\mathrm{M}}}{\delta \omega}, \\ \mathcal{E}_A &:= \frac{\delta \mathcal{S}_{\mathrm{M}}}{\delta A}, \quad \mathcal{E}_\Phi := \frac{\delta \mathcal{S}_{\mathrm{M}}}{\delta \Phi_H}, \\ \mathcal{E}_\sigma &:= \frac{\delta \mathcal{S}_{\mathrm{M}}}{\delta \sigma}, \quad \mathcal{E}_\Psi := \frac{\delta \mathcal{S}_{\mathrm{M}}}{\delta \Psi}, \\ \mathcal{E}_\chi &:= \frac{\delta \mathcal{S}_{\mathrm{M}}}{\delta \chi}. \end{aligned} \tag{174}$$

Here A is the residual internal connection, and the omitted entries are any additional explicitly dynamical auxiliary-field equations. The reference information parameter is fixed in this formulation. The fixed-coframe connection component of (174) is $\mathcal{E}_a := \iota_{\mathfrak{h}}^*(\mathbb{DP} - \mathbb{J}_{\mathrm{ext}}) = 0$. In a Cartan decomposition, its rotational part is the ω equation, whereas the Einstein tensor comes from the independent coframe (or metric) equation $\mathcal{E}_e = 0$. This distinction is essential because the Hodge map and the volume form in the master pairing may themselves depend on e.

The precise sector-recovery statement used below is the following.

THEOREM 9 (Controlled sector recovery from one unified Euler system). *Assume that, after gauge fixing or passage to the physical quotient, the selected phase has a light-sector splitting into a gravitational Cartan block and a residual internal block, with the fixed-coframe rotational and internal projections π_ω and π_{int} defined above. Assume that the constitutive tensor is block compatible, that the gravitational block contains an isolated Palatini term with a nonzero, spatially constant coefficient κ_P, and that the coframe is non-degenerate. Here "isolated" means that, at the retained effective order, $\mathcal{E}_\omega$ receives no unsuppressed curvature-square, torsion-square, or mixed contribution. The exact Palatini implication below uses zero connection remainder. More generally, if heavy connection modes have been integrated out, assume on specified normed spaces that the retained spinless equation has the form $0 = \mathcal{L}_e T + \mathcal{R}_\omega$, where $\mathcal{L}_e$ is invertible, $\|\mathcal{L}_e^{-1}\| \le C_e$, and $\|\mathcal{R}_\omega\| \le \delta_\omega$. Assume that the matter spin current in the ω equation vanishes (or is negligible at the matching scale), $\mathcal{J}_\omega^{\mathrm{spin}} = 0$; otherwise the same calculation gives the Einstein–Cartan branch with torsion sourced by spin. Assume also that the internal block has a positive Ad-invariant form $\widehat{\kappa}_{AB}$ compatible with the Hodge operator. The hat records that this form may depend on the selected scalar and coframe; on a constant scalar/metric branch it is denoted simply by κ_{AB}. Assume further that, after the stated reduction and continuation, the retained coframe-dependent Lorentzian action has the*

effective basis displayed in (208)*, with every other retained coframe-dependent term included in* $S_{\mathrm{nongrav},L}$ *rather than silently discarded. This is the action induced after the retained connection equation has been solved, or after the indicated connection modes have been integrated out consistently; it is not obtained by restricting an unreduced independent-connection action before varying it. Assume moreover that every fixed information, reference, regulator, and matching datum entering the coframe variation is a diffeomorphism-covariant spurion and either belongs to the varied on-shell system or satisfies the associated Noether balance law. Then the single system* (174) *has the following three linked low-energy consequences, corresponding to the connection, coframe, and residual internal-connection components:*

$$\mathcal{E}_\omega = 0 \text{ in the Palatini truncation} \Longrightarrow T^a = 0. \tag{175}$$

If the controlled connection remainder just described is retained instead, the same equation and the inverse bound give

$$\|T\| \le \|\mathcal{L}_e^{-1}\|\,\|\mathcal{R}_\omega\| \le C_e \delta_\omega. \tag{176}$$

After imposing the torsionless branch and the stated continuation, the coframe equation $\mathcal{E}_e = 0$ *gives*

$$G_{\mu\nu} + \Lambda_L g_{\mu\nu} + 16\pi G_{\mathrm{eff}} \sum_i \bar{\alpha}_i \bar{\mathcal{H}}^{(i)}_{\mu\nu} \qquad = 8\pi G_{\mathrm{eff}} T^L_{\mu\nu}. \tag{177}$$

and

$$\pi_{\mathrm{int}}\mathcal{E}_a = 0 \Longleftrightarrow D\big(\widehat{\kappa}_{AB} \star F^B\big) \qquad = -\star J_A, \Longleftrightarrow D_\mu\big(\widehat{\kappa}_{AB} F^{B\mu\nu}\big) = J^\nu_A. \tag{178}$$

On a frozen constant-kinetic branch, canonical normalization reduces (178) *to the textbook form* (319)*. The Noether hypothesis ensures that the stress tensor in* (177) *has no unaccounted external exchange term. If it is not satisfied, a fixed non-on-shell datum can spoil covariant conservation and the coframe equation must include the corresponding exchange contribution. The ordinary Einstein equation is the controlled regime in which the last higher-curvature term in* (177) *is negligible. Thus the two familiar equations are separate projections of one full variational system: Einstein comes from its coframe/metric component after the connection equation selects the torsionless branch, whereas Yang–Mills comes from the residual internal-connection component. The hypotheses specify the phase, constitutive structure, and retained scale; they do not assume either field equation. The two equations are obtained by varying the same master action, so the implication is conditional but not circular. In particular, a spatially varying coefficient multiplying the Palatini term is not covered by the torsionless implication. For the joint candidate below this coefficient is proportional to* $w(\sigma)$*, so a constant scalar branch or a controlled scalar-gradient approximation is required before applying the displayed Einstein reduction. The exact implication*

$\mathcal{E}_\omega = 0 \Rightarrow T = 0$ *is therefore a statement about the retained constant-coefficient Palatini truncation; with a nonzero controlled connection remainder, the full theory gives the quantitative torsion estimate* (176)*. It is not an identity for the unreduced* $SO(5)$ *curvature-square witness, whose independent connection equation contains additional* $D_\omega \star R$ *and torsion terms and therefore represents the more general higher-derivative theory before the controlled sector is taken.*

Proof. The equality $\mathcal{E}_a = 0$ is exactly (172). Block compatibility gives (173). On the isolated Palatini branch, the variation with respect to ω is computed in (194); its algebraic inversion is given in (195)–(196), and proves (175). On the controlled-remainder branch, invertibility gives $T = -\mathcal{L}_e^{-1}\mathcal{R}_\omega$; taking the declared norms proves (176). With $T^a = 0$, the independent coframe variation is the metric variation of the induced effective action. Equations (205)–(210), using the retained effective-action hypothesis, then give (177), including the stated Euclidean-to-Lorentzian continuation. Finally, $\mathbb{P}_H^A = \widehat{\kappa}_{AB} \star F^B$ by Hodge compatibility, so the internal component of $\mathcal{E}_a = 0$ is the first equality in (178); the coordinate calculation in (314)–(318) proves the last equality. This also shows why a field-dependent or mixed constitutive tensor would leave the more general restricted constitutive equation $\iota_{\mathfrak{h}}^*[\mathbb{D}(\partial\mathcal{L}/\partial\mathbb{F}) - \mathbb{J}_{\text{ext}}] = 0$ instead. □

The word "controlled" records the domain of the theorem, not an unfinished step in its proof. Once its hypotheses hold, the displayed equations follow from the variational calculation and no classification of all global solutions or global regularity theorem for the full gauge–gravity evolution is needed. The light-sector splitting, constitutive form, continuation, and scale separation are sector and effective-matching hypotheses; non-degeneracy, admissibility of the variations, and the Noether balance are mathematical consistency hypotheses. Showing that a particular ultraviolet completion selects this domain uniquely would be a stronger result about model selection and predictivity, not a missing step in the conditional recovery theorem.

The next two subsections provide the detailed gravitational and internal calculations used in this theorem. They are projections of the same master Euler system, not independent sector actions.

Suppose the selected phase suppresses internal components at a length scale L, leaves a gravitational Cartan connection (e, ω) light, and selects an invariant pairing/order-parameter insertion whose curvature cross-term is of Palatini type. Concretely, this means that the reduced density contains, for some coefficient κ fixed by the microscopic pairing,

$$\left\langle \mathbf{F}_{\mathrm{M}}^{\mathrm{ext}}, \mathbf{F}_{\mathrm{M}}^{\mathrm{ext}} \right\rangle_{\mathbf{h}} \mathrm{vol}_g \supset \kappa\, \epsilon_{abcd} e^a \wedge e^b \wedge R^{cd}. \tag{179}$$

The left-hand side is a scalar density written as a four-form by multiplication with vol_g. Thus the displayed inclusion is an equality of four-forms; equivalently, after division by the nowhere-vanishing volume form on the coframe chart, it reads

$$\left\langle \mathbf{F}_{\mathrm{M}}^{\mathrm{ext}}, \mathbf{F}_{\mathrm{M}}^{\mathrm{ext}} \right\rangle_{\mathbf{h}} \supset \kappa \, \frac{\epsilon_{abcd} e^a \wedge e^b \wedge R^{cd}}{\mathrm{vol}_g}. \tag{180}$$

The quotient in (180) is the Hodge-type block of the extended pairing, not an untyped identification of a scalar with a differential form. This is an additional algebraic assumption; it does not follow from a generic positive curvature-square norm. One sufficient mechanism for the term is a symmetry-breaking J-sector curvature

$$F_J^{ab} = R^{ab} + \lambda \, e^a \wedge e^b \tag{181}$$

and an induced contraction proportional to ϵ_{abcd}. The parameter λ has the inverse-length-squared dimension required by the chosen coframe normalization. In this display R^{ab} denotes the curvature of the Lorentz connection after any $C_{P_a P_b}{}^{J_{cd}} e^a \wedge e^b$ contribution has been separated; if that contribution is retained in R^{ab}, its coefficient must instead be absorbed into λ. Such a tensor is required to be invariant under the residual subgroup used in the effective theory; it need not be invariant under the full microscopic group before symmetry breaking. Its algebraic expansion is

$$\begin{aligned} \epsilon_{abcd} F_J^{ab} \wedge F_J^{cd} = \epsilon_{abcd} R^{ab} \wedge R^{cd} + 2\lambda \, \epsilon_{abcd} e^a \wedge e^b \wedge R^{cd} \\ + \lambda^2 \epsilon_{abcd} e^a \wedge e^b \wedge e^c \wedge e^d. \end{aligned} \tag{182}$$

The overall factors depend on the normalization of J_{ab} and are absorbed into κ. Thus the Palatini term is an output of the specified symmetry-breaking insertion, not a consequence of an arbitrary positive inner product. The ϵ-contraction is a signed residual invariant; it is compatible with the positive Euclidean master norm only if it arises from a cross-block or order-parameter insertion whose full graded pairing remains positive on the chosen real slice. Positivity of that full pairing must be checked in the concrete model. Under the stated assumption, the finite-dimensional analogue makes the check explicit: if the relevant curvature/order-parameter block of $\mathbf{h}$ has matrix $\left(\begin{smallmatrix} A & B \\ B^* & C \end{smallmatrix}\right)$ with $A > 0$, then nonnegativity requires the Schur complement

$$C - B^* A^{-1} B \succeq 0. \tag{183}$$

For a positive definite, non-degenerate pairing in finite dimensions the inequality must be strict. In a Hilbert realization, a uniformly positive norm additionally requires a coercive lower bound on this complement and boundedness of the operators used in the factorization. Thus a signed cross term can occur without making the full Euclidean pairing indefinite, but only when (183) (or its operator

analogue) is verified. The reduced curvature is then

$$\mathbb{F} \rightsquigarrow \ell^{-1} T^a P_a + \frac{1}{2}\left(R^{ab} + \lambda\, e^a \wedge e^b\right) J_{ab}. \tag{184}$$

If the selected vacuum imposes the torsionless branch,

$$T^a = 0, \tag{185}$$

then, for a non-degenerate coframe, ω is identified with the Levi–Civita spin connection of that coframe.

The linear Einstein term requires specified curvature components and a specified pairing. The Palatini-type pairing above is one mechanism; Section 5.3 gives another using a coframe-dependent positive Hodge norm. With the convention

$$\epsilon_{abcd} e^a \wedge e^b \wedge R^{cd} = 2R \ \mathrm{vol}_g \tag{186}$$

up to convention-dependent normalization. In an oriented orthonormal coframe, write $R^{cd} = \frac{1}{2} R^{cd}{}_{ef}\, e^e \wedge e^f$. Then

$$\begin{aligned} \epsilon_{abcd} e^a \wedge e^b \wedge R^{cd} &= \frac{1}{2} \epsilon_{abcd} R^{cd}{}_{ef}\, e^a \wedge e^b \wedge e^e \wedge e^f \\ &= \frac{1}{2} \epsilon_{abcd} \epsilon^{abef} R^{cd}{}_{ef}\ \mathrm{vol}_g \\ &= \left(\delta_c^{\,e}\delta_d^{\,f} - \delta_c^{\,f}\delta_d^{\,e}\right) R^{cd}{}_{ef}\ \mathrm{vol}_g = 2R\ \mathrm{vol}_g, \end{aligned} \tag{187}$$

where $\epsilon_{abcd}\epsilon^{abef} = 2(\delta_c^{\,e}\delta_d^{\,f} - \delta_c^{\,f}\delta_d^{\,e})$ and the last equality uses the scalar-curvature convention $R := R^{cd}{}_{cd}$ and the antisymmetry of $R^{cd}{}_{ef}$ in e, f together with the chosen curvature convention. Reversing the orientation or the sign convention for R^{cd} reverses the displayed sign. The low-energy gravitational action therefore has the form

$$\begin{aligned} S_{\mathrm{grav,eff}} = \int_M \sqrt{g}\, \Big[\Lambda_{\mathrm{eff}} - \frac{R}{16\pi G_{\mathrm{eff}}} + \alpha_1 R^2 \\ + \alpha_2 R_{\mu\nu} R^{\mu\nu} + \alpha_3 R_{\mu\nu\rho\sigma} R^{\mu\nu\rho\sigma} + \cdots \Big]\, \mathrm{d}^4 x. \end{aligned} \tag{188}$$

The coefficients are not predicted by geometry alone; they depend on the precise master algebra, measure, regulator, and vacuum. The Einstein term is therefore a structural consequence conditional on those data, whereas a numerical prediction for G_{eff} is a separate problem. The geometric normalization is to be compared with the classical gravitational field equation only after the convention for R^{ab} has been fixed [63]. The boundedness and positivity assumptions imposed on the regulated master functional should not be confused with boundedness of this truncated Einstein–higher-curvature expansion; the latter is an effective description and can require additional stabilizing terms.

The logical origin of the gravitational equation can now be stated without introducing a second action. The gravitational projection of the connection

equation in (173) supplies the rotational connection equation and, on the isolated Palatini branch, the torsionless condition. The Einstein tensor is supplied by the independent coframe equation in (174); it is not obtained by applying a connection projection alone. Under the block-projection assumptions, the torsionless Palatini branch, and the specified coframe variation, the exact conditional chain is

$$\begin{aligned} \mathcal{E}_\omega = 0 \quad &\Longrightarrow \quad T^a = 0, \\ \mathcal{E}_e = 0 \quad &\Longrightarrow \quad \begin{aligned} &G_{\mu\nu} + \Lambda_L g_{\mu\nu} + 16\pi G_{\text{eff}} \sum_i \bar{\alpha}_i \bar{\mathcal{H}}^{(i)}_{\mu\nu} \\ &\qquad = 8\pi G_{\text{eff}} T^L_{\mu\nu} \end{aligned} \end{aligned} \tag{189}$$

Both lines are understood after the stated continuation and matching. The first line is the ω component of the unified Euler system and is proved in (194)– (196). The second line is the coframe/metric component after the connection equation has selected the torsionless branch; the Euclidean-to-Lorentzian continuation and the normalization of the Palatini coefficient are included in the phrase "stated continuation and matching." Thus (189) is a conditional projection of the single master variational system, not an independent Einstein action appended to it. In the controlled low-curvature regime in which the higher-curvature term is negligible, it reduces to the ordinary Einstein equation with cosmological constant.

5.2. *Metric variation and controlled recovery of the Einstein equation.* The occurrence of the scalar-curvature term in (188) is not by itself a derivation of Einstein's field equation. The latter is an Euler–Lagrange equation and requires a variation with respect to the coframe, or equivalently with respect to the induced metric on a non-degenerate branch. We make this step explicit. Write

$$I_1 = R^2, \qquad I_2 = R_{\rho\sigma} R^{\rho\sigma}, \qquad I_3 = R_{\rho\sigma\lambda\tau} R^{\rho\sigma\lambda\tau}. \tag{190}$$

For any curvature invariant I_i, define its metric variational tensor by

$$\mathcal{H}^{(i)}_{\mu\nu} := \frac{1}{\sqrt{g}} \frac{\delta}{\delta g^{\mu\nu}} \int_M \sqrt{g}\, I_i \, \mathrm{d}^4 x. \tag{191}$$

This definition includes the variation of the volume density. For example, with variations of compact support (or boundary conditions that remove the boundary term),

$$\mathcal{H}^{(1)}_{\mu\nu} = 2R R_{\mu\nu} - \frac{1}{2} g_{\mu\nu} R^2 + 2\big(g_{\mu\nu}\Box - \nabla_\mu \nabla_\nu\big) R. \tag{192}$$

For I_2 and I_3, equation (191) is the unambiguous definition; their expanded expressions contain the corresponding curvature contractions and second covariant derivatives. This choice avoids hiding a sign convention for the Riemann tensor in a formula that is later continued to Lorentzian signature.

The torsionless statement also has a precise variational status. If the Palatini block is isolated with a nonzero constant coefficient κ_P as

$$S_P = \frac{\kappa_P}{2}\int_M \epsilon_{abcd}\, e^a \wedge e^b \wedge R^{cd}, \tag{193}$$

then, using $\delta R^{cd} = D\delta\omega^{cd}$ and discarding the boundary term,

$$\delta_\omega S_P = -\kappa_P \int_M \epsilon_{abcd}\, T^a \wedge e^b \wedge \delta\omega^{cd}. \tag{194}$$

For a non-degenerate coframe, the connection equation implies $\epsilon_{abcd}T^a \wedge e^b = 0$. For completeness, the elementary algebraic inversion is as follows. Write $T^a = \frac{1}{2}T^a{}_{mn}e^m \wedge e^n$ and set $V_n := T^a{}_{an}$. Taking the Hodge dual of the three-form equation and using $\star(e^m \wedge e^n \wedge e^b) = \epsilon^{mnb}{}_s e^s$ gives

$$0 = \frac{1}{2}\epsilon_{abcd}T^a{}_{mn}\epsilon^{mnb}{}_s e^s = -\left(T^s{}_{cd} + \delta^s_d V_c - \delta^s_c V_d\right) e^s. \tag{195}$$

Here the displayed contraction uses the Euclidean orthonormal frame before Lorentzian continuation. Reversing orientation changes both epsilon tensors in this contraction, leaving their product unchanged. The contraction used in (195), with δ^{mns}_{acd} denoting the generalized Kronecker delta, is $\epsilon_{abcd}\epsilon^{mnb}{}_s = -\delta^{mns}_{acd}$, together with $\delta^{mns}_{acd}T^a{}_{mn} = 2(T^s{}_{cd} + \delta^s_d V_c - \delta^s_c V_d)$. Consequently,

$$T^s{}_{cd} = V_d\delta^s_c - V_c\delta^s_d. \tag{196}$$

Taking the trace $s = c$ and summing over c gives $V_d = 4V_d - V_d = 3V_d$, hence $V_d = 0$; equation (196) then gives $T^s{}_{cd} = 0$. Thus $T^a = 0$ on the non-degenerate torsionless branch. This statement is for the spinless or vacuum sector. If matter has a nonzero spin current, the connection equation is instead $\epsilon_{abcd}T^a \wedge e^b = \mathcal{J}^{\rm spin}_{cd}$, and the appropriate low-energy theory is Einstein–Cartan with torsion sourced by spin. The ordinary Einstein branch therefore requires $\mathcal{J}^{\rm spin}_\omega = 0$ (or a controlled suppression) at the matching scale. The torsionless implication is also not automatic if the full master pairing contains independent torsion-square or mixed terms; in that case the additional terms must be included in the connection equation. Likewise, variation of the coframe gives

$$\delta_e S_P = \kappa_P \int_M \epsilon_{abcd}\, \delta e^a \wedge e^b \wedge R^{cd}, \tag{197}$$

which must be combined with the cosmological, higher-curvature, and matter variations before it can be identified with an Einstein equation.

For the joint candidate, the common scalar generally makes the Palatini coefficient position dependent. The distinction can be derived without assuming a torsion ansatz. For a smooth positive function w, put

$$S_P[w, e, \omega] = \frac{\kappa_P}{2}\int_M w\, \epsilon_{abcd}e^a \wedge e^b \wedge R^{cd}, \qquad E^a := \sqrt{w}\, e^a. \tag{198}$$

Holding e and w fixed while varying ω, integration by parts gives

$$\begin{aligned}\delta_\omega S_P[w,e,\omega] &= -\frac{\kappa_P}{2}\int_M \epsilon_{abcd} D_\omega(we^a\wedge e^b)\wedge\delta\omega^{cd}\\ &= -\kappa_P\int_M \epsilon_{abcd}\left(wT^a\wedge e^b+\frac{1}{2}\mathrm{d}w\wedge e^a\wedge e^b\right)\wedge\delta\omega^{cd}.\end{aligned} \tag{199}$$

Since $we^a\wedge e^b = E^a\wedge E^b$, the same algebraic inversion as in (195)–(196), now applied to the non-degenerate coframe E, shows that the spinless connection equation is $D_\omega E^a = 0$. Expanding this identity yields

$$0 = D_\omega E^a = \sqrt{w}\left(T^a+\frac{1}{2}\mathrm{d}\log w\wedge e^a\right), \qquad T^a = \frac{1}{2}e^a\wedge\mathrm{d}\log w. \tag{200}$$

Thus ω is the Levi–Civita spin connection of the conformally rescaled coframe E, but it is generally not the torsionless connection of the original coframe e. The reduction to the ordinary Einstein equation for the metric g_e therefore requires $\mathrm{d}w = 0$, or a specified approximation that controls the scalar gradient and the remaining connection terms. Even if one imposes $\omega = \omega(e)$ before variation, the metric variation already displays the missing derivative terms:

$$\frac{1}{\sqrt{g}}\frac{\delta}{\delta g^{\mu\nu}}\int_M \sqrt{g}\, wR(g)\,\mathrm{d}^4x = wG_{\mu\nu} + (g_{\mu\nu}\Box - \nabla_\mu\nabla_\nu)\, w. \tag{201}$$

Here w is held fixed in the metric variation. Eliminating the independent connection from (198) also produces terms quadratic in $\mathrm{d}w$; it is not the same operation as imposing $\omega(e)$ at the outset. Consequently, the constant-coefficient equations (206) and (210) describe a constant-scalar branch or a controlled effective limit, rather than every solution of the coupled weighted theory.

To display the remaining signs, first stay on the Euclidean slice used in (188). In this subsection $S_{\mathrm{mat},E}$ denotes the total non-gravitational effective action, including the Yang–Mills, scalar, and matter sectors. Define the Euclidean stress tensor by

$$T^E_{\mu\nu} := \frac{2}{\sqrt{g}}\frac{\delta S_{\mathrm{mat},E}}{\delta g^{\mu\nu}}. \tag{202}$$

The elementary identities

$$\delta\sqrt{g} = -\frac{1}{2}\sqrt{g}\, g_{\mu\nu}\delta g^{\mu\nu}, \qquad \delta R = R_{\mu\nu}\delta g^{\mu\nu} + g_{\mu\nu}\Box\delta g^{\mu\nu} - \nabla_\mu\nabla_\nu\delta g^{\mu\nu} \tag{203}$$

and covariant integration by parts give

$$\delta\int_M \sqrt{g}\, R\,\mathrm{d}^4x = \int_M \sqrt{g}\, G_{\mu\nu}\delta g^{\mu\nu}\,\mathrm{d}^4x, \qquad G_{\mu\nu} := R_{\mu\nu} - \frac{1}{2}Rg_{\mu\nu}. \tag{204}$$

Consequently, varying the complete Euclidean effective action, including the matter term, yields

$$0 = -\frac{1}{16\pi G_{\mathrm{eff}}}G_{\mu\nu} - \frac{1}{2}\Lambda_{\mathrm{eff}}g_{\mu\nu} + \sum_i \alpha_i\mathcal{H}^{(i)}_{\mu\nu} + \frac{1}{2}T^E_{\mu\nu} \tag{205}$$

$$\begin{aligned} G_{\mu\nu} \quad &+ 8\pi G_{\mathrm{eff}}\Lambda_{\mathrm{eff}} g_{\mu\nu} - 16\pi G_{\mathrm{eff}} \sum_i \alpha_i \mathcal{H}^{(i)}_{\mu\nu} \\ &= 8\pi G_{\mathrm{eff}} T^E_{\mu\nu}. \end{aligned} \tag{206}$$

The first displayed line is the direct variation; the following two lines are the same equation after multiplication by $-16\pi G_{\mathrm{eff}}$. It is therefore the precise Euclidean statement associated with the sign convention in (188). Here Λ_{eff} is a vacuum-energy density in the Euclidean action. The curvature cosmological constant has dimension two and is related, up to the sign fixed by the continuation, by $\Lambda_E = 8\pi G_{\mathrm{eff}}\Lambda_{\mathrm{eff}}$; it must not be identified with Λ_{eff} itself.

The usual Lorentzian Einstein equation requires an additional analytic continuation and a Lorentzian matter convention. To make the continuation explicit, choose the mostly-plus Lorentzian convention $g_L = -(e^0_L)^2 + \sum_{j=1}^3 (e^j_L)^2$ and the Wick map

$$\begin{gathered} e^4_E \longmapsto i e^0_L, e^j_E \longmapsto e^j_L \quad (j = 1,2,3), \\ g_E \longmapsto g_L, \sqrt{g_E}\,\mathrm{d}^4x \longmapsto i\sqrt{-g_L}\,\mathrm{d}^4x, SO(5) \longmapsto SO(1,4), R_E \longmapsto R_L. \end{gathered} \tag{207}$$

The volume multiplier in (207) includes an orientation and contour convention. We take the oriented Euclidean volume in the order $e^4_E \wedge e^1_E \wedge e^2_E \wedge e^3_E$ and the Lorentzian volume in the order $e^0_L \wedge e^1_L \wedge e^2_L \wedge e^3_L$. The declared map then multiplies the volume by i. If instead the Euclidean wedge order is 1234, the associated orientation or contour Jacobian must also be reversed to retain this convention. All Levi–Civita symbols are defined relative to the chosen orientation; no additional sign is suppressed. The last line uses the curvature convention transported by the complexified coframe and spin connection; components with a time index acquire the corresponding factors of i. Writing $\mathcal{W}$ for this continuation, the relation between the path-integral weights is fixed by $S_L = i\mathcal{W}(S_E)$, so that $\exp[-\mathcal{W}(S_E)] = \exp(iS_L)$. In particular, the Euclidean density $\Lambda_{\mathrm{eff}} - R_E/(16\pi G_{\mathrm{eff}})$ continues to the Lorentzian density $R_L/(16\pi G_{\mathrm{eff}}) - \Lambda_{\mathrm{eff}}$. Thus this convention gives $\Lambda_L = 8\pi G_{\mathrm{eff}}\Lambda_{\mathrm{eff}}$; for unchanged real scalar curvature-square coefficients it gives $\bar{\alpha}_i = -\alpha_i$ at this continuation step. Other real-form or signature conventions are equivalent after changing all associated signs consistently. The map is a continuation of the regulated fields and boundary data; a formal substitution alone does not establish Lorentzian hyperbolicity, causality, or a globally defined solution. In particular, the Euclidean $SO(5)/SO(4)$ round-sphere vacuum is not itself a Lorentzian solution until this continuation and the relevant boundary conditions have been supplied. When the stated continuation exists, write the continued action as

$$S_L = \int_M \sqrt{-g}\left[\frac{R - 2\Lambda_L}{16\pi G_{\mathrm{eff}}} + \sum_i \bar{\alpha}_i I_i + \mathcal{L}_{\mathrm{nongrav},L}\right]\mathrm{d}^4x, \tag{208}$$

where $\mathcal{L}_{\mathrm{nongrav},L}$ contains the continued Yang–Mills, scalar, and matter terms, and where its action is $S_{\mathrm{nongrav},L} := \int_M \sqrt{-g}\,\mathcal{L}_{\mathrm{nongrav},L}\,\mathrm{d}^4x$. Define

$$T^L_{\mu\nu} := -\frac{2}{\sqrt{-g}}\frac{\delta S_{\mathrm{nongrav},L}}{\delta g^{\mu\nu}}, \qquad \bar{\mathcal{H}}^{(i)}_{\mu\nu} := \frac{1}{\sqrt{-g}}\frac{\delta}{\delta g^{\mu\nu}}\int_M \sqrt{-g}\,I_i\,\mathrm{d}^4x. \tag{209}$$

The Lorentzian Euler–Lagrange equation is then

$$G_{\mu\nu} + \Lambda_L g_{\mu\nu} + 16\pi G_{\mathrm{eff}} \sum_i \bar{\alpha}_i \bar{\mathcal{H}}^{(i)}_{\mu\nu} = 8\pi G_{\mathrm{eff}} T^L_{\mu\nu}. \tag{210}$$

The barred coefficients include the specified Wick sign and any separately declared renormalization or matching changes. Thus the ordinary Einstein equation is recovered, with an explicit error estimate, in a controlled low-curvature regime. A scale-based condition that remains meaningful near an exact vacuum is the following. Let L be a characteristic curvature length and suppose, for the displayed curvature invariants, that $\|\bar{\mathcal{H}}^{(i)}\| \le C_i L^{-4}$ for fixed dimensionless constants C_i. Require

$$16\pi G_{\mathrm{eff}} \sum_i |\bar{\alpha}_i| C_i L^{-2} \le \varepsilon, \qquad 0 < \varepsilon \ll 1. \tag{211}$$

Define the residual of the ordinary Einstein equation by

$$\mathscr{R}^{\mathrm{E}}_{\mu\nu} := G_{\mu\nu} + \Lambda_L g_{\mu\nu} - 8\pi G_{\mathrm{eff}} T^L_{\mu\nu}. \tag{212}$$

Equation (210), the triangle inequality, and (211) give the quantitative bound

$$\left\|\mathscr{R}^{\mathrm{E}}\right\| \le 16\pi G_{\mathrm{eff}} \sum_i |\bar{\alpha}_i|\,\|\bar{\mathcal{H}}^{(i)}\| \le \varepsilon L^{-2}. \tag{213}$$

Equivalently, the total higher-curvature contribution is bounded by an ε-fraction of a fixed leading curvature scale of order L^{-2}. This is a scale-separation condition, not a pointwise identity. If $G + \Lambda_L g = 0$ exactly, no ratio with that tensor is defined; an exact solution then requires $\sum_i \bar{\alpha}_i \bar{\mathcal{H}}^{(i)} = 0$, or a constant part of this correction must be absorbed into the definition of Λ_L. The continuation, the torsionless coframe branch, and the estimate (211) define the domain and accuracy of the recovery statement. They are not claims of global regularity and need not hold for every solution of the unreduced equations. In particular, the fixed-background connection calculation in Appendix A does not replace this metric/coframe variation; conversely, proving the local variational identity does not require a global existence theory for all solutions.

For the displayed quadratic-curvature basis, a sufficient local version of the assumed Euler-tensor bound controls derivatives as well as curvature. Fix a positive reference tensor norm on a compact observation region and suppose

$$\|\mathrm{Rm}\| \le c_0 L^{-2}, \qquad \|\nabla \mathrm{Rm}\| \le c_1 L^{-3}, \qquad \|\nabla^2 \mathrm{Rm}\| \le c_2 L^{-4}. \tag{214}$$

Products of two curvatures and second derivatives of curvature are then bounded by constants times L^{-4}. These are the terms appearing in the quadratic-curvature Euler tensors, so the constants C_i above can be chosen from c_0, c_1, c_2 and the fixed contraction norms. An indefinite Lorentzian contraction is not used as a positive error norm. Small $\|\mathrm{Rm}\|$ alone does not control a rapidly varying $\nabla^2\mathrm{Rm}$; higher-derivative operators require corresponding additional derivative estimates.

The conclusion of (213) is an equation residual bound on the matched branch. A bound on the distance between an effective solution and an Einstein solution additionally requires common admissible initial or boundary data, a stability estimate in a declared norm, constraint propagation, and exclusion or treatment of additional higher-derivative modes. No such solution-distance bound follows from the residual estimate alone.

5.3. *A positive Cartan-curvature realization.* A concrete gravitational choice removes the need to leave the Einstein coefficient as an unspecified algebraic insertion. Take the compact Cartan pair $(SO(5), SO(4))$, fix $\ell > 0$ and $g_{\mathrm{c}} > 0$, and use the defining real matrix representation. On an oriented orthonormal frame bundle the local connection matrix is

$$\mathbb{A}_{\mathrm{c}} = \begin{pmatrix} \omega^a{}_b & \ell^{-1}e^a \\ -\ell^{-1}e_b & 0 \end{pmatrix}, \qquad a, b \in \{1, 2, 3, 4\}. \tag{215}$$

The matrix is skew symmetric, so its values belong to $\mathfrak{so}(5)$. The inclusion of $\mathfrak{so}(4)$ is the upper-left block, and the four off-diagonal components are the soldering form. The ordinary transformation laws for ω and e prove $SO(4)$-equivariance and reproduction of vertical generators. Non-degeneracy of the soldering form makes the map from the four horizontal directions an isomorphism onto $\mathfrak{so}(5)/\mathfrak{so}(4)$. Together with the six vertical directions this verifies the Cartan isomorphism axiom. The matrix commutator supplies all brackets and their Jacobi identities. This construction uses the frame bundle and requires no global trivialization of its coframe.

Matrix multiplication of forms gives

$$\mathbb{F}_{\mathrm{c}} = \begin{pmatrix} R^a{}_b - \ell^{-2}e^a \wedge e_b & \ell^{-1}T^a \\ -\ell^{-1}T_b & 0 \end{pmatrix}, \qquad T^a = \mathrm{d}e^a + \omega^a{}_b \wedge e^b. \tag{216}$$

Let $\star_e$ be the spacetime Hodge operator of $g_e = \delta_{ab}e^a \otimes e^b$. With $I, J \in \{1, \ldots, 5\}$, define a single curvature norm

$$S_{\mathrm{c}}[e, \omega] = \frac{1}{2g_{\mathrm{c}}^2} \int_M \sum_{I<J} F_{\mathrm{c}}^{IJ} \wedge \star_e F_{\mathrm{c}}^{IJ}. \tag{217}$$

The Lie-algebra pairing is the positive multiple of the negative trace form in the defining representation. Its norm, and hence the integrand in (217),

is nonnegative on the Euclidean slice. The Hodge operator is part of the coframe-dependent data and must vary when the coframe varies. The gauge transformations used here are those of the declared Cartan isotropy group $SO(4)$.

THEOREM 10 (Exact coefficients of a Cartan norm). *Write* $R^{ab} = \frac{1}{2}R^{ab}{}_{cd}e^c \wedge e^d$, *set* $R(\omega) = R^{ab}{}_{ab}$, *and define* $\tau^2 = \sum_a |T^a|^2_{g_e}$. *Then*

$$S_{\mathrm{c}} = \frac{1}{2g_{\mathrm{c}}^2}\int_M \left[\frac{1}{4}R^{ab}{}_{cd}R^{ab}{}_{cd} - \frac{R(\omega)}{\ell^2} + \frac{6}{\ell^4} + \frac{\tau^2}{\ell^2}\right]\mathrm{vol}_{g_e}\,. \tag{218}$$

On the torsionless restriction $\omega = \omega(e)$, *its coefficients in* (188) *are*

$$G_{\mathrm{eff}} = \frac{g_{\mathrm{c}}^2\ell^2}{8\pi}, \Lambda_{\mathrm{eff}} = \frac{3}{g_{\mathrm{c}}^2\ell^4}, \qquad \alpha_1 = \alpha_2 = 0, \alpha_3 = \frac{1}{8g_{\mathrm{c}}^2}, \tag{219}$$

in the unreduced curvature-invariant basis used there. The associated Euclidean curvature cosmological constant obeys

$$\Lambda_E = \frac{3}{\ell^2}, \qquad 64\pi G_{\mathrm{eff}}\Lambda_E\alpha_3 = 3. \tag{220}$$

Proof. The two-forms $e^a \wedge e^b$, $a < b$, form an orthonormal basis. There are six such forms. Antisymmetry in each curvature index pair gives

$$\begin{gathered}\sum_{a<b}|R^{ab}|^2 = \frac{1}{4}\sum_{a,b,c,d}(R^{ab}{}_{cd})^2, \quad \sum_{a<b}\langle R^{ab}, e^a\wedge e^b\rangle = \sum_{a<b}R^{ab}{}_{ab} = \frac{1}{2}R(\omega),\\ \sum_{a<b}|e^a\wedge e^b|^2 = 6.\end{gathered} \tag{221}$$

Expand each square $|R^{ab} - \ell^{-2}e^a\wedge e^b|^2$. Its cross term is $-2\ell^{-2}\langle R^{ab}, e^a\wedge e^b\rangle$, whose sum is $-\ell^{-2}R(\omega)$. The $(a,5)$ components add $\ell^{-2}\tau^2$. These four contributions prove (218). Under the torsionless restriction the curvature is Riemannian, and comparison of the coefficient of $-R$ gives $1/(16\pi G_{\mathrm{eff}}) = 1/(2g_{\mathrm{c}}^2\ell^2)$. The constant and curvature-square coefficients give the other entries of (219). Substitution into $\Lambda_E = 8\pi G_{\mathrm{eff}}\Lambda_{\mathrm{eff}}$ and then into $64\pi G_{\mathrm{eff}}\Lambda_E\alpha_3$ proves (220). □

The round four-sphere of radius ℓ gives an exact Euclidean configuration with $T^a = 0$ and $R^{ab} = \ell^{-2}e^a\wedge e^b$. Thus $\mathbb{F}_{\mathrm{c}} = 0$ and $S_{\mathrm{c}} = 0$. Every first variation vanishes: both the variation of the curvature and that of the Hodge operator occur multiplied by at least one curvature factor. This configuration is a minimum of the positive action and has $R_{\mu\nu} = 3\ell^{-2}g_{\mu\nu}$. It supplies an explicit Einstein vacuum of the Euclidean example.

For general configurations, imposing $\omega = \omega(e)$ before variation defines a restricted metric theory. It is not equivalent without further analysis to varying the independent connection in (217): the curvature-square and torsion-square

terms contribute to that connection equation. The existence of the round vacuum proves neither uniqueness of the selected phase nor suppression of all torsional fluctuations.

The coefficient relation also exposes a scale restriction. In the metric equation, $16\pi G_{\mathrm{eff}}\alpha_3 = \ell^2/4$. For fields with curvature and derivatives characterized by a length L, the curvature-square correction has the relative derivative-expansion scale ℓ^2/L^2. The round vacuum itself has curvature scale ℓ^{-2}; its stationarity does not imply a small higher-derivative correction for arbitrary perturbations. An independently justified vacuum-energy mechanism would be needed to separate these two scales. Additional matter thresholds or independent finite counterterms can also change (220). In four dimensions the Euler density allows a change of curvature-invariant basis, so the relation is stated in the specified basis and is not by itself an invariant scattering prediction.

This gravitational example belongs to the established Cartan and gauge-geometric setting [145] and [116]. Its algebra, pairing, and coefficients are explicit inputs and consequences. The next construction places this Cartan block and the three Standard Model gauge factors in one specified master system and makes the remaining selection assumptions explicit.

5.4. *A joint microscopic candidate with one order parameter.* The phrase "one microscopic model" has a precise dimension constraint in Cartan geometry. Let

$$\begin{gathered} G_{\mathrm{SM}} := SU(3)_c \times SU(2)_L \times U(1)_Y, \quad \widetilde{G}_0 := SO(5) \times G_{\mathrm{SM}}, \\ H_0 := SO(4) \times G_{\mathrm{SM}}. \end{gathered} \tag{222}$$

Then

$$\begin{gathered} \dim \widetilde{G}_0 = 10 + 8 + 3 + 1 = 22, \quad \dim H_0 = 6 + 8 + 3 + 1 = 18, \\ \dim(\widetilde{G}_0/H_0) = 4. \end{gathered} \tag{223}$$

The quotient dimension is therefore the dimension of the spacetime manifold. This condition rules out simply choosing a larger group whose quotient has many extra directions and then silently identifying all of them with a four-dimensional coframe.

Let Γ_0 denote the full master-data package (55) obtained by supplementing $(\widetilde{G}_0, H_0)$ with the specified principal bundle, representations, invariant pairing, order-parameter map, reference measure, regularization, mobility, and information data. It is an explicit candidate witness for the coupled construction, not a selected minimizer of the selection problem in Section 6.1. Accordingly, $\widehat{\mathbb{M}}_{\Gamma_0}$ below denotes the tangent mobility induced by that entire package, including its gauge fixing or quotient prescription.

The group G_{SM}, the hypercharge normalization, and the one-generation representation displayed below are prescribed inputs in this candidate. They

are included to exhibit one common, well-typed realization and are not outputs of the minimization problem in Section 6.1. Moreover, the Lie algebra is a direct product: the candidate is coupled through the shared scalar and mobility data, but it is not a proof of an algebraically indecomposable master algebra. The no-factorization test in Definition 2 remains an additional requirement.

On a principal H_0-bundle, use the single Cartan-type master field

$$\mathbb{A}_0 = \left(\begin{pmatrix} \omega^a{}_b & \ell^{-1} e^a \\ -\ell^{-1} e_b & 0 \end{pmatrix},\ A \right), \qquad A = A^A T_A \in \Omega^1(M, \mathfrak{g}_{\mathrm{SM}}). \tag{224}$$

The first entry is an $\mathfrak{so}(5)$-valued Cartan connection of type $SO(5)/SO(4)$; its displayed matrix is the descended vector-representation expression. The Spin(4) lift is included so that spinor matter can be defined globally; if no spin lift exists, only the bosonic Cartan block is available. The second entry is the internal connection. Its curvature is the single ordered tuple

$$\mathbb{F}_0 = \left(R^{ab} - \ell^{-2} e^a \wedge e^b,\ \ell^{-1} T^a,\ F^A \right), \qquad F^A = \mathrm{d}A^A + \frac{1}{2} f_{BC}{}^A A^B \wedge A^C. \tag{225}$$

All three entries are components of one connection; they are not three independently postulated actions.

To make the coupling between the two geometric blocks explicit, introduce a dimensionless scalar coordinate σ, use

$$w(\sigma) := \exp(-\alpha_\sigma \sigma) > 0, \qquad \alpha_\sigma \in \mathbb{R}, \tag{226}$$

and let Φ_H be a scalar in the representation $(\mathbf{1}, \mathbf{2})_{1/2}$ of G_{SM}. The scalar σ is a shared master coordinate: the same function $w(\sigma)$ multiplies the Cartan and internal curvature blocks. With $\mathbf{F}_{\mathrm{joint}}$ denoting the tuple consisting of $\mathbb{F}_0, D\Phi_H, \mathrm{d}\sigma, \mathfrak{U}_H, D\Psi$, define the one-norm action by

$$\mathcal{S}_{\mathrm{joint}} := \frac{1}{2} \int_M \langle \mathbf{F}_{\mathrm{joint}}, \mathbf{h}_{\mathrm{joint}}(\sigma) \mathbf{F}_{\mathrm{joint}} \rangle \, \mathrm{vol}_{g_e} . \tag{227}$$

The prefactor $1/2$ is fixed by the master normalization. Let T embed the displayed joint tuple into the extended master tuple, including the reference-scale factors in (51). With T^* denoting the adjoint for the background fiber pairings, set

$$\mathbf{h}_{\mathrm{joint}} = \tfrac{1}{2} T^* \mathbf{h} T. \tag{228}$$

Thus $\frac{1}{2}\langle U, \mathbf{h}_{\mathrm{joint}} U \rangle = \frac{1}{4}\langle TU, \mathbf{h} TU \rangle$. When the component scales coincide, this is one half of the restricted master pairing. Equation (227) is therefore the corresponding restriction of (52). The final matter term below is shorthand for the regularized fermionic block contraction contained in the same extended pairing; it is not an additional primitive action. The following displayed form

fixes the relevant blocks and their normalization:

$$\begin{aligned}\mathcal{S}_{\text{joint}} = \frac{1}{2g_{\text{c}}^2}\int_M w(\sigma)\left[\sum_{a<b} F_{\text{c}}^{ab}\wedge\star_e F_{\text{c}}^{ab} + \sum_a F_{\text{c}}^{a5}\wedge\star_e F_{\text{c}}^{a5}\right] \\ + \frac{1}{2}\int_M w(\sigma)\,\kappa_{AB}F^A\wedge\star_e F^B + \frac{1}{2}\int_M \big[|D\Phi_H|^2 + f_\sigma^2|\mathrm{d}\sigma|^2 \\ +|\mathfrak{U}_H(\Phi_H,\sigma)|^2\big]\,\mathrm{vol}_{g_e} \\ + \mathcal{S}_{\text{matter}}[\Psi;\mathbb{A}_0,\Phi_H,\sigma,\mu_{\text{info}}].\end{aligned} \tag{229}$$

Here $F_{\text{c}}^{ab} = R^{ab} - \ell^{-2}e^a\wedge e^b$ and $F_{\text{c}}^{a5} = \ell^{-1}T^a$. The last line is included as a component of the extended norm after the fermionic regularization; it is not an independently added fourth action. The internal bilinear form κ_{AB} is positive on the Euclidean residual sector. The explicit choice

$$\mathfrak{U}_H(\Phi_H,\sigma) = \sqrt{\lambda_H}\left(\Phi_H^\dagger\Phi_H - \frac{v_H^2}{2}\right) \tag{230}$$

with $\lambda_H > 0$ produces a quartic component $\frac{1}{2}|\mathfrak{U}_H|^2$ bounded below. Here $f_\sigma > 0$ is a reference mass scale for the dimensionless coordinate σ; setting $f_\sigma = 1$ is allowed only after declaring a fully nondimensionalized convention. The parameters λ_H, v_H are selected microscopic data at this stage.

The same σ prevents a decomposition into two independent functionals. For example, differentiation of (229) gives

$$\frac{\partial}{\partial\sigma}\frac{\delta^2\mathcal{S}_{\text{joint}}}{\delta F_{\text{c}}\,\delta F_{\text{c}}} = -\alpha_\sigma w(\sigma)\,\frac{1}{g_{\text{c}}^2}, \qquad \frac{\partial}{\partial\sigma}\frac{\delta^2\mathcal{S}_{\text{joint}}}{\delta F^A\,\delta F^B} = -\alpha_\sigma w(\sigma)\,\kappa_{AB}. \tag{231}$$

The displayed factors use the standard form-Hessian normalization in (229); fixed form-index contractions are understood. These derivatives would vanish for a sum of a gravitational functional, an internal functional, and a separate scalar functional. A field-dependent rescaling that removes w from one block transfers the coupling to the derivative terms, so it does not produce two independent stochastic systems. The candidate is therefore one coupled master system whenever $\alpha_\sigma \neq 0$ and the shared coordinate is retained. A full proof of irreducibility in a continuum realization still requires the no-factorization test in Definition 2 after gauge fixing and regularization.

The stochastic law uses one mobility on the complete coordinate vector. In the finite-dimensional affine realization of the candidate, let $\mathbb{B}_{\Gamma_0}$ be the complete reversible Itô drift obtained from (61) by replacing the master action, the contravariant mobility, and the reference density with those of Γ_0. With the field-space noise frame of (60), the law is

$$\mathrm{d}\mathbb{X}_t = \mathbb{B}_{\Gamma_0}(\mathbb{X}_t)\,\mathrm{d}t + \sqrt{2\theta}\,\widehat{\mathbb{M}}^{1/2}_{\Gamma_0,\mathbb{G}}(\mathbb{X}_t)\mathcal{E}_{\mathbb{X}_t}\,\mathrm{d}W_t. \tag{232}$$

In these coordinates, if the reference measure is $m_{\nu,\Gamma_0}(x)\,\mathrm{d}x$, then

$$\mathbb{B}^i_{\Gamma_0} = -M^{ij}_{\Gamma_0}\partial_j \mathcal{S}_{\mathrm{joint}} + \theta m^{-1}_{\nu,\Gamma_0}\partial_j\left(m_{\nu,\Gamma_0} M^{ij}_{\Gamma_0}\right). \tag{233}$$

The second term vanishes for constant mobility and a flat reference density; otherwise it is part of the drift that enters the path cost and the equilibrium equation. The composite noise coefficient has coordinate covariance $2\theta M_{\Gamma_0}$; its Hilbert-space realization requires the admissibility conditions stated for (62). The covariance is allowed to contain gravitational, internal, and scalar blocks. It must be symmetric and nonnegative; in a two-block regulator the condition is the Schur complement inequality, provided that $\mathbb{M}_c$ is strictly positive on the retained gravitational range:

$$\mathbb{M}_K - C^*\mathbb{M}_c^{-1}C \succeq 0. \tag{234}$$

If $\mathbb{M}_c$ is only nonnegative, the ordinary inverse in this display is replaced by the Moore–Penrose inverse and the corresponding range condition is imposed. Thus the action, the mobility, the Wiener process, and the path cost belong to the same specified model.

For completeness, the left-handed matter content of one anomaly-free generation may be chosen as

$$\begin{gathered} Q_L = (\mathbf{3},\mathbf{2})_{1/6}, u^c = (\overline{\mathbf{3}},\mathbf{1})_{-2/3}, \quad d^c = (\overline{\mathbf{3}},\mathbf{1})_{1/3}, L_L = (\mathbf{1},\mathbf{2})_{-1/2}, \\ e^c = (\mathbf{1},\mathbf{1})_1. \end{gathered} \tag{235}$$

with an optional neutral $\nu^c = (\mathbf{1},\mathbf{1})_0$. The anomaly calculations use the left-handed convention. With $T(\mathbf{3}) = T(\mathbf{2}) = 1/2$,

$$\begin{aligned} \mathcal{A}_{SU(3)^3} &= 2 - 1 - 1 = 0, \\ \mathcal{A}_{SU(3)^2U(1)} &= 2\left(\frac{1}{6}\right)\frac{1}{2} - \frac{2}{3}\frac{1}{2} + \frac{1}{3}\frac{1}{2} = 0, \\ \mathcal{A}_{SU(2)^2U(1)} &= 3\left(\frac{1}{6}\right)\frac{1}{2} - \frac{1}{2}\frac{1}{2} = 0, \\ \mathcal{A}_{\mathrm{grav}^2U(1)} &= 6\left(\frac{1}{6}\right) + 3\left(-\frac{2}{3}\right) + 3\left(\frac{1}{3}\right) + 2\left(-\frac{1}{2}\right) + 1 = 0, \\ \mathcal{A}_{U(1)^3} &= 6\left(\frac{1}{6}\right)^3 + 3\left(-\frac{2}{3}\right)^3 + 3\left(\frac{1}{3}\right)^3 + 2\left(-\frac{1}{2}\right)^3 + 1 = 0. \end{aligned} \tag{236}$$

There are four $SU(2)$ doublets after color multiplicity is counted, so the global Witten anomaly is absent. This verifies consistency of the displayed residual representation; it does not derive the representation from the master algebra.

Suppose a homogeneous value σ_* is selected by a specified stabilization or boundary condition, and write $w_* = w(\sigma_*)$. On this constant-scalar, torsionless branch, the explicit Cartan expansion and the internal kinetic term give, at

tree level,

$$\frac{1}{16\pi G_{\mathrm{eff}}} = \frac{w_*}{2g_{\mathrm{c}}^2\ell^2}, \qquad g_a^{-2} = w_*\kappa_a, \qquad \alpha_3 = \frac{w_*}{8g_{\mathrm{c}}^2}. \tag{237}$$

These equalities identify coefficients in a restricted homogeneous background; they are not the field equations for an arbitrary varying σ. In particular, when $\mathrm{d}\sigma \neq 0$, (200) supplies a nonzero connection response and the coframe equation contains scalar-derivative terms. Consequently,

$$G_{\mathrm{eff}} g_a^{-2} = \frac{g_{\mathrm{c}}^2\ell^2\kappa_a}{8\pi}, \qquad 64\pi G_{\mathrm{eff}}\Lambda_E\alpha_3 = 3, \qquad \Lambda_E = \frac{3}{\ell^2}. \tag{238}$$

The first relation is independent of the shared order-parameter value σ_* at tree level. It becomes a physical prediction only if $g_{\mathrm{c}}, \ell, \kappa_a$ are fixed by the same selection problem and if loop, threshold, and basis corrections are computed. Writing the one-loop and threshold terms as Δ_a and Δ_G, the measured quantities obey instead

$$g_a^{-2} = w_*\kappa_a + \Delta_a, \qquad G_{\mathrm{eff}}^{-1} = \frac{8\pi w_*}{g_{\mathrm{c}}^2\ell^2} + \Delta_G. \tag{239}$$

These correction terms are part of the calculation required for a numerical prediction.

Section 14.39 completes a concrete orbital recovery test on the specified torsionless, scalar-decoupled stationary sector. It retains the curvature-square coefficient inherited from the Cartan norm, verifies its exact cancellation on the constructed Einstein exterior, and derives the test-body orbit from the same matter metric. The zero-vacuum-energy matching gives the standard periapsis advance; the unmodified Cartan constant gives an additional cosmological term. Thus the matching assumptions remain visible in the observable itself.

The internal group and representation in (222) and (235) are explicit inputs of this candidate witness. To claim that they are predicted, the minimization over a candidate class must select this Γ_0 uniquely up to gauge and field redefinitions. The candidate therefore proves existence of a single well-typed coupled realization; it does not by itself prove uniqueness, ultraviolet completeness, or a parameter-free Standard Model.

5.4.1. *The scalar equation and confinement of its constant mode.* The common positive weight couples the curvature blocks, but positivity alone does not confine the shared scalar. This point is relevant both to the classical vacuum and to the equilibrium construction. Work first on a smooth connected closed Riemannian four-manifold, keep the coframe fixed while varying σ, and consider the bosonic action with the auxiliary map (230). Define the nonnegative curvature density

$$\mathcal{K}(e,\omega,A) := \frac{1}{2g_{\mathrm{c}}^2}\sum_{I<J}|F_{\mathrm{c}}^{IJ}|_{g_e}^2 + \frac{1}{2}\kappa_{AB}\langle F^A, F^B\rangle_{g_e}. \tag{240}$$

Thus the part depending on σ is $\int_M [w(\sigma)\mathcal{K} + \frac{1}{2} f_\sigma^2 |\mathrm{d}\sigma|^2] \,\mathrm{vol}_{g_e}$. For a real test function η, the two variations are

$$\begin{aligned} \delta_\eta \int_M w(\sigma)\mathcal{K} \,\mathrm{vol}_{g_e} &= -\alpha_\sigma \int_M \eta w(\sigma)\mathcal{K} \,\mathrm{vol}_{g_e}, \\ \delta_\eta \int_M \tfrac{1}{2} f_\sigma^2 |\mathrm{d}\sigma|^2 \,\mathrm{vol}_{g_e} &= -f_\sigma^2 \int_M \eta \Delta_g \sigma \,\mathrm{vol}_{g_e}. \end{aligned} \tag{241}$$

There is no derivative of (230) with respect to σ. Therefore the scalar Euler equation is

$$-f_\sigma^2 \Delta_g \sigma - \alpha_\sigma w(\sigma)\mathcal{K} = 0. \tag{242}$$

Integration over M removes the Laplacian. If $\alpha_\sigma \neq 0$, it gives $\int_M w(\sigma)\mathcal{K} \,\mathrm{vol}_{g_e} = 0$. Since $w > 0$ and $\mathcal{K} \geq 0$, smoothness implies $\mathcal{K} = 0$ everywhere. Positive definiteness of the curvature pairings then gives $F_{\mathrm{c}} = 0$ and $F = 0$. Equation (242) reduces to $\Delta_g \sigma = 0$; multiplication by σ and integration by parts give $\int_M |\mathrm{d}\sigma|^2 \,\mathrm{vol}_{g_e} = 0$, so σ is constant. A nonzero scalar-dependent matter source, a boundary flux, or an additional scalar potential changes this argument and must appear explicitly in the scalar equation. A prescribed constant σ_* is consequently not an arbitrary solution with nonzero master-curvature density $\mathcal{K}$ in the unstabilized closed bosonic model. This does not force the Riemann curvature of the coframe metric to vanish: $F_{\mathrm{c}} = 0$ permits $R^{ab} = \ell^{-2} e^a \wedge e^b$, as on the round-sphere branch.

The same omission obstructs the simplest Gibbs construction. In a regulator that retains the constant scalar mode, write $\sigma = s + \sigma_\perp$, with $\int_M \sigma_\perp \,\mathrm{vol}_{g_e} = 0$. At fixed values of the other regulated coordinates,

$$\mathcal{S}_{\mathrm{joint}}(s) = e^{-\alpha_\sigma s} C + \mathcal{S}_0, \qquad C := \int_M e^{-\alpha_\sigma \sigma_\perp} \mathcal{K} \,\mathrm{vol}_{g_e} \geq 0, \tag{243}$$

where $\mathcal{S}_0$ is independent of s in this bosonic calculation. For $\alpha_\sigma \neq 0$, along $\alpha_\sigma s \to +\infty$, the Gibbs integrand tends to $\exp(-\mathcal{S}_0/\theta) > 0$. Hence its integral over the Lebesgue variable s diverges. For $\alpha_\sigma = 0$ it is independent of s and diverges as well. With a product reference measure, Tonelli's theorem extends this divergence to the full regulated partition function whenever the remaining finite-action coordinates have positive measure. This conclusion is specific to the stated unconfined reference measure; a prescribed confining reference density is additional model data.

An explicit bosonic modification within the same extended-norm construction is to enlarge its algebraic auxiliary fiber and replace the displayed map by

$$\mathfrak{U}_H^{\mathrm{stab}}(\Phi_H, \sigma) := \begin{pmatrix} \sqrt{\lambda_H}(\Phi_H^\dagger \Phi_H - v_H^2/2) \\ m_\sigma f_\sigma (\sigma - \sigma_0) \end{pmatrix}, \qquad m_\sigma > 0. \tag{244}$$

Both entries have mass dimension two; m_σ and f_σ have mass dimension one, and σ_0 is dimensionless. This declares new microscopic data rather than inferring

a potential from the weight w. The same single squared norm now contains $\frac{1}{2}m_\sigma^2 f_\sigma^2(\sigma-\sigma_0)^2$, and the scalar equation becomes

$$-f_\sigma^2\Delta_g\sigma - \alpha_\sigma w(\sigma)\mathcal{K} + m_\sigma^2 f_\sigma^2(\sigma-\sigma_0) = 0. \tag{245}$$

This additional force can balance the curvature source. It does not prove existence of a solution of the coupled coframe and connection equations.

THEOREM 11 (Fixed-background stabilized scalar). *Let (M,g) be a smooth connected closed Riemannian manifold, let $\mathcal{K}\in C^\infty(M)$ be nonnegative, and let $f_\sigma, m_\sigma > 0$, $\alpha_\sigma, \sigma_0 \in \mathbb{R}$ be fixed. With $\Delta_g = \operatorname{div}_g \operatorname{grad}_g$, equation (245) has exactly one smooth solution. It is the unique finite-energy minimizer of the fixed-background scalar action*

$$J_\sigma[\sigma] = \int_M \left[\frac{f_\sigma^2}{2}|\nabla\sigma|^2 + \frac{m_\sigma^2 f_\sigma^2}{2}(\sigma-\sigma_0)^2 + \mathcal{K}e^{-\alpha_\sigma\sigma}\right]\operatorname{vol}_g. \tag{246}$$

For $\alpha_\sigma = 0$ the solution is $\sigma = \sigma_0$. For $\alpha_\sigma \neq 0$, put

$$u = \alpha_\sigma(\sigma-\sigma_0), \qquad a = \frac{\alpha_\sigma^2 e^{-\alpha_\sigma\sigma_0}}{f_\sigma^2}\mathcal{K}, \qquad (-\Delta_g + m_\sigma^2)u = ae^{-u}. \tag{247}$$

Then

$$0 \le u \le b, \qquad be^b = \frac{\|a\|_\infty}{m_\sigma^2}, \quad b \ge 0. \tag{248}$$

Equivalently $b = W_0(\|a\|_\infty/m_\sigma^2)$, where W_0 is the nonnegative inverse of $z\mapsto ze^z$. If $\mathcal{K}\not\equiv 0$, then $u > 0$. For $\alpha_\sigma \neq 0$, the solution is constant if and only if $\mathcal{K}$ is constant.

Proof. The case $\alpha_\sigma = 0$ follows by testing $(-\Delta_g + m_\sigma^2)(\sigma-\sigma_0) = 0$ with $\sigma-\sigma_0$. Suppose $\alpha_\sigma \neq 0$. The substitution in (247) gives the stated equation. Define on $H^1(M)$ the extended nonnegative functional

$$E[u] = \int_M \left[\frac{1}{2}|\nabla u|^2 + \frac{m_\sigma^2}{2}u^2 + ae^{-u}\right]\operatorname{vol}_g. \tag{249}$$

It is finite at zero and coercive in $H^1(M)$. For $\phi_x(t) = m_\sigma^2 t^2/2 + a(x)e^{-t}$, one has $\phi_x'(t) < 0$ for $t < 0$, while for $t > b$,

$$\phi_x'(t) = m_\sigma^2 t - a(x)e^{-t} \ge m_\sigma^2 b - \|a\|_\infty e^{-b} = 0. \tag{250}$$

The truncation $T(t) = \min\{b, \max\{0,t\}\}$ therefore decreases the potential pointwise and, being 1-Lipschitz, does not increase the gradient energy. Replace a minimizing sequence by its truncations. Weak compactness in H^1, compactness in L^2, and passage to an almost-everywhere convergent subsequence give a limit u with $0 \le u \le b$. Weak lower semicontinuity of the quadratic energy and Fatou's lemma for the exponential term show that u minimizes E. Since truncation decreases E on its entire domain, this is an unrestricted minimizer.

For every smooth test function η, boundedness of u and η justifies differentiating $E[u+t\eta]$ under the integral. Its first variation is

$$\int_M \left[\langle \nabla u, \nabla \eta\rangle + m_\sigma^2 u\eta - a e^{-u}\eta\right] \mathrm{vol}_g = 0. \tag{251}$$

The right-hand side of the weak equation is bounded. Elliptic regularity first gives $u \in W^{2,p}(M)$ for every finite p, and then smoothness by Sobolev embedding and bootstrapping. If u, v are two smooth solutions, subtract their equations and test with $u - v$ to obtain

$$\int_M \left[|\nabla(u-v)|^2 + m_\sigma^2 (u-v)^2\right] \mathrm{vol}_g = \int_M a(e^{-u} - e^{-v})(u-v)\,\mathrm{vol}_g \le 0. \tag{252}$$

Thus $u = v$. Strict convexity gives uniqueness of the energy minimizer, and $J_\sigma = (f_\sigma^2/\alpha_\sigma^2)E$ under the substitution. The strong maximum principle gives $u > 0$ if $a \not\equiv 0$. Finally a constant u satisfies $a(x) = m_\sigma^2 u e^u$, so a must be constant. Conversely, constant a has the unique constant solution $u = W_0(a/m_\sigma^2)$. □

The fixed-background second variation at this solution is

$$\begin{aligned}\delta^2 J_\sigma[\eta,\eta] &= \int_M \left[f_\sigma^2 |\nabla\eta|^2 + \left(m_\sigma^2 f_\sigma^2 + \alpha_\sigma^2 \mathcal{K} e^{-\alpha_\sigma \sigma_*}\right)\eta^2\right] \mathrm{vol}_g \\ &\ge m_\sigma^2 f_\sigma^2 \|\eta\|^2_{L^2(g)}.\end{aligned} \tag{253}$$

Hence the canonically normalized scalar block has operator

$$H_\sigma = -\Delta_g + m_\sigma^2 + \frac{\alpha_\sigma^2 \mathcal{K} e^{-\alpha_\sigma\sigma_*}}{f_\sigma^2} \succeq m_\sigma^2 I. \tag{254}$$

For constant $\mathcal{K}$ and $\alpha_\sigma \neq 0$, the squared scalar mass in this block is $m_\sigma^2(1+u_*)$. For variable $\mathcal{K}$, the solution and the added multiplication potential are generally spatially variable; a prescribed constant σ_* is then not the exact scalar solution. These conclusions concern the scalar at fixed coframe and connection. They do not establish a solution of the coupled field equations or a lower bound for the full Hessian after mixing with the other fields.

For the constant mode, nonnegativity of the other bosonic norm components gives a direct integrability estimate. Let $V_g := \int_M \mathrm{vol}_{g_e} > 0$. The zero-mean property of $\sigma_\perp$ removes the mixed term in the potential, and consequently

$$\begin{aligned}\mathcal{S}^{\mathrm{stab}}_{\mathrm{joint}} &\ge \frac{m_\sigma^2 f_\sigma^2}{2}\left[V_g(s-\sigma_0)^2 + \|\sigma_\perp\|^2_{L^2(g_e)}\right], \\ \int_{\mathbb{R}} e^{-\mathcal{S}^{\mathrm{stab}}_{\mathrm{joint}}/\theta}\,\mathrm{d}s &\le \left(\frac{2\pi\theta}{m_\sigma^2 f_\sigma^2 V_g}\right)^{1/2} \exp\left[-\frac{m_\sigma^2 f_\sigma^2}{2\theta}\|\sigma_\perp\|^2_{L^2(g_e)}\right].\end{aligned} \tag{255}$$

Thus the modification removes this particular scalar zero-mode divergence at fixed geometry. Controlling the gauge quotient, degenerate coframes, the remaining field coordinates, a fermion determinant, and the continuum limit

still requires separate estimates. In particular, (255) is not a construction of a four-dimensional interacting field measure. The tree-level curvature identities (237) are unchanged at a prescribed constant scalar value. If that value differs from σ_0, the new potential contributes to the vacuum energy; the cosmological relation (238) then refers only to the Cartan curvature contribution and must be corrected for this added energy.

5.5. *Inertia, gravitation, and the absence of ordinary material shielding.* The controlled recovery theorem identifies the low-energy gravitational field equation under its stated matching hypotheses. We now distinguish its physical interpretation from the stronger, still conditional claim that a microscopic equilibrium principle has derived the origin of the selected geometry. Let $e^a_{*\mu}$ be a non-degenerate Lorentzian coframe on the selected low-energy branch, and define

$$g^*_{\mu\nu} := \eta_{ab} e^a_{*\mu} e^b_{*\nu}. \tag{256}$$

The asterisk records the branch under discussion. Equation (256) is a coframe representation of its metric; by itself it does not prove that a global equilibrium problem has selected e_* from all admissible coframes.

5.5.1. *Universal coupling and free motion.* Assume that ordinary low-energy matter fields ψ^A have the covariant action

$$S_{\mathrm{m}}[g^*, \psi] = \int_M \mathcal{L}_{\mathrm{m}}\big(g^*, \psi, \nabla^{(g^*)}\psi\big)\, \sqrt{-g^*}\, \mathrm{d}^4x, \tag{257}$$

with no fixed, non-covariant background that exchanges energy–momentum with the matter sector. Equivalently, one may use $S_{\mathrm{m}}[e_*, \omega_*, \psi]$ on the torsionless branch, on which ω_* is the Levi–Civita spin connection of e_*. Fix the stress-tensor convention by

$$\delta S_{\mathrm{m}} = \frac{1}{2}\int_M \sqrt{-g^*}\, T^{\mu\nu}\, \delta g^*_{\mu\nu}\, \mathrm{d}^4x + \int_M E_A\, \delta\psi^A\, \mathrm{d}^4x. \tag{258}$$

For a compactly supported infinitesimal diffeomorphism generated by ζ^μ, covariance gives $\delta_\zeta g^*_{\mu\nu} = 2\nabla^{(g^*)}_{(\mu}\zeta_{\nu)}$ and $\delta_\zeta \psi^A = \mathcal{L}_\zeta \psi^A$. Thus, when the matter equations $E_A = 0$ hold, integration by parts in (258) gives

$$\nabla^{(g^*)}_\mu T^{\mu\nu} = 0. \tag{259}$$

The qualification concerning fixed backgrounds is necessary: a non-dynamical datum that is neither varied on shell nor transformed as a diffeomorphism-covariant spurion contributes an exchange term to (259). This is precisely the Noether-balance condition appearing in Theorem 9.

For pressureless, spinless matter, set

$$T^{\mu\nu} = \rho u^\mu u^\nu, \qquad J^\mu = \rho u^\mu, \qquad \nabla^{(g^*)}_\mu J^\mu = 0, \tag{260}$$

where $u^\mu u_\mu = -1$ and $\rho > 0$ on the support of the dust. Equations (259) and (260) yield

$$0 = \nabla_\mu^{(g^*)}(\rho u^\mu u^\nu) = u^\nu \nabla_\mu^{(g^*)}(\rho u^\mu) + \rho u^\mu \nabla_\mu^{(g^*)} u^\nu = \rho u^\mu \nabla_\mu^{(g^*)} u^\nu. \tag{261}$$

Hence a freely falling dust element obeys

$$u^\mu \nabla_\mu^{(g^*)} u^\nu = 0. \tag{262}$$

This is the standard test-body limit of universally coupled matter [63] and [158]. Spinning, extended, pressured, or non-minimally coupled bodies can acquire additional multipole, spin-curvature, pressure, or direct-curvature forces, so (262) is not a trajectory equation for every possible material model.

In this precise low-energy sense, inertia and gravitation are represented by one geometry. Inertia is free propagation relative to the connection of g^*, whereas the invariant tidal content of gravitation is curvature of the same connection. For neighboring geodesics with tangent u^μ and separation ξ^μ,

$$\frac{D^2\xi^\mu}{D\tau^2} = -R^\mu{}_{\alpha\nu\beta}[g^*]\, u^\alpha \xi^\nu u^\beta. \tag{263}$$

Thus vanishing coordinate acceleration in a local inertial frame does not remove the tidal observable in (263). On the controlled low-curvature branch, this curvature is governed by (177), which arises from the coframe component of the master Euler system.

5.5.2. *Spectral mass, inertial propagation, and gravitational response.* The preceding dust argument starts from a stress tensor and therefore does not yet identify the origin of the mass that appears in that tensor. The effective-action formulation supplies the missing interface. Let ϕ denote collectively the physical matter and order-parameter coordinates after gauge fixing, removal of constraints, and passage to the physical quotient. At a selected stationary background (e_*, ϕ_*), write $\eta := \phi - \phi_*$. The renormalized effective action has the local expansion

$$\begin{gathered}\left.\frac{\delta\Gamma_{\mathrm{eff}}}{\delta\phi}\right|_{(e_*,\phi_*)} = 0, \quad \Gamma_{\mathrm{eff}}[e_*, \phi_* + \eta] = \Gamma_* + \frac{1}{2}\langle \eta, \mathcal{K}_*\eta\rangle + O(\|\eta\|^3), \\ \mathcal{K}_* := \left.\frac{\delta^2\Gamma_{\mathrm{eff}}}{\delta\phi\,\delta\phi}\right|^{\mathrm{phys}}_{(e_*,\phi_*)}.\end{gathered} \tag{264}$$

The superscript *phys* is essential. Before the gauge and constraint quotients, $\mathcal{K}_*$ contains gauge zero modes, and its raw eigenvalues are not particle masses. Even after this reduction, $\mathcal{K}_*$ is a spacetime two-point operator: its eigenvalues generally include kinetic momentum and boundary spectra. For a bosonic second-order channel in a local derivative expansion, separate the positive

kinetic form K_*^{kin} from the zero-momentum potential Hessian $\mathcal{V}_*$. Curvature masses are then defined by

$$\mathcal{V}_* v_j = m_{H,j}^2 K_*^{\mathrm{kin}} v_j, \qquad K_*^{\mathrm{kin}} \succ 0, \qquad \mathcal{V}_* := \left.\frac{\partial^2 V_{\mathrm{eff}}}{\partial\phi\,\partial\phi}\right|_{\phi_*}^{\mathrm{phys}}. \tag{265}$$

The positive eigenvalues of this kinetic-normalized potential pencil give the bosonic curvature mass squared, not the eigenvalues of the full spacetime Hessian. Fermionic first-order channels instead use the singular values of the matched Dirac mass map, or the appropriate Majorana diagonalization, before quantum pole corrections. On a translation-invariant Lorentzian branch, a stable physical mass is instead a pole of the gauge-invariant or gauge-reduced two-point function. With the mostly-plus convention used here, put $s := -p_L^2$. For a possibly mixed channel j, define

$$\mathscr{P}_j(s;\mathbf{q}_*,\mu) := \det\left[\Gamma^{(2)}_{j,\mathrm{phys}}(p_L;\mathbf{q}_*,\mu)\right]_{-p_L^2=s}, \qquad \mathscr{P}_j(M^2_{j,\mathrm{pole}};\mathbf{q}_*,\mu) = 0. \tag{266}$$

Here $\mathbf{q}_*$ denotes the selected vacuum coordinates and renormalized couplings. A simple, isolated real zero with positive residue defines a stable one-particle mass. An unstable excitation has a complex pole on the appropriate continued sheet; a confined channel must be defined through a gauge-invariant composite correlator. On a generic curved background there need not be a global momentum p_L, and the corresponding invariant statement uses spectral thresholds or the long-distance decay of covariant two-point functions. These qualifications prevent a stochastic relaxation rate, a gauge-dependent Hessian eigenvalue, or an arbitrary inverse length from being renamed a physical mass.

The connection between the pole in (266) and inertial motion can be seen without postulating a separate inertial force. Consider, for clarity, a minimally coupled scalar representative. In this paragraph $m = M_{\mathrm{pole}}$ is the matched physical mass. Its short-wavelength equation is

$$\left(\hbar^2\Box_{g^*} - m^2 - \hbar^2\xi R[g^*]\right)\psi = 0. \tag{267}$$

For $\psi = a\exp(iS/\hbar)$, the order-$\hbar^0$ term is

$$g_*^{\mu\nu}\partial_\mu S\,\partial_\nu S + m^2 = 0. \tag{268}$$

The curvature coupling and amplitude transport enter at subsequent eikonal orders. Put $p_\mu := \partial_\mu S$. Since covariant derivatives commute on a scalar phase,

$$p^\nu\nabla_\nu^{(g^*)}p_\mu = p^\nu\nabla_\mu^{(g^*)}p_\nu = \frac{1}{2}\nabla_\mu^{(g^*)}(p^\nu p_\nu) = 0. \tag{269}$$

For $m > 0$, $u^\mu := p^\mu/m$ therefore obeys $u^\nu\nabla_\nu^{(g^*)}u^\mu = 0$. This eikonal reduction assumes a stable narrow excitation and background variation on scales large compared with its Compton wavelength. The analogous principal-symbol calculation gives the same timelike characteristic for minimally coupled spinor

and vector wave packets after their physical polarizations have been selected. Here the geodesic statement concerns a freely propagating, neutral mode with constant matched mass. For a charged Abelian mode with constant charge q_{el}, define the gauge-invariant eikonal momentum by $k_\mu = \partial_\mu S - q_{\mathrm{el}} A_\mu$, with $F_{\mu\nu} = \partial_\mu A_\nu - \partial_\nu A_\mu$. If a background scalar makes the effective mass position dependent, the leading eikonal relation and its differentiated characteristic are

$$\begin{aligned} k^\mu k_\mu = -m(x)^2, \quad k^\nu \nabla_\nu k_\mu &= \tfrac{1}{2}\partial_\mu (k^\nu k_\nu) + q_{\mathrm{el}} F_{\mu\nu} k^\nu \\ &= q_{\mathrm{el}} F_{\mu\nu} k^\nu - \tfrac{1}{2}\partial_\mu m(x)^2. \end{aligned} \tag{270}$$

The first equality in the second line uses $\nabla_\nu k_\mu - \nabla_\mu k_\nu = q_{\mathrm{el}} F_{\mu\nu}$. Thus universal gravitational coupling coexists with a Lorentz force or scalar force; a pure geodesic follows when those terms vanish or are negligible in the declared approximation. Thus inertia is the characteristic propagation of a spectral excitation of the selected vacuum; it is not an extra force appended to the geometric field equation.

The same conclusion, including the gravitational source, follows from the localized worldline limit. For a stable, structureless excitation, let

$$S_{\mathrm{pp}}[z; g^*] = -m \int \mathrm{d}s = -m \int \sqrt{-g^*_{\mu\nu}(z) \dot{z}^\mu \dot{z}^\nu}\, \mathrm{d}\lambda. \tag{271}$$

This worldline action must be obtained by matching the isolated matter pole and the stress-tensor Ward identity; merely postulating it would build the mass equivalence into the assumption. Once that matching has been made, endpoint-fixed variation of z, followed by the proper-time choice of parameter, gives

$$\frac{\mathrm{d}^2 z^\mu}{\mathrm{d}\tau^2} + \Gamma^\mu{}_{\alpha\beta}[g^*] \frac{\mathrm{d}z^\alpha}{\mathrm{d}\tau} \frac{\mathrm{d}z^\beta}{\mathrm{d}\tau} = 0. \tag{272}$$

Metric variation of the same term gives

$$\delta_g S_{\mathrm{pp}} = \frac{m}{2} \int u^\mu u^\nu \delta g^*_{\mu\nu}(z(\tau))\, \mathrm{d}\tau = \frac{1}{2} \int_M \sqrt{-g^*}\, T^{\mu\nu}_{\mathrm{pp}}(x) \delta g^*_{\mu\nu}(x)\, \mathrm{d}^4 x, \tag{273}$$

where

$$T^{\mu\nu}_{\mathrm{pp}}(x) = \frac{m}{\sqrt{-g^*(x)}} \int u^\mu u^\nu \delta^{(4)}\big(x - z(\tau)\big)\, \mathrm{d}\tau. \tag{274}$$

Equations (272) and (274) are not two independent assignments: they are the worldline and coframe variations of one covariant functional. At the quantum level, the corresponding non-circular normalization is the zero-momentum stress-tensor form factor. For a stable normalized spin-zero one-particle state, write

$$\langle p' | T_{\mu\nu}(0) | p \rangle = 2P_\mu P_\nu A(q^2) + (q_\mu q_\nu - g^*_{\mu\nu} q^2) C(q^2), \quad P := \frac{p + p'}{2}, \quad q := p' - p. \tag{275}$$

For a spinning state, additional spin-dependent tensors occur, but its spin-averaged forward normalization has the same Ward-identity content. An anomaly-free diffeomorphism Ward identity and canonical state normalization give $A(0) = 1$. This condition matches the pole four-momentum to the long-wavelength tensor gravitational charge, including loop corrections. It is not available for a confined colored state, an infraparticle without an isolated pole, or a theory with an anomalous Ward identity.

For clarity, the normalization does not involve division by a distributional state overlap. Use $\langle p'|p\rangle = 2E_{\mathbf{p}}(2\pi)^3\delta^{(3)}(\mathbf{p}' - \mathbf{p})$ and the translation charge $\widehat{P}^\mu = \int T^{0\mu}(0,\mathbf{x})\,\mathrm{d}^3x$. Spatial translation covariance of the matrix element gives

$$\langle p'|\widehat{P}^\mu|p\rangle = (2\pi)^3\delta^{(3)}(\mathbf{p}' - \mathbf{p})\langle p'|T^{0\mu}(0)|p\rangle = 2E_{\mathbf{p}}p^\mu(2\pi)^3\delta^{(3)}(\mathbf{p}' - \mathbf{p}). \quad (276)$$

The forward limit of the form-factor decomposition is $\langle p|T^{0\mu}(0)|p\rangle = 2E_{\mathbf{p}}p^\mu A(0)$. Equality of the coefficients of the common delta distribution therefore gives $A(0) = 1$, or equivalently the same result follows after smearing with normalizable wave packets. This uses the total conserved stress tensor and its translation generator. A partial-sector stress tensor, a gauge-dependent excitation, or an independently normalized extra scalar force need not have this forward gravitational interpretation.

This identity becomes especially transparent in the Newtonian limit. Write $g^*_{00} = -(1 + 2\Phi_N)$, take $g^*_{0i} = 0$, and retain first order in Φ_N and second order in $|\mathbf{v}|$. Then

$$\frac{\mathrm{d}s}{\mathrm{d}t} = 1 + \Phi_N - \frac{1}{2}|\mathbf{v}|^2 + O(\Phi_N^2, \Phi_N|\mathbf{v}|^2, |\mathbf{v}|^4), \quad (277)$$

so, after removal of the constant rest term,

$$L_{\mathrm{NR}} = \frac{1}{2}m|\mathbf{v}|^2 - m\Phi_N, \qquad m\ddot{\mathbf{x}} = -m\nabla\Phi_N. \quad (278)$$

Moreover, $T^{00}_{\mathrm{pp}} = m\delta^{(3)}(\mathbf{x} - \mathbf{z})$ to this order, and $\nabla^2\Phi_N = 4\pi G_{\mathrm{eff}}T^{00}$ after neglecting the cosmological and higher-curvature remainders. The same m therefore enters the active source. Inertial, passive gravitational, and active monopole mass are one coefficient in the same generally covariant effective action, rather than two or three masses whose equality is imposed after the fact.

This statement is restricted to the tensor branch with universal minimal coupling. The shared-scalar sector in Section 11.11 can carry composition-dependent scalar charges and then produces a fifth force and an Eötvös signal. Nonminimal curvature terms, spin, finite size, radiation reaction, or strong self-gravity also require a corrected effective action. They can invalidate the elementary point-particle reduction without invalidating the diffeomorphism Ward identity in its proper domain.

The resulting interpretation is more specific than the phrase *mass resists acceleration*. Mass is the pole or spectral stiffness of a physical excitation around the selected equilibrium; inertia is the covariant phase propagation of that excitation; gravitational charge is the coframe response of the same effective term; and observable gravity is the tidal curvature relating neighboring characteristics. The extension sought by the present framework is not a replacement of this general-relativistic low-energy mechanism. It is a derivation, from one selected microscopic package, of the vacuum, its physical Hessian, the coframe, and their universal coupling.

5.5.3. *What would determine numerical inertial masses?* The preceding argument identifies what mass means, but it does not by itself calculate any observed mass. A non-circular calculation requires the selected data $\mathbf{q}_*$ to be fixed independently of the masses that will test the theory. In a declared renormalization scheme, the closed system to be solved is schematically

$$\nabla_{\mathbf{q}}\mathscr{S}_{\mathrm{sel}}(\mathbf{q}_*)=0, \qquad \mathscr{C}_A(\mathbf{q}_*)=0, \qquad \mathscr{P}_j(M_j^2;\mathbf{q}_*,\mu)=0, \qquad \mu\frac{\mathrm{d}M_j}{\mathrm{d}\mu}=0. \tag{279}$$

Here $\mathscr{C}_A$ contains the gauge, anomaly, vacuum, and matching constraints, and the last identity states renormalization-group invariance of the physical pole after all threshold terms have been included. At a simple pole, an uncertainty or a change in selected microscopic data propagates as

$$\delta M_j^2=-\frac{\partial_{\mathbf{q}}\mathscr{P}_j(M_j^2;\mathbf{q}_*,\mu)\cdot\delta\mathbf{q}_*}{\partial_s\mathscr{P}_j(M_j^2;\mathbf{q}_*,\mu)}. \tag{280}$$

If the microscopic construction selects only dimensionless coordinates, then one can at most obtain

$$\frac{M_i}{M_j}=\frac{\mathfrak{m}_i(\mathbf{q}_*)}{\mathfrak{m}_j(\mathbf{q}_*)}. \tag{281}$$

Absolute masses additionally require a selected scale μ_*, for example through a rigorously controlled dimensional-transmutation mechanism,

$$\Lambda_{\mathrm{dyn}}=\mu\exp\left[-\int^{g(\mu)}\frac{\mathrm{d}g}{\beta(g)}\right], \tag{282}$$

with a declared renormalization boundary condition. One then has $M_j=\mu_*\mathfrak{m}_j(\mathbf{q}_*)$. Fitting $\mathbf{q}_*$, μ_*, or Yukawa matrices to the target masses and reproducing them through (279) is matching, not prediction. The present paper supplies the equations and some conditional mass relations, but it does not yet solve this closed system for all observed masses.

5.5.4. *A precise Machian response criterion.* The statement that inertia is influenced by the rest of the universe has several inequivalent meanings. Universal geodesic motion proves none of them by itself. A formula-level

version can, however, be stated in the present selection framework. Let φ collect the physical non-coframe variables, introduce physical sources through $\Gamma_J = \Gamma_{\rm eff} - \langle J_e, e\rangle - \langle J_\varphi, \varphi\rangle$, and evaluate the reduced Hessian at a selected solution. On the gauge quotient it has the block form

$$\mathcal{K}_*^{\rm red} = \begin{pmatrix} K_{ee} & K_{e\varphi} \\ K_{\varphi e} & K_{\varphi\varphi} \end{pmatrix}. \tag{283}$$

Linearizing the two stationarity equations gives

$$\begin{pmatrix} K_{ee} & K_{e\varphi} \\ K_{\varphi e} & K_{\varphi\varphi} \end{pmatrix} \begin{pmatrix} \delta e_* \\ \delta\varphi_* \end{pmatrix} = \begin{pmatrix} \delta J_e \\ \delta J_\varphi \end{pmatrix}. \tag{284}$$

Assume that $K_{\varphi\varphi}$ is invertible on the physical subspace and define the coframe Schur complement

$$K_{\rm Mach} := K_{ee} - K_{e\varphi} K_{\varphi\varphi}^{-1} K_{\varphi e}. \tag{285}$$

If the boundary conditions and global selection rule also make $K_{\rm Mach}$ invertible, elimination of $\delta\varphi_*$ yields

$$\boxed{\delta e_* = K_{\rm Mach}^{-1}\left(\delta J_e - K_{e\varphi} K_{\varphi\varphi}^{-1} \delta J_\varphi\right).} \tag{286}$$

The integral kernel of the second term,

$$\chi_{e\varphi}(x,y) := -\left[K_{\rm Mach}^{-1} K_{e\varphi} K_{\varphi\varphi}^{-1}\right](x,y), \tag{287}$$

is a quantitative Mach susceptibility: it measures how a physical change of matter or order-parameter data at y changes the selected local coframe at x. It is nonlocal because it contains Green operators, not because the theory permits superluminal signalling. Causal response requires the corresponding retarded Lorentzian kernel; the Euclidean inverse is used only for equilibrium selection.

Equation (286) distinguishes three levels of claim. First, the off-diagonal block $K_{e\varphi} \neq 0$ gives a weak relational statement: matter and inertial geometry respond to common data. Second, a strong Machian closure requires the physical kernel of $K_{\rm Mach}$ to vanish after boundary conditions, so that there is no freely specifiable homogeneous coframe perturbation independent of the selected global state. Third, a complete origin theorem must derive those boundary conditions and the selected state rather than insert them. One may state the strong condition without coordinate ambiguity as

$$\frac{\{X : \mathcal{E}_{\rm M}[X] = 0,\ \mathcal{O}_{\rm mat}[X] = \mathcal{D},\ \mathcal{B}_{\rm rel}[X] = 0\}}{\mathrm{Diff}(M) \ltimes \mathfrak{G}} = \{[X_*(\mathcal{D})]\}. \tag{288}$$

Here $\mathcal{D}$ is the complete declared relational matter data and $\mathcal{B}_{\rm rel}$ is a physically fixed boundary condition. Vacuum Einstein solutions and freely propagating gravitational waves show that ordinary general relativity does not satisfy this strong requirement in an unqualified form. The current master theory provides the response operator and a route by which global equilibrium data could

impose the stronger closure, but it has not proved (288) for the physical branch. This is the precise boundary between a formula-derived Machian mechanism and a verbal appeal to Mach's principle.

5.5.5. *Quantum geometry and the vacuum-curvature balance.* Classical stochastic fluctuations of e are not, by themselves, quantum gravity. A quantum interpretation would require a physical finite-regulator Euclidean measure, schematically

$$\mathrm{d}\mu^{\mathrm{phys}}_{a,N}(\Phi) = \frac{1}{Z_{a,N}} \exp\left[-\frac{S_E^{a,N}(\Phi)}{\hbar}\right] \mathrm{d}\nu^{\mathrm{phys}}_{a,N}(\Phi), \tag{289}$$

where the quotient, gauge fixing, determinants, and physical observables are defined consistently. One would then have to prove the regulator-independent Schwinger limits (857), reflection positivity, the remaining Osterwalder–Schrader axioms, and the gravitational constraint or relational-observable conditions stated in the quantum-completion section. Identifying the classical noise scale θ with $\hbar$ is not a derivation of any of these properties.

For a direct Lorentzian construction, the Gauss, local Lorentz, diffeomorphism, and Hamiltonian constraints, collectively $\widehat{\mathcal{C}}_A$, would have to satisfy

$$\widehat{\mathcal{C}}_A \Psi_{\mathrm{phys}} = 0, \qquad [\widehat{\mathcal{C}}_A, \widehat{\mathcal{C}}_B] = i\hbar\, \widehat{f}_{AB}{}^{C} \widehat{\mathcal{C}}_C, \qquad Q^2_{\mathrm{BRST}} = 0, \tag{290}$$

with the field-dependent structure functions, domains, regularization, and possible boundary charges treated explicitly. An anomaly in this algebra, an indefinite physical inner product, or the absence of relational observables prevents the construction from being a quantum theory of geometry.

If such a quantum completion exists, the in-in effective action gives two related response equations. Its first coframe variation yields the semiclassical fixed point

$$G_{\mu\nu} + \Lambda_{\mathrm{ren}} g_{\mu\nu} + \mathcal{H}^{\mathrm{ren}}_{\mu\nu} = 8\pi G_{\mathrm{ren}} \langle \widehat{T}_{\mu\nu} \rangle^{\mathrm{ren}}_{\omega_*, g}, \tag{291}$$

while its second physical variation determines the connected coframe two-point function through

$$\int \Gamma^{(2)}_{ee,\mathrm{phys}}(x,z) G^{\mathrm{phys}}_{ee}(z,y)\, \mathrm{d}z = P_{\mathrm{phys}}(x,y). \tag{292}$$

Here P_{phys} projects away gauge directions and enforces the constraints. Real-time response must also be causal:

$$\frac{\delta \langle \widehat{T}_{\mu\nu}(x) \rangle^{\mathrm{ren}}_{\omega_*, g}}{\delta g_{\rho\sigma}(y)} = 0 \qquad \text{when } y \notin J^-(x). \tag{293}$$

This condition is naturally formulated by the Schwinger–Keldysh effective action and does not follow from an in-out or Euclidean Hessian alone. Formula (292) gives the proposed extension of the classical interpretation: the mean coframe is the first-response variable selected by the effective action, whereas quantum

geometry is encoded by the physical inverse Hessian and higher connected coframe correlations. These are completion conditions, not a construction of a positive graviton Hilbert space in the present manuscript.

The same effective action separates a possible explanation of the cosmological constant from an unsupported cancellation claim. On a constant vacuum branch write

$$\Gamma_{\rm vac}[g,\varphi]=\int_M\sqrt{-g}\left[\frac{R-2\Lambda_L(\mathbf{q},\mu)}{16\pi G(\mathbf{q},\mu)}-V_{\rm eff}(\varphi;\mathbf{q},\mu)+\mathcal{L}_{\rm hc}\right]\mathrm{d}^4x. \tag{294}$$

Let φ_* satisfy the renormalized vacuum equations. On a maximally symmetric four-dimensional branch with $R_{\mu\nu}=3H_*^2g_{\mu\nu}$, define $\mathcal{Q}_{\rm hc}(H_*^2)g_{\mu\nu}$ to be the complete higher-curvature and nonlocal vacuum contribution after multiplication by $8\pi G$. The coframe equation reduces to the scalar balance

$$\boxed{3H_*^2=\Lambda_L(\mathbf{q}_*,\mu)+8\pi G(\mathbf{q}_*,\mu)V_{\rm eff}(\varphi_*;\mathbf{q}_*,\mu)+\mathcal{Q}_{\rm hc}(H_*^2;\mathbf{q}_*,\mu).} \tag{295}$$

Thus the observed curvature is a renormalized balance among the geometric Cartan term, the selected vacuum energy, and the remaining quantum and higher-curvature response. It is not equal to any one bare zero-point sum. When all beta functions and counterterms are included consistently, the physical root must satisfy

$$\mu\frac{\mathrm{d}}{\mathrm{d}\mu}\left[\Lambda_L+8\pi GV_{\rm eff}+\mathcal{Q}_{\rm hc}\right]_{(\varphi_*,\mathbf{q}_*,H_*)}=0. \tag{296}$$

Renormalization-scale invariance removes an unphysical scale dependence; it does not explain why the resulting root is small. For a field of mass M_i, a typical one-loop threshold contribution has the form

$$\Delta V_i=\frac{(-1)^{F_i}n_iM_i^4}{64\pi^2}\left(\log\frac{M_i^2}{\mu^2}-c_i\right), \tag{297}$$

so every threshold must be included in the matching and stability test.

Ordinary equilibrium minimization alone cannot solve the additive vacuum-energy problem. To see this directly, fix the coframe while selecting an internal vacuum coordinate q, and let

$$V_C(q):=V_0(q)+C,\qquad \partial_qV_0(q_*)=0,\qquad \partial_q^2V_0(q_*)>0. \tag{298}$$

Then

$$\begin{aligned}&\frac{\mathrm{d}q_*}{\mathrm{d}C}=0,\qquad \frac{\mathrm{d}}{\mathrm{d}C}V_C(q_*)=1,\\ &\frac{\partial}{\partial C}\left(\Lambda_L+8\pi GV_C(q_*)+\mathcal{Q}_{\rm hc}\right)\Big|_{q_*,G,\Lambda_L,\mathcal{Q}_{\rm hc}}=8\pi G.\end{aligned} \tag{299}$$

The first equality follows because an additive constant does not enter the internal stationarity equation; the second is the envelope identity; and the third is the direct change of the curvature source with its other inputs held fixed. It is not the full implicit response when the higher-curvature term depends on the

root. To retain that feedback, put $y(C) := H_*^2(C)$ and hold G, Λ_L, and $V_0(q_*)$ fixed while solving

$$3y(C) = \Lambda_L + 8\pi G\big(V_0(q_*) + C\big) + \mathcal{Q}_{\mathrm{hc}}(y(C)). \tag{300}$$

At a differentiable simple root, implicit differentiation gives

$$\frac{\mathrm{d}y}{\mathrm{d}C} = \frac{8\pi G}{3 - \mathcal{Q}'_{\mathrm{hc}}(y)}, \qquad 3 - \mathcal{Q}'_{\mathrm{hc}}(y) \neq 0. \tag{301}$$

In the ordinary Einstein limit the derivative is $8\pi G/3$; for the curvature quantity $3y$ it is $8\pi G$. A vanishing denominator invalidates the simple-root argument rather than proving insensitivity. If the selected matter vacuum, couplings, or counterterms also vary, their chain-rule terms must be included. Thus higher-curvature feedback changes the response but does not automatically cancel the vacuum-energy sensitivity. A global volume constraint, a symmetry, a sequestering variable, or another dynamical zero-mode could modify this response, but it must be part of the master data and must satisfy the radiative-stability test

$$\frac{\mathrm{d}}{\mathrm{d}C}\left[\Lambda_L(\mathbf{q}_*(C)) + 8\pi G(\mathbf{q}_*(C))V_C(\varphi_*(C), \mathbf{q}_*(C)) + \mathcal{Q}_{\mathrm{hc}}(H_*^2(C), \mathbf{q}_*(C))\right] \approx 0 \tag{302}$$

over the declared range of threshold corrections. The present local master action does not yet prove this criterion or calculate the observed value of H_*. Its explanatory content is a common response architecture and a sharp obstruction test: inertia, gravitation, quantum coframe correlations, and vacuum curvature are successive first- and second-variation data of one selected effective functional, while numerical mass and cosmological-constant predictions require the additional selection and radiative-stability equations displayed above.

5.5.6. *Relation to the stochastic control cost.* The functional (65) measures the quadratic deviation of an admissible absolutely continuous skeleton from a specified uncontrolled drift. Therefore

$$\mathcal{J}_T[x] = 0 \quad \Longleftrightarrow \quad \dot{x}_t = \mathbb{B}(x_t) \quad \text{for almost every } t, \tag{303}$$

on the range of the mobility and under the hypotheses of Section 3.9. If a test-body reduction of that drift is independently derived in the form

$$\mathbb{B}_{\mathrm{tb}}(x, v) = \left(v^\mu, -\Gamma^\mu{}_{\alpha\beta}[g^*]v^\alpha v^\beta\right), \tag{304}$$

then (303) gives the geodesic equation (262). The order of this implication matters. Specifying (304) in advance and then calling its paths "zero-cost" does not derive the origin of inertial motion; it merely assigns zero control expenditure to a preselected drift.

A microscopic origin result would require the same independently calibrated selection data to determine the coframe, universal matter coupling, and reduced drift. Schematically, the required stronger conclusion is

$$\Gamma_* \in \operatorname*{arg\,min}_{\Gamma\in\mathscr{G}_{\mathrm{adm}}} \mathscr{S}_{\mathrm{sel}}(\Gamma) \quad\Longrightarrow\quad \big(e_*, \omega_*, S_{\mathrm{m}}[e_*, \omega_*, \psi], \mathbb{B}_{\mathrm{tb}}\big). \tag{305}$$

The right-hand side includes the universal coupling in (257) and the derivation of (304). Equation (305) is a mathematically definite target for a concrete realization; it is not implied solely by the notation (256).

5.5.7. *Ordinary material response and shielding.* Let a source, a passive material layer, and a probe have stress tensors $T^{\mathrm{src}}_{\mu\nu}$, $T^{\mathrm{mat}}_{\mu\nu}$, and $T^{\mathrm{pr}}_{\mu\nu}$, respectively. The controlled metric equation then has the decomposed form

$$G_{\mu\nu}[g^*] + \Lambda_L g^*_{\mu\nu} + 16\pi G_{\mathrm{eff}} \sum_i \bar{\alpha}_i \bar{\mathcal{H}}^{(i)}_{\mu\nu}[g^*] = 8\pi G_{\mathrm{eff}} \big(T^{\mathrm{src}}_{\mu\nu} + T^{\mathrm{mat}}_{\mu\nu} + T^{\mathrm{pr}}_{\mu\nu}\big). \tag{306}$$

The material layer can change the total stress tensor and hence the solution g^*, but it does not remove the probe from the universal coupling (257). The present ordinary-matter branch therefore contains no material parameter that changes (262) into free motion with respect to a second, shielded metric. This is the structural reason that it has no electromagnetic Faraday-cage analogue for externally imposed gravitational response.

This assertion is intentionally narrower than a no-go theorem for every gravitational configuration. Material distributions can modify curvature; a symmetric shell can make the Newtonian field generated by that shell vanish in its interior; selected source configurations can cancel the acceleration of a particular probe; and gravitational radiation can be scattered, absorbed, or phase shifted. Such effects alter the solution of (306); they do not universally decouple interior probes from g^*. A general no-shielding theorem would require an operational definition of shielding, a class of material stress tensors, boundary conditions, and suitable energy and regularity hypotheses. Neither universal coupling alone nor the absence of a simple negative gravitational charge supplies that theorem.

At low energy, this interpretation is intended to recover, rather than replace, the geometric content of general relativity. General relativity takes a metric and its universal matter coupling as fundamental low-energy structure. The additional programme here is to derive, from common selection data, why the effective coframe, its field equation, and universal coupling occur together. Until one concrete microscopic realization proves the selection statement (305) and derives the drift (304), that origin claim remains a well-specified conditional objective rather than a consequence of the master cost alone.

5.6. *Yang–Mills sectors and electromagnetism.* For the residual internal block, the same master equation has $\mathbb{P}_H^A = \widehat{\kappa}_{AB} \star F^B$, where $\widehat{\kappa}_{AB}$ is the internal constitutive form induced by the single master pairing. It may contain the shared order-parameter weight; for the joint candidate in (229), $\widehat{\kappa}_{AB}(\sigma) = w(\sigma)\kappa_{AB}$. The second projection in (173) is then

$$\pi_{\mathrm{int}} \iota_{\mathfrak{h}}^* (\mathbb{D}\mathbb{P} - \mathbb{J}_{\mathrm{ext}}) = 0 \quad \Longleftrightarrow \quad D\Big(\widehat{\kappa}_{AB} \star F^B\Big) = - \star J_A. \tag{307}$$

In local coordinates, after fixing the Hodge convention and lowering the form index, this is precisely $D_\mu(\widehat{\kappa}_{AB} F^{B\mu\nu}) = J_A^\nu$, which is derived by direct variation below. A scalar-dependent but Hodge-compatible coefficient is already included inside the derivative in this equation. If the constitutive tensor has off-diagonal blocks or is not Hodge-compatible, one must instead retain the appropriate internal component of $\iota_{\mathfrak{h}}^* \mathbb{D}(\partial \mathcal{L}/\partial \mathbb{F})$; the displayed Yang–Mills form is the rigorously recovered residual equation on the stated Hodge-compatible branch. The displayed Hodge equation is Euclidean, because positivity of the master pairing and the stochastic construction are formulated on the Euclidean slice. If the Wick map (207) extends analytically to the internal connection and its source, write

$$\star_E F_E \longmapsto \varsigma_\star \star_L F_L, \qquad J_E \longmapsto \varsigma_J J_L, \qquad \varsigma_\star, \varsigma_J \in \{\pm 1, \pm i\}. \tag{308}$$

The continuation must fix these factors together with the Lorentzian action and real source normalization. An arbitrary imaginary factor cannot be absorbed into a coupling while retaining a real, physically admissible theory. With the real convention $D_{L,\mu}(\widehat{\kappa}_{L,AB} F_L^{B\mu\nu}) = J_{L,A}^\nu$, the corresponding differential-form equation is $D_L(\widehat{\kappa}_{L,AB} \star_L F_L^B) = - \star_L J_{L,A}$. Thus, under the specified continuation and real source convention, the physical Lorentzian Yang–Mills equation is recovered from the same projected Euler system. Establishing global hyperbolicity, global existence, or regularity for every solution is a separate analytic problem and is not a prerequisite for this local variational identity.

On a phase in which the internal connection survives as a light connection on a residual compact group G_H, the master curvature contains

$$F = \mathrm{d}A + A \wedge A. \tag{309}$$

In components, the wedge-product convention is $(A \wedge A)^A = \frac{1}{2} f_{BC}{}^A A^B \wedge A^C$, which is equivalent to (312) below. Let $\widehat{\kappa}_{AB}$ denote the internal bilinear form induced by the reduced master pairing after the residual symmetry and field normalization have been fixed. It is not an additional microscopic pairing. The corresponding quadratic curvature invariant is

$$S_{\mathrm{YM,eff}} = \frac{1}{2} \int_M \widehat{\kappa}_{AB} F^A \wedge \star F^B = \frac{1}{4} \int_M \sqrt{g}\, \widehat{\kappa}_{AB} F^A_{\mu\nu} F^{B\mu\nu} \mathrm{d}^4 x. \tag{310}$$

On a branch on which the scalar and coframe are frozen, $\widehat{\kappa}_{AB} = \kappa_{AB}$ is constant; only on that branch does the following variation omit derivatives of the constitutive coefficient. After canonical normalization and symmetry breaking, this may take the familiar form

$$S_{\mathrm{YM,eff}} = \int_M \sqrt{g}\left[\frac{1}{4g_3^2}G^a_{\mu\nu}G^{a\mu\nu} + \frac{1}{4g_2^2}W^i_{\mu\nu}W^{i\mu\nu} + \frac{1}{4g_1^2}B_{\mu\nu}B^{\mu\nu}\right]\mathrm{d}^4x. \quad (311)$$

Electromagnetism then appears after electroweak breaking as the unbroken $U(1)_{\mathrm{em}}$ connection. The photon is not a fourth microscopic connection in this construction; it is the massless residual gauge mode of the broken electroweak phase. The conventional gauge-theoretic and electroweak structures are recalled in [167], [81], [160], and [143], while the standard symmetry-breaking mechanism is represented by [95] and [65].

5.7. *Internal-connection variation.* We now verify the corresponding gauge equation rather than identifying the Yang–Mills term at the level of the action only. Choose a basis $\{T_A\}$ of the residual Lie algebra with $[T_B, T_C] = f^A{}_{BC}T_A$, and write

$$F = F^A T_A, \qquad F^A_{\mu\nu} = 2\partial_{[\mu}A^A_{\nu]} + f^A{}_{BC}A^B_\mu A^C_\nu. \quad (312)$$

The invariant form $\widehat{\kappa}_{AB}$ is assumed here to be positive definite on the Euclidean residual sector and $\mathrm{Ad}(G_H)$-invariant. It is constant in the following subcalculation, as on the frozen scalar/coframe branch; for a dynamical $\widehat{\kappa}$, the same integration by parts keeps it inside the covariant derivative. These assumptions are precisely what permit the following covariant integration by parts. The curvature variation is

$$\delta F^A_{\mu\nu} = 2(D_{[\mu}\delta A_{\nu]})^A, \qquad (D_\mu X)^A = \partial_\mu X^A + f^A{}_{BC}A^B_\mu X^C. \quad (313)$$

Varying (310) and using the antisymmetry of $F^{A\mu\nu}$ gives

$$\begin{aligned}\delta S_{\mathrm{YM,eff}} &= \frac{1}{2}\int_M \sqrt{g}\,\widehat{\kappa}_{AB}F^{A\mu\nu}\delta F^B_{\mu\nu}\,\mathrm{d}^4x \\ &= \int_M \sqrt{g}\,\widehat{\kappa}_{AB}F^{A\mu\nu}(D_\mu\delta A_\nu)^B\,\mathrm{d}^4x. \end{aligned} \quad (314)$$

Assume that the boundary term vanishes. Gauge-covariant integration by parts, together with the invariance of κ, then yields

$$\delta S_{\mathrm{YM,eff}} = -\int_M \sqrt{g}\,D_\mu\big(\widehat{\kappa}_{AB}F^{B\mu\nu}\big)\,\delta A^A_\nu\,\mathrm{d}^4x. \quad (315)$$

Define the connection current of the remaining low-energy matter and order-parameter action by

$$\delta S_{\mathrm{src}} = \int_M \delta A^A \wedge \star J_A = \int_M \sqrt{g}\,J^\nu_A\delta A^A_\nu\,\mathrm{d}^4x, \qquad J^\nu_A := \frac{1}{\sqrt{g}}\frac{\delta S_{\mathrm{src}}}{\delta A^A_\nu}. \quad (316)$$

Here $J_A = J_{A,\mu}\mathrm{d}x^\mu$, and the order of the forms fixes the sign: $\star J_A \wedge \delta A^A = -\delta A^A \wedge \star J_A$. Thus the three-form source in (171) is $\mathbb{J}_{\mathrm{ext},A} = -\star J_A$. Equivalently,

$$D(\widehat{\kappa}_{AB} \star F^B) = -\star\left[g_{\nu\lambda} D_\mu(\widehat{\kappa}_{AB} F^{B\mu\nu})\,\mathrm{d}x^\lambda\right]. \tag{317}$$

In this identity D_μ contains both the gauge connection and the Levi–Civita connection on spacetime indices. The latter is essential for integration against $\sqrt{g}\,\mathrm{d}^4x$. The stationarity condition is exactly

$$D_\mu\left(\widehat{\kappa}_{AB} F^{B\mu\nu}\right) = J^\nu_A. \tag{318}$$

In a basis with $\kappa_{AB} = \delta_{AB}$, this becomes

$$D_\mu F^{A\mu\nu} = J^{A\nu}. \tag{319}$$

For a canonically normalized simple factor on the frozen branch with $\kappa_{AB} = \delta_{AB}/g_a^2$, the same equation reads $D_\mu F^{A\mu\nu} = g_a^2 J^{A\nu}$; absorbing g_a^2 into the definition of the source gives the displayed canonical convention. If $\widehat{\kappa}$ depends on a scalar or coframe, the derivative in (318) must be expanded and the corresponding variation contributes to the scalar and metric equations. The covariant conservation law can be checked directly from the equation of motion. Set $K^{\mu\nu}_A := \widehat{\kappa}_{AB} F^{B\mu\nu}$. Antisymmetry and an exchange of dummy indices give

$$D_\nu J^\nu_A = D_\nu D_\mu K^{\mu\nu}_A = \tfrac{1}{2}[D_\nu, D_\mu] K^{\mu\nu}_A = 0. \tag{320}$$

The spacetime-curvature contractions vanish because the Ricci tensor is symmetric and $K^{\mu\nu}_A$ is antisymmetric. The gauge-curvature contraction vanishes by the symmetric Ad-invariant pairing: in a simple factor it is a scalar multiple of $[F_{\nu\mu}, F^{\mu\nu}] = 0$. Abelian factors contribute no commutator. Gauge invariance of the source action yields the same identity on its matter equations. This is compatible with, but does not follow merely from, the differential Bianchi identity $D_{[\mu}F_{\nu\rho]} = 0$. Equations (318)–(319) are the internal low-energy projection of the fixed-coframe unified connection equation $\iota_{\mathfrak{h}}^*(\mathbb{DP} - \mathbb{J}_{\mathrm{ext}}) = 0$ in (172), after the residual pairing has become block-diagonal and the background metric is fixed. In the present Hodge-compatible case, its internal constitutive momentum is $\mathbb{P}^A_H = \widehat{\kappa}_{AB} \star F^B$, so the projected equation is exactly $D(\widehat{\kappa}_{AB} \star F^B) = -\star J_A$. A mixed or non-Hodge-compatible master pairing instead gives the restricted constitutive equation $\iota_{\mathfrak{h}}^*[\mathbb{D}(\partial\mathcal{L}/\partial\mathbb{F}) - \mathbb{J}_{\mathrm{ext}}] = 0$. Therefore the displayed Yang–Mills equation is the exact internal projection under the stated constitutive hypotheses. Its conditional scope makes it a controlled recovery theorem, not an additional microscopic action.

5.8. *From the common action to a controlled Einstein–Yang–Mills comparison.* The preceding variations identify a common origin for the gravitational and internal equations. To compare their solutions with familiar physics, one must also specify which coefficients are held fixed, which additional terms

are small, and which stability estimate turns an equation error into a field error. These questions connect the variational construction to the physical matching problem. They also distinguish a numerical approximation of the mother equations from a low-energy reduction of those equations.

The geometric source of the Einstein term. The coframe supplies a length-valued one-form that relates local frame components to spacetime distances. Its occurrence in the Cartan connection therefore carries more information than an independent internal gauge connection. In the geometric branch of (217), the curvature has components

$$F_{\mathrm{c}}^{ab} = R^{ab} - \ell^{-2} e^a \wedge e^b, \qquad F_{\mathrm{c}}^{a5} = \ell^{-1} T^a. \tag{321}$$

For an orthonormal Euclidean coframe in four dimensions, the six forms $e^a \wedge e^b$, $a < b$, have unit squared norm. With the curvature convention of (1097),

$$\sum_{a<b} |R^{ab}|^2 = \tfrac{1}{4} |\operatorname{Rm}|^2, \qquad \sum_{a<b} \langle R^{ab}, e^a \wedge e^b \rangle = \tfrac{1}{2} \mathcal{S}. \tag{322}$$

Expanding the square gives the geometric contribution

$$S_{\mathrm{c},E} = \frac{w_*}{2 g_{\mathrm{c}}^2} \int_M \left(\tfrac{1}{4} |\operatorname{Rm}|^2 - \ell^{-2} \mathcal{S} + 6 \ell^{-4} + \ell^{-2} \sum_a |T^a|^2 \right) \operatorname{vol}_g. \tag{323}$$

Thus the Einstein term comes from the cross contraction in the Cartan curvature norm. The continuation and consistent reduction stated in Section 14.39 yield $M_{\mathrm{P}}^2 = w_* / (g_{\mathrm{c}}^2 \ell^2)$ and the unmodified vacuum coefficient $\Lambda = 3\ell^{-2}$. Neither a generic connection norm nor an arbitrary additional scalar supplies this conclusion. In particular, changing the vacuum coefficient is additional matching data. The exact Einstein critical points under independent connection and coframe variation are proved in Proposition 159.

The generalized curvature in (52) is a typed tuple. Its matter and potential entries need not be differential forms of the same degree. The common pairing makes their contraction well defined; it does not identify the tuple with the square of an unspecified superconnection. Likewise, the coupling of sectors is a property of the action, reference law and admissible reductions together. A mixed Hessian can display a coupling in chosen coordinates, but is not an invariant criterion for the factorization in Definition 2. For example, an interaction $x^2 y^2$ has zero mixed Hessian at the origin while coupling the variables away from it.

Two coefficient errors in the internal equation. Write $H = \widehat{\kappa}$ for the symmetric invariant kinetic pairing in the preceding calculation. Invariance permits independent constants on distinct compact simple ideals; abelian factors can have kinetic mixing. The comparison pairing H_0 is fixed, parallel and invertible. Both act from the adjoint bundle to its dual. All statements below use one

gauge and one source convention, namely (316). On a fixed branch define the equation defect r and the canonical comparison residual $\mathcal{R}_A$ by

$$D_\mu(HF^{\mu\nu}) = J^\nu + r^\nu, \qquad \mathcal{R}_A^\nu = D_\mu F^{\mu\nu} - H_0^{-1}J^\nu. \tag{324}$$

Here a defect can represent a retained physical term or a numerical equation error; its origin must be specified before taking a limit.

Proposition 12 (The coefficient-normalized gauge residual). *Suppose the terms in* (324) *are defined and* $DH_0 = 0$. *Then*

$$H_0\mathcal{R}_A^\nu = r^\nu - (D_\mu H)F^{\mu\nu} - (H - H_0)D_\mu F^{\mu\nu}. \tag{325}$$

For $1 \le p \le \infty$, *use a positive auxiliary bundle norm and the induced norms for the displayed contractions. If their right-hand side is in* L^p, *then*

$$\|\mathcal{R}_A\|_{L^p} \le \|H_0^{-1}\|\big(\|r\|_{L^p} + \|DH\|_\infty\|F\|_{L^p} + \|H - H_0\|_\infty\|D_\mu F^{\mu\cdot}\|_{L^p}\big). \tag{326}$$

If H *is pointwise symmetric and Ad-invariant, the same equation also implies the distributional compatibility condition*

$$D_\nu J^\nu = -D_\nu r^\nu. \tag{327}$$

Proof. The product rule gives $D_\mu(HF^{\mu\nu}) = HD_\mu F^{\mu\nu} + (D_\mu H)F^{\mu\nu}$. Subtract J, split $H = H_0 + (H - H_0)$, and move both coefficient terms to the other side. This proves (325). Apply H_0^{-1}, the triangle inequality and the multiplication bound $\|Bu\|_{L^p} \le \|B\|_\infty\|u\|_{L^p}$. The contraction norm incorporates the sum over the spacetime index, so no unspecified component factor is suppressed. Finally, antisymmetry gives $D_\nu D_\mu(HF^{\mu\nu}) = \frac{1}{2}[D_\nu, D_\mu](HF^{\mu\nu}) = 0$. The Ricci contractions and the internal commutator vanish for the reasons given after (320). Taking the divergence of (324) proves (327). □

Small derivatives of H alone are insufficient for recovery with a prescribed source normalization. A nonmatching constant coefficient has zero derivative and still changes $H_0^{-1}J$. Conversely, a variable coefficient can give a canonical equation on a special solution if the two coefficient terms cancel. The proposition gives a sufficient bound, not a necessary characterization of every such solution. If a charged background replaces the invariant pairing, its own variation and the corresponding Noether identity must be included; the last conclusion does not extend by simply dropping that equation.

Variations, boundary data and physical units. The preceding local statements use compactly supported variations on the interior of M, or a closed Euclidean manifold. For a nonempty boundary the gauge surface variation contains $\int_{\partial M}\delta A^A \wedge H_{AB} \star F^B$, with the orientation inherited from Stokes' theorem. Fixing the tangential connection removes this term. Prescribing flux instead requires a different boundary variational problem. There is no universal boundary functional $\langle F, A\rangle$ that simultaneously supplies the gauge, coframe and

independent-connection conditions. For the metric Einstein–Hilbert action, fixing the induced metric uses the corresponding Gibbons–Hawking–York term on a non-null boundary; higher-curvature terms require their own boundary data. These choices are unnecessary for the compact-support statements proved here.

All comparisons must also respect units. In four dimensions with $\hbar = c = 1$, the component quantities $A_\mu, F_{\mu\nu}, J^\nu$ have dimensions L^{-1}, L^{-2}, L^{-3}, while H is dimensionless. Every term in (325) consequently has dimension L^{-3}. The Einstein residual $G_{\mu\nu} + \Lambda g_{\mu\nu} - 8\pi G T_{\mu\nu}$ has dimension L^{-2}. Choosing a reference length L_0 makes these residuals dimensionless by multiplying them by L_0^3 and L_0^2, respectively, before defining a combined error. Their unscaled numerical values cannot be added as if they were the same observable.

Four distinct steps in recovery. Equation consistency asks whether a given configuration has a small Einstein–Yang–Mills residual. Compactness asks whether a family of configurations has a convergent subsequence. Stability asks whether a small residual implies proximity to a selected solution. Physical evolution asks whether the proximity persists on a time interval. Each step has assumptions not supplied by the preceding one.

For example, fix a compact smooth four-dimensional manifold, a finite bundle atlas, and compatible diffeomorphism and internal gauge choices. Suppose e_j are bounded in H^s, A_j, ω_j are bounded in H^{s-1}, and $s > 4$. Also impose a uniform lower bound on the smallest singular value of e_j, measured using fixed positive reference metrics. Sobolev compactness then gives a subsequence with $e_j \to e$ in C^2 and $A_j, \omega_j \to A, \omega$ in C^1. This assertion does not provide bounds or gauges for an arbitrary sequence of mother-theory solutions. In particular, on these regularity assumptions $D_\mu F^{\mu\nu}$ is naturally in H^{s-3}, not H^{s-1}.

If, in addition, $H_j \to H_0$ in C^1, $J_j \to J$ in L^1, and $r_j \to 0$ in distributions, testing (324) against a smooth one-form and integrating by parts passes the equation to $H_0 D_\mu F^{\mu\nu} = J^\nu$. The integrated terms involve $H_j F_j$ and first derivatives of the test form, with the convergent metric and connection coefficients. They therefore converge under the stated assumptions without demanding pointwise convergence of second derivatives of A_j. If instead $r_j \to r_\infty \neq 0$, this source remains in the limiting equation. Applying the same argument to a quantitatively matched coframe equation requires convergence of the stress tensor and of its actual geometric remainder. The Einstein tensor itself is continuous under the above C^2 convergence. These conclusions do not imply C^∞ convergence or removal of all physical scales.

For local stationary stability, Proposition 157 requires an invertible gauge-fixed linearization with a bounded inverse, together with bounds on the nonlinear and remainder terms. Gauge modes and physical zero modes must first be treated. Under its hypotheses, an equation defect bounded by δ gives a field

displacement at most $2K\delta$, where K bounds the inverse. The dependence on K is indispensable: the scalar equation $\varepsilon^2 z - \varepsilon = 0$ has residual ε at zero but solution $z = \varepsilon^{-1}$.

For Lorentzian evolution, an elliptic inverse cannot replace an energy estimate. Suppose a specified hyperbolic reduction and its propagated constraints yield, on $[0,T]$, an energy $E(t) \geq 0$ for the difference of two solutions satisfying

$$E'(t) \leq C(t)E(t) + f(t)^2, \qquad C \in L^1(0,T), \quad f \in L^2(0,T). \tag{328}$$

Multiplication by $\exp(-\int_0^t C)$ and integration give

$$E(t) \leq e^{\int_0^t C(u)\,\mathrm{d}u} E(0) + \int_0^t e^{\int_v^t C(u)\,\mathrm{d}u} f(v)^2\,\mathrm{d}v. \tag{329}$$

Here f must be obtained from the actual forcing and matching defect of the reduced equations, and E must control the chosen solution norm. The calculation does not establish the required hyperbolic reduction for an unrestricted higher-derivative branch. It specifies the estimate that a finite-time recovery argument must justify, including its initial data and constraint equations.

Finite examples that separate the errors. The following calculations use dimensionless synthetic fields. They isolate individual implications of the recovery argument; they are not observations or a nonlinear simulation of the entire mother theory. On the periodic interval $[0, 2\pi)$, prescribe a transverse abelian potential and its kinetic coefficient, with $|\alpha| < 1$, by

$$A_y = \sin x, \quad F_{xy} = \cos x, \quad H = 1 + \alpha \cos x, \quad J_y = -\sin x - \alpha \sin(2x). \tag{330}$$

Then $\partial_x(HF_{xy}) = J_y$, whereas $\partial_x F_{xy} - J_y = \alpha \sin(2x)$. Each of the two coefficient terms in (325) contributes half this canonical residual. With $h = 2\pi/N$, the centered difference of the exact flux gives the exact discrete root-mean-square error

$$e_h^2 = \tfrac{1}{2}\left[(1 - \operatorname{sinc} h)^2 + \alpha^2(1 - \operatorname{sinc}(2h))^2\right], \qquad \operatorname{sinc} z = \frac{\sin z}{z}. \tag{331}$$

The formula holds for the uniform meshes below, by discrete orthogonality of the two resolved sine modes. Its leading order is $e_h = h^2\sqrt{(1 + 16\alpha^2)/72} + O(h^4)$. The canonical continuum residual instead has root-mean-square norm $|\alpha|/\sqrt{2}$. Thus a convergent discretization can converge accurately to a constitutive equation different from the canonical one.

A second comparison uses the actual quadratic gravitational multiplier of (1775). For Fourier modes $k = 1, \ldots, 12$ and a unit source in each mode, compare

$$h_0(k) = k^{-2}, \quad h_\ell(k) = [k^2(1 + \ell^2 k^2)]^{-1}, \quad h_{\ell,h}(k) = [q_h(k)(1 + \ell^2 q_h(k))]^{-1}, \tag{332}$$

Table 2. Synthetic periodic gauge calculation at $\alpha = 0.2$. The second column tests the constitutive equation; the third compares with the constant-coefficient equation using the same source.

N	Flux residual	Canonical residual	Observed order
32	$5.79431 \cdot 10^{-3}$	0.14149404	—
64	$1.45312 \cdot 10^{-3}$	0.14142591	1.99548
128	$3.63565 \cdot 10^{-4}$	0.14142164	1.99887
256	$9.09090 \cdot 10^{-5}$	0.14142137	1.99972
512	$2.27284 \cdot 10^{-5}$	0.14142136	1.99993
1024	$5.68216 \cdot 10^{-6}$	0.14142136	1.99998

where $q_h(k) = 4h^{-2}\sin^2(kh/2)$ is the centered Laplacian symbol. At $\ell = 0.1$, increasing N from 64 to 1024 reduces $\|h_{\ell,h} - h_\ell\|_2/\|h_\ell\|_2$ from $2.45772 \cdot 10^{-3}$ to $9.35572 \cdot 10^{-6}$. The separate continuum correction $\|h_\ell - h_0\|_2/\|h_0\|_2 = 0.02435798$ is unchanged. The sharp band bound (1776) is a worst-source bound; a source concentrated in low modes need not saturate it.

The role of stability can be seen without an infinite-dimensional existence assumption. For $0 < \varepsilon < 1$, consider

$$V_\varepsilon(x, y) = \tfrac{1}{2}(x^2 + y^2) + \varepsilon xy + \varepsilon x. \tag{333}$$

Its Hessian has eigenvalues $1 \pm \varepsilon$, so it has the unique global minimizer

$$(x_\varepsilon, y_\varepsilon) = \left(-\frac{\varepsilon}{1-\varepsilon^2}, \frac{\varepsilon^2}{1-\varepsilon^2}\right), \qquad \|(x_\varepsilon, y_\varepsilon)\|_2 \le \frac{\varepsilon}{1-\varepsilon}. \tag{334}$$

Indeed, solving the two linear stationarity equations gives the displayed point, and the inverse Hessian has norm $(1-\varepsilon)^{-1}$. This finite example demonstrates the mechanism of a residual-to-distance bound, rather than verifying the Einstein linearization hypotheses.

Finally, a periodic 4×4 $SU(2)$ lattice tests the internal covariance. Let $T_a = i\sigma_a/2$, with σ_a the Pauli matrices, and use link variables $U_{x\mu}$. The Wilson functional and a local gauge transformation are

$$S_W = \sum_p (1 - \tfrac{1}{2}\operatorname{Re}\operatorname{tr} U_p), \qquad U_{x\mu} \mapsto G_x U_{x\mu} G_{x+\mu}^\dagger. \tag{335}$$

For reproducibility, the link exponent vectors are drawn as 0.3ξ and the gauge exponent vectors as η, with independent standard Gaussian components and generator seed 20261028. The force $f_{x\mu,a} = \partial_t S_W(e^{tT_a}U_{x\mu})\big|_{t=0}$ is computed by differentiating each plaquette product. It transforms by $f'_{x\mu,a} = R_{ab}(G_x) f_{x\mu,b}$, where $R_{ab}(G) = -2\operatorname{Re}\operatorname{tr}(T_a G T_b G^\dagger)$. In double precision, the action difference is $8.89 \cdot 10^{-16}$ or less, and the largest component of the analytic force-covariance

defect is $3.06 \cdot 10^{-16}$ or less. Central differences provide a separate check of the derivative. For a single varied link, $S_W(t) = a + b\cos(t/2) + c\sin(t/2)$, so the central derivative equals the exact force multiplied by $\mathrm{sinc}(t/2)$. This supplies its truncation error without choosing an arbitrary acceptance threshold. At very small steps, floating-point subtraction eventually dominates that error.

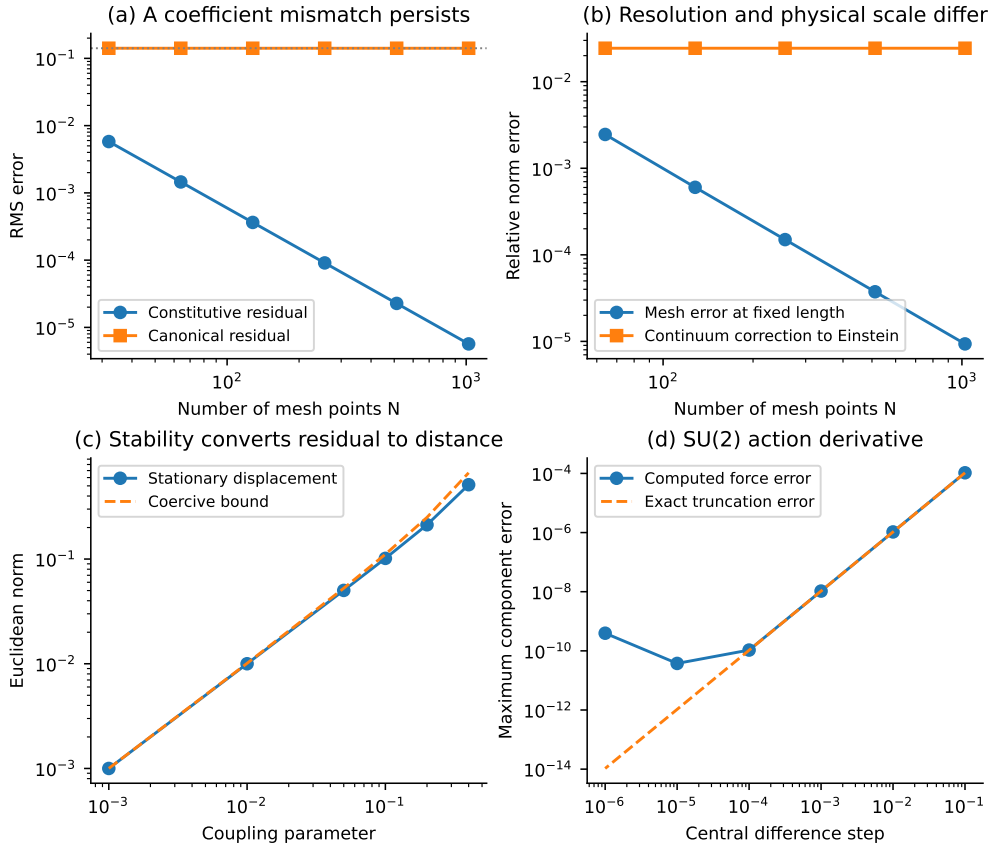


Figure 3. Four synthetic comparisons. (a) A variable-coefficient gauge equation is resolved with second-order accuracy while its canonical mismatch persists. (b) Mesh error and the fixed physical curvature correction have different limits. (c) A coercive finite stationary model obeys its explicit displacement bound. (d) Independent central differences of the lattice action agree with its analytic derivative until roundoff competes with truncation. These calculations test the stated finite mechanisms, not a full nonlinear or quantum continuum completion.

These comparisons make the next field-theoretic task precise. The common action supplies the coefficients and the exact projected equations. A selected

branch must then supply uniform regularity, constraint propagation and stability, with the physical correction kept separate from the discretization error. The matter equations considered next determine the sources in that comparison and their exchange with the geometric and internal fields.

5.9. *Matter, order parameter, and information.*

5.10. *Matter coupling.* The master Dirac-type operator is written schematically as

$$\mathscr{D}_{\mathbb{A}} = \gamma^{\mu}\mathbb{D}_{\mu} + \mathcal{Y}(\Phi_H, \chi), \tag{336}$$

where $\mathcal{Y}$ is a master Yukawa-type endomorphism. The following notation denotes the matter component of the low-energy expansion of (52), not an additional primitive action:

$$\mathcal{S}_{\mathrm{mat}} = \int_M \sqrt{g}\,\overline{\Psi}\mathscr{D}_{\mathbb{A}}\Psi\,\mathrm{d}^4x. \tag{337}$$

The displayed first-order Grassmann expression is a conditional effective identification. The extended norm in (51) contains the quadratic component $\langle \mathbb{D}\Psi, \mathbb{D}\Psi\rangle$; obtaining a first-order Dirac action requires an additional fermionic construction, such as a supertrace, a spectral determinant, or the elimination of auxiliary variables. No such construction is assumed in the abstract framework, so the Dirac term is not claimed to follow from the norm alone. For a complete physical theory, the representations of Ψ, chirality, reality conditions, and anomaly cancellation must all follow from the master representation problem. The conventional normalization and chiral-field bookkeeping can be compared with [128] and [162].

More explicitly, whenever the selected Euclidean geometry admits a spin structure, the matter field has the form

$$\Psi \in \Gamma\big(S_{g[\mathbb{X}]} \otimes E_{\mathcal{R}}\big), \qquad E_{\mathcal{R}} := P_H \times_{\mathcal{R}} V_{\mathcal{R}}, \tag{338}$$

where $S_{g[\mathbb{X}]}$ is the spinor bundle of the induced metric and $\mathcal{R}$ is a representation supplied by the master representation problem. In the worked candidate, the familiar fields Q_L, u_R, d_R, L_L, e_R are prescribed representation components. In a predictive realization, the selection problem must instead determine why these components, and any additional fields, are retained. Equation (338) is conditional on the existence of a spin lift and on the extension of the relevant H-representation; it does not by itself prove the observed chiral spectrum.

5.11. *Information as a state coordinate.* The information variable χ is defined as a coordinate on the state manifold rather than as an independently added force. If its state space carries a linear representation ρ_χ of the master group, a minimal covariant coupling is

$$\mathbb{D}\chi = \mathrm{d}\chi + \rho_\chi(\mathbb{A})\chi. \tag{339}$$

The model may then admit an information–geometry interaction through the same master metric,

$$\|\mathbb{D}\chi\|^2_{\mathbb{G}}\,. \tag{340}$$

The physical status of χ remains open. It may ultimately be eliminated as an auxiliary variable, identified with an information-theoretic order parameter, or promoted to a microscopic field. The present formulation does not assume which interpretation is correct. Related geometric treatments of matter and internal data in a unified spectral setting include [45], [44], [10], [155], [83], [46], [28], and [30].

5.12. *Spectral and heat-kernel reduction.* The classical variations identify the field equations on a specified branch. Fluctuations around that branch contribute further local operators. The heat kernel organizes those operators by dimension; the determinant also tests whether the chosen background admits a stable Gaussian expansion. Positivity of a principal symbol and stability of the entire quadratic operator are different requirements.

5.13. *One operator, one spectral object.* Suppose the quadratic fluctuation operator around a selected background $\mathbb{X}_*$ is a Laplace-type operator

$$L = -\left(g^{\mu\nu}\nabla_\mu\nabla_\nu + E\right). \tag{341}$$

Here g is the metric induced by the selected coframe as in (37); on a preliminary regulator it means the auxiliary $\bar{g}$. Thus the heat kernel is a low-energy/effective expansion around a selected master geometry. It can generate the local invariants R, F^2, and matter endomorphism terms once the operator and the selected background are specified, but it does not by itself construct a metric, a Cartan bundle, or a residual gauge group from no prior geometric data. For the determinant calculation, assume that the Euclidean manifold is smooth and closed and that L has a self-adjoint elliptic realization. After removing its finite-dimensional kernel, assume in addition that the remaining spectrum is strictly positive. Let $P_{\ker L}$ denote the orthogonal projection onto the kernel, and write

$$\mathrm{Tr}'(e^{-tL}) := \mathrm{Tr}(e^{-tL}) - \dim\ker L = \sum_{\lambda_j>0} e^{-t\lambda_j}. \tag{342}$$

The equality with the last sum uses the absence of negative eigenvalues. On a compact manifold the positive spectrum has a lower bound $\lambda_1 > 0$. For $t \geq 1$,

$$\mathrm{Tr}'(e^{-tL}) \leq e^{-(t-1)\lambda_1}\,\mathrm{Tr}'(e^{-L}), \tag{343}$$

so the large-t part of the proper-time integral converges. The Laplace-type principal symbol alone does not imply this positivity. For example, $L = -\Delta_g - m^2$, with $m > 0$, has a negative constant mode on a closed connected manifold; that mode contributes e^{tm^2}. Such a background requires a separate

treatment of unstable directions and cannot be integrated as a positive Gaussian equilibrium.

The factor of the fluctuation scale can be fixed without a formal infinite-dimensional integral. Retain N positive modes, write their coordinates as y_j, and let L_N be the restricted Hessian. Gaussian integration gives

$$\begin{aligned}\int_{\mathbb{R}^N} \exp\left(-\frac{y^{\mathsf{T}} L_N y}{2\theta}\right) \mathrm{d}y &= (2\pi\theta)^{N/2} (\det L_N)^{-1/2}, \\ \Delta\mathcal{S}_{1-\mathrm{loop},N} &= \frac{\theta}{2} \sum_{j=1}^{N} \log\left(\frac{\lambda_j}{\mu_{\mathrm{ref}}^2}\right) + C_N.\end{aligned} \tag{344}$$

Here $\mu_{\mathrm{ref}} > 0$ is a fixed mass unit and C_N records the chosen finite-dimensional reference normalization. The effective action is defined by the weight $\exp(-\mathcal{S}_{\mathrm{eff}}/\theta)$; therefore its one-loop term contains θ. Dividing the entire effective action by θ instead gives the frequently used dimensionless $\frac{1}{2}\log\det$ expression. These conventions agree with the explicit heavy-field integration in Section 11.10.

For positive λ and μ_{ref}^2, the identity

$$\log\frac{\lambda}{\mu_{\mathrm{ref}}^2} = -\int_0^\infty \frac{e^{-t\lambda} - e^{-t\mu_{\mathrm{ref}}^2}}{t}\,\mathrm{d}t \tag{345}$$

follows by differentiation with respect to λ and evaluation at $\lambda = \mu_{\mathrm{ref}}^2$. The numerator is $O(t)$ at zero and decays at infinity. Summing this identity over the retained modes explains both the sign and the subtraction in a proper-time regulator.

In the continuum, the reference and scale must remain visible. If a positive reference operator L_{ref} is chosen with the same zero-mode convention and the relative heat trace has the required trace-class and small-time properties, define

$$\begin{aligned}\log \det{}'_{\epsilon}(L, L_{\mathrm{ref}}) &:= -\int_\epsilon^\infty \frac{\mathrm{d}t}{t}\left\{\mathrm{Tr}'(e^{-tL}) - \mathrm{Tr}'(e^{-tL_{\mathrm{ref}}})\right\}, \\ \Delta\mathcal{S}^{(\epsilon)}_{1-\mathrm{loop}} &:= \frac{\theta}{2}\log \det{}'_{\epsilon}(L, L_{\mathrm{ref}}).\end{aligned} \tag{346}$$

This relative definition reduces in N dimensions to the sum of the Frullani identities after taking $L_{\mathrm{ref}} = \mu_{\mathrm{ref}}^2 I_N$. An alternative absolute definition uses spectral zeta continuation:

$$\begin{aligned}\zeta_{L/\mu_{\mathrm{ref}}^2}(s) &:= \mathrm{Tr}'\left[(L/\mu_{\mathrm{ref}}^2)^{-s}\right] = \mu_{\mathrm{ref}}^{2s}\zeta_L(s), \\ \log \det{}'_{\zeta}(L/\mu_{\mathrm{ref}}^2) &:= -\zeta'_{L/\mu_{\mathrm{ref}}^2}(0) = -\zeta'_L(0) - 2\zeta_L(0)\log\mu_{\mathrm{ref}},\end{aligned} \tag{347}$$

provided ζ_L is regular at zero. Thus the normalization-scale dependence is explicit rather than hidden in an unspecified additive constant. If the

relative small-time cancellations do not hold, removing the ultraviolet cutoff requires the local counterterms determined by the heat expansion. Their background dependence cannot in general be absorbed into a numerical constant. Finite scheme-dependent local terms must be fixed by declared renormalization conditions. Zero modes require collective coordinates or a quotient construction in addition to their removal from the determinant. Fermionic and ghost determinants have their own signs and multiplicities, fixed by the specified quadratic field content. The unprimed local heat trace has the asymptotic expansion [156]

$$\operatorname{Tr}(e^{-tL}) \sim \frac{1}{(4\pi t)^2} \sum_{k=0}^{\infty} t^k \int_M \operatorname{tr}(a_{2k}(x, L))\ \operatorname{vol}_g . \tag{348}$$

The coefficients contain curvature, bundle curvature, and endomorphism invariants. Consequently, a single master fluctuation operator can generate gravitational and gauge invariants in the same expansion. The sign convention and integrated heat coefficients used here are summarized in Appendix D.

For example, in a standard Laplace-type convention,

$$a_0 = \mathrm{Id}, \tag{349}$$

$$a_2 = E + \frac{1}{6} R\,\mathrm{Id}, \tag{350}$$

$$\begin{aligned} a_4 = \frac{1}{360}\Big[&60\nabla^\mu\nabla_\mu E + 60RE + 180E^2 + 30\Omega_{\mu\nu}\Omega^{\mu\nu} \\ &+ \left(12\Box R + 5R^2 - 2R_{\mu\nu}R^{\mu\nu} + 2R_{\mu\nu\rho\sigma}R^{\mu\nu\rho\sigma}\right)\mathrm{Id}\Big], \end{aligned} \tag{351}$$

where $\Omega_{\mu\nu} = [\nabla_\mu, \nabla_\nu]$. On a closed manifold the displayed $\nabla^2 E$ and $\Box R$ terms integrate to zero, but they are part of the local coefficient. The precise signs and multiplicities depend on the convention for L and the bundle connection; the convention must be fixed before numerical matching. Standard references for these coefficients and their geometric applications are [78], [59], [17], and [158].

5.14. *Effective action.* After renormalization and symmetry reduction, one obtains schematically

$$\begin{aligned} \mathcal{S}_{\mathrm{eff}} = \int_M \sqrt{g}\,\Big[&\Lambda_{\mathrm{eff}} - \frac{R}{16\pi G_{\mathrm{eff}}} + \sum_a \frac{1}{4g_a^2} F^a_{\mu\nu} F^{a\mu\nu} \\ &+ |D\Phi_H|^2 + V_{\mathrm{eff}}(\Phi_H) + \overline{\Psi}\not{\mathcal{D}}\Psi + \mathcal{S}_{\mathrm{higher}}\Big]\,\mathrm{d}^4x. \end{aligned} \tag{352}$$

Equation (352) is a target effective structure. It is not a numerical prediction until the complete microscopic operator, field content, measure, regularization, and renormalization conditions are specified.

6. **Group selection and the conditional (331) phase**

6.1. *The group-selection problem.* The preceding reductions begin with a fixed candidate. Selecting among candidates adds a comparison problem: the equilibrium free energy must be defined with compatible units, normalization, and admissibility rules. Existence of an equilibrium within each candidate does not imply existence or uniqueness of a minimizer across candidates. The next results specify the additional compactness conditions and exhibit an obstruction when positive curvature coefficients remain unrestricted.

6.2. *Why the gauge group cannot be inserted.* A circular construction would begin with

$$\mathfrak{g}_{\mathrm{int}} = \mathfrak{su}(3) \oplus \mathfrak{su}(2) \oplus \mathfrak{u}(1) \tag{353}$$

and then recover the Standard Model action from it. That is a reconstruction, not a derivation of the group. The construction first defines a type-admissible candidate class $\mathscr{G}_{\mathrm{cand}}$ of master-data packages Γ of the form (55). The notation $\mathscr{A}$ below is retained only as a short name for this class: $\mathscr{A} := \mathscr{G}_{\mathrm{cand}}$. Membership means that the candidate has a well-defined configuration and reference-measure class, an invariant pairing, admissible representations, and a positive Euclidean regularization. The anomaly, stability, locality, and stochastic well-posedness requirements are imposed in the consistency-admissible subclass $\mathscr{G}_{\mathrm{adm}}$ defined below; they are not inferred from the desired residual group.

For each candidate $\Gamma \in \mathscr{A}$, use the full master-data package (55); the notation $\Gamma = (\mathfrak{g}, \mathbf{h}, \mathcal{R}, \mathcal{B})$ in the next display is only a projection onto the algebra, pairing, representation, and vacuum components. All omitted components of the package, including the configuration space, reference measure, mobility, regularization, and information data, remain part of the candidate label. Fix a normalized reference measure ν_Γ, a dimensionless normalization scale, and an explicitly specified candidate configuration space $\mathfrak{X}_\Gamma$. The admissible probability class $\mathcal{P}_\Gamma$ consists of normalized densities p on $\mathfrak{X}_\Gamma$, not of pairs containing a second copy of the random configuration. Here $\mathcal{B}$ denotes vacuum or order-parameter data and is distinct from the stochastic diffusion coefficient. If a candidate contains an externally fixed background β, it is included in the label Γ; if it is to be optimized, one must instead specify a separate class $\mathcal{B}_\Gamma$ and take an explicitly stated additional infimum over $\beta \in \mathcal{B}_\Gamma$. These choices, as well as the consistency class below, must be fixed before the low-energy target is inspected; otherwise the selection rule can encode the desired answer by construction. Cross-candidate comparison also requires a common dimensionless unit convention, a reference-measure normalization rule fixed for the entire candidate class, a common fluctuation scale θ, and a common additive zero for the renormalized action and free energy. If an embedding or quotient map is used to compare configuration spaces, its treatment of the reference

measure must be specified explicitly. Such a map is not required merely to evaluate the real-valued scores on different spaces. For the finite compact-group examples below, the common rule is product Haar probability on every compact group factor and the same declared scalar reference law. This rule is part of the comparison problem; it is not inferred from equilibrium of an individual candidate. Candidate-dependent shifts, rescalings, or regulator-dependent constants are not allowed. A prescribed common reference configuration, when available, can fix the additive action zero by subtraction of its action value. That subtraction does not fix the reference-measure normalization, which must still be supplied separately. Finally, assume that every $\mathcal{P}_\Gamma$ is nonempty and that the stated coercivity/compactness hypotheses make the infimum finite and attained whenever $\mathscr{C}_{\mathrm{cons}}(\Gamma) < \infty$. For a candidate Γ, let $\mathcal{F}_\Gamma[p]$ denote the free-energy functional of Section 4.1 restricted to $\mathfrak{X}_\Gamma$, ν_Γ, and the candidate master action. Define the selection functional

$$\mathscr{S}_{\mathrm{sel}}(\Gamma) := \inf_{p \in \mathcal{P}_\Gamma} \left\{ \mathcal{F}_\Gamma[p] + \mathscr{C}_{\mathrm{cons}}(\Gamma) \right\}, \tag{354}$$

where $\mathscr{C}_{\mathrm{cons}}$ is not a phenomenological fit penalty but the indicator of a previously stated consistency class encoding normalization, anomaly, positivity, stability, locality, stochastic well-posedness, and any explicitly declared renormalization or effective-field-theory consistency constraints. It contains no adjustable group-dependent weights and does not refer to the observed group label. In the strict version, inconsistency is assigned infinite cost:

$$\mathscr{C}_{\mathrm{cons}}(\Gamma) = +\infty \tag{355}$$

whenever the candidate violates a required consistency condition.

The selected phase is

$$\Gamma_* \in \operatorname*{arg\,min}_{\Gamma \in \mathscr{G}_{\mathrm{adm}}} \mathscr{S}_{\mathrm{sel}}(\Gamma). \tag{356}$$

The Standard Model group is predicted only if the minimizer is unique up to the declared notion of isomorphism and its residual group is the observed one. This statement has three logically distinct levels:

(S1) *Existence*: the admissible infimum is attained, so that

$$\operatorname*{arg\,min}_{\Gamma \in \mathscr{G}_{\mathrm{adm}}} \mathscr{S}_{\mathrm{sel}}(\Gamma) \neq \varnothing. \tag{357}$$

(S2) *Uniqueness*: the minimizing equivalence class is unique (or a finite list of classes is obtained together with a stated residual degeneracy).

(S3) *Identification*: the residual stabilizer of that class is $SU(3)_c \times SU(2)_L \times U(1)_Y$, and the subsequent electroweak stabilizer is $U(1)_{\mathrm{em}}$.

Only the first two levels are variational existence or compactness questions; the third additionally requires the representation and symmetry-breaking calculation. None of the three levels is silently inferred from the notation G_{SM}.

6.3. *Anomaly cancellation as a constraint.* For anomaly bookkeeping, let $\mathcal{R}_L$ and $\mathcal{R}_R$ denote the original left- and right-handed Weyl representations, respectively. A right-handed contribution enters with the opposite chirality sign. Equivalently, one may convert every right-handed field to a left-handed field in $\mathcal{R}_R^*$ and add the corresponding conjugate trace. We use the equivalent two-chirality notation below, with T_R acting in the original right-handed representation. The perturbative cubic gauge-anomaly tensor is schematically

$$\mathcal{A}^{abc} := \mathrm{tr}_{\mathcal{R}_L}\Big(T^a\{T^b,T^c\}\Big) - \mathrm{tr}_{\mathcal{R}_R}\Big(T^a\{T^b,T^c\}\Big) = 0, \tag{358}$$

where the indices range over all gauge generators. The mixed gauge–gravitational condition is a separate linear trace constraint for each abelian generator,

$$\mathcal{A}^a_{\mathrm{grav}} := \mathrm{tr}_{\mathcal{R}_L}(T^a) - \mathrm{tr}_{\mathcal{R}_R}(T^a) = 0. \tag{359}$$

Thus the cubic equation covers $U(1)^3$ and mixed abelian–nonabelian gauge anomalies, whereas the second equation covers the gauge–gravitational anomaly. Independent global conditions, such as the mod–2 $SU(2)$ anomaly when applicable, must be checked separately. All of these tests must be carried out in a concrete representation. A candidate master phase that fails any required condition cannot define a consistent chiral quantum gauge theory in the usual framework.

Accordingly, in a realization in which these anomalies are part of the quantum consistency requirements, the admissible class can be written more explicitly as

$$\mathscr{G}_{\mathrm{adm}} := \left\{ \Gamma \in \mathscr{G}_{\mathrm{cand}} : \begin{array}{ll} \mathcal{A}^{abc}(\Gamma) = 0, & \mathcal{A}^a_{\mathrm{grav}}(\Gamma) = 0, \\ \mathcal{A}_{\mathrm{global}}(\Gamma) = 0, & \mathscr{C}_{\mathrm{reg}}(\Gamma) < \infty \end{array} \right\}. \tag{360}$$

where $\mathcal{A}_{\mathrm{global}}$ denotes the collection of required global tests (for example, the mod–2 $SU(2)$ condition when applicable) and $\mathscr{C}_{\mathrm{reg}}$ collects the previously stated positivity, stability, locality, compactness/coercivity, stochastic well-posedness, and the declared renormalization or effective-field-theory consistency criterion. Equation (360) is a definition of the candidate class, not an assertion that any particular master algebra has yet been found in it. If a proposed realization does not contain a chiral quantum sector, the corresponding anomaly conditions must be removed explicitly rather than silently declared satisfied.

6.4. *Coercive selection and uniqueness modulo equivalence.* The preceding definition specifies what may be compared, but it does not by itself prove that a comparison has a minimizer or that the minimizer is unique. Those are separate

compactness questions. We make the relevant notion of sameness explicit before stating a selection result. Two master packages Γ and Γ' are called *package-equivalent*, written $\Gamma \sim \Gamma'$, if there is a bundle and field redefinition that consists of a Lie-group isomorphism $u : \widetilde{G}_\Gamma \to \widetilde{G}_{\Gamma'}$ on the master groups, an isomorphism of the associated bundles and representations, and a configuration-space bijection $\mathscr{T} : \mathfrak{X}_\Gamma \to \mathfrak{X}_{\Gamma'}$, such that the following data are preserved (with v, w tangent vectors):

$$\begin{gathered}\mathbb{F}_{\Gamma'}(\mathscr{T}x) = u_*\mathbb{F}_\Gamma(x), \qquad u^*\mathbf{h}_{\Gamma'} = \mathbf{h}_\Gamma, \qquad \mathscr{T}^*\nu_{\Gamma'} = \nu_\Gamma, \qquad \mathcal{S}_{\Gamma'}[\mathscr{T}x] = \mathcal{S}_\Gamma[x], \\ \mathbb{G}_{\Gamma'}(\mathscr{T}_*v, \mathscr{T}_*w) = \mathbb{G}_\Gamma(v, w), \qquad \mathbb{M}_{\Gamma'}(\mathscr{T}x) \circ \mathscr{T}^{-*} = \mathscr{T}_* \circ \mathbb{M}_\Gamma(x),\end{gathered} \tag{361}$$

and the order-parameter and information maps intertwine under the same identifications. Here $\mathscr{T}^{-*}$ denotes the cotangent pushforward, the dual inverse of $\mathscr{T}_*$, so that both sides of the mobility identity have type $T^*_x\mathfrak{X}_\Gamma \to T_{\mathscr{T}x}\mathfrak{X}_{\Gamma'}$. The equality of measures in (361) is understood after the common dimensionless normalization fixed above. Thus a smooth invertible change of coordinates, an admissible gauge transformation, or a representation relabeling does not create a new candidate when it satisfies all these requirements. In particular the map $\mathscr{T}$ is required to be a diffeomorphism on the regularized configuration manifolds, to transport $\mathcal{P}_\Gamma$ bijectively onto $\mathcal{P}_{\Gamma'}$, and to preserve the consistency indicator and regularization domains. Preservation of the displayed action and measure alone would not guarantee preservation of a separately restricted admissible density class. Conversely, a change of a coupling, a change of the reference measure, a different regularization, or a different residual stabilizer is not declared equivalent unless an isomorphism satisfying (361) is supplied. We write $\mathscr{Q} := \mathscr{G}_{\mathrm{adm}}/\!\sim$ for the resulting set of equivalence classes and $[\Gamma]$ for the class of Γ.

The package-equivalence requirement is also what makes the selection functional independent of the representative. Indeed, if $p \in \mathcal{P}_\Gamma$, pushforward by $\mathscr{T}$ gives a density $\mathscr{T}_\# p \in \mathcal{P}_{\Gamma'}$. Equation (361), together with the common entropy reference, then gives

$$\mathcal{F}_{\Gamma'}[\mathscr{T}_\# p] = \mathcal{F}_\Gamma[p], \qquad \mathscr{S}_{\mathrm{sel}}(\Gamma') = \mathscr{S}_{\mathrm{sel}}(\Gamma). \tag{362}$$

Consequently $\mathscr{S}_{\mathrm{sel}}$ descends to a well-defined extended-real functional $\overline{\mathscr{S}}_{\mathrm{sel}}$ on $\mathscr{Q}$.

For an infinite candidate class, a precise coercivity assumption is the following. Equip $\mathscr{Q}$ with the topology induced by the chosen topology on the master data and assume that it is Hausdorff. We call the selection functional *coercive on the quotient* if, for every finite R,

$$\mathscr{K}_R := \big\{ q \in \mathscr{Q} : \overline{\mathscr{S}}_{\mathrm{sel}}(q) \le R \big\} \quad \text{is compact,} \tag{363}$$

and if $\overline{\mathscr{S}}_{\mathrm{sel}}$ is lower semicontinuous. In a metrizable parameterization, (363) means that every sequence of bounded selection cost has a convergent subsequence whose limit remains in the corresponding sublevel. In particular, any sequence escaping every compact subset has cost tending to infinity. This condition is a property to be proved for a concrete class; it is not a consequence of merely listing the possible groups.

THEOREM 13 (Coercive existence and uniqueness modulo package equivalence). *Assume the following conditions.*

(E1) The consistency class $\mathscr{G}_{\mathrm{adm}}$ and the indicator $\mathscr{C}_{\mathrm{cons}}$ are fixed before the observed low-energy group is inspected. They use only intrinsic algebraic, analytic, stochastic, locality, positivity, anomaly, and renormalization conditions; in particular, they do not contain the statement that a specified residual group is preferred.

(E2) For every $\Gamma \in \mathscr{G}_{\mathrm{adm}}$ with $\mathscr{C}_{\mathrm{cons}}(\Gamma) < \infty$, the class $\mathcal{P}_\Gamma$ is nonempty and sequentially compact in the topology used for probability measures, and $\mathcal{F}_\Gamma$ is proper and lower semicontinuous on that class. The value $\inf_{p\in\mathcal{P}_\Gamma} \mathcal{F}_\Gamma[p]$ is finite.

(E3) The common units, reference-measure normalization, fluctuation scale, and additive zero of the renormalized free energy have been fixed as in the preceding subsection, and package-equivalent candidates satisfy (362).

(E4) The quotient $\mathscr{Q}$ is Hausdorff and $\overline{\mathscr{S}}_{\mathrm{sel}}$ is proper, lower semicontinuous, and coercive in the sense of (363)*; in particular, it is bounded below and finite for at least one admissible class.*

Then the following conclusions hold.

(i) For every admissible Γ with finite consistency cost, there exists $p_\Gamma \in \mathcal{P}_\Gamma$ satisfying $\mathcal{F}_\Gamma[p_\Gamma] = \inf_{p\in\mathcal{P}_\Gamma} \mathcal{F}_\Gamma[p]$.

(ii) The quotient minimizer set

$$\operatorname*{argmin}_{q\in\mathscr{Q}} \overline{\mathscr{S}}_{\mathrm{sel}}(q) \tag{364}$$

is nonempty and compact.

(iii) The microscopic package is uniquely selected modulo the declared equivalence precisely when this minimizer set consists of one class. If q_* denotes that class and the quotient is not a singleton, a sufficient and directly checkable condition is the strict gap

$$\Delta_{\mathrm{sel}} := \inf_{q\in\mathscr{Q},\ q\neq q_*} \big(\overline{\mathscr{S}}_{\mathrm{sel}}(q) - \overline{\mathscr{S}}_{\mathrm{sel}}(q_*)\big) > 0. \tag{365}$$

A zero gap leaves uniqueness undecided by this criterion: distinct minimizing classes give a degeneracy, but a unique minimizer can also have zero gap. For example, $s(q) = q^2$ on $\mathbb{R}$ has the unique minimizer $q = 0$, while $\inf_{q\neq 0} s(q) = 0$.

The theorem gives no identification of a particular physical group. Such an identification is an additional statement that the residual stabilizer map of the selected class has the claimed value.

Proof. Fix Γ with finite consistency cost and let $(p_n)_{n\geq 1} \subset \mathcal{P}_\Gamma$ be a minimizing sequence for $\mathcal{F}_\Gamma$. By (E2), a subsequence converges in the prescribed weak topology to some $p_\Gamma \in \mathcal{P}_\Gamma$. Lower semicontinuity gives

$$\mathcal{F}_\Gamma[p_\Gamma] \leq \liminf_{n\to\infty} \mathcal{F}_\Gamma[p_n] = \inf_{p\in\mathcal{P}_\Gamma} \mathcal{F}_\Gamma[p], \tag{366}$$

while the reverse inequality follows from the definition of the infimum. This proves (i), and hence the inner infimum in (354) is an attained value.

Let s_* be the infimum of $\overline{\mathscr{S}}_{\mathrm{sel}}$ on $\mathscr{Q}$, and choose a minimizing sequence (q_n). Since at least one finite-cost class exists, $s_* < +\infty$; after discarding finitely many terms, the sequence lies in the sublevel set $\mathscr{K}_{s_*+1}$. Coercivity makes this set compact, so a subnet (or a subsequence in the metrizable case) converges to some $q_* \in \mathscr{K}_{s_*+1}$. Lower semicontinuity yields

$$\overline{\mathscr{S}}_{\mathrm{sel}}(q_*) \leq \liminf \overline{\mathscr{S}}_{\mathrm{sel}}(q_n) = s_*. \tag{367}$$

The definition of s_* gives the opposite inequality, so equality holds. The minimizer set is a closed subset of the compact sublevel set and is therefore compact. By definition, it consists of one element exactly when the selected package is unique modulo $\sim$. If (365) holds, every other class has strictly larger cost, so the minimizer set is the singleton $\{q_*\}$. Conversely, a singleton minimizer does not in general imply a positive gap on a non-discrete quotient; therefore the gap is stated as a sufficient, not a necessary, criterion in that case. No step of the argument uses the name of an observed residual group. □

The finite comparison used in an explicit regularization can be stated without any topological assumption. It is useful because it separates the existence of a candidate list from the physical identification of the selected phase.

THEOREM 14 (Finite candidate selection). *Let $N \geq 1$ and let $\mathscr{Q}_{\mathrm{fin}} = \{q_1, \ldots, q_N\} \subset \mathscr{Q}$ be a finite list of pairwise inequivalent, target-blind admissible package classes, and suppose that each class has a finite real, attained inner free-energy minimum. Put*

$$s_i := \overline{\mathscr{S}}_{\mathrm{sel}}(q_i), \qquad s_{\min} := \min_{1\leq i\leq N} s_i, \qquad I_* := \{i : s_i = s_{\min}\}. \tag{368}$$

Then the selected classes in the finite list are exactly $\{q_i : i \in I_*\}$. In particular, the selection is unique modulo package equivalence if and only if $|I_*| = 1$. When $N > 1$ and $|I_*| = 1$, the strict finite gap

$$\Delta_{\mathrm{fin}} := \min_{i\neq i_*}(s_i - s_{i_*}) > 0 \tag{369}$$

is an explicit certificate of uniqueness within the listed class. If $|I_*| > 1$, the tied classes are not distinguishable by the stated selection functional and no unique physical group may be claimed from this finite comparison.

Proof. The set of real numbers $\{s_1, \dots, s_N\}$ is finite, so its minimum $s_{\min}$ exists. A class q_i belongs to the finite-list argmin precisely when $s_i = s_{\min}$, which is the definition of I_*. If $|I_*| = 1$, every other value exceeds $s_{\min}$; the minimum of the finitely many positive differences is therefore positive and equals Δ_{fin}. If $|I_*| > 1$, at least two inequivalent classes have exactly the same cost, so the selection rule leaves a genuine degeneracy. The argument is purely a comparison of the pre-specified target-blind costs and does not use the desired low-energy label. □

Thus, in a concrete model, uniqueness is a theorem only after one supplies the candidate topology or a finite exhaustive list, proves the inner free-energy compactness, fixes the common normalization, and verifies either the singleton quotient argmin or the strict gap in (365) or (369). The residual group is then computed from the stabilizer of the selected vacuum; it is not inserted into the selection cost. The explicit candidate Γ_0 of Section 5.4 can therefore serve as one member of such a list, but it is an existence witness until all competing classes have been included and compared.

6.5. *An obstruction to unrestricted coupling and group selection.* The compactness and separation assumptions in the selection theorems are substantive restrictions on the candidate class. A common positive norm and a unique equilibrium for each candidate do not supply them. First, the absolute selection score must be distinguished from the normalized equilibrium law. If the admissible density class contains the Gibbs minimizer, its score is $-\theta \log Z$. Replacing an action and reference measure by $S + A$ and $c\nu$, respectively, gives

$$Z' = ce^{-A/\theta} Z, \qquad -\theta \log Z' = -\theta \log Z + A - \theta \log c. \tag{370}$$

The normalized Gibbs probability and reversible generator are unchanged. This proves the necessity of the previously imposed common additive zero and reference normalization. Such candidate-dependent changes are excluded from the selection problem stated here. The following obstruction persists even after excluding them.

THEOREM 15 (Monotonicity obstruction for a free positive coefficient). *Fix a reference measure ν, a scale $\theta > 0$, and measurable functions S_0, V, with V finite and nonnegative almost everywhere. Assume*

$$0 < Z_0 := \int e^{-S_0/\theta} \, \mathrm{d}\nu < \infty, \qquad \int_{\{V>0\}} e^{-S_0/\theta} \, \mathrm{d}\nu > 0. \tag{371}$$

For $\kappa > 0$, let $S_\kappa = S_0 + \kappa V$ and suppose each package has zero consistency indicator and an admissible density class containing its Gibbs density. Use the relative free-energy extension just defined; alternatively, require the Gibbs energy moment to be finite and restrict the class to densities with separately integrable energy and entropy. Then its selection score is

$$s(\kappa) = -\theta \log Z_\kappa, \qquad Z_\kappa = \int e^{-(S_0+\kappa V)/\theta} \, \mathrm{d}\nu, \tag{372}$$

and s is continuous and strictly increasing on $(0, \infty)$. Moreover,

$$s'(\kappa) = \int V \, \mathrm{d}\pi_\kappa > 0, \qquad \lim_{\kappa \downarrow 0} s(\kappa) = -\theta \log Z_0. \tag{373}$$

Consequently the candidate family with every $\kappa > 0$ has no minimizer. If zero curvature coefficient is inadmissible, its infimum is approached only at an excluded endpoint. If instead the permitted interval is $[\kappa_{\min}, \kappa_{\max}]$ with $\kappa_{\min} > 0$, minimization selects the prescribed boundary $\kappa_{\min}$.

Proof. The Gibbs identity gives (372). If $0 < \kappa_1 < \kappa_2$, the integrand defining Z_{κ_2} is at most that defining Z_{κ_1} and is strictly smaller on a set of positive weighted measure. Hence $0 < Z_{\kappa_2} < Z_{\kappa_1} \le Z_0$. Dominated convergence proves continuity and the limit at zero. For κ in a compact subinterval of $(0, \infty)$, the bound $v e^{-\kappa v/\theta} \le \theta/(e\kappa)$ for $v \ge 0$ supplies an integrable dominator after multiplication by $e^{-S_0/\theta}$. Differentiation under the integral gives

$$Z_\kappa' = -\theta^{-1} \int V e^{-S_\kappa/\theta} \, \mathrm{d}\nu, \qquad s'(\kappa) = -\theta Z_\kappa'/Z_\kappa, \tag{374}$$

which proves (373). Every positive κ is strictly improved by $\kappa/2$, proving nonattainment on the open family. Strict monotonicity also proves the endpoint assertion on a closed permitted interval. □

For the bosonic joint action, an independently variable internal coefficient has precisely this form, with

$$V_a = \frac{1}{2} \int_M e^{-\alpha_\sigma \sigma} |F_a|^2 \, \mathrm{vol}_g \ge 0. \tag{375}$$

This application fixes the regulator, reference measure, and all remaining data while varying that coefficient. If all positive values are retained, the sequence $\kappa_j \downarrow 0$ has bounded selection score but no limit in the positive-coefficient class. The coercivity hypothesis therefore fails in its ordinary parameter topology. A restriction excluding this sequence may be physically appropriate, but must be separately supplied.

There are also inequivalent gauge groups with the same scalar confinement and finite-regulator equilibrium mechanism. For each integer $n \ge 2$, set

$$\widetilde{G}_n = SO(5) \times SU(n), \qquad H_n = SO(4) \times SU(n). \tag{376}$$

The quotient dimension is four for every n. Take a common fixed Cartan background and a bosonic matter choice. No chiral fermionic anomaly is introduced by this choice; a chiral spectrum is not being derived.

An explicit compact gauge regulator has four links $U_1, \dots, U_4 \in SU(n)$ with product Haar probability $\mathrm{d}U$ and

$$P(U) = U_1 U_2 U_3^{-1} U_4^{-1}, \qquad C_n(U) = \tfrac{1}{2}\|I - P(U)\|_{\mathrm{F}}^2 = n - \operatorname{Re}\operatorname{tr} P(U). \quad (377)$$

It is a smooth nonnegative gauge-invariant squared curvature coordinate. Conditional on three links, the plaquette is Haar distributed. Since a point has Haar measure zero in $SU(n)$, $C_n > 0$ almost everywhere. This is a declared finite plaquette regulator, not an assertion of a continuum limit for the dynamical coframe.

Fix the same dimensionless constants $v, m, f, \theta > 0$, $\alpha_\sigma \neq 0$, s_0, and $C_{\mathrm{c}} \geq 0$ for every group. Use the explicit common normalization rule

$$\nu_n(\mathrm{d}U\, \mathrm{d}s) = \mathrm{d}U\, \frac{e^{-s^2/(2v)}}{\sqrt{2\pi v}}\, \mathrm{d}s, \qquad \nu_n(1) = 1, \quad (378)$$

and the same additive action zero in

$$S_{n,\kappa}(U, s) = e^{-\alpha_\sigma s}[C_{\mathrm{c}} + \kappa C_n(U)] + \frac{m^2 f^2}{2}(s - s_0)^2. \quad (379)$$

The compact factors always have Haar mass one, and the scalar reference law is identical; no group-dependent measure multiplier is used. This is an application of the common normalization prescription. It does not assert that the Haar laws for different groups are pushforwards under their natural inclusions. For example, the inclusion of $SU(2)^4$ into $SU(3)^4$ has a lower-dimensional image, of zero ambient Haar measure. Its pushed-forward probability is therefore singular relative to the Haar probability on $SU(3)^4$. Each action is a single positive extended norm with the same exponential weight and quadratic stabilizer. Its partition function lies in $(0, 1]$. The corresponding reversible scalar drift includes the reference term $-\theta s/v$ in addition to $-\partial_s S_{n,\kappa}$. For the Lyapunov function $V_0(s) = 1 + s^2$, put $a = m^2 f^2$ and use $C_n \leq 2n$ and $ze^{-z} \leq e^{-1}$. Direct differentiation gives

$$\mathcal{L}V_0 \leq 2\theta + a s_0^2 + \frac{2(C_{\mathrm{c}} + 2\kappa n)}{e} - (a + 2\theta/v)s^2. \quad (380)$$

The finite-regulator proof in Theorem 19 therefore applies, with the reference drift included. Compactness of the links, ellipticity, and connectedness are unchanged. Hence each candidate has global regulated dynamics and a unique Gibbs equilibrium.

Write $s_n(\kappa) = -\theta \log Z_{n,\kappa}$. At $\kappa = 0$ the normalized link integral is one, so $s_n(0)$ is the same number s_* for every n. The preceding theorem gives

strict increase and continuity. Since $C_n > 0$ almost everywhere, dominated convergence also gives

$$Z_{n,\kappa} \longrightarrow 0 \quad (\kappa \to \infty), \qquad s_n((0,\infty)) = (s_*, \infty). \tag{381}$$

Thus, for any declared score $r > s_*$, each group has exactly one positive κ_n with $s_n(\kappa_n) = r$. Two such packages for $SU(2)$ and $SU(3)$ have equal selection score but cannot be package-equivalent: their master groups have different dimensions. In the declared finite bosonic regulator class, assume that both packages satisfy the same previously specified consistency conditions, so that both indicators are zero. A class containing just these two packages then has two minimizers; the class retaining all their positive coefficients has no minimizer. Choosing other allowed coefficients can give either ordering. These choices demonstrate underdetermination; they are not a prescription for tuning a desired group into the minimum.

The examples establish an obstruction within the explicit algebraic, bosonic, and regulated class. A completed chiral, continuum, or Lorentzian consistency condition could exclude some of them, but an actual exclusion argument is required. Finally, even at a prescribed $w_* > 0$, the tree relations $g_a^{-2} = w_*\kappa_a$ reproduce any positive gauge-coupling triple by choosing $\kappa_a = g_a^{-2}/w_*$. Numerical coupling prediction therefore requires independent constraints fixing those normalizations; the common exponential weight alone does not fix them.

6.5.1. *A quantitative one-plaquette check.* A single $U(1)$ plaquette makes the obstruction quantitatively explicit. Use a plaquette angle $u \in [-\pi, \pi)$ with Haar measure $\mathrm{d}u/(2\pi)$, one scalar $s \in \mathbb{R}$ with Lebesgue reference, and the dimensionless data

$$S_\kappa(u,s) = \frac{1}{2}s^2 + \kappa e^{-\alpha_\sigma s}(1 - \cos u), \qquad \theta = 1, \quad \alpha_\sigma = 0.6, \quad \kappa > 0. \tag{382}$$

The scalar action is confining, the curvature term is nonnegative, and the finite-regulator proof in Theorem 19 applies. Angular integration gives

$$\begin{aligned} I_0(a) &:= \frac{1}{2\pi}\int_{-\pi}^{\pi} e^{a\cos u}\,\mathrm{d}u, & I_1(a) &:= I_0'(a), \\ R(\kappa) &:= \frac{Z_\kappa}{Z_0} = \mathbb{E}_{s\sim N(0,1)}\left[e^{-a}I_0(a)\right], & a &= \kappa e^{-\alpha_\sigma s}, \\ Z_0 &= \sqrt{2\pi}, & F(\kappa) - F(0) &= -\log R(\kappa). \end{aligned} \tag{383}$$

The scaled Bessel function $e^{-a}I_0(a)$ is bounded by one for $a \geq 0$, so this formula avoids a large-exponential cancellation in numerical integration. Differentiation, with the domination established in the selection argument, yields

$$F'(\kappa) = \frac{\mathbb{E}\left[e^{-\alpha_\sigma s}e^{-a}\{I_0(a) - I_1(a)\}\right]}{R(\kappa)} > 0. \tag{384}$$

The numerator is the Gaussian expectation of the nonnegative angular integral $e^{-\alpha_\sigma s}(1-\cos u)e^{-a(1-\cos u)}$. It is strictly positive because the angle is not concentrated at zero.

The scalar drift is $-s+\alpha_\sigma\kappa e^{-\alpha_\sigma s}(1-\cos u)$. All its terms are integrable in equilibrium by the Gaussian domination and the derivative estimate. Either taking stationary expectations of the scalar equation or integrating the scalar Gibbs density by parts therefore gives the independent balance identity

$$\mathbb{E}_{\pi_\kappa} s = \alpha_\sigma \kappa F'(\kappa). \tag{385}$$

This is a relation for a nonlinear coupled scalar–gauge equilibrium, not a small-fluctuation Gaussian identity.

Figure 4 evaluates (383)–(385) at 241 logarithmically spaced values of κ in $[10^{-3}, 10^2]$. Gauss–Hermite orders 256 and 384 differ by at most 9.13×10^{-16} over all reported quantities. The maximum stationary-balance residual is 4.56×10^{-15}. A fourth-order centered finite difference with relative step 2×10^{-3} differs from (384) by at most 5.39×10^{-11}. As an independent check, adaptive quadrature on $s\in[-12,12]$ at $\kappa=10^{-3},10^{-2},10^{-1},1,10,10^2$ differs from the order-384 Gauss–Hermite values by at most 3.72×10^{-15}; the omitted standard normal tail probability is below 4×10^{-33}. These comparisons are numerical consistency checks, not certified global quadrature error bounds. The exact integral inequalities prove monotonicity independently of the plot.

6.6. *A conditional 331 family and flavor extension.* The selection results above distinguish a consistency condition from a selection theorem. We now give a concrete chiral candidate class in which that distinction can be followed through anomaly cancellation, symmetry breaking, flavor, and threshold matching. The candidate package Γ_{331} contains the group, representations, scalar potential, flavor maps, regulator, mobility, reference measure, and matching conditions. It is admitted to the anomaly part of (360) only after all of those data have been specified. Neither the anomaly identities below nor the equilibrium construction bypasses the nonattainment result of Theorem 15 or the equal-score examples in (376). Accordingly, Γ_{331} is an additional conditional realization, rather than a uniquely selected phase of the master theory.

6.7. *Conditional anomaly and family-count mechanism.* Let

$$\widetilde{G}_{331} := \mathrm{SU}(3)_c\times\mathrm{SU}(3)_L\times\mathrm{U}(1)_x, \qquad Q = T_3 - \frac{T_8}{\sqrt{3}} + X_{331}. \tag{386}$$

For the global statements below, the compact U(1) factor is normalized by an integral character charge $x\in\mathbb{Z}$. We use the phenomenological generator $X_{331}=x/3$, and the corresponding coupling normalization is fixed by

$$g_x\, x = g_X\, X_{331}, \qquad \text{equivalently} \qquad g_x = \frac{g_X}{3}. \tag{387}$$

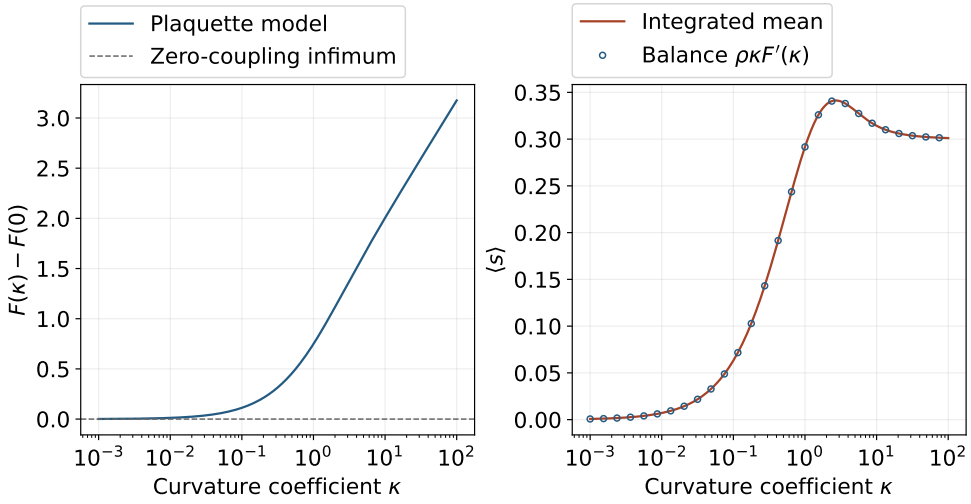


Figure 4. Deterministic integrals for the scalar–$U(1)$ plaquette model. Left: the strictly increasing free-energy difference, whose infimum corresponds to the excluded zero coefficient. Right: the directly integrated scalar mean and the independent stationary-balance formula. The curves represent the specified mathematical model and contain no observational data.

Thus the fractional labels in the following display are conventional X_{331}-charges, while the compact-group characters are the integral charges $x = 3X_{331}$. This convention leaves the vanishing of all local anomaly coefficients unchanged and will be used again in the global quotient test below. The following matter class is a 331 realization with right-handed neutrinos. Early 331 constructions were introduced in [70] and [130], and the stated right-handed-neutrino realization is described in [69]. We state its complete covering-group charged chiral content used in the anomaly count because the family-number conclusion depends on these representations, on the absence of additional active colored fields, and on the chosen normalization of X_{331}. The displayed subscripts denote X_{331}-charges. For $i = 1, \dots, N_g$, $r = 1, \dots, k$, and $\alpha = 1, \dots, N_g - k$, take

$$\begin{aligned} \mathsf{L}_{iL} &\sim (\mathbf{1}, \mathbf{3})_{-1/3}, \mathsf{E}_{iR} \sim (\mathbf{1}, \mathbf{1})_{-1}, \mathsf{Q}^t_{rL} \sim (\mathbf{3}, \mathbf{3})_{1/3}, \mathsf{Q}^a_{\alpha L} \sim (\mathbf{3}, \overline{\mathbf{3}})_0, \\ \mathsf{U}_{iR} &\sim (\mathbf{3}, \mathbf{1})_{2/3}, \mathsf{D}_{iR} \sim (\mathbf{3}, \mathbf{1})_{-1/3}, \mathsf{T}_{rR} \sim (\mathbf{3}, \mathbf{1})_{2/3}, \mathsf{B}_{\alpha R} \sim (\mathbf{3}, \mathbf{1})_{-1/3}. \end{aligned} \tag{388}$$

The declared representations have a common central kernel. With $\omega_3 = e^{2\pi i/3}$, the faithful continuous gauge group is

$$\begin{aligned} K_{331} &= \{(\omega_3^m \mathbf{1}_3, \omega_3^m \mathbf{1}_3, \omega_3^m) : m = 0, 1, 2\}, \\ G_{331} &= \widetilde{G}_{331}/K_{331} \simeq \{(U, V) \in \mathrm{U}(3)^2 : \det U = \det V\}. \end{aligned} \tag{389}$$

To verify that the kernel is complete, an element (C, L, z) acting trivially on $\mathsf{E}_R, \mathsf{L}_L, \mathsf{U}_R$ must satisfy $z^3 = 1$, $L = z\mathbf{1}_3$, and $C = z^{-2}\mathbf{1}_3 = z\mathbf{1}_3$. Each remaining multiplet has trialities a_c, b_L and character x with $a_c + b_L + x = 0 \pmod 3$, so these three elements act trivially on all of them. The unitary-pair isomorphism is induced by $(C, L, z) \mapsto (z^{-1}C, z^{-1}L)$. A cube root of the common determinant proves surjectivity, and its kernel is exactly K_{331}. Local Lie-algebra computations below are unchanged, but principal bundles and the global anomaly problem refer to this quotient rather than its cover.

The lepton triplet has electric charges $(0, -1, 0)$; we therefore write

$$\mathsf{L}_{iL} = (\nu_{iL}, e_{iL}, n^c_{iL})^T. \tag{390}$$

The embedded neutral field n^c_{iL} is distinct from the gauge-singlet field N_{iR} introduced below for the even type-I seesaw. In the declared matching action, n^c_{iL} instead obtains its odd-sector Dirac partner through S_R. The gauge-singlet fermions introduced below have $X_{331} = 0$ and do not alter these gauge or mixed gauge–gravitational anomaly coefficients. The symbols in (388) are local to this candidate and are distinct from the prescribed Standard-Model fields in the earlier joint realization. In anomaly sums every right-handed field is replaced by its charge-conjugate left-handed field. With $T(\mathbf{3}) = 1/2$, the potentially nonzero local anomaly coefficients are

$$\begin{aligned}
\mathcal{A}^{331}_{\mathrm{SU}(3)^3_c} &= 3N_g - \big(2N_g + k + N_g - k\big) = 0,\\
\mathcal{A}^{331}_{\mathrm{SU}(3)^2_c X_{331}} &= \frac{1}{2}\left[k - \frac{N_g}{3} - \frac{2k}{3} + \frac{N_g - k}{3}\right] = 0,\\
\mathcal{A}^{331}_{\mathrm{SU}(3)^3_L} &= N_g + 3(2k - N_g) = 6k - 2N_g,\\
\mathcal{A}^{331}_{\mathrm{SU}(3)^2_L X_{331}} &= \frac{1}{2}\left[-\frac{N_g}{3} + k\right] = \frac{3k - N_g}{6},\\
\mathcal{A}^{331}_{X^3_{331}} &= N_g\left[3\left(-\frac{1}{3}\right)^3 + 1\right] + 3\left[-\frac{4k}{9} - \frac{2(N_g - k)}{9}\right] = \frac{2(N_g - 3k)}{9},\\
\mathcal{A}^{331}_{\mathrm{grav}^2 X_{331}} &= 0.
\end{aligned} \tag{391}$$

For example, the first line counts the three $\mathrm{SU}(3)_L$ components of each left-handed colored multiplet and then subtracts the charge-conjugated right-handed color fundamentals. The last coefficient vanishes separately in each lepton and quark family. All anomalies with one generator of a simple factor and generators of independent simple factors vanish by tracelessness. Thus the local anomaly conditions in this specified class reduce exactly to

$$N_g = 3k. \tag{392}$$

THEOREM 16 (Conditional 331 three-family statement). *Assume* (388), *color-singlet scalar fields, no additional colored degrees of freedom in the energy interval in which the one-loop color criterion is imposed, and one-loop color asymptotic freedom. Then local anomaly cancellation together with that asymptotic-freedom condition implies* $N_g = 3$ *and* $k = 1$.

Proof. Equation (392) gives $N_g = 3k$. Since $N_g > 0$, k is a positive integer. Each family contains two ordinary and one exotic Dirac color fundamental above the exotic thresholds. Hence there are $3N_g$ Dirac color fundamentals. In the convention $\mu\,\partial_\mu g_c = -b_{0,c}^{(331)} g_c^3/(16\pi^2) + \cdots$,

$$b_{0,c}^{(331)} = 11 - \frac{2}{3}(3N_g) = 11 - 2N_g. \tag{393}$$

Color asymptotic freedom gives $N_g < 11/2$. The only positive multiple of three below $11/2$ is $N_g = 3$; substitution into (392) gives $k = 1$. □

Ordinary-spin global consistency. The quotient admits two universal rank-three unitary bundles with the same determinant line. Write their common first Chern class as d. The classifying-space fibration has fiber $B\mathrm{SU}(3)_c \times B\mathrm{SU}(3)_L$ over $B\mathrm{U}(1)$. All integral fiber Chern monomials lift to the universal bundles on the total space. Leray–Hirsch [92, Theorem 4D.1] therefore gives

$$H^*(BG_{331};\mathbb{Z}) = \mathbb{Z}[d, c_{2c}, c_{2L}, c_{3c}, c_{3L}], \qquad |d| = 2, \quad |c_{2j}| = 4, \quad |c_{3j}| = 6. \tag{394}$$

The actual lifted generators remove multiplicative extension ambiguity; finite-type universal coefficients give free even-degree homology and zero odd-degree homology. In the ordinary spin-bordism spectral sequence, the only total-degree-five term is $E^2_{4,1} = (\mathbb{Z}/2)^3$. The incoming and outgoing differentials are the homology duals of Sq^2, including mod-two reduction for the incoming integral group [55]. In the degree-four basis (d^2, c_{2c}, c_{2L}) and the degree-six basis $(d^3, dc_{2c}, dc_{2L}, c_{3c}, c_{3L})$, they are

$$A = \begin{pmatrix} 1 & 0 & 0 \end{pmatrix}, \qquad B = \begin{pmatrix} 0 & 0 & 0 & 0 & 0 \\ 0 & 1 & 0 & 1 & 0 \\ 0 & 0 & 1 & 0 & 1 \end{pmatrix}, \qquad \ker A = \operatorname{im} B. \tag{395}$$

Indeed, $\mathrm{Sq}^2 d = d^2$, $\mathrm{Sq}^2(d^2) = 0$, and $\mathrm{Sq}^2 c_{2j} = dc_{2j} + c_{3j}$. These are operations on the actual quotient-bundle classes, not on hypothetical generators of its cover. No other degree-five entry or extension survives, and hence

$$\Omega_5^{\mathrm{Spin}}(BG_{331}) = 0. \tag{396}$$

This excludes a residual continuous-group fermion anomaly on ordinary spin spacetime after the local anomaly polynomial vanishes. Non-liftable quotient bundles are included. Paper II supplies the degree-by-degree integral and differential proofs. A spin–gauge identification, a gauged discrete parity, and

ultraviolet line-operator choices are different questions and are not resolved by (396).

The three-family theorem is conditional in two independent ways. Asymptotic freedom is an additional dynamical requirement rather than a universal quantum consistency condition, and colored messengers or other threshold states change (393). For the minimal three-family content with three complex $\mathrm{SU}(3)_L$ triplet scalars, the remaining one-loop coefficients are

$$b_{0,L}^{(331)} = \frac{13}{2}, \qquad b_{X_{331}}^{(331)} = -\frac{26}{3}, \qquad \beta_X(g_X) = +\epsilon_{\mathrm{loop}} \frac{26\, g_X^3}{3(16\pi^2)} + O(\epsilon_{\mathrm{loop}}^2 g_X^5). \tag{397}$$

Here and below the one-loop convention is $\mu\, \partial_\mu g = -\epsilon_{\mathrm{loop}} b_0 g^3/(16\pi^2) + \cdots$. The sign of $b_{X_{331}}^{(331)}$ is therefore consistent with the manuscript-wide convention (451). The explicitly displayed positive β_X signals abelian ultraviolet growth and therefore requires a cutoff or a further ultraviolet completion. The numerical magnitude of $b_{X_{331}}^{(331)}$ is tied to the generator normalization in (387); its sign and the matched products $g_X X_{331}$ are unchanged by a consistent rescaling. The family mechanism itself is established 331 physics, not a new derivation of the observed family number from the master action.

The flavor and spectrum construction below the generalized-color and parent-group obstruction analyses specializes to the branch $N_g = 3$, $k = 1$ selected in Theorem 16. There is therefore one gauge-triplet quark multiplet and two gauge-antitriplet quark multiplets. Whenever a 3×3 ordinary-flavor matrix is used in that construction, its left-handed rows are ordered as

$$(\mathsf{Q}_{1L}, \mathsf{Q}_{2L}, \mathsf{Q}_{3L}) := (\mathsf{Q}_{1L}^t, \mathsf{Q}_{1L}^a, \mathsf{Q}_{2L}^a). \tag{398}$$

This is a gauge-basis bookkeeping convention; it is not an identification of the special gauge triplet with a physical mass generation, which is defined only after the Yukawa matrices are diagonalized.

6.8. *Why anomaly cancellation does not select three colors.* The preceding theorem must not be read as an independent derivation of $\mathrm{SU}(3)_c$. To see the limitation directly, replace color by $\mathrm{SU}(N_c)$, retain $\mathrm{SU}(3)_L$, and allow the ordinary quark-doublet hypercharge to be an unknown Y_q. The triplet and antitriplet charges are then

$$X_t = Y_q + \frac{1}{6}, \qquad X_a = Y_q - \frac{1}{6}, \tag{399}$$

whereas the corresponding right-handed ordinary and exotic charges are

$$X_{\mathsf{U}} = Y_q + \frac{1}{2}, \qquad X_{\mathsf{D}} = Y_q - \frac{1}{2}. \tag{400}$$

The two independent left-handed anomaly equations are

$$\begin{aligned}\mathcal{A}^{331}_{\mathrm{SU}(3)_L^3} &= N_g + N_c(2k - N_g) = 0,\\ \mathcal{A}^{331}_{\mathrm{SU}(3)_L^2 X_{331}} &= -\frac{N_g}{6} + \frac{N_c}{2}\left[N_g Y_q + \frac{2k - N_g}{6}\right] = 0.\end{aligned} \tag{401}$$

Substitution of the first equation into the second gives $Y_q = 1/(2N_c)$. At that value, direct substitution in the cubic abelian sum gives

$$\mathcal{A}^{331}_{\mathrm{SU}(3)_L^2 X_{331}} = \frac{\mathcal{A}^{331}_{\mathrm{SU}(3)_L^3}}{12}, \qquad \mathcal{A}^{331}_{X_{331}^3} = -\frac{\mathcal{A}^{331}_{\mathrm{SU}(3)_L^3}}{9}, \tag{402}$$

and the color and mixed gravitational anomalies vanish. Consequently the remaining anomaly and color-asymptotic-freedom conditions are

$$2N_c k = (N_c - 1)N_g, \qquad b^{(331)}_{0,c} = \frac{11N_c}{3} - 2N_g > 0. \tag{403}$$

For odd N_c, coprimality of N_c and $(N_c - 1)/2$ makes N_g a multiple of N_c; the inequality in (403) then leaves

$$N_g = N_c, \qquad k = \frac{N_c - 1}{2}. \tag{404}$$

For even N_c, integrality makes N_g a multiple of $2N_c$, which violates the same inequality. Thus every odd $N_c \geq 3$ survives these two tests. With the three scalar triplets used below, the $\mathrm{SU}(3)_L$ coefficient is

$$b^{(331)}_{0,L} = 11 - \frac{N_g(N_c + 1)}{3} - \frac{1}{2}. \tag{405}$$

The explicit alternative $(N_c, N_g, k) = (5, 5, 2)$ has

$$b^{(331)}_{0,c} = \frac{25}{3}, \qquad b^{(331)}_{0,L} = \frac{1}{2}, \tag{406}$$

so both nonabelian factors are asymptotically free. Its ordinary quark charges are $3/5$ and $-2/5$. If the observed charges $2/3$ and $-1/3$ are instead imposed, then $Y_q = 1/6 = 1/(2N_c)$ forces $N_c = 3$; those observed charges are then empirical inputs. The anomaly mechanism therefore correlates the number of families and colors in this class but does not select three colors by itself.

6.9. *An illustrative* SU(6) *splitting, global orientation, and chiral obstruction.* It is useful to distinguish a calculable residual Lie algebra from a full global embedding of the matter representations. Fix an SU(6) parent, a traceless Hermitian adjoint Σ_6, and the positive potential

$$\mathfrak{U}_6(\Sigma_6) = \lambda_6 \,\mathrm{tr}\left[\left(\Sigma_6^2 - \frac{v_6^2}{6}\mathbf{1}_6\right)^2\right], \qquad \lambda_6, v_6 > 0. \tag{407}$$

The potential in (407) is a sum of squares. After diagonalizing Σ_6, every zero of this sum has eigenvalues $\pm v_6/\sqrt{6}$. If r eigenvalues are positive, tracelessness

gives $(2r-6)v_6/\sqrt{6}=0$, hence $r=3$. All zero-cost vacua therefore lie in the one SU(6) orbit of

$$\Sigma_{6,*}=\frac{v_6}{\sqrt{6}}\,\mathrm{diag}(\mathbf{1}_3,-\mathbf{1}_3). \tag{408}$$

Its stabilizer is $S(\mathrm{U}(3)\times\mathrm{U}(3))$, with Lie algebra

$$\mathfrak{su}(3)\oplus\mathfrak{su}(3)\oplus\mathfrak{u}(1). \tag{409}$$

This is a conditional algebraic splitting into two SU(3) factors. The Lie ranks of SU(6) and SU(3) are five and two, respectively; the calculation does not distinguish which factor would be color.

The global quotient is essential. The homomorphism

$$(U,V,z)\longmapsto \mathrm{diag}(zU,z^{-1}V) \tag{410}$$

from $\mathrm{SU}(3)\times\mathrm{SU}(3)\times\mathrm{U}(1)$ has kernel

$$\left\{(\omega_3^{-m}\mathbf{1}_3,\omega_3^m\mathbf{1}_3,\omega_3^m) : m=0,1,2\right\}\cong\mathbb{Z}_3,\qquad \omega_3=e^{2\pi i/3}. \tag{411}$$

A representation with the two trialities (a,b) and integral U(1) charge n_X descends through this quotient only if

$$-a+b+n_X=0 \pmod 3. \tag{412}$$

In the normalization of (387), the charge appearing here is $n_X=x=3X_{331}$. The condition is consequently a global representation condition and not another local anomaly equation. The proposed quark antitriplet $(\mathbf{3},\overline{\mathbf{3}})_0$ has $(a,b,n_X)=(1,-1,0)$ and violates (412). This excludes the direct identification of the parent blocks with physical color and the left group, not every global identification. Composing the color factor with complex conjugation instead gives

$$\psi(C,L,z)=\mathrm{diag}(z\overline{C},z^{-1}L),\qquad \ker\psi=K_{331}. \tag{413}$$

The first block has determinant z^3 and the second z^{-3}, so the image lies in $S(\mathrm{U}(3)\times\mathrm{U}(3))$. Conversely a cube root of the first determinant supplies a preimage. The induced global-group isomorphism is therefore correct, and the descent condition becomes $a_c+b_L+x=0 \pmod 3$, exactly the condition in (389).

Global compatibility nevertheless does not supply a chiral ultraviolet completion. The following obstruction is independent of the direct orientation failure and agrees with the full calculation in Paper II. Let $P=e^{i\pi/6}\left(\begin{smallmatrix}0 & \mathbf{1}_3\\ \mathbf{1}_3 & 0\end{smallmatrix}\right)$. The block exchange has determinant -1, so $\det P=1$, and

$$P\psi(C,L,z)P^{-1}=\psi(\overline{L},\overline{C},z^{-1}). \tag{414}$$

Thus the normalizer acts on residual irreducible labels by $\tau(R_c,R_L)_x=(\overline{R_L},\overline{R_c})_{-x}$. For every finite-dimensional parent representation, its action of P intertwines the restricted representation with this pullback. Uniqueness of

compact-group decomposition forces $n(r) = n(\tau r)$. Since τ commutes with conjugation, the chiral index $I(r) = n(r) - n(\overline{r})$ obeys

$$I(\tau r) = I(r). \tag{415}$$

In the following chiral-index counts the subscripts denote the integer character $x = 3X_{331}$, rather than the fractional labels in (388). In the three-family left-handed spectrum, $r = (\mathbf{1}, \mathbf{3})_{-1}$ has index 3, whereas $\tau r = (\overline{\mathbf{3}}, \mathbf{1})_{+1}$ has index 5 from the three ordinary and two exotic down-type singlet conjugates. Already $3 \neq 5$ contradicts (415). Independently, $(\mathbf{1}, \mathbf{1})_{+3}$ has index 3 and is sent to its conjugate, which would require that index to vanish. Additional vectorlike pairs change neither index. Thus no finite collection of complete four-dimensional SU(6) multiplets yields this target spectrum through the stated adjoint breaking. A completion must change the parent, breaking pattern, spectrum, or restriction mechanism, and must still verify its own anomaly and unwanted-state conditions.

6.10. *A 331 auxiliary-map vacuum, parity, and flavor sector.* We next give a scalar realization in the G_{331} candidate itself. It is to be understood as a candidate square-norm component of the auxiliary map entering the master scalar potential $\mathfrak{U}_H$, rather than as an unrelated fundamental action. At this point $\mathfrak{U}_{331}$ is an effective scalar block; it becomes a member of $\mathscr{G}_{\mathrm{adm}}$ only after an equivariant auxiliary map, regulator, mobility, reference measure, and continuation and matching data have been fixed. Use three distinct fields

$$\Phi_\eta, \Phi_\Xi \sim (\mathbf{1}, \mathbf{3})_{-1/3}, \qquad \Phi_\rho \sim (\mathbf{1}, \mathbf{3})_{2/3}. \tag{416}$$

Take $v_\eta, v_\rho, v_\Xi, \Lambda_D > 0$. An explicit positive component that imposes the desired orbit is

$$\begin{aligned} \mathfrak{U}_{331} = {} & \sum_{a \in \{\eta,\rho,\Xi\}} \lambda_a^{331} \left(\Phi_a^\dagger \Phi_a - \frac{v_a^2}{2} \right)^2 + \sum_{\substack{a,b \in \{\eta,\rho,\Xi\} \\ a<b}} \zeta_{ab} |\Phi_a^\dagger \Phi_b|^2 \\ & + \frac{\zeta_D}{\Lambda_D^2} \left| \det(\Phi_\eta, \Phi_\rho, \Phi_\Xi) - \frac{v_\eta v_\rho v_\Xi}{2\sqrt{2}} \right|^2, \qquad \lambda_a^{331}, \zeta_{ab}, \zeta_D > 0. \end{aligned} \tag{417}$$

The determinant has total X_{331}-charge zero. Every summand in (417) is nonnegative and all vanish at

$$\langle \Phi_\eta \rangle = \frac{v_\eta}{\sqrt{2}} e_1, \qquad \langle \Phi_\rho \rangle = \frac{v_\rho}{\sqrt{2}} e_2, \qquad \langle \Phi_\Xi \rangle = \frac{v_\Xi}{\sqrt{2}} e_3. \tag{418}$$

Conversely, a zero of the potential fixes the three lengths, their pairwise orthogonality, and the determinant phase. Hence the normalized column matrix

$$\mathsf{U}_\Phi := \sqrt{2} \left(\frac{\Phi_\eta}{v_\eta}, \frac{\Phi_\rho}{v_\rho}, \frac{\Phi_\Xi}{v_\Xi} \right) \tag{419}$$

obeys $\mathsf{U}_\Phi^\dagger \mathsf{U}_\Phi = \mathbf{1}_3$ and $\det \mathsf{U}_\Phi = 1$, and so belongs to $\mathrm{SU}(3)_L$. Every zero-cost vacuum is consequently gauge-equivalent to (418). The final term in (417) contains a dimension-six effective interaction and requires a cutoff or an auxiliary-field completion. The hierarchy $v_\Xi \gg v_\eta, v_\rho$ and its radiative stability remain additional input.

The e_3 expectation value is invariant under the upper-block $\mathrm{SU}(2)_L$ and under $Y = -T_8/\sqrt{3} + X_{331}$, whereas the three aligned expectations preserve precisely $Q = T_3 + Y$. Thus, under the stated hierarchy, the alignment realizes the breaking chain at the Lie-algebra level, with finite central quotients suppressed in this display,

$$G_{331} \longrightarrow \mathrm{SU}(3)_c \times \mathrm{SU}(2)_L \times \mathrm{U}(1)_Y \longrightarrow \mathrm{SU}(3)_c \times \mathrm{U}(1)_{\mathrm{em}}. \tag{420}$$

The three displayed $\langle\Phi\rangle$ are representatives of the selected orbit on the gauge-fixed realization used for this calculation. The gauge-invariant content of the breaking chain is the orbit stabilizer and the mass spectrum of $(D_\mu\Phi)^\dagger D^\mu\Phi$; it is not an assertion of a gauge-noninvariant local order parameter in a finite-volume unfixed measure. At this order, write

$$v_{\mathrm{EW}}^2 := v_\eta^2 + v_\rho^2, \qquad M_W^2 = \frac{g_{3L}^2 v_{\mathrm{EW}}^2}{4} \quad \text{at tree level after the electroweak stage,} \tag{421}$$

with the coupling evaluated at the chosen common matching scale.

An ordinary–exotic separation can be imposed rather than assumed. Give $\Phi_\Xi, \mathsf{U}_R, \mathsf{D}_R, \mathsf{E}_R$ intrinsic parity $+1$, and give $\Phi_\eta, \Phi_\rho, \mathsf{Q}_L^t, \mathsf{Q}_L^a, \mathsf{L}_L, \mathsf{T}_R, \mathsf{B}_R$ intrinsic parity -1. The product of this parity with $\mathrm{diag}(-1,-1,1) \in \mathrm{SU}(3)_L$ defines a residual parity Π_{sp} that preserves (418). The ordinary doublet components are Π_{sp}-even and the exotic third components are Π_{sp}-odd. In particular, the parity-even ordinary Yukawa operators can be written as

$$\begin{aligned} -\mathcal{L}_{Y,\mathrm{ord}} = {}& \overline{\mathsf{Q}}_{rL}^{\,t} \Phi_\eta (\mathbf{Y}_t^u)_{ri} \mathsf{U}_{iR} + \overline{\mathsf{Q}}_{rL}^{\,t} \Phi_\rho (\mathbf{Y}_t^d)_{ri} \mathsf{D}_{iR} \\ & + \overline{\mathsf{Q}}_{\alpha L}^{\,a} \Phi_\rho^* (\mathbf{Y}_a^u)_{\alpha i} \mathsf{U}_{iR} + \overline{\mathsf{Q}}_{\alpha L}^{\,a} \Phi_\eta^* (\mathbf{Y}_a^d)_{\alpha i} \mathsf{D}_{iR} + \mathrm{h.c.}, \end{aligned} \tag{422}$$

where repeated family indices are summed. The exotic operators

$$\overline{\mathsf{Q}}_{rL}^{\,t} \Phi_\Xi (\mathbf{Y}_{\mathsf{T}})_{rs} \mathsf{T}_{sR} \quad \text{and} \quad \overline{\mathsf{Q}}_{\alpha L}^{\,a} \Phi_\Xi^* (\mathbf{Y}_{\mathsf{B}})_{\alpha\beta} \mathsf{B}_{\beta R} \tag{423}$$

are also parity even, whereas ordinary–exotic mass mixing is forbidden. Full rank of both $\mathbf{Y}_{\mathsf{T}}$ and $\mathbf{Y}_{\mathsf{B}}$ is necessary and sufficient for every exotic quark to have a nonzero tree-level mass. On the $k = 1$ branch, $\mathbf{Y}_{\mathsf{T}} \neq 0$ is equivalent to full rank. The exotic masses are uniformly of order v_Ξ only when the corresponding singular values are bounded above and below by positive constants independent of v_{EW}/v_Ξ and of the flavor expansion parameter. A quantum-consistent realization of Π_{sp} and an acceptable fate for its lightest odd state are still required; in particular, a stable colored lightest state is not viable.

Introduce a G_{331}-singlet, Π_{sp}-even flavor spurion $\varphi_{\mathrm{FN}} \sim (\mathbf{1},\mathbf{1})_0$ of flavor charge -1, and fix its phase convention by

$$\varepsilon_{\mathrm{FN}} := \frac{\langle \varphi_{\mathrm{FN}} \rangle}{\Lambda_F}, \qquad 0 < \varepsilon_{\mathrm{FN}} \ll 1. \tag{424}$$

After choosing an ordering of the ordinary flavor rows in (422), assign

$$F(\mathsf{Q}_{iL}) = -q_i, \qquad F(\mathsf{U}_{jR}) = u_j, \qquad F(\mathsf{D}_{jR}) = d_j, \tag{425}$$

and give the scalar triplets zero flavor charge. The effective operators then carry powers $q_i + u_j$ and $q_i + d_j$. This is the Froggatt–Nielsen mechanism [74]. For the illustrative choice

$$q = (3,2,0), \qquad u = (5,2,0), \qquad d = (4,3,3), \tag{426}$$

the Yukawa matrices have the factorized form

$$\mathbf{Y}_u = \mathbf{D}_q \mathbf{C}_u \mathbf{D}_u, \qquad \mathbf{Y}_d = \mathbf{D}_q \mathbf{C}_d \mathbf{D}_d, \qquad \mathbf{D}_f = \mathrm{diag}(\varepsilon_{\mathrm{FN}}^{f_1}, \varepsilon_{\mathrm{FN}}^{f_2}, \varepsilon_{\mathrm{FN}}^{f_3}). \tag{427}$$

The row-dependent electroweak vacuum factors in (422) are included in $\mathbf{C}_u, \mathbf{C}_d$; the statements below require them to introduce no additional powers of $\varepsilon_{\mathrm{FN}}$. Assume that the relevant minors of $\mathbf{C}_u, \mathbf{C}_d$ remain nonzero and of order one as $\varepsilon_{\mathrm{FN}} \to 0$.

For a matrix $\mathbf{Y}$ with descending singular values $\sigma_1(\mathbf{Y}) \geq \sigma_2(\mathbf{Y}) \geq \sigma_3(\mathbf{Y})$, the exterior powers satisfy

$$\left\| \bigwedge^r \mathbf{Y} \right\|_{\mathrm{op}} = \prod_{j=1}^{r} \sigma_j(\mathbf{Y}). \tag{428}$$

The generic-minor assumptions and (427) give

$$\begin{aligned} \left(\|\mathbf{Y}_u\|_{\mathrm{op}}, \left\| \bigwedge^2 \mathbf{Y}_u \right\|_{\mathrm{op}}, |\det \mathbf{Y}_u| \right) &\asymp (1, \varepsilon_{\mathrm{FN}}^4, \varepsilon_{\mathrm{FN}}^{12}), \\ \left(\|\mathbf{Y}_d\|_{\mathrm{op}}, \left\| \bigwedge^2 \mathbf{Y}_d \right\|_{\mathrm{op}}, |\det \mathbf{Y}_d| \right) &\asymp (\varepsilon_{\mathrm{FN}}^3, \varepsilon_{\mathrm{FN}}^8, \varepsilon_{\mathrm{FN}}^{15}). \end{aligned} \tag{429}$$

Dividing the second and third products in (429) by their preceding products yields

$$m_u : m_c : m_t \sim \varepsilon_{\mathrm{FN}}^8 : \varepsilon_{\mathrm{FN}}^4 : 1, \qquad m_d : m_s : m_b \sim \varepsilon_{\mathrm{FN}}^7 : \varepsilon_{\mathrm{FN}}^5 : \varepsilon_{\mathrm{FN}}^3. \tag{430}$$

Absent cancellations between the two left rotations, the same charge differences give the scaling estimates

$$|V_{us}| \sim \varepsilon_{\mathrm{FN}}, \qquad |V_{cb}| \sim \varepsilon_{\mathrm{FN}}^2, \qquad |V_{ub}| \sim \varepsilon_{\mathrm{FN}}^3. \tag{431}$$

These are power laws, not numerical predictions: the coefficients, phases, charges in (426), and $\varepsilon_{\mathrm{FN}}$ remain independent microscopic data. A gauged flavor symmetry also requires its own anomaly analysis, while a global continuous version requires a mechanism for the associated would-be Goldstone mode. The spurion presentation is an effective description and contains no messenger fields in the spectrum used in Theorem 16. If the asymptotic-freedom premise of that theorem is imposed through a scale at which colored flavor messengers

are active, their Dynkin indices and thresholds must be included in (393); the family-count proof applies only on a range with no additional active colored states.

6.11. *Neutral fermions, alignment-dependent FCNCs, and heavy masses.* The neutral third component of L_L is not automatically made heavy by $\langle\Phi_\Xi\rangle$. To give a fully declared tree-level candidate, introduce three Π_{sp}-even gauge singlets $\mathsf{N}_R \sim (\mathbf{1},\mathbf{1})_0$ and three Π_{sp}-odd gauge singlets $\mathsf{S}_R \sim (\mathbf{1},\mathbf{1})_0$. The corresponding neutral-sector Lagrangian is

$$-\mathcal{L}_{Y,\nu} = \overline{\mathsf{L}}\Phi_\eta \mathbf{Y}_\nu \mathsf{N}_R + \overline{\mathsf{L}}\Phi_\Xi \mathbf{Y}_S \mathsf{S}_R + \frac{1}{2}\overline{\mathsf{N}_R^c}\,\mathbf{M}_{\mathsf{N}}\mathsf{N}_R + \mathrm{h.c.} \tag{432}$$

Here $\mathbf{Y}_S$ is a 3×3 matrix. To assert that every odd neutral third component is heavy, assume constants $0 < c_S \le C_S < \infty$ independent of v_{EW}/v_Ξ and of $\varepsilon_{\mathrm{FN}}$ such that

$$c_S \le \sigma_{\min}(\mathbf{Y}_S) \le \sigma_{\max}(\mathbf{Y}_S) \le C_S. \tag{433}$$

For the matching action used here, the independently allowed odd-singlet Majorana block $\mathbf{M}_{\mathsf{S}}$ is set to zero and independent dimension-five neutrino operators are excluded at the matching scale. These are explicit action assumptions, not consequences of the gauge group or parity. On this $\mathbf{M}_{\mathsf{S}} = 0$ branch, the odd neutral components and S_R then form three Dirac fermions with mass singular values

$$\sigma_i(m_S) = \frac{v_\Xi}{\sqrt{2}}\sigma_i(\mathbf{Y}_S), \qquad m_S = \frac{v_\Xi}{\sqrt{2}}\mathbf{Y}_S, \qquad i = 1,2,3, \tag{434}$$

and are uniformly of order v_Ξ. Without (433), the displayed gauge-invariant operator alone establishes neither full rank nor a common heavy scale. The charged-lepton operator and its mass matrix are

$$-\mathcal{L}_Y^\ell = \overline{\mathsf{L}}\Phi_\rho \mathbf{Y}_e \mathsf{E}_R + \mathrm{h.c.}, \qquad \mathbf{M}_e = \frac{v_\rho}{\sqrt{2}}\mathbf{Y}_e. \tag{435}$$

If $\mathbf{M}_{\mathsf{S}}$ is retained, the complete odd mass matrix must be diagonalized; a parametrically large block can generate light odd states despite full-rank $\mathbf{Y}_S$.

For the even sector, assume $\mathbf{M}_{\mathsf{N}} = \mathbf{M}_{\mathsf{N}}^T$, $\det \mathbf{M}_{\mathsf{N}} \neq 0$, and $\|m_{\nu D}\mathbf{M}_{\mathsf{N}}^{-1}\| \ll 1$. The leading type-I seesaw expression is

$$m_\nu = -m_{\nu D}\mathbf{M}_{\mathsf{N}}^{-1} m_{\nu D}^T, \qquad m_{\nu D} = \frac{v_\eta}{\sqrt{2}}\mathbf{Y}_\nu. \tag{436}$$

Let $\mathbf{D}_\ell$ and $\mathbf{D}_n$ be invertible diagonal flavor-power matrices. In particular, $\mathbf{D}_\ell^T = \mathbf{D}_\ell$ and $\mathbf{D}_n^T = \mathbf{D}_n$. If

$$\begin{aligned} &\mathbf{Y}_\nu = \mathbf{D}_\ell \mathbf{C}_D \mathbf{D}_n, \quad \mathbf{M}_{\mathsf{N}} = M_0 \mathbf{D}_n \mathbf{C}_{\mathsf{N}} \mathbf{D}_n, \\ &\mathbf{C}_{\mathsf{N}} = \mathbf{C}_{\mathsf{N}}^T, \qquad \det \mathbf{C}_{\mathsf{N}} \neq 0, \qquad M_0 > 0, \end{aligned} \tag{437}$$

then $\mathbf{M}_{\mathsf{N}}$ is symmetric and invertible, and the inverse is

$$\mathbf{M}_{\mathsf{N}}^{-1} = \frac{1}{M_0}\mathbf{D}_n^{-1}\mathbf{C}_{\mathsf{N}}^{-1}\mathbf{D}_n^{-1}. \tag{438}$$

Using the transpose of the first line in (437) in (436), the adjacent $\mathbf{D}_n$ and $\mathbf{D}_n^{-1}$ factors cancel, and therefore

$$m_\nu = -\frac{v_\eta^2}{2M_0}\mathbf{D}_\ell\mathbf{C}_D\mathbf{C}_{\mathsf{N}}^{-1}\mathbf{C}_D^T\mathbf{D}_\ell. \tag{439}$$

Equal lepton-doublet charges can allow large mixing, but do not determine its angles.

The remaining numerical freedom can be proved without a fit. For any positive diagonal masses and any unitary V_{CKM}, choose

$$\mathbf{M}_u = \mathbf{D}_u^{\mathrm{mass}}, \qquad \mathbf{M}_d = V_{\mathrm{CKM}}\mathbf{D}_d^{\mathrm{mass}}. \tag{440}$$

The left diagonalizations give the prescribed V_{CKM}. Similarly, for any positive diagonal $\mathbf{D}_\nu$, any unitary U_{PMNS}, and $\mathbf{M}_{\mathsf{N}} = M\mathbf{1}_3$ with M sufficiently large for the seesaw expansion, the choice

$$m_{\nu D} = i\sqrt{M}\,U_{\mathrm{PMNS}}^*\sqrt{\mathbf{D}_\nu} \tag{441}$$

gives, at the leading seesaw order stated in (436), $m_\nu = U_{\mathrm{PMNS}}^*\mathbf{D}_\nu U_{\mathrm{PMNS}}^\dagger$ through (436). With diagonal charged-lepton masses, $U_{\mathrm{PMNS}}^T m_\nu U_{\mathrm{PMNS}} = \mathbf{D}_\nu$, so U_{PMNS} is the Takagi matrix. Gauge invariance and the displayed flavor power counting therefore do not fix numerical CKM or PMNS data without a further selection principle.

Anomaly cancellation distinguishes one quark representation, but it does not identify that representation with a measured generation before the Yukawa matrices are diagonalized. Let $\mathsf{P}_{\mathrm{fam}} = \mathbf{e}_{\mathrm{fam}}\mathbf{e}_{\mathrm{fam}}^\dagger$ project onto the special gauge triplet. In a quark mass basis, a nonuniversal neutral interaction has the form

$$\mathbf{G}_q = c_{\mathrm{o}}\mathbf{1} + \Delta c\,\mathbf{U}_{qL}^\dagger\mathsf{P}_{\mathrm{fam}}\mathbf{U}_{qL}, \qquad (\mathbf{G}_q)_{ij} = \Delta c\,(\mathbf{U}_{qL})_{\mathrm{fam},i}^*(\mathbf{U}_{qL})_{\mathrm{fam},j} \quad (i \neq j). \tag{442}$$

The CKM matrix alone is insufficient to determine these couplings. Indeed, for every unitary W, the pair $\mathbf{U}_{uL} = W$, $\mathbf{U}_{dL} = WV_{\mathrm{CKM}}$ has the same $\mathbf{U}_{uL}^\dagger\mathbf{U}_{dL} = V_{\mathrm{CKM}}$, but in general produces different projectors in (442). Neutral meson mixing consequently probes flavor alignment and the heavy neutral boson scale jointly.

For canonically normalized gauge fields,

$$D_\mu = \partial_\mu - ig_{3L}T_aA_\mu^a - ig_X X_{331}B_\mu, \tag{443}$$

the leading v_Ξ-scale masses follow directly from $|D_\mu\langle\Phi_\Xi\rangle|^2$. The off-diagonal vectors have

$$M_{\mathrm{off}}^2 = \frac{g_{3L}^2 v_\Xi^2}{4}. \tag{444}$$

Since the neutral third component has $T_8 = -1/\sqrt{3}$ and $X_{331} = -1/3$, the neutral mass matrix is

$$\mathbf{M}^2_{0,331} = v_\Xi^2 \begin{pmatrix} g_{3L}^2/3 & g_{3L}g_X/(3\sqrt{3}) \\ g_{3L}g_X/(3\sqrt{3}) & g_X^2/9 \end{pmatrix}. \tag{445}$$

Its determinant is zero, and its nonzero eigenvalue gives

$$M^2_{Z'_{331}} = v_\Xi^2 \left(\frac{g_{3L}^2}{3} + \frac{g_X^2}{9} \right), \quad \frac{M^2_{Z'_{331}}}{M^2_{\rm off}} = \frac{4}{3} + \frac{4g_X^2}{9g_{3L}^2}, \qquad \frac{1}{g_Y^2} = \frac{1}{3g_{3L}^2} + \frac{1}{g_X^2}. \tag{446}$$

The final identity matches the canonically normalized massless combination to $Y = -T_8/\sqrt{3} + X_{331}$, so the unbroken charge convention agrees with $Q = T_3 + Y$ used for the Standard-Model phase. It requires all couplings to be evaluated at a common matching scale. Positivity of the abelian kinetic normalization requires

$$\frac{1}{g_X^2} = \frac{1}{g_Y^2} - \frac{1}{3g_{3L}^2} > 0, \qquad \sin^2\theta_W < \frac{3}{4}, \qquad \tan\theta_W = \frac{g_Y}{g_{3L}}. \tag{447}$$

This is a consistency condition of the declared 331 embedding, not a prediction of v_Ξ. Electroweak corrections are relatively $O(v_{\rm EW}^2/v_\Xi^2)$, and loop and threshold corrections require a separate calculation. Exotic-quark masses are the singular values of $v_\Xi \mathbf{Y}_{\mathsf{T},\mathsf{B}}/\sqrt{2}$. For the isolated radial potential $\lambda_\Xi(\Phi_\Xi^\dagger\Phi_\Xi - v_\Xi^2/2)^2$, one obtains $m^2_{h_\Xi} = 2\lambda_\Xi v_\Xi^2$; the complete multi-scalar theory instead requires the full canonically normalized Hessian.

6.12. *What remains to be selected.* At fixed dimensionless couplings, the replacement $v_\Xi \mapsto a v_\Xi$ rescales all leading heavy masses by a. The common master action does not eliminate this scaling freedom. The physical masses to be compared with experiment are propagator poles after continuation and matching; stochastic relaxation eigenvalues are not automatically those poles. A predictive completion must therefore supply a global-group-compatible chiral parent, a selected flavor map and vacuum scale, threshold matching, and a target-independent comparison proving uniqueness of the candidate class. Before those further constructions, the anomaly identities, vacuum orbit, flavor power laws, flavor-changing-neutral-current structure, and leading mass ratio above are conditional consequences of the explicitly stated data. This intermediate-scale 331 block can obey the existing conditional Yang–Mills projection once its kinetic and continuation hypotheses are verified; it does not add a separate derivation of the Einstein equation, whose status remains that of the Cartan branch analyzed earlier.

7. Well-posedness, conditional recovery, and parameter matching

7.1. *Conditional emergence theorem.* The following theorem states precisely what the framework can establish once a concrete master algebra and

measure have been supplied. Because the hypotheses explicitly include the residual group and the effective-sign and stability conditions, the result is a conditional implication; it is not an existence proof for a master algebra or an independent derivation of the observed group.

THEOREM 17 (Conditional effective-sector implication). *Assume the following hypotheses.*

(H1) The master configuration space is well-defined and the master action $\mathcal{S}_{\mathrm{M}}$ is bounded below on the admissible class.

(H2) A specified realization of the stochastic law (62) *admits a global weak solution, and its invariant probability measure is unique in the selected phase. If this probability is identified with a Gibbs law for state-dependent mobility or a nonconstant reference density, the realization uses the complete reversible drift* (80)*, or its intrinsic counterpart* (81)*, rather than the uncorrected gradient drift alone.*

(H3) The group-selection problem (356) *has a unique admissible minimizer Γ_*, whose residual internal symmetry is $SU(3)_c \times SU(2)_L \times U(1)_Y$.*

(H4) The selected matter representation is anomaly-free and contains the required low-energy chiral representations. If the claim includes propagating Dirac fermions, the microscopic or regularized action must additionally specify a non-degenerate first-order Dirac kinetic operator on those representations; this is an extra hypothesis and does not follow from the quadratic norm alone.

(H5) The fluctuation operator about the selected phase is of Laplace type after gauge fixing, and the heat-kernel expansion is valid in the relevant low-energy regime.

(H6) The Lorentzian continuation exists and satisfies the required positivity, causality, and unitarity conditions.

(H7) After gauge fixing or passage to the quotient by gauge orbits, the selected phase admits a reductive decomposition with a non-degenerate physical potential Hessian on the broken directions. Its positive kinetic pencil defines the tree-level curvature-mass scales. A positive mobility-weighted relaxation spectrum, when available, is a separate stochastic property and is not identified with a physical pole mass. The residual gauge symmetry protects the unbroken directions from an explicit mass term at that order. In addition, the quadratic form induced by $|D\Phi_H|^2$ on the broken gauge generators has full rank on $\mathfrak{g}_{\mathrm{broken}}$ after the vacuum is inserted; this is the condition that actually gives masses to all claimed broken vector modes.

(H8) The scalar/order-parameter representation contains the required electroweak doublet with its stated hypercharge, and its renormalized potential is bounded below and has a stable, non-degenerate vacuum implementing $SU(2)_L \times$

$U(1)_Y \to U(1)_{\mathrm{em}}$. *The regularization and matching prescription gives nonzero, finite coefficients for the scalar-curvature, gauge-curvature, scalar, and matter terms at the claimed effective order; moreover* $G_{\mathrm{eff}} > 0$*, the gauge kinetic matrix is positive on the Euclidean slice, and the scalar kinetic and potential terms have the signs required for stability. If a propagating fermionic matter action is claimed, the regularized matter block is additionally assumed to contain a non-degenerate first-order Dirac operator compatible with the selected representation. Without this extra hypothesis the conclusion about matter is only the selected representation content, not a derived Dirac kinetic term.*

Then the low-energy effective action contains, to the corresponding order in the heat-kernel expansion, an Einstein term with positive Newton coefficient, Yang–Mills fields of the residual gauge group with positive kinetic form, and a stable Higgs-type symmetry-breaking sector. It also contains the matter terms associated with those selected representations for which a kinetic operator has been explicitly included. Electromagnetism appears as the unbroken $U(1)_{\mathrm{em}}$ *subgroup after electroweak symmetry breaking. The theorem does not by itself derive a first-order Dirac kinetic term; that conclusion is conditional on the additional Dirac clause in (H8).*

Proof. By (H3), the selected residual group is the stated product. By (H7), the reductive decomposition and the full-rank broken-vector quadratic form give mass terms to the claimed broken vector modes, while residual gauge symmetry forbids an explicit local mass term for the unbroken connections at that order. The latter statement is not a claim that every residual sector has a massless physical excitation: a confining sector may have a physical mass gap without such a local mass term. By (H4), the selected representations are consistent with the residual gauge symmetry. A Dirac kinetic term is available only when the additional first-order hypothesis in (H8) is satisfied. By (H5) and (H8), the one-loop determinant has a valid heat-kernel expansion and its renormalized coefficients include the scalar-curvature, gauge-curvature, scalar, and any explicitly specified matter structures displayed in (352). By (H6), the Euclidean effective action can be continued to a Lorentzian effective theory without violating the stated physical consistency requirements. The final electromagnetic subgroup follows from the residual stabilizer of the electroweak order parameter. The theorem still does not determine numerical coupling values without an explicit matching calculation. □

If the selected propagating matter has a non-negligible spin current, the connection component of Theorem 9 lies on its Einstein–Cartan branch. The torsionless Einstein reduction additionally requires the spin-current suppression stated there. When algebraic torsion can be integrated out with an invertible

local field equation, the effective action instead acquires the corresponding local spin-current interactions; the Dirac-operator hypothesis alone does not remove them.

The hypotheses identify the mathematical conditions that must be verified in a concrete realization. In particular, (H3) and (H8) are not proved by the abstract master-action definitions: they supply the group-selection and renormalized matching information needed to turn the implication into a physical derivation. The theorem therefore records the logical dependence of the effective-sector statement without claiming that the Standard Model group or its numerical couplings have already been selected. All of these hypotheses are mathematical premises of the implication, but those selecting the residual group, vacuum, kinetic signs, scale separation, and Lorentzian continuation specify the physical effective branch rather than merely technical regularity.

7.2. *A non-circular definition of prediction.* A parameter is predicted by the framework only if it is not inserted into the microscopic model as an independent free datum and is uniquely determined by the selection, normalization, and matching procedures. Let λ denote a low-energy parameter. We call λ a structural prediction if

$$\lambda = \Lambda(\Gamma_*) \tag{448}$$

for a uniquely selected microscopic object Γ_*, where Λ is fixed by the theory and not by fitting the measured value of λ.

In particular, the following hierarchy should be distinguished:

(1) *Structural consequence*: follows algebraically from the master definitions.
(2) *Conditional consequence*: follows once explicitly stated hypotheses are assumed.
(3) *Matching result*: follows after fixing renormalization and normalization conditions.
(4) *Empirical input*: supplied by experiment and not predicted.

This distinction specifies which observables can be compared with data after matching without using those same observations as inputs.

7.3. *Renormalized parameter matching and identifiability.* The preceding definition of prediction becomes operational only after the microscopic data have been mapped to renormalized observables. We make this map explicit in order to keep three logically different operations separate: the evaluation of the selected microscopic action, the integration of modes between two scales, and the choice of quantities that are calibrated from experiment. Let $\mathcal{Q}_\Gamma \subset \mathbb{R}^d$ be a local coordinate space for the finite collection of microscopic parameters that remains after the algebraic constraints, gauge quotient, and vacuum equations for a candidate Γ have been imposed. Typical coordinates, when they are

independent in a particular realization, include w_*, g_{c}, ℓ, entries of the invariant pairing κ, and heavy masses and coupling vectors. The notation $\mathcal{Q}_\Gamma$ does not assume that these quantities are free: a successful selection problem may reduce it to a single point.

Fix a matching scale μ_{match}, a renormalization prescription $\mathcal{R}$, and reference units for dimensionful observables. The renormalized matching map is

$$\mathcal{M}_{\mu,\mathcal{R}}(\Gamma,\mathbf{q}) = \mathbf{O}(\mu) := \begin{pmatrix} G_{\mathrm{eff}}^{-1}(\mu) \\ g_1^{-2}(\mu) \\ g_2^{-2}(\mu) \\ g_3^{-2}(\mu) \\ \lambda_H(\mu) \\ m_H^2(\mu) \\ \vdots \end{pmatrix}, \qquad \mathbf{q} \in \mathcal{Q}_\Gamma. \tag{449}$$

Here the target space is the finite product of the corresponding observable spaces, with dimensions and units fixed by the chosen reference convention. The ellipsis denotes only observables for which the selected realization supplies a renormalized operator and a finite matching prescription; it does not silently add an independently postulated sector. The map is defined only after the regulator, field normalization, subtraction scheme, and residual operator basis have been specified. A change of scheme changes the coordinates of $\mathbf{O}$ and the finite terms below, but not a scheme-consistent observable relation.

For the joint candidate, the tree-level component of $\mathcal{M}$ is the previously derived relation

$$g_a^{-2}(\mu_{\mathrm{match}}) = w_*\kappa_a, \qquad G_{\mathrm{eff}}^{-1}(\mu_{\mathrm{match}}) = \frac{8\pi w_*}{g_{\mathrm{c}}^2\ell^2}, \qquad \Lambda_E = \frac{3}{\ell^2}. \tag{450}$$

The first two identities are the components of (237); the last one fixes the curvature convention used in the Cartan witness. They are relations among selected microscopic coordinates, not numerical values, until the selection problem fixes those coordinates.

To state the perturbative part without assigning uncomputed constants, introduce a dimensionless loop-counting parameter ϵ_{loop}, set to one after the perturbative order has been identified. This parameter is distinct from the fixed fluctuation scale θ. Choose the convention

$$\beta_a(g_a) := \mu\,\frac{\mathrm{d}g_a}{\mathrm{d}\mu} = -\epsilon_{\mathrm{loop}}\frac{b_a g_a^3}{16\pi^2} + O(\epsilon_{\mathrm{loop}}^2 g_a^5). \tag{451}$$

The chain rule gives $\mathrm{d}(g_a^{-2})/\mathrm{d}\log\mu = -2g_a^{-3}\beta_a(g_a)$. Integrating between μ_{match} and μ, and adding the finite threshold and subtraction contributions, gives

$$\begin{aligned} g_a^{-2}(\mu) &= w_*\kappa_a + \epsilon_{\mathrm{loop}}\frac{b_a}{8\pi^2}\log\Big(\frac{\mu}{\mu_{\mathrm{match}}}\Big) \\ &\quad +\Delta_a^{\mathrm{th}}(\mu_{\mathrm{match}};\Gamma,\mathbf{q},\mathcal{R}) + \Delta_a^{\mathrm{fin}}(\mu_{\mathrm{match}};\Gamma,\mathbf{q},\mathcal{R}) \\ &\quad +O(\epsilon_{\mathrm{loop}}^2) + O\Big(\frac{E^2}{M_H^2}\Big), \quad G_{\mathrm{eff}}^{-1}(\mu) = \frac{8\pi w_*}{g_{\mathrm{c}}^2\ell^2} + \Delta_G^{\mathrm{loop}}(\mu,\mu_{\mathrm{match}};\Gamma,\mathbf{q},\mathcal{R}) \\ &\quad +\Delta_G^{\mathrm{th}}(\mu_{\mathrm{match}};\Gamma,\mathbf{q},\mathcal{R}) + M_{\mathrm{ref}}^2 O(\epsilon_{\mathrm{loop}}^2). \end{aligned} \tag{452}$$

Here $M_{\mathrm{ref}} > 0$ is a fixed matching mass, introduced to state the dimension-two gravitational remainder in dimensionless units. The Δ-terms include their declared loop orders and any retained tree-level threshold. The order symbols concern a specified perturbative truncation on a fixed range of scales; they are not nonperturbative error bounds unless such bounds are proved separately. The coefficient b_a is determined by the selected light spectrum and representations. The scale E is the largest external momentum in the effective calculation and M_H is the smallest integrated-out mass in the retained expansion. The displayed remainder is therefore a controlled statement only when E/M_H is small and the loop expansion is valid. A different beta-function convention changes the sign assigned to b_a and the logarithm together, leaving the integrated equation unchanged. No numerical value of b_a, a threshold, or a coupling is asserted here.

The heavy-mode calculation in Section 11.10 supplies an explicit component of the threshold term. For one scalar and the operator basis used there,

$$\Delta C_{ij}^{(\phi)} = \frac{c_i c_j}{m_\phi^2 m_*^2}, \qquad C_{\mathrm{eff}} = C_{\mathrm{direct}} + \Delta C^{(\phi)} + C_{\mathrm{loop}}, \tag{453}$$

where the second identity is understood in one fixed nonredundant basis and renormalization scheme. Equation (453) is the rank-one contribution of the specified exchange; it does not replace the determinant, direct terms, other heavy fields, or finite counterterms. Those terms are part of Δ^{th} or Δ^{fin} in the full map and must be calculated before a physical coefficient is compared with data.

We next state the local inverse-problem criterion used to decide whether a matching calculation actually determines the microscopic coordinates. Let N be the number of selected observable components and write $\mathcal{M}_*(\mathbf{q}) := \mathcal{M}_{\mu,\mathcal{R}}(\Gamma_*,\mathbf{q})$. In local coordinates, the matching Jacobian is

$$J_{A\alpha}(\mathbf{q}_*) := \left.\frac{\partial \mathcal{M}_{*,A}}{\partial q^\alpha}\right|_{\mathbf{q}=\mathbf{q}_*}, \qquad 1 \le A \le N, \quad 1 \le \alpha \le d. \tag{454}$$

Theorem 18 (Conditional matching and local identifiability). *Assume the following.*

(M1) The selection functional has a unique minimizer Γ_* modulo package equivalence, and the selected vacuum determines a point $\mathbf{q}_* \in \mathcal{Q}_{\Gamma_*}$ independently of the measured values of the observables under consideration.

(M2) The regulator, residual operator basis, and renormalization prescription $\mathcal{R}$ are fixed, and the perturbative and heavy-mode expansions in (452) *have a specified error bound.*

(M3) The point $\mathbf{q}_*$ lies in the interior of a d-dimensional smooth coordinate chart of the physical quotient. In this chart, the map $\mathcal{M}_* : \mathcal{Q}_{\Gamma_*} \to \mathbb{R}^N$ is C^1, after dimensionful coordinates have been expressed in the fixed reference units.

Then the following statements hold.

(i) The tree-level, loop, and threshold expressions define one matching map, with the tree component given by (450) *and the corrections separated as in* (452)*.*

(ii) If $N = d$ and $\det J(\mathbf{q}_*) \neq 0$, there are neighborhoods U of $\mathbf{q}_*$ and V of $\mathcal{M}_*(\mathbf{q}_*)$ for which $\mathcal{M}_* : U \to V$ has a unique C^1 inverse. Thus the selected matching data determine the microscopic coordinates locally, modulo the package equivalence already removed in defining $\mathcal{Q}_{\Gamma_*}$.

(iii) If $N \geq d$ and $\operatorname{rank} J(\mathbf{q}_*) = d$, a set of d observable components has a nonsingular Jacobian minor. Those components locally identify $\mathbf{q}_*$; the remaining components are consistency relations and can be tested without refitting the identified coordinates.

(iv) If $\operatorname{rank} J(\mathbf{q}_*) < d$, there is a nonzero tangent direction $h \in \ker J(\mathbf{q}_*)$ with

$$\mathcal{M}_*(\mathbf{q}_* + \varepsilon h) = \mathcal{M}_*(\mathbf{q}_*) + o(\varepsilon). \tag{455}$$

The linearized matching problem is then non-identifiable. Higher-order terms can remove this degeneracy only after an additional nonlinear calculation; rank deficiency alone cannot be reported as a unique parameter determination.

Proof. The first assertion is a bookkeeping identity: the tree term is obtained by evaluating the selected invariant pairing on the low-energy operators, the renormalization-group term is the integral of the beta function between the two displayed scales, and the threshold term is the finite contribution of the modes removed at μ_{match}. The separation is meaningful once the scheme and operator basis in (M2) have been fixed. The one-loop formula follows directly from $\mu\,\mathrm{d}(g_a^{-2})/\mathrm{d}\mu = \epsilon_{\mathrm{loop}} b_a/(8\pi^2) + O(\epsilon_{\mathrm{loop}}^2 g_a^2)$, which is the derivative of the beta-function convention stated above. The heavy-scalar part is the Gaussian elimination identity already proved in Theorem 41; its contribution is therefore exactly the first term in (453).

For (ii), the hypotheses make $\mathcal{M}_*$ a C^1 map between two finite-dimensional spaces of equal dimension. The inverse-function theorem applied at $\mathbf{q}_*$ gives neighborhoods U, V and a unique C^1 inverse because $\det J(\mathbf{q}_*) \neq 0$. Package-equivalent directions have already been quotiented out, so this is the claimed physical local identifiability.

For (iii), full column rank provides a set of d rows whose $d \times d$ minor is invertible. Apply the inverse-function theorem to the submap made of those rows. Its local inverse determines all coordinates in $\mathbf{q}_*$; composing the remaining rows with that inverse gives well-defined local consistency relations. These relations are not used to choose a second set of fitted coordinates.

For (iv), choose a nonzero h in the kernel of $J(\mathbf{q}_*)$. The first-order Taylor formula for the C^1 map gives $\mathcal{M}_*(\mathbf{q}_* + \varepsilon h) = \mathcal{M}_*(\mathbf{q}_*) + \varepsilon J(\mathbf{q}_*)h + o(\varepsilon) = \mathcal{M}_*(\mathbf{q}_*) + o(\varepsilon)$, proving the stated linearized non-identifiability. No assertion about an exact nonlinear family is made without further hypotheses. □

The theorem also fixes the status of a numerical statement. If (M1) fixes $\mathbf{q}_*$ without using the measured values of $\mathbf{O}$, every component of $\mathcal{M}_*(\mathbf{q}_*)$ is a prediction in principle, subject to the stated truncation error. If instead r coordinates are calibrated from r observables, the calibrated coordinates are empirical inputs; only independent relations among the remaining observables are predictions. More invariantly, a relation $\mathcal{R}_0$ is parameter-free on the selected class when

$$\mathcal{R}_0(\mathcal{M}_{\mu,\mathcal{R}}(\Gamma_*, \mathbf{q})) = 0 \quad \text{for every admissible } \mathbf{q} \text{ retained by selection.} \tag{456}$$

Thus a successful fit, by itself, is a reconstruction. A prediction requires either a uniquely selected $\mathbf{q}_*$ or a relation such as (456) that survives all still-allowed microscopic coordinates and the calculated loop and threshold corrections.

7.4. *Gauge invariance and stochastic covariance.* Let g denote a smooth deterministic gauge transformation, possibly depending on time. For the Cartan bundle specified above, g is at least an H-valued transformation; a transformation by the full $\widetilde{G}$ requires an additional extension of the bundle and is not assumed automatically. The master connection transforms as

$$\mathbb{A} \mapsto g\mathbb{A}g^{-1} + g\mathrm{d}g^{-1}, \tag{457}$$

and the curvature transforms covariantly,

$$\mathbb{F} \mapsto g\mathbb{F}g^{-1}. \tag{458}$$

If the invariant pairing satisfies (46) and the extension data satisfy (49), then

$$\langle \mathbb{F}, \mathbb{F} \rangle_{\mathfrak{g}} \tag{459}$$

is gauge invariant. The matter and information terms are gauge invariant provided their representations and covariant derivatives are chosen consistently.

The stochastic mobility must transform as a tensor on configuration space. If R_g denotes the tangent action of a gauge transformation, assume that the chosen field-space metric is R_g-isometric and let R_g^* denote the corresponding dual action on cotangent vectors. Covariance then requires

$$\mathbb{M}(g \cdot \mathbb{X}) = R_g \mathbb{M}(\mathbb{X}) R_g^*. \tag{460}$$

Here the right-hand side uses the cotangent action on the dual slot; in the metric-identified tangent notation this is equivalently

$$\widehat{\mathbb{M}}(g \cdot \mathbb{X}) = R_g \widehat{\mathbb{M}}(\mathbb{X}) R_g^{-1}, \qquad \boldsymbol{\sigma}(g \cdot \mathbb{X}) \boldsymbol{\sigma}(g \cdot \mathbb{X})^* = R_g \big(\boldsymbol{\sigma}\boldsymbol{\sigma}^*\big)(\mathbb{X}) R_g^{-1}. \tag{461}$$

This is a covariance condition on the second-order symbol. For a smooth deterministic coordinate transformation $y = \Upsilon(t, x)$, Itô's formula also gives the transformed drift

$$\widetilde{b}^a = \partial_t \Upsilon^a + \partial_i \Upsilon^a \, b^i + \frac{1}{2} a^{ij} \partial_i \partial_j \Upsilon^a. \tag{462}$$

The time-derivative term is present even for an affine time-dependent transformation; the quadratic-variation term is present for a nonlinear transformation even when it is time independent. A stochastic gauge transformation requires additional Itô–Wentzell and cross-variation terms and is not covered by this deterministic change of coordinates. Stratonovich notation absorbs the latter into the ordinary chain rule, but retains the former. A mathematically complete construction must either work on the quotient configuration space or introduce a gauge-fixing and BRST/BV treatment. The covariance condition alone does not complete the global quotient construction.

7.5. *Well-posedness requirements.* An infinite-dimensional stochastic equation requires an analytic configuration space in addition to its geometric notation. In particular, a realization of (62) must specify the operator domains, the boundary conditions, the treatment of gauge orbits, the covariance of the noise, and the sense in which the stochastic integral is defined. A quotient by gauge orbits need not be a Hilbert space. The Hilbert-space statements below apply to a specified Hilbert realization of a gauge slice, or to quotient coordinates for which that structure has actually been established.

On a finite-dimensional slice, write M_N for the tangent mobility and S_N for the projected action. In Euclidean coordinates with Lebesgue reference volume, the reversible Itô approximation is

$$\mathrm{d}X_t^N = \big[-M_N \nabla S_N + \theta \, \mathrm{div}\, M_N\big](X_t^N)\, \mathrm{d}t + \sqrt{2\theta M_N(X_t^N)}\, \mathrm{d}W_t^N. \tag{463}$$

Here $(\mathrm{div}\, M_N)^i = \sum_j \partial_j M_N^{ij}$. For constant mobility the divergence vanishes. With a positive reference density r_N, it is replaced by $r_N^{-1} \, \mathrm{div}(r_N M_N)$. Thus a projection of the formal gradient and a projection of the noise do not, by

themselves, specify a reversible approximation for a variable mobility or a nonconstant reference density.

A useful first estimate is

$$\sup_N \mathbb{E}\left[\sup_{t\le T}\mathcal{V}(X_t^N)+\int_0^T \mathcal{D}(X_t^N)\,\mathrm{d}t\right]<\infty. \tag{464}$$

Its consequences depend on what the functionals control. A bound on the Hilbert norm alone does not give compactness in an infinite-dimensional Hilbert space. Spatial compactness, control of time increments, and identification of the limiting martingales are distinct requirements. The general stochastic-evolution and invariant-measure framework is developed in [53] and [54]; the martingale-problem and measure-theoretic background is given in [148] and [19].

7.6. *A complete finite-regulator equilibrium construction.* The scalar confinement estimate can be extended to all variables of a specified bosonic regulator. This supplies an existence and uniqueness result in which the coefficients and the reference measure are fixed. It also separates the finite-regulator problem from the continuum geometry problem. In this construction the lattice geometry is fixed; the coframe is not an additional integration variable.

Let $\mathcal{V}$ be a finite set of n vertices, let $\mathcal{E}$ be a finite set of oriented links, and choose finitely many oriented closed plaquette paths $\mathcal{P}$. Set

$$\begin{aligned} K &= SO(5)\times SU(3)\times SU(2)\times U(1),\\ \mathcal{X}_{\mathrm{lat}} &= K^{\mathcal{E}}\times\mathbb{R}^{\mathcal{V}}, \qquad \nu_{\mathrm{lat}} = \mathrm{d}U\,\mathrm{d}s. \end{aligned} \tag{465}$$

Here $\mathrm{d}U$ is product Haar probability and $\mathrm{d}s$ is ordinary Lebesgue measure in the declared dimensionless scalar coordinates. For each plaquette p, let U_p be the ordered link product, using an inverse when its orientation opposes that of a link. Choose a base vertex $v(p)$, fixed positive coefficients β_a, and unitary representations R_a of dimensions d_a for the four factors. Define

$$\begin{aligned} k_p(U) &= \sum_a \beta_a\big[d_a-\mathrm{Re}\,\mathrm{tr}\,R_a(U_{p,a})\big],\\ 0\le k_p(U) &\le k_{p,\max} := 2\sum_a \beta_a d_a. \end{aligned} \tag{466}$$

The lower bound follows by summing $1-\cos\vartheta$ over the eigenphases of a unitary matrix. These are smooth gauge-invariant functions. Their plaquette form is a declared regulator of curvature energy; no convergence to the dynamical-coframe Cartan theory is inferred from this definition.

Fix $f, m, q, \theta > 0$, $\alpha_\sigma, s_0 \in \mathbb{R}$, and nonnegative edge weights a_{ij}. The edge sum below counts each unordered scalar edge once:

$$\begin{aligned} S_{\mathrm{lat}}(U,s) = \sum_{p\in\mathcal{P}} e^{-\alpha_\sigma s_{v(p)}} k_p(U) + \frac{f^2}{2}\sum_{\{i,j\}} a_{ij}(s_i - s_j)^2 \\ + \frac{m^2 f^2}{2}\sum_{i\in\mathcal{V}} (s_i - s_0)^2. \end{aligned} \tag{467}$$

The scalar weight and quadratic stabilizer are precisely the mechanisms in Section 5.4.1. Higgs and fermion coordinates are omitted from this bosonic realization; their measures cannot be deduced from the following construction.

Equip $K^{\mathcal{E}}$ with a fixed product bi-invariant Riemannian metric. Write ∇_U, Δ_U for its gradient and Laplacian, with Δ_U nonpositive in the L^2 pairing. The generator is

$$\mathcal{L}_{\mathrm{lat}} F = \theta \Delta_U F - \langle \nabla_U S_{\mathrm{lat}}, \nabla_U F\rangle + q\big(\theta \Delta_s F - \nabla_s S_{\mathrm{lat}} \cdot \nabla_s F\big). \tag{468}$$

This is an intrinsic generator. In local group coordinates its Itô drift includes the metric-volume term; it is not obtained by dropping the correction in (80).

THEOREM 19 (Finite-regulator equilibrium). *The diffusion with generator* (468) *has a unique nonexplosive realization from every initial point. Its unique invariant probability, among all probability measures on* $\mathcal{X}_{\mathrm{lat}}$*, is*

$$\pi_{\mathrm{lat}}(\mathrm{d}U\,\mathrm{d}s) = Z_{\mathrm{lat}}^{-1} e^{-S_{\mathrm{lat}}(U,s)/\theta}\,\mathrm{d}U\,\mathrm{d}s, \qquad 0 < Z_{\mathrm{lat}} < \infty. \tag{469}$$

It is reversible. Every polynomial scalar moment and every fixed linear-exponential scalar moment is finite under this probability.

Proof. Put $y_i = s_i - s_0$. Positivity of every summand gives

$$0 < Z_{\mathrm{lat}} \le \int_{\mathbb{R}^n} \exp\left(-\frac{m^2 f^2}{2\theta}|y|^2\right)\mathrm{d}y = \left(\frac{2\pi\theta}{m^2 f^2}\right)^{n/2}. \tag{470}$$

For strict positivity, restrict to a scalar cube of positive volume: the continuous action is bounded there because the group factor is compact, so the integrand has a strictly positive lower bound. Multiplication by $|y|^r$ or $e^{b\cdot y}$ preserves integrability of the bounding Gaussian. Division by $Z_{\mathrm{lat}} > 0$ proves the moment assertions.

Smooth coefficients give a pathwise unique local diffusion on this finite-dimensional manifold. To prove that its lifetime is infinite, use $V(U,s) = 1 + |y|^2$. A direct differentiation yields

$$\begin{aligned} \mathcal{L}_{\mathrm{lat}} V = 2q\theta n - 2qm^2 f^2 |y|^2 - 2qf^2 \sum_{\{i,j\}} a_{ij}(y_i - y_j)^2 \\ + 2q\sum_p \alpha_\sigma y_{v(p)} e^{-\alpha_\sigma(s_0 + y_{v(p)})} k_p(U) \le A_0 - 2qm^2 f^2 |y|^2, \end{aligned} \tag{471}$$

where

$$A_0 = 2q\theta n + \frac{2qe^{-\alpha_\sigma s_0}}{e} \sum_p k_{p,\max}. \tag{472}$$

Indeed, $ze^{-z} \le e^{-1}$ for every real z: it is negative for $z < 0$, and differentiation gives its maximum at $z = 1$ on $[0, \infty)$. This also covers $\alpha_\sigma = 0$, when the corresponding force is zero.

Let $\tau_R = \inf\{t : |y_t| \ge R\}$ with $R > |y_0|$. Before τ_R, coefficients and derivatives are bounded on a compact set, so the stopped stochastic integral has mean zero. Dynkin's formula and (471) imply

$$\mathbb{E}V(U_{t\wedge\tau_R}, s_{t\wedge\tau_R}) \le V(U_0, s_0^{\text{init}}) + A_0 t. \tag{473}$$

Here s_0^{init} denotes the initial vector, not the scalar center s_0. Continuity gives $V \ge 1 + R^2$ on $\{\tau_R \le t\}$, and therefore

$$\mathbb{P}(\tau_R \le t) \le \frac{V(U_0, s_0^{\text{init}}) + A_0 t}{1 + R^2} \longrightarrow 0. \tag{474}$$

The compact group coordinates cannot escape. Thus the local lifetime is infinite for every initial point, which completes the existence and pathwise-uniqueness argument.

We next verify invariance without relying solely on a formal stationarity equation. For compactly supported smooth functions F, G, integration by parts on the group and Euclidean factors gives

$$\int F\mathcal{L}_{\text{lat}} G \, \mathrm{d}\pi_{\text{lat}} = -\theta \int \left[\langle \nabla_U F, \nabla_U G\rangle + q\nabla_s F \cdot \nabla_s G\right] \mathrm{d}\pi_{\text{lat}}. \tag{475}$$

On the bounded smooth domain $K^{\mathcal{E}} \times \{|y| < R\}$, the killed diffusion has a symmetric Dirichlet transition semigroup $P_t^{(R)}$ for this divergence-form operator. This follows from the Dirichlet integration-by-parts identity and uniqueness of its uniformly elliptic heat equation. For nonnegative bounded functions, the killed expectations increase to the full diffusion expectations as $R \to \infty$. Monotone convergence passes symmetry to P_t. Nonexplosion gives $P_t 1 = 1$. Taking one argument equal to 1 in the resulting semigroup identity proves

$$\int P_t F \, \mathrm{d}\pi_{\text{lat}} = \int F P_t 1 \, \mathrm{d}\pi_{\text{lat}} = \int F \, \mathrm{d}\pi_{\text{lat}}. \tag{476}$$

The extension from bounded nonnegative functions to bounded measurable functions follows by positive and negative parts. Thus the probability in (469) is invariant and reversible.

Finally, the manifold is connected and the diffusion matrix is positive definite. On every bounded domain its smooth transition density is strictly positive between interior points for positive time, by the strong maximum principle for the uniformly elliptic heat equation. Any two points lie in a common connected bounded domain. The full transition kernel consequently

has a strictly positive density relative to π_{lat}; local heat-kernel existence and this exhaustion are within the finite-dimensional diffusion theory of [148].

If η is another invariant probability, invariance and absolute continuity of each positive-time transition give $\eta = h\pi_{\mathrm{lat}}$ for some $h \geq 0$ with $\int h \, \mathrm{d}\pi_{\mathrm{lat}} = 1$. Semigroup symmetry extends to a nonnegative L^1 argument by applying it to truncations and then using monotone convergence. Reversibility implies $P_t h = h$ almost everywhere: test this identity against a bounded function, use invariance of η, and interchange the semigroup by symmetry. For the strictly concave bounded function $\varphi(r) = r/(1+r)$ on $[0,\infty)$, Jensen's inequality gives $P_t\varphi(h) \leq \varphi(P_t h) = \varphi(h)$ almost everywhere. Both sides have equal π_{lat} integral by invariance. Equality therefore holds almost everywhere. Equality in the strict Jensen inequality forces h to be constant almost surely under a positive-time transition from any point where equality holds. Such a transition is equivalent to π_{lat}, so h is constant π_{lat}-almost everywhere. Its integral is one, hence $h = 1$ and $\eta = \pi_{\mathrm{lat}}$. □

The lattice gauge group has finite Haar volume, so gauge invariance does not create the infinite group-volume obstruction of an unreduced continuum functional integral. Gauge-invariant observables may also be pushed to the finite quotient. The theorem supplies no estimates uniform in the number of lattice sites, no integration over a degenerating coframe, and no interacting fermion measure. Those are separate questions when this regulator is compared with the original continuum geometry.

8. **A concrete four-dimensional interacting regulator and its thermodynamic reduction**

The preceding construction is abstract until one declares a finite branch on which every integration variable, coefficient, and boundary condition is visible. This section supplies such a branch. Its purpose is deliberately limited: it gives a fully specified four-dimensional Euclidean regulator with interacting gauge, coframe, and order-parameter variables, and proves the finite-regulator thermodynamic theorem on that branch. It does not identify this regulator with the complete Lorentzian gravitational theory, and it does not claim a regulator-independent quantum limit.

8.1. *Finite four-dimensional state space and mother-data registry.* Let Λ_h be a finite periodic hypercubic lattice approximating the four-dimensional torus $\mathbb{T}^4$. Write $\mathcal{V}_h$, $\mathcal{E}_h$, and $\mathcal{P}_h$ for its vertices, oriented links, and oriented plaquettes. The compact gauge group used at the finite regulator is

$$K = \mathrm{SO}(5) \times \mathrm{SU}(3) \times \mathrm{SU}(2) \times \mathrm{U}(1), \qquad \mathcal{X}_h = K^{\mathcal{E}_h} \times \mathbb{R}^{16|\mathcal{V}_h|} \times \mathbb{R}^{|\mathcal{V}_h|}. \quad (477)$$

The first factor contains link variables U_ℓ. The second contains the four-by-four coframe coefficients e_v at each vertex, flattened into $\mathbb{R}^{16}$, and the last contains the scalar/order-parameter values σ_v. The coframe variables in this section are Euclidean regulator coordinates. The oriented nondegenerate sector and its Lorentzian continuation are treated as additional matching conditions below. In this particular finite model, e_v and σ_v are invariant under link gauge transformations. The differences $e_v - e_w$ below are ordinary differences, not covariant differences of local Lorentz vectors. Thus the sixteen variables at a vertex are coordinates for a proposed geometric sector; identifying them with a gravitational coframe requires a further covariant construction. The finite thermal argument does not assume that identification.

All numerical coefficients are recorded before any evolution or comparison with data. The registry is

$$\mathscr{R}_h = \big(\beta_a, \alpha, \eta, \kappa_e, m_e, \lambda_e, f, m_\sigma, \theta, e_\star, \sigma_\star, \Gamma_h\big), \tag{478}$$

where $\beta_a, \kappa_e, m_e, \lambda_e, f, m_\sigma, \theta > 0$, $\eta, \alpha \geq 0$, and Γ_h is a fixed positive mobility matrix. In the unified-field interpretation each entry of $\mathscr{R}_h$ must be the value of a specified pairing, regulator, vacuum datum, or bath coupling in the mother data. A value selected after inspecting an observable is a fit and is not counted as a mother prediction. The graph, the positive symmetric edge weights a_{vw}, and the unitary representations R_a of dimensions d_a are also fixed data. Each geometric plaquette is assigned one orientation and one anchor vertex $v(p)$.

For a plaquette p let $U_{p,a}$ be the ordered product in the ath group factor and define

$$k_p(U) = \sum_a \beta_a \big[d_a - \operatorname{Re}\operatorname{tr} R_a(U_{p,a})\big] \geq 0. \tag{479}$$

Let

$$w_v(e,\sigma) = \exp(-\alpha\sigma_v)\left[1 + \eta\,\frac{\|e_v - e_\star\|^2}{1 + \|e_v - e_\star\|^2}\right]. \tag{480}$$

The coframe factor lies in $[1, 1+\eta]$. The full weight is positive but is unbounded as $\sigma_v \to -\infty$ when $\alpha > 0$. Its multiplication by $k_p \geq 0$ preserves the lower bound on the action; boundedness of the full weight is not needed for the partition integral. With each unoriented edge counted once, set

$$\begin{aligned} S_h(U,e,\sigma) = {} & \sum_{p\in\mathcal{P}_h} w_{v(p)}(e,\sigma) k_p(U) + \frac{\kappa_e}{2}\sum_{\{v,w\}} \|e_v - e_w\|^2 \\ & + \frac{m_e^2}{2}\sum_v \|e_v - e_\star\|^2 + \frac{\lambda_e}{4}\sum_v \|e_v - e_\star\|^4 \\ & + \frac{f^2}{2}\sum_{\{v,w\}} a_{vw}(\sigma_v - \sigma_w)^2 + \frac{m_\sigma^2 f^2}{2}\sum_v (\sigma_v - \sigma_\star)^2. \end{aligned} \tag{481}$$

This is a specified finite candidate for matching to the positive norm-square branch of the extended curvature. The plaquette term is the gauge-curvature block, the coframe terms are the regulated geometric block, and the scalar terms are the order-parameter block. The common weight in (480) is the retained mixed interaction. Equality with the primitive mother norm is a matching condition on the selected pairing and regulator; it is not obtained merely by reusing the word "action". If that matching condition is established, the displayed terms must all be accounted for by the same primitive pairing. The finite theorem below holds for the displayed action without presupposing that the matching has been proved.

8.2. *Exact finite generator and Gibbs law.* Equip $K^{\mathcal{E}_h}$ with the product bi-invariant metric and use the Euclidean metric on the coframe and scalar factors. Let ∇_h and div_h denote the corresponding gradient and divergence. For the fixed temperature parameter $\theta > 0$ define

$$\mathcal{L}_h F = \theta \,\mathrm{div}_h(\Gamma_h \nabla_h F) - \langle \Gamma_h \nabla_h S_h, \nabla_h F \rangle_h \,, \qquad \Gamma_h = \Gamma_h^{\mathsf{T}} \succ 0. \tag{482}$$

The intrinsic form includes the metric-volume drift; writing an Itô equation in local coordinates without that drift would change the invariant measure. Here a fixed matrix on the group factors means its components in a fixed product frame of left-invariant and Euclidean vector fields. More generally, Γ_h may be a smooth symmetric bundle map satisfying $\gamma_- I \le \Gamma_h \le \gamma_+ I$ for fixed positive constants. These are assumptions at a fixed regulator, not bounds uniform in h.

Gauge covariance imposes a further restriction on the mobility. Let Φ_g be the site-gauge action on the links, acting trivially on the coframe and scalar coordinates of this particular model. In addition to the gauge-invariant action and reference volume, a covariant generator requires

$$\Gamma_h(\Phi_g x) = D\Phi_g(x)\, \Gamma_h(x)\, D\Phi_g(x)^*, \tag{483}$$

where the adjoint uses the specified product metric. This condition makes $\mathcal{L}_h(F \circ \Phi_g) = (\mathcal{L}_h F) \circ \Phi_g$ by invariance of the gradient and divergence. It is not implied by positive definiteness. For example, in an SU(2) link block, a left-frame matrix $\mathrm{diag}(1,2,3)$ is positive but a right gauge rotation can exchange its first two principal axes. The resulting covariance is then $\mathrm{diag}(2,1,3)$, so the generator is not gauge covariant. A sufficient choice is a block-diagonal mobility with a fixed positive scalar multiple of the identity on each link-factor tangent block and an arbitrary fixed positive symmetric block on the Euclidean variables. In this sufficient choice, all mixed blocks involving a link factor vanish. The equilibrium theorem below holds for the full stated class of positive mobilities on the unreduced finite space; its gauge-covariant interpretation uses

the subclass satisfying (483). Invariance of a Gibbs law alone does not justify passage of the dynamics to gauge equivalence classes.

THEOREM 20 (Finite four-dimensional interacting equilibrium). *For every fixed finite lattice, every registry satisfying* (478) *and the fixed geometric data above, the diffusion generated by* (482) *is nonexplosive and has the unique invariant probability*

$$\pi_h(\mathrm{d}U\,\mathrm{d}e\,\mathrm{d}\sigma) = Z_h^{-1}\exp[-S_h(U,e,\sigma)/\theta]\mathrm{d}U\,\mathrm{d}e\,\mathrm{d}\sigma, \qquad 0 < Z_h < \infty. \tag{484}$$

It is reversible with respect to π_h, and all polynomial moments of the Euclidean variables are finite.

Proof. The compact gauge factor has finite Haar volume. Since $k_p \geq 0$ and the quadratic and quartic coframe terms are nonnegative, the integrand in (484) is bounded above by a product of Gaussian–quartic integrable factors in (e,σ). Restricting these variables to a compact box gives a strictly positive lower bound, so $0 < Z_h < \infty$. Smoothness and uniform ellipticity on each bounded coordinate domain give local existence and pathwise uniqueness. For nonexplosion, we use an energy argument that does not require an unproved comparison between exponential derivatives and polynomial confinement. Write $z = (e-e_\star, \sigma-\sigma_\star)$ and choose smooth cutoffs $\chi_R(z) = \chi(z/R)$ with $0 \leq \chi_R \leq 1$, $\chi_R \to 1$, and $|\nabla\chi_R| \leq C/R$. The gradient form on $L^2(\pi_h)$ is closable because its density is smooth and positive and its coefficients are locally uniformly elliptic. For its closure $\mathcal{E}_h$, finite total mass gives

$$\|1-\chi_R\|_{L^2(\pi_h)} \to 0, \qquad \mathcal{E}_h(\chi_R,\chi_R) \leq \theta\gamma_+ C^2/R^2 \to 0. \tag{485}$$

Consequently 1 belongs to the closed form domain with zero energy. The associated symmetric semigroup preserves 1, so its diffusion has no killing or explosion for π_h-almost every initial state. Local smooth ellipticity upgrades this to every starting point. Indeed, the minimal diffusion has an absolutely continuous transition law before its lifetime; the Markov property at time $\varepsilon > 0$ then rules out an explosion after ε, and local existence rules out explosion at time zero. The local strong solution therefore extends globally. This is the conservative-form criterion of [75]. Integration by parts gives

$$\int F\mathcal{L}_h G\,\mathrm{d}\pi_h = -\theta\int \langle\nabla_h F, \Gamma_h\nabla_h G\rangle_h\,\mathrm{d}\pi_h, \tag{486}$$

which proves reversibility and invariance. Strict positivity of the finite dimensional heat kernel and connectedness imply uniqueness by the standard irreducibility argument. □

8.3. *Second-law identity on the declared branch.* For a law $\rho_t \ll \pi_h$, let $r_t = \mathrm{d}\rho_t/\mathrm{d}\mu_h$ and $f_t = \mathrm{d}\rho_t/\mathrm{d}\pi_h$, where $\mu_h = \mathrm{d}U\,\mathrm{d}e\,\mathrm{d}\sigma$. Define $F_h[\rho] = \int S_h\,\mathrm{d}\rho + \theta\int \log r\,\mathrm{d}\rho$. Then

Table 3. Synthetic finite-regulator quadrature check. The numbers are not experimental data and are not a continuum test.

Quantity	Value
Estimated partition integral Z_h	12.0485034910
Left side $\int g\mathcal{L}_h g \,\mathrm{d}\pi_h$	−0.3744077978
Right side $-\theta \int \nabla g^{\mathsf{T}} \Gamma \nabla g \,\mathrm{d}\pi_h$	−0.3744077978
Absolute discrepancy	5.6×10^{-17}

THEOREM 21 (Finite-regulator entropy production). *For every smooth positive solution of the Fokker–Planck equation generated by* (482)*, with finite Fisher information,*

$$F_h[\rho_t] - F_h[\pi_h] = \theta D(\rho_t \| \pi_h), \tag{487}$$

$$\frac{\mathrm{d}}{\mathrm{d}t} D(\rho_t \| \pi_h) = -\theta \int r_t \left(\nabla_h \log \frac{\rho_t}{\pi_h} \right)^{\mathsf{T}} \Gamma_h \left(\nabla_h \log \frac{\rho_t}{\pi_h} \right) \mathrm{d}\mu_h \le 0. \tag{488}$$

For a physical heat interpretation, additionally assume $\theta = k_B T$ and that S_h is the effective energy in fixed units. The Euclidean regulator and its sampling parameter do not by themselves specify a physical bath or physical time. If the bath coupling obeys local detailed balance and the heat convention is $\dot{Q}_{\mathrm{bath}} = -\mathrm{d}\mathbb{E}[S_h]/\mathrm{d}t$, then

$$\dot{S}_{\mathrm{tot}} = -T^{-1} \frac{\mathrm{d}F_h[\rho_t]}{\mathrm{d}t} \ge 0. \tag{489}$$

Proof. Equation (486) gives the symmetric Dirichlet form. Applying it to $f_t = \rho_t/\pi_h$ yields the second line of (488); positive definiteness of Γ_h gives the sign. The first line is the exact Gibbs identity and follows by expanding $\log(d\rho_t/d\pi_h)$. The final statement uses the first-law balance and local detailed balance; it is not inferred from Gibbs invariance alone. □

8.4. *Reproducible finite diagnostic.* As a numerical check of the analytic identity, we evaluated the one-plaquette U(1) subbranch with one coframe and one scalar coordinate. The potential was the restriction of (481) with $(\theta, \beta, \alpha, \eta, m_e^2, \lambda_e, m_\sigma^2) = (0.8, 1, 0.3, 0.2, 1, 0.1, 1)$ and $\Gamma = \mathrm{diag}(0.7, 0.5, 0.4)$. A tensor-product quadrature on $64 \times 161 \times 161$ points was applied to a smooth test function $g(\vartheta, e, \sigma) = \sin\vartheta + 0.2e^2 + 0.1\sigma e$. The two sides of the Dirichlet identity were computed independently: The angular reference measure in this table is $\mathrm{d}\vartheta$ with total mass 2π; normalizing Haar measure changes Z_h but not either expectation. The discrepancy is a floating-point residual, not a certified bound on quadrature or truncation error. The calculation checks the finite integration-by-parts identity only; it supplies no evidence for a regulator-independent or quantum theory.

8.5. *Relation to Lorentzian and continuum dynamics.* The use of polynomially confined matrix coordinates leaves a geometric integrability issue even at fixed resolution. A matrix can be invertible almost surely while its inverse has no finite first moment.

PROPOSITION 22 (Inverse-coframe moments in the finite reference law). *For the Gibbs law* (484)*, at every vertex* v *and for every* $r \geq 1$*,*

$$\mathbb{E}_{\pi_h} |\det e_v|^{-r} = \infty, \qquad \mathbb{E}_{\pi_h} \|e_v^{-1}\|_{\mathrm{F}}^r = \infty.$$

These statements persist on conditioning on $\det e_v > 0$*.*

Proof. Choose a rank-three matrix E_0. At least one cofactor is nonzero, so the determinant has nonzero differential there. The inverse function theorem gives local coordinates $(u, y) \in \mathbb{R} \times \mathbb{R}^{15}$ with $u = \det e_v$, with a smooth nonzero change-of-volume factor. Restrict y and all remaining noncompact variables to small compact boxes and the group variables to a set of positive Haar measure. The Gibbs density is continuous and strictly positive on this compact set, including $u = 0$. Its contribution to the first expectation is therefore bounded below by $c \int_{-\varepsilon}^{\varepsilon} |u|^{-r} du = \infty$. The selected cofactor remains bounded away from zero on a smaller box. The inverse-matrix formula consequently bounds one inverse entry below in magnitude by $c'/|u|$, proving the second assertion. On the positive orientation sector the same argument uses $\int_0^{\varepsilon} u^{-r} du$; conditioning divides by a finite positive probability and cannot remove the divergence. □

The singular matrices themselves have zero probability. The divergence comes from their neighborhoods and is compatible with finiteness of all polynomial moments proved above. Interpreting this reference law as a measure on fluctuating nondegenerate geometry therefore requires additional control near singular coframes. A change of measure or action for that purpose must be matched to the mother data and its quantum positivity checked separately.

On this fixed four-dimensional lattice, the same declared action supplies the gauge-curvature energy, the coframe/order-parameter coupling, the Gibbs law, and the entropy-production identity. It is not a proof of the full unified theory. In particular, the following implications remain to be established before a continuum or quantum claim is made:

(1) the oriented nondegenerate coframe sector and Lorentzian continuation must be selected without changing the registry;
(2) the nonlinear Hamiltonian and gauge constraints must close and be preserved for all lattice modes;
(3) estimates uniform in h must give a regulator-independent limit;
(4) a physical interacting Hilbert space, positive inner product, and anomaly-free quantum constraint algebra must be constructed.

The finite theorem connects the declared energy, probability law, and dissipation on the same state space. The next section examines which additional structures can be constructed explicitly and which require further matching to the gravitational theory.

9. **A discrete finite four-dimensional certification branch**

The continuous compact-group branch introduced above and the discrete branch below serve different purposes. The former carries the coframe and compact gauge variables used for the proposed geometric interface. The present $\mathbb{Z}_2$ branch is a smaller, completely enumerable certification model. It supplies an exact finite state space, an explicit stochastic kernel, and an independently reproducible no-refit check. No identification of the two regulators, and no inference about a continuum limit, is made.

The preceding structural discussion becomes mathematically testable only after one model, one state space, and one parameter registry have been fixed. We therefore give a complete finite example. The example is not introduced as a continuum limit in disguise: every sum below is finite, and every conclusion is stated at the regulator level.

9.1. *Lattice, fields, and gauge constraint.* Fix the periodic lattice

$$\Lambda_3 = (\mathbb{Z}/3\mathbb{Z})^4, \qquad |\Lambda_3| = 81,$$

with four positive coordinate directions labelled by $\mu \in \{0, 1, 2, 3\}$. There are therefore 324 oriented links. A raw configuration is

$$\omega = (U, \sigma, \tau), \qquad U_{x,\mu}, \sigma_x, \tau_x \in \{+1, -1\}.$$

The finite gauge group is $\mathcal{G} = \{\eta : \Lambda_3 \to \{+1, -1\}\}$, acting by

$$U_{x,\mu} \longmapsto \eta_x U_{x,\mu} \eta_{x+\hat{\mu}}, \qquad \sigma_x \longmapsto \eta_x \sigma_x, \qquad \tau_x \longmapsto \eta_x \tau_x.$$

The physical finite state space is the orbit quotient

$$\Omega_{\text{phys}} = \Omega/\mathcal{G}.$$

The quotient is finite and nonempty because the raw state space is finite and nonempty. All observables used below are orbit invariant and hence are well-defined on this quotient.

9.2. *Gauge-invariant action.* Define the three sufficient statistics

$$P(U) = \sum_{x \in \Lambda_3} \sum_{0 \le \mu < \nu \le 3} U_{x,\mu} U_{x+\hat{\mu},\nu} U_{x+\hat{\nu},\mu} U_{x,\nu}, \tag{490}$$

$$H(U, \sigma) = \sum_{x \in \Lambda_3} \sum_{\mu=0}^{3} \sigma_x U_{x,\mu} \sigma_{x+\hat{\mu}}, \tag{491}$$

$$R(\sigma,\tau)=\sum_{x\in\Lambda_3}\sigma_x\tau_x. \tag{492}$$

Each factor of η appears twice in every summand of (490) and (491), and the two factors cancel because $\eta_x^2=1$. The same cancellation is immediate in (492). Thus P, H, R and the action

$$S_{\beta,\kappa,\rho}(\omega)=-\beta P(U)-\kappa H(U,\sigma)-\rho R(\sigma,\tau)$$

are constant on gauge orbits. The Lean quotient construction in the finite gauge–Higgs verification module formalizes precisely the descent step: an orbit-invariant function is lifted to a function on Ω_{phys}.

9.3. *Finite Gibbs law.* For $\theta=(\beta,\kappa,\rho)$, define

$$Z_\theta=\sum_{\omega\in\Omega_{\mathrm{phys}}}\exp[-S_\theta(\omega)], \tag{493}$$

$$\pi_\theta(\omega)=Z_\theta^{-1}\exp[-S_\theta(\omega)]. \tag{494}$$

The quotient is finite and nonempty, and every summand in Z_θ is strictly positive. Consequently,

$$Z_\theta>0,\qquad \pi_\theta(\omega)>0,\qquad \sum_{\omega\in\Omega_{\mathrm{phys}}}\pi_\theta(\omega)=1.$$

These statements are proved by the finite Gibbs lemmas in the Lean module; they do not use a thermodynamic limit or an integrability estimate.

9.4. *Reversible finite dynamics and entropy balance.* Let $q(i,j)\ge 0$ be a symmetric proposal weight on Ω_{phys}. Set

$$w_\theta(i,j)=q(i,j)\exp\!\left(\frac{S_\theta(i)-S_\theta(j)}{2}\right).$$

The rate is nonnegative and satisfies detailed balance by direct algebra:

$$\exp[-S_\theta(i)]w_\theta(i,j)=q(i,j)\exp\!\left[-\frac{S_\theta(i)+S_\theta(j)}{2}\right] \tag{495}$$

$$=\exp[-S_\theta(j)]w_\theta(j,i). \tag{496}$$

The common factor Z_θ^{-1} therefore gives the same identity for π_θ. A probability vector p_t evolves according to

$$\dot p_i(t)=\sum_j\big[p_j(t)w_\theta(j,i)-p_i(t)w_\theta(i,j)\big].$$

For the relative entropy

$$\mathcal{H}(p_t\mid\pi_\theta)=\sum_i p_i(t)\log\frac{p_i(t)}{\pi_\theta(i)},$$

the finite-state calculation gives

$$\frac{\mathrm{d}}{\mathrm{d}t}\mathcal{H}(p_t \mid \pi_\theta) = -\frac{1}{2}\sum_{i,j}\bigl(p_i w_{ij} - p_j w_{ji}\bigr)\log\frac{p_i w_{ij}}{p_j w_{ji}} \tag{497}$$

$$= -\mathcal{D}_\theta(p_t) \le 0, \tag{498}$$

where $\mathcal{D}_\theta \ge 0$ follows from $(a-b)(\log a - \log b) \ge 0$ for positive a, b. The Lean theorem for the finite entropy balance makes the dependence on the master-equation derivative, positivity, normalization, and symmetric-support hypotheses explicit. Thus the entropy sign is derived from the finite dynamics; it is not inserted as an independent axiom.

9.5. *Parameter registration.* Let c_0 be the all-plus configuration. Let c_1 flip one link, c_2 flip one σ-spin, and c_3 flip one τ-spin. An independent lattice enumeration gives

$$\Delta(P, H, R)_{c_1} = (-12, -2, 0), \tag{499}$$

$$\Delta(P, H, R)_{c_2} = (0, -16, -2), \tag{500}$$

$$\Delta(P, H, R)_{c_3} = (0, 0, -2). \tag{501}$$

The first number follows because one link belongs to six plaquettes in four dimensions and each affected plaquette changes by -2. The second follows because one site belongs to eight oriented links. The third is the single on-site cross-field factor. The Python checker records these counts and rejects the registry if any one differs.

Because the partition function cancels in a probability ratio,

$$y_i := \log\frac{\pi_\theta(c_i)}{\pi_\theta(c_0)}$$

satisfies

$$\begin{pmatrix} y_1 \\ y_2 \\ y_3 \end{pmatrix} = \begin{pmatrix} -12 & -2 & 0 \\ 0 & -16 & -2 \\ 0 & 0 & -2 \end{pmatrix} \begin{pmatrix} \beta \\ \kappa \\ \rho \end{pmatrix}.$$

The determinant is -384, so the registry is injective. Explicitly,

$$\rho = -\frac{y_3}{2}, \qquad \kappa = -\frac{y_2 + 2\rho}{16}, \qquad \beta = -\frac{y_1 + 2\kappa}{12}.$$

The Lean declarations `registry_injective` and `registry_inverse` prove these identities over $\mathbb{R}$.

9.6. *Frozen no-refit prediction.* In an empirical application, a calibration split would be used once to estimate the three ratios in (9.5); after solving for $\widehat{\theta}$, the parameters would be frozen. In the finite check reported below, the ratios

are supplied by the exact registry construction, so no statistical calibration sample is used. For a held-out observable O, the prediction is

$$\widehat{\mathbb{E}}[O] = \frac{\sum_{\omega\in\Omega_{\mathrm{phys}}} O(\omega)\exp[-S_{\widehat{\theta}}(\omega)]}{Z_{\widehat{\theta}}}.$$

The primary declared observable is the plaquette mean $P/486$; the matter-link and cross-field means are secondary observables. The Lean registry theorems prove that equal registered ratios imply equal parameters and hence equality of the resulting finite expectations. The numerical report must still provide Monte–Carlo uncertainty and held-out error; the exact finite theorem alone is not an experimental confirmation. In the numerical check below, "held-out" denotes an independent simulation chain, not an independent physical data set.

9.7. *Uniformization, nonnegativity, and normalization.* The entropy identity above was initially stated for a strictly positive, normalized solution of the master equation. The finite construction below first establishes a nonnegative, normalized law from the jump rates. Let

$$r_i = \sum_j q(i,j), \qquad K_{ij} = \delta_{ij}\left(1 - \frac{r_i}{\lambda}\right) + (1-\delta_{ij})\frac{q(i,j)}{\lambda},$$

where $\lambda > 0$, $q(i,j) \geq 0$, $q(i,i) = 0$, and $r_i \leq \lambda$. The finite generator is

$$L_{ij} = \begin{cases} -r_i, & i = j, \\ q(i,j), & i \neq j, \end{cases} \qquad L = \lambda(K - I).$$

The verified generator–uniformization bridge proves

$$K_{ij} \geq 0, \qquad \sum_j K_{ij} = 1, \qquad \lambda(K_{ij} - \delta_{ij}) = L_{ij}.$$

For an initial probability vector p_0 and $t \geq 0$, define the Poisson-uniformized law, with $a = \lambda t \geq 0$, by

$$p_t(j) = \sum_{n=0}^{\infty} e^{-a}\frac{a^n}{n!}(p_0 K^n)_j.$$

The Lean module 'UniformizedFiniteMarkov20261118' proves termwise nonnegativity, summability, and

$$p_t(j) \geq 0, \qquad \sum_j p_t(j) = 1.$$

The remaining analytic bridge is termwise differentiation of (9.7), which yields $\dot{p}_t = p_t L$ (or the transpose convention for column vectors). It is a finite-series estimate and is kept separate from the completed positivity and mass proof. The present formal result therefore establishes nonnegativity and unit mass, but does not by itself establish strict positivity. Strict positivity for positive

times requires an irreducibility condition together with a full-support initial law; alternatively, the entropy identity can be stated with the standard convention $0 \log 0 = 0$.

9.8. *Independent frozen-parameter check.* The registry equations were solved once before either Monte–Carlo chain was inspected. We used

$$(\beta, \kappa, \rho) = (0.08, 0.06, 0.04), \qquad (y_1, y_2, y_3) = (-1.08, -1.04, -0.08),$$

and froze this parameter vector. Two independent chains, with seeds 2026111801 and 2026111802, each retained 12000 samples after 3000 burn-in steps and thinning by 10. The differences between the chains were

observable	difference	95% bootstrap interval
$P/486$	0.0017476	$[-0.0041344, 0.0075542]$
$H/324$	-0.0038256	$[-0.0089635, 0.0013575]$
$R/81$	0.0036914	$[-0.0061728, 0.0144897]$.

All three intervals contain zero. This verifies reproducibility of the frozen finite regulator at the reported Monte–Carlo precision. It is not an experimental confirmation: no public physical observable has yet been mapped to the three discrete lattice statistics.

9.9. *Limits of the result.* This section closes one finite interacting regulator. It does not prove that the family has a regulator-independent continuum limit, that the infinite volume limit is unique, or that the construction yields a positive physical Hilbert space for interacting Lorentzian gravity. Those are separate claims requiring uniform estimates and a reconstruction theorem. The present model is valuable precisely because every finite statement is explicit, auditable, and falsifiable before those harder limits are attempted.

10. **Identifiable finite models, constrained motion, and positive quantum evolution**

A common variational structure becomes predictive only after its parameters, admissible motions, and observation rules have been fixed. Recovering coefficients from responses does not select those coefficients from first principles. Preserving a constraint does not identify it with a gravitational constraint. Likewise, constructing positive quantum evolution at fixed spatial resolution leaves a separate problem of removing that resolution. We develop explicit constructions that provide a starting point for these three distinct extensions.

10.1. *What the finite responses determine.* Fix the graph, its edge weights and representations, the reference fields $e_\star, \sigma_\star$, and units of field amplitude, energy, and time. Consider (478) with constant mobility in the specified product frame. We ask whether different coefficients can give the same complete

responses. This inverse problem within a selected model differs from whether primitive mother data select one model and one registry.

An actual configuration variation avoids treating plaquette energies as independent coordinates. Choose a link ℓ contained in $n_\ell > 0$ distinct plaquettes and X_a in one Lie-algebra factor, with $c_a = \operatorname{tr}[dR_a(X_a)^\dagger dR_a(X_a)] > 0$. Vary $U_{\ell,a}(t) = \exp(tX_a)$, set all other links to the identity, and take constant fields $\sigma = s$ and $\|e - e_\star\|^2/(1 + \|e - e_\star\|^2) = r$. Then

$$Q_a(r, s) := \frac{1}{n_\ell c_a} \frac{\mathrm{d}^2}{\mathrm{d}t^2} S_h(U(t), e, s)\Big|_{t=0} = \beta_a e^{-\alpha s}(1 + \eta r). \tag{502}$$

Indeed, either orientation of an incident plaquette gives $d_a - \operatorname{Re}\operatorname{tr} R_a(e^{\pm tX_a}) = c_a t^2/2 + O(t^4)$; the remaining energy terms are independent of t. Consequently

$$\beta_a = Q_a(0, 0), \qquad \alpha = -\partial_s \log Q_a(0, s)|_{s=0}, \qquad \eta = \partial_r \log Q_a(r, 0)|_{r=0+}. \tag{503}$$

The last derivative can equivalently be obtained from a unit-vector coframe variation: $\partial_t^2 Q_a(r(e_\star + tv), 0)|_{t=0} = 2\beta_a \eta$. No extension to negative r is required.

At identity links and reference fields, let L_0, L_a be the unweighted and weighted graph Laplacians, with each edge counted once. The noncompact Hessians and an onsite fourth derivative are

$$H_e = (\kappa_e L_0 + m_e^2 I) \otimes I_{16}, \qquad H_\sigma = f^2 L_a + m_\sigma^2 f^2 I, \qquad \partial^4_{e_{v,i}} S_h = 6\lambda_e. \tag{504}$$

The mixed gauge energy vanishes at identity links. An off-diagonal edge entry of H_e identifies κ_e, and a row sum identifies m_e^2. A scalar edge entry with known positive weight identifies f^2; a row sum then identifies $m_\sigma^2 f^2$. Positivity fixes the square roots. This argument does not require a nondegenerate full gauge Hessian.

For temperature and mobility, let $p_h = \mathrm{d}\pi_h/\mathrm{d}\mu_h$ be the Gibbs density relative to the fixed volume and choose $S_h(x) \neq S_h(y)$. Then

$$\theta = -\frac{S_h(x) - S_h(y)}{\log p_h(x) - \log p_h(y)}, \qquad \frac{1}{2} \lim_{\Delta t \downarrow 0} \frac{\operatorname{Cov}(\Delta Y \mid Y_t = y)}{\Delta t} = \theta \Gamma_h(y). \tag{505}$$

The covariance uses the fixed local frame. Equivalently, the carré du champ, defined as $[\mathcal{L}_h(FG) - F\mathcal{L}_h G - G\mathcal{L}_h F]/2$, equals $\theta\langle \nabla F, \Gamma_h \nabla G\rangle$. These are ideal response and density probes; estimation from noisy finite observations remains a separate inverse problem.

Proposition 23 (Finite response identifiability). *If the fixed graph has the stated link and edge probes and all responses are given in fixed units, the coefficients $(\beta_a, \alpha, \eta, \kappa_e, m_e, \lambda_e, f, m_\sigma, \theta, \Gamma_h)$ are uniquely determined by the preceding probes. The graph, reference fields, representations, and functional form are held fixed.*

Proof. Equation (503) recovers the gauge coefficients and shared couplings. Edge entries, row sums, and fourth derivatives in (504) recover the confinement and edge coefficients. Since $f > 0$, division recovers m_σ^2. Equation (505) then gives θ and Γ_h. Two registries with the same probes therefore coincide. This does not select the graph, vacuum, or group from primitive data. □

Absolute energy calibration is essential. For every $c > 0$,

$$(S_h, \theta, \Gamma_h) \longmapsto (cS_h, c\theta, \Gamma_h/c) \tag{506}$$

preserves both π_h and $\mathcal{L}_h$. It is realized within the registry by multiplying $\beta_a, \kappa_e, m_e^2, \lambda_e, f^2$ by c, leaving m_σ^2, α, η fixed, and changing θ, Γ_h as displayed. Probability laws alone cannot distinguish this family. One independent energy normalization removes this ambiguity; it does not prove unique selection of every constant by the mother theory.

For quadratic potentials one may instead use the Ornstein–Uhlenbeck relations $A_* = -\Gamma_h H_*$ and $C_* = \theta H_*^{-1}$. The covariance relation is not exact for a nonlinear Gibbs equilibrium. For example, $V(x) = m^2x^2/2 + \lambda x^4/4$ gives, by integration by parts, $m^2\mathbb{E}x^2 + \lambda\mathbb{E}x^4 = \theta$. For $\lambda > 0$, setting $\mathbb{E}x^2 = \theta/m^2$ is incorrect.

10.2. *Finite response measurements and stable prediction.* The ideal inverse formulas identify coefficients from exact derivatives. An experiment, however, returns a finite collection of responses with uncertainty. We therefore retain the response law already obtained from the finite action and ask what three measurements can determine. Fix one gauge factor, suppress its index, choose $h > 0$ and $0 < r < 1$, and write

$$Q(r', s') = \beta \exp(-\alpha s')(1 + \eta r'), \qquad \beta > 0, \quad \alpha, \eta \geq 0. \tag{507}$$

All response logarithms below use numerical values in one fixed positive response unit; the same unit is used for β. Ratios and the final four-response contrast are independent of this choice of unit. The calibration settings are $(0, 0)$, $(0, h)$, and $(r, 0)$. Here Q remains the normalized link-response coefficient defined in (502); a measurement protocol must control the error in extracting that coefficient as well as the error in recording it. Finite settings in (r, s) do not by themselves remove the link-derivative measurement requirement.

Let their measured positive responses be Y_0, Y_h, Y_r. Assume a deterministic simultaneous log-error bound with $\delta \geq 0$

$$Y_0 = \beta e^{e_0}, \quad Y_h = \beta e^{-\alpha h + e_h}, \quad Y_r = \beta(1 + \eta r)e^{e_r}, \qquad |e_0|, |e_h|, |e_r| \leq \delta. \tag{508}$$

This hypothesis may be supplied by a metrological error budget or by an appropriately simultaneous confidence event. Three separate confidence statements are not automatically one event of the same confidence level.

Put

$$z_0 = \log Y_0, \quad z_h = \log Y_h, \quad z_r = \log Y_r, \qquad b = \log \beta, \quad v = \log(1 + \eta r). \tag{509}$$

The observation map becomes affine in (b, α, v):

$$(z_0, z_h, z_r) = (b, b - \alpha h, b + v) + (e_0, e_h, e_r), \qquad \alpha, v \geq 0. \tag{510}$$

This coordinate choice makes both positivity and common calibration uncertainty visible.

PROPOSITION 24 (Exact feasible coefficients from three finite settings). *Define*

$$B_- := \max\{z_0 - \delta, z_h - \delta\}, \qquad B_+ := \min\{z_0 + \delta, z_r + \delta\}. \tag{511}$$

A parameter triple satisfying (507) *and* (508) *exists if and only if* $B_- \leq B_+$. *When it exists, the exact joint feasible set consists of*

$$\begin{aligned} B_- \leq b \leq B_+, \qquad A_-(b) \leq \alpha \leq A_+(b), \qquad V_-(b) \leq v \leq V_+(b), \\ A_-(b) := \max\{0, (b - z_h - \delta)/h\}, \qquad A_+(b) := (b - z_h + \delta)/h, \\ V_-(b) := \max\{0, z_r - \delta - b\}, \qquad V_+(b) := z_r + \delta - b, \end{aligned} \tag{512}$$

with $\beta = e^b$ *and* $\eta = (e^v - 1)/r$. *In particular the exact marginal intervals are*

$$\begin{aligned} &\beta \in [e^{B_-}, e^{B_+}], \\ &\alpha \in [\max\{0, (B_- - z_h - \delta)/h\}, (B_+ - z_h + \delta)/h], \\ &\eta \in \left[\frac{\exp(\max\{0, z_r - \delta - B_+\}) - 1}{r}, \frac{\exp(z_r + \delta - B_-) - 1}{r}\right]. \end{aligned} \tag{513}$$

These marginal intervals are individually sharp. Their Cartesian product generally contains triples outside the joint feasible set.

Proof. The first observation gives $b \in [z_0 - \delta, z_0 + \delta]$. The second gives $b - z_h - \delta \leq \alpha h \leq b - z_h + \delta$. Its intersection with $\alpha \geq 0$ is nonempty exactly when $b \geq z_h - \delta$. The third gives $z_r - \delta - b \leq v \leq z_r + \delta - b$. Its intersection with $v \geq 0$ is nonempty exactly when $b \leq z_r + \delta$. Their combined requirement is precisely (511). For every b in this interval, the two remaining intervals are nonempty and independent conditional on b. Conversely, every point in these intervals supplies errors $e_0 = z_0 - b$, $e_h = z_h - b + \alpha h$, and $e_r = z_r - b - v$ in $[-\delta, \delta]$. Thus the description is exact. Both endpoints for α increase with b, whereas both endpoints for v decrease with b. Taking their extrema on $[B_-, B_+]$ and using the monotonicity of the exponential proves (513). □

An empty set has a direct meaning: the stated response family, sign conditions and simultaneous error budget cannot all explain the three measurements. It does not identify which of these inputs failed. A nonempty set also does

not establish that the physical system realizes the response family; an unused response setting tests that additional claim.

PROPOSITION 25 (A positive estimator and a uniform target-response bound). *Define*

$$\begin{aligned} \widehat{b} &= z_0, \qquad \widehat{\alpha} = \max\{0, (z_0 - z_h)/h\}, \\ \widehat{v} &= \max\{0, z_r - z_0\}, \qquad \widehat{\eta} = (e^{\widehat{v}} - 1)/r. \end{aligned} \tag{514}$$

For an unused setting $0 \le r_* < 1$, $s_* \in \mathbb{R}$, let $t = r_*/r$ and set

$$\widehat{Q}_* = e^{\widehat{b} - \widehat{\alpha} s_*}(1 + \widehat{\eta} r_*), \qquad L_t = \begin{cases} 0, & t = 0, \\ \max\{1, t\}, & t > 0. \end{cases} \tag{515}$$

Under (508),

$$\begin{gathered} |\widehat{b} - b| \le \delta, \quad |\widehat{\alpha} - \alpha| \le 2\delta/h, \quad |\widehat{v} - v| \le 2\delta, \\ |\widehat{\eta} - \eta| \le \frac{1 + \eta r}{r}(e^{2\delta} - 1), \\ \left| \log \frac{\widehat{Q}_*}{Q(r_*, s_*)} \right| \le E_* := \delta + \frac{2\delta |s_*|}{h} + 2\delta L_t. \end{gathered} \tag{516}$$

Consequently $e^{-E_*} \le \widehat{Q}_*/Q(r_*, s_*) \le e^{E_*}$. No division by η or its estimate is required, so the result also holds at $\eta = 0$.

Proof. The raw slope errors are $(e_0 - e_h)/h$ and $e_r - e_0$. Projection onto $[0, \infty)$ does not increase distance from a nonnegative true value, which proves the first three bounds. The estimate $|\widehat{v} - v| \le 2\delta$ yields $|e^{\widehat{v}} - e^v| \le e^v(e^{2\delta} - 1)$ and hence the coefficient bound. For the target define $g_t(v) = \log(1 - t + te^v)$ on $v \ge 0$. Its argument is positive because $1 - t + te^v = 1 + t(e^v - 1) \ge 1$. If $t = 0$ then $g_t = 0$. Otherwise

$$g_t'(v) = \frac{te^v}{1 - t + te^v}, \qquad 0 \le g_t'(v) \le \max\{1, t\}. \tag{517}$$

For $0 < t \le 1$ the upper bound follows by adding the nonnegative $1 - t$ to the denominator; for $t \ge 1$, the inequality $g_t' \le t$ is equivalent to $(t - 1)(e^v - 1) \ge 0$. The target logarithm is $b - \alpha s_* + g_t(v)$. Applying the triangle inequality and the preceding Lipschitz bound proves the assertion. □

The clipped estimate is always physically signed, although it need not belong to the joint feasible set for a particular data realization. When feasibility itself is part of the inference, use (512). Assuming $B_- \le B_+$, for $s_* \ge 0$ the exact minimum and maximum of the target logarithm over that set reduce to

$$\ell_*^- = \min_{b \in [B_-, B_+]} \{b - s_* A_+(b) + g_t(V_-(b))\},$$

$$\ell_*^+ = \max_{b\in[B_-,B_+]} \{b - s_* A_-(b) + g_t(V_+(b))\}. \tag{518}$$

For $s_* < 0$, exchange A_+ and A_- in these two expressions. The functions are continuous on a compact interval, so the extrema are attained. Monotonicity in α and v proves that $[e^{\ell_*^-}, e^{\ell_*^+}]$ is the exact prediction interval. This one-dimensional optimization retains the shared-baseline uncertainty that is lost by independently combining marginal endpoints.

An especially simple unused setting is the fourth corner (r, h). The response law itself gives the exact relation

$$Q(r,h) = \frac{Q(0,h)Q(r,0)}{Q(0,0)}. \tag{519}$$

Thus $Y_h Y_r / Y_0$ is a prediction formed entirely from the three calibration measurements. Its log error relative to the true fourth response is $e_h + e_r - e_0$, of magnitude at most 3δ. If an independent measurement Y_* at (r, h) has log error $|e_*| \le \delta$, the observable contrast obeys

$$|\log Y_* - \log Y_h - \log Y_r + \log Y_0| \le 4\delta. \tag{520}$$

No parameter is refitted to Y_*. A violation rejects the conjunction of the separable response law and its stated error budget. Agreement tests this structural relation, which is also shared by other separable response families, and cannot uniquely identify the mother functional. With independent log errors of known variance σ_e^2, the contrast variance is $4\sigma_e^2$; a Gaussian test additionally requires centered Gaussian errors (or independently known biases removed) and a test fixed before observing the target. If data are correlated, their full covariance replaces this variance.

What the measurement spacings control. Increasing h reduces the deterministic slope uncertainty $2\delta/h$ provided the same log-error budget remains justified. This proviso matters: an instrument with fixed additive error has increasing relative error when $Q(0, h)$ becomes small. The factor $1/r$ likewise shows why a very small coframe perturbation is poor for estimating η in absolute units. Taking r close to one is not free: the defining coframe displacement has squared norm $r/(1 - r)$ and therefore becomes large. Admissible perturbation size, signal-to-noise ratio and the range of the response model must all enter the design.

The common baseline also creates a statistical correlation. If the three log errors are independent, centered, and have variance σ_e^2, then the covariance of the raw, unclipped coordinates $(z_0, (z_0 - z_h)/h, z_r - z_0)$ is exactly

$$\sigma_e^2 \begin{pmatrix} 1 & 1/h & -1 \\ 1/h & 2/h^2 & -1/h \\ -1 & -1/h & 2 \end{pmatrix}. \tag{521}$$

Clipping changes this covariance near the sign boundaries. Equation (521) must therefore not be used as the exact covariance of the clipped estimator. A deterministic error budget and a probabilistic covariance model are separate statements; either requires support from the specified measurement procedure.

These results extend the three-coefficient response law to finite uncertainty. They do not select the graph or representation, establish the physical availability of the probes, identify the entire remaining registry, or prove unique selection of fundamental constants.

10.3. *Constraint tangency and the physical quotient.* A constraint selects admissible states; gauge symmetry identifies admissible states with the same physical meaning. A dynamics must respect both operations. Let $\mathcal{C} = (\mathcal{C}_1, \dots, \mathcal{C}_m)$ be C^3 on an open subset of $\mathbb{R}^n$, with $G = D\mathcal{C}$ of full row rank near $\mathcal{S} = \{\mathcal{C} = 0\}$. Set

$$P_T = I - G^{\mathsf{T}}(GG^{\mathsf{T}})^{-1}G, \qquad v = P_T b, \qquad B_k = P_T \sigma_k, \tag{522}$$

and assume sufficient smoothness for the local Stratonovich equation

$$\mathrm{d}Y_t = v(Y_t)\mathrm{d}t + \sum_k B_k(Y_t) \circ \mathrm{d}W_t^k. \tag{523}$$

Proposition 26 (Constraint preservation). *If $Y_0 \in \mathcal{S}$, the process remains in $\mathcal{S}$ until its lifetime or exit from the regular neighborhood. Its Itô drift is $v + \frac{1}{2}\sum_k DB_k B_k$.*

Proof. Since $GP_T = 0$, the Stratonovich chain rule gives $\mathrm{d}\mathcal{C}(Y_t) = 0$. For a direct Itô check, differentiate $D\mathcal{C}_i B_k = 0$ along B_k:

$$D^2\mathcal{C}_i[B_k, B_k] + D\mathcal{C}_i(DB_k B_k) = 0. \tag{524}$$

The curvature drift cancels the quadratic-variation term. Projecting only the noise in an Itô equation would generally omit this drift. □

Hamiltonian first-class closure is a separate requirement:

$$\{\mathcal{C}_\alpha, \mathcal{C}_\beta\} = f_{\alpha\beta}{}^{\gamma}\mathcal{C}_\gamma, \qquad \{\mathcal{C}_\alpha, H\} = u_\alpha{}^{\gamma}\mathcal{C}_\gamma. \tag{525}$$

It makes $J\nabla H$ tangent on $\mathcal{S}$. Enforcing tangency by a projection does not prove either bracket identity. For a smooth quotient $q : \mathcal{S} \to \mathcal{S}/\mathcal{G}$, physical evolution further requires

$$\mathcal{L}(f \circ q) = (\mathcal{L}_{\mathrm{phys}} f) \circ q \quad \text{for every smooth quotient function } f. \tag{526}$$

Gauge invariance of H and tangent ellipticity alone do not guarantee this: the diffusion and drift must respect gauge orbits. Nor does pure tangent noise preserve a Gibbs law without a matching dissipative drift and the appropriate surface and quotient volumes.

For a nonlinear example, take canonical coordinates (q_1, q_2, p_1, p_2) and

$$C = q_1 p_2 - q_2 p_1, \qquad H = \tfrac{1}{2}|p|^2 + \tfrac{\omega^2}{2}|q|^2 + \tfrac{\lambda}{4}|q|^4, \qquad \lambda \geq 0. \tag{527}$$

Direct differentiation gives $\{C, H\} = \{C, C\} = 0$ and $|DC|^2 = |q|^2 + |p|^2$. Away from the origin the constraint is regular. Simultaneous rotations of q, p are orthogonal, and P_T is equivariant. For $b = J\nabla H$ and isotropic ambient noise, the full projected generator commutes with rotations and descends to the regular quotient. On $q \neq 0$, the coordinates $r = |q|$, $p_r = q \cdot p/r$ give $H = p_r^2/2 + \omega^2 r^2/2 + \lambda r^4/4$ on $C = 0$. This verifies nonlinear tangency and projectability in a concrete model; its rotational constraint is not the ADM constraint system.

10.4. *The limit required for entropy dissipation.* Convergence of linear generators does not by itself control dissipation along nonlinear densities. Embed probabilities π_N in a common Polish space, with $\pi_N \Rightarrow \pi$. Let $\mathcal{E}_N$ be symmetric, strongly local diffusion forms, including the temperature coefficient. For $\rho_s^N = f_s^N \pi_N$, their chain rule gives

$$\mathcal{I}_N(\rho_s^N) = 4\mathcal{E}_N(\sqrt{f_s^N}, \sqrt{f_s^N}). \tag{528}$$

This expression is not asserted for arbitrary jump forms.

THEOREM 27 (Conditional transfer of entropy dissipation). *Fix $T > 0$. Assume the finite laws obey integrated entropy inequalities, their initial entropies converge to $D(\rho_0\|\pi) < \infty$, and $\rho_T^N \Rightarrow \rho_T$. Assume that for almost every $s \in (0, T)$ the limiting density $\rho_s = f_s\pi$ is identified and $\sqrt{f_s^N}$ converges to $\sqrt{f_s}$ in the weak comparison topology for the Mosco lower-bound condition. Then*

$$D(\rho_T\|\pi) + 4\int_0^T \mathcal{E}(\sqrt{f_s}, \sqrt{f_s})\,\mathrm{d}s \leq D(\rho_0\|\pi). \tag{529}$$

Proof. The variational formula $D(\rho\|\pi) = \sup_{g \in C_b}\{\int g\,\mathrm{d}\rho - \log\int e^g\,\mathrm{d}\pi\}$ gives joint lower semicontinuity at T. Square-root convergence and the Mosco lower bound give $\mathcal{E}(\sqrt{f_s}, \sqrt{f_s}) \leq \liminf_N \mathcal{E}_N(\sqrt{f_s^N}, \sqrt{f_s^N})$ almost everywhere in s. Fatou's lemma passes this through the integral. Add the lower bounds and use initial entropy convergence. □

For varying Hilbert spaces the comparison maps are part of the hypothesis; see [107]. Weak convergence of laws does not alone identify their square roots in this topology. The required compactness, or a direct integrated Fisher lower bound, must be established for the chosen sequence. The theorem specifies a passage to the limit; it does not supply uniform estimates for the full dynamical-coframe theory. It concerns thermal probability evolution, not quantum reconstruction.

10.5. *Positive quantum evolution at fixed spatial resolution.* Quantum positivity can be achieved constructively before taking a spatial limit. The following is an alternative temporal regularization: its time-crossing kernel replaces the temporal plaquette weight of (481). Equality of the two measures is not assumed. In particular, anchoring a weight to one vertex of a time-crossing plaquette need not preserve time reflection.

Fix a finite three-dimensional spatial lattice and set $Q_h = K^{\mathcal{E}_h^{\mathrm{sp}}} \times \mathbb{R}^{17|\mathcal{V}_h^{\mathrm{sp}}|}$, with product volume μ_h^{sp}. Let $V_h \geq 0$ be the spatial part of the finite action, including its shared interaction and confinement. Then $\int e^{-aV_h}\,\mathrm{d}\mu_h^{\mathrm{sp}} < \infty$ for every $a > 0$. Fix all field units and use $\hbar = 1$, so a has inverse-energy units. For a kinetic coefficient $\nu > 0$ with corresponding units, define on $\mathcal{H}_h = L^2(Q_h, \mu_h^{\mathrm{sp}})$

$$H_{0,h} = -\nu\Delta_{Q_h}, \qquad M_a = e^{-aV_h/2}, \qquad T_{a,h} = M_a e^{-aH_{0,h}} M_a. \tag{530}$$

The heat kernel propagates configurations between time slices; M_a assigns half the potential weight to each endpoint. This symmetric assignment yields positivity without assuming it for an arbitrary Gibbs weight.

Proposition 28 (An interacting quantum model with a spatial cutoff). *At fixed spatial lattice, $T_{a,h}$ is an injective positive self-adjoint trace-class contraction. It defines $H_{a,h} = -a^{-1}\log T_{a,h} \geq 0$ on a dense domain. Bounded positive-time cylinder observables on an even periodic time lattice satisfy reflection positivity, and the link-gauge- invariant subspace is preserved. Also, for every $t > 0$,*

$$(T_{t/n,h})^n \longrightarrow e^{-tH_h} \text{ strongly}, \qquad H_h = H_{0,h} \dot{+} V_h, \tag{531}$$

where $\dot{+}$ denotes the closed nonnegative form sum. The spatial regulator is fixed throughout this time-continuum limit.

Proof. Set $B = e^{-aH_{0,h}/2} M_a$. Then $T_{a,h} = B^*B$ and $\langle\psi, T_{a,h}\psi\rangle = \|B\psi\|^2 \geq 0$. Both factors are injective contractions. The heat kernel p_a has bounded diagonal on the compact group factor and constant diagonal $(4\pi\nu a)^{-d/2}$ on the Euclidean factor. Hence

$$\|B\|_{\mathrm{HS}}^2 = \int e^{-aV_h(x)} p_a(x,x)\,\mathrm{d}\mu_h^{\mathrm{sp}}(x) < \infty. \tag{532}$$

This makes $T_{a,h}$ trace class. Spectral calculus gives its densely defined self-adjoint nonnegative logarithmic Hamiltonian.

The transfer kernel is real, symmetric, and nonnegative. Reflect an even periodic time lattice through two opposite bonds. Multiplication by bounded observables and transfer along one half assemble into an operator A; integrating the reflected half gives the quadratic form

$$\mathrm{Tr}(A^* T_{a,h} A T_{a,h}) = \|T_{a,h}^{1/2} A T_{a,h}^{1/2}\|_{\mathrm{HS}}^2 \geq 0. \tag{533}$$

Linear combinations of cylinder observables give the corresponding linear combination of A. The normalization $\mathrm{Tr}(T_{a,h}^{2n})$ is finite and positive.

The finite site gauge group acts isometrically by left and right link multiplication. It preserves V_h: spatial plaquette traces are invariant, and e, σ are singlets in this model. Thus the group commutes with both transfer factors. Haar averaging projects orthogonally onto the invariant subspace, preserved by the transfer and Hamiltonian operators.

Finally, $\nu \int |\nabla\psi|^2 \, \mathrm{d}\mu_h^{\mathrm{sp}} + \int V_h |\psi|^2 \, \mathrm{d}\mu_h^{\mathrm{sp}}$ is densely defined, closed, and nonnegative. On this complete product manifold the smooth nonnegative potential gives essential self-adjointness on smooth compactly supported functions. The contraction product formula [151] then yields (531), with symmetric half-potentials at the endpoints. No bound uniform in spatial lattice size has been used. □

This is interacting quantum mechanics of finitely many field coordinates, with a positive inner product and link gauge symmetry. It does not impose the gravitational Hamiltonian and momentum constraints. The selection of ν, V_h by mother data, and their matching to a physical Lorentzian action, remain separate questions. Removing the spatial regulator requires uniform estimates and renormalized limiting observables. Time reflection here acts on Euclidean time slices, not on the relaxation parameter of the earlier stochastic sampling process.

Positivity of a classical density is insufficient even if it is reflection symmetric. The density proportional to $\exp[-(x^2 + y^2 + 2cxy)/2]$, $0 < c < 1$, is positive and invariant under $x \leftrightarrow y$. For $F(x) = x$, however,

$$\mathbb{E}[(\Theta F)F] = \mathbb{E}[xy] = -\frac{c}{1 - c^2} < 0. \tag{534}$$

Truncation of F supplies bounded counterexamples as well. This explains why the transfer construction is a genuine extra requirement.

10.6. *Finite calculations and the next matching problem.* In a single-gauge-factor example, group the coordinates as $u = (\beta, \alpha, \eta, \kappa_e, m_e^2)$ and $v = (\lambda_e, f^2, m_\sigma^2, \theta, \gamma_1, \gamma_2, \gamma_3)$. The first five responses equal u; the remaining seven are $(6\lambda_e, f^2, f^2 m_\sigma^2, \theta^{-1}, \theta\gamma_1, \theta\gamma_2, \theta\gamma_3)$. Their Jacobian determinant is $-6f^2\theta \neq 0$. This checks the selected inverse map, not selection of primitive constants.

For a transfer calculation choose $H = -\frac{1}{2}\partial_x^2 + x^2/2 + 0.1x^4$ on $[-6, 6]$ with Dirichlet boundaries. A centered finite-difference kinetic matrix and its exact matrix exponential define T_a. We compare $-a^{-1} \log \lambda_{\max}(T_a)$ with the smallest eigenvalue of the unsplit Hamiltonian on the same grid, separating time-splitting from spatial discretization error. Units are dimensionless and data synthetic.

Table 4. Synthetic transfer calculation with 200 interior points on $[-6, 6]$. The reference is the unsplit matrix on the same grid; no continuum error bound is inferred.

a	Transfer ground energy	Absolute splitting error
0.200	0.557420583	1.568×10^{-3}
0.100	0.558593069	3.950×10^{-4}
0.050	0.558889138	9.896×10^{-5}
0.025	0.558963344	2.475×10^{-5}

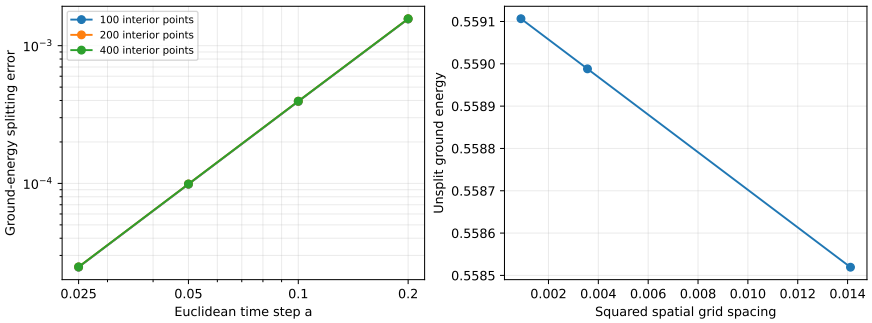


Figure 5. Synthetic quartic-oscillator calculation. Left: transfer energy error relative to the unsplit Hamiltonian on each identical grid. Right: spatial-grid variation of the unsplit energy. These finite diagnostics are not observations of gravity or a quantum-field spatial continuum limit.

Further work now has a definite order. First derive or independently calibrate the registry and freeze it before predicting a held-out observable. Next derive the actual Lorentzian constraints and prove propagation and projectability. Then establish uniform estimates and the nonlinear density convergence required by the entropy theorem. Finally match a positive quantum construction to that same Lorentzian branch and remove its spatial regulator. The finite results above provide components of this programme, with the remaining implications kept explicit.

10.7. *Matching a shared temporal weight to canonical quantum dynamics.* The positive transfer operator above leaves a specific matching question: which kinetic operator represents the same field-dependent weight as the regulated gauge action? A constant configuration-space diffusion does not in general answer that question. We can resolve it in a retained compact gauge mode coupled to the scalar. This calculation keeps a genuine shared interaction and makes the temporal normalization explicit.

Freeze the coframe coordinates at their reference values. Let $q \in S^1$ denote a retained $U(1)$ holonomy angle and shift the scalar reference to $\sigma_\star = 0$, absorbing the constant weight into both β and the temporal gauge inertia I. In fixed dimensionless reference units, with $\hbar = 1$, define

$$w(\sigma) = e^{-\alpha\sigma}, \qquad V(q,\sigma) = \beta w(\sigma)(1-\cos q) + \tfrac{1}{2}K_\sigma \sigma^2, \quad \beta, K_\sigma > 0. \tag{535}$$

Here K_σ is the scalar onsite coefficient $m_\sigma^2 f^2$ in the fixed normalization. Temporal coefficients require their own regulator scaling: write $I = \lim_{a\downarrow 0} a\beta_t(a) > 0$ for the gauge coefficient and $J > 0$ for the analogously normalized scalar inertia. These limits are matching conditions on temporal edge coefficients. The unscaled four-dimensional plaquette coefficient alone does not determine them without the spatial cell volume and field normalization.

The local Lorentzian mechanical action associated with these temporal coefficients is

$$L_L = \tfrac{1}{2} I w(\sigma)\dot{q}^2 + \tfrac{1}{2} J\dot{\sigma}^2 - V(q,\sigma), \qquad H_L = \frac{p_q^2}{2Iw(\sigma)} + \frac{p_\sigma^2}{2J} + V. \tag{536}$$

Both inertias are positive. The momenta are $p_q = Iw\dot{q}$ and $p_\sigma = J\dot{\sigma}$, so the Legendre map is invertible at every finite scalar value. Its Euler–Lagrange equations read

$$Iw\ddot{q} + Iw'\dot{\sigma}\dot{q} + V_q = 0, \qquad J\ddot{\sigma} - \tfrac{1}{2} Iw'\dot{q}^2 + V_\sigma = 0. \tag{537}$$

The two terms containing w' exchange energy between the retained gauge and scalar modes. Direct differentiation of H_L along the canonical equations gives $\dot{H}_L = 0$. The Wick substitution $t = -i\tau$ gives the positive kinetic Euclidean action $S_E = \int [Iw(q')^2/2 + J(\sigma')^2/2 + V]d\tau$. This is an explicit finite-mode continuation; it is not an analytic continuation theorem for the full fluctuating-coframe measure.

The kinetic mismatch and its correction. Choose flat canonical volume $dq\, d\sigma$ and the symmetric divergence ordering. The corresponding differential expression is

$$\mathsf{H} = -\frac{1}{2Iw(\sigma)}\partial_q^2 - \frac{1}{2J}\partial_\sigma^2 + V. \tag{538}$$

Since w is independent of q, the gauge kinetic term is exactly $-\partial_q[(2Iw)^{-1}\partial_q]$. There is no missing scalar drift in this chosen flat-volume ordering. A constant gauge coefficient $\nu = (2Iw(0))^{-1}$ instead changes the kinetic energy of a Fourier mode e^{inq} at a fixed scalar value by

$$\delta E_n(\sigma) = \frac{n^2}{2I}\big(w(\sigma)^{-1} - w(0)^{-1}\big). \tag{539}$$

Thus agreement at the reference vacuum does not imply agreement on the interacting branch. On $|\sigma| \le S$, $|n| \le N$, the exact operator norm of this

kinetic difference is

$$\|\delta \mathsf{H}_q\| = \frac{N^2}{2I}(e^{\alpha S} - 1) \quad (\alpha \geq 0). \tag{540}$$

This is a kinetic norm bound on a declared finite Fourier band, not a bound for full gravitational field evolution.

A positive transfer operator with the corrected coefficient. First restrict the scalar to $(-S, S)$ with Dirichlet boundary conditions, keeping the angle periodic. This additional field-amplitude regulator makes the coefficient smooth and uniformly elliptic. Let $\mathsf{K}_q = -(2Iw)^{-1}\partial_q^2$ and $\mathsf{K}_\sigma = -(2J)^{-1}\partial_\sigma^2$. Define

$$\mathsf{T}_a = e^{-aV/2} e^{-a\mathsf{K}_\sigma/2} e^{-a\mathsf{K}_q} e^{-a\mathsf{K}_\sigma/2} e^{-aV/2}. \tag{541}$$

The gauge heat operator acts independently at each scalar value and has the explicit fiber kernel

$$p_a(q' - q; \sigma) = \frac{1}{2\pi} \sum_{n \in \mathbb{Z}} e^{-an^2/(2Iw(\sigma))} e^{in(q'-q)}. \tag{542}$$

Its Gaussian image representation has variance $a/(Iw)$ and includes the normalizing factor $(Iw/(2\pi a))^{1/2}$. Both the exponent and this field-dependent factor matter in comparison with a configuration integral.

Proposition 29 (Matched positive evolution on the retained branch). *For fixed $S < \infty$, the operator* (541) *is an injective positive self-adjoint trace-class contraction. Its even periodic-time cylinder measure is reflection positive. For every $t > 0$, $\mathsf{T}_{t/n}^n \to e^{-t\mathsf{H}_S}$ strongly, where H_S is the Dirichlet realization of* (538)*. After restoring $\hbar$ in the kinetic terms, its leading semiclassical symbol is the Hamiltonian in* (536)*.*

Proof. Put $B = e^{-a\mathsf{K}_q/2} e^{-a\mathsf{K}_\sigma/2} e^{-aV/2}$. Every factor is an injective contraction, and $\mathsf{T}_a = B^*B$. For the trace, expand in angle Fourier modes and let $s_{a/2}$ be the Dirichlet scalar heat kernel. Since $V \geq 0$,

$$\|B\|_{\mathrm{HS}}^2 \leq \int_{-S}^{S}\int_{-S}^{S} |s_{a/2}(\sigma', \sigma)|^2 \sum_{n \in \mathbb{Z}} e^{-an^2/(2Iw(\sigma'))} d\sigma \, d\sigma' < \infty. \tag{543}$$

Boundedness above and below of w on this interval controls the Gaussian sum, and the scalar heat operator is Hilbert–Schmidt. The same folding argument as (533) proves reflection positivity because the kernel is nonnegative and $\mathsf{T}_a \geq 0$. The uniformly elliptic Dirichlet operator on the compact cylinder is self-adjoint, with the smooth Dirichlet functions as a core. The symmetric contraction product formula gives the stated time limit. Taking the principal symbol, or performing the Legendre calculation in (536), identifies the kinetic coefficient Iw. □

The amplitude restriction can also be removed for this two-coordinate Hamiltonian. On $S^1 \times \mathbb{R}$, close the nonnegative form

$$\mathfrak{q}[\psi] = \int \left[\frac{|\partial_q \psi|^2}{2Iw} + \frac{|\partial_\sigma \psi|^2}{2J} + V|\psi|^2 \right] dq\, d\sigma \tag{544}$$

initially on smooth functions with compact scalar support. Such a closure exists by local ellipticity and positivity. The increasing union of the finite-interval Dirichlet form domains is dense in this closed form by its definition. Monotone convergence of closed forms therefore gives strong resolvent, and then strong positive-time semigroup, convergence as $S \to \infty$, with the natural zero extensions. This constructs a positive Hamiltonian after removing an amplitude cutoff at fixed spatial and modal content. It does not remove a spatial field regulator or prove the remaining relativistic reconstruction requirements.
What normalization of a Wilson temporal link changes. The same matching can be checked against the actual compact-link interaction rather than only a quadratic approximation. At fixed σ the temporal Wilson factor and its row integral are

$$r_a(\delta;\sigma) = e^{-z(1-\cos\delta)}, \qquad z = \frac{Iw(\sigma)}{a}, \qquad c_a(\sigma) = 2\pi e^{-z} I_0(z). \tag{545}$$

Here $I_n(z) = (2\pi)^{-1} \int_{-\pi}^{\pi} e^{z\cos\delta} e^{-in\delta} d\delta$ is the modified Bessel coefficient. The normalized convolution r_a/c_a has positive Fourier multipliers $I_n(z)/I_0(z) \le 1$. For fixed Fourier band and a compact scalar interval, their energy satisfies, uniformly as $a \downarrow 0$,

$$-a^{-1} \log \frac{I_n(z)}{I_0(z)} = \frac{n^2}{2Iw} + \frac{an^2}{4I^2w^2} + O(a^2). \tag{546}$$

The fixed-order Bessel expansion is given in [123], formula 10.40.1 of its online companion. For completeness, the first two logarithmic terms follow by expanding $I_n(z) = e^z(2\pi z)^{-1/2}[1-(4n^2-1)/(8z)+(4n^2-1)(4n^2-9)/(128z^2)+O(z^{-3})]$. Subtracting the logarithmic series for $n = 0$ gives $\log(I_n/I_0) = -n^2/(2z) - n^2/(4z^2) + O(z^{-3})$.

The unnormalized factor is not equivalent to the normalized one when σ fluctuates. Relative to the reference row integral, the additional multiplication factor can be written $e^{-aU_a(\sigma)}$, with

$$\begin{aligned} U_a(\sigma) &= -a^{-1} \log \frac{c_a(\sigma)}{c_a(0)}, \\ &= \frac{1}{2a} \log \frac{w(\sigma)}{w(0)} - \frac{1}{8I} \left(\frac{1}{w(\sigma)} - \frac{1}{w(0)} \right) + O(a). \end{aligned} \tag{547}$$

For the exponential weight the leading term is $-\alpha\sigma/(2a)$. This term is field dependent and generally divergent at fixed nonzero σ as $a \downarrow 0$. It cannot be discarded as a constant partition normalization. One must specify the temporal

measure or a compensating local factor. The compact-interval asymptotic statement does not assert a limiting vacuum for the unnormalized full field model. Section 10.13 specifies a symmetric endpoint arrangement and calculates its exact compensating factor, including the finite term left by leading-power normalization alone.

Quantum ordering is a separate declared choice. The metric kinetic interpretation uses $ds_Q^2 = Iw(\sigma)dq^2 + Jd\sigma^2$. Its natural volume is proportional to $\sqrt{w}\,dq\,d\sigma$. Quantization by $-\Delta_Q/2+V$, followed by the unitary map $\psi \mapsto w^{1/4}\psi$ to flat volume, gives

$$U(-\tfrac{1}{2}\Delta_Q + V)U^{-1} = \mathsf{H} + V_{\mathrm{ord}}, \qquad V_{\mathrm{ord}} = \frac{(\log w)''}{8J} + \frac{[(\log w)']^2}{32J}. \tag{548}$$

To check the formula, the scalar part of Δ_Q is $J^{-1}[\partial_\sigma^2 + \frac{1}{2}(\log w)'\partial_\sigma]$; conjugation removes the first derivative and gives the displayed potential. For $w = e^{-\alpha\sigma}$, $V_{\mathrm{ord}} = \alpha^2/(32J)$ is constant, so the two choices have identical energy gaps in this reduced example. For more general retained weights this need not be a constant. The classical action alone therefore does not settle the quantum ordering.

The nonabelian lattice extension and its exact Gauss constraints. The kinetic correction extends to the full compact link group at a fixed spatial graph. Keep e, σ as the gauge singlets specified in the finite branch, and choose positive temporal weights $w_\ell(e,\sigma)$ from the same retained weight. For source and target vertices $s(\ell), t(\ell)$, introduce a temporal gauge multiplier $A_{0,v}$ and the covariant velocity

$$D_t U_\ell = \dot{U}_\ell + A_{0,s(\ell)}U_\ell - U_\ell A_{0,t(\ell)}, \qquad L_g = \sum_\ell \frac{I_\ell w_\ell}{2}\|U_\ell^{-1}D_tU_\ell\|^2 - V_h. \tag{549}$$

Add the declared positive kinetic terms for the singlet variables. The group norm is bi-invariant. Under a time-dependent site transformation, $U_\ell \mapsto g_s U_\ell g_t^{-1}$ and $A_{0,v} \mapsto g_v A_{0,v} g_v^{-1} - \dot{g}_v g_v^{-1}$, the covariant velocity transforms as $D_tU_\ell \mapsto g_s(D_tU_\ell)g_t^{-1}$. Thus the spatial Wilson potential and the full kinetic expression are gauge invariant even when the weights fluctuate.

Let $\mathcal{G} = K^{\mathcal{V}_h^{\mathrm{sp}}}$ act by this link transformation. On the cotangent phase space, choose the equivariant moment-map convention $\{G[\xi], G[\zeta]\} = G[[\xi,\zeta]]$. The components of G are the sums of outgoing left and incoming minus right link momenta, with this fixed momentum convention. Variation of A_0 imposes $G_v^a = 0$.

Proposition 30 (Finite lattice Gauss closure and positive quantization). *For the continuous-time lattice action* (549)*, the Gauss constraints are first class and preserved by its Hamiltonian:*

$$\{G_v^a, G_u^b\} = \delta_{vu} f^{ab}{}_c G_v^c, \qquad \{G_v^a, H_h\} = 0. \tag{550}$$

At a fixed finite scalar/coframe amplitude box with Dirichlet boundary, replace the constant link kinetic coefficient by

$$\mathsf{K}_g = -\sum_{\ell} \frac{1}{2I_\ell w_\ell(e,\sigma)} \Delta_{K,\ell}. \tag{551}$$

The symmetric transfer construction using K_g, the singlet kinetic operator, and V_h is positive and preserves the gauge-invariant Hilbert subspace. On smooth gauge vectors, the quantum Gauss generators close without a central term.

Proof. The cotangent lift of a site action has the canonical moment map obtained by pairing each link momentum with the corresponding infinitesimal link variation. Left and right actions on the same link commute, actions on different links commute, and the action at a vertex has Lie bracket $[\xi_v, \zeta_v]$. The canonical moment-map brackets consequently give the first equation in (550). Invariance of the Hamiltonian gives the second. The covariant time action therefore preserves Gauss constraints; it is not an unconstrained evolution with an added numerical projection.

For quantization, let $\mathcal{U}(g)$ be the unitary pullback representation on product Haar and singlet volume. Define $\widehat{G}^a_v = i\, d\mathcal{U}(T^a_v)$, so that $\mathcal{U}(e^{tT^a_v}) = e^{-it\widehat{G}^a_v}$. Differentiating the representation identity gives $[\widehat{G}^a_v, \widehat{G}^b_u] = i\delta_{vu} f^{ab}{}_c \widehat{G}^c_v$ on smooth vectors. This calculation contains no central term. The bi-invariant link Laplacian, the singlet weights, and V_h commute with the site action. Each transfer factor therefore commutes with the Haar projection $\Pi_{\mathcal{G}} = \int_{\mathcal{G}} \mathcal{U}(g) dg$. Its range is precisely the invariant subspace, equivalently the joint kernel of the infinitesimal generators for the connected group used here. Positivity follows from the same B^*B factorization as (541). On the finite amplitude box the link diffusion coefficients have a common positive lower bound; the compact-group heat trace is uniformly finite. Together with the singlet Dirichlet heat trace this gives the trace-class estimate as in (543). □

This proves the full finite-graph internal Gauss algebra for this selected continuous-time action and its invariant quantum subspace. The lapse, shift, and dynamical spacetime coframe have not been introduced in this construction. Accordingly the hypersurface-deformation algebra of gravity, spatial regulator removal, and their quantum realization remain additional requirements.
Calculations with the same parameter registry. The following synthetic calculations fix $I = J = \beta = K_\sigma = 1$, $\alpha = 0.3$ and $\sigma_\star = 0$ before any comparison. Fourier modes $-N, \ldots, N$ represent the angle; centered scalar differences use Dirichlet data at $\sigma = \pm 6$. The matched kinetic operator and the reference-frozen constant coefficient use identical potentials and identical numerical spaces. No parameter is refitted between them. The scalar mean in the table is the quantum ground-state expectation, not a classical thermal mean.

Table 5. Synthetic coupled spectrum on 200 scalar interior points and angle modes $-6, \ldots, 6$. Parameters, potential, and discretization are identical in both rows. Grid and Fourier refinements are recorded separately.

Kinetic coefficient	Ground energy	First energy gap	$\langle\sigma\rangle_0$
Matched shared weight	0.96746453	0.89250524	0.01522086
Frozen at reference	0.96571572	0.86815162	0.07642631

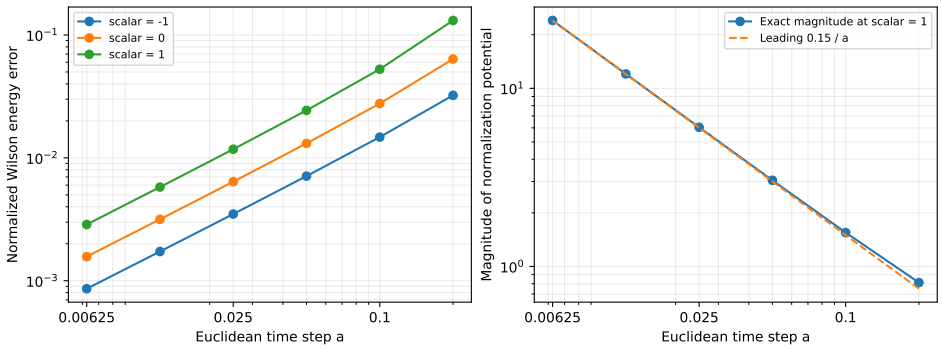


Figure 6. Synthetic retained-mode matching. Left: normalized Wilson-link energy error relative to the matched heat energy, for $n = 1$ and fixed scalar values. Right: the field-dependent normalization term at $\sigma = 1$ compared with its calculated leading divergence. These are tests of a finite shared-weight branch, not gravitational observations.

The calculation resolves a specific part of the earlier matching problem: on this retained interacting branch the common temporal weight fixes the classical inertia and the principal quantum kinetic coefficient, and a positive transfer operator implements both. It also identifies the measure normalization and ordering data still required. Gravitational coframe variation, the full nonlinear constraint algebra, and a spatial quantum continuum are not supplied by freezing those degrees of freedom.

10.8. *Dynamical geometry, material clocks, and the physical inner product.* The retained gauge–scalar interaction provides a controlled setting in which to compare temporal measures and kinetic operators. A dynamical spacetime requires an additional distinction. A coframe determines lengths and causal cones, whereas a material reference system assigns readings to events. These roles can interact without being identified. We now give the local geometric construction, an exactly soluble constrained quantum example, and a sufficient estimate for taking limits of constraint products.

Geometry and reference readings. Use a, b for Lorentz indices, μ, ν for spacetime indices, and I, J for labels of four scalar reference fields. With signature $(-,+,+,+)$, an invertible coframe and its matrix inverse satisfy

$$g_{\mu\nu} = \eta_{ab} e^a{}_\mu e^b{}_\nu, \qquad g^{\mu\nu} = \eta^{ab} e_a{}^\mu e_b{}^\nu, \qquad e^a{}_\mu e_b{}^\mu = \delta^a_b. \tag{552}$$

The inverse is a matrix inverse; it is not obtained by raising an index with an independently prescribed background metric. Four scalar fields X^I do not replace this coframe. In particular, if $e^a = dX^a$ and the Jacobian has full rank, the X^a are local coordinates and $g = \eta_{ab}\, dX^a dX^b$ is locally flat. Thus this identification excludes general curved metrics. The statement concerns the equality $e^a = dX^a$: a common nonconstant factor $e^a = \Omega\, dX^a$ can give a curved, conformally flat metric. Also, $de^a = 0$ alone is not a torsion condition when an independent connection is present, since $T^a = de^a + \omega^a{}_b \wedge e^b$.

To use $T = X^0$ as a local clock, its level sets must be spacelike. On an injective reference chart the relevant conditions and normal are

$$\begin{gathered} g^{\mu\nu}\partial_\mu T \partial_\nu T < 0, \qquad \det(\partial_\mu X^I) \neq 0, \\ n_\mu = -\frac{\partial_\mu T}{\sqrt{-g^{\alpha\beta}\partial_\alpha T \partial_\beta T}}, \qquad h_{\mu\nu} = g_{\mu\nu} + n_\mu n_\nu. \end{gathered} \tag{553}$$

The sign of n is chosen to give the desired future orientation. The weaker condition $dT \neq 0$ allows both spacelike and null gradients: in Minkowski space $T = x^1$ and $T = t + x^1$ are elementary examples. If a clock ceases to define a chart, one may need another clock or another patch. Such failure does not by itself exclude the underlying physical configuration.

The inverse map $x = x(X)$ defines a relational scalar and metric by

$$O_{\mathrm{rel}}(X) = O(x(X)), \qquad g^{\mathrm{rel}}_{IJ}(X) = g_{\mu\nu}(x(X)) \frac{\partial x^\mu}{\partial X^I} \frac{\partial x^\nu}{\partial X^J}. \tag{554}$$

They are invariant under simultaneous spacetime diffeomorphisms of the fields, within the chosen chart. A coframe component evaluated at the same relational event still transforms under local Lorentz rotations. Its use as a fully invariant observable requires a frame choice or an additional Lorentz-invariant construction. Relational quantum descriptions can be related by reduction maps under specified clock and spectral assumptions [97]; this does not assert an equivalence for every gravitational constraint system.

Reference matter and its gravitational response. A physical clock carries energy. One explicit extension of the two-derivative gravitational branch is a scalar reference action

$$S_X = -\int \sqrt{-g}\, \left[\tfrac{1}{2} Q_{IJ} g^{\mu\nu} \partial_\mu X^I \partial_\nu X^J + U_X(X)\right] d^4x, \qquad Q_{IJ} = Q_{JI} > 0. \tag{555}$$

Here Q is constant. In four spacetime dimensions, with $c = \hbar = 1$, one may normalize X^I to have mass dimension one, Q to be dimensionless, and U_X to have dimension four. The readings X^I need not have the units of coordinate time or length. Positive Q gives ordinary healthy scalar kinetic terms; the Lorentz metric on coframes is not a target metric for these four scalars. This action is a declared matter extension. Identifying its coefficients with primitive mother data is a separate matching condition.

Variation gives $Q_{IJ}\Box_g X^J - \partial_I U_X = 0$ and

$$T^X_{\mu\nu} = Q_{IJ}\partial_\mu X^I \partial_\nu X^J - g_{\mu\nu}\left(\tfrac{1}{2}Q_{IJ}g^{\alpha\beta}\partial_\alpha X^I \partial_\beta X^J + U_X\right). \tag{556}$$

The ADM Legendre transform gives the two constraint contributions

$$\begin{gathered}\mathcal{H}_X = \frac{Q^{IJ}P_I P_J}{2\sqrt{h}} + \frac{\sqrt{h}}{2}Q_{IJ}h^{ij}\partial_i X^I \partial_j X^J + \sqrt{h}\,U_X, \\ \mathcal{H}_{i,X} = P_I \partial_i X^I.\end{gathered} \tag{557}$$

Indeed $P_I = \sqrt{h}\,Q_{IJ}(\dot{X}^J - N^i\partial_i X^J)/N$, so substitution into $P_I\dot{X}^I - \mathcal{L}_X$ gives $N\mathcal{H}_X + N^i\mathcal{H}_{i,X}$. For the Einstein–Hilbert branch this stress enters $M_{\mathrm{P}}^2(G_{\mu\nu} + \Lambda g_{\mu\nu}) = T^X_{\mu\nu} + T^{\mathrm{other}}_{\mu\nu}$. Reference matter therefore changes the constraints rather than merely labelling a pre-existing solution. Neither a free scalar action nor the ADM decomposition guarantees a globally valid clock, and the lapse, shift, and Lorentz gauge directions do not acquire independent physical momenta merely because a coframe is used.

Gauge averaging also affects how semiclassical geometry should be tested. Consider the four proper spatial rotations

$$\begin{aligned} R_0 &= \mathrm{diag}(1,1,1), \quad R_1 = \mathrm{diag}(1,-1,-1), \\ R_2 &= \mathrm{diag}(-1,1,-1), \quad R_3 = \mathrm{diag}(-1,-1,1). \end{aligned} \tag{558}$$

Each coframe $e_{(r)} = \mathrm{diag}(1, R_r)$ is invertible and induces the same Minkowski metric. Nevertheless, $\frac{1}{4}\sum_r e_{(r)} = \mathrm{diag}(1,0,0,0)$ is degenerate. A degenerate mean of a gauge-dependent coframe therefore need not signal degenerate physical geometry. Metric, volume, or relational observables give appropriate geometric tests. A semiclassical Einstein equation also requires a specified state, renormalized stress, and control of geometric fluctuations: in general $G(\langle e\rangle) \neq \langle G(e)\rangle$.

Ordering and a nontrivial test of constraint covariance. Coordinate covariance and a symmetric inner product restrict quantization but need not select it uniquely. On a compact smooth configuration manifold with metric γ and without boundary, the operators

$$\mathsf{H}_\xi = -\frac{\hbar^2}{2m}(\Delta_\gamma - \xi\mathcal{R}_\gamma) + V, \qquad \xi \in \mathbb{R}, \tag{559}$$

have the same principal symbol and are coordinate covariant. For smooth real V, each has a self-adjoint realization with domain H^2 in $L^2(d\,\mathrm{vol}_\gamma)$. The continuous curvature parameter is not fixed by these requirements. Earlier gravitational ordering analyses likewise distinguish ordering conditions from algebraic anomalies [34]. In a separate companion paper, Christodoulakis and Zanelli obtained a formally consistent constraint algebra using a minimal modification of canonical commutation relations [35]. That construction changes the algebraic input; it does not by itself provide a regulator-independent representation, a physical inner product, or a quantization of the present interacting mother action. Formal symmetry, self-adjoint realization, and a common invariant domain for products are separate requirements.

In the metric Einstein–Yang–Mills benchmark, let C_i denote the gauge-covariant momentum constraint, G_A the Gauss constraint with internal gauge label A, and $V_i = C_i + A_i^A G_A$ the ordinary spatial diffeomorphism constraint. With $G_A = -D_i E_A^i$ and the usual canonical Poisson bracket, the Hamiltonian bracket is

$$\{H[N], H[M]\} = C[Z] = V[Z] - G[Z^i A_i], \qquad Z^i = h^{ij}(N\partial_j M - M\partial_j N). \tag{560}$$

The right-hand side is a momentum constraint, with a field-dependent structure function. It is not another scalar Hamiltonian constraint. This distinction persists when a quantum representative and an ordering for the right-hand side are chosen.

Let Φ be a common invariant dense test domain on which the required products exist. If $\widehat{C}_\alpha \psi = 0$ for every constraint, then $[\widehat{C}_\alpha, \widehat{C}_\beta]\psi = 0$ already follows algebraically. Thus a calculation only on this common kernel cannot establish the required spacetime covariance. One must also establish a nonzero physical space and examine the commutator on a suitable domain, or its matrix elements in controlled semiclassical states, with the correct structure functions and regulator estimates. A term that adds independent restrictions may change the physical sector; its effect cannot be decided by simply discarding it on the kernel.

Changing canonical commutators is one possible additional hypothesis, not a consequence of the ordering problem. It must define a consistent adjoint algebra and a representation. For example, the proposal $[q_i, p_j] = i\hbar f(q)\delta_{ij}$ together with $[q_i, q_j] = [p_i, p_j] = 0$ gives the Jacobi expression

$$[p_i, [p_j, q_k]] + [p_j, [q_k, p_i]] + [q_k, [p_i, p_j]] = \hbar^2 f\big(\delta_{ik}\partial_j f - \delta_{jk}\partial_i f\big). \tag{561}$$

For nonconstant positive f in dimension at least two this generally fails. Alternative regulators, counterterms, reduced quantization, or other constraint constructions must be assessed on their own assumptions.

From a positive form to physical states. For a unitary representation of a compact internal gauge group, normalized Haar averaging gives an orthogonal projection $P_{\mathrm{inv}} = \int U(g)\, dg$. Hence

$$\begin{gathered} q(u,v) = \langle u, P_{\mathrm{inv}} v\rangle, \qquad q(u,u) = \|P_{\mathrm{inv}} u\|^2 \geq 0, \\ \mathcal{H}_{\mathrm{phys}} \simeq \mathcal{H}_{\mathrm{aux}} / \ker P_{\mathrm{inv}} \simeq \operatorname{Ran} P_{\mathrm{inv}}. \end{gathered} \tag{562}$$

Nonzero auxiliary vectors can have zero physical norm. The quotient removes these vectors and gives a positive definite inner product. For noncompact constraints, a rigging form instead requires a test space, a justified integral or distributional prescription, positivity, compatibility with physical observables, and completion of the null quotient. Uniqueness is an additional question. The Giulini–Marolf theorem assumes a finite-dimensional Lie group, an appropriate L^1 test space invariant under their group algebra, and a nonzero averaging form; under those conditions any compatible rigging map, if it exists, is proportional to group averaging [80]. Convergence alone is not that theorem. The field-dependent structure functions in (560) do not provide an ordinary constraint group with Haar measure for all gravitational constraints.

An explicit noncompact example shows both the construction and its scope. Set $\hbar = 1$, choose a Hermitian $d \times d$ matrix H_s, and take

$$\mathcal{H}_{\mathrm{aux}} = L^2(\mathbb{R}_T) \otimes \mathbb{C}^d, \qquad \Phi = \mathcal{S}(\mathbb{R}) \otimes \mathbb{C}^d, \qquad C = -i\partial_T + H_s. \tag{563}$$

In an orthonormal eigenbasis $H_s|\ell\rangle = E_\ell|\ell\rangle$, use the unitary Fourier transform in T. Group averaging is then exactly

$$\eta(u)[v] = \int_{\mathbb{R}} \frac{ds}{2\pi} \langle u, e^{isC} v\rangle = \sum_{\ell=1}^{d} \overline{\widetilde{u}_\ell(-E_\ell)}\, \widetilde{v}_\ell(-E_\ell). \tag{564}$$

For these test vectors the matrix coefficient is Schwartz in s, so the integral is absolutely convergent. Fourier inversion proves the displayed evaluation formula. It is positive semidefinite. Its null space consists precisely of the vectors for which all evaluations $\widetilde{u}_\ell(-E_\ell)$ vanish. Evaluation maps onto $\mathbb{C}^d$, since one may prescribe these finitely many values with Schwartz functions. The completed physical space is therefore $\mathbb{C}^d$. A corresponding history is $\Psi(T) = e^{-iH_s T}\chi$, and $C\Psi = 0$ follows by direct differentiation. For $\chi \neq 0$ this history is not square integrable in the clock variable, even though its physical norm $\|\chi\|$ is finite. This example realizes a deparametrized clock constraint; it does not realize the full gravitational hypersurface-deformation algebra.

The sign of an inner product must also be tied to its construction. For the relativistic mass-shell constraint $C = p_0^2 - |\mathbf{p}|^2 - m^2$, $m > 0$, put $\omega_{\mathbf{p}} = \sqrt{|\mathbf{p}|^2 + m^2}$. Averaging with $\delta(C)$ gives the positive shell form

$$q(u,v) = \int \frac{d^3p}{2\omega_{\mathbf{p}}} \left[\overline{u(\omega_{\mathbf{p}}, \mathbf{p})} v(\omega_{\mathbf{p}}, \mathbf{p}) + \overline{u(-\omega_{\mathbf{p}}, \mathbf{p})} v(-\omega_{\mathbf{p}}, \mathbf{p})\right]. \tag{565}$$

The conserved Klein–Gordon charge form has opposite signs on the two frequency sectors. These are different forms; positivity of one does not turn the other into a positive form. Enlarging a test space while retaining a negative-norm vector cannot remove that negative norm. Similarly, positivity of a temporal transfer operator $B^\dagger B$ does not identify its Hilbert space with a physical constraint quotient without a reconstruction or intertwining map.

Spatial refinement and products of constraints. Clock resolution, temporal step size, spatial field truncation, and amplitude cutoffs are different parameters. Finer clock readings do not add missing spatial field modes. A relational resolution can describe spatial refinement only after an explicit map to physical geometry and observables has been given. Projective consistency, a renormalization group fixed point, and convergence of a chosen sequence are also distinct properties. A fixed point is one possible route to a continuum theory; failure to find one in a truncation is not a nonexistence proof.

Even convergent matrix elements are insufficient for constraint products. Let $\{e_0, e_1, \ldots\}$ be the standard basis of ℓ^2 and set

$$A_n = |e_0\rangle\langle e_n| + |e_n\rangle\langle e_0|, \qquad B_n = i\big(|e_n\rangle\langle e_0| - |e_0\rangle\langle e_n|\big). \tag{566}$$

Both self-adjoint sequences have norm one and converge weakly to zero. However, $[A_n, B_n] = 2i(P_0 - P_n)$ converges weakly to $2iP_0$, where $P_j = |e_j\rangle\langle e_j|$. Thus the commutator of the limits differs from the limit of the commutators.

The following stronger estimate gives a sufficient replacement.

Proposition 31 (Control of commutators on a scale of spaces). *Let $V_2 \hookrightarrow V_1 \hookrightarrow V_0$ be Banach spaces. Suppose A_n, B_n, A, B act consistently on both successive levels $V_2 \to V_1$ and $V_1 \to V_0$, with every such operator norm at most M. If, on both levels, $\|A_n - A\| \le \epsilon_A(n)$ and $\|B_n - B\| \le \epsilon_B(n)$, then*

$$\|[A_n, B_n] - [A, B]\|_{V_2 \to V_0} \le 2M\big(\epsilon_A(n) + \epsilon_B(n)\big). \tag{567}$$

Proof. Write $A_nB_n - AB = (A_n - A)B_n + A(B_n - B)$. Composition between the successive spaces bounds this difference by $M(\epsilon_A + \epsilon_B)$. Apply the same argument to $B_nA_n - BA$ and use the triangle inequality. □

For changing Hilbert spaces the operators must first be transported by specified comparison maps. For unbounded gravitational constraints, the required domains and bounds remain to be established. The proposition is a conditional analytic criterion, rather than an estimate already proved for those constraints.

Quantization data and comparison of branches. The shared-weight example shows concretely why a path-integral measure and a kinetic expression must be matched. In general the quantization data also include the regulator, counterterms, boundary conditions, operator domains, and state preparation.

A measure alone need not select an ordering. Terms of order $\hbar^2$ need not be negligible at low energy, and equations of motion need not uniquely select a boundary state or a reference-field preparation.

Agreement of one relational expectation value is not physical equivalence. For example, $H_1 = \mathrm{diag}(0,1)$ and $H_2 = \mathrm{diag}(0,2)$ have the same ground-state expectation of σ_z but different excitation gaps. Exact equivalence requires a unitary map W that preserves the physical observable representation and evolution:

$$W\pi_1(O)W^{-1} = \pi_2(O), \qquad WU_1(t) = U_2(t)W. \tag{568}$$

An effective low-energy comparison can instead specify a family of observables and states and bound their differences after comparison. Distinct vacua, superselection sectors, and inequivalent quantizations must be distinguished in that analysis. Their presence leaves the conditional branch constructions meaningful, while preventing a claim that the primitive mother data have already selected a unique physical quantum theory.

These results separate three tasks that a material-clock formulation must connect: dynamical geometric constraints, a positive physical state space, and spatial cutoff removal. The local reference construction and the clock model complete explicit parts of this connection. The full nonlinear gravitational operator algebra and its interacting continuum representation require additional constructions beyond the finite gauge sector.

10.9. *Logarithmic coframes and integrability near degenerate geometry.* An invertible coframe can approach a singular matrix while every matrix entry remains bounded. Inverse metric observables can therefore fail to be integrable even when the partition function is finite. Proposition 22 establishes this obstruction for the smooth positive matrix-entry density of the finite mother branch. Logarithmic coordinates locate the relevant tail precisely and provide an explicit alternative measure with finite inverse moments. The distinction between changing coordinates and changing the probability law is essential.

The polar change of variables. Work at one vertex in fixed dimensionless Euclidean coframe coordinates. If a dimensional coframe is used, it must first be divided by a specified reference scale. Every $e \in \mathrm{GL}^+(4,\mathbb{R})$ has the unique polar representation $e = R\exp S$, where $R \in \mathrm{SO}(4)$ and $S = S^{\mathsf{T}}$. Let dS_F be Lebesgue measure in the ten orthonormal Frobenius coordinates, namely S_{ii} and $\sqrt{2}S_{ij}$ for $i < j$, and normalize Haar measure dR to have mass one. For eigenvalues $\lambda_1, \dots, \lambda_4$ of S, the matrix-entry volume is

$$de = J(S)\, dR\, dS_F, \qquad J(S) = c_4 e^{4\,\mathrm{tr}\,S} \prod_{i<j} \frac{\sinh(\lambda_i - \lambda_j)}{\lambda_i - \lambda_j}. \tag{569}$$

Here $c_4 > 0$ depends only on the volume normalizations, and each ratio at a repeated eigenvalue has value one. To derive the formula, first write $e = RP$ with $P > 0$. At diagonal P with entries s_i, the differential $de = \Omega P + dP$, $\Omega^{\mathsf{T}} = -\Omega$, has Jacobian proportional to $\prod_{i<j}(s_i + s_j)$. Indeed the two off-diagonal entries for each pair (i, j) have determinant s_i+s_j. Next, the differential of $P = \exp S$ multiplies the diagonal direction i by e^{λ_i} and the symmetric direction (i, j) by $(e^{\lambda_i} - e^{\lambda_j})/(\lambda_i - \lambda_j)$. Multiplying these factors and using $e^{2\lambda_i} - e^{2\lambda_j} = 2e^{\lambda_i+\lambda_j} \sinh(\lambda_i - \lambda_j)$ gives (569).

In particular, $S = 0$ means $e = R$ and $\det e = 1$. No inverse-coframe singularity occurs there. The singular values of e are e^{λ_i}, so the dangerous direction is $\lambda_{\min} \to -\infty$. For the illustrative matrix Gaussian $d\mu \propto e^{-a \operatorname{tr}(e^{\mathsf{T}}e)} de$, $a > 0$, conditioned on positive orientation, integration over the angular coordinates gives the joint logarithmic singular-value density

$$p_a(\lambda) \propto e^{-a \sum_i e^{2\lambda_i}} e^{\sum_i \lambda_i} \prod_{i<j} |e^{2\lambda_i} - e^{2\lambda_j}|. \tag{570}$$

The ordinary real-symmetric spectral volume contributes $|\Delta(\lambda)| = \prod_{i<j} |\lambda_i - \lambda_j|$; these factors cancel the denominators in (569). The eigenvalues are not independent.

Keep $\lambda_2, \lambda_3, \lambda_4$ in compact disjoint intervals. As $\lambda_1 \to -\infty$, the density in (570) is bounded above and below by positive multiples of e^{λ_1}, uniformly on smaller such intervals. Both $(\det e)^{-r}$ and $\|e^{-1}\|_F^r$ then have a lower bound proportional to $e^{-r\lambda_1}$. Consequently their integrals contain

$$\int_{-\infty}^{-L} e^{(1-r)\lambda_1} \, d\lambda_1 = \infty, \qquad r \geq 1. \tag{571}$$

Thus the logarithmic change of variables preserves, and makes visible, the original divergence. In the interacting mother measure the exact pullback is instead $J(S)e^{-S_h(U,Re^S,\sigma)/\theta}$, with the remaining fields and angular variables retained. It need not have the factorized spectral form of (570).

For comparison, a bounded neighborhood of $S = 0$ gives an elementary finite integral. Ordering the four eigenvalues and integrating the Vandermonde polynomial yields

$$\int_{[0,\varepsilon]^4} |\Delta(\lambda)| \, d^4\lambda = \frac{\varepsilon^{10}}{1050}. \tag{572}$$

The power ten is the sum of four integration dimensions and the six Vandermonde factors. The coefficient follows from $4! \int_{0<x_1<x_2<x_3<x_4<1} \prod_{i<j}(x_j - x_i) \, d^4x = 1/1050$. For $r \geq 0$, inserting $e^{-r\sum_i \lambda_i}$ bounds the integral between $e^{-4r\varepsilon}\varepsilon^{10}/1050$ and $\varepsilon^{10}/1050$. Even without the Vandermonde factor the bounded integrand is integrable on this cube. A weight vanishing at $S = 0$ is therefore unnecessary for inverse-moment control and cannot repair the negative tail by its behavior at the origin alone.

A different measure with explicit inverse moments. Consider the declared logarithmic Gaussian law

$$d\nu_a(R,S) = \left(\frac{a}{\pi}\right)^5 e^{-a\,\mathrm{tr}\,S^2}\,dS_F\,dR, \qquad a>0. \tag{573}$$

It is not the pullback of the matrix Gaussian above. Relative to matrix-entry volume its density contains $J(S)^{-1}$. This change suppresses nearly singular configurations rather than merely renaming them. The Euclidean construction is invariant under fixed left and right SO(4) rotations. It is not, on that account, a Lorentz-invariant probability law or a solution of the gravitational constraints.

Proposition 32 (Inverse moments of a logarithmic Gaussian coframe). *For* (573) *and every* $r \ge 0$,

$$\mathbb{E}_{\nu_a}(\det e)^{-r} = e^{r^2/a}, \qquad \mathbb{E}_{\nu_a}\|e^{-1}\|_F^r \le 2^{r+5}e^{r^2/(2a)} < \infty. \tag{574}$$

If $d\nu_{a,W} = Z_W^{-1}e^{-W}d\nu_a$, *where* $W \ge -C$ *and* $0 < Z_W < \infty$, *each corresponding moment is at most* e^C/Z_W *times its value or bound under* ν_a.

Proof. The ten orthonormal matrix coordinates give the partition integral $(\pi/a)^5$. Since $\det e = e^{\mathrm{tr}\,S}$, complete the square:

$$-a\,\mathrm{tr}\,S^2 - r\,\mathrm{tr}\,S = -a\,\mathrm{tr}\left(S + \frac{r}{2a}I_4\right)^2 + \frac{r^2}{a}. \tag{575}$$

Translation invariance of dS_F proves the determinant formula. Moreover $\|e^{-1}\|_F \le 2e^{\|S\|_F}$ and $r\rho \le a\rho^2/2 + r^2/(2a)$. Integrating the resulting Gaussian with precision $a/2$ rather than a contributes 2^5, giving the second bound. Finally $e^{-W} \le e^C$ proves the assertion for the tilt. □

The parameter a remains free: integrability holds for every $a > 0$. For example, $\mathbb{E}\,\mathrm{tr}\,S^2 = 5/a$ and $\mathrm{Var}(\log\det e) = 2/a$ offer possible calibration relations, but do not determine their observed values. A dynamical realization of the un-tilted law is equally explicit. If B_s^F is Brownian motion in the ten orthonormal symmetric coordinates, then

$$dS_s = -2\theta a S_s\,ds + \sqrt{2\theta}\,dB_s^F, \qquad \theta > 0, \tag{576}$$

has invariant density proportional to $e^{-a\,\mathrm{tr}\,S^2}$. An independent rotation diffusion with invariant Haar measure gives (573). Every finite-time sample has an invertible coframe. Here s is an auxiliary diffusion parameter; its identification with a physical clock requires further dynamics.

These estimates also explain the limit of a finite-lattice construction. For N_v vertices with marginal law (573), no independence assumption is needed for the union bound

$$\mathbb{P}\{\min_v \det e_v < \delta\} \le \min\left\{1, N_v \exp\left[-\frac{a}{4}\left(\log\frac{1}{\delta}\right)^2\right]\right\}, \qquad 0<\delta<1. \tag{577}$$

Table 6. Synthetic inverse moments for a single logarithmic Gaussian coframe with $a = 1$. The matrix-entry Gaussian has divergent values in all four rows. Numerical values refer to the different law ν_1.

Observable	Value under ν_1	Evaluation
$(\det e)^{-1}$	$e = 2.7182818\ldots$	Exact Gaussian integral
$(\det e)^{-2}$	$e^4 = 54.5981500\ldots$	Exact Gaussian integral
$\|e^{-1}\|_F$	4.92466	Randomized quadrature
$\|e^{-1}\|_F^2$	31.11929	Gaussian quadrature

Indeed Markov's inequality gives $N_v \delta^r e^{r^2/a}$, minimized at $r = (a/2)\log(1/\delta)$. The bound deteriorates as N_v grows. This loss of an upper bound is not itself evidence of degeneration. Section 10.14 compares different joint laws with the same marginals and proves a bound for a fixed list of averaged observations. Section 10.12 embeds the logarithmic reference in a finite locally rotation-covariant interaction, retaining the interaction-dependent normalization in its moment estimates. Individual inverse moments therefore do not establish a uniform nondegenerate continuum geometry; spatial regularity, correlations, and regulator-uniform estimates remain necessary.

Finite-dimensional numerical illustration. Table 6 gives synthetic values for $a = 1$. The determinant moments are exact. For the second Frobenius moment, one can reduce the spectral integral to one-dimensional Gaussian quadratures. Define the antisymmetric matrix, with indices $0 \le i, j \le 3$,

$$A_{ij}(t) = \int_{x<y} (x^i y^j - y^i x^j) e^{-x^2-y^2} (1 + te^{-2x})(1 + te^{-2y})\, dx\, dy. \tag{578}$$

Expansion of the Vandermonde determinant on the ordered chamber gives $\mathcal{Z}(t) = 4!\,\mathrm{Pf}\, A(t)$, where $\mathrm{Pf}\, A = A_{01}A_{23} - A_{02}A_{13} + A_{03}A_{12}$. Thus $\mathcal{Z}(0) = 3\pi/2$ and

$$\mathbb{E}_{\nu_1} \|e^{-1}\|_F^2 = \frac{d}{dt} \log \mathcal{Z}(t)\bigg|_{t=0} \simeq 31.1192891. \tag{579}$$

The substitution $x = u - v$, $y = u + v$, $v > 0$, factors each polynomial term into a full-line and a half-line Gaussian moment. The derivative in (579) is justified by Gaussian integrability; $\mathcal{Z}(t)$ is a generating polynomial near zero, not a claim of a positive density for negative t.

An independent calculation in matrix coordinates uses twelve scrambled Sobol replicates of 2^{17} points each. Writing $S = (q/2)I_4 + S_0$, with $\mathrm{tr}\, S_0 = 0$, $q \sim N(0, 1/2)$ independent of S_0, integrates the trace exactly: the factor for the rth inverse norm is $e^{r^2/16}$. The remaining nine-dimensional calculation

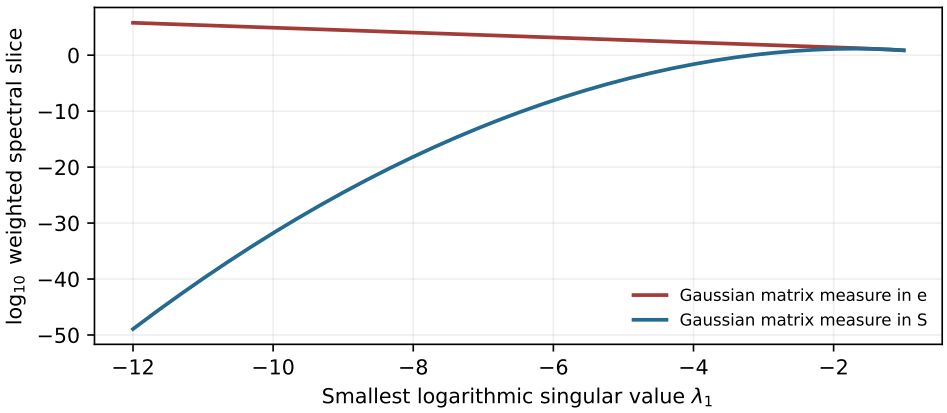


Figure 7. Synthetic conditional spectral slices, weighted by $e^{-2\lambda_1}$, with the other three logarithmic singular values fixed at $\log(1,2,3)$. Each unweighted slice is normalized to one at $\lambda_1 = -1$. The matrix-entry Gaussian grows after inverse-square weighting toward $\lambda_1 = -\infty$, whereas the logarithmic Gaussian decays. These slices are neither marginal densities nor observational data.

gives 4.9246643 for the first moment and 31.1112707 for the second. Replicate-based standard error estimates are 0.0000451 and 0.002582, respectively. The second-moment difference from (579) is -0.0080184, approximately 0.026% or 3.1 estimated standard errors. The replicate estimates do not provide rigorous integration bounds. Figure 7 illustrates the different negative tails responsible for the integrability change.

10.10. *Constraint reduction and quantum consistency beyond moment bounds.* Finite inverse moments make geometric observables integrable. They do not determine the number of propagating degrees of freedom or the sign of a physical inner product. Those questions concern the action, its constraints, and its quantization. A finite mechanical example separates the constraint issue from the measure issue.

Second-class constraints can remove a higher-derivative mode. On a regular irreducible constraint stratum with N canonical pairs, F independent first-class constraints and S_c independent second-class constraints, the reduced number of canonical pairs is

$$N_{\mathrm{phys}} = N - F - \tfrac{1}{2}S_c. \tag{580}$$

Each first-class constraint removes one constraint direction and one gauge direction. Each second-class constraint removes one phase-space dimension. A degenerate velocity Hessian produces primary constraints, but preservation can generate further constraints or fix multipliers. The entire Dirac–Bergmann

procedure, on a specified rank stratum, is needed before applying (580). The higher-derivative scalar–tensor analysis of Langlois and Noui provides a field-theoretic example of this distinction [108].

Consider the mechanical Lagrangian, with $\omega_x, \omega_y > 0$,

$$L = \tfrac{1}{2}(\dot{q} + \ddot{x})^2 + \tfrac{1}{2}\dot{x}^2 - \tfrac{1}{2}\omega_x^2 x^2 - \tfrac{1}{2}\omega_y^2 (q + \dot{x})^2. \tag{581}$$

Introduce $Q = \dot{x}$ and a multiplier enforcing this identity. After eliminating the multiplier's auxiliary canonical pair, the coordinates are (x, Q, q) and

$$H = \tfrac{1}{2}p_q^2 - \tfrac{1}{2}Q^2 + p_x Q + \tfrac{1}{2}\omega_x^2 x^2 + \tfrac{1}{2}\omega_y^2 (q + Q)^2, \qquad \phi = p_Q - p_q = 0. \tag{582}$$

The two momenta p_Q, p_q coincide because the Hessian in $(\dot{Q}, \dot{q})$ is the rank-one matrix with every entry equal to one. Canonical brackets give

$$\chi = \{\phi, H\} = Q - p_x, \qquad \{\phi, \chi\} = -1, \qquad N_{\mathrm{phys}} = 3 - 0 - 2/2 = 2. \tag{583}$$

Preserving χ fixes the multiplier of ϕ; it generates no gauge freedom. On the constraint surface put $y = q + Q$. The canonical one-form reduces to $p_x\,dx + p_q\,dy$, and the Hamiltonian becomes

$$H_{\mathrm{red}} = \tfrac{1}{2}(p_x^2 + p_q^2 + \omega_x^2 x^2 + \omega_y^2 y^2). \tag{584}$$

Two second-class constraints remove the extra pair and leave two stable oscillators, although there are no first-class constraints. For a coframe–connection action the analogous calculation must retain the independent connection until its constraints are classified. Elimination is justified by a map preserving the reduced symplectic structure and dynamics, not solely by equality of expressions after setting constraints to zero. Quantization adds domain and ordering requirements to this classical equivalence.

Real characteristic speeds are not a complete evolution estimate. Strong hyperbolicity of a first-order reduction requires a uniformly controlled diagonalization of its principal symbol, or an appropriate uniformly positive symmetrizer, in addition to real characteristic speeds. The constant system $\partial_t u = A\partial_x u$ with

$$A = \begin{pmatrix} 1 & 1 \\ 0 & 1 \end{pmatrix}, \qquad e^{ikAt} = e^{ikt}\left[I + ikt\begin{pmatrix} 0 & 1 \\ 0 & 0 \end{pmatrix}\right] \tag{585}$$

has real eigenvalues but growth proportional to $|k|t$, precluding a frequency-uniform estimate at the same Sobolev order. Gauge-dependent characteristic speeds can occur in legitimate gauge evolution equations. Their presence alone neither removes a mode nor proves a physical instability. Gauge fixing, the constraint subsystem, principal-symbol estimates, and boundary conditions must be considered together.

A vanishing physical expectation can miss an anomaly. Suppose provisionally that a physical subspace is represented by an orthogonal projection P in an auxiliary Hilbert space. Even vanishing of all compressed matrix elements only states $P\mathcal{A}P = 0$. For example,

$$P = \begin{pmatrix} 1 & 0 \\ 0 & 0 \end{pmatrix}, \qquad \mathcal{A} = \begin{pmatrix} 0 & 1 \\ 1 & 0 \end{pmatrix}, \qquad P\mathcal{A}P = 0, \quad \mathcal{A}\begin{pmatrix} 1 \\ 0 \end{pmatrix} = \begin{pmatrix} 0 \\ 1 \end{pmatrix}. \tag{586}$$

The operator takes a physical vector outside the physical subspace. Moreover, commutators vanish algebraically on a common constraint kernel whenever the products exist, and an empty physical space satisfies every such test vacuously. In refined algebraic quantization physical states can instead be distributions, as in (563); an auxiliary orthogonal projection onto their kernel is then not available.

A substantive sufficient estimate uses a common domain and the correct classical structure functions. For the benchmark (560), write, at fixed $\hbar > 0$,

$$\begin{gathered} \mathcal{A}_h[N, M] = (i\hbar)^{-1}[\widehat{H}_h[N], \widehat{H}_h[M]] - \widehat{C[Z]}_h, \\ \|\mathcal{A}_h[N, M]\psi\|_{V_0} \le \epsilon_h(N, M)\|\psi\|_{V_2}, \qquad \epsilon_h(N, M) \longrightarrow 0. \end{gathered} \tag{587}$$

The ordering of $\widehat{C[Z]}_h$ must include the metric dependence of Z. Comparison maps are needed when the regulated spaces differ. Proposition 31 supplies one sufficient product estimate, but not these gravitational bounds. This off-shell test must be accompanied by a nontrivial positive physical construction with the intended classical observables. An $O(\hbar)$ remainder can describe a semiclassical approximation; at fixed $\hbar$ it is not a vanishing cutoff error or a proof of exact anomaly cancellation.

Group averaging has similarly specific hypotheses. Under the Giulini–Marolf assumptions, including their L^1 test-space condition, invariance under the relevant group algebra, and a nonzero averaging form, a compatible rigging map is unique up to normalization if it exists [80]. Their integrability requirements include the specified modularly weighted measures for nonunimodular groups. Mere convergence of one Haar integral, or an arbitrary convergent regularization, does not supply these hypotheses. Louko and Molgado exhibit a convergent indefinite averaging form for the $(1, 1)$ oscillator representation; under the uniqueness hypotheses it rules out a rigging map for their chosen test space and observable structure [115]. This is not a universal nonexistence statement for every quantization of that classical system. Likewise, the relational trinity of [97] uses particular clock–system constraints and spectral assumptions; it is not a theorem for all ordinary Lie-group constraints, much less the full field-dependent gravitational algebra.

Higher-derivative poles, physical positivity, and effective theory. The BFV formulation organizes gauge constraints and their ghost sector. It does not by

itself remove every negative-residue propagating mode. In the quadratic-gravity calculation of Bellorin, Bórquez, and Droguett, the stated sign choice gives a massive transverse-traceless tensor and one scalar with negative norm, while the massive transverse vector has positive norm [14]. These are statements about that calculation; classifying the present model requires its own constraint reduction and physical observables.

A fakeon prescription changes the quantization of selected poles rather than deriving their removal from the classical constraint algebra. Fakeons can contribute internally to tree and loop amplitudes, but are excluded from physical asymptotic states and the corresponding unitarity cuts. The construction uses a specified nonanalytic continuation, with average continuation across fake thresholds [3]. Its physical cutting equations sum over physical states. It therefore does not dispense with positive physical probabilities, nor does it supply a positive physical space for an arbitrary mother action. It also does not preserve ordinary microscopic causality: the one-loop gravity analysis explicitly finds a causality violation associated with the fakeon scale [4]. A perturbative fakeon construction and a reflection-positive Euclidean reconstruction impose different conditions; neither may be inferred merely by choosing a propagator pole.

The low-energy alternative admits a simple quantitative statement. For a Euclidean scalar polarization with $G_\ell(p) = [p^2(1+\ell^2p^2)]^{-1}$, let $G_\ell^{(n)}(p) = p^{-2}\sum_{j=0}^{n}(-\ell^2p^2)^j$. At $p^2 > 0$, the finite geometric-series identity gives

$$G_\ell - G_\ell^{(n)} = \frac{(-\ell^2p^2)^{n+1}}{p^2(1+\ell^2p^2)}, \qquad \frac{|G_\ell - G_\ell^{(n)}|}{|G_\ell|} \le (\ell^2\Lambda^2)^{n+1}, \quad 0 < p^2 \le \Lambda^2. \tag{588}$$

The bound is useful when $\ell\Lambda < 1$. It bounds this propagator expansion, not an interacting amplitude without further estimates, and not the negative part of a physical inner product. Treating higher-derivative operators perturbatively in an effective theory avoids using its truncated action as an exact high-energy propagator; it does not establish a positive ultraviolet completion of that propagator.

Power counting must use the actual high-momentum behavior. For a connected four-dimensional graph, with propagator decay p^{-r_e} on internal line e and d_v derivatives at vertex v,

$$D = 4L + \sum_v d_v - \sum_e r_e, \qquad L = I - V + 1. \tag{589}$$

Two-derivative Einstein power counting gives $D = 2L + 2$; if all relevant propagators decay as p^{-4} and all vertices carry at most four derivatives, it gives $D \le 4$. Mixed matter and gauge sectors require their own line and vertex counts. Neither estimate proves positive physical spectral weights. A negative component of a gauge-fixed auxiliary propagator also cannot alone

decide physical unitarity: positivity tests concern physical observables under the stated spectral assumptions. Finally, a Euclidean renormalization-group fixed point does not supply Lorentzian constraint closure, causal reconstruction, or the physical inner product without the corresponding additional results.

10.11. *Constraint-preserving diffusions and pathwise clock readings.* The geometric constraint problem also appears before quantization: noise tangent to a curved surface produces a normal Itô drift. This drift is fixed by the curvature of the constraint surface. Keeping it explicit separates geometric invariance from the choice of an optimal approximation to an unconstrained stochastic model.

For a smooth regular constraint surface $\mathcal{M} = \{C_A = 0\}$ and an Itô diffusion $dZ = b\,ds + \sum_r \sigma_r\,dW^r$, Itô's formula gives the local invariance conditions on $\mathcal{M}$:

$$DC_A\sigma_r = 0, \qquad DC_A b + \tfrac{1}{2}\sum_r D^2C_A[\sigma_r,\sigma_r] = 0. \tag{590}$$

Under smooth local existence and uniqueness assumptions, these conditions ensure invariance up to the lifetime of the solution. They are independent of a particular projection convention. Stratonovich, Itô-vector and Itô-jet projections are all manifold-valued constructions when defined intrinsically. Armstrong, Brigo, and Ferrucci identify different local approximation criteria: in their setting the Itô-vector projection minimizes the stated leading weak error after fixing the diffusion approximation, whereas the Itô-jet projection minimizes the stated mean-square error relative to the metric-projected process [6]. These criteria are distinct from constraint preservation. A numerical constraint residual can compare discretizations but cannot by itself choose a unique continuous projection.

On the unit sphere $\mathbb{S}^{d-1}$, $d \geq 2$, put $P_x = I - xx^{\mathsf{T}}$ and let U be smooth. The intrinsic Stratonovich diffusion and its equivalent Itô equation are

$$\begin{aligned} dX &= -P_X\nabla U\,ds + \sqrt{2\theta}\,P_X \circ dW, \\ dX &= [-P_X\nabla U - \theta(d-1)X]\,ds + \sqrt{2\theta}\,P_X\,dW. \end{aligned} \tag{591}$$

Here an arbitrary smooth ambient extension of U can be used; its projected gradient on the sphere is intrinsic. For the diffusion columns $V_r(x) = P_x e_r$, differentiation gives $\sum_r DV_r(x)V_r(x) = -(d-1)x$ on the sphere. Therefore the Stratonovich-to-Itô correction is $-\theta(d-1)x$. Since $x^{\mathsf{T}}P_x = 0$ and $\operatorname{tr} P_x = d-1$,

$$d|X|^2 = [-2\theta(d-1) + 2\theta\operatorname{tr} P_X]\,ds = 0. \tag{592}$$

The generator is $\mathcal{L} = \theta\Delta_{\mathbb{S}} - \nabla_{\mathbb{S}}U\cdot\nabla_{\mathbb{S}}$. Integration by parts on the compact sphere gives the invariant law $Z^{-1}e^{-U/\theta}d\operatorname{vol}_{\mathbb{S}}$, and, for smooth f, g,

$$\int f\mathcal{L}g\,d\nu = -\theta\int \nabla_{\mathbb{S}}f\cdot\nabla_{\mathbb{S}}g\,d\nu. \tag{593}$$

This example verifies both the constraint and the Gibbs reference. A time-stepping rule must still be checked separately: a generic Euler step does not preserve the sphere exactly, and geometric projection of a step does not automatically preserve the invariant law.

Finally, a clock function $T(Z)$ has Itô differential and quadratic variation

$$dT = (\mathcal{L}T)\,ds + \sum_r DT\sigma_r\,dW^r, \qquad [T]_s = \int_0^s \sum_r |DT\sigma_r|^2\,du. \tag{594}$$

A positive drift does not ensure increasing readings along individual paths: $T_s = s + \varepsilon W_s$ fails to be monotone for every $\varepsilon > 0$. A continuous monotone path has finite variation and zero quadratic variation. Thus monotone diffusion clocks necessarily satisfy $DT\sigma_r = 0$ almost everywhere along their paths. Together with $\mathcal{L}T \geq 0$, this condition is sufficient for nondecreasing readings; a uniform positive lower bound gives strictly increasing readings while the chart remains valid. The spacetime condition that dT is timelike, the probabilistic condition of pathwise monotonicity, and the identification of a physical clock with an auxiliary diffusion parameter are three separate requirements.

The finite calculations above give explicit measure, reduction, and stochastic-invariance results. Connecting them to an interacting quantum geometry requires a single action and measure to satisfy the complete gravitational constraints, regulator-uniform evolution and moment estimates, and a nontrivial positive physical quantum construction. Those connections are additional physical and analytic requirements; the logarithmic Gaussian example alone does not select them.

10.12. *A finite covariant extension with controlled inverse coframes.* The preceding constructions isolate three physical requirements: a coframe must transform with the local reference frame, inverse geometric observables must be integrable, and the time evolution must use the declared interaction. These requirements can be satisfied together in a finite Euclidean model. The construction below changes both the coframe representation and its probability law. It is an extension to be matched to the original mother branch, rather than a change of coordinates in that branch.

Take a fixed finite graph with oriented edges, a finite list of plaquettes, and four-dimensional internal Euclidean frames. At vertex v, set $e_v = R_v \exp S_v$, with $R_v \in \mathrm{SO}(4)$ and $S_v \in \mathrm{Sym}(4)$; let $\sigma_v \in \mathbb{R}$. On edge (v, w) take $U_{vw} \in \mathrm{SO}(4)$. For local rotations L_v, prescribe

$$R_v \mapsto L_v R_v, \qquad U_{vw} \mapsto L_v U_{vw} L_w^{-1}, \qquad S_v \mapsto S_v, \quad \sigma_v \mapsto \sigma_v. \tag{595}$$

Thus $e_v - U_{vw} e_w$ transforms as $L_v(e_v - U_{vw} e_w)$. The graph and coordinate column indices remain fixed: local internal rotations are being restored, not arbitrary changes of spacetime coordinates.

Normalize each Haar measure and put independent logarithmic Gaussians ν_a of (573) on the coframes, and normalized densities proportional to $e^{-b\sigma_v^2}$ on the scalars, with $a, b > 0$. Call the product reference measure $\nu_{a,b,h}$. For nonnegative κ, f^2, η and $\alpha \geq 0$, define

$$W_h = \frac{\kappa}{2} \sum_{(v,w)} \|e_v - U_{vw} e_w\|_F^2 + \sum_p \omega_{v(p)} k_p(U) + \frac{f^2}{2} \sum_{(v,w)} (\sigma_v - \sigma_w)^2, \tag{596}$$

$$\omega_v = e^{-\alpha\sigma_v} \left(1 + \eta \frac{\operatorname{tr} S_v^2}{1 + \operatorname{tr} S_v^2}\right), \qquad k_p(U) = 4 - \operatorname{tr} U_p.$$

Here $v(p)$ is a declared base vertex of each plaquette and U_p is its oriented holonomy. Since $U_p \in \mathrm{SO}(4)$, $k_p \geq 0$. All quantities in this construction are dimensionless after fixing a coframe scale, a scalar scale, and an energy unit.

PROPOSITION 33 (A finite covariant Gibbs law). *The law $d\mu_h = Z_h^{-1} e^{-W_h} d\nu_{a,b,h}$ is well defined, locally* SO(4) *invariant, and has all positive inverse-coframe moments at each vertex. More precisely, for $r > 0$,*

$$0 < Z_h \leq 1, \qquad \mathbb{E}_{\mu_h} (\det e_v)^{-r} \leq Z_h^{-1} e^{r^2/a}, \qquad \mathbb{E}_{\mu_h} \|e_v^{-1}\|_F^r \leq Z_h^{-1} 2^{r+5} e^{r^2/(2a)}. \tag{597}$$

On the product Riemannian configuration space, its gradient Dirichlet form has a conservative reversible realization and only constants have zero Dirichlet energy. It therefore has a unique invariant probability density relative to μ_h.

Proof. Every summand of W_h is nonnegative and smooth. The integrand e^{-W_h} is strictly positive at every finite configuration, proving $0 < Z_h \leq 1$. Equation (595), orthogonal invariance of the Frobenius norm, and conjugation invariance of the plaquette trace give invariance of W_h. Left invariance of Haar measure gives invariance of the reference law. For a nonnegative observable F, $\mathbb{E}_{\mu_h} F \leq Z_h^{-1} \mathbb{E}_{\nu_{a,b,h}} F$. Apply the previously calculated logarithmic Gaussian moments to obtain (597).

Write $\Phi_h = a \sum_v \operatorname{tr} S_v^2 + b \sum_v \sigma_v^2 + W_h$. The smooth positive density proportional to $e^{-\Phi_h}$ defines the closed gradient form $\mathcal{E}_h(f, f) = \theta \int |\nabla f|^2 d\mu_h$. Choose smooth radial cutoffs in the noncompact coordinates, equal to one on a ball of radius R, vanishing outside radius $2R$, and with gradient bounded by C/R. They converge to one in $L^2(\mu_h)$ and their energies are at most $\theta C^2/R^2$. Hence the constant function belongs to the form domain with zero energy, and the associated symmetric Markov semigroup is conservative. A function of zero energy has zero weak gradient; connectedness and the strictly positive density imply that it is constant. This gives irreducibility and uniqueness of the invariant probability density. The generator on compactly supported smooth

functions is

$$\mathcal{L}_h = \theta\Delta - \theta\nabla\Phi_h \cdot \nabla, \qquad \frac{d}{dt}\left[\theta \int f_t \log f_t \, d\mu_h\right] = -\theta^2 \int \frac{|\nabla f_t|^2}{f_t} \, d\mu_h. \quad (598)$$

The identity follows by integration by parts for positive smooth densities with finite dissipation; approximation extends the integrated inequality to the usual finite-entropy domain. □

The thermodynamic content of this model is specific. The reference energy is $E_h = \theta\Phi_h$, the chosen mobility is the identity in the specified product metric, and its covariance is 2θ times that mobility. Equation (598) is therefore a free-energy balance for this declared isothermal dynamics. Identification with measured bath entropy still uses the heat convention and local detailed balance developed earlier. Neither the equilibrium density alone nor local rotation invariance fixes the mobility, the clock, or a, b.

There is also an exact internal constraint statement. On the cotangent bundle, the infinitesimal site action now moves R_v as well as the links. With the moment-map convention of Proposition 30, its Gauss generator pairs the momenta with these variations:

$$G[\xi] = \sum_{(v,w)} p_{U_{vw}}(\xi_v U_{vw} - U_{vw}\xi_w) + \sum_v p_{R_v}(\xi_v R_v). \quad (599)$$

Cotangent-lift equivariance gives the same internal Lie algebra and any invariant Hamiltonian preserves $G = 0$. Omitting the second sum would omit the coframe charge. These are internal rotation constraints on a fixed graph; lapse and shift constraints have not been constructed here. Moreover, the positive Euclidean action above has not been derived by reducing the full mother group. Its matching, Lorentzian continuation, and regulator dependence remain distinct questions. In particular, Z_h^{-1} in (597) need not be uniformly bounded as the graph grows.

10.13. *Exact temporal normalization and the retained inertia.* A second connection concerns the time coordinate. A field-dependent normalization repeated at each time slice can change the limiting Hamiltonian, even when it seems harmless in a single integral. The retained $U(1)$ mode allows this effect to be computed without an expansion of the full field theory. Put $w = e^{-\alpha\sigma}$, $w(0) = 1$, and let $\epsilon > 0$ denote the temporal spacing. The Wilson row integral is

$$c_\epsilon(\sigma) = \int_{-\pi}^{\pi} e^{-Iw(\sigma)(1-\cos q)/\epsilon} \, dq = 2\pi e^{-z} I_0(z), \quad z = \frac{Iw(\sigma)}{\epsilon}, \quad R_\epsilon = \frac{c_\epsilon(\sigma)}{c_\epsilon(0)}. \quad (600)$$

I_0 is the modified Bessel function. To specify how this row factor enters a transfer operator, consider the symmetric arrangement $T_{\mathrm{raw}} = R_\epsilon^{1/2} T_{\mathrm{norm}} R_\epsilon^{1/2}$,

where each R_ϵ acts by multiplication. This is a declared kernel arrangement; an arbitrary mother kernel need not factor this way.

PROPOSITION 34 (Endpoint compensation for one compact mode). *In this arrangement the exact compensating kernel multiplier is*

$$N_\epsilon(\sigma,\sigma') = R_\epsilon(\sigma)^{-1/2} R_\epsilon(\sigma')^{-1/2}. \tag{601}$$

Uniformly on each fixed compact scalar interval,

$$\log R_\epsilon = -\tfrac{1}{2}\log w + \frac{\epsilon}{8I}(w^{-1}-1) + O(\epsilon^2). \tag{602}$$

Thus its leading endpoint multiplier is $w(\sigma)^{1/4} w(\sigma')^{1/4}$.

Proof. Multiplication by (601) cancels the two endpoint factors algebraically. The large-z formula $I_0(z) = e^z(2\pi z)^{-1/2}(1 + 1/(8z) + O(z^{-2}))$ gives (602), since w is bounded above and below on the specified interval. Taking minus one half of this logarithm gives the quarter power at each endpoint. □

For a constant scalar value, the uncompensated effective contribution $U_\epsilon = -\epsilon^{-1}\log R_\epsilon$ is

$$U_\epsilon = -\frac{\alpha\sigma}{2\epsilon} - \frac{e^{\alpha\sigma}-1}{8I} + O(\epsilon). \tag{603}$$

A half power of w at each endpoint overcompensates and leaves the opposite divergence $+\alpha\sigma/(2\epsilon)$. A quarter power at each endpoint cancels the divergence but leaves the finite term $-(e^{\alpha\sigma}-1)/(8I)$. Exact compensation cancels the entire declared row factor. For d independent Gaussian kinetic coordinates with the same scalar weight, the leading endpoint exponent is $d/4$; with a general kinetic matrix it is the corresponding determinant factor. The exponent must therefore be computed for the retained variables.

For example, the synthetic values $I = 1$, $\alpha = 0.3$, $\sigma = 1$ give the following direct Bessel evaluations. The last column concerns only the row contribution, not the complete Hamiltonian.

ϵ	$\epsilon U_{\mathrm{raw}}$	$\epsilon U_{1/2}$	$U_{1/4}$
0.10000	−0.15501838	0.14498162	−0.05018378
0.05000	−0.15232871	0.14767129	−0.04657415
0.02500	−0.15112701	0.14887299	−0.04508030
0.01250	−0.15055487	0.14944513	−0.04438996
0.00625	−0.15027536	0.14972464	−0.04405726
Limit	−0.15	0.15	−0.04373235

Normalization does not remove the matched inertia $Iw(\sigma)$ in (536). Rescaling the angle by a scalar-dependent factor would change its periodicity and introduce mixed derivatives when the scalar moves. Nor does the factor $J(\Delta\sigma)^2/(2\epsilon)$ in a short-time action imply a Hamiltonian inertia proportional to ϵ^{-1}: the factor ϵ^{-1} arises from integrating a squared velocity over a time step. Temporal

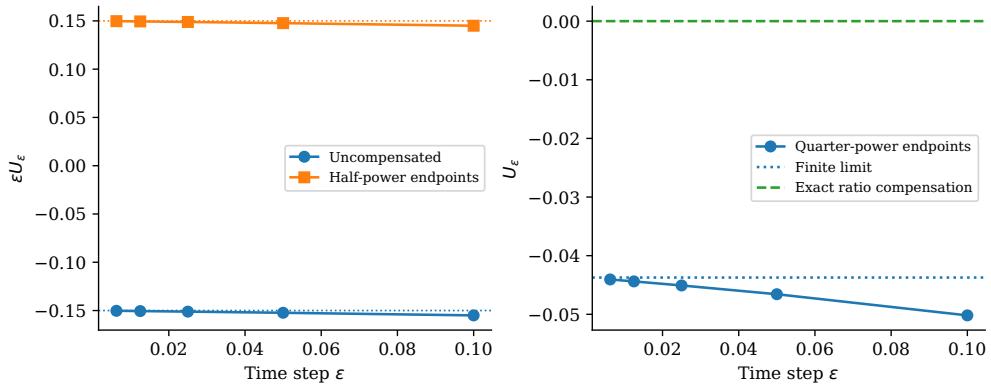


Figure 8. Synthetic normalization calculation for one retained compact mode. Left: the uncompensated and half-power choices have opposite divergent potentials. Right: quarter-power compensation leaves a finite potential, whereas the exact Bessel ratio removes the declared row factor.

normalization, kinetic matching, and spatial regulator removal are separate operations.

10.14. *Nondegeneracy at a stated observation scale.* An observation averages fields over a finite region. This gives a useful nondegeneracy question that is weaker than controlling the smallest coframe determinant at every regulator vertex. Fix the coordinate reference volume used to define $D_v = \det e_v > 0$, and deterministic weights $b_{jv} \geq 0$ with $\sum_v b_{jv} = 1$ for $j = 1, \dots, M$. Define $\bar{D}_j = \sum_v b_{jv} D_v$; these are averages of a density relative to that fixed volume, not coordinate-independent scalars without an observation prescription.

Proposition 35 (Finite-resolution determinant bound). *Suppose, for every $r > 0$ and vertex v, $\mathbb{E} D_v^{-r} \leq C_h e^{r^2/a}$, with $C_h \geq 1$. Then, for $0 < \delta < 1$,*

$$\mathbb{E}\bar{D}_j^{-r} \leq C_h e^{r^2/a}, \qquad \mathbb{P}\{\min_j \bar{D}_j < \delta\} \leq \min\{1, M C_h e^{-a \log^2(1/\delta)/4}\}. \tag{604}$$

No independence assumption is required.

Proof. Convexity of $x \mapsto x^{-r}$ gives $\bar{D}_j^{-r} \leq \sum_v b_{jv} D_v^{-r}$. Markov's inequality and a union bound then give $M C_h \delta^r e^{r^2/a}$. Its exponent $r \log \delta + r^2/a$ is minimized at $r = (a/2)\log(1/\delta)$, proving the assertion. □

For the product logarithmic law, $C_h = 1$. For the interacting model of Proposition 33, $C_h = Z_h^{-1}$ is available and must be retained. If $\bar{D}(x)$ is also defined for continuously located observations, assume its Lipschitz constant is at most K_L outside an event of probability ζ. An η-net with $M(\eta)$ centers

then gives, for every $r > 0$,

$$\mathbb{P}\{\inf_x \bar{D}(x) < \delta\} \le \min\{1, \zeta + M(\eta) C_h (\delta + K_L \eta)^r e^{r^2/a}\}. \tag{605}$$

Indeed an observation below δ has a net center below $\delta + K_L\eta$ on the Lipschitz event. Spatial regularity and uniform control of C_h would still have to be proved for a continuum claim.

The need for joint control can be seen without asymptotics. Under the one-vertex logarithmic law, $\log D$ is Gaussian with variance $2/a$. For $a = 1$ and $\delta = 0.1$, the one-vertex probability is approximately 0.05174405. For $N = 10$ independent vertices the minimum falls below δ with probability 0.41216455; for $N = 100$ the probability is 0.99507328. Perfectly correlated copies keep the one-vertex probability for every N. The same marginals therefore do not determine the large-graph event. A union upper bound that grows beyond one proves neither degeneration nor nondegeneration. Finally, $e = \mathrm{diag}(z, z^{-1}, 1, 1)$ has determinant one while $\|e^{-1}\|_F^2 = z^2 + z^{-2} + 2$ diverges as $z \to \infty$. Determinant control must be supplemented by shape control when inverse metrics are the observable of interest.

10.15. *Equilibrium preservation does not select a physical clock.* The equilibrium reference constrains admissible dynamics, but a reference density does not determine the rate of physical evolution. This is particularly relevant when a thermodynamic model is matched to a field-theoretic clock. Let $\pi \propto e^{-U/\theta}$, and write the reversible diffusion generator in fixed Euclidean coordinates as

$$Lf = \theta \pi^{-1} \nabla \cdot (\pi \Gamma \nabla f) = \theta \nabla \cdot (\Gamma \nabla f) - \Gamma \nabla U \cdot \nabla f. \tag{606}$$

Here Γ is symmetric positive definite. Under the time change $dt = r(X_s)ds$, with smooth $0 < c \le r \le C$, the new generator and stationary law are

$$L_r = r^{-1} L, \qquad d\pi_r = Z_r^{-1} r \, d\pi, \qquad Z_r = \int r \, d\pi. \tag{607}$$

To verify stationarity, integrate $L_r f$ against π_r and cancel r. More explicitly, choose $\Gamma_r = \Gamma / r$ and $U_r = U - \theta \log r$. The derivative of r^{-1} in the divergence term cancels the derivative of $-\theta \log r$ in the drift, leaving L/r. The Dirichlet form becomes $\mathcal{E}_r = \mathcal{E}/Z_r$. Although U_r represents the new occupation density, this algebra does not show that a mechanical energy has changed solely because a clock has been relabelled. Physical heat and work must use the calibrated generator and the declared bath model.

For a concrete obstruction, take $L_a = \theta \partial_y^2 - 2\theta a y \partial_y$ and $r(y) = e^{-(a'-a)y^2}$ with $a, a' > 0$. The stationary density after time change is still Gaussian, proportional to $e^{-a' y^2}$, but its diffusion coefficient is $\theta / r(y)$ and is nonconstant if $a' \ne a$. Thus the Gaussian Gibbs family is preserved while the constant-diffusion Ornstein–Uhlenbeck family is not. Although this r need not be bounded, its stationary mean is finite and positive; ergodicity of the original process gives

$\int_0^s r(X_u)du \to \infty$, so the time change remains conservative. Even a constant r leaves a global clock-scale freedom. Selecting a physical time therefore requires a dynamical matching or a clock observable beyond membership in a Gibbs family.

10.16. *Backreaction from the same shared weight.* The retained mechanical model now gives a quantitative test of how a common weight affects an observable. A changing scalar changes both the gauge kinetic energy and its restoring force. The leading frequency at a fixed scalar value is consequently independent of that weight, while energy exchanged with a moving scalar gives an amplitude-dependent correction. This distinction determines which experiment the model would require.

Write $K = K_\sigma > 0$, $x = \sigma - \sigma_0$, and $w_0 = e^{-\alpha\sigma_0}$. The previous branch has $\sigma_0 = 0$; a displaced reference requires an explicitly included preparation or stabilizing potential $K(\sigma - \sigma_0)^2/2$. With $\omega_0^2 = \beta/I$ and $\Omega^2 = K/J$, the exact equations are

$$\ddot{q} - \alpha\dot{x}\dot{q} + \omega_0^2 \sin q = 0, \tag{608}$$

$$J\ddot{x} + Kx = \alpha w_0 e^{-\alpha x}[\beta(1 - \cos q) - I\dot{q}^2/2]. \tag{609}$$

Their conserved energy is

$$E = \tfrac{1}{2} I w_0 e^{-\alpha x}\dot{q}^2 + \tfrac{1}{2} J\dot{x}^2 + \beta w_0 e^{-\alpha x}(1 - \cos q) + \tfrac{1}{2} K x^2. \tag{610}$$

The scalar source contains a potential contribution and a kinetic contribution with opposite signs. Substitution of $q = A\cos\omega_0 t$ gives $F\cos 2\omega_0 t$ to order A^2, where

$$F = \tfrac{1}{2}\alpha\beta w_0 A^2, \qquad \Delta = K - 4J\omega_0^2, \qquad B = F/\Delta. \tag{611}$$

Its mean vanishes at this order. For $\Delta \neq 0$, the periodic particular solution is $B\cos 2\omega_0 t$, whereas zero scalar position and velocity initially give

$$x_a(t) = B(\cos 2\omega_0 t - \cos\Omega t). \tag{612}$$

At $\Omega = 2\omega_0$, direct resonant forcing instead gives

$$x_a(t) = \frac{\alpha\beta w_0 A^2}{8J\omega_0}\, t \sin 2\omega_0 t.$$

The static denominator K cannot replace Δ in an oscillatory response, and proximity to resonance requires a different approximation.

For a smooth small-amplitude periodic branch admitting a regular expansion, the order-A^3 equation for q contains the fundamental forcing $\omega_0^2 A^3/8 + \alpha B A\omega_0^2$. The first term follows from $\cos^3 t = (3\cos t + \cos 3t)/4$; the second follows from $2\sin 2t \sin t = \cos t - \cos 3t$ in $\alpha\dot{x}\dot{q}$. Removing the secular fundamental

term therefore gives the coefficient

$$\frac{\omega-\omega_0}{\omega_0}=-\frac{A^2}{16}-\frac{\alpha^2\beta w_0A^2}{4\Delta}+O(A^4). \tag{613}$$

This coefficient calculation presumes such a regular branch and excludes the displayed resonance. It does not establish its global existence or a uniform remainder for arbitrary preparations. A finite-time estimate for an explicitly prepared trajectory can, however, be proved directly.

PROPOSITION 36 (Finite-time response estimate). *Assume $I,J,\beta,K,w_0>0$, $\alpha\ge 0$, $0<A<\pi$ and $\Delta\neq 0$. Let the exact solution start at $(q,\dot q,x,\dot x)=(A,0,0,0)$, and set $y_a=(A\cos\omega_0t,-A\omega_0\sin\omega_0t,x_a,\dot x_a)$. Define $E_0=\beta w_0(1-\cos A)$ and*

$$\begin{aligned}&S_e=\sqrt{2E_0/K},\qquad w_-=w_0e^{-\alpha S_e},\quad Q_e=\arccos(1-E_0/(\beta w_-)),\\&V_e=\sqrt{2E_0/(Iw_-)},\quad Z_e=\sqrt{2E_0/J},\quad S_a=2|B|,\quad Z_a=|B|(2\omega_0+\Omega).\end{aligned} \tag{614}$$

Require $E_0<2\beta w_-$ and put

$$\begin{aligned}&Q=\max(Q_e,A),\quad V=\max(V_e,A\omega_0),\quad S=\max(S_e,S_a),\\&Z=\max(Z_e,Z_a),\qquad w_+=w_0e^{\alpha S}.\end{aligned} \tag{615}$$

In the norm $\|y\|_E^2=\omega_0^2q^2+v^2+\Omega^2x^2+z^2$, the exact error obeys, for every finite $t\ge 0$,

$$\|y(t)-y_a(t)\|_E\le\eta\frac{e^{L_Et}-1}{L_E}, \tag{616}$$

with the continuous interpretation ηt if $L_E=0$, where

$$\begin{aligned}\eta_v&=\omega_0^2A^3/6+\alpha Z_aA\omega_0,\\\eta_z&=\frac{\alpha\beta w_0}{J}\left[\frac{A^2}{2}(e^{\alpha S_a}-1)+e^{\alpha S_a}\frac{A^4}{24}\right],\qquad \eta=(\eta_v^2+\eta_z^2)^{1/2},\end{aligned} \tag{617}$$

$$\begin{aligned}L_E^2=&\left(\frac{\omega_0Q^2}{2}\right)^2+(\alpha Z)^2+(\alpha V)^2+\left(\frac{\alpha\beta w_+Q}{J\omega_0}\right)^2\\&+\left(\frac{\alpha Iw_+V}{J}\right)^2+\left[\frac{\alpha^2w_+(\beta Q^2+IV^2)}{2J\Omega}\right]^2.\end{aligned} \tag{618}$$

Proof. Energy conservation gives $|x|\le S_e$, $|\dot x|\le Z_e$ and $|\dot q|\le V_e$. A continuous trajectory from $A\in(0,\pi)$ cannot reach either $q=\pi$ or $q=-\pi$, because its potential energy there is at least $2\beta w_->E_0$. On this connected potential well it therefore satisfies $|q|\le Q_e$. The approximate trajectory lies in the enlarged box (615), so every line segment between the two trajectories lies in that box. These bounds also prevent finite-time escape of the exact solution.

Separate the first-order vector field as $\dot{y} = \mathsf{A}y + N(y)$, where A is the direct sum of the two harmonic oscillators and

$$N(y) = \left(0, \alpha z v + \omega_0^2(q - \sin q), 0, \frac{\alpha w_0 e^{-\alpha x}}{J}[\beta(1 - \cos q) - I v^2/2]\right). \quad (619)$$

The linear group is an isometry in $\|\cdot\|_E$. The six possibly nonzero entries of the weighted Jacobian of N have the bounds whose squares appear in (618). Here one uses $|\sin q| \le |q|$ and $1 - \cos q \le q^2/2$. Their Frobenius norm bounds the operator norm, giving a Lipschitz constant L_E on the box.

Only the velocity equations have a residual at y_a. The bound $|q - \sin q| \le |q|^3/6$ gives η_v. For the scalar equation,

$$\beta(1 - \cos q_a) - I v_a^2/2 = \tfrac{1}{2}\beta A^2 \cos 2\omega_0 t + \rho(t), \qquad |\rho(t)| \le \beta A^4/24. \quad (620)$$

Multiply by $e^{-\alpha x_a}$ and use $|e^{-\alpha x_a} - 1| \le e^{\alpha S_a} - 1$ to obtain η_z. Variation of constants then bounds the error by $\int_0^t (L_E \|y(s) - y_a(s)\|_E + \eta) ds$. Gronwall's inequality gives (616) because the initial error is zero. □

The estimate controls a complete trajectory in fixed time units, not only the scalar amplitude. It can be conservative over long observation windows because it grows exponentially. A small frequency correction therefore still needs a phase-error estimate, a sufficiently long calibrated measurement, and detector noise below the signal. In particular, (616) supplies no automatic experimental resolution.

Synthetic comparisons without changing the parameters. Fix $I = J = \beta = 1$, $K = 9$, $\alpha = 0.3$, and $\sigma_0 = 0$. For zero scalar initial data, integrate the complete equations (608)–(609) for $T = 2\pi$. An eighth-order DOP853 calculation uses relative tolerance $2 \cdot 10^{-12}$, absolute tolerance $2 \cdot 10^{-14}$, and maximum step 0.025. The table compares the largest error on 2001 equally spaced samples with the analytic bound at T, which also bounds all earlier times.

A	L_E	Sampled maximum error	Bound at T
0.05	0.03015577	$5.26033 \cdot 10^{-5}$	$1.83037 \cdot 10^{-4}$
0.10	0.06072202	$4.20385 \cdot 10^{-4}$	$1.61928 \cdot 10^{-3}$
0.20	0.12368627	$3.34897 \cdot 10^{-3}$	$1.60915 \cdot 10^{-2}$

The maximum sampled relative energy drift is below $7.5 \cdot 10^{-14}$. This is a numerical conservation check; floating-point integration is not an interval enclosure of the exact trajectory.

A separate long-time calculation uses the same coefficients and $(q, \dot{q}, x, \dot{x}) = (A, 0, B, 0)$, which matches the periodic preparation through order A^2. DOP853 tolerances are $2 \cdot 10^{-11}$ and $2 \cdot 10^{-13}$, the maximum step is 0.15, and the duration is 240π; frequency is measured from successive peaks after 40π. For $A = 0.05, 0.10, 0.20$, respectively, the measured frequencies are 0.999832510370, 0.999330165599, and 0.997322636213. Equation (613) gives 0.999832500000,

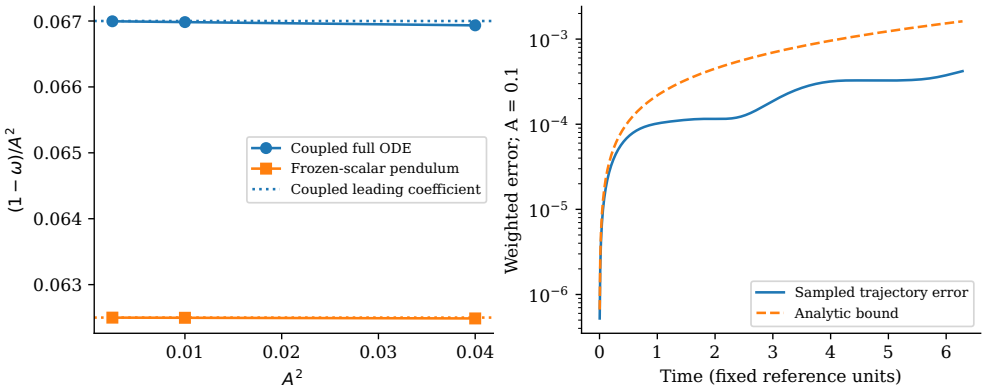


Figure 9. Synthetic shared-weight response. Left: frequencies from the coupled equations, compared with the frozen-scalar pendulum and the perturbative coefficient, using the same registered parameters. Right: the zero-scalar preparation at $A = 0.1$, compared with the analytic finite-time error bound. These simulations are finite-model calculations, not observations of a new interaction.

0.999330000000, and 0.997320000000. The coefficients approach $(1-\omega)/A^2 = 0.067$, whereas the frozen-scalar pendulum has leading coefficient $1/16 = 0.0625$. Its exact comparator is $\pi/[2\mathsf{K}(\sin^2(A/2))]$, where $\mathsf{K}(m) = \int_0^{\pi/2}(1 - m\sin^2 u)^{-1/2}du$. No coefficient is fitted between these comparisons. The two initial preparations must be distinguished: the finite-time theorem above addresses the zero-scalar preparation, not the long-time peak estimator.

10.17. *What the finite construction requires of the field theory.* The finite results give concrete tests for an extension to fluctuating geometry. Such an extension must identify its independent fields and reduce their complete constrained spectrum. Up to ten broken symmetry directions can be represented in a vierbein in suitable spontaneous Lorentz- and diffeomorphism-breaking models [18]; this is not a count of ten propagating massless particles. Gauge directions, first- and second-class constraints, and kinetic degeneracies change the physical count. Massive negative-norm or tachyonic modes must be tested as well as massless polarizations. The teleparallel equivalent of general relativity is equivalent to GR under its defining assumptions [117]; extra modes in modified teleparallel theories cannot be assigned to TEGR itself. An independent Palatini connection can be auxiliary. Its spectrum depends on its action and cannot be inferred from a universal "two plus five" count.

Constraint closure must likewise refer to the specified generators. Loll's lattice calculation concerns the spatial diffeomorphism commutator in a particular

construction and its small-spacing behavior [114]. It does not preclude exact finite internal Gauss closure, and it does not supply the missing Hamiltonian and mixed brackets of the present mother theory. If a deformed gravitational algebra is used, its generators, structure functions, Jacobi identities, error topology, and common continuum limit must all be specified. These requirements cannot be replaced by the fact that a finite symmetry exists.

Finally, a local one-loop expansion cannot decide a far negative log-coframe tail without a uniform remainder and a coercive estimate there. Nor does a nonzero projection of a constraint onto a Hessian nullspace establish ghost removal: the full reduced Hamiltonian and its inner product are needed. A fakeon prescription is a distinct physical choice involving analytic continuation and microscopic causality [3] and [4]. Discrete spatial momentum alone is not a no-go theorem for that prescription; lattice dispersion functions can have analytic extensions and time can remain continuous. Conversely, the present finite construction does not implement such a prescription. The earlier negative-residue reflection test for the unchanged higher-derivative tensor kernel remains applicable. A positive transfer operator for the retained compact model cannot remove that obstruction in a different physical sector. The new finite estimates identify what can be matched and calculated now, while leaving a precise spectral and dynamical task for the complete theory.

10.18. *A conditional Galerkin continuum theorem.* We give explicit sufficient hypotheses for a compactness and identification argument. They include uniform control of a stronger spatial norm and are stronger than the assumptions used in many variational SPDE existence theorems. This strength makes the convergence topology and every passage to a limit unambiguous.

Let $V \Subset H \equiv H^* \hookrightarrow V^*$ be a Gelfand triple of separable Hilbert spaces with dense continuous embeddings and compact embedding $V \hookrightarrow H$. Let U be another separable Hilbert space. Choose nested finite-dimensional spaces $H_N \subset V$ with dense union in V, and let $P_N : H \to H_N$ be their orthogonal projections. Assume $P_N v \to v$ in V for every $v \in V$. The uniform boundedness principle then gives $\sup_N \|P_N\|_{V\to V} < \infty$. Extend P_N to V^* by $\langle P_N \ell, v\rangle_{V^*,V} = \langle \ell, P_N v\rangle_{V^*,V}$.

Let

$$B : V \to V^*, \qquad \Sigma : V \to \mathcal{L}_2(U, H) \tag{621}$$

be Borel maps, where $\mathcal{L}_2$ denotes the Hilbert–Schmidt class. The drift B includes any correction required by the reference measure and the mobility. For the constant-mobility, flat-reference version of (62), it is $-\widehat{\mathbb{M}}\,\mathrm{grad}_{\mathbb{G}}\,\mathcal{S}_{\mathrm{M}}$ on its domain. Assume that the finite-dimensional equations

$$\mathrm{d}X_t^N = B_N(X_t^N)\,\mathrm{d}t + \Sigma_N(X_t^N)\,\mathrm{d}W_t, \qquad X_0^N \in H_N, \tag{622}$$

have non-explosive continuous solutions. The driving process is cylindrical on U, and $\Sigma_N(x) \in \mathcal{L}_2(U, H_N)$. For $R < \infty$, set

$$\begin{aligned} r^B_{N,R} &= \sup_{\substack{x \in H_N \\ \|x\|_V \le R}} \|B_N(x) - P_N B(x)\|_{V^*}, \\ r^\Sigma_{N,R} &= \sup_{\substack{x \in H_N \\ \|x\|_V \le R}} \|\Sigma_N(x) - P_N \Sigma(x)\|_{\mathcal{L}_2(U,H)}. \end{aligned} \tag{623}$$

The initial laws converge weakly to a probability ν_0 on H. One sufficient, stronger initial-data condition on a common space is

$$\mathbb{E}\|X^N_0 - P_N X_0\|^2_H \longrightarrow 0, \qquad \mathrm{Law}(X_0) = \nu_0, \quad \mathbb{E}\|X_0\|^2_H < \infty. \tag{624}$$

THEOREM 37 (Conditional Galerkin-to-continuum convergence). *Suppose that the preceding setup and the following assumptions hold for every $T < \infty$.*

(G1) For every $R < \infty$, $r^B_{N,R} + r^\Sigma_{N,R} \to 0$. On the ball $K_R = \{v \in V : \|v\|_V \le R\}$, the norms $\|B(v)\|_{V^*}$ and $\|\Sigma(v)\|_{\mathcal{L}_2(U,H)}$ are bounded. Whenever $v_n, v \in K_R$ and $v_n \to v$ in H, one has

$$\langle B(v_n), \varphi\rangle_{V^*,V} \to \langle B(v), \varphi\rangle_{V^*,V} \quad (\varphi \in V), \|\Sigma(v_n) - \Sigma(v)\|_{\mathcal{L}_2(U,H)} \to 0. \tag{625}$$

(G2) For some $\delta > 0$ and $C_T < \infty$, independent of N,

$$\begin{aligned} \sup_N \mathbb{E}\Bigg[\sup_{t \le T} \|X^N_t\|^{2+\delta}_V + \left(\int_0^T \|B_N(X^N_s)\|_{V^*}\, \mathrm{d}s \right)^{2+\delta} \\ + \left(\int_0^T \|\Sigma_N(X^N_s)\|^2_{\mathcal{L}_2(U,H)}\, \mathrm{d}s \right)^{1+\delta/2} \Bigg] \le C_T. \end{aligned} \tag{626}$$

In particular, this supplies the spatial localization

$$\sup_N \mathbb{P}\left(\sup_{t \le T} \|X^N_t\|_V > R \right) \le C_T R^{-(2+\delta)}. \tag{627}$$

(G3) For some $p > 2$, $\alpha > 0$, and $C_{T,p} < \infty$,

$$\sup_N \mathbb{E}\|X^N_t - X^N_s\|^p_{V^*} \le C_{T,p}|t-s|^{1+\alpha}, \qquad 0 \le s \le t \le T. \tag{628}$$

Then the laws of X^N are tight in $C([0,T]; H)$. Every subsequential limit solves the martingale problem for

$$\mathrm{d}X_t = B(X_t)\,\mathrm{d}t + \Sigma(X_t)\,\mathrm{d}W_t, \qquad \mathrm{Law}(X_0) = \nu_0, \tag{629}$$

in the following precise sense. For every $\varphi \in V$,

$$M^\varphi_t = (X_t - X_0, \varphi)_H - \int_0^t \langle B(X_s), \varphi\rangle_{V^*,V}\, \mathrm{d}s \tag{630}$$

is a continuous square-integrable martingale, and for $\varphi, \psi \in V$,

$$[M^{\varphi}, M^{\psi}]_t = \int_0^t (\Sigma(X_s)^*\varphi, \Sigma(X_s)^*\psi)_U \, \mathrm{d}s. \tag{631}$$

These identities define the weak stochastic equation through its drift and covariance. If a representation by a cylindrical Wiener process is desired, the usual Hilbert-space martingale representation may be performed on an enlarged probability space. If this martingale problem is unique in law in the stated solution class, the entire sequence converges to that law.

Proof. We first prove compactness in a Polish path space. The moment estimate in (628) gives tight bounds for the V^*-Hölder seminorm with any exponent $0 < \beta < \alpha/p$, by the moment form of the Kolmogorov criterion. Together with (627), this places the paths, with arbitrarily high probability, in sets of the form

$$\sup_{t \le T} \|u(t)\|_V \le R, \qquad \|u(t) - u(s)\|_{V^*} \le L|t-s|^{\beta}. \tag{632}$$

For $z \in V$, the pivot-space identity and duality give

$$\|z\|_H^2 = \langle z, z \rangle_{V^*,V} \le \|z\|_{V^*}\|z\|_V. \tag{633}$$

Consequently these paths have the common H-modulus $\|u(t) - u(s)\|_H^2 \le 2RL|t-s|^{\beta}$. The closed ball K_R is compact in H: compactness gives relative compactness, and weak lower semicontinuity of the V-norm makes it closed in H. The metric-space Arzelà–Ascoli theorem now gives relative compactness of the path sets in $C([0,T];H)$. Their closures are compact, so the laws are tight.

Choose a weakly convergent subsequence. Since $C([0,T];H)$ is Polish, its Skorokhod representation gives copies, still denoted X^N, X, such that $X^N \to X$ uniformly in H, almost surely. No common Wiener process is asserted for these copies. The map

$$u \longmapsto \sup_{t \le T} \|u(t)\|_V \tag{634}$$

is lower semicontinuous on this path space, where the V-norm is extended by $+\infty$ off V. This follows by taking the supremum of the lower semicontinuous functions $u \mapsto \|u(t)\|_V$. The limit therefore inherits the V-moment bound in (G2). In particular, its paths are bounded in V almost surely.

Fix $\varphi \in V$ and $R < \infty$. On the event that both paths remain in K_R, decompose the drift discrepancy as

$$\begin{aligned} \langle B_N(X_s^N), \varphi\rangle - \langle B(X_s), \varphi\rangle = \langle B_N(X_s^N) - P_N B(X_s^N), \varphi\rangle \\ + \langle B(X_s^N), P_N\varphi - \varphi\rangle + \langle B(X_s^N) - B(X_s), \varphi\rangle. \end{aligned} \tag{635}$$

The first term is bounded by $r_{N,R}^B \|\varphi\|_V$, and the second by $C_R\|P_N\varphi - \varphi\|_V$. The scalar map $v \mapsto \langle B(v), \varphi\rangle$ is continuous on the compact H-space K_R, hence

uniformly continuous there. Uniform convergence of the paths makes the last term tend to zero uniformly in time. The probability of the complementary event is at most $2C_T R^{-(2+\delta)}$, using the inherited bound for the limit. First taking $N \to \infty$, then $R \to \infty$, proves convergence in probability of the drift integrals, uniformly in their upper limit.

The same argument applies to the covariance. On K_R the image $\Sigma(K_R)$ is compact in $\mathcal{L}_2(U, H)$. The operators $A \mapsto P_N A$ are contractions on that space and converge strongly to the identity; they consequently converge uniformly on this compact image. Using the noise residual, we obtain

$$\sup_{s \le T} \|\Sigma_N(X_s^N) - \Sigma(X_s)\|_{\mathcal{L}_2(U,H)} \longrightarrow 0 \tag{636}$$

in probability after localization. Products of the adjoint coefficients against φ, ψ therefore converge in their time integrals. This passage concerns covariance integrals; it does not identify stochastic integrals across the new probability space.

We next pass the martingale identities themselves to the limit. Let M_N^φ be the coordinate martingale defined as in (630), with B_N, X^N in place of B, X. The finite-dimensional stochastic equation and the Burkholder–Davis–Gundy inequality imply

$$\begin{aligned} &\sup_N \mathbb{E} \sup_{t \le T} |M_N^\varphi(t)|^{2+\delta} \\ &\quad \le C_{\delta,T} \|\varphi\|_H^{2+\delta} \sup_N \mathbb{E} \left(\int_0^T \|\Sigma_N(X_s^N)\|_{\mathcal{L}_2}^2 \, \mathrm{d}s \right)^{1+\delta/2} < \infty. \end{aligned} \tag{637}$$

Thus these martingales are uniformly integrable, as are their pairwise products. Their covariance integrals are uniformly integrable by the last term of (G2). The drift convergence and uniform path convergence identify the limit M^φ.

For $0 \le s < t \le T$, let F be a bounded continuous function of the path restricted to $[0, s]$. Each approximate law satisfies

$$\mathbb{E}\big[(M_N^\varphi(t) - M_N^\varphi(s)) F(X^N|_{[0,s]})\big] = 0. \tag{638}$$

Uniform integrability permits passage to the limit in this identity. Apply the same argument to $M_N^\varphi M_N^\psi - \int_0^\cdot (\Sigma_N^* \varphi, \Sigma_N^* \psi)_U \, \mathrm{d}r$. A monotone-class argument extends these identities from bounded continuous past-path functions to all bounded functions measurable with respect to the past. Hence M^φ is a martingale and (631) holds. A countable dense set in V, followed by approximation using the integrability bounds, gives the assertions for every test vector. The initial law is ν_0, because evaluation at time zero is continuous. This constructs a limiting martingale solution; its existence was not an assumption. Finally, uniqueness in law makes all subsequential limits equal, which proves convergence of the entire sequence. □

For completeness, a convergence-in-probability upgrade requires more than pathwise uniqueness stated without reference to the approximations. On a common stochastic basis, one must prove joint tightness of (X^N, X^M, W) in a Polish realization of the noise and show that every joint subsequential limit consists of two solutions driven by the same limiting noise with the same initial condition. Pathwise uniqueness then puts every joint limit on the diagonal. The Gyöngy–Krylov criterion gives convergence in probability in $C([0,T];H)$. These joint identification hypotheses are additional to convergence of the marginal martingale problems.

For the master model, the preceding theorem is a conditional criterion. Its coefficient continuity, moment estimates, noise factorization, and uniqueness hypothesis must be verified for a specified realization. In particular, a formal Galerkin projection or a finite-dimensional calculation does not establish any of those analytic properties.

10.19. *Infinite-dimensional invariant measures.* A finite-time continuum limit and a stationary continuum law answer different questions. We now fix a time-homogeneous Markov realization of

$$\mathrm{d}X_t = B(X_t)\,\mathrm{d}t + \Sigma(X_t)\,\mathrm{d}W_t \tag{639}$$

on H, with transition semigroup $\mathsf{P}_t f(x) = \mathbb{E}[f(X_t^x)]$. The next result states exactly the Lyapunov and coupling assumptions used in the existence and uniqueness arguments.

THEOREM 38 (Conditional existence and uniqueness of an infinite-dimensional invariant measure). *Assume (I1)–(I4).*

(I1) The chosen realization is a conservative Markov family with continuous H-paths, and P_t maps $C_b(H)$ into $C_b(H)$.

(I2) There is a lower semicontinuous function $\mathcal{W} : H \to [0,\infty]$, finite at some x_*, with compact sublevel sets and constants $c_H > 0, C_H \geq 0$ such that

$$\mathcal{W}(x) \geq c_H \|x\|_H^2 - C_H. \tag{640}$$

(I3) For each initial point with finite $\mathcal{W}$, the process $\mathcal{W}(X_t)$ has the local decomposition

$$\mathcal{W}(X_t) = \mathcal{W}(X_0) + \int_0^t a_s\,\mathrm{d}s + M_t, \tag{641}$$

with a local martingale M, and

$$a_s \leq c_0 - c_1 \mathcal{W}(X_s) \quad \text{for almost every } s, \qquad c_0 \geq 0, \quad c_1 > 0. \tag{642}$$

A justified generalized Itô formula may supply this decomposition; lower semicontinuity of $\mathcal{W}$ alone does not.

(I4) There are increasing stopping times $\tau_n \to \infty$ almost surely such that $M_{t\wedge\tau_n}$ is a true martingale with mean zero and all terms in the stopped decomposition are integrable for finite t. The exhaustion $\tau_n \to \infty$ is part of this assumption and must be proved when constructing a realization.

Then there exists an invariant probability π, with $\int \mathcal{W}\,\mathrm{d}\pi \le c_0/c_1$ and finite second moment, satisfying

$$\int_H \mathsf{P}_t f\,\mathrm{d}\pi = \int_H f\,\mathrm{d}\pi, \qquad t \ge 0, \quad f \in C_b(H). \tag{643}$$

For the uniqueness assertion assume, in addition:

(I5) Solutions from any coupling of two initial laws with finite second moment admit a common-noise variational realization. Their paths belong to V for almost every time, the variational Itô formula for their squared H-distance holds, and

$$\begin{aligned} &2\langle B(x) - B(y), x - y\rangle_{V^*,V} \\ &\qquad + \|\Sigma(x) - \Sigma(y)\|^2_{\mathcal{L}_2(U,H)} \le -2\kappa\|x - y\|_H^2, \qquad x, y \in V, \end{aligned} \tag{644}$$

for some $\kappa > 0$. The semigroup preserves finite second moments.

Then

$$W_2(\mathsf{P}_t^*\mu, \mathsf{P}_t^*\nu) \le e^{-\kappa t} W_2(\mu, \nu) \tag{645}$$

for all probability measures μ, ν with finite second moment. Consequently π is the unique invariant probability measure on H. The Wasserstein estimate concerns finite-second-moment laws, but the uniqueness conclusion does not impose a moment condition on a competing invariant probability.

Proof. Start at x_*. Stop the decomposition in (I3), apply (I4), and use nonnegativity of $\mathcal{W}$. This gives

$$\mathbb{E}\mathcal{W}(X_{t\wedge\tau_n}) + c_1\mathbb{E}\int_0^{t\wedge\tau_n} \mathcal{W}(X_s)\,\mathrm{d}s \le \mathcal{W}(x_*) + c_0 t. \tag{646}$$

For each fixed t, exhaustion implies $X_{t\wedge\tau_n} = X_t$ for all sufficiently large n, almost surely. Fatou's lemma for the first term and monotone convergence for the integral therefore yield

$$\mathbb{E}\mathcal{W}(X_t) + c_1\mathbb{E}\int_0^{t} \mathcal{W}(X_s)\,\mathrm{d}s \le \mathcal{W}(x_*) + c_0 t. \tag{647}$$

This argument needs no unproved uniform integrability of the terminal Lyapunov values. It does need the exhausting stopping times: a continuous H-path need not remain in bounded sublevels of an arbitrary extended lower semicontinuous function.

Define the time-averaged laws

$$\mu_T = \frac{1}{T}\int_0^T \operatorname{Law}(X_s^{x_*})\,\mathrm{d}s. \tag{648}$$

Tonelli's theorem and the preceding estimate give

$$\int_H \mathcal{W}\,\mathrm{d}\mu_T \le \frac{\mathcal{W}(x_*)}{c_1 T} + \frac{c_0}{c_1}. \tag{649}$$

For $K_R = \{\mathcal{W} \le R\}$, Markov's inequality consequently gives

$$\mu_T(H \setminus K_R) \le \frac{1}{R}\left(\frac{\mathcal{W}(x_*)}{c_1 T} + \frac{c_0}{c_1}\right). \tag{650}$$

The sets K_R are compact, so $\{\mu_T : T \ge 1\}$ is tight. Prokhorov's theorem supplies $T_n \to \infty$ and $\mu_{T_n} \Rightarrow \pi$. Lower semicontinuity and the Portmanteau theorem show

$$\int_H \mathcal{W}\,\mathrm{d}\pi \le \liminf_n \int_H \mathcal{W}\,\mathrm{d}\mu_{T_n} \le c_0/c_1. \tag{651}$$

Together with (640), this proves the claimed finite second moment.

For $f \in C_b(H)$ and $t \ge 0$, the semigroup property gives the exact boundary-term identity

$$\int_H \mathsf{P}_t f\,\mathrm{d}\mu_T - \int_H f\,\mathrm{d}\mu_T = \frac{1}{T}\left[\int_T^{T+t} \mathsf{P}_s f(x_*)\,\mathrm{d}s - \int_0^t \mathsf{P}_s f(x_*)\,\mathrm{d}s\right]. \tag{652}$$

Its absolute value is at most $2t\|f\|_\infty/T$. The Feller property makes both integrands on the left bounded and continuous as functions of the initial state. Weak convergence therefore proves (643). Bounded continuous functions determine Borel probability measures on H; hence this is invariance of the probability measure.

Now impose (I5), put $D_t = X_t - Y_t$, and use the same driving Wiener process. The variational Itô identity reads

$$\begin{aligned} \mathrm{d}\|D_t\|_H^2 &= \left[2\langle B(X_t) - B(Y_t), D_t\rangle + \|\Sigma(X_t) - \Sigma(Y_t)\|_{\mathcal{L}_2}^2\right]\mathrm{d}t + \mathrm{d}N_t, \\ N_t &= 2\int_0^t (\Sigma(X_s)^* D_s - \Sigma(Y_s)^* D_s, \mathrm{d}W_s)_U. \end{aligned} \tag{653}$$

All pairings are evaluated at times for which the paths lie in V. No continuous extension of the unbounded drift pairing to H is required. Multiplication by $e^{2\kappa t}$ and (644) show that $e^{2\kappa t}\|D_t\|_H^2$ has nonpositive drift and a local martingale part. Stop that martingale at a localizing sequence, take expectations, and apply Fatou's lemma to the nonnegative left-hand side as the stopping times increase to infinity. We obtain

$$\mathbb{E}\|X_t - Y_t\|_H^2 \le e^{-2\kappa t}\mathbb{E}\|X_0 - Y_0\|_H^2. \tag{654}$$

For any initial coupling, the joint law of X_t, Y_t is a coupling of the two evolved laws. Taking the infimum over initial couplings and then square roots proves (645). If π_1, π_2 are invariant and have finite second moment,

$$W_2(\pi_1, \pi_2) \le e^{-\kappa t} W_2(\pi_1, \pi_2). \tag{655}$$

For $t > 0$ the multiplier is strictly less than one, so the finite distance must vanish. Thus $\pi_1 = \pi_2$.

To remove the moment restriction on a competing invariant law, fix $x \in H$. Since the constructed π has finite second moment,

$$W_2(\delta_x, \pi)^2 = \int_H \|x - y\|_H^2 \, \pi(\mathrm{d}y) < \infty. \tag{656}$$

For any bounded Lipschitz function $f : H \to \mathbb{R}$, integrate $|f(u) - f(v)| \le \mathrm{Lip}(f)\|u - v\|_H$ against a coupling and apply Cauchy–Schwarz. Taking the infimum over couplings and using invariance of π gives

$$|\mathsf{P}_t f(x) - \pi(f)| \le \mathrm{Lip}(f) W_2(\mathsf{P}_t^* \delta_x, \pi) \le \mathrm{Lip}(f) e^{-\kappa t} W_2(\delta_x, \pi) \longrightarrow 0. \tag{657}$$

Let η be any invariant probability on H, with no moment assumption. Invariance gives $\eta(f) = \int_H \mathsf{P}_t f(x) \, \eta(\mathrm{d}x)$. The integrand converges pointwise to $\pi(f)$, and its absolute value is bounded by $\|f\|_\infty$. Dominated convergence therefore yields $\eta(f) = \pi(f)$. Bounded Lipschitz functions determine probability measures on the Polish space H, so $\eta = \pi$. □

The existence proof uses compactness and time averaging; the uniqueness proof uses the additional contraction. A spectral gap or a logarithmic Sobolev inequality for one prescribed equilibrium does not, without further irreducibility or accessibility assumptions, rule out a different invariant probability supported on another invariant component. Alternative uniqueness arguments must state their own state-space, regularity, and irreducibility hypotheses.

10.20. *Reference measures and reversible continuum dynamics.* There is no infinite-dimensional analogue of translation-invariant Lebesgue probability. A continuum Gibbs formula must specify a reference probability and the generator compatible with it. Let $\{e_j\}_{j \ge 1}$ be an orthonormal basis of H, and let γ be the centered Gaussian probability with covariance $Ce_j = c_j e_j$, where $c_j > 0$ and $\sum_j c_j < \infty$. For a measurable interaction $\mathcal{U}$, suppose

$$\pi_{\mathrm{G}}(\mathrm{d}x) = Z^{-1} e^{-\mathcal{U}(x)/\theta} \gamma(\mathrm{d}x), \qquad 0 < Z = \int_H e^{-\mathcal{U}(x)/\theta} \, \gamma(\mathrm{d}x) < \infty. \tag{658}$$

The interaction $\mathcal{U}$ is the part of the energy not already encoded in γ. If the full formal action is placed in this density, the reference Gaussian contributes an additional quadratic energy; the resulting model must be interpreted accordingly.

Here is a precise reversible construction. Choose diagonal, constant mobilities $m_j > 0$. For smooth cylindrical functions define

$$\mathcal{E}(f,g) = \theta \int_H \sum_{j\geq 1} m_j \partial_j f \, \partial_j g \, \mathrm{d}\pi_{\mathrm{G}}. \tag{659}$$

Each integrand has only finitely many nonzero derivatives. Assume the cylindrical domain, including constants, is dense in $L^2(\pi_{\mathrm{G}})$, the displayed integrals are finite, and the form is closable. Its closure is a symmetric Dirichlet form: the contraction property follows from the ordinary chain rule and passage to the closure. Let Q_t be its associated self-adjoint Markov semigroup. Since 1 belongs to the form domain and $\mathcal{E}(1,g) = 0$ for every form-domain g, the definition of the associated generator gives 1 in its operator domain and $\mathscr{L}_{\mathrm{G}} 1 = 0$. Consequently $\mathsf{Q}_t 1 = 1$, and self-adjointness proves

$$\int_H \mathsf{Q}_t f \, \mathrm{d}\pi_{\mathrm{G}} = (\mathsf{Q}_t f, 1)_{L^2(\pi_{\mathrm{G}})} = (f, \mathsf{Q}_t 1)_{L^2(\pi_{\mathrm{G}})} = \int_H f \, \mathrm{d}\pi_{\mathrm{G}}. \tag{660}$$

This establishes invariance at the semigroup level.

If the coordinate weak derivatives of $\mathcal{U}$ and the relevant integration-by-parts identities exist with the required integrability, the generator on its cylindrical operator domain is

$$\mathscr{L}_{\mathrm{G}} f = \sum_j m_j \left[\theta \partial_{jj} f - \left(\partial_j \mathcal{U} + \frac{\theta x_j}{c_j} \right) \partial_j f \right]. \tag{661}$$

To check the coefficient, the one-coordinate Gaussian identity gives

$$\int \partial_j h \, \mathrm{d}\pi_{\mathrm{G}} = \int h \left(\frac{x_j}{c_j} + \frac{\partial_j \mathcal{U}}{\theta} \right) \mathrm{d}\pi_{\mathrm{G}}. \tag{662}$$

Apply this with $h = f \partial_j g$, multiply by θm_j, and sum over the finitely many active coordinates. The result is $-\int f \mathscr{L}_{\mathrm{G}} g \, \mathrm{d}\pi_{\mathrm{G}} = \mathcal{E}(f,g)$. Thus the reference drift $-\theta m_j x_j / c_j$ is essential. The expression $C^{-1}x$ need not be H-valued at a typical Gaussian sample, so (661) is initially a cylindrical or variational identity.

To identify Q_t with the transition semigroup of a specified SPDE, one must also establish that the constructed process solves that SPDE and that the relevant martingale problem is well posed. The identity $\int \mathscr{L} f \, \mathrm{d}\pi_{\mathrm{G}} = 0$ on a merely formal test class, without this generator or semigroup justification, is insufficient. For the four-dimensional master field, normalizability, the gauge construction, closability, and identification remain conditions on the chosen continuum realization.

10.21. *An explicit infinite-dimensional equilibrium example.* The analytic requirements are nonempty. The following realization gives an exact continuum process and stationary measure, while keeping its relation to the nonlinear

master model explicit. Take $H = \ell^2$ and

$$V = \left\{ x : \sum_{j \geq 1} j^2 x_j^2 < \infty \right\}, \qquad \|x\|_V^2 = \sum_{j \geq 1} j^2 x_j^2. \tag{663}$$

The embedding $V \Subset H$ is compact: on a V-ball of radius R, the squared H-norm of the tail after coordinate J is at most $R^2/(J+1)^2$, uniformly in the point. Consider independent Brownian motions β_j and the equations

$$\mathrm{d}X_j(t) = -j^2 X_j(t)\,\mathrm{d}t + \sqrt{2\theta}\, j^{-2}\mathrm{d}\beta_j(t). \tag{664}$$

Their explicit solution is

$$X_j(t) = e^{-j^2 t} x_j + \sqrt{2\theta}\, j^{-2} \int_0^t e^{-j^2(t-s)}\,\mathrm{d}\beta_j(s). \tag{665}$$

This series defines an H-continuous process. To see this directly, integration by parts gives, for $a > 0$,

$$\int_0^t e^{-a(t-s)}\,\mathrm{d}\beta(s) = \beta(t) - a \int_0^t e^{-a(t-s)}\beta(s)\,\mathrm{d}s, \tag{666}$$

whose absolute supremum on $[0,T]$ is at most $2\sup_{s \leq T} |\beta(s)|$. The L^2 maximal inequality for Brownian motion therefore bounds the expected squared supremum of the j-th stochastic coordinate by $32\theta T j^{-4}$. The sum of these bounds is finite. Its tails tend to zero, so the finite-coordinate processes converge in $L^2(\Omega; C([0,T]; H))$. The deterministic series is continuous by dominated convergence.

The covariance of the stochastic convolution at time t is diagonal, with entries

$$c_j(t) = \frac{\theta}{j^6}(1 - e^{-2j^2 t}). \tag{667}$$

Hence the Gaussian probability

$$\pi_\infty = \bigotimes_{j \geq 1} \mathcal{N}(0, \theta j^{-6}) \tag{668}$$

is supported on H, because $\int \|x\|_H^2\,\mathrm{d}\pi_\infty = \theta \sum_j j^{-6} < \infty$. If $X(0)$ has this law and is independent of the Brownian motions, each coordinate at time t has variance

$$e^{-2j^2 t}\theta j^{-6} + \theta j^{-6}(1 - e^{-2j^2 t}) = \theta j^{-6}. \tag{669}$$

The coordinates remain independent. Equality of all finite-coordinate laws proves invariance of π_∞.

Solutions with the same noise satisfy

$$\|X^x(t) - X^y(t)\|_H^2 = \sum_j e^{-2j^2 t}|x_j - y_j|^2 \leq e^{-2t}\|x - y\|_H^2. \tag{670}$$

This proves the Feller property by bounded convergence and gives Wasserstein contraction with $\kappa = 1$. It also proves uniqueness among finite-second-moment stationary laws. In this example uniqueness holds among all stationary probabilities: for fixed $x \in H$, (665) converges in law to π_∞, as follows by coupling its initial point with a sample from π_∞ and applying (670). For $f \in C_b(H)$ this gives $\mathsf{P}_t f(x) \to \int f \, \mathrm{d}\pi_\infty$. If η is any invariant probability, bounded convergence in $\int \mathsf{P}_t f \, \mathrm{d}\eta = \int f \, \mathrm{d}\eta$ gives $\eta(f) = \pi_\infty(f)$, and hence $\eta = \pi_\infty$.

The compact Lyapunov mechanism is visible without a formal infinite-dimensional differentiation. Set $\mathcal{W}_J(x) = \sum_{j=1}^{J} j^2 x_j^2$. Itô's formula gives

$$\mathscr{L}\mathcal{W}_J = -2\sum_{j=1}^{J} j^4 x_j^2 + 2\theta \sum_{j=1}^{J} j^{-2} \le -2\mathcal{W}_J + 2\theta \sum_{j\ge 1} j^{-2}. \tag{671}$$

For $x \in V$, take expectations of the integrated identity and let $J \to \infty$, using monotone convergence. The result is

$$\mathbb{E}\mathcal{W}(X_t) + 2\mathbb{E}\int_0^t \mathcal{W}(X_s)\, \mathrm{d}s \le \mathcal{W}(x) + 2\theta t \sum_{j\ge 1} j^{-2}, \qquad \mathcal{W}(x) = \|x\|_V^2. \tag{672}$$

Its sublevels are compact in H, and $\int \mathcal{W} \, \mathrm{d}\pi_\infty = \theta \sum_j j^{-4} < \infty$. Moreover $B(x) = (-j^2 x_j)_j$ is a map $V \to V^*$, $\|B(x)\|_{V^*} = \|x\|_V$, and the noise coefficient is Hilbert–Schmidt. This example therefore has a genuine unbounded variational drift; an extension of its energy pairing as a continuous function on all of H would be an inappropriate extra requirement.

Finally, the coordinate gradient representation uses mobility j^{-4} and the formal quadratic energy $\frac{1}{2}\sum_j j^6 x_j^2$. That energy is infinite π_∞-almost surely: its first J terms equal $\frac{\theta}{2}\sum_{j=1}^{J} Z_j^2$ for independent standard normal Z_j, and their averages tend to $\theta/2$. The measure is consequently specified by its Gaussian covariance, not by a density with respect to nonexistent infinite-dimensional Lebesgue volume. In (658) one takes $\gamma = \pi_\infty$ and $\mathcal{U} = 0$. The example establishes feasibility of the analytic equilibrium mechanism; it does not identify this linear model with the nonlinear four-dimensional gauge–gravity theory.

10.22. *A nonlinear exponential scalar field on a fixed background.* The preceding linear example can be extended while retaining the exponential weight of the shared scalar. The construction below keeps the Riemannian background and its nonnegative curvature density fixed. It also specifies a stronger Gaussian smoothing than the scalar kinetic term alone provides. These choices define an additional continuum realization; their removal, or their replacement by the full gauge–gravity dynamics, is a different problem.

Let M be a smooth connected compact Riemannian four-manifold without boundary. Fix $m, \theta > 0$, $\alpha_\sigma \in \mathbb{R} \setminus \{0\}$, and $K \in C^\infty(M)$ with $K \ge 0$, $K \not\equiv 0$.

All fields and parameters in this subsection are expressed in fixed dimensionless reference units. Set

$$L = m^2 - \Delta_g, \qquad \mathcal{H} = D(L^{3/2}), \qquad (x,y)_{\mathcal{H}} = (L^{3/2}x, L^{3/2}y)_{L^2(M)}. \tag{673}$$

The Laplacian convention is $-\Delta_g \geq 0$. The Sobolev embedding in four dimensions gives $\mathcal{H} = H^3(M) \hookrightarrow C(M)$. Choose a real orthonormal eigenbasis $Le_j = \lambda_j e_j$ in $L^2(M)$, ordered with multiplicity. Its least eigenvalue is $\lambda_1 = m^2$, and

$$\sum_{j\geq 1} \lambda_j^{-a} < \infty \quad \text{for every } a > 2. \tag{674}$$

This follows from the Weyl eigenvalue estimate $\lambda_j \asymp j^{1/2}$ in dimension four. An entirely explicit instance is the flat torus $M = (\mathbb{R}/2\pi\mathbb{Z})^4$, for which the complex Fourier eigenvalues are $m^2 + |n|^2$, $n \in \mathbb{Z}^4$; real sine and cosine functions give the corresponding real basis. The number of lattice points in a shell of radius R and unit thickness is $O(R^3)$, so the trace sum is bounded by a constant times $\sum_{R\geq 1} R^{3-2a}$, which converges exactly when $a > 2$. The vectors $f_j = \lambda_j^{-3/2} e_j$ are an orthonormal basis of $\mathcal{H}$. Define

$$\begin{aligned} U(x) &= \int_M K(q) e^{-\alpha_\sigma x(q)} \, \mathrm{vol}_g(\mathrm{d}q), \\ F(x) &= -\alpha_\sigma K e^{-\alpha_\sigma x}, \qquad G(x) = L^{-3} F(x). \end{aligned} \tag{675}$$

Pointwise values in this expression refer to the continuous representative of $x \in \mathcal{H}$. In particular, U is finite and continuous everywhere on $\mathcal{H}$.

The mobility in $L^2(M)$ is L^{-3}. The equation is

$$\mathrm{d}X_t = -\big[L^4 X_t + L^{-3} F(X_t)\big] \, \mathrm{d}t + \sqrt{2\theta}\, L^{-3/2} \mathrm{d}W_t^0, \tag{676}$$

where W^0 is cylindrical on $L^2(M)$. Its noise coefficient is Hilbert–Schmidt into $L^2(M)$, because $\sum_j \lambda_j^{-3} < \infty$. For solutions in $\mathcal{H}$, it is convenient to write $A = L^4$ and to use the cylindrical Wiener process $W^{\mathcal{H}} = \sum_j \beta_j f_j$ on $\mathcal{H}$. The precise interpretation is the mild equation

$$X_t = e^{-tA}x - \int_0^t e^{-(t-s)A} G(X_s) \, \mathrm{d}s + Z_t, \quad Z_t = \sqrt{2\theta} \int_0^t e^{-(t-s)A} \, \mathrm{d}W_s^{\mathcal{H}}. \tag{677}$$

No $\mathcal{H}$-valued Wiener process with identity covariance is assumed; the semigroup in the stochastic convolution supplies the smoothing.

THEOREM 39 (A nonlinear continuum equilibrium with exponential coupling). *For the data just specified, the following assertions hold.*

(i) For every $x \in \mathcal{H}$, equation (677) *has a unique global adapted solution with continuous $\mathcal{H}$-paths. The solutions form a time-homogeneous Feller Markov family.*

(ii) Spectral Galerkin solutions driven by the same Brownian coordinates and started at the spectral projections of x converge almost surely in $C([0,T];\mathcal{H})$, for every finite T.

(iii) Let γ be the centered Gaussian law whose covariance on $L^2(M)$ is θL^{-7}, equivalently whose covariance on $\mathcal{H}$ is θA^{-1}. Then

$$\pi(\mathrm{d}x) = \mathcal{Z}^{-1} e^{-U(x)/\theta}\gamma(\mathrm{d}x), \qquad 0 < \mathcal{Z} = \int_{\mathcal{H}} e^{-U/\theta}\,\mathrm{d}\gamma \le 1 \tag{678}$$

is invariant. It has finite moments of every polynomial order in $\mathcal{H}$.

(iv) If $\kappa = m^8$, solutions driven by the same noise satisfy

$$\|X_t^x - X_t^y\|_{\mathcal{H}} \le e^{-\kappa t}\|x-y\|_{\mathcal{H}}. \tag{679}$$

Consequently, for $\mu,\nu \in \mathcal{P}_2(\mathcal{H})$,

$$W_2(P_t^*\mu, P_t^*\nu) \le e^{-\kappa t} W_2(\mu,\nu). \tag{680}$$

The invariant probability π is unique among all invariant probabilities on $\mathcal{H}$, without a moment assumption on competing invariant laws.

Proof. We first establish the deterministic properties of the nonlinear term. For $x, h \in \mathcal{H}$, differentiation under the integral gives

$$DU(x)[h] = \int_M F(x)h \ \mathrm{vol}_g = (G(x), h)_{\mathcal{H}}. \tag{681}$$

The identity in the last step follows from the spectral definition of L^{-3}. Thus G is the gradient of U in $\mathcal{H}$. If $\|x\|_{\mathcal{H}}, \|y\|_{\mathcal{H}} \le R$, Sobolev embedding bounds their uniform norms by $C_{\mathrm{emb}}R$. The ordinary mean-value theorem then gives

$$\begin{aligned} \|F(x) - F(y)\|_{L^2} &\le \alpha_\sigma^2 \|K\|_\infty e^{|\alpha_\sigma| C_{\mathrm{emb}} R}\|x-y\|_{L^2}, \\ \|G(x) - G(y)\|_{\mathcal{H}} = \|L^{-3/2}(F(x)-F(y))\|_{L^2} &\le m^{-3}\|F(x)-F(y)\|_{L^2}. \end{aligned} \tag{682}$$

Hence $G : \mathcal{H} \to \mathcal{H}$ is locally Lipschitz and bounded on bounded sets. Moreover, the scalar function $r \mapsto -\alpha_\sigma K(q) e^{-\alpha_\sigma r}$ is nondecreasing for every q. Therefore

$$(G(x) - G(y), x-y)_{\mathcal{H}} = \int_M \big(F(x) - F(y)\big)(x-y)\ \mathrm{vol}_g \ge 0. \tag{683}$$

The positive operator A satisfies $(Av, v)_{\mathcal{H}} \ge \kappa \|v\|_{\mathcal{H}}^2$ on its domain.

Next we construct Z with continuous $\mathcal{H}$-paths. The second moment at a fixed time is bounded by

$$\mathbb{E}\|Z_t\|_{\mathcal{H}}^2 = \theta \sum_j \lambda_j^{-4}(1 - e^{-2t\lambda_j^4}) \le \theta \sum_j \lambda_j^{-4} < \infty. \tag{684}$$

For path continuity, fix $\alpha = 1/8$ and define

$$Y_\alpha(t) = \int_0^t (t-s)^{-\alpha} e^{-(t-s)A}\,\mathrm{d}W_s^{\mathcal{H}}. \tag{685}$$

The Itô isometry and the substitution $v = 2\lambda_j^4 u$ give

$$\begin{aligned}\mathbb{E}\|Y_\alpha(t)\|_{\mathcal{H}}^2 &= \sum_j \int_0^t u^{-2\alpha} e^{-2u\lambda_j^4}\,\mathrm{d}u \\ &\le 2^{2\alpha-1}\Gamma(1-2\alpha)\sum_j \lambda_j^{4(2\alpha-1)} = C_\alpha \sum_j \lambda_j^{-3} < \infty.\end{aligned} \tag{686}$$

Gaussian moment bounds imply $\mathbb{E}\int_0^T \|Y_\alpha(t)\|_{\mathcal{H}}^p \mathrm{d}t < \infty$ for every finite p. Choose $p > 8$, so $\alpha > 1/p$. Stochastic Fubini and the beta-integral identity yield

$$Z_t = \frac{\sqrt{2\theta}\sin(\pi\alpha)}{\pi}\int_0^t (t-s)^{\alpha-1} e^{-(t-s)A} Y_\alpha(s)\,\mathrm{d}s. \tag{687}$$

Indeed, after interchanging the two integrals, the scalar kernel at a fixed Brownian time $r < t$ is

$$\int_r^t (t-s)^{\alpha-1}(s-r)^{-\alpha}\,\mathrm{d}s = \Gamma(\alpha)\Gamma(1-\alpha) = \frac{\pi}{\sin(\pi\alpha)}. \tag{688}$$

The moment estimate above justifies that interchange. The deterministic convolution in (687) maps $L^p(0,T;\mathcal{H})$ continuously into $C([0,T];\mathcal{H})$: Hölder's inequality applies because $(\alpha-1)p/(p-1) > -1$, and continuity follows by approximation with continuous functions and strong continuity of e^{-tA}. This proves the required continuous version of Z.

Fix one of its continuous sample paths and put $V = X - Z$. The local contraction-mapping argument for

$$V_t = e^{-tA}x - \int_0^t e^{-(t-s)A} G(V_s + Z_s)\,\mathrm{d}s \tag{689}$$

gives a unique local solution, because G is locally Lipschitz. We prove that its maximal existence time is infinite. On an interval of local existence, the energy identity is

$$\frac{1}{2}\frac{\mathrm{d}}{\mathrm{d}t}\|V_t\|_{\mathcal{H}}^2 + \|A^{1/2}V_t\|_{\mathcal{H}}^2 = -(G(V_t+Z_t), V_t)_{\mathcal{H}} \quad \text{for almost every } t. \tag{690}$$

For a mild solution this identity follows by applying spectral projections to its integral equation, integrating the resulting finite-coordinate identities, and passing to the limit. The forcing is continuous and bounded on each such interval. The projected pairings converge by dominated convergence, and the nonnegative $A^{1/2}$-energy converges monotonically. In particular the integrated energy is finite and the identity is justified without presupposing a classical $D(A)$-valued path.

Subtract $G(Z_t)$ inside the pairing and use (683). Young's inequality gives

$$-(G(V_t+Z_t), V_t)_{\mathcal{H}} \le \|G(Z_t)\|_{\mathcal{H}}\|V_t\|_{\mathcal{H}} \le \frac{\kappa}{2}\|V_t\|_{\mathcal{H}}^2 + \frac{1}{2\kappa}\|G(Z_t)\|_{\mathcal{H}}^2. \tag{691}$$

The integrating-factor calculation therefore gives

$$\|V_t\|_{\mathcal{H}}^2 \le e^{-\kappa t}\|x\|_{\mathcal{H}}^2 + \frac{1}{\kappa}\int_0^t e^{-\kappa(t-s)}\|G(Z_s)\|_{\mathcal{H}}^2\,\mathrm{d}s. \tag{692}$$

For every finite T, the continuous path Z is bounded on $[0,T]$, and G is bounded on that ball. The right-hand side is therefore finite uniformly for $t \le T$. The blow-up alternative in the local contraction-mapping construction excludes a finite maximal time. The construction is adapted and measurable in the initial state and driving noise. Uniqueness and independent Wiener increments give the Markov property and time homogeneity.

For two solutions driven by the same noise, the difference satisfies a deterministic evolution equation. The same projected-energy argument and (683) give

$$\frac{1}{2}\frac{\mathrm{d}}{\mathrm{d}t}\|X_t^x - X_t^y\|_{\mathcal{H}}^2 \le -\kappa\|X_t^x - X_t^y\|_{\mathcal{H}}^2. \tag{693}$$

Integration proves (679). Bounded convergence then proves the Feller property.

We next construct and identify the invariant law. Let P_N be the orthogonal projection onto $\operatorname{span}\{f_1,\dots,f_N\}$, and let X^N solve

$$\mathrm{d}X_t^N = -\big[AX_t^N + P_N G(X_t^N)\big]\mathrm{d}t + \sqrt{2\theta}\sum_{j=1}^N f_j\,\mathrm{d}\beta_j(t), \qquad X_0^N = P_N x. \tag{694}$$

Its stochastic convolution is $Z^N = P_N Z$. The estimate (692) holds uniformly in N, because P_N is a contraction and, for $v \in P_N\mathcal{H}$, $(P_N G(v+Z^N) - P_N G(Z^N), v)_{\mathcal{H}} \ge 0$. Also $\sup_t \|Z_t^N\|_{\mathcal{H}} \le \sup_t \|Z_t\|_{\mathcal{H}}$. Consequently, on each fixed continuous noise path and finite interval, all X^N and X lie in one finite $\mathcal{H}$-ball.

Strong convergence of the contractions P_N is uniform on a compact subset of $\mathcal{H}$. It follows that $P_N Z \to Z$ uniformly in time. The same statement applies to the compact image $\{G(X_t) : 0 \le t \le T\}$. Subtract the two mild equations, use the local Lipschitz constant on the common ball, and obtain

$$\sup_{r\le t}\|X_r^N - X_r\|_{\mathcal{H}} \le a_N + C_R\int_0^t \sup_{u\le s}\|X_u^N - X_u\|_{\mathcal{H}}\,\mathrm{d}s, \tag{695}$$

where

$$a_N = \|P_N x - x\|_{\mathcal{H}} + \sup_{t\le T}\|P_N Z_t - Z_t\|_{\mathcal{H}} + T\sup_{t\le T}\|(P_N - I)G(X_t)\|_{\mathcal{H}} \longrightarrow 0. \tag{696}$$

Gronwall's inequality proves assertion (ii).

On $P_N\mathcal{H}$, set

$$V_N(y) = \tfrac{1}{2}(Ay, y)_{\mathcal{H}} + U(y). \tag{697}$$

Its Hessian is at least κI, and (694) is the ordinary gradient diffusion $\mathrm{d}Y = -\nabla V_N(Y)\mathrm{d}t + \sqrt{2\theta}\mathrm{d}B^N$ in its orthonormal coordinates. The probability

$$\pi_N(\mathrm{d}y) = \mathcal{Z}_N^{-1} e^{-U(y)/\theta}\gamma_N(\mathrm{d}y), \qquad \gamma_N = (P_N)_*\gamma, \tag{698}$$

is invariant. We give a semigroup justification of this finite-dimensional statement to distinguish it from formal infinitesimal stationarity. In orthonormal coordinates its smooth density r_N is proportional to $e^{-V_N/\theta}$, and

$$L_N u = \theta r_N^{-1}\,\mathrm{div}(r_N \nabla u). \tag{699}$$

For $f \in C_c^\infty(P_N\mathcal{H})$, $L_N f$ is bounded. Dynkin's formula, nonexplosion, and the backward equation give $\partial_t P_t^N f = L_N P_t^N f = P_t^N L_N f$; in particular this derivative is bounded by $\|L_N f\|_\infty$. The backward equation may be justified locally by the uniformly elliptic finite-dimensional equation and then by localization, as in the standard diffusion construction [105] and [54]. The derivative flow solves $\dot J_t = -D^2 V_N(Y_t)J_t$, so $\|J_t\| \le e^{-\kappa t}$. Differentiating the expectation therefore gives $\|\nabla P_t^N f\|_\infty \le e^{-\kappa t}\|\nabla f\|_\infty$. Choose cutoffs χ_R with $\chi_R \to 1$, $0 \le \chi_R \le 1$, and $\|\nabla \chi_R\|_\infty \le C/R$. Integration by parts yields

$$\int \chi_R L_N P_t^N f\, r_N\,\mathrm{d}y = -\theta \int (\nabla\chi_R, \nabla P_t^N f) r_N\,\mathrm{d}y \longrightarrow 0. \tag{700}$$

The left side converges by the bounded-generator estimate. Thus $\frac{\mathrm{d}}{\mathrm{d}t}\int P_t^N f\,\mathrm{d}\pi_N = 0$, proving invariance first for compactly supported smooth f, and then for bounded continuous functions because such test functions determine finite Borel measures.

The Gaussian law in the theorem exists on $\mathcal{H}$, since $\mathrm{Tr}_{\mathcal{H}}(\theta A^{-1}) = \theta\sum_j \lambda_j^{-4} < \infty$. If ξ has that law, then $P_N\xi \to \xi$ in $\mathcal{H}$ almost surely. Continuity and nonnegativity of U imply

$$e^{-U(P_N\xi)/\theta} \longrightarrow e^{-U(\xi)/\theta}, \qquad 0 < e^{-U(P_N\xi)/\theta} \le 1. \tag{701}$$

Dominated convergence gives $\mathcal{Z}_N \to \mathcal{Z}$. The limit is strictly positive because its integrand is positive everywhere on $\mathcal{H}$. This also proves $\pi_N \Rightarrow \pi$. Polynomial moments of π are finite, because

$$\int \|x\|_{\mathcal{H}}^p\,\pi(\mathrm{d}x) \le \mathcal{Z}^{-1}\int \|x\|_{\mathcal{H}}^p\,\gamma(\mathrm{d}x) < \infty. \tag{702}$$

For $f \in C_b(\mathcal{H})$, invariance of π_N is the identity

$$\int_{\mathcal{H}} P_t^N f(P_N x) e^{-U(P_N x)/\theta}\,\gamma(\mathrm{d}x) = \int_{\mathcal{H}} f(P_N x) e^{-U(P_N x)/\theta}\,\gamma(\mathrm{d}x). \tag{703}$$

The Galerkin convergence proved above gives $P_t^N f(P_N x) \to P_t f(x)$ for every $x \in \mathcal{H}$. Both integrands are bounded in absolute value by $\|f\|_\infty$. Dominated convergence, followed by division by $\mathcal{Z}$, proves $\pi(P_t f) = \pi(f)$. This proves continuum invariance without using a formal infinite-dimensional Lebesgue density or an unverified generator-core claim.

To verify the second moments required by (680), couple a solution started from an arbitrary $\mu \in \mathcal{P}_2(\mathcal{H})$ with an independent initial sample of π, and then use the same noise. Invariance gives a finite second moment for the latter solution at every time. The pathwise contraction then gives a finite second moment for the former. Taking the infimum over all initial couplings proves (680).

Finally, for every $x \in \mathcal{H}$, contraction against π gives $W_2(P_t^*\delta_x, \pi) \to 0$. Hence $P_t f(x) \to \pi(f)$ for every bounded Lipschitz function f. If η is any invariant probability, bounded convergence gives

$$\eta(f) = \int P_t f \, \mathrm{d}\eta \longrightarrow \pi(f). \tag{704}$$

Bounded Lipschitz functions separate probabilities on the separable Hilbert space $\mathcal{H}$. Therefore $\eta = \pi$, proving the last assertion. □

The partition function also has an explicit positive lower bound. Let $v(q) = \mathbb{E}_\gamma[\xi(q)^2]$. Continuity of point evaluation on $\mathcal{H}$ gives

$$0 \le v(q) \le C_{\mathrm{emb}}^2 \theta \sum_j \lambda_j^{-4}. \tag{705}$$

Tonelli's theorem and the scalar Gaussian exponential moment give

$$\mathbb{E}_\gamma U = \int_M K(q) e^{\alpha_\sigma^2 v(q)/2} \, \mathrm{vol}_g(\mathrm{d}q) < \infty. \tag{706}$$

Jensen's inequality applied to $r \mapsto e^{-r/\theta}$ therefore yields

$$\exp\left[-\frac{1}{\theta}\int_M K(q) e^{\alpha_\sigma^2 v(q)/2} \, \mathrm{vol}_g(\mathrm{d}q)\right] \le \mathcal{Z} \le 1. \tag{707}$$

Thus normalizability in this realization is a proved estimate, not an additional existence assumption.

10.22.1. *A stationary balance identity for the shared scalar.* The construction supplies a quantitative identity that is absent from the unstabilized scalar model. Let $\bar{x} = \mathrm{vol}_g(M)^{-1} \int_M x \, \mathrm{vol}_g$. Projection of (676) onto the constant eigenfunction and taking stationary expectations gives

$$m^{14} \mathbb{E}_\pi \bar{X} = \frac{\alpha_\sigma}{\mathrm{vol}_g(M)} \, \mathbb{E}_\pi U(X). \tag{708}$$

To justify the expectation, observe that π has a finite second moment, and $\mathbb{E}_\pi U \le \mathcal{Z}^{-1} \mathbb{E}_\gamma U < \infty$. The constant-coordinate martingale has mean zero. Its integrated drift is integrable, so stationarity makes the expected increment vanish. Since $L1 = m^2 1$, the drift projection is $-m^8 \int X + m^{-6} \alpha_\sigma U(X)$, which gives the displayed factor m^{14}. In particular, $\mathbb{E}_\pi \bar{X}$ is strictly positive for $\alpha_\sigma > 0$ and strictly negative for $\alpha_\sigma < 0$.

For the flat-torus example with $K \equiv k > 0$, the measure is translation invariant: both its Gaussian reference and its interaction are unchanged by spatial translations. Thus $\mu := \mathbb{E}_\pi X(q)$ is independent of q. Point evaluation is continuous on $\mathcal{H}$, so this expectation is well defined. The balance identity and Jensen's inequality give

$$m^{14}\mu = \alpha_\sigma k\, \mathbb{E}_\pi e^{-\alpha_\sigma X(q)}, \qquad m^{14}\alpha_\sigma\mu \geq \alpha_\sigma^2 k e^{-\alpha_\sigma \mu}. \tag{709}$$

Writing $a = \alpha_\sigma\mu > 0$, we obtain the quantitative bound

$$ae^a \geq \frac{\alpha_\sigma^2 k}{m^{14}}, \qquad \alpha_\sigma\mu \geq W_0\Big(\frac{\alpha_\sigma^2 k}{m^{14}}\Big), \tag{710}$$

where $W_0 : [0,\infty) \to [0,\infty)$ is the inverse of $a \mapsto ae^a$. This bound is an observable statement for the specified scalar equilibrium and its chosen parameters; it is not an experimental prediction for gravity or the Standard Model.

The quadratic Gaussian completion provides the balancing force. For the finite-coordinate actions it is $\frac{1}{2}(x, L^7 x)_{L^2}$; it contains a positive constant-mode term $\frac{1}{2}m^{14}\|x\|_{L^2}^2$, the gradient term $\frac{7}{2}m^{12}\|\nabla x\|_{L^2}^2$, and higher derivative terms. Those finite-coordinate energies determine the reference covariance θL^{-7}. Their infinite-coordinate quadratic energy is typically infinite under γ, so the continuum law remains the relative density (678). Identity (708) is an exact stationary response of this specified scalar realization. It does not determine a parameter-free observable of the full gauge–gravity theory.

The assumptions $K \geq 0$, fixed compact geometry, and the stated smoothing operator are essential to the proof. A varying metric would require uniform geometric estimates, and integrating over gauge fields would make K a random coupled field. Neither operation is performed here. Removing the higher derivative smoothing in four dimensions would also require a new definition and analysis of the pointwise exponential interaction. The theorem establishes an interacting scalar continuum realization with the original exponential mechanism while leaving the nonlinear gauge–gravity continuum problem separate.

11. **Equilibrium observables, sector separation, and falsifiability**

11.1. *The master equilibrium and spontaneous sector separation.* The equilibrium measure p_* may possess several metastable basins. Let $\mathcal{V}_1, \ldots, \mathcal{V}_k$ be local minimizers of $\mathcal{S}_{\mathrm{M}}$. Since gauge orbits otherwise generate zero directions and an infinite gauge volume, fix a local gauge slice or work on the quotient configuration space $\mathfrak{X}/\mathfrak{G}$. In a local exponential chart on that slice (or quotient), write

$$\mathbb{X} = \exp_{\mathcal{V}_i}(\eta). \tag{711}$$

Then

$$\mathcal{S}_{\mathrm{M}}[\exp_{\mathcal{V}_i}(\eta)] = \mathcal{S}_{\mathrm{M}}[\mathcal{V}_i] + \frac{1}{2}\langle \eta, H_i\eta\rangle + O(\|\eta\|^3), \tag{712}$$

where H_i is the Hessian restricted to the physical tangent space of the slice or quotient. Stable directions correspond to positive quadratic-form directions, while zero modes correspond to residual symmetries or moduli. The relaxation or mass gap is not determined by the raw eigenvalues of H_i alone: if K_i is the positive kinetic metric, the physical fluctuation operator is $K_i^{-1/2} H_i K_i^{-1/2}$, whereas the stochastic relaxation operator is, when defined, $\widehat{\mathbb{M}}_i^{1/2} H_i \widehat{\mathbb{M}}_i^{1/2}$. The relevant gap must therefore be stated for the operator appropriate to the claimed scale separation.

Assume here that the selected phase is a C^3 critical point on the gauge-fixed slice or quotient Hilbert space, with locally bounded third derivative, for which the Hessian is self-adjoint with the relevant spectral decomposition, and that the broken directions have a positive gap for the appropriate kinetic or mobility-weighted operator. Under these hypotheses the low-energy spectrum is controlled at quadratic order by the Hessian of the same master action. A gap identifies candidate heavy directions, but does not alone justify eliminating their interactions. Controlled elimination additionally requires estimates for the derivative expansion, nonlinear couplings, and induced threshold operators. Section 11.10 gives an explicit Gaussian elimination in which the light-field operators are retained.

Together with a separately established symmetry-breaking pattern, these spectral data describe how a common equilibrium can organize effective sectors. Identifying those sectors with the observed interactions still requires the representation and matching conditions stated above.

11.2. *Observable consequences and falsifiability.* A unified theory is scientifically useful only if it eventually constrains observations. The present architecture leads to several classes of potential predictions.

11.3. *Coupling relations.* The invariant pairing h_{IJ} determines the relative normalization of curvature components before symmetry breaking. In the following matching formula, μ denotes the renormalization scale and is distinct from the fixed information parameter μ_{info}. If the microscopic theory uniquely fixes h_{IJ}, then the low-energy couplings satisfy matching relations of the form

$$g_a^{-2}(\mu) = \mathcal{M}_a[h, \Gamma_*, \mu], \qquad G_{\mathrm{eff}}^{-1}(\mu) = \mathcal{M}_g[h, \Gamma_*, \mu], \tag{713}$$

where $\mathcal{M}_a$ are calculable matching functionals. Numerical values require explicit evaluation and renormalization conditions.

11.4. *Higher-curvature terms.* The heat-kernel expansion generically produces higher-curvature terms. Precision tests constrain them once their coefficients and the observable map are fixed. Section 5.3 gives an exact coefficient relation for a specified Cartan action, and Section 11.10 derives a different relation for a specified heavy-field threshold. The contributions of other modes,

operator-basis changes, and renormalization must be included before either relation is compared with observations.

11.5. *Correlated sector responses.* Because the sectors originate from one master Hessian, a perturbation of the microscopic equilibrium may induce correlated shifts in several effective parameters. If λ_i are low-energy parameters, one expects

$$\delta\lambda_i = \sum_A \frac{\partial \lambda_i}{\partial q_A} \delta q_A, \tag{714}$$

where q_A are master vacuum coordinates. This identity is the chain rule. It constrains observations only after the dependence on the vacuum coordinates is specified. Section 11.8 provides an explicit response calculation and identifies its observable assumptions.

11.6. *Scale-dependent fluctuation law.* Projection of the master noise determines the quadratic covariation of the effective noise increments. Equal-time equilibrium correlations also depend on the restoring drift and on the chosen observables. Block diagonality of the noise covariance alone therefore does not imply statistical independence at equilibrium. The distinction can be calculated exactly in the following finite-dimensional realization.

11.7. *An exactly solvable coupled equilibrium.* Fix dimensionless coordinates $x \in \mathbb{R}^n$ on a physical configuration space after removal of gauge zero modes. Let $H = H^\top > 0$ and $M_0 = M_0^\top > 0$ be constant matrices. Here H is the Hessian of the quadratic action, and M_0 represents the tangent mobility $\widehat{\mathbb{M}}$. For this realization the complete data are

$$S_0(x) = \frac{1}{2} x^\top H x = \frac{1}{2} \|H^{1/2} x\|^2, \qquad \nu(\mathrm{d}x) = \mathrm{d}x, \qquad \theta > 0. \tag{715}$$

Thus the action is one positive quadratic norm; its decomposition into sectors is determined by specified coordinate projections. The stochastic law and its path cost are

$$\mathrm{d}X_t = -M_0 H X_t \, \mathrm{d}t + \sqrt{2\theta M_0} \, \mathrm{d}W_t, \tag{716}$$

$$\mathcal{J}_T[x] = \frac{1}{4\theta} \int_0^T (\dot{x} + M_0 H x)^\top M_0^{-1} (\dot{x} + M_0 H x) \, \mathrm{d}t. \tag{717}$$

The cost is defined for absolutely continuous paths with square-integrable residual drift. This example fixes the finite-dimensional stochastic data explicitly; the identification of these coordinates with gravitational or internal gauge observables is a separate geometric step.

THEOREM 40 (Equilibrium covariance and sector coupling). *The diffusion* (716) *has a unique invariant law* $\pi_0 = N(0, C_0)$*, where*

$$C_0 = \theta H^{-1}, \qquad Z_0 = \frac{(2\pi\theta)^{n/2}}{\sqrt{\det H}}, \qquad \pi_0(\mathrm{d}x) = Z_0^{-1} e^{-S_0(x)/\theta}\,\mathrm{d}x. \tag{718}$$

For a decomposition $x = (x_1, x_2)$*, write*

$$H = \begin{pmatrix} A & B \\ B^\top & D \end{pmatrix}, \qquad Q = D - B^\top A^{-1} B. \tag{719}$$

Then $A > 0$*,* $Q > 0$*, and the full cross-covariance block satisfies*

$$(C_0)_{12} = -\theta A^{-1} B Q^{-1}, \qquad (C_0)_{12} = 0 \iff B = 0. \tag{720}$$

Proof. Put $L_0 = M_0 H$. The similarity identity

$$L_0 = M_0^{1/2} (M_0^{1/2} H M_0^{1/2}) M_0^{-1/2} \tag{721}$$

shows that all eigenvalues of L_0 are strictly positive. The linear coefficients are globally Lipschitz, so the stochastic equation has the global solution

$$X_t = e^{-L_0 t} X_0 + \int_0^t e^{-L_0(t-s)} \sqrt{2\theta M_0}\,\mathrm{d}W_s. \tag{722}$$

The Itô isometry gives the covariance of the stochastic integral as

$$C_t = 2\theta \int_0^t e^{-L_0 s} M_0 e^{-L_0^\top s}\,\mathrm{d}s. \tag{723}$$

To evaluate this integral, use $L_0 H^{-1} = M_0 = H^{-1} L_0^\top$. Differentiation yields

$$\frac{\mathrm{d}}{\mathrm{d}s}\left(e^{-L_0 s} \theta H^{-1} e^{-L_0^\top s}\right) = -2\theta e^{-L_0 s} M_0 e^{-L_0^\top s}. \tag{724}$$

Integration from zero to t therefore gives

$$C_t = \theta H^{-1} - e^{-L_0 t} \theta H^{-1} e^{-L_0^\top t} \longrightarrow \theta H^{-1}. \tag{725}$$

The deterministic part in (722) converges to zero. Starting from $N(0, \theta H^{-1})$ preserves that covariance and the zero mean, which proves invariance. For uniqueness even among invariant laws without an assumed second moment, let φ be the characteristic function of such a law. Independence of the future noise gives

$$\varphi(k) = \varphi(e^{-L_0^\top t} k) \exp\left(-\frac{1}{2} k^\top C_t k\right). \tag{726}$$

As $t \to \infty$, continuity at zero and $\varphi(0) = 1$ determine $\varphi(k) = \exp(-\theta k^\top H^{-1} k/2)$. Diagonalizing H orthogonally and evaluating the one-dimensional Gaussian integrals gives the displayed value of Z_0.

Since $H > 0$, its principal block A is positive definite. For any nonzero y, evaluate the quadratic form of H on $(-A^{-1}By, y)$; the result is $y^{\top}Qy > 0$. Finally the factorization

$$H = \begin{pmatrix} I & 0 \\ B^{\top}A^{-1} & I \end{pmatrix} \begin{pmatrix} A & 0 \\ 0 & Q \end{pmatrix} \begin{pmatrix} I & A^{-1}B \\ 0 & I \end{pmatrix} \tag{727}$$

has inverse with upper-right block $-A^{-1}BQ^{-1}$. Multiplication by θ proves (720); invertibility of A and Q proves its converse. In a Gaussian law this vanishing block is also equivalent to independence of the two full coordinate sectors. □

The quadratic covariation of the noise obeys a different identity:

$$\mathrm{d}[X_i, X_j]_t = 2\theta(M_0)_{ij}\,\mathrm{d}t, \qquad \mathrm{Cov}_{\pi_0}(X_i, X_j) = \theta(H^{-1})_{ij}. \tag{728}$$

For example, taking $M_0 = I$ and $H = \left(\begin{smallmatrix} 2 & 1 \\ 1 & 2 \end{smallmatrix}\right)$ makes the cross quadratic covariation zero but gives covariance $-\theta/3$. Interchanging these choices makes the cross quadratic covariation $2\theta\,\mathrm{d}t$ while the equal-time covariance vanishes. Both models use a single action, one mobility, and one vector Wiener process.

For general two-mode data,

$$H = \begin{pmatrix} a & c \\ c & b \end{pmatrix}, \qquad a, b > 0, \qquad \Delta = ab - c^2 > 0, \tag{729}$$

direct inversion gives

$$C_0 = \frac{\theta}{\Delta} \begin{pmatrix} b & -c \\ -c & a \end{pmatrix}, \qquad \rho_{12} = \frac{(C_0)_{12}}{\sqrt{(C_0)_{11}(C_0)_{22}}} = -\frac{c}{\sqrt{ab}}. \tag{730}$$

Thus the sign and magnitude of the correlation follow from specified couplings. For projected observables $u^{\top}X_1$ and $v^{\top}X_2$, the covariance is $-\theta u^{\top}A^{-1}BQ^{-1}v$; a particular projection can annihilate this expression even when $B \neq 0$.

11.8. *Response relations and the observable map.* Couple an external source by $S_f(x) = S_0(x) - f^{\top}x$. Completing the square gives

$$S_f(x) = \frac{1}{2}(x - H^{-1}f)^{\top}H(x - H^{-1}f) - \frac{1}{2}f^{\top}H^{-1}f. \tag{731}$$

Consequently $\mathbb{E}_f X = H^{-1}f$. Defining the static susceptibility $\chi_{ij} := \partial_{f_j}\mathbb{E}_f X_i$ gives

$$\chi = H^{-1}, \qquad C_0 = \theta\chi, \qquad \rho_{12} = \frac{\chi_{12}}{\sqrt{\chi_{11}\chi_{22}}}. \tag{732}$$

The last relation eliminates the fluctuation scale. It is an equilibrium fluctuation–response identity, also satisfied by other reversible Gibbs models; its physical use requires that the sources and observables be defined independently of the measured correlations [137].

For the stationary process let $K(t) = \mathbb{E}[X_t X_0^\top]$, $t \geq 0$. Equation (722) gives $K(t) = e^{-L_0 t} C_0$. A time-dependent source enters the drift as $M_0 f(t)$, and variation of constants gives its impulse response $\mathscr{R}(t) = e^{-L_0 t} M_0$. Since $L_0 C_0 = \theta M_0$,

$$\mathscr{R}(t) = -\theta^{-1} K'(t), \qquad K'(0) = -\theta M_0, \qquad \int_0^\infty \mathscr{R}(t)\,\mathrm{d}t = H^{-1}. \tag{733}$$

The last equality follows by integrating $e^{-L_0 t}$, whose integral is L_0^{-1}, and using $L_0^{-1} M_0 = H^{-1}$. No commutation of M_0 and H is needed. The lag t here is stochastic time. A prediction for measured temporal spectra requires a justified map to physical time.

There is also an exact nonlinear response identity. For gauge-invariant observables O_i, introduce a source through $S_f = S - f O_j$. Assume the Gibbs integral is finite for f in an open interval about zero and that its derivative, including the insertion $O_i O_j$, can be passed under the integral. Differentiating its numerator and denominator separately gives

$$\frac{\partial}{\partial f} \mathbb{E}_f O_i \bigg|_{f=0} = \theta^{-1} \left(\mathbb{E}_0[O_i O_j] - \mathbb{E}_0[O_i] \mathbb{E}_0[O_j] \right). \tag{734}$$

For a nonlinear action the formula $C_0 = \theta H^{-1}$ is not exact. If a unique non-degenerate minimum dominates the Gibbs integral and the rescaled fluctuations have uniformly integrable second moments, Laplace asymptotics give $C_\theta = \theta H^{-1} + o(\theta)$. The global concentration and moment assumptions are needed in addition to a positive local Hessian. A physical application must fix the selected vacuum, the gauge-invariant observable map, and the normalization of the sources before (720) or (734) can constrain measurements.

11.9. *A reproducible numerical benchmark.* The exact identities above admit a finite-dimensional numerical comparison in which time-discretization error and sampling error can be distinguished. Use the two-mode data

$$H = \begin{pmatrix} 2 & 0.8 \\ 0.8 & 1.5 \end{pmatrix}, \qquad M_0 = \begin{pmatrix} 1 & 0.25 \\ 0.25 & 0.75 \end{pmatrix}, \quad \theta = 0.5, \qquad \Delta t = 0.02. \tag{735}$$

The leading principal minors are $2, 2.36$ for H and $1, 0.6875$ for M_0, so both matrices are positive definite. Direct multiplication and inversion give

$$\begin{gathered} L_0 = \begin{pmatrix} 2.2 & 1.175 \\ 1.1 & 1.325 \end{pmatrix}, \quad C_0 = \frac{0.5}{2.36} \begin{pmatrix} 1.5 & -0.8 \\ -0.8 & 2 \end{pmatrix}, \\ H^{-1} \begin{pmatrix} 0.7 \\ -0.4 \end{pmatrix} = \frac{1}{2.36} \begin{pmatrix} 1.37 \\ -1.36 \end{pmatrix}. \end{gathered} \tag{736}$$

Set $A_\Delta = \exp(-L_0 \Delta t)$, and

$$C_0 = \theta H^{-1}, \qquad Q_\Delta = C_0 - A_\Delta C_0 A_\Delta^\top. \tag{737}$$

The exact sampled Markov chain is

$$X_{n+1} = A_\Delta X_n + Q_\Delta^{1/2}\xi_n, \qquad \xi_n \sim N(0, I_2), \tag{738}$$

with independent standard Gaussian vectors ξ_n. Equation (738) follows by integrating the linear SDE over one interval; its noise covariance is $2\theta \int_0^{\Delta t} e^{-L_0 s} M_0 e^{-L_0^\top s}\,\mathrm{d}s$, which equals Q_Δ by (725). It therefore tests the continuous-time formulas while introducing no time-discretization bias.

For the retained spacing $\tau = 20\Delta t = 0.4$, the semigroup property allows the twenty base transitions to be compressed without approximation. Indeed, writing $A_\tau = \exp(-L_0\tau)$, repeated conditioning gives

$$A_\tau = A_\Delta^{20}, \qquad Q_\tau = \sum_{j=0}^{19} A_\Delta^j Q_\Delta (A_\Delta^j)^\top = C_0 - A_\tau C_0 A_\tau^\top. \tag{739}$$

Thus direct simulation of the τ-kernel has exactly the same retained finite-dimensional distributions as simulating twenty Δt-updates and discarding nineteen intermediate states. It does not reproduce the same sample path for a fixed pseudorandom stream, and it contains no statistics of the nineteen ungenerated intermediate states.

The exact-transition chain was initialized in its invariant law $N(0, C_0)$ and first advanced through 20,000 exact base-kernel updates of size $\Delta t = 0.02$. It was then advanced with the compressed kernel (739) to obtain $N = 2{,}000{,}000$ retained states at stochastic-time spacing $\tau = 0.4$. This is distributionally identical to a base-step span of 40,020,000 updates. Since the initial law is already invariant, the initial omission is not needed for equilibration; it is retained as a fixed reproducibility convention. For the response test, the source $f = (0.7, -0.4)^\top$ was applied and independent samples were drawn from the shifted invariant law $N(H^{-1}f, C_0)$. The analytic values and the sample estimates are shown in Table 7.

The computation uses IEEE–754 double precision, NumPy 2.4.6, SciPy 1.18.0, and the PCG64 generator. The matrix exponential is evaluated by SciPy's scaling-and-squaring implementation. A master `SeedSequence` with entropy 20260928 spawns distinct streams for the initial state, chain innovations, independent response sample, and replicate calculation. Thus neither the response estimates nor the replicate check reuse random numbers from the reported chain. Standard normal innovations are multiplied by the lower-triangular Cholesky factor of the exact transition covariance. These conventions and the seed sequence fix the sampling procedure. In binary64 arithmetic, direct evaluation of A_Δ^{20} and of the covariance sum in (739) differs from the independently evaluated τ-kernel by relative Frobenius residuals 1.01×10^{-15} and 2.05×10^{-15}, respectively.

Table 7. Exact two-mode benchmark. The simulation uses the compressed exact transition in (739); the source means use the same covariance with the shifted mean $H^{-1}f$. The numerical discrepancies are sampling errors, not parameter fits. The penultimate column is the non-overlapping batch-means standard error defined below; the final column is the analytic Gaussian Markov-chain asymptotic standard error.

Quantity	Analytic	Simulation	Abs. error	Batch SE	Analytic SE
C_{11}	0.3177966102	0.3187088589	0.0009122487	0.0004896335	0.0005098973
C_{12}	-0.1694915254	-0.1703786744	0.0008871490	0.0005798761	0.0005770144
C_{22}	0.4237288136	0.4245362175	0.0008074039	0.0008181636	0.0008336947
ρ_{12}	-0.4618802154	-0.4631917274	0.0013115120	0.0009348570	0.0009313465
$\mathbb{E}_f X_1$	0.5805084746	0.5804640080	0.0000444665	0.0003806697	0.0003986205
$\mathbb{E}_f X_2$	-0.5762711864	-0.5765309774	0.0002597909	0.0004605228	0.0004602873

The retained chain is stationary but its samples are correlated. To estimate Monte Carlo variability without treating thinned states as independent, let $g_{ij,n} = (X_{i,n} - \bar{X}_i)(X_{j,n} - \bar{X}_j) - \widehat{C}_{ij}$ be the centered first-order influence sequence for a covariance entry. For the correlation, use

$$g_{\rho,n} = \frac{g_{12,n}}{\sqrt{\widehat{C}_{11}\widehat{C}_{22}}} - \frac{\widehat{\rho}}{2}\left(\frac{g_{11,n}}{\widehat{C}_{11}} + \frac{g_{22,n}}{\widehat{C}_{22}}\right). \tag{740}$$

Divide each influence sequence into $b = 400$ non-overlapping batches of $m =$ 5,000 retained states. If $\bar{g}_j$ is the mean in batch j and $\bar{g}_\bullet = b^{-1}\sum_{j=1}^{b}\bar{g}_j$, the batch-means standard error is

$$\widehat{\mathrm{se}}(\widehat{T}) = \left\{\frac{1}{b(b-1)}\sum_{j=1}^{b}(\bar{g}_j - \bar{g}_\bullet)^2\right\}^{1/2}. \tag{741}$$

The response means use the analogous centered observation sequences. The approximate 95-percent intervals use $t_{399,0.975} = 1.96592729592$. They are asymptotic diagnostics, without an assertion of exact finite-sample coverage. All six analytic values lie inside their reported intervals; the largest absolute residual divided by its batch standard error is 1.863. The covariance estimator uses divisor N and is not asserted to be unbiased in a finite correlated sample.

There is also an analytic long-run-variance check. Put $A_\tau = \exp(-M_0 H\tau)$. For a centered quadratic observable $g_P(x) = x^\top Px - \mathrm{tr}(PC_0)$, Isserlis' identity

gives

$$\gamma_P(k) = 2\,\mathrm{tr}\left[P A_\tau^k C_0 P (A_\tau^k C_0)^\top\right], \quad \Gamma_P = \gamma_P(0) + 2\sum_{k=1}^{\infty}\gamma_P(k), \\ \mathrm{se}_{\mathrm{asy}}(\widehat{T}) = \sqrt{\Gamma_P/N}, \qquad N_{\mathrm{eff}} = N\gamma_P(0)/\Gamma_P. \tag{742}$$

Here $P_{11} = e_1 e_1^\top$, $P_{22} = e_2 e_2^\top$, and $P_{12} = (e_1 e_2^\top + e_2 e_1^\top)/2$. The delta-method influence matrix for the correlation is

$$P_\rho = \frac{P_{12}}{\sqrt{C_{11}C_{22}}} - \frac{\rho_{12}}{2}\left(\frac{P_{11}}{C_{11}} + \frac{P_{22}}{C_{22}}\right). \tag{743}$$

For $C_{11}, C_{12}, C_{22}, \rho_{12}$, respectively, the exact integrated autocorrelation times and the resulting effective sample sizes are

$$(\tau_{\mathrm{int}}^{11}, \tau_{\mathrm{int}}^{12}, \tau_{\mathrm{int}}^{22}, \tau_{\mathrm{int}}^{\rho}) = (2.57435, 4.07555, 3.87113, 2.80331), \tag{744}$$

$$(N_{\mathrm{eff}}^{11}, N_{\mathrm{eff}}^{12}, N_{\mathrm{eff}}^{22}, N_{\mathrm{eff}}^{\rho}) = (776{,}896, 490{,}732, 516{,}645, 713{,}442). \tag{745}$$

The corresponding batch estimates are $848{,}143, 488{,}285, 537{,}673, 705{,}577$. Finally, 128 independently seeded exact-transition chains, each containing 50,000 retained states at spacing 0.4, provide a second check of the static covariance and correlation statistics: the four replicate-average standardized residuals have absolute value below 1.22. These replicates are not used to validate the separate lag-product standard errors below.

The uncertainty in the lag-covariance plot can also be computed from the Gaussian law rather than inferred only from batches. Let $Y_n = e_1^\top X_n$ for the retained chain and set $r_k = \mathbb{E}[Y_k Y_0] = (A_\tau^{|k|} C_0)_{11}$ for $k \in \mathbb{Z}$. Because the invariant mean is known to vanish, the plotted estimator at the integer lag h is

$$\widehat{K}_h = \frac{1}{N-h}\sum_{n=0}^{N-h-1} Y_{n+h} Y_n. \tag{746}$$

It is unbiased for r_h. If $Z_n^{(h)} = Y_{n+h}Y_n$, a direct application of Isserlis' identity gives

$$\gamma_h(d) := \mathrm{Cov}(Z_0^{(h)}, Z_d^{(h)}) = r_d^2 + r_{d+h} r_{d-h}, \quad \Gamma_h := \gamma_h(0) + 2\sum_{d=1}^{\infty}\gamma_h(d), \\ \mathrm{se}_{\mathrm{asy}}(\widehat{K}_h) = \sqrt{\frac{\Gamma_h}{N-h}}. \tag{747}$$

The series is absolutely convergent because the spectral radius of A_τ is strictly less than one. Over the 26 plotted lags, the ratios of the batch standard errors to the analytic standard errors range from 0.902 to 1.080, with mean 0.985. The vertical bars use $z_{0.975} = 1.95996398454$ and are pointwise asymptotic intervals; they are not a simultaneous 95-percent band for the whole curve. At lag zero

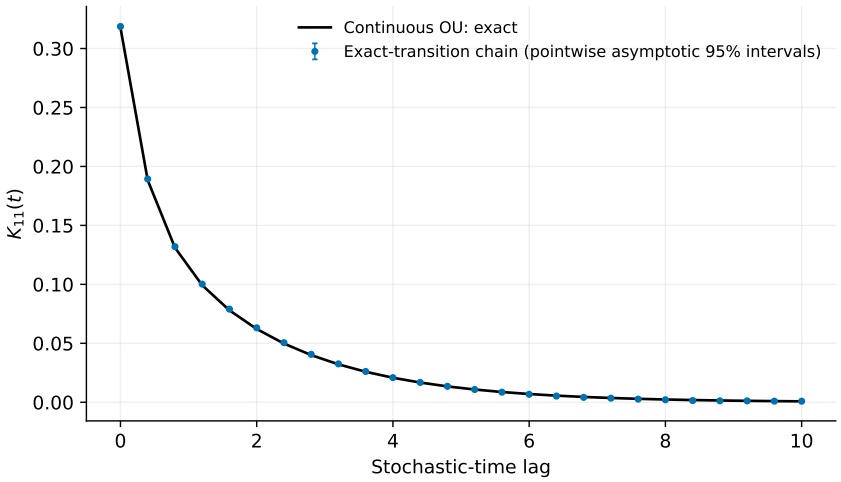


Figure 10. Dynamical check of the exact two-mode Ornstein–Uhlenbeck chain. The solid curve is the analytic stationary lag covariance $K_{11}(t) = [\exp(-M_0 H t) C_0]_{11}$; circles are the empirical covariance from the compressed exact transition in (739). Vertical bars are the pointwise asymptotic 95-percent intervals from (747); they do not form a simultaneous confidence band. No Euler time-discretization is used.

the analytic standard error is 5.0990×10^{-4}, while at the largest plotted lag it is 3.6058×10^{-4}. Consequently, the far tail is resolved on an absolute, but not a high-relative-precision, scale.

The dynamical comparison in Figure 10 shows the analytic lag covariance and the exact-chain estimates on the same time grid; the prefix convergence in Figure 11 checks the three independent covariance entries against their analytic values. The comparison illustrates the inverse-Hessian covariance, the sign of the cross-correlation, and the static response relation in one coupled stochastic system. The analytic identities follow from the preceding proofs; these simulations describe their finite-sample behavior. The coordinates are dimensionless, and no identification with measured physical channels or physical time is used.

11.9.1. *An explicit discretization comparison.* An Euler scheme for the same diffusion has a different stationary covariance. This difference can be calculated without fitting simulation output. For step size $h > 0$, let

$$Y_{k+1} = (I - hL_0)Y_k + \sqrt{2\theta h M_0}\,\xi_k, \qquad \xi_k \sim N(0, I_2). \tag{748}$$

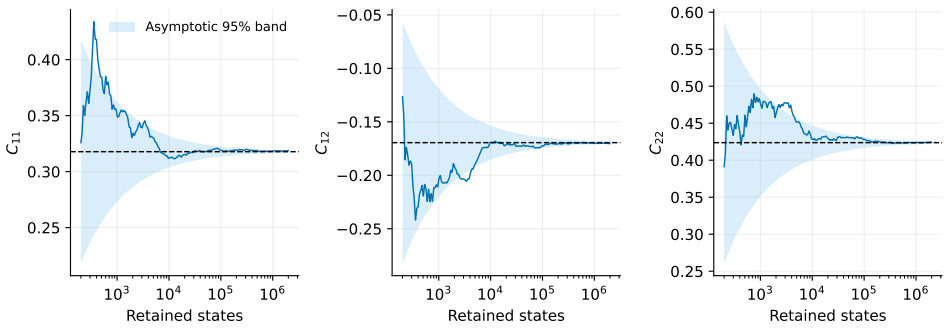


Figure 11. Prefix convergence of the exact-chain covariance estimates. The blue curves use the retained states in the prescribed order; the dashed lines are the analytic entries of $C_0 = \theta H^{-1}$. Sample covariances use the empirical mean and divisor equal to the prefix length. The shaded regions are analytic Gaussian Markov-chain asymptotic 95-percent bands computed from the long-run variance in (742). They are pointwise in the prefix length and do not constitute a simultaneous confidence band.

Write $S = M_0^{1/2} H M_0^{1/2} > 0$ and let $S = U\,\mathrm{diag}(\lambda_1, \lambda_2) U^\top$ with U orthogonal. In coordinates $z = U^\top M_0^{-1/2} Y$, each component satisfies $z_{i,k+1} = (1 - h\lambda_i) z_{i,k} + \sqrt{2\theta h}\,\eta_{i,k}$ with independent standard normal innovations. A stationary variance exists precisely when $|1 - h\lambda_i| < 1$ for each i. Consequently the stability condition is $0 < h < 2/\lambda_{\max}(S)$, which equals $h < 0.6709930268$ for the specified matrices. The scalar variance equation is

$$v_i = (1 - h\lambda_i)^2 v_i + 2\theta h, \qquad v_i = \frac{\theta}{\lambda_i (1 - h\lambda_i/2)}. \tag{749}$$

Transforming back gives

$$C_h^{\mathrm{E}} = \theta M_0^{1/2} \left(S - \frac{h}{2} S^2 \right)^{-1} M_0^{1/2}. \tag{750}$$

Because all matrix functions between the square roots of M_0 are functions of the same symmetric matrix S, subtraction of $C_0 = \theta M_0^{1/2} S^{-1} M_0^{1/2}$ is legitimate without assuming that M_0 commutes with H. It yields

$$\begin{aligned} C_h^{\mathrm{E}} - C_0 &= \frac{\theta h}{2} M_0^{1/2} \left(I - \frac{h}{2} S \right)^{-1} M_0^{1/2} > 0, \\ C_h^{\mathrm{E}} - C_0 &= \frac{\theta h}{2} M_0 + O(h^2), \qquad h \downarrow 0. \end{aligned} \tag{751}$$

Thus every nonzero linear observable has an upward stationary variance bias under Euler sampling. In contrast, the exact transition satisfies $A_h C_0 A_h^\top +$

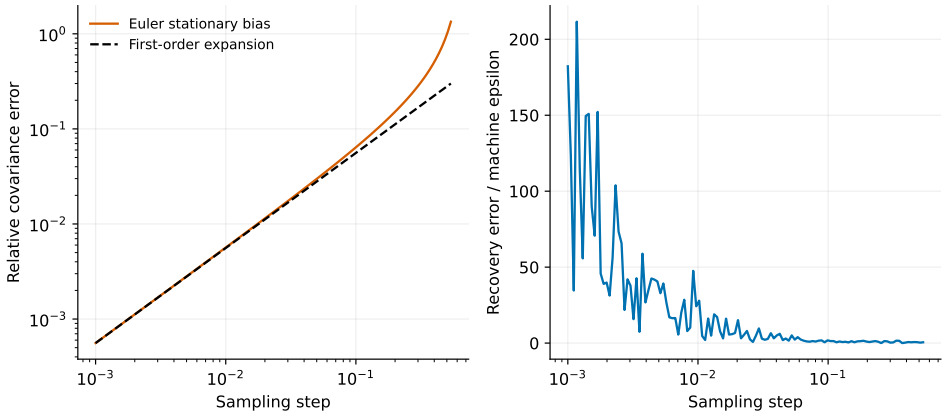


Figure 12. Stationary covariance under Euler and exact-transition sampling. Left: the Euler bias and its first-order expansion. Right: the relative covariance residual for the exact transition, divided by the double-precision machine epsilon. Both panels evaluate discrete Lyapunov equations; they contain no Monte Carlo samples.

$Q_h = C_0$ for every $h > 0$. Figure 12 compares the relative Frobenius error $\|C_h^{\mathrm{E}} - C_0\|_{\mathrm{F}}/\|C_0\|_{\mathrm{F}}$ with its first-order value $\theta h\|M_0\|_{\mathrm{F}}/(2\|C_0\|_{\mathrm{F}})$. The discrete Lyapunov equation provides an independent numerical evaluation:

$$\operatorname{vec}(C_h) = (I - T_h \otimes T_h)^{-1} \operatorname{vec}(Q_h), \tag{752}$$

where vec stacks columns and T_h, Q_h are the transition matrix and innovation covariance of the chosen chain. All 120 plotted step sizes lie between 0.001 and $0.8\,[2/\lambda_{\max}(S)]$. The exact-transition residual from this independent linear solve is at most 4.70×10^{-14} in relative Frobenius norm. The directly evaluated discrete invariance residual is at most 6.76×10^{-17}. Both reflect floating-point conditioning.

11.10. *A heavy-mode matching calculation.* A specified heavy direction provides a second calculable restriction, this time on effective-action coefficients. Fix an oriented Lorentzian background with signature $(-+++)$ and a gauge-invariant operator basis at a matching scale μ_{match}. The Lorentzian realization is an additional input here. The operators

$$\mathcal{O}_R = \mu_0^2 R, \qquad \mathcal{O}_a = \frac{1}{4}\kappa_{AB}^{(a)} F_a^{A\mu\nu} F_{a\mu\nu}^{B} \tag{753}$$

have mass dimension four; $\mu_0 > 0$ is a fixed reference mass and $\kappa^{(a)}$ is a fixed invariant normalization for gauge factor a. The factor μ_0 only aligns dimensions and is not a new prediction. Its redefinition must be accompanied by the

inverse change of the corresponding coefficient. Let $\mathcal{O}$ be the column of these operators, c a real dimensionless column, and $m_* > 0$ a reference mass. A single real heavy scalar ϕ of mass $m_\phi > 0$ couples through

$$\mathcal{L}_{\phi,L} = -\frac{1}{2}\nabla_\mu\phi\nabla^\mu\phi - \frac{1}{2}m_\phi^2\phi^2 + \phi J, \qquad J = \frac{1}{m_*}c^\top\mathcal{O}. \tag{754}$$

All terms have mass dimension four, since $[\phi] = 1$ and $[J] = 3$. The couplings to $\mathcal{O}_a$ are effective interactions with their own cutoff; this matching problem concerns momenta below that cutoff.

The relation to the one-norm formulation can be specified on the Euclidean regulator. Put $o = \mathcal{O}/\mu_0^4$ and $z = \phi/\mu_0$, with the Euclidean operator basis and continuation signs fixed, and take

$$\mathcal{L}_{\mathrm{block},E} = \frac{1}{2}|\nabla\phi|^2 + \frac{\mu_0^4}{2}\begin{pmatrix} o \\ z \end{pmatrix}^\top \begin{pmatrix} Q & -d \\ -d^\top & r \end{pmatrix}\begin{pmatrix} o \\ z \end{pmatrix}, \qquad r = \frac{m_\phi^2}{\mu_0^2}. \tag{755}$$

Here Q is symmetric and $r > 0$. Let c_E be the dimensionless coupling column determined by the specified continuation, so that

$$J_E = m_*^{-1}c_E^\top\mathcal{O}_E, \qquad d = \frac{\mu_0}{m_*}c_E, \qquad J_E = \mu_0^3 d^\top o. \tag{756}$$

Thus no equality of Euclidean and Lorentzian operator signs is presumed. Completing the scalar square gives

$$o^\top Qo - 2z\,d^\top o + rz^2 = r\left(z - r^{-1}d^\top o\right)^2 + o^\top\left(Q - r^{-1}dd^\top\right)o. \tag{757}$$

For instance $Q = I + r^{-1}dd^\top$ makes this quadratic form strictly positive. Thus the mixed block can be part of one positive extended norm, with explicit algebraic entries in $\mathscr{E}_{\mathrm{ext}}$, once the scalar operators and their reference scales have been supplied. Those entries are extra model data; they are not implied by the abstract notation $\mathbb{F}$. The remaining regulator, reference measure, and constraints must still make the full functional integral well-defined.

On a fixed smooth closed Euclidean background, or with self-adjoint boundary conditions for which $-\nabla_E^2 \geq 0$ (such as Dirichlet or Neumann conditions), $K_E = m_\phi^2 - \nabla_E^2 \geq m_\phi^2$. At a finite spectral cutoff, project J_E onto the retained modes. The exact Gaussian integration on those modes is obtained from

$$\frac{1}{2}\langle\phi, K_E\phi\rangle - \langle\phi, J_E\rangle = \frac{1}{2}\langle\phi - K_E^{-1}J_E, K_E(\phi - K_E^{-1}J_E)\rangle - \frac{1}{2}\langle J_E, K_E^{-1}J_E\rangle. \tag{758}$$

It produces the source contribution $-\langle J_E, K_E^{-1}J_E\rangle/2$ and the determinant contribution $\theta\log\det K_E/2$ to the Euclidean effective action, up to a source-independent normalization fixed by the finite-mode reference measure. Equivalently, each eigenvalue inside the logarithm is divided by the fixed reference unit of the quadratic form, so that the determinant is dimensionless. The parameter θ here is the scale in $\exp(-S_E/\theta)$. Although K_E is independent of the source,

its determinant depends on the background metric. The determinant therefore gives additional gravitational terms of the type discussed in Section 5.1; it cannot be discarded when comparing full curvature coefficients.

THEOREM 41 (Single-mode threshold relations). *At tree level, eliminating the scalar in* (754) *gives*

$$\Delta S_L = \frac{1}{2}\langle J, (m_\phi^2 - \Box)^{-1} J\rangle_L. \tag{759}$$

The inverse in this variational expression uses a symmetric boundary prescription; causal real-time responses require the corresponding causal construction. At leading order in the local low-momentum expansion,

$$\Delta\mathcal{L}_L^{(0)} = \frac{1}{2}\sum_{i,j}\Delta C_{ij}\mathcal{O}_i\mathcal{O}_j, \qquad \Delta C_{ij} = \frac{c_i c_j}{m_\phi^2 m_*^2}. \tag{760}$$

The symmetric coefficient matrix has rank at most one, and every two-by-two minor vanishes:

$$\Delta C_{ij}\Delta C_{k\ell} - \Delta C_{i\ell}\Delta C_{kj} = 0, \qquad (\Delta C_{ij})^2 = \Delta C_{ii}\Delta C_{jj}. \tag{761}$$

Proof. With compactly supported variations, the scalar equation is $(m_\phi^2 - \Box)\phi = J$. Integration by parts writes the quadratic Lorentzian action as $-\langle\phi, (m_\phi^2 - \Box)\phi\rangle_L/2 + \langle\phi, J\rangle_L$. Substitution of its stationary solution therefore leaves $\langle J, (m_\phi^2 - \Box)^{-1}J\rangle_L/2$, which proves (759).

The local expansion starts with

$$(m_\phi^2 - \Box)^{-1} = m_\phi^{-2} + m_\phi^{-4}\Box + \cdots. \tag{762}$$

Its controlled meaning can be given on a Euclidean spectral band: if $-\nabla_E^2$ has eigenvalues in $[0, E^2]$ on the projected sources, then

$$\left\|(m_\phi^2 - \nabla_E^2)^{-1} - m_\phi^{-2} I\right\| \le \frac{E^2}{m_\phi^4}. \tag{763}$$

Indeed, for each eigenvalue λ the absolute difference is $\lambda/[m_\phi^2(m_\phi^2+\lambda)] \le E^2/m_\phi^4$. Consequently the source-action error is at most $E^2\|J_E\|^2/(2m_\phi^4)$. Continuing the local coefficients under the stated Lorentzian prescription gives the leading term $J^2/(2m_\phi^2)$. Substituting $J = m_*^{-1}\sum_i c_i\mathcal{O}_i$ proves (760). Finally,

$$\Delta C_{ij}\Delta C_{k\ell} = \frac{c_i c_j c_k c_\ell}{m_\phi^4 m_*^4} = \Delta C_{i\ell}\Delta C_{kj}, \tag{764}$$

which proves both identities in (761). □

For example, with just $\mathcal{O}_R$ and one gauge operator $\mathcal{O}_a$, expansion without a matrix convention reads

$$\Delta\mathcal{L}_L^{(0)} = A_R R^2 + B_{Ra} R\mathcal{O}_a + C_a\mathcal{O}_a^2, \tag{765}$$

where

$$A_R = \frac{c_R^2 \mu_0^4}{2 m_\phi^2 m_*^2}, B_{Ra} = \frac{c_R c_a \mu_0^2}{m_\phi^2 m_*^2}, \qquad C_a = \frac{c_a^2}{2 m_\phi^2 m_*^2}, B_{Ra}^2 = 4 A_R C_a. \tag{766}$$

The coefficient dimensions are respectively $0, -2, -4$, so the last relation has dimension -4 on both sides. Its factor four follows from the convention that the mixed term appears once in (765). This is a calculated relation among the scalar-exchange contributions to the curvature and gauge terms.

It is essential to keep the threshold contribution ΔC distinct from the full Wilson-coefficient matrix. In a fixed renormalization scheme,

$$C_{\text{eff}}(\mu_{\text{match}}) = C_{\text{direct}}(\mu_{\text{match}}) + \Delta C(\mu_{\text{match}}) + C_{\text{loop}}(\mu_{\text{match}}). \tag{767}$$

The positive Euclidean completion (755) itself contains direct quadratic operator terms. They need not have rank one. Other heavy particles, the determinant, and independent finite counterterms also contribute. Thus (761) constrains the specified tree-level exchange contribution, and constrains the full action only when the other contributions are fixed or controlled independently. Curvature identities and field redefinitions can mix the operators, so a physical test must compare coefficients in one nonredundant basis or compare gauge-invariant amplitudes.

For independent heavy scalars with positive masses and diagonal quadratic kinetic terms, the same calculation gives

$$\Delta C = \sum_{r=1}^{N_h} \frac{c^{(r)} c^{(r)\top}}{m_r^2 m_{*,r}^2}, \qquad \operatorname{rank} \Delta C \le N_h. \tag{768}$$

The Cauchy–Schwarz inequality applied to the vectors $(c_i^{(r)}/(m_r m_{*,r}))_r$ gives $(\Delta C_{ij})^2 \le \Delta C_{ii} \Delta C_{jj}$. Equality holds precisely when the two vectors are linearly dependent, including the case in which one of them vanishes. These restrictions distinguish single- and multiple-mode matching mechanisms under the stated assumptions.

An invariant version of single-mode factorization is the residue of an isolated scalar pole in physical scattering channels. If g_i is the on-shell coupling of a scalar mass eigenstate to channel i, normalized so that its propagator has unit residue, the simple-pole part has coefficient $\mathcal{P}_{ij} = g_i g_j^*$. Hence

$$|\mathcal{P}_{ij}|^2 = \mathcal{P}_{ii} \mathcal{P}_{jj}. \tag{769}$$

This statement assumes an isolated stable pole and well-defined physical external states. Regular local contact terms do not change its residue. Degenerate states or overlapping resonances require the corresponding sum over states. Factorization is a general property of single-particle exchange, not unique to a unified model [161]. To turn this calculation into a prediction of the master construction, the selected vacuum must determine the heavy spectrum, the

operator couplings, and the physical channels; their identification cannot be inferred from the existence of one norm alone.

11.11. *Conditional observable relations of the shared scalar.* The common weight in (226) determines relative couplings once a propagating scalar mode has been identified. A fluctuation of that weight changes the gauge kinetic terms and the gravitational coefficient together. Converting this observation into a scattering or force prediction requires diagonalizing the scalar–metric kinetic terms. The required distinction is particularly relevant for the Cartan realization: on its round-sphere branch the full master curvature vanishes, whereas the separate Einstein and curvature-squared contributions need not have small scalar variations. A two-derivative truncation is not justified on that branch merely because the metric is an Einstein metric.

The following calculation concerns a specified low-energy branch. Assume that a Lorentzian continuation exists, the torsion and other heavy modes have been eliminated consistently, and their effects admit an expansion at a scale $M_{\mathrm{hd}} > 0$. Let all momenta and the scalar mass be small compared with M_{hd}, and let background curvatures be small compared with M_{hd}^2. These conditions are additional to the Euclidean construction. The coefficients in (237) do not by themselves prove this separation.

Choose the scalar vacuum as $\sigma_* = \sigma_0$ for the explicit vacuum-matched branch below, and define

$$\phi = f_\sigma(\sigma - \sigma_0), \qquad c = \frac{\rho}{f_\sigma}, \qquad F(\phi) = \frac{w(\sigma)}{w(\sigma_0)} = e^{-c\phi}. \tag{770}$$

Here ϕ has mass dimension one and c has mass dimension minus one. Absorb the constant $w(\sigma_0)\kappa_a$ into the normalization of each gauge field and its coupling. In these coordinates the Jordan-frame two-derivative action is

$$\begin{aligned} S_J = \int \sqrt{-g_J}\,\mathrm{d}^4x \Big\{ \frac{M_{\mathrm{P}}^2}{2} F(\phi) R_J - \frac{1}{2} g_J^{\mu\nu} \partial_\mu\phi\, \partial_\nu\phi - V_J(\phi) \\ - \frac{F(\phi)}{4} \sum_a \mathcal{F}^{aA}_{\mu\nu} \mathcal{F}^{\mu\nu}_{aA} \Big\} + S_{\mathrm{m}}[g_J, \Psi; \phi]. \end{aligned} \tag{771}$$

The reduced Planck mass satisfies $M_{\mathrm{P}}^{-2} = 8\pi G_*$. To connect this scalar-observable branch to the tensor Newton coefficient used in the Einstein recovery, one must impose the matching condition

$$G_*(\mu_*) = G_{\mathrm{eff}}(\mu_*) \tag{772}$$

on the same renormalized tensor branch and at the same matching scale μ_*, or else include the explicitly computed threshold conversion between them. The equality is therefore a matching condition, not a consequence of the notation M_{P}. The field strengths $\mathcal{F}^a = \mathrm{d}\mathcal{A}^a + g_a \mathcal{A}^a \wedge \mathcal{A}^a$ are canonically normalized at

$\phi = 0$; invariant color contractions are understood. The matter term must be specified separately when material bodies or massive-particle decay channels are considered.

11.11.1. *Vacuum matching and its additional assumptions.* The stabilizing quadratic term alone does not guarantee the flat vacuum used in a scattering calculation. Suppose the Cartan cosmological contribution on this branch is $V_C F(\phi)$, where V_C is a constant energy density. With only $V_C e^{-c\phi} + \frac{1}{2}m_\sigma^2\phi^2$, the value and derivative of the potential at zero are V_C and $-cV_C$. They cannot both be set to zero by choosing $\sigma = \sigma_0$.

One explicit local vacuum-matching prescription adds the constant and linear terms $-V_C + cV_C\phi$. This gives

$$V_J(\phi) = \frac{1}{2}m_\sigma^2\phi^2 + V_C\big(e^{-c\phi} - 1 + c\phi\big). \tag{773}$$

For $V_C \geq 0$, the inequality $e^u \geq 1 + u$ shows that $V_J \geq \frac{1}{2}m_\sigma^2\phi^2$. In particular,

$$V_J(0) = V_J'(0) = 0, \qquad m_J^2 := V_J''(0) = m_\sigma^2 + c^2 V_C > 0. \tag{774}$$

Consequently Minkowski space with vanishing gauge fields and $\phi = 0$ solves this effective vacuum system. Curvature-squared terms have no background tadpole at a flat metric, although they do affect propagators and interactions beyond the low-energy order retained here.

The two matching terms are additional model data. Their values have been fixed by the stated zero-vacuum-energy and zero-tadpole conditions. Those conditions are not consequences of the original positive Euclidean norm, and the modified action does not automatically inherit its positivity or equilibrium-measure construction. Formula (773) supplies a concrete conditional branch for observable calculations; it is not a derivation of the cosmological constant from the unstated continuum completion. More generally, the results below use only a correctly matched local potential with $V_J(0) = V_J'(0) = 0$ and $V_J''(0) = m_J^2 > 0$.

11.11.2. *Diagonalization of scalar–metric mixing.* Set $g^E_{\mu\nu} = F(\phi)g^J_{\mu\nu}$. Since $F > 0$, this change is locally invertible. In four dimensions,

$$\begin{aligned} \sqrt{-g_J} &= F^{-2}\sqrt{-g_E}, & g_J^{\mu\nu} &= F g_E^{\mu\nu}, \\ R_J &= F\left\{R_E + 3\Box_E \log F - \frac{3}{2}(\partial \log F)^2_E\right\}. \end{aligned} \tag{775}$$

After discarding the total divergence with compatible boundary conditions, the Einstein-frame action has the scalar part

$$\int \sqrt{-g_E}\,\mathrm{d}^4x\,\left\{\frac{M_{\mathrm{P}}^2}{2}R_E - \frac{1}{2}K(\phi)(\partial\phi)^2_E - U(\phi)\right\}, \tag{776}$$

where

$$K(\phi) = F^{-1} + \frac{3M_{\rm P}^2}{2}\left(\frac{F'}{F}\right)^2 = e^{c\phi} + \frac{3}{2}c^2M_{\rm P}^2, \qquad U(\phi) = \frac{V_J(\phi)}{F(\phi)^2}. \tag{777}$$

The first contribution to K comes from the Jordan scalar kinetic term. The second comes from the curvature transformation, so it cannot be omitted when the metric is dynamical. Define the local canonical field by

$$\varphi(\phi) = \int_0^\phi \sqrt{K(s)}\,\mathrm{d}s, \qquad Z_* := K(0) = 1 + \frac{3}{2}c^2M_{\rm P}^2. \tag{778}$$

It follows that $\varphi = \sqrt{Z_*}\phi + O(\phi^2)$. Applying the chain rule twice to U, and using $U'(0) = 0$, gives

$$m_\varphi^2 = \left.\frac{\mathrm{d}^2U}{\mathrm{d}\varphi^2}\right|_0 = \frac{U''(0)}{Z_*} = \frac{m_J^2}{Z_*}. \tag{779}$$

The last equality uses both vacuum conditions in (774). For the explicit matched potential, $m_J^2 = m_\sigma^2 + c^2V_C$, not merely m_σ^2. For the displayed potential, $\phi = 0$ is the unique minimum among finite field values, but its large-field behavior in the Einstein frame requires a separate check. For $c \neq 0$, put $t = c\phi$. Equations (773) and (777) give

$$\begin{gathered} U(t/c) = \frac{m_\sigma^2}{2c^2}t^2e^{2t} + V_C\big(e^t - e^{2t} + te^{2t}\big), \\ \lim_{t\to-\infty} U(t/c) = 0, \qquad \lim_{t\to-\infty} K(t/c) = \frac{3}{2}c^2M_{\rm P}^2 > 0. \end{gathered} \tag{780}$$

In particular, the canonical-field distance along this direction is infinite: $\sqrt{K(\phi)} \geq \sqrt{3/2}\,|c|M_{\rm P}$, so the integral of $\sqrt{K}\,|\mathrm{d}\phi|$ diverges as $|\phi| \to \infty$. The inequality $V_J(\phi) \geq m_\sigma^2\phi^2/2$ still implies $U(\phi) > 0$ for every finite $\phi \neq 0$; thus this limit does not by itself show a lower-energy vacuum or a dynamical instability. It does show that the two-derivative Einstein-frame potential is not globally coercive. Neither a full field-theoretic equilibrium measure nor control of the large-field dynamics follows from the Jordan-frame bound. Those questions also depend on the omitted operators and on the range of validity of the low-energy expansion. When $c = 0$, the exponential coupling is absent and this asymptotic direction does not occur.

The local mass relation above uses a metric scalar–tensor reduction. An independent Palatini connection, unsuppressed curvature-squared poles, or additional scalar mixing changes the kinetic diagonalization and must be treated before using Z_*.

The four-dimensional gauge kinetic density is conformally invariant: the factor F^{-2} from the measure cancels the two factors F from inverse metrics. Therefore its Einstein-frame coefficient is still $F(\phi)$. At linear order in the

canonical scalar,

$$-\frac{1}{4}F(\phi)\sum_a \mathcal{F}_a^2 = -\frac{1}{4}\sum_a \mathcal{F}_a^2 + \gamma\varphi\sum_a \mathcal{O}_a + O(\varphi^2),$$
$$\mathcal{O}_a := \frac{1}{4}\mathcal{F}_a^2, \qquad \gamma := \frac{c}{\sqrt{Z_*}}. \tag{781}$$

The common coefficient γ, rather than independently assigned heavy-scalar couplings, follows from the same weight that multiplies the Cartan and internal blocks. No equality of the gauge couplings g_a is implied.

THEOREM 42 (Tree-level relations on the matched scalar branch). *Under the low-energy, vacuum, and normalization assumptions above, retain one isolated scalar mass eigenstate φ. Its exchange between the normalized gauge operators has residue matrix*

$$\mathcal{R}_{ab} = \gamma^2, \qquad \Delta C_{ab} = \frac{\gamma^2}{m_\varphi^2} = \frac{c^2}{m_J^2}. \tag{782}$$

The residue formula uses the scalar propagator normalized to unit residue; external polarization and momentum tensors are factored out. For a massless gauge factor of dimension d_a, its leading two-gauge-boson partial width is

$$\Gamma(\varphi \longrightarrow aa) = \frac{d_a\gamma^2 m_\varphi^3}{64\pi}. \tag{783}$$

For elementary nonrelativistic bodies whose Jordan-frame masses are independent of ϕ, unscreened scalar exchange gives

$$V_{12}(r) = -\frac{G_* m_1 m_2}{r}\left(1 + \alpha_\varphi e^{-m_\varphi r}\right), \qquad \alpha_\varphi = \frac{\gamma^2 M_{\rm P}^2}{2}. \tag{784}$$

Consequently,

$$\alpha_\varphi = 32\pi M_{\rm P}^2\frac{\Gamma(\varphi\to\gamma\gamma)}{m_\varphi^3}, \qquad 0 \le \alpha_\varphi < \frac{1}{3}. \tag{785}$$

The upper limit is approached as $|c|M_{\rm P}\to\infty$. The relation concerns the direct tree-level photon amplitude and the stated elementary-body charges, rather than an inclusive width with arbitrary loop contributions or a generic composite-material force.

Proof. The linear source in the scalar equation is $J = \gamma\sum_a \mathcal{O}_a$. Eliminating the scalar at tree level gives $\frac{1}{2}\langle J, (m_\varphi^2 - \Box)^{-1}J\rangle_L$. The coefficient of its isolated pole is γ^2 for every ordered operator pair. Expanding at momenta below m_φ gives $\Delta C_{ab} = \gamma^2/m_\varphi^2$. Substituting $\gamma^2 = c^2/Z_*$ and $m_\varphi^2 = m_J^2/Z_*$ proves the last equality in (782). Thus the wave-function factor cancels from this leading local coefficient; it does not cancel from the separate mass or on-shell width.

The vertex from $\gamma\varphi\mathcal{F}_a^2/4$, up to an overall phase, is

$$\mathcal{M}_{\mu\nu}^{AB} = \gamma\delta^{AB}\left[(k_1\cdot k_2)g_{\mu\nu} - k_{1\nu}k_{2\mu}\right]. \tag{786}$$

It is transverse in both external momenta. In the scalar rest frame, two transverse parallel polarization pairs have squared amplitude $\gamma^2 m_\varphi^4/4$ each; orthogonal pairs give zero. The color sum gives $\delta^{AB}\delta^{AB} = d_a$. Therefore

$$\sum_{\mathrm{pol},A,B} |\mathcal{M}|^2 = \frac{1}{2} d_a \gamma^2 m_\varphi^4. \tag{787}$$

The integrated massless two-body phase space is $1/(8\pi)$. Multiplying by the initial normalization $1/(2m_\varphi)$ and the identical-boson factor $1/2!$ yields (783).

For a point particle of Jordan mass m_i, the conformal transformation of its line element gives

$$-m_i\int \mathrm{d}s_J = -m_i\int A(\varphi)\,\mathrm{d}s_E, \qquad A = F^{-1/2}, \qquad \left.\frac{\mathrm{d}\log A}{\mathrm{d}\varphi}\right|_0 = \frac{\gamma}{2}. \tag{788}$$

Thus its linear scalar charge is $q_i = \gamma m_i/2$. Exchange of a canonical scalar between two such sources produces $-q_1q_2e^{-m_\varphi r}/(4\pi r)$, because the three-dimensional Fourier transform of $(|\mathbf{k}|^2 + m_\varphi^2)^{-1}$ is $e^{-m_\varphi r}/(4\pi r)$. Dividing by the tensor Newton potential $-m_1m_2/(8\pi M_{\mathrm{P}}^2 r)$ gives $\alpha_\varphi = \gamma^2 M_{\mathrm{P}}^2/2$. For the photon $d_a = 1$; eliminating γ^2 proves (785). Finally, writing $q = |c|M_{\mathrm{P}}$ gives $\alpha_\varphi = q^2/(2+3q^2)$, which lies in the stated range. □

11.11.3. *The hierarchy constraint for the tree-level Cartan coefficients.* There is a further restriction when the vacuum-matched illustration retains the magnitudes of the displayed Cartan coefficients. They give

$$V_C = \frac{3M_{\mathrm{P}}^2}{\ell^2}, \qquad \frac{|\bar\alpha_3|}{M_{\mathrm{P}}^2} = \frac{\ell^2}{8}. \tag{789}$$

Here $\bar\alpha_3$ is the Lorentzian coefficient of the Riemann-squared term; its sign must be fixed by the continuation. The relation for V_C specifies the positive cosmological-energy branch used in (773). To identify a scale rather than merely a dimensional estimate, freeze the scalar at the flat background and use the four-dimensional identity $R^2_{\mu\nu\rho\sigma} = 4R^2_{\mu\nu} - R^2 + \mathcal{G}$. The constant-coefficient Gauss–Bonnet integral does not affect the local quadratic metric equation. For a transverse, traceless perturbation h, $R^{(1)}_{\mu\nu} = -\Box h_{\mu\nu}/2$ and $R^{(1)} = 0$. Its quadratic Lagrangian, after integration by parts, is therefore

$$\mathcal{L}^{(2)}_{\mathrm{TT}} = \frac{M_{\mathrm{P}}^2}{8} h^{\mu\nu}\Box h_{\mu\nu} + \bar\alpha_3(\Box h_{\mu\nu})^2. \tag{790}$$

Variation gives $\Box[1 + (8\bar\alpha_3/M_{\mathrm{P}}^2)\Box]h_{\mu\nu} = 0$. The magnitude of the higher-derivative expansion parameter is consequently $p^2\ell^2$. The formal extra root

has magnitude $|m_2^2| = \ell^{-2}$; its residue and stability are not those of an automatically acceptable new particle. Here the higher-derivative term is used only perturbatively at $p^2\ell^2 \ll 1$, and no ultraviolet completion is inferred by extrapolating the truncated propagator. Proposition 160 computes the corresponding Euclidean source-response error and exhibits a strictly negative reflection form for the positive four-derivative quadratic kernel.

The same coefficients tie the scalar mass to its force strength:

$$\begin{gathered} m_\varphi^2\ell^2 = \frac{m_\sigma^2\ell^2 + 3q^2}{1 + \frac{3}{2}q^2} \geq 6\alpha_\varphi, m_\varphi\ell \leq \varepsilon \quad \Longrightarrow \quad \alpha_\varphi \leq \frac{\varepsilon^2}{6}, \\ \frac{\Gamma_{\gamma\gamma}M_{\mathrm{P}}^2}{m_\varphi^3} = \frac{\alpha_\varphi}{32\pi} \leq \frac{\varepsilon^2}{192\pi}. \end{gathered} \tag{791}$$

Thus a parametrically light scalar in this minimally vacuum-matched branch also has a parametrically small elementary fifth-force strength. The formal large-q limit of the two-derivative formulas is not simultaneously a controlled on-shell limit with these unaltered Cartan coefficients. Changing this conclusion requires additional matching that changes the potential's quadratic term or the higher-curvature coefficients.

11.11.4. *Observable channels and limitations of the relations.* The common coefficient fixes the direct tree-level ratio

$$\frac{\Gamma(\varphi \to gg)}{\Gamma(\varphi \to \gamma\gamma)} = 8 \tag{792}$$

when $c \neq 0$ and m_φ is sufficiently above the confinement scale for the gluon partial width to be interpreted perturbatively. At $c = 0$, both direct widths vanish and their ratio is undefined. This is a ratio of partial widths, not a branching-fraction prediction: Higgs, fermion, massive-vector, or other channels may also contribute to the total width. Non-Abelian gauge bosons in an unbroken perturbative description give the multiplicity ratios $8 : 3 : 1$ for $SU(3), SU(2), U(1)$. Physical electroweak final states require symmetry breaking and thresholds.

At quadratic order in the neutral electroweak gauge fields, write $B_{\mu\nu} = c_W F^\gamma_{\mu\nu} - s_W F^Z_{\mu\nu}$ and $W^3_{\mu\nu} = s_W F^\gamma_{\mu\nu} + c_W F^Z_{\mu\nu}$. Then

$$B_{\mu\nu}B^{\mu\nu} + W^3_{\mu\nu}W^{3\mu\nu} = F^\gamma_{\mu\nu}F_\gamma^{\mu\nu} + F^Z_{\mu\nu}F_Z^{\mu\nu}. \tag{793}$$

The cross coefficient cancels since $-2c_W s_W + 2s_W c_W = 0$. Hence there is no direct tree-level $\varphi Z\gamma$ kinetic vertex on this common-weight branch. Unequal running coefficients, threshold corrections, and loop amplitudes can generate that channel. For massive vector bosons the matter-sector conformal coupling also contributes to the amplitude, so a field-strength phase-space factor alone would not give the complete WW or ZZ width.

Ordinary laboratory bodies are composite and do not generally satisfy the scalar-independent Jordan-mass assumption. Their measured force depends on their scalar charges

$$\beta_i = M_{\rm P}\left[\frac{\gamma}{2} + \left.\frac{\partial \log m_{i,J}}{\partial\varphi}\right|_0\right], \qquad \alpha_{12} = 2\beta_1\beta_2. \tag{794}$$

For example, keeping a fixed Jordan renormalization scale μ and fixed thresholds in one-loop asymptotically free gauge theory,

$$\begin{gathered}\Lambda_{\rm QCD}(\varphi) = \mu\exp\!\left[-\frac{8\pi^2}{b_0 g_s^2(\varphi)}\right], \quad g_s^{-2}(\varphi) = g_s^{-2}(0)\big[1-\gamma\varphi+O(\varphi^2)\big], \\ \partial_\varphi \log\Lambda_{\rm QCD}\big|_0 = \frac{8\pi^2\gamma}{b_0 g_s^2(0)}, \qquad b_0 > 0.\end{gathered} \tag{795}$$

Thus even a Jordan-frame Lagrangian with scalar-independent elementary masses can produce scalar-dependent hadron masses through the gauge coupling. Hadronic matrix elements, quark-mass dependence, thresholds, and binding energies are needed before applying a material-body force bound. The elementary bound $\alpha_\varphi < 1/3$ is not a bound on arbitrary composite α_{12}.

For elementary charges, differentiating (784) gives the attractive force ratio

$$\frac{|F_{12}(r)|}{G_* m_1 m_2/r^2} = 1 + \alpha_\varphi(1+x)e^{-x}, \qquad x = m_\varphi r. \tag{796}$$

The denominator uses the tensor coefficient G_*. A Cavendish determination at distances much smaller than m_φ^{-1} would instead infer $G_*(1+\alpha_\varphi)$ for these charges; normalization to that measured constant changes the plotted ratio accordingly. For the explicit illustration, choose $m_\sigma\ell = 0.01$ and $|q| \le 0.05$. Equation (791) gives $m_\varphi\ell < 0.088$, so the on-shell higher-derivative expansion parameter is below 0.0076. The force curves use $r/\ell \ge 10$, where the spatial derivative parameter is at most 0.01. These small ratios control the displayed tree-level derivative expansion; they do not bound uncomputed loop or matching corrections. They also do not by themselves show that the scalar signal exceeds all omitted contributions. An experimental sensitivity estimate requires bounding those contributions for the actual sources and apparatus. Figure 13 displays the resulting theoretical curves. It contains no fitted observations, experimental confidence regions, or measured residuals. Each force curve is evaluated at 801 values of r/ℓ, and the width curve at 1001 values of q. At $q = 10^{-4}, 0.005, 0.02, 0.05$, the scalar coupling, mass, and photon-width coefficient were recomputed with 80-decimal-digit arithmetic. For the three force-curve values of q, both the potential and force ratios were also recomputed at $r/\ell = 10, 10^{3/2}, 10^2, 10^{5/2}, 10^3$. The largest absolute discrepancy from binary64 is 1.08×10^{-16} for the ratios and 7.24×10^{-18} for the parameter relations. The hierarchy and photon-width identity residuals are at most 2.58×10^{-18} and

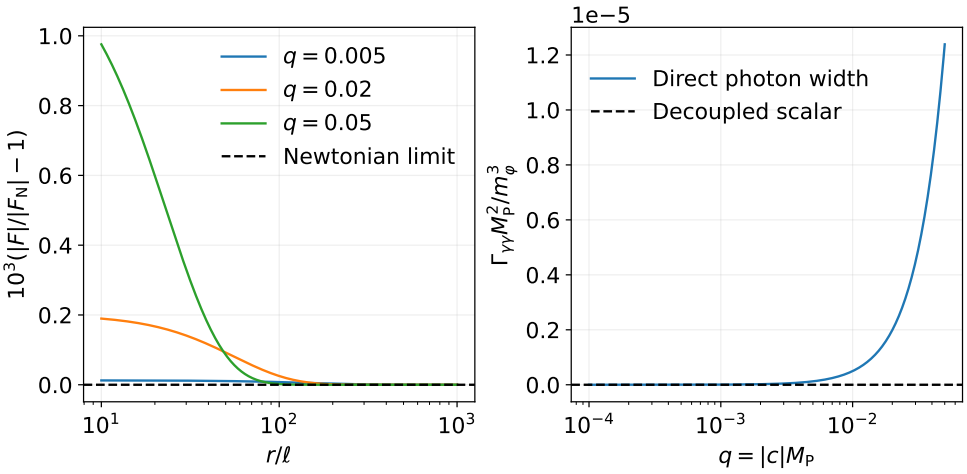


Figure 13. Conditional tree-level scalar relations on the vacuum-matched Cartan branch with $m_\sigma \ell = 0.01$. Left: elementary-body force excess for $q = |c|M_P = 0.005, 0.02, 0.05$ at $r/\ell \geq 10$, compared with the tensor Newtonian limit. Right: the photon partial-width coefficient $\Gamma_{\gamma\gamma} M_P^2/m_\varphi^3$, with the decoupled value indicated, for $q \leq 0.05$. These are analytic parameter illustrations of the specified effective branch, not experimental data.

1.09×10^{-19}, respectively. These residuals quantify numerical evaluation of the analytic formulas, not omitted physical corrections.

The accuracy of these relations is set by several distinct expansions: external momenta and background curvature relative to the scale of omitted operators, loop corrections in the specified renormalization scheme, and possible mixing with other scalar modes. In the local exchange coefficient, the derivative expansion additionally requires $E^2 \ll m_\varphi^2$; the on-shell decay calculation instead requires $m_\varphi^2 \ll M_{\rm hd}^2$ and an isolated narrow pole. Radiative scalar-mass corrections must be included in the matched m_J^2; smallness of that mass is not protected by the displayed quadratic potential alone. Without numerical bounds on these corrections, the formulas do not supply numerical theoretical error bars. They are falsifiable relations for this specified branch once the parameters, observables, and corrections are fixed independently. Other scalar–tensor or dilaton models can share the same relations, so their confirmation alone would not uniquely identify the master construction.

11.11.5. *Tabletop cross-sector prediction program.* The preceding scalar relations need not be tested first through a new high-energy resonance. In the same matched branch, a sufficiently light canonical scalar also changes the

quantities that determine clock and optical-cavity frequencies and produces a composition-dependent Yukawa correction to gravity. These are laboratory precision observables. Existing tests of short-range forces, equivalence-principle violation, time variation of constants, and clock-based searches for ultralight scalar backgrounds provide the relevant experimental language [2], [50], [57], [142], and [153]. The point made here is narrower than a complete data analysis: if the scalar in Section 11.11 is the common equilibrium mode, then the clock/cavity and fifth-force signals are not independent anomalies. They must be fitted by the same scalar-charge vector.

Let X_A denote dimensionless low-energy quantities controlling a set of precision frequencies, for instance ratios built from α, mass ratios, and hadronic scales. Define the linear scalar sensitivities

$$d_A := M_{\rm P}\,\frac{\partial \log X_A}{\partial \varphi}\bigg|_{\varphi=0}. \tag{797}$$

For a clock transition, resonator, or interferometric frequency standard i, let

$$K_i^A := \frac{\partial \log \nu_i}{\partial \log X_A}\bigg|_0, \qquad D_i := \sum_A K_i^A d_A. \tag{798}$$

The coefficients K_i^A are properties of the chosen atomic, molecular, or optical system. They are not fitted by the master action. To first order, the fractional frequency residual is therefore

$$y_i(t) := \delta \log \nu_i(t) = D_i \frac{\varphi(t)}{M_{\rm P}} + n_i(t) + O(\varphi^2), \tag{799}$$

where n_i denotes instrumental, environmental, and readout noise after ordinary deterministic corrections. The same scalar charge vector also determines the mass response of a material body A:

$$\beta_A := M_{\rm P}\,\frac{\partial \log m_A(\varphi)}{\partial \varphi}\bigg|_0. \tag{800}$$

Equation (794) is a special case of (800); hadronic matrix elements, binding energies, and thresholds decide how the fundamental d_A's enter β_A.

THEOREM 43 (Single-scalar tabletop signatures). *Assume that one light scalar φ is the only unresolved common mode in the frequency and force channels, that the linear approximations* (799) *and* (800) *are valid, and that the instruments sample the same scalar time series after synchronization and response calibration. This last assumption requires spatial coherence or a specified common-mode reduction; one scalar field species alone does not imply it at separated sites. Assume the local noises are mutually uncorrelated and uncorrelated with the scalar. Define the signal spectrum by subtracting their auto-spectra:*

$$S_{ij}^{\rm res}(f) := S_{ij}^{\rm obs}(f) - \delta_{ij} S_{n_i}(f). \tag{801}$$

Then this signal matrix has rank at most one:

$$S_{ij}^{\mathrm{res}}(f) = D_i D_j \frac{S_\varphi(f)}{M_{\mathrm{P}}^2}, \qquad S_{ij}^{\mathrm{res}} S_{k\ell}^{\mathrm{res}} - S_{i\ell}^{\mathrm{res}} S_{kj}^{\mathrm{res}} = 0. \tag{802}$$

Moreover, for two test bodies A, B falling toward a source S, the signed Eotvos ratio in the weak-scalar regime is

$$\begin{aligned} \eta_{AB;S}^{\mathrm{sgn}}(r) &= 2\beta_S(\beta_A - \beta_B)(1 + m_\varphi r)e^{-m_\varphi r} + O(\beta^4), \\ \beta &:= \max\{|\beta_A|, |\beta_B|, |\beta_S|\}. \end{aligned} \tag{803}$$

Consequently, changing the material pair must change the sign and relative size of the signal according to

$$\operatorname{sgn} \eta_{AB;S}^{\mathrm{sgn}} = \operatorname{sgn}\{\beta_S(\beta_A - \beta_B)\}, \tag{804}$$

at the displayed leading order. For the exact observable, the sign follows only when the absolute total remainder is smaller than the magnitude of that leading term. A nonzero but nearly cancelling charge difference does not by itself ensure this inequality. The same vector of scalar sensitivities must fit D_i in clocks or cavities and β_A in force experiments.

Proof. Equation (799) is a linear observation equation with a single common stochastic or coherent scalar component. If the residual local noise auto-spectra have been removed as specified, then

$$S_{ij}^{\mathrm{res}}(f) = \frac{D_i D_j}{M_{\mathrm{P}}^2} S_\varphi(f). \tag{805}$$

This matrix is the scalar number $S_\varphi(f)/M_{\mathrm{P}}^2$ multiplied by the outer product $DD^\top$. Every 2×2 minor therefore vanishes, which proves (802). The statement also shows how the prediction can fail: two independent light modes, an unmodelled environmental common mode, or nonlinear response generally raises the rank.

Uncorrelated instrumental noises do not make the full observed matrix rank one: they add a generally nonzero diagonal matrix. If their auto-spectra are not known, the displayed tetrad can instead be tested with four distinct channels, so that all four entries are off diagonal. Finite-sample uncertainty and correlations introduced by a shared frequency reference must be retained. Frequency-dependent complex transfer functions replace $D_i D_j$ by $h_i(f)h_j(f)^*$ before deconvolution. The corresponding common-signal matrix still has rank at most one, but the real-coefficient formula requires the response convention stated above.

For the force channel, the linearized coupling of φ to body A is $\beta_A m_A \varphi / M_{\mathrm{P}}$. Canonical scalar exchange between A and S gives

$$V_{AS}(r) = -\frac{G_* m_A m_S}{r}\left[1 + 2\beta_A \beta_S e^{-m_\varphi r}\right], \tag{806}$$

where $G_* = (8\pi M_{\mathrm{P}}^2)^{-1}$ is the tensor Newton coefficient. Differentiating in r gives

$$a_A(r) = \frac{G_* m_S}{r^2}\left[1 + 2\beta_A\beta_S(1 + m_\varphi r)e^{-m_\varphi r}\right] + O(\beta^4). \tag{807}$$

The signed Eotvos ratio is $\eta^{\mathrm{sgn}}_{AB;S} = 2(a_A - a_B)/(a_A + a_B)$. Substituting (807) gives, for the displayed tree potential with $Y = (1 + m_\varphi r)e^{-m_\varphi r}$,

$$\eta^{\mathrm{tree}}_{AB;S} = \frac{2\beta_S(\beta_A - \beta_B)Y}{1 + \beta_S(\beta_A + \beta_B)Y}.$$

The denominator is positive for sufficiently small β. Its expansion introduces an error of order β^4, proving the stated leading formula with fixed charge ratios. The same order is retained for the acceleration remainders displayed above, provided they are uniform in this limit. Unincluded screening, nonlinear matching, post-Newtonian and instrumental corrections need their own bounds. For the total remainder R_η, the sufficient sign condition is $|R_\eta| < |2\beta_S(\beta_A - \beta_B)Y|$. Since both (798) and (800) are derivatives with respect to the same canonical scalar, clock/cavity data and material-force data must be compatible with one common set of fundamental d_A's after the ordinary atomic, nuclear, and materials matching calculations have been supplied. □

The theorem gives a practical falsification route. A single unmodelled disturbance can mimic one anomalous clock pair or one force curve, but it is harder to mimic the simultaneous conditions

$$\operatorname{rank} S^{\mathrm{res}}(f) \le 1, \qquad \eta^{\mathrm{sgn}}_{AB;S}(r) \propto \beta_S(\beta_A - \beta_B)(1 + m_\varphi r)e^{-m_\varphi r}, \tag{808}$$

with the same d_A's across dissimilar clock species, resonator materials, source masses, and test bodies. Conversely, a signal that is scalar-like in a clock channel but requires incompatible material charges in a torsion-balance, atom-interferometric, microcantilever, or optomechanical force channel would rule out this one-scalar matched branch even if each experiment separately could be fitted by a generic scalar model.

This prediction program is conditional and deliberately low energy. It does not assert a new numerical value for m_φ, ℓ_φ, or the fundamental charges before the vacuum selection and matching problem has fixed them. It also does not claim that scalar-tensor or dilaton phenomenology is unique to the present master action. The distinctive requirement is the cross-sector lock: the same equilibrium mode that perturbs curvature and gauge weights must control, after materials matching, both the rank-one metrological correlation and the signed composition dependence of a Yukawa force. This makes the branch experimentally vulnerable with existing or near-tabletop precision platforms rather than only with large accelerators.

12. Quantum completion, mass-gap boundary, entanglement, and Bell correlations

12.1. *Quantum completion, entanglement, and Bell correlations.* The Gibbs measures, Ornstein–Uhlenbeck processes, controlled diffusions, filtrations, and response covariances constructed above all belong to ordinary Kolmogorov probability theory. Their joint laws may be nonfactorizing and their correlations may be strong, but those facts alone do not define a noncommutative observable algebra or a quantum state. The distinction is essential: a classical common cause can correlate two sectors, whereas quantum entanglement is nonseparability of a state relative to specified commuting observable algebras. We first prove the Bell-local obstruction for every classical realization of the present stochastic framework.

12.2. *The classical boundary of the stochastic equilibrium.* Let Alice choose a setting $x \in \{0,1\}$, let Bob choose $y \in \{0,1\}$, and let their respective outcomes lie in $[-1,1]$. The hidden variable λ may contain the complete master-field path, the common initial condition, all shared classical noise, all local random seeds, and any memory used by a feedback controller. Measurement independence means that the sampling law of this complete variable is not changed by the later setting choices:

$$\rho(\mathrm{d}\lambda \mid x, y) = \rho(\mathrm{d}\lambda). \tag{809}$$

Bell locality means that, conditional on the complete classical state, the two response kernels factorize:

$$P(\mathrm{d}a, \mathrm{d}b \mid x, y, \lambda) \qquad = P_A(\mathrm{d}a \mid x, \lambda) P_B(\mathrm{d}b \mid y, \lambda). \tag{810}$$

At fixed λ, this condition is the conjunction of parameter independence and outcome independence. Together with measurement independence and the law of total probability it implies operational no-signalling; without measurement independence, factorization alone need not do so.

Theorem 44 (Classical CHSH bound for the master equilibrium). *Assume* (809) *and* (810). *Define*

$$E_{xy} := \int_{[-1,1]^2} ab\, P(\mathrm{d}a, \mathrm{d}b \mid x, y), \qquad x, y \in \{0,1\}. \tag{811}$$

Then the CHSH combination satisfies

$$|E_{00} + E_{01} + E_{10} - E_{11}| \le 2. \tag{812}$$

Proof. For each setting and each hidden state, introduce the conditional response means

$$\alpha_x(\lambda) := \int_{[-1,1]} a\, P_A(\mathrm{d}a \mid x, \lambda), \qquad \beta_y(\lambda) := \int_{[-1,1]} b\, P_B(\mathrm{d}b \mid y, \lambda). \tag{813}$$

Because both outcome spaces are contained in $[-1,1]$,

$$|\alpha_x(\lambda)| \le 1, \qquad |\beta_y(\lambda)| \le 1. \tag{814}$$

Equations (809) and (810) first give the observed hidden-state marginal

$$P(\mathrm{d}a, \mathrm{d}b \mid x, y) = \int P_A(\mathrm{d}a \mid x, \lambda) P_B(\mathrm{d}b \mid y, \lambda)\, \rho(\mathrm{d}\lambda). \tag{815}$$

Fubini's theorem then gives

$$E_{xy} = \int \alpha_x(\lambda)\beta_y(\lambda)\, \rho(\mathrm{d}\lambda). \tag{816}$$

For a fixed λ, abbreviate $\alpha_x = \alpha_x(\lambda)$ and $\beta_y = \beta_y(\lambda)$. The pointwise CHSH integrand obeys

$$\begin{aligned} &|\alpha_0\beta_0 + \alpha_0\beta_1 + \alpha_1\beta_0 - \alpha_1\beta_1| \\ &\quad = |\alpha_0(\beta_0 + \beta_1) + \alpha_1(\beta_0 - \beta_1)| \\ &\quad \le |\beta_0 + \beta_1| + |\beta_0 - \beta_1| \\ &\quad = 2\max\{|\beta_0|, |\beta_1|\} \le 2. \end{aligned} \tag{817}$$

The equality in the penultimate line follows by considering whether $\beta_0\beta_1$ is nonnegative or nonpositive. Integrating (817) against the probability measure ρ and using (816) proves (812). □

Theorem 44 allows arbitrary nonlinear Gibbs interactions, arbitrary memory, an arbitrarily high-dimensional hidden state, correlated classical noise, and arbitrary local HJB feedback. Therefore the nonzero cross covariance in Section 11.7 is a classical nonfactorization result; it cannot by itself violate (812). Allowing ρ to depend on (x, y), or allowing Alice's response kernel to depend on y or Bob's to depend on x, abandons a hypothesis of the theorem rather than deriving a quantum violation from the classical equilibrium. For four $\{+1, -1\}$-valued observables in the consistently connected $2 \times 2 \times 2$ marginal scenario, where one-party marginals do not depend on the remote setting, Fine's theorem equates a joint law for A_0, A_1, B_0, B_1 with satisfaction of all eight sign variants of the CHSH inequalities, equivalently the corresponding CH inequalities [13], [39], and [66]. The bounded-outcome estimate in Theorem 44 is more general, but Fine's equivalence is not being asserted outside its dichotomic marginal setting.

The logical distinctions used below can be summarized as

$$\begin{aligned} \text{classical nonfactorization} &\neq \text{quantum entanglement}, \\ \text{quantum entanglement} &\neq \text{superluminal signalling}. \end{aligned} \tag{818}$$

12.3. *Local observable algebras and the definition of entanglement.* A quantum completion must replace the commutative algebra of classical random variables by a unital C^*-algebra $\mathfrak{A}_{\mathrm{M}}$ of master observables. A quantum state is a linear functional

$$\omega : \mathfrak{A}_{\mathrm{M}} \longrightarrow \mathbb{C}, \qquad \omega(C^*C) \geq 0, \qquad \omega(\mathbf{1}) = 1. \tag{819}$$

Let $\mathcal{O}_A$ and $\mathcal{O}_B$ be spacelike separated regions and let

$$\mathfrak{A}_A := \mathfrak{A}(\mathcal{O}_A), \qquad \mathfrak{A}_B := \mathfrak{A}(\mathcal{O}_B) \subset \mathfrak{A}_{\mathrm{M}}. \tag{820}$$

Microcausality requires

$$[A, B] = 0 \quad \text{for every } A \in \mathfrak{A}_A,\ B \in \mathfrak{A}_B. \tag{821}$$

This commutativity across spacelike regions does not require either local algebra to be commutative internally.

Equation (821) concerns the physical observable net, whose elements are even. A larger charged or fermionic field net may instead obey graded locality: for homogeneous fields of parities $|F_A|, |F_B| \in \{0, 1\}$,

$$F_A F_B = (-1)^{|F_A||F_B|} F_B F_A \quad \text{at spacelike separation.} \tag{822}$$

A complete reconstruction must connect the field and observable nets and establish the spin–statistics and CPT properties under their stated hypotheses; bosonic commutativity alone does not construct the chiral fermion sector [87].

A product state on the algebra generated by $\mathfrak{A}_A \cup \mathfrak{A}_B$ is a state satisfying

$$\omega_{\mathrm{prod}}(AB) = \omega_A(A)\omega_B(B), \qquad A \in \mathfrak{A}_A, \quad B \in \mathfrak{A}_B. \tag{823}$$

The state ω is *separable* relative to this pair of algebras when its restriction belongs to the weak-* closed convex hull of the product states that exist on the generated algebra. It is *entangled* when it does not. In finite dimensions this reduces to the familiar condition

$$\rho_{AB} = \sum_k p_k \, \rho_k^A \otimes \rho_k^B, \qquad p_k \geq 0, \qquad \sum_k p_k = 1. \tag{824}$$

The algebraic definition is primary in continuum quantum field theory: local von Neumann algebras are generally of type III, and a canonical factorization $\mathcal{H} = \mathcal{H}_A \otimes \mathcal{H}_B$ need not exist [87] and [40]. A tensor-product interpretation for suitably separated regions requires an additional split-property hypothesis, not merely spacelike commutativity [62].

12.4. *The quantum CHSH bound and an explicit recovery test.* Let $A_0, A_1 \in \mathfrak{A}_A$ and $B_0, B_1 \in \mathfrak{A}_B$ be self-adjoint dichotomic observables,

$$A_i^* = A_i, \quad B_j^* = B_j, \quad A_i^2 = B_j^2 = \mathbf{1}. \tag{825}$$

Define the CHSH operator

$$\mathcal{B}_{\mathrm{CHSH}} := A_0(B_0 + B_1) + A_1(B_0 - B_1). \tag{826}$$

THEOREM 45 (Separable and quantum CHSH bounds). *Under* (821) *and* (825)*, the following statements hold.*

(i) Every separable state satisfies

$$|\omega(\mathcal{B}_{\mathrm{CHSH}})| \le 2. \tag{827}$$

(ii) Every quantum state satisfies the Tsirelson bound

$$|\omega(\mathcal{B}_{\mathrm{CHSH}})| \le 2\sqrt{2}. \tag{828}$$

(iii) Consequently, $|\omega(\mathcal{B}_{\mathrm{CHSH}})| > 2$ *certifies entanglement relative to* $(\mathfrak{A}_A, \mathfrak{A}_B)$.

Proof. For a product state, set

$$a_i := \omega_A(A_i), \qquad b_j := \omega_B(B_j). \tag{829}$$

Positivity and normalization imply $|a_i|, |b_j| \le 1$. Product factorization then gives

$$\begin{aligned} |\omega_{\mathrm{prod}}(\mathcal{B}_{\mathrm{CHSH}})| &= |a_0(b_0 + b_1) + a_1(b_0 - b_1)| \\ &\le |b_0 + b_1| + |b_0 - b_1| \\ &\le 2. \end{aligned} \tag{830}$$

Convex combinations preserve this inequality, and weak-* convergence preserves the value of the fixed observable $\mathcal{B}_{\mathrm{CHSH}}$. This proves (827) for every separable state.

For the quantum bound, cross-region commutativity permits Alice and Bob operators to be reordered. Expanding the square and using $A_i^2 = B_j^2 = \mathbf{1}$ yields

$$\mathcal{B}_{\mathrm{CHSH}}^2 = 4\mathbf{1} - [A_0, A_1][B_0, B_1]. \tag{831}$$

For completeness, the two mixed products used in this calculation are

$$(B_0 + B_1)(B_0 - B_1) = -[B_0, B_1], \qquad (B_0 - B_1)(B_0 + B_1) = [B_0, B_1]. \tag{832}$$

Since self-adjoint unitaries have norm one,

$$\|[A_0, A_1]\| \le 2, \qquad \|[B_0, B_1]\| \le 2. \tag{833}$$

It follows from (831) that

$$\|\mathcal{B}_{\mathrm{CHSH}}^2\| \le 4 + 2 \cdot 2 = 8, \qquad \|\mathcal{B}_{\mathrm{CHSH}}\| \le 2\sqrt{2}. \tag{834}$$

Finally, the state Cauchy–Schwarz inequality gives

$$|\omega(\mathcal{B}_{\mathrm{CHSH}})|^2 \le \omega(\mathcal{B}_{\mathrm{CHSH}}^2) \le \|\mathcal{B}_{\mathrm{CHSH}}^2\| \le 8. \tag{835}$$

This proves (828); comparison with (827) proves the final assertion [38]. □

A violation of the separable bound is sufficient but not necessary for entanglement. In particular, neither same-side noncommutativity by itself nor entanglement by itself guarantees that a prescribed quartet of observables violates CHSH; entangled states admitting relevant local hidden-variable models are known [163].

The standard two-qubit singlet supplies a precise recovery target for any proposed quantum completion. Let

$$|\Psi^-\rangle := \frac{|0\rangle \otimes |1\rangle - |1\rangle \otimes |0\rangle}{\sqrt{2}} \tag{836}$$

and choose

$$A_0 = \sigma_z \otimes I, A_1 = \sigma_x \otimes I, \qquad B_0 = I \otimes \frac{\sigma_z + \sigma_x}{\sqrt{2}}, B_1 = I \otimes \frac{\sigma_z - \sigma_x}{\sqrt{2}}. \tag{837}$$

The singlet identity

$$\langle \Psi^-|(\boldsymbol{\sigma} \cdot \mathbf{a}) \otimes (\boldsymbol{\sigma} \cdot \mathbf{b})|\Psi^-\rangle = -\mathbf{a} \cdot \mathbf{b} \tag{838}$$

gives, for the convention in (826),

$$E_{00} = E_{01} = E_{10} = -\frac{1}{\sqrt{2}}, \qquad E_{11} = \frac{1}{\sqrt{2}}. \tag{839}$$

Therefore

$$|E_{00} + E_{01} + E_{10} - E_{11}| = 2\sqrt{2}. \tag{840}$$

Equations (836)–(840) are a standard quantum-mechanical benchmark, not a prediction derived from the present master Gibbs law. Local quantum field theory can contain vacuum states with Bell-nonclassical correlations, but that general result likewise does not establish the required state for this model [149] and [150].

An exact noisy benchmark makes the prediction boundary quantitative. For $0 \le v \le 1$, consider the two-qubit state

$$\rho_v := v|\Psi^-\rangle\langle\Psi^-| + (1 - v)\frac{I_4}{4}. \tag{841}$$

This family also quantifies the gap between entanglement and CHSH detection. Partial transposition on Bob's factor gives

$$\mathrm{Spec}(\rho_v^{T_B}) = \left\{ \frac{1+v}{4}, \frac{1+v}{4}, \frac{1+v}{4}, \frac{1-3v}{4} \right\}. \tag{842}$$

Every separable state's partial transpose is positive, because transposition preserves positivity on each product factor and convex combinations preserve positivity. Thus $v > 1/3$ implies entanglement. Conversely, the boundary state has the explicit separable representation

$$\rho_{1/3} = \int_{S^2} \frac{I + \mathbf{n} \cdot \boldsymbol{\sigma}}{2} \otimes \frac{I - \mathbf{n} \cdot \boldsymbol{\sigma}}{2} \frac{\mathrm{d}\Omega(\mathbf{n})}{4\pi}. \tag{843}$$

Indeed, $\int_{S^2} n_i n_j \, \mathrm{d}\Omega/(4\pi) = \delta_{ij}/3$, so the right-hand side equals $\frac{1}{4}[I_4 - \frac{1}{3}\sum_i \sigma_i \otimes \sigma_i] = \rho_{1/3}$. For $0 \le v \le 1/3$,

$$\rho_v = 3v\,\rho_{1/3} + (1-3v)\frac{I_4}{4}, \tag{844}$$

and both terms are separable. Hence ρ_v is entangled exactly when $v > 1/3$. Because every Pauli matrix is traceless, the maximally mixed term contributes zero to each product correlation. Hence

$$\mathrm{Tr}[\rho_v(\boldsymbol{\sigma}\cdot\mathbf{a}) \otimes (\boldsymbol{\sigma}\cdot\mathbf{b})] = -v\,\mathbf{a}\cdot\mathbf{b}. \tag{845}$$

For the settings in (837),

$$|S(v)| = 2\sqrt{2}\,v, \qquad |S(v)| > 2 \quad\Longleftrightarrow\quad v > \frac{1}{\sqrt{2}}. \tag{846}$$

These settings maximize the absolute CHSH value among nondegenerate local projective spin observables $A_i = \mathbf{a}_i \cdot \boldsymbol{\sigma}$ and $B_j = \mathbf{b}_j \cdot \boldsymbol{\sigma}$. Indeed, for arbitrary unit vectors the absolute CHSH expression is at most

$$v\big(|\mathbf{b}_0 + \mathbf{b}_1| + |\mathbf{b}_0 - \mathbf{b}_1|\big) \le 2\sqrt{2}\,v, \tag{847}$$

where the last inequality follows by writing $|\mathbf{b}_0+\mathbf{b}_1| = 2\cos(\vartheta/2)$ and $|\mathbf{b}_0-\mathbf{b}_1| = 2\sin(\vartheta/2)$, followed by $\sin u + \cos u \le \sqrt{2}$. Equality occurs for orthogonal Bob settings and the corresponding bisecting Alice settings. If degenerate dichotomic observables $\pm I$ are also admitted, the unrestricted two-qubit maximum is $\max\{2, 2\sqrt{2}\,v\}$. Such degenerate choices do not create a Bell violation, so the threshold in (846) is unchanged.

Combining (842) with (846) gives the nonempty interval

$$\frac{1}{3} < v \le \frac{1}{\sqrt{2}}, \tag{848}$$

in which the state is entangled but no CHSH violation is obtained, even after optimizing its local projective spin settings. This statement concerns CHSH detection for this state family; it is not a claim about every possible Bell scenario or every POVM.

Equation (846) is still not, by itself, a new prediction of the master theory: v was introduced in (841). It becomes a model-specific prediction only if the reconstructed master dynamics independently determines a function $v = v(q_1, \ldots, q_r; L, E)$ from already calibrated microscopic parameters, scale L, and energy E. The resulting absolute CHSH value, threshold crossing, and scale dependence could then be tested without fitting the Bell outcomes. A measured discrepancy outside propagated theoretical and detector uncertainties would falsify that completed branch. This is the same non-circular prediction standard used in Section 7.2.

12.5. *No-signalling and the resolution of the apparent paradox.* Let $\{M_a^x\}_a \subset \mathfrak{A}_A$ and $\{N_b^y\}_b \subset \mathfrak{A}_B$ be local POVMs. Thus their effects are positive and complete:

$$M_a^x \geq 0, \quad N_b^y \geq 0, \quad \sum_a M_a^x = \mathbf{1}, \quad \sum_b N_b^y = \mathbf{1}. \tag{849}$$

Microcausality makes $M_a^x N_b^y$ positive, so the Born probabilities

$$p(a, b \mid x, y) := \omega(M_a^x N_b^y) \tag{850}$$

form a normalized joint distribution.

THEOREM 46 (No-signalling for complete local measurements). *Under* (821) *and* (849)*, Alice's marginal is independent of Bob's setting and Bob's marginal is independent of Alice's setting:*

$$\sum_b p(a, b \mid x, y) = \omega(M_a^x), \qquad \sum_a p(a, b \mid x, y) = \omega(N_b^y). \tag{851}$$

Proof. Linearity of ω and completeness of Bob's POVM give

$$\begin{aligned} \sum_b p(a, b \mid x, y) &= \sum_b \omega(M_a^x N_b^y) \\ &= \omega\left(M_a^x \sum_b N_b^y \right) \\ &= \omega(M_a^x), \end{aligned} \tag{852}$$

which contains no y. Interchanging Alice and Bob gives the second identity in (851). □

A CHSH value above 2 is consequently compatible with operational no-signalling. Bell-local factorization, spacelike commutativity, and no-signalling are three different conditions. Bell's theorem rules out the joint use of measurement independence, Bell-local factorization, and a single classical hidden-variable explanation for the observed violating correlations. It neither removes microcausality nor opens a superluminal communication channel. This identification of the incompatible premises is the precise resolution of the apparent Bell paradox; it is not an elimination of Bell's theorem.

The POVM probabilities in (850) also expose an additional assumption. The classical equilibrium construction does not derive the Born rule, selective state update, or detector dynamics. A full measurement model must supply normalized completely positive local instruments $\{\mathcal{I}_{a|x}\}_a$, whose nonselective sum is trace-preserving in the Schrödinger picture, or the equivalent unital condition in the Heisenberg picture. Normalization alone is insufficient for

locality. If $\mathcal{J}^*_{b|y}$ are Bob's Heisenberg instrument maps, one must also require the nonselective remote operation to leave Alice's algebra unchanged,

$$\mathcal{J}^*_y := \sum_b \mathcal{J}^*_{b|y}, \qquad \mathcal{J}^*_y(A) = A \quad \text{for every } A \in \mathfrak{A}_A, \tag{853}$$

and impose the analogous condition for Alice together with spacelike compatibility of the two instruments. Filtration and classical conditioning cannot substitute for this quantum instrument structure.

12.6. *A conditional Euclidean-to-Lorentzian route.* The master equilibrium could support a quantum interpretation only after a separate reconstruction theorem. Let N denote a regulator. The regulated classical equilibrium has the form

$$\pi_{*,N}(\mathrm{d}\mathbb{X}) = Z_N^{-1} \exp\!\left[-\frac{\mathcal{S}_{\mathrm{M},N}(\mathbb{X})}{\theta}\right] \mu_{0,N}(\mathrm{d}\mathbb{X}). \tag{854}$$

A Euclidean quantum-field measure would instead be represented schematically as

$$\mu_{E,N}(\mathrm{d}\mathbb{X}) = \widetilde{Z}_N^{-1} \exp\!\left[-\frac{S_{E,N}(\mathbb{X})}{\hbar}\right] \nu_N(\mathrm{d}\mathbb{X}). \tag{855}$$

Equations (854) and (855) are literal positive-measure representations only for bosonic physical variables. Chiral fermions and gauge-fixed ghost sectors require graded Schwinger functionals, Berezin integration, and the corresponding graded reflection operation; they are not ordinary positive probability measures. Reflection positivity must ultimately be established on the gauge-invariant physical Schwinger functional rather than inferred from a formal ghost-extended density. Thus setting $\theta = \hbar$ is neither necessary nor sufficient. If $\mu_{0,N} \ll \nu_N$, equality of the two measures up to normalization requires the complete matching relation

$$\frac{S_{E,N}}{\hbar} = \frac{\mathcal{S}_{\mathrm{M},N}}{\theta} - \log\!\left(\frac{\mathrm{d}\mu_{0,N}}{\mathrm{d}\nu_N}\right) + c_N, \tag{856}$$

where c_N is field independent. The reference-measure contribution in (856) cannot be discarded merely because the same formal action appears in both exponents.

For gauge-invariant smeared observables $F_1, \dots, F_n$, one must then prove regulator-independent Schwinger limits

$$S_n(F_1, \dots, F_n) := \lim_{N\to\infty} \int F_1(\mathbb{X}) \cdots F_n(\mathbb{X})\, \mu_{E,N}(\mathrm{d}\mathbb{X}). \tag{857}$$

On a Euclidean background carrying a specified time reflection $\vartheta(\tau, \mathbf{x}) = (-\tau, \mathbf{x})$, let Θ denote the induced antilinear reflection on functionals, including the appropriate tensor and fermionic transformations; for a real scalar, $(\Theta F)(\mathbb{X}) = \overline{F(\vartheta\mathbb{X})}$. The limiting Schwinger functions must satisfy the full Osterwalder–Schrader hypotheses: Euclidean covariance, symmetry or graded symmetry,

regularity, reflection positivity, and the appropriate cluster condition. Reflection positivity requires, for every positive-time cylinder functional F,

$$\int (\Theta F)(\mathbb{X}) F(\mathbb{X})\, \mu_E(\mathrm{d}\mathbb{X}) \geq 0. \tag{858}$$

More generally, applying (858) to $F = \sum_i c_i F_i$ requires the whole reflected Gram matrix to be positive, not only its diagonal entries.

Under the complete Osterwalder–Schrader axioms, quotienting the resulting positive-time pre-Hilbert space by its null space and completing it yields a physical Hilbert space $\mathcal{H}$, a vacuum Ω, a nonnegative Hamiltonian H, and the Euclidean semigroup $e^{-\tau H}$. With the remaining reconstruction hypotheses, analytic continuation produces a Lorentzian Wightman theory and its local observable algebras [124] and [125]. Pointwise positivity of the Gibbs density, boundedness below of a Euclidean action, and finiteness of the partition function do not separately imply (858). For a non-flat selected background or a fluctuating metric, the standard flat-space theorem cannot simply be quoted: a reflection structure and an appropriate covariant reconstruction theorem must first be supplied. A fully diffeomorphism-invariant integral over metrics has no canonical common time reflection, preferred vacuum, or Hamiltonian. It therefore requires a relational or generalized reconstruction, or the direct Lorentzian route in Definition 3. On a generic curved Lorentzian branch there may likewise be no global positive-energy vacuum; the appropriate replacement is a locally covariant state satisfying the Hadamard microlocal spectrum condition, unless a stationary or asymptotically stationary branch supplies the additional spectral structure [158].

The stochastic relaxation parameter used in Sections 3.9 and 4.5 is auxiliary. It cannot be identified with Euclidean coordinate time or physical Lorentzian time without an additional theorem. Moreover, Osterwalder–Schrader reconstruction alone does not prove entanglement. After reconstruction one must still identify two physical local algebras, construct the selected state, and calculate a Bell witness such as (826).

12.7. *Gauge constraints, local subsystems, and dynamical geometry.* A relativistic quantum completion should provide a covariant net $\mathcal{O} \mapsto \mathfrak{A}(\mathcal{O})$ of physical observable algebras. At minimum it must establish isotony, covariance, microcausality, and the time-slice property. Schematically,

$$\mathcal{O}_1 \subset \mathcal{O}_2 \Longrightarrow \mathfrak{A}(\mathcal{O}_1) \subset \mathfrak{A}(\mathcal{O}_2), \qquad \mathcal{O}_1 \perp \mathcal{O}_2 \Longrightarrow [\mathfrak{A}(\mathcal{O}_1), \mathfrak{A}(\mathcal{O}_2)] = 0. \tag{859}$$

Covariance must act consistently on the regions and algebras, and observables in any neighborhood of a Cauchy surface must generate the algebra of its causal development.

Gauge theories add a regional-factorization obstruction. Gauss constraints tie flux through a boundary to enclosed charge, so a physical Hilbert space does not automatically factorize across that boundary. One must specify the gauge-invariant regional algebra, its possible centre and superselection sectors, or a declared edge-mode extension. Entanglement quantities depend on this choice [24]. Gauge-fixed fields and ghost integrals are useful computational devices, but their indefinite or graded state spaces are not by themselves positive physical probability spaces.

A BRST/BV realization must therefore prove, after renormalization, a nilpotent quantum differential and the relevant Slavnov–Taylor identity:

$$s_{\mathrm{ren}}^2 = 0, \qquad \mathcal{S}(\Gamma_{\mathrm{ren}}) = 0, \qquad \mathfrak{A}_{\mathrm{phys}} = H^0(s_{\mathrm{ren}}). \tag{860}$$

In an operator realization the corresponding physical state space must be a positive completion of

$$\mathcal{H}_{\mathrm{phys}} = \ker Q_{\mathrm{BRST}} / \overline{\mathrm{Ran}\, Q_{\mathrm{BRST}}}. \tag{861}$$

Here Q_{BRST} must be a closed operator, or a specified closed extension of a closable operator, on a common invariant dense domain; its nilpotency must give $\overline{\mathrm{Ran}\, Q_{\mathrm{BRST}}} \subset \ker Q_{\mathrm{BRST}}$. The inner product induced on the quotient must then be proved positive and nondegenerate before its completion is a physical Hilbert space. This requires cancellation of perturbative gauge and diffeomorphism anomalies, mixed gauge–gravitational anomalies, global gauge anomalies, and any anomaly of a gauged discrete symmetry. By contrast, a 't Hooft anomaly of a genuine global symmetry need not vanish; it must be matched along the renormalization-group flow and obstructs gauging that symmetry. The proposed residual parity must therefore first be classified as gauged or global. Its discrete gauge anomaly must cancel in the former case, whereas its anomaly matching and protection status must be stated in the latter. The representation traces checked in Sections 6.1 and 6.6 address only part of this problem [12] and [94].

The gravitational sector is still more delicate. On a fully dynamical geometry, a coordinate-local field is generally not a diffeomorphism-invariant observable. Physical observables require relational, asymptotic, or gravitational dressing, and such dressing can obstruct exact compact localization [61]. The full theory must close the Lorentz and diffeomorphism constraint algebra without anomaly and derive and control the commutators of its physical dressed observables; exact spacelike vanishing cannot be assumed when the dressing has nonlocal tails. The ordinary local net in (859) can be used on the selected semiclassical branch only as a controlled approximation until that task is completed.

12.8. *Information filtering is not automatically holography.* The information coordinate and finite-resolution filtration in the classical master process describe which observables are retained under conditioning or coarse graining. This structure is not, by definition, a holographic duality. If Π is a measurable coarse-graining map, the data-processing inequality gives

$$D_{\mathrm{KL}}(\Pi_{\#}P\|\Pi_{\#}Q) \le D_{\mathrm{KL}}(P\|Q). \tag{862}$$

The inequality normally expresses information loss. Calling the image a holographic screen does not produce a boundary theory capable of recovering the discarded bulk observables.

A precise bridge requires recoverability. In the Schrodinger-picture state description, let $\mathcal{E}$ be a completely positive trace-preserving encoding channel from a declared bulk code space to a boundary system. A restriction of observable algebras is instead a Heisenberg-picture unital completely positive map and should not be conflated with this state channel. Holographic reconstruction on that code has the following sufficient operational criterion: there is a recovery channel $\mathcal{R}$ such that

$$(\mathcal{R}\circ\mathcal{E})(\rho) = \rho \qquad \text{for every state } \rho \text{ in the code family.} \tag{863}$$

For a faithful reference state σ, saturation of relative-entropy monotonicity for every state in the code family, together with the support and domain hypotheses of the Petz theorem, is a sufficient algebraic signal of such recoverability,

$$D(\rho\|\sigma) = D(\mathcal{E}(\rho)\|\mathcal{E}(\sigma)), \tag{864}$$

with the corresponding Petz recovery map under its standard domain hypotheses. Equality for one isolated pair (ρ,σ) is insufficient to establish a duality. Approximate reconstruction requires quantitative recovery-error bounds and a declared code algebra (for example, an entanglement-wedge algebra), rather than a change of terminology [129].

Consequently, the present filtration can serve as a candidate coarse-grained input to a holographic construction only after (863), boundary algebra reconstruction, and compatible bulk and boundary dynamics have been proved. No-signalling is a causal property of local instruments; it neither creates this encoding nor causes the Einstein and Yang–Mills equations to emerge from a lossy filter. The distinction is operational: a generic filter satisfies only the inequality (862), whereas a genuine duality must preserve and reconstruct the physical information on its stated code subspace.

12.9. *Completion criteria for a genuinely unified quantum theory.* It is neither necessary nor realistic for one paper to settle every global regularity, constructive-field-theory, and quantum-gravity problem before it can make a substantive unification result. Three levels must instead be kept separate.

Structural unification identifies one action and one dynamical package and proves the relations among its sectors. A *controlled effective recovery* derives the Einstein and Yang–Mills equations in a stated low-energy regime with declared matching and scale-separation hypotheses. *Constructive quantum completeness* asks for a regulator-independent nonperturbative realization of the entire package. Open global existence or regularity questions at the third level do not invalidate theorems at the first two levels, just as an unsolved global regularity problem does not alter the local content of a field equation.

The hypotheses in a controlled recovery theorem and open global regularity problems have different logical roles. A sector or matching hypothesis, such as dominance of a constant-coefficient Palatini block with controlled curvature-square, torsion, mixed, and scalar-gradient remainders, specifies the physical regime in which the theorem applies. It is therefore part of the mathematical domain of the implication, not an unresolved step inside its proof. Global existence and regularity ask whether all relevant initial data generate solutions with prescribed long-time behavior. Neither question has to be solved in every phase before the conditional low-energy equations are valid. Deriving the matched sector uniquely from a particular ultraviolet completion would strengthen universality and predictivity; it is not required for the validity of the recovery theorem. The conditions below define the still stronger claim of a quantum-complete fundamental realization. They are a research program, not prerequisites for the conditional theorems proved in this paper.

Definition 3 (Quantum-complete realization and predictive extension). *A selected master package is called a quantum-complete unified realization when conditions (Q1)–(Q9) below are established from that same package. It is additionally called predictive and empirically discriminating, at its stated accuracy, when (Q10) is also established without using the target data both to choose the package and to test it.*

(Q1) On a selected reflection-equipped Euclidean phase or background, a regulator-independent family of gauge-invariant Schwinger functions as in (857) satisfies all Osterwalder–Schrader axioms. Alternatively, a direct Lorentzian construction provides a positive physical Hilbert space and unitary dynamics, together with the global spectrum condition where it is meaningful or the locally covariant Hadamard microlocal spectrum condition on a generic curved branch.

(Q2) A covariant net of physical observable algebras satisfies isotony, microcausality, clustering, and the time-slice property, with a compatible CAR/graded-local fermionic field net, spin–statistics and CPT properties, and a proved relational or dressed replacement where gravitational constraints forbid strict localization. With massless photons or gravitons, the construction

also specifies infrared-dressed charged states, infraparticle sectors where present, and inclusive infrared-finite observables.

(Q3) A complete quotient or BRST/BV construction identifies the physical observables and positive physical states. All perturbative and global gauge or diffeomorphism anomalies, mixed gauge–gravitational anomalies, and gauged discrete anomalies cancel; anomalies of genuine global symmetries satisfy the required 't Hooft matching. The renormalized Ward or Slavnov–Taylor identities hold.

(Q4) The regulator can be removed with finite renormalized observables and a closed counterterm structure. Predictivity at the fundamental level requires a controlled ultraviolet limit with a finite-dimensional relevant parameter space, or another explicitly justified predictive mechanism. An effective theory must instead state its cutoff and retain every operator needed at the claimed accuracy.

(Q5) The curvature-square sector is either demonstrably perturbative below that cutoff or has a positive spectral realization without physical negative-norm modes. A pole of a truncated higher-derivative propagator may not be declared physical while simultaneously treating the term only as a low-energy expansion.

(Q6) The spacetime dimension and Lorentzian signature, spin or Spin^c structure, global gauge group and quotient, topological bundle sectors, $N_c = 3$, chiral family content, all charges, symmetry-breaking vacuum, fermion masses and mixings, neutrino sector, and the relevant confinement or mass-gap properties are selected or derived rather than reinserted as fitted labels.

(Q7) The same quantum master equations recover the anomaly-free chiral Yang–Mills theory and the semiclassical Einstein equation in controlled limits, with compatible stress-energy Ward identities, a positive graviton sector, causal propagation, and the equivalence-principle limit. They also recover the appropriate low-energy scattering amplitudes or locally covariant precision observables, not only the formal field equations.

(Q8) A stable physical state is selected. Its vacuum or thermal properties, cluster behavior, superselection sectors, and phase structure must be proved; the classical uniqueness results above do not imply uniqueness of this quantum state.

(Q9) Born probabilities and normalized completely positive local instruments are specified or derived, and at least one state-dependent Bell experiment has calculable local observables and no-signalling marginals. The setting generators, spacetime localization, detector response, no-click outcomes, and any event-ready selection rule are included, so fair sampling or postselection is not imposed silently.

(Q10) Renormalization-group evolution, threshold matching, theoretical uncertainties, and detector-level observable maps produce at least one finite, independently calibrated prediction that distinguishes the realization from the Standard Model coupled to general relativity.

Conditions (Q1)–(Q9) concern quantum consistency and internal low-energy recovery; (Q10) adds empirical discriminability. This separation also shows why adding a discussion of entanglement does not by itself complete unification. The conditional Einstein and Yang–Mills equations derived earlier address part of (Q7), the anomaly calculation in the 331 example addresses part of (Q3) and (Q6), and the finite-regulator equilibrium theorem addresses part of the existence problem preceding (Q1). None of these partial results supplies the other conditions automatically.

A phenomenologically comprehensive realization should also state how it treats the cosmological constant and vacuum energy, strong CP, proton stability, neutrino masses, dark matter, the baryon asymmetry, early-universe initial conditions, and black-hole thermodynamics. Not every item is a logical prerequisite for unifying the four interactions, but leaving their status unspecified would leave the physical domain of the proposed theory unclear.

Finally, a model-specific Bell prediction requires a state ω_*, four independently fixed local observables, and the calculation

$$S_{\mathrm{M}} := \omega_*(A_0B_0) + \omega_*(A_0B_1) + \omega_*(A_1B_0) - \omega_*(A_1B_1). \tag{865}$$

The state, settings, detector model, and visibility corrections must be fixed without fitting the Bell-test outcomes. If $|S_{\mathrm{M}}| > 2$, Theorem 44 excludes every measurement-independent Bell-local classical representation of those data, while Theorem 46 establishes no-signalling for the specified commuting complete POVMs. The singlet value in (840) is a recovery test of standard quantum mechanics. A genuinely new prediction would require an independently determined correction, scale dependence, channel relation, or other observable departure supplied by the selected master dynamics. No numerical Bell correction follows from the present classical master law. A future quantum completion would have to derive, without fitting Bell data, either $v(L, E)$ in (841) or a non-Werner correction

$$E_{\mathrm{M}}(\mathbf{a}, \mathbf{b}; L, E) = -\mathbf{a} \cdot \mathbf{b} + \Delta E_{\mathrm{M}}(\mathbf{a}, \mathbf{b}; L, E). \tag{866}$$

It would then have to prove positivity of all outcome probabilities, no-signalling, the quantum CHSH bound, a controlled standard-quantum limit, and the detector response including no-click outcomes. Until such a function is derived from the selected master package, it is a prospective observable, not a prediction.

12.10. *Scope of the conclusions.* The construction yields the following structural consequences under the stated hypotheses.

12.11. *Structural consequences under the stated hypotheses.* Under the stated functional-analytic assumptions, the following are structural:

(1) the definition of one master connection;
(2) the definition of one master curvature;
(3) the definition of one master action;
(4) the definition of one path-deviation cost;
(5) the zero-cost characterization of the deterministic drift;
(6) the Girsanov representation of the same cost as relative entropy when the hypotheses hold;
(7) the free-energy dissipation identity;
(8) the Gibbs characterization of equilibrium in the finite-dimensional or rigorously controlled setting;
(9) the classical CHSH bound in Theorem 44 for every measurement-independent Bell-local use of that equilibrium, irrespective of shared noise, memory, or local feedback;
(10) the macroscopic ODE and stochastic microscopic scaling limits under the corresponding assumptions, with randomness in the former retained when its initial condition is random.

12.12. *Explicit realization results and their domains.* Theorem 9 proves the effective-sector recovery of the Einstein–higher-curvature and Yang–Mills equations on its stated domain; the quantitative ordinary-Einstein remainder is (213). This local variational conclusion is independent of a global classification or regularity theory for all solutions.

The fixed-background variational problem and two stochastic realizations supply unconditional conclusions within their stated data. Theorem 11 treats smooth prescribed geometry and curvature density; it determines the scalar while holding those fields fixed. Theorem 19 treats compact link variables and finitely many confined scalar coordinates. Its proof establishes nonexplosion, normalizability, semigroup invariance, and uniqueness; it does not assume that formal stationarity already implies invariance. Theorem 39 treats a nonlinear continuum scalar with the specified smoothing operator. It proves the limiting dynamics and equilibrium directly, including convergence of the approximations.

These existence results do not imply selection of the microscopic data. Theorem 15 rules out a minimum in the stated unrestricted positive-coupling class, and its examples show that distinct group packages can have identical optimized free energy. Additional candidate-class restrictions must be justified independently if they are to restore selection.

Section 6.6 supplies an additional conditional intermediate-scale realization. Theorem 16 derives three families only in its restricted representation and threshold class. The generalized-color calculation in Section 6.8 shows that

this does not separately select three colors, while Section 6.12 records the independent flavor, scale, global-representation, and matching conditions still required.

Theorem 42 establishes observable relations for the explicitly vacuum-matched Lorentzian effective branch. The relation between the photon partial width and the elementary-body force strength concerns a common canonically normalized scalar. Composite-body charges, running coefficients, other decay channels, and the hierarchy bound in (791) must be included when comparing that relation with measurements.

Section 12.1 supplies two kinds of results with different domains. Theorem 44 is an obstruction theorem for the classical stochastic framework itself. Theorem 45 and Theorem 46 are exact operator-algebraic statements once commuting local quantum algebras, a state, and local measurements are supplied. The manuscript has not yet constructed those quantum data from the master equilibrium. Consequently, the singlet calculation is a recovery benchmark and not a new output of the model.

12.13. *Open conditions for quantum-complete and predictive realization.* The following require additional constructions or verification:

(1) uniqueness of a physically admissible irreducible master algebra;
(2) derivation of $SU(3)_c \times SU(2)_L \times U(1)_Y$ from first principles;
(3) derivation of the complete observed chiral fermion spectrum;
(4) anomaly cancellation for the ultimately selected representation unless explicitly verified;
(5) numerical prediction of the gauge couplings and Newton's constant;
(6) regulator-independent gauge-invariant Schwinger functions satisfying the complete Osterwalder–Schrader axioms, or a direct positive-metric Lorentzian quantization with the spectrum condition;
(7) construction of the physical local or relational observable net, including the treatment of gauge centres, edge modes, and gravitational dressing;
(8) a BRST/BV or equivalent quotient construction with a positive physical Hilbert space and renormalized Ward identities; perturbative and global gauge or diffeomorphism anomalies, mixed gauge–gravitational anomalies, and gauged discrete anomalies must cancel, while exact global-symmetry anomalies must satisfy 't Hooft matching;
(9) a renormalized continuum limit and ultraviolet completion, or an explicit finite effective-field-theory cutoff with controlled higher-curvature poles and a complete operator basis;
(10) selection of a physical quantum state and a Born-rule measurement model with completely positive local instruments;

(11) a model-derived Bell experiment whose state and observables are fixed independently of the measured Bell data, together with calculated no-signalling marginals and uncertainties;
(12) proof that the information field χ is a new fundamental physical degree of freedom;
(13) experimental confirmation of any new cross-sector fluctuation relation;
(14) a global-group-compatible chiral completion of the conditional 331 candidate in Section 6.6;
(15) independent selection of $N_c = 3$, the flavor charges and coefficients, the 331 symmetry-breaking scale, and the complete odd-neutral matching action.

These problems have different logical weights. The conditional and effective theorems of this paper do not require every item to be solved. Meeting Definition 3 is instead required only for the stronger claim of a regulator-independent, nonperturbative, predictive quantum unification. Before that stage, each result should be described at its proved structural or effective level rather than being discounted for unrelated open regularity problems or promoted beyond its matching hypotheses.

12.14. *Comparison with existing unification architectures.* The framework organizes the geometric action, stochastic control problem, equilibrium measure, and matching calculation using one specified set of microscopic data. Each of these ingredients has established precedents. Writing them together does not alone reduce the number of independent couplings or establish a new observable relation. The additional restriction proposed here is selection over equivalence classes of complete data packages. A conventional grand-unified model normally fixes an internal group before symmetry breaking; the abstract selection problem allows that group to vary, whereas the worked joint candidate fixes it explicitly.

The approach is conceptually related to gauge-geometric unification, spectral action methods, and stochastic quantization. MacDowell and Mansouri demonstrated that gravitational dynamics can be encoded in a gauge-geometric curvature framework [116]. Chamseddine and Connes constructed a spectral action whose low-energy expansion contains gravitational and Standard-Model structures [26], [27], and [43]. Heat-kernel analysis provides the mathematical machinery underlying such asymptotic expansions [156]. Parisi and Wu introduced stochastic quantization through relaxation in an auxiliary stochastic time [126], while subsequent work clarified gauge-field implementations [170]. The framework combines a different logical chain: the stochastic cost is generated by the same master action whose equilibrium determines the selected effective phase.

The phrase "same master action" is the central restriction. If future calculations reveal that the required algebra, pairing, or measure necessarily factorizes into independent sectors, then the theory should be classified as an effective aggregation rather than genuine microscopic unification. This criterion makes the proposal falsifiable at the mathematical level.

The thermodynamic and fluid branches also have specific precedents, which should not be presented as new physical laws. The Fokker–Planck and Gibbs identities are standard diffusion results [137]; the control-cost representation uses Girsanov change of measure [105]; and the path-reversal formulation follows stochastic thermodynamics [31], [144], and [146]. The Crooks and Jarzynski relations require the additional reservoir and protocol assumptions in (150)–(151). Their appearance in one regulated construction is an interface calculation, not an independent discovery of the fluctuation theorems.

Similarly, the skew-transport and positive-mobility decomposition is GENERIC-inspired [84]. A full GENERIC structure needs the Poisson and degeneracy properties specified in (895); a stochastic HJB objective does not supply them automatically. The Mori–Zwanzig memory equation and stress Green–Kubo formula give a conditional route from unresolved microscopic variables to viscosity [121], [169], and [106]. The finite Galerkin energy identity is the standard Itô balance for a divergence-free stochastic fluid, not a derivation of universal turbulent closure. The additional requirement proposed here is that the constitutive and projection data come from the same fixed microscopic package rather than be fitted independently. Verifying that requirement is separate from testing a supplied finite fluid equation numerically.

The programme is also distinct from a completed quantum-gravity construction. String theory, loop quantum gravity, and functional-renormalization-group approaches introduce different microscopic degrees of freedom or quantization strategies [132], [140], and [136]. The present Euclidean stochastic sampler is not a world-sheet theory, a physical spin-network Hilbert space, or a proof of an ultraviolet fixed point. Its auxiliary stochastic time does not replace their physical time or causal structure. On a semiclassical branch, the stress-response equation (291) still requires a physical state and renormalized causal response; random coframe coordinates alone do not meet that requirement. Thus comparison concerns the declared degrees of freedom, the matching map, and the eventual observable predictions, not an unsupported ranking of competing approaches.

12.15. *A regulated topology-switching extension.* A switching control problem can be formulated without identifying its free boundary with a spacetime singularity. Let $\mathcal{I} = \{1, \dots, K\}$ index a finite family of regulated geometric

sectors, each with state space $\mathcal{X}_\alpha^{a,N}$, generator $\mathcal{L}_\alpha^u$, and running cost ℓ_α. A switch from α to β has cost $c_{\alpha\beta}(x) > 0$ and reset map $R_{\alpha\beta} : \mathcal{X}_\alpha^{a,N} \to \mathcal{X}_\beta^{a,N}$. Define $M_\alpha V(x) := \inf_{\beta\neq\alpha}\{c_{\alpha\beta}(x) + V_\beta(R_{\alpha\beta}x)\}$. The value functions satisfy the switching quasi-variational inequality

$$\max\Big\{-\partial_t V_\alpha - \inf_u\big[\mathcal{L}_\alpha^u V_\alpha + \ell_\alpha(x,u)\big],\ V_\alpha - M_\alpha V\Big\} = 0. \tag{867}$$

The first branch is the continuation equation inside one regulated sector. The second defines a switching region. The terminal condition is

$$V_\alpha(T,x) = g_\alpha(x). \tag{868}$$

Admissible strategies must have finitely many switches on compact time intervals (or a specified non-Zeno relaxation), and every directed switching cycle must have strictly positive total cost. These conditions, together with comparison, compactness or coercivity, and well-posed martingale problems, are required before (867) has a unique value solution.

To interpret the sector labels as distinct spacetime topologies requires substantially more. One must specify admissible cobordisms, Lorentzian and spin structures, continuation of gauge bundles and anomalies, junction data, causal propagation, the action assigned to a transition, and a quantum or statistical rule producing the jump rates. A blow-up of ∇V_α or $D^2 V_\alpha$ is a regularity failure of the value function. It is not equivalent to curvature blow-up, geodesic incompleteness, trapped-surface formation, or any other geometric singularity criterion. Conversely, introducing a switch before an escape time regulates the control model but does not prove that the underlying spacetime singularity has been resolved.

A physically meaningful singularity-avoidance theorem would at least have to derive the switching law from the same master data and establish regulator-uniform estimates such as

$$\begin{aligned} &\sup_{a,N}\mathbb{E}\left[\sup_{0\le t\le T}\mathcal{I}_{\mathrm{curv}}(g_{\alpha_t}^{a,N}(t))\right] < \infty,\\ &\lim_{K\to\infty}\sup_{a,N}\mathbb{P}\left(\sup_{0\le t\le T}\mathcal{I}_{\mathrm{curv}}(g_{\alpha_t}^{a,N}(t)) > K\right) = 0, \end{aligned} \tag{869}$$

for a declared coercive curvature observable $\mathcal{I}_{\mathrm{curv}}$ defined compatibly with the reset maps so that values in different sectors are comparable, followed by a causal continuum identification. Equation (867) is therefore a well-defined research extension for comparing geometric phases. It is not, without (869) and the structural conditions above, a theory of black-hole singularity excision, spacetime foam, or topology change in nature.

12.16. *Further mathematical problems.* A complete development should solve the following problems in order.

1. Construct an explicit master Lie or super-Lie algebra and complete data package satisfying the invariant-pairing and Jacobi identities together with Definition 2.
2. If the Euclidean construction is claimed to admit a four-dimensional Lorentzian asymptotic S-matrix, state whether the hypotheses of the Coleman–Mandula theorem hold. With a nontrivial analytic S-matrix, finitely many particle types below each mass, a mass gap, and the usual regularity assumptions, ordinary bosonic spacetime and internal symmetries cannot mix beyond the Coleman–Mandula form; a graded extension is constrained by the Haag–Lopuszanski–Sohnius theorem [41] and [88]. The present Cartan–Euclidean data do not automatically satisfy those hypotheses, so any mixed master algebra must either verify them or state explicitly which assumption is absent.
3. Construct the corresponding principal or generalized bundle and prove global existence conditions.
4. Specify the exact field-space metric and mobility operator.
5. Establish gauge covariance of the stochastic process on the quotient configuration space.
6. Extend the fixed-background scalar construction and the nonlinear continuum result of Theorem 39 to dynamical coframes, gauge connections, and the declared matter variables, with estimates uniform in the regulator and a justified treatment of gauge symmetry.
7. Extend the complete finite-regulator equilibrium theorem to that coupled continuum. This requires tightness and identification estimates that survive regulator removal; the smoothing in the scalar example cannot be removed merely by invoking its contraction bound.
8. Construct a reflection-positive regulator family for gauge-invariant master observables, prove convergence of every required Schwinger function, and verify Euclidean covariance, graded symmetry, regularity, reflection positivity, and clustering rather than only positivity of the Gibbs density.
9. Carry out Osterwalder–Schrader reconstruction on a selected Euclidean vacuum and prove positivity of the physical inner product, the spectrum condition, unitary Lorentzian evolution, microcausality, clustering, and the time-slice property. The auxiliary stochastic time must remain distinct unless an additional identification theorem is proved.
10. Specify an independently justified selection class that avoids the positive-coupling nonattainment in Theorem 15, then determine whether the observed residual group is its unique minimizer.
11. Derive the matter representation and verify all gauge and mixed anomalies.

12. Construct the BRST/BV complex for the selected gauge and gravitational constraints; prove its quantum nilpotency, the renormalized Slavnov–Taylor identities, cancellation of every gauge, diffeomorphism, mixed, global-gauge, and gauged-discrete anomaly, the required 't Hooft matching for genuine global symmetries, and positivity of the physical cohomology.
13. Compute the complete one-loop determinant and heat-kernel coefficients for the selected master operator.
14. Derive the low-energy matching equations for G, g_1, g_2, g_3, masses, and scalar couplings.
15. Establish a Lorentzian continuation satisfying positivity and causality.
16. Construct the covariant physical observable net. Treat Gauss-law centres and edge modes in the gauge sector, and construct relational or gravitationally dressed observables with controlled causal commutators in the diffeomorphism-invariant sector.
17. Specify normalized completely positive local instruments, derive or explicitly adopt the Born rule, and compute a spacelike Bell experiment from the selected state. Verify both its CHSH value and its no-signalling marginals without using the experimental outputs as selection inputs.
18. Determine whether the stochastic formulation is merely a Euclidean mathematical device or has a deeper physical interpretation.
19. Determine whether the conditional width and force relations in Section 11.11 survive full matching, running, mixing, and composite-source corrections, and calculate their theoretical uncertainties. An observable that distinguishes the construction from other scalar–tensor theories requires further restrictions beyond the common tree-level weight.
20. For a candidate such as Section 6.6, construct a global representation-compatible parent or an alternative ultraviolet completion; then compute its full threshold matching, including flavor alignment, neutral-sector operators, and all additional beta-function contributions.

These dependencies determine how predictions are tested. Fitting can guide model comparison, but observations used for calibration must be distinguished from independent tests of the selected model. For the variational mechanics and geometric gauge theory used in the construction, we refer to [7] and [71]; these references provide the mathematical background, not a proof of the selection or parameter-matching assertions of this framework.

12.17. *Discussion.* The construction combines geometric and probabilistic data in a master stochastic variational system, summarized by

$$\boxed{\left(\mathfrak{g}, \mathbb{A}, \mathbf{F}_{\mathrm{M}}^{\mathrm{ext}}, \mathcal{S}_{\mathrm{M}}, \widehat{\mathbb{M}}, \theta\right).} \tag{870}$$

The connection determines the curvature, and the extended curvature and pairing determine the action. The action, mobility, reference measure, and stochastic convention together determine a compatible drift. The drift and covariance then determine the control energy. When its partition function is finite and the reversible dynamics is well posed, the same action also defines an equilibrium probability.

The proposed unification criterion asks whether the observed distinctions between interactions can be determined by the spectrum, symmetry, and scaling of one selected microscopic package. The worked candidate establishes some component relations for prescribed group and representation data. It does not yet establish that those data are the unique output of the selection problem.

The minimum-cost principle also acquires a precise probabilistic meaning. The cost does not represent four physical penalties added together. It measures the squared displacement of an admissible skeleton from the selected master drift in the geometry determined by the noise covariance. The deterministic theory is the zero-cost sector. The equilibrium distribution is the zero-dissipation state of the probability dynamics. These are therefore three descriptions of one structure rather than three independent postulates.

This common probabilistic structure does not erase the classical–quantum boundary. Its nonfactorizing equilibrium law remains a positive measure on a commutative event space and hence satisfies Theorem 44 whenever measurement independence and Bell locality hold. Quantum entanglement would instead be nonseparability of a reconstructed state on two commuting but individually noncommutative local algebras. The conditional route in Section 12.1 locates the failure of a Bell-local classical explanation, while the specified commuting complete local POVMs satisfy no-signalling. It does not claim that the present Gibbs construction has already made that reconstruction.

A sufficiently flexible master algebra, potential, mobility, and measure can reproduce almost any effective theory. Flexibility is therefore not evidence of unification. Predictivity requires independently constrained microscopic data and unique selection of the observed low-energy structure. The group-selection and numerical-matching problems are consequently central components of the construction.

12.18. *Interim synthesis.* The variational–stochastic framework contains one master configuration, one master connection, one master curvature, one master action, one stochastic dynamical equation, one path-space cost, and one equilibrium principle. The four familiar interactions are interpreted as low-energy sectors of the same master object rather than as four independent costs.

For an absolutely continuous skeleton x, the control energy is

$$\boxed{\mathcal{J}_T[x] = \frac{1}{4\theta}\int_0^T \|\dot{x}_t - \mathbb{B}(x_t)\|^2_{\widehat{\mathbb{M}}(x_t)^\dagger}\,\mathrm{d}t.} \tag{871}$$

Here $\mathbb{B}$ is the complete reference drift, including the reference-volume correction in (80) when required. The norm is the quadratic form in (66), with value $+\infty$ off $\operatorname{Ran}\widehat{\mathbb{M}}^{1/2}$; in a finite-dimensional nondegenerate realization it is the ordinary inverse-mobility norm. For random controls, the expected control energy equals path-space relative entropy under the state-path measurability, Girsanov integrability, and uniqueness-in-law hypotheses of Section 3.9. Absolute continuity alone is not the full hypothesis of this identity.

If $0 < Z < \infty$, the corresponding equilibrium density is

$$p_* = Z^{-1}e^{-\mathcal{S}_{\mathrm{M}}/\theta}. \tag{872}$$

It is invariant for the compatible reversible dynamics under the semigroup and boundary assumptions established above. Its free-energy difference is the state-space relative entropy in Appendix B. The confining modification in Section 5.4.1 resolves the displayed scalar constant-mode obstruction. Theorem 11 proves the associated fixed-background vacuum theorem, and Theorem 19 proves finiteness and uniqueness of equilibrium for the specified compact gauge–scalar regulator. Theorem 39 gives a nonlinear scalar continuum with a unique invariant law and exponential contraction. The global nonperturbative gauge–gravity partition function and coupled continuum require estimates beyond these fixed-background constructions.

At the effective level, Theorem 9 proves that the coframe/metric component gives (210) and the residual internal-connection component gives (318). On the stated torsionless, matched Lorentzian branch, the Yang–Mills constitutive equation is exact, becoming canonical on the frozen constant-kinetic branch, and the ordinary Einstein equation has the quantified residual (213). The branch, continuation, higher-curvature scale separation, block-compatible residual pairing, and Noether-balanced treatment of fixed data define the theorem's domain; they are not unfinished steps in its proof. In particular, this recovery does not wait for a global regularity theory of the full nonlinear gauge–gravity system. The unreduced $SO(5)$ curvature-square witness obeys the more general constitutive equation described in Appendix A; proving that its dynamics uniquely selects the matched sector would be a distinct, stronger statement.

Section 5.4 supplies one explicit bosonic joint candidate: $\widetilde{G}_0 = SO(5) \times G_{\mathrm{SM}}$, $H_0 = SO(4) \times G_{\mathrm{SM}}$, a shared order parameter, one extended norm, and one stochastic mobility. When spinor matter is included, this candidate must additionally be lifted to a compatible Spin(4) bundle (and, where required, to the double cover of the Cartan group); the dimension and bosonic curvature

formulas are unchanged. The Cartan norm in Section 5.3 fixes the coefficients of its specified torsionless curvature-invariant expansion and admits an exact Euclidean Einstein vacuum. The quadratic dynamics in Section 11.7 distinguish noise cross variation from equilibrium covariance, with a necessary and sufficient condition for vanishing full sector covariance. The numerical benchmark in Section 11.9 provides numerical checks of those identities using the exact transition law. The heavy-mode calculation in Section 11.10 determines rank restrictions on a specified exchange contribution. The candidate gives a concrete algebraic realization of coupled sectors, and the finite-regulator construction supplies a corresponding bosonic equilibrium example on fixed geometry. The finite-regulator and nonlinear scalar constructions resolve specific existence questions within that system's proposed analytic realizations; they do not select its group or construct the global nonperturbative coupled continuum.

The equilibrium correlations just summarized remain classical correlations. Theorem 44 proves that shared noise, a nonfactorizing Gibbs law, a common history, or local stochastic control cannot violate CHSH while measurement independence and Bell-local factorization are retained. Section 12.1 therefore adds no hidden assertion that classical nonfactorization is entanglement. It instead specifies the required quantum completion: reflection-positive Euclidean correlators or a direct positive Lorentzian construction, anomaly-free physical observable algebras, a selected nonseparable state, and a Born-rule measurement model. In such a completion, $|S_{\mathrm{M}}| > 2$ would exclude the Bell-local classical representation, whereas commuting complete local POVMs obey the no-signalling identities in (851); local instruments must additionally satisfy (853). These are completion criteria, not results already derived by the current classical equilibrium.

The conditional 331 realization in Section 6.6 gives a complementary chiral calculation. For its specified matter class, anomaly cancellation and color asymptotic freedom imply $N_g = 3$ and $k = 1$ by Theorem 16; the five-color example in Section 6.8 shows why this does not independently derive $N_c = 3$. The auxiliary-map vacuum and residual parity forbid the displayed ordinary–exotic mixings at the matching scale. Their physical protection still requires a quantum-consistent realization of Π_{sp}, including discrete gauge-anomaly cancellation if it is gauged or the appropriate anomaly matching and protection mechanism if it is global, together with an acceptable fate for the lightest odd state. The flavor construction gives power laws rather than numerical CKM or PMNS predictions. The relation (446) is a relative leading-order threshold relation, not an absolute mass prediction. Its physical use requires the global representation, flavor alignment, continuation, and matching data listed in Section 6.12.

The observable calculation in Section 11.11 includes scalar–metric kinetic mixing and yields a common normalized gauge vertex, a direct tree-level gauge-width ratio, and a relation between the photon partial width and an elementary-source Yukawa force. Vacuum matching is explicit. The curvature coefficients also impose a mass–force hierarchy, so a large formal coupling cannot be used indiscriminately in a low-energy on-shell prediction. The numerical plots evaluate the stated approximations and contain no experimental observations. These local effective-field relations do not establish a globally coercive scalar potential or an invariant probability for the matched Lorentzian branch; the large-field limitation is explicit in (780).

Irreducibility is a condition on the complete dynamical package in Definition 2. A direct-product Lie algebra with an orthogonal invariant pairing can still support coupled dynamics through a shared scalar, a dynamical metric, matter, or mobility. Conversely, a single action symbol does not prove that those couplings are independently fixed. The relevant comparison is therefore factorization of the action, configuration, measure, and dynamics together.

The selection problem must first overcome the concrete obstruction in Theorem 15. The unrestricted positive-coupling family cannot uniquely retain this candidate because its infimum is approached at the excluded zero-coupling boundary. A restricted class would have to justify its measure, coupling normalizations, matter realization, Lorentzian continuation, and threshold corrections independently of the desired output. A successful result would turn the structural relation (238) and the covariance criterion (720) into parameter-constrained tests. A failure would identify which part of the one-action and equilibrium principle is insufficient.

12.19. *Mass definitions and the Yang–Mills mass-gap boundary.* The effective-sector discussion distinguishes a regulated Hessian mass from a physical pole mass. After gauge and constraint reduction, let $K_N^{\mathrm{kin}} \succ 0$ be the kinetic quadratic form and let $\mathcal{H}_N$ be the zero-momentum potential Hessian. The regulated curvature masses solve the generalized eigenvalue problem

$$\begin{gathered}\mathcal{H}_N u_{N,j} = m_{H,N,j}^2 K_N^{\mathrm{kin}} u_{N,j}, \quad \mathcal{M}_{H,N}^2(\mu) := (K_N^{\mathrm{kin}})^{-1/2} \mathcal{H}_N (K_N^{\mathrm{kin}})^{-1/2}, \\ s := -p_L^2, \quad \mathcal{F}_N(s) := \det\left[s\mathbf{1} - \mathcal{M}_{H,N}^2(\mu) - \widehat{\mathbf{\Pi}}_N^T(s;\mu)\right], \\ \mathcal{F}_N(s_{*,N}) = 0.\end{gathered} \tag{873}$$

The variable s in this display is available at finite regulator only when the regulated model has a translation-invariant transfer-matrix or two-point function with an analytic continuation; otherwise the finite-regulator mass is the generalized Hessian eigenvalue, and no continuous Lorentzian momentum is being asserted. More generally, denote a regulated pole by $s_{*,a,N,V}$ (with volume V) and define a continuum pole only through a declared nested limit, when that

limit exists. Here $\widehat{\mathbf{\Pi}}_N^T$ is the matrix-valued renormalized physical transverse self-energy remainder on the selected mixed vector channel, with its local counterterms and tree-level Hessian subtraction fixed by the same renormalization scheme. This prevents double counting between $\mathcal{H}_N$ and $\widehat{\mathbf{\Pi}}_N^T$. For a scalar or mixed channel, the transverse superscript is omitted and the determinant is taken on the full reduced physical channel; the transverse form above is only the vector-boson specialization. Canonical normalization corresponds to $K_N^{\mathrm{kin}} = \mathbf{1}$. The first line defines a curvature mass; the last line defines a regulated pole proxy. It represents a stable physical pole mass only after the continuum limit exists and the zero is simple, real, gauge independent, and has positive residue. An unstable state has a complex continued pole $s_* = (M_* - i\Gamma_*/2)^2$; a confined channel must instead be tested by gauge-invariant composite correlators. A generic curved background need not admit the global momentum used in this formula. A stochastic relaxation eigenvalue is none of these quantities without an independent spectral identification. When translation invariance and analytic continuation are available at every stage, a physical pole is defined by the ordered procedure

$$s_{*,\mathrm{phys}} := \lim_{\mathcal{R} \nearrow \mathbb{R}^4} \lim_{a \downarrow 0} s_{*,a,N(a),V(a)}, \tag{874}$$

with the volume and mode cutoffs, the renormalization conditions, and the order of limits explicitly declared. Existence, regulator independence, and positivity of the residue are additional hypotheses rather than consequences of the finite Hessian calculation.

For compact simple G, the pure Yang–Mills Wilson regulator [165] with $\beta(a) \geq 0$ is

$$S_{W,a} = \beta(a) \sum_p \left(1 - \frac{1}{\dim R} \operatorname{Re} \operatorname{tr}_R U_p\right), \qquad \mathrm{d}\mu_a = Z_a^{-1} e^{-S_{W,a}} \prod_\ell \mathrm{d}U_\ell. \tag{875}$$

Haar measure gives gauge invariance at fixed lattice and volume. With a reflection-compatible lattice, reflection plane, and boundary condition, the antilinear Euclidean time reflection Θ defined in (858) gives

$$\int (\Theta F) F \, \mathrm{d}\mu_a \geq 0 \tag{876}$$

for positive-time gauge-invariant cylinder functionals. Complex conjugation is already part of Θ; it is applied exactly once. In particular, for a constant functional $F = z$, the reflected form equals $|z|^2$.

A continuum limit means $a \downarrow 0$, $\Lambda_a \nearrow \mathbb{R}^4$, and distributional convergence of all required gauge-invariant Schwinger functions. Under the full Osterwalder–Schrader hypotheses, the positive-time quotient and completion give a physical Hilbert space, vacuum Ω, and positive self-adjoint Hamiltonian H with $H\Omega = 0$

and its spectral decomposition. The pure-glue gap is the conditional statement

$$\Delta_{\mathrm{YM}} = \inf\big(\mathrm{Spec}(H) \setminus \{0\}\big) > 0. \tag{877}$$

Finite-volume transfer gaps and reflection positivity do not imply this uniform continuum inequality. The four-dimensional nonperturbative Yang–Mills mass-gap problem remains open; this paper does not claim to prove it.

PROPOSITION 47 (Conditional gap from reconstructed Euclidean decay). *Suppose that gauge-invariant continuum Schwinger functions satisfy the full reconstruction hypotheses and give a nontrivial physical Hilbert space $\mathcal{H}_{\mathrm{phys}}$, a normalized vacuum Ω, and a nonnegative self-adjoint Hamiltonian H. Assume that* $\ker H = \mathrm{span}\{\Omega\}$. *Let $\mathcal{D}_0$ be a set of centered gauge-invariant observable states whose linear span is dense in $\Omega^{\perp}$. Assume that an independently established Euclidean correlation estimate supplies $\Delta_0 > 0$ such that, for every $\psi \in \mathcal{D}_0$, there is a finite C_ψ with*

$$0 \le \langle \psi, e^{-tH}\psi\rangle \le C_\psi e^{-\Delta_0 t}, \qquad t \ge 0. \tag{878}$$

Then

$$\mathrm{Spec}(H) \subset \{0\} \cup [\Delta_0, \infty), \qquad \Delta_{\mathrm{YM}} \ge \Delta_0 > 0 \tag{879}$$

when this reconstructed theory is the declared pure Yang–Mills theory. The time t is physical Euclidean time in the reconstructed semigroup, not the auxiliary stochastic relaxation time. The scale Δ_0 therefore has energy units in the convention $\hbar = c = 1$.

Proof. Let E_H be the spectral measure of H, and set $\mu_\psi(B) = \langle \psi, E_H(B)\psi\rangle$. Self-adjointness and nonnegativity give

$$\langle \psi, e^{-tH}\psi\rangle = \int_{[0,\infty)} e^{-t\lambda}\, \mathrm{d}\mu_\psi(\lambda). \tag{880}$$

Centeredness and vacuum uniqueness give $\mu_\psi(\{0\}) = 0$. Fix $0 < \varepsilon < \Delta_0$. If $b_\varepsilon := \mu_\psi((0, \Delta_0 - \varepsilon]) > 0$, then (880) implies

$$b_\varepsilon e^{-(\Delta_0-\varepsilon)t} \le \langle \psi, e^{-tH}\psi\rangle \le C_\psi e^{-\Delta_0 t}, \qquad b_\varepsilon \le C_\psi e^{-\varepsilon t}. \tag{881}$$

Letting $t \to \infty$ contradicts $b_\varepsilon > 0$. Taking a countable sequence $\varepsilon \downarrow 0$ therefore gives $\mu_\psi((0, \Delta_0)) = 0$, or equivalently $E_H((0, \Delta_0))\psi = 0$, for every $\psi \in \mathcal{D}_0$. This spectral projection is bounded and hence annihilates the closure of their linear span, namely $\Omega^{\perp}$. It also annihilates Ω. Thus the projection is zero on the whole physical Hilbert space. The spectral theorem excludes spectrum in $(0, \Delta_0)$, which proves (879). □

A sufficient regulated input for (878) would be convergence of the connected gauge-invariant transfer correlations at fixed physical time, together with bounds $C_\psi e^{-\Delta_0 t_a}$ whose constants and positive physical scale are independent of the cutoff and volume, where the allowed lattice times t_a converge to t. Positivity

and convergence then pass the bound to the reconstructed correlation. A cutoff-dependent positive gap is insufficient if it tends to zero; decay of only one observable is insufficient if the associated states do not span all physical excitation channels. Establishing the uniform decay estimate, the continuum limit, and vacuum structure in four dimensions remains the nonperturbative Yang–Mills task. The proposition proves the spectral implication, not those premises. It neither proves a Wilson-loop area law nor identifies an auxiliary control relaxation rate with a particle mass.

12.19.1. *A control representation of a confinement criterion.* Asymptotic freedom makes the color coupling weak at high energy and short distance; the confinement problem concerns the low-energy, long-distance strong-coupling regime. Neither anomaly cancellation in the 331 branch nor an HJB equation proves confinement. The gauge-invariant criterion must first be stated independently of the proposed control interpretation. In pure Yang–Mills theory, for rectangular Wilson loops of spatial width R and Euclidean duration T, define

$$V_{\mathrm{stat}}(R) := -\lim_{T\to\infty} \frac{1}{T} \log\langle W(R,T)\rangle, \qquad \sigma_{\mathrm{str}} := \liminf_{R\to\infty} \frac{V_{\mathrm{stat}}(R)}{R}. \tag{882}$$

An area law has $\sigma_{\mathrm{str}} > 0$. With dynamical fundamental matter, string breaking changes the asymptotic Wilson-loop diagnostic, and one must instead formulate the absence of colored asymptotic states and the gauge-invariant hadron spectrum. Chiral symmetry breaking is a further, logically distinct statement.

There is nevertheless an exact variational identity behind a possible control-theoretic confinement reformulation. Let $P_{a,N}$ be a regulated reference path law, let $\theta > 0$, and let $\mathcal{I}^{+}_{R,T}$ be a strictly positive, measurable, gauge-invariant heavy-source or flux-tube insertion with $0 < \mathbb{E}_{P_{a,N}} \mathcal{I}^{+}_{R,T} < \infty$. Put $\mathcal{O}_{R,T} := -\theta \log \mathcal{I}^{+}_{R,T}$. A Wilson loop is not assumed to be pointwise positive; its use here would require a separate reflection-positive heavy-source construction proving equivalence to this positive insertion. The Gibbs variational formula gives

$$-\theta \log \mathbb{E}_{P_{a,N}} \exp\!\left(-\frac{\mathcal{O}_{R,T}}{\theta}\right) = \inf_{Q \ll P_{a,N}} \left\{ \mathbb{E}_Q \mathcal{O}_{R,T} + \theta D_{\mathrm{KL}}(Q \| P_{a,N}) \right\}. \tag{883}$$

Indeed, if

$$\frac{\mathrm{d}Q_*}{\mathrm{d}P_{a,N}} = \frac{\exp(-\mathcal{O}_{R,T}/\theta)}{\mathbb{E}_{P_{a,N}} \exp(-\mathcal{O}_{R,T}/\theta)},$$

then the right-hand side of (883) differs from its left-hand side by $\theta D_{\mathrm{KL}}(Q\|Q_*) \geq 0$. For a class $\mathcal{Q}^{\mathrm{G}}_{a,N}$ of laws generated by admissible Follmer/Girsanov drifts satisfying the range, true-martingale, and uniqueness hypotheses, one has

$$\inf_{Q \in \mathcal{Q}^{\mathrm{G}}_{a,N}} \left\{ \mathbb{E}_Q \mathcal{O}_{R,T} + \theta D_{\mathrm{KL}}(Q \| P_{a,N}) \right\} \geq -\theta \log \mathbb{E}_{P_{a,N}} e^{-\mathcal{O}_{R,T}/\theta}, \tag{884}$$

with equality only when the exponentially tilted law Q_* is itself realizable by such a drift. Thus a positive area-order lower bound for the optimized admissible energy-plus-information cost is a separate criterion. For the volume-dependent regulator, define the admissible finite-regulator cost density by

$$\mathcal{C}_{a,N,V}(R,T) := \inf_{Q\in\mathcal{Q}^{\mathrm{G}}_{a,N,V}} \left\{\mathbb{E}_Q\mathcal{O}_{R,T} + \theta D_{\mathrm{KL}}(Q\|P_{a,N,V})\right\}. \tag{885}$$

The precise area-order obstruction is then

$$\liminf_{R\to\infty}\liminf_{T\to\infty}\liminf_{\mathfrak{R}=(a,N,V)\to(0,\infty,\infty)} \frac{\mathcal{C}_{\mathfrak{R}}(R,T)}{RT} \geq \sigma_{\mathrm{ctrl}} > 0. \tag{886}$$

would be a precise control obstruction to maintaining a separated color-flux history at subarea cost. The regulator symbol $\mathfrak{R}$ denotes a declared cofinal continuum and infinite-volume net; it is not an undefined simultaneous limit. To identify the resulting free-energy density with the physical string tension, the positive insertion must be proved equivalent to the Wilson-loop or heavy-source observable, including the normalization by θ, and the limits must exist in the stated order while gauge, reflection-positivity, and continuum conditions survive. Degeneration of an information filtration by itself implies none of these facts and cannot force a colored trajectory to become a singlet. Equation (886) is therefore a mathematically testable completion criterion, not a claimed solution of confinement or the Yang–Mills mass-gap problem.

The inertial–gravitational interface is also conditional: with a covariant renormalized action, define

$$T_{\mu\nu} = -\frac{2}{\sqrt{-g}}\frac{\delta S_{\mathrm{m}}}{\delta g^{\mu\nu}}, \qquad \nabla^\mu T_{\mu\nu} = 0. \tag{887}$$

Common metric coupling, anomaly-free Ward identities, and controlled nonminimal terms then identify pole rest energy with the zero-momentum gravitational form factor and the integrated rest energy. There is no independent pointwise stress-tensor mass. All loop and threshold corrections require a declared regulator, renormalization scheme, RG flow, counterterms, and matching of renormalized gauge-invariant Green functions.

13. **Nonequilibrium thermodynamics and regulated turbulence**

13.1. *Nonequilibrium thermodynamics and a regulated turbulence branch.* The equilibrium construction developed above has a nonequilibrium extension. The pathwise control problem, the law of the controlled process, and the hydrodynamic projection of that law are distinct mathematical objects. A minimum of a path cost does not by itself imply convergence to equilibrium, and a nonzero drift and diffusion do not by themselves define turbulence. We therefore begin with a finite lattice and finite Galerkin regulator.

13.2. *A common finite-regulator data package.* In this section all displayed regulator variables are numerical quantities in fixed state, energy, and stochastic-time units. More precisely, they are the barred quantities of Appendix E, with bars suppressed: $x_i = X_i/x_{i,\mathrm{ref}}$, $t = t_{\mathrm{s}}/t_{\mathrm{ref}}$, $E = E_{\mathrm{dim}}/E_{\mathrm{ref}}$, and $\theta = \theta_{\mathrm{dim}}/E_{\mathrm{ref}}$. The state scales are positive and constant. Mobilities, transport operators, control maps, observations, and target generators are transformed at the same time, as in (1486)–(1488). Thus the displayed running and terminal costs below are dimensionless. Restoring the reference units does not change the admissible optimization problem when all its data, initial laws, and endpoint conditions are transformed together. The regulator time t_{s} is not identified with Lorentzian or laboratory time by this choice of units.

Fix a lattice spacing $a > 0$, a finite Galerkin rank N, a gauge slice (or a finite gauge quotient), and a compact time interval $[0, T]$. Let $\mathcal{X}_{a,N}$ be the resulting finite-dimensional physical configuration space. It contains the regulated metric, internal connections, matter, and scalar modes. The velocity variable used below is not an additional coordinate: it is the derived projection $U^N = \Pi^{a,N}_{\mathrm{NS}}(X)$. A concrete model must derive this map from its conserved currents or fluid observables and prevent double counting of the underlying matter coordinates. The probability density ρ_t is a density on $\mathcal{X}_{a,N}$, not an additional spacetime field. Let $\nu_{a,N}$ be a strictly positive reference measure and let $E, s \in C^2(\mathcal{X}_{a,N})$, where s is dimensionless. For the remainder of the equilibrium and entropy calculation, write $m = m_{a,N}$ for its coordinate density and assume $\theta > 0$. The deterministic case $\theta = 0$ is a separate zero-noise limit and is not covered by the normalized Gibbs density below.

More precisely, in a regulator chart we write

$$\nu_{a,N}(\mathrm{d}x) = m_{a,N}(x)\,\mathrm{d}x, \qquad \rho_t^u = \frac{\mathrm{d}\mu_t^u}{\mathrm{d}x}, \qquad p_t^u = \frac{\mathrm{d}\mu_t^u}{\mathrm{d}\nu_{a,N}} = \frac{\rho_t^u}{m_{a,N}}. \tag{888}$$

Thus ρ_t^u always means the coordinate-volume density of the controlled law, whereas p_t^u is its density relative to the reference measure. With $p_\theta := \pi_\theta/m_{a,N}$, this convention makes $\nabla \log(\rho_t^u/\pi_\theta) = \nabla \log(p_t^u/p_\theta)$ and prevents a change of reference density from being mistaken for a thermodynamic force.

The coordinate content of a regulated state is inherited from (43). More explicitly, after choosing the local Cartan splitting in (36), we may display it as

$$x = (\mathbb{A}, \Psi, \Phi_H, \sigma, \chi) \equiv (e, \omega, A, \Psi, \Phi_H, \sigma, \chi) \in \mathcal{X}_{a,N}. \tag{889}$$

Here Ψ is reserved for the matter multiplet, Φ_H for the scalar order parameter, σ for the shared scalar, and χ for the information-state coordinate. In particular, the terminal cost below is not denoted by Ψ. The density ρ_t is the law of X_t relative to the declared coordinate volume; it is constrained by the forward equation and is not an independent spacetime field.

For the baseline control problem, fix a continuous running cost $\ell^{E}_{\mathrm{cl}} : \mathcal{X}_{a,N} \to \mathbb{R}$ and a terminal cost $\mathcal{G}^{\mathrm{term},0}_{a,N} : \mathcal{X}_{a,N} \to \mathbb{R}$, both bounded below and integrable under every admissible controlled law. For the ergodic quadratic-control specialization, fix a control-space operator

$$\mathcal{R}_{\mathrm{u}} = \mathcal{R}_{\mathrm{u}}^{*} \succ 0. \tag{890}$$

The subscript distinguishes this cost weight from the matter-representation datum $\mathcal{R}$ used earlier. Existence of a finite ergodic value will additionally require recurrence and uniform integrability; it is not implied by these definitions.

Let $\mathbb{L}(x)$ and $\mathbb{M}(x)$ satisfy

$$\mathbb{L}(x)^{\mathsf{T}} = -\mathbb{L}(x), \qquad \mathbb{M}(x)^{\mathsf{T}} = \mathbb{M}(x) \succeq 0. \tag{891}$$

Algebraic skewness $\mathbb{L}^{\mathsf{T}} = -\mathbb{L}$ alone does not make the induced transport generator anti-self-adjoint in the equilibrium L^2-space. The terminology in the next display follows the operator decomposition (134) only after the invariant-density, boundary, and parity conditions in (987)–(988) have been imposed. The $\mathbb{M}$-sector carries the fluctuation–dissipation current. Statistical reversibility of the complete stationary process still requires (133); it is not inferred merely from either label. Define

$$b_{\mathrm{rev}} = \mathbb{L}\nabla E, \qquad b_{\mathrm{irr}} = \mathbb{M}(\theta\nabla s - \nabla E) + \theta\beta_m, \qquad \beta_{m,i} := m^{-1}\partial_j(m\mathbb{M}_{ij}). \tag{892}$$

An external force f_{ext} and the control operator $\mathbb{B}_{0,a,N}$ are added separately. We do not denote the latter by $\mathbb{G}$, because $\mathbb{G}$ already denotes the positive field-space metric. The unified regulated stochastic equation is

$$\mathrm{d}X_t = \Big[b_{\mathrm{rev}}(X_t) + b_{\mathrm{irr}}(X_t) + f_{\mathrm{ext}}(X_t) + \mathbb{B}_{0,a,N}(X_t)u_t\Big]\mathrm{d}t + \sqrt{2\theta\,\mathbb{M}(X_t)}\,\mathrm{d}W_t. \tag{893}$$

Here W_t is a standard finite-dimensional Wiener process. In an infinite-dimensional version one must specify whether W is cylindrical or a Q-Wiener process and impose the corresponding Cameron–Martin and trace-class conditions. The two conventions must not be combined by inserting a covariance square root twice. For later linearization, abbreviate

$$b^{u}(t,x) := b_{\mathrm{rev}}(x) + b_{\mathrm{irr}}(x) + f_{\mathrm{ext}}(x) + \mathbb{B}_{0,a,N}(x)u(t,x), \qquad B(x) := \sqrt{2\theta\mathbb{M}(x)}. \tag{894}$$

The following are GENERIC-inspired degeneracy conditions [84]:

$$\mathbb{L}\nabla s = 0, \qquad \mathbb{M}\nabla E = 0, \tag{895}$$

when the state space includes the heat reservoir needed for total-energy conservation. In a reduced fluid model the heat reservoir is omitted from the displayed state, so the reduced kinetic energy is allowed to decrease. To restore a closed energy balance one must enlarge the state by an explicit heat variable;

viscous loss of kinetic energy is then the gain of the reservoir energy. Adding that variable is an extension of the model, not a replacement of the degeneracy condition by a new identity. They are not, by themselves, a complete GENERIC structure. For that stronger statement the bracket $\{F, G\}_{\mathbb{L}} := \nabla F \cdot \mathbb{L}\nabla G$ must also satisfy the Jacobi identity on a declared algebra and common domain, and the $\mathbb{M}$-bracket must satisfy its stated symmetry, positivity, and domain requirements. The finite-regulator results below use only the displayed skewness, positivity, and degeneracy identities.

13.3. *Why the variational and dissipative descriptions are compatible.* An ordinary time-translation-invariant action for a closed set of mechanical variables produces a conservative Euler–Lagrange equation and a Noether energy. A positive local viscosity term cannot be obtained by simply varying the same single-field conservative action: under the usual boundary conditions, the resulting energy balance has no strictly negative production term. This is the familiar reason that a phenomenological dissipative system requires either a reservoir, a doubled or history-dependent action, or a statistical path-space formulation.

Two logical qualifications prevent a common overstatement of this argument. The stationary-action principle does not itself require time-translation symmetry: Noether's energy balance follows only when the action, its boundary conditions, and all external data are invariant under that symmetry. Likewise, an ordinary Hamiltonian description is reversible only after the time-reversal parities of the variables have been specified. A finite-dimensional time-independent Hamiltonian flow preserves its symplectic volume, but a Hamiltonian description enlarged by reservoir variables can project to a dissipative reduced equation. The obstruction addressed here is therefore the use of a *single, local, conservative, resolved-field action* as a complete description of viscosity; it is not a no-go theorem for every variational or Hamiltonian representation of a dissipative system.

The Hamiltonian appearing in stochastic control is a different object from the canonical Hamiltonian of a time-translation-invariant mechanical action. For a controlled diffusion it is the dynamic-programming operator

$$\mathscr{H}_{\mathrm{HJB}}(x, p, X) := \inf_{u \in \mathcal{U}} \left\{ \big[b(x) + B(x)u\big] \cdot p + \theta \,\mathrm{Tr}\big(\mathbb{M}(x)X\big) + \ell(x, u) \right\}. \quad (896)$$

It is not a conserved energy and it is not the Noether charge associated with time translations. The HJB equation is oriented by a terminal or asymptotic value condition, while the controlled path law is oriented by the chosen forward filtration. A nonzero HJB direction therefore does not contradict a conservative Noether identity for a closed enlarged system. Physical irreversibility enters only after comparing the forward and parity-corrected reverse path laws, as in

(125); the HJB formalism by itself does not assert that this relative entropy is positive.

The present construction uses the third description while retaining the first one for the reversible sector. With the notation above, the drift separates as

$$\mathbb{B} = \underbrace{\mathbb{L}\nabla E}_{\text{conservative transport}} + \underbrace{\mathbb{M}(\theta\nabla s - \nabla E) + \theta\beta_m}_{\text{reversible-measure-corrected dissipation}} + \underbrace{f_{\text{ext}} + \mathbb{B}_{0,a,N}u}_{\text{drive and control}}. \tag{897}$$

Several qualifications are essential for this interpretation. For a diffusion with coordinate density ρ, the probability current is componentwise

$$J_i[\rho] = b_i^u\rho - \frac{1}{2}\partial_j\big[(\sigma\sigma^{\mathsf{T}})_{ij}\rho\big]. \tag{898}$$

The condition $\nabla\cdot J = 0$ is only stationarity. A stationary process may have a nonzero solenoidal current and still satisfy detailed balance in a parity-corrected conservative sector. Nonnegative entropy production is obtained from the forward/reverse path-law relative entropy, or from the irreversible part of the current after the parity, boundary, absolute continuity, and fluctuation–dissipation hypotheses have been imposed. It does not follow from a nonzero current or from a nonzero diffusion coefficient alone.

The ergodic control objective is rigorously written as a limsup unless the long-time limit is proved:

$$\lambda(u) := \limsup_{T\to\infty}\frac{1}{T}\mathbb{E}^{\mathbb{P}^u}\int_0^T \ell(X_t,u_t)\,\mathrm{d}t. \tag{899}$$

Under recurrence, integrability, comparison, and a sufficiently regular value function, dynamic programming yields the stationary HJB equation

$$-\lambda_* + \inf_{u\in\mathcal{U}}\big\{\ell(x,u) + b^u(x)\cdot\nabla V(x) + \theta\,\mathrm{Tr}\big(\mathbb{M}(x)D^2V(x)\big)\big\} = 0. \tag{900}$$

The pointwise minimizer is an optimal feedback only when it is measurable, admissible, attained, and compatible with the martingale problem. The gradient ∇V is a value-function sensitivity (a costate in the dynamic-programming sense); it is not automatically a physical force.

The relation with a most-probable path is conditional. In a small-noise scaling in which a Freidlin–Wentzell or Onsager–Machlup principle has been proved, minimizers of the corresponding rate functional describe the dominant path asymptotics. An expected running-cost problem and a small-noise large-deviation problem are different optimization problems unless their scaling and admissible classes are explicitly identified.

The antisymmetric part is the Hamiltonian-type response and is the part to which the ordinary Noether argument applies. The symmetric mobility part is paired with the noise covariance $2\theta\mathbb{M}$. The forward and backward path laws then differ by a relative entropy whose density is the quadratic irreversible-current

norm proved in (130). This entropy production is a property of the stochastic law and its reservoir bookkeeping; it is not a claim that the conservative Euler–Lagrange equation has acquired a preferred time direction.

For the enlarged state containing the reservoir, the degeneracy condition $\mathbb{M}\nabla E = 0$ gives exact conservation of the total energy on each finite regulator energy leaf. The apparent loss of kinetic energy in a resolved subsystem is the compensating gain of unresolved or reservoir modes. After projection, the finite Galerkin equation contains the effective term $-\nu_{\mathrm{v}} A_N U^N$, and its Itô identity (1023) has the negative viscous contribution and the positive stochastic injection term. Thus the framework resolves the logical conflict at the level of bookkeeping: conservative symmetry belongs to the closed enlarged dynamics, whereas irreversible dissipation belongs to the reduced path law.

The coefficient ν_{v}, however, is not fixed by the algebraic split alone. A derivation from the microscopic master action must identify the resolved projection, the memory kernel, and the noise covariance, and then prove a controlled short-memory limit of (1007). The generalized Langevin fluctuation– dissipation relation (1008) constrains the noise and memory together; a transport coefficient additionally requires the appropriate stress autocorrelation Green–Kubo formula. Consequently, the paper proves the finite-regulator dissipative identities and states the precise matching problem for deriving physical viscosity, while a direct derivation of the universal turbulent closure from the bare conservative action remains an open completion condition.

For the closed enlarged system with $f_{\mathrm{ext}} = u = 0$, these conditions and the Itô reference correction imply

$$\mathrm{d}E(X_t) = 0 \quad \text{almost surely.} \tag{901}$$

Indeed, skewness removes $\langle \nabla E, \mathbb{L}\nabla E \rangle$, degeneracy removes the $\mathbb{M}$-drift and martingale terms, and differentiating $\mathbb{M}\nabla E = 0$ cancels the Itô Hessian term against $\theta\beta_m \cdot \nabla E$. The full state space therefore decomposes into invariant energy leaves. On a regular leaf $E = E_0$, the natural conditional equilibrium has the formal coarea notation

$$\pi_{E_0}(\mathrm{d}x) = Z_{E_0}^{-1} m(x) e^{s(x)} \delta(E(x) - E_0)\, \mathrm{d}x, \tag{902}$$

interpreted as the induced surface measure with its coarea factor. The canonical density below is a mixture of such leaf measures and is not generally unique for the closed dynamics. Ergodicity claims must therefore be leafwise. A subsystem obtains a canonical law from an open or enlarged reservoir construction, not from exact total-energy degeneracy plus full-space irreducibility.

Definition 4 (Baseline quadratic path–entropy objective). *Let $\mathbb{P}^0$ be the path law of* (893) *with $u = 0$, and let $\mathbb{P}^u$ be the controlled path law. The baseline*

quadratic finite-regulator objective is

$$\mathscr{J}_{a,N,T}(u) := \mathbb{E}^{\mathbb{P}^u}\left[\int_0^T \ell^E_{\mathrm{cl}}(X_t)\,\mathrm{d}t + \mathcal{G}^{\mathrm{term},0}_{a,N}(X_T)\right] + \theta\, D_{\mathrm{KL}}(\mathbb{P}^u \,\|\, \mathbb{P}^0). \quad (903)$$

The running cost contains the regulated Euclidean geometric, gauge, matter, and hydrodynamic contributions. The terminal cost specifies the endpoint objective, and the KL term measures departure from the reference path law. In dimensional stochastic time these quantities are restored as

$$\ell_{\mathrm{dim}} = \frac{E_{\mathrm{ref}}}{t_{\mathrm{ref}}}\ell^E_{\mathrm{cl}}, \qquad G_{\mathrm{dim}} = E_{\mathrm{ref}}\mathcal{G}^{\mathrm{term},0}_{a,N}, \qquad J_{\mathrm{dim}} = E_{\mathrm{ref}}\,\mathscr{J}_{a,N,T}. \quad (904)$$

Consequently the running cost has energy per unit stochastic time, while the terminal cost and $\theta_{\mathrm{dim}} D_{\mathrm{KL}}$ have energy units. A geometric energy inserted into a running cost requires a declared rate factor. Changing that factor while leaving the terminal and KL weights fixed changes the model; it is not a change of units.

13.4. *A genuinely joint nonlinear objective.* The geometric antecedent of the construction is the one-norm master action (52); its entries are components of one extended curvature, not separately postulated sector actions. Its path-space antecedent is the single inverse-mobility norm in (65). Definition 4 is retained because it is the convenient quadratic relative-entropy representation for the proved control identities. It is not used as the definition of the stronger joint objective below, and its explicit KL term is not added a second time.

Let $\mathscr{D}_{a,N}$ be a declared open set of strictly positive normalized C^2 densities on $\mathcal{X}_{a,N}$. On a noncompact regulator chart, the same notation denotes a weighted Sobolev class with the decay needed for all integrations by parts. If a density does not have a well-defined finite score, the objective below is assigned the extended value $+\infty$. The regulator maps the extended master curvature to a finite vector $\mathbf{F}_{\mathrm{M}}^{\mathrm{ext},a,N}(x)$. Introduce the finite direct sum

$$\mathscr{R}_{a,N} := \mathscr{R}_{\mathrm{F}} \oplus \mathscr{R}_{\mathrm{u}} \oplus \mathscr{R}_{\mathrm{th}} \oplus \mathscr{R}_{\mathrm{NS}}, \quad (905)$$

where every summand, its inner product, and its transformation law are part of the finite-regulator data.

Fix positive reference scales $(\ell_{\mathrm{F}}, \ell_{\mathrm{u}}, \ell_{\mathrm{th}}, \ell_{\mathrm{NS}})$ with the dimensions of the four channels. Let $F_1, \dots, F_m \in C^2_b(H_N)$ be a declared family of hydrodynamic test functions. Write $\mathcal{L}^u_{a,N}$ for the generator of (893) under a deterministic Markov feedback $u = u(t,x)$, and let $\mathcal{L}^{\mathrm{NS}}_N$ be (1020). The controlled finite-test projection defect is

$$r^{a,N;u}_{\mathrm{NS},\alpha}(t,x) := \mathcal{L}^u_{a,N}(F_\alpha \circ \Pi^{a,N}_{\mathrm{NS}})(x) - \mathcal{L}^{\mathrm{NS}}_N F_\alpha\big(\Pi^{a,N}_{\mathrm{NS}}(x)\big), \qquad 1 \le \alpha \le m. \quad (906)$$

The reference defect is $\mathbf{r}_{\mathrm{NS}}^{a,N;0}$. Since the control changes only the drift,

$$r_{\mathrm{NS},\alpha}^{a,N;u} = r_{\mathrm{NS},\alpha}^{a,N;0} + \left\langle \mathbb{B}_{0,a,N} u, \nabla(F_\alpha \circ \Pi_{\mathrm{NS}}^{a,N}) \right\rangle . \tag{907}$$

Thus the controlled defect must be used when the projected controlled law is being compared with Navier–Stokes; the reference defect is used only for the uncontrolled branch. Vanishing for a finite test family means finite weak generator matching. Equality of generators, and hence equality of laws, requires a determining core together with well-posedness of both martingale problems.

Proposition 48 (Coordinate identification of a projected diffusion). *Fix a regulator and a deterministic Markov control. In a Euclidean chart, let the nonexplosive mother diffusion have generator $\mathcal{L}_t = b_t \cdot \nabla + \frac{1}{2} a_t : D^2$, with $a_t = \Sigma_t \Sigma_t^{\mathsf{T}}$, and let $\Pi : \mathcal{X}_{a,N} \to \mathbb{R}^d$ be C^2. Define*

$$\begin{aligned} c_i(t,x) &= \mathcal{L}_t \Pi_i(x), \\ A_{ij}(t,x) &= \mathcal{L}_t(\Pi_i \Pi_j)(x) - \Pi_i(x) c_j(t,x) - \Pi_j(x) c_i(t,x) \\ &= \nabla \Pi_i(x)^{\mathsf{T}} a_t(x) \nabla \Pi_j(x). \end{aligned} \tag{908}$$

Suppose $c(t,x) = \beta(t, \Pi(x))$ and $A(t,x) = \mathsf{a}(t, \Pi(x))$, where the target diffusion with generator $\mathcal{K}_t = \beta \cdot \nabla + \frac{1}{2} \mathsf{a} : D^2$ has a well-posed, nonexplosive martingale problem. Then $\Pi(X_t)$ has the target law with the projected initial distribution. Conversely, pointwise generator matching on the coordinate and quadratic tests y_i and $y_i y_j$, $1 \le i \le j \le d$, implies these coefficient equalities. The tests are understood locally, with stopping and smooth bounded extensions where an unbounded test is not in the global generator domain.

Proof. The product rule for a second-order generator gives $\mathcal{L}_t(fg) = f \mathcal{L}_t g + g \mathcal{L}_t f + \nabla f^{\mathsf{T}} a_t \nabla g$, proving (908). For $y = \Pi(x)$, the ordinary chain rule for first and second derivatives gives

$$\mathcal{L}_t(F \circ \Pi)(x) = c(t,x) \cdot \nabla F(y) + \tfrac{1}{2} A(t,x) : D^2 F(y). \tag{909}$$

Indeed, its second derivative is

$$D^2(F \circ \Pi) = \sum_i (\partial_i F) D^2 \Pi_i + \sum_{ij} (\partial_{ij} F) \nabla \Pi_i \nabla \Pi_j^{\mathsf{T}}. \tag{910}$$

The first contribution is already included in c; omitting it would lose the Itô correction for a nonlinear projection.

For a compactly supported smooth F, Itô's formula, localized on exhausting compact sets, now shows that $F(\Pi(X_t)) - F(\Pi(X_0)) - \int_0^t \mathcal{K}_s F(\Pi(X_s))\, \mathrm{d}s$ is a local martingale. The projected process therefore solves the target martingale problem; well-posedness identifies its law. No prior Markov property of the projection is assumed. The coefficient descent through Π is the step that closes its dynamics. For the converse, coordinate tests identify c_i. Subtracting the two first-order product terms from each quadratic test then identifies A_{ij}.

Localization removes the need to assume global integrability of polynomial tests. □

REMARK 49 (Quantitative projection error). *When exact matching fails, define* $r_i = c_i - \beta_i(t,y)$ *and* $r_{ij} = \mathcal{L}_t(\Pi_i\Pi_j) - \mathcal{K}_t(y_iy_j)$, *with* $y = \Pi(x)$. *The diffusion defect is*

$$\delta A_{ij} := A_{ij} - \mathsf{a}_{ij}(t,y) = r_{ij} - y_ir_j - y_jr_i. \tag{911}$$

Thus quadratic-test errors are not themselves covariance errors when the drift also mismatches. Equation (909) *implies the pointwise bound*

$$\big|\mathcal{L}_t(F\circ\Pi) - \mathcal{K}_tF(y)\big| \le |r|\,|\nabla F(y)| + \tfrac{1}{2}\|\delta A\|_{\mathrm{F}}\|D^2F(y)\|_{\mathrm{F}}, \tag{912}$$

where $\|\cdot\|_{\mathrm{F}}$ *denotes the Frobenius norm in the fixed finite-dimensional coordinates. To turn this into an observable error, let* $v(s,y) = \mathbb{E}[F(Y_t) \mid Y_s = y]$ *solve the target backward equation* $\partial_s v + \mathcal{K}_s v = 0$, *with* $v(t,\cdot) = F$. *Assume* $v \in C^{1,2}$, $\sup|\nabla v| \le K_1$, $\sup\|D^2v\|_{\mathrm{F}} \le K_2$, *and the integrability needed to remove stopping in Itô's formula. For matching projected initial laws,*

$$\begin{aligned}\big|\mathbb{E}F(\Pi(X_t)) - \mathbb{E}F(Y_t)\big| \le \int_0^t \big[&K_1\mathbb{E}|r(s,X_s)| \\ &+\tfrac{1}{2}K_2\mathbb{E}\|\delta A(s,X_s)\|_{\mathrm{F}}\big]\,\mathrm{d}s.\end{aligned} \tag{913}$$

This follows by applying Itô's formula to $v(s,\Pi(X_s))$, *subtracting its initial expectation, and using the backward equation. The derivative bounds and the mismatch norms are additional quantitative inputs, not consequences of testing a few arbitrary observables.*

The special coordinate family identifies a local second-order diffusion only because its differential form and coefficient descent are specified. An arbitrary finite family in (906) *does not have that property. Nor does identifying a declared Navier–Stokes target derive its viscosity, forcing, or physical clock from microscopic data. For hydrodynamic use, the projected drift and covariance must first be calculated independently; the formulas above then provide a precise comparison and, when their bounds hold, a finite-time observable estimate.*

For $\rho \in \mathscr{D}_{a,N}$, define the joint channel vector

$$\mathfrak{R}_{a,N}(t,x,\rho,u) := \begin{pmatrix} \ell_{\mathrm{F}}^{-1}\mathbf{F}_{\mathrm{M}}^{\mathrm{ext},a,N}(x) \\ \ell_{\mathrm{u}}^{-1}\mathbb{B}_{0,a,N}(x)u(t,x) \\ \ell_{\mathrm{th}}^{-1}\nabla_x\log(\rho(x)/\pi_\theta(x)) \\ \ell_{\mathrm{NS}}^{-1}\mathbf{r}_{\mathrm{NS}}^{a,N;u}(t,x) \end{pmatrix}. \tag{914}$$

The first entry is the regulated master-curvature channel, the second is the controlled drift displacement, the third is the thermodynamic score relative to the common Gibbs state, and the fourth is the controlled finite-test generator

defect. The first entry is not the Euler residual $\delta\mathcal{S}_{\mathrm{M}}/\delta\mathbb{X}$: varying its norm produces the master Euler equation, whereas setting the curvature entry itself to zero would impose a generally unwarranted flatness condition. If a least-squares equation-residual objective is desired instead, that entry must be replaced by the regulated Euler tuple $\mathcal{E}_{\mathrm{M}}^{a,N}$ from (174); its stationary normal equation can have nonzero-residual critical points and is therefore a different problem.

Let the joint metric be a map

$$\mathbb{H}_{a,N} : \mathcal{X}_{a,N} \times \mathscr{D}_{a,N} \longrightarrow \mathcal{L}_{\mathrm{sa}}(\mathscr{R}_{a,N}), \qquad (x,\rho) \longmapsto \mathbb{H}_{a,N}[x;\rho], \tag{915}$$

which is C^1 in x, Frechet differentiable in ρ, measurable in time when evaluated along a density curve, and uniformly positive:

$$0 < h_- I \preceq \mathbb{H}_{a,N}[x;\rho] \preceq h_+ I < \infty. \tag{916}$$

Its derivatives are locally bounded on the admissible set. In the physical channel decomposition it has the form

$$\mathbb{H}_{a,N}[x;\rho] = \begin{pmatrix} H_{\mathrm{F}} & C_{\mathrm{F}u} & C_{\mathrm{F}th} & C_{\mathrm{F}NS} \\ C_{\mathrm{F}u}^{*} & H_{\mathrm{u}} & C_{\mathrm{u}th} & C_{\mathrm{u}NS} \\ C_{\mathrm{F}th}^{*} & C_{\mathrm{u}th}^{*} & H_{\mathrm{th}} & C_{thNS} \\ C_{\mathrm{F}NS}^{*} & C_{\mathrm{u}NS}^{*} & C_{\mathrm{th}NS}^{*} & H_{\mathrm{NS}} \end{pmatrix}. \tag{917}$$

Here every block may depend on $[x;\rho]$, and * is the adjoint in the declared channel pairings. For real residual spaces it is the transpose. The blocks must descend to the gauge quotient (or transform equivariantly on a gauge slice), and a cross block must be an allowed intertwiner between the two channel representations. In particular, no invariant pairing between unrelated simple Lie algebras is inserted merely to manufacture coupling.

A useful uniform Schur criterion makes positivity explicit. Put $D = \mathrm{diag}(H_{\mathrm{F}}, H_{\mathrm{u}}, H_{\mathrm{th}}, H_{\mathrm{NS}})$ and $C = \mathbb{H} - D$. If every diagonal block is positive and, for some $\varepsilon_H \in (0,1]$,

$$\left\| D^{-1/2} C D^{-1/2} \right\| \le 1 - \varepsilon_H, \tag{918}$$

then $\mathbb{H} \succeq \varepsilon_H D \succ 0$. For two channels this contains the familiar condition

$$\left\| H_1^{-1/2} C H_2^{-1/2} \right\| < 1 \tag{919}$$

when both diagonal blocks are positive. Although an unrestricted unitary change of basis diagonalizes any finite positive matrix, such a change is not physically admissible if it mixes the fixed geometric, control, thermodynamic, and hydrodynamic representations. Hence a cross block is called non-removable only relative to sector-preserving, gauge-equivariant, dimension-preserving changes of variables.

Set

$$q_{a,N}(t,x,\rho,u) := \langle \mathfrak{R}_{a,N}(t,x,\rho,u), \mathbb{H}_{a,N}[x;\rho]\mathfrak{R}_{a,N}(t,x,\rho,u) \rangle \tag{920}$$

and, for $\kappa \geq 0$,

$$\varphi_\kappa(q) := \begin{cases} (e^{\kappa q} - 1)/(4\kappa), & \kappa > 0, \\ q/4, & \kappa = 0. \end{cases} \tag{921}$$

The reference scales and channel pairings are chosen so that q is dimensionless; otherwise κ has the reciprocal dimension of q. The four channel scales are not all lengths. When components within a channel have different physical units, the corresponding scale is a diagonal or block normalization map, equivalently absorbed into the declared channel pairing. In particular, tests F_α of different units require their own observation scales. The precise construction is given in (1495); it also transforms every cross block. A single scalar scale is sufficient only for an already commensurate channel. Let $\mathcal{G}^{\mathrm{term}}_{a,N}(x,\rho)$ be a lower-bounded terminal cost, distinct from the matter field Ψ. On admissible triples satisfying (893), $\rho_t = \rho^u_t$, and the associated Fokker–Planck equation, define

$$\boxed{\begin{aligned} \mathfrak{J}^{a,N}_{\kappa,T}[X,\rho,u] &:= \mathbb{E}^{\mathbb{P}^u}\left[\int_0^T \varphi_\kappa\big(q_{a,N}(t,X_t,\rho_t,u_t)\big)\,\mathrm{d}t + \mathcal{G}^{\mathrm{term}}_{a,N}(X_T,\rho_T)\right] \\ &= \int_0^T \int_{\mathcal{X}_{a,N}} \rho_t(x)\varphi_\kappa(q_{a,N}(t,x,\rho_t,u_t))\,\mathrm{d}x\,\mathrm{d}t \\ &\quad + \int_{\mathcal{X}_{a,N}} \rho_T(x)\mathcal{G}^{\mathrm{term}}_{a,N}(x,\rho_T)\,\mathrm{d}x. \end{aligned}} \tag{922}$$

The second line is written in a fixed regulator chart with respect to coordinate volume $\mathrm{d}x$. If the declared base measure is

$$\nu_{a,N}(\mathrm{d}x) = m_{a,N}(x)\,\mathrm{d}x, \qquad p_t = \frac{\rho_t}{m_{a,N}}, \qquad p_\theta = \frac{\pi_\theta}{m_{a,N}}, \tag{923}$$

then the invariant form is obtained by replacing $\rho_t\,\mathrm{d}x$ with $p_t\,\nu_{a,N}$. In particular, $\nabla \log(\rho_t/\pi_\theta) = \nabla \log(p_t/p_\theta)$. The objective is therefore relative to the declared reference measure and regulator chart; it is not automatically invariant under an arbitrary nonlinear change of coordinates or a change of quotient measure. If $m_{a,N}$, π_θ, or the score reference is varied, their variations must be included in the first variation. The time convention is the one fixed in Section 13.2: $t = t_{\mathrm{s}}/t_{\mathrm{ref}}$. For a positive cost unit C_{ref}, a dimensional version is

$$J_{\mathrm{joint,dim}} = C_{\mathrm{ref}}\mathbb{E}^{\mathbb{P}^u}\left[\int_0^{T_{\mathrm{s}}} \varphi_\kappa(q_{t_{\mathrm{s}}})\frac{\mathrm{d}t_{\mathrm{s}}}{t_{\mathrm{ref}}} + \mathcal{G}^{\mathrm{term}}_{a,N}(X_T,\rho_T)\right], \qquad T = T_{\mathrm{s}}/t_{\mathrm{ref}}. \tag{924}$$

The state and law arguments in this expression remain normalized; they are evaluated at $t = t_{\mathrm{s}}/t_{\mathrm{ref}}$. Choosing $C_{\mathrm{ref}} = E_{\mathrm{ref}}$ gives an energy-valued cost. This is a conversion of the already specified objective, not an additional penalty. It is independent of the physical-time calibration of the fluid projection. The

variables X, ρ, and u in this notation are constrained: ρ must be the law generated by X and u. Treating them as three independent minimization variables without the forward equation would define a different and underconstrained problem.

PROPOSITION 50 (Coercivity and integrability of the joint integrand). *Under* (916)*, for every admissible channel vector,*

$$\varphi_\kappa(q) \geq \frac{q}{4} \geq \frac{h_-}{4}\|\mathfrak{R}\|^2_{\mathscr{R}_{a,N}}, \qquad \varphi'_\kappa(q) = \frac{1}{4}e^{\kappa q}, \qquad \varphi''_\kappa(q) = \frac{\kappa}{4}e^{\kappa q}. \tag{925}$$

For $\kappa = 0$, square integrability of the channels and integrability of the terminal cost make $\mathfrak{J}$ finite. For $\kappa > 0$, finiteness requires exponential integrability of q. Differentiation along a given admissible family q^ε additionally requires a domination condition. Assume first that q^ε_t is differentiable at zero for $(dt \otimes \mathbb{P}^u)$-almost every point, with the path law fixed in this differentiation. A sufficient domination condition is the existence of $\delta > 0$ and an integrable nonnegative envelope K_t such that, for $|\varepsilon| \leq \delta$,

$$|q^\varepsilon_t - q_t| \leq |\varepsilon| K_t, \qquad \mathbb{E}^{\mathbb{P}^u}\int_0^T e^{\kappa(q_t + \delta K_t)}(1 + K_t)\,\mathrm{d}t < \infty. \tag{926}$$

This condition is not implied by an ordinary second-moment estimate. The Lipschitz bound alone does not prove differentiability: the family $q^\varepsilon = q + |\varepsilon|$ is a counterexample. If the path law also varies, its variation must be included through a justified density derivative or a common-noise state-sensitivity argument.

Proof. The metric bound gives $q \geq h_-\|\mathfrak{R}\|^2$. For $q \geq 0$, the elementary inequality $e^{\kappa q} \geq 1 + \kappa q$ gives $\varphi_\kappa(q) \geq q/4$. Direct differentiation gives the remaining identities. The stated integrability assumptions then permit Tonelli's theorem and differentiation under the integral; they do not by themselves prove existence of an optimizer. □

PROPOSITION 51 (Attainment on a compact admissible class). *Let the regulated state chart be a locally compact Polish space. Suppose the admissible Markov pairs (ρ, u) form a nonempty sequentially compact set $\mathcal{A}_{a,N}$, and the forward constraint and initial law are closed in its topology. Require that convergence of admissible pairs implies weak convergence of their finite occupation measures and terminal laws:*

$$\mu_n(dt\,dx) = dt\,\rho_n(t,x)\,dx \implies \mu(dt\,dx), \qquad \nu_n(dx) = \rho_n(T,x)\,dx \implies \nu(dx).$$

The occupation measures have the common mass T. Along each such sequence, suppose that the continuous functions

$$f_n(t,x) = \varphi_\kappa(q_n(t,x)), \qquad g_n(x) = \mathcal{G}^{\mathrm{term}}_{a,N}(x, \rho_n(T))$$

converge locally uniformly to the corresponding functions f, g of the limit pair. Assume uniform integrability with respect to these varying measures, in the precise form

$$\lim_{R\to\infty} \sup_n \left\{ \int (|f_n| - R)_+ \, d\mu_n + \int (|g_n| - R)_+ \, d\nu_n \right\} = 0.$$

For $\kappa > 0$, uniform integrability of $e^{\kappa q_n}$ with respect to μ_n suffices for the running term; a uniform second-moment bound does not suffice. Assume that at least one admissible pair has finite cost. No common positive density bound is imposed on an infinite-volume domain. Then

$$\inf_{(\rho,u)\in\mathcal{A}_{a,N}} \mathfrak{J}^{a,N}_{\kappa,T}[\rho, u] \tag{927}$$

is attained.

Proof. Choose a minimizing sequence and a convergent subsequence supplied by sequential compactness. Closedness makes its limit admissible. Write $T_R(s) = \max(-R, \min(s, R))$. Weak convergence makes the occupation measures uniformly tight. On a compact set, local uniform convergence of f_n gives uniform convergence of $T_R(f_n)$; outside that set both clipped functions have modulus at most R. Consequently

$$\int T_R(f_n) \, d\mu_n \longrightarrow \int T_R(f) \, d\mu$$

for each fixed R. Apply the same argument to the bounded continuous functions $\min(K, (|f_n| - R)_+)$, and then let K increase to infinity. It follows that the integral of $(|f| - R)_+$ is bounded by the uniform tail bound in the hypothesis. Thus f is integrable and its tail vanishes with that bound. Since $|s - T_R(s)| = (|s| - R)_+$, letting R tend to infinity proves $\int f_n \, d\mu_n \to \int f \, d\mu$. The identical argument with (g_n, ν_n) proves terminal-cost convergence. Hence the cost of the admissible limit equals the infimum. Pointwise convergence under moving measures would not justify this argument; the local uniform convergence and the stated measure-dependent tail bounds are essential sufficient conditions here. □

The proposition isolates rather than hides the compactness problem. Its hypotheses can be verified directly for a compact finite state space with a compact control set and uniformly regular positive densities, but they do not follow merely from $\mathbb{H} \succ 0$. Uniqueness is not asserted: the master-curvature channel, the NS defect, and the state-dependent cross blocks are generally nonconvex.

PROPOSITION 52 (Quantitative meaning of the generator channel). *Let*

$$\mathfrak{J}_{\mathrm{run}} := \mathbb{E}^{\mathbb{P}^u} \int_0^T \varphi_\kappa(q_t)\,\mathrm{d}t.$$

Under the lower metric bound in (916)*,*

$$\mathbb{E}^{\mathbb{P}^u} \int_0^T \left|\mathbf{r}_{\mathrm{NS}}^{a,N;u}(t,X_t)\right|^2 \mathrm{d}t \le \frac{4\ell_{\mathrm{NS}}^2}{h_-}\mathfrak{J}_{\mathrm{run}}. \tag{928}$$

For a declared test F_α, assume additionally that its composition with the projection belongs to the extended generator domain with an integrable Dynkin identity: its martingale part is a true martingale, the endpoint values and generator integrals are integrable, and any reflection boundary term vanishes. Bounded smooth tests in the reflecting generator domain, or a square-integrable martingale together with the stated drift integrability, give sufficient conditions. For such tests and $0 \le t \le T$, Dynkin's formula gives

$$\begin{aligned}\left|\mathbb{E}^{\mathbb{P}^u}\left[F_\alpha(U_t^N) - F_\alpha(U_0^N) - \int_0^t \mathcal{L}_N^{\mathrm{NS}} F_\alpha(U_s^N)\,\mathrm{d}s\right]\right| \\ \le 2\ell_{\mathrm{NS}}\sqrt{\frac{t\,\mathfrak{J}_{\mathrm{run}}}{h_-}}.\end{aligned} \tag{929}$$

A zero joint running cost forces every normalized channel to vanish almost everywhere. A positive-cost minimizer generally trades the channels and need not make the Navier–Stokes defect vanish.

Proof. The fourth component of $\mathfrak{R}$, together with (925), gives

$$\varphi_\kappa(q_t) \ge \frac{h_-}{4\ell_{\mathrm{NS}}^2}\left|\mathbf{r}_{\mathrm{NS}}^{a,N;u}(t,X_t)\right|^2.$$

Integrating proves (928). Dynkin's formula, the definition (906), Cauchy–Schwarz in time, and then Cauchy–Schwarz in probability give (929). The final assertion follows from strict positivity of the joint metric and nonnegativity of φ_κ. □

Writing R_i for the four normalized entries of $\mathfrak{R}$, the quadratic argument expands as

$$q = \sum_i \langle R_i, H_i R_i\rangle + 2\sum_{i<j} \mathrm{Re}\langle R_i, C_{ij} R_j\rangle. \tag{930}$$

For example, it contains

$$\frac{2}{\ell_{\mathrm{F}}\ell_{\mathrm{th}}}\,\mathrm{Re}\big\langle \mathbf{F}_{\mathrm{M}}^{\mathrm{ext},a,N}, C_{\mathrm{F}th}\nabla\log(\rho/\pi_\theta)\big\rangle \tag{931}$$

and the analogous F–NS term with coefficient $2/(\ell_{\mathrm{F}}\ell_{\mathrm{NS}})$. Thus a nonzero admissible cross block gives bilinear cross-channel coupling already at $\kappa = 0$. If all cross blocks vanish and $\kappa = 0$, the running integrand is algebraically

additive by channel, although the optimization problem can remain coupled through shared states, coefficients, dynamics, or terminal data. If $\kappa > 0$, even a block-diagonal metric is non-additive, since for distinct channel energies q_i, q_j,

$$\frac{\partial^2}{\partial q_i \partial q_j} \varphi_\kappa \left(\sum_r q_r \right) = \frac{\kappa}{4} e^{\kappa \sum_r q_r} > 0. \tag{932}$$

This is outer nonlinear coupling, distinct from a representation-theoretic cross pairing. The time integral in (922) is nevertheless an ordinary time-additive running cost; it is not the risk-sensitive criterion $\kappa^{-1} \log \mathbb{E} \exp[\kappa \int_0^T q_t \, \mathrm{d}t]$.
Recovery of the Girsanov direction. Suppose $\kappa = 0$, retain only the control channel, restrict it to the noise range, and choose

$$H_{\mathrm{u}} = \ell_{\mathrm{u}}^2 \mathbb{M}^\dagger \quad \text{on } \operatorname{Ran} \mathbb{M}^{1/2}. \tag{933}$$

If $\mathbb{B}_{0,a,N} u \in \operatorname{Ran} \mathbb{M}^{1/2}$, the minimum Brownian shift is progressively measurable on canonical path space, its stochastic exponential is a true martingale, and the tilted martingale problem is unique in law, then Girsanov's formula gives

$$\frac{1}{4} \mathbb{E}^{\mathbb{P}^u} \int_0^T \left\langle \mathbb{B}_{0,a,N} u_t, \mathbb{M}^\dagger \mathbb{B}_{0,a,N} u_t \right\rangle \mathrm{d}t = \theta D_{\mathrm{KL}}(\mathbb{P}^u \,\|\, \mathbb{P}^0). \tag{934}$$

Thus the quadratic control block is the KL cost and is not added again to the joint functional. The full joint functional is not itself a relative entropy. For $\kappa > 0$, for nonzero control cross blocks, or away from the calibration (933), no such identification holds. Novikov integrability and (926) are distinct assumptions. Likewise, the thermodynamic-score block is a Fisher-information-type channel; it equals the entropy-production norm only after calibrating it to the range of $\mathbb{M}$. Since the GENERIC-inspired degeneracy condition makes $\mathbb{M}$ semidefinite, that calibration is positive definite only on the corresponding range quotient.

13.4.1. *Complete first variation.* We first record the differential of the scalar argument. For an admissible tangent (ξ, η, v), where ξ varies the state, η varies the density, and v varies the feedback, put

$$\dot{\mathfrak{R}} := D_x \mathfrak{R}[\xi] + D_\rho \mathfrak{R}[\eta] + D_u \mathfrak{R}[v], \qquad \dot{\mathbb{H}} := D_x \mathbb{H}[\xi] + D_\rho \mathbb{H}[\eta]. \tag{935}$$

At fixed x and fixed π_θ, the two characteristic derivatives are

$$D_\rho R_{\mathrm{th}}[\eta] = \ell_{\mathrm{th}}^{-1} \nabla(\eta/\rho), \qquad D_u R_{\mathrm{u}}[v] = \ell_{\mathrm{u}}^{-1} \mathbb{B}_{0,a,N} v. \tag{936}$$

If the controlled NS defect is used, its control derivative is

$$\left(D_u r_{\mathrm{NS}}^{a,N;u}[v] \right)_\alpha = \left\langle \mathbb{B}_{0,a,N} v, \nabla(F_\alpha \circ \Pi_{\mathrm{NS}}^{a,N}) \right\rangle. \tag{937}$$

Self-adjointness gives the exact pointwise identity

$$\boxed{\dot{q} = 2 \operatorname{Re} \langle \dot{\mathfrak{R}}, \mathbb{H} \mathfrak{R} \rangle + \langle \mathfrak{R}, \dot{\mathbb{H}} \mathfrak{R} \rangle.} \tag{938}$$

This identity retains the field- and law-dependent metric variation. It is the differential of the pointwise quadratic argument, not yet the variation of the expectation or of the law.

For the full law variation, restrict for clarity to deterministic Markov feedbacks. Let $u^\varepsilon = u + \varepsilon v$, $\rho^\varepsilon = \rho + \varepsilon\eta + o(\varepsilon)$, and keep the initial density fixed. For law-independent base coefficients, differentiating the forward equation gives

$$\partial_t \eta_t = (\mathcal{L}^{u_t}_{a,N})^* \eta_t - \nabla\cdot(\rho_t \mathbb{B}_{0,a,N} v_t)\,, \qquad \eta_0 = 0, \qquad \int_{\mathcal{X}_{a,N}} \eta_t(x)\,\mathrm{d}x = 0, \tag{939}$$

with the linearized zero-flux boundary condition. A law-dependent drift or feedback contributes its additional Frechet derivative to this equation.

Proposition 53 (Full Eulerian first variation). *Assume* (926)*, differentiability of the residuals, metric, and terminal functional, and domination sufficient to differentiate under the integrals. If* (η, v) *satisfies* (939)*, then*

$$\begin{aligned} D\mathfrak{J}[\rho,u][\eta,v] = \int_0^T \int_{\mathcal{X}_{a,N}} \Big\{ & \eta\, \varphi_\kappa(q) \\ & + \rho\, \varphi'_\kappa(q) \big[2\,\mathrm{Re}\langle \dot{\mathfrak{R}}^E, \mathbb{H}\mathfrak{R}\rangle + \langle \mathfrak{R}, D_\rho \mathbb{H}[\eta]\mathfrak{R}\rangle \big] \Big\}\,\mathrm{d}x\,\mathrm{d}t \\ & + \int_{\mathcal{X}_{a,N}} \Big\{ \eta_T \mathcal{G}^{\mathrm{term}}_{a,N}(x,\rho_T) + \rho_T D_\rho \mathcal{G}^{\mathrm{term}}_{a,N}(x,\rho_T)[\eta_T] \Big\}\,\mathrm{d}x, \end{aligned} \tag{940}$$

where, at fixed Eulerian coordinate x*,*

$$\dot{\mathfrak{R}}^E = D_\rho \mathfrak{R}[\eta] + D_u \mathfrak{R}[v], \qquad \varphi'_\kappa(q) = \tfrac{1}{4} e^{\kappa q}. \tag{941}$$

If the configuration itself is varied by ξ*, the bracket in* (940) *additionally contains*

$$2\,\mathrm{Re}\langle D_x \mathfrak{R}[\xi], \mathbb{H}\mathfrak{R}\rangle + \langle \mathfrak{R}, D_x \mathbb{H}[\xi]\mathfrak{R}\rangle, \tag{942}$$

together with the corresponding state and terminal variations.

Proof. Use the Eulerian representation in (922). The product rule produces the outer-density term $\eta\varphi_\kappa(q)$, while the chain rule and (938) produce the second term. Applying the same product rule to the terminal integral gives its two displayed terms. The domination assumption justifies interchanging derivative and integration. Equation (939) identifies the admissible tangent to the law constraint. This proves the formula. □

There are two equivalent ways to account for the changing path law, and they must not be combined. The Eulerian formula above uses the outer-density terms and the linearized forward equation. In a fixed-noise strong realization, one instead differentiates the state process. For this strong formulation, assume a boundaryless chart, a periodic state space, or nonexplosive dynamics on the full Euclidean chart, with differentiable coefficients and feedback. At a reflecting

boundary, differentiation of the Skorokhod reflection and its local-time term is additionally required; it is not included in the formula below. On the stated boundaryless branch the tangent Y_t satisfies

$$\begin{aligned} \mathrm{d}Y_t &= [D_x b^u(t,X_t)Y_t + \mathbb{B}_{0,a,N}(X_t)v(t,X_t)]\,\mathrm{d}t \\ &\quad + D_x\sqrt{2\theta\mathbb{M}}(X_t)[Y_t]\,\mathrm{d}W_t, \qquad Y_0 = 0. \end{aligned} \tag{943}$$

Then $\xi = Y$, η is the density tangent in (939), and expectation is taken on the fixed noise space. With independent state and control arguments in the residual, put

$$\dot{\mathfrak{R}}^{\mathrm{str}} := D_x\mathfrak{R}[Y] + D_\rho\mathfrak{R}[\eta] + D_u\mathfrak{R}[v + D_x u\, Y]. \tag{944}$$

Here $D_x\mathfrak{R}$ holds the instantaneous control argument fixed. The additional term $D_x u\, Y$ differentiates $u^\varepsilon(t, X_t^\varepsilon)$; it is absent only for an open-loop state-independent control. Equivalently, it can be absorbed in the state derivative of the composed-feedback residual, but not counted in both places. The derivative $D_x b^u$ in (943) already differentiates the composed drift. the complete strong first variation is

$$\boxed{\begin{aligned} D\mathfrak{J}(u)[v] = \mathbb{E}\Bigg[\int_0^T \varphi_\kappa'(q_t)\Big\{ & 2\,\mathrm{Re}\langle \dot{\mathfrak{R}}_t^{\mathrm{str}}, \mathbb{H}_t\mathfrak{R}_t\rangle \\ & + \langle \mathfrak{R}_t, [D_x\mathbb{H}_t[Y_t] + D_\rho\mathbb{H}_t[\eta_t]]\mathfrak{R}_t\rangle \Big\}\,\mathrm{d}t \\ & + D_x\mathcal{G}_{a,N}^{\mathrm{term}}(X_T,\rho_T)[Y_T] + D_\rho\mathcal{G}_{a,N}^{\mathrm{term}}(X_T,\rho_T)[\eta_T] \Bigg]. \end{aligned}} \tag{945}$$

No likelihood term is added to (945). Alternatively, on canonical path space, if

$$Z_T^v := \int_0^T \left\langle (\sqrt{2\theta\mathbb{M}})^\dagger \mathbb{B}_{0,a,N} v_t,\, \mathrm{d}W_t^u \right\rangle \tag{946}$$

is square integrable and the Girsanov hypotheses hold, then for the complete canonical cost C^u,

$$D\mathfrak{J}(u)[v] = \mathbb{E}^{\mathbb{P}^u}\left[\dot{C}^{\mathrm{can}} + C^u Z_T^v\right]. \tag{947}$$

Here the coordinate path is held fixed, so $\dot{C}^{\mathrm{can}}$ contains the direct u- and ρ-derivatives but no state tangent Y. Adding both Y and Z_T^v would count the same change of law twice.

For completeness, the constrained first-order system can be displayed with a law multiplier $\lambda(t,x)$. Introduce the augmented functional

$$\mathscr{L}(\rho,u,\lambda) := \mathfrak{J}_{\kappa,T}^{a,N}[\rho,u] - \int_0^T \int_{\mathcal{X}_{a,N}} \lambda\big(\partial_t\rho - (\mathcal{L}_{a,N}^u)^*\rho\big)\,\mathrm{d}x\,\mathrm{d}t. \tag{948}$$

Variation with respect to λ gives the forward equation $\partial_t \rho = (\mathcal{L}^u_{a,N})^* \rho$, with the prescribed initial law. Write

$$\mathfrak{g}_\rho(t,x) := \frac{\delta}{\delta \rho(x)} \int_{\mathcal{X}_{a,N}} \rho(y) \varphi_\kappa(q(t,y,\rho,u))\,\mathrm{d}y, \tag{949}$$

$$\mathfrak{g}_T(x) := \frac{\delta}{\delta \rho_T(x)} \int_{\mathcal{X}_{a,N}} \rho_T(y) \mathcal{G}^{\mathrm{term}}_{a,N}(y,\rho_T)\,\mathrm{d}y. \tag{950}$$

To specify the density derivative and its boundary condition, write $W_{\mathrm{th}} = (\mathbb{H}\mathfrak{R})_{\mathrm{th}}$ and

$$K_{\mathrm{th}} = \frac{2\rho \varphi'_\kappa(q)}{\ell_{\mathrm{th}}} W_{\mathrm{th}}. \tag{951}$$

The score contribution is

$$\int_\Omega K_{\mathrm{th}} \cdot \nabla(\eta/\rho)\,\mathrm{d}x = -\int_\Omega \frac{\operatorname{div} K_{\mathrm{th}}}{\rho} \eta\,\mathrm{d}x \quad + \int_{\partial\Omega} (K_{\mathrm{th}} \cdot n) \frac{\eta}{\rho}\,\mathrm{d}S. \tag{952}$$

On a periodic or boundaryless domain the surface term is absent; on an unbounded domain its vanishing requires the stated decay. On a bounded domain with free density variations at the boundary, impose the natural cost condition $K_{\mathrm{th}} \cdot n = 0$, or retain the corresponding boundary Euler equation. Fixed boundary density instead gives $\eta|_{\partial\Omega} = 0$. Reflecting probability flux alone does not eliminate this surface term: cross blocks can give W_{th} a normal component.

If the law derivative of the metric has the bulk representation

$$\int_\Omega \rho \varphi'_\kappa(q) \langle \mathfrak{R}, D_\rho \mathbb{H}[\eta]\mathfrak{R}\rangle\,\mathrm{d}x = \int_\Omega m_\rho(x)\eta(x)\,\mathrm{d}x, \tag{953}$$

the declared residual yields

$$\mathfrak{g}_\rho = \varphi_\kappa(q) - \frac{\operatorname{div} K_{\mathrm{th}}}{\rho} + m_\rho. \tag{954}$$

The representation and regularity of m_ρ are assumed when a classical bulk equation is used; otherwise it is a functional derivative in the chosen dual space. The derivative on normalized laws is defined up to a time-dependent spatial constant, which can be absorbed into the multiplier. With the cost and forward-adjoint boundary terms eliminated under these conditions, variation with respect to ρ gives the adjoint equation

$$-\partial_t \lambda - \mathcal{L}^u_{a,N} \lambda = \mathfrak{g}_\rho, \qquad \lambda(T,\cdot) = \mathfrak{g}_T. \tag{955}$$

The minus sign in (948) fixes this convention: time integration by parts gives the terminal coefficient $\mathfrak{g}_T - \lambda(T,\cdot)$ and the interior coefficient $\mathfrak{g}_\rho + \partial_t\lambda + \mathcal{L}^u_{a,N}\lambda$. The initial density is fixed, so there is no free initial boundary variation. On a smooth bounded chart with reflecting forward probability flux, the corresponding fixed-domain backward condition is $n \cdot a\nabla\lambda = 0$, where $a = 2\theta\mathbb{M}$. This removes the adjoint surface term; it is separate from $K_{\mathrm{th}} \cdot n = 0$. One may restrict admissible

control variations to $n \cdot \mathbb{B}_{0,a,N} v = 0$ to preserve that boundary domain. If controls change the normal flux or the domain itself, the linearized boundary law and its associated surface variation must instead be retained. The displayed bulk system alone is not the complete boundary-control problem. For an open control set, stationarity is the variational identity

$$D_u \Big[\int \rho \, \varphi_\kappa(q) \, \mathrm{d}x + \int \lambda (\mathcal{L}^u_{a,N})^* \rho \, \mathrm{d}x \Big] [v] = 0 \tag{956}$$

for every admissible variation v; for a closed convex control set it is replaced by the corresponding normal-cone inequality. Configuration variations add $D_x \mathbb{H}$, $D_x \mathfrak{R}$, induced law variations, and the gauge/constraint tangent conditions. Thus this forward–adjoint system is distinct from both the pointwise master Euler equation and the density-space Bellman equation below.

13.4.2. *Existence in a positive finite-state realization.* The first variation identifies admissible stationary points. To show that a minimizing control actually exists in a concrete class, consider an additional finite-state realization of the regulated law. Its nodes $x_1, \dots, x_K$ represent declared physical configurations, and $p_i(t)$ denotes a probability, not a continuum density. Let $U \subset \mathbb{R}^d$ be nonempty, compact, and convex, and let $Q(u) = Q_0 + \sum_{r=1}^d u^r Q_r$ be a continuous affine matrix with nonnegative off-diagonal entries and zero row sums for every $u \in U$. Controls may encode a separate feedback at each node by taking a product control set. The forward law is

$$\dot{p} = Q(u)^{\mathsf{T}} p, \qquad p_i(0) > 0, \qquad \sum_{i=1}^K p_i(0) = 1. \tag{957}$$

With a fixed positive reference probability π, a discrete score channel can be defined by $D_i \log(p/\pi)$, where D_i is a declared finite-difference matrix annihilating constants. This does not identify a probability vector with a smooth field density; convergence of the score approximation is a further discretization question.

Suppose that the joint residual at node i has the form $R_i(p,u) = r_i(p) + B_i(p)u$, with coefficients continuous for positive p, and that the field- and law-dependent joint metric $H_i(p)$ is continuous, symmetric, and positive definite there. Cross-channel blocks are allowed. The affine form includes an affine controlled-generator defect and the control residual, while the score enters $r_i(p)$. Keep H_i independent of u in this realization. The objective is

$$\mathfrak{J}_K(u) = \int_0^T \sum_{i=1}^K p_i(t) \varphi_\kappa\big(R_i^{\mathsf{T}} H_i R_i\big) \, \mathrm{d}t + G_K(p(T)), \qquad \kappa \geq 0, \tag{958}$$

where G_K is continuous on the attainable probability vectors. The sum is the expectation over states; it is not a sum of independent physical-sector objectives. The same coupled residual and metric are used at each node.

PROPOSITION 54 (Attainment of the regulated joint minimum). *Under the preceding assumptions,* (958) *attains its minimum over measurable U-valued controls on every finite horizon. The controlled probabilities remain strictly positive, the exponential cost is integrable, and a minimizer satisfies the forward law. This is an existence result; it does not imply uniqueness, smoothness of a Bellman value, or convergence to the diffusion or field-theory continuum.*

Proof. Compactness of U bounds all rates. Choose $\Lambda \geq \sup_{u\in U,i}(-Q_{ii}(u))$. The forward equation preserves the probability simplex, and its componentwise inflow is nonnegative. Thus $\dot{p}_i \geq -\Lambda p_i$, which gives

$$p_i(t) \geq p_i(0)e^{-\Lambda t} \geq \delta, \qquad \delta := e^{-\Lambda T} \min_i p_i(0) > 0. \tag{959}$$

The attainable laws consequently lie in the compact set $\Delta_\delta = \{p : \sum_i p_i = 1,\ p_i \geq \delta\}$, and bounded rates give a common Lipschitz bound in time. On $\Delta_\delta \times U$, all residuals and metrics are bounded, the score logarithms are finite, and the running and terminal costs are bounded. In particular no unproved exponential moment is needed in this finite-state realization.

Take a minimizing sequence u_n. It is bounded in $L^2([0,T];\mathbb{R}^d)$ and therefore has a weakly convergent subsequence $u_n \rightharpoonup u$. The set of U-valued controls is norm-closed and convex, hence weakly closed; thus $u(t) \in U$ almost everywhere. Arzela–Ascoli gives $p_n \to p$ uniformly after taking another subsequence. In the integrated forward equation, the terms $\int_0^t u_n^r(s)Q_r^{\mathsf{T}}p_n(s)\,\mathrm{d}s$ converge to the corresponding terms for (u,p): uniform convergence controls the factor $p_n - p$, and weak convergence applies to $1_{[0,t]}Q_r^{\mathsf{T}}p$. Hence p solves (957) with control u.

At fixed p, set $q_i = R_i^{\mathsf{T}}H_iR_i$. Direct differentiation shows convexity in the control:

$$\begin{aligned} \nabla_u^2\varphi_\kappa(q_i) &= 2\varphi_\kappa'(q_i)B_i^{\mathsf{T}}H_iB_i + \varphi_\kappa''(q_i)\nabla_u q_i \nabla_u q_i^{\mathsf{T}} \succeq 0, \\ \varphi_\kappa'(q) &= \tfrac{1}{4}e^{\kappa q}, \qquad \varphi_\kappa''(q) = \tfrac{\kappa}{4}e^{\kappa q}. \end{aligned} \tag{960}$$

Continuity on the compact domain implies uniform continuity in p. Replacing p_n by p in the running cost therefore changes its integral by a quantity tending to zero, uniformly for $u_n \in U$. The remaining integral at fixed p is convex and continuous in the bounded control domain, and its extension by $+\infty$ outside that domain is weakly lower semicontinuous. Consequently $\mathfrak{J}_K(u) \leq \liminf_n \mathfrak{J}_K(u_n)$, using continuity of $G_K(p_n(T))$. Since the sequence is minimizing and u is admissible, the infimum is attained. □

This construction gives a directly computable nonempty class in which law dependence, field dependence, and nonzero cross blocks coexist with attainment.

Strict convexity at fixed p does not imply convexity of the full law-constrained problem, so multiple optimal histories remain possible. To approximate the diffusion problem, one must additionally establish generator consistency, tightness, score convergence, and uniform integrability of the costs; finite-state attainment alone does not justify a regulator limit.

13.4.3. *Dynamic programming and the status of the sector equations.* A concrete finite-state example. To make the attainment class explicit, take three nodes, initial law $p(0) = \pi = (0.2, 0.3, 0.5)$, horizon $T = 5$, $U = [-0.2, 0.2]$, and

$$Q(u) = \begin{pmatrix} -0.4 - u & 0.4 + u & 0 \\ 0.2 & -0.5 & 0.3 \\ 0.1 & 0 & -0.1 \end{pmatrix}. \tag{961}$$

All off-diagonal rates are nonnegative and each row sums to zero. Here π is a prescribed score reference, not an asserted invariant law of every $Q(u)$. A Gibbs-invariant branch would require the additional calibration of the reference generator. The maximum exit rate is $\Lambda = 0.6$. With cyclic indices, put $s_i = \log(p_i/\pi_i) - \log(p_{i-1}/\pi_{i-1})$, and choose

$$\begin{aligned} R_i &= (i-2,\ u,\ s_i,\ 0.1(i-2) + 0.5u)^{\mathsf{T}}, \\ H_i &= \begin{pmatrix} 1 + 0.1(i-1) & 0 & 0.12 & 0 \\ 0 & 1 & 0 & 0.08 \\ 0.12 & 0 & 1 + p_i & 0 \\ 0 & 0.08 & 0 & 1.2 \end{pmatrix}, \qquad i = 1, 2, 3. \end{aligned} \tag{962}$$

The two coupled principal pairs have positive Schur complements for every p in the probability simplex; hence $H_i \succ 0$. Set $\kappa = 0.08$ and $G_K = 0$. This example contains a discrete score, an affine controlled defect, and law-dependent nonzero cross blocks without losing the compactness or convex control slices used in Proposition 54.

Figure 14 shows the forward law under the prescribed feasible policy $u(t) = 0.15 \sin t$, and the cost slices at its terminal law. The policy is not asserted to be an optimizer. Adaptive eighth-order integration with relative tolerance 10^{-12} and absolute tolerance 10^{-14} preserves normalization to 2.23×10^{-16} and satisfies the positivity bound $p_i(t) \geq p_i(0)e^{-0.6t}$ at all 201 displayed times. Central differences with step 10^{-4} on 303 node/control pairs agree with (960) to a maximum normalized error 2.94×10^{-8}. Separately, 300 nonlinear-projection cases verify the chain rule (909) to normalized finite-difference error 2.27×10^{-8}, and the covariance recovery formula (911) to absolute error 4.11×10^{-15}. A periodic 4096-point density calculation tests (954), including metric dependence and the score derivative, against a central density variation; its absolute discrepancy is 8.27×10^{-13}. All inputs are

synthetic and dimensionless. These finite calculations illustrate the stated formulas, not a parameter fit or a continuum existence proof.

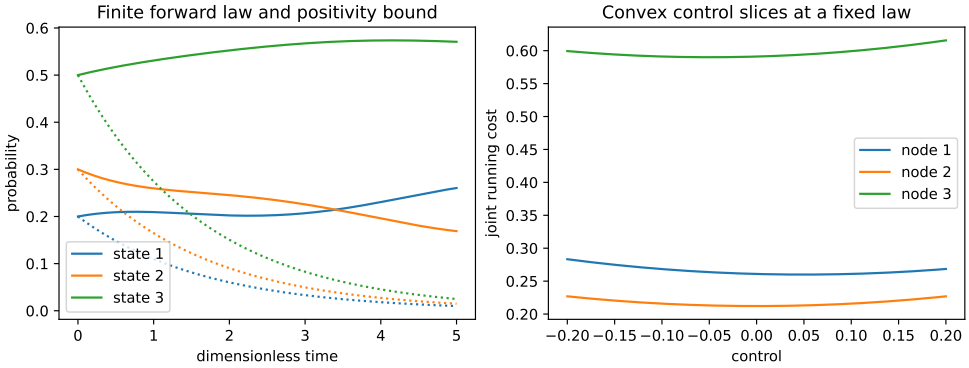


Figure 14. A coupled finite-state realization. Solid curves are the probabilities under a prescribed feasible control; dotted curves are their analytical lower bounds. The right panel shows convex control slices at one fixed law, not convexity of the full constrained problem.

13.4.4. *A globally optimal coupled law-control branch.* The preceding three-node calculation illustrates a feasible control. A separate two-node branch permits an exact optimality proof and a uniform error bound when the full logarithmic thermodynamic force and a state-dependent residual metric are restored. The verification method is the standard finite-horizon HJB and completion-of-squares argument [111]; the particular normalization and perturbation bound are specified below. This is a regulated law-control model, not a solution of the complete geometric field-control problem.

Let the reference probabilities be $\pi_0 = \pi_1 = 1/2$, and write the probability of node 1 as $p_1 = 1/2 + z$. The transition rates are $q_{01} = k + u$ and $q_{10} = k - u$, where $k > 0$. Controls in this branch are measurable deterministic functions of time, applied to both nodes with the declared rate convention. They are not arbitrary state-adapted controls of an individual jump trajectory. The forward equation is consequently

$$\dot{z} = (k+u)(1/2 - z) - (k-u)(1/2+z) = -2kz + u. \tag{963}$$

Fix $0 < \delta < 1/2$, $|z(0)| \le \delta$, and $|u(t)| \le u_{\max} := 2k\delta$. The rates remain strictly positive. At $z = \delta$ the velocity is nonpositive, and at $z = -\delta$ it is nonnegative. Equivalently, variation of constants gives

$$|z(t)| \le e^{-2kt}\delta + \int_0^t e^{-2k(t-s)} 2k\delta \, \mathrm{d}s = \delta. \tag{964}$$

Thus all admissible laws remain a fixed distance from the simplex boundary.

For dimensionless constants $a, r > 0$, $c \in \mathbb{R}$, $ar > c^2$, and $\beta \geq 0$, define

$$J_0(t, z; u) = \frac{1}{4} \int_t^T \left(a z_s^2 + 2 c z_s u_s + r u_s^2 \right) \mathrm{d}s + \frac{\beta}{4} z_T^2. \tag{965}$$

The residual metric $H_0 = \left(\begin{smallmatrix} a & c \\ c & r \end{smallmatrix}\right)$ is positive definite. The mixed term is a genuine coupling in these declared probability/control coordinates. An algebraic change of coordinates can complete its square, but cannot at the same time leave both the forward equation and the interpretation of the controlled rates unchanged.

Proposition 55 (Exact optimal control in the invariant interval). *Set*

$$P_\pm = -2kr - c \ \pm \sqrt{(2kr + c)^2 + ar - c^2}, \qquad \Delta_P = P_+ - P_- > 0. \tag{966}$$

Suppose

$$|c| + \max\{\beta, P_+\} \leq 2kr. \tag{967}$$

Then the value of (965) *is* $V_0(t, z) = P(t) z^2 / 4$, *where*

$$\begin{aligned} \dot{P} &= 4kP + \frac{(c + P)^2}{r} - a, \qquad P(T) = \beta, \\ R(t) &= \frac{\beta - P_+}{\beta - P_-} \exp\left[-\frac{\Delta_P}{r} (T - t) \right], \qquad P(t) = \frac{P_+ - R(t) P_-}{1 - R(t)}. \end{aligned} \tag{968}$$

The unique optimal control, up to equality almost everywhere along the optimal law, is $u_*(t) = -(c + P(t)) z_*(t) / r$.

Proof. The determinant condition implies $P_+ > 0 > P_-$. In reversed time $\tau = T - t$, the Riccati equation becomes $\partial_\tau P = -(P - P_+)(P - P_-)/r$. Its solution remains between β and P_+; integrating the ratio $(P - P_+)/(P - P_-)$ gives (968). Since $(\beta - P_+)/(\beta - P_-) < 1$ and the exponential lies in $(0, 1]$, the denominator never vanishes on the finite horizon. In particular $0 \leq P(t) \leq \max\{\beta, P_+\}$.

The finite-horizon Bellman equation in the interior is

$$0 = \partial_t V_0 + \min_{|u| \leq u_{\max}} \left\{ \frac{a z^2 + 2 c z u + r u^2}{4} + (-2kz + u) \partial_z V_0 \right\}. \tag{969}$$

Substitution of $V_0 = P z^2 / 4$ gives the control-dependent expression $r u^2 / 4 + (c + P) z u / 2$, whose unconstrained minimizer is $-(c + P) z / r$. Condition (967) bounds its absolute value by $2k\delta$ throughout the invariant interval. The remaining coefficient of z^2 is $(\dot{P} + a - 4kP - (c + P)^2 / r)/4$, which is zero.

For completeness, global optimality does not require invoking comparison for this boundary problem. Along any admissible absolutely continuous law, differentiation and the Riccati equation give

$$\frac{a z_s^2 + 2 c z_s u_s + r u_s^2}{4} + \frac{\mathrm{d}}{\mathrm{d}s} \frac{P(s) z_s^2}{4} = \frac{r}{4} \left(u_s + \frac{c + P(s)}{r} z_s \right)^2. \tag{970}$$

Integrating, including the terminal value, yields

$$J_0(t,z;u) - V_0(t,z) = \frac{r}{4}\int_t^T \left(u_s + \frac{c+P(s)}{r} z_s\right)^2 \,\mathrm{d}s \geq 0. \tag{971}$$

The displayed feedback is admissible and makes this integral zero. Conversely, equality forces that feedback almost everywhere; uniqueness of the resulting linear forward equation proves the claimed uniqueness. □

Restoring the logarithmic force and metric variation. The exact normalized two-node force is

$$d(z) = \frac{1}{4}\left[\log\frac{p_1}{\pi_1} - \log\frac{p_0}{\pi_0}\right] = \frac{1}{2}\operatorname{artanh}(2z), \qquad d'(z) = \frac{1}{1-4z^2}. \tag{972}$$

The factor $1/4$ fixes the residual scale so that $d(z) = z + O(z^3)$. For $\zeta \geq 0$ and a symmetric positive semidefinite matrix D, let $H(z) = H_0 + \zeta z^2 D$ and $R_z = (d(z), u)^{\mathsf{T}}$. The exact branch uses running cost $\ell_{\mathrm{ex}}(z,u) = R_z^{\mathsf{T}} H(z) R_z/4$, the same terminal cost as (965), and $\kappa = 0$. At fixed u its variation contains both required terms:

$$\partial_z \ell_{\mathrm{ex}} = \frac{1}{2} d'(z)(1,0)H(z)R_z + \frac{\zeta z}{2} R_z^{\mathsf{T}} D R_z. \tag{973}$$

The second term would be lost by holding the field-dependent metric fixed.

Proposition 56 (Uniform value and policy bounds for the exact branch). *Define*

$$\begin{aligned} \eta_\delta = \frac{4\delta^3}{3(1-4\delta^2)}, \quad \epsilon_\delta = \frac{a}{4}(2\delta\eta_\delta + \eta_\delta^2) + \frac{|c|}{2}\eta_\delta u_{\max} \\ + \frac{\zeta\delta^2\|D\|}{4}\big[(\delta+\eta_\delta)^2 + u_{\max}^2\big]. \end{aligned} \tag{974}$$

For every admissible control, $|J_{\mathrm{ex}}(t,z;u) - J_0(t,z;u)| \leq (T-t)\epsilon_\delta$. Consequently the exact value satisfies

$$\begin{aligned} |V_{\mathrm{ex}}(t,z) - V_0(t,z)| &\leq (T-t)\epsilon_\delta, \\ 0 \leq J_{\mathrm{ex}}(t,z;u_*) - V_{\mathrm{ex}}(t,z) &\leq 2(T-t)\epsilon_\delta. \end{aligned} \tag{975}$$

At fixed k, a, c, r, ζ, D, T, these are fourth-order bounds as $\delta \downarrow 0$.

Proof. The power series for artanh gives $d(z) - z = \sum_{n\geq 1} 2^{2n} z^{2n+1}/(2n+1)$. Bounding every denominator by 3 and summing the resulting geometric series proves $|d(z) - z| \leq \eta_\delta$ on the invariant interval. Therefore $|d^2 - z^2| \leq 2\delta\eta_\delta + \eta_\delta^2$ and $|(d-z)u| \leq \eta_\delta u_{\max}$. The added metric term obeys $0 \leq \zeta z^2 R_z^{\mathsf{T}} D R_z/4 \leq \zeta\delta^2\|D\|[(\delta+\eta_\delta)^2 + u_{\max}^2]/4$. These three estimates give $|\ell_{\mathrm{ex}} - \ell_0| \leq \epsilon_\delta$, hence the cost bound. Taking infima over the same admissible controls gives the value bound. Applying it to the exact quadratic optimizer yields $J_{\mathrm{ex}}(u_*) \leq V_0 + (T-t)\epsilon_\delta \leq V_{\mathrm{ex}} + 2(T-t)\epsilon_\delta$. The fourth-order scaling follows from

$\eta_\delta = O(\delta^3)$ and $u_{\max} = O(\delta)$. No differentiability of the exact nonlinear value function is assumed. □

For the synthetic benchmark $k = 1, a = 1, c = 0.2, r = 2, \beta = 0.5, T = 3$, $\zeta = 0.5$, and $D = \left(\begin{smallmatrix} 1 & 0.25 \\ 0.25 & 0.5 \end{smallmatrix}\right)$, Fig. 15 displays the optimal quadratic law and the guaranteed policy-gap bound for its exact extension. Two hundred synthetic parameter and piecewise-constant-control cases compare the closed Riccati solution with an independent adaptive ODE integration; the maximum discrepancy is 1.01×10^{-11}. Analytically integrated piecewise-control costs agree with (971) to 2.78×10^{-17}, while the integrated optimal cost agrees with the value to 1.33×10^{-16}. All sampled exact-score costs satisfy the uniform bound. Numerical agreement checks the declared formulas; global optimality and the unsampled error bound follow from the proofs, not from the finite sample. The guarantee is conservative and is not a claim that the true nonlinear policy gap attains its upper bound.

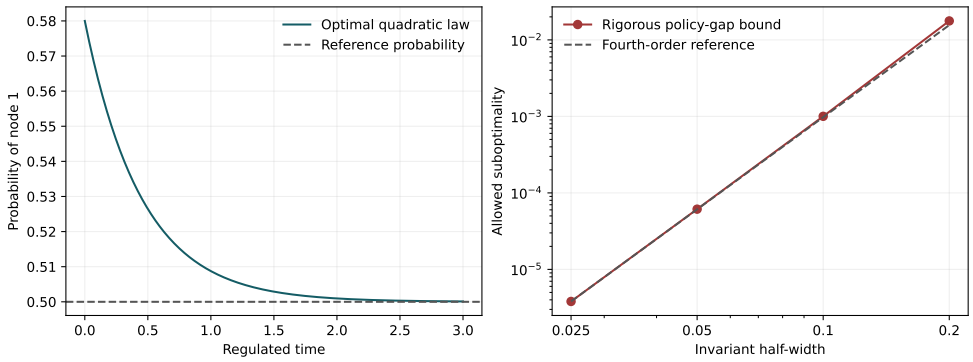


Figure 15. An exactly optimized regulated probability-law branch (left) and a rigorous bound on the suboptimality of that policy when the full logarithmic force and variable metric are retained (right). Inputs are synthetic and dimensionless. The fourth-order reference is an asymptotic comparison, not an empirical scaling law for turbulent or particle data.

The example closes an optimization question for one explicit common-cost branch. Extending the bound to the full field system requires estimates for its constraints, projection residuals, and regulator dependence. It does not follow from placing a desired target equation in the cost.

13.4.5. *Density-space dynamic programming.* If a positive density curve $\bar{\rho}_t$ is prescribed exogenously, then $\ell_\kappa(t, x, a) := \varphi_\kappa(q(t, x, \bar{\rho}_t, a))$ is an ordinary time-dependent running cost. Under the usual finite-dimensional nonexplosion,

coercivity, and comparison hypotheses, its state-space value function obeys

$$\begin{aligned} -\partial_t V = \inf_a \Big\{ & (b_{\mathrm{rev}} + b_{\mathrm{irr}} + f_{\mathrm{ext}} + \mathbb{B}_{0,a,N} a) \cdot \nabla V \\ & + \theta \,\mathrm{Tr}(\mathbb{M} D^2 V) + \ell_\kappa(t,x,a) \Big\}, \quad V(T,x) = \mathcal{G}^{\mathrm{term}}_{a,N}(x, \bar{\rho}_T). \end{aligned} \tag{976}$$

For the self-consistent problem, however, the score channel makes the cost law-dependent even when $\mathbb{H}$ is fixed. Define the value on the positive-density state space by

$$\mathcal{V}(t,\rho) := \inf_u \left\{ \int_t^T \int \rho_s \varphi_\kappa(q_s) \,\mathrm{d}x \,\mathrm{d}s + \int \rho_T \mathcal{G}^{\mathrm{term}}_{a,N}(x,\rho_T) \,\mathrm{d}x \right\}, \tag{977}$$

where $\partial_s \rho_s = (\mathcal{L}^{u_s}_{a,N})^* \rho_s$. If a dynamic programming principle and a classically differentiable value functional have been established, then the Bellman equation is

$$\boxed{-\partial_t \mathcal{V}(t,\rho) = \inf_u \left\{ \int \rho(x) \varphi_\kappa(q(t,x,\rho,u)) \,\mathrm{d}x + D_\rho \mathcal{V}(t,\rho)[(\mathcal{L}^u_{a,N})^* \rho] \right\}.} \tag{978}$$

Its terminal value is the final integral in (977). Equation (978) is a density-space, or equivalently smooth Wasserstein-space, Bellman equation. A rigorous classical or viscosity solution theory requires a separately specified topology, parabolic or hypoelliptic regularization, Frechet or Lions differentiability, a dynamic programming theorem, and comparison. The stationary state-space HJB below belongs to the earlier law-independent quadratic objective and is not silently reused for (922).

The formal feedback condition also shows exactly where the cross blocks enter. Let

$$\mathsf{S}_u(t,x,\rho,u)v := D_u \mathfrak{R}(t,x,\rho,u)[v], \qquad \zeta(t,x) := \frac{\delta \mathcal{V}}{\delta \rho}(t,\rho)(x).$$

If the control set is open, $\mathbb{H}$ is independent of u, and a minimizer is attained at a differentiability point, then variation of the Hamiltonian in (978) gives

$$\boxed{\mathbb{B}^*_{0,a,N} \nabla \zeta + 2\varphi'_\kappa(q)\, \mathsf{S}^*_u \mathbb{H} \mathfrak{R} = 0.} \tag{979}$$

The second term contains every allowed control cross block and, through (937), the controlled NS-generator channel. For a closed convex control set, (979) is replaced by the corresponding normal-cone variational inequality. This is a necessary formal optimality condition, not an existence or uniqueness theorem for the optimizer.

Finally, the joint objective organizes the equations but does not make them logical consequences of a single unqualified differentiation. The Fokker–Planck equation is the law constraint; the HJB or (978) is the optimality equation; field variation uses (942); and the NS block enforces only the declared generator tests. In particular, stationarity of a path-law expectation generally

gives a forward–adjoint optimality system, not the pointwise master Euler equation. The Einstein–Yang–Mills projection proved earlier therefore remains the independent matched branch condition

$$\mathcal{E}_e = 0, \qquad \mathcal{E}_\omega = 0, \qquad \mathcal{E}_A = 0, \tag{980}$$

with its hypotheses in Theorem 9. For a solution of (980) also to be stationary under the added joint channels, a useful noncontamination design condition on a branch $\mathcal{B}$ is

$$D_{(e,\omega,A)}\,\mathbb{E}^{\mathbb{P}^u}\Bigg[\int_0^T \Big\{\varphi_\kappa(q_t) - \frac{1}{4}\langle R_{\mathrm{F},t}, H_{\mathrm{F}} R_{\mathrm{F},t}\rangle\Big\}\,\mathrm{d}t + \mathcal{G}^{\mathrm{term}}_{a,N}(X_T,\rho_T)\Bigg]_{\mathcal{B}} = 0. \tag{981}$$

Here the derivative includes the state variation and the induced terminal-law variation described above, and H_{F} is calibrated to the master pairing. Condition (981) removes only the additional channels. It does not convert

$$D_{(e,\omega,A)}\mathbb{E}\int_0^T \tfrac{1}{4}\langle R_{\mathrm{F}}, H_{\mathrm{F}} R_{\mathrm{F}}\rangle\,\mathrm{d}t = 0$$

into the pointwise equation $\delta\mathcal{S}_{\mathrm{M}} = 0$. Such an inference would require a separately proved localization theorem, for example a static or concentrating law, admissible localized field variations, positivity on their support, and vanishing of every induced law and adjoint contribution. No such theorem is assumed here.

A useful special case is that the terminal functional is field-independent on $\mathcal{B}$ and the first variation of every cross and remaining channel vanishes there. At $\kappa = 0$ these extra variations must vanish or be retained as quantified sources or remainders. Thus $\kappa = 0$ is useful but is not by itself sufficient to preserve the old field solutions when nonzero cross blocks are present. For an isolated static scalar q with fixed $\mathbb{H}$, composition with the strictly increasing φ_κ preserves its critical points; in the coupled path-and-law problem, the nonconstant weight $\varphi'_\kappa(q_t)$ changes the feedback and adjoint equations and must be rederived.

For comparing the joint objective with the independently established low-energy branch, the conservative implementation is therefore $\kappa = 0$, symmetry-allowed cross blocks satisfying (918), and the compatibility target (981). This choice retains bilinear cross-channel coupling without the additional exponential weight $\varphi'_\kappa(q)$. It does not prove (980) from the stochastic control problem.

13.5. *Generator, Fokker–Planck equation, and probability current.* For $F \in C^2(\mathcal{X}_{a,N})$, the controlled generator is

$$\mathcal{L}^u F = \langle b_{\mathrm{rev}} + b_{\mathrm{irr}} + f_{\mathrm{ext}} + \mathbb{B}_{0,a,N}u, \nabla F\rangle + \theta\,\mathrm{Tr}\big(\mathbb{M}D^2F\big). \tag{982}$$

It is useful to collect all nonreference drift into

$$h_t(x) := f_{\mathrm{ext}}(x) + \mathbb{B}_{0,a,N}(x)u_t(x). \tag{983}$$

Writing ρ_t for the law of X_t, integration by parts gives

$$\partial_t\rho_t = -\partial_i\big(b_i^u\rho_t\big) + \theta\partial_i\partial_j\big(\mathbb{M}_{ij}\rho_t\big), \qquad \partial_t\rho_t = -\nabla\cdot J_{\rho_t}, \tag{984}$$

where

$$(J_\rho)_i = b_i^u\rho - \theta\partial_j(\mathbb{M}_{ij}\rho). \tag{985}$$

The reference equilibrium density is

$$\pi_\theta(x) = Z_\theta^{-1}m(x)\exp\left(\frac{\theta s(x) - E(x)}{\theta}\right). \tag{986}$$

Assume that the boundary has zero probability flux and that

$$\nabla\cdot\big(\pi_\theta\mathbb{L}\nabla E\big) = 0. \tag{987}$$

If the regulator domain has a boundary, assume in addition that the reversible vector field is tangent to it,

$$(\mathbb{L}\nabla E)\cdot n = 0, \tag{988}$$

or impose periodic boundary conditions. On a noncompact domain the same role is played by sufficient decay of the reversible boundary term at infinity. Then, when the total drive h vanishes,

$$J_{\mathrm{irr}}[\rho] = -\theta\mathbb{M}\rho\nabla\log\left(\frac{\rho}{\pi_\theta}\right). \tag{989}$$

Substitution of $\rho = \pi_\theta$ proves $J_{\mathrm{irr}}[\pi_\theta] = 0$. Stationarity alone would only give $\nabla\cdot J = 0$, not detailed balance.

THEOREM 57 (Finite-regulator free-energy dissipation). *Under* (891)–(987)*, assume* (988)*, periodic boundary conditions, or the stated decay at infinity. Assume $0 < Z_\theta < \infty$ and a conservative realization with a positive smooth probability density ρ_t and vanishing boundary flux. Put $f_t = \rho_t/\pi_\theta$. On every compact time interval I, require finite entropy and dissipation, and an integrable function $G_I(x)$ with*

$$\rho_t|\log f_t| + |\partial_t\rho_t|(1 + |\log f_t|) \le G_I(x) \quad (t\in I).$$

On a noncompact state space, choose smooth cutoffs $\chi_R \to 1$ and assume the two entropy boundary remainders vanish in $L^1(I;\mathrm{d}t)$:

$$\int \log f_t\, J_{\rho_t}\cdot\nabla\chi_R\,\mathrm{d}x \to 0, \qquad \int \rho_t b_{\mathrm{rev}}\cdot\nabla\chi_R\,\mathrm{d}x \to 0.$$

These are conditions on the solution and its tails. They hold automatically on a compact smooth state space for a strictly positive smooth solution and the

stated boundary conditions; smoothness and normalization alone do not imply them on an unbounded domain. Define

$$\mathcal{F}_\theta(\rho) := \theta \int_{\mathcal{X}_{a,N}} \rho \log\left(\frac{\rho}{\pi_\theta}\right) \mathrm{d}x. \tag{990}$$

If $h = 0$, then

$$\frac{\mathrm{d}}{\mathrm{d}t}\mathcal{F}_\theta(\rho_t) = -\theta^2 \int \rho_t \left\langle \nabla \log\left(\frac{\rho_t}{\pi_\theta}\right), \mathbb{M}\nabla \log\left(\frac{\rho_t}{\pi_\theta}\right)\right\rangle \mathrm{d}x \le 0. \tag{991}$$

Proof. Differentiate (990) and use $\int \partial_t \rho_t \, \mathrm{d}x = 0$. This gives

$$\frac{\mathrm{d}}{\mathrm{d}t}\mathcal{F}_\theta(\rho_t) = \theta \int \partial_t \rho_t \log\left(\frac{\rho_t}{\pi_\theta}\right) \mathrm{d}x.$$

Insert $\partial_t \rho_t = -\nabla \cdot J_{\rho_t}$ and integrate by parts. For an unbounded domain, first use χ_R in this calculation. The integrable envelope justifies differentiation and passage to the limit on the entropy side; the stated flux remainders remove the boundary contributions. To check the reversible term explicitly, write

$$\int \rho_t b_{\mathrm{rev}} \cdot \nabla \log f_t \, \mathrm{d}x = \int \pi_\theta b_{\mathrm{rev}} \cdot \nabla f_t \, \mathrm{d}x = 0.$$

This uses $\nabla \cdot (\pi_\theta b_{\mathrm{rev}}) = 0$ and its own boundary condition. Inserting (989) gives the factor θ^2 in (991): one factor comes from the definition of $\mathcal{F}_\theta$, and the second from the irreversible current. Positive semidefiniteness of $\mathbb{M}$ gives the inequality. Under the exact degeneracy $\mathbb{M}\nabla E = 0$, total energy is conserved and the state space decomposes into energy leaves. Irreducibility, Poincare, log-Sobolev, or Harris hypotheses can therefore give uniqueness only on a declared leaf (or within another invariant component). A unique globally attracting law requires an open reservoir that breaks exact total-energy conservation or an enlarged state description in which the conserved total energy is fixed. □

With a general external or controlled drive,

$$\frac{\mathrm{d}}{\mathrm{d}t}\mathcal{F}_\theta(\rho_t) = -\theta\Sigma(\rho_t) + \mathcal{W}_h(\rho_t), \tag{992}$$

where

$$\Sigma(\rho) := \int \frac{J_{\mathrm{irr}}[\rho]^{\mathsf{T}}(\theta\mathbb{M})^{\dagger} J_{\mathrm{irr}}[\rho]}{\rho} \, \mathrm{d}x \ge 0. \tag{993}$$

With (989), this is equivalently

$$\Sigma(\rho) = \theta \int \rho \, \langle \nabla \log(\rho/\pi_\theta), \mathbb{M}\nabla \log(\rho/\pi_\theta)\rangle \, \mathrm{d}x,$$

so the unforced identity is $\mathrm{d}\mathcal{F}_\theta/\mathrm{d}t = -\theta\Sigma$, consistently with (991). The drive term in (992) is, under the same zero-flux boundary condition,

$$\mathcal{W}_h(\rho) := \theta \int_{\mathcal{X}_{a,N}} \rho \left\langle h, \nabla \log\left(\frac{\rho}{\pi_\theta}\right)\right\rangle \mathrm{d}x. \tag{994}$$

This term is not sign-definite: it is the external-plus-control drive measured against the thermodynamic score. Optimality of u, positivity of the joint metric, or a nonzero cross block does not imply that this term vanishes. The expression assumes that time-reversal parities and boundary conditions have been specified. Momentum-, magnetic-, and gauge-odd variables require the corresponding generalized time-reversal decomposition. This is the parity-aware convention of (133)–(135), not a classification based only on whether the drift or diffusion coefficient is zero.

THEOREM 58 (Finite-regulator entropy-increase law). *Assume the hypotheses of Theorem 57, the degeneracy conditions* (895)*, and the pointwise energy-compatibility condition*

$$\mathbb{M}(x)\nabla E(x) = 0.$$

Assume in addition that the reference-measure correction is included in the drift as in (892)*, that the boundary flux vanishes, and that the heat-reservoir variables have been included so that this degeneracy represents conservation of total energy. At a reflecting boundary, use conormal reflection in the direction $\mathbb{M}n$, or require separately that the reflection field annihilate E; zero probability flux alone does not remove the energy change caused by an arbitrary reflection direction. Assume that the total drive $h = f_{\mathrm{ext}} + \mathbb{B}_{0,a,N}u$ vanishes. Require, at every time in question,*

$$\int \rho_t\big(|E| + |s| + |\log(\rho_t/m)|\big)\,\mathrm{d}x < \infty.$$

This condition makes the following energy–entropy decomposition an identity of finite quantities. A finite partition function alone is insufficient. Define the dimensionless entropy and mean energy by

$$\begin{aligned} \mathscr{S}(\rho) &:= \int_{\mathcal{X}_{a,N}} \rho(x)s(x)\,\mathrm{d}x \quad - \int_{\mathcal{X}_{a,N}} \rho(x)\log\Big(\frac{\rho(x)}{m(x)}\Big)\,\mathrm{d}x, \\ \mathscr{E}(\rho) &:= \int_{\mathcal{X}_{a,N}} \rho(x)E(x)\,\mathrm{d}x. \end{aligned} \tag{995}$$

Then

$$\frac{\mathrm{d}}{\mathrm{d}t}\mathscr{E}(\rho_t) = 0, \qquad \frac{\mathrm{d}}{\mathrm{d}t}\mathscr{S}(\rho_t) = \Sigma(\rho_t) \geq 0. \tag{996}$$

Thus the entropy-increase law is a consequence of the irreversible current and energy degeneracy, not of the mere presence of a nonzero diffusion coefficient.

Proof. The definition of the Gibbs density in (986) gives the exact algebraic identity

$$\mathcal{F}_\theta(\rho) = \mathscr{E}(\rho) - \theta\mathscr{S}(\rho) + \theta\log Z_\theta. \tag{997}$$

We first verify energy conservation. The reversible contribution to the generator applied to E is

$$\langle \nabla E, \mathbb{L}\nabla E\rangle = 0$$

because $\mathbb{L}^{\mathsf{T}} = -\mathbb{L}$. The term $\langle \nabla E, \mathbb{M}\nabla s\rangle$ vanishes because $\mathbb{M}\nabla E = 0$, and the term $-\langle \nabla E, \mathbb{M}\nabla E\rangle$ vanishes by the same condition. Finally, the Itô correction and the reference-measure drift combine as

$$\theta\, \mathbb{M}_{ij}\partial_{ij}E + \theta\, \beta_{m,i}\partial_i E = \theta\, m^{-1}\partial_j\big(m\mathbb{M}_{ij}\partial_i E\big) = 0,$$

where the last equality uses $\mathbb{M}\nabla E = 0$ pointwise. There is also a direct pathwise justification: positive semidefiniteness gives $\mathbb{M}^{1/2}\nabla E = 0$, so both the Itô drift $\mathcal{L}E$ and the stochastic coefficient of $E(X_t)$ vanish. The boundary term vanishes by the stated reflection condition. Stopped Itô identities and conservativeness therefore give $E(X_t) = E(X_0)$ almost surely. The finite initial energy moment then proves conservation of its expectation without using an unjustified unbounded test in the generator domain. The free-energy theorem and the driven free-energy formula with $h = 0$ give

$$\frac{\mathrm{d}}{\mathrm{d}t}\mathcal{F}_\theta(\rho_t) = -\theta\Sigma(\rho_t).$$

Differentiate (997), use $\mathrm{d}\mathscr{E}/\mathrm{d}t = 0$ and the constancy of θ and Z_θ, and divide by $-\theta$. This yields $\mathrm{d}\mathscr{S}/\mathrm{d}t = \Sigma \geq 0$, as claimed. □

The condition $h = 0$ is essential for the monotonicity statement as written: it requires both zero external drive and zero control drift, unless a separate orthogonality or reservoir cancellation is proved. More generally, the same calculation gives the exact controlled balances

$$\begin{aligned}\frac{\mathrm{d}}{\mathrm{d}t}\mathscr{E}(\rho_t) = \int \rho_t\langle h_t, \nabla E\rangle\,\mathrm{d}x, \quad \frac{\mathrm{d}}{\mathrm{d}t}\mathscr{S}(\rho_t) = \Sigma(\rho_t) + \frac{1}{\theta}\int \rho_t\langle h_t, \nabla E\rangle\,\mathrm{d}x \\ - \int \rho_t\,\langle h_t, \nabla\log(\rho_t/\pi_\theta)\rangle\,\mathrm{d}x.\end{aligned} \tag{998}$$

Indeed, the reference generator annihilates E by the antisymmetry, degeneracy, and reservoir hypotheses used in the proof, leaving only the first displayed drive term. Combining this identity with (992) and (997) gives the second. Neither term has a fixed sign for a general control. The theorem is therefore stated for the total energy of the enlarged, undriven finite regulator rather than for an isolated kinetic-energy equation.

13.6. *Ergodic control and the HJB constant.* For the long-time objective

$$\lambda(u) := \limsup_{T\to\infty}\frac{1}{T}\mathbb{E}^u\int_0^T\left[\ell^E_{\mathrm{cl}}(X_t) + \frac{1}{2}\langle u_t, \mathcal{R}_{\mathrm{u}}u_t\rangle\right]\mathrm{d}t, \tag{999}$$

the stationary HJB equation is

$$-\lambda_* + \inf_u \left\{ \mathcal{L}^u v(x) + \ell^E_{\mathrm{cl}}(x) + \frac{1}{2}\langle u, \mathcal{R}_{\mathrm{u}} u\rangle \right\} = 0. \tag{1000}$$

The constant λ_* is an ergodic average cost per unit stochastic time. Adding a constant to the running cost shifts λ_*, but this normalization has no automatic interpretation as a Lorentzian vacuum-energy density. Such an interpretation would require a separately derived, dimensionally consistent, diffeomorphism-covariant, and regulator-independent matching map. In particular, one would have to prove the existence of a finite limit of the form

$$\rho^{\mathrm{ctrl}}_\Lambda = \lim_{a\downarrow 0,\, N\to\infty} c_{a,N}\lambda_*^{a,N} \tag{1001}$$

with a fixed conversion coefficient $c_{a,N}$, and then show that this quantity enters the covariant effective action. No such identification is assumed here.

13.7. *Finite Galerkin stochastic Navier–Stokes branch.* We now make the hydrodynamic part of the regulated construction explicit. This subsection is a finite-dimensional realization of the common stochastic law, not a proof of global regularity for the three-dimensional Navier–Stokes equations. Let $\mathbb{T}^3$ be the periodic three-torus, let H be the real L^2-space of mean-zero divergence-free vector fields, and let $P_N : H \to H_N$ be the orthogonal projection onto a finite set of Fourier modes. Write $A_N = P_N(-\Delta)P_N$ for the positive Galerkin Stokes operator and

$$B_N(x,y) := P_N\, P\big((x\cdot\nabla)y\big), \qquad x, y \in H_N,$$

where P is the Leray projection. The periodic integration-by-parts identity $\nabla\cdot x = 0$ gives

$$\langle x, B_N(x,x)\rangle_H = 0, \qquad x \in H_N. \tag{1002}$$

Indeed, projection does not change the pairing with $x \in H_N$, and

$$\langle x, (x\cdot\nabla)x\rangle_H = \frac{1}{2}\int_{\mathbb{T}^3} x\cdot\nabla|x|^2\,\mathrm{d}z = -\frac{1}{2}\int_{\mathbb{T}^3}(\nabla\cdot x)|x|^2\,\mathrm{d}z = 0.$$

Let $Q_N = Q_N^{\mathsf{T}} \succeq 0$ be a finite-dimensional covariance, let $f_N \in H_N$, and let W_t^N be a standard Brownian motion in H_N. The regulated stochastic Navier–Stokes equation is

$$\begin{aligned} \mathrm{d}X_t^N = {} & \big[-\nu_{\mathrm{v}} A_N X_t^N - B_N(X_t^N, X_t^N) + f_N\big]\,\mathrm{d}t \\ & + \sqrt{2\theta Q_N}\,\mathrm{d}W_t^N, \qquad \nu_{\mathrm{v}} > 0, \quad \theta \geq 0. \end{aligned} \tag{1003}$$

The coefficients ν_{v} and Q_N in this realization are initially effective data. Their thermodynamic consistency can be tested before attempting a microscopic

derivation. If the unforced linearized process has stationary covariance C_N, then its covariance equation is

$$\nu_{\mathrm{v}}(A_N C_N + C_N A_N) = 2\theta Q_N. \tag{1004}$$

For the kinetic Gibbs law with $C_N = \theta I_{H_N}$ and $\theta > 0$, this reduces to

$$Q_N = \nu_{\mathrm{v}} A_N. \tag{1005}$$

At $\theta = 0$, the Lyapunov equation becomes $0 = 0$ for this formal choice and does not imply $Q_N = \nu_{\mathrm{v}} A_N$. Moreover, a stationary covariance is not by itself detailed balance. The unforced linear process has zero stationary probability current only if

$$\nu_{\mathrm{v}} A_N C_N = \theta Q_N \quad \text{and hence} \quad \nu_{\mathrm{v}} C_N A_N = \theta Q_N, \tag{1006}$$

with the required commutation and domain conditions. Driven turbulence is generically outside this zero-current case. For the nonlinear Galerkin equation, invariance of that law additionally requires the finite-mode convection vector field to be divergence free in phase space as well as energy preserving. General driven turbulence need not satisfy (1005); its stationary current then records detailed-balance breaking.

A derivation from the master dynamics would start with a projection onto the resolved velocity modes and an orthogonal unresolved force. The exact Mori–Zwanzig form is schematically

$$\dot{U}_t^N = \mathcal{B}_N(U_t^N) - \int_0^t K_N(t-s) U_s^N \, \mathrm{d}s + \eta_N(t), \tag{1007}$$

and equilibrium microscopic reversibility would impose a generalized Langevin second fluctuation–dissipation relation of the form

$$\mathbb{E}_{\pi_\theta}\big[\eta_N(t) \otimes \eta_N(s)\big] = \theta K_N(|t-s|) \tag{1008}$$

in the chosen normalization [121] and [169]. A transport coefficient requires in addition the relevant stress autocorrelation Green–Kubo formula; for a homogeneous shear channel, one conventional normalization is

$$\nu_{\mathrm{v}} = \frac{1}{\rho_{\mathrm{m}} \theta V} \int_0^\infty \mathbb{E}_{\pi_\theta}[\Pi_{xy}(t)\Pi_{xy}(0)]_c \, \mathrm{d}t, \tag{1009}$$

where V is the volume, $\rho_{\mathrm{m}} > 0$ is the mean mass density, and Π_{xy} is the volume-integrated shear stress in this convention. The formula without ρ_{m} gives dynamic viscosity, whereas ν_{v} is kinematic viscosity. Unit mass density recovers the normalized convention. Other stress normalizations require their corresponding volume and density factors [106]. A controlled short-memory limit must then show that the memory term converges to $\nu_{\mathrm{v}} A_N U_t^N$ and that the noise converges to the covariance Q_N. Equations (1004)–(1008) are the

missing constitutive interface; the energy identity below does not derive them by itself.

13.7.1. *An exactly eliminable memory channel.* The projection methods of Zwanzig and Mori preserve the unresolved dynamics as memory rather than replacing it immediately by viscosity [169] and [121]. An exactly soluble regulated example shows what this approach contributes to the present interface. Let x be a resolved coordinate, z an unresolved coordinate, and W_1, W_2 independent Brownian motions. Fix $a, b, \theta > 0$, $c \in \mathbb{R}$, and consider

$$\begin{aligned} \mathrm{d}x_t &= (-ax_t + cz_t)\,\mathrm{d}t + \sqrt{2a\theta}\,\mathrm{d}W_{1,t}, \\ \mathrm{d}z_t &= (-cx_t - bz_t)\,\mathrm{d}t + \sqrt{2b\theta}\,\mathrm{d}W_{2,t}. \end{aligned} \tag{1010}$$

Its energy is $E = (x^2+z^2)/2$. The cross coupling is generated by the antisymmetric matrix $\left(\begin{smallmatrix} 0 & c \\ -c & 0 \end{smallmatrix}\right)$; it conserves E and is not an external drive. The mobility is $\mathrm{diag}(a, b)$, and the invariant density is $\pi_\theta(x, z) = (2\pi\theta)^{-1} e^{-(x^2+z^2)/(2\theta)}$. Writing the drift matrix as B, direct substitution verifies

$$\begin{aligned} B(\theta I) + (\theta I)B^{\mathsf{T}} + 2\theta\,\mathrm{diag}(a, b) = 0, \\ PBP = B^{\mathsf{T}}, \qquad P = \mathrm{diag}(1, -1). \end{aligned} \tag{1011}$$

Thus the stationary mother law is reversible under the declared parity $(x, z) \mapsto (x, -z)$, despite its reversible circulating current.

Variation of constants in the second equation gives

$$z_t = e^{-bt} z_0 - c \int_0^t e^{-b(t-s)} x_s\,\mathrm{d}s + \sqrt{2b\theta} \int_0^t e^{-b(t-s)}\,\mathrm{d}W_{2,s}. \tag{1012}$$

Substituting this expression into the first equation yields the exact generalized Langevin equation

$$\begin{aligned} \mathrm{d}x_t &= \left[-ax_t - \int_0^t K_b(t-s) x_s\,\mathrm{d}s + \eta_t \right] \mathrm{d}t + \sqrt{2a\theta}\,\mathrm{d}W_{1,t}, \\ K_b(t) &= c^2 e^{-bt}, \qquad t \geq 0, \quad \eta_t = ce^{-bt} z_0 + c\sqrt{2b\theta} \int_0^t e^{-b(t-s)}\,\mathrm{d}W_{2,s}. \end{aligned} \tag{1013}$$

For Gibbs initial data, $z_0 \sim \mathcal{N}(0, \theta)$ is independent of x_0 and the future Brownian increments. For $t \geq s$, the initial contribution to $\mathbb{E}\eta_t\eta_s$ is $c^2\theta e^{-b(t+s)}$; the Brownian contribution is $c^2\theta[e^{-b(t-s)} - e^{-b(t+s)}]$. Their sum gives

$$\mathbb{E}\eta_t\eta_s = \theta c^2 e^{-b|t-s|} = \theta K_b(|t-s|). \tag{1014}$$

The initial term cannot be dropped for an exact stationary fluctuation–dissipation relation. Non-Gibbs initial data introduce an initial-slip transient and need not satisfy this covariance identity. At finite b, the resolved process is generally non-Markovian; $\mathcal{L}x = -ax + cz$ does not descend through

the projection onto x. Proposition 48 therefore does not license an exact one-coordinate Markov closure.

The short-memory limit is explicit. Set $c^2 = \gamma b$, with $\gamma > 0$ fixed, and let $b \to \infty$. The causal kernel has total integral γ. For a differentiable resolved test history, integration by parts gives

$$\begin{aligned} &\int_0^t \gamma b e^{-b(t-s)} x_s \, \mathrm{d}s - \gamma x_t = -\gamma e^{-bt} x_0 - \gamma \int_0^t e^{-b(t-s)} \dot{x}_s \, \mathrm{d}s, \\ &\left| \int_0^t K_b(t-s) x_s \, \mathrm{d}s - \gamma x_t \right| \le \gamma e^{-bt} |x_0| + \frac{\gamma}{b} \sup_{0 \le s \le t} |\dot{x}_s|. \end{aligned} \tag{1015}$$

This bound applies to smooth histories, not to individual Brownian paths. For the stationary Gaussian diffusion, convergence can instead be checked from its exact spectral density. With the two-sided convention $\mathbb{E} x_t x_0 = (2\pi)^{-1} \int e^{i\omega t} S_x(\omega) \, \mathrm{d}\omega$, solving the two linear Fourier equations gives

$$S_x(\omega) = \frac{2\theta\{a(b^2+\omega^2) + bc^2\}}{(ab + c^2 - \omega^2)^2 + (a+b)^2\omega^2}. \tag{1016}$$

At every fixed frequency, and uniformly on each bounded frequency band, this tends to

$$S_x^{\mathrm{eff}}(\omega) = \frac{2\theta(a+\gamma)}{(a+\gamma)^2 + \omega^2}. \tag{1017}$$

The limit is the spectrum of $\mathrm{d}x_t = -(a+\gamma) x_t \, \mathrm{d}t + \sqrt{2\theta(a+\gamma)} \, \mathrm{d}W_t$. Both the added damping and its thermal noise follow from the eliminated channel. Each nonnegative spectrum has integral $2\pi\theta$, as follows from the exactly stationary covariance. Pointwise convergence and this common integral imply L^1 spectral convergence by Scheffe's lemma. The covariance functions therefore converge uniformly, and the centered stationary Gaussian finite-dimensional distributions converge to those of the effective OU process. This argument does not assert an arbitrary nonlinear or nonstationary path-space limit. More directly, $\widehat{K}_b(\omega) = \gamma b/(b + i\omega)$, so

$$|\widehat{K}_b(\omega) - \gamma| \le \gamma|\omega|/b, \qquad S_\eta(\omega) = \frac{2\theta\gamma b^2}{b^2 + \omega^2}. \tag{1018}$$

Thus a finite-frequency colored component and a dispersive response provide a measurable rejection criterion for the instantaneous white-noise approximation. They are conditional finite-model relations, not a new universal law. Importantly, the exact equilibrium model has zero physical-parity entropy production: memory alone does not create a time arrow. The example establishes a mechanism and its error scale; deriving a nonlinear fluid kernel from the master fields still requires its specified projection and independently calculated stress correlations.

Finite-memory spectral comparison. For the dimensionless synthetic values $a = 0.6$, $\gamma = 0.9$, $\theta = 0.7$, Figure 16 compares (1016) with the instantaneous limit for $b \in \{1, 5, 20, 100\}$. On $0 \le \omega \le 3$, the maximum relative spectral differences are respectively 0.622, 0.208, 0.0658, and 0.0143, rounded upward. The variance remains θ in every case; spectral shape, rather than variance alone, distinguishes the memory channel. Numerical integration of $S_x/2\pi$ gives variance errors below 1.12×10^{-16} for these examples. In 100 independently generated parameter cases, the stationary covariance identity has maximum normalized residual 8.12×10^{-16}, and deterministic variation-of-constants elimination agrees with an independently integrated auxiliary memory coordinate to normalized error 3.05×10^{-12}. These results concern specified linear models and do not supply a nonlinear Navier–Stokes closure.

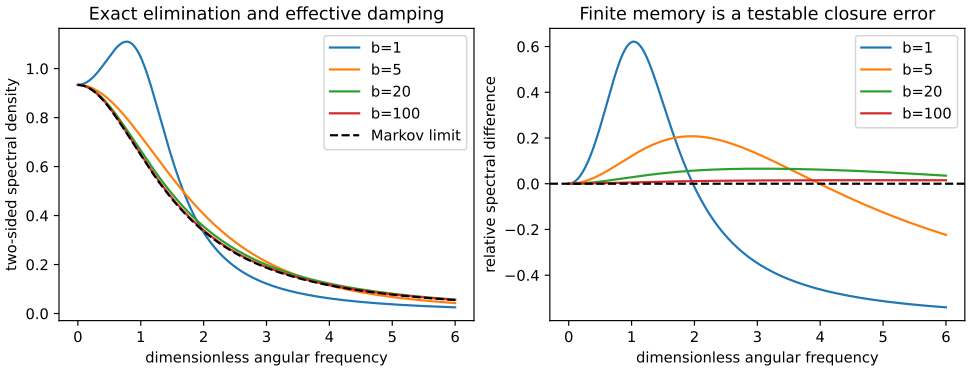


Figure 16. Exact resolved spectra for increasing unresolved relaxation rate b, with $c^2/b = \gamma$ fixed. The dashed curve is the Markov-limit spectrum. The right panel shows relative spectral differences; equal equilibrium variances do not imply equal transport responses. All parameters are synthetic and dimensionless.

The hydrodynamic variables enter through a declared projection, rather than through a change of notation. Let $\Pi_{\mathrm{NS}}^{a,N} : \mathcal{X}_{a,N} \to H_N$ be a chosen C^2 map from the regulated master variables to the velocity modes and write $U_t^N = \Pi_{\mathrm{NS}}^{a,N}(X_t)$. Denote the generator of the unprojected reference process (with $u = 0$) by $\mathcal{L}_{a,N}$. The statement that the projected process is the Navier–Stokes branch is the generator-matching condition

$$\mathcal{L}_{a,N}(F \circ \Pi_{\mathrm{NS}}^{a,N})(x) = \mathcal{L}_N^{\mathrm{NS}} F\big(\Pi_{\mathrm{NS}}^{a,N}(x)\big), \qquad F \in C_b^2(H_N), \tag{1019}$$

where

$$\mathcal{L}_N^{\mathrm{NS}} F(u) = \langle -\nu_{\mathrm{v}} A_N u - B_N(u,u) + f_N, \nabla F(u) \rangle_H + \theta \,\mathrm{Tr}\big(Q_N D^2 F(u)\big). \tag{1020}$$

Equation (1019) is an interface hypothesis to be checked for a concrete master model; it is not a consequence of the existence of a common action symbol. If the two associated martingale problems are well posed, the matching condition gives equality of the finite-dimensional laws for matching initial data, and the energy identities below then apply to the projected master process.

The time parameter in this equality is initially the regulated stochastic evolution parameter. Interpreting it as laboratory fluid time requires a calibration and limit theorem, for example

$$t_{\mathrm{phys}} = c_{a,N} t_{\mathrm{stoch}}, \qquad c_{a,N} > 0, \qquad c_{a,N}^{-1} \mathcal{L}_{a,N}^{\mathrm{proj}} \longrightarrow \mathcal{L}_{\mathrm{phys}}^{\mathrm{NS}} \tag{1021}$$

on a determining core. The finite-mode identities remain exact in the auxiliary parameter, but no identification with measured time is claimed until (1021) is proved.

If the projected branch is to be interpreted as a relativistic fluid coupled to the Lorentzian geometric sector, an additional constitutive interface is required. The candidate equations must include

$$\nabla_\mu T_{\mathrm{tot}}^{\mu\nu} = 0, \qquad D_\mu J_a^\mu = 0, \qquad \nabla_\mu s^\mu \geq 0, \tag{1022}$$

with the stress tensor, gauge currents, entropy current, and their frame conditions defined by the same renormalized effective action. Causal and stable dissipative closure requires a hyperbolic transient theory, such as a specified Israel–Stewart or BDNK-type realization, together with a proof that all characteristic speeds lie inside the physical light cone [102]. The nonrelativistic Galerkin identities in this section do not supply that proof. At the quantum interface, a Schwinger–Keldysh construction would additionally have to satisfy unitarity, reality, KMS, and dynamical-KMS constraints. These are completion conditions for a relativistic thermodynamic realization, not assumptions hidden in the finite $\mathbb{T}^3$ Navier–Stokes regulator.

The coefficients are smooth on the finite-dimensional space H_N, so a unique maximal strong solution exists. The energy estimate below prevents finite-time escape and therefore makes the solution global. This is the precise sense in which the present construction supplies a stochastic Navier–Stokes branch: both the mode cutoff N and the covariance Q_N are part of the statement.

Proposition 59 (Finite-regulator energy identity). *For a solution of* (1003)*,*

$$\begin{aligned} \mathrm{d}\frac{|X_t^N|_H^2}{2} &= \left[-\nu_{\mathrm{v}} \|A_N^{1/2} X_t^N\|_H^2 + \langle f_N, X_t^N \rangle_H + \theta \,\mathrm{Tr}\, Q_N\right] \mathrm{d}t \\ &\quad + \sqrt{2\theta}\, \langle Q_N^{1/2} X_t^N, \mathrm{d}W_t^N \rangle_H. \end{aligned} \tag{1023}$$

In particular, if $\lambda_{1,N} > 0$ is the smallest eigenvalue of A_N, then

$$\begin{aligned} \mathrm{d}\frac{|X_t^N|_H^2}{2} \le \Big[-\frac{\nu_{\mathrm{v}}\lambda_{1,N}}{2}|X_t^N|_H^2 + \frac{|f_N|_H^2}{2\nu_{\mathrm{v}}\lambda_{1,N}} + \theta \operatorname{Tr} Q_N\Big]\,\mathrm{d}t \\ + \sqrt{2\theta}\,\big\langle Q_N^{1/2}X_t^N, \mathrm{d}W_t^N\big\rangle_H. \end{aligned} \tag{1024}$$

Consequently the finite-dimensional solution is global and has a second-moment bound on every bounded time interval. The bound is uniform in time for fixed N; no uniformity in the cutoff N is asserted.

Proof. Apply Itô's formula to $V(x) = |x|_H^2/2$. Its first derivative is $DV(x)h = \langle x, h\rangle_H$, and its second derivative is the identity on H_N. The drift contribution is therefore

$$\Big\langle X_t^N, -\nu_{\mathrm{v}}A_N X_t^N - B_N(X_t^N, X_t^N) + f_N\Big\rangle_H = -\nu_{\mathrm{v}}\|A_N^{1/2}X_t^N\|_H^2 + \langle f_N, X_t^N\rangle_H,$$

where (1002) removes the quadratic term. The quadratic variation of the martingale part is $2\theta\langle Q_N X_t^N, X_t^N\rangle_H\,\mathrm{d}t$, while the Hessian term in Itô's formula contributes $\theta \operatorname{Tr} Q_N\,\mathrm{d}t$. This proves (1023). The inequality follows from $\langle f_N, x\rangle_H \le \frac{\nu_{\mathrm{v}}\lambda_{1,N}}{2}|x|_H^2 + \frac{|f_N|_H^2}{2\nu_{\mathrm{v}}\lambda_{1,N}}$ and $\|A_N^{1/2}x\|_H^2 \ge \lambda_{1,N}|x|_H^2$. Localizing at the exit time from a ball, taking expectations, and then letting the radius tend to infinity gives the stated moment bound. The bound rules out explosion of a finite-dimensional locally Lipschitz SDE. □

Proposition 60 (Existence and moments at a fixed fluid regulator). *For the coefficients in* (1003)*, assume $\nu_{\mathrm{v}} > 0$, $\lambda_{1,N} > 0$, fixed $f_N \in H_N$, and fixed nonnegative covariance Q_N. The finite-dimensional process has a Feller semigroup and at least one invariant probability μ_N with every finite polynomial moment. This statement does not assert uniqueness, detailed balance, or estimates uniform in N.*

Proof. For fixed N, the coefficients are locally Lipschitz and the solution is global by Proposition 59. Solutions depend continuously on their initial data before exit from a compact ball. The stopped energy estimate bounds the probability of exit before any fixed time by $C_{N,t,K}/R^2$, uniformly for initial states in a compact set K. Letting $R \to \infty$ and using bounded convergence for a bounded continuous test proves the Feller property. Thus local continuous dependence is sufficient even though the quadratic convection field is not globally Lipschitz.

Writing $c_N = \nu_{\mathrm{v}}\lambda_{1,N}$, the energy inequality gives

$$\mathbb{E}|X_t^N|_H^2 \le e^{-c_N t}|X_0^N|_H^2 + K_N(1 - e^{-c_N t}), \quad K_N = \frac{|f_N|_H^2}{\nu_{\mathrm{v}}^2\lambda_{1,N}^2} + \frac{2\theta \operatorname{Tr} Q_N}{\nu_{\mathrm{v}}\lambda_{1,N}}. \tag{1025}$$

For a deterministic initial state x, define the occupation laws by

$$\mu_T = \frac{1}{T}\int_0^T \mathrm{Law}(X_s^{N,x})\,\mathrm{d}s. \tag{1026}$$

They satisfy $\sup_{T\ge 1}\mu_T(\{|y|_H > R\}) \le (|x|_H^2 + K_N)/R^2$. In finite dimension closed balls are compact, so these laws are tight. If $\mu_{T_j} \Rightarrow \mu_N$, the semigroup identity gives, for $F \in C_b(H_N)$ and $s \ge 0$,

$$\left|\int P_s F\,\mathrm{d}\mu_T - \int F\,\mathrm{d}\mu_T\right| \le \frac{2s\|F\|_\infty}{T}. \tag{1027}$$

The Feller property permits passage to the weak limit, proving invariance. This is the finite-dimensional application of the occupation-measure argument given in (652).

Higher moments require no new cancellation. Put $V_p(x) = (1+|x|_H^2)^p$, for an integer $p \ge 1$, and $z = 1 + |x|_H^2$. Direct differentiation yields

$$\begin{aligned}\mathcal{L}_N V_p(x) &= 2pz^{p-1}\big[-\nu_{\mathrm{v}}\langle A_N x, x\rangle_H + \langle f_N, x\rangle_H\big] \\ &\quad + 2\theta p z^{p-1}\,\mathrm{Tr}\,Q_N + 4\theta p(p-1)z^{p-2}\langle Q_N x, x\rangle_H \\ &\le -\tfrac{1}{2}p\nu_{\mathrm{v}}\lambda_{1,N}V_p(x) + C_{p,N}.\end{aligned} \tag{1028}$$

The convection term vanishes because ∇V_p is radial and $\langle x, B_N(x,x)\rangle_H = 0$. For the inequality, first use $2\langle f_N, x\rangle_H \le \nu_{\mathrm{v}}\lambda_{1,N}|x|_H^2 + |f_N|_H^2/(\nu_{\mathrm{v}}\lambda_{1,N})$ and $\langle Q_N x, x\rangle_H \le \|Q_N\||x|_H^2$. The remaining positive terms have order at most z^{p-1}, whereas the negative term has order z^p; absorbing the former gives the finite constant $C_{p,N}$. Localization and Fatou's lemma now bound $\sup_{t\ge 0}\mathbb{E}V_p(X_t^{N,x})$ for every fixed p. Lower semicontinuity along the same convergent occupation subsequence gives $\int V_p\,\mathrm{d}\mu_N < \infty$ for every integer p. These moments justify the cubic shell-flux averages below. They need not be uniform as the number of retained modes grows. □

Proposition 61 (A classical small-set route to regulated uniqueness). *Fix $h > 0$ and let $P = P_h$ be the transition operator of the fixed-regulator fluid process. Put $V(x) = |x|_H^2$. Suppose*

$$\begin{aligned} &PV \le \zeta V + K, \qquad 0 < \zeta < 1, \quad K > 0, \\ &P(x,\cdot) \ge \alpha\nu_0(\cdot) \quad \text{for } V(x) \le R, 0 < \alpha < 1, \qquad R > 2K/(1-\zeta), \end{aligned} \tag{1029}$$

where ν_0 is a probability measure. The first condition follows from (1025) *with $\zeta = e^{-c_N h}$, and with any positive upper bound on $K_N(1-e^{-c_N h})$. The minorization condition is additional. Choose $0 < \alpha_0 < \alpha$, set $w = \alpha_0/K$, and define*

$$\zeta_0 = \zeta + 2K/R < 1, \qquad r = \max\left\{1 - \alpha + \alpha_0, \frac{2 + wR\zeta_0}{2 + wR}\right\} < 1. \tag{1030}$$

Then P contracts the weighted total-variation distance $\|\mu-\nu\|_w := \int(1+wV)\,|\mu-\nu|$ by the factor r on probability measures with finite V-moment. In particular, the fluid invariant probability is unique and

$$\|P_{nh}^{*}\mu-\mu_N\|_w \le r^n\|\mu-\mu_N\|_w. \tag{1031}$$

This is the weighted-norm form of the classical Harris argument [89]*, applied to the regulated fluid model.*

Proof. For $x\neq y$, put $d_w(x,y)=2+wV(x)+wV(y)$, and put $d_w(x,x)=0$. If a test function satisfies $|F(x)-F(y)|\le d_w(x,y)$, it can be shifted by a constant so that $|F(x)|\le 1+wV(x)$. To see this, the intervals $[-1-wV(x)-F(x),1+wV(x)-F(x)]$ have pairwise intersections by the assumed difference bound. Intersecting with any one finite interval gives a nonempty intersection of the whole family. A constant from this intersection has the required property. Conversely, the weighted bound implies the difference bound. Since constants integrate to zero against $\mu-\nu$, the corresponding dual distance is exactly $\|\mu-\nu\|_w$.

Let $s=V(x)+V(y)$. If $s\ge R$, the drift condition gives

$$|PF(x)-PF(y)|\le 2+w\zeta s+2wK\le 2+w\zeta_0 s\le \frac{2+wR\zeta_0}{2+wR}d_w(x,y). \tag{1032}$$

The last inequality follows because $(2+w\zeta_0 s)/(2+ws)$ decreases with $s\ge 0$. If $s<R$, both points satisfy the minorization condition. Write $P(x,\cdot)=\alpha\nu_0+(1-\alpha)\widetilde{P}(x,\cdot)$, and similarly for y. The common component cancels, so

$$\begin{aligned}|PF(x)-PF(y)| &\le 2(1-\alpha)+w[PV(x)+PV(y)]\\ &\le 2(1-\alpha+\alpha_0)+w\zeta s\le r\,d_w(x,y).\end{aligned} \tag{1033}$$

Here $wK=\alpha_0$, and $r\ge\zeta_0>\zeta$. Duality proves the one-step contraction; iteration proves (1031). Existence and the needed moment are already supplied by Proposition 60. This proves uniqueness among finite-moment invariant laws. For any other invariant probability, apply the pointwise convergence of $P_{nh}F(x)$ for bounded tests and integrate it against that probability. Bounded convergence gives the same limiting expectations, proving uniqueness without a moment assumption on a competing invariant law. □

The condition is operational rather than a synonym for equilibrium. If the fixed-time transition density is continuous and strictly positive on $\{V\le R\}\times B$, with B a compact ball of positive volume, its positive minimum gives minorization with ν_0 the uniform law on B. Establishing that density property is the additional step, especially for degenerate forcing. A canonical Gibbs density is not inferred from Harris convergence: the invariant law may carry a driven current. Likewise, the constants can deteriorate with N. This classical method

supplies a route to regulated mixing; it neither proves regulator-independent turbulence nor replaces the physical constitutive matching.

PROPOSITION 62 (Stationary injection–dissipation balance). *Assume that* (1003) *has an invariant probability* μ_N *with* $\int |x|_H^2 \, \mu_N(\mathrm{d}x) < \infty$. *Since* H_N *is finite-dimensional,* A_N *is bounded for fixed* N, *so this moment assumption also controls* $\|A_N^{1/2} x\|_H^2$. *Then*

$$\nu_{\mathrm{v}} \int \|A_N^{1/2} x\|_H^2 \, \mu_N(\mathrm{d}x) = \int \langle f_N, x \rangle_H \, \mu_N(\mathrm{d}x) + \theta \, \mathrm{Tr}\, Q_N. \tag{1034}$$

Thus the mean viscous dissipation equals deterministic power input plus stochastic noise injection. Proposition 60 supplies an invariant law for the declared fixed-regulator coefficients. Uniqueness requires a separate irreducibility or contraction argument; existence alone does not give a uniquely selected turbulent state.

Proof. The generator applied to $V(x) = |x|_H^2/2$ is

$$\mathcal{L}_N V(x) = -\nu_{\mathrm{v}} \|A_N^{1/2} x\|_H^2 + \langle f_N, x \rangle_H + \theta \, \mathrm{Tr}\, Q_N,$$

again by (1002). Invariance gives $\int \mathcal{L}_N V \, \mu_N = 0$. To justify this identity when only a second moment is assumed, use radial cutoffs $V_R(x) = R^2 \eta(V(x)/R^2)$, where $\eta(s) = s$ near zero and η is smooth and constant for large s. Their radial gradients retain the exact convection cancellation. Their generator values are dominated by $C_N(1 + |x|_H^2)$, uniformly in R. Invariance for the bounded cutoff and dominated convergence therefore give the unbounded-test identity. Rearranging gives (1034). □

For later comparison with cascade diagnostics, let $P_{\le K}$ be an orthogonal Fourier-shell projection with $P_{\le K} H_N \subset H_N$ and $P_{\le K} A_N = A_N P_{\le K}$, and set

$$\Pi_{K,N}(x) := \langle P_{\le K} x, \, B_N(x, x) \rangle_H \, . \tag{1035}$$

The nonlinear contribution to the low-mode energy is $-\Pi_{K,N}(X_t^N)$; hence positive $\Pi_{K,N}$ denotes mean transfer out of the low shell under this sign convention. Applying Itô's formula to $|P_{\le K} X_t^N|_H^2/2$ and integrating against an invariant law with a finite third moment gives

$$\begin{aligned} \int \Pi_{K,N}(x) \, \mu_N(\mathrm{d}x) &= \int \langle P_{\le K} f_N, P_{\le K} x \rangle_H \, \mu_N(\mathrm{d}x) \\ -\nu_{\mathrm{v}} \int \|A_N^{1/2} P_{\le K} x\|_H^2 \, \mu_N(\mathrm{d}x) \quad &+ \theta \, \mathrm{Tr}(P_{\le K} Q_N P_{\le K}). \end{aligned} \tag{1036}$$

When $P_{\le K} = I_{H_N}$, in particular when the shell label contains all retained modes, the left side vanishes by (1002), and (1036) reduces to (1034). The shell identity may display nonzero fluxes when its right-hand side is nonzero; this is a finite-regulator signature of nonlinear transfer, not a theorem about a

universal inertial-range law or an intermittency exponent. The invariant law constructed in Proposition 60 meets the finite-third-moment requirement for the cubic flux. For a different invariant law, a second moment alone does not establish its integrability.

13.7.2. *A three-dimensional finite-mode numerical realization.* The energy identities can be tested on an explicit Fourier regulator without claiming an inertial range. Use $\mathbb{T}^3 = [0, 2\pi)^3$ with normalized spatial inner product and retain the wave set

$$\mathcal{K} = \{-1, 0, 1\}^3 \setminus \{0\}, \qquad |\mathcal{K}| = 26. \tag{1037}$$

Choose one member of each pair $\{k, -k\}$ by requiring the first nonzero component to be positive. For each of the 13 retained representatives, put $\widehat{k} = k/|k|$, and let a_k be the coordinate unit vector whose index minimizes $|k_i|$, breaking ties in the order x, y, z. Define

$$e_{k,1} = \frac{\widehat{k} \times a_k}{|\widehat{k} \times a_k|}, \qquad e_{k,2} = \widehat{k} \times e_{k,1}. \tag{1038}$$

These are real orthonormal vectors perpendicular to k, with a nonzero denominator for every retained wave. This prescription fixes the polarization of the deterministic forcing. The functions $\sqrt{2}e_{k,r}\cos(k \cdot x)$ and $\sqrt{2}e_{k,r}\sin(k \cdot x)$, for $r = 1, 2$, are orthonormal. Thus the regulator has 52 real coordinates X, and

$$\begin{aligned} \widehat{U}_k &= \frac{1}{\sqrt{2}} \sum_{r=1}^{2} e_{k,r}(X_{k,r,c} - iX_{k,r,s}), \qquad \widehat{U}_{-k} = \overline{\widehat{U}_k}, \\ E_N(X) &= \tfrac{1}{2}\|X\|^2 = \tfrac{1}{2} \sum_{k \in \mathcal{K}} |\widehat{U}_k|^2, \\ \widehat{B}_k &= iP_k \sum_{\substack{p,q \in \mathcal{K} \\ p+q=k}} (\widehat{U}_p \cdot q)\widehat{U}_q, \qquad P_k = I - kk^{\mathsf{T}}/|k|^2. \end{aligned} \tag{1039}$$

Only retained convolution pairs are summed; no pseudospectral aliasing is introduced. The zero mode is absent and its mean is fixed to zero. Symmetry of the wave set, solenoidality, and periodic integration by parts give $X \cdot B_N(X, X) = 0$, exactly as in (1002). Independent spatial quadrature on a five-point grid in each coordinate checks the retained convolution without using the convolution implementation itself.

The dimensionless parameters are

$$\begin{aligned} &\nu_{\mathrm{v}} = 0.5, \qquad \theta = 0.05, \\ &(A_N)_{jj} = |k_j|^2, \qquad (Q_N)_{jj} = \begin{cases} 0.2, & |k_j|^2 = 1, \\ 0.02, & |k_j|^2 > 1, \end{cases} \\ &\operatorname{Tr} Q_N = 12(0.2) + 40(0.02) = 3.2, \qquad \theta \operatorname{Tr} Q_N = 0.16. \end{aligned} \tag{1040}$$

The force has magnitude 0.4 in the first transverse cosine coordinate at $k = (1, 0, 0)$, and is zero in all other coordinates. Noise injects 0.12 units of energy per unit time into the $|k| = 1$ shell. These are prescribed input data. In particular, $Q_N \neq \nu_{\mathrm{v}} A_N$; the benchmark does not impose the equilibrium fluctuation–dissipation relation (1005). Neither a physical temperature nor a thermodynamic entropy rate is inferred from its noise amplitude.

Integration and exact discrete energy accounting. We compose an exact linear/noise half step, an explicit-midpoint convection step, and a second exact half step. For a linear substep of duration h, put $a_j = \nu_{\mathrm{v}}|k_j|^2$. Its exact transition is

$$\begin{aligned} m_{h,j}(x) &= e^{-a_j h} x_j + \frac{f_j}{a_j}(1 - e^{-a_j h}), \\ y_j &= m_{h,j}(x) + \zeta_j, \qquad \mathbb{E}\zeta_j^2 = v_{h,j} = \frac{\theta(Q_N)_{jj}}{a_j}(1 - e^{-2a_j h}). \end{aligned} \tag{1041}$$

Here $\zeta \sim \mathcal{N}(0, V_h)$, with independent components and $V_h = \mathrm{diag}(v_{h,j})$. Each realized energy increment is decomposed, without dropping its random part, as

$$\begin{aligned} E_N(y) - E_N(x) = {} & \tfrac{1}{2}\big(\|m_h(x)\|^2 - \|x\|^2 + \operatorname{Tr} V_h\big) \\ & + m_h(x) \cdot \zeta + \tfrac{1}{2}\big(\|\zeta\|^2 - \operatorname{Tr} V_h\big), \end{aligned} \tag{1042}$$

The last line is a conditionally centered random increment. The convection step is

$$x_{1/2} = x - \tfrac{1}{2}\Delta t B_N(x, x), \qquad x^+ = x - \Delta t B_N(x_{1/2}, x_{1/2}). \tag{1043}$$

It is not exactly energy preserving, despite the cancellation of the continuous vector field. We retain its realized defect $\delta E_{\mathrm{c}} = E_N(x^+) - E_N(x)$. Summing (1042) over both linear half steps and adding δE_{c} telescopes to the observed boundary energy. This identity distinguishes stochastic fluctuations from numerical convection error. The composition is still a finite-step approximation to the nonlinear diffusion; exact linear substeps do not make the nonlinear transition exact.

Sampling, uncertainty, and measured results. At each $\Delta t \in \{0.04, 0.02, 0.01\}$, 16 independently seeded paths start at zero, evolve for a preparation time 20, and are observed for $T_{\mathrm{obs}} = 80$. A deterministic seed sequence with entropy 20261008 specifies all streams and their child indices. Observation integrals use the trapezoidal rule on the endpoint values. Preparation time is not itself a proof of stationarity, so boundary energy is retained. For one path define

$$R_E := \frac{E_N(X_{t_0+T_{\mathrm{obs}}}) - E_N(X_{t_0})}{T_{\mathrm{obs}}} + \overline{D} - \overline{P} - \theta \operatorname{Tr} Q_N, \tag{1044}$$

where $D = \nu_{\mathrm{v}}\|A_N^{1/2} X\|^2$, $P = f \cdot X$, and bars denote the numerical time averages. The continuous identity makes the exact counterpart of R_E a martingale

Table 8. Finite-mode NS benchmark. Entries are means plus or minus one replicate standard error. $\overline{\Pi}$ is outward transfer from the $|k| = 1$ shell, and $\overline{\delta E_{\mathrm{c}}}$ is the sum of convection-step energy defects divided by observation time. All quantities are dimensionless.

Δt	$\overline{E}$	$\overline{\Pi}$	R_E	$10^8\overline{\delta E_{\mathrm{c}}}$
0.04	0.43650 ± 0.00667	0.02455 ± 0.00087	0.00253 ± 0.00426	-3.493 ± 2.024
0.02	0.42488 ± 0.00575	0.02432 ± 0.00091	-0.00165 ± 0.00335	-3.872 ± 0.628
0.01	0.42710 ± 0.00586	0.02493 ± 0.00091	-0.00181 ± 0.00322	-1.727 ± 0.179

contribution divided by T_{obs}, not zero on each trajectory. Its numerical version also contains time-step and quadrature error. Standard errors are computed across the 16 independent path averages, not by treating correlated time samples as independent.

At the finest step, mean dissipation is 0.46247 with standard error 0.00610, deterministic input is 0.30400 with standard error 0.00305, and mean boundary rate is -0.000283. Adding the known noise input 0.16 yields the balance residual in Table 8. The pointwise Student intervals use 15 degrees of freedom; they are approximate replicate intervals, not simultaneous confidence bands or a convergence-order proof. The measured mean outward low-shell flux is positive, but the three steps are not coupled to the same Brownian trajectories and do not establish a strong error rate.

Direct numerical checks on 64 independently sampled test states give $\max |X \cdot B_N| < 9 \times 10^{-15}$ and a normalized cancellation error below 7.2×10^{-17}. The Fourier divergence, reality, and Parseval checks are below 2.3×10^{-15}, 2.7×10^{-15}, and 2.2×10^{-14}, respectively. Independent spatial quadrature differs from the retained convolution by less than 5.4×10^{-15}. A separate linear test propagates 65,536 independent stationary Gaussian draws through one exact OU transition; its covariance identity residual is below 3.5×10^{-18}. These finite tests complement, but do not replace, the analytic cancellation proof or stochastic energy identity.

The benchmark tests the declared finite fluid equation. It does not verify the generator-matching map from an interacting microscopic gauge–gravity model, and it does not establish $N \to \infty$ convergence. That further numerical programme must refine the spatial cutoff as well as time steps, hold the physical forcing and noise conventions fixed, and resolve statistics with independent replicas or correlation-aware errors. Uniform energy and compactness estimates and identification of the limit must still be proved before a continuum conclusion can be drawn.

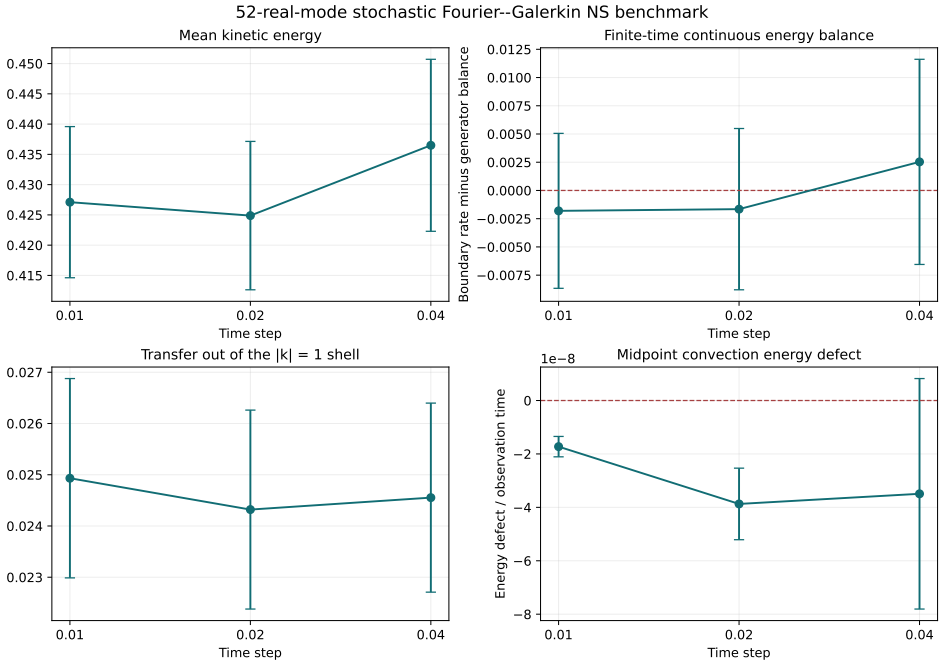


Figure 17. Step comparison for the 52-real-mode stochastic NS realization. Bars are pointwise approximate 95-percent Student intervals across 16 independent paths. The continuous balance residual includes the finite-time boundary term; the convection defect is recorded separately. Positive outward shell transfer concerns this forced finite regulator, not an inertial-range exponent or a regulator-independent turbulent law.

Remark 63 (Scope of the turbulence claim). *The preceding identities establish a mathematically controlled stochastic fluid branch at each finite N. They do not establish global regularity of the three-dimensional continuum equation, convergence as $N \to \infty$, or universality of the limiting energy spectrum. Such statements require uniform estimates and a separately proved continuum compactness and identification theorem.*

14. **A single mother equation for thermodynamics and hydrodynamic transport**

The phrase "recovered from the mother model" has a precise meaning in this paper. It does not mean that an arbitrary stochastic equation can be renamed as a fluid equation or that a Gibbs identity automatically becomes a physical second law. It means that one regulated state equation is fixed first, and that the thermodynamic and hydrodynamic equations are obtained by

two declared maps from that same equation. The maps must satisfy generator identities; otherwise the reduced equations are separate model inputs.

14.1. *The regulated mother equation.* Fix a finite regulator $r = (a, N, V)$, where a is a spatial cutoff when present, N is a mode cutoff, and V is a finite volume or compact domain. After gauge reduction and restriction to the admissible constraint manifold, let $X_t \in \mathcal{X}_r \subset \mathbb{R}^{d_r}$ satisfy

$$\mathrm{d}X_t = \big[-M_r(X_t)\nabla S_r(X_t) + \theta\ \mathrm{div}\, M_r(X_t) + c_r(X_t)\big]\mathrm{d}t + \sqrt{2\theta M_r(X_t)}\mathrm{d}W_t. \tag{1045}$$

Here S_r is the regulated master energy obtained from the master action after the declared spatial and modal reduction, $M_r = M_r^{\mathsf{T}} \succ 0$ is the physical reduced mobility, $\theta > 0$ is the calibrated fluctuation energy, and c_r is a reversible or maintained-circulation drift. The divergence in (1045) is taken row by row in the chosen reference coordinates. The noise covariance is therefore $2\theta M_r$. A different stochastic convention changes the displayed noise-induced drift and must be transformed consistently. For dimensional time, S_r is the energy-normalized functional U_{M} restricted to this regulator, not the unscaled Lorentzian action. The covariance square root is interpreted in the chosen normalized coordinates or through a factor Σ_r with $\Sigma_r\Sigma_r^{\mathsf{T}} = 2\theta M_r$. Componentwise unit conversion is given in Appendix E.

Assume that

$$Z_r := \int_{\mathcal{X}_r} e^{-S_r/\theta}\mathrm{d}x < \infty, \qquad \pi_r := Z_r^{-1}e^{-S_r/\theta}, \qquad \nabla\cdot(\pi_r c_r) = 0, \tag{1046}$$

with either periodic boundary conditions or reflecting conditions $n \cdot M_r\nabla(p/\pi_r) = 0$ and $n \cdot c_r = 0$. The first two conditions make the Gibbs law a candidate probability law; the last condition states that c_r preserves that measure. It does not separately imply that c_r is divergence free in coordinate volume or tangent to every energy level. It is not automatic for a drift extracted from a master action.

The generator of (1045) is

$$L_r f = \big[-M_r\nabla S_r + \theta\,\mathrm{div}\, M_r + c_r\big]\cdot\nabla f + \theta M_r : D^2 f. \tag{1047}$$

The corresponding Fokker–Planck current for a density p_t relative to coordinate volume is

$$j_r[p_t] = p_t c_r - \theta p_t M_r \nabla \log(p_t/\pi_r), \qquad \partial_t p_t = -\nabla\cdot j_r[p_t]. \tag{1048}$$

Indeed, $\nabla \log \pi_r = -\nabla S_r/\theta$, and substitution of (1045) into the adjoint of (1047) gives $j_r = p_r[-M_r\nabla S_r + \theta\,\mathrm{div}\, M_r + c_r] - \theta\,\mathrm{div}(M_r p_r)$, which is exactly (1048). At $p_t = \pi_r$, the current is $\pi_r c_r$, whose divergence vanishes by (1046).

14.2. *The second law as a consequence of the same equation.* Define the regulated relative free energy

$$\mathcal{F}_r[p] - \mathcal{F}_r[\pi_r] := \theta\ \mathrm{KL}(p\|\pi_r) = \theta \int p \log(p/\pi_r)\mathrm{d}x. \tag{1049}$$

For positive smooth solutions with finite weighted Fisher information, the continuity equation and integration by parts give

$$\begin{aligned}\frac{\mathrm{d}}{\mathrm{d}t}\,\mathrm{KL}(p_t\|\pi_r) &= \int j_r[p_t]\cdot\nabla\log(p_t/\pi_r)\mathrm{d}x \\ &= -\theta\int p_t\,\nabla\log(p_t/\pi_r)^{\mathsf{T}} M_r \nabla\log(p_t/\pi_r)\mathrm{d}x \le 0.\end{aligned} \tag{1050}$$

The circulation term vanishes because, with $f = p_t/\pi_r$, $\int \pi_r c_r\cdot\nabla f\mathrm{d}x = 0$. Hence

$$\frac{\mathrm{d}}{\mathrm{d}t}\mathcal{F}_r[p_t] = -\theta^2\int p_t\,\nabla\log(p_t/\pi_r)^{\mathsf{T}} M_r\nabla\log(p_t/\pi_r)\mathrm{d}x \le 0. \tag{1051}$$

This is an ensemble-level second-law statement for the declared finite regulator. It does not assert that every sample path has monotonically decreasing energy. If $c_r \neq 0$, the limiting Gibbs density can still carry a stationary current. Under all-even time reversal and mutual absolute continuity of forward and reversed path laws, the stationary path-entropy rate is instead

$$\sigma_r := \lim_{T\to\infty}\frac{1}{T}\,\mathrm{KL}(P^r_{[0,T]}\|\Theta_{\#}P^r_{[0,T]}) = \frac{1}{\theta}\int \pi_r c_r^{\mathsf{T}} M_r^{-1} c_r\mathrm{d}x \ge 0. \tag{1052}$$

For odd variables, Θ must reverse the declared odd coordinates and external parameters before the Girsanov comparison. Thus (1051) measures relaxation of a distribution, whereas (1052) measures maintained path irreversibility; they are not the same quantity.

14.3. *Dynamic programming is generated by the same drift and cost.* Use the uncontrolled reference drift $b^0_r = c_r + \theta\,\mathrm{div}\,M_r$, with covariance $2\theta M_r$. Add a drift control u_t to this reference, and use the running cost

$$\ell_r(x,u) = W_r(x) + \frac{1}{2}u^{\mathsf{T}} M_r(x)^{-1}u. \tag{1053}$$

Here u is a drift increment. With dimensional stochastic time, $u^{\mathsf{T}}M_r^{-1}u$, ℓ_r, W_r, and the ergodic value λ_r have units of energy per unit time, whereas $V_r = S_r$ has energy units. Under $t = t_{\mathrm{s}}/t_{\mathrm{ref}}$, the numerical running and ergodic costs are multiplied by $t_{\mathrm{ref}}/E_{\mathrm{ref}}$, and the value by $1/E_{\mathrm{ref}}$. Thus every term in the HJB equation below has the same units. If a smooth function $V_r = S_r$ and constant λ_r obey

$$W_r = \lambda_r + \frac{1}{2}\nabla S_r^{\mathsf{T}} M_r\nabla S_r - c_r\cdot\nabla S_r - \theta\,\mathrm{div}(M_r\nabla S_r), \tag{1054}$$

define $L_r^{0,u} f = (b_r^0 + u) \cdot \nabla f + \theta M_r : D^2 f$. Direct substitution into the ergodic HJB equation gives

$$\ell_r + L_r^{0,u} V_r - \lambda_r = \frac{1}{2}(u + M_r \nabla S_r)^{\mathsf{T}} M_r^{-1} (u + M_r \nabla S_r) \geq 0,$$
$$u_r^* = -M_r \nabla S_r. \tag{1055}$$

The selected drift is $b_r^0 + u_r^* = b_r$. Adding the control to the already dissipative drift b_r would count the gradient term twice. The completed-square identity supplies a smooth HJB candidate. An ergodic optimality conclusion also requires admissibility, nonexplosion, integrability of the martingale, and the transversality condition $\mathbb{E} V_r(X_T)/T \to 0$ for the compared controls. Integrating the identity and dividing by T then gives the lower bound λ_r, with equality for the admissible selector. Thus the HJB selector, the Gibbs reference and the dissipative drift are generated by one explicitly matched data set. Equation (1054) is a compatibility condition, not a claim that every residual cost in the larger programme automatically has this form. Dynamic programming and the stochastic maximum principle must use the same filtration, endpoint data, admissible controls and clock.

14.4. *Hydrodynamic projection and recovery of a finite Galerkin equation.* Let V_N be a divergence-free Galerkin space on the regulated spatial domain, with orthogonal projector P_N, Stokes operator A_N, and bilinear convection map B_N. Let $\Pi_N : \mathcal{X}_r \to V_N$ be the declared velocity observation map. It may depend on the coframe, matter momentum and the bath variables, but it is fixed before the fluid validation data are used. Put $U_t^N = \Pi_N(X_t)$. The exact finite-regulator recovery condition is the generator identity

$$L_r(F \circ \Pi_N)(x) = \mathcal{L}_N^{\mathrm{NS}} F(\Pi_N x) \quad \text{for every } F \in \mathscr{C}_N, \tag{1056}$$

where $\mathscr{C}_N$ is a determining cylinder core and

$$\mathcal{L}_N^{\mathrm{NS}} F(U) = DF(U)\big[-\nu A_N U - P_N B_N(U,U) + f_N\big] + \frac{1}{2} Q_N : D^2 F(U). \tag{1057}$$

For a smooth projection, (1056) is equivalent to the two coefficient identities

$$D\Pi_N \, b_r + \frac{1}{2}\big[\mathrm{tr}(a_r D^2 \Pi_{N,i})\big]_i = -\nu A_N \Pi_N - P_N B_N(\Pi_N, \Pi_N) + f_N,$$
$$D\Pi_N \, a_r D\Pi_N^{\mathsf{T}} = Q_N, \tag{1058}$$

where b_r and $a_r = 2\theta M_r$ are the drift and covariance of the mother equation. The first line contains the Itô correction; it vanishes only for an affine projection. The second line fixes the projected noise, so the fluid covariance cannot be fitted independently after the drift has been matched.

Under (1056), Itô's formula gives the finite-dimensional stochastic Navier–Stokes equation

$$\mathrm{d}U_t^N = \big[-\nu A_N U_t^N - P_N B_N(U_t^N, U_t^N) + f_N\big]\mathrm{d}t + Q_N^{1/2}\mathrm{d}W_t^N. \tag{1059}$$

This is the precise sense in which the hydrodynamic equation is recovered from the mother equation. It is not a proof of the unregularized three-dimensional Navier–Stokes regularity problem.

Assume the Galerkin convection is energy preserving, $\langle U, B_N(U,U)\rangle = 0$, and use the energy $E_N(U) = \frac{1}{2}\|U\|^2$. Itô's formula applied to (1059) yields

$$\mathrm{d}E_N(U_t^N) = \left[-\nu\|A_N^{1/2}U_t^N\|^2 + \langle f_N, U_t^N\rangle + \frac{1}{2}\operatorname{tr} Q_N\right]\mathrm{d}t + \langle U_t^N, Q_N^{1/2}\mathrm{d}W_t^N\rangle. \tag{1060}$$

Taking expectations gives the injection–dissipation identity. If P_k partitions the retained modes and $T_k(U) := -\langle P_k U, P_k B_N(U,U)\rangle$, then

$$\sum_k T_k(U) = 0, \qquad \frac{\mathrm{d}}{\mathrm{d}t}\mathbb{E}E_N = \mathbb{E}\langle f_N, U_N\rangle + \frac{1}{2}\operatorname{tr} Q_N - \nu\mathbb{E}\|A_N^{1/2}U_N\|^2. \tag{1061}$$

The first identity is conservative redistribution among retained shells; it is not itself an inertial-range law. A continuum cascade would require uniform estimates as $a \downarrow 0$, $N \to \infty$, and $V \uparrow \mathbb{R}^3$, with a compatible sequence of projections and tightness. Those estimates remain a separate completion problem.

14.5. *The projected second law and its physical normalization.* The Galerkin energy budget and the projected entropy law require different calculations. Suppose the mother process has invariant probability π_r, the observation $U = \Pi_N(X)$ is autonomous Markov, and its well-posed martingale problem has the generator fixed by the drift and covariance matching identities. Write $\pi_N = (\Pi_N)_{\#}\pi_r$. If $X_0 \sim \pi_r$, then $X_t \sim \pi_r$ and $U_t \sim \pi_N$; hence π_N is invariant for the projected semigroup. The same Markov kernel acts on every admissible initial law, so data processing gives

$$\mathrm{KL}(p_t^N\|\pi_N) \le \mathrm{KL}(p_s^N\|\pi_N), \qquad t \ge s. \tag{1062}$$

This conclusion needs neither detailed balance nor a quadratic Gibbs law for the resolved velocity.

For a projected diffusion with covariance $Q_N(U)$, let $f_t = dp_t^N/d\pi_N > 0$. Assume that the logarithmic chain rule, generator adjoint relation, and boundary integrations are valid, with finite entropy and Fisher integral. Invariance and

$$L_N(f\log f) = (1+\log f)L_N f + \frac{1}{2f}\nabla f^{\mathsf{T}} Q_N \nabla f$$

give, using $\partial_t f_t = L_N^\dagger f_t$ in $L^2(\pi_N)$,

$$\frac{d}{dt}\,\mathrm{KL}(p_t^N\|\pi_N) = -\frac{1}{2}\int f_t\,\nabla\log f_t^{\mathsf{T}} Q_N \nabla\log f_t\,d\pi_N \le 0. \tag{1063}$$

Indeed, $\int f_t L_N \log f_t\,d\pi_N$ is the entropy derivative, and $L_N \log f = f^{-1}L_N f - (2f^2)^{-1}\nabla f^{\mathsf{T}} Q_N \nabla f$, whose first term integrates to zero after multiplication by f. This derivation avoids an unjustified assumption that the projected generator is symmetric.

If $\pi_N = Z_N^{-1} e^{-E_N/(k_B T)}$ relative to the declared reference measure at a calibrated constant temperature, the excess isothermal free energy is $k_B T\,\mathrm{KL}(p^N\|\pi_N)$. Thus $-T^{-1}d\mathcal{F}_N/dt \ge 0$ is the corresponding relaxation contribution to the entropy-production rate. For a maintained nonequilibrium stationary law, that contribution need not equal total entropy production: external work and housekeeping production must also be included. A stationary law need not be a Gibbs law for the kinetic energy. Marginalizing a Gibbs measure generally produces a potential of mean force, not the original microscopic energy evaluated at a projection.

These results establish a finite Galerkin second law when the projected generator, covariance, and invariant measure really are inherited from the same mother process. They do not establish an unconditional second law for arbitrary reversible microscopic dynamics or a continuum turbulence theorem. The latter would require a compatible family of generators, uniform bounds, tightness, and control of entropy and boundary terms in the limit.

14.6. *A precise correspondence inclusion.* The phrase "the classical theories are contained in the unified theory" is made precise by restricting the statement to a declared class of classical equations and to declared reduction maps. Let $\mathfrak{T}_{\mathrm{cl}}^{(r)}$ denote the set of finite-regulator classical mechanical, geometric, gauge, and Galerkin-fluid generators listed below, and let $\mathfrak{T}_{\mathrm{un}}^{(r)}$ denote the images of the mother generator under the admissible projections and parameter scalings. The intended correspondence statement is

$$\mathfrak{T}_{\mathrm{cl}}^{(r)} \subseteq \mathfrak{T}_{\mathrm{un}}^{(r)}, \tag{1064}$$

provided the generator identities, constraint maps, and boundary conditions listed in this section hold. For an unregulated theory the mathematically appropriate statement is the closure relation

$$\mathfrak{T}_{\mathrm{cl}} \subseteq \overline{\bigcup_r \mathfrak{T}_{\mathrm{un}}^{(r)}}, \tag{1065}$$

where the closure is taken in the declared topology of generators or finite-time laws. Equation (1065) is a completion criterion, not an automatic consequence of a common notation.

For classical mechanics, choose the canonical antisymmetric matrix J_{can}, let $M_r \to 0$, $\theta \to 0$, and identify the master energy with a Hamiltonian $H(q,p)$. The limiting drift is then

$$\dot z = J_{\mathrm{can}} \nabla H(z), \qquad \dot q = \partial_p H, \quad \dot p = -\partial_q H, \tag{1066}$$

with the usual Hamiltonian conservation law $\mathrm{d}H/\mathrm{d}t = 0$ whenever H has no explicit time dependence.

The corresponding stochastic-to-classical scaling can be stated without identifying the control Hamiltonian with the mechanical Hamiltonian. Let $\widetilde{M}_r = \widetilde{M}_r^{\mathsf{T}} \succeq 0$, let $J_{\mathrm{can}}^{\mathsf{T}} = -J_{\mathrm{can}}$, and set $M_r = \gamma \widetilde{M}_r$, $S_r = H$, and $c_r = J_{\mathrm{can}} \nabla H$. The regulated equation then reads

$$\begin{aligned} \mathrm{d}Z_t^{\gamma,\theta} = {} & \Big[J_{\mathrm{can}} \nabla H(Z_t^{\gamma,\theta}) - \gamma \widetilde{M}_r \nabla H(Z_t^{\gamma,\theta}) \Big] \mathrm{d}t \\ & + \theta\gamma \ \mathrm{div}\, \widetilde{M}_r(Z_t^{\gamma,\theta}) \mathrm{d}t + \sqrt{2\theta\gamma \widetilde{M}_r(Z_t^{\gamma,\theta})}\, \mathrm{d}W_t. \end{aligned} \tag{1067}$$

The canonical drift preserves H and the Gibbs density because $\nabla \cdot (J_{\mathrm{can}} \nabla H) = 0$ and $(J_{\mathrm{can}} \nabla H) \cdot \nabla H = 0$. Thus it is a Hamiltonian transport part; statistical reversal additionally requires the declared momentum parity and symmetry of H. The terms proportional to γ are the reservoir coupling. If $H \in C^2$, the mobility and its divergence are locally bounded, the stochastic equations are well posed, and the solutions with the same initial condition remain in a common compact set, then for every finite T,

$$\sup_{t \le T} \big| Z_t^{\gamma,\theta} - z_t \big| \longrightarrow 0 \quad \text{in probability} \qquad \text{as } \gamma \downarrow 0, \quad \theta\gamma \downarrow 0, \tag{1068}$$

where z solves $\dot z = J_{\mathrm{can}} \nabla H(z)$. The assertion is a finite-time convergence statement; it does not claim convergence of invariant measures. Dissipative relaxation estimates need not be uniform as $\gamma \downarrow 0$.

For completeness, stop both solutions on exiting a compact set K. The Lipschitz constant of $J_{\mathrm{can}} \nabla H$ and the coefficient bounds on K, followed by the martingale maximal inequality and Gronwall's inequality, give

$$\mathbb{E} \sup_{t \le T \wedge \tau_K} |Z_t^{\gamma,\theta} - z_t|^2 \le C_{T,K} \{ \gamma^2 + (\theta\gamma)^2 + \theta\gamma \}.$$

The first two terms bound the integrated drift perturbations; the last comes from the quadratic variation of the noise. The right side tends to zero in the stated scaling. Removing the stop requires a common compact containment estimate; it does not follow from smoothness alone.

For the mechanical Hamiltonian

$$H(q,p) = \frac{|p|^2}{2m} + V(q), \tag{1069}$$

the canonical equations in (1066) give

$$\dot{q} = \frac{p}{m}, \qquad \dot{p} = -\nabla V(q), \qquad m\ddot{q} = -\nabla V(q).$$

Consequently Newton's equation is the zero-noise, zero-reservoir-coupling subsector of the regulated mother equation, subject to the regularity and finite-time compactness assumptions above. This is the precise content of the inclusion of classical mechanics; it is not a claim that every classical Hamiltonian system is recovered without specifying its phase space, symplectic form, boundary conditions, and scaling.

For a globally defined C^2 charge Q generating the canonical symmetry $\xi = J_{\mathrm{can}}\nabla Q$, invariance of H implies $\{Q, H\} = \nabla Q^{\mathsf{T}} J_{\mathrm{can}} \nabla H = 0$. Itô's formula then gives the finite-coupling charge balance

$$\begin{aligned} dQ(Z_t) = {} & \left[-\gamma \nabla Q^{\mathsf{T}} \widetilde{M}_r \nabla H + \theta\gamma \operatorname{div}(\widetilde{M}_r \nabla Q)\right] dt \\ & + \nabla Q^{\mathsf{T}} \sqrt{2\theta\gamma \widetilde{M}_r}\, dW_t. \end{aligned}$$

Under the same local bounds the drift terms and martingale converge to zero on finite intervals, recovering $dQ(z_t)/dt = 0$. At finite coupling this is a balance law; conservation requires the additional cancellation of its drift, and pathwise conservation also requires vanishing quadratic variation. A general symplectic vector field need not have a globally defined Hamiltonian charge.

For the geometric branch, the coframe and connection projections must obey

$$\left\|\mathcal{E}^{(r)}_{\mathrm{grav}}\right\|_X \le \varepsilon_{\mathrm{grav}}(r), \qquad \varepsilon_{\mathrm{grav}}(r) \longrightarrow 0 \tag{1070}$$

under the stated low-curvature and scale-matching limit. The target equation is the Einstein equation plus the declared higher-curvature remainder; ordinary Einstein dynamics is recovered only when the remainder estimate tends to zero.

For the internal connection, the corresponding requirement is

$$\left\|\mathcal{E}^{(r)}_{\mathrm{YM}}\right\|_Y \le \varepsilon_{\mathrm{YM}}(r), \qquad \varepsilon_{\mathrm{YM}}(r) \longrightarrow 0, \tag{1071}$$

with constant or separately matched kinetic coefficients on the declared branch. Gauge covariance and positivity of the kinetic form are hypotheses; they are not inferred from the existence of a larger connection.

For the fluid branch, the exact finite-dimensional inclusion is the generator identity (1056). If it is replaced by an approximate identity, define

$$\begin{aligned} \varepsilon^{(r,N)}_{\mathrm{rec}} := {} & \left\| D\Pi_N b_r + \tfrac{1}{2}[\mathrm{tr}(2\theta M_r D^2 \Pi_{N,i})]_i - b^{\mathrm{NS}}_N \circ \Pi_N \right\| \\ & + \| D\Pi_N (2\theta M_r) D\Pi_N^{\mathsf{T}} - Q_N \circ \Pi_N \|, \end{aligned} \tag{1072}$$

where the norms are evaluated on the declared regulated domain. The finite Galerkin equation is recovered only when $\varepsilon^{(r,N)}_{\mathrm{rec}} = 0$; convergence to a continuum fluid equation requires a separate uniform estimate.

The mechanical scaling and the finite fluid generator identity therefore give explicit correspondence calculations. Einstein and Yang–Mills equations concern field variations and require their separate low-energy matching results; they are not established by the diffusion calculation alone. Simultaneous recovery with one frozen coefficient vector requires the admissible parameter sets of all branches to have a common point. Separate nonempty branch sets need not intersect. Approximate recovery also requires stability of the solution maps and residual convergence in the topology used for the limit. The displayed inclusion is consequently a conditional correspondence target until these compatibility requirements are verified for the specified physical mother model.

14.7. *No-refit cross-sector prediction.* The correspondence inclusion becomes a physical prediction only after the mother data have been frozen. Let

$$\vartheta = (c_\alpha, \mu_\beta, p_\gamma, \theta, \bar{\kappa}, \text{boundary and scale data})$$

denote all coefficients that enter the regulated generator and the declared projection maps. Partition the available information into a calibration set D_{cal} and a statistically independent validation set D_{val}. The calibration problem is

$$\vartheta_* \in \operatorname*{arg\,min}_{\vartheta\in\Theta_r,\ \mathcal{C}(\vartheta)=0} \left\{ \|\mathcal{O}_{\mathrm{cal}}(\vartheta) - D_{\mathrm{cal}}\|^2_{\Sigma_{\mathrm{cal}}^{-1}} \right\}, \tag{1073}$$

where the constraint residual $\mathcal{C}$ includes positivity, gauge, parity, conservation, generator-matching, and boundary conditions. Once ϑ_* has been fixed, it is not changed when computing any target observable in D_{val}.

For each branch b (thermodynamic, hydrodynamic, gauge, or black-hole), the prediction is the deterministic map

$$\widehat{\mathcal{O}}_b = \mathcal{P}_b(\vartheta_*; \mathcal{I}_b), \tag{1074}$$

where $\mathcal{I}_b$ contains only independently specified initial, boundary, and instrument data. The branch maps are not allowed to contain a target-dependent adjustment of ϑ_*.

The principal black-hole candidate is the correlated relation

$$\frac{M\Delta\omega^{\mathrm{res}}_{\ell m}}{C_{\ell m}(a/M)} = \frac{\Delta\mathcal{D}_{\mathrm{acc}}/\mathcal{D}_0}{D(a/M, \dot{M}, \ldots)} = \bar{\kappa}_* + O(\bar{\kappa}_*^2), \tag{1075}$$

provided both coefficients are nonzero first-order responses derived from the same physical model, $\mathcal{D}_0 \neq 0$, and $G = c = 1$. Each displayed equality holds to the indicated order, with its own controlled remainder. Higher leading orders require a different relation. The first residual uses independently inferred Kerr mass and spin,

$$\Delta\omega^{\mathrm{res}}_{\ell m} = \omega^{\mathrm{obs}}_{\ell m} - \omega^{\mathrm{Kerr}}_{\ell m}(M, a),$$

so ordinary Kerr rotational splitting is not misidentified as a new effect. Equation (1075) is a prediction protocol, not a numerical claim: $C_{\ell m}$ and D must be computed before the validation data are inspected.

The validation statistic is the whitened residual

$$\chi^2_{\mathrm{val}} = \big(\mathcal{O}_{\mathrm{val}} - \widehat{\mathcal{O}}_{\mathrm{val}}(\vartheta_*)\big)^T \Sigma_{\mathrm{val}}^{-1} \big(\mathcal{O}_{\mathrm{val}} - \widehat{\mathcal{O}}_{\mathrm{val}}(\vartheta_*)\big). \tag{1076}$$

The null comparison must include general-relativistic Kerr, the declared standard fluid closure, and a separable-channel model with the same number of calibration parameters. A failure of the correlated relation or of the predeclared validation bound is a falsification of this realization, not a reason to refit the target sector.

This procedure is the precise sense in which the same mother equation can predict an independent observation without target-dependent fitting. It also prevents a formal common notation from being counted as physical unification.

Equations (1051) and (1059) are consequences of the same finite-regulator law only when the displayed Gibbs, boundary, generator-matching, and covariance conditions hold. The theorem therefore supplies a falsifiable bridge: one may estimate S_r, M_r, c_r in one calibration sector and test the predicted fluid drift, noise covariance, free-energy decay and stationary path asymmetry in another sector without introducing a second independently fitted generator.

It does not determine the numerical viscosity, bath temperature, projection, or physical clock merely from notation. It also does not derive a full quantum field theory, a regulator-independent Navier–Stokes continuum, or a universal cosmological arrow. Those claims require additional matching and limit theorems. This explicit boundary is part of the proposed unification: the mother equation is a common source only to the extent that its physical data and its reduction maps are actually fixed and verified.

14.8. *Causal order, clock duration, and a statistical arrow.* Time enters this construction in three distinct ways. A Lorentzian metric specifies which events can be connected by causal signals. A material clock measures duration along a timelike trajectory. A path law specifies whether forward histories can be distinguished statistically from physically reversed histories. The last property does not define either of the first two. In signature $(-+++)$ and coordinates $x^0 = ct$, proper time satisfies

$$d\tau^2 = -c^{-2} g_{\mu\nu}\, dx^\mu dx^\nu.$$

This formula applies to timelike worldlines, not to an arbitrary Brownian path in a configuration space. An auxiliary sampling parameter acquires a physical interpretation only after a clock map has been supplied.

The following result makes the effect of a clock map explicit. It is an application of the standard time-change construction for Markov processes, not a derivation of relativistic proper time from a probability law.

PROPOSITION 64 (A state-dependent clock changes the invariant law). *Let X_s be a conservative diffusion on a connected compact smooth manifold without boundary, with smooth uniformly elliptic generator*

$$Lf = b^i \partial_i f + D^{ij} \partial_i \partial_j f, \qquad D = D^{\mathsf{T}} > 0.$$

Suppose that it has invariant probability π and a unique martingale problem. Let a be smooth and $0 < a_- \le a(x) \le a_+ < \infty$. Define $T(s) = \int_0^s a(X_v)\, dv$, its inverse $S(t) = T^{-1}(t)$, and $Y_t = X_{S(t)}$. Then the generator and invariant law of Y are

$$\widetilde{L} = a^{-1} L, \qquad \widetilde{\pi}(dx) = \frac{a(x)}{Z_a} \pi(dx), \qquad Z_a = \int a \, d\pi. \tag{1077}$$

The invariant probability is unique. Reversibility is preserved under this clock change, with respect to the new invariant probability.

Proof. For a smooth f, the process $f(X_s) - f(X_0) - \int_0^s Lf(X_v)\, dv$ is a local martingale. Substituting $s = S(t)$ and using $dS/dt = 1/a(Y_t)$ gives the martingale problem for $\widetilde{L}$. The bounds on a prevent clock explosion or stopping. The smooth uniformly elliptic diffusion on the compact connected state space has a conservative, irreducible, smoothing semigroup. Its invariant probability is therefore unique. Integration gives

$$\int \widetilde{L} f \, d\widetilde{\pi} = Z_a^{-1} \int Lf \, d\pi = 0.$$

Smooth elliptic well-posedness identifies this infinitesimal identity with invariance. Finally,

$$\langle f, \widetilde{L} g \rangle_{\widetilde{\pi}} = Z_a^{-1} \langle f, Lg \rangle_{\pi}.$$

Thus symmetry of one generator is equivalent to symmetry of the other on their smooth cores, and hence of their closed realizations. □

The identity extends to compatible reflecting realizations when the time-changed martingale problem, conormal boundary condition, and invariant measure criterion are established. An unbounded clock, a vanishing lapse, or a singular boundary requires a separate theorem. In particular, this compact uniformly elliptic result cannot be extended to a black-hole horizon by substitution.

14.9. *Entropy rates and relaxation after calibration.* For an explicit calculation take a flat torus and assume all state variables are even under time reversal. Write $\pi(x)$ for the smooth positive stationary density and

$$J_i = b_i\pi - \partial_j(D_{ij}\pi).$$

Assume the stationary forward and reversed laws satisfy the usual finite path-energy and absolute-continuity hypotheses. Their relative entropy per unit s is

$$e_s = \int \frac{J^{\mathsf{T}} D^{-1} J}{\pi}\, dx.$$

Under (1077), direct substitution yields

$$\widetilde{D} = D/a, \qquad \widetilde{J} = J/Z_a, \qquad e_t = \int \frac{\widetilde{J}^{\mathsf{T}}\widetilde{D}^{-1}\widetilde{J}}{\widetilde{\pi}}\, dx = \frac{e_s}{Z_a}.$$

The cancellation follows from $\partial_j[(D_{ij}/a)(a\pi/Z_a)] = Z_a^{-1}\partial_j(D_{ij}\pi)$. This also proves that a positive clock change cannot turn a reversible diffusion into an irreversible one. For odd variables the reversal must include their parity; preservation of generalized detailed balance requires a parity-even clock and the corresponding operator domains.

On a finite path window the informational asymmetry is $D(P_F\|P_R\circ\mathcal{T}^{-1})$. Under mutual absolute continuity, normalization gives

$$\mathbb{E}_F \exp(-\Sigma/k_B) = 1, \qquad \mathbb{E}_F\Sigma = k_B D(P_F\|P_R\circ\mathcal{T}^{-1}) \geq 0,$$

where $\Sigma = k_B \log[dP_F/d(P_R\circ\mathcal{T}^{-1})]$. The equality of Σ with thermodynamic total entropy requires local detailed balance, reservoir bookkeeping, and the specified endpoint laws. It does not follow solely from normalization.

An invariant Gibbs law can support irreversible relaxation from a prepared nonequilibrium distribution while its stationary process is reversible. Conversely, a stationary circulating law can have positive path entropy production even though its state relative entropy is constant. Thus duration, relaxation, and stationary path asymmetry are different physical quantities.

PROPOSITION 65 (A calibrated spectral-gap bound). *Under Proposition 64, suppose that L is reversible and obeys $\operatorname{Var}_\pi f \leq C_P\mathcal{E}(f,f)$, where $\mathcal{E}(f,f) = -\langle f, Lf\rangle_\pi$. Then*

$$\operatorname{Var}_{\widetilde{\pi}} f \leq a_+ C_P\, \widetilde{\mathcal{E}}(f,f), \qquad \widetilde{\mathcal{E}}(f,f) = Z_a^{-1}\mathcal{E}(f,f).$$

In particular the new spectral gap is at least $(a_+C_P)^{-1}$.

Proof. Use the variational characterization of variance and choose the old mean:

$$\operatorname{Var}_{\widetilde{\pi}} f \leq \int (f-\pi f)^2\, d\widetilde{\pi} \leq (a_+/Z_a)\operatorname{Var}_\pi f.$$

Insert the old Poincare inequality and the displayed Dirichlet-form identity. The spectral theorem gives exponential $L^2(\widetilde{\pi})$ relaxation for densities initially in that space. This argument does not claim uniform total-variation convergence from every singular initial law. □

14.10. *An exactly normalized clock experiment.* Consider $dX_s = b\,ds + \sqrt{2D}\,dW_s$ modulo 2π, with $D > 0$, and $a(x) = a_0(1 + \eta\cos x)$, where $a_0 > 0$ and $|\eta| < 1$. The original invariant density is $1/(2\pi)$, whereas

$$\widetilde{\pi}(x) = \frac{1 + \eta\cos x}{2\pi}, \qquad \widetilde{J} = \frac{b}{2\pi a_0}, \qquad e_t = \frac{b^2}{Da_0}.$$

Consequently equilibrium histograms alone cannot identify the clock or the current: changing b preserves this histogram and changes the arrow. The example is dimensionless; a_0 converts its two declared time units.

For an integer $N \geq 3$, set $h = 2\pi/N$ and $q_\pm = D/h^2 \pm b/(2h) > 0$, and divide the two outgoing rates at node i by $a_i = a(ih)$. The resulting Markov chain has $\widetilde{\pi}_i = a_i/\sum_j a_j$. Its stationary oriented edge flows are $q_\pm/\sum_j a_j$, so its entropy rate is exactly

$$e_{t,N} = \frac{b}{a_0 h}\log\frac{D/h^2 + b/(2h)}{D/h^2 - b/(2h)} = \frac{b^2}{Da_0} + \frac{b^4h^2}{12D^3a_0} + O(h^4). \tag{1078}$$

The restriction $N \geq 3$ keeps the two neighbours distinct. For $N = 2$, clockwise and counterclockwise jumps reach the same state, so the state-observed off-diagonal rate is $(q_+ + q_-)/a_i$. The stationary flux in either direction is then $(q_+ + q_-)/\sum_{j=0}^{1} a_j$, and the state-path entropy production is zero. Formula (1078) can still describe the two-state system if jump orientations are recorded as distinct channels; it is not the entropy rate of the state path alone. The series uses $\log[(1+z)/(1-z)] = 2z+2z^3/3+O(z^5)$, with $|z| = |b|h/(2D) < 1$. Thus positivity and second-order entropy-rate convergence can be checked independently of a stochastic sampling error. The matrix-exponential experiment uses $(b, D, a_0, \eta) = (0.7, 0.4, 1.6, 0.5)$. It compares transient densities with the exact stationary law and checks relative-entropy contraction toward that law. It is a synthetic clock calibration example, not an observation of fundamental time.

14.11. *A finite-state proof of the three entropy statements.* A clock orders events and measures duration. Entropy production asks a different question: how well can the statistics of a history be distinguished from those of its specified reverse? The distinction can be proved without a continuum limit. Throughout this subsection all variables are even under reversal, and rates refer to one fixed physical clock. Odd variables, magnetic protocols, and time-dependent reservoirs require their corresponding reversed dynamics.

Table 9. Synthetic clock experiment. The exact continuum entropy rate is 0.76562500; the invariant residual is the maximum component of $Q^{\mathsf{T}}\widetilde{\pi}$.

N	Entropy rate	Absolute error	Invariant residual
16	0.79809013	3.25e-02	8.33e-17
32	0.77329434	7.67e-03	1.11e-16
64	0.76751664	1.89e-03	1.67e-16
128	0.76609634	4.71e-04	4.44e-16
256	0.76574274	1.18e-04	8.88e-16

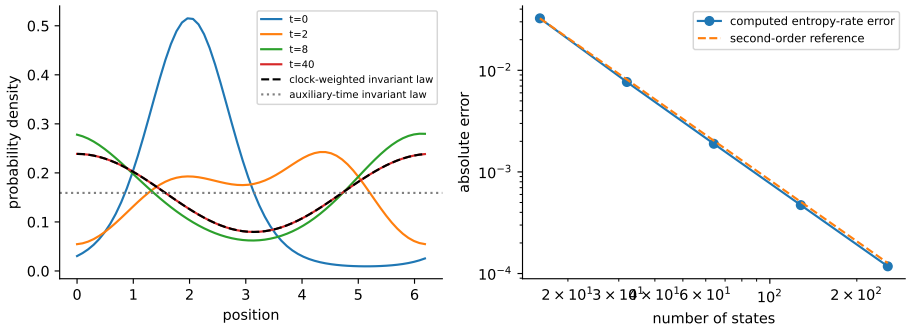


Figure 18. A state-dependent clock reweights the invariant density. The left panel shows deterministic Markov-semigroup evolution and its exact target. The right panel compares discrete stationary path entropy rates with the continuum value. The calculation tests a clock transformation, not a derivation of a spacetime metric.

Proposition 66 (Relaxation and stationary path asymmetry). *Let q_{ij}, $i \neq j$, be the rates of an irreducible finite continuous-time Markov chain. Assume reciprocal support: $q_{ij} > 0$ if and only if $q_{ji} > 0$. Let π be its unique stationary probability, and let $p(t) > 0$ solve the master equation. Put $f_i = p_i/\pi_i$. Sums below run over directed edges with positive rate. Then*

$$\sigma_{\mathrm{tot}} = \sum_{i \neq j} p_i q_{ij} \log \frac{p_i q_{ij}}{p_j q_{ji}}, \tag{1079}$$

$$\sigma_{\mathrm{hk}} = \sum_{i \neq j} p_i q_{ij} \log \frac{\pi_i q_{ij}}{\pi_j q_{ji}}, \tag{1080}$$

$$\sigma_{\mathrm{na}} = \sum_{i \neq j} p_i q_{ij} \log \frac{f_i}{f_j} = -\frac{d}{dt} D(p(t) \| \pi). \tag{1081}$$

All three rates are nonnegative and $\sigma_{\mathrm{tot}} = \sigma_{\mathrm{hk}} + \sigma_{\mathrm{na}}$. These rates have units of inverse time. Multiplication by k_B gives entropy units, but their physical reservoir interpretation additionally requires a thermodynamic identification of the rates.

Proof. Stationarity gives $\sum_{j\neq i} \pi_j q_{ji} = \pi_i \sum_{j\neq i} q_{ij}$. Define $q^\dagger_{ij} = \pi_j q_{ji}/\pi_i$. Thus the original and adjoint chains have the same escape rate at every state. Since $x\log(x/y) \geq x - y$ for $x, y > 0$,

$$\sigma_{\mathrm{hk}} = \sum_i p_i \sum_{j\neq i} q_{ij} \log(q_{ij}/q^\dagger_{ij}) \geq \sum_i p_i \sum_{j\neq i} (q_{ij} - q^\dagger_{ij}) = 0.$$

The same inequality yields

$$\sigma_{\mathrm{na}} = \sum_{i\neq j} \pi_i q_{ij} f_i \log(f_i/f_j) \geq \sum_{i\neq j} \pi_i q_{ij}(f_i - f_j) = 0,$$

where the final cancellation uses stationarity after summing over i. Differentiate $D(p\|\pi) = \sum_i p_i \log f_i$ and use $\sum_i \dot{p}_i = 0$:

$$\frac{d}{dt} D(p\|\pi) = \sum_i \dot{p}_i \log f_i = \sum_{i\neq j} p_i q_{ij} (\log f_j - \log f_i).$$

Splitting the logarithm in σ_{tot} proves the decomposition. Alternatively, pairing opposite edges gives

$$\sigma_{\mathrm{tot}} = \frac{1}{2} \sum_{i\neq j} (p_i q_{ij} - p_j q_{ji}) \log \frac{p_i q_{ij}}{p_j q_{ji}} \geq 0.$$

This last formula also fixes the factor-of-two convention. □

At $p = \pi$, the state relative entropy and σ_{na} vanish, but σ_{hk} can remain positive. Detailed balance, $\pi_i q_{ij} = \pi_j q_{ji}$, makes $\sigma_{\mathrm{hk}} = 0$. In a reversible chain prepared away from π, σ_{na} is instead generally positive during relaxation. Consequently an invariant law, relaxation to that law, and a stationary arrow are three distinct properties.

14.12. *The initial law is part of the reversal experiment.* Let $\mathcal{T}_T \omega(t) = \omega(T - t)$ and let $P^{[0,T]}_\pi$ be the stationary path law of the preceding chain. Reciprocal rates and positive π ensure mutual absolute continuity of forward and reversed laws. For a history with jumps $i_0 \to i_1 \to \cdots \to i_n$, the waiting-time factors cancel and

$$\log \frac{dP_\pi}{d(P_\pi \circ \mathcal{T}_T^{-1})} = \log \frac{\pi_{i_0}}{\pi_{i_n}} + \sum_{\alpha=1}^{n} \log \frac{q_{i_{\alpha-1} i_\alpha}}{q_{i_\alpha i_{\alpha-1}}}.$$

Taking its expectation, the endpoint term has zero mean by stationarity. Expected jump counts are $T\pi_i q_{ij}$. Hence

$$D(P_\pi \| P_\pi \circ \mathcal{T}_T^{-1}) = T\sigma_{\mathrm{tot}}(\pi). \tag{1082}$$

Detailed balance is therefore equivalent to vanishing stationary path asymmetry in this finite irreducible setting. Motion does not cease: a reversible chain still jumps.

The word *stationary* cannot be omitted. Consider two states with $q_{12} = q_{21} = 1$ and initial law $p(0) = (0.8, 0.2)$. The generator is reversible with $\pi = (1/2, 1/2)$, while $p_1(T) = 1/2 + 0.3e^{-2T}$. Reversing the same nonstationary path law gives

$$D(P_{p(0)} \| P_{p(0)} \circ \mathcal{T}_T^{-1}) = [0.8 - p_1(T)] \log 4 > 0 \quad (T > 0).$$

To prove this formula, detailed balance reduces the path log ratio to $\log f_0(X_0) - \log f_0(X_T)$; take expectations with the two endpoint laws. This is not the same comparison as an experiment whose reverse is initialized in $p(T)$. With that reverse initialization and the same reversible rates, the expected log ratio is instead $D(p(0)\|\pi) - D(p(T)\|\pi)$. Thus the self-reversed path law and a thermodynamic reverse protocol must not be silently exchanged.

14.13. *Local detailed balance supplies the physical interpretation.* If an edge represents one resolved reservoir mechanism and Q_{ij} is heat delivered to the system on a jump, one common convention is

$$\log(q_{ij}/q_{ji}) = -Q_{ij}/(k_B T_b).$$

This local detailed-balance law must follow from, or be imposed as, the specified system–bath model. Internal degeneracies, particle exchange, and multiple mechanisms add their own entropy and chemical terms. For several reservoirs one must retain the reservoir label on a jump; aggregating the rates can hide physical entropy production. The endpoint contribution is the change in stochastic system entropy, and the rate ratio accounts for the bath contribution under this convention. Only after these identifications does a path log ratio equal the total thermodynamic entropy change.

For mutually absolutely continuous forward and specified reverse path laws, write $\Sigma = k_B \log(dP_F/dP_R^{\mathrm{rev}})$. Normalization gives

$$\mathbb{E}_F e^{-\Sigma/k_B} = 1, \qquad \mathbb{E}_F \Sigma = k_B D(P_F \| P_R^{\mathrm{rev}}) \geq 0.$$

The first identity follows by integrating dP_R^{rev}/dP_F; the second follows from the definition of relative entropy. Neither identity creates a light cone, determines a proper-time metric, or proves a thermodynamic interpretation without the specified bath and reversal data.

14.14. *Existence, uniqueness, and convergence are separate claims.* Even in finite dimension, a normalizable formal Gibbs expression must be compatible with the realized generator and its boundary before it is an invariant law. Irreducibility establishes uniqueness for the finite chain above, and a finite irreducible continuous-time chain then converges to that law. The corresponding

diffusion results require their own nonexplosion, domain, boundary, and mixing hypotheses.

In particular, existence does not imply uniqueness: two disconnected communicating classes have distinct invariant laws. Uniqueness alone does not imply relaxation for a general dynamical semigroup: a deterministic rotation at nonzero speed on a circle has a unique probability invariant under the full continuous-time flow, but a point mass remains a point mass and does not converge weakly to the uniform law. Entropy decay alone need not establish a strict rate. Spectral-gap, Harris, or other suitable mixing estimates are additional arguments. These logical distinctions persist when a finite regulator is removed.

14.15. *A common projection must transport dynamics, cost, and clock.* The physical proposal is to use one specified stochastic variational structure to constrain several effective descriptions. This requires more than reproducing their equations with separately chosen coefficients. The configuration space, action, reference measure, covariance, mobility, control cost, boundary conditions, physical clock, and observation map form one model package. A conditional branch retains each inherited datum and records each independently added matching assumption.

Suppose $dX_s = b(X_s)\,ds + \sigma(X_s)\,dW_s$, put $A = \sigma\sigma^{\mathsf{T}}$, and let $z = \Pi(X)$ be a C^2 projection. Itô's formula gives

$$b_\Pi^\alpha = \partial_i \Pi^\alpha b^i + \tfrac{1}{2} A^{ij} \partial_i \partial_j \Pi^\alpha, \qquad A_\Pi^{\alpha\beta} = \partial_i \Pi^\alpha A^{ij} \partial_j \Pi^\beta.$$

An autonomous Markov law for z follows only if the projected martingale problem closes and is well posed. A sufficient condition is that these coefficients depend on X only through $\Pi(X)$, with compatible boundary conditions. Otherwise conditioning over hidden variables generally produces memory and correlated unresolved forcing.

Clock calibration belongs to this calculation. If $dt = a(X_s)\,ds$, the projected physical generator is obtained from $a^{-1}L$, not from L. Even an autonomous s-projection can fail to be autonomous in t if a depends on unresolved coordinates. For an invariant mother law π, the physical-clock marginal is

$$\widetilde{\pi}_\Pi(dz) = \frac{\mathbb{E}_\pi[a(X) \mid \Pi(X) = z]}{\pi(a)} \pi_\Pi(dz). \tag{1083}$$

This is proved by integrating a bounded test function of $\Pi(X)$ against $a\pi/\pi(a)$. A conditional mean in this formula specifies stationary occupation probabilities; it does not by itself close transition laws.

Proposition 67 (Control cost inherited under a finite projection). *At a fixed regulated state let R be a symmetric positive definite real matrix and let $B : \mathbb{R}^m \to \mathbb{R}^r$ have full row rank. The minimum mother control cost at a*

prescribed resolved force v is

$$\min_{Bu=v} \frac{1}{2} u^{\mathsf{T}} R u = \frac{1}{2} v^{\mathsf{T}} Q^{-1} v, \qquad Q = B R^{-1} B^{\mathsf{T}},$$

and the unique minimizing lift is $u_* = R^{-1} B^{\mathsf{T}} Q^{-1} v$.

Proof. Full row rank and positivity of R imply $Q > 0$. The displayed lift satisfies $Bu_* = v$. Every admissible control is $u_* + w$ with $Bw = 0$, and $u_*^{\mathsf{T}} R w = v^{\mathsf{T}} Q^{-1} B w = 0$. Expanding the square gives the stated minimum and strict uniqueness. □

Thus a resolved Helmholtz metric is inherited only if its inverse equals the specified matrix $B R^{-1} B^{\mathsf{T}}$ after units and constraints are fixed. Choosing that metric independently produces an additional effective model. With a running cost $\int \ell(X_s, u_s)\, ds$, time change gives ℓ/a and $\widetilde{B} = B/a$. At a fixed state the matrix for the resolved physical force in the preceding minimization is Q/a, so the induced force cost is $a\, v_t^{\mathsf{T}} Q^{-1} v_t/2$. This pointwise calculation presupposes a control-independent clock and does not identify two different terminal-time control problems.

14.16. *The existing superfluid and quantum-vortex branches.* The finite-temperature two-fluid closure of [98] already treats two tensor stresses and an equal-and-opposite friction defect with a joint constrained cost. The GP study [99] separately treats a complex order parameter, particle transfer, and an energy-work bound. They supply concrete effective branches. Their constitutive equations, temperature fractions, regularizations, and quantum normalizations are not uniquely selected by the present mother model. Proposition 67 specifies the comparison that would establish an inherited control metric. Generator matching and (1083) supply independent checks.

The strongest resulting claim is a conditional common-origin relation: given the same mother package and a verified projection, the effective force cost, covariance, clock, and constraints cannot be fitted independently. The existence of a unique optimal control for this package does not select the physical package itself. Gauge and unit redundancies must first be removed; any additional selection principle remains an explicit assumption. Likewise an equilibrium measure alone determines neither a unique current nor a quantum phase. These limitations leave a concrete task: compute the projected matrices and compare their constrained predictions across sectors.

14.17. *One definition source and the status of branch data.* The primitive model remains the package Γ in (55), with the action (52) and the realized drift and stochastic equation (61)–(62). The following operational record supplements those definitions; it does not replace them with a different mother

equation. For a regulator N, a usable branch specifies

$$\mathcal{B}_N = (\Gamma, N, \mathcal{X}_N, S_N, \nu_N, L_N, A_N, M_N, \mathcal{C}_N, \mathcal{D}_N, \Pi_N, a_N, \mathcal{O}_N).$$

Here $A_N = \sigma_N \sigma_N^{\mathsf{T}}$ is the covariance, M_N the mobility, $\mathcal{C}_N$ the constraints, and $\mathcal{D}_N$ the operator domain including its boundary. The map Π_N resolves physical variables, $dt_{\mathrm{phys}} = a_N\, ds$ specifies a clock if one is available, and $\mathcal{O}_N$ is the observation map. A cost and admissible control class are also recorded for a controlled branch.

Every entry has one of three meanings. It is derived if the fixed primitive package and stated realization determine it. It is fixed under matching conditions if a specified low-energy or physical identification determines it only after those conditions are supplied. It is an input if it is still chosen, measured, or fitted independently. Taking a derivative of an input action derives an equation from that action; it does not derive the input coefficient from the mother model.

In the present family, finite projected drifts, covariances, and minimum lift costs are derived once the full primitive data and the projection are fixed. Lorentzian kinetic normalization, physical state and instrument selection, bath identification, and the clock map are conditional matching data. Unselected relative invariant-pairing weights, curvature–scalar couplings, scalar masses, and branch reservoir coefficients remain inputs unless a separate selection argument fixes them. Equality of sector symbols supplies no such argument.

The notations κ_{cost}, κ_P, κ_H, κ_{trap}, and $\bar{\kappa}$ retain their different definitions: control penalty, Palatini-action normalization, horizon surface gravity, laboratory trap stiffness, and a proposed shared coupling, respectively. Their physical dimensions are computed from the defining cost, action, clock, or force equation. There is no default equality among them. In diffusion notation $D_N = A_N/2$ when the generator is written $b \cdot \nabla + D_N : \nabla^2$. Neither the noise amplitude σ_N nor its covariance A_N can be silently substituted for this D_N.

14.18. *Conditional selection and what a rank calculation proves.* Fix units and the gauge equivalence relation before defining $\Theta_{\mathrm{phys}} = \Theta/\!\sim$. Let F_{sel} be a proper, lower-semicontinuous function bounded below on this space, and suppose it has nonempty compact sublevel sets in a metrizable topology. A minimizing sequence lies in one such sublevel set, has a convergent subsequence, and lower semicontinuity gives a minimizer. This is an existence proof.

For uniqueness, one sufficient condition is a one-to-one coordinate representation of the admissible quotient as a convex domain on which F_{sel} is strictly convex. If two different points minimized it, their midpoint would have a strictly smaller value. The argument cannot be transferred to an arbitrary nonconvex quotient without the coordinate and convexity hypotheses. Alternatively a discrete branch can have a separately proved strict global gap above one candidate. The origin of F_{sel} remains a physical issue: an independently

added selector is a new axiom, even when this minimization proof is valid. Gibbs invariance, HJB well-posedness, and stochastic symmetry alone do not supply that axiom.

For differentiable constraints $C(\vartheta) = 0$ of constant rank r near a regular point in d physical coordinates, the constant-rank theorem gives a local admissible dimension $d - r$. Choose a basis Z of $\ker DC$ there. The observation sensitivity on this tangent space is

$$J_{\mathrm{obs}} = D\mathcal{O}(\vartheta)\, Z.$$

Full column rank implies local identification by a suitable selection of observables, by the inverse-function theorem in local coordinates. It does not prove global injectivity. Singular values and a condition number are meaningful only after units and uncertainty weights for parameters and observations have been fixed. A shared notation does not establish rank or remove a parameter. The existing finite examples test specific projection and calibration matrices; they do not constitute the rank calculation of the entire thermodynamic–fluid–particle–gravitational observation map.

14.19. *Consistent scope across the physical branches.* A finite-regulator theorem includes its state space, generator domain, boundary, and fixed parameters. A conditional physical recovery adds its matching, state, clock, and limiting hypotheses. A proposed forward calculation or a validation protocol remains an unfinished problem until its result is supplied. Existence of an invariant measure, uniqueness of that measure, and convergence from a specified initial class must be stated separately at every level.

In particular, the fluctuation law on black-hole labels is not a regularity theorem for the interior metric. A scalar scattering calculation is not a tensor resonance calculation. A positive classical density is not a reconstructed quantum state. The finite Galerkin energy and entropy identities do not pass to a continuum without uniform estimates, tightness, identification of the limiting generator, and control of defect terms in the energy and entropy balances. Quantum removal of a regulator is a separate limit.

For independent prediction, calibration determines one parameter vector using only the declared calibration data. The observation map, physical clock, detector, nuisance treatment, baseline, failure criterion, and uncertainty model are then frozen before evaluation on held-out data. The genuine restriction is a multi-sector relation produced by the same parameters, compared with a model that fits sectors separately. No single signal is claimed to be impossible for every other effective theory to reproduce.

14.20. *A conditional relativistic limit and its measurable waves.* A flat stationary metric is one necessary ingredient of a relativistic vacuum, but

matter propagation must be checked as well. In the declared Lorentzian branch suppose the matched vacuum is Minkowski, the retained matter action is Poincare covariant, its physical quadratic modes have positive kinetic energy, and the reduced equations have a well-posed causal initial-value problem. Fix the matter metric, mass normalization, and boundary conditions. For a canonical scalar this gives

$$\left(c^{-2}\partial_t^2 - \Delta + m^2c^2/\hbar^2\right)\varphi = 0.$$

Substitution of $\varphi = \exp[-iEt/\hbar + i\mathbf{p}\cdot\mathbf{x}/\hbar]$ yields $E^2 = c^2|\mathbf{p}|^2 + m^2c^4$. This verifies the dispersion relation of this specified quadratic action. It does not derive the action, the clock, or $\hbar$ from a classical sampling measure. Higher-order operators must be retained within their validity range or consistently order reduced; their extra poles cannot silently be discarded.

A thermal bath can supply a material rest frame without changing the covariance of the underlying laws. A preferred frame built into vacuum noise is a different assertion and requires an observational bound. Relativistic particle noise may be formulated on the future mass shell with timelike trajectories, but a coordinate Brownian displacement is not thereby a relativistic model. When the recovery uses vanishing noise, the convergence of the physical equations and clocks must be controlled.

For the Einstein tensor branch in vacuum, linearization in transverse traceless gauge yields, at leading two-derivative order,

$$(\partial_t^2 - c^2\Delta)h_{ij}^{\mathrm{TT}} = 0.$$

An observable wave is a relative tidal acceleration. With the curvature convention defined by

$$\frac{D^2\xi^\mu}{D\tau^2} = -R^\mu{}_{\nu\alpha\beta}u^\nu\xi^\alpha u^\beta,$$

the geodesic-deviation equation connects a metric perturbation to nearby freely falling detectors. In the weak-wave, long-wavelength limit an arm in direction n has $\delta L/L = \frac{1}{2}n^i h_{ij}^{\mathrm{TT}} n^j$. A detector compares arms and includes antenna geometry and propagation; a coordinate component alone is not the strain measurement.

The complete matched action must be linearized before declaring its polarizations, speeds, or mode count. Extra scalar or higher-curvature terms can mix with the tensor branch. Recovery of the displayed equation requires their controlled decoupling, not merely a Minkowski solution. A shared coupling is most usefully tested through relations among several responses. Exclusion of every possible effective field theory is neither implied nor needed: a sufficiently general effective description can represent many of the same low-energy operators.

14.21. *A conditional branch with finite propagation speed.* A flat solution does not by itself recover special relativity. To obtain a causal matter branch, suppose the matching procedure supplies the Lorentz-scalar quadratic action with positive kinetic coefficient and mass parameter $\mu_\varphi = mc/\hbar \geq 0$. In Minkowski coordinates it gives

$$\partial_t^2\varphi - c^2\Delta\varphi + c^2\mu_\varphi^2\varphi = 0.$$

Here $t = x^0/c$ is the Minkowski clock coordinate, not an auxiliary sampling parameter. The action is Poincare invariant, its principal symbol is proportional to $g^{ab}k_ak_b$, and a plane wave satisfies $\omega^2 = c^2|k|^2 + c^2\mu_\varphi^2$. With the supplied quantum identification $E = \hbar\omega$ and $p = \hbar k$, this becomes $E^2 = c^2|p|^2 + m^2c^4$. The value of $\hbar$ is not derived by this calculation.

Proposition 68 (Domain of dependence for the matched scalar). *For a smooth finite-energy solution of the displayed equation, let both initial position and velocity vanish outside the ball of radius R. Then the solution vanishes outside the ball of radius $R + ct$ for $t \geq 0$.*

Proof. Define

$$e = \tfrac{1}{2}\big((\partial_t\varphi)^2 + c^2|\nabla\varphi|^2 + c^2\mu_\varphi^2\varphi^2\big), \qquad F = -c^2(\partial_t\varphi)\nabla\varphi.$$

Multiplication of the equation by $\partial_t\varphi$ gives $\partial_t e + \nabla\cdot F = 0$. The inequality $2c|\partial_t\varphi||\nabla\varphi| \leq (\partial_t\varphi)^2 + c^2|\nabla\varphi|^2$ implies $|F| \leq ce$. Let $E_{\mathrm{ext}}(t) = \int_{|x|>R+ct} e\,dx$. Integration over the moving exterior region, with a vanishing outer flux obtained by finite-energy approximation, yields

$$\frac{dE_{\mathrm{ext}}}{dt} = \int_{|x|=R+ct} (F\cdot n - ce)\,dS \leq 0,$$

where n points radially outward from the ball. Since $E_{\mathrm{ext}}(0) = 0$ and $e \geq 0$, this exterior energy remains zero. For $\mu_\varphi > 0$ the field vanishes there directly. For $\mu_\varphi = 0$ its space and time derivatives vanish there, and the zero initial exterior value fixes the remaining constant. Approximation extends the support statement to the usual finite-energy solution class. □

This is a proof for the specified canonical scalar, not for every mode of the proposed mother theory. Coupled tensor, vector, and higher-derivative branches require their own constrained principal symbols and stability analysis. For a linear effective correction bounded by δK from the chosen energy domain to L^2, with unchanged stable principal part, the difference from the uncorrected solution obeys the forced energy estimate

$$\sqrt{E_{\mathrm{diff}}(T)} \leq \frac{\delta K}{\sqrt{2}} \int_0^T \|\varphi_\delta(t)\|_{\text{energy domain}}\,dt$$

for equal initial data. It follows by pairing the forced difference equation with its time derivative. The required uniform norm bound is part of the hypothesis; an uncontrolled higher-derivative term cannot be assigned this error estimate or the same light cone.

14.22. *A proper-time particle process on the future mass shell.* Ordinary Brownian increments directly added to a spacetime position do not define timelike paths. A different conditional construction puts noise in velocity. Let U_τ be a continuous, nonexplosive diffusion on the future unit mass hyperboloid in Minkowski spacetime,

$$g(U,U) = -c^2, \qquad U^0 > 0, \qquad X_\tau = X_0 + \int_0^\tau U_v \, dv.$$

The velocity generator is tangent to the hyperboloid; for example it may contain its Laplace–Beltrami operator and a smooth tangent drift. Then X has continuously differentiable timelike paths, $dX^\mu = U^\mu d\tau$, and the metric length of each path is exactly $d\tau = c^{-1}\sqrt{-g_{\mu\nu}\, dX^\mu dX^\nu}$. Writing $x^0 = ct$ gives

$$\frac{dt}{d\tau} = \frac{U^0}{c} = \sqrt{1 + \frac{|\boldsymbol{U}|^2}{c^2}} \geq 1, \qquad \left|\frac{d\boldsymbol{X}}{dt}\right| = \frac{c|\boldsymbol{U}|}{U^0} < c.$$

These statements follow path by path and do not require differentiating the Brownian velocity. They prove causality of position trajectories under the given construction, not a mother-derived particle law.

The relativistic factor U^0/c is unbounded on the full hyperboloid. Consequently a theorem assuming a bounded positive clock on a compact state space does not automatically give an invariant laboratory-time law here. Nonexplosion, integrability of this clock under a proposed proper-time invariant law, and physical bath covariance require separate verification. A thermal bath supplies a physical rest frame; Lorentz-covariant equations may include its four-velocity without asserting a vacuum preferred frame.

14.23. *Which conservation laws are recovered.* A common variational origin is useful only if the projected equations retain the corresponding balance laws. Three statements must be distinguished: pathwise constancy of a quantity, constancy of its expectation, and a balance in which resolved energy is exchanged with other fields or a bath.

Stochastic Noether theory in optimal control relates suitable contact symmetries of a sufficiently regular HJB equation to local martingales along optimal states [58]. The Itô criterion below tests a proposed charge; it does not construct a symmetry by itself. Its drift cancellation must follow from the actual symmetry theorem or from a direct calculation for the specified dynamics.

For a regular classical Lagrangian $L(q, \dot{q}, t)$ and an infinitesimal configuration symmetry $\delta q = \xi(q)$ at fixed time, suppose $\delta L = dB/dt$. On an

Euler–Lagrange solution, writing $p = \partial_{\dot{q}} L$ gives

$$\frac{d}{dt}(p \cdot \xi - B) = (\dot{p} - \partial_q L) \cdot \xi + \delta L - \frac{dB}{dt} = 0.$$

This is the classical Noether charge. Time translation of an autonomous regular Lagrangian gives conservation of $H = p \cdot \dot{q} - L$; spatial translation and rotation give the corresponding momentum and angular momentum when external fields and boundaries share those symmetries. The recovery requires an identified mechanical action and the relevant symmetry, not only a noise coefficient tending to zero.

PROPOSITION 69 (Stochastic charge and pathwise criterion). *Let $dX_t = b\,dt + \sigma\,dW_t$ be a well-posed finite-dimensional Itô diffusion and $Q \in C^{1,2}$ with $\mathbb{E}|Q(0, X_0)| < \infty$. Up to localization,*

$$dQ(t, X_t) = \left(\partial_t Q + b \cdot \nabla Q + \tfrac{1}{2}\sigma\sigma^{\mathsf{T}} : D^2 Q\right) dt + (\sigma^{\mathsf{T}} \nabla Q) \cdot dW_t.$$

If the drift vanishes, $Q(t, X_t)$ is a local martingale. It is a martingale, with constant expectation, when its stochastic integral is square integrable and its initial value is integrable. It is pathwise constant if both the drift and $\sigma^{\mathsf{T}} \nabla Q$ vanish along the trajectories. Conversely pathwise constancy forces these two terms to vanish almost everywhere along the trajectories.

Proof. Itô's formula gives the decomposition. Its quadratic variation is $\int_0^t |\sigma^{\mathsf{T}} \nabla Q|^2\,ds$. A constant process has zero quadratic variation and zero finite-variation part; uniqueness of the semimartingale decomposition gives necessity. The zero-integrand conditions give sufficiency. Square integrability upgrades the local stochastic integral to a true martingale. □

For a time-independent charge in a Stratonovich Hamiltonian realization, $dQ = \{Q, H_0\}dt + \sum_k \{Q, H_k\} \circ dW^k$, a charge commuting with every H_k, including H_0, is pathwise conserved. A symmetry of the drift Hamiltonian alone is insufficient. For a time-independent charge, a state-dependent positive clock divides LQ by its rate and the stochastic coefficient by its square root; it preserves their vanishing when the time-change theorem applies. An explicitly time-dependent charge requires changing the time coordinate of the augmented process as well: replacing $Q(s, x)$ by $Q(t, x)$ without this transformation need not preserve a martingale. A vanishing-noise limit recovers a classical charge only if the actions, symmetries, coefficients, solutions, and relevant moment bounds converge. Classical Noether theory is therefore contained in a matched conservative limit, rather than in every deterministic limit.

PROPOSITION 70 (A finite-time conservative limit). *On $\mathbb{R}^{2n}$ let $b_0 = J\nabla H$ be globally Lipschitz, where J is the canonical symplectic matrix. Let r_ϵ and*

σ_ϵ be uniformly bounded and globally Lipschitz coefficients, and let $0 < \epsilon \le 1$. Couple

$$dX_t^\epsilon = [b_0(X_t^\epsilon) + \epsilon r_\epsilon(X_t^\epsilon)]\,dt + \sqrt{\epsilon}\,\sigma_\epsilon(X_t^\epsilon)\,dW_t, \qquad \dot{x}_t = b_0(x_t).$$

If $\mathbb{E}|X_0^\epsilon - x_0|^2 \le C_0\epsilon$, then for every finite T there is C_T independent of ϵ such that

$$\mathbb{E}\sup_{t\le T}|X_t^\epsilon - x_t|^2 \le C_T\epsilon.$$

Every continuous classical conserved charge Q therefore satisfies

$$\sup_{t\le T}|Q(X_t^\epsilon) - Q(x_0)| \longrightarrow 0 \quad \textit{in probability.}$$

Convergence of the corresponding expectations additionally requires uniform integrability.

Proof. Write the difference as the initial error, the integral of the b_0 difference, the ϵr_ϵ integral, and a martingale. If the Lipschitz constant of b_0 is L and the coefficient bounds are R, S (the latter in Hilbert–Schmidt norm), Cauchy–Schwarz, the inequality $|\sum_{i=1}^4 z_i|^2 \le 4\sum_i |z_i|^2$, and Doob's L^2 inequality give, for $t \le T$,

$$F(t) \le 4C_0\epsilon + 4TL^2\int_0^t F(s)\,ds + 4\epsilon^2T^2R^2 + 16\epsilon TS^2,$$
$$F(t) = \mathbb{E}\sup_{v\le t}|X_v^\epsilon - x_v|^2.$$

Gronwall's inequality proves the estimate. Continuity of Q and the continuous-mapping theorem on finite-time path space give the last assertion, since $Q(x_t) = Q(x_0)$. Uniform integrability is the extra condition needed to pass to expectations. □

These assumptions describe a finite-dimensional conservative branch. For locally Lipschitz physical forces the same estimate is first localized; a uniform exit or moment estimate is needed to remove the stopping time. Neither an arbitrary long-time limit nor removal of the field regulator follows from this finite-T argument. In particular, leaving a nonzero friction term as $\epsilon \to 0$ changes the limiting equation and need not preserve mechanical energy.

14.24. *A stochastic Hamiltonian example with exact conservation.* Take $X = (q, p)$, $H(X) = |X|^2/2$, and the canonical matrix $J = \left(\begin{smallmatrix} 0 & 1 \\ -1 & 0 \end{smallmatrix}\right)$. For a scalar Brownian motion and constant β,

$$dX = JX\,dt + \beta JX \circ dW = \left(JX - \frac{\beta^2}{2}X\right)dt + \beta JX\,dW.$$

Both driving Hamiltonians are multiples of H. Directly,

$$LH = -\frac{\beta^2}{2}|X|^2 + \frac{\beta^2}{2}|JX|^2 = 0, \qquad (\beta JX)\cdot\nabla H = 0.$$

Thus $H(X_t) = H(X_0)$ on every sample path. Equivalently $X_t = \exp[J(t + \beta W_t)]X_0$ is an orthogonal rotation. Omitting the Itô drift correction changes the model: for $dX = JX\,dt + \beta JX\,dW$ one instead obtains $dH = \beta^2 H\,dt$. This example identifies the precise cancellation needed for conservation; it also shows why stochasticity alone does not imply mechanical dissipation.

14.25. *Dissipation is compatible with a total energy balance.* Consider the isothermal Langevin momentum $dp = -(\gamma/m)p\,dt + \sqrt{2\gamma k_B T}\,dW_t$, with $E = p^2/(2m)$. Itô's formula yields

$$dE = \left(-\gamma p^2/m^2 + \gamma k_B T/m\right)dt + (p/m)\sqrt{2\gamma k_B T}\,dW_t.$$

The positive trace term must accompany the random work. If heat delivered to the reservoir is defined by the model's first-law convention,

$$dQ_{\mathrm{bath}} = \left(\gamma p^2/m^2 - \gamma k_B T/m\right)dt - (p/m)\sqrt{2\gamma k_B T}\,dW_t,$$

then $dE + dQ_{\mathrm{bath}} = 0$. At the Gibbs variance $\mathbb{E}p^2 = mk_BT$, the mean energy injection and friction loss cancel. This is the open-system energy ledger under a specified bath model, not a derivation of that bath's microscopic dynamics.

14.26. *Fluid, geometric, and gauge balances.* For an orthogonal, divergence-free Fourier–Galerkin projection on a periodic domain, let

$$du_N = [-\Pi_N((u_N\cdot\nabla)u_N) + \nu\Delta u_N + f_N]\,dt + G_N\,dW_t.$$

The kinetic-energy pairing gives

$$d\frac{\|u_N\|_2^2}{2} = \left[-\nu\|\nabla u_N\|_2^2 + \langle f_N, u_N\rangle + \frac{1}{2}\|G_N\|_{\mathrm{HS}}^2\right]dt + \langle u_N, G_N\,dW_t\rangle.$$

The nonlinear term vanishes because orthogonality removes Π_N from the pairing and $\int u_N\cdot(u_N\cdot\nabla)u_N\,dx = \int\nabla\cdot(|u_N|^2u_N/2)\,dx = 0$. If the zero Fourier mode is included, spatial integration gives $d\int u_N\,dx = (\int f_N\,dx)dt + \int G_N\,dW_t$. Thus momentum is conserved pathwise when both integrated sources vanish. If a mean-zero subspace is imposed instead, its prescribed mean is fixed as part of the phase space. Kinetic energy is conserved in the unforced inviscid deterministic branch; viscosity converts it into unresolved or internal energy in a thermodynamic completion. For a compressible smooth branch, $\partial_t\rho + \nabla\cdot(\rho u) = 0$ conserves total mass under periodic or impermeable boundaries. A proposed projection must retain this conservative form, or explicitly account for its mass source.

For interacting relativistic fields, diffeomorphism invariance of the complete matched action and the on-shell matter equations give the covariant total-stress

balance. In an Einstein representation with higher-curvature terms consistently retained or placed in an effective stress tensor, it has the form $\nabla_\mu T^{\mu\nu}_{\rm tot} = 0$. Individual sectors can obey $\nabla_\mu T^{\mu\nu}_i = Q^\nu_i$ with $\sum_i Q^\nu_i = 0$. Local covariant balance does not imply a globally defined conserved energy in an arbitrary spacetime. A Killing symmetry and suitable boundary flux conditions provide such a charge; dynamical geometries require the corresponding boundary or asymptotic construction. Indeed, for symmetric $T_{\rm tot}$ and a Killing field ξ,

$$\nabla_\mu(T^{\mu\nu}_{\rm tot}\xi_\nu) = T^{\mu\nu}_{\rm tot}\nabla_{(\mu}\xi_{\nu)} = 0.$$

The divergence theorem then equates the charges on two spacelike slices when the intervening boundary flux vanishes.

Likewise the matched gauge equations imply a covariant current identity $D_\mu J^\mu = 0$ on shell under the appropriate gauge symmetry. For $D_\mu F^{\mu\nu} = g^2_{\rm YM} J^\nu$ with a constant coupling, antisymmetry gives $D_\nu D_\mu F^{\mu\nu} = \frac{1}{2}[D_\nu, D_\mu]F^{\mu\nu} = 0$: the spacetime curvature contractions are symmetric–antisymmetric contractions, and the gauge-curvature contraction is proportional to $[F_{\nu\mu}, F^{\mu\nu}] = 0$. A field-dependent coupling instead requires differentiating the full gauge displacement in its field equation. The scalar and interaction terms cannot be dropped. An anomaly-free quantum realization and a well-defined boundary charge are additional requirements. The two-fluid internal-force cancellation, MHD Lorentz exchange, and conservative GP particle balance are concrete instances of this common bookkeeping principle. Controls, reservoirs, and unresolved modes must appear in the balance whenever they exchange the relevant quantity.

14.27. *Simultaneous compatibility of projected branches.* A common notation becomes a common physical model only after its primitive data have been fixed. For each branch b, let Θ_b denote the subset of physical parameters on which its matching, boundary conditions and estimates hold. Simultaneous recovery requires

$$\Theta_{\rm joint} = \bigcap_b \Theta_b \neq \varnothing.$$

Separate existence statements for the sets Θ_b do not prove this intersection property. A constructive realization consists of a parameter point in the intersection, together with the branch maps and their error bounds. If a branch uses a different potential or reservoir, that change belongs to its primitive data. Conditional selection of a minimizer and identification of parameters from observations remain different operations.

The finite example below supplies such a realization for mechanics, stationary statistics, reservoir heat and a projected memory equation. Its coefficients are declared inputs. It does not identify its oscillator coordinates with gravitational, gauge or quantum fields, and it does not select a unique physical

coupling. The purpose is to exhibit the complete compatibility calculation at a resolution where each step can be verified.

14.28. *One energy, one generator and several consequences.* Use fixed dimensionless coordinate and time units, unit masses, and $k_B = 1$. Two coordinates x_1, x_2 interact through a third coordinate r. Put $q = (x_1, x_2, r)^T$, and let p be the conjugate momentum. Set

$$K_{\mathrm{f}} = \begin{pmatrix} k_1 & 0 & -c_1 \\ 0 & k_2 & -c_2 \\ -c_1 & -c_2 & k_0 \end{pmatrix}, \qquad H_{\mathrm{f}}(q,p) = \tfrac{1}{2} p^T p + \tfrac{1}{2} q^T K_{\mathrm{f}} q.$$

Here $k_1, k_2, k_0 > 0$, and $c = (c_1, c_2)^T$ is a supplied coupling vector. Completing the square in x_1, x_2 gives the exact criterion

$$K_{\mathrm{f}} > 0 \quad \Longleftrightarrow \quad k_0 - \frac{c_1^2}{k_1} - \frac{c_2^2}{k_2} > 0. \tag{1084}$$

In particular, $\det K_{\mathrm{f}} = k_1 k_2 (k_0 - c_1^2/k_1 - c_2^2/k_2)$. The cross terms cannot be chosen independently of stability.

Let $\Lambda_{\mathrm{f}} = \mathrm{diag}(\gamma_1, \gamma_2, \gamma_0) > 0$ and let the reservoir temperatures $\Theta_i > 0$, $i = 1, 2, 0$, be independently specified. With independent Wiener processes, define

$$dq = p\,dt, \qquad dp = (-K_{\mathrm{f}} q - \Lambda_{\mathrm{f}} p)\,dt + \sqrt{2\Lambda_{\mathrm{f}}\Theta_{\mathrm{f}}}\,dW, \qquad \Theta_{\mathrm{f}} = \mathrm{diag}(\Theta_1, \Theta_2, \Theta_0). \tag{1085}$$

Its physical reversal is $(q, p) \mapsto (q, -p)$. The temperatures, frictions and reversal are part of this thermal realization; no entropy interpretation is inferred solely from a positive covariance.

Proposition 71 (A nonempty finite compatibility class). *Under* (1084), *the process* (1085) *is nonexplosive and has a unique nondegenerate Gaussian invariant law. Its covariance C_{f} is the unique solution of*

$$B_{\mathrm{f}} C_{\mathrm{f}} + C_{\mathrm{f}} B_{\mathrm{f}}^T + A_{\mathrm{f}} = 0, \qquad B_{\mathrm{f}} = \begin{pmatrix} 0 & I \\ -K_{\mathrm{f}} & -\Lambda_{\mathrm{f}} \end{pmatrix}, \quad A_{\mathrm{f}} = \begin{pmatrix} 0 & 0 \\ 0 & 2\Lambda_{\mathrm{f}}\Theta_{\mathrm{f}} \end{pmatrix}. \tag{1086}$$

For equal temperatures $\Theta_i = \Theta$,

$$C_{\mathrm{f}} = \mathrm{diag}(\Theta K_{\mathrm{f}}^{-1}, \Theta I), \qquad \rho_{\mathrm{f}} \propto e^{-H_{\mathrm{f}}/\Theta}.$$

This equal-temperature process satisfies detailed balance with momentum reversal. Its Gaussian law is attracting in W_2 for initial laws with finite second moment, with a rate depending on the displayed coefficients.

Proof. All coefficients are globally Lipschitz. If z is an eigenvalue of B_{f}, its position eigenvector $v \neq 0$ satisfies $(z^2 I + z\Lambda_{\mathrm{f}} + K_{\mathrm{f}})v = 0$. Multiplication by v^*

gives $az^2 + bz + d = 0$, with $a = v^*v > 0$, $b = v^*\Lambda_{\mathrm{f}}v > 0$, and $d = v^*K_{\mathrm{f}}v > 0$. Both roots have negative real part. Consequently

$$C_{\mathrm{f}} = \int_0^\infty e^{tB_{\mathrm{f}}} A_{\mathrm{f}} e^{tB_{\mathrm{f}}^T}\, dt$$

is finite and satisfies (1086). Noise acts in every momentum direction; applying B_{f} to these directions produces every position direction. The resulting controllability matrix has rank six, so $C_{\mathrm{f}} > 0$. The explicit linear solution converges to this Gaussian, establishing existence and uniqueness. Coupling two solutions with the same noise gives $\delta Z_t = e^{tB_{\mathrm{f}}}\delta Z_0$, and hence W_2 convergence from exponential matrix decay. Substitution verifies the equal-temperature covariance. In its Gaussian L^2 space the Hamiltonian transport is antisymmetric and changes sign under momentum reversal, while the momentum Ornstein–Uhlenbeck part is symmetric and parity invariant. This proves generalized detailed balance. □

14.29. *Heat, dissipation and the reversible limit.* Itô's formula, including the momentum quadratic variation, yields

$$dH_{\mathrm{f}} = \sum_i dQ_i, \qquad dQ_i = \gamma_i(\Theta_i - p_i^2)\, dt + \sqrt{2\gamma_i\Theta_i}\, p_i\, dW_i. \tag{1087}$$

Positive Q_i denotes heat entering the oscillator system. The reservoir entropy increment has mean $-\mathbb{E}[dQ_i]/\Theta_i$. At stationarity put

$$\dot{Q}_i = \gamma_i(\Theta_i - C_{p_ip_i}), \qquad \sigma_{\mathrm{f}} = -\sum_i \dot{Q}_i/\Theta_i.$$

Stationary energy balance gives $\sum_i \dot{Q}_i = 0$. The dissipative momentum current is $j_i = -\gamma_i(p_i\rho_{\mathrm{f}} + \Theta_i\partial_{p_i}\rho_{\mathrm{f}})$.

Proposition 72 (Thermal and probabilistic entropy rates agree). *For the invariant law in Proposition 71,*

$$\sigma_{\mathrm{f}} = \sum_i \int \frac{j_i^2}{\gamma_i\Theta_i\rho_{\mathrm{f}}}\, dq\, dp \geq 0. \tag{1088}$$

If $c_1c_2 \neq 0$, equality holds exactly when all three temperatures are equal.

Proof. The Gaussian tails justify integration by parts. Hamiltonian transport has zero divergence. Stationarity of Shannon entropy therefore gives

$$\sum_i \gamma_i \left[-1 + \Theta_i \int (\partial_{p_i}\log\rho_{\mathrm{f}})^2\rho_{\mathrm{f}}\right] = 0.$$

Expanding the squared currents, and using $\int p_i\partial_{p_i}\rho_{\mathrm{f}} = -1$, proves (1088). If its right-hand side vanishes, every j_i vanishes, so $\rho_{\mathrm{f}} = f(q)\exp[-\sum_i p_i^2/(2\Theta_i)]$. The remaining Hamiltonian equation requires $\nabla_q \log f = -\Theta_{\mathrm{f}}^{-1}K_{\mathrm{f}}q$. Symmetry of the Hessian implies $(K_{\mathrm{f}})_{ij}(\Theta_i^{-1} - \Theta_j^{-1}) = 0$. The coupling graph is connected

when $c_1 c_2 \neq 0$, forcing equal temperatures. The converse follows from the Gibbs covariance. □

Thus one coupled finite model has both a reversible equilibrium branch and a maintained irreversible branch. Unequal reservoir temperatures, rather than noise alone, produce the latter. The model is open; (1087) is an energy exchange law, not pathwise conservation of oscillator energy in isolation.

To recover Hamiltonian dynamics, replace Λ_{f} by $\varepsilon\Lambda_{\mathrm{f}}$, keeping the temperatures and initial data fixed. The noise amplitude is then $O(\sqrt{\varepsilon})$. The limiting equation is $dq = p\,dt,\ dp = -K_{\mathrm{f}} q\,dt$. Variation of constants and the martingale maximal inequality give, on each fixed interval $[0,T]$,

$$\mathbb{E}\sup_{t\le T}|Z_t^{\varepsilon} - Z_t^{0}|^2 \le C_T\varepsilon(1+\mathbb{E}|Z_0|^2), \qquad 0<\varepsilon\le 1.$$

Indeed, the drift difference is $\varepsilon(0,-\Lambda_{\mathrm{f}}p^{\varepsilon})$; its time integral has squared norm bounded by $\varepsilon^2 T\int_0^T \mathbb{E}|p^{\varepsilon}|^2 dt$. The noise integral contributes at most a constant times εT; the linear Gronwall estimate supplies the stated bound. Uniform finite-time second moments follow from (1087). In contrast, taking temperatures to zero at fixed friction leaves damped dynamics. The long-time and zero-friction limits need not commute.

14.30. *The same coupling fixes memory and a static restriction.* Write $D_{\mathrm{f}} = \mathrm{diag}(k_1,k_2)$. Eliminating r at fixed x in the energy gives

$$r_*(x) = c^T x/k_0, \qquad H_{\mathrm{eff}}^{\mathrm{stat}}(x) = \tfrac{1}{2}x^T(D_{\mathrm{f}} - cc^T/k_0)x.$$

Dynamical elimination uses instead the retarded Green function G_0 of $\partial_t^2 + \gamma_0\partial_t + k_0$. Substitution of

$$r(t) = r_{\mathrm{hom}}(t) + \int_0^t G_0(t-s)c^T x(s)\,ds + \sqrt{2\gamma_0\Theta_0}\int_0^t G_0(t-s)\,dW_0(s)$$

in the x equation produces the memory kernel

$$\mathcal{K}_{\mathrm{f}}(t) = cc^T G_0(t), \qquad \widehat{\mathcal{K}}_{\mathrm{f}}(s) = \frac{cc^T}{s^2+\gamma_0 s + k_0}. \tag{1089}$$

The initial mediator term and its colored noise remain in the reduced equation. At points where the denominator is nonzero, $\widehat{\mathcal{K}}_{11}\widehat{\mathcal{K}}_{22} - \widehat{\mathcal{K}}_{12}^2 = 0$. This rank-one identity concerns the induced correction to the inverse response, after the local response is separated; it does not say that the complete two-channel susceptibility has rank one. Such a restriction is a standard consequence of a single linear mediator. Its physical use requires deriving the mediator and its coefficients from a specified branch rather than treating the restriction as unique evidence for one theory.

14.31. *A frozen-parameter synthetic comparison.* Choose

$$(k_1, k_2, k_0) = (2, 3, 5), \quad c = \eta_{\mathrm{f}}(1, 0.6)^T, \quad (\gamma_1, \gamma_2, \gamma_0) = (0.7, 0.9, 0.8).$$

The admissible interval is $|\eta_{\mathrm{f}}| < \sqrt{5/0.62} = 2.839809\ldots$. The synthetic generating value is 0.7. At calibration temperature $\Theta = 0.8$, the Gibbs covariance obeys

$$\eta_{\mathrm{f}} = 2C_{q_1 r}/C_{rr}.$$

This follows from the $(1, 3)$ entry of $K_{\mathrm{f}} C_{qq} = \Theta I$. It determines this one parameter once the remaining coefficients are fixed. It is observational identification within this family, not fundamental selection of the family or its coupling direction.

From 80000 independent zero-mean Gaussian calibration draws, $\widehat{\eta}_{\mathrm{f}} = 0.69559058$, with delta-method standard error 0.01076504. For sample second moments the variance formula is

$$\mathrm{Var}(\widehat{\eta}_{\mathrm{f}}) \simeq \frac{4}{n}\left(\frac{C_{q_1 q_1}}{C_{rr}} - \frac{C_{q_1 r}^2}{C_{rr}^2}\right).$$

It follows from the Gaussian fourth-moment identity; the known mean is zero. The estimated parameter is frozen before three new temperature settings are evaluated. Each uses 120000 independent stationary Gaussian draws. No target covariance enters the calibration.

Reservoir temperatures	Predicted rate	Sample estimate	Standard error
$(1.2, 0.7, 0.9)$	0.00479634	0.00736950	0.00571119
$(1.4, 0.5, 0.9)$	0.01558864	0.00668704	0.00573660
$(1.6, 0.3, 0.9)$	0.04138724	0.04951965	0.00598202

The errors combine independent target sampling and propagated calibration uncertainty to first order. They are asymptotic standard errors, not exact or simultaneous confidence guarantees. If $a_i = \gamma_i/\Theta_i$, the target estimator has variance

$$\frac{2}{n}\sum_{i,j} a_i a_j C_{p_i p_j}^2.$$

The first setting has weak statistical power at this sample size. Agreement within these errors illustrates the prediction procedure; it does not establish observational support for the physical field programme. The covariance equation, energy balance and the two entropy expressions agree numerically within 6×10^{-15}; an independently formed full resolvent and its Schur reduction agree within 4×10^{-16}. These residuals concern algebraic computations, not experimental accuracy.

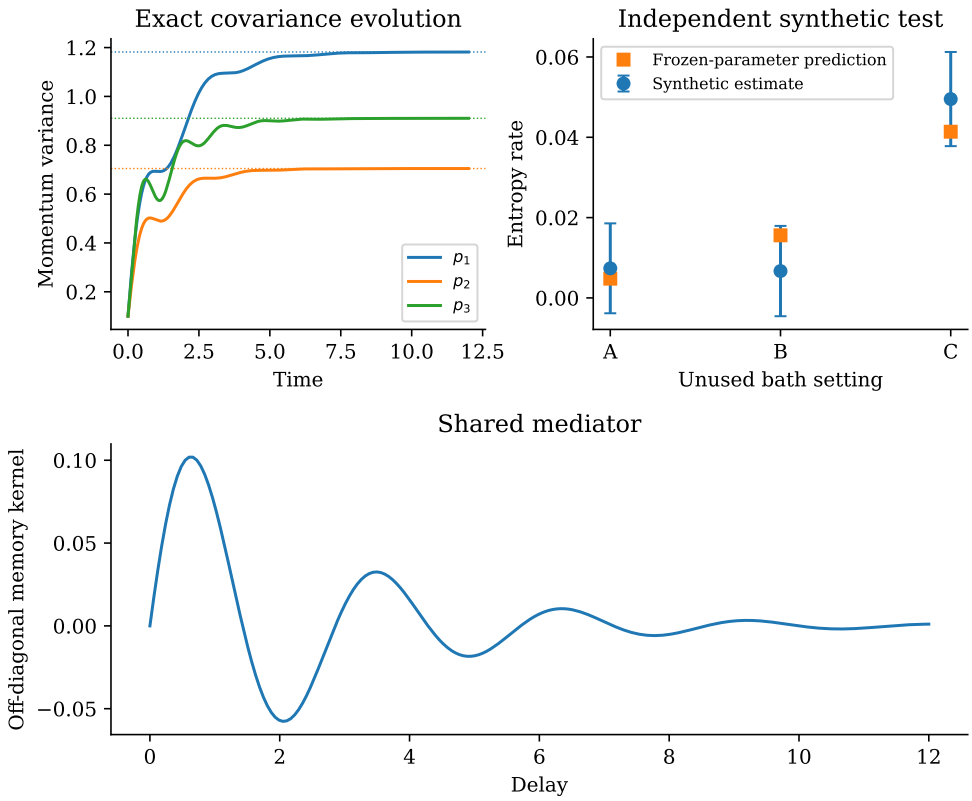


Figure 19. The fixed three-coordinate realization. Upper left: exact covariance relaxation from an initial covariance $0.1I$; dotted lines are stationary values. Upper right: frozen-parameter entropy predictions and independent synthetic estimates, with bars of 1.96 combined standard errors. Bottom: the off-diagonal memory kernel obtained by eliminating the same mediator. The samples are generated from the stated model.

14.32. *Exact projection and a controlled recovery error.* A common action is useful only if its realized dynamics and its physical projections agree. This requirement can be stated independently of a choice of coordinates for the other branches. Fix a conservative diffusion with generator

$$Lf = b \cdot \nabla f + \tfrac{1}{2} A : \nabla^2 f, \qquad A = \sigma\sigma^T,$$

and a twice continuously differentiable map $y = \Pi(x)$. For this paragraph there is no reflecting local-time term. A reflected realization needs its projected boundary term and domain as additional data. Define

$$\beta_i(x) = L\Pi_i(x), \qquad \mathsf{a}(x) = D\Pi(x) A(x) D\Pi(x)^T.$$

The second derivative in $L\Pi_i$ is essential for a nonlinear projection.

PROPOSITION 73 (A sufficient condition for an exact Markov projection). *Suppose* $\beta = \bar{b} \circ \Pi$ *and* $\mathsf{a} = \bar{A} \circ \Pi$. *Assume the martingale problem for* $\bar{L} = \bar{b} \cdot \nabla + \frac{1}{2}\bar{A} : \nabla^2$ *is conservative and well posed for the projected initial laws, and the test functions below belong to the realized generator domains, or admit valid localization. Then* $\Pi(X_t)$ *has the law of that Markov diffusion. In particular, for its semigroup* $\bar{P}_t$,

$$P_t(f \circ \Pi) = (\bar{P}_t f) \circ \Pi.$$

If π *is invariant for the mother process,* $\Pi_{\#}\pi$ *is invariant for the projected process.*

Proof. The chain rule gives

$$L(f \circ \Pi) = \beta \cdot (\nabla f) \circ \Pi + \tfrac{1}{2}\mathsf{a} : (\nabla^2 f) \circ \Pi = (\bar{L} f) \circ \Pi.$$

The corresponding stopped martingales therefore solve the projected martingale problem. Its well-posedness identifies the law, and conservativity removes the stopping under the assumed localization conditions. Integrating the semigroup identity against π proves invariance of its pushforward. No uniqueness of that invariant law is needed in this step. □

Matching only the projected drift is insufficient: the quadratic variation must match as well. If the coefficients depend on unresolved coordinates, the projected process need not be Markov. Replacing that dependence by a conditional mean requires a specified conditional law and generally introduces memory or an approximation.

There is also a quantitative weak form. Let $v(t, y)$ solve $\partial_t v + \bar{L} v = 0$ on $[0, T]$ with $v(T, y) = f(y)$, with enough regularity and integrability for Itô's formula. For approximate matching, put

$$r_v(t, x) = (\beta - \bar{b} \circ \Pi) \cdot \nabla v(t, \Pi x) + \tfrac{1}{2}(\mathsf{a} - \bar{A} \circ \Pi) : \nabla^2 v(t, \Pi x).$$

For the same projected initial law, Itô's formula and expectation give

$$|\mathbb{E} f(\Pi X_T) - \mathbb{E} f(Y_T)| \le \int_0^T \mathbb{E}|r_v(t, X_t)|\, dt. \tag{1090}$$

Indeed the difference before taking absolute values is the integral of $\mathbb{E} r_v$. This estimate includes the projection, observable, time interval and derivative regularity; it is not an unrestricted continuum or path-space error bound.

14.33. *Joint branch realization and the remaining physical inputs.* The finite mechanical realization in Section 14.27 already connects one energy, one generator, stationary statistics, reservoir heat and memory. It does not identify its coordinates with spacetime or quantum observables. For the physical

family the same test must be applied to one primitive package, allowing distinct declared environments and background solutions. Separate choices of a potential that are incompatible at the mother level cannot count as simultaneous recovery.

A reproducible branch specifies the projection, covariance, clock, boundary, physical reservoir and observation map. The preceding proposition makes one of these requirements testable. The quotient selection argument in Section 14.18 addresses a different requirement: selection of primitive parameters. Neither generator matching nor uniqueness of a projected solution selects those parameters. Where a selector is supplied independently, it is an additional physical assumption. Where a parameter remains identifiable only from data, it remains an input to predictions in the other branches.

The unresolved mass–curvature direction in the present matched scalar branch therefore persists. A common prediction must carry that direction through its uncertainty analysis, or constrain it using an independent observable. Declaring a massless potential is a different branch unless the original matching constraints permit that limit. These distinctions preserve the content of the finite recovery statements while specifying what a stronger simultaneous physical realization must demonstrate.

14.34. *Why strict stability inequalities do not select a coupling.* The remaining calibration fiber in Section 14.36 cannot generally be removed by imposing additional strict stability inequalities. At a point with $q_\sigma > 0$, parameterize that fiber by L_c while keeping (A_φ, m_φ^2) fixed. It is an open interval locally, with $q_\sigma(L_c) = m_\varphi^2 - 6A_\varphi/L_c$.

Proposition 74 (Persistence under finitely many strict constraints). *Suppose finitely many added conditions take the form $g_j(\vartheta) > 0$, with each g_j continuous, and all hold at an interior point of the calibration fiber. Then an interval of that fiber still satisfies all the conditions. Its curvature coupling is not unique.*

Proof. For each j, positivity and continuity give an open neighborhood of the point on the fiber. The intersection of finitely many such neighborhoods contains an interval. On it $K_{\mathrm{curv}} = A_\varphi L_c^2/32$ has derivative $A_\varphi L_c/16 > 0$, so different points have different curvature couplings. □

This statement applies only to strict continuous inequalities at an interior point. A derived equality, a proved global minimization principle, or a constraint saturated at a physical boundary can have a different effect. The proposition does not prohibit a future physical selection mechanism. It shows why selecting an arbitrary stable member of the present family would not establish such a mechanism. An extra independent curvature measurement can identify the magnitude through the explicit inverse already given, but that is observational

identification rather than a determination of a fundamental constant from the mother dynamics.

14.35. *Memory, loss of confinement, and the meaning of criticality.* Eliminating the mediator in Section 14.30 produces a dependence on earlier states. It does not add a spatial metric or a quantum state space. The distinction matters when interpreting a slowly decaying signal or a large fluctuation as evidence for new physics. In this finite example the location and nature of the stability boundary can be determined exactly.

PROPOSITION 75 (A tuned stability boundary of the finite mediator model). *Assume equal positive temperatures Θ, positive fixed frictions, and the three-coordinate model of Section 14.28. Define*

$$d_{\mathrm{f}} = k_0 - c^T D_{\mathrm{f}}^{-1} c.$$

For $d_{\mathrm{f}} > 0$, the mediator variance is $\mathrm{Var}(r) = \Theta/d_{\mathrm{f}}$. At $d_{\mathrm{f}} = 0$, the process has no invariant probability law. Approaching this boundary with fixed frictions and a convergent positive set of diagonal stiffnesses makes at least one drift decay rate tend to zero. The retarded representation has exactly the same boundary as the full Markovian system when its initial mediator and noise are retained.

Proof. Block inversion of K_{f} gives $(K_{\mathrm{f}}^{-1})_{rr} = 1/d_{\mathrm{f}}$, proving the variance formula from the Gibbs covariance. At equality let $v = (D_{\mathrm{f}}^{-1}c, 1)^T \neq 0$, so that $K_{\mathrm{f}} v = 0$. The row vector $w^T = ((\Lambda_{\mathrm{f}} v)^T, v^T)$ obeys $w^T B_{\mathrm{f}} = 0$. Therefore the scalar projection $Y = w^T Z$ satisfies

$$dY = \sqrt{2\Theta}\, v^T \Lambda_{\mathrm{f}}^{1/2} dW.$$

Its variance grows at strictly positive rate $2\Theta v^T \Lambda_{\mathrm{f}} v$. More generally, convolution with a nondegenerate Gaussian has no invariant probability on the real line: the characteristic function identity would force it to vanish at every nonzero frequency, contradicting continuity at zero. An invariant law for Z would project to such a law for Y, which is impossible. Continuity of the roots of the drift characteristic polynomial shows that a zero eigenvalue is approached from the stable side. Finally, substitution of the exact mediator Green solution is an identity, so it cannot create a new instability absent from the original dynamics. □

For the coefficients used in the synthetic comparison, $d_{\mathrm{f}} = 5 - 0.62\eta_{\mathrm{f}}^2$. Growing variance and slow relaxation near $|\eta_{\mathrm{f}}| = \sqrt{5/0.62}$ thus have a precise classical explanation. This boundary must be approached by changing an input. No feedback equation drives the input there, so this example does not establish self-organized criticality. A claim of that kind would require a specified adaptive or driven mechanism, robustness to parameter changes and finite-size scaling of

independently defined observables. A broad fitted power spectrum alone would not supply those properties.

Classical phase mixing and loss of a measured phase correlation are also distinct from quantum decoherence. The latter requires a quantum reduced density operator and a declared system–environment coupling; even disappearance of its off-diagonal entries depends on the basis and operational measurement. The present positive classical path law does not derive this structure. Similarly the loss of quadratic confinement is not gravitational collapse: there is no evolving spacetime metric, gravitational constraint or trapped-surface condition in this oscillator model. These distinctions permit memory to be studied as a testable dynamical mechanism without assigning it physical consequences that the specified variables cannot express.

14.36. *The remaining parameter in a laboratory-to-curvature prediction.* A cross-sector relation is useful only if calibration determines every parameter that changes its target. The shared scalar branch permits an explicit test of this requirement. Work at one fixed matching scale and in fixed units, with the same metric reduction, vacuum subtraction and elementary unscreened matter convention as in Section 11.11. Retain the Cartan coefficient relations $V_C = 3M_{\mathrm{P}}^2/\ell^2$ and $|\bar{\alpha}_3| = M_{\mathrm{P}}^2\ell^2/8$. Independent threshold operators, composite-body charges and screening would require additional matching rather than this three-parameter reduction.

Use coordinates

$$A_\varphi := \alpha_\varphi \in (0, 1/3), \qquad q_\sigma := m_\sigma^2/Z_* \geq 0, \qquad L_c := \ell^2 > 0.$$

Here L_c has dimensions of length squared; it is not a generator. The nonnegative coordinate q_σ is a mass squared, not the bare mass itself. The inherited relations give

$$m_\varphi^2 = q_\sigma + \frac{6A_\varphi}{L_c}, \qquad K_{\mathrm{curv}} := \frac{\lambda_3^2}{M_{\mathrm{P}}^2} = \frac{A_\varphi L_c^2}{32}. \tag{1091}$$

The symbol K_{curv} denotes a dimensional coupling combination, not a measured curvature scalar. To obtain the first identity, substitute $\gamma^2 = 2A_\varphi/M_{\mathrm{P}}^2$ in $m_\varphi^2 = m_\sigma^2/Z_* + \gamma^2 V_C$. The second follows from $\lambda_3 = -\bar{\alpha}_3\gamma$.

Proposition 76 (Calibration degeneracy and its removal). *On the interior $q_\sigma > 0$, calibration of (A_φ, m_φ^2) alone leaves a continuous family of different K_{curv}. The enlarged map $(A_\varphi, q_\sigma, L_c) \mapsto (A_\varphi, m_\varphi^2, K_{\mathrm{curv}})$ is locally invertible. For positive $A_\varphi, K_{\mathrm{curv}}$, its inverse on the physical domain is*

$$L_c = \sqrt{\frac{32K_{\mathrm{curv}}}{A_\varphi}}, \qquad q_\sigma = m_\varphi^2 - \frac{6A_\varphi}{L_c} \geq 0. \tag{1092}$$

Neither statement determines the sign of λ_3.

Proof. The Jacobian, with columns ordered as $(A_\varphi, q_\sigma, L_c)$, is

$$J = \begin{pmatrix} 1 & 0 & 0 \\ 6/L_c & 1 & -6A_\varphi/L_c^2 \\ L_c^2/32 & 0 & A_\varphi L_c/16 \end{pmatrix}, \qquad \det J = \frac{A_\varphi L_c}{16} > 0.$$

Its first two rows annihilate $(0, 6A_\varphi/L_c^2, 1)^T$; its last row does not. More directly, at fixed calibration values the exact fiber is

$$L_c \geq \frac{6A_\varphi}{m_\varphi^2}, \qquad q_\sigma = m_\varphi^2 - \frac{6A_\varphi}{L_c}.$$

Along this fiber $K_{\mathrm{curv}} = A_\varphi L_c^2/32$ varies strictly. This proves nonidentification without relying on parameter counting. Solving the last identity for its positive root gives (1092); the determinant proves regular local invertibility. The dependence on λ_3^2 leaves its sign absent. □

For an explicit comparison, measure lengths in the same geometrical black-hole mass $\mathcal{M}$. Take $A_\varphi = 10^{-6}$ and $m_\varphi \mathcal{M} = 0.1$. The two choices $\ell/\mathcal{M} = 0.05, 0.1$ require, respectively, $q_\sigma \mathcal{M}^2 = 0.0076, 0.0094$. Both are positive. Nevertheless they give

$$\frac{K_{\mathrm{curv}}}{\mathcal{M}^4} = 1.953125\,10^{-13}, \qquad 3.125000\,10^{-12},$$

a factor of sixteen. These are supplied parameter examples, not measurements. They satisfy the displayed algebraic and scale conditions; they do not establish a common admissible vacuum for all other branches.

There are consequently two distinct ways to close this particular prediction. An independent observation can constrain L_c or K_{curv} through a specified forward map, or an additional physical principle can fix one of them. An assigned value of a renormalized coefficient is not automatically such an observation: redundant operators, field redefinitions and matter matching must be included. Likewise setting $q_\sigma = 0$ would remove one freedom, but is a new physical restriction unless a separate derivation enforces it. The direct photon width is not a third independent calibration here, because $\Gamma_{\gamma\gamma} = A_\varphi m_\varphi^3/(32\pi M_{\mathrm{P}}^2)$ is already fixed by the first two entries.

Conditional on these inputs, the massive stationary Kerr calculation provides a definite intermediate response. Let $I_\chi(\mu_s) > 0$ be its normalized curvature-source susceptibility, with $\mu_s = m_\varphi \mathcal{M}$. Its scalar energy-form strength is

$$\mathcal{B}_\chi = \frac{A_\varphi}{32} \left(\frac{\ell}{\mathcal{M}}\right)^4 I_\chi(\mu_s). \tag{1093}$$

The Kerr companion derives this function by a coercive stationary field problem and computes it with radial and angular refinement. The factor I_χ is independent of the overall linear scalar source amplitude; it is not a fitted

black-hole coupling. Formula (1093) therefore supplies a conditional connection, while Proposition 76 specifies exactly what additional calibration it needs. A detector prediction still requires metric backreaction, wave propagation and the observation likelihood. No thermodynamic temperature or turbulent transport coefficient has been identified with K_{curv} by this calculation.

14.37. *Conditional global identification from resolved response channels.* Unique dynamics at fixed parameters and identification of those parameters from observations are different questions. The shared scalar branch permits a global identification result for a deliberately restricted ideal experiment. Fix units, one matching scale, the reference source mass, the asymptotic time convention, and the elementary unscreened matter map. Retain the three positive-branch coordinates $A_\varphi > 0$, $m_\varphi > 0$, $K_{\mathrm{curv}} > 0$ and the matching relations

$$K_{\mathrm{curv}} = \frac{A_\varphi \ell^4}{32}, \qquad q_\sigma = m_\varphi^2 - \frac{6A_\varphi}{\ell^2} \geq 0. \tag{1094}$$

The sign of a scalar coordinate is fixed by convention or quotiented out when every coupling transforms under the same scalar reflection. This does not identify signs of additional independently coupled operators.

At two prescribed distances $0 < r_1 < r_2$, suppose the measured fractional force corrections are positive resolved values

$$Y_j = A_\varphi (1 + m_\varphi r_j) e^{-m_\varphi r_j}, \quad j = 1, 2. \tag{1095}$$

Also suppose that a calibrated zero-spin source of known geometrical mass M supplies its complex fundamental odd-parity frequency shift

$$\Delta w_2 = \frac{K_{\mathrm{curv}}}{M^4} C_2^{\mathrm{ax}}(m_\varphi M). \tag{1096}$$

These equations define the exact leading-order ideal observation model. For a finite-error physical test, their remainders, source uncertainties, body charges, noise and instrument maps have to be retained.

Proposition 77 (Global identification in the ideal matched branch). *If $0 < Y_2/Y_1 < 1$, the two force values determine unique $m_\varphi > 0$ and $A_\varphi > 0$. If also $C_2^{\mathrm{ax}}(m_\varphi M) \neq 0$, a frequency shift of the form* (1096) *determines a unique positive K_{curv}. The implied positive ℓ is unique, and so is the nonnegative q_σ whenever the reconstructed parameters satisfy the branch conditions. Data satisfy this branch only if the complex shift has the required phase and amplitude sign and the reconstructed q_σ is nonnegative.*

Proof. Define

$$R(m) = \frac{1 + m r_2}{1 + m r_1} e^{-m(r_2 - r_1)}.$$

It is continuous, tends to 1 as $m \downarrow 0$ and tends to 0 as $m \to \infty$. Its logarithmic derivative is

$$(\log R)' = -m\left[\frac{r_2^2}{1+mr_2} - \frac{r_1^2}{1+mr_1}\right] < 0 \quad (m > 0),$$

because the derivative of $r^2/(1+mr)$ with respect to r is $r(2+mr)/(1+mr)^2 > 0$. The intermediate value theorem and strict monotonicity give exactly one solution of $R(m) = Y_2/Y_1$. Then

$$A_\varphi = \frac{Y_1 e^{m_\varphi r_1}}{1+m_\varphi r_1}.$$

Write $C = C_2^{\mathrm{ax}}(m_\varphi M)$. Multiplication of the complex mode equation by $\overline{C}$ gives the unique real value

$$K_{\mathrm{curv}} = M^4 \frac{\mathrm{Re}(\overline{C}\Delta w_2)}{|C|^2}.$$

The exact consistency conditions are $\mathrm{Im}(\overline{C}\Delta w_2) = 0$ and $\mathrm{Re}(\overline{C}\Delta w_2) > 0$. Solving (1094) gives $\ell = (32K_{\mathrm{curv}}/A_\varphi)^{1/4} > 0$ and the stated q_σ. The branch is rejected when $q_\sigma < 0$. □

The required phase condition uses both components of the complex shift; discarding it would lose a testable constraint. A second axial mode then has the retained prediction $\Delta w_3 = (K_{\mathrm{curv}}/M^4)C_3^{\mathrm{ax}}(m_\varphi M)$, and no additional response amplitude is fitted. For a different prescribed source mass M', both $m_\varphi M'$ and K_{curv}/M'^4 change by their fixed dimensional scaling rather than by recalibration.

14.37.1. *Identification accuracy and a synthetic recovery.* The inverse is poorly conditioned when the two force distances do not resolve the range. For perturbations to the force ratio,

$$\delta m \simeq \frac{\delta \log(Y_2/Y_1)}{(\log R)'(m)}.$$

The denominator tends to zero as $m \downarrow 0$ and becomes small when the distances approach one another. Likewise the frequency inverse amplifies noise when $|C|$ is small or its dimensional shift is unresolved. Global uniqueness in an exact ideal map therefore does not assert practical identifiability in noisy data.

As a numerical exercise, use units $M_0 = 1$ and supply $A_\varphi = 10^{-5}$, $m_\varphi = 0.3$, $\ell = 0.03$ once. At $r_1 = 2$, $r_2 = 5$, the synthetic force values are $8.78098618\,10^{-6}$ and $5.57825400\,10^{-6}$. The computed zero-spin axial coefficient gives the synthetic calibration shift

$$\Delta w_2 = (1.12191156 + 0.56695278i)10^{-14}.$$

The inverse recovers the supplied parameters to a maximum relative arithmetic difference below $4.3\,10^{-15}$. This same-model, noiseless exercise tests

the inverse calculation. It is not an independent observation test. With the recovered parameters frozen, the second mode is predicted as $(2.64441419 + 0.61467463i)10^{-14}$ at $M = M_0$; the companion zero-spin calculation also supplies predictions at $M/M_0 = 1/3$ and $10/3$ with no separate response fit.

14.37.2. *Relation to a physical selector and other sectors.* The proposition selects one parameter vector from specified ideal data; it does not derive a physical parameter vector from the mother dynamics. A dynamical selector on $\Theta/\sim$ still requires its independently justified functional and its uniqueness hypotheses. Conversely, a normalizable invariant law, an HJB solution or a stochastic symmetry does not replace the three observation channels used here.

The frequency coefficients require the matched vacuum action, the corrected metric, and ingoing/outgoing tensor boundary conditions. They are computed for the odd-parity zero-spin branch. Applying them to a rotating remnant would alter the stated observation model. A genuine frozen physical test must fix the source and nuisance treatment, noise model and observation map on calibration data, then evaluate disjoint test data without a response refit. The existing conditional public strain comparisons concern a different massless rotating representative; they cannot calibrate this massive branch without additional matching. No equation in this inverse map identifies K_{curv} with a fluid viscosity, a reservoir temperature or a quantum reconstruction parameter.

14.38. *Conditional identifiability and a frozen cross-event check.* This section records two computations that sharpen, but do not erase, the remaining closure conditions. The first concerns local identifiability in the already specified massless tensor branch. The second applies the analysis protocol frozen on GW150914 to an event that was not used to set its scenario weights. Neither calculation selects a fundamental coupling from the mother action.

14.38.1. *A rank test for a multi-mode response.* Let M_0 be a fixed reference mass and let the three local coordinates be

$$q = (\log(M/M_0),\, \chi,\, \zeta), \qquad y^{(p)}_{\ell mn}(q) := M_0 \omega^{(p)}_{\ell mn}.$$

$$y^{(p)}_{\ell mn}(q) = e^{-q_1}\left[z^{\mathrm{Kerr}}_{\ell mn}(\chi) + \zeta C^{(p)}_{\ell mn}(\chi) + O(\zeta^2)\right],$$

where p denotes the parity and the coefficients C are the explicitly normalized published coefficients of the declared scalar–Gauss–Bonnet branch [36]. Here $z^{\mathrm{Kerr}} = M\omega^{\mathrm{Kerr}}$, whereas y uses the fixed reference mass: their mass derivatives differ. The Jacobian is evaluated at $q_1 = 0$ and $\zeta = 0$. A single complex mode supplies two real equations, so its Jacobian has rank at most two and cannot identify all three coordinates. For the fundamental $(2, 2, 0)$ and $(3, 3, 0)$ modes, direct finite differences of the public Kerr continued-fraction solver and the

tabulated response coefficients give, at $\chi = 0.7$,

$$J_A = \begin{pmatrix} -0.53260024 & 0.44489913 & 0.18708640 \\ 0.08079287 & 0.03794290 & -0.24911726 \\ -0.84368686 & 0.65773127 & 0.06752952 \\ 0.08285568 & 0.04424175 & -0.20511071 \end{pmatrix},$$

$$J_P = \begin{pmatrix} -0.53260024 & 0.44489913 & -1.23866143 \\ 0.08079287 & 0.03794290 & 0.31015384 \\ -0.84368686 & 0.65773127 & -4.73566406 \\ 0.08285568 & 0.04424175 & 0.56924229 \end{pmatrix}.$$

Both matrices have rank three. Their smallest singular values are, respectively, 5.91×10^{-2} and 1.07×10^{-1}; halving the finite-difference step changes every displayed Jacobian entry by less than 1.46×10^{-8}. The same rank is obtained with the $(2, 1, 0)$ mode, and with all three modes. Thus multiple modes can identify a coupling *locally within this declared branch*, provided the source parameters and mode assignment are specified and both frequencies are resolved. This is an identifiability result, not a proof that the mother model chooses ζ.

The calculation also gives a precise version of the selection limitation. For one mode the coupling column lies in the span of the mass and spin columns (projected norms below 4×10^{-16} in the calculation), whereas the two-mode projected norms are 0.1754 (axial) and 1.4560 (polar). Consequently, a multi-mode observation can remove a degeneracy that a single mode cannot remove, but only by supplying an additional datum. It does not turn an observational estimate into a first-principles selection principle.

PROPOSITION 78 (Local identification in the prescribed spectral branch). *Assume the displayed spectral map is continuously differentiable near the reference point and its real Jacobian has full column rank three. Then the map is locally one-to-one in these three coordinates. The same holds on its physical restriction $\zeta \geq 0$ if a continuously differentiable extension through zero has the same full-rank derivative.*

Proof. Write F for the real spectral map and $A = DF(q_*)$. Full column rank in finite dimension gives $K > 0$ such that $\|v\| \leq K\|Av\|$. Continuous differentiability yields a neighborhood U of q_* on which

$$\|F(x) - F(y) - A(x - y)\| \leq (2K)^{-1}\|x - y\|, \qquad x, y \in U.$$

The triangle inequality then gives $\|x - y\| \leq \frac{1}{2}\|x - y\| + K\|F(x) - F(y)\|$, and hence

$$\|x - y\| \leq 2K\|F(x) - F(y)\|, \qquad x, y \in U.$$

This proves local injectivity and a local stability estimate. Restriction to $U \cap \{\zeta \geq 0\}$ preserves injectivity. The continuously differentiable extension does not interpret negative ζ as a physical squared coupling. □

This is a local statement: it excludes neither distant degeneracies nor additional nuisance parameters. Its conditioning depends on coordinate units and on the observational noise covariance. The displayed unweighted singular values are numerical rank diagnostics, not measured precision or confidence intervals. At fixed dimensionful coupling $\zeta \propto M^{-4}$; the extra contribution to the mass derivative vanishes at the reference $\zeta = 0$ used here. The massless nonzero-coupling branch uses the explicitly modified potential discussed above. It does not satisfy the massive-scalar constraint of the unaltered common-weight potential.

14.38.2. *Frozen prediction on GW170104.* The original GW150914 protocol, coefficient registry, source grid, nuisance model and three fixed scenarios $\sqrt{|\alpha|} = 0, 1, 10\,\mathrm{km}$ were frozen before downloading the GWOSC H1 and L1 4096-Hz, 32-s HDF5 files for GW170104 [1]. Noise spectra were estimated from the declared off-event interval, and the test segment was chosen from the catalog GPS time by the predeclared +0.05-s offset. No coupling, source grid, waveform amplitude or test-data processing choice was re-estimated. Event-specific off-source noise is calibrated by the same fixed procedure. Source mass, spin and redshift are marginalized over the unchanged 27-point grid, and Gaussian amplitude priors are integrated analytically rather than optimized on the new strain. The frozen scenario weights, transferred from the earlier calibration, are $(0.33331978, 0.33331979, 0.33336043)$. The network log marginal likelihood for the three scenarios is -2.98016882, -2.98016883, and -2.98030047. After applying the frozen weights, the predictive value is -2.98021271; relative to the zero-coupling reference it is

$$\Delta \log \mathcal{B} = -4.3891 \times 10^{-5}.$$

More precisely, if b_{ej} is the event-e log marginal likelihood relative to noise in scenario j, equal calibration priors give

$$w_j = \frac{e^{b_{\mathrm{cal},j}}}{\sum_k e^{b_{\mathrm{cal},k}}}, \qquad b_{\mathrm{pred}} = \log\left(\sum_j w_j e^{b_{\mathrm{test},j}}\right).$$

This transfers a discrete calibrated distribution, not a uniquely selected physical constant. The almost equal weights already show that GW150914 did not identify these scenarios under the adopted model. The direct covariance calculation and its Woodbury implementation agree to 6.53×10^{-14}. These numbers show that this particular short, single-event analysis has essentially no resolving power for the tested scenarios. It is therefore a reproducible null

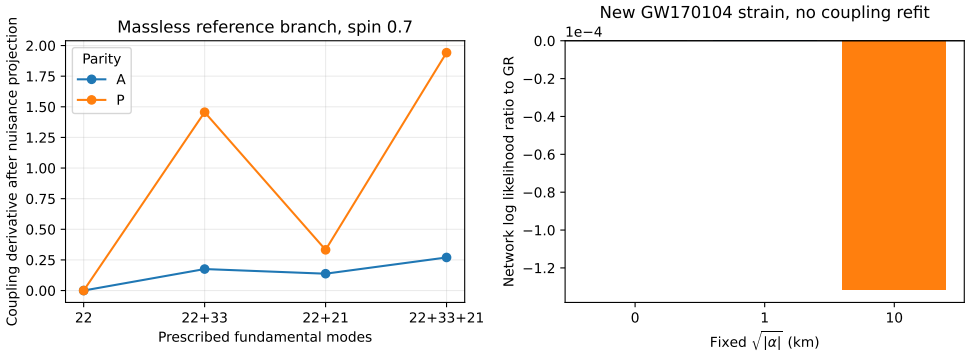


Figure 20. Left: coupling derivatives after projection against mass and spin derivatives for prescribed fundamental modes in the massless reference branch. Right: the fixed GW170104 scenario likelihoods relative to the zero-coupling reference. The first panel concerns local algebraic identification; the second shows negligible scenario discrimination under the frozen conditional model. Neither panel is a massive tensor spectrum or a validation of the mother theory.

result, not evidence for or against the full unified theory. A genuine cross-sector validation still requires the missing massive coupled tensor operator, a complete radiation map, and an independently fixed calibration and test protocol. This new strain split was frozen locally, not externally preregistered. The late catalog-based window is not established to isolate the full linear ringdown. The raw noise covariance has condition numbers of order 10^{11}–10^{12}; agreement of two Gaussian formulas does not bound noise-model or covariance conditioning errors. The tiny ratio must not be interpreted as a precise physical exclusion. Calibration errors, overtone excitation and an inspiral–merger model are absent from this restricted analysis.

14.38.3. *Relation to physical selection and the massive branch.* The rank calculation supplies a concrete route by which independent multi-mode data could identify a declared coupling combination. The frozen GW170104 calculation uses strain from an event excluded from calibration to compare the existing conditional reference scenarios. Its negligible discrimination and the stated covariance limitations remain part of the interpretation. Neither calculation supplies a physical selector functional F_{sel}, nor does it compute the massive rotating tensor pencil required for a genuine $C_{\ell m}(a/M, \mu_s)$. Those remain explicit theorems and computations to be established before unconditional claims of unique coupling or unified empirical validation are justified.

The next calculation links the Cartan coefficient expansion in Section 5.3, the joint restriction (227), the declared Lorentzian continuation (208), and the matter equation (262). Its flat-vacuum version uses the existing matching prescription (773). The recovered orbital observable is a consequence of these specified interfaces, with the classical interpretation of [63].

14.39. *From the specified mother action to a physical orbit.* An orbital recovery result requires three linked calculations: expansion of the mother action, solution of its metric equation, and motion of matter coupled to that metric. A standard metric cannot be inserted at the last step without checking the preceding two. We complete this chain on the declared stationary, torsionless Lorentzian metric branch. The result is a conditional classical sector of the specified model.

The continuation and the consistent elimination of torsion are the same conditions used in the earlier metric reduction. Compactly supported variations are used below, so boundary counterterms do not change the local equations. The common scalar weight is taken in its decoupling limit: its logarithmic slope is zero, and its stationary value is $w_* > 0$. This limit is allowed by the existing parameter family; it does not select that value for nature. Gauge fields vanish in the exterior, the scalar is at an unsourced stationary vacuum, and the probe has no independent scalar or gauge charge. The matter block is universally coupled to the induced metric. Additional retained operators would have to be included in the following variation if their coefficients were nonzero.

At a finite regulator the complete mother drift is $-M^{ij}\partial_j S + \theta m_\nu^{-1}\partial_j(m_\nu M^{ij})$, with covariance $2\theta M$. At zero noise its stationary configurations obey $M\,dS = 0$. If M is injective on the allowed physical variations, this gives $dS = 0$, the Euler system used for the stationary field sector. This finite statement neither identifies the Euclidean relaxation parameter with proper time nor proves the existence of a Lorentzian continuum limit. The continued, consistently reduced action below is used under precisely that matching hypothesis.

14.39.1. *Coefficients inherited from the curvature norm.* For the displayed Cartan block,

$$F_{\mathrm{c}}^{ab} = R^{ab} - \ell^{-2} e^a \wedge e^b, \qquad F_{\mathrm{c}}^{a5} = \ell^{-1} T^a.$$

The Euclidean gravitational part of the one-norm mother action is

$$S_{\mathrm{c},E} = \frac{w_*}{2g_{\mathrm{c}}^2} \int \sum_{I<J} F_{\mathrm{c}}^{IJ} \wedge \star_e F_{\mathrm{c}}^{IJ}.$$

There are six orthonormal two-forms $e^a \wedge e^b$ with $a < b$. Antisymmetry gives

$$\sum_{a<b} |R^{ab}|^2 = \tfrac{1}{4} R_{abcd} R^{abcd}, \qquad \sum_{a<b} \langle R^{ab}, e^a \wedge e^b \rangle = \tfrac{1}{2} R.$$

Expansion of the squares therefore gives, before continuation,

$$S_{\mathrm{c},E} = \frac{w_*}{2g_{\mathrm{c}}^2} \int \sqrt{g_E} \left[\tfrac{1}{4} R_{abcd} R^{abcd} - \frac{R}{\ell^2} + \frac{6}{\ell^4} + \frac{\sum_a |T^a|^2}{\ell^2} \right] d^4x. \tag{1097}$$

Thus the Einstein term and the curvature-square term arise from the same norm. Under the stated Wick convention and torsionless metric reduction, the retained Lorentzian action is

$$S_{\mathrm{ext}} = \int \sqrt{-g} \left[\frac{M_{\mathrm{P}}^2}{2} (R - 2\Lambda_{\mathrm{vac}}) + \bar{\alpha}_3 R_{abcd} R^{abcd} \right] d^4x + S_{\mathrm{m}}[g, \Psi], \tag{1098}$$

where, at the displayed tree matching scale,

$$M_{\mathrm{P}}^2 = \frac{w_*}{g_{\mathrm{c}}^2 \ell^2}, \qquad G_* = \frac{1}{8\pi M_{\mathrm{P}}^2} = \frac{g_{\mathrm{c}}^2 \ell^2}{8\pi w_*}, \qquad \bar{\alpha}_3 = -\frac{w_*}{8 g_{\mathrm{c}}^2}. \tag{1099}$$

These relations use natural units. Any threshold conversion of the tensor Newton coefficient is required at the same matching scale.

The cosmological term needs explicit bookkeeping. The unmodified Cartan constant has energy density $V_C = 3M_{\mathrm{P}}^2/\ell^2$ and hence $\Lambda_{\mathrm{vac}} = 3/\ell^2$. The already specified vacuum-matched scalar branch subtracts this constant and its scalar tadpole. On that branch $V_J(0) = V_J'(0) = 0$, giving $\Lambda_{\mathrm{vac}} = 0$ at the retained order. The subtraction is additional matching data, not a consequence of the positive norm. Both values of Λ_{vac} are retained below; the flat-vacuum calculation uses the latter branch explicitly.

The spacetime metric is induced by the Lorentzian coframe, $g_{\mu\nu} = \eta_{ab} e^a{}_\mu e^b{}_\nu$, with $\eta = \mathrm{diag}(-1, 1, 1, 1)$. On the scalar-decoupled, vacuum-normalized branch the Jordan and Einstein physical metrics coincide. Orbital matter consequently sees this metric. No metric on mass labels or positive configuration-space mobility enters its definition.

14.39.2. *Why the retained quadratic curvature does not obstruct this sector.* Let $I_1 = R^2$, $I_2 = R_{ab}R^{ab}$ and $I_3 = R_{abcd}R^{abcd}$, and define $H_{ab}^{(i)} = (-g)^{-1/2} \delta \int \sqrt{-g} I_i / \delta g^{ab}$. The exterior metric equation obtained by varying (1098) is

$$M_{\mathrm{P}}^2 (G_{ab} + \Lambda_{\mathrm{vac}} g_{ab}) + 2\bar{\alpha}_3 H_{ab}^{(3)} = T_{ab}, \qquad T_{ab} = -\frac{2}{\sqrt{-g}} \frac{\delta S_{\mathrm{m}}}{\delta g^{ab}}. \tag{1100}$$

The factor two follows from the $M_{\mathrm{P}}^2/2$ normalization. It is not an independently chosen gravitational weight.

On a four-dimensional Einstein metric $R_{ab} = \Lambda_{\mathrm{vac}} g_{ab}$, the scalar curvature is constant, $R = 4\Lambda_{\mathrm{vac}}$. The algebraic part of $H^{(1)}$ is $2RR_{ab} - \frac{1}{2} g_{ab} R^2 = 0$; its

derivative terms vanish as well. For $H^{(2)}$ the derivative terms vanish because the Ricci tensor is parallel. Its algebraic part reduces to

$$2R_{acbd}R^{cd} - \tfrac{1}{2}g_{ab}R_{cd}R^{cd} = 2\Lambda_{\rm vac}R_{ab} - 2\Lambda_{\rm vac}^2 g_{ab} = 0.$$

In four dimensions the local variation of the Euler density $I_3-4I_2+I_1$ vanishes for compactly supported metric variations. Consequently $H^{(3)} = 4H^{(2)} - H^{(1)} = 0$ on the same metric.

This is an exact cancellation in the retained action. It proves that an Einstein exterior solves the full displayed metric equation even when $\bar{\alpha}_3 \neq 0$. It does not require deleting the quadratic term or estimating its ratio to a vanishing Einstein tensor. The quadratic theory can also have other solutions and extra modes; their stability and elimination are separate questions. The calculation constructs the recovered Einstein solution sector, rather than proving that it exhausts the fourth-order theory.

14.39.3. *Deriving the spherical exterior.* Write $x^0 = c_{\rm light}t$, where $c_{\rm light}$ denotes the speed of light and is distinct from a scalar-weight slope. On a static exterior with $F_o > 0$, use the areal-radius ansatz

$$ds^2 = -e^{2d_o(r)}F_o(r)(dx^0)^2 + F_o(r)^{-1}dr^2 + r^2d\Omega^2.$$

To construct the Einstein solution sector, first solve its second-order vacuum equation and then use the previous cancellation to verify the full equation (1100). Its independent components are

$$G^t{}_t = \frac{F_o - 1}{r^2} + \frac{F_o'}{r}, \qquad G^r{}_r - G^t{}_t = \frac{2F_o d_o'}{r}.$$

The second identity gives $d_o' = 0$; a constant time rescaling removes d_o. The first equation is

$$[r(F_o - 1)]' = -\Lambda_{\rm vac}r^2.$$

Integration, with the mass parameter written as $\mathcal{M}$, yields

$$F_o(r) = 1 - \frac{2\mathcal{M}}{r} - \frac{\Lambda_{\rm vac}r^2}{3}, \qquad ds^2 = -F_o(dx^0)^2 + F_o^{-1}dr^2 + r^2d\Omega^2. \quad (1101)$$

The angular equation independently gives $G^\theta{}_\theta = F_o''/2 + F_o'/r = -\Lambda_{\rm vac}$. Thus $R_{ab} = \Lambda_{\rm vac}g_{ab}$, and the quadratic tensors vanish, which verifies (1100) with $T_{ab} = 0$. Equation (1101) has been obtained from the retained mother coefficients and their metric variation.

For the flat-vacuum matching, asymptotic time normalization fixes the meaning of t and $\mathcal{M} = G_*M/c_{\rm light}^2$ is the geometrical mass. For $\Lambda_{\rm vac} \neq 0$ there is no asymptotically flat ADM definition; $\mathcal{M}$ is the spherical integration constant matched to a local source. On a weak-field static patch, $g_{tt} = -(1 + 2\Phi/c_{\rm light}^2)$ gives $\Phi = -G_*M/r - \Lambda_{\rm vac}c_{\rm light}^2r^2/6$. The value of M is fixed by source or

boundary data. This exterior calculation does not compute the stellar equation of state or its mass from the mother action.

PROPOSITION 79 (A conditional mother-action orbit sector). *Under the stated metric reduction, scalar decoupling, stationary vacuum and universal matter coupling,* (1101) *is an exact vacuum solution of the retained action* (1098)*. Neutral spinless test matter follows its physical timelike geodesics. On the vacuum-matched branch, the leading periapsis advance is* $6\pi\mathcal{M}/[a(1-e^2)]$ *per radial period. The result proves recovery in this specified sector, with the matching conditions shown.*

Proof. The preceding metric construction and vanishing of $H^{(3)}$ prove the first assertion. The matter and orbit variations establishing the remaining assertions are given next. □

14.39.4. *Obtaining the trajectory from the same matter coupling.* For the universally coupled matter block, its on-shell diffeomorphism variation is

$$0 = \delta_\xi S_{\mathrm{m}} = \int \sqrt{-g}\, T^{ab}\nabla_a\xi_b\, d^4x = -\int \sqrt{-g}\, (\nabla_a T^{ab})\xi_b\, d^4x.$$

Arbitrary compactly supported ξ therefore gives $\nabla_a T^{ab} = 0$. For a pressureless spinless test element, $T^{ab} = \rho U^a U^b$ and $\nabla_a(\rho U^a) = 0$, so $\rho U^a \nabla_a U^b = 0$. On its matter support $\rho > 0$, and hence $U^a\nabla_a U^b = 0$.

An explicit massive scalar probe gives the same result without assigning a worldline in advance. Its matched minimally coupled equation is $(\hbar^2\Box_g - m_b^2 c_{\mathrm{light}}^2)\Psi_b = 0$. Substituting $\Psi_b = b\exp(iS_b/\hbar)$ and retaining the leading eikonal order gives $g^{ab}\partial_a S_b \partial_b S_b = -m_b^2 c_{\mathrm{light}}^2$. With $p_a = \partial_a S_b$, symmetry of its derivatives yields

$$p^a\nabla_a p_b = p^a\nabla_b p_a = \tfrac{1}{2}\nabla_b(p^a p_a) = 0.$$

The massive wave packet therefore has the same geodesic characteristic. This step uses the matter principal symbol of the declared branch; a nonminimal matter operator or a variable mass can change it. A planet is treated as a neutral test body at leading multipole order. Spin, self-gravity, tides and pressure corrections require the corresponding extended-body matching and are not supplied by the scalar wave-packet calculation alone.

14.39.5. *Exact radial first integral and the periapsis.* Use equatorial motion and proper length $s = c_{\mathrm{light}}\tau$. The dimensionless energy and angular momentum per unit rest mass in geometrical units are

$$\mathcal{E}_o = F_o\frac{dx^0}{ds}, \qquad J_o = r^2\frac{d\phi_o}{ds},$$

$$-1 = -F_o \left(\frac{dx^0}{ds}\right)^2 + F_o^{-1}\left(\frac{dr}{ds}\right)^2 + r^2\left(\frac{d\phi_o}{ds}\right)^2.$$

The cyclic-coordinate variations conserve $\mathcal{E}_o, J_o$, and normalization gives

$$\left(\frac{dr}{ds}\right)^2 = \mathcal{E}_o^2 - F_o\left(1 + \frac{J_o^2}{r^2}\right).$$

Set $u_o = 1/r$. Then $dr/ds = -J_o u_o'$ where a prime here denotes $d/d\phi_o$. The radial first integral becomes

$$(u_o')^2 = \frac{\mathcal{E}_o^2}{J_o^2} - F_o(1/u_o)\left(J_o^{-2} + u_o^2\right).$$

Differentiating, first away from a turning point and then extending by continuity to it, gives the exact Binet equation

$$u_o'' + u_o = \frac{\mathcal{M}}{J_o^2} + 3\mathcal{M}u_o^2 - \frac{\Lambda_{\rm vac}}{3J_o^2 u_o^3}. \tag{1102}$$

Every coefficient in this equation came from (1101); no relativistic orbit term was added separately.

For $\Lambda_{\rm vac} = 0$, define the Newtonian semilatus rectum $p_o = a(1-e^2)$ and $\epsilon_o = \mathcal{M}/p_o \ll 1$, with $0 < e < 1$ fixed away from the endpoints. At leading order $J_o^2 = \mathcal{M}p_o[1 + O(\epsilon_o)]$ and $u_0 = (1 + e\cos\phi_o)/p_o$. The nonlinear forcing is

$$3\mathcal{M}u_0^2 = \frac{3\mathcal{M}}{p_o^2}\left[1 + \frac{e^2}{2} + 2e\cos\phi_o + \frac{e^2}{2}\cos(2\phi_o)\right].$$

The resonant coefficient is $6\mathcal{M}e/p_o^2$. Since $(d^2/d\phi_o^2 + 1)(\phi_o \sin\phi_o) = 2\cos\phi_o$, its particular solution is $3\mathcal{M}e\phi_o \sin\phi_o/p_o^2$. The other terms are bounded first-order changes of the orbit and its element definitions. The resonant term is the first-order expansion of $(e/p_o)\cos[(1-3\epsilon_o)\phi_o]$. The advance between successive periapses is therefore

$$\Delta\varpi_o = 6\pi\epsilon_o + O(\epsilon_o^2) = \frac{6\pi G_* M}{c_{\rm light}^2 a(1-e^2)} + O(\epsilon_o^2). \tag{1103}$$

The exact relation between J_o and the two turning radii differs at first order from its Newtonian value; that difference changes bounded orbital terms and cannot change the leading resonant coefficient.

14.39.6. *An independent geodesic computation and numerical benchmark.* For a bound Schwarzschild orbit, define a, e from its turning radii, $r_p = a(1-e)$ and $r_a = a(1+e)$, and put $r = p_o/(1 + e\cos\chi_o)$. Substitution in the two turning-point equations gives

$$\frac{J_o^2}{\mathcal{M}p_o} = \frac{1}{1 - (3+e^2)\epsilon_o}, \qquad \frac{d\phi_o}{d\chi_o} = [1 - (6 + 2e\cos\chi_o)\epsilon_o]^{-1/2}.$$

For $\epsilon_o(6+2e)<1$, the exact advance is

$$\Delta\varpi_o^{\mathrm{exact}}=\int_0^{2\pi}\left\{[1-(6+2e\cos\chi_o)\epsilon_o]^{-1/2}-1\right\}d\chi_o. \tag{1104}$$

The binomial series is uniformly convergent on each compact subdomain of this inequality. Termwise integration gives

$$\Delta\varpi_o^{\mathrm{exact}}=6\pi\epsilon_o+\frac{3\pi}{2}(18+e^2)\epsilon_o^2+O(\epsilon_o^3).$$

This checks the leading frequency calculation and specifies its next error term with the turning-radius convention.

As a reproducible solar-system benchmark, prescribe $G_*M_\odot = 1.32712440018\times10^{20}\,\mathrm{m^3s^{-2}}$, $c_{\mathrm{light}}=299792458\,\mathrm{m\,s^{-1}}$, $a=5.7909227\times10^{10}\,\mathrm{m}$, $e=0.205630$, and period 87.9691 days. These external rounded inputs are not predictions of the mother model, nor are they a fitted planetary ephemeris. They give

$$\begin{aligned}\mathcal{M}_\odot&=1476.62503825\,\mathrm{m},\\ p_o&=5.54606107978\times10^{10}\,\mathrm{m},\\ \epsilon_o&=2.66247525407\times10^{-8}.\end{aligned}$$

Multiplying (1103) by $180\times3600/\pi$ converts radians to arcseconds. A Julian century has 36525 days, so the conversion uses 415.202611 orbital periods:

$$\Delta\varpi_o^{(1)}=0.1035170379''/\mathrm{orbit}=42.9805444''/\mathrm{century}.$$

Stable quadrature of (1104) gives $42.9805496''$/century with the turning-radius input convention, a higher-order difference of 5.16×10^{-6} arcsec/century. No measured precession was used to choose a mother coefficient. This is the isolated relativistic contribution; planetary interactions, solar quadrupole, solar rotation and ephemeris inference are not included.

Numerical integration of the nonlinear Binet equation provides a separate check. At $e=0.2$ and $\epsilon_o=10^{-3},3\times10^{-4},10^{-4}$, the next periapsis obtained as a zero of u_o' agrees with (1104) to within 2.6×10^{-13} radians. These finite-tolerance numerical differences are not rigorous interval error bounds. The comparison in Figure 21 shows the expected first omitted order.

14.39.7. *The cosmological term and the coupled scalar sector.* The cosmological term in (1102) must be retained when the original Cartan constant is not subtracted. At first order in $\xi_o=|\Lambda_{\mathrm{vac}}|a^3/\mathcal{M}\ll1$, its periapsis contribution is

$$\Delta\varpi_\Lambda=\frac{\pi\Lambda_{\mathrm{vac}}a^3}{\mathcal{M}}\sqrt{1-e^2}. \tag{1105}$$

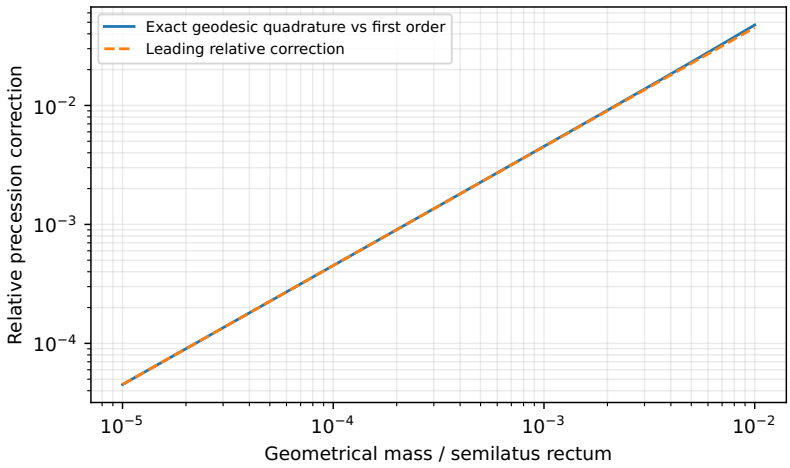


Figure 21. Computed Schwarzschild geodesic quadrature on the recovered stationary sector. The relative correction to the leading periapsis advance agrees with $(9/2 + e^2/4)\epsilon_o$ at small compactness, here with $e = 0.2$. These are theoretical orbit calculations with supplied inputs, rather than a fit to planetary observations.

For completeness, differentiating $\int_0^{2\pi}(1 + e\cos\phi_o)^{-2}d\phi_o = 2\pi(1 - e^2)^{-3/2}$ gives

$$\int_0^{2\pi} \frac{\cos\phi_o\, d\phi_o}{(1 + e\cos\phi_o)^3} = -\frac{3\pi e}{(1 - e^2)^{5/2}}.$$

Inserting this Fourier coefficient in the last term of (1102) gives (1105). Joint small-parameter expansion has neglected terms of orders ϵ_o^2, $\epsilon_o\xi_o$ and ξ_o^2 at fixed eccentricity. For the quoted solar inputs, the linear response is $3.46279 \times 10^{37}\Lambda''_{\rm vac}$/century when $\Lambda_{\rm vac}$ is in m^{-2}. For illustration, a prescribed tolerance of $0.1''$/century would require $|\Lambda_{\rm vac}| < 2.88784 \times 10^{-39}\,\mathrm{m}^{-2}$. If the unmodified relation $\Lambda_{\rm vac} = 3/\ell^2$ is imposed, this would require $\ell > 3.22310 \times 10^{19}\,\mathrm{m}$. The tolerance is illustrative, not a measured confidence limit. This calculation makes the need for vacuum matching explicit; it does not solve the cosmological-constant or extra-mode problem.

At nonzero common scalar slope, a constant scalar cannot generally be inserted into the exterior. In the retained Ricci-flat perturbative branch,

$$(\Box - m_\varphi^2)\varphi = -\lambda_3 R_{abcd}R^{abcd} + \text{matter sources},$$
$$\lambda_3 = -\bar{\alpha}_3\gamma, \qquad g^J_{ab} = A_{\rm m}(\varphi)^2 g^E_{ab}.$$

For a nonzero mass Schwarzschild reference metric, $R_{abcd}R^{abcd} = 48\mathcal{M}^2/r^6$, so a vanishing scalar is not a solution when $\lambda_3 \neq 0$. The scalar, its stress and the conformal matter force must then be solved together. A star requires

regular-centre and surface matching; a black-hole horizon condition cannot be reused as a solar scalar boundary condition.

Once that coupled exterior is determined, the physical metric supplies a direct orbital map. For $ds_J^2 = -A_J(dx^0)^2 + B_J dr^2 + C_J d\Omega^2$,

$$\frac{d\phi_o}{dr} = \frac{J_o\sqrt{B_J}}{C_J\sqrt{\mathcal{E}_o^2/A_J - 1 - J_o^2/C_J}}, \qquad \Delta\varpi_o = 2\int_{r_p}^{r_a} \frac{d\phi_o}{dr}\, dr - 2\pi.$$

The constants are fixed by the two turning points:

$$J_o^2 = \frac{A_J(r_a) - A_J(r_p)}{A_J(r_p)/C_J(r_p) - A_J(r_a)/C_J(r_a)}, \qquad \mathcal{E}_o^2 = A_J(r_p)\left[1 + \frac{J_o^2}{C_J(r_p)}\right].$$

This formula is invariant under a monotone radial-coordinate change with $B_J dr^2$ transformed consistently. It specifies the actual forward map for a scalar correction; that correction has not been inferred from the classical recovery calculation.

The established implication is therefore the selected mother norm, its continued metric variation, the constructed physical exterior, the universal matter equation, and the orbital observable in one conditional sector. It uses the already declared flat-vacuum matching and the scalar-decoupling limit. It does not identify a unique physical coupling, select that sector dynamically, or prove the full continuum Lorentzian completion. No identification of stochastic relaxation time with proper time is needed: orbital proper time is defined by the physical metric itself.

15. **Cross-sector response and independent validation**

A common origin becomes predictive when its reduction maps constrain observables that have not been used to select the model. This section specifies that requirement at a finite regulator. It distinguishes a calculation within a specified model from a derivation of that model's physical coefficients. In particular, eliminating unresolved variables usually introduces memory; the resulting static stiffness is not by itself a Kerr propagation operator.

15.1. *Shared hypotheses, parameters, and observable consequences.* A shared reduction starts from one specified state space, action, residual metric, mobility, path cost, reference law, and projection. Its consequences depend on matching the action, generator, covariance, boundaries, and clock in the physical branch. The curvature-sourced scalar response provides one example: its massless charge relation uses the topological result of Prabhu and Stein [134], while the common-weight hypothesis relates its coefficient to coefficients in the other retained terms.

The numerical weights, invariant-form normalizations, physical projections, scalar mass, and constitutive maps are supplied or independently matched

data unless a separate selection argument determines them. In particular, $(S, \theta, M) \mapsto (aS, a\theta, M/a)$, $a > 0$, leaves the finite diffusion law unchanged. Uniqueness of a stationary response for fixed coefficients does not remove this freedom. The following identifiability calculation determines precisely which observations are unchanged by that scaling.

The stationary scalar boundary problem and cross stress determine part of the gravitational reduction. Tensor resonance coefficients $C_{\ell m}(a/M)$ additionally require the coupled metric calculation. A non-vacuum accretion observable $D(a/M, \dot{M}, \ldots)$ requires its transport and radiation map. The Kerr companion supplies selected leading tensor coefficients on an explicitly matched massless vacuum branch by normalizing published coupled spectral results. This does not evaluate the general massive tensor response. A separate massive zero-spin calculation now supplies the local surface-flux response of a prescribed steady test thin disc, including the leading conformal matter contribution. It does not supply a rotating radiative accretion flow or a detector map. For a strictly positive scalar mass, a separate coercive stationary problem gives a unique finite-energy weak scalar response and a residual-controlled numerical susceptibility. Its shared-weight amplitude still needs an independently constrained curvature scale; calibrating the elementary force strength and scalar mass alone leaves that scale free. Their use in prediction requires a parameter vector fixed from independent calibration, followed by propagation of source, instrument, and model uncertainty.

Numerical refinement and symbolic residuals test the specified equations. An observational comparison instead uses the full forward map and the held-out protocol in Section 15.13. GWOSC strain, NICER timing and spectra, and EHT interferometry require their respective instrument likelihoods; JHTDB supplies numerical fluid data. Access to those products alone establishes neither a fit nor a common-parameter validation.

15.2. *Identifiability theorem for the present mother data.* The coupling question can be settled rigorously at the level of the present finite diffusion data. Let $\mathscr{L}_{S,\theta,M,c}$ denote the law of

$$\mathrm{d}X_t = \big[-M\nabla S + \theta\ \mathrm{div}\, M + c\big](X_t)\,\mathrm{d}t + \sqrt{2\theta M}\,\mathrm{d}W_t,$$

with fixed domain, reference measure, boundary condition, and a unique martingale problem. For every $a > 0$, define

$$T_a(S, \theta, M, c) = (aS, a\theta, M/a, c).$$

Then

$$-\frac{M}{a}\nabla(aS) + a\theta\ \mathrm{div}(M/a) + c = -M\nabla S + \theta\ \mathrm{div}\, M + c, \qquad 2(a\theta)(M/a) = 2\theta M.$$

The Gibbs exponent is also unchanged: $(aS)/(a\theta) = S/\theta$. Hence

$$\mathscr{L}_{T_a(S,\theta,M,c)} = \mathscr{L}_{S,\theta,M,c}$$

for every path observable defined in the declared physical time. The map from these coefficients to the state-path law is therefore non-injective. No estimator based only on that law can distinguish two points on this normalization orbit. In particular, its likelihood cannot select the absolute normalization without independent thermodynamic calibration. An HJB value or a Noether charge is a law-only statistic only after its cost and observable definitions have also been fixed. For example, the same uncontrolled state process with running costs 1 and a, zero terminal cost, and horizon T has values $T - t$ and $a(T - t)$. Thus equality of state-path laws alone does not imply equality of externally normalized costs or charges.

There is a second obstruction after this normalization is fixed. For a direct sum of r compact simple ideals, every invariant positive form has

$$h = \sum_{i=1}^{r} c_i h_i, \qquad c_i > 0.$$

One linear trace normalization removes at most one degree of freedom; the admissible coefficient set still has local dimension $r - 1$. The matrices

$$H_h = \begin{pmatrix} 1 & h \\ h & 1 \end{pmatrix}, \qquad |h| < 1,$$

give an elementary finite counterfamily with distinct cross-couplings, strict positivity, normalizable Gibbs laws, and well-posed linear diffusions. Thus positivity, Gibbs invariance, finite HJB well-posedness, and stochastic symmetry identities do not imply unique relative couplings.

The first calculation establishes non-identifiability of absolute normalization from the state-path law. The second establishes that positivity, invariance, and well-posedness do not select the relative couplings. These are different conclusions. Once the normalization orbit has been quotiented out, a relative coupling can still be identifiable from data. For example, the diffusion with drift $-H_h x$ and covariance $2\theta I$ has stationary covariance

$$C_h = \frac{\theta}{1 - h^2} \begin{pmatrix} 1 & -h \\ -h & 1 \end{pmatrix}, \qquad h = -\frac{(C_h)_{12}}{(C_h)_{11}}.$$

Thus its exact stationary law determines h, even when the common variance scale is unknown. This identification does not derive the value of h from positivity or invariance. One route to an independently selected coupling is a functional F_{sel} on the physical quotient with the existence and strictness properties stated below. It is a sufficient route, not the only possible selection mechanism. Introducing such a functional to reproduce a desired value adds

model data rather than deriving it from the existing Gibbs, HJB, or Noether conditions.

The scaling calculation exhibits a nontrivial equivalence orbit of the coefficient-to-law map; it does not classify its entire kernel. The relative weight example separately disproves selection from positivity and invariance alone. Additional measurements can distinguish relative weights, but they do not turn those weights into deductions of the original premises.

15.3. *Conditional coupling-selection theorem.* The normalization obstruction does not prevent a conditional selection theorem once the missing physical data are supplied. Let Θ be the admissible parameter space and let $\sim$ identify gauge, normalization, and operationally indistinguishable descriptions. Assume that the quotient $\Theta/\sim$ carries the declared topology and that the energy, temperature, and physical-time units have been fixed independently. Suppose the mother model derives a functional

$$F_{\mathrm{sel}} : \Theta/\sim \longrightarrow \mathbb{R} \cup \{+\infty\}$$

THEOREM 80 (Conditional unique-coupling selection). *Assume that the quotient has a fixed metrizable realization, that F_{sel} is proper, bounded below, and lower semicontinuous, and that every finite sublevel set is compact. For uniqueness, assume either that its effective domain is identified with a convex subset of a real vector space on which it is strictly convex, or that an explicitly identified candidate ϑ_0 satisfies $F_{\mathrm{sel}}(\vartheta) - F_{\mathrm{sel}}(\vartheta_0) \geq \delta > 0$ for every other admissible class. In the latter case the gap must be established by a separate calculation. Then there is one and only one equivalence class*

$$\vartheta_* = \operatorname*{arg\,min}_{\vartheta \in \Theta/\sim} F_{\mathrm{sel}}(\vartheta).$$

Proof. A minimizing sequence is eventually contained in a compact sublevel set and therefore has a convergent subsequence; lower semicontinuity attains the infimum. If two distinct minimizers existed, strict convexity would make the value at their midpoint strictly smaller. In the strict-gap case the strict gap gives the same contradiction. The selected representative is unique only if an additional gauge or normalization convention selects exactly one representative of that equivalence class. □

This theorem is conditional. It becomes a deduction of the mother model only if the displayed F_{sel}, the quotient, the units, and the coercivity/strictness estimates are derived independently from that model. Adding F_{sel} solely to obtain a preferred numerical coupling would instead add a new physical postulate. The normalization obstruction and the failure of positivity alone to select relative weights remain in force; neither excludes identification from additional observations.

15.4. *Declared mother-cost selection principle.* To turn the conditional selection theorem into a testable model extension, we declare the following additional principle explicitly. After fixing the energy, temperature, and physical-time units and passing to $\Theta/\!\sim$, let π_ϑ denote the stationary law of the specified regulated generator whenever it exists. For a dimensionless joint residual q_ϑ and a fixed positive residual metric $\mathsf{H}_{\mathrm{ref}}$, define

$$\Phi_\kappa(q) = \begin{cases} (e^{\kappa q} - 1 - \kappa q)/\kappa^2, & \kappa \neq 0, \\ q^2/2, & \kappa = 0, \end{cases} \qquad \Phi_\kappa(q) \geq 0,$$

and

$$F_{\mathrm{sel}}([\vartheta]) := \limsup_{T\to\infty} \frac{1}{T}\mathbb{E}_{\pi_\vartheta}\left[\int_0^T \left\{\frac{1}{2}R_\vartheta^{\mathsf{T}}\mathsf{H}_{\mathrm{ref}}^{-1}R_\vartheta + \eta_{\mathrm{sel}}\Phi_{\kappa_{\mathrm{risk}}}(q_\vartheta)\right\}\mathrm{d}t\right].$$

Here $\eta_{\mathrm{sel}} \geq 0$ is a separately declared dimensionless penalty weight, and $\kappa_{\mathrm{risk}} \geq 0$ is the dimensionless risk parameter. Neither symbol redefines the original exponential-cost coefficient κ_{cost}. The residual metric, residuals, and score must descend to the quotient; otherwise the minimization is not a well-defined operation on physical equivalence classes. The *mother-cost selection principle* (SP) chooses the equivalence class that minimizes this dimensionless long-time cost, subject to the exact positivity, conservation, gauge, parity, and generator-matching constraints. The subtraction $1 + \kappa q$ makes the risk term continuous at $\kappa = 0$; no sign or convexity claim is made for a dimensional q before its normalization is declared.

SP is a new, explicitly declared physical postulate unless a microscopic derivation of this stationary score from the mother action is supplied. Consequently the conditional theorem above proves uniqueness only when SP's functional is independently shown to be lower semicontinuous, coercive, and strictly convex (or separated by a certified discrete gap) on the quotient. The finite construction below tests SP directly. These analytic properties and a unique numerical physical coupling have not been established for the full continuum theory.

15.4.1. *Stationary averaging, integrability, and parameter sensitivity.* Let $c_\vartheta(x)$ denote the nonnegative integrand in SP, with $\mathsf{H}_{\mathrm{ref}} > 0$ and $\eta_{\mathrm{sel}} \geq 0$. For a stationary initial law, Tonelli's theorem gives, for every $T > 0$,

$$\frac{1}{T}\mathbb{E}_{\pi_\vartheta}\int_0^T c_\vartheta(X_t)\,\mathrm{d}t = \int c_\vartheta\,\mathrm{d}\pi_\vartheta.$$

Thus the stated long-time score is exactly a one-time stationary expectation, including the possibility of the value $+\infty$. No ergodic theorem is needed for this equality. Almost-sure estimation from a single trajectory additionally requires ergodicity and integrability. For positive risk, finite polynomial moments do

not suffice: the score requires the relevant exponential moment. For example, if a residual is quartic in a nondegenerate Gaussian state, its positive exponential moment is generally infinite. A nonempty finite-score domain must be established before applying the selection theorem.

This stationary expectation must also be distinguished from the path cumulant rate

$$\Lambda_\vartheta(k) = \lim_{T\to\infty} T^{-1} \log \mathbb{E} \exp\left(k \int_0^T c_\vartheta(X_t)\, \mathrm{d}t \right).$$

SP, as defined above, is not this cumulant rate or a path relative entropy. The two functions have different integrability and spectral requirements. Calling the stationary penalty informational does not identify it with a Girsanov likelihood or a large-deviation rate function.

A useful conditional existence result is elementary. Suppose the parameter quotient is represented by a compact metric space K, the state space is fixed and Polish, $\vartheta \mapsto \pi_\vartheta$ is weakly continuous, and the continuous costs c_ϑ converge uniformly on compact state sets as the parameter converges. Suppose also that the stationary laws are uniformly tight and the costs are uniformly integrable under these laws. Truncation to a compact set followed by bounded continuous convergence shows that $\pi_\vartheta(c_\vartheta)$ is continuous. Compactness then gives a minimum. For unbounded costs, the tail estimate is an essential part of this argument. These conditions give existence; they do not give strict convexity or uniqueness.

Even strict convexity of the integrand in the parameter need not survive averaging against a parameter-dependent law. To see this, let

$$\mathrm{d}X_t = -[X_t - (v + \sin v)]\, \mathrm{d}t + \sqrt{2}\, \mathrm{d}W_t, \qquad c_v(x) = (v - x)^2, \qquad v \in [-\pi, \pi].$$

The unique stationary law is $N(v + \sin v, 1)$. Although $\partial_v^2 c_v(x) = 2$, its averaged score is $F(v) = 1 + \sin^2 v$, with three minimizers at $-\pi, 0, \pi$. This is a counterexample to inferring uniqueness of the selection score from convexity of the residual penalty alone.

For a differentiable stationary family, the missing derivative can be computed. Assume that differentiation under stationary integration is justified and that the centered Poisson problem has a solution in a common generator domain:

$$\mathcal{L}_\vartheta u_\vartheta = c_\vartheta - F(\vartheta), \qquad \pi_\vartheta(u_\vartheta) = 0.$$

Differentiating $\pi_\vartheta \mathcal{L}_\vartheta = 0$, and using $\partial_i \pi_\vartheta(1) = 0$, gives

$$\partial_i F = \pi_\vartheta(\partial_i c_\vartheta) - \pi_\vartheta((\partial_i \mathcal{L}_\vartheta) u_\vartheta).$$

The second term is the stationary-law response. Omitting it generally changes both the stationary point and the Hessian. A strong-convexity certificate

therefore concerns the complete derivative, in the tangent directions of the constrained quotient.

There is also a temporal identifiability limitation. If different circulation drifts preserve the same π_ϑ, and if c_ϑ does not depend on those drifts, SP gives them the same score. For an isotropic Gaussian law, the diffusions with drift $-x+\omega Jx$, $J^{\mathsf{T}} = -J$, illustrate this freedom. Choosing a stationary distribution alone therefore does not select a nonzero stationary current or an arrow of time. Those require the generator, parity convention, and appropriate path observables.

15.4.2. *A selection problem solved without an assumed convexity claim.* The following finite example tests what the new principle actually selects. Fix the noise scale $\theta > 0$, the reference residual metric $\mathsf{H}_{\mathrm{ref}} = I$, and all units. Let

$$H_g = \begin{pmatrix} 1 & g \\ g & 1 \end{pmatrix}, \qquad \mathrm{d}X_t = -H_g X_t \,\mathrm{d}t + \sqrt{2\theta}\,\mathrm{d}W_t, \qquad |g| < 1.$$

The solution is a Gaussian Ornstein–Uhlenbeck process. Since the drift eigenvalues are $1 \pm g > 0$, its invariant law is uniquely $\pi_g = N(0, \theta H_g^{-1})$, and its mean and covariance converge to that law. Declare the residual $R_g = gJX$, where $J = \left(\begin{smallmatrix} 0 & 1 \\ 1 & 0 \end{smallmatrix}\right)$, and put $q_g = |R_g|^2/2 = g^2|X|^2/2$. These residual choices are additional model data; they are not consequences of invariance. Orthogonal diagonalization gives independent coordinates with variances $\theta/(1+g)$ and $\theta/(1-g)$. Hence

$$m_g := \mathbb{E}_{\pi_g} q_g = \frac{\theta g^2}{1-g^2}, \qquad M_g(k) := \mathbb{E}_{\pi_g} e^{kq_g} = \prod_{\sigma\in\{-1,1\}} \left(1 - \frac{k\theta g^2}{1+\sigma g}\right)^{-1/2}.$$

For $k > 0$, the last expression is finite exactly when $k\theta g^2 < 1 - |g|$. The score is therefore

$$F(g) = m_g + \frac{\eta_{\mathrm{sel}}}{k^2}[M_g(k) - 1 - km_g]$$

on this finite-moment domain. With positive η_{sel}, it is $+\infty$ outside the domain. If $\eta_{\mathrm{sel}} = 0$, the risk term is absent rather than interpreted as $0 \cdot \infty$. At $k = 0$, Gaussian fourth moments instead give

$$F(g) = \frac{\theta g^2}{1-g^2} + \frac{\eta_{\mathrm{sel}}\theta^2 g^4(2+g^2)}{2(1-g^2)^2}.$$

These expressions follow directly by integrating the two Gaussian marginals; they do not use fitted coefficients.

Proposition 81 (A unique but vanishing cross coupling). *For the displayed residual model, $g_* = 0$ is the unique global minimizer of SP for $\theta > 0$, $\eta_{\mathrm{sel}} \geq 0$, and $k \geq 0$, with the finite-score convention above.*

Proof. The inequality $e^z \geq 1 + z$ makes the risk contribution nonnegative. At $g = 0$, the residual vanishes identically, so $F(0) = 0$. At any $g \neq 0$ in the finite-score domain, $F(g) \geq m_g > 0$. Infinite scores cannot minimize it. This proves global uniqueness without an unverified global Hessian condition. □

For $(\theta, k, \eta_{\mathrm{sel}}) = (0.7, 0.5, 0.3)$, the computed scores at $g = (0, 0.2, 0.5, 0.7)$ are respectively 0, 0.0294309860515, 0.254795800047, and 1.00268822460. Independent Gaussian quadrature agrees with the closed exponential moments to less than 10^{-12} in these cases. This is a numerical check of the finite example, not a measurement of a physical coupling. At zero noise the attracting stationary law is δ_0 for every g, and every score vanishes. Thus uniqueness in this example is not uniform in the zero-noise limit. A nonzero selected physical coupling needs independently justified competing terms or constraints; it cannot be inferred from the name of the selection principle.

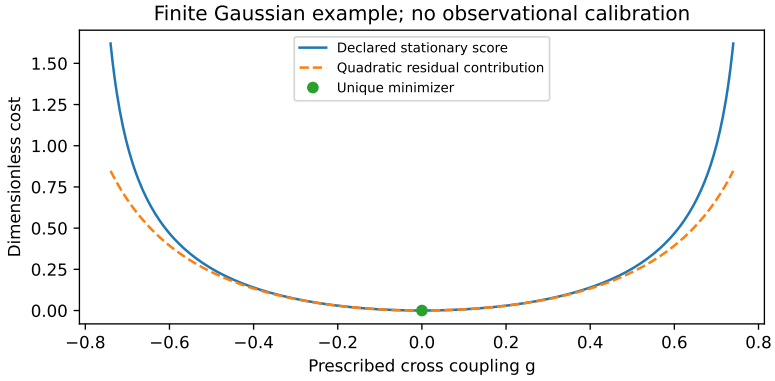


Figure 22. The exactly specified Gaussian selection example at $\theta = 0.7$, $\kappa_{\mathrm{risk}} = 0.5$, and $\eta_{\mathrm{sel}} = 0.3$. The risk penalty increases the cost away from zero, while the minimum is already fixed by the declared quadratic residual. The curve is a finite-model computation.

15.5. *Perturbative tensor response and observable matching.* For the matched action used in the Kerr branch, a consistent tensor prediction requires the following background and perturbation equations. Let $h^{(2)}$ solve

$$M_{\mathrm{P}}^2\, \delta G^{\mathrm{K}}_{ab}[h^{(2)}] = T^{\varphi}_{ab}[\varphi_1] + T^{\mathrm{int}}_{ab}[\varphi_1]$$

with a specified gauge, regular future-horizon data, fixed asymptotic mass and spin, and no unlisted homogeneous perturbation. Let Π_{phys} be the corresponding constraint and gauge projection and $G^{\mathrm{stat}}_{\mathrm{K}}$ an inverse, on the chosen stationary source and solution spaces, of $M_{\mathrm{P}}^2 \delta G^{\mathrm{K}}$ after those zero modes are removed.

Existence of this inverse is an additional analytic hypothesis; it is not supplied by the scalar boundary problem. The first backreaction is then

$$h^{(2)} = G_{\mathrm{K}}^{\mathrm{stat}}\Pi_{\mathrm{phys}}\big(T^{\varphi}[\varphi_1] + T^{\mathrm{int}}[\varphi_1]\big).$$

After differentiating the complete operator, including the background change, direct metric terms, scalar-mediated term, and the boundary domain, the first nonzero resonant correction must have the form

$$\mathcal{N}_{\ell m} := \big\langle v_{\ell m}, \big(\mathcal{L}_{\mathrm{direct}}^{[p]} + \mathcal{L}_{\mathrm{bg}}^{[p]}[h^{(2)}] + \mathcal{L}_{\mathrm{scalar}}^{[p]}\big)u_{\ell m}\big\rangle,$$

$$C_{\ell m} := -\frac{\mathcal{N}_{\ell m}}{\langle v_{\ell m}, \partial_{\widehat{\omega}}\mathcal{L}_{\mathrm{Kerr}}u_{\ell m}\rangle}, \qquad M\Delta\omega_{\ell m} = \varepsilon^p C_{\ell m} + o(\varepsilon^p).$$

The stationary correction is an argument of the background-dependent operator; that operator acts on the oscillating right mode, not on the stationary correction itself. The left and right resonant states, their bilinear pairing, the boundary variation, and the order p must all be supplied. A scalar profile, static Schur complement, or mass–spin diffusion does not determine these objects. A reliable computation requires that (i) the coupled boundary-value solve converges under radial and angular refinement, (ii) the constraint residual converges in the same gauge, (iii) the result is invariant under an allowed gauge change, and (iv) the same frozen ϑ_* is used in every held-out observable.

For an accretion observable, the response requires the non-vacuum equations

$$\nabla_a T^{ab}_{\mathrm{total}} = 0, \qquad T_{\mathrm{total}} = T_{\mathrm{fluid}} + T_{\mathrm{EM}} + T_{\mathrm{rad}} + T_{\mathrm{cross}},$$

an equation of state and closure, radiation transport, boundary and initial data, and an instrument map. For nonzero reference observable $\mathcal{D}_0$, define its dimensionless leading response at a declared positive integer order q_D by

$$\mathcal{D}(\varepsilon) = \mathcal{D}_0[1 + \varepsilon^{q_D} D + o(\varepsilon^{q_D})].$$

All lower derivatives must vanish if $q_D > 1$; a vanishing linear derivative is not evidence for the absence of a quadratic signal. The coefficient is determined only after those equations are solved with the same frozen ϑ_*. It cannot be recovered from T^{ab}_{cross} alone.

15.6. *Frozen-parameter validation is a reproducible procedure.* The no-refit claim is accepted only if the following sequence is recorded:

(1) Freeze the action, regulator, units, clock, projection, and nuisance parameterization.
(2) Select ϑ_* using only $\mathcal{D}_{\mathrm{cal}}$ and exact structural constraints.
(3) Publish hashes of source code, input data, and the frozen parameter file.
(4) Open the held-out data only after the preceding steps.
(5) Evaluate the complete forward map and likelihood without refitting ϑ_*.

(6) Report uncertainty, model discrepancy, nuisance treatment, baseline comparison, and a predeclared decision rule.

Application to the gravitational branch requires independently calibrated λ_3, m_φ, the backreacted tensor waveform, and the complete accretion forward map. Those physical inputs and calculations remain necessary before this procedure yields an observational test.

15.7. *Parameter definitions and selection.* For every coefficient, the model record must specify its defining equation, units, regulator and renormalization scale, physical clock, admissible range, and origin: prescribed, derived, or independently calibrated. In particular, the following symbols have different meanings:

Symbol	Definition	Present role
κ_{cost}	Coefficient multiplying the residual cost in an exponential	Input; $\kappa_{\mathrm{cost}} q$ must be dimensionless
κ_P	Coefficient of the declared curvature term	Branch coefficient, with units fixed by the action convention
κ_H	Surface gravity of the normalized horizon generator	Derived geometric quantity, not a universal coupling
κ_{trap}	Stiffness in a specified physical displacement coordinate	Local experimental coefficient
$\bar{\kappa}$	Normalized common perturbation parameter	Requires an independent selection or calibration map
η_{sel}	Weight of the additional stationary selection penalty	New SP input; not selected by naming the score
κ_{risk}	Exponent parameter in $\Phi_\kappa(q)$	New dimensionless SP input; requires exponential integrability

This list distinguishes the original five symbols and the two SP inputs; it does not identify them. The rest of the record includes the energy coefficients, mobility, covariance, observation maps, reference measure, boundary data, and clock. Derived quantities such as $\kappa_H(M, a)$ are not counted again as free coordinates. A function-valued coefficient requires either a fixed function or a declared finite basis, not an unrecorded fit.

A unique minimizer for a fixed cost is not a unique physical parent theory. For example, all matrices

$$H_h = \begin{pmatrix} 1 & h \\ h & 1 \end{pmatrix}, \qquad |h| < 1,$$

define strictly positive quadratic energies and well-posed reversible diffusions with identity mobility and normalizable Gibbs laws. Their cross-couplings differ. Thus positivity, Gibbs invariance, and well-posedness alone do not select a

common weight. Additional symmetry or variational restrictions must actually eliminate this freedom.

A sufficient finite-dimensional selection theorem would specify a convex admissible coefficient set and an independently fixed, coercive, strictly convex objective on it. Existence and strict convexity would then give a unique minimizer within that class. Gauge-equivalent representations must first be quotiented out. Selection of a physical projection requires, in addition, its operational definition and generator-matching identity. These hypotheses have not been established for all physical couplings and all projections of the unified field programme.

There is an exact normalization freedom even before physical selection. For any positive constant a, the simultaneous replacement

$$(S_r, \theta, M_r) \longmapsto (aS_r, a\theta, M_r/a)$$

leaves S_r/θ, the drift $-M_r\nabla S_r + \theta \operatorname{div} M_r + c_r$, and the covariance $2\theta M_r$ unchanged, with the same reference measure, domain, and c_r. The same conclusion holds for a weighted divergence. Thus it leaves the state-path law unchanged whenever the martingale problem is unique. Absolute energy and temperature units, or independently measured thermodynamic responses, can fix this normalization; the state trajectory alone cannot. This is a redundancy of this diffusion identification, not a statement that every independently defined control cost is invariant.

Nor does removing this normalization fix all relative weights. For a direct sum of r compact simple ideals, invariant positive forms can have r independent positive coefficients. One trace normalization leaves an $(r-1)$-dimensional open simplex. Minimizing over the fields does not vary these external coefficients. A penalty favoring equal coefficients would be additional model data unless derived from a stated microscopic selection problem.

15.8. *Constrained linearization and exact elimination.* All matrices below are expressed in fixed physical coordinates after constraint reduction. If constraints $G_j(Y) = 0$ are imposed before linearization, the energy Hessian on an orthonormal tangent basis Q at a constrained critical point is

$$H_* = Q^{\mathsf{T}} \left(D^2 S_r + \sum_j \lambda_j D^2 G_j \right) Q, \qquad \nabla S_r + \sum_j \lambda_j \nabla G_j = 0.$$

It is generally not the unrestricted Hessian. A nonlinear state reduction also contributes an Itô drift correction. Those terms, the transformed reference measure, and boundary conditions must be included before forming a reduced generator.

In the resulting coordinates, write the mother drift as $b = -M_r \nabla S_r + \theta \operatorname{div} M_r + c_r$. Its differential in a direction v is

$$Db(Y_*)v = -M_* H_* v - (DM_r(Y_*)[v])\nabla S_r(Y_*) + \theta D(\operatorname{div} M_r)(Y_*)v + Dc_r(Y_*)v. \tag{1106}$$

The simpler expression $B_* = -M_* H_* + C_*$ applies when $\nabla S_r(Y_*) = 0$, with $C_* = \theta D(\operatorname{div} M_r)(Y_*) + Dc_r(Y_*)$. An expansion about a constant deterministic background also requires $b(Y_*) = 0$. Existence of a stationary probability law does not imply either of these pointwise conditions.

Partition the retained fluctuation into $Y = (\xi, \eta)$ and set

$$H_* = \begin{pmatrix} H_{\xi\xi} & H_{\xi\eta} \\ H_{\eta\xi} & H_{\eta\eta} \end{pmatrix}, \qquad M_* = \begin{pmatrix} M_{\xi\xi} & M_{\xi\eta} \\ M_{\eta\xi} & M_{\eta\eta} \end{pmatrix}, \qquad B_* = Db(Y_*). \tag{1107}$$

For the additive-noise linear realization $dY = B_* Y\, dt + \Sigma_*\, dW$, variation of constants gives

$$\begin{aligned} \eta_t &= e^{tB_{\eta\eta}}\eta_0 + \int_0^t e^{(t-s)B_{\eta\eta}} B_{\eta\xi}\xi_s\, ds + \int_0^t e^{(t-s)B_{\eta\eta}}\Sigma_\eta\, dW_s, \\ d\xi_t &= \left[B_{\xi\xi}\xi_t + \int_0^t K(t-s)\xi_s\, ds + B_{\xi\eta}e^{tB_{\eta\eta}}\eta_0 + \zeta_t \right] dt + \Sigma_\xi\, dW_t, \\ K(t) &= B_{\xi\eta}e^{tB_{\eta\eta}}B_{\eta\xi}, \qquad \zeta_t = B_{\xi\eta}\int_0^t e^{(t-s)B_{\eta\eta}}\Sigma_\eta\, dW_s. \end{aligned} \tag{1108}$$

This is exact for the specified linear model. The inherited colored noise, its correlation with retained noise, and the initial transient cannot be deleted while claiming the same reduced stochastic law. For nonlinear multiplicative noise, the additive model itself is an additional approximation.

For z outside the spectrum of $B_{\eta\eta}$, the corresponding deterministic response pencil is

$$\mathcal{P}(z) = zI - B_{\xi\xi} - B_{\xi\eta}(zI - B_{\eta\eta})^{-1}B_{\eta\xi}. \tag{1109}$$

Only at zero frequency does this reduce to

$$B_{\mathrm{eff}}(0) = B_{\xi\xi} - B_{\xi\eta}B_{\eta\eta}^{-1}B_{\eta\xi}. \tag{1110}$$

If $A = B_{\eta\eta}$ is invertible and $|z|\|A^{-1}\| < 1$, the resolvent identity and a Neumann series yield

$$\|(zI - A)^{-1} + A^{-1}\| \le \frac{|z|\|A^{-1}\|^2}{1 - |z|\|A^{-1}\|}.$$

Multiplication by the two off-diagonal block norms bounds the error in replacing the full response by its static approximation. This condition controls both frequency and possible nonnormal amplification.

15.9. *Perturbation order and the Kerr identification.* Let $\varepsilon = \bar{\kappa}$ be a declared dimensionless parameter. A response coefficient is a derivative, not the entire finite-coupling difference:

$$\mathcal{L}_{\mathrm{cross}}(z) := \partial_\varepsilon \mathcal{P}(z;\varepsilon)|_0\,, \qquad \mathcal{P}(z;\varepsilon) = \mathcal{P}(z;0) + \varepsilon \mathcal{L}_{\mathrm{cross}}(z) + O(\varepsilon^2). \quad (1111)$$

The background, blocks, projectors, and boundary conditions that depend on ε must all be differentiated. If $R = (zI - B_{\eta\eta})^{-1}$, then $R' = RB'_{\eta\eta}R$, and

$$\mathcal{P}' = -B'_{\xi\xi} - B'_{\xi\eta}RB_{\eta\xi} - B_{\xi\eta}RB'_{\eta\xi} - B_{\xi\eta}RB'_{\eta\eta}RB_{\eta\xi}.$$

If both off-diagonal drift blocks are $O(\varepsilon)$ and the diagonal blocks have no first-order correction, the first nonzero elimination term is $O(\varepsilon^2)$. A nonzero linear signal cannot be assumed.

For example, take the fully specified two-coordinate energy and mobility

$$S = \tfrac{1}{2}a_0x^2 + \varepsilon g_0 xy + \tfrac{1}{2}b_0y^2, \qquad M = \mathrm{diag}(\mu,\nu),$$
$$a_0, b_0, \mu, \nu > 0, \quad a_0b_0 > \varepsilon^2 g_0^2.$$

The process with drift $-M\nabla S$ and covariance $2\theta M$ has

$$\mathcal{P}(z;\varepsilon) = z + \mu a_0 - \frac{\mu\nu\varepsilon^2 g_0^2}{z + \nu b_0}, \qquad \mathrm{Var}(x) = \frac{\theta}{a_0 - \varepsilon^2 g_0^2/b_0}. \quad (1112)$$

The second identity follows by integrating out y in the Gibbs density. The first follows directly by substituting the four drift blocks into (1109). Thus $\partial_\varepsilon \mathcal{P}|_0 = 0$, although the finite-coupling response and equilibrium covariance change. The pole $-\nu b_0$ also shows why a static Schur complement is not a full dynamical description. This is a finite mathematical benchmark, not a black-hole prediction.

For the prescribed dimensionless values $(a_0, b_0, g_0, \varepsilon, \mu, \nu, \theta) = (2, 3, 0.4, 0.6, 0.8, 1.4, 0.7)$, the effective static stiffness is 1.9808 and the exact variance is 0.3533925687. An independent sample of 50,000 Gaussian equilibrium draws gives variance 0.3547202593, with theoretical standard error 0.0022350732 for the unbiased sample variance. Solving the full Lyapunov equation agrees with θH_*^{-1} to a maximum entrywise error of 2.3×10^{-16}. These results check the specified finite realization; none of its coefficients has been inferred from observations.

To apply the construction to Kerr, a separate field identification must show that the physical perturbation pencil at zero coupling is the declared Kerr operator, with its gauge conditions, physical time, and ingoing and outgoing boundary conditions. A mass–spin label diffusion does not establish that identification. In units $G = c = 1$, put $\widehat{\omega} = M\omega$ and $\chi = a/M$. If that identification and a simple resonance perturbation theory hold, one may write

$$\mathcal{L}_{\mathrm{BH}}(\widehat{\omega}, \chi; \varepsilon) = \mathcal{L}_{\mathrm{Kerr}}(\widehat{\omega}, \chi) + \varepsilon^p \mathcal{L}^{[p]}_{\mathrm{cross}}(\widehat{\omega}, \chi) + o(\varepsilon^p),$$

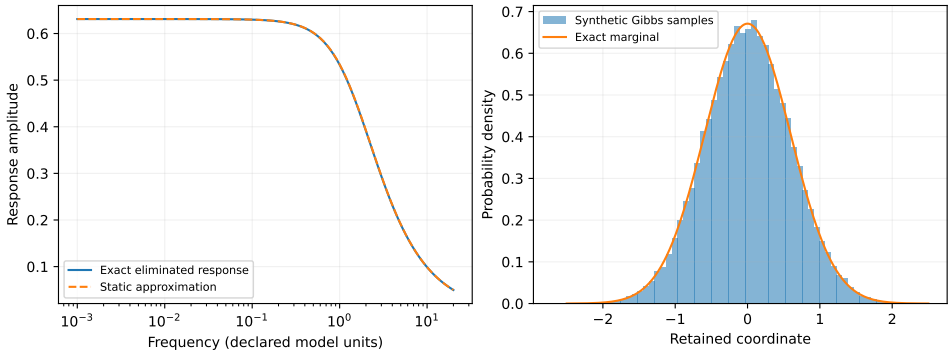


Figure 23. Finite synthetic benchmark for the prescribed two-coordinate model. Left: exact frequency response and its zero-frequency elimination approximation. Right: independent equilibrium samples and the analytical Gaussian marginal. The agreement concerns the declared mathematical model and is not an astronomical or laboratory validation.

$$C_{\ell m}(\chi) = -\frac{\langle v_{\ell m}, \mathcal{L}_{\mathrm{cross}}^{[p]} u_{\ell m}\rangle}{\langle v_{\ell m}, \partial_{\widehat{\omega}} \mathcal{L}_{\mathrm{Kerr}} u_{\ell m}\rangle}, \qquad M\Delta\omega_{\ell m} = \varepsilon^p C_{\ell m} + o(\varepsilon^p). \quad (1113)$$

Here p is the first nonzero order. The left and right resonant modes and their pairing must be defined in the specified spectral realization; ordinary square-integrable normalization is generally unavailable for outgoing resonances. The denominator must be nonzero. Differentiating the eigen-equation and pairing with the left null vector removes the unknown mode derivative and gives the displayed formula. Perturbations of the boundary domain must be included in the differentiated operator.

15.10. *Resonance perturbation under fixed analytic hypotheses.*

THEOREM 82 (Conditional existence and uniqueness of the Kerr coefficient). *Let the horizon and infinity conditions be represented on fixed complex Banach spaces X, Y after a specified analytic change of domain. If scalar or auxiliary fields are eliminated, assume that their elimination is analytic and retains every contribution at the stated order. Assume that the resulting gauge-fixed tensor operator is analytic in $(\widehat{\omega}, \varepsilon)$, is Fredholm of index zero, and has the operator-norm expansion*

$$\mathcal{L}(\widehat{\omega}, \varepsilon) = \mathcal{L}_0(\widehat{\omega}) + \varepsilon^p \mathcal{L}_p(\widehat{\omega}) + O(\varepsilon^{p+1}), \qquad p \geq 1.$$

Require $\mathcal{L}_0(\widehat{\omega}) = \mathcal{L}_{\mathrm{Kerr}}(\widehat{\omega}, \chi) : X \to Y$ in this same boundary and gauge realization. The equality of the unperturbed operators is part of the hypothesis; properties of a different Kerr operator do not suffice. Assume that the gauge-fixed Kerr boundary-value operator $\mathcal{L}_{\mathrm{Kerr}}(\widehat{\omega}, \chi)$ is an analytic Fredholm family

of index zero near a simple resonance $\widehat{\omega}_0$, with right and left null vectors $u_{\ell m}$ and $v_{\ell m}$. Assume that the kernel and cokernel are both one dimensional and that

$$\left\langle v_{\ell m}, \partial_{\widehat{\omega}} \mathcal{L}_{\mathrm{Kerr}}(\widehat{\omega}_0, \chi) u_{\ell m} \right\rangle \neq 0.$$

Then, for sufficiently small ε, there is a unique resonance branch $\widehat{\omega}_{\ell m}(\varepsilon)$ near $\widehat{\omega}_0$, modulo the declared mode normalization, and

$$\widehat{\omega}_{\ell m}(\varepsilon) = \widehat{\omega}_0 + \varepsilon^p C_{\ell m}(\chi) + O(\varepsilon^{p+1}),$$

where $C_{\ell m}$ is the quotient in (1113)*. A bound uniform over a compact spin interval additionally requires uniform operator bounds, a uniformly bounded inverse on the complementary subspaces, a uniform lower bound on the displayed nonzero pairing, and isolation from other resonances. Being away from extremality alone does not establish those conditions.*

Proof. Write $T_0 = \mathcal{L}_0(\widehat{\omega}_0)$, $u_0 = u_{\ell m}$, and let $v_0 = v_{\ell m} \in Y^*$ annihilate the range of T_0. Choose a bounded functional $\ell \in X^*$ with $\ell(u_0) = 1$. Then $X = \operatorname{span}\{u_0\} \oplus X_1$, where $X_1 = \ker \ell$. Since the range is closed with codimension one, $Y_1 = \operatorname{ran} T_0 = \ker v_0$. Choose $y_0 \in Y$ with $v_0(y_0) = 1$, and set $Qy = y - v_0(y) y_0$. The restriction $T_0 : X_1 \to Y_1$ is a bounded bijection and has a bounded inverse.

Apply the analytic implicit-function theorem to

$$Q\mathcal{L}(\widehat{\omega}, \varepsilon)(u_0 + w) = 0, \qquad w \in X_1.$$

Its w-derivative at the base point is the preceding bijection. It therefore determines a unique analytic $w = w(\widehat{\omega}, \varepsilon)$ nearby. The remaining equation is the scalar equation

$$g(\widehat{\omega}, \varepsilon) = v_0(\mathcal{L}(\widehat{\omega}, \varepsilon)[u_0 + w(\widehat{\omega}, \varepsilon)]) = 0.$$

At the base point,

$$\partial_{\widehat{\omega}} g = v_0((\partial_{\widehat{\omega}} \mathcal{L}_0) u_0),$$

because $v_0 T_0 = 0$. This derivative is nonzero by hypothesis, so a second analytic implicit-function theorem gives the unique local resonance branch with normalization $\ell(u) = 1$.

The operator expansion has no positive powers below p. Successively comparing these powers in the normalized equation forces the corresponding frequency and mode coefficients to vanish. At order p the equation is

$$T_0 u_p + C_{\ell m}(\partial_{\widehat{\omega}} \mathcal{L}_0) u_0 + \mathcal{L}_p u_0 = 0.$$

Applying v_0 removes u_p and proves the quotient. Analyticity gives the local remainder. The stated uniform inverse, pairing, and isolation bounds are additionally needed to control that remainder uniformly in spin. □

The theorem is a conditional closure statement. It does not manufacture $\mathcal{L}^{[p]}_{\mathrm{cross}}$: all same-order curvature operators, metric backreaction, scalar mass, gauge, horizon data, and asymptotic conditions must be supplied before a numerical $C_{\ell m}$ can be reported.

15.10.1. *The dynamical scalar elimination and its range of validity.* The operator entering the frequency quotient can be identified more precisely before computing its matrix elements. After fixing the action, field normalizations, gauge, and frequency-dependent boundary conditions, suppose the coupled perturbation pencil has the block expansion

$$\begin{pmatrix} L_g(\widehat{\omega}) + \varepsilon^2 A_2(\widehat{\omega}) + O(\varepsilon^3) & \varepsilon B_1(\widehat{\omega}) + O(\varepsilon^2) \\ \varepsilon C_1(\widehat{\omega}) + O(\varepsilon^2) & L_s(\widehat{\omega}) + O(\varepsilon) \end{pmatrix} \begin{pmatrix} u \\ v \end{pmatrix} = 0.$$

Here A_2 includes the change of the metric background, direct tensor terms, and the pulled-back change of the boundary domain. This expansion assumes that no retained operator produces a first-order tensor term. It must be derived from the specified action, not from a stationary Hessian alone. All compositions below are between the stated function spaces and must be bounded in the chosen operator topology.

If $L_s(\widehat{\omega})$ has a holomorphic inverse near the tensor resonance, the scalar equation gives

$$v = -\varepsilon L_s^{-1} C_1 u + O(\varepsilon^2), \qquad L_{\mathrm{eff}} = L_g + \varepsilon^2 \underbrace{(A_2 - B_1 L_s^{-1} C_1)}_{L^{[2]}_{\mathrm{cross}}} + O(\varepsilon^3).$$

The minus sign follows from solving the scalar equation and substituting it into the tensor equation. The inverse must carry the actual horizon and outgoing-wave conditions. A zero-frequency elliptic inverse generally cannot replace it. The background contribution within A_2 is $(D_g L_g)[h^{(2)}]$; it acts on the right resonant mode u.

With the left functional w annihilating the range of $L_g(\widehat{\omega}_0)$, the leading coefficient is

$$C = -\frac{\langle w, (A_2 - B_1 L_s^{-1} C_1) u \rangle}{\langle w, \partial_{\widehat{\omega}} L_g \, u \rangle}.$$

Differentiating the frequency dependence of the Schur term contributes at the next order: its prefactor is already ε^2, whereas $\Delta\widehat{\omega} = O(\varepsilon^2)$. The zeroth-order denominator is therefore correct in the isolated simple-mode problem. If a scalar resonance coincides with the tensor resonance, L_s^{-1} has a pole and this elimination fails. One must retain the coupled resonant subspace; an $O(\varepsilon)$ splitting can then occur.

An elementary complex matrix checks the algebra without claiming a Kerr computation. Set

$$L = \begin{pmatrix} \widehat{\omega} - w_g + \varepsilon^2 a & \varepsilon b \\ \varepsilon c & \widehat{\omega} - w_s \end{pmatrix}, \qquad C = -a + \frac{bc}{w_g - w_s}.$$

For $w_g = 0.37 - 0.09i$, $w_s = 0.50 - 0.10i$, $a = 0.03 + 0.02i$, $b = 0.08 - 0.01i$, and $c = 0.11 + 0.015i$, direct solution of the quadratic determinant gives $C = -0.0983823529412 - 0.02602941176 47i$. For $\varepsilon = 0.1, 0.05, 0.025, 0.0125$, the absolute errors after subtracting $w_g + \varepsilon^2 C$ are 5.292×10^{-6}, 3.338×10^{-7}, 2.091×10^{-8}, and 1.308×10^{-9}. Their fourth-order scaling follows here from the exact even dependence of this matrix on the coupling. These values are a finite algebraic benchmark, not values of $C_{\ell m}$ for a black hole.

15.10.2. *What a numerical coefficient would certify.* Small residuals alone are insufficient near a nonnormal resonance. Let N and d be the exact numerator and denominator of the frequency quotient. If independent bounds satisfy

$$|N - \widetilde{N}| \le \delta_N, \qquad |d - \widetilde{d}| \le \delta_d < |\widetilde{d}|,$$

then elementary subtraction of the two quotients yields

$$\left| C + \frac{\widetilde{N}}{\widetilde{d}} \right| \le \frac{\delta_N}{|\widetilde{d}| - \delta_d} + \frac{|\widetilde{N}|\delta_d}{|\widetilde{d}|(|\widetilde{d}| - \delta_d)}.$$

Obtaining δ_N, δ_d requires errors in the background, both resonant modes, operator matching, and the regularized pairing. The inverse on the complementary spectral subspace converts equation residuals into mode errors. Grid refinement is useful numerical evidence, but does not supply that inverse bound by itself. No such certified full Kerr computation is asserted here.

15.11. *Covariant cross stress.* A state-space quadratic cost is not automatically a covariant spacetime action. Suppose an independent reduction supplies a differentiable, diffeomorphism-invariant action $S_{\mathrm{phys}} = S_0 + \varepsilon S_1 + O(\varepsilon^2)$. With signature $(-+++)$ and variation of the covariant metric, define

$$\delta_g S_1 = \frac{1}{2} \int \sqrt{-g}\, T^{\mu\nu}_{\mathrm{cross}} \delta g_{\mu\nu}\, d^4x, \qquad T^{\mu\nu}_{\mathrm{cross}} = \frac{2}{\sqrt{-g}} \frac{\delta S_1}{\delta g_{\mu\nu}}. \tag{1114}$$

Equivalently, $T^{\mathrm{cross}}_{\mu\nu} = -2(\sqrt{-g})^{-1} \delta S_1 / \delta g^{\mu\nu}$. The sign changes when the varied metric is inverted. Metric dependence of the volume, contractions, field operators, and projections must all be varied, including boundary terms.

As a convention check, a prescribed scalar cross action $S_1 = -h_0 \int \sqrt{-g}\, g^{\alpha\beta} \partial_\alpha \phi \partial_\beta \psi\, d^4x$ gives

$$T^{\mu\nu}_{\mathrm{cross}} = h_0 \big(\nabla^\mu \phi \nabla^\nu \psi + \nabla^\nu \phi \nabla^\mu \psi - g^{\mu\nu} \nabla_\alpha \phi \nabla^\alpha \psi \big).$$

This follows from $\delta\sqrt{-g} = \frac{1}{2}\sqrt{-g} g^{\mu\nu} \delta g_{\mu\nu}$ and $\delta g^{\alpha\beta} = -g^{\alpha\mu} g^{\beta\nu} \delta g_{\mu\nu}$. It illustrates the variation; it does not select this interaction or its coefficient from the

mother model. Only the total stress is conserved on the coupled field equations; the cross contribution can exchange energy and momentum with other sectors. Dissipative contributions from eliminated reservoirs require their own covariant constitutive construction.

For a specified accretion observable $\mathcal{D}$, the fractional response at linear order $q_D = 1$ is

$$\mathcal{D}(\varepsilon) = \mathcal{D}_0[1 + \varepsilon D + o(\varepsilon)], \qquad D = \mathcal{D}_0^{-1} \frac{\partial \mathcal{D}}{\partial \varepsilon}\bigg|_0, \qquad \mathcal{D}_0 \neq 0. \tag{1115}$$

This derivative requires the coupled fluid, electromagnetic, radiation, and observation equations at fixed independently specified boundary data. If the leading order is higher, the expansion must be changed accordingly. It cannot be computed from a stress symbol alone.

THEOREM 83 (Conditional accretion-response closure). *Suppose a covariant initial–boundary value problem for $T^{ab}_{\mathrm{total}} = T^{ab}_{\mathrm{fluid}} + T^{ab}_{\mathrm{EM}} + T^{ab}_{\mathrm{rad}} + T^{ab}_{\mathrm{cross}}$ is well posed in a Banach space, $\nabla_a T^{ab}_{\mathrm{total}} = 0$ holds, and the equation of state, radiation closure, source data, and detector map are fixed independently of ε. Write its equations, constraints, and lifted boundary conditions as $\mathscr{F}(U, \varepsilon) = 0$, a C^2 map between specified Banach spaces, with $\mathscr{F}(U_0, 0) = 0$. Assume that $A_0 = D_U \mathscr{F}(U_0, 0)$ is a bounded isomorphism after gauge and constraint reduction. Let the observation map $\mathcal{D}(U, \varepsilon)$ be C^2, with $\mathcal{D}_0 = \mathcal{D}(U_0, 0) \neq 0$. Then D in* (1115) *exists and is unique. Its value is obtained by solving the linearized coupled conservation, constitutive, and instrument equations with the same boundary data; changing any of those inputs changes the response problem.*

Proof. The implicit-function theorem supplies the local solution branch and

$$U_1 = -A_0^{-1} \partial_\varepsilon \mathscr{F}(U_0, 0), \qquad D = \frac{D_U \mathcal{D}(U_0, 0)[U_1] + \partial_\varepsilon \mathcal{D}(U_0, 0)}{\mathcal{D}_0}.$$

This proves the stated uniqueness and gives the computation. Ordinary nonlinear well-posedness alone does not imply invertibility of its linearization. Shocks, changing domains, marginal stability, and long-time limits therefore require separate estimates. If the first nonzero response is quadratic, the parameter in this theorem may instead be the declared squared coupling, with the corresponding smoothness checked. □

This theorem is conditional on the complete non-vacuum forward model. The present manuscripts have not supplied that model and therefore do not report a numerical accretion coefficient.

For a quadratic leading response, the same assumptions give a more explicit formula without presuming an even reparameterized solution. Write

$$U(\varepsilon) = U_0 + \varepsilon U_1 + \varepsilon^2 U_2 + o(\varepsilon^2),$$

where $U_2 = \frac{1}{2}\partial_\varepsilon^2 U(0)$. Taylor expansion of $\mathscr{F}(U(\varepsilon),\varepsilon) = 0$ gives

$$U_1 = -A_0^{-1}\mathscr{F}_\varepsilon,$$
$$U_2 = -A_0^{-1}\left\{\tfrac{1}{2}\mathscr{F}_{UU}[U_1,U_1] + \mathscr{F}_{U\varepsilon}[U_1] + \tfrac{1}{2}\mathscr{F}_{\varepsilon\varepsilon}\right\}.$$

Every derivative on the right is evaluated at $(U_0, 0)$, and includes the fixed constraint and boundary realization. If the linear observable coefficient vanishes, its coefficient D at $q_D = 2$ is therefore

$$D = \mathcal{D}_0^{-1}\left\{\mathcal{D}_U[U_2] + \tfrac{1}{2}\mathcal{D}_{UU}[U_1,U_1] + \mathcal{D}_{U\varepsilon}[U_1] + \tfrac{1}{2}\mathcal{D}_{\varepsilon\varepsilon}\right\}.$$

This expansion retains the direct observable response and the change of the state at both orders. The first-order scalar state may be nonzero even when the first-order tensor or luminosity response vanishes. Consequently a substitution $\delta = \varepsilon^2$ is justified only for a reduced problem that is smooth in δ, not for an arbitrary coupled scalar–metric state with an odd scalar component.

15.12. *Which constraints actually remove free parameters?* Work in one ambient parameter vector $\alpha \in \mathbb{R}^d$ containing the independent sector coefficients. Let $F_0(\alpha) = 0$ encode the within-sector constraints and $C(\alpha) = 0$ encode proposed additional cross-sector relations. At a feasible regular point, define

$$J_0 = DF_0, \qquad J_{\text{joint}} = \begin{pmatrix} DF_0 \\ DC \end{pmatrix}, \qquad \Delta r = \operatorname{rank} J_{\text{joint}} - \operatorname{rank} J_0. \tag{1116}$$

With constant ranks in a neighborhood, the solution manifold dimensions are $d - \operatorname{rank} J_0$ and $d - \operatorname{rank} J_{\text{joint}}$. Their difference is Δr. If N_0 spans $\ker J_0$, then $\Delta r = \operatorname{rank}(DC\, N_0)$: one restricts the new constraints to directions left free by the old ones. This proves precisely what is removed. A stacked shared-parameter Jacobian and a block-diagonal Jacobian with duplicated parameter columns are not comparable by a direct rank subtraction.

For instance, $F_0(\alpha) = \alpha_1 + \alpha_2 + \alpha_3 - s_0$ has rank one. Adding $C = (\alpha_1 - \alpha_2, \alpha_2 - \alpha_3)$ gives total rank three and removes two local degrees of freedom. This is a transparent algebraic example. It is a physical result only after the two equalities are derived from the specified mother model, not imposed for the calculation.

Observational identifiability is a separate test. If N spans the tangent space of the fully constrained parameter set, $D_\alpha\mathcal{O}$ is the observable derivative, $D_\beta\mathcal{O}$ the nuisance derivative, and W a fixed whitening matrix, use

$$J_{\text{obs}}^{\text{phys}} = (I - P_\beta)W(D_\alpha\mathcal{O})N,$$

where P_β is the orthogonal projector onto $\operatorname{range}(WD_\beta\mathcal{O})$. Full column rank is a sufficient regular local test for distinguishing all allowed physical directions from nuisance directions. Rank deficiency is an infinitesimal degeneracy, not

a proof of global non-identifiability. Singular values, dimensionless scaling, tolerance, and numerical derivative errors must be reported.

15.13. *Frozen calibration and the status of the data.* Let ϑ parameterize the admissible model after structural constraints are imposed. Exact constraints are enforced as constraints, not silently replaced by a soft penalty:

$$\vartheta_* \in \operatorname*{arg\,min}_{\vartheta\in\Theta,\,\mathcal{C}(\vartheta)=0} \|\mathcal{O}_{\mathrm{cal}}(\vartheta) - D_{\mathrm{cal}}\|^2_{\Sigma_{\mathrm{cal}}^{-1}}. \tag{1117}$$

Approximate constraints require independently justified residual bounds. A nonunique minimizer requires a declared selection rule or propagation of the entire allowed set. It must not be chosen with the validation data.

For branch b, independently specified source and instrument data $\mathcal{I}_b$ define

$$\widehat{\mathcal{O}}_b = \mathcal{P}_b(\vartheta_*; \mathcal{I}_b), \qquad R_{\mathrm{test}} = \|\widehat{\mathcal{O}}_b - D_{\mathrm{test}}\|^2_{\Sigma_{\mathrm{pred}}^{-1}}. \tag{1118}$$

The prediction covariance includes measurement noise, propagated calibration uncertainty, and specified model discrepancy. Gaussian quadratic statistics are used only when their sampling assumptions apply. Event-count likelihoods and visibility likelihoods generally require different statistical models. Instrument processing, data exclusions, nuisance estimation, and rejection thresholds are fixed before opening the held-out observations. No-refit refers to shared theory parameters; new sources can still require independently constrained masses, spins, viewing angles, or accretion rates. Baseline GR/Kerr, GRMHD, and sector-specific models must use comparable nuisance treatment.

The public sources have different evidential roles:

- GWOSC supplies measured detector strain. Public posterior products incorporate their original waveform models and priors; they are not independent raw data from which an arbitrary new likelihood follows.
- HEASARC/NICER products require event filtering, background estimation, instrument responses, and source selection before a timing or spectral test.
- Released EHT observational products must be distinguished from EHT GRMHD code-comparison simulations; the latter test forward models.
- JHTDB is a direct-numerical-simulation benchmark for fluid statistics, not an astronomical or laboratory observation.

A GW150914 H1 4-kHz, 32-s strain file is archived with SHA-256

`C5EA87BECED5094B56B4D694F3A36E6D59F7`
`4D3A46E546B980A6A199D1F252A9`.

The two lines concatenate to one hash. Archiving the file does not constitute a frozen-parameter test. A data-access route is likewise not a completed NICER, EHT, or JHTDB validation.

Keeping the physical couplings as supplied inputs, as in the conditional branch used here, permits forward calculations over those inputs. It does not

create an independently selected parameter vector. In particular, using the published GW150914 remnant posterior to set mass and spin and then calling the same event an independent ringdown test would require accounting for the data reused in that posterior. Independent calibration must be independent of the tested statistic, or the shared likelihood must explicitly account for the dependence. A second detector does not by itself remove this issue if the calibration posterior already used both detectors.

For a fixed detector template $h(\vartheta)$, Gaussian noise with a separately estimated covariance Σ would give

$$-2\log\mathscr{L}(\vartheta) = (d - h(\vartheta))^{\mathsf{T}}\Sigma^{-1}(d - h(\vartheta)) + \log\det\Sigma + \text{constant}.$$

The covariance and template must describe the same filtering and sampling. The normalized stationary scalar profile is not h. Without the tensor waveform, source-to-detector projection, and declared nuisance model, this formula has no computable theory likelihood. Assigning a parameter value or a likelihood merely because a raw file is available would supply uncomputed physical information.

15.14. *A conditional local curvature response.* The companion Kerr analysis makes a local field response explicit. Suppose the matched Lorentzian metric action retains $f_3(\varphi)R^2_{\alpha\beta\gamma\delta}$, with a canonical scalar of mass m_φ, and suppose the other operators of the retained order are controlled. Put $\lambda_3 = f_3'(0)$. On a Ricci-flat Kerr background the leading scalar equation is

$$(\Box_{\mathrm{K}} - m_\varphi^2)\varphi_1 = -\lambda_3 R^{\mathrm{K}}_{\alpha\beta\gamma\delta}R_{\mathrm{K}}^{\alpha\beta\gamma\delta}.$$

Horizon regularity, axis regularity, and decay at infinity give at most one stationary axisymmetric response for $m_\varphi^2 \geq 0$ under the stated finite-energy conditions. In the massless case, direct integration of the monopole equation gives

$$Q_{\mathrm{BH}} = 8\lambda_3\kappa_H, \qquad \varphi_1 = Q_{\mathrm{BH}}/r + O(r^{-2}).$$

This recovers the known curvature-induced scalar-charge mechanism [134]. Its relation to the common-weight branch is $\lambda_3 = -\bar{\alpha}_3\gamma = -2\bar{\alpha}_3 a_{\mathrm{m}}$, where $f_3(0) = \bar{\alpha}_3$, $\gamma = -\partial_\varphi \log B_\gamma|_0$, and $a_{\mathrm{m}} = \partial_\varphi \log A|_0$. These signed relations require matched common weights and constant elementary Jordan masses; they are not general consequences of Gibbs invariance.

For the specified curvature interaction, metric variation gives an explicit covariant cross stress; on the Ricci-flat background its leading form is

$$T^{\mathrm{int}}_{ab} = -8\lambda_3 R^{\mathrm{K}}_{acbd}\nabla^c\nabla^d\varphi_1.$$

Its divergence cancels the scalar stress exchange on the sourced scalar equation. The full expression, the nonvacuum terms, and the scalar–metric differential coupling are given in the Kerr companion. The charge formula applies to

the massless response; a positive scalar mass changes the asymptotics. These calculations determine a conditional exterior field response and its source. On their own they do not evaluate a tensor resonance shift or a disk luminosity. The separate coupled spectral matching in the Kerr companion supplies leading tensor coefficients only under its additional massless vacuum conditions.

With geometrical mass $\mathcal{M} = G_N M$, the dimensionless backreaction scale is $\lambda_3^2/(M_{\mathrm{P}}^2\mathcal{M}^4)$. One universal dimensionful λ_3 therefore produces different dimensionless strengths for different source masses. The mass, canonical normalization, curvature coefficient, and physical matter coupling must all be fixed before a shared-parameter observational comparison.

The unaltered tree-level Cartan potential imposes a further restriction: with $|\bar{\alpha}_3|/M_{\mathrm{P}}^2 = \ell^2/8$ and $m_\varphi^2\ell^2 \geq 6\alpha_\varphi$,

$$\frac{\lambda_3^2}{M_{\mathrm{P}}^2\mathcal{M}^4} \leq \frac{(m_\varphi\mathcal{M})^2}{192}\left(\frac{\ell}{\mathcal{M}}\right)^6.$$

Thus a light scalar and a controlled curvature expansion suppress this particular branch's tensor backreaction. An exactly massless scalar with these unaltered coefficients has zero coupling. The nonzero massless charge calculation is a reference for other matched branches, not an additional prediction obtained by discarding that constraint.

15.15. *Logical status.* The finite-regulator Gibbs and relative-entropy identities hold under the stated analytic hypotheses. The block elimination, perturbation-order calculation, metric-variation convention, and rank identity above are finite mathematical results. Classical mechanics and the geometric, gauge, and fluid branches require their stated projections, generator matching, scalings, and boundary conditions. In particular, finite Galerkin energy balance alone is not a proof of a thermodynamic entropy-production formula; the invariant measure and projected generator must also be matched.

The solved massless zero-spin reference branch further supplies the first exterior metric backreaction and a circular-orbit binding diagnostic. At fixed ADM mass, its minimally coupled fractional efficiency coefficient is $D_{\mathrm{geo}} = 0.420800563657\ldots$ per unit $\zeta = \lambda_3^2/(M_{\mathrm{P}}^2\mathcal{M}^4)$. With the stated Jordan matter projection, a separate term $-2.64578589957\ldots\, a_{\mathrm{m}}\lambda_3/\mathcal{M}^2$ appears in the fractional binding efficiency at the same retained level. The Schwarzschild and Kerr companion calculations give the derivation and normalization. This orbit-energy quantity is not the full radiation and instrument-dependent accretion response D, and the nonzero massless reference is unavailable in an unaltered potential that forces its coupling to vanish.

A single independently fixed physical parameter vector, the general massive tensor response, a closed accretion and radiation model, and their joint

independent observational validation have not been obtained by these identities. The Kerr companion now gives 60 source-attributed, normalized leading tensor coefficients for three fundamental modes, two parities and ten spins in a specified massless vacuum branch. They are inherited coupled spectral results, not newly solved tensor equations or uniquely selected physical constants.

A fixed conditional likelihood has also been evaluated on real GW150914 H1 and L1 strain, with off-source noise calibration. Its supplied coupling scenarios have negligible discrimination: the joint log likelihood contrast is about 1.22×10^{-4} even for the declared $\sqrt{|\alpha|} = 10\,\mathrm{km}$ scenario. Source and excitation priors remain inputs; this comparison is not a common-parameter validation of thermodynamics, fluids and gravity. The one-mode mass–spin–coupling degeneracy and the conditional two-mode rank calculation specify what additional information is needed. Neither a physical $\bar{\kappa}_*$ nor a radiative D is selected by these calculations. The continuum and quantum limits remain separate problems.

15.16. *Invariant-measure claims: existence, uniqueness, and convergence.* The word "equilibrium" is used only after three logically separate questions have been answered. For a regulated Markov generator $\mathcal{L}_N$ on a state space $\mathcal{X}_N$, existence means that at least one probability π_N satisfies

$$P_t^{N,*}\pi_N = \pi_N \quad (t \geq 0), \qquad \text{equivalently} \qquad \int_{\mathcal{X}_N} \mathcal{L}_N f \,\mathrm{d}\pi_N = 0$$

for every function in the generator domain. Uniqueness means that no other probability has this property. Convergence means that $P_t^{N,*}\nu$ tends to that particular π_N in a declared topology for the stated class of initial laws ν. Existence alone implies neither uniqueness nor convergence, and uniqueness alone does not supply convergence or a rate.

For a reversible gradient branch, the calculation is explicit. If

$$\mathcal{L}_N f = \theta_N \pi_N^{-1} \nabla \cdot \big(\pi_N M_N \nabla f\big),$$
$$\pi_N(\mathrm{d}x) = Z_N^{-1} e^{-S_N(x)/\theta_N} m_N(x)\,\mathrm{d}x, \quad Z_N < \infty.$$

then integration by parts and the declared zero-flux or reflecting boundary condition give

$$\int \mathcal{L}_N f \,\mathrm{d}\pi_N = \theta_N \int_{\partial \mathcal{X}_N} \pi_N M_N \nabla f \cdot n \,\mathrm{d}\sigma = 0.$$

This proves invariance, but not uniqueness. Uniqueness requires, for example, strong Feller regularisation together with topological irreducibility, or a separately verified Harris or contraction theorem. Likewise, a quantitative convergence statement requires a mixing estimate. For instance, a Poincaré

inequality

$$\operatorname{Var}_{\pi_N}(f) \le C_{P,N} \int (\nabla f)^T M_N \nabla f \, \mathrm{d}\pi_N$$

combined with the symmetric generator yields

$$\operatorname{Var}_{\pi_N}(P_t^N f) \le e^{-2\theta_N t / C_{P,N}} \operatorname{Var}_{\pi_N}(f),$$

with the rate changed according to the normalization of $\mathcal{L}_N$. An invariant density, a free-energy minimizer, or a positive diffusion coefficient alone does not supply either of the latter two conclusions.

For a nonreversible nonequilibrium stationary state, the same existence and uniqueness questions remain, but the stationary current need not vanish and the invariant law need not have Gibbs form. Thus path-space irreversibility and stationarity must not be identified with failure of existence or with nonuniqueness. In the finite Galerkin branch, a coercive Lyapunov estimate and the Feller property give existence by tight occupation measures; uniqueness and convergence are conditional on the stated irreducibility, smoothing, or weak-Harris hypotheses. In the Schwarzschild one-dimensional reflected diffusion, normalisability, ellipticity, reflection, and irreducibility give the unique reversible law, while a Poincaré estimate supplies exponential relaxation. In the bounded reflected Kerr mass–spin model, the weighted Poincaré estimate gives the positive spectral gap and hence uniqueness and L^2 relaxation for that regulated label process. These are theorems for the declared generators; they are not global uniqueness theorems for the continuum spacetime, arbitrary turbulent flow, or quantum theory.

Accordingly, every claim of "equilibrium" in this programme is tagged as one of the following: (E) existence of an invariant probability, (U) uniqueness for the fixed generator and boundary data, or (C) convergence in a specified metric. A physical interpretation as thermodynamic equilibrium requires all relevant tags and the declared energy, temperature, parity, and time calibration. This bookkeeping prevents a finite-regulator identity or a numerical attractor from being promoted silently to a universal theorem.

Conditional closure theorem and proof. The following implication is used whenever a branch is labelled "conditional." Assume (A1) that the fixed-regulator martingale problem is well posed and its Markov semigroup P_t^N is Feller; (A2) that a nonnegative Lyapunov function V_N has compact sublevel sets and satisfies

$$\mathcal{L}_N V_N \le -c_N V_N + C_N, \qquad c_N > 0;$$

(A3) that either strong Feller regularisation and topological irreducibility hold, or a stated Harris/weak-Harris contraction holds; and (A4), for a quantitative rate, that the displayed Poincare inequality or the corresponding Harris/hypocoercive estimate holds. Then the fixed-regulator process has an invariant probability;

it is unique under (A3), and it converges to that law in the metric specified by (A4).

Indeed, Dynkin's formula and Gronwall's inequality give

$$\mathbb{E}_x V_N(X_t) \le e^{-c_N t} V_N(x) + \frac{C_N}{c_N}(1 - e^{-c_N t}).$$

Averaging this estimate over $0 \le t \le T$ gives a T-independent bound on the mass of the occupation measure outside each compact sublevel set. The occupation measures are therefore tight. Every weak limit of a Krylov–Bogoliubov subsequence is invariant because the Feller property allows $P_t^N f$ to pass to the limit for bounded continuous f. This proves existence.

If two invariant probabilities existed, the strong Feller and irreducibility assumptions in (A3) would make the semigroup positivity improving; the standard Doob argument then gives equality of the two measures. In the alternative Harris route, the contraction estimate applied to both invariant measures gives a zero distance and hence equality. This proves uniqueness without using a free-energy minimum as a substitute for mixing.

Finally, in the symmetric gradient case, set $u_t = P_t^N f - \int f \, d\pi_N$. Integration by parts gives

$$\frac{d}{dt}\|u_t\|^2_{L^2(\pi_N)} = -2\theta_N \int (\nabla u_t)^T M_N \nabla u_t \, d\pi_N.$$

Applying (A4) and Gronwall yields

$$\|u_t\|^2_{L^2(\pi_N)} \le e^{-2\theta_N t / C_{P,N}} \|u_0\|^2_{L^2(\pi_N)}.$$

The nonsymmetric case uses the declared Harris or hypocoercive estimate in the same final step. Thus the proof establishes exactly the conditional existence, uniqueness, and convergence claim and no stronger continuum statement.

15.17. *Primitive data, derived consequences, and testable predictions.* The word "unified" is used here in a precise logical sense. The model has primitive data, mathematical consequences conditional on those data, and predictions that can be compared with observations. These three classes must not be conflated. In particular, a stationary law for a prescribed generator does not select the generator, and a numerical solution of one sector does not constitute an independent test of another sector.

15.18. *Primitive data of a realization.* A finite realization is specified by the tuple

$$\mathfrak{D}_r = \big(\mathfrak{X}_r, \mathbb{A}_r, \mathbf{h}_r, S_r, M_r, c_r, \theta_r, \nu_r, \mathcal{B}_r, \Pi_r, \mathcal{C}_r\big). \tag{1119}$$

Here $\mathfrak{X}_r$ is the regulated configuration space, $\mathbb{A}_r$ is the master connection, $\mathbf{h}_r$ is the invariant pairing including its dimensional scales, S_r is the energy-normalized master functional, and M_r is the mobility. The symbols c_r, θ_r,

and ν_r denote respectively the maintained circulation, fluctuation scale, and reference measure. $\mathcal{B}_r$ contains the boundary and constraint realization, Π_r contains the declared physical projections, and $\mathcal{C}_r$ contains the physical clock and unit calibration. A parameter is primitive if its value is fixed in this tuple or by an independently justified calibration rule; it is not made a consequence merely by placing it inside one displayed integral.

The parameter-to-law map has a genuine normalization orbit. For $a > 0$,

$$(S_r, \theta_r, M_r, c_r) \mapsto (aS_r, a\theta_r, M_r/a, c_r) \tag{1120}$$

leaves both the drift and covariance of the regulated diffusion unchanged. Consequently, Gibbs invariance, HJB well-posedness, and stochastic symmetry identities cannot determine this normalization without an independent energy, temperature, and clock calibration. The same conclusion applies to relative positive weights on independent invariant factors unless an additional selection principle or an independent observation removes that freedom.

15.19. *Consequences conditional on the primitive data.* Once $\mathfrak{D}_r$ and the admissibility hypotheses are fixed, the following are mathematical consequences rather than additional inputs:

$$dX_t = \big[-M_r \nabla S_r + \theta_r \operatorname{div} M_r + c_r\big](X_t)\, dt + \sqrt{2\theta_r M_r(X_t)}\, dW_t, \tag{1121}$$

$$L_r f = \big[-M_r \nabla S_r + \theta_r \operatorname{div} M_r + c_r\big] \cdot \nabla f + \theta_r M_r : D^2 f, \tag{1122}$$

$$\pi_r(dx) = Z_r^{-1} e^{-S_r(x)/\theta_r}\, \nu_r(dx), \tag{1123}$$

provided $Z_r < \infty$, the generator domain is well defined, and the boundary conditions preserve the stated reference law. If $\operatorname{div}_{\nu_r}(\pi_r c_r) = 0$, then the relative free energy obeys

$$\frac{d}{dt} \operatorname{KL}(p_t \| \pi_r) = -\theta_r \int p_t \, \|\nabla \log(p_t/\pi_r)\|_{M_r}^2 \, d\nu_r \le 0. \tag{1124}$$

This is an ensemble statement. Uniqueness of π_r and convergence from all admissible initial laws require separate irreducibility, coercivity, spectral-gap, Harris, or hypocoercivity hypotheses.

The same distinction applies to the effective sectors. A projected equation is derived from the mother generator only when the declared projection obeys, for every test function in its domain,

$$L_r(f \circ \Pi_r) = (L_{\mathrm{eff},r} f) \circ \Pi_r + \varepsilon_{r,f}, \qquad \|\varepsilon_{r,f}\| \le \delta_r(f). \tag{1125}$$

The term $\delta_r(f)$ is part of the result. Without this generator intertwining, a familiar effective equation is a separately supplied model.

The finite odd-parity zero-spin massive axial coefficients reported in the Kerr companion are consequences of a specified curvature–scalar action, boundary realization, perturbative order, and numerical discretization. They are not

consequences of the abstract stochastic architecture alone. Their logical form is

$$M\Delta\omega_j = \frac{K_{\mathrm{curv}}}{M^4} C_j^{\mathrm{ax}}(m_\varphi M) + \mathcal{R}_j, \qquad j = 2, 3, \tag{1126}$$

with the displayed remainder and numerical refinement diagnostics stated in the companion calculation.

15.20. *Predictions and independent tests.* A prediction is a quantity computed after the relevant parameters, nuisance model, source model, and observation map have been frozen without using the target datum. The current finite results have the following status.

Object	Status already established	Status not established
Finite generator and Gibbs branch	Invariance, free-energy identity, and specified conditional convergence results under their hypotheses	A universal continuum invariant law or a unique law for every field sector
Coupling selection	A normalization no-go result and a conditional selector theorem on $\Theta/\sim$	A mother-derived numerical value of the physical coupling
Massive tensor response	Eight checked odd-parity coefficients at zero spin	The complete nonzero-spin massive Kerr tensor, polar–scalar, and constraint blocks
Cross-sector propagation	Frozen synthetic force–frequency propagation for one supplied parameter vector	A real multi-sector test with independently calibrated parameters
Public rotating archive	Integrity, parity, and branch-comparability checks	Same-action, same-spin empirical agreement or observational confirmation

The unique-coupling problem is therefore reduced to a definite mathematical requirement. Let $\Theta/\sim$ be the physical quotient and let F_{sel} be derived from $\mathfrak{D}_r$, rather than inserted to reproduce a preferred number. If F_{sel} is proper, lower semicontinuous, coercive on the quotient, and strictly convex on its effective domain (or has a separately proved positive gap), then it has one minimizing equivalence class. This proves conditional uniqueness. It does not prove that the present mother data already contain such a selector.

The complete Kerr calculation has an equally definite closure criterion. One must specify all same-order curvature operators, the massive scalar and matter couplings, gauge and constraint conditions, horizon and asymptotic boundary data, and then solve the coupled background and perturbation Hessian. Only after the resulting nonzero-spin operator has a controlled simple resonance can $C_{\ell m}(a/M)$ be called a full Kerr prediction. The zero-spin axial calculation satisfies a strict subset of this criterion.

Finally, a real independent test requires a calibration set, a frozen parameter and nuisance vector, a disjoint target set, and a prespecified likelihood or error statistic. Public data availability alone does not meet this condition. The existing GWOSC calculation is a real-data conditional comparison on a massless reference branch with negligible discrimination; it is not a validation of the massive mother theory. The synthetic force– frequency inversion is an internal arithmetic check and is labelled as such.

15.21. *Logical closure statement.* The strongest statement justified by the present construction is therefore

$$\begin{gathered}\mathfrak{D}_r + \text{matching hypotheses} \Longrightarrow \text{finite regulated consequences} \\ \text{and frozen conditional predictions,}\end{gathered} \tag{1127}$$

whereas

$$\begin{gathered}\text{unique physical coupling} \quad + \quad \text{full massive Kerr response} \\ + \text{ independent physical validation}\end{gathered} \tag{1128}$$

requires, respectively, a derived selector, the complete rotating Hessian calculation, and a genuine calibration–holdout data analysis. Keeping these implications separate is part of the theory's mathematical content: it prevents an internal consistency check from being counted twice as an empirical test.

15.22. *An explicit structural-selection extension.* The normalization obstruction in Eq. (1120) has a precise consequence: the original mother data do not select an absolute physical coupling. We therefore introduce the following extension as a new physical postulate. It is stated separately from the original model so that a conditional result cannot be mistaken for a derivation from the unextended stochastic law.

15.23. *The quotient and the calibrated physical scale.* Let Θ denote the finite-dimensional parameter space of a regulated realization. The equivalence relation $\sim$ removes changes of field coordinates, gauge representatives, and other descriptions that leave every declared observable and the regulated path law unchanged. The quotient is written $\bar{\Theta} = \Theta/\!\sim$. The normalization orbit (1120) is not silently removed: it is removed only after the model declares a

physical energy, temperature, and clock calibration

$$E = E_{\mathrm{clk}}, \qquad \theta = \theta_{\mathrm{clk}}, \qquad t = t_{\mathrm{clk}}, \tag{1129}$$

where the three standards are fixed before any target observation is used. Equation (1129) is part of the extension's physical content; it is not a consequence of Gibbs invariance or of an HJB equation. Without it, the normalization orbit remains a genuine non-identifiability and no absolute coupling can be selected.

15.24. *Dimensionless structural residuals.* For each regulator r, choose a finite, declared probe family $\{f_{r,k}\}_{k=1}^{K_r}$ in the common generator domain. All probes, constraints, and boundary functionals are fixed before data are inspected. After division by the scales in Eq. (1129), define the following dimensionless residuals for $\bar{\vartheta} \in \bar{\Theta}$:

$$R^{r,k}_{\mathrm{int}}(\bar{\vartheta}) = L_r(f_{r,k} \circ \Pi_r) - \big(L_{\mathrm{eff},r}(\bar{\vartheta}) f_{r,k}\big) \circ \Pi_r, \tag{1130}$$

$$R^{r}_{\mathrm{con}}(\bar{\vartheta}) = \big(DC_r\, b_r(\bar{\vartheta}) + \tfrac{1}{2} Q_r : D^2 C_r,\ DC_r\, \sigma_r\big), \tag{1131}$$

$$R^{r}_{\mathrm{bd}}(\bar{\vartheta}) = \mathcal{F}_{\partial \mathfrak{X}_r}[J_r], \qquad (J_r)^i = \pi_r b_r^i - \tfrac{1}{2}\partial_j(\pi_r Q_r^{ij}), \tag{1132}$$

$$R^{r,s}_{\mathrm{reg}}(\bar{\vartheta}) = \mathcal{T}_{r\to s}\mathcal{O}_r(\bar{\vartheta}) - \mathcal{O}_s(\bar{\vartheta}). \tag{1133}$$

Here C_r is the declared constraint map, b_r is the Itô drift, $Q_r = \sigma_r \sigma_r^{\top}$, and π_r is the coordinate density. The two constraint residuals are evaluated on $C_r^{-1}(0)$; they are the drift and martingale terms in Itô's formula for $C_r(X_t)$. Omitting the Hessian term or noise tangency does not ensure constraint preservation. In a reflecting realization, the boundary condition is zero normal total probability current, including diffusion. Finally, $\mathcal{F}_{\partial \mathfrak{X}_r}$ is the boundary flux functional. $\mathcal{T}_{r\to s}$ is the prescribed matching map between two regulators, and $\mathcal{O}_r$ is an off-shell structural observable, not a datum from the calibration or test set. The matching maps and probe norms are part of the model specification. They may not be adjusted after a target datum is seen.

Let $\widehat{R}_\alpha$ denote the residuals in Eqs. (1130)–(1133) after canonical variance normalization with the primitive reference measure. The proposed selector is

$$F_{\mathrm{sel}}(\bar{\vartheta}) = \frac{1}{2}\sum_{\alpha \in \mathcal{I}} \|\widehat{R}_\alpha(\bar{\vartheta})\|_\alpha^2, \qquad \bar{\vartheta}_* = \operatorname*{arg\,min}_{\bar{\vartheta}\in\bar{\Theta}} F_{\mathrm{sel}}(\bar{\vartheta}). \tag{1134}$$

The index set $\mathcal{I}$, the probe family, the normalization, and the norms are fixed before calibration. Equal weighting in the dimensionless residual space is a declared minimal-structural-mismatch convention. It is therefore a physical axiom of the extension, not a theorem and not a hidden fit.

Assumption 84 (Structural-selection axiom). *The physical coupling is the equivalence class $\bar{\vartheta}_*$ in Eq.* (1134)*, provided the minimizer exists. The selector uses only the mother generator, constraints, boundary realization, regulator maps, and the calibrated units in Eq.* (1129)*; it uses no target observation. If*

the minimizer is not unique, the extended theory is declared under-specified rather than choosing one member by convention.

15.25. *What the axiom proves, and what it does not prove.*

THEOREM 85 (Conditional existence and uniqueness). *Assume that* $\bar{\Theta}$ *is a complete finite-dimensional metric space,* F_{sel} *is lower semicontinuous and proper, and every sublevel set* $\{F_{\mathrm{sel}} \le q\}$ *is compact. Then* $\arg\min F_{\mathrm{sel}}$ *is nonempty. If, in addition,* F_{sel} *is geodesically* μ*-strongly convex for some* $\mu > 0$ *on* $\bar{\Theta}$*, and every two admissible points are joined by a geodesic lying in this domain, then the minimizer is unique.*

Proof. Choose a minimizing sequence. Compactness of a sublevel set gives a convergent subsequence, and lower semicontinuity gives attainment of the infimum. If two distinct minimizers existed, strong convexity along a geodesic joining them would give a strictly smaller value at its midpoint, which is a contradiction. □

There is also a local certificate that can be checked without using observations. Suppose the residual map $\widehat{R} : \bar{\Theta} \to \mathcal{H}$ is C^2 into a finite-dimensional inner-product space and $\widehat{R}(\bar{\vartheta}_*) = 0$. At that point,

$$D^2 F_{\mathrm{sel}}(\bar{\vartheta}_*)[v, v] = \|D\widehat{R}(\bar{\vartheta}_*)v\|^2_{\mathcal{H}}. \tag{1135}$$

Consequently, a full-column-rank Jacobian gives a strict local minimum. A global uniqueness claim still requires strong convexity or a separately certified positive gap away from that minimum. A numerical optimizer, positive configuration Hessian, or one successful sector fit is not such a certificate.

The scale calibration and Assumption 84 remove the original normalization ambiguity only in the enlarged theory. They do not retroactively prove that the unextended mother model selected a coupling. The logically correct implication is therefore

$$\begin{aligned} &\text{mother data} + \text{explicit selection axiom} \\ &\quad + \text{verified convexity/gap} \Longrightarrow \text{unique conditional coupling.} \end{aligned} \tag{1136}$$

whereas the mother data alone imply only the no-go statement in Eq. (1120).

15.26. *A reproducible certification protocol.* For a claimed numerical selector, the following four quantities must be reported: (i) the complete list of probes and residual norms; (ii) the singular values of $D\widehat{R}(\bar{\vartheta}_*)$ on the quotient tangent space; (iii) a lower bound for the smallest constrained Hessian eigenvalue; and (iv) a regulator-refinement bound for $|F^{(r)}_{\mathrm{sel}} - F^{(s)}_{\mathrm{sel}}|$. The same frozen $\bar{\vartheta}_*$ is then propagated to observables. If any of these four certificates is absent, the result is a conditional construction and must not be reported as an unconditional physical determination.

15.27. *Selection after solving the nuisance field equations.* A consistency condition tests whether a proposed field solves its equations. A selection condition must also distinguish physical parameter values after the fields have been solved. These are different questions. Let ξ denote coordinates on a smooth gauge-fixed chart of the admissible parameter quotient, and let Y collect the background fields, projected states and boundary data that are solved for at a given ξ.

PROPOSITION 86 (Vanishing profiled residuals do not select a coupling). *Suppose $R(\xi, Y)$ is C^2 into a finite-dimensional inner-product space and a C^2 solution family $Y(\xi)$ satisfies $R(\xi, Y(\xi)) = 0$ on an open parameter set U. Then*

$$F_{\mathrm{prof}}(\xi) = \tfrac{1}{2}\|R(\xi, Y(\xi))\|^2 = 0, \qquad DF_{\mathrm{prof}} = 0, \qquad D^2F_{\mathrm{prof}} = 0 \quad \text{on } U.$$

Neither strict convexity nor an isolated selected parameter follows from these residuals. In particular, full rank of $\partial_\xi R$ while holding Y fixed is not a rank certificate for the profiled problem.

Proof. The composite residual is identically zero, so the asserted derivatives vanish. The chain rule gives

$$J_{\mathrm{prof}} = \partial_\xi R + \partial_Y R\, D_\xi Y = 0.$$

At zero residual, differentiating its squared norm gives $D^2F_{\mathrm{prof}} = J_{\mathrm{prof}}^\top J_{\mathrm{prof}} = 0$. As an explicit example, $R(\xi, Y) = Y - \xi$, $Y(\xi) = \xi$ has $\partial_\xi R = -1$ but $J_{\mathrm{prof}} = 0$. □

There is a useful form when the fields are obtained by a local least-squares solve rather than an exact prescribed family. Let J_Y be full column rank after removing its gauge kernel. At a zero residual, elimination of the field variation gives the reduced quadratic form

$$H_{\mathrm{prof}} = J_\xi^\top (I - P_Y) J_\xi, \qquad P_Y = J_Y (J_Y^\top J_Y)^{-1} J_Y^\top. \tag{1137}$$

Indeed, minimizing $\|J_\xi v + J_Y w\|^2$ over w gives $w = -(J_Y^\top J_Y)^{-1} J_Y^\top J_\xi v$ and the value $v^\top H_{\mathrm{prof}} v$. If an exact field family absorbs a parameter variation, then $J_\xi v$ lies in $\operatorname{Ran} J_Y$ and the reduced curvature in that direction is zero. Equation (1137) is local; it does not prove global uniqueness and assumes an interior smooth chart with the stated rank.

Thus the conditional selector theorem applies only to residuals or an additional physical functional that remain parameter-sensitive after field elimination. An independently specified off-shell mother matching condition could supply such information, but its reduced rank and global selection property must be established. Equations solved separately for each coupling do not do so. A new selection postulate is legitimate if stated explicitly; its physical objective and

weights require independent justification. Choosing a quadratic penalty centred at a desired coupling would prescribe that coupling rather than derive it.

All global strong-convexity statements here require a geodesically convex admissible domain, or an ordinary convex coordinate domain with its stated metric. Completeness alone does not supply a joining geodesic. Existence uses properness, lower semicontinuity and compact sublevels, with a finite lower bound or an equivalent exclusion of descent to $-\infty$; for the nonnegative squared-residual score the lower bound is automatic. Coercivity must mean compact sublevels, or be combined with a proper metric/finite-dimensional closed-domain assumption that ensures them. A positive global gap on a continuous parameter space can be asserted outside a fixed neighbourhood of an isolated minimizer, not between the minimizer and every arbitrarily close point.

The parameter-freezing operation used in a statistical analysis remains distinct from this selection theorem. Freezing an input or a posterior mixture prevents subsequent parameter adjustment; it does not change the source of that input or prove a unique physical coupling.

15.28. *Selection by information projection of a fixed mother path law.* A candidate field can satisfy its equations at many different couplings. To select among those couplings, the comparison must contain information that is held fixed while the candidate is varied. We now supply such a comparison at a finite regulator. It uses a specified mother path law, a specified physical projection, and calibrated units. It does not use a target observation or a penalty centred at a desired answer.

The change-of-measure identity is the standard Girsanov construction [79]; the hidden linear filter below uses the Kalman–Bucy covariance equation [104]. The physical interpretation is a new conditional principle: among a declared family of effective dynamics, use the member that loses the least information about the fixed projected mother dynamics. The resulting mathematical minimizer is derived below. Calling that minimizer a physical coupling additionally requires this principle and the coefficient-to-coupling map as physical hypotheses. The reference law itself cannot be changed when the candidate coupling changes.

15.28.1. *Path laws, covariance matching, and the new principle.* Let X be a stationary, finite-dimensional mother diffusion on a fixed probability space, and let $Y = \Pi(X)$ take values in $\mathbb{R}^n$. Fix the physical energy, temperature and clock units, the map Π, and the time-reversal parity of all coordinates. Suppose that, in its own filtration, the projected process has the semimartingale representation

$$dY_t = \beta_t\,dt + \sigma(Y_t)\,dW_t^Y, \qquad Q(y) = \sigma(y)\sigma(y)^\top > 0. \tag{1138}$$

The drift β_t may depend on the observed past. Thus this hypothesis does not assume that projection removes memory. Assume a stationary current law π_Y and a measurable function $\bar{\beta}$ such that

$$\mathbb{E}[\beta_t \mid Y_t] = \bar{\beta}(Y_t) \quad \text{for almost every } t. \tag{1139}$$

For a smooth projection of a stationary Itô diffusion, this identity follows from conditional expectation of $D\Pi\, b + \frac{1}{2} Q_X : D^2\Pi$, provided the projected covariance is the function $Q(Y)$ appearing in (1138) and the indicated semimartingale representation is valid.

Represent a gauge-fixed physical parameter chart by a nonempty closed convex set $K \subset \mathbb{R}^d$. Introduce nuisance drift coordinates $\eta \in \mathbb{R}^q$. They are coefficients of specified drift features, not an unrestricted family of background fields. The candidate dynamics are

$$dY_t = [b_0(Y_t) + \Phi(Y_t)\xi + \Psi(Y_t)\eta]dt + \sigma(Y_t)dW_t, \qquad \xi \in K. \tag{1140}$$

Here b_0, the $n \times d$ matrix Φ, and the $n \times q$ matrix Ψ are fixed before minimization. The initial law of every candidate is π_Y. Assume nonexplosion and well-posedness for the declared candidate laws. On each finite time interval assume the change of drift satisfies the Girsanov martingale and integrability conditions, so that the projected reference law $\mathbb{R}_T$ is absolutely continuous with respect to the candidate law $\mathbb{P}_{\xi,\eta,T}$ and has finite relative entropy. These analytic conditions are separate from parameter identifiability. The chart identifies distinct points with distinct declared physical equivalence classes. Global uniqueness on the entire admissible quotient requires that this chart cover that quotient; otherwise the conclusion is global only on the declared branch K.

The covariance in (1140) is the same as that in (1138). This is essential: for two different constant covariances, the sets of continuous paths with quadratic variation tQ_1 and tQ_2 are disjoint. Their diffusion path laws are mutually singular, and a drift-only relative-entropy formula cannot compare them.

ASSUMPTION 87 (Fixed-reference information projection). *The effective coefficients minimize*

$$F_T(\xi, \eta) = T^{-1} D(\mathbb{R}_T \| \mathbb{P}_{\xi,\eta,T}), \qquad T > 0,$$

over the declared family. The mother law, units, covariance, projection, features, nuisance family and coefficient-to-physical-coupling map are fixed independently of target data. If these primitive inputs still contain an unselected fundamental parameter, the minimization does not select that parameter without further information.

15.28.2. *Derivation and elimination of nuisance directions.* All expectations below use the reference law. Write $\delta_t = \beta_t - b_0(Y_t)$ and define

$$\begin{aligned} H &= \mathbb{E}_{\pi_Y}[\Phi^\top Q^{-1}\Phi], & B &= \mathbb{E}_{\pi_Y}[\Phi^\top Q^{-1}\Psi], \\ V &= \mathbb{E}_{\pi_Y}[\Psi^\top Q^{-1}\Psi], & h &= \mathbb{E}_{\pi_Y}[\Phi^\top Q^{-1}(\bar\beta - b_0)], \\ g &= \mathbb{E}_{\pi_Y}[\Psi^\top Q^{-1}(\bar\beta - b_0)]. \end{aligned} \tag{1141}$$

Assume these quantities and $c_T = (2T)^{-1}\mathbb{E}\int_0^T \delta_t^\top Q^{-1}\delta_t dt$ are finite. When $q > 0$, assume V is positive definite after redundant nuisance coordinates have been removed. When $q = 0$, all expressions involving Ψ, V, B, g are absent.

THEOREM 88 (Conditional unique effective coupling). *Under the preceding hypotheses, the relative-entropy score has the exact form*

$$F_T = c_T + \frac{1}{2}\xi^\top H\xi + \xi^\top B\eta + \frac{1}{2}\eta^\top V\eta - h^\top\xi - g^\top\eta. \tag{1142}$$

Eliminating the nuisance coordinates gives

$$\begin{aligned} \eta_*(\xi) &= V^{-1}(g - B^\top\xi), \\ F_T^{\mathrm{red}}(\xi) &= c_T - \tfrac{1}{2}g^\top V^{-1}g + \tfrac{1}{2}\xi^\top H_{\mathrm{red}}\xi - h_{\mathrm{red}}^\top\xi, \\ H_{\mathrm{red}} &= H - BV^{-1}B^\top, \qquad h_{\mathrm{red}} = h - BV^{-1}g. \end{aligned} \tag{1143}$$

If $H_{\mathrm{red}} \geq \lambda I$ for some $\lambda > 0$, this score has one and only one minimizer on K. It is independent of T. If $H_{\mathrm{red}}^{-1}h_{\mathrm{red}} \in K$, then

$$\xi_* = H_{\mathrm{red}}^{-1}h_{\mathrm{red}}. \tag{1144}$$

Otherwise it is the unique point satisfying $\langle H_{\mathrm{red}}\xi_* - h_{\mathrm{red}}, \xi - \xi_*\rangle \geq 0$ for every $\xi \in K$. A fixed physical map $k(\xi)$ then assigns the unique conditional coupling $k(\xi_*)$.

Proof. Let $u_t = \sigma(Y_t)^{-1}[\beta_t - b_0 - \Phi\xi - \Psi\eta]$; for a rectangular noise factor the same argument uses its minimum-norm right inverse. The assumed Girsanov identity and martingale integrability give

$$D(\mathbb{R}_T\|\mathbb{P}_{\xi,\eta,T}) = \frac{1}{2}\mathbb{E}\int_0^T |\beta_t - b_0 - \Phi\xi - \Psi\eta|^2_{Q^{-1}}dt.$$

The stochastic integral in the log likelihood has zero reference expectation. The identical initial laws give no initial entropy term. Expanding the square proves (1142); stationarity fixes the quadratic terms, and (1139) fixes the linear terms. The constant c_T may depend on T because the observed filter can retain memory, but it has no parameter dependence.

Differentiate with respect to η to obtain $V\eta + B^\top\xi - g = 0$. Positive definiteness of V gives the displayed nuisance minimizer. Substitution and completion of the square give (1143). Its Hessian is exactly H_{red}; there is no

parameter-dependent reference measure whose derivative was omitted. The inequality $H_{\mathrm{red}} \geq \lambda I$ gives

$$F_T^{\mathrm{red}}(\xi) \geq c_T - \tfrac{1}{2} g^\top V^{-1} g + \tfrac{\lambda}{2}|\xi|^2 - |h_{\mathrm{red}}|\,|\xi|.$$

Thus sublevel sets on the closed finite-dimensional set K are compact. A minimizing sequence converges along a subsequence and continuity gives attainment. Strict convexity on the convex domain gives uniqueness. Differentiation gives the variational inequality and, at an admissible unconstrained critical point, (1144). The T-dependent constant does not change this minimizer. □

The hypothesis on the reduced matrix has a concrete meaning. In the Hilbert space of drift features with norm $\|f\|^2 = \mathbb{E}_{\pi_Y} f^\top Q^{-1} f$,

$$v^\top H_{\mathrm{red}} v = \inf_{w \in \mathbb{R}^q} \|\Phi v + \Psi w\|^2. \tag{1145}$$

Indeed, expanding this norm and minimizing gives $w = -V^{-1} B^\top v$. Hence positive reduced rank means that no nonzero physical parameter direction can be absorbed by the declared nuisance drifts. Full rank before this elimination is insufficient.

If the quotient needs finitely many disjoint branch charts K_j, use the same reference law and time interval in every score. Suppose each branch satisfies the theorem and has minimum score m_j. If one branch j_* has $m_j - m_{j_*} \geq \delta > 0$ for every $j \neq j_*$, the minimizer on their union is unique: every other branch has strictly larger score, and the selected branch has a unique minimizer. The positive gap is an extra comparison of branch minima, not a gap to arbitrarily nearby points in a continuous chart. Branch-dependent constants in the entropy score must be retained in this comparison. Without this coverage or strict branch comparison, chart uniqueness is not quotient uniqueness.

15.28.3. *Stability of the selected coefficients under refinement.* The information projection also supplies an error estimate. Suppose $H_r \geq \lambda I$ and $H \geq \lambda I$ are reduced matrices on the same closed convex K, with linear coefficients h_r, h and minimizers ξ_r, ξ_*. The two variational inequalities imply

$$|\xi_r - \xi_*| \leq \frac{\|H_r - H\|\,|\xi_*| + |h_r - h|}{\lambda}. \tag{1146}$$

To prove it, use ξ_* as a comparison in the first inequality and ξ_r in the second. Subtracting gives $\lambda|\xi_r - \xi_*|^2 \leq |(H_r - H)\xi_* - (h_r - h)|\,|\xi_r - \xi_*|$. Cancel the nonzero distance; the zero case is immediate. Uniform reduced rank and convergent reference Gram integrals therefore imply convergence of the conditional selector. They do not establish removal of a physical field regulator unless those integrals and their physical matching also converge.

15.28.4. *A finite mother model with an explicit nonzero selected drift.* Consider the dimensionless, fully specified example

$$dX = -AX\,dt + \sqrt{2}\,dW, \qquad A = \begin{pmatrix} 1 & 0.25 & 0.15 \\ -0.15 & 1.4 & 0.2 \\ 0.1 & -0.2 & 2 \end{pmatrix}, \qquad Y = (X_1, X_2). \tag{1147}$$

The symmetric part of A is positive definite, so every eigenvalue has positive real part. The unique Gaussian invariant covariance is

$$C_X = 2\int_0^\infty e^{-At}e^{-A^\top t}dt, \qquad AC_X + C_X A^\top = 2I.$$

Write $C = (C_X)_{YY}$, $a = A_{Y3}$ and $r = (C_X)_{3Y}C^{-1}$. Gaussian conditional expectation gives

$$\bar\beta(y) = -[A_{YY} + ar]y =: -B_* y.$$

The candidate damping matrix is $B_\xi = \left(\begin{smallmatrix} k_1 & g-\omega_c \\ g+\omega_c & k_2 \end{smallmatrix}\right)$. Take $K = \mathbb{R}^4$ and no nuisance coordinates. Every candidate is a nonexplosive linear diffusion on a finite time interval; it need not have an invariant law for the path comparison to be defined. The reference observation and its conditional hidden mean form an augmented linear filter with bounded deterministic coefficients on each such interval. Replacing the observation drift by $-B_\xi Y$ leaves this augmented system linear. Localization of the change-of-drift exponential therefore gives shifted laws with uniform finite-time second-moment bounds. Their probability of reaching a localization radius R is $O(R^{-2})$, so no mass is lost when the radius tends to infinity and the exponential has mean one. This proves the finite-time Girsanov martingale condition here; Gaussian second moments also give the required entropy integrability. Its four independent linear features and $Q_Y = 2I$ give a positive Gram matrix: a nonzero matrix difference D has $\mathbb{E}|DY|^2 = \operatorname{tr}(DCD^\top) > 0$ since $C > 0$. Thus the theorem uniquely selects B_*. The YY block of the covariance equation gives $B_*C + CB_*^\top = 2I$, which also proves stability of B_*.

This selection does not make the projected process Markovian. For the hidden coordinate, stationary filtering has variance P satisfying

$$0 = -2A_{33}P + 2 - \tfrac{1}{2}|a|^2P^2, \qquad P = \frac{2}{A_{33} + \sqrt{A_{33}^2 + |a|^2}}.$$

This follows from the scalar Kalman–Bucy covariance equation after observing $dY + A_{YY}Y dt = -aX_3 dt + \sqrt{2}dW_Y$; the hidden noise is independent of the observation noise. Conditioning on the full past leaves P, whereas conditioning on the current Y leaves $v_0 = (C_X)_{33} - (C_X)_{3Y}C^{-1}(C_X)_{Y3}$. The limiting minimum path entropy rate is

$$F_{\min} = \tfrac{1}{4}|a|^2(v_0 - P) \ge 0. \tag{1148}$$

It follows from the conditional variance of $\mathbb{E}[X_3 \mid Y_{(-\infty,t]}] - rY_t$ and the same Girsanov formula. The finite-time filter initialized from Y_0 converges to the positive stationary Riccati root; its transient contribution vanishes in the entropy rate. A nonzero minimum records unresolved memory rather than an exact generator intertwining.

Solving the covariance equation in exact rational arithmetic gives

$$B_* \simeq \begin{pmatrix} 0.991086457297 & 0.251978689569 \\ -0.161884723605 & 1.402638252758 \end{pmatrix}.$$

The selected coefficients are approximately

$$k_1 = 0.991086457297, \quad k_2 = 1.402638252758,$$
$$g = 0.045046982982, \quad \omega_c = -0.206931706587.$$

The four Gram eigenvalues are approximately 0.356056, 0.505232, 0.712284 and 1.010710; exact positive leading minors also establish its positive definiteness. If a nuisance feature duplicates the circulation feature, the reduced rank is three and that parameter is not selected. The memory floor in (1148) is $3.470142914 \times 10^{-5}$ per declared time unit. These are exact-formula finite-model quantities rounded for display, not physical measurements.

For any real s, the alternatives $B_s = B_* + sJC^{-1}$, $J = \left(\begin{smallmatrix} 0 & -1 \\ 1 & 0 \end{smallmatrix}\right)$, have exactly the same stationary covariance. Their excess path score is $\mathrm{tr}[(B_s - B_*)^\top (B_s - B_*)C]/4$, strictly positive for $s \neq 0$. This illustrates why a stationary density alone misses circulation information. All numbers in this example are mother-model inputs or derived effective drift coefficients. None is a determination of λ_3, m_φ or a universal physical coupling.

15.28.5. *What the conditional selection closes.* The result replaces an assumed convexity assertion by a derived quadratic functional and an explicit reduced-rank condition. It closes the selection problem for a specified projected reference law and a specified effective feature family. Applying it to the unified physical model requires its parameter-independent primitive reference, physical projection and coefficient map. If changing ξ also changes that reference, or if all physical features lie in the nuisance span, the theorem does not apply. Thus adding its conditions is mathematically sufficient, while verifying those conditions in the full physical branch remains a separate task.

15.29. *Reconstructing a mother realization and locating its uniqueness boundary.* The conditional selector in Section 15.28 compares effective models with a fixed mother law. A further question remains: which parts of that mother law are themselves determined? Three different mathematical problems occur. An initial-value problem concerns a solution for fixed coefficients. An invariant-measure problem concerns the long-time law of that fixed dynamics. A structural reconstruction problem concerns the coefficients, state space and

physical meaning of the dynamics. We now give a constructive finite-regulator result for the third problem, together with examples that identify its necessary qualifications.

Throughout this subsection, physical time and field coordinates have been calibrated. A change of clock or state coordinates is not used to identify two physically different candidates. The regulator, constraint reduction, state space, boundary condition and generator domain are fixed. The statements concern the finite-dimensional stochastic realization; they do not assert uniqueness of an unregularized field theory or of its gauge group and matter content.

15.29.1. *What the generator determines.* Let $\Omega \subset \mathbb{R}^d$ be a connected domain. Suppose the martingale problem is conservative and well posed for

$$Lf = b^i \partial_i f + \tfrac{1}{2} A^{ij} \partial_i \partial_j f, \qquad A = A^{\mathsf{T}} > 0. \tag{1149}$$

The coefficients are continuous, with enough local regularity for the derivatives below. Compactly supported smooth functions are available as interior test functions. A reflecting boundary, if present, has its domain specified separately. An assertion about the generator includes that domain, not only its differential expression.

Proposition 89 (Local coefficient reconstruction). *Knowledge of L on interior test functions determines b and A at every interior point. Together with the fixed well-posed boundary realization and initial law, these coefficients determine one path law. The factor σ in $A = \sigma\sigma^{\mathsf{T}}$ is not separately determined by the state path law.*

Proof. Fix an interior point and multiply the coordinate polynomials by a smooth cutoff that equals one in a neighborhood of that point. At that point the cutoff derivatives vanish, so the resulting generator values give

$$b^i = Lx_i, \qquad A^{ij} = L(x_i x_j) - x_i Lx_j - x_j Lx_i. \tag{1150}$$

These are pointwise formulas; globally unbounded coordinates need not be in the generator domain. If the coefficients extend continuously to a boundary, their boundary values follow by continuity, while the prescribed operator domain fixes how the process behaves there. Well-posedness of the martingale problem gives the path-law assertion. Replacing a square invertible σ by $\sigma O(x)$ with $O(x)$ orthogonal leaves A and the generator unchanged. It therefore leaves that state path law unchanged, although a specified coupling to an observed bath could carry additional information about the noise representation. □

Knowledge of every transition operator P_t on a common generator core determines L by the limit $(P_t f - f)/t$ as $t \downarrow 0$. A single observed trajectory does not give these expectations exactly. Statistical estimation and coverage of the

state space are additional tasks. Moreover, an interior differential expression without its boundary realization does not define the full transition semigroup.

15.29.2. *Energy, mobility and stationary current.* Fix a positive reference density $m(x)$, fluctuation energy $\theta > 0$ and a positive normalized invariant coordinate density $p(x)$. Suppose the mother realization has the Gibbs form

$$\begin{aligned} &p = Z^{-1} m \exp(-S/\theta), \\ &b = -M\nabla S + \theta m^{-1}\partial_j(mM^{ij}) + c, \qquad A = 2\theta M. \end{aligned} \tag{1151}$$

The vector $m^{-1}\partial_j(mM^{ij})$ is the reference-volume divergence of the mobility. Indices in this formula specify the ith component. This decomposition uses the usual diffusion probability current [137]; the reconstruction below keeps its physical inputs explicit.

THEOREM 90 (Conditional reconstruction of a Gibbs mother realization). *Under* (1151), *the fixed data* (L, p, m, θ) *determine*

$$M = \frac{A}{2\theta}, \qquad S = -\theta \log(p/m) + C, \qquad c^i = b^i - \frac{1}{2p}\partial_j(A^{ij}p). \tag{1152}$$

Thus the reduced energy is unique up to a configuration-independent constant, and the stationary probability current is uniquely $j = pc$. *Conversely, these formulas reproduce* L *and its invariant density whenever the assumed regularity and boundary conditions hold. If* L *has more than one positive invariant density, one must specify which* p *is used; the theorem does not prove invariant-measure uniqueness.*

Proof. The covariance identity gives M. Taking logarithms of the Gibbs formula gives the displayed S, with the normalizing constant absorbed in C. Substitution into the reversible part of the drift yields

$$\begin{aligned} -M^{ij}\partial_j S + \theta m^{-1}\partial_j(mM^{ij}) &= \theta M^{ij}\partial_j \log(p/m) + \theta\partial_j M^{ij} + \theta M^{ij}\partial_j \log m \\ &= \theta\partial_j M^{ij} + \theta M^{ij}\partial_j \log p = \frac{1}{2p}\partial_j(A^{ij}p). \end{aligned}$$

Subtracting this drift from b proves the formula for c. The stationary Fokker–Planck equation says $\partial_i[b^i p - \frac{1}{2}\partial_j(A^{ij}p)] = 0$, which is exactly $\nabla \cdot (pc) = 0$. The normal-current condition is inherited from the fixed boundary realization. These computations also prove the converse. □

This result reconstructs a specified reduced realization. It does not derive the physical inputs m, θ, the clock or the state space. If these are allowed to vary, the conclusion changes. For example, $(S, \theta, M) \mapsto (aS, a\theta, M/a)$ for $a > 0$ preserves the drift, covariance and Gibbs coordinate density when m and c are fixed. An independent physical energy or temperature calibration removes this orbit. The constant C in (1152) is a constant on configuration space. A

spacetime vacuum-energy contribution $\int \sqrt{-g}\, V_\Lambda \, d^4x$ depends on the metric configuration and is not such a constant. The reconstruction theorem therefore does not eliminate the gravitational vacuum-energy matching problem.

15.29.3. *Why a unique equilibrium cannot select the whole dynamics.* Consider the fully explicit two-dimensional family

$$\begin{aligned} dX_t &= B_{m,\omega} X_t \, dt + \sqrt{2m}\, dW_t, \qquad m > 0, \\ B_{m,\omega} &= -mI + \omega J, \qquad J = \begin{pmatrix} 0 & -1 \\ 1 & 0 \end{pmatrix}. \end{aligned} \tag{1153}$$

Here m is a scalar damping parameter and has no relation to the reference density $m(x)$ used above. The example uses reference density one and $\theta = 1$. Its energy is $S = |x|^2/2$, mobility mI, and circulation $c = \omega J x$. Since $x \cdot Jx = 0$ and $\operatorname{tr} J = 0$, $\nabla \cdot (c e^{-|x|^2/2}) = 0$. Every member has the same invariant law $N(0, I)$. It is the unique invariant law for each member: the explicit solution has mean $e^{Bt} X_0 \to 0$ and noise covariance $(1 - e^{-2mt})I \to I$, so its characteristic functions converge to those of $N(0, I)$ for every initial probability law. A second invariant law would remain constant under this evolution and must have the same limit.

Nevertheless the stationary ordered covariance is

$$C(t) := \mathbb{E}[X_t X_0^{\mathsf{T}}] = e^{-mt}\{\cos(\omega t) I + \sin(\omega t) J\}. \tag{1154}$$

It identifies $B = C'(0)$ if its full right derivative is known in the calibrated clock. In a general stationary nondegenerate linear model with covariance Q, the corresponding formulas are

$$B = C'(0) Q^{-1}, \qquad A = -(BQ + QB^{\mathsf{T}}). \tag{1155}$$

They follow from $C(t) = e^{Bt} Q$ and the stationary covariance equation. They recover coefficients from a dynamic law, not from the equilibrium density alone.

Proposition 91 (An exact sampling ambiguity). *Fix a sampling interval $\Delta > 0$ and stationary initial law $N(0, I)$. The processes* (1153) *with rotations ω and $\omega + 2\pi k/\Delta$, $k \in \mathbb{Z}$, have identical laws on every finite sample $(X_0, X_\Delta, \dots, X_{n\Delta})$. Their continuous-time laws differ when $k \neq 0$. Observing only X_t^1 cannot distinguish ω from $-\omega$, even with its entire stationary continuous-time law.*

Proof. The sampled Gaussian Markov transition has conditional mean $e^{B\Delta} x$ and covariance $(1 - e^{-2m\Delta})I$. Both are unchanged by the stated frequency shift; the same initial law then gives equality of every sampled joint law. The generators differ through their drift, so their full continuous-time transition families differ. For the single coordinate, its stationary process is centered

Gaussian with covariance $e^{-m|t-s|}\cos(\omega(t-s))$. This function is even in ω, and the covariance determines every finite-dimensional Gaussian law. □

A restriction to one unaliased frequency interval can remove the first ambiguity, but that restriction is an additional input. Ordered cross-channel measurements or adequately resolved lags supply information that the single-channel equilibrium record lacks.

15.29.4. *A constructive finite-dimensional rank condition.* For a declared physical chart, suppose a vector of generator probes has the exact affine form

$$r(\vartheta) = r_0 + D\vartheta, \qquad \vartheta \in K \subset \mathbb{R}^q. \tag{1156}$$

The probes may contain the local drift and covariance values in (1150). Units, gauge directions, boundary data, feature functions and nuisance treatment are fixed before constructing D. The probe values must come from primitive structural information or a declared observation model, rather than from the same equations solved separately for each candidate.

Proposition 92 (Unique compatible coefficients and a quantitative margin). *Define the minimum gain over all parameter directions by* $s_* := \inf_{|v|=1} |Dv|$. *If* $s_* > 0$, *at most one point in* K *can satisfy a prescribed compatibility equation* $r(\vartheta) = y$. *If* ϑ_* *satisfies it and another point obeys* $|r(\widehat{\vartheta}) - y| \le \eta$, *then*

$$|\widehat{\vartheta} - \vartheta_*| \le \eta / s_*. \tag{1157}$$

Conversely, if $Dv = 0$ *for* $v \neq 0$ *and* $\vartheta_* + sv \in K$ *for a nontrivial interval of* s, *that interval has exactly the same probe values. Uniqueness fails there.*

Proof. Subtract the two probe vectors and use $|D(\vartheta - \vartheta_*)| \ge s_*|\vartheta - \vartheta_*|$. The converse follows by direct substitution. Existence is not implied by the rank condition: the prescribed y must lie in $r_0 + D(K)$. □

All parameter directions are included in this definition. For a wide rectangular matrix, the smallest entry of a reduced singular-value list need not be its minimum gain. For example, $D = (1 \;\; 0)$ has the listed singular value one, whereas $D(0,1)^{\mathsf{T}} = 0$. Thus it has minimum gain zero and cannot identify the second parameter. Full column rank, rather than a positive reduced singular value, is required. When the minimum gain is positive, injectivity in the fixed parameter chart follows, independently of the number of probes.

This compatibility theorem adds no minimization postulate. It states exactly when already supplied structural information determines the coefficients within the declared affine family. A least-squares selector for incompatible probes is a different modeling step. A full-rank calculation in one chart also leaves other gauge groups, field contents, operator bases and disconnected charts to be compared separately.

For (1153), drift probes at the two fixed states e_1, e_2 have feature matrix

$$D = \begin{pmatrix} -1 & 0 \\ 0 & 1 \\ 0 & -1 \\ -1 & 0 \end{pmatrix}, \qquad D^{\mathsf{T}} D = 2I.$$

Thus m, ω are uniquely determined by those complete drift probes, with $s_* = \sqrt{2}$. The covariance $A = 2mI$ alone has no sensitivity to ω, and the invariant density has sensitivity to neither parameter. These are explicit, different ranks for different information sets.

15.29.5. *Uniqueness of coefficients in a fixed reduced action family.* The reconstruction can also be stated directly for the reduced energy obtained after the specified regulator and constraint reduction. Let

$$S_\vartheta(x) = S_0(x) + \sum_{j=1}^{q} \vartheta_j \mathcal{U}_j(x). \tag{1158}$$

Here the basis functions $\mathcal{U}_j \in C^1(\Omega)$, the mobility $M(x) > 0$, the circulation c, reference density, fluctuation energy and clock are fixed independently of ϑ. This S_ϑ is the regulated reduced energy in (1151); it is not a Lorentzian action reinterpreted as a positive energy without a specified reduction. Coordinates and coefficient units are nondimensionalized by fixed physical scales before taking the norms and eigenvalues below. Choose a fixed probability density $\varrho > 0$ almost everywhere on the connected open domain Ω, and assume the entries of

$$G_{ij} = \int_\Omega (\nabla \mathcal{U}_i)^{\mathsf{T}} M \nabla \mathcal{U}_j \, \varrho \, dx \tag{1159}$$

are finite. The density ϱ is a comparison weight, not an additional invariant-density assumption.

Proposition 93 (Identifiable reduced-action coefficients). *Suppose the basis is linearly independent modulo constants: a constant linear combination $\sum_j z_j \mathcal{U}_j$ on Ω implies $z = 0$. Then G is positive definite. Within the fixed family* (1158)*, identical drift fields imply identical coefficients. More quantitatively, with $\|h\|^2_{M^{-1},\varrho} := \int h^{\mathsf{T}} M^{-1} h \, \varrho dx$,*

$$|\widehat{\vartheta} - \vartheta_*| \le \frac{\|b_{\widehat{\vartheta}} - b_{\vartheta_*}\|_{M^{-1},\varrho}}{\sqrt{\lambda_{\min}(G)}}. \tag{1160}$$

This is an at-most-one statement; it does not imply that a prescribed target drift belongs to the family.

Proof. For $z \in \mathbb{R}^q$ put $F_z = \sum_j z_j \mathcal{U}_j$. Then $z^{\mathsf{T}} G z = \int (\nabla F_z)^{\mathsf{T}} M \nabla F_z \, \varrho dx \ge 0$. If this integral vanishes, positivity of M and ϱ gives $\nabla F_z = 0$ almost

everywhere. Continuity of ∇F_z makes it zero everywhere on Ω. Connectedness therefore makes F_z constant. Independence modulo constants gives $z = 0$, proving positive definiteness. Since the reference-volume drift and circulation are fixed, their differences cancel, and

$$b_{\widehat{\vartheta}} - b_{\vartheta_*} = -M\nabla F_{\widehat{\vartheta}-\vartheta_*}.$$

Consequently the squared norm in (1160) equals $(\widehat{\vartheta} - \vartheta_*)^{\mathsf{T}} G(\widehat{\vartheta} - \vartheta_*)$. The smallest-eigenvalue bound proves the estimate and uniqueness. □

For example, with one coordinate, $M = 1$, standard Gaussian comparison weight, $\mathcal{U}_1 = x^2/2$ and $\mathcal{U}_2 = x^4/4$, the second, fourth and sixth Gaussian moments are $1, 3, 15$. Hence

$$G = \begin{pmatrix} 1 & 3 \\ 3 & 15 \end{pmatrix}, \qquad \det G = 6, \qquad \lambda_{\min}(G) = 8 - \sqrt{58} > 0.$$

This is a direct coefficient-identification example. Taking $S_0 = 0$, reference density one and $\theta > 0$, the quartic energy has a normalizable Gibbs density when its leading quartic coefficient is positive; if that coefficient is zero, a positive quadratic coefficient is required. The Gram calculation alone does not establish admissibility of every parameter value.

The theorem holds within the chosen physical basis. It does not select that basis, a gauge group, a matter representation, or a boundary realization. Allowing the circulation to change would remove the cancellation used in the proof and requires a new identification argument. Different actions related by a total derivative, a constraint identity or a field redefinition must first be reduced to a declared equivalence class. Those equivalences cannot be removed merely by counting coefficients.

15.29.6. *Hidden extensions and the continuum question.* There is a further obstruction when the state space is not fixed. Let an observed Markov model X be any candidate, and let Z be an independent Ornstein–Uhlenbeck process in an additional coordinate. The product model (X, Z) with observation map $(x, z) \mapsto x$ gives exactly the same observed path law as X. If X is a reversible nondegenerate Gaussian diffusion with a strictly convex energy, both models can have these properties, including unique invariant probability measures. They still have different state spaces and different hidden energies. Integrating the independent Z law out of every cylinder probability proves the observational equality. No record of X alone can reconstruct that unobserved extension. A minimality or observability requirement, if used to exclude it, must be stated as a premise and its physical justification must be supplied.

At increasing regulators, the preceding singular-value margin must also be controlled. For aligned physical parameter coordinates, suppose $y = D\vartheta_*$,

$s_{\min}(D_N) \geq s_* > 0$ and $|D_N\vartheta_N - y_N| \leq \eta_N$. Then

$$|\vartheta_N - \vartheta_*| \leq \frac{\eta_N + |y_N - y| + \|D_N - D\|\,|\vartheta_*|}{s_*}. \tag{1161}$$

Indeed, apply the lower singular-value bound to $D_N(\vartheta_N - \vartheta_*)$ and add and subtract y_N, y. This proves convergence when the numerator tends to zero. It is a conditional coefficient-identification limit, not the construction of a continuum field measure: tightness, operator convergence, renormalization and physical matching still have their own hypotheses.

15.29.7. *Synthetic calculation and physical interpretation.* The numerical example fixes $m = 0.7$, $\omega = 0.8$ and $\Delta = 0.5$. The drift-probe inverse recovers both parameters with maximum absolute error 4.45×10^{-16}. The alias rotation is $\omega + 4\pi = 13.3663706144$. The largest operator difference between the two transition matrices over the first ten sampled lags is below 1.8×10^{-14}, while their difference at $\Delta/3$ is about 1.54132. These values evaluate the exact formulas above; they are not observed field data.

The right-derivative approximation

$$\widehat{B}_h = \frac{-3I + 4C(h) - C(2h)}{2h}, \qquad \widehat{A}_h = -(\widehat{B}_h + \widehat{B}_h^{\mathsf{T}})$$

has second-order truncation error because Taylor expansion cancels the constant and quadratic powers of h. The remaining leading derivative error is $-B^3h^2/3$. Table 10 gives the actual finite-step errors for the stated example.

h	Drift error	Covariance error
0.02	1.585e-04	2.620e-04
0.01	3.983e-05	6.612e-05
0.005	9.984e-06	1.661e-05
0.0025	2.499e-06	4.161e-06
0.00125	6.252e-07	1.042e-06

Table 10. Synthetic recovery from positive-time covariance values. Errors are matrix operator norms relative to the exact generator coefficients.

The resulting uniqueness claim is precise: the full calibrated generator determines a well-posed regulated path law, and the stated Gibbs data determine its mobility, reduced energy and stationary current. Finite structural probes determine compatible parameters when their physical sensitivity has full rank. Selecting the primitive action, field content, clock, energy scale and hidden-state interpretation from more basic physical principles remains

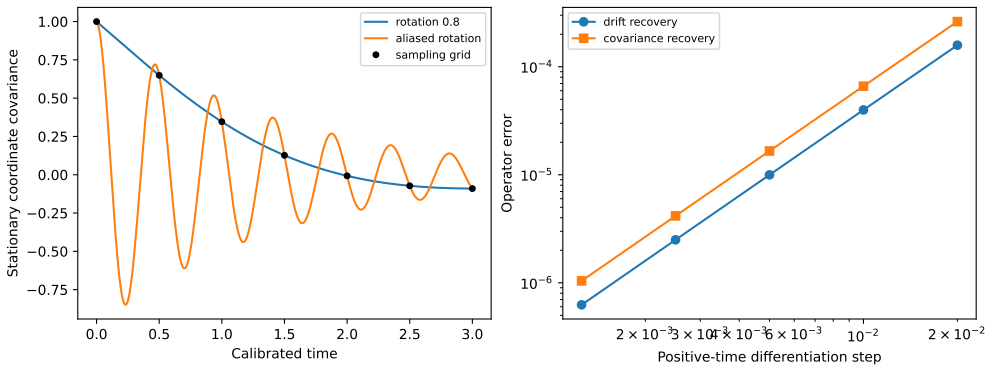


Figure 24. The same stationary sample law can hide different continuous-time mother generators. Left: the coordinate covariances agree on the indicated sampling grid. Right: resolving short positive lags recovers the known synthetic generator with second-order differentiation error.

a stronger problem. The reconstruction and the explicit ambiguities identify which additional information that problem must contain.

15.30. *Coefficient identification in a specified lattice mother realization.* An abstract reconstruction criterion becomes useful only after its independent operators and its observation requirements have been identified in a particular model. We now apply the criterion to a member of the bosonic lattice family in Section 7.6. The configuration includes all four declared group factors and four scalar sites. Its group, representations, lattice and clock are specified before identification. The result determines six coefficients in that realization; it does not select those primitive structures from competing field theories.

15.30.1. *The square plaquette and its independent coefficients.* Use one square with vertices $1, 2, 3, 4$, four distinct links, and cyclic scalar edges $\{1,2\},\{2,3\},\{3,4\},\{4,1\}$. Retain $K = SO(5) \times SU(3) \times SU(2) \times U(1)$ and the defining representations. Their dimensions and real-character variances are

$$d = (5,3,2,1)^{\mathsf{T}}, \qquad \zeta = (1, \tfrac{1}{2}, 1, \tfrac{1}{2})^{\mathsf{T}}, \qquad Z_\chi = \operatorname{diag}(\zeta). \tag{1162}$$

The metric on each group is fixed by normalizing its defining-character Casimir to one: $-\Delta_a \operatorname{Re}\chi_a = \operatorname{Re}\chi_a$. This is a choice of physical coefficient coordinates, not a group-selection argument. Each factor admits such a positive rescaling of its bi-invariant metric.

Let $U_{p,a}$ be the plaquette product in factor a and set $k_a = d_a - \operatorname{Re}\chi_a(U_{p,a})$. Fix the scalar center at zero, scalar mobility at one, and $|\alpha| \le 1/2$. Define six

gauge-invariant functions by

$$F_a(U,s) = e^{-\alpha s_1} k_a(U), \quad 1 \le a \le 4,$$

$$F_E(s) = \tfrac{1}{2} \sum_{\{i,j\}\ \text{cyclic}} (s_i - s_j)^2, \qquad F_M(s) = \tfrac{1}{2} \sum_{i=1}^{4} s_i^2. \tag{1163}$$

The action and its coefficient vector are

$$S_\vartheta = \sum_{a=1}^{4} \beta_a F_a + \kappa F_E + \nu F_M, \qquad \vartheta = (\beta_1, \beta_2, \beta_3, \beta_4, \kappa, \nu). \tag{1164}$$

For the positive coefficient region, this is exactly (467), with $f^2 = \kappa$ and $m^2 f^2 = \nu$. Theorem 19 consequently supplies nonexplosion and the unique invariant Gibbs probability for each fixed coefficient vector. The lattice geometry is fixed; dynamical coframe, Higgs and fermion coordinates are not added to that theorem.

Use the fixed comparison probability

$$\varrho(dU\, ds) = dU\, (2\pi)^{-2} e^{-|s|^2/2}\, d^4 s. \tag{1165}$$

This is product Haar probability and an independent standard Gaussian on the scalar coordinates. It is a weight for identification, not the unknown invariant law. Gradients below use the stated product metric. All weighted gradient moments are finite: group variables are compact, and Gaussian moments remain finite after multiplication by any fixed polynomial and linear exponential.

15.30.2. *Exact Haar and Gaussian calculation.* For a nontrivial irreducible unitary representation, Haar orthogonality gives $\int \chi_a = 0$ and $\int |\chi_a|^2 = 1$. The defining characters of $SO(5)$ and $SU(2)$ are real, whereas the $SU(3)$ and charge-one $U(1)$ representations are inequivalent to their conjugates. In the latter cases $\int \chi_a^2 = 0$, and $\int (\operatorname{Re} \chi_a)^2 = 1/2$. These facts give (1162). For clarity, the unit character norm follows by averaging matrix units in the irreducible representation: Haar invariance and Schur's lemma give $\int R_{ij} \overline{R_{kl}} = \delta_{ik}\delta_{jl}/d_a$; summing the diagonal entries gives $\int |\chi_a|^2 = 1$. The same orthogonality applied to inequivalent representations gives $\int \chi_a^2 = 0$ when R_a and its conjugate are inequivalent. For the defining $SU(3)$ representation this inequivalence is already seen from the distinct actions of its nonreal central elements; for $U(1)$ it is the difference between charges $+1$ and -1. Independence of group factors gives

$$\mathbb{E} k_a = d_a, \qquad \mathbb{E}(k_a k_b) = d_a d_b + \delta_{ab} \zeta_a. \tag{1166}$$

The product of four independent Haar links is Haar. By bi-invariance, differentiating with respect to any one link gives the same integrated gradient norm as differentiating the plaquette product. Integration by parts and the Casimir

normalization therefore yield

$$\mathbb{E}\langle \nabla_U k_a, \nabla_U k_b \rangle = 4\delta_{ab}\zeta_a. \tag{1167}$$

The factor four counts links. Gauge invariance does not remove it: these are derivatives along all link coordinates of the specified intrinsic generator, with a fixed product metric.

The scalar edge Laplacian is

$$L_\square = \begin{pmatrix} 2 & -1 & 0 & -1 \\ -1 & 2 & -1 & 0 \\ 0 & -1 & 2 & -1 \\ -1 & 0 & -1 & 2 \end{pmatrix}, \qquad \nabla F_E = L_\square s, \qquad \nabla F_M = s.$$

Its eigenvalues are $0, 2, 2, 4$, so $\operatorname{tr} L_\square = 8$ and $\operatorname{tr} L_\square^2 = 24$. Put $E_1 = e^{\alpha^2/2}$ and $E_2 = e^{2\alpha^2}$. Gaussian differentiation of $\mathbb{E}e^{ts_1} = e^{t^2/2}$ gives

$$\mathbb{E}e^{-\alpha s_1} = E_1, \quad \mathbb{E}[s_1 e^{-\alpha s_1}] = -\alpha E_1, \quad \mathbb{E}e^{-2\alpha s_1} = E_2.$$

Combining these identities gives the complete coefficient Gram matrix

$$G_\alpha = \begin{pmatrix} E_2[4Z_\chi + \alpha^2(dd^{\mathsf{T}} + Z_\chi)] & 2\alpha^2 E_1 d & \alpha^2 E_1 d \\ 2\alpha^2 E_1 d^{\mathsf{T}} & 24 & 8 \\ \alpha^2 E_1 d^{\mathsf{T}} & 8 & 4 \end{pmatrix}. \tag{1168}$$

For example, the first off-diagonal scalar block is

$$\mathbb{E}\langle \nabla_s F_a, \nabla_s F_E \rangle = -\alpha d_a \mathbb{E}[e^{-\alpha s_1}(2s_1 - s_2 - s_4)] = 2\alpha^2 E_1 d_a.$$

The Gaussian scalar variables have zero means and are independent; the mixed s_2, s_4 terms vanish. This calculation also fixes the sign of the group–scalar cross terms.

THEOREM 94 (A uniform coefficient margin for the square regulator). *For the fixed realization above and every $|\alpha| \le 1/2$,*

$$G_\alpha \succeq \frac{2}{25} I_6. \tag{1169}$$

Consequently identical full regulated generators imply identical coefficients in (1164)*. If their covariant first-order drift fields are b_ϑ, then*

$$|\widehat{\vartheta} - \vartheta_*| \le \frac{5}{\sqrt{2}} \| b_{\widehat{\vartheta}} - b_{\vartheta_*} \|_{L^2(\varrho)}. \tag{1170}$$

Here the diffusion, metric, clock, reference volume, scalar exponent and circulation are fixed. Local coordinate corrections from the metric volume cancel when the two generators are subtracted.

Proof. Write a coefficient difference as $z = (u, a, b)$ with $u \in \mathbb{R}^4$. Let $\mathcal{E} = z^{\mathsf{T}} G_\alpha z$ and put $A = |u|^2$. The group-gradient part alone gives

$$\mathcal{E} \ge hA, \qquad h = 2E_2 \ge 2,$$

because every $\zeta_a \geq 1/2$. The scalar gradient of the curvature combination is

$$g = -\alpha e^{-\alpha s_1} \left(\sum_a u_a k_a \right) e_1.$$

Since $|d|^2 = 39$ and $\|Z_\chi\| = 1$,

$$\mathbb{E}|g|^2 \leq CA, \qquad C = 40\alpha^2 E_2, \qquad C/h \leq 5. \tag{1171}$$

The remaining scalar gradient is $r = aL_\square s + bs$. Its norm is

$$\mathbb{E}|r|^2 = 24a^2 + 16ab + 4b^2 \geq a^2 + b^2.$$

For an elementary proof of this last inequality, multiply its difference by 23 and complete squares:

$$23(23a^2 + 16ab + 3b^2) = (23a + 8b)^2 + 5b^2 \geq 0. \tag{1172}$$

Using $r = (r + g) - g$ now gives

$$a^2 + b^2 \leq 2\mathbb{E}|r + g|^2 + 2\mathbb{E}|g|^2 \leq 2\mathcal{E} + 2CA \leq 12\mathcal{E}.$$

Also $A \leq \mathcal{E}/2$. Hence $|z|^2 = A + a^2 + b^2 \leq 25\mathcal{E}/2$, proving (1169). The drift difference is $-\nabla(S_{\widehat{\vartheta}} - S_{\vartheta_*})$, whose squared $L^2(\varrho)$ norm is $\mathcal{E}$. This proves (1170) and coefficient uniqueness. □

The proof is an integral estimate on the actual regulated field space. It does not infer the uniform bound from a sampled eigenvalue plot. In particular, it remains valid at $\alpha = 0$, where the curvature and scalar channels decouple and the coefficient Gram matrix remains full rank. Decoupling and loss of coefficient identification are different properties.

15.30.3. *Generator probes, parameter coordinates and numerical results.* After subtracting the known diffusion and reference-volume parts, the first-order vector field is $b_\vartheta = -\nabla S_\vartheta$. Define the integrated probes

$$y_j = -\int \langle \nabla F_j, b_\vartheta \rangle \, d\varrho, \qquad y = G_\alpha \vartheta. \tag{1173}$$

If $\widehat{y}$ is supplied with $|\widehat{y} - y| \leq \eta$, the unconstrained inverse satisfies

$$|G_\alpha^{-1}\widehat{y} - \vartheta| \leq \frac{25}{2}\eta. \tag{1174}$$

Compatibility with the positive physical parameter region must also be checked. An algebraic inverse need not lie in that region. The formula presumes that the generator probes are available; it does not extract a full generator from one finite, noisy observation record.

For $\alpha = 1/2$ and $\vartheta = (0.7, 0.5, 0.4, 0.3, 1.2, 0.8)$, synthetic exact-formula probes recover the six coefficients with maximum floating-point difference 4.45×10^{-16}. The computed smallest Gram eigenvalue is approximately 1.1811357444. Independently, an outward-rounded LDL^{T} factorization of $G_{1/2} - I$ has strictly

positive pivot intervals, with the smallest lower endpoint exceeding 0.20286. This proves $G_{1/2} \succ I$ within the stated interval evaluation of the exact matrix. The uniform analytic bound remains (1169), valid across the entire exponent interval.

A synthetic probe perturbation of norm 10^{-4} in the computed least-sensitive direction changes the coefficients by approximately 8.46643×10^{-5}. Its induced drift difference has norm 9.20132×10^{-5}; the analytic drift bound gives 3.25316×10^{-4}. These values illustrate stability for the declared probes and do not constitute physical parameter measurements.

The independent primitive parameters are recovered only after their coordinate redundancies are removed. With known unit scalar edge weights,

$$f = \sqrt{\kappa}, \qquad m = \sqrt{\nu/\kappa}.$$

If the edge weights are unknown, the products $f^2 a_{ij}$ replace f^2 as directly visible coefficients. A rescaling of f can then be compensated by edge weights and m. Even with fixed weights, inverse sensitivity becomes large as $\kappa \downarrow 0$. On a fixed rectangle $\kappa \geq \kappa_{\min} > 0$, $\nu \geq \nu_{\min} > 0$, $\nu \leq \nu_{\max}$, the mean-value theorem gives

$$|\delta m| \leq \frac{|\delta \nu|}{2\sqrt{\nu_{\min}\kappa_{\min}}} + \frac{\sqrt{\nu_{\max}}}{2\kappa_{\min}^{3/2}}|\delta\kappa|. \tag{1175}$$

The square-root conversion is therefore a separate calibrated step.

15.30.4. *From complete drift fields to a specified observation system.* The norm in (1170) uses a complete drift field and a prescribed comparison distribution. Neither is automatically available from measurements. The following estimate states the additional information needed to retain the coefficient margin. It also separates loss of spatial coverage from loss caused by an observation map.

Use the normalized coefficient coordinates of Section 15.29. In a local orthonormal frame, collect the columns $M^{1/2}\nabla F_j$ in a matrix $D(x)$. The quantity $M^{-1/2}(b_\vartheta - b_0) = -D(x)\vartheta$ is then the mobility-weighted drift. On a manifold the following quadratic forms are independent of the local orthonormal frame. Let μ be a specified sampling probability and let $T(x)$ be a calibrated linear observation operator acting on this weighted drift. Define

$$G_{\mu,T} = \int D(x)^{\mathsf{T}} T(x)^{\mathsf{T}} T(x) D(x)\, \mu(dx). \tag{1176}$$

Its entries are assumed finite. The observation operator acts on state directions; it is distinct from the parameter-to-probe matrix in (1156).

Proposition 95 (A margin under coverage and observation bounds). *Suppose $G_{\varrho,I} \succeq \gamma_* I$ with $\gamma_* > 0$. Let K be a measurable observed region and*

assume

$$\mu(E) \geq c_0 \varrho(E) \quad (E \subset K \text{ measurable}), \qquad c_0 > 0,$$
$$\left\| \int_{K^c} D^{\mathsf{T}} D \, d\varrho \right\|_{\mathrm{op}} \leq \eta_K < \gamma_*,$$
$$|T(x)D(x)z| \geq s_0 |D(x)z| \quad (z \in \mathbb{R}^6, \ \varrho\text{-almost every } x \in K), \qquad s_0 > 0. \tag{1177}$$

Then

$$G_{\mu,T} \succeq \gamma_{\mathrm{obs}} I, \qquad \gamma_{\mathrm{obs}} = c_0 s_0^2 (\gamma_* - \eta_K) > 0. \tag{1178}$$

In particular, an observed drift discrepancy of $L^2(\mu)$ norm at most ε_b implies $|\widehat{\vartheta} - \vartheta_*| \leq \varepsilon_b / \sqrt{\gamma_{\mathrm{obs}}}$.

Proof. For any coefficient vector z, the integrand $|TDz|^2$ is nonnegative. Restricting its integral to K, using the measure domination and then the observation bound, gives

$$\begin{aligned} z^{\mathsf{T}} G_{\mu,T} z &\geq c_0 s_0^2 \int_K |Dz|^2 \, d\varrho \\ &= c_0 s_0^2 \left(z^{\mathsf{T}} G_{\varrho,I} z - \int_{K^c} |Dz|^2 \, d\varrho \right) \\ &\geq c_0 s_0^2 (\gamma_* - \eta_K) |z|^2. \end{aligned}$$

Apply this inequality to $z = \widehat{\vartheta} - \vartheta_*$ and take square roots to obtain the discrepancy bound. □

For the square regulator, $\gamma_* = 2/25$ is supplied by Theorem 94. The constants c_0, s_0, η_K are additional quantities: their positivity or smallness is not a consequence of that theorem. In particular, a finite empirical measure cannot dominate a continuous ϱ on a region of positive volume. The measure μ in the proposition is the population sampling law; finite observations require a separate error bound.

To state that bound, let $h = G_{\mu,T} \vartheta_*$, where the sign of the drift has been included in the definition of the probe h. Suppose a symmetric numerical Gram matrix $\widehat{G}$ and probe $\widehat{h}$ satisfy

$$\|\widehat{G} - G_{\mu,T}\|_{\mathrm{op}} \leq \varepsilon_G < \gamma_{\mathrm{obs}}, \qquad |\widehat{h} - h| \leq \varepsilon_h, \qquad |\vartheta_*| \leq R_\vartheta.$$

The matrix inequality $\widehat{G} \succeq (\gamma_{\mathrm{obs}} - \varepsilon_G) I$ proves that $\widehat{\vartheta} = \widehat{G}^{-1} \widehat{h}$ exists. Subtraction of the normal equations gives the exact relation

$$\widehat{G}(\widehat{\vartheta} - \vartheta_*) = \widehat{h} - h - (\widehat{G} - G_{\mu,T}) \vartheta_*.$$

Consequently

$$|\widehat{\vartheta} - \vartheta_*| \leq \frac{\varepsilon_h + \varepsilon_G R_\vartheta}{\gamma_{\mathrm{obs}} - \varepsilon_G}. \tag{1179}$$

This deterministic estimate includes uncertainty in both the probe and the Gram matrix. Probabilistic bounds for those errors must use the actual sampling law; consecutive points on one diffusion path cannot be treated as independent without justification. A numerical inverse must also be checked against the admissible coefficient region.

Coverage alone is insufficient. For example, if $D = I_2$ and the only sensor is $T = (1, 0)$, then $G_{\varrho,I} = I_2$ for every sampling probability, whereas $G_{\mu,T} = \operatorname{diag}(1, 0)$. The second coefficient remains invisible even with unlimited repeated measurements. More generally, any nonzero z satisfying $T(x)D(x)z = 0$ for μ-almost every x is an unresolved coefficient direction. These examples explain why the complete-generator reconstruction is a conditional mathematical statement rather than a claim of identification from arbitrary observational data.

15.30.5. *A volume-uniform family of periodic regulators.* The number of scalar sites can increase without losing a normalized coefficient bound in one explicitly specified family. Let the vertices be $(\mathbb{Z}/\ell\mathbb{Z})^4$, where $\ell \geq 3$, and set $n = \ell^4$. At each vertex retain the four positively oriented link variables and the six elementary plaquettes with direction pairs $\mu < \nu$. Use each plaquette once, with that vertex as its base. Scalar edges join nearest neighbors and have unit weights. The lattice has $4n$ links and $6n$ plaquettes. The restriction $\ell \geq 3$ keeps the scalar graph simple and gives four distinct links in each plaquette, with different supports for different plaquettes.

Keep the product group, character normalization, scalar exponent and comparison measure used above, now with n independent standard Gaussian scalar coordinates. Replace the curvature features by

$$F_a = \sum_p e^{-\alpha s_{v(p)}}(d_a - \operatorname{Re}\chi_a(U_{p,a})),$$

and use the scalar edge and mass energies on this graph. The six coefficients remain common to all sites and plaquettes. They are not independent coefficients for each individual link or site.

Distinct elementary plaquettes have a link belonging to one and not the other. Conditional integration over that link sets their character cross moment to zero, since every defining representation here has zero Haar mean. For a cross term between link derivatives, only a shared differentiated link can contribute to the gradient pairing. The private link is different from that differentiated link; integrating it again gives zero. This argument uses the independent Haar comparison measure. It does not assert independence of plaquette observables under an interacting Gibbs law.

For a fixed base vertex i, put $K_{a,i} = \sum_{p:v(p)=i} k_{p,a}$. The six plaquettes based there give

$$\mathbb{E}K_{a,i} = 6d_a, \qquad \mathbb{E}(K_{a,i}K_{b,i}) = 36d_a d_b + 6\delta_{ab}\zeta_a. \tag{1180}$$

All group-gradient cross terms between distinct plaquettes vanish by the same private-link argument. Each of the $6n$ plaquettes contributes four link derivatives. If L is the scalar graph Laplacian, every vertex has degree eight, and hence

$$\operatorname{tr} L = 8n, \qquad \operatorname{tr} L^2 = \sum_i \big(L_{ii}^2 + \sum_{j\neq i} L_{ij}^2\big) = 72n.$$

For example, the curvature–edge cross term is $\alpha^2 E_1 d_a \sum_i 6L_{ii} = 48n\alpha^2 E_1 d_a$. The volume-normalized Gram matrix is therefore exactly

$$\overline{G}_\alpha := \frac{G_{\alpha,n}}{n} = \begin{pmatrix} A_\alpha & 48\alpha^2 E_1 d & 6\alpha^2 E_1 d \\ 48\alpha^2 E_1 d^{\mathsf{T}} & 72 & 8 \\ 6\alpha^2 E_1 d^{\mathsf{T}} & 8 & 1 \end{pmatrix}, \tag{1181}$$

$$A_\alpha = E_2[24Z_\chi + \alpha^2(36dd^{\mathsf{T}} + 6Z_\chi)].$$

In these fixed coordinates the normalized matrix does not depend on ℓ. The Gaussian weight is an identification weight throughout.

THEOREM 96 (Volume-uniform identification in the periodic family). *For every $\ell \geq 3$ and $|\alpha| \leq 1/2$, the stated periodic regulator satisfies*

$$\frac{G_{\alpha,n}}{n} \succeq \frac{96}{53225} I_6. \tag{1182}$$

In particular, all six common coefficients are identifiable from the full generator. With $\|b\|_{\mathrm{av}}^2 = n^{-1}\int |b|^2\, d\varrho_n$,

$$|\widehat{\vartheta} - \vartheta_*| \leq \sqrt{\frac{53225}{96}}\|b_{\widehat{\vartheta}} - b_{\vartheta_*}\|_{\mathrm{av}}. \tag{1183}$$

The constant is independent of the number of sites in this fixed metric and operator normalization.

Proof. Write $z = (u, a, b)$ and $\mathcal{E} = z^{\mathsf{T}}\overline{G}_\alpha z$. The group part gives $\mathcal{E} \geq h|u|^2$ with $h = 12E_2 \geq 12$. The normalized squared norm of the scalar curvature gradient is at most $C|u|^2$, where

$$C = \alpha^2 E_2(36|d|^2 + 6\|Z_\chi\|) = 1410\alpha^2 E_2, \qquad \frac{C}{h} = \frac{235}{2}\alpha^2 \leq \frac{235}{8}.$$

The remaining scalar gradient $r = aLs + bs$ satisfies

$$\frac{1}{n}\mathbb{E}|r|^2 = 72a^2 + 16ab + b^2 \geq \frac{8}{73}(a^2 + b^2).$$

Indeed, its two-by-two Gram matrix has trace 73 and determinant 8, and both eigenvalues are positive. The larger is at most 73, so the smaller is at least $8/73$. Equivalently, the inequality has the polynomial certificate

$$\begin{aligned} 5248\{73(72a^2+16ab+b^2)-8(a^2+b^2)\} \\ = (5248a+584b)^2+64b^2 \geq 0. \end{aligned}$$

Apply $|r|^2 \leq 2|r+g|^2+2|g|^2$ to the scalar curvature gradient g. After dividing by n, the preceding inequalities imply

$$a^2+b^2 \leq \frac{73}{4}\left(1+\frac{C}{h}\right)\mathcal{E} \leq \frac{17739}{32}\mathcal{E}, \qquad |u|^2 \leq \frac{1}{12}\mathcal{E}.$$

Since $1/12+17739/32 = 53225/96$, summing proves (1182). The normalized squared drift difference equals $z^{\mathsf{T}}\overline{G}_\alpha z$, which proves (1183). □

An independent enumeration of vertices, links, scalar edges and plaquette supports for side lengths $3, 4, 5$ reproduces (1181); the largest floating-point entry difference after division by n is below 3×10^{-14}. At $\alpha = 1/2$, the calculated smallest eigenvalue is approximately 0.10713271, larger than the conservative analytic margin $96/53225 \simeq 0.00180366$. Table 11 lists these geometry checks. The theorem applies to every stated side length, not just the three enumerated sizes.

Side	Sites	Links	Plaquettes	$\lambda_{\min}(G/n)$
3	81	324	486	0.10713271
4	256	1024	1536	0.10713271
5	625	2500	3750	0.10713271

Table 11. The periodic-regulator calculation at $\alpha = 1/2$. The matrix normalization divides the integrated squared drift by the number of scalar sites; it does not rescale the physical clock.

This is uniformity with respect to volume within a declared finite lattice family. A continuum limit normally changes the lattice spacing, field normalization, metric, coefficient scaling and reference laws. Those changes are not part of the theorem. Tightness, identification of the limiting generator and compatibility of the physical observation maps remain necessary before a continuum reconstruction can be claimed. Duplicate plaquettes, site-dependent unknown coefficients or unfixed metrics likewise require a new Gram calculation.

15.30.6. *Loss of information at the boundary of the model class.* Multiply all known scalar edge weights by $\rho \geq 0$. The new feature is ρF_E, and its Gram matrix is $G_{\alpha,\rho} = T_\rho^{\mathsf{T}} G_\alpha T_\rho$ with $T_\rho = \mathrm{diag}(1,1,1,1,\rho,1)$. For $\rho > 0$, the rank is six; at $\rho = 0$, the edge coefficient disappears and the rank is five. The uniform

bound for fixed unit edges cannot be transferred to this degenerating family. Table 12 shows the calculated loss of conditioning. Adding a duplicate operator

Edge scale	Smallest Gram eigenvalue	Rank
1	1.18114	6
0.1	0.0768629	6
0.01	0.00079968	6
0.001	7.99997e-06	6
0	0	5

Table 12. Conditioning of the exact square-regulator Gram matrix at $\alpha = 1/2$ as known edge weights vanish. Values are numerical evaluations; the rank loss at zero follows directly from the missing feature.

is another explicit failure: replacing $\beta_1 F_1$ by $\beta_1 F_1 + \widetilde{\beta}_1 F_1$ leaves only $\beta_1 + \widetilde{\beta}_1$ identifiable. The enlarged Gram matrix has null vector $(1, 0, 0, 0, 0, 0, -1)$. More measurements of the same generator cannot remove an algebraic redundancy of this kind.

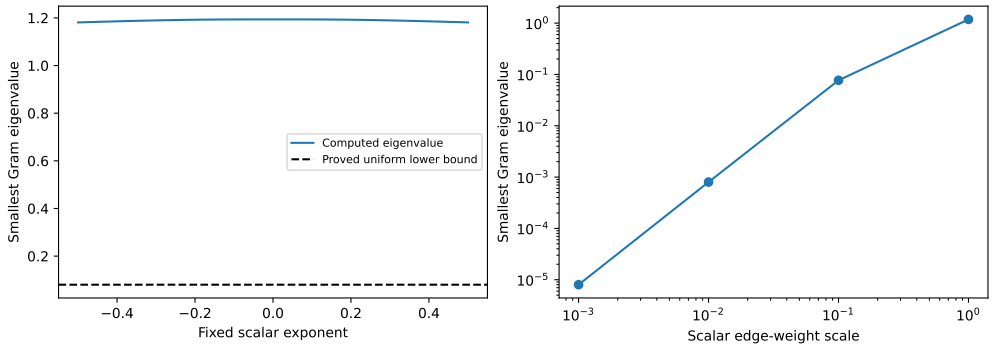


Figure 25. Coefficient sensitivity in the specified lattice realization. Left: computed eigenvalues on an exponent grid and the separately proved uniform lower bound. Right: deterioration as the known edge weights vanish. The first panel does not prove a continuum or group-selection result.

This construction connects the earlier existence theorem to a concrete identification result. Its assumptions are supplied by one stated regulated model, and its coefficient margin follows from analytic Haar and Gaussian integrals. The periodic family gives one volume-uniform extension with a fixed operator basis. Other lattices require their own conditioning estimates; extending the

Statement	Inputs used	Mathematical consequence
Finite-regulator equilibrium	fixed lattice, positive coefficients, compact group metric, scalar confinement	nonexplosion and one Gibbs invariant probability
Coefficient identification	fixed basis, reference weight, clock, mobility and exponent	the full generator determines six coefficients
Stable inverse	a bound on generator or integrated-probe error	the explicit coefficient error bounds
Primitive-model selection	comparison of groups, fields, clocks and hidden extensions	not implied by the coefficient theorem

Table 13. The logical dependencies of the square-regulator construction.

result to a continuum field theory requires the separate uniform estimates and limit identification discussed in Section 10.18.

16. **Joint recovery maps and quantitative defect certificates**

This section makes the word "shared" quantitative. A common symbol or a common equilibrium density is not, by itself, a joint reconstruction. The statement below fixes the regulated data, the branch maps, and the errors that are allowed when a branch is reduced from the common process. All assertions in this section concern finite regulators and the hypotheses displayed here; they do not establish a regulator-independent mother theory.

16.1. *Common data and branch maps.* For a regulator or branch index r, collect the data in

$$\mathfrak{M}_{r,\Theta} := \big(\mathcal{X}_r, \mathcal{A}_r, S_r, M_r, c_r, \theta_r, \nu_r, \mathcal{D}(L_r), \mathcal{T}_r\big). \tag{1184}$$

Here $\mathcal{X}_r$ is the regulated state space, $\mathcal{A}_r$ the action, S_r the reduced energy, M_r the mobility, c_r the circulation or antisymmetric part, θ_r the fluctuation scale, ν_r the reference measure, $\mathcal{D}(L_r)$ the generator domain, and $\mathcal{T}_r$ the map from regulator time to the operational time used by the branch. The action, the reduced energy, and a control cost are different objects and are not identified by notation.

Let Θ denote parameters required to be shared and let η_a denote branch data that are independently supplied, such as geometry, temperature, material composition, initial state, or detector calibration. A branch is specified by

$$\beta_a = F_a(\Theta, \eta_a; \mu_a), \qquad \mathcal{O}_a = \mathcal{G}_a(\beta_a, \eta_a), \tag{1185}$$

where μ_a is the declared regulator or discretisation. Thus a parameter advertised as common cannot be refitted separately in each a. Conversely, branch-specific material constants are not silently promoted to universal constants.

For an approximate common parameter $\widehat{\Theta}$, define the matching residual

$$r_a(\widehat{\Theta}) := F_a(\widehat{\Theta}, \eta_a; \mu_a) - \widehat{\beta}_a. \tag{1186}$$

If F_a is $L_{F,a}$-Lipschitz in Θ on the declared compact set, then the observable error obeys

$$\big\|\mathcal{G}_a(\widehat{\beta}_a, \eta_a) - \mathcal{G}_a(F_a(\Theta, \eta_a; \mu_a), \eta_a)\big\| \le L_{G,a}\big(L_{F,a}\|\widehat{\Theta} - \Theta\| + \|r_a(\widehat{\Theta})\|\big), \tag{1187}$$

provided $\mathcal{G}_a$ is $L_{G,a}$-Lipschitz on a set containing both branch parameters. Indeed, insert $F_a(\widehat{\Theta}, \eta_a; \mu_a)$ between $\widehat{\beta}_a$ and $F_a(\Theta, \eta_a; \mu_a)$ and use the triangle inequality. The first argument of $\mathcal{G}_a$ is a branch parameter; it is not the common parameter Θ. This is a propagation bound, not an identifiability theorem: it does not say that a small residual uniquely determines Θ.

16.2. *Predictable observables when parameters are not fully identifiable.* Full parameter identification is sufficient but not necessary for a cross-branch prediction. The appropriate question is whether the unresolved parameter directions change the proposed observable. All coordinates and norms in this subsection use fixed physical normalizations, including observation-noise whitening when it is available. A change of units must transform those normalizations.

Consider affine calibration and target maps

$$y - y_0 = Jz, \qquad o - o_0 = Kz. \tag{1188}$$

The vector z may include independently specified nuisance parameters as well as the shared physical parameters. It ranges over the full finite-dimensional vector space for the following exact statement. Restrictions to a physical subset can weaken the necessity direction and must be analyzed on that subset.

Proposition 97 (Observable identification on calibration fibres). *The following conditions are equivalent: (i) every two parameters with the same calibration have the same target; (ii)* $\ker J \subseteq \ker K$*; (iii)* $K = LJ$ *for a linear map* L *on the observation space. When they hold,* $L_0 = KJ^\dagger$ *is one such map, where* $J^\dagger$ *is the Euclidean Moore–Penrose inverse in the fixed normalized coordinates. For measured data* $y = y_0 + Jz + e$, $\|e\| \le \epsilon$,

$$\|\widehat{o} - o\| \le \|L_0\|\epsilon, \qquad \widehat{o} = o_0 + L_0(y - y_0). \tag{1189}$$

Among linear exact predictors, L_0 *has minimum operator norm, although the minimum need not be unique.*

Proof. Applying (i) to z and $z + h$ for $h \in \ker J$ proves (ii). Conversely, $Jz = Jz'$ implies $z - z' \in \ker J$, so (ii) implies (i). Under (ii), define $L(Jz) = Kz$ on $\operatorname{ran} J$. This is well-defined and linear. Extend it by zero on the orthogonal

complement. Since $J^\dagger J$ is the orthogonal projection onto $(\ker J)^\perp$, $KJ^\dagger J = K$; hence this extension is L_0. Condition (iii) immediately implies (ii). Finally, $\widehat{o} - o = L_0 e$ proves the bound. Every exact extension agrees with L_0 on $\operatorname{ran} J$, and therefore has norm at least the norm of that restriction. The zero extension attains this norm. □

For exact linear nuisance dependence $y = J_\Theta \Theta + N\nu + e$ and a nuisance-independent target $o = K_\Theta \Theta$, an exact predictor must satisfy both $LJ_\Theta = K_\Theta$ and $LN = 0$. Equivalently, with $P_N = I - NN^\dagger$, the criterion is $\ker(P_N J_\Theta) \subseteq \ker K_\Theta$. Indeed, $P_N J_\Theta h = 0$ means $J_\Theta h$ can be cancelled by a nuisance change. Necessity follows from the previous proposition; sufficiency follows by factoring through $P_N J_\Theta$ and multiplying the predictor by P_N. Ignoring this projection can create apparent information that is actually an uncalibrated nuisance offset.

Proposition 98 (Local nonlinear and design-error allowance). *On a convex ball $\|z\| \le R$, let calibration F and target G have the expansions*

$$F(z) = F(0) + Jz + r_F(z), \quad G(z) = G(0) + Kz + r_G(z),$$

with $\|r_F(z)\| \le M_F R^2/2$ and $\|r_G(z)\| \le M_G R^2/2$. Suppose $\|\widehat{J} - J\| \le \delta_J$, $\|\widehat{K} - K\| \le \delta_K$, and a computed map L satisfies $\|\widehat{K} - L\widehat{J}\| \le \delta_{\mathrm{fac}}$. For $y = F(z) + e$, $\|e\| \le \epsilon$, define $\widehat{o} = G(0) + L(y - F(0))$. Then

$$\|\widehat{o} - G(z)\| \le \|L\|\epsilon + (\delta_{\mathrm{fac}} + \delta_K + \|L\|\delta_J)R + \tfrac{1}{2}(M_G + \|L\|M_F)R^2. \quad (1190)$$

Proof. Subtract $G(z)$ from the predictor to obtain $(LJ-K)z + Lr_F - r_G + Le$. The decomposition

$$K - LJ = (K - \widehat{K}) + (\widehat{K} - L\widehat{J}) + L(\widehat{J} - J)$$

and the triangle inequality prove the claim. Bounds on the second derivatives throughout the ball imply the displayed remainder bounds by the integral Taylor formula. A sampled Hessian or a rank at one point alone does not establish those uniform bounds. □

This estimate does not recover full nonlinear identifiability from a linear rank calculation. Rather, it retains the unresolved quadratic error and the error in a numerically imposed factorization. If $h \in \ker J$ but $Kh \neq 0$, the affine target varies along the exact calibration fibre. Without a bound on that direction, no finite target-error bound can be inferred from calibration alone. For a bounded physical region, one must instead optimize the target over the entire compatible region. For two scalar predicted intervals, $[o_1 - r_1, o_1 + r_1]$ and $[o_2 - r_2, o_2 + r_2]$, discrimination requires $|o_1 - o_2| > r_1 + r_2$. Overlap is a limitation of the proposed observation, not evidence that the two underlying models are equal.

16.2.1. *An exact shared-parameter example with a common offset.* Consider dimensionless synthetic calibration data with

$$J_\Theta = \begin{pmatrix} 1 & 1 & 0 \\ 0 & 1 & 1 \\ 1 & 0 & -1 \end{pmatrix}, \qquad N = \begin{pmatrix} 1 \\ 1 \\ 1 \end{pmatrix}, \qquad K_\Theta = \begin{pmatrix} 1 & 2 & 1 \end{pmatrix}.$$

The augmented calibration matrix has null direction $(1, -1, 1, 0)$. The target annihilates this direction, although the three physical parameters are not uniquely determined. The exact predictor is $L = (3, -1, -2)$: direct multiplication gives $LJ_\Theta = K_\Theta$ and $LN = 0$. Thus a Euclidean observation error of 0.01 permits target error at most $\sqrt{14}/100 = 0.03741657387$. For $\Theta = (0.4, -0.2, 0.7)$ and $\nu = 0.05$, the exact observations are $(0.25, 0.55, -0.25)$ and the target is 0.7. The deterministic perturbation $e = 0.01L^T/\sqrt{14}$ attains the bound. This is an extremal calculation, not a measured dataset.

If only the first two calibration channels are retained, the change $\Delta\Theta = (1, 0, 1)$, $\Delta\nu = -1$ leaves both data unchanged while changing the target by 2. Conversely, replacing the third channel by an offset-only reference gives $L = (1, 1, -2)$ and reduces the allowance to $\sqrt{6}/100 = 0.02449489743$ at the same normalized observation-error radius. The comparison assumes equally normalized noise and acquisition cost; it is not an automatic physical advantage of a particular detector.

Figure 26 shows these two exact error allowances. The calculation illustrates how to select an informative branch observation before fitting all mother parameters. For an actual cross-sector claim, the matrices must be obtained from the common physical forward model, and their uncertainties must enter (1190); they cannot be chosen to force a preferred prediction. The linear-algebra criterion is standard. Its role here is to state the precise target-identification condition needed by the shared-parameter construction.

16.3. *Projection, generator defects, and cross-covariances.* Let X be the common regulated Markov process with generator L and let $\Pi_a : \mathcal{X} \to \mathcal{X}_a$ be a C^2 reduction map. For a smooth test function f on $\mathcal{X}_a$, define the generator defect

$$\mathcal{D}_a f(x) := L(f \circ \Pi_a)(x) - (L_a f)(\Pi_a x). \tag{1191}$$

If P_t and P_t^a are the common and branch semigroups, respectively, Dynkin's formula gives the exact defect identity

$$\mathbb{E}_x f(\Pi_a X_T) - P_T^a f(\Pi_a x) = \int_0^T \mathbb{E}_x\big[\mathcal{D}_a P_{T-s}^a f(X_s)\big]\, \mathrm{d}s, \tag{1192}$$

provided $u(s, y) = P_{T-s}^a f(y)$ solves the backward equation, $u(s, \Pi_a \cdot)$ belongs to the common generator domain, and the time-dependent Dynkin formula is justified. More explicitly, assume nonexplosion through T, integrability of

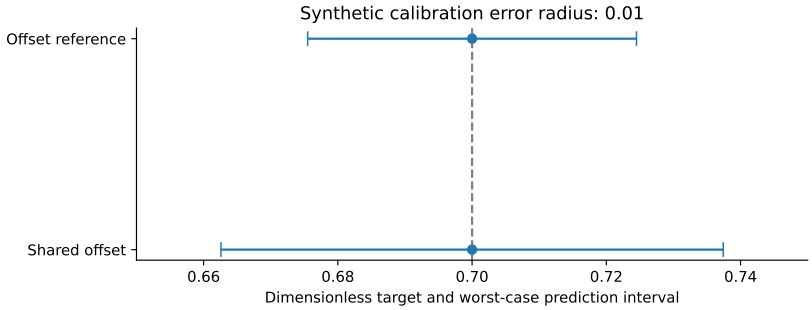


Figure 26. Synthetic shared-parameter prediction under a bounded calibration error. Two exact nuisance-cancelling designs predict the same target 0.7 with different worst-case radii. The first two channels alone leave the target unbounded without a parameter prior. The displayed intervals are deterministic allowances, not confidence intervals from an experiment.

the displayed defect, and uniform integrability of $u(T \wedge \tau_j, \Pi_a X_{T\wedge\tau_j})$ along a localization sequence $\tau_j \uparrow \infty$. Apply Itô's formula to $u(s, \Pi_a X_s)$ stopped at $T\wedge\tau_j$; the backward equation cancels $L_a u$ and uniform integrability removes the stopping. If localization cannot be removed, its terminal boundary contribution must instead be retained. Consequently, if $\sup_{0\le s\le T} \|\mathcal{D}_a P^a_{T-s} f\|_\infty \le d_a(f,T)$, then the weak observable discrepancy is at most $T d_a(f,T)$. The identity shows exactly where a finite reduction enters; it cannot be replaced by the assertion that the two generators are "the same".

Write the common diffusion matrix as $a = \sigma\sigma^{\mathsf{T}}$. For $F = f \circ \Pi_a$ and $G = g \circ \Pi_b$, the joint carré du champ is

$$\Gamma_L(F,G) := L(FG) - F\,LG - G\,LF = \nabla F^{\mathsf{T}} a \nabla G. \tag{1193}$$

In particular, the cross-covariance carried by the common noise is

$$a_{ab}(x) := D\Pi_a(x)\, a(x)\, D\Pi_b(x)^{\mathsf{T}}. \tag{1194}$$

This matrix is an output of the common diffusion and the two maps. It is not an independent fit to a desired cross-spectrum. The identity also supplies a direct numerical check: an independently assembled covariance must agree with (1194) within the stated arithmetic and discretisation error.

16.4. *Action-to-Hamiltonian matching with a remainder.* The conservative mechanical limit is conditional on a regular Legendre map. For a configuration q, velocity v, mass matrix $\mathsf{M}(q)$, vector potential $A(q)$, charge e, and scalar potential $U(q)$, take

$$L_0(q,v) = \tfrac{1}{2} v^{\mathsf{T}} \mathsf{M}(q) v + eA(q)\cdot v - U(q), \qquad p = \partial_v L_0 = \mathsf{M}(q)v + eA(q). \tag{1195}$$

If $\mathsf{M}(q)$ is positive definite, the inverse Legendre map is $v = \mathsf{M}^{-1}(p - eA)$ and

$$H_0(q,p) = p\cdot v - L_0(q,v) = \tfrac{1}{2}(p-eA)^{\mathsf{T}}\mathsf{M}^{-1}(p-eA) + U(q). \tag{1196}$$

The following elementary estimate is the form used when a regulated action is only approximately of the form (1195). Let $L_\delta = L_0 + R_\delta$ on a compact configuration set and a common convex compact velocity set K_v. Fix a compact momentum set on which both Legendre maximizers lie in the interior of K_v. Assume that L_0, R_δ are C^2 in a neighbourhood of these sets, that $D_v^2 L_\delta \succeq m_\delta I$ with $m_\delta > 0$, and that

$$\|R_\delta\|_\infty \le \eta_0, \qquad \|D_v R_\delta\|_\infty \le \eta_v, \qquad \|D_q R_\delta\|_\infty \le \eta_q, \qquad D_v^2 L_0 \succeq m_* I, \tag{1197}$$

with $m_* > 0$. These assumptions give unique interior maximizers v_δ, v_0 and differentiable local Legendre transforms. A sufficient curvature condition is $\|D_v^2 R_\delta\| < m_*$. Uniform bounds on R_δ and its first derivatives alone would not ensure this regularity. The two stationarity equations give

$$D_v L_0(q, v_\delta) - D_v L_0(q, v_0) = -D_v R_\delta(q, v_\delta).$$

Taking the inner product with $v_\delta - v_0$ and using strong monotonicity gives

$$\|v_\delta - v_0\| \le \frac{\eta_v}{m_*}. \tag{1198}$$

The Hamiltonian definition as a supremum immediately yields

$$|H_\delta - H_0| \le \eta_0, \qquad \|D_p H_\delta - D_p H_0\| \le \frac{\eta_v}{m_*}. \tag{1199}$$

If $\|D_q D_v L_0\| \le K_{qv}$ on the same set, the envelope theorem gives

$$\|D_q H_\delta - D_q H_0\| \le \eta_q + K_{qv}\frac{\eta_v}{m_*}. \tag{1200}$$

These inequalities quantify a conditional recovery statement. They do not prove that an arbitrary Hamiltonian, or an arbitrary continuum theory, is selected uniquely by the regulated stochastic model.

16.5. *Relativistic and generally covariant constrained Hamiltonian recovery.* General covariance does not remove constraints; it generates them. Start from a declared diffeomorphism-invariant action and perform an ADM split,

$$ds^2 = -N^2 dt^2 + h_{ij}(dx^i + N^i dt)(dx^j + N^j dt).$$

The lapse N and shift N^i have vanishing canonical momenta, $p_N \approx 0$ and $p_i \approx 0$. For canonical pairs (h_{ij}, π^{ij}) and (ψ, p_ψ), the total Hamiltonian has the form

$$H_{\mathrm{T}} = \int_\Sigma \left(N\mathcal{H} + N^i\mathcal{H}_i + \lambda p_N + \lambda^i p_i\right) \mathrm{d}^3x + B_{\partial\Sigma}. \tag{1201}$$

Preservation of the primary constraints gives the Hamiltonian and momentum constraints $\mathcal{H} \approx 0$ and $\mathcal{H}_i \approx 0$. For the Einstein–Hilbert action with

the Gibbons–Hawking–York boundary term, their Poisson brackets form the hypersurface-deformation algebra,

$$\{\mathcal{H}[N],\mathcal{H}[M]\}=\mathcal{H}_i[h^{ij}(N\partial_j M-M\partial_j N)],\quad \{\mathcal{H}_i[N^i],\mathcal{H}[M]\}=\mathcal{H}[\mathcal{L}_N M], \tag{1202}$$

with the analogous Lie-bracket relation for two momentum constraints. These smeared relations use compactly supported smearings, or boundary conditions for which the surface terms vanish; boundary charges otherwise require the corresponding additional terms. The displayed matter pair is a canonical scalar. Gauge matter adds its own primary and Gauss constraints. The structure functions h^{ij} are why this is not an ordinary finite-dimensional Lie algebra. First-class closure and a well-posed boundary variation are the required tests; writing a covariant action alone does not prove them for a modified action.

For a finite regulator, let $C^A(z)=0$ collect all declared constraints and let $\chi_A(z)=0$ be gauge-fixing conditions for a regular, irreducible first-class constraint family. If the matrix $\{\chi_A,C^B\}$ is invertible on the gauge patch, the Dirac bracket $\{\cdot,\cdot\}_D$ gives a reduced Hamiltonian flow on the constraint surface of the combined constraints and gauge conditions. This is a local construction on the stated gauge patch. For a constraint family C (including gauge conditions when that surface is intended), an Itô stochastic extension

$$\mathrm{d}z=X_{H_{\mathrm{T}}}(z)\,\mathrm{d}t+\sum_\alpha b_\alpha(z)\,\mathrm{d}W_t^\alpha$$

preserves the regular surface under local well-posedness and the tangency conditions, for every A,

$$DC^A\,b_\alpha=0,\qquad LC^A=DC^A X_{H_{\mathrm{T}}}+\tfrac12\sum_\alpha D^2C^A[b_\alpha,b_\alpha]=0\quad\text{on } C=0. \tag{1203}$$

For approximate preservation define $q(z)=LC(z)$ and $A_C(z)=DC(z)\sigma(z)$, with columns $\sigma_\alpha=b_\alpha$. Suppose that on a compact tube, up to its exit time τ, the Euclidean and Frobenius norms satisfy

$$|q(z)|\le L_C|C(z)|+\varepsilon_C,\qquad \|A_C(z)\|_{\mathrm{F}}\le\varepsilon_\sigma.$$

Stopped Itô gives $C(Z_{t\wedge\tau})=C(Z_0)+\int_0^{t\wedge\tau}q(Z_s)\,ds+M_t$. The Itô isometry and the L^2 maximal inequality give $\mathbb{E}\sup_{s\le t}|M_s|\le 2\varepsilon_\sigma\sqrt{t}$. Taking the expected running maximum and applying Gronwall therefore yields

$$\mathbb{E}\sup_{s\le T}|C(Z_{s\wedge\tau})|\le e^{L_C T}\big(|C(Z_0)|+\varepsilon_C T+2\varepsilon_\sigma\sqrt{T}\big). \tag{1204}$$

Exact tangency throughout the tube sets $\varepsilon_\sigma=0$; a bound on LC alone cannot remove the martingale term. For example, $C(z)=z$ and $dZ=dW$ have $LC=0$ but nonzero constraint fluctuations. For a curved surface even tangent noise may need an Itô drift correction: on $|z|=1$ in $\mathbb{R}^2$, $dZ=JZ\,dW$ with

$J^{\mathsf{T}} = -J$ and $J^{\mathsf{T}}J = I$ satisfies $DC\,Jz = 0$ for $C = |z|^2 - 1$, but $LC = |z|^2$. The added drift $-Z/2$ cancels this term. Thus relativistic and generally covariant constrained Hamiltonian mechanics can be recovered in a finite, gauge-fixed branch, with a measurable constraint residual. The result is conditional on the declared action, boundary term, constraint closure, gauge patch, and stochastic tangency. It is not an unconditional derivation of general relativity or a unique covariant Hamiltonian from the shared stochastic notation.

PROPOSITION 99 (Finite joint-recovery certificate). *Consider four versions of the same observable. Write O_{com}, O_{red}, O_{par}, and O_{num} for its successive evaluations in the common process, its reduced branch, the matched parameter approximation, and its mechanical approximation. Assume the hypotheses of the preceding three subsections apply to these consecutive pairs. If the last observable is Lipschitz in H, D_pH, D_qH with constants K_0, K_p, K_q, respectively, then*

$$\begin{aligned}|O_{\mathrm{com}} - O_{\mathrm{num}}| \le{}& T d_a(f,T) + L_{G,a}\big(L_{F,a}\|\widehat{\Theta} - \Theta\| + \|r_a(\widehat{\Theta})\|\big) \\ &+ K_0\eta_0 + K_p\eta_v/m_* + K_q(\eta_q + K_{qv}\eta_v/m_*). \end{aligned} \tag{1205}$$

The consecutive observable maps and constants must refer to the same initial state, time, units, and boundary convention. These compatibility requirements are additional hypotheses, not consequences of the triangle inequality.

Proof. Insert O_{red} and O_{par} between the endpoint observables. Bound the three differences by the Dynkin identity, the parameter bound, and the three Hamiltonian estimates, respectively. Add the bounds. For a trajectory observable the mechanical constants also include flow sensitivity. For example, two Hamiltonian flows with equal initial data, vector-field difference at most ε_H, and one field with Lipschitz constant L_H on a common invariant compact set satisfy $|z_\delta(T) - z_0(T)| \le \varepsilon_H(e^{L_H T} - 1)/L_H$. This follows by integrating the vector-field difference and applying Gronwall; the factor is T at $L_H = 0$. Thus a pointwise Hamiltonian bound cannot be used as a long-time observable bound without a stability factor. □

16.6. *A shared-coupling calculation with simultaneous prediction bounds.* A finite oscillator model illustrates the distinction between common calibration and separate branch fitting. It is a dimensionless example, not a derivation of the physical couplings of the fundamental interactions. For $q = (x_1, x_2, r)$ and $p \in \mathbb{R}^3$, set

$$K_\eta = \begin{pmatrix} 2 & 0 & -\eta \\ 0 & 3 & -3\eta/5 \\ -\eta & -3\eta/5 & 5 \end{pmatrix}, \qquad \Gamma = \mathrm{diag}(7/10, 9/10, 4/5).$$

The mechanical Hamiltonian is

$$H_\eta = \tfrac{1}{2}p^{\mathsf{T}}p + \tfrac{1}{2}q^{\mathsf{T}}K_\eta q.$$

The drift and diffusion covariance are

$$B_\eta = \begin{pmatrix} 0 & I \\ -K_\eta & -\Gamma \end{pmatrix}, \qquad D_{\mathsf{T}} = \begin{pmatrix} 0 & 0 \\ 0 & 2\Gamma\mathsf{T} \end{pmatrix}, \quad \mathsf{T} = \operatorname{diag}(T_1, T_2, T_3).$$

For $\eta \in [0.65, 0.75]$, the row diagonal-dominance bounds give $K_\eta \succeq (5/4)I$. Positive friction and stiffness make B_η Hurwitz: the mechanical energy derivative is $-p^{\mathsf{T}}\Gamma p$, whose invariant zero set contains only the origin. Equivalently, the Lyapunov construction below gives a uniform quantitative test. The stationary covariance C is the unique solution of

$$B_\eta C + C B_\eta^{\mathsf{T}} + D_{\mathsf{T}} = 0. \tag{1206}$$

This determines both branch covariances and their cross blocks.

At the calibration temperature $T_0 = 4/5$, the position law is $\mathcal{N}(0, T_0 K_\eta^{-1})$. Completing the square in x_1 gives $x_1 \mid r \sim \mathcal{N}(\eta r/2, T_0/2)$. For n_0 independent equilibrium snapshots define

$$\widehat{\eta} = \frac{2\sum_j x_{1j} r_j}{\sum_j r_j^2}, \qquad s_\eta = \sqrt{\frac{2T_0}{\sum_j r_j^2}}.$$

Conditionally on the r_j, $(\widehat{\eta} - \eta)/s_\eta$ is standard normal. The interval $\widehat{\eta} \pm 3s_\eta$ therefore has exact model-based coverage $\operatorname{erf}(3/\sqrt{2})$ before outward rounding. The synthetic run with $n_0 = 80{,}000$ and generating value $\eta = 0.7$ gives

$$\widehat{\eta} = 0.7056258967501134, \qquad I_\eta = [0.673225, 0.738026].$$

The same interval is used in all three thermal settings below.

To enclose the covariance without fitting it to target samples, pack its 21 symmetric entries into c. Let $\mathcal{L}_\eta c$ represent $B_\eta C + C B_\eta^{\mathsf{T}}$, and set $c_0 = -\mathcal{L}_{0.7}^{-1} d$ and $S = \mathcal{L}_{0.7}^{-1}\partial_\eta \mathcal{L}_\eta$. For $r_\eta = 0.038026$ and $\eta \in I_\eta$,

$$c - c_0 = -(\eta - 0.7)S(c_0 + c - c_0), \qquad |c - c_0| \le (I - r_\eta |S|)^{-1} r_\eta |S c_0|.$$

The inverse is nonnegative because $r_\eta \| |S| \|_\infty < 0.131575 < 1$, so its Neumann series converges. These matrices and endpoint bounds are evaluated with rational arithmetic. A separate uniform stability check solves $B_{0.7}^{\mathsf{T}} P + P B_{0.7} = -I$. Exact positive LDL pivots verify $P \succ 0$ and $-B_\eta^{\mathsf{T}} P - P B_\eta \succeq I/2$ at $\eta = 0.65, 0.75$; affinity in η extends the inequality to the entire interval.

The target observable is the stationary reservoir entropy-production rate

$$s(\eta, \mathsf{T}) = \sum_{i=1}^{3} \Gamma_{ii}(C_{p_i p_i}/T_i - 1).$$

It follows from the mean heat flow $\Gamma_{ii}(\mathbb{E}p_i^2 - T_i)$ into reservoir i divided by T_i. For $n = 120{,}000$ fresh independent stationary momentum samples per setting, the

sample statistic replaces each covariance entry by its sample second moment. Put $W = \operatorname{diag}(\Gamma_{ii}/T_i)$ and $V = \operatorname{tr}[(C_{pp}^{1/2} W C_{pp}^{1/2})^2]$. A simultaneous upper bound $V \le V_+$ follows from the entrywise covariance enclosure. Diagonalization reduces the centered statistic to a weighted sum of independent centered chi-squares. Its moment generating function uses $\mathbb{E}e^{t(Z^2-1)} = e^{-t}(1-2t)^{-1/2}$ for $2t < 1$. The inequality $-\log(1-z) - z \le z^2/[2(1-z)]$, $0 \le z < 1$, and a Chernoff bound give the two-sided allowance

$$a_n(s) = 2\sqrt{V_+ s/n} + 2\sqrt{V_+}\, s/n$$

with failure probability at most $2e^{-s}$. The second term bounds the largest eigenvalue by $\sqrt{V_+}$ and safely covers the smaller lower-tail allowance as well. With $s = 6.4$, a union bound over the three settings and the calibration event gives total coverage at least

$$\operatorname{erf}(3/\sqrt{2}) - 6e^{-6.4} = 0.9873308602976962.$$

This statement refers to the sampling procedure, not to a posterior probability assigned to the realized intervals. If a calibration interval leaves the certified parameter region, the procedure must report no finite prediction bound (or an unbounded interval), rather than resample until it passes. The present realized interval lies inside that region.

(T_1, T_2, T_3)	predicted mean	new sample	simultaneous interval
$(1.2, 0.7, 0.9)$	0.00493445	0.01140159	$[-0.018682, 0.028395]$
$(1.4, 0.5, 0.9)$	0.01604643	0.01226907	$[-0.010203, 0.041780]$
$(1.6, 0.3, 0.9)$	0.04262323	0.03529602	$[0.011740, 0.072116]$

Table 14. Three synthetic predictions using one frozen coupling calibration. Interval endpoints are widened outwards. The intervals include sampling error and need not remain nonnegative even when the population rate is.

An independent floating-point Lyapunov solver agrees with the rational covariance calculation to at most 2.221×10^{-15} in maximum entry error at the generating parameter. This checks two implementations of the same finite equations; it is not an independent empirical test of the model.

Remark 100 (Interpretation of the synthetic example). *The accompanying finite-oscillator calculation uses synthetic Gaussian calibration data. It estimates a shared coupling and checks independent stationary samples against simultaneous predictive intervals. The samples are not experimental observations. In particular, a sample lying outside a population-confidence interval but inside the wider predictive interval is not evidence against the model. A*

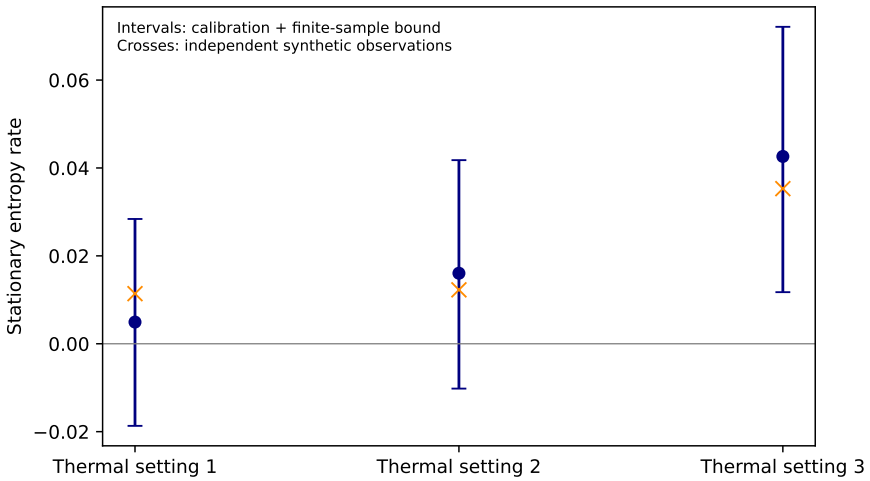


Figure 27. Frozen shared-coupling predictions and independent synthetic samples. The intervals propagate the calibration and finite-sample errors derived in the text.

population interval, a prediction interval, a calibration interval, and a physical detection claim must be reported separately.

17. **A conditional kinetic interface and macroscopic conservation**

A Gibbs invariant density does not determine a collision operator. Recovering a dilute-gas transport equation requires particle kinematics, a collision law and a justified reduction of pair statistics. We make these additional inputs explicit here. The construction is the classical elastic Boltzmann interface [25]; its use below does not assert that molecular chaos follows from a one-particle stationary density.

17.1. *Collision law and the entropy calculation.* Let $f(t,x,v) \geq 0$ be a number density in phase space, and let $m_p > 0$ be the mass of one particle. In logarithms, f is divided by a fixed phase-space reference density; that constant changes entropy by a conserved multiple of particle number. For equal-mass elastic binary collisions, write $g = v - v_*$ and, for $n \in S^2$, set

$$v' = v - (g \cdot n)n, \qquad v'_* = v_* + (g \cdot n)n.$$

This transformation is an involution with absolute Jacobian one, preserves $v+v_*$ and $|v|^2 + |v_*|^2$, and reverses $g \cdot n$. Take a nonnegative collision kernel $B(g,n)$ invariant under this transformation and exchange of the particles. Under the incoming-pair factorization assumption, the collision term is

$$Q(f,f)(v) = \int_{\mathbb{R}^3 \times S^2} B(g,n)\,[f(v')f(v'_*) - f(v)f(v_*)]\,dv_*\,dn.$$

The transport equation is

$$\partial_t f + v \cdot \nabla_x f + \frac{\mathbf{F}}{m_p} \cdot \nabla_v f = Q(f, f),$$

with a specified velocity-independent force $\mathbf{F}(t, x)$. The calculation is for classical positive solutions with integrable moments, entropy and collision entropy production, sufficient to justify the changes of variables and differentiation under the integrals. The global entropy statement uses periodic spatial boundaries or vanishing fluxes, together with decay in velocity.

PROPOSITION 101 (Collision balance and entropy sign). *Let $a = f'f'_*$, $b = ff_*$. For admissible test functions ψ,*

$$\int \psi Q \, dv = \frac{1}{4} \int B(a - b)(\psi + \psi_* - \psi' - \psi'_*) \, dv \, dv_* \, dn.$$

Consequently $1, v, |v|^2$ are collision invariants and

$$\frac{d}{dt} \int f \log f \, dx \, dv = -\frac{1}{4} \int B(a - b) \log(a/b) \, dx \, dv \, dv_* \, dn \leq 0.$$

At zero values the nonnegative integrand is interpreted by its lower-semicontinuous extension.

Proof. Exchange v, v_* in the weak collision integral and average. Next apply the collision involution, which interchanges a, b, and average again. This gives the factor $1/4$ and the displayed weak form. The three collision invariants follow from the explicit velocity transformation. For strictly positive f, put $\psi = \log f$; then $\psi + \psi_* - \psi' - \psi'_* = \log(b/a)$. The inequality follows from monotonicity of the logarithm. The transport integrals vanish by integration by parts. The term from differentiating $f \log f$ without its logarithm vanishes by number conservation. Extension to nonnegative solutions requires a positive approximation for which these identities hold and for which the entropy, transport fluxes and integrated collision production converge. Under these additional hypotheses the same formula follows by passage to the limit; arbitrary weak solutions are not covered. □

For $n_p > 0$, $T > 0$ and velocity u, the Maxwellian

$$f_M(v) = n_p \left(\frac{m_p}{2\pi k_{\mathrm{B}} T} \right)^{3/2} \exp\left[-\frac{m_p |v - u|^2}{2 k_{\mathrm{B}} T} \right]$$

satisfies $f'_M f'_{M*} = f_M f_{M*}$ and hence $Q(f_M, f_M) = 0$. This is an equilibrium calculation for the specified collision law. A local Maxwellian need not solve the transport equation, and uniqueness of collision equilibria requires the nondegeneracy hypotheses for the classification of collision invariants.

17.2. *Exact moment equations and the constitutive step.* Define $\rho = m_p \int f\,dv$, $\rho u = m_p \int v f\,dv$, $c_v = v - u$,

$$P = m_p \int c_v \otimes c_v f\,dv, \qquad \rho e = \frac{m_p}{2}\int |c_v|^2 f\,dv, \qquad q = \frac{m_p}{2}\int |c_v|^2 c_v f\,dv.$$

Let $E = \rho|u|^2/2 + \rho e$. Multiplication of the kinetic equation by $m_p, m_p v, m_p|v|^2/2$ gives, without a constitutive closure,

$$\begin{aligned} \partial_t \rho + \nabla\cdot(\rho u) &= 0,\\ \partial_t(\rho u) + \nabla\cdot(\rho u\otimes u + P) &= \rho\mathbf{F}/m_p,\\ \partial_t E + \nabla\cdot(Eu + Pu + q) &= \rho u\cdot\mathbf{F}/m_p. \end{aligned}$$

The signs follow by integrating the force term in velocity; symmetry of P follows directly from its definition. Euler closure uses $P = pI$, $q = 0$. Compressible Navier–Stokes–Fourier closure uses

$$P = pI - 2\eta D^0 u - \zeta(\nabla\cdot u)I, \qquad q = -\kappa\nabla T, \qquad D^0 u = \tfrac{1}{2}(\nabla u + \nabla u^{\mathsf{T}}) - \tfrac{1}{3}(\nabla\cdot u)I.$$

With $\eta, \zeta, \kappa \geq 0$, the local constitutive entropy production is

$$\frac{2\eta|D^0 u|^2 + \zeta(\nabla\cdot u)^2}{T} + \frac{\kappa|\nabla T|^2}{T^2} \geq 0.$$

These formulas display which step is conservation and which is closure. They do not derive water's equation of state or viscosity from dilute gas kinetics.

17.3. *Linear response and the remaining limiting problem.* Suppose the negative linearized collision operator $\mathcal{A}$ is self-adjoint, nonnegative, and has a bounded inverse on the orthogonal complement of its collision invariants. For projected microscopic currents χ_i, define

$$\mathcal{K}_{ij} = \langle \chi_i, \mathcal{A}^{-1}\chi_j\rangle.$$

Self-adjointness implies $\mathcal{K}_{ij} = \mathcal{K}_{ji}$, while $b_i\mathcal{K}_{ij}b_j = \langle \sum_i b_i\chi_i, \mathcal{A}^{-1}\sum_j b_j\chi_j\rangle \geq 0$. This is the reversible linear-response step. With a magnetic field or time-reversal-odd variables, the appropriate statement is an Onsager–Casimir relation between reversed parameters, not unrestricted matrix symmetry.

A microscopic derivation still has to control incoming-pair correlations, recollisions and the chosen dilute limit. A hydrodynamic derivation must then control the Knudsen expansion, boundary layers, the inverse of $\mathcal{A}$, and a remainder in a specified norm and time interval. A Fokker–Planck diffusion limit is a different scaling and does not supply those conclusions automatically. The calculation above therefore provides the explicit kinetic matching interface, not an unconditional derivation of the Boltzmann equation from the mother generator.

18. **Physical matching of additional interactions**

Recovering an established equation and predicting a deviation from that equation are different mathematical tasks. A deviation requires a physical coupling, its normalization and range, a source, and a detector response. This section develops one such conditional response for a finite scalar source. It also identifies assumptions that cannot be replaced by the existence of a regulator or by positivity of entropy production.

18.1. *A finite source and a common scalar response.* Use a canonically normalized scalar perturbation φ with a constant nonnegative mass m_φ, reduced Planck mass M_{P}, and source charge α_E. In units $\hbar = c = 1$, suppose the weak-field, static, unscreened equations reduce to

$$(\nabla^2 - m_\varphi^2)\varphi = \frac{\alpha_E}{M_{\mathrm{P}}}\rho_E, \qquad \varphi \longrightarrow 0 \quad \text{at spatial infinity.} \tag{1207}$$

The source is a ball of radius R, uniform density $\rho_E = 3M_E/(4\pi R^3)$, and negligible scalar backreaction on that density. A sufficiently small test body has acceleration $-\alpha_A \nabla\varphi/M_{\mathrm{P}}$, where $\alpha_A = M_{\mathrm{P}}\partial_\varphi \log m_A$ is evaluated on the background. These assumptions exclude nonlinear screening and appreciable source redistribution.

Proposition 102 (Finite-source transfer and two detector channels). *For $r > R$, the unique decaying solution of* (1207)*, regular at the origin, is*

$$\begin{aligned} \frac{\varphi(r)}{M_{\mathrm{P}}} &= -\frac{2G\alpha_E M_E}{r}\, F(m_\varphi R) e^{-m_\varphi r}, \\ F(z) &= \frac{3(z\cosh z - \sinh z)}{z^3}, \qquad F(0) = 1. \end{aligned} \tag{1208}$$

Let $C(r) = \delta \log(\nu_a/\nu_b) = D\,\varphi(r)/M_{\mathrm{P}}$ be a background-subtracted clock-ratio response, with constant nonzero D. Let Δa_{AB} be the signed difference of the scalar radial accelerations of two test bodies. Then

$$D\,\Delta a_{AB} = (\alpha_A - \alpha_B)(m_\varphi + r^{-1})\, C(r). \tag{1209}$$

Proof. The Yukawa Green function gives

$$\varphi(\mathbf{r}) = -\frac{\alpha_E}{4\pi M_{\mathrm{P}}} \int_{|\mathbf{s}|\le R} \rho_E \frac{e^{-m_\varphi|\mathbf{r}-\mathbf{s}|}}{|\mathbf{r}-\mathbf{s}|}\, d^3 s.$$

For $r > s$, angular integration yields

$$\int_{S^2} \frac{e^{-m_\varphi|\mathbf{r}-\mathbf{s}|}}{|\mathbf{r}-\mathbf{s}|}\, d\Omega_s = \frac{4\pi e^{-m_\varphi r}\sinh(m_\varphi s)}{m_\varphi r s}.$$

The remaining integral is $\int_0^R s\sinh(m_\varphi s)\, ds = [m_\varphi R\cosh(m_\varphi R) - \sinh(m_\varphi R)]/m_\varphi^2$. Substitute the density and $G = (8\pi M_{\mathrm{P}}^2)^{-1}$ to obtain (1208). The zero-mass value follows by continuity. A regular decaying

homogeneous difference vanishes, either by integration of its positive Dirichlet form for positive mass or by the harmonic uniqueness theorem at zero mass. Finally, $\partial_r\varphi = -(m_\varphi + r^{-1})\varphi$; subtract the two accelerations and use the definition of C. □

For SI observables write $\mu = m_\varphi c/\hbar$, replace GM_E/r in (1208) by $GM_E/(c^2 r)$, and replace the right-hand side of (1209) by $c^2(\alpha_A - \alpha_B)(\mu + r^{-1})C(r)$. The dimensions are then acceleration on both sides. A universal test-body charge makes the differential acceleration vanish even when the common scalar acceleration is nonzero. If $\alpha_E = 0$, there is no source response; if $D = 0$, this clock pair does not measure the scalar. Neither case is excluded by the variational construction alone.

The factor F is a linear finite-source correction, not a screening factor. In particular,

$$F(z) = 1 + \frac{z^2}{10} + \frac{z^4}{280} + O(z^6).$$

At the surface the transfer relative to the massless monopole is $F(z)e^{-z}$, which behaves as $3/(2z^2)$ for large z. A numerical cutoff does not set the physical inverse range μ. That range is fixed here by the canonically normalized field equation.

18.2. *Range identification with a held-out radius.* For the same static source and identical clock pairs at two exterior radii, $C(r) = Ke^{-\mu r}/r$ with a common nonzero signed amplitude K. Therefore

$$\mu = \frac{\log(r_1|C_1|) - \log(r_2|C_2|)}{r_2 - r_1}, \qquad C_3 = C_1 \frac{r_1}{r_3} e^{-\mu(r_3 - r_1)}. \tag{1210}$$

The amplitude, source form factor, and common scalar charge cancel from the first identity. A third radius tests the spatial law without changing these quantities. This cancellation does not remove environmental clock shifts or an incorrectly subtracted tensor gravitational redshift.

If measured values $\widehat{C}_i$ obey deterministic error bounds $|\widehat{C}_i - C_i| \le d_i < |\widehat{C}_i|$, the signs are fixed and the mean-value theorem for $\log|x|$ gives

$$|\widehat{\mu} - \mu| \le \frac{1}{|r_2 - r_1|} \sum_{i=1}^{2} \frac{d_i}{|\widehat{C}_i| - d_i}. \tag{1211}$$

Here the radii are exact inputs; uncertain radii require their own propagation terms. The bound becomes uninformative near a null signal, as it should. If $|\widehat{\mu} - \mu| \le d_\mu$, the third-radius prediction, with $L = |r_3 - r_1|$, satisfies

$$|\widehat{C}_3 - C_3| \le \frac{r_1}{r_3} e^{-\widehat{\mu}(r_3 - r_1)} \left[d_1 + (|\widehat{C}_1| + d_1)(e^{d_\mu L} - 1) \right].$$

This follows by adding and subtracting $C_1(r_1/r_3)e^{-\widehat{\mu}(r_3-r_1)}$. It is a conditional prediction interval from bounded errors, not a confidence statement or a detection claim.

A synthetic unit-radius calculation compares the analytic exterior field with direct three-dimensional source integration reduced only by azimuthal symmetry. The inverse ranges are $0, 0.1, 1, 3, 10$ and the observation radius is 1.4. The largest absolute difference between the two calculations is 1.45×10^{-15}; this is numerical agreement, not an interval enclosure. Figure 28 also shows a specified response with $\mu R = 0.8$, amplitude -0.03, calibration radii $1.4R, 2R$, and prediction radius $2.7R$. These dimensionless inputs are synthetic. No measured laboratory sensitivity or physical selection of the amplitude is inferred from them.

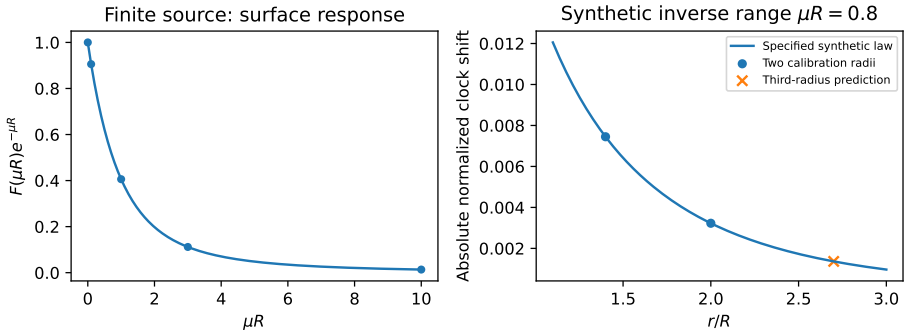


Figure 28. Linear scalar response of a finite spherical source (left) and synthetic range identification with a third-radius prediction (right). The source correction is distinguished from nonlinear screening.

18.3. *Entropy production does not supply an interaction law.* There is a direct counterexample to deriving an additional mechanical force merely from positive path entropy production. Let $z \in \mathbb{R}^2$ solve

$$dz = (-aI + \Omega J)z\,dt + \sqrt{2a}\,dW_t, \qquad J = \begin{pmatrix} 0 & -1 \\ 1 & 0 \end{pmatrix}, \quad a > 0.$$

Its stationary covariance is I. With both components even under the declared time reversal, the stationary current is $j(z) = \Omega J z\, p(z)$, where p is the standard Gaussian density. The current formula gives the dimensionless entropy-production rate

$$\sigma = \int \frac{|j|^2}{ap}\,dz = \frac{2\Omega^2}{a} > 0 \quad (\Omega \neq 0).$$

Couple this process to a mechanical Hamiltonian system by a direct product: the Hamilton equations have no z-dependence. Their force is exactly unchanged for every Ω, despite the positive entropy production. An additional force therefore requires a nonzero, specified cross-coupling. The time-reversal convention in this example is not spatial parity.

Likewise, at fixed temperature an equilibrium generalized force is $-\partial_q \mathcal{F} = -\partial_q U + T\partial_q S$, where $\mathcal{F} = U - TS$. This does not give a force $-T\nabla S_{\mathrm{path}}$ from a path-relative-entropy rate. A dimensionless entropy requires k_{B}; a rate requires an additional time scale even before a force dimension is obtained.

Let P be a forward path measure and Q its specified reversed comparison measure. If they are mutually absolutely continuous and $\Sigma = \log(dP/dQ)$, then $\mathbb{E}_P e^{-\Sigma} = \int dQ = 1$. Projection to observed paths obeys the same identity for the projected Radon–Nikodym ratio, whenever the projected measures are equivalent. Discarding hidden heat or replacing a memory process by a Markov approximation can misidentify that ratio; it does not by itself modify the identity. Interpreting Σ as work minus free energy requires the additional bath, preparation and protocol assumptions of the work relations.

18.4. *Regulators, boundaries and distinguishable signals.* For a central spatial difference with mesh h, the wave-number symbol is $4h^{-2}\sin^2(kh/2) = k^2 - h^2k^4/12 + O(h^4k^6)$. The correction vanishes at fixed k as the computational mesh is refined. Interpreting it as a physical dispersion correction requires a physical cutoff, symmetry analysis, a matched operator coefficient, and a regulator-independent observable. Finite-mode turbulence errors have the same logical distinction from measured intermittency.

A static Schur complement describes a static response. A ringdown frequency instead depends on the dynamical perturbation operator, its physical boundary conditions, and left and right resonant modes. Positive path entropy does not determine a frequency shift or its sign. Similarly, a boundary-dependent inertial response is an additional physical effect only after subtracting the response already present in general relativity for the same matter and boundary data. The conditional scalar relation (1209) supplies an explicit way to compare two channels. It does not establish that nature has a nonzero scalar charge, or uniquely select that charge from the mother family.

19. **Binary-pulsar constraints on a conditional scalar interaction**

An additional interaction becomes testable when its source charges and propagation law determine an observable that was not used to choose those charges. A static force and radiative energy loss provide different such observables. We now apply the scalar normalization of Section 18 to published orbital-decay measurements of two pulsar–white-dwarf binaries. The data are

observational summaries from Freire et al. [73] and Antoniadis et al. [5]; the analysis below is a reanalysis of those historical summaries, with an explicitly specified Gaussian approximation. It is neither a new fit to pulse arrival times nor a determination of the present strongest observational bound.

19.1. *Physical charges and the distinction between force and radiation.* In this subsection use $\hbar = c = 1$. Suppose that the effective branch, about a stable background $\varphi = 0$, contains

$$S_{\text{eff}} = \int \sqrt{-g}\left[\frac{M_{\text{P}}^2}{2}R - \frac{1}{2}(\nabla\varphi)^2 - \frac{1}{2}m_\varphi^2\varphi^2\right] d^4x - \sum_A \int m_A(\varphi)\, ds_A. \quad (1212)$$

Here $G_* = (8\pi M_{\text{P}}^2)^{-1}$, and

$$\alpha_A = M_{\text{P}}\left.\frac{\partial \log m_A}{\partial \varphi_\infty}\right|_{N_A, \mathcal{E}_A}, \qquad \Delta\alpha_b = \alpha_A - \alpha_B. \quad (1213)$$

For a compact star the derivative holds its baryon number N_A and matter equation of state $\mathcal{E}_A$ fixed and refers to a family of stellar solutions with asymptotic field φ_∞. Its mass includes binding energy. Thus a neutron-star charge is not generally the charge of one constituent particle, and different neutron-star masses need not have the same charge.

For weak, unscreened sources with constant charges, the point-source potential is, to the retained order,

$$V_{AB}(r) = -\frac{G_* m_A m_B}{r}\left[1 + 2\alpha_A\alpha_B e^{-m_\varphi r}\right]. \quad (1214)$$

A finite extended source instead requires its source integral, as in Proposition 102. The scalar part of the static potential depends on $\alpha_A\alpha_B$. The leading circular dipole luminosity depends on $(\Delta\alpha_b)^2$. Equal nonzero charges therefore remove this dipole while retaining a static scalar interaction. Conversely, a bound on the charge difference alone does not bound the charge product.

The convention in the binary literature can be obtained by writing $\varphi = \sqrt{2}M_{\text{P}}\varphi_{\text{DEF}}$. Its scalar kinetic term is then $-2(\nabla\varphi_{\text{DEF}})^2/(16\pi G_*)$, and

$$\alpha_A^{\text{DEF}} = \sqrt{2}\alpha_A. \quad (1215)$$

This conversion is necessary when comparing numerical charge limits; omitting it changes a squared-charge coefficient by a factor of two.

19.2. *Radiative transfer and its mass threshold.* Assume slowly moving, nearly circular bodies, constant effective charges over an orbit, a linear unscreened exterior scalar equation, outgoing boundary conditions, and perturbatively small conservative corrections. Let $M_b = m_A + m_B$, $\mu_b = m_A m_B/M_b$, a_b be the separation, $\Omega_b = 2\pi/P_b$, and P_b the orbital period.

For the massless scalar, its charge dipole in the center-of-mass frame is

$$\mathbf{D}(t) = \sum_A \frac{\alpha_A m_A}{M_{\rm P}} \mathbf{x}_A(t) = \frac{\mu_b \Delta\alpha_b}{M_{\rm P}} \mathbf{r}(t).$$

The radiative far field is $\varphi_{\rm rad} = -\mathbf{n}\cdot\dot{\mathbf{D}}(t-r)/(4\pi r)$. The monopole is constant under the assumptions above. Its flux gives

$$\mathcal{P}_\varphi = \frac{1}{16\pi^2}\int_{S^2} (\mathbf{n}\cdot\ddot{\mathbf{D}})^2\, d\Omega = \frac{|\ddot{\mathbf{D}}|^2}{12\pi} = \frac{2G_*}{3}\mu_b^2(\Delta\alpha_b)^2 a_b^2 \Omega_b^4.$$

The angular identity used here is $\int n_i n_j\, d\Omega = (4\pi/3)\delta_{ij}$.

Restoring SI units, and retaining the Newtonian orbit at the same order,

$$\mathcal{P}_\varphi = \frac{2G_*}{3c^3}\mu_b^2(\Delta\alpha_b)^2 a_b^2\Omega_b^4, \qquad E_b = -\frac{G_{AB}\mu_b M_b}{2a_b}, \qquad a_b^3\Omega_b^2 = G_{AB}M_b. \tag{1216}$$

Here G_{AB} is the constant leading orbital coupling in the long-range limit. The approximation requires corrections to the conservative orbit and to the tensor luminosity to be negligible at the required accuracy; it does not cover arbitrary large scalar charges. Since $\dot{E}_b = -\mathcal{P}_\varphi$, $\dot{a}_b/a_b = \mathcal{P}_\varphi/E_b$, and $\dot{P}_b/P_b = 3\dot{a}_b/(2a_b)$. Substitution yields

$$\dot{P}_b^{\rm dip} = -C_b(\Delta\alpha_b)^2, \qquad C_b = \frac{8\pi^2 G_*\mu_b}{c^3 P_b}. \tag{1217}$$

Both $\dot{P}_b$ and C_b are dimensionless: $G_*\mu_b/c^3$ has units of time. Equation (1215) converts the coefficient $8\pi^2$ to the $4\pi^2$ coefficient multiplying $(\Delta\alpha_b^{\rm DEF})^2$ in Antoniadis et al. [5].

For a massive scalar, a harmonic of angular frequency ω has outgoing wave number

$$k_\varphi^2 = \frac{\omega^2}{c^2} - \frac{m_\varphi^2 c^2}{\hbar^2}.$$

In the long-wavelength dipole expansion, the source amplitude is proportional to $k_\varphi \mathbf{n}\cdot\mathbf{D}$, and the outgoing flux is proportional to ωk_φ times its squared amplitude. Relative to the massless value, the factor is therefore $(ck_\varphi/\omega)^3$. For the circular dipole $\omega = \Omega_b$,

$$\begin{aligned} f_b(m_\varphi) &= \left[1 - \left(\frac{m_\varphi c^2}{\hbar\Omega_b}\right)^2\right]_+^{3/2}, \qquad [x]_+ = \max(x,0), \\ \dot{P}_b^{\rm dip} &= -C_b(\Delta\alpha_b)^2 f_b(m_\varphi). \end{aligned} \tag{1218}$$

This factor applies to the linear leading circular dipole. Above its threshold there can still be a static force, higher multipoles, or higher harmonics in an eccentric orbit. Variable charges, strong scalarization, screening, and changes of the binary background require a different coupled calculation.

19.3. *Published observations and the general-relativistic baseline.* An observed period derivative contains line-of-sight acceleration effects in addition to intrinsic orbital evolution. For the usual timing conventions,

$$\dot{P}_b^{\rm int} = \dot{P}_b^{\rm obs} - \frac{P_b \mu_{\rm sky}^2 d}{c} - \frac{P_b a_{\rm los}}{c} - \dot{P}_b^{\rm other}. \tag{1219}$$

The second term is the Shklovskii correction, with angular proper motion $\mu_{\rm sky}$ and distance d; $a_{\rm los}$ is the relative line-of-sight acceleration of the system and the Solar System. Mass loss, tides, or variation of gravitational couplings must be included or independently bounded when relevant. In particular, $\dot{P}_b^{\rm obs} - \dot{P}_b^{\rm GR}$ is not automatically a scalar-radiation measurement.

For a circular GR orbit, with masses $\bar{m}_A, \bar{m}_B$ in solar units and $T_\odot = GM_\odot/c^3 = 4.925490947\,\mu$s,

$$\dot{P}_b^{\rm GR} = -\frac{192\pi}{5}\left(\frac{2\pi T_\odot}{P_b}\right)^{5/3} \frac{\bar{m}_A \bar{m}_B}{(\bar{m}_A + \bar{m}_B)^{1/3}}. \tag{1220}$$

The binaries used here have negligible eccentricity at the precision of this summary calculation. The optical companion masses and measured mass ratios provide the input masses; masses inferred by imposing the same GR period-decay relation are not substituted as independent data. Weak-field stellar modeling and spectroscopy remain part of the input assumptions.

For PSR J1738+0333, Freire et al. [73] report

$$\dot{P}_b^{\rm int} = (-25.9 \pm 3.2) \times 10^{-15}, \quad \dot{P}_b^{\rm GR} = (-27.7^{+1.5}_{-1.9}) \times 10^{-15},$$
$$y_b := \dot{P}_b^{\rm int} - \dot{P}_b^{\rm GR} = (2.0^{+3.7}_{-3.6}) \times 10^{-15}.$$

We use their published excess, which incorporates their Monte Carlo propagation, and take 3.7×10^{-15} as the standard deviation of the declared symmetric approximation. Subtracting the rounded medians in the first two lines would instead give 1.8×10^{-15}; that arithmetic difference does not replace the published residual distribution.

For PSR J0348+0432, Antoniadis et al. [5] report $\dot{P}_b^{\rm obs} = (-2.73 \pm 0.45) \times 10^{-13}$, a small combined external correction $(0.016 \pm 0.003) \times 10^{-13}$, and $\dot{P}_b^{\rm GR} = (-2.58^{+0.07}_{-0.11}) \times 10^{-13}$. Their correction includes the allowed contribution of a varying G; it is a nuisance estimate, not evidence that G varies. Using these summaries gives

$$\begin{aligned} y_b &= (-2.73 - 0.016 + 2.58) \times 10^{-13} = -1.66 \times 10^{-14}, \\ \sigma_b &= \sqrt{0.45^2 + 0.003^2 + 0.11^2} \times 10^{-13} \\ &= 4.6325911 \times 10^{-14}. \end{aligned} \tag{1221}$$

The quadrature combination is an independent-Gaussian summary model, using the larger quoted GR error. It is not the authors' joint timing likelihood. If

the proposed scalar also changes the allowed $\dot{G}$, Galactic acceleration, or mass inference appreciably, those terms must be fitted consistently instead.

Quantity	J1738+0333	J0348+0432
P_b (days)	0.3547907398724	0.102424062722
$\bar{m}_B$ (white dwarf)	0.181	0.172
$q = m_A/m_B$	8.1	11.70
$\bar{m}_A = q\bar{m}_B$	1.4661	2.0124
$y_b/(10^{-15})$	2.0	−16.6
$\sigma_b/(10^{-15})$	3.7	46.325911
C_b	2.0439743×10^{-9}	6.9636046×10^{-9}

Table 15. Published historical inputs and the resulting leading scalar coefficient. The first residual is the published distribution summary; the second uses (1221). Charges use (1213). For the numerical coefficient we identify G_* with the measured G at the retained weak-coupling order. The table is not a raw arrival-time fit.

As an arithmetic consistency check, inserting the rounded central masses into (1220) gives $-2.7541583 \times 10^{-14}$ and $-2.5930002 \times 10^{-13}$. These differ slightly from the published nonlinear distribution summaries. The published GR values remain the baselines for the residual analysis.

19.4. *A one-sided constraint and its statistical scope.* Let $B_b = C_b(\Delta\alpha_b)^2 f_b \geq 0$ denote the magnitude of additional dipole decay. For each binary separately, use

$$Y_b = -B_b + \epsilon_b, \qquad \epsilon_b \sim \mathcal{N}(0, \sigma_b^2). \tag{1222}$$

The variance and C_b are fixed inputs of this approximate model. Write Φ_{N} for the standard normal distribution function, and $z_{0.95} = \Phi_{\mathrm{N}}^{-1}(0.95) = 1.64485362695$.

Proposition 103 (One-sided bound in the Gaussian residual model). *For* (1222)*, the interval*

$$0 \leq B_b \leq U_b(Y_b), \qquad U_b(y) = \max\{0, z_{0.95}\sigma_b - y\}$$

has coverage 0.95 *for every* $B_b > 0$*, and coverage one at* $B_b = 0$*. If* $f_b > 0$*, it gives*

$$|\Delta\alpha_b| \leq \left(\frac{U_b(y_b)}{C_b f_b}\right)^{1/2}. \tag{1223}$$

Proof. For $B_b > 0$, the event $B_b \leq U_b(Y_b)$ is equivalent to $Y_b + B_b \leq z_{0.95}\sigma_b$. Its probability is $\Phi_{\mathrm{N}}(z_{0.95}) = 0.95$. At $B_b = 0$ the interval contains the

parameter for every observation. Monotonicity of $B_b = C_b f_b |\Delta\alpha_b|^2$ proves the final assertion. □

This proposition establishes coverage in the stated Gaussian model. It does not establish Gaussianity of the full observational likelihood or bound unmodeled astrophysical and theoretical effects. If an additional deterministic residual b_b is known to satisfy $|b_b| \le d_b$, so that $Y_b = -B_b + b_b + \epsilon_b$, the replacement

$$U_b(y) = \max\{0, z_{0.95}\sigma_b + d_b - y\}$$

has at least 95% coverage in the same noise model. No numerical bound d_b for all omitted scalar effects is assumed here.

In the massless limit the calculated endpoints are

	J1738+0333	J0348+0432
$U_b(y_b)$	$4.0859584 \times 10^{-15}$	$9.2799342 \times 10^{-14}$
$\lvert\Delta\alpha_b\rvert_{95}$	1.4138693×10^{-3}	3.6505256×10^{-3}
$\lvert\Delta\alpha_b^{\mathrm{DEF}}\rvert_{95}$	1.9995131×10^{-3}	5.1626228×10^{-3}

(1224)

These are separate one-sided conditional bounds, not a joint 95% statement for both stars. Their different neutron-star masses preclude identifying their charge differences without a specified stellar-response model.

For J0348+0432, arbitrary correlations between the three quoted Gaussian error contributions give $\sigma_b \le (0.45 + 0.003 + 0.11) \times 10^{-13} = 5.63 \times 10^{-14}$. Using this upper standard deviation instead yields $|\Delta\alpha_b|_{95} \le 3.9600870 \times 10^{-3}$, with at least nominal coverage if the joint Gaussian and marginal-error assumptions hold. This sensitivity calculation does not establish those assumptions.

A separate deterministic mass sensitivity calculation uses the rectangles

$$\mathcal{R}_{1738} = [0.160, 0.205] \times [7.5, 8.7], \qquad \mathcal{R}_{0348} = [0.163, 0.181] \times [11.31, 12.09]$$

for $(\bar{m}_B, q)$. They are chosen from three times the quoted one-standard-deviation sides and are not joint confidence regions. Since

$$C_b = \frac{8\pi^2 T_\odot}{P_b} \frac{\bar{m}_B q}{1+q}$$

increases with both arguments, its smallest value is at the lower corner. Holding the residual model fixed, the resulting largest massless charge endpoints are 1.5103903×10^{-3} and 3.7550404×10^{-3}. This isolates coefficient sensitivity; it does not rerun the correlated mass–GR-baseline inference.

19.5. *Interpretation and complementary observations.* The leading dipole thresholds are

	J1738+0333	J0348+0432
$\hbar\Omega_b$ (eV)	$1.3491481 \times 10^{-19}$	$4.6733671 \times 10^{-19}$
c/Ω_b (AU)	9.7769060	2.8224819

where the second line is the reduced Compton wavelength at threshold. For $m_\varphi c^2 < \hbar\Omega_b$, the massless charge bound is multiplied by $[1-(m_\varphi c^2/\hbar\Omega_b)^2]^{-3/4}$. Its divergence toward threshold expresses loss of sensitivity, not permission to use the weak-coupling approximation at arbitrarily large charge.

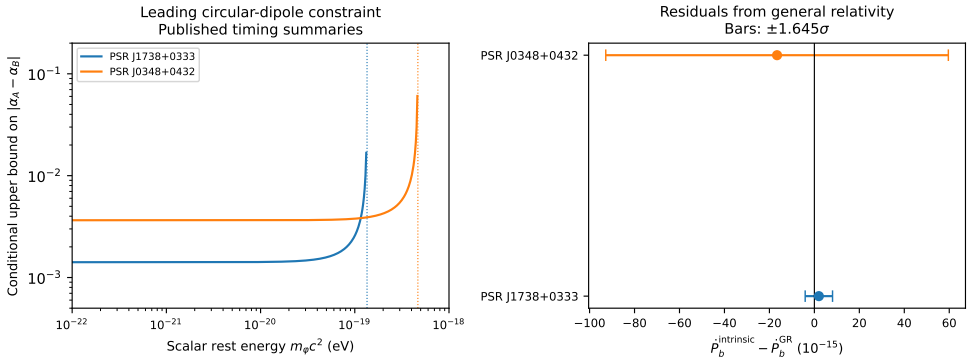


Figure 29. Conditional scalar-dipole constraints calculated from two published observational summaries. Left: the leading circular-dipole upper endpoints as a function of scalar rest energy, with dotted thresholds. Above each threshold this channel gives no bound. Right: residuals about the published GR baselines; bars extend 1.645 Gaussian standard deviations on each side and are not two-sided 95% intervals. The two effective charge differences are treated separately.

The residuals are 0.541 and −0.358 standard deviations from zero. The constrained best-fit decay amplitudes are $\widehat{B}_b = \max(0, -y_b)$. Relative to $B_b = 0$, their reductions of the Gaussian squared residual are 0 and 0.1284, respectively. Neither summary provides significant evidence of additional radiation. The calculation restricts a declared effective scalar branch; it does not confirm the scalar's existence or identify the mother construction.

Three further steps would convert this conditional constraint into a test of common fundamental coefficients. Section 20 now implements the first for a specified conditional coupling and explains why its identification with the original mother branch remains restricted. In general, first solve the stellar interior and matching equations for the same matter couplings and equation-of-state family, obtaining $\alpha_A(\theta, N_A, \mathcal{E}_A, \varphi_\infty)$, the scalar mass, and their uncertainties. Second, propagate the same coefficients into the timing model, conservative orbit, radiation, kinematic corrections, and any variation of G. Third, combine distinct binary systems and static-force or clock observations using a shared parameter likelihood with independent nuisance parameters. Choosing each charge to fit its own residual would not complete these steps.

A gravitational-wave polarization test requires an additional response calculation. For detector I, a possible scalar breathing component enters as

$$h_I = F_I^{+} h_{+} + F_I^{\times} h_{\times} + F_I^{\mathrm{b}} h_{\mathrm{b}} + n_I.$$

The source dynamics must predict h_{b}, its propagation, and its coupling to the detector. Detector geometry, sky position, calibration, and noise determine whether this component can be separated from tensor signals. Nearly aligned detectors cannot generally identify three independent polarization amplitudes without further assumptions. Massive scalars may also have a longitudinal response. In many scalar models an isolated stationary black hole has zero scalar charge, so a binary-black-hole signal is not automatically the most sensitive dipole source. A tensor-only ringdown comparison therefore does not constitute a breathing-mode measurement. The published binary constraints above are the observational result established here; a scalar waveform analysis requires these further physical inputs.

The historical J0348 input above is not the latest timing determination. Section 20 treats the newer result and the dependence of its revised masses on the GR decay assumption.

20. Stellar charges from common couplings and their observational transfer

A scalar charge measures how the total mass of a body responds to its ambient scalar field. For a star, the total mass contains gravitational binding energy as well as the rest energy of its constituents. Its charge must therefore be obtained from a stellar boundary-value problem before it is used in a radiation calculation. We carry out this step for an explicit conditional matter coupling, compare two prescribed equations of state, and transfer the resulting charges to three published binary summaries. We then examine whether that conditional model is a realization of the original common-weight scalar branch. The last question is essential: solving the stellar equations does not select their fundamental couplings.

The stellar equations and the fixed-baryon definition of charge belong to established scalar–tensor theory [51]. Batrakov et al. [11] already combine stellar response grids with a common-parameter pulsar timing model. The calculation here implements that physical interface within the present normalization; it does not introduce a new theory of stellar scalarization.

20.1. *A declared matter branch and its units.* Write $\varphi = \sqrt{2} M_{\mathrm{P}} x$, so that x is dimensionless. In geometrized units $G_* = c = 1$, consider

$$S = \frac{1}{16\pi} \int \sqrt{-g}\, [R - 2(\nabla x)^2] d^4x + S_m[A(x)^2 g, \Psi], \qquad A(x) = e^{a_0 x}. \quad (1225)$$

The numerical example fixes

$$a_0 = 10^{-3}, \qquad \frac{d^2 \log A}{dx^2} = 0, \qquad x_\infty = 0,$$

and a zero scalar potential. These values define a massless, constant-coupling benchmark. They were not obtained by fitting any of the orbital-decay residuals below. The assumed Jordan-frame equation of state has no additional explicit dependence on x. This last assumption excludes, for example, a scalar-dependent nuclear scale unless its effect has already been incorporated consistently into the matter action.

In physical units, weakly bound bodies measure $G_N = G_* A(x_\infty)^2(1 + a_0^2)$. Thus the calculation uses $G_* = G_N/(1 + a_0^2)$, rather than silently identifying both constants. A cgs rest-mass density or energy density divided by c^2 is converted to geometrized inverse-square kilometres by multiplication by $10^{10} G_*/c^2$. A solar mass corresponds to $G_* M_\odot/(10^5 c^2)$ kilometres. These conversions distinguish the stellar units from the observed period P_b in seconds.

20.2. *Interior equations and the regular centre.* Let

$$ds^2 = -e^{\nu(r)} dt^2 + (1 - 2m(r)/r)^{-1} dr^2 + r^2 d\Omega^2,$$
$$\psi = x', \qquad h(p) = \int_0^p \frac{d\widetilde{p}}{\varepsilon(\widetilde{p}) + \widetilde{p}}.$$

Here r is the Einstein-frame areal radius, ρ is the Jordan-frame rest-mass density, and ε and p are its total energy density and pressure in geometrized units. The scalar stress contributes to the gravitational mass. The field equations give

$$m' = 4\pi r^2 A^4 \varepsilon + \tfrac{1}{2} r(r - 2m)\psi^2, \tag{1226}$$

$$\nu' = \frac{2(m + 4\pi r^3 A^4 p)}{r(r - 2m)} + r\psi^2, \qquad x' = \psi, \tag{1227}$$

$$\psi' = \frac{4\pi r A^4}{r - 2m}[a_0(\varepsilon - 3p) + r\psi(\varepsilon - p)] - \frac{2(r - m)}{r(r - 2m)}\psi, \tag{1228}$$

$$h' = -\tfrac{1}{2}\nu' - a_0\psi, \qquad M_b' = \frac{4\pi r^2 A^3 \rho}{\sqrt{1 - 2m/r}}. \tag{1229}$$

The factor A^3 in the conserved baryon mass M_b is the spatial volume conversion. Replacing it by A^4, or holding the gravitational mass fixed when differentiating the charge, changes the physical problem. The enthalpy equation follows from $p' = -(\varepsilon + p)(\nu'/2 + a_0\psi)$.

At a regular centre, prescribe $h_c > 0$ and x_c, with $m(0) = M_b(0) = \psi(0) = 0$. Put

$$s_c = \frac{4\pi}{3} A_c^4 a_0(\varepsilon_c - 3p_c), \qquad g_c = 4\pi A_c^4(\varepsilon_c/3 + p_c).$$

The starting expansions are

$$m(r) = \tfrac{4\pi}{3} A_c^4 \varepsilon_c r^3 + O(r^5), \qquad M_b(r) = \tfrac{4\pi}{3} A_c^3 \rho_c r^3 + O(r^5),$$
$$x(r) = x_c + \tfrac{1}{2} s_c r^2 + O(r^4), \qquad \psi(r) = s_c r + O(r^3),$$
$$h(r) = h_c - \tfrac{1}{2}(g_c + a_0 s_c) r^2 + O(r^4), \qquad \nu(r) = \nu_c + g_c r^2 + O(r^4).$$

Integration stops at the first surface $h(R) = 0$. A central scalar shooting condition enforces $x_\infty = 0$; the additive constant in ν is fixed by $\nu(\infty) = 0$. The physical surface radius is $R_J = A(x_s)R$. For a specified mass, the central enthalpy selects the stellar configuration. It is not selected from a radiation residual.

20.3. *Thermodynamically consistent matter models.* For neutron stars we use the SLy and AP4 piecewise-polytropic fits of Read et al. [135]. In cgs notation set $\bar{p} = p/c^2 = K_i \rho^{\Gamma_i}$. The cold first law requires

$$\frac{\varepsilon}{c^2} = (1 + b_i)\rho + \frac{K_i \rho^{\Gamma_i}}{\Gamma_i - 1}, \qquad h = \log\left[1 + b_i + \frac{\Gamma_i K_i \rho^{\Gamma_i - 1}}{\Gamma_i - 1}\right]. \tag{1230}$$

At a joining density ρ_i, pressure continuity determines the neighbouring K_i, and energy continuity gives

$$b_{i+1} = b_i + \frac{K_i \rho_i^{\Gamma_i - 1}}{\Gamma_i - 1} - \frac{K_{i+1} \rho_i^{\Gamma_{i+1} - 1}}{\Gamma_{i+1} - 1}.$$

Consequently $d\varepsilon/d\rho = (\varepsilon + p)/\rho$ and $dp/d\varepsilon = \Gamma_i p/(\varepsilon + p)$ on each piece. Continuity is imposed using the exact intersections of the printed polytropes; the rounded joining densities are not independently imposed.

The four crust pairs (K_i, Γ_i), with K_i in the units of p/c^2, are

$$(6.80110 \times 10^{-9}, 1.58425), \quad (1.06186 \times 10^{-6}, 1.28733),$$
$$(53.2697, 0.62223), \quad (3.99874 \times 10^{-8}, 1.35692).$$

For the three core pieces, at joining densities $\rho_1 = 10^{14.7}$ and $\rho_2 = 10^{15}$ $\mathrm{g\,cm^{-3}}$, the parameters are

	$\log_{10}[p(\rho_1)/(\mathrm{dyn\,cm^{-2}})]$	Γ_1	Γ_2	Γ_3
SLy	34.384	3.005	2.988	2.851
AP4	34.269	2.830	3.445	3.348

These are two prescribed approximations to possible matter equations of state, not a statistical determination of the actual neutron-star equation of state. In particular, the fits must not be extrapolated beyond their causal range without examination.

For white dwarfs we use a separate, explicit cold electron model with mean mass per electron $2m_u$. Let $y = p_F/(m_e c)$, $K_e = (m_e c/\hbar)^3/(3\pi^2)$, and

$\eta = m_e/(2m_u)$. Then

$$\rho = 2m_u K_e y^3, \qquad h = \log[1 + \eta(\sqrt{1+y^2} - 1)], \tag{1231}$$

$$\frac{p}{c^2} = K_e m_e I(y), \quad I(y) = \int_0^y \frac{z^4\,dz}{\sqrt{1+z^2}} = \frac{y(2y^2-3)\sqrt{1+y^2} + 3\,\operatorname{arsinh} y}{8}, \tag{1232}$$

$$\frac{\varepsilon}{c^2} = \rho e^h - \frac{p}{c^2}. \tag{1233}$$

The small-y expansion $I(y) = y^5/5 - y^7/14 + y^9/24 - 5y^{11}/176 + 35y^{13}/1664 + O(y^{15})$ avoids subtraction of nearly equal terms. This model includes the electron kinetic energy but omits temperature, envelopes, Coulomb corrections and nuclear composition effects beyond the specified mass per electron. Its radius is therefore not an independent fit to the observed white dwarf.

20.4. *Exterior matching and two definitions of charge.* In the massless exterior,

$$x(r) = x_\infty - \frac{a_A M}{r} + O(r^{-2}), \qquad a_A = \left.\frac{\partial \log M}{\partial x_\infty}\right|_{M_b}, \qquad \alpha_A = \frac{a_A}{\sqrt{2}}.$$

The last equality returns to the canonical charge in (1213). The mass derivative uses the same matter equation of state and baryon mass along a neighbouring family of solutions. It assumes that this family exists and is differentiable.

At the surface define

$$v_s = R\psi_s^2 + \frac{2m_s}{R(R-2m_s)}, \qquad a_A = \frac{2\psi_s}{v_s}, \qquad q_s = \sqrt{1+a_A^2}.$$

Exact vacuum matching [51] gives

$$\widehat{\nu}_s = -\frac{2}{q_s}\operatorname{artanh}\frac{q_s}{1 + 2/(Rv_s)}, \tag{1234}$$

$$x_\infty = x_s - \tfrac{1}{2}a_A\widehat{\nu}_s, \qquad M = \tfrac{1}{2}v_s R^2\sqrt{1-2m_s/R}\,e^{\widehat{\nu}_s/2}. \tag{1235}$$

An independent exterior integration uses $z = 1/r$ and $Q = r^2\psi$:

$$\begin{aligned} \frac{dm}{dz} &= -\tfrac{1}{2}Q^2(1-2mz), & \frac{dx}{dz} &= -Q, \\ \frac{dQ}{dz} &= \frac{2mQ}{1-2mz}, & \frac{d\nu}{dz} &= -\frac{2m}{1-2mz} - Q^2 z. \end{aligned} \tag{1236}$$

At $z = 0$, it returns $M = m(0)$, $x_\infty = x(0)$, and $a_A = Q(0)/M$. No finite outer-radius replacement for infinity is needed.

The scalar equation also displays the physical source of charge:

$$a_A M = 4\pi a_0 \int_0^R \frac{r^2 e^{\nu/2} A^4(\varepsilon - 3p)}{\sqrt{1-2m/r}}\,dr. \tag{1237}$$

Indeed, the derivative of $r^2 e^{\nu/2}\sqrt{1-2m/r}\,\psi$ is the integrand on the right, and its value at infinity is $a_A M$. The pressure contribution, the redshift and the binding energy explain why a compact star does not have the weak-binding charge a_0. Equation (1237) does not assert that charge decreases monotonically for every possible equation of state or scalar coupling.

20.5. *Computed charges and numerical comparisons.* Table 16 gives the computed response at the input masses. The coupling is identical in every row; each neutron-star equation of state is also used unchanged across all three systems.

System	$M_{\rm NS}/M_\odot$	$M_{\rm WD}/M_\odot$	$10^3 a_{\rm NS}^{\rm SLy}$	$10^3 a_{\rm NS}^{\rm AP4}$	$10^3 a_{\rm WD}$
J1738	1.4661	0.1810	0.643077	0.632443	0.999970
J0348 (2013)	2.0124	0.1720	0.336333	0.389325	0.999972
J2222	1.8200	1.3153	0.493726	0.496618	0.998566

Table 16. Synthetic stellar predictions at specified observational input masses, for $a_0 = 10^{-3}$. Charges use the dimensionless DEF convention $a_A = \sqrt{2}\alpha_A$. The J0348 mass is the historical optical input; the newer mass inference is treated separately below.

The neutron-star radii span approximately 10.54–11.66 km. All nine retained stellar configurations have a positive metric factor $1-2m/r$, subluminal sound speed and positive local mass slope along the chosen central-enthalpy sequence. The largest sampled squared sound speed is $0.9074c^2$. Positive mass slope is a branch diagnostic, not a complete radial-mode stability proof.

Three distinct numerical comparisons were performed. First, exact exterior matching and (1236) agree to within 1.34×10^{-15} in the recorded mass in kilometres, charge and asymptotic scalar components. Second, tighter integration tolerances change a charge by at most 9.86×10^{-12}; comparison with a different Runge–Kutta method gives at most 2.16×10^{-11}. Third, central differences of $\log M$ at fixed M_b, using $x_\infty = \pm 0.1$ and ± 0.05, agree with the asymptotic charge to relative error below 9.08×10^{-6}. Although these scalar increments are dimensionless, the corresponding changes of $\log A$ are only 10^{-4} and 5×10^{-5}. The zero-coupling equations give zero charge and reproduce a separately integrated GR mass to relative differences below 9.0×10^{-9}. These are measured numerical comparisons, not rigorous enclosures of the continuum solution or bounds on matter-model error.

20.6. *Transfer to a third binary without charge adjustment.* For a massless scalar and a Keplerian orbit, the leading dipole term is

$$\dot{P}_b^{\rm dip} = -\frac{4\pi^2 G_* \mu_b}{c^3 P_b}(a_A - a_B)^2 \frac{1 + e_b^2/2}{(1-e_b^2)^{5/2}}. \tag{1238}$$

The circular limit is (1217) after the charge conversion. The eccentricity factor follows by averaging the squared relative acceleration: $\langle r^{-4}\rangle = a_b^{-4}(1 + e_b^2/2)/(1-e_b^2)^{5/2}$, using $dt = r^2 d\theta/\sqrt{G_{AB} M_b a_b (1-e_b^2)}$.

The additional target J2222–0137 has $P_b = 2.44576436$ days and $e_b = 0.00038092$. Guo et al. [86], Table 4, give the DDGR input masses 1.820(14) and 1.3153(56) in solar units. In that fit an extra $\dot{P}_b$ is a fitted parameter; the masses are not fixed by imposing that the total observed decay equal the GR quadrupole prediction. Their Section 7 uses a GR contribution $-8.09(5)\times 10^{-15}$ and a residual $y = (-6.3 \pm 7.6)\times 10^{-15}$. These are still GR-based conservative timing inputs. Their use here is a weak-coupling approximation, not a full scalar–tensor refit of arrival times. The alternative 1.831(10) solar-mass estimate in the same paper comes from a different combined inference and is not substituted silently into this baseline.

System	$10^{15}\dot{P}_b^{\rm dip}$, SLy	$10^{15}\dot{P}_b^{\rm dip}$, AP4	$10^{15} y$	$10^{15}\sigma$
J1738 (2012)	−0.13017	−0.13805	2.0	3.7
J0348 (2013)	−1.53344	−1.29832	−16.6	46.32591
J2222 (2021)	−0.17906	−0.17702	−6.3	7.6

Table 17. Common-parameter leading-dipole predictions and published residual summaries. The first two observational inputs are those of Section 19; the third is from Guo et al. [86]. No row is a new observation.

The predicted dipoles are only 0.0233–0.0374 times the respective summary standard deviations. They are therefore much smaller than the quoted observational uncertainties. For a descriptive Gaussian comparison define

$$\Delta\chi_b^2 = \frac{(y_b - \dot{P}_b^{\rm dip})^2 - y_b^2}{\sigma_b^2}.$$

Across the two equations of state it is positive for J1738 (0.0393–0.0418) and slightly negative for the historical J0348 and J2222 summaries (absolute values below 0.039). Such small changes do not identify a scalar signal or discriminate the framework. All three comparisons are retrospective. Neither the published residual covariances nor a joint nuisance posterior are reconstructed here.

The J2222 residual also depends on the Galactic acceleration model. The models tabulated by Guo et al. give central excesses between −6.8 and −2.6,

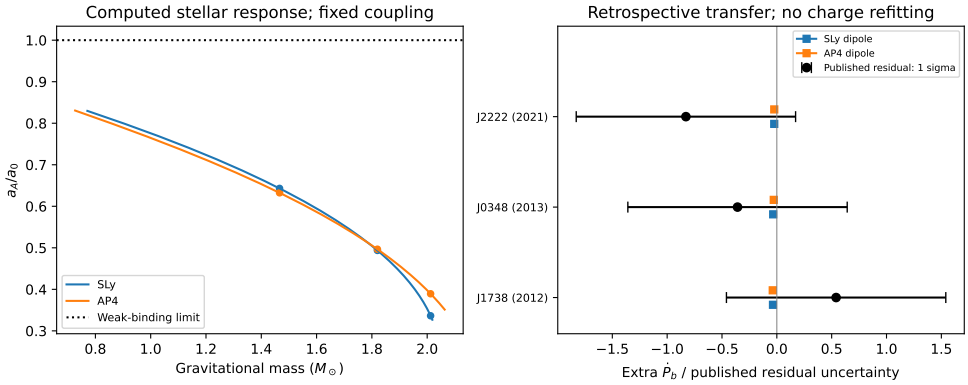


Figure 30. Left: computed neutron-star charge relative to the same fixed coupling for two prescribed equations of state; markers denote the input masses. Right: synthetic dipole predictions compared with real published residuals, each divided by its own quoted standard deviation. Black bars are one-standard-deviation summary errors. The J0348 comparison uses the historical 2013 inputs, not the newer GR-derived mass.

in units of 10^{-15}, with similar uncertainties. This variation exceeds the predicted dipole in Table 17. Rotational corrections, uncertain stellar interiors, conservative scalar timing effects and scalar corrections to tensor radiation must also be propagated before these leading terms are used for precision parameter inference.

20.7. *The newer J0348 result and the direction of the residual.* Saffer et al. [141] report $\dot{P}_b^{\rm obs} = (-2.17 \pm 0.07) \times 10^{-13}$. Their neutron-star mass $1.806(37)M_\odot$ and white-dwarf mass $0.154(3)M_\odot$ are inferred by combining the optical mass ratio with the assumption that orbital decay follows GR. Those masses cannot then be inserted as independent measurements in a test of the same decay relation. In particular, agreement produced this way is not an additional confirmation of either GR or the present scalar branch.

For the old optical masses, that paper quotes a GR prediction $(-2.593 \pm 0.078) \times 10^{-13}$. Direct subtraction of the two reported values gives

$$\begin{aligned} \delta\dot{P}_b &= 4.23 \times 10^{-14}, \\ \sigma_\delta &= \sqrt{0.07^2 + 0.078^2} \times 10^{-13} = 1.04805 \times 10^{-14}. \end{aligned} \tag{1239}$$

The ratio is approximately 4.04. This reproduces a comparison of the published summaries; it is not a joint new-gravity significance. The kinematic corrections and the old white-dwarf atmosphere and interior assumptions require consistent reassessment.

The sign already gives useful information. An outgoing positive-energy scalar dipole has $\dot{P}_b^{\rm dip} \le 0$. At fixed old masses, adding it increases the positive difference in (1239); it cannot explain that difference. The newer mass-model tension is therefore not evidence for this additional radiation channel. A defensible updated test requires masses constrained independently of the tested decay, or a joint matter and timing model that does not reuse a GR-derived mass as an independent input.

20.8. *Matching back to the original common-weight branch.* The massless example above is not automatically an exact reduction of the common-weight construction. To see the obstruction, denote its Jordan scalar by σ, write $F(\sigma) = e^{-b\sigma}$, and put $q = bM_{\rm P}$. For the metric scalar–tensor reduction at the stated vacuum, the canonical normalization and linear elementary-body coupling are

$$Z_0 = 1 + \tfrac{3}{2}q^2, \qquad \gamma = \frac{b}{\sqrt{Z_0}}, \qquad a_0 = \frac{\gamma M_{\rm P}}{\sqrt{2}}, \qquad a_0^2 = \frac{q^2}{2+3q^2}. \tag{1240}$$

The elementary weak-source Yukawa strength is a_0^2, not a_0. This matches a derivative of $A = F^{-1/2}$ at the vacuum; it does not make $\log A$ linear in the canonical scalar at every field value.

Retaining the original Cartan coefficients, the same branch has $V_C = 3M_{\rm P}^2/\ell^2$, and its vacuum-matched quadratic coefficient is $m_J^2 = m_\sigma^2 + b^2 V_C$. In units $\hbar = c = 1$,

$$(m_\varphi \ell)^2 = \frac{m_\sigma^2 \ell^2 + 3q^2}{1 + 3q^2/2} = 6a_0^2 + \frac{m_\sigma^2 \ell^2}{Z_0}. \tag{1241}$$

This relation concerns the minimally matched branch with those coefficients. Additional potential matching or additional fields can change it, but such a change is an extra physical specification.

Proposition 104 (A necessary common-weight dipole condition). *Assume $m_\sigma^2 \ge 0$, a single canonically normalized scalar, and* (1241)*. A strictly massless scalar then has $a_0 = 0$. More generally, suppose that the derivative expansion is used at a specified inverse length k_* with $\ell k_* \le \epsilon$. Propagating leading circular scalar-dipole radiation at frequency Ω_b requires*

$$|a_0| < \frac{\epsilon \Omega_b}{\sqrt{6}\, c k_*}. \tag{1242}$$

This is a necessary condition; it does not imply a nonzero source charge difference, an observable signal or uniform validity of the derivative expansion.

Proof. Equation (1241) implies $m_\varphi \ell \ge \sqrt{6}|a_0|$ in natural units. If the mass is zero, its two nonnegative squared contributions vanish. Restoring

units, set $\mu_\varphi = m_\varphi c/\hbar$. The circular-dipole threshold is $\mu_\varphi < \Omega_b/c$. Hence $\sqrt{6}|a_0| \le \mu_\varphi \ell < \Omega_b \ell/c \le \epsilon\Omega_b/(ck_*)$, which proves the condition. □

Here ℓ is finite and positive. In a family of models, the limit $m_\varphi \to 0$ by itself does not force $a_0 \to 0$ if $\ell \to \infty$ simultaneously. The sufficient dimensionless condition is $m_\varphi \ell \to 0$ in natural units, or fixed finite ℓ and vanishing physical mass. Such a joint limit must separately preserve the derivative expansion. Also, $m_\sigma = 0$ alone leaves $m_\varphi \ell = \sqrt{6}|a_0|$; it is not the massless physical-scalar limit. These are algebraic matching statements, not a proof that a time-dependent solution dynamically drives its coupling to zero.

For illustration only, choose $k_* = 1/R_{\rm NS}$ using the SLy benchmark radii and $\epsilon = 0.1$. The necessary upper values of $|a_0|$ are approximately 3.26×10^{-10}, 1.02×10^{-9}, and 4.55×10^{-11} for J1738, J0348 and J2222, respectively. At the benchmark $a_0 = 10^{-3}$, radiation would instead require $\ell > 0.02395$, 0.006914, and 0.1651 AU, incompatible with this illustrative stellar derivative-scale requirement. The radius choice is not a proof that all interior derivatives obey a uniform remainder bound. It makes the scale assumption and the resulting incompatibility explicit. In particular, the massless charge table must not be presented as a prediction of the unaltered minimal Cartan branch.

There is a second matching issue for composite matter. The common weight also changes gauge coefficients. A scalar-dependent nuclear equation of state need not reduce to $S_m[A^2 g, \Psi]$ with fixed Jordan masses. For a zero-temperature fluid with Jordan energy density $\varepsilon_J(n_J, x)$, vary x at fixed Einstein-frame conserved particle current. Then $n_J = A^{-3} n_E$, and

$$\partial_x[A^4 \varepsilon_J(A^{-3} n_E, x)]\big|_{n_E} = A^4 \left[a(x)(\varepsilon_J - 3p_J) + \partial_x \varepsilon_J|_{n_J}\right], \tag{1243}$$

where $a(x) = \partial_x \log A$ and $p_J = n_J \partial_{n_J} \varepsilon_J - \varepsilon_J$. The identity follows by the chain rule. The second term is absent in the benchmark but is generally present when the same scalar changes nuclear or electromagnetic binding energies. It enters the scalar source and requires a consistently varied stellar matter model. Assigning a new effective charge to each observed star does not supply this missing common matter matching.

20.9. *What the common-parameter calculation establishes.* For a specified action, equation of state and background, the calculation now determines charges from stellar structure and transfers them across different binaries without fitting individual charges. It also exhibits a concrete restriction on using the original mother coefficients in this channel. Neither step selects b, ℓ, the scalar potential or the nuclear scalar response from independent physical information.

For example, keeping the SLy equation of state and the J1738 input mass fixed, the alternative couplings $a_0 = 5 \times 10^{-4}$ and $a_0 = 2 \times 10^{-3}$ give

charges approximately 3.21538×10^{-4} and 1.28616×10^{-3}, respectively. The stellar equations are solvable for both. Their existence does not choose one coupling. The subsequent physical task is to determine the canonical scalar potential and composition-dependent matter response from one specified mother action, constrain its remaining parameters without the target orbital decay, and propagate those same parameters through the conservative timing and radiative equations. Present observational compatibility of the conditional benchmark is not evidence for a uniquely identified mother theory.

20.10. *Radiative thresholds, evanescent fields and static range.* It is useful to make the propagation restriction explicit rather than replace it by a qualitative suppression factor. For a stable linear massive scalar in an asymptotically flat exterior, a Fourier component of frequency $\omega > 0$ has

$$k^2 = \frac{\omega^2}{c^2} - \mu_\varphi^2, \qquad \mu_\varphi = \frac{m_\varphi c}{\hbar}.$$

If $k^2 > 0$, outgoing waves can carry energy to infinity. For the leading circular dipole, $\omega = \Omega_b$, and the flux factor is

$$f_b = \left[1 - \left(\frac{m_\varphi c^2}{\hbar \Omega_b}\right)^2\right]_+^{3/2}.$$

If $k^2 < 0$, the steady Fourier component is evanescent: $\varphi_\omega \propto e^{-\kappa r}/r$, with $\kappa = \sqrt{\mu_\varphi^2 - \omega^2/c^2}$. Its time-averaged outgoing flux at spatial infinity vanishes. The decay exponent depends on distance through κr; it is not universally $m_\varphi c^2/(\hbar\Omega_b)$. The threshold value also has zero leading flux. Transient signals with broader frequency support require their own spectral calculation.

The static Yukawa field instead contains $e^{-\mu_\varphi r}$, with reduced Compton range $\lambda_\varphi = 1/\mu_\varphi$. This mass-induced finite range is not a nonlinear screening mechanism. At the three dipole thresholds, the ranges are approximately 9.777, 2.822, and 67.40 AU for J1738, J0348 and J2222. Thus a mass just above a binary's dipole threshold need not correspond to a short range on laboratory scales.

For fixed ℓ and $m_\sigma = 0$, (1241) becomes the lower boundary

$$m_\varphi c^2 = \frac{\sqrt{6}\hbar c}{\ell}|a_0|, \qquad |a_0|_{\rm cross} = \frac{\ell \Omega_b}{\sqrt{6}c}.$$

For general $m_\sigma^2 \geq 0$ it is a lower bound, and the coupling crossing is only a necessary condition for an open dipole channel. Figure 31 displays this distinction.

A closed leading dipole channel does not exclude every binary signature. An eccentric orbit has harmonics $n\Omega_b$, and other scalar multipoles can radiate at their own frequencies. For example, $\Omega_b < m_\varphi c^2/\hbar < 2\Omega_b$ closes the fundamental

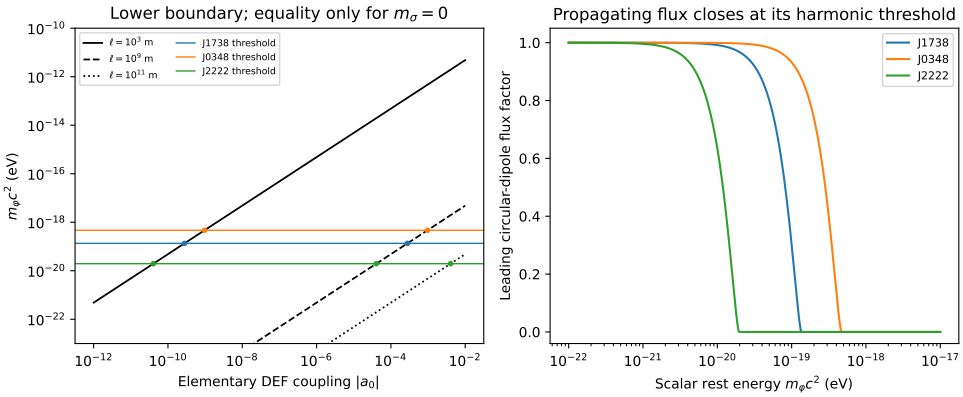


Figure 31. Left: conditional common-weight mass–coupling lower boundaries at three specified values of ℓ; equality assumes $m_\sigma = 0$. Horizontal lines give the three binary dipole thresholds, and dots mark intersections within the displayed coupling range. The large values of ℓ are parameter illustrations, not viable stellar derivative expansions. Right: the leading circular-dipole propagation factor for each binary. These are analytic model curves, not measured signals.

dipole but does not kinematically close a component at $2\Omega_b$. Whether such a component is sourced, and whether it is measurable, requires its amplitude and detector response. Static forces and conservative orbital changes also remain separate observables. No claim that all binary signals disappear above one dipole threshold follows.

21. Composite-matter response and identifiable stellar predictions

A comparison across stars becomes predictive only when their scalar charges follow from the same matter theory. A measured or tabulated equation of state at one scalar background does not specify its response to a change of that background. This section identifies the missing derivatives, gives their linear transfer to stellar charges, and measures the separation of the preceding benchmark predictions from GR. The transfer calculation extends the conditional stellar example; it does not supply a new nuclear equation of state or select a fundamental coupling. Composite scalar charges and stellar sensitivities have the established antecedents [50] and [51].

21.1. *What the mother relation fixes.* Use $x = \varphi/(\sqrt{2}M_{\rm P})$, $a_0 = \partial_x \log A|_0$, and $\mu_\varphi = m_\varphi c/\hbar$. Thus a_0 is dimensionless and μ_φ has units of inverse length.

In natural units the original common-weight relation can be inverted:

$$q^2 = \frac{2a_0^2}{1-3a_0^2}, \qquad Z_0 = \frac{1}{1-3a_0^2}, \qquad |a_0| < \frac{1}{\sqrt{3}}, \\ m_\sigma^2 = \frac{\mu_\varphi^2 - 6a_0^2/\ell^2}{1-3a_0^2}. \tag{1244}$$

Here m_σ is also expressed as an inverse length. The sign of q agrees with the sign of a_0 under the previously fixed scalar orientation. For any finite positive ℓ, the choices $\mu_\varphi \ell \geq \sqrt{6}|a_0|$ give nonnegative m_σ^2. Consequently the relation restricts a continuous parameter family. It does not provide a numerical value for a_0, ℓ, or μ_φ. Stability, a controlled derivative expansion, matter matching, and observations impose further conditions. Selecting a member using an orbital-decay residual would be calibration, not a prediction of that residual.

21.2. *From gauge coefficients to a matter derivative.* The distinction between an elementary coupling and a hadronic response can already be seen in one-loop running. Fix a Jordan-frame reference scale U above the top threshold, choose six active quarks there, and put $H_U(x) = g_s^{-2}(U,x)$. All reference scales and the renormalization prescription in the following derivative are held fixed. With $b_{N_f} = 11 - 2N_f/3$, continuity of the one-loop inverse coupling at the three heavy-quark thresholds gives

$$\log \Lambda_3 = \frac{7}{9}\log U - \frac{8\pi^2}{9} H_U + \frac{2}{27}\log(m_c m_b m_t) - \frac{8\pi^2}{9}\Delta_{\mathrm{fin}}. \tag{1245}$$

The logarithms use one fixed reference unit; their dimensionful powers sum to one, so the exponentiated formula has mass dimension one. Δ_{fin} denotes the net additive finite matching correction to the inverse coupling; it is zero in the strict one-loop continuity approximation. To obtain the formula, run successively with $b_6 = 7$, $b_5 = 23/3$, $b_4 = 25/3$, and $b_3 = 9$, and use $\log \Lambda_3 = \log \mu - 8\pi^2 g_s^{-2}(\mu)/9$. The intermediate low scale μ cancels.

At the common-weight matching point, $\partial_x \log H_U = -2a_0$. Define $d_\Lambda = \partial_x \log \Lambda_3|_0$ and $\kappa_h^J = \partial_x \log m_{h,J}|_0$. Differentiating (1245) yields

$$d_\Lambda = \frac{16\pi^2}{9 g_s^2(U,0)} a_0 + \frac{2}{27}\sum_{h=c,b,t} \kappa_h^J - \frac{8\pi^2}{9}\,\partial_x \Delta_{\mathrm{fin}}|_0\,. \tag{1246}$$

This is a leading matching relation for the stated particle content. It is not a nonperturbative determination of nuclear matter. Moving the reference scale with the scalar adds its scale derivative; crossing a new threshold changes the formula. Heavy-quark mass slopes, finite matching terms, light-quark matrix elements and nuclear interactions must be determined consistently. The equality $\partial_x \log H_U = -2a_0$ is imposed at the common-weight matching scale, not at every scale after running.

At zero temperature, express a thermodynamically complete Jordan energy density as

$$\varepsilon_J(n,x) = \Lambda(x)^4 f\Big(\frac{n}{\Lambda(x)^3}, X_1(x), \dots, X_s(x)\Big), \qquad p_J = n\partial_n\varepsilon_J - \varepsilon_J. \quad (1247)$$

Here n is conserved baryon number per proper volume, and the dimensionless ratios X_p include the relevant quark and lepton mass ratios, electromagnetic coupling and any other independent matter parameters retained by the approximation. Any additional dimensionful scale must be represented by a ratio; omitting one would invalidate this dimensional decomposition. Put $d_p = \partial_x \log X_p|_0$ and $\mathcal{E}_p = \partial_{\log X_p}\varepsilon_J|_0$. At fixed n, the chain rule gives

$$\partial_x\varepsilon_J|_n = d_\Lambda(\varepsilon_0 - 3p_0) + \sum_p d_p\mathcal{E}_p. \quad (1248)$$

Indeed the scale derivative is $4\varepsilon_0 - 3n\partial_n\varepsilon_0 = \varepsilon_0 - 3p_0$.

Combining this identity with (1243), at $A(0) = 1$ the linear matter source is

$$J_0 = (a_0 + d_\Lambda)(\varepsilon_0 - 3p_0) + \sum_p d_p\mathcal{E}_p. \quad (1249)$$

The conformal contribution a_0 and the Jordan mass-scale contribution d_Λ are distinct. Counting the conformal factor once in d_Λ and again in a_0 would give a wrong charge. If composition is determined by smooth constrained chemical equilibrium, the stationary composition terms cancel in the first derivative at fixed baryon density. This envelope argument requires composition constraints independent of x; phase changes require one-sided derivatives or explicit phase matching.

Proposition 105 (A background equation of state does not identify its scalar source). *Let $\varepsilon_0(n)$ be a differentiable background energy density on a positive-density interval. For each constant d, define*

$$\varepsilon_d(n,x) = e^{4dx}\varepsilon_0(e^{-3dx}n). \quad (1250)$$

Every member has the same energy density and pressure at $x = 0$, but its scalar derivative is $d(\varepsilon_0 - 3p_0)$. Thus background energy and pressure data alone cannot determine that derivative wherever $\varepsilon_0 - 3p_0 \neq 0$.

Proof. At $x = 0$, both the energy density and its density derivative agree with those of ε_0; hence so does $n\partial_n\varepsilon - \varepsilon$. Differentiation with respect to x gives $d(4\varepsilon_0 - 3n\partial_n\varepsilon_0) = d(\varepsilon_0 - 3p_0)$. □

On a compact density interval, strict local positivity and strict sound-speed inequalities persist for sufficiently small $|x|$ by continuity. This is a counterexample to identification from the background EOS, not a claim that every member follows from the full mother action. A completed microscopic

matching could select or exclude members. A second useful response direction is $\varepsilon(n, x) = \varepsilon_0(n) + dx m_b n$: its scalar source changes by $dm_b n$, whereas its pressure has zero x derivative. Here m_b is a fixed reference baryon rest mass.

21.3. *A linear response map for stellar charges.* To separate matter uncertainty from gravitational propagation, use a regular GR stellar background

$$ds^2 = -N(r)^2 dt^2 + \frac{dr^2}{f(r)} + r^2 d\Omega^2, \qquad f(r) = 1 - \frac{2\mathfrak{m}(r)}{r} > 0, \qquad N(\infty) = 1. \tag{1251}$$

In this subsection $G_* = c = 1$, so energy densities have dimension length^{-2}. Linearize about an unscalarized background with small source couplings and no matter-induced scalar instability. Retaining a specified nonnegative scalar mass, the radial equation is

$$(Px')' - \mu_\varphi^2 W x = 4\pi W J_0, \qquad P = Nr^2\sqrt{f}, \qquad W = \frac{Nr^2}{\sqrt{f}}. \tag{1252}$$

This follows by writing the covariant scalar wave operator in divergence form. Metric and fluid backreaction are neglected at this retained order. A finite matter susceptibility multiplying x, a nonlinear scalarized branch, or an environment-dependent effective mass changes the operator and must be included before applying this map.

For a fixed nonnegative μ_φ^2, regularity at the centre and a vanishing asymptotic field make a solution unique in the finite-energy decaying class. In fact the difference u of two solutions satisfies the homogeneous equation. Multiplication by u and integration, with vanishing endpoint term $[Puu']_0^\infty$, give

$$\int_0^\infty P(u')^2\, dr + \mu_\varphi^2 \int_0^\infty W u^2\, dr = 0. \tag{1253}$$

Both terms are nonnegative. For zero mass the remaining constant is removed by the asymptotic condition. This proves uniqueness, not an existence or error theorem for an arbitrary singular background.

In the massless case the flux outside the stellar surface is constant. Define the linear DEF charge by $x(r) = -a_A^{\mathrm{lin}}\mathfrak{M}/r + O(r^{-2})$, where $\mathfrak{M} = \mathfrak{m}(R)$. Integrating (1252) gives

$$a_A^{\mathrm{lin}} = \mathcal{K}_A[J_0], \qquad \mathcal{K}_A[q] = \frac{4\pi}{\mathfrak{M}} \int_0^R \frac{Nr^2}{\sqrt{f}}\, q(r)\, dr. \tag{1254}$$

The sign agrees with a positive source and a negative asymptotic scalar field. The same solution satisfies $x' = a_A^{\mathrm{lin}}\mathfrak{M}/(r^2 f)$ in the exterior, providing an independent way to compute the charge. The factors of lapse and proper radial volume cannot be omitted for a compact star.

Consequently the matter-to-charge map is

$$a_A^{\mathrm{lin}} = (a_0 + d_\Lambda)C_A^{\mathrm{tr}} + \sum_p d_p C_A^p, \quad C_A^{\mathrm{tr}} = \mathcal{K}_A[\varepsilon_0 - 3p_0], \quad C_A^p = \mathcal{K}_A[\mathcal{E}_p]. \tag{1255}$$

The same coefficient vector acts on every star. Different masses and equations of state change the response rows, not the microscopic coefficients. For a massive scalar, the linear source decomposition remains useful, but one must solve (1252) with the decaying massive exterior and use its correctly normalized transfer function. There is no nonzero massless $1/r$ asymptotic charge to extract in that case.

21.4. *Computed response rows and finite-coupling checks.* Using the same Read EOS inputs [135] and target masses as the preceding stellar calculation, we integrate the GR equations together with the two source responses $q_{\mathrm{tr}} = \varepsilon_0 - 3p_0$ and $q_b = m_b n$. The latter is a basis direction for a rest-energy perturbation, not an assigned quark or nuclear sensitivity. Hydrostatic balance implies $N(r) = \sqrt{f(R)}e^{-h(r)}$, where $h = \int_0^p dp/(\varepsilon + p)$. This identity normalizes the lapse without a second lapse shooting problem.

System	EOS	$M/M_\odot$	C_A^{tr}	C_A^b
J1738	SLy	1.4661	0.643076	0.777694
J1738	AP4	1.4661	0.632443	0.773384
J0348, historical	SLy	2.0124	0.336327	0.600851
J0348, historical	AP4	2.0124	0.389323	0.637891
J2222	SLy	1.8200	0.493724	0.691873
J2222	AP4	1.8200	0.496616	0.697720

Table 18. Calculated dimensionless response coefficients on GR backgrounds. These are model outputs, not observed stellar charges. The two columns respond to different common matter derivatives.

The cold white-dwarf model gives trace coefficients approximately 0.999970, 0.999972, and 0.998566 for the three companion masses. Across all nine configurations, the volume-integral and exterior-flux trace coefficients differ by at most 3.35×10^{-11}; the largest change between the two numerical integration methods is 1.50×10^{-9}. These comparisons measure floating-point agreement, not a rigorous enclosure or a nuclear uncertainty.

The largest difference between C_A^{tr} and the previous nonlinear charge divided by $a_0 = 10^{-3}$ is 5.3883×10^{-6}, for the heavier SLy star. Reducing the coupling to 5×10^{-4} reduces that difference to 1.3489×10^{-6}. The approximately fourfold reduction is consistent with the quadratic correction to the charge divided by a_0 on this symmetric constant-coupling branch. It must not be

reported as an integration error. The computation supplies response rows but leaves the actual nuclear derivatives $\mathcal{E}_p$ and their common coefficients to microscopic matching.

21.5. *How much separation do the current predictions provide?* Before interpreting agreement as support, compare the sizes of the predicted differences with the measurement errors. Consider two simple Gaussian hypotheses with means f_0, f_1 and a common known positive covariance Σ. Their mean separation and relative entropy are

$$D^2 = (f_1 - f_0)^\top \Sigma^{-1} (f_1 - f_0), \qquad D_{\mathrm{KL}}(P_1 \| P_0) = \tfrac{1}{2} D^2. \tag{1256}$$

Whitening the data and projecting onto the mean difference reduces the optimal likelihood-ratio test to two unit-variance normal variables whose means are separated by D. With equal prior probabilities, its minimum average classification error is $\Phi(-D/2)$, where Φ is the standard normal cumulative distribution function. This is a design property of the two specified distributions, not a significance assigned to the observed residual.

For the three historical summaries, take the quoted marginal errors as independent and hold the masses and EOS fixed. Using the preceding massless $a_0 = 10^{-3}$ predictions gives

comparison	D	D_{KL}	$\Phi(-D/2)$
SLy benchmark versus GR	0.053745	0.0014443	0.48928
AP4 benchmark versus GR	0.052153	0.0013600	0.48960
SLy versus AP4 benchmarks	0.005510	0.00001518	0.49890

(1257)

Thus these declared predictions are nearly indistinguishable with this summary error model. Uniformly reducing all three errors by a factor of about 93 or 96, while holding the respective signals fixed, would give $D = 5$ against GR. That conditional scaling is neither a forecast of achievable precision nor an observed five-standard-deviation detection. It also does not turn the massless benchmark into the original minimal mother branch. Correlated errors, EOS uncertainty, revised masses and a complete timing likelihood must be treated before a physical inference.

For completeness, if freely fitted linear nuisance shifts span the columns of a whitened matrix B, profiling those shifts replaces a whitened mean difference z by

$$z_\perp = (I - BB^+)z, \qquad D^2_{\mathrm{prof}} = \|z_\perp\|^2 \le \|z\|^2, \tag{1258}$$

where B^+ is the Moore–Penrose inverse. The inequality follows because BB^+ is an orthogonal projection. Constrained nuisance parameters and independent calibration information require their actual likelihood; they are not represented by an arbitrary projection.

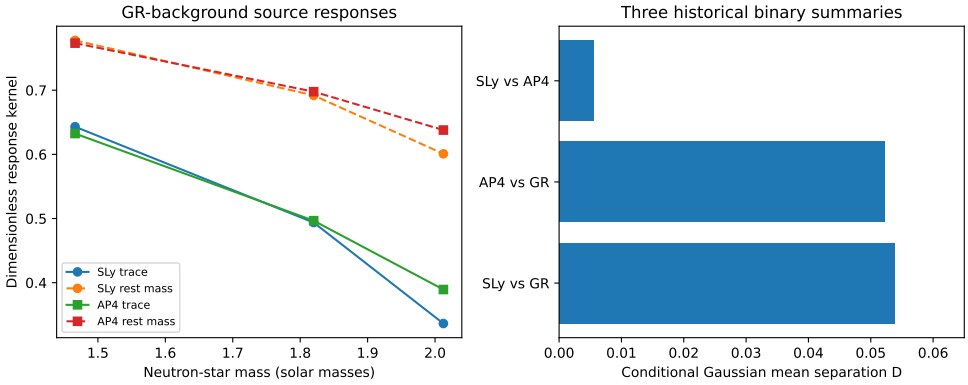


Figure 32. Left: computed neutron-star response rows for a trace source and a rest-energy source. Right: conditional Gaussian separations of the previous fixed benchmark predictions using three historical timing summaries. The panels show calculated response and design quantities; neither panel presents a newly detected fifth force.

21.6. *Eliminating common responses across three binaries.* Unknown microscopic parameters need not prevent every prediction: a relation between observables can remain after they are eliminated. The important question is whether that relation survives the matter responses allowed by the theory. We examine this question using the two calculated response columns in Table 18. This is a conditional truncation of (1249); it does not identify the missing nuclear derivatives with those columns.

Let $q_i = a^{\mathrm{lin}}_{\mathrm{NS},i} - a^{\mathrm{lin}}_{\mathrm{WD},i}$ denote a signed charge difference. Retain the common source $J_0 = \theta_1(\varepsilon_0 - 3p_0) + \theta_2 m_b n$, where $\theta_1 = a_0 + d_\Lambda$ and θ_2 is a separate rest-energy response coefficient. Then

$$q_i = B_{i1}\theta_1 + B_{i2}\theta_2, \qquad B_{i1} = C^{\mathrm{tr}}_{\mathrm{NS},i} - C^{\mathrm{tr}}_{\mathrm{WD},i}, \quad B_{i2} = C^{b}_{\mathrm{NS},i} - C^{b}_{\mathrm{WD},i}. \tag{1259}$$

No coefficient is chosen separately for an individual star. Number the historical systems J1738, J0348 and J2222 by $1, 2, 3$, and write B_{12} for the first two rows. If B_{12} is invertible, define the row $\lambda = B_{3,:}B_{12}^{-1}$. Direct substitution gives

$$q_3 = \lambda_1 q_1 + \lambda_2 q_2. \tag{1260}$$

Thus signed calibration of the first two charge differences determines the third without determining either coefficient from the third system.

Proposition 106 (A squared-signal relation with two common responses). *Assume* (1259), *an invertible* B_{12}, *and a retained dipole model* $s_i = -\mathscr{K}_i q_i^2$, *with known* $\mathscr{K}_i > 0$. *Put* $y_i = -s_i/\mathscr{K}_i$. *For unrestricted real* θ_1, θ_2, *the three*

signals are attainable if and only if $y_i \geq 0$ *and*

$$\left(y_3 - \lambda_1^2 y_1 - \lambda_2^2 y_2\right)^2 - 4\lambda_1^2\lambda_2^2 y_1 y_2 = 0. \tag{1261}$$

In particular, the first two exact squared signals give at most two values for the third:

$$y_3 = \left(\lambda_1\sqrt{y_1} \pm \lambda_2\sqrt{y_2}\right)^2. \tag{1262}$$

Additional restrictions on the coefficients can remove branches; they cannot add values to this set.

Proof. Squaring (1260) and isolating the cross term gives the necessity of (1261). For sufficiency, the left side factors as

$$\left[y_3 - (\lambda_1\sqrt{y_1} + \lambda_2\sqrt{y_2})^2\right]\left[y_3 - (\lambda_1\sqrt{y_1} - \lambda_2\sqrt{y_2})^2\right].$$

One factor must vanish. Select $q_1 = \sqrt{y_1}$ and the corresponding sign of $q_2 = \pm\sqrt{y_2}$, and solve $\theta = B_{12}^{-1}(q_1, q_2)^\top$. Equation (1260) gives the required third square. The argument also covers a zero signal or a zero component of λ. □

The square roots in this proposition apply to exact model means. An observed timing residual can be positive because of measurement noise or other contributions. Taking its negative square root, or discarding that observation, is not a valid implementation. Inference must use the likelihood of the original timing observables with their nuisance parameters. The response rows used here are massless static rows. They can only support the corresponding conditional long-range, quasistatic dipole approximation. At a fixed nonzero mass the response rows and propagation factors must both be recomputed. A closed channel has $\mathscr{K}_i = 0$ and cannot enter this division. The exact minimal common-weight massless branch has $a_0 = 0$, as explained above; the present example is not a nonzero-coupling realization of it.

EOS	$\det B_{12}$	$\mathrm{cond}_2 B_{12}$	λ_1	λ_2
SLy	−0.00507092	153.12	0.423875	0.532762
AP4	−0.00529151	130.47	0.389913	0.587320

Table 19. Computed transfer coefficients for the fixed GR stellar backgrounds. The condition number refers to the stated normalization of the two source columns. It measures the recovery of their coefficients, not the conditioning of every observable.

For example, the synthetic choice $\theta = (10^{-3}, 2 \times 10^{-4})$ gives $q_1 = -4.01350 \times 10^{-4}$ and $q_2 = -7.43470 \times 10^{-4}$ for SLy. Their two squares alone allow J2222 extra-decay means of approximately −0.225247 and −0.035876 fs/s. The chosen input realizes the former. For AP4 the

corresponding alternatives are -0.222027 and -0.040538 fs/s. These values are calculated examples, not measured charge differences or a blind validation.

21.7. *A missing response and a quantitative closure condition.* The preceding elimination is useful only if the two-source truncation has an independently controlled remainder. Suppose, more generally,

$$q_i = B_{i,:}\theta + e_i, \qquad |e_i| \le \epsilon_i. \tag{1263}$$

Then exact cancellation of the retained coefficients gives

$$\begin{aligned} q_3 - \lambda_1 q_1 - \lambda_2 q_2 &= e_3 - \lambda_1 e_1 - \lambda_2 e_2, \\ |q_3 - \lambda_1 q_1 - \lambda_2 q_2| &\le E, \qquad E = \epsilon_3 + |\lambda_1|\epsilon_1 + |\lambda_2|\epsilon_2. \end{aligned} \tag{1264}$$

For a signed prediction $\widehat{q}_3$, the associated mean-signal error is bounded by

$$|s_3 - \widehat{s}_3| \le \mathscr{K}_3\big(2|\widehat{q}_3|E + E^2\big). \tag{1265}$$

These follow from the triangle inequality and $q_3^2 - \widehat{q}_3^2 = 2\widehat{q}_3(q_3 - \widehat{q}_3) + (q_3 - \widehat{q}_3)^2$. A response-row error bounded by $\|\delta B_{i,:}\| \le \eta_i$ can be included by adding $\eta_i\|\theta\|$ to ϵ_i. Without a coefficient bound, a small row error alone does not bound the prediction error.

A concrete unretained source is supplied by the common Jordan energy perturbation

$$\delta\varepsilon_J(n,x) = d_3 x\,\frac{m_b n^2}{n_{\mathrm{ref}}}, \qquad h(n) = \frac{m_b n^2}{n_{\mathrm{ref}}}. \tag{1266}$$

It vanishes at $x = 0$, and so does its pressure perturbation. Nevertheless, both its scalar energy derivative and its scalar pressure derivative equal $d_3 h$. This is a possible local matter response left unspecified by the background EOS; it is not a microscopic prediction of the mother action. On a compact density interval with strict thermodynamic inequalities, sufficiently small perturbations preserve those inequalities. No claim of nonlinear stellar stability follows from this observation.

Use the same reference rest-mass density $m_b n_{\mathrm{ref}} = 2.8 \times 10^{14}\,\mathrm{g\,cm^{-3}}$ for all stars, and compute $z_i = \mathcal{K}_{\mathrm{NS},i}[h] - \mathcal{K}_{\mathrm{WD},i}[h]$. The full linear map becomes $q = B\theta + d_3 z$. Its third direction cannot be absorbed into the first two if

$$\kappa_3 = z_3 - \lambda_1 z_1 - \lambda_2 z_2 \neq 0. \tag{1267}$$

Indeed, choosing the common shift $\delta\theta = -d_3 B_{12}^{-1}(z_1, z_2)^{\top}$ leaves the first two signed charges unchanged but changes the third by $d_3\kappa_3$. Equivalently,

$$\det[B\ z] = (\det B_{12})\kappa_3. \tag{1268}$$

This construction changes common matter coefficients, not independent charges assigned to each star.

The density responses were integrated both as a weighted volume source and as a radial scalar flux. Across nine configurations their largest absolute

EOS	z_1	z_2	z_3	κ_3	$\det[B\ z]$
SLy	1.571585	1.880036	1.761733	0.0939665	-4.76496×10^{-4}
AP4	1.684014	1.850105	1.804565	0.0613412	-3.24587×10^{-4}

Table 20. New density-source calculations on the same GR backgrounds. The nonzero determinants belong to these computed response matrices; they are not rigorous interval enclosures for the continuum ODE.

difference is 4.36×10^{-13}; comparison of two integration methods changes the response by at most 4.52×10^{-9}. These checks concern numerical agreement, not physical EOS uncertainty. In the synthetic example, taking $d_3 = 10^{-4}$ and compensating the first two responses changes the SLy target from -0.225247 to -0.217833 fs/s; for AP4 it changes -0.222027 to -0.217208 fs/s. Both are leading linear-response calculations.

This also gives a concrete accuracy requirement. If this is the only missing direction, a sufficient condition for at most one percent error in the nonzero synthetic target mean is

$$|d_3| \le \frac{(\sqrt{1.01} - 1)|\widehat{q}_3|}{|\kappa_3|}. \tag{1269}$$

It is approximately 3.005×10^{-5} for SLy and 4.571×10^{-5} for AP4 in this example. These are required matching accuracies in the specified source normalization, not measured limits on a fundamental coefficient. Other omitted directions require their own contributions to (1264).

Finally, fitting the original three historical residual summaries in their original variables, with the same diagonal uncertainty convention, gives $\chi^2_{\mathrm{GR}} = 1.107739$. The enlarged two-source linear model gives approximately 0.715977 for SLy and 0.664830 for AP4. The improvements, 0.391761 and 0.442908, provide no substantial fit preference. The unrestricted fitted coefficients reach order 0.1, outside a weak-response regime justified by the earlier small-coupling calculation; these extrema are therefore diagnostics of the enlarged linear model, not established physical stellar solutions. Polynomial stationary-direction calculations agree with a separate angular search. Neither method reconstructs a full timing likelihood or assigns a detection significance.

The result specifies both a useful conditional prediction and its missing physical input. To promote the relation to a consequence of the mother theory, microscopic matching must exclude additional response directions or bound their projections in (1264). An arbitrary common scalar-dependent EOS does not provide that bound.

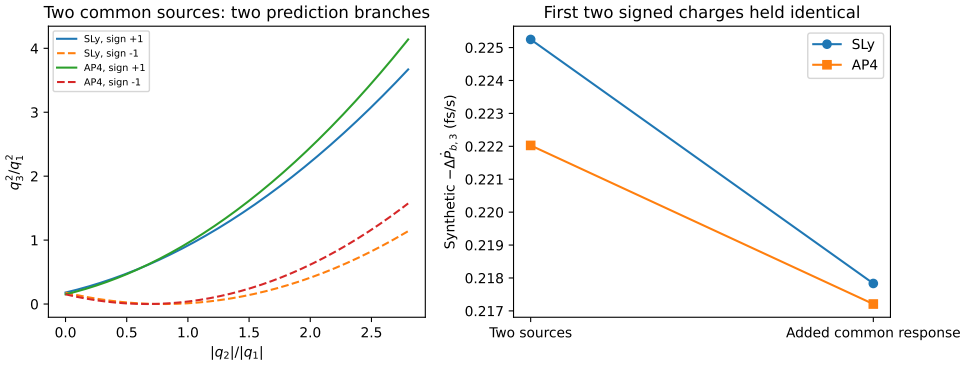


Figure 33. Conditional cross-binary prediction. Left: the two allowed third-signal branches after eliminating two common coefficients. Right: synthetic target decay before and after adding a common density response while keeping the first two signed charges identical. The added source illustrates missing physical matching, not evidence for a new force.

21.8. *Prediction, calibration, and distinguishability.* An operational prediction can use externally calibrated parameters; they need not all be parameter-free constants. What is essential is that the target data are not reused to choose its coupling, matter derivatives or nuisance adjustment. A suitable sequence fixes one matched action and its parameter family, determines the common matter response from independent inputs, and freezes the resulting parameter distribution before examining the target. Propagating that distribution through the stellar and timing equations gives a predictive distribution without a new source-charge fit. Previously inspected public targets remain retrospective comparisons.

Distinctiveness requires an additional test. A competing scalar theory with the same matched effective action, state preparation, background conditions and measurement model has the same observable probabilities at the retained order. No experiment confined to those observables can identify which larger construction motivated that identical action. The mother framework therefore needs additional independently derived restrictions across coefficients, scales or channels. Its mass–coupling relation is one conditional restriction, but an allowed parameter family containing arbitrarily small couplings need not be separated from GR by a positive minimum signal. The response map above states precisely which remaining physical inputs are needed to turn the conditional stellar calculation into a stronger prediction.

22. Common-weight response, stellar balance, and a conditional radiation envelope

A scalar radiation calculation involves three different questions. The action fixes the field normalization and the elementary coupling. The matter model and stellar boundary problem determine the source response. The orbit and propagation law then determine which part of that response can radiate. Increasing an elementary coupling need not increase the observable signal when the same parameter also increases the scalar mass. We make this competition explicit for the original common-weight branch. We first derive its nonlinear conformal coupling, then give the static fluid equations and a scalar-response error bound, and finally combine the mass relation with the leading circular dipole formula. The resulting bound is conditional on a specified source-response bound; a tabulated background equation of state does not provide that missing input.

22.1. *The nonlinear canonical coupling of the metric branch.* Use natural units in this subsection. To keep field dimensions explicit, write the relevant Jordan-frame terms as

$$S_J = \int \sqrt{-g_J}\left[\frac{M_{\rm P}^2}{2}F(\sigma)R_J - \frac{1}{2}g_J^{\mu\nu}\partial_\mu\sigma\partial_\nu\sigma - V_J(\sigma)\right]d^4z + S_{m,J}, \qquad F(\sigma) = e^{-b\sigma}. \tag{1270}$$

Here σ has mass dimension one, b has inverse mass dimension, and $M_{\rm P}^{-2} = 8\pi G_*$. If an earlier information coordinate s is dimensionless and has a constant kinetic coefficient K_s^2, this convention means $\sigma = K_s s$ and $b\sigma = (bK_s)s$. Changing that kinetic coefficient changes the canonical map; the formula below assumes the unit Jordan kinetic term in (1270). We use the metric, rather than an independent Palatini, conformal transformation.

With $g_E = Fg_J$, the Jordan metric is $g_J = A^2 g_E$, where $A = F^{-1/2}$. The curvature transformation and the original scalar kinetic term give, respectively, the two terms in

$$\left(\frac{d\varphi}{d\sigma}\right)^2 = Z(\sigma),$$
$$Z(\sigma) = F^{-1} + \frac{3}{2}M_{\rm P}^2\left(\frac{F'}{F}\right)^2 = e^{b\sigma} + \frac{3}{2}q^2, \tag{1271}$$
$$q = bM_{\rm P}, \qquad x = \frac{\varphi}{\sqrt{2}M_{\rm P}}.$$

Choose the positive square root and set $x = 0$ at $\sigma = 0$. Then $Z > 0$, so the map is locally invertible everywhere on this real scalar branch. The dimensionless

conformal coupling and its slope are

$$a(x) = \partial_x \log A = \frac{q}{\sqrt{2Z}}, \qquad \beta(x) = \partial_x a = -\frac{q^2 e^{b\sigma}}{2Z^2}. \tag{1272}$$

Indeed $\partial_x \sigma = \sqrt{2} M_{\mathrm{P}}/\sqrt{Z}$, and differentiating $q(2Z)^{-1/2}$ gives the second expression. This calculation keeps the field-dependent normalization; replacing $Z(\sigma)$ by $Z(0)$ before differentiating would lose that term.

Proposition 107 (A conformal-slope bound for the specified branch). *For* (1270) *with the canonical convention* (1271),

$$-\frac{1}{12} \le \beta(x) \le 0, \qquad \beta_0 = -a_0^2(1 - 3a_0^2), \qquad |a_0| < \frac{1}{\sqrt{3}}. \tag{1273}$$

These are restrictions on the conformal coupling, not a stability theorem for arbitrary composite matter.

Proof. Put $E = e^{b\sigma} > 0$. Direct completion of the square yields

$$\beta + \frac{1}{12} = \frac{(E - 3q^2/2)^2}{12(E + 3q^2/2)^2} \ge 0. \tag{1274}$$

The upper bound follows from (1272). At $\sigma = 0$, $a_0^2 = q^2/(2 + 3q^2)$ and $1 - 3a_0^2 = (1 + 3q^2/2)^{-1}$. Their product gives the stated value of $-\beta_0$. The strict range of a_0 holds for finite real q. □

Thus the preceding constant-coupling massless example, which used $\beta_0 = 0$ at nonzero a_0, is a different conditional matter branch. At very small coupling its difference from the present conformal slope can be perturbatively small, but it is not an exact identification. Moreover, the total matter derivative in (1243) contains explicit Jordan responses. Its second derivative, including composition relaxation, can alter the scalar perturbation operator. The bound on β therefore cannot exclude every matter-induced scalar instability.

22.2. *A consistent massive scalar–fluid boundary problem.* State the action before specifying stellar equilibrium. With a zero-temperature, isentropic conserved baryon current, use

$$S_E = \frac{1}{16\pi G_*} \int \sqrt{-g} \left[R - 2(\partial x)^2 - 4\mathcal{V}(x) \right] d^4 z + S_m[g, x]. \tag{1275}$$

The canonical physical potential is $U_E = 2M_{\mathrm{P}}^2 \mathcal{V}$. In natural units, $U_{E,\varphi\varphi}(0) = \mathcal{V}_{xx}(0) = \mu_\varphi^2$. Define the Einstein-frame fluid variables at fixed conserved number by

$$\begin{aligned} n_J &= A^{-3} n_E, & \mathcal{E}(n_E, x) &= A^4 \varepsilon_J(n_J, x), \\ \mathcal{P} &= n_E \mathcal{E}_{n_E} - \mathcal{E} = A^4 p_J, & \mathcal{J} &= \mathcal{E}_x|_{n_E} = A^4 \left[a(\varepsilon_J - 3p_J) + \varepsilon_{J,x}|_{n_J} \right]. \end{aligned} \tag{1276}$$

The two contributions in the last expression have different origins: the first changes volume and energy units through the conformal metric; the second changes the Jordan matter theory itself.

Varying (1275) gives $\Box x = \mathcal{V}_x + 4\pi G_* \mathcal{J}$. The diffeomorphism identity gives $\nabla_\mu T_m^{\mu\nu} = -\mathcal{J}\nabla^\nu x$; the scalar carries the opposite exchange. In geometrized units $G_* = c = 1$, set

$$ds^2 = -e^{\nu(r)}dt^2 + f(r)^{-1}dr^2 + r^2 d\Omega^2, \qquad f = 1 - \frac{2\mathfrak{m}}{r}, \qquad \psi = x'. \quad (1277)$$

The static equations are

$$\begin{aligned} \mathfrak{m}' &= 4\pi r^2 \mathcal{E} + \frac{1}{2} r^2 f \psi^2 + r^2 \mathcal{V}, \\ \frac{\nu'}{2} &= \frac{\mathfrak{m} + 4\pi r^3 \mathcal{P} - r^3 \mathcal{V}}{r^2 f} + \frac{1}{2} r \psi^2, \\ \left(e^{\nu/2} r^2 \sqrt{f}\, \psi\right)' &= \frac{e^{\nu/2} r^2}{\sqrt{f}} (\mathcal{V}_x + 4\pi \mathcal{J}), \\ \mathcal{P}' &= -(\mathcal{E} + \mathcal{P}) \frac{\nu'}{2} - \mathcal{J}\psi, \\ N_b' &= \frac{4\pi r^2 n_E}{\sqrt{f}}. \end{aligned} \quad (1278)$$

The first two equations are the independent temporal and radial metric equations. The third retains the exact radial volume and lapse factors. The fourth follows from the radial matter exchange law, and the fifth counts baryons on a static proper-volume slice. Energy densities and $\mathcal{V}$ have geometrized dimension length^{-2}, ψ has dimension length^{-1}, and $\mathfrak{m}$ has dimension length. Every term in each equation has the corresponding dimension. A physical EOS must be converted using the same G_* and matter-frame convention throughout.

There is a useful independent derivation of the pressure equation. For an isentropic fluid the local chemical potential is $\mathcal{E}_{n_E}$, and equilibrium implies $(e^{\nu/2}\mathcal{E}_{n_E})' = 0$. Differentiating $\mathcal{P} = n_E \mathcal{E}_{n_E} - \mathcal{E}$ gives $\mathcal{P}' = n_E (\mathcal{E}_{n_E})' - \mathcal{J}\psi$. Since $n_E \mathcal{E}_{n_E} = \mathcal{E} + \mathcal{P}$, this is the fourth line of (1278). In Jordan variables the same equation becomes

$$p_J' = -(\varepsilon_J + p_J)\left(\frac{\nu'}{2} + a\psi\right) - \varepsilon_{J,x}\big|_{n_J}\psi. \quad (1279)$$

To verify the conversion, differentiate $\mathcal{P} = A^4 p_J$, substitute (1276), and combine $a(\varepsilon_J - 3p_J) + 4ap_J = a(\varepsilon_J + p_J)$. Dropping the explicit derivative in (1279) is justified only for a matter model with that derivative zero.

For finite central density and scalar value, regularity gives

$$\begin{aligned} \mathfrak{m}(r) &= \frac{4\pi\mathcal{E}_c + \mathcal{V}_c}{3} r^3 + O(r^5), \\ \psi(r) &= \frac{\mathcal{V}_{x,c} + 4\pi\mathcal{J}_c}{3} r + O(r^3), \\ N_b(r) &= \frac{4\pi n_{E,c}}{3} r^3 + O(r^5). \end{aligned} \tag{1280}$$

At a free surface use the correct vanishing-pressure condition and continue through the scalar exterior. Asymptotic flatness at $x = 0$ requires $\mathcal{V}(0) = \mathcal{V}_x(0) = 0$. A nonzero cosmological background instead requires a matched local exterior. A material interface or phase transition requires its own junction and chemical-equilibrium conditions.

The equations specify a common massive-fluid model once $\varepsilon_J(n_J, x)$, $A(x)$, $\mathcal{V}(x)$ and the boundary data are supplied. They do not by themselves determine the missing nuclear derivatives. Nor does positive sound speed alone prove stability of the coupled scalar–fluid configuration. A massless sensitivity derivative must hold N_b, rather than a scalar-dependent mass $m_b(x)N_b$, fixed. For a massive potential that pins the asymptotic vacuum, the physically relevant response must instead be defined by its specified external field or retarded transfer problem; an arbitrary variation of a constant asymptotic scalar need not remain a solution.

22.3. *Coercivity and an explicit static-response error bound.* The scalar source can be small while its response is large near an unstable or nearly neutral mode. To expose this dependence, fix a regular GR background and a prescribed scalar susceptibility $\chi(r)$. Linearization at fixed background matter gives $\mathcal{J} = J_0 + \chi x$. With $P = Nr^2\sqrt{f}$ and $W = Nr^2/\sqrt{f}$, the equation on $0 < r < L$ is

$$\begin{aligned} \mathscr{L}u &:= -(Pu')' + W\kappa u = \mathcal{F}, \\ \kappa &= \mu_\varphi^2 + 4\pi\chi, \qquad \mathcal{F} = -4\pi W J_0, \\ P(L)u'(L) &+ hu(L) = 0. \end{aligned} \tag{1281}$$

The positive coefficient h is a specified exterior response map. It must be computed from the same decaying exterior when that exterior is curved. In a flat vacuum exterior, $h = L^2(\mu_\varphi + 1/L)$. The susceptibility here is prescribed on a fixed background; eliminating fluid or composition perturbations generally changes this operator.

Proposition 108 (A residual estimate for a coercive radial response). *Assume P and W are bounded above and below by positive constant multiples of r^2, κ is bounded, $\kappa \geq \kappa_0 > 0$, and $h > 0$. Use the radial energy space obtained*

by completing smooth regular radial functions in the norm

$$\|v\|_B^2 = \int_0^L \left[P(v')^2 + W\kappa v^2\right] dr + hv(L)^2. \tag{1282}$$

For $\int_0^L \mathcal{F}^2/W\, dr < \infty$, (1281) *has a unique weak solution in this space. Let* $\widetilde{u}$ *be a smooth approximation with the regular central endpoint term zero. Assume that its flux is absolutely continuous on each material interval, that the weighted residual below is finite, and that there are no interface flux jumps. Define*

$$\begin{aligned} \mathcal{R} &= \mathcal{F} + (P\widetilde{u}')' - W\kappa\widetilde{u}, \\ \eta &= -P(L)\widetilde{u}'(L) - h\widetilde{u}(L), \\ \delta^2 &= \frac{1}{\kappa_0}\int_0^L \frac{\mathcal{R}^2}{W} dr + \frac{\eta^2}{h}. \end{aligned} \tag{1283}$$

Then

$$\|u-\widetilde{u}\|_B \le \delta, \qquad |u(L)-\widetilde{u}(L)| \le \frac{\delta}{\sqrt{h}}, \qquad \left|\int_0^L W\zeta(u-\widetilde{u})dr\right| \le \frac{\|\zeta\|_{L^2(W)}}{\sqrt{\kappa_0}}\delta. \tag{1284}$$

The last inequality assumes $\zeta \in L^2(W dr)$.

Proof. The symmetric bilinear form associated with (1282) is coercive and continuous in this energy space. The source functional is continuous by weighted Cauchy–Schwarz and $\kappa \ge \kappa_0$, so the Lax–Milgram theorem gives existence and uniqueness. Integration by parts shows that the error $e = u - \widetilde{u}$ satisfies

$$B[e,v] = \int_0^L \mathcal{R}v\, dr + \eta v(L). \tag{1285}$$

Applying Cauchy–Schwarz to the two displayed residual terms together gives

$$|B[e,v]| \le \delta\left(\kappa_0\int_0^L Wv^2 dr + hv(L)^2\right)^{1/2} \le \delta\|v\|_B.$$

Set $v = e$ and divide by $\|e\|_B$ when nonzero. The boundary and volume readout bounds then follow directly from the two positive terms in the norm. □

The assumptions are sufficient, not necessary. A zero-mass operator can still be coercive by a radial Poincaré inequality and the exterior boundary term, but the particular $1/\kappa_0$ estimate above does not cover that case. If the susceptibility is negative, a lower bound on the full operator, rather than the scalar mass alone, is needed. Approach to a zero eigenvalue can make a small residual compatible with a large field error. A comparable estimate for the coupled fluid problem requires its full linearized operator. Likewise, the static estimate is not a certificate for a response at nonzero orbital frequency.

22.4. *Boundary control when the scalar potential is not positive.* A light scalar need not have a strictly positive local restoring term. Matter can also contribute a negative susceptibility. In either case, the preceding estimate based on $\kappa_0 > 0$ may cease to apply even though the exterior boundary still controls a static response. Physically, the exterior is part of the field problem: fixing its decaying solution prevents an arbitrary constant interior shift. The following estimate makes this mechanism explicit before a response is interpreted as a large stellar charge.

Write $R > 0$ for the outer radius. Suppose that P and W are bounded above and below by positive multiples of r^2, and retain constants $P \geq p_- r^2$ and $W \leq w_+ r^2$. Let $h > 0$ be the exterior boundary coefficient and define

$$E_0[v] = \int_0^R P(v')^2 \, dr + h v(R)^2, \qquad C_P = w_+ \left(\frac{R^3}{3h} + \frac{R^2}{6p_-} \right). \tag{1286}$$

The energy space is the completion of smooth regular radial functions in $E_0^{1/2}$. In these definitions C_P has the dimensions of an inverse potential coefficient; when P, W have the usual radial normalization, it has dimensions of length squared.

Proposition 109 (A boundary-controlled response estimate). *Assume that the bounded potential satisfies $\kappa \geq -K$, with $K \geq 0$, and that $\gamma = 1 - KC_P > 0$. Then*

$$\int_0^R W v^2 \, dr \leq C_P E_0[v], \qquad B[v,v] := E_0[v] + \int_0^R W \kappa v^2 \, dr \geq \gamma E_0[v]. \tag{1287}$$

For a source with $\int_0^R \mathcal{F}^2/W \, dr < \infty$, the radial equation with boundary condition $Pu'(R) + hu(R) = 0$ has a unique weak solution in this space. For a smooth approximation $\widetilde{u}$, let $\mathcal{R}$ and η be the interior and boundary residuals of Eq. (1283)*, with the regular central flux term zero. The flux $P\widetilde{u}'$ is assumed absolutely continuous on each smooth material interval, and the displayed weighted residual norm must be finite. In the estimate as stated there are no interface flux jumps; when such jumps occur their trace functionals must be added. Put*

$$a_R = \left(\int_0^R \frac{\mathcal{R}^2}{W} \, dr \right)^{1/2}, \qquad \delta_B = \frac{\sqrt{C_P}\, a_R + |\eta|/\sqrt{h}}{\sqrt{\gamma}}. \tag{1288}$$

Then, for $e = u - \widetilde{u}$,

$$\|e\|_B \leq \delta_B, \qquad |e(R)| \leq \frac{\delta_B}{\sqrt{\gamma h}}, \qquad \|e\|_{L^2(W)} \leq \sqrt{C_P/\gamma}\, \delta_B. \tag{1289}$$

Proof. For a smooth regular v, write $v(r) = v(R) - \int_r^R v'(s)\,ds$. Weighted Cauchy–Schwarz gives

$$|v(r) - v(R)|^2 \le \frac{1}{p_-}\left(\frac{1}{r} - \frac{1}{R}\right)\int_0^R P(v')^2\,ds.$$

The apparent singularity at zero is integrable against $r^2 dr$. Since $\int_0^R (r - r^2/R)\,dr = R^2/6$, the triangle inequality in $L^2(W dr)$ yields

$$\|v\|_{L^2(W)} \le \sqrt{\frac{w_+ R^3}{3h}}\,\sqrt{h}\,|v(R)| + \sqrt{\frac{w_+ R^2}{6p_-}}\left(\int_0^R P(v')^2\,dr\right)^{1/2}.$$

Cauchy–Schwarz for these two terms proves the first inequality in Eq. (1287). Density extends it to the completed energy space. The lower bound $\kappa \ge -K$ then proves the second inequality. Boundedness of κ makes B continuous in $E_0^{1/2}$, and the source is a continuous functional by the first inequality. Lax–Milgram gives the asserted weak solution.

The residual identity remains $B[e, v] = \int_0^R \mathcal{R} v\,dr + \eta v(R)$. Hence

$$|B[e, v]| \le \left(\sqrt{C_P}\,a_R + \frac{|\eta|}{\sqrt{h}}\right)\sqrt{E_0[v]} \le \delta_B \|v\|_B.$$

Taking $v = e$ proves the energy estimate, with the zero-error case immediate. The boundary and weighted-volume estimates follow from $B[e, e] \ge \gamma E_0[e]$. □

The sufficient condition $KC_P < 1$ is not a necessary stability criterion. Its failure means that this estimate is inconclusive. For piecewise smooth coefficients, a discontinuity of the approximate flux contributes an interface term to the residual functional; such a term must be retained rather than absorbed into a smooth volume residual. More explicitly, let $r_j \in (0, R)$ be finitely many interfaces and assume that $\widetilde{u}$ is continuous there. Write $q_j = [P\widetilde{u}']_{r_j^-}^{r_j^+}$, with the right limit minus the left limit. Integration by parts on each interval gives

$$B[e, v] = \int_0^R \mathcal{R} v\,dr + \eta v(R) + \sum_j q_j v(r_j).$$

The same weighted Cauchy–Schwarz argument, now applied before radial integration, gives

$$|v(r_j)| \le C_j \sqrt{E_0[v]}, \qquad C_j^2 = \frac{1}{h} + \frac{1}{p_-}\left(\frac{1}{r_j} - \frac{1}{R}\right).$$

Thus the bounds in Eq. (1289) remain valid when δ_B is replaced by

$$\delta_{B,\mathrm{int}} = \frac{\sqrt{C_P}\,a_R + |\eta|/\sqrt{h} + \sum_j |q_j| C_j}{\sqrt{\gamma}}. \tag{1290}$$

Here the volume residual is evaluated within the individual intervals. A physical surface source would change the prescribed jump condition and must be included in q_j as a jump residual. This extension makes the interface contribution explicit for piecewise material models.

An exact example shows why the extra term is necessary. Take $P = W = r^2$, $R = h = 1$, $\kappa = \mathcal{F} = 0$, and $0 < a < 1$. The true solution is zero. Define a continuous approximation by $\widetilde{u}(r) = 1$ for $r \le a$ and $\widetilde{u}(r) = a/r$ for $r \ge a$. Both volume residuals and the outer boundary residual vanish, but the interface flux jump is $q = -a$. Direct integration gives

$$E_0[\widetilde{u}] = a, \qquad \widetilde{u}(1) = a, \qquad C_a^2 = 1/a, \qquad |q|C_a = \sqrt{a}.$$

Omitting the interface term would give the false error bound zero. Including it recovers the exact energy-error norm in this example.

22.4.1. *The matter derivative at fixed conserved number.* To connect the estimate to a specified scalar branch, consider the conditional matter model $\varepsilon_J = \varepsilon_J(n_J)$, with no explicit Jordan-frame scalar dependence. At $A(0) = 1$, use $n_J = A^{-3}n_E$, $a = \partial_x \log A$, $\beta = \partial_x a$, and the causal barotropic sound-speed ratio $c_s^2 = dp_J/d\varepsilon_J$. The trace source is $\mathcal{J} = A^4 a(\varepsilon_J - 3p_J)$. Holding n_E fixed gives $\partial_x n_J = -3an_J$, while the isentropic first law gives $n_J\varepsilon_{J,n_J} = \varepsilon_J + p_J$ and $n_J p_{J,n_J} = c_s^2(\varepsilon_J + p_J)$. Therefore

$$\begin{aligned}\chi_0 := \partial_x \mathcal{J}|_{n_E, x=0} &= (\beta_0 + 4a_0^2)(\varepsilon_J - 3p_J) - 3a_0^2(1 - 3c_s^2)(\varepsilon_J + p_J) \\ &= \beta_0(\varepsilon_J - 3p_J) + a_0^2\{\varepsilon_J - 15p_J + 9c_s^2(\varepsilon_J + p_J)\}. \quad (1291)\end{aligned}$$

Holding n_J fixed instead would omit the second term in the first line and would describe a different perturbation. For the common-weight conformal branch, $\beta_0 = -a_0^2(1 - 3a_0^2)$ is inserted at this stage; it is not replaced by zero. Explicit scalar dependence of nuclear or binding energies would add further derivatives. The displayed formula does not determine those additional physical responses.

For a fixed GR background with nonnegative density and pressure and $0 \le c_s^2 \le 1$, a useful conservative bound is

$$|\chi_0| \le |\beta_0|(\varepsilon_J + 3p_J) + a_0^2(10\varepsilon_J + 24p_J).$$

If density and pressure decrease outwards, their central values bound the right-hand side. With $\kappa = \mu_\varphi^2 + 4\pi\chi_0$ and $\mu_\varphi^2 \ge 0$, this supplies an explicit K. This frozen-density operator is one component of the stellar response; eliminating fluid and metric perturbations changes the full operator.

22.4.2. *A computable exterior bound and numerical illustrations.* For a GR star in geometrized units, let M and R be its mass and radius, and let h_c be its central fluid enthalpy. If $f_- = 1 - 8\pi\varepsilon_c R^2/3 > 0$, monotonicity of the density implies $f(r) \ge f_-$. Hydrostatic balance gives $N_c = N_R e^{-h_c}$, where

$N_R = \sqrt{1 - 2M/R}$. Consequently one may take

$$p_- = N_c\sqrt{f_-}, \qquad w_+ = N_R/\sqrt{f_-}.$$

In the massless Schwarzschild exterior the decaying static solution is proportional to $\log(1 - 2M/r)$, so its boundary coefficient is $h_0 = -2M/\log(1 - 2M/R) > 0$. Adding a nonnegative exterior mass potential increases the minimum exterior energy for a fixed surface value, and hence its boundary coefficient is at least h_0. Using h_0 in C_P is therefore conservative. This comparison does not set the physical mass of a nonzero-coupling common-weight branch to zero.

For numerical GR stars of mass $1.4661M_\odot$, the retained SLy and AP4 EOS approximations give $C_P \simeq 370.94$ and $269.53\,\mathrm{km}^2$, respectively. At $a_0 = 10^{-3}$ and the common-weight value of β_0, the resulting margins $1 - KC_P$ are approximately 0.9999443 and 0.9999583. These values illustrate the size of the sufficient margin under the stated matter assumptions. The background integrations have not been enclosed by interval arithmetic, so the displayed decimal margins are numerical illustrations of the analytic estimate, not validated error bounds for observed stars or a proof of coupled stellar stability.

An exact rational calculation tests the residual estimate without that background uncertainty. On $0 < r < 1$, take $P = W = r^2$, $h = 1$, $\mathcal{F} = -3r^2$, and $\kappa = -s$. Then $C_P = 1/2$ and $\gamma = 1 - s/2 > 0$ for $0 \le s < 2$. The exact solution is

$$u_s(r) = \frac{3}{s}\left[1 - \frac{\sin(\sqrt{s}\,r)}{\sqrt{s}\,r\cos\sqrt{s}}\right] \quad (s > 0), \qquad u_0(r) = \frac{r^2 - 3}{2}. \tag{1292}$$

The central quotient has its continuous value. Direct differentiation verifies the equation and $u_s'(1) + u_s(1) = 0$. The first homogeneous zero mode actually occurs at $s = \pi^2/4$; the sufficient threshold $s < 2$ is deliberately conservative.

For $\widetilde{u} = \sum_i c_i r^{2i}$, the Galerkin matrix and right-hand side are

$$M_{ij} = \frac{4ij}{2i + 2j + 1} - \frac{s}{2i + 2j + 3} + 1, \qquad f_i = -\frac{3}{2i + 3}.$$

At rational s, solving this finite system and integrating the polynomial residual use exact rational arithmetic. In this normalization, the surface estimate is bounded above by the square root of $\{a_R^2 + 2\eta^2\}/\gamma^2$; the square root is rounded upwards using integer inequalities. This calculation includes the zero-potential case and negative potentials, for which the earlier $1/\kappa_0$ estimate is unavailable.

22.5. *A controlled frequency band with an outgoing exterior.* A static charge describes the response to a source that does not change with time. Radiation requires a further ingredient: the field must carry energy away from an oscillating source. We now include this boundary condition in an explicitly solvable radial setting. It provides a first frequency-dependent extension of

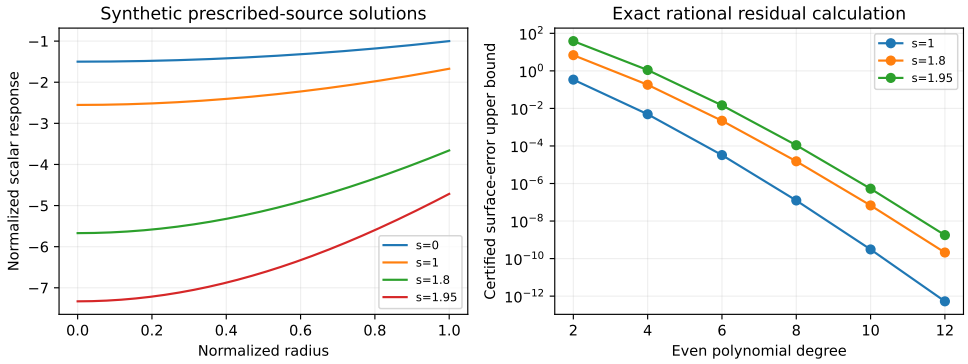


Figure 34. Synthetic prescribed-source response with a negative interior potential and a positive exterior boundary term. Left: exact profiles. Right: upper bounds on the surface error from exact rational residuals. The zero-potential polynomial solution is exact and has zero residual. No experimental data are represented by these curves.

the preceding estimate, with the source and the background still specified independently.

Use units with $c = 1$ and a canonical real scalar with time dependence $\mathrm{Re}(u(r)e^{-i\omega t})$, where $\omega \geq 0$. Let $R > 0$, $\mu \geq 0$, and let χ be a bounded real susceptibility on $(0, R)$. The radial source equation and its vacuum exterior are

$$\begin{aligned} -(r^2u')' + r^2(\mu^2 + \chi - \omega^2)u &= r^2 f, \\ u_{\mathrm{ext}}(r) = \frac{R}{r}u(R)e^{ik(r-R)}, &\quad k = \sqrt{\omega^2 - \mu^2}. \end{aligned} \tag{1293}$$

Choose the square root with nonnegative real and imaginary parts. Above threshold $\omega > \mu$, this is an outgoing wave; below threshold it decays exponentially. At threshold it is the continuous $1/r$ limit. Continuity of the field and its radial derivative gives

$$u'(R) + (R^{-1} - ik)u(R) = 0. \tag{1294}$$

We impose the regular central condition and initially exclude surface sources. The quantities ω and μ have inverse-length units, while χ has inverse-length-squared units.

For complex radial functions set

$$\begin{aligned} E_0[v] &= \int_0^R r^2|v'|^2\,\mathrm{d}r + R|v(R)|^2, \qquad C_P = R^2/2, \\ a_\omega(u,v) &= \int_0^R r^2\{u'\overline{v'} + (\mu^2+\chi-\omega^2)u\overline{v}\}\,\mathrm{d}r \\ &\quad + (R - ikR^2)u(R)\overline{v(R)}. \end{aligned} \tag{1295}$$

The space is the complex completion of smooth regular radial functions in the norm $E_0^{1/2}$. The preceding weighted Poincare argument, applied to real and imaginary parts, gives $\|v\|^2_{L^2(r^2\mathrm{d}r)} \le C_P E_0[v]$.

Proposition 110 (Frequency-dependent source and residual estimates). *Suppose $\mu^2+\chi \ge -K$ almost everywhere, with $K \ge 0$, and*

$$\gamma_\omega := 1 - (K+\omega^2)C_P > 0. \tag{1296}$$

For $f \in L^2((0,R), r^2\mathrm{d}r)$ there is a unique weak solution of (1293)–(1294). It satisfies

$$E_0[u]^{1/2} \le \frac{\sqrt{C_P}}{\gamma_\omega}\|f\|_{L^2(r^2\mathrm{d}r)}, \qquad |u(R)| \le \frac{\sqrt{C_P/R}}{\gamma_\omega}\|f\|_{L^2(r^2\mathrm{d}r)}. \tag{1297}$$

For a continuous, piecewise smooth regular approximation $\widetilde{u}$, define the volume and boundary residuals by

$$\begin{aligned} \mathcal{R} &= r^2 f + (r^2\widetilde{u}')' - r^2(\mu^2+\chi-\omega^2)\widetilde{u}, \\ \eta_R &= -\{R^2\widetilde{u}'(R) + (R - ikR^2)\widetilde{u}(R)\}, \qquad a_R = \left(\int_0^R |\mathcal{R}|^2/r^2\,\mathrm{d}r\right)^{1/2}. \end{aligned} \tag{1298}$$

Assume this norm is finite. At each interior interface $r_j > 0$ retain the flux jump $q_j = [r^2\widetilde{u}']_{r_j^-}^{r_j^+}$; if there are no jumps the following sum is zero. Then $e = u - \widetilde{u}$ obeys

$$E_0[e]^{1/2} \le \frac{\sqrt{C_P}a_R + |\eta_R|/\sqrt{R} + \sum_j |q_j|/\sqrt{r_j}}{\gamma_\omega}, \qquad |e(R)| \le E_0[e]^{1/2}/\sqrt{R}. \tag{1299}$$

Proof. For the chosen square root, $\mathrm{Re}(-ik) = \mathrm{Im}\,k \ge 0$. Thus the exterior contributes at least $R|v(R)|^2$ to the real part of the form. The potential bound and Poincare inequality give

$$\mathrm{Re}\,a_\omega(v,v) \ge E_0[v] - (K+\omega^2)\|v\|^2_{L^2(r^2\mathrm{d}r)} \ge \gamma_\omega E_0[v].$$

Boundedness of χ and continuity of the surface trace make a_ω a continuous sesquilinear form on this Hilbert space. The source functional is continuous, with

norm at most $\sqrt{C_P}\|f\|_{L^2(r^2\mathrm{d}r)}$. The complex Lax–Milgram theorem therefore gives existence and uniqueness. Testing with u, taking real parts and dividing by $E_0[u]^{1/2}$ when it is nonzero proves (1297); the zero case is immediate.

Integration by parts on the smooth material intervals yields

$$a_\omega(e,v) = \int_0^R \mathcal{R}\overline{v}\,\mathrm{d}r + \eta_R\overline{v(R)} + \sum_j q_j\overline{v(r_j)}.$$

The central flux term vanishes by regularity. The trace estimate from the preceding subsection becomes $|v(r_j)| \le E_0[v]^{1/2}/\sqrt{r_j}$, because $h = R$ and $p_- = 1$. Weighted Cauchy–Schwarz now bounds the absolute value of this functional by the numerator of (1299) times $E_0[v]^{1/2}$. Set $v = e$ and use coercivity. A physical surface source changes the required jump and must be subtracted in the definition of the corresponding jump residual. □

The condition $\gamma_\omega > 0$ defines a sufficient band, not the exact resonance boundary. Losing this estimate is not evidence for an instability. Its gain is a calculable response bound uniform on any closed frequency interval with a positive minimum margin. If $f = a_0 f_0$ with f_0 fixed independently of a_0, the surface bound is explicitly proportional to $|a_0|$ for a fixed operator on such an interval. If the operator itself varies with a_0, the same statement across that family requires a common positive lower bound on γ_ω and a uniform upper bound on $\|f_0\|_{L^2(r^2\mathrm{d}r)}$. This identifies the constant in a linear source estimate for the stated problem. Nuclear response, curved backgrounds, and coupled metric and fluid perturbations require further matching.

The radiated energy also follows from the same normalization. For a canonical scalar the outward energy flux density is $-\partial_t\varphi\,\partial_r\varphi$. Time averaging the real harmonic field gives $(\omega/2)\,\mathrm{Im}(u'\overline{u})$. Consequently the outgoing power is

$$\overline{\mathcal{P}}_{\mathrm{out}} = 2\pi R^2\omega k|u(R)|^2 \quad (\omega > \mu), \qquad \overline{\mathcal{P}}_{\mathrm{out}} = 0 \quad (0 \le \omega \le \mu). \tag{1300}$$

The evanescent solution has zero averaged outward power despite a nonzero near field. This monopole calculation has angular momentum $l = 0$; it does not supply the $l = 1$ dipole response of a binary system.

An explicit approximation with a checkable error. For $R = 1$, constant $z = \mu^2 + \chi - \omega^2 < 0$ and $f = 1$, set $s = \sqrt{-z}$, $H(r) = \sin(sr)/(sr)$ and $h_\omega = 1 - ik$. Whenever the denominator is nonzero the exact solution is

$$u(r) = z^{-1} + AH(r), \qquad A = -\frac{h_\omega}{z\{H'(1) + h_\omega H(1)\}}. \tag{1301}$$

The continuous central value of H is one. Substitution verifies the equation and the boundary condition. For $u_N = \sum_{j=0}^{N} c_j r^{2j}$, Galerkin testing gives

$$\sum_{j=0}^{N} M_{ij} c_j = \frac{1}{2i+3}, \qquad M_{ij} = \frac{4ij}{2i+2j+1} + \frac{z}{2i+2j+3} + h_\omega, \quad 0 \le i \le N. \tag{1302}$$

Thus N is the basis order and $2N$ the polynomial degree. All residual integrals involve explicit polynomials.

In this constant-source example the surface error converges unusually fast. Let b_ω be the complex symmetric bilinear form obtained from a_ω by removing the conjugations. Since the approximation space is invariant under conjugation, Galerkin orthogonality gives $b_\omega(e, u_N) = b_\omega(e, 1) = 0$. The exact equation gives $b_\omega(u, e) = \int_0^1 r^2 e \, \mathrm{d}r$. Symmetry therefore yields $b_\omega(e, e) = \int_0^1 r^2 e \, \mathrm{d}r$, while testing with one yields $z \int_0^1 r^2 e \, \mathrm{d}r + h_\omega e(1) = 0$. Hence

$$h_\omega e(1) = -z b_\omega(e, e). \tag{1303}$$

The surface error is quadratic in the energy error for this special problem. This fact explains why double-precision surface differences can reach roundoff before the interior approximation does. The numerical comparison below therefore reports the energy error and uses 80-decimal-digit arithmetic for the small-error comparison.

22.6. *An exactly solvable radial example and rational error bounds.* Consider a declared flat-background example with radius R, constant source density ρ, $M = 4\pi\rho R^3/3$, and $J_0 = a_0\rho$. Neglect metric and fluid backreaction. For $z = \mu_\varphi R > 0$ the regular interior and decaying exterior are

$$\begin{aligned} u_{\mathrm{in}}(r) &= \frac{4\pi a_0 \rho}{\mu_\varphi^2} \left[(1+z) e^{-z} \frac{\sinh(\mu_\varphi r)}{\mu_\varphi r} - 1 \right], \\ u_{\mathrm{out}}(r) &= -\frac{a_0 M}{r} \, \mathcal{Y}(z) e^{-\mu_\varphi r}, \qquad \mathcal{Y}(z) = \frac{3(z\cosh z - \sinh z)}{z^3}. \end{aligned} \tag{1304}$$

The ratio $\sinh(\mu_\varphi r)/(\mu_\varphi r)$ takes its continuous value one at the centre. Substitution verifies the interior equation $(r^2 u')' - \mu_\varphi^2 r^2 u = 4\pi a_0 \rho r^2$. Matching u and u' at R fixes both constants. The small-mass limit gives $\mathcal{Y}(0) = 1$. The physical surface amplitude contains $e^{-z}\mathcal{Y}(z)$, not just $\mathcal{Y}(z)$; for large z it is $3(1 - 1/z)/(2z^2) + O(e^{-2z}/z^2)$. This is finite-source attenuation, without a nonlinear screening model.

For nonzero source amplitude, use r/R and $u/(a_0 M/R)$ as dimensionless variables, and drop the bars. This normalizes a linear response; it does not set the physical common-weight coupling to one. Then $\mathcal{F} = -3r^2$, $P = W = r^2$, $\kappa_0 = z^2$, and $h = 1 + z$, with $z = \mu_\varphi R$. For $\widetilde{u} = \sum_{i=0}^{d/2} c_i r^{2i}$, exact Galerkin

integration gives

$$\sum_j \left[\frac{4ij}{2i+2j+1}+\frac{z^2}{2i+2j+3}+h\right]c_j=-\frac{3}{2i+3}. \tag{1305}$$

At rational mass, every coefficient, residual integral and squared bound in (1283) is rational. Upper square roots can therefore be bounded with integer arithmetic before displaying rounded decimal values. Table 21 gives degree-twelve results. The much smaller direct errors show why an error estimate and a floating-point comparison answer different questions.

$\mu_\varphi R$	Exact surface field	Surface-error bound	Direct surface error
0.1	-0.905742578670067	1.368×10^{-24}	2.05×10^{-56}
1	-0.406005849709838	7.651×10^{-14}	6.37×10^{-31}
10	-0.013500000034009	1.285×10^{-5}	1.37×10^{-10}

Table 21. Dimensionless uniform-source model outputs. The surface-error bounds are rounded upward from exact rational residual bounds. Direct errors use a separate 70-digit evaluation of (1304); they are numerical comparisons. No stellar EOS, observed charge or orbital-frequency response is inferred from this example.

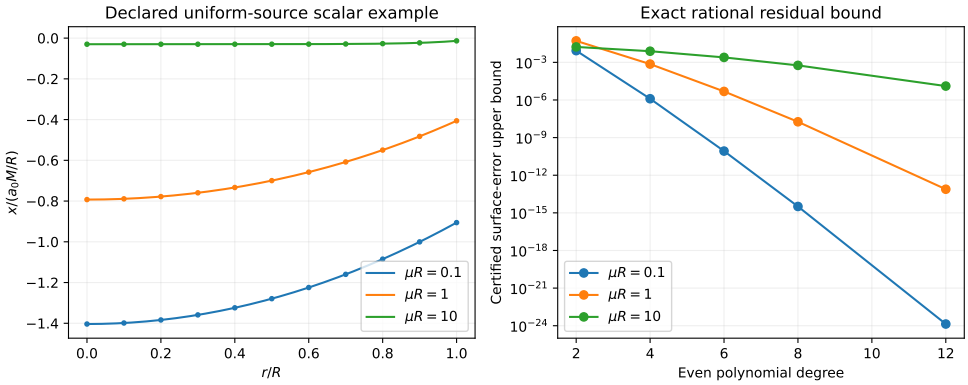


Figure 35. The declared radial example. Left: analytic scalar profiles (lines) and degree-twelve polynomial approximations (markers). Right: certified surface-error bounds versus polynomial degree. The background and source are prescribed; these are synthetic calculations.

22.7. *A source-conditioned circular-dipole envelope.* Restore physical units and write $\mu_\varphi = m_\varphi c/\hbar$. Let $C > 0$ be the fixed leading circular orbital coefficient, including its chosen mass and tensor-gravity convention. Suppose that a stable, adiabatic, point-source reduction supplies a uniform bound

$$|a_A - a_B| \le B|a_0|, \qquad S := |\dot{P}_b^{\rm dip}| = C(a_A - a_B)^2 \left[1 - \left(\frac{\mu_\varphi c}{\Omega_b}\right)^2\right]_+^{3/2}. \tag{1306}$$

Here $[v]_+ = \max(v, 0)$. The coefficient B bounds the effective response difference on the entire parameter set being tested; it is not automatically the elementary coupling or a static massless charge. The exponent $3/2$ is the leading dipole phase-space factor for the propagating linear massive mode. Below threshold that harmonic is evanescent. This is not the universal exponential rule e^{-m/Ω_b}, and it does not close higher harmonics of an eccentric orbit.

Proposition 111 (A conditional radiation envelope). *Assume* (1306)*, the original minimal common-weight mass relation with $m_\sigma^2 \ge 0$, and a finite $\ell > 0$. Define $a_* = \ell\Omega_b/(\sqrt{6}c)$. Then*

$$S \le \mathfrak{c}\, CB^2 a_*^2, \qquad \mathfrak{c} = \frac{2}{5}\left(\frac{3}{5}\right)^{3/2} = 0.185903200617956\ldots. \tag{1307}$$

If additionally $\ell k_* \le \epsilon$, then

$$S \le \frac{\mathfrak{c}\, CB^2\epsilon^2\Omega_b^2}{6c^2k_*^2}. \tag{1308}$$

The shape constant is optimal on $0 \le t \le 1$; equality for a physical source additionally requires saturation of the assumed mass and charge bounds and access to the maximizing coupling.

Proof. The mass relation gives $\mu_\varphi\ell \ge \sqrt{6}|a_0|$. Since the propagation factor decreases with nonnegative mass,

$$S \le CB^2 a_0^2[1 - (a_0/a_*)^2]_+^{3/2}.$$

For $|a_0| \ge a_*$ the bound is zero. Otherwise set $t = (a_0/a_*)^2$. Dividing by $CB^2a_*^2$ leaves $f(t) = t(1-t)^{3/2}$. Its derivative is

$$f'(t) = \sqrt{1-t}\left(1 - \frac{5}{2}t\right), \qquad f(0) = f(1) = 0. \tag{1309}$$

It is positive before $t = 2/5$ and negative afterwards, proving (1307). The scale condition then bounds a_* and gives (1308). □

The maximum also has an algebraic proof. Put $s = \sqrt{3/5}$ and $r = \sqrt{1-t}/s \ge 0$. Then $f(t) = s^3r^3(1 - 3r^2/5)$ and

$$\mathfrak{c} - f(t) = \frac{s^3}{5}(r-1)^2(3r^3 + 6r^2 + 4r + 2) \ge 0. \tag{1310}$$

This isolates the exact polynomial inequality from the square-root change of variable and the physical source assumptions.

The proof isolates the physical input that remains necessary. Without a justified uniform B, the mass relation alone is not an observational exclusion. Near a scalar mode or a composition transition the linear response bound may fail. A static coercivity bound can help establish a static response estimate, but a radiating binary additionally needs frequency-dependent source matching. If C, source masses or response coefficients vary in a parameter comparison, they must be bounded or propagated on that same set. An eccentric calculation must treat the individual harmonic thresholds and their source amplitudes.

22.8. *An elementary static-force envelope and its calibration.* The common mass–coupling relation also constrains a simpler observable than binary radiation: the static force between two ideal weak sources. This calculation isolates the role of the common matching length before composition, finite size, and nonlinear stellar response are introduced. Let $\mu = \mu_\varphi$ be the physical inverse range and put $\alpha = \alpha_\varphi = a_0^2$. For the stable minimal branch,

$$0 \le \alpha < \frac{1}{3}, \qquad 6\alpha \le \mu^2 \ell^2. \tag{1311}$$

Assume a canonically normalized scalar, linear weak fields, unscreened point sources, and scalar-independent elementary Jordan masses. With G_* denoting the tensor Newton constant, the matched potential is

$$V(r) = -\frac{G_* m_1 m_2}{r}(1 + \alpha e^{-\mu r}), \qquad \frac{|F_\varphi(r)|}{G_* m_1 m_2 / r^2} = \alpha(1 + \mu r)e^{-\mu r}. \tag{1312}$$

The second formula follows by differentiating $e^{-\mu r}/r$; omitting the factor $1 + \mu r$ would confuse a potential ratio with a force ratio.

Proposition 112 (Point-source force bound). *Under these hypotheses, for $r > 0$,*

$$\begin{aligned} \frac{|F_\varphi(r)|}{G_* m_1 m_2 / r^2} &\le C_* \left(\frac{\ell}{r}\right)^2, \\ C_* &:= \frac{(1+\sqrt{3})^2(2+\sqrt{3})e^{-(1+\sqrt{3})}}{6} = 0.3021755006588408\ldots. \end{aligned} \tag{1313}$$

Proof. Set $x = \mu r$. Inequality (1311) bounds the force ratio by $(\ell/r)^2 x^2(1+x)e^{-x}/6$. The derivative of its x-dependent factor $x^2(1+x)e^{-x}/6$ is $x(2+2x-x^2)e^{-x}/6$. On $x \ge 0$ this factor increases up to $x = 1+\sqrt{3}$ and then decreases to zero. Substitution gives the result. At $\mu = 0$ the branch relation forces $\alpha = 0$, so the endpoint is included. □

This bound is relative to the tensor force. A measured Newton constant need not have that normalization. To see the distinction exactly, suppose

an ideal calibration uses a separation r_c and define $f_0(x) = (1+x)e^{-x}$ and $G_{\rm cal} = G_*[1+\alpha f_0(\mu r_c)]$. The fractional force excess relative to that calibration is

$$\frac{|F_{\rm tot}(r)|}{G_{\rm cal} m_1 m_2/r^2} - 1 = \frac{\alpha\{f_0(\mu r) - f_0(\mu r_c)\}}{1+\alpha f_0(\mu r_c)}. \tag{1314}$$

Its absolute value does not generally satisfy (1313): for fixed $\mu > 0$ and $\alpha > 0$, the right-hand side of (1314) tends to a nonzero negative constant as $r \to \infty$, whereas $(\ell/r)^2$ tends to zero. Experimental comparison must therefore retain the calibration map.

For completeness, the two algebraic bounds on α can be combined without losing their shared dependence on μ. With $s = \ell/r > 0$ and $x_* = 1+\sqrt{3}$, the supremum over those two bounds alone is

$$\sup_{x\ge 0} \min\{s^2x^2/6, 1/3\}(1+x)e^{-x} = \begin{cases} C_* s^2, & s \le \sqrt{2}/x_*, \\ (1+\sqrt{2}/s)e^{-\sqrt{2}/s}/3, & s > \sqrt{2}/x_*. \end{cases} \tag{1315}$$

Indeed the cap changes branch at $x = \sqrt{2}/s$; before that point the uncapped factor rises until x_*, while beyond the cap $f_0'(x) = -xe^{-x} \le 0$. The strict inequality $\alpha < 1/3$ can make the displayed value a supremum rather than an attained maximum. Additional restrictions of the mother branch may lower it further.

If the mass is restricted by $\mu\ell \le \varepsilon < \sqrt{2}$, the same proof instead uses $x_E = \min\{x_*, \varepsilon r/\ell\}$ and gives $s^2x_E^2(1+x_E)e^{-x_E}/6$. A low-energy interpretation also requires the exchanged momenta and separation to lie in its controlled regime. Neither the mass restriction alone nor the static force bound controls omitted higher-order interactions. Composite charges, screening, source geometry and detector calibration must be computed before this result becomes an experimental exclusion statement.

22.9. *An illustrative common-scale calculation.* To assess scale rather than claim a nuclear prediction, retain the previous GR trace responses and orbital coefficients. For each fixed EOS use one cap for all three binaries,

$$\ell_{\rm max} = 0.1 \min_j R_{{\rm NS},j}, \qquad B_j = |C^{\rm tr}_{{\rm NS},j} - C^{\rm tr}_{{\rm WD},j}|. \tag{1316}$$

This gives $\ell_{\rm max} = 1054.4184\,\mathrm{m}$ for SLy and $1084.2243\,\mathrm{m}$ for AP4. The radius cap is an illustrative derivative-scale choice, not a uniform bound on all stellar EFT remainders. Likewise, the trace coefficients define a static linear scenario rather than a bound on the missing massive composite response. The historical J0348 mass inputs are retained to avoid substituting its new decay-derived mass. For the very weakly eccentric J2222 system, the retained leading coefficient is used as a near-circular approximation; no complete massive eccentric harmonic sum is evaluated.

System	EOS	a_*	Envelope for S	Envelope / σ_j
J1738	SLy	2.9431×10^{-10}	2.0962×10^{-30}	5.6654×10^{-16}
J1738	AP4	3.0263×10^{-10}	2.3504×10^{-30}	6.3525×10^{-16}
J0348, historical	SLy	1.0195×10^{-9}	2.9629×10^{-28}	6.3959×10^{-15}
J0348, historical	AP4	1.0483×10^{-9}	2.6525×10^{-28}	5.7256×10^{-15}
J2222	SLy	4.2694×10^{-11}	6.0678×10^{-32}	7.9840×10^{-18}
J2222	AP4	4.3901×10^{-11}	6.3424×10^{-32}	8.3453×10^{-18}

Table 22. Synthetic trace-response envelopes using the published summary uncertainties σ_j. Each entry maximizes its own circular dipole shape over the common-weight mass boundary; these separate maxima need not occur at the same a_0. They are not measured signals, fitted source charges, or limits on arbitrary scalar models.

One common a_0 must be used when combining sources. Under the previous diagonal Gaussian summary convention define $D(a_0)^2 = \sum_j [S_j(a_0)/\sigma_j]^2$. The individual analytic envelopes imply

$$D(a_0) \le \begin{cases} 6.421 \times 10^{-15}, & \text{SLy}, \\ 5.761 \times 10^{-15}, & \text{AP4}, \end{cases} \tag{1317}$$

where the displayed bounds round upward. A numerical one-parameter search on the mass-boundary scenario gives maxima approximately 6.39586×10^{-15} and 5.72563×10^{-15}, at $|a_0| = 6.44779 \times 10^{-10}$ and 6.63005×10^{-10}, respectively. Agreement with a 10001-point grid is a numerical comparison; the analytic bound in (1317) does not depend on that search being globally optimal. Published nuisance covariances are not reconstructed by this diagonal illustration.

For the SLy J0348 example, an envelope as large as one quoted summary standard deviation would require B at least approximately 8.30×10^6, rather than the retained trace value 0.6636. Such an amplification cannot be assumed while continuing to use an unmodified stable linear stellar model. The calculation therefore gives a precise reason why the earlier massless benchmark separation $D \simeq 0.054$ must not be attributed to the unaltered minimal common-weight branch. It does not exclude additional matched potentials, matter responses or interactions, whose restrictions and observables must instead be derived separately.

A useful next physical test must therefore do more than improve the ODE tolerance. It must determine or bound the same scalar-dependent matter responses, establish a stable source transfer at the relevant frequency, and use a channel with sufficient sensitivity on the allowed parameter set. Changing the

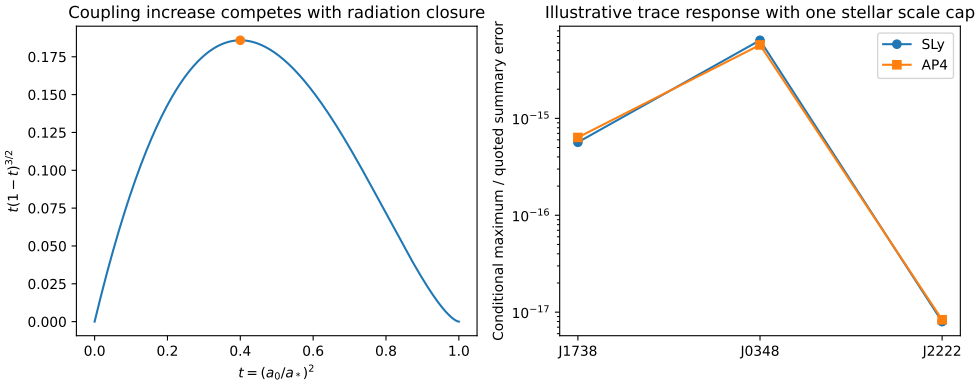


Figure 36. Left: the exact competition between coupling growth and closure of the leading circular radiation channel. Right: the illustrative trace-response envelopes relative to the published summary errors. The two panels describe the stated conditional model and scale choice; they do not constitute a fifth-force detection or a universal exclusion.

potential or matter theory is a different declared branch; refitting a separate charge to every target would remove the cross-source restriction that makes the test informative.

23. **Identifiability and eccentric-orbit radiation in the shared scalar branch**

The stellar calculation above supplies a response map, but a response map is not identifiable merely because it can be evaluated. This section makes the calibration–prediction distinction explicit and then treats the finite mass threshold for an eccentric orbit. Both calculations use the same declared normalization as the preceding stellar and pulsar sections. The numerical values are conditional diagnostics based on the archived response kernels and the published timing-summary scales; they are not a fit to the complete timing likelihood.

23.1. *A local no-refit test for the stellar response.* Let the two calibrated response coefficients be collected in $\theta = (\theta_1, \theta_2)^T$, and let an additional matter derivative d_3 enter the three source charges through

$$q_i(\theta, d_3) = B_i\theta + d_3 z_i, \qquad i = 1, 2, 3, \tag{1318}$$

where B_i is a row of the archived response matrix and z_i is the declared common-source response. The leading dipole diagnostic has the form $s_i = -K_i q_i^2$, with

Table 23. Local identifiability diagnostic for the archived response map. The input point is synthetic and the two quoted timing scales are used only as a diagonal summary covariance. The target interval uses $|d_3| \le 10^{-4}$ and compensates θ to keep the first two charges fixed. It is therefore a sensitivity interval, not an experimental bound.

EOS	$\kappa(D_{12})$	$\mathrm{sd}(\theta_1)$	$\mathrm{sd}(\theta_2)$	$\mathrm{sd}_{\mathrm{lin}}(s_3)$	$s_3(d_3\text{-interval})$
SLy	7.5191×10^2	5.2903×10^{-1}	8.6315×10^{-1}	4.0865×10^{-15}	$[-2.3279, -2.1783] \times 10^{-16}$
AP4	5.4314×10^2	5.1377×10^{-1}	8.4476×10^{-1}	4.7159×10^{-15}	$[-2.2690, -2.1721] \times 10^{-16}$

$K_i > 0$ fixed by the orbital summary. Its exact local Jacobian is therefore

$$D_{ij} := \frac{\partial s_i}{\partial \theta_j} = -2K_i q_i B_{ij}. \tag{1319}$$

This derivative exposes two distinct sources of non-identifiability. First, if $q_i = 0$, the squared observable has zero first derivative even when the underlying charge map has full rank. Second, a near-dependent pair of rows of the calibration map amplifies coefficient errors. The relevant condition number is that of the weighted two-row Jacobian, not merely the determinant of the unsquared charge map.

For a declared diagonal summary covariance Σ_y, the local Fisher diagnostic and the propagated variance of an unused third signal are

$$\mathcal{I} = D_{12}^T \Sigma_y^{-1} D_{12}, \qquad \mathrm{Var}_{\mathrm{lin}}(s_3) = D_3 \mathcal{I}^{-1} D_3^T. \tag{1320}$$

The notation $\mathrm{Var}_{\mathrm{lin}}$ emphasizes that this is a local linearization. It is not a posterior distribution and does not include uncertainty in the equation of state, distances, masses, orbital nuisance parameters or the scalar background.

For the archived synthetic point $\theta = (10^{-3}, 2 \times 10^{-4})$, the two calibration rows have rank two but are ill-conditioned after the squared-signal map. The values are shown in Table 23. The very large coefficient standard deviations obtained from the quoted summary scales are a useful negative result: the displayed timing summaries do not by themselves identify the two coefficients at the precision needed to claim a parameter-free fifth-force prediction.

The calculation also gives an exact algebraic countercheck on the no-refit logic. Solving $B_{12}\,\delta\theta = -d_3 z_{12}$ leaves the first two charges unchanged, whereas the third changes by

$$\delta q_3 = d_3 \kappa_3, \qquad \kappa_3 = z_3 - B_3 B_{12}^{-1} z_{12}. \tag{1321}$$

For SLy and AP4, $\kappa_3 = 0.0939665$ and 0.0613412, respectively. Thus a common source derivative that is invisible to the two calibration objects changes the unused prediction. A mother-selected prediction would require an independent derivation or measurement of this derivative, together with a complete likelihood

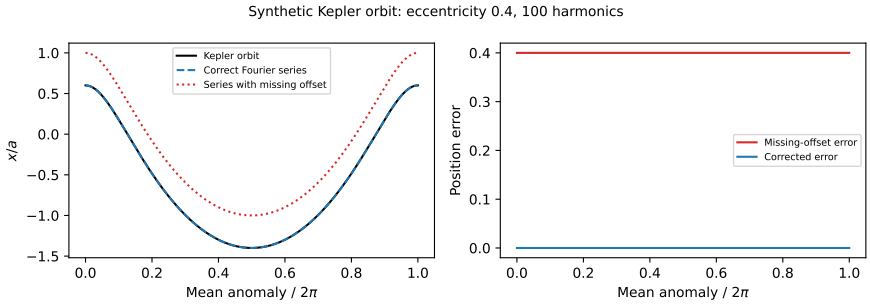


Figure 37. Synthetic eccentric orbit at $e = 0.4$. Solving Kepler's equation on 8192 uniform mean-anomaly nodes agrees with the corrected 100-harmonic position series to 8.4×10^{-16} in x/a. Replacing the constant term $-3e/2$ by $-e/2$ produces a uniform offset e. The nonzero-frequency coefficients, and hence the point-dipole radiation sum, are unchanged.

for the calibration data. The present result establishes the identifiability condition and its failure mode; it does not establish a fifth-force signal.

23.2. *All open harmonics of an eccentric massive scalar dipole.* The circular threshold in Eq. (1218) is not the threshold for an eccentric binary. Let M be the mean anomaly, E the eccentric anomaly, and $e < 1$ the eccentricity. Kepler's equation and the orbital coordinates are

$$M = E - e\sin E, \qquad \frac{x}{a} = \cos E - e, \qquad \frac{y}{a} = \sqrt{1-e^2}\sin E. \tag{1322}$$

The Bessel expansions give, for $n \geq 1$,

$$\frac{x}{a} = -\frac{3e}{2} + \sum_{n\geq 1} A_n \cos(nM), \qquad \frac{y}{a} = \sum_{n\geq 1} B_n \sin(nM), \tag{1323}$$

with

$$A_n = \frac{2J_n'(ne)}{n}, \qquad B_n = \frac{2\sqrt{1-e^2}}{ne} J_n(ne). \tag{1324}$$

The constant term follows directly from the time measure:

$$\left\langle \frac{x}{a} \right\rangle_M = \frac{1}{2\pi}\int_0^{2\pi} (\cos E - e)(1 - e\cos E)\, dE = -\frac{3e}{2}.$$

Its second time derivative is zero, so it does not contribute to dipole radiation. The coefficient formulas above are used for $0 < e < 1$; at $e = 0$ their continuous limits give $A_1 = B_1 = 1$ and all higher coefficients zero.

Figure 37 compares the Fourier position with an independent solution of Kepler's equation.

At leading point-dipole order, the massless power in the n-th harmonic is proportional to

$$W_n(e) = \frac{1}{2} n^4 (A_n^2 + B_n^2) = 2n^2 \left[J_n'(ne)^2 + \frac{1-e^2}{e^2} J_n(ne)^2 \right]. \tag{1325}$$

The identity

$$\sum_{n=1}^{\infty} W_n(e) = \frac{1 + e^2/2}{(1-e^2)^{5/2}} \tag{1326}$$

recovers the standard eccentric enhancement and provides an internal check on the normalization.

Write $x_\varphi = m_\varphi c^2/(\hbar\Omega_b)$. The n-th harmonic is propagating only for $n > x_\varphi$, and its leading flux factor is $[1 - (x_\varphi/n)^2]_+^{3/2}$. The finite, explicitly computable radiation factor is consequently

$$S_N(e, x_\varphi) = \sum_{n=1}^{N} W_n(e) \left[1 - \left(\frac{x_\varphi}{n} \right)^2 \right]_+^{3/2}. \tag{1327}$$

It multiplies the massless *circular-orbit* dipole power at the same semimajor axis, mean motion, masses, and charges. If the reference prediction already includes the eccentric enhancement, the appropriate multiplier is $S_N(e, x_\varphi)(1 - e^2)^{5/2}/(1 + e^2/2)$, with the omitted-tail error stated below. This distinction prevents counting eccentricity twice. A massive field can therefore have a static Yukawa force even when the fundamental radiative harmonic is closed, while higher harmonics remain open in an eccentric orbit.

For completeness, the truncation is controlled analytically. If $\eta > 0$ satisfies $\delta = \eta - e \sinh \eta > 0$, the contour estimate $|J_n(ne)| \le e^{-n\delta}$ and $|J_n'(ne)| \le \cosh(\eta) e^{-n\delta}$ imply

$$\begin{aligned} 0 \le \sum_{n>N} W_n(e) &\le C_\eta \frac{r^{N+1}}{1-r} \left[(N+1)^2 + \frac{2(N+1)r}{1-r} + \frac{r(1+r)}{(1-r)^2} \right], \\ C_\eta &= 2 \left[\cosh^2 \eta + \frac{1-e^2}{e^2} \right], \qquad r = e^{-2\delta}. \end{aligned} \tag{1328}$$

The threshold factor is at most one, so the same expression bounds the omitted massive flux. At $e = 0.4$, $\eta = 0.5$, and $N = 100$, the bound is 8.16×10^{-21}. The computed massless sum is 1.670034874255044, agreeing with Eq. (1326) to double precision. An independent uniform-mean-anomaly solution of Kepler's equation and FFT quadrature agrees with every retained W_n to 2.3×10^{-16}. Figure 38 shows the resulting threshold curve.

The calculation closes the harmonic bookkeeping and supplies a controlled tail for the stated approximation. It does not include scalarization, screening,

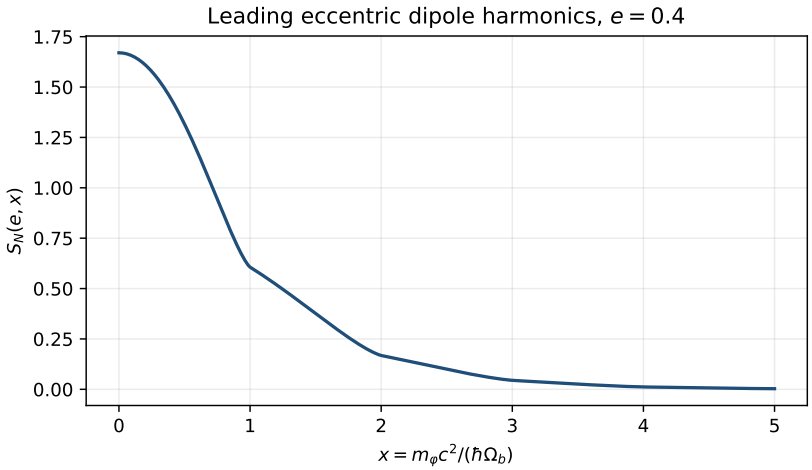


Figure 38. Leading point-dipole eccentric radiation factor $S_{100}(0.4, x_\varphi)$ from Eq. (1327). The curve is a conditional harmonic calculation, not a timing measurement or a complete scalar–tensor waveform.

conservative orbital corrections, higher multipoles, finite-size effects, or correlated timing nuisance parameters. Those effects must be included before the result can be used as an observational exclusion or as a new-physics detection.

24. **A frozen-parameter public-data holdout test**

The preceding stellar calculation supplies a response template, but it does not by itself determine whether the same template is compatible with more than one binary. We therefore separate calibration from evaluation. The published residual summary for PSR J1738+0333 is used once to set a one-sided envelope for one global amplitude. The resulting amplitude is then carried unchanged to PSR J0348+0432 and PSR J2222–0137. No target charge, equation of state, or coupling is re-fitted. This is a retrospective holdout test of the declared effective branch; it is not a new pulse-arrival-time analysis.

24.1. *Frozen response map.* Fix one of the two EOS choices, SLy or AP4, and let $a_{0,\mathrm{ref}}^{\mathrm{DEF}} = 10^{-3}$ denote the illustrative coupling used in the stellar solve of Section 20. In the linear weak-coupling regime write the common amplitude as $\rho = a_0/a_{0,\mathrm{ref}}$. The already computed charge differences obey

$$\Delta\alpha_i(\rho) = \rho\,\Delta\alpha_i^{(0)}, \qquad B_i(\rho) := C_i\{\Delta\alpha_i(\rho)\}^2 = \rho^2 B_i^{(0)}, \tag{1329}$$

where B_i is the positive magnitude of the leading dipole contribution $-\dot{P}_{b,i}^{\mathrm{dip}}$. The canonical and DEF conventions give the same $B_i^{(0)}$: $C_i^{\mathrm{can}} = 2C_i^{\mathrm{DEF}}$ and

$\Delta\alpha_i^{\mathrm{DEF}} = \sqrt{2}\Delta\alpha_i^{\mathrm{can}}$. Consequently, the ratio

$$R_{j1} := \frac{B_j^{(0)}}{B_1^{(0)}} \tag{1330}$$

is independent of the amplitude that is calibrated from the first system.

For a residual summary $Y_i = -B_i + \epsilon_i$, with the Gaussian approximation used in Proposition 103, the J1738+0333 upper endpoint is

$$U_1 = \max\{0, z_{0.95}\sigma_1 - y_1\} = 4.0859584197 \times 10^{-15}, \qquad z_{0.95} = 1.64485362695. \tag{1331}$$

The amplitude envelope and the corresponding holdout envelope are therefore

$$\rho_{95} = \sqrt{\frac{U_1}{B_1^{(0)}}}, \qquad B_{j,95} = R_{j1}U_1. \tag{1332}$$

Only the calibrator enters U_1. Equations (1329)–(1332) are thus a no-refit transfer rule rather than three independent fits.

EOS	holdout	R_{j1}	ρ_{95}	$-B_{j,95}$ (fs/s)	$(y_j + B_{j,95})/\sigma_j$
SLy	J0348+0432	11.780040	5.602561	−48.1328	0.6807
SLy	J2222–0137	1.375579	5.602561	−5.6206	−0.0894
AP4	J0348+0432	9.405051	5.440464	−38.4286	0.4712
AP4	J2222–0137	1.282314	5.440464	−5.2395	−0.1395

Table 24. Frozen-parameter public-data holdout envelopes. The calibrator is J1738+0333; its residual is not re-used as a holdout. The observed target summaries are -16.6 ± 46.3259 fs/s for J0348+0432 and -6.3 ± 7.6 fs/s for J2222–0137. The last column measures the distance between the observed target residual and the upper-envelope mean in units of the quoted target summary error. It is a diagnostic comparison, not a new confidence level.

The ratios in Table 24 are obtained from the same stellar response rows used in Table 17; the archived benchmark predictions are reproduced before the amplitude is rescaled. For both EOS choices, the two target summaries lie within two quoted standard deviations of the calibration-derived envelopes. The J0348 result is compatible with an envelope as large as −48.13 fs/s (SLy) or −38.43 fs/s (AP4), while the J2222 envelope is close to its observed central residual. Since the calibrator has a positive residual and hence a constrained best-fit extra decay of zero, the calculation provides an upper envelope rather than a nonzero point estimate.

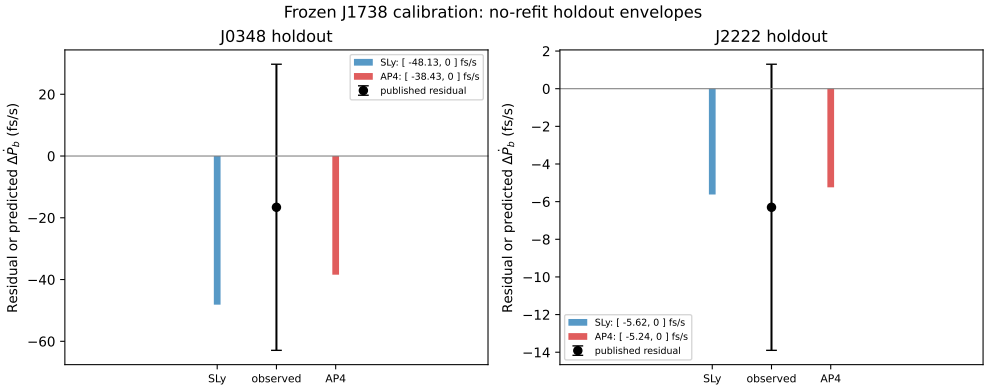


Figure 39. The J1738+0333 calibration is propagated to two unused published summary records. Thick vertical segments are the allowed leading-dipole envelopes $[-B_{j,95}, 0]$ for the two fixed EOS choices; the point and error bar are the published target residual summaries. The figure displays a conditional no-refit constraint and contains no fitted target signal.

The common amplitude and common stellar-response map connect the additional orbital decay across different masses without assigning an independent scalar charge to each binary. It does not establish that the illustrative coupling is selected by the mother functional. It also does not include the full scalar–tensor timing likelihood, correlated nuisance parameters, EOS uncertainty, screening, or conservative strong-field corrections. A positive fifth-force claim would require a predeclared source model, a complete timing likelihood, independent calibration of those effects, and replication on data not used in the present retrospective summaries.

24.2. *An additional target and a comparison without a fitted amplitude.* An orbital clock measures the cumulative loss of binary binding energy. If the two stars carry different scalar charge per unit mass, their orbital motion can radiate a scalar dipole in addition to the tensor quadrupole. The distinctive prediction is therefore a common relation between the charges of different stars and their additional orbital decay. An individual charge fitted to each residual would remove this test. We instead retain the action, coupling and two EOS choices of the preceding calculation and compute a further stellar pair before using its period-decay residual. The target selection is retrospective: its published residual was already available, although it was not used to choose these retained parameters.

Ding et al. [60] report for PSR J1012+5307 the excess $y = 10.6 \pm 6.1\,\mathrm{fs/s}$, where $1\,\mathrm{fs/s} = 10^{-15}$. Their adopted optical inputs are $m_c = 0.174 \pm 0.011\,M_\odot$

and the spectroscopic mass ratio $q = 10.44 \pm 0.11$. Thus the central neutron-star mass used here is $m_p = qm_c = 1.81656\,M_\odot$. We use the rounded period $P_b = 0.60$ days in their Table 4; a rounding interval of ± 0.005 day changes the leading dipole coefficient by less than 0.85%. These inputs are historical published summaries, not a new timing solution. Their excess includes the reported subtraction of the Shklovskii, Galactic and GR quadrupole terms. A varying gravitational coupling or a revised acceleration model would require a joint treatment.

At the retained coupling $a_0^{\mathrm{DEF}} = 10^{-3}$, the same stellar boundary-value calculation gives the white-dwarf charge $\alpha_c^{\mathrm{DEF}} = 9.99971258 \times 10^{-4}$. The neutron-star charges are $4.95644445 \times 10^{-4}$ for SLy and $4.98219654 \times 10^{-4}$ for AP4. These are computed source responses, not charges inferred from y. They give the following comparison. For the added star, tightening the integration

Target	Published residual	SLy prediction	AP4 prediction
J0348+0432	-16.6 ± 46.3259	-1.53344	-1.29832
J2222–0137	-6.3 ± 7.6	-0.17906	-0.17702
J1012+5307	10.6 ± 6.1	-0.15149	-0.14995

Table 25. Additional orbital decay in fs/s at the single retained reference coupling. The first two observational inputs and their mass-inference assumptions are those of Table 17; the additional target uses Ding et al. [60]. All predictions use central input masses. The quoted observational errors are not complete theory-error bars.

tolerance and independently integrating the exterior provide numerical checks of the charge. Such checks do not remove uncertainty in the EOS, the cold white-dwarf model, or the measured source masses. The grid described below gives predicted decays from -0.2257 to -0.1077 fs/s for SLy, and from -0.2075 to -0.1104 fs/s for AP4. A finite grid of the optical mass and mass ratio at their central values and one quoted standard deviation on either side tests source sensitivity separately; it is not a posterior credible region because their joint distribution has not been supplied.

The common-amplitude hypothesis also admits a test that eliminates the amplitude algebraically. Write $B_i = gb_i$, where $b_i = B_i^{(0)} > 0$ and $g = \rho^2 \geq 0$, and let index 1 denote J1738+0333. For each remaining target set

$$R_j = \frac{b_j}{b_1}, \qquad d_j = Y_j - R_j Y_1, \qquad V_{jk} = \delta_{jk}\sigma_j^2 + R_j R_k \sigma_1^2. \tag{1333}$$

Under independent Gaussian summary errors with fixed b_i, $Y_i = -gb_i + \epsilon_i$, the amplitude cancels exactly: $d_j = \epsilon_j - R_j\epsilon_1$. The second term in V is essential:

the targets share the same calibration error and are not independent after this subtraction. Since the diagonal matrix of target variances is positive definite, so is V. Whitening $d \sim N(0, V)$ then gives

$$Q = d^T V^{-1} d \sim \chi^2_3. \tag{1334}$$

No value of g is chosen from the target residuals in this statistic. For SLy and AP4 respectively, $Q = 3.8571$ and 3.7891, with conditional upper-tail probabilities 0.2773 and 0.2852. These values test the shared response pattern. They are not probabilities that the theory is true, and the null pattern includes $g = 0$. Shared Galactic or mass-inference errors would change V; the numerical values above apply to the explicitly stated independent-summary approximation.

To ask whether the data prefer the fixed nonzero benchmark to GR, one must compare predictions rather than only ask whether they are compatible. At $g = 1$, retaining all three target summaries gives

$$\log \frac{\mathcal{L}_{\rm ref}}{\mathcal{L}_{\rm GR}} = -\frac{1}{2} \sum_{j \in \mathcal{H}} \frac{2 y_j b_j + b_j^2}{\sigma_j^2} = \begin{cases} -0.01290, & \text{SLy}, \\ -0.01433, & \text{AP4}. \end{cases} \tag{1335}$$

The corresponding likelihood ratios are 0.9872 and 0.9858. These nearly equal likelihoods do not distinguish the benchmark from GR. In particular, the positive J1012 residual does not provide evidence for an additional negative dipole contribution. No EOS is selected by taking the more favorable of these results.

24.3. *Sensitivity required for a discriminating observation.* The same calculation specifies a quantitative experimental target. For a fixed predicted vector b and independent target errors, define

$$D_{\mathcal{H}} = \left(\sum_{j \in \mathcal{H}} b_j^2 / \sigma_j^2 \right)^{1/2}, \qquad Z = -\frac{\sum_j b_j Y_j / \sigma_j^2}{D_{\mathcal{H}}}. \tag{1336}$$

Under GR, $Z \sim N(0, 1)$; at the fixed benchmark, $Z \sim N(D_{\mathcal{H}}, 1)$. The separation is only 0.04762 for SLy and 0.04396 for AP4 at the present quoted errors. If all these standard errors could be reduced by a factor f, with the same source prediction and no additional systematic error, the power of a one-sided threshold $Z > 5$ would be $1 - \Phi(5 - f D_{\mathcal{H}})$. Requiring 95% power gives

$$f \geq \frac{5 + \Phi^{-1}(0.95)}{D_{\mathcal{H}}} \simeq 140 \text{ (SLy)}, \qquad 151 \text{ (AP4)}. \tag{1337}$$

This is an idealized sensitivity calculation, not a prediction that longer timing alone can deliver these factors. Distances, proper motions, optical masses, Galactic acceleration and stellar modeling must all support the target error. At the larger upper-envelope amplitudes allowed by the historical J1738 calibration, the corresponding factors would be about 4.45 and 5.11, conditional on the linear

response scaling. Those envelope endpoints are upper limits, not measured nonzero signals.

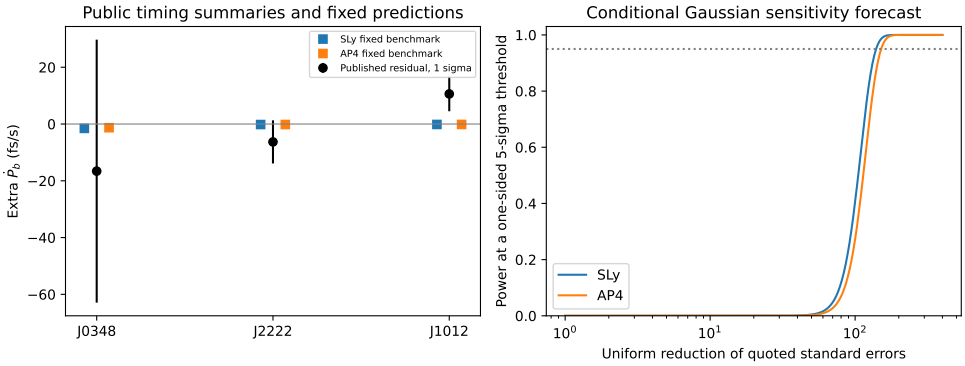


Figure 40. Left: historical public timing summaries and computed predictions at a common fixed coupling. Right: the conditional Gaussian power forecast of Eq. (1337). The curves are analytic sensitivity forecasts; they are not additional observational data.

The empirical interpretation depends on the branch being tested. This calculation retains the independently specified massless scalar reference action with nonzero coupling. It does not realize the minimal common-weight branch in which exact zero scalar mass forces the matter coupling to vanish. For that branch, its parameter map must be inserted before comparison with data: the same parameters must determine the scalar mass, stellar charges and radiative transfer for every binary. In the leading circular regime, the response is

$$b_i(\vartheta) = C_i\{\Delta\alpha_i(\vartheta)\}^2 \left[1 - \left\{\frac{m_\varphi(\vartheta)c^2}{\hbar\Omega_i}\right\}^2\right]_+^{3/2}.$$

If the calibration system has zero response, the ratio in Eq. (1333) is undefined and a direct joint likelihood is needed. A different parameter fit for each binary would no longer test the proposed shared parameter map. The present results therefore provide a reproducible conditional scalar test and an explicit sensitivity requirement; a distinctive empirical test of the mother functional still requires that map and the associated timing model.

24.4. *Independent solar-system calibration and transfer to binary clocks.* A solar-system propagation experiment supplies a physically different calibration of the same reference coupling. Radio light passing the Sun experiences a propagation delay determined by both the temporal and spatial parts of the metric. In the unscreened, constant-coupling, massless reference branch, with

weak solar self-gravity neglected at the retained order, the physical Jordan-frame metric has coefficients proportional to $G_*M(1+a_0^2)$ in its Newtonian temporal potential and $G_*M(1-a_0^2)$ in its spatial potential. Here $a_0 = a_0^{\mathrm{DEF}}$ and $A(0) = 1$. Their ratio gives

$$G_N = G_*(1+a_0^2), \qquad \gamma = \frac{1-a_0^2}{1+a_0^2}, \qquad \gamma - 1 = -\frac{2a_0^2}{1+a_0^2}. \tag{1338}$$

Thus this experiment constrains the weak-field coupling independently of the strong-field neutron-star charge. This is the usual scalar–tensor weak-field relation, not a new prediction unique to the mother functional.

Bertotti, Iess and Tortora [16] report $\gamma - 1 = (2.1 \pm 2.3) \times 10^{-5}$ from the Cassini radio links. Treating this reported uncertainty as a Gaussian standard deviation, write $Y_\gamma = -B_\gamma + \epsilon_\gamma$, where $B_\gamma = 2a_0^2/(1+a_0^2) \geq 0$. The same one-sided construction as above gives

$$U_\gamma = \max\{0, \Phi^{-1}(0.95)\sigma_\gamma - y_\gamma\}, \qquad |a_0| \leq \sqrt{\frac{U_\gamma}{2-U_\gamma}} = 0.00290101. \tag{1339}$$

This is a conditional one-sided 95% upper limit reconstructed from the published summary. It is not a new fit to the spacecraft Doppler data or a determination of the strongest present bound. The boundary value zero is retained if the unconstrained upper limit is negative; coverage is then at least 95% for the nonnegative parameter.

The coupling in Eq. (1339) is now fixed using only the solar-system observation. Re-solving the nonlinear stellar boundary-value problem at this endpoint, for the same central source masses and EOS choices, gives the rates in Table 26.

Target	SLy endpoint	AP4 endpoint	Published residual
J0348+0432	−12.9036	−10.9258	-16.6 ± 46.3259
J2222–0137	−1.5069	−1.4897	-6.3 ± 7.6
J1012+5307	−1.2749	−1.2619	10.6 ± 6.1

Table 26. Cross-observable transfer in fs/s. A single coupling determined by the Cassini summary upper endpoint is used for every star. The columns are predictions at that endpoint, not separately fitted binary signals or simultaneous confidence intervals. Source-mass and timing-model assumptions are retained from the preceding tables.

The endpoint predictions differ from scaling the reference rates by $(0.00290101/0.001)^2$ by at most 1.29×10^{-4} in relative value. This direct calculation checks the weak-coupling scaling at the tested endpoint; it does

not prove a uniform error bound throughout the parameter interval. No period-decay residual is used to set the endpoint or to adjust an individual stellar charge.

The solar-system limit is more restrictive than the earlier pulsar-only amplitude envelope in this particular massless reference branch. Using the recomputed endpoint signals in Eq. (1336) gives idealized error-reduction factors of about 16.6 and 18.0 for 95% power at a one-sided 5σ threshold. The more optimistic pulsar-only factors quoted above therefore cannot be used once this independent constraint is imposed. At the smaller fixed benchmark $a_0 = 10^{-3}$, the factors remain approximately 140 and 151.

The test connects light propagation and binary radiation through one specified action and one coupling. Its current outcome is a conditional constraint without a detected extra force. A finite scalar range, screening, nonconstant coupling, or the minimal common-weight mass–coupling relation changes Eq. (1338); in those cases the solar propagation and stellar radiation problems must both be recomputed before making this transfer.

25. **Physical-time evolution of the homogeneous constrained branch**

The nonlinear constraint family constructed earlier supplies initial data. Initial-data preservation alone does not show that the family follows a physical Lorentzian evolution. Here we evolve the same diagonal family in the vacuum Einstein equations with a positive cosmological constant. This is a matched Einstein branch and is therefore a controlled test of physical-time evolution, rather than a claim about the full independent-connection mother system.

Use the Bianchi-I metric

$$ds^2 = -dt^2 + \sum_{i=1}^{3} A_i(t)^2 (dx^i)^2, \qquad H_i = \frac{\dot{A}_i}{A_i}, \qquad H = \frac{1}{3}\sum_i H_i, \tag{1340}$$

and define $s_i = H_i - H$. With the convention $K^i{}_j = H_i \delta^i_j$, the vacuum equations are

$$\dot{H}_i + 3H H_i = \Lambda, \qquad 3H^2 = \Lambda + \frac{1}{2}\sum_i s_i^2. \tag{1341}$$

The initial branch is

$$H_i(0) = \frac{\tau_0}{3} + c_i, \qquad (c_1, c_2, c_3) = (a, -a, 0), \qquad \tau_0 = \sqrt{3(a^2 + \Lambda)}. \tag{1342}$$

Thus $\sum_i c_i = 0$ and $\sum_i c_i^2 = 2a^2$, so the Hamiltonian constraint holds at $t = 0$.

Let $V = A_1 A_2 A_3$. Subtracting the mean of the first equation in Eq. (1341) gives

$$\dot{s}_i = -3H s_i, \qquad s_i(t) = \frac{c_i}{V(t)}, \qquad \dot{H} = \Lambda - 3H^2. \tag{1343}$$

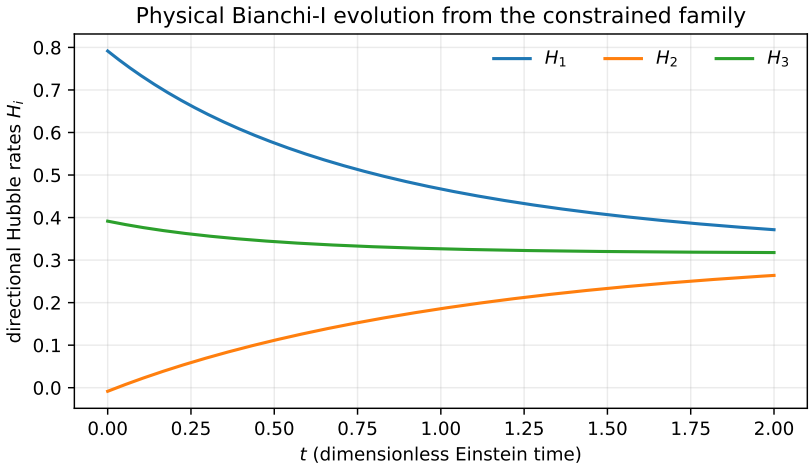


Figure 41. Directional expansion rates for the matched Bianchi-I Einstein–Λ branch with $(\Lambda, a) = (0.3, 0.4)$. The shear decays as V^{-1}, while the three rates approach the same de Sitter value. The plotted curve is a dimensionless synthetic calculation.

The constraint then reduces the volume equation to

$$\dot{V} = \sqrt{3\Lambda V^2 + 3a^2}, \qquad V(t) = \cosh(kt) + \frac{\tau_0}{k}\sinh(kt), \qquad k = \sqrt{3\Lambda}, \tag{1344}$$

where the positive root corresponds to the expanding branch and $V(0) = 1$. The directional scale factors are then given without another differential equation by

$$A_i(t) = V(t)^{1/3} \exp\left(c_i \int_0^t \frac{du}{V(u)} \right), \qquad H_i(t) = \frac{\dot{V}(t)}{3V(t)} + \frac{c_i}{V(t)}. \tag{1345}$$

Direct substitution gives

$$3H^2 - \Lambda - \frac{1}{2}\sum_i s_i^2 = 0, \qquad -\sum_i (\dot{H}_i + H_i^2) + \Lambda = 0, \qquad \dot{H}_i + 3HH_i - \Lambda = 0. \tag{1346}$$

These identities establish the constraint and the two independent Ricci equations analytically for every finite time on the expanding branch.

For the dimensionless test $(\Lambda, a) = (0.3, 0.4)$, a DOP853 integration of the first-order equations was compared with Eqs. (1344)– (1345). On $0 \le t \le 2$, the maximum absolute error over V, A_i, H_i was 1.83×10^{-12}. The analytic constraint and Ricci residuals were below 3.4×10^{-16} in these units. The values are numerical verification of the declared Einstein branch; they are not observational data. Figure 41 displays the directional expansion rates.

The construction has a precise scope. It proves physical evolution of a homogeneous diagonal subset after matching to the Einstein equations. It does

not derive the Lorentzian equations from the complete independent connection action, prove nonlinear constraint propagation for arbitrary inhomogeneous data, or construct an interacting quantum theory. Those questions remain separate closure problems.

26. **Relativistic clock rates and gravitation without rest mass**

The physical meaning of time requires a specification of both geometry and clocks. A Lorentzian metric determines causal relations and lengths of timelike paths. A material clock converts that length into a count of cycles. The orientation of nonequilibrium evolution is a further question about dynamical laws and initial conditions. These three roles need not be supplied by the same mathematical parameter.

26.1. *Proper time and relative clock rates.* Let $\widetilde{g}$ be the physical metric to which the clock matter is minimally coupled, with signature $(-+++)$ and $x^0 = ct$. Along a timelike path, its proper time is

$$d\tau^2 = -c^{-2}\widetilde{g}_{\mu\nu}dx^\mu dx^\nu. \tag{1347}$$

An ideal clock measures this interval under the clock hypothesis. A coordinate time is a label used to compare events; it is not a clock carried by every observer. For a flat physical metric,

$$d\tau = dt\sqrt{1 - v^2/c^2}. \tag{1348}$$

This follows directly by substituting $d\mathbf{x}^2 = v^2dt^2$. Different timelike paths between the same two events can accumulate different proper durations even though each ideal clock functions normally along its own path.

In a static region with zero shift, write

$$d\widetilde{s}^2 = -N(\mathbf{x})^2c^2dt^2 + h_{ij}(\mathbf{x})dx^idx^j, \qquad N > 0.$$

The local speed relative to the static observers is $v_{\mathrm{loc}}^2 = h_{ij}(dx^i/dt)(dx^j/dt)/N^2$. Equation (1347) then gives the exact relation

$$\frac{d\tau}{dt} = N\sqrt{1 - v_{\mathrm{loc}}^2/c^2}. \tag{1349}$$

For $|\Phi|/c^2 \ll 1$, $v_{\mathrm{loc}}^2/c^2 \ll 1$, and $N = 1 + \Phi/c^2 + O(c^{-4})$, this becomes

$$\frac{d\tau}{dt} = 1 + \frac{\Phi}{c^2} - \frac{v_{\mathrm{loc}}^2}{2c^2} + O\left(\frac{\Phi^2 + |\Phi|v_{\mathrm{loc}}^2 + v_{\mathrm{loc}}^4}{c^4}\right). \tag{1350}$$

The coefficient in the O-term also depends on the controlled remainder in the weak-field metric. At equal local speed, a clock at a lower potential accumulates less proper time per unit of this coordinate time. At equal lapse, the moving clock accumulates less. This comparison does not assert the existence of a universal time whose intrinsic rate varies.

For example, in a Schwarzschild exterior with $r_s = 2GM/c^2$, static clocks satisfy

$$\frac{d\tau_B}{d\tau_A} = \sqrt{\frac{1 - r_s/r_B}{1 - r_s/r_A}}.$$

At $r_A = 10r_s$ and $r_B = 20r_s$, the ratio is $\sqrt{19/18} \simeq 1.02740$. These radii are an illustrative geometry, not observational data. A photon emitted at A and received at B has local frequency ratio $\nu_B/\nu_A = N_A/N_B$, since its conserved Killing energy is proportional to $N\nu$. The inverse relation between photon frequency and clock-rate ratio fixes the sign of gravitational redshift.

The lapse is coordinate dependent, whereas the accumulated proper time and a specified frequency comparison are physical observables. In a spatially homogeneous cosmology, comoving observers may use a common cosmic proper-time coordinate. Expansion and cosmological redshift do not by themselves mean that all local clocks change their intrinsic rates together.

26.2. *Clock matter, conformal frames and stochastic time.* On the conformal branch used for the stellar calculation, $\widetilde{g} = A(x)^2 g$, and hence $d\tau_J = A(x) d\tau_E$. Consistently transforming masses and clock frequencies leaves dimensionless observations unchanged. Comparing a Jordan proper time with an Einstein-frame frequency while leaving their unit conversion implicit would introduce a spurious clock effect.

If the scalar also changes dimensionless matter parameters, a clock is specified more fully by its phase count,

$$d\mathcal{N}_i = \nu_i(x)\, d\tau_J, \qquad \delta \log \frac{\nu_i}{\nu_j} = D_{ij}\, \frac{\delta\varphi}{M_{\mathrm{P}}} + O(\delta\varphi^2). \tag{1351}$$

Here $\mathcal{N}_i$ counts cycles, and the sensitivity D_{ij} must be derived from the same matter couplings or measured independently. An additional scalar clock response is therefore distinct from the geometric redshift. The finite-source calculation gives one conditional way of transferring such a response between radii; it does not choose D_{ij} from the existence of stochastic noise.

A stochastic parameter s can instead be related to a calibrated clock through $t = \int_0^s a(X_u)du$, with $a > 0$. Under the stated well-posedness hypotheses, a Markov generator L is then changed to $a^{-1}L$, and an invariant probability π becomes $a\pi/\int a\, d\pi$. This is a change in residence times and their statistics. It is not a derivation of the Lorentzian metric or of the clock hypothesis. Similarly, a nonnegative entropy-production rate describes a statistical arrow; it does not determine the gravitational lapse. The recovery of relativistic clock effects in this framework is conditional on the physical metric and matter matching already specified.

26.3. *What determines a clock and a causal signature.* The reference action and the physical clock play different roles even before a continuum limit. On a finite orthonormal affine realization, keep the action, reference density and fluctuation scale fixed, and replace the mobility by $M_\gamma = \gamma M$, with constant $\gamma > 0$. The complete drift, including its reference-density correction, and the generator then satisfy

$$B_\gamma = \gamma B, \qquad L_\gamma = \gamma L, \qquad \pi_\gamma = \pi.$$

These identities use the same domain and compatible boundary realization. They describe distinct transport rates if the laboratory clock is held fixed. If the clock parameter is also rescaled, they instead describe the same paths with different labels. Indeed, for a finite-dimensional absolutely continuous admissible skeleton $y(t) = x(\gamma t)$,

$$\mathcal{J}^{(\gamma)}_{T/\gamma}[y] = \frac{1}{4\theta}\int_0^{T/\gamma} \gamma\|\dot{x}(\gamma t) - B(x(\gamma t))\|^2_{M^\dagger}\, dt = \mathcal{J}_T[x].$$

Here $(\gamma M)^\dagger = \gamma^{-1}M^\dagger$, and the range constraint is unchanged. Thus the family of admissible mobilities and the path-cost form do not select a clock normalization. Once a mobility and its physical calibration are fixed, this freedom is no longer a freedom to change the same physical model. The explicit correlations in Proposition 127 separate equilibrium identification from transport identification.

The causal signature asks a different question. For a local second-order scalar propagation equation, its principal symbol is the quadratic expression in a wave covector that multiplies the highest derivatives. Its zeros describe candidate characteristic wavefronts. Gauge constraints and unphysical components must be eliminated before this interpretation is applied to a field system.

Proposition 113 (Quadratic hyperbolicity fixes a Lorentzian signature). *Let V be a four-dimensional real covector space, let B be a nondegenerate symmetric bilinear form, and put $q(k) = B(k,k)$. Suppose $q(n) > 0$ for some n, and suppose every polynomial $\lambda \mapsto q(k+\lambda n)$, $k \in V$, has only real roots. Then B has one positive and three negative eigenvalues. Consequently its characteristic cone is Lorentzian; multiplication by -1 gives the convention $(-+++)$.*

Proof. The discriminant condition is

$$B(n,k)^2 - q(n)q(k) \geq 0 \qquad (k \in V).$$

On the three-dimensional subspace $W = \{k : B(n,k) = 0\}$, it implies $q(k) \leq 0$. This restriction is negative definite. To see the strictness, suppose $w \in W$ and $q(w) = 0$. For every $z \in W$, $q(w+tz) = 2tB(w,z) + t^2 q(z) \leq 0$ for both signs of sufficiently small t, so $B(w,z) = 0$. Also $B(w,n) = 0$. Since

$V = \mathbb{R}n \oplus W$, nondegeneracy gives $w = 0$. In this orthogonal decomposition $q(an + w) = a^2 q(n) + q(w)$, which proves the signature. □

This result determines the signature from a quadratic hyperbolic propagation law. Applying it to the mother theory requires deriving that law on a specified physical branch. In particular, retained fourth-order curvature terms cannot be treated as second-order equations without a controlled reduction. Different matter fields may also have different principal symbols. A common light cone requires their physical characteristic sets to agree; the first-order Dirac symbol reaches the quadratic form through its square. These are additional dynamical requirements, not consequences of positivity of the configuration-space mobility. Even a common cone fixes a metric only up to a positive conformal factor; material-clock matching supplies the duration scale. Initial and boundary data then determine a solution, whereas the statistical arrow additionally depends on the prepared law and the specified reversal experiment.

26.4. *A common characteristic cone on the matched two-derivative branch.* Signals and clocks enter an observation in different ways. A signal connects two events; a clock assigns a duration to the interval along its own trajectory. To relate these operations, the physical fields must first have compatible propagation equations. The following calculation uses the retained Lorentzian branch of Theorem 9. It determines the characteristic sets of that branch, rather than selecting the branch from the Euclidean probability law.

Use units $c = \hbar = 1$ in this subsection and the convention $g_{\mu\nu} = \mathrm{diag}(-1, 1, 1, 1)$ in a local orthonormal frame. The retained kinetic terms are

$$I_2 = \int \sqrt{-g} \left[\frac{M_{\mathrm{P}}^2}{2} R - \frac{1}{2} K_{AB} g^{\mu\nu} D_\mu \phi^A D_\nu \phi^B - \frac{1}{4} H_{ab} F^a_{\mu\nu} F^{b\mu\nu} - V \right] d^4x + I_\psi^{(1)}. \tag{1352}$$

Here K and H are positive definite on the retained physical scalar and gauge components. The matched first-order fermion action $I_\psi^{(1)}$ has principal operator $Z_\psi \gamma^\mu D_\mu$, with $Z_\psi > 0$; its overall phase and spinor-adjoint convention are fixed by that matching and do not affect its characteristic set. This is notation for the matched kinetic terms, not an additional microscopic action. In particular, the first-order fermion construction retains the separate hypothesis stated after (336). Masses and algebraic interactions do not enter the principal symbols.

Linearize around an Einstein background with constant scalar vacuum, zero background gauge curvature and zero fermion background. At a fixed point, freeze the coefficients of the highest derivatives and replace ∂_μ by a real covector k_μ. This convention omits the harmless factors of i used in a Fourier transform. Put $q_g(k) = g^{\mu\nu} k_\mu k_\nu$. The background restrictions ensure that the

displayed free physical blocks have no unsuppressed mixed principal derivatives. More general backgrounds require the symbol of the full coupled system.
Scalar perturbations. Variation of the scalar kinetic term gives $\nabla_\mu(K_{AB}\nabla^\mu\delta\phi^B)$ at highest order. Consequently

$$P_\phi(k) = Kq_g(k), \qquad \det P_\phi(k) = \det(K)q_g(k)^{n_\phi}.$$

Since K is invertible, the characteristic covectors are precisely the nonzero zeros of q_g. Derivatives of a smooth scalar kinetic coefficient multiply at most first derivatives of the perturbation and do not alter this frozen principal block.
Gauge perturbations. The highest-order part of $D_\mu(H_{ab}F^{b\mu\nu}) = J^\nu_a$, with the vector index lowered, has symbol

$$(P_A(k)a)_{a\nu} = H_{ab}\{q_g(k)a^b_\nu - k_\nu k^\rho a^b_\rho\}.$$

The amplitude $a^b_\nu = k_\nu\chi^b$ lies in its kernel for every k. Thus the determinant of the ungauged operator vanishes identically and cannot identify the physical cone. In Lorenz gauge, $k^\rho a^b_\rho = 0$, the reduced principal operator is $Hq_g(k)$; quotienting the residual gauge amplitudes leaves the transverse physical modes. A variable H contributes terms such as $(\partial_\mu H_{ab})\delta F^{b\mu\nu}$, which are lower order. Hence constant kinetic coefficients are needed for the canonical constant-coupling equation, but are not needed for this pointwise cone calculation when the metric constitutive form and invertibility remain.
Fermion perturbations. Let $\Gamma(k) = \gamma^\mu k_\mu$, with $\gamma^\mu\gamma^\nu+\gamma^\nu\gamma^\mu = 2g^{\mu\nu}I$. Symmetry of $k_\mu k_\nu$ gives

$$\Gamma(k)^2 = q_g(k)I.$$

When $q_g(k) \neq 0$, $\Gamma(k)^{-1} = \Gamma(k)/q_g(k)$. For a null covector its square is zero, so it is not invertible on the nonzero spinor space. The characteristic set is again $q_g = 0$. The first-order symbol itself is not a multiple of q_g; its square is. Confusing these statements would obscure the different differential orders of the matter equations.
Metric perturbations. Write $h_{\mu\nu} = \delta g_{\mu\nu}$, $h = g^{\mu\nu}h_{\mu\nu}$, and $\bar h_{\mu\nu} = h_{\mu\nu} - g_{\mu\nu}h/2$. In a normal frame the principal part of the linearized Einstein tensor is

$$\begin{aligned}(\delta G_{\mu\nu})_{\mathrm{pr}} = \tfrac{1}{2}\{&k_\mu k^\rho h_{\rho\nu} + k_\nu k^\rho h_{\rho\mu} - q_g h_{\mu\nu} - k_\mu k_\nu h\\ &- g_{\mu\nu}(k^\rho k^\sigma h_{\rho\sigma} - q_g h)\}.\end{aligned} \tag{1353}$$

Harmonic gauge imposes $k^\mu\bar h_{\mu\nu} = 0$, reducing this expression to $-q_g\bar h_{\mu\nu}/2$. Curvature and the cosmological constant enter lower-order terms. The constraints and gauge quotient select the physical tensor polarizations; they do not generate an additional characteristic cone in this Einstein branch.

Proposition 114 (Shared cone of the retained free physical blocks). *Under the kinetic, background and gauge hypotheses above, the scalar, gauge, Dirac and Einstein perturbation blocks in* (1352) *have the same characteristic*

set $\{k \neq 0 : q_g(k) = 0\}$. *Smooth nonvanishing scalar prefactors and algebraic masses do not change these principal characteristic sets.*

Proof. The scalar and gauge reductions are invertible for $q_g \neq 0$ because their internal kinetic matrices are invertible. The Clifford identity gives the same assertion for the fermion symbol. Trace reversal is invertible in four dimensions, so the harmonic Einstein symbol has the same zeros. Null covectors support the corresponding physical polarizations. All omitted terms in these specified blocks have lower differential order, as shown in the preceding variations. □

The proposition establishes compatibility of the retained branch. It does not derive Lorentzian continuation, the fermion construction or this kinetic basis from positivity of the mother norm. A general constitutive tensor, derivative coupling to a background field, or unsuppressed mixed principal term can change the conclusion. For example, adding a scalar kinetic contraction $\eta u^\mu u^\nu \partial_\mu \phi \partial_\nu \phi$ changes its principal form. Its sign and admissible range must be tested directly; the existence of one positive equilibrium measure does not remove it.

The distinction is also important for curvature-square terms. A small coefficient in a low-frequency expansion does not bound a higher-order operator at arbitrary frequency. Such terms may be removed only on a specified reduced branch with controlled initial data, frequency range and remainder. The present proposition concerns the displayed two-derivative physical blocks and makes no assertion about all extra modes of the unreduced fourth-order equations.

26.5. *Wavefronts, group delay, and a finite-frequency comparison.* The common cone describes the fastest characteristic propagation of the specified local equations. It does not require the peaks of all wave packets to move at the same speed. For $\partial_t^2 u - c_*^2 \partial_x^2 u + \mu^2 u = 0$,

$$\omega(k) = \sqrt{c_*^2 k^2 + \mu^2}, \qquad v_{\mathrm{group}}(k) = \frac{c_*^2 k}{\sqrt{c_*^2 k^2 + \mu^2}}.$$

The principal cone has speed c_* for every μ, whereas a massive narrow-band packet travels more slowly. This distinction is necessary when arrival times are used to compare matter clocks and signals through a fluctuating medium.

For a finite Fourier representation with orthonormal coefficients $\widehat{u}_j$, two positive-frequency evolutions satisfy the exact bound

$$\|u_1(t) - u_0(t)\|_2^2 \leq \sum_j |\widehat{u}_j|^2 \min\{4, t^2 |\omega_{1j} - \omega_{0j}|^2\}. \tag{1354}$$

Indeed, Parseval reduces the difference to individual phase factors, and $|e^{-iat} - e^{-ibt}| \leq \min\{2, |a-b||t|\}$. If $\omega_{1j}^2 = \omega_{0j}^2 + r_j$, with both frequencies positive, then $|\omega_{1j} - \omega_{0j}| = |r_j|/(\omega_{1j} + \omega_{0j})$. Thus a stated spectral error gives an explicit

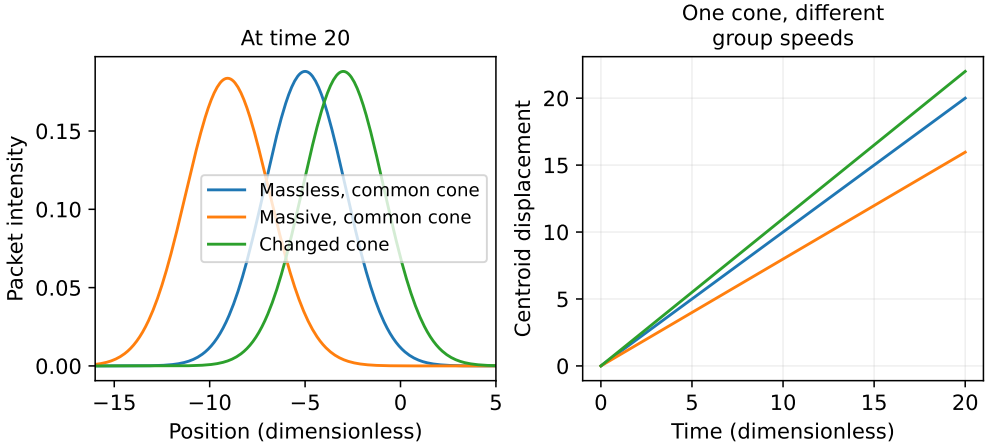


Figure 42. Synthetic packet propagation. Equal principal cones permit different group delays. The third model changes the propagation cone. All variables are dimensionless and the periodic Gaussian packets have noncompact tails.

finite-time signal error. This estimate does not extend a finite frequency window to an uncontrolled ultraviolet limit.

A synthetic periodic calculation uses length 160, 2048 Fourier nodes and the initial complex packet $u_0(x) \propto e^{-(x+25)^2/18} e^{3ix}$, normalized to unit squared norm. Exact Fourier phases evolve it to $t = 20$. The massless and massive cases have $c_* = 1$; the latter has $\mu = 2.25$. A third comparison uses $c_* = 1.1, \mu = 0$, which changes the cone itself. The Gaussian has tails and is periodic here; this calculation does not measure a compact-support wavefront.

case	cone speed	carrier group speed	centroid speed
massless	1	1	1.00000000
massive	1	0.8	0.79828095
changed cone	1.1	1.1	1.10000000

The massive centroid agrees with the spectral average of the group velocity; replacing that average by the carrier value would introduce the displayed bandwidth error. The largest squared-norm drift is 3.4×10^{-16}. Independent adaptive integration of 32 occupied Fourier-mode amplitudes differs by at most 1.1×10^{-10}. For the separate small kinetic perturbation $\omega_1^2 = (1+10^{-3})k^2 + 2.25^2$ of the massive case, the final norm difference is 0.024134206, below the bound 0.024134818 from (1354).

26.6. *Calibrating a transport clock and transferring its prediction.* A dynamical observation can determine information that an equilibrium histogram cannot. In the scalar specialization of (1509), let the independently specified

stiffness and mobility product be $a_* = M_* K_* > 0$, and let $\gamma > 0$ multiply the mobility. With an externally calibrated lag $\tau > 0$,

$$R(\tau) = \frac{\mathbb{E}[X_\tau X_0]}{\mathbb{E}[X_0^2]} = e^{-\gamma a_* \tau}, \qquad \gamma = -\frac{\log R(\tau)}{a_* \tau}.$$

This identifies the transport rate relative to the specified clock. It does not create a unit of proper time or identify the stochastic parameter with the metric length of a worldline.

PROPOSITION 115 (Finite-data clock interval and transfer). *Suppose a population correlation obeys $R(\tau) \in [R_-, R_+] \subset (0,1)$, with a_* and τ known. Then*

$$\frac{-\log R_+}{a_* \tau} \le \gamma \le \frac{-\log R_-}{a_* \tau}, \qquad R(\tau') \in [R_-^{\tau'/\tau}, R_+^{\tau'/\tau}] \quad (\tau' > 0).$$

For N independent centered Gaussian pairs with common known variance v and correlation R, the estimator $\widehat{R} = N^{-1} \sum_j X_j Y_j / v$ satisfies

$$\operatorname{Var}(\widehat{R}) = \frac{1 + R^2}{N} \le \frac{2}{N}, \qquad \Pr\{|\widehat{R} - R| \ge \varepsilon\} \le \frac{2}{N \varepsilon^2}.$$

Proof. The logarithm is increasing and $a_* \tau > 0$, which gives the rate interval. The identity $R(\tau') = R(\tau)^{\tau'/\tau}$ and monotonicity of a positive power give the transfer interval. Write $X = \sqrt{v}\,\xi$ and $Y = \sqrt{v}(R\xi + \sqrt{1 - R^2}\,\zeta)$, with independent standard normal ξ, ζ. Their second and fourth moments give $\mathbb{E}(XY/v) = R$ and $\mathbb{E}[(XY/v)^2] = 1 + 2R^2$. Independence across pairs gives the stated variance, and Chebyshev's inequality gives the finite-sample bound. No asymptotic normal approximation is used. □

Unknown equilibrium variance, measurement noise, overlapping time pairs and uncertainty in the lag or in a_* require additional uncertainty bounds. In particular, consecutive pairs from one trajectory cannot be treated as independent by increasing their nominal sample count.

For a synthetic example take $a_* = 1.2$, $\gamma = 0.7$, known variance one, and $N = 200000$ independent pairs at each of two lags. At calibration lag 0.8, the estimate is 0.51092535; at the independent test lag 1.7, it is 0.24136602. The conservative 95-percent marginal half-width is $\sqrt{2/(0.05N)} = 0.01414214$. Calibration alone gives $\widehat{\gamma} = 0.69951228$, rate interval $[0.67107134, 0.72875160]$, and test-lag prediction interval $[0.22612818, 0.25436488]$. Both marginal intervals contain their generating values in this realization. Their simultaneous coverage is at least 90 percent by the union bound. A 95-percent simultaneous statement requires a different allocation of the two error probabilities. The test data are not used to fit the rate or change the intervals.

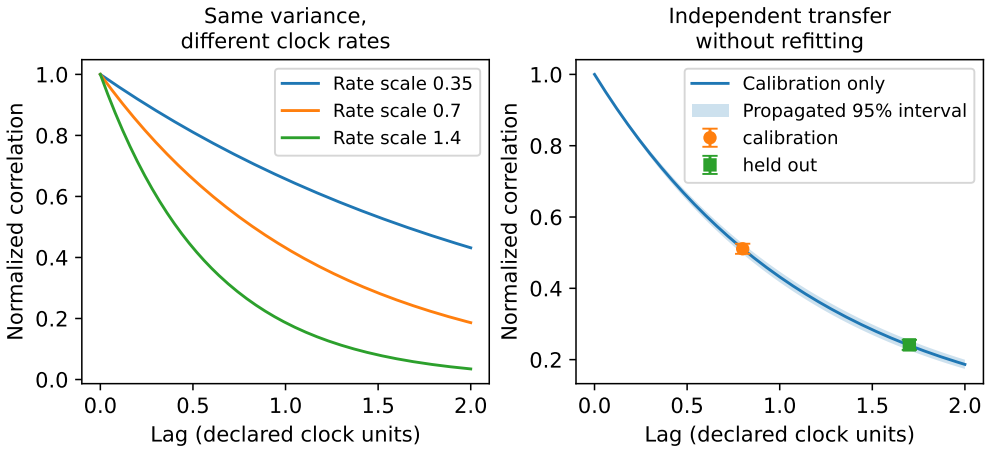


Figure 43. Synthetic transport-clock calibration. Left: identical equilibrium variance permits different correlation times. Right: calibration at one lag transfers to an independent lag without refitting. Shading propagates the calibration interval; pointwise error bars are conservative finite-sample marginal intervals.

The time structure therefore has three linked but distinct interfaces. The physical principal symbols determine propagation cones; material clocks calibrate durations and observed response rates; a specified path reversal determines statistical irreversibility. On a reversible stationary branch the path entropy rate is zero although clocks run and signals propagate. On a maintained nonequilibrium branch the stationary density can remain fixed while path entropy production is positive. These alternatives prevent a clock-rate estimate from being interpreted as a measurement of an entropy-generated spacetime metric.

26.7. *Local vacuum, vacuum energy and massless fields.* The absence of local ordinary matter is different from the absence of curvature. With zero cosmological constant, the vacuum Einstein equations give $R_{\mu\nu} = 0$, but need not give $R_{\mu\nu\rho\sigma} = 0$. In a Schwarzschild exterior,

$$R_{\mu\nu} = 0, \qquad R_{\mu\nu\rho\sigma}R^{\mu\nu\rho\sigma} = \frac{48G^2M^2}{c^4r^6}.$$

The Weyl curvature can therefore remain nonzero in a locally vacuum region. The exterior mass parameter describes global or boundary data; $T_{\mu\nu} = 0$ in that region does not assert zero total mass of the whole spacetime. Vacuum gravitational waves provide another example of curvature without a local material stress tensor. Such a region need not have strong curvature: its magnitude depends on the solution and the location.

In this subsection use $\hbar = c = 1$. A Lorentz-invariant vacuum contribution with renormalized energy density ρ_{vac} has $T^{\mathrm{vac}}_{\mu\nu} = -\rho_{\mathrm{vac}} g_{\mu\nu}$. It can be combined with the cosmological term as $\Lambda_{\mathrm{eff}} = \Lambda_{\mathrm{bare}} + \rho_{\mathrm{vac}}/M_{\mathrm{P}}^2$. This form does not determine the finite observed value of Λ_{eff} by summing unrenormalized zero-point energies. A positive effective cosmological constant permits an accelerating de Sitter solution. The Casimir force between material boundaries is instead an electromagnetic, boundary-dependent quantum interaction; it is not the gravitational force of a cosmological constant. Stress associated with a particular quantum state and apparatus can gravitate, but that is a separate statement about its stress tensor.

For a canonical scalar,

$$T^{\varphi}_{\mu\nu} = \partial_\mu\varphi\partial_\nu\varphi - g_{\mu\nu}\left[\tfrac{1}{2}(\nabla\varphi)^2 + V(\varphi)\right]. \tag{1355}$$

The physical mass at a stationary background is $m_\varphi^2 = V''(\varphi_0)$ after kinetic diagonalization. Vanishing mass does not imply a vanishing potential value, vanishing higher self-interactions, or a constant field. In a local orthonormal frame its energy density is $\frac{1}{2}\dot\varphi^2 + \frac{1}{2}|\nabla\varphi|^2 + V$. Temporal variation can therefore source gravity even without a spatial gradient. Electromagnetic radiation likewise has nonzero energy and stress despite zero photon rest mass.

26.8. *Vanishing direct coupling does not remove scalar stress.* Proposition 104 constrains the direct elementary matter coupling on the specified common-weight branch. For fixed finite ℓ and the stated nonnegative quadratic coefficient, a strictly massless physical scalar has $a_0 = 0$. This does not make (1355) vanish. In a general scalar–tensor model, zero linear coupling at one background also need not remove higher matter couplings; the retained common-weight family must be distinguished from those more general theories.

There is a simple exact illustration. Retain Einstein gravity and a free canonical massless scalar, with no ordinary matter and no cosmological constant. In a flat FLRW geometry, for $t > 0$, set

$$a(t) = a_*\left(\frac{t}{t_*}\right)^{1/3}, \qquad \varphi(t) = \varphi_* + \sqrt{\frac{2}{3}}M_{\mathrm{P}}\log\frac{t}{t_*}. \tag{1356}$$

Then $H = 1/(3t)$, $\rho_\varphi = p_\varphi = M_{\mathrm{P}}^2/(3t^2)$, and direct substitution gives

$$3M_{\mathrm{P}}^2H^2 = \rho_\varphi, \qquad \ddot\varphi + 3H\dot\varphi = 0, \qquad R = 6(\dot H + 2H^2) = -\frac{2}{3t^2}.$$

Thus a scalar with zero rest mass and no direct matter coupling can support a non-vacuum curved geometry. This example concerns the retained Einstein–scalar equations and does not assume that an arbitrary large-curvature epoch satisfies the original derivative expansion.

The accurate decoupling statement is consequently conditional. If direct scalar matter couplings vanish but scalar initial data carry energy, the remaining

theory contains Einstein gravity sourced by that scalar (and by any ordinary matter). To recover the ordinary-matter Einstein equations without this extra source, its gradients and kinetic energy must vanish or be negligible, its potential contribution must be fixed or negligible, and the other retained corrections must be controlled. A constant remaining potential can be absorbed into the cosmological term. Vacuum Einstein equations require the corresponding matter stress to vanish as well. Neither the disappearance of a fifth-force vertex nor a mass–coupling identity alone supplies all of these conditions.

26.9. *Frozen prediction and an exact condition for statistical separation.* A frozen prediction is a distribution for new data, not a promise that those data will support the theory. This distinction can be expressed without a particular detector. Let $\mathcal{C}$ contain every calibration datum and every design choice. Conditional on $\mathcal{C}$, freeze the physical parameters, source treatment, forward map, detector response, noise model, analysis window and decision rule. The test likelihood is the sampling law conditional on this calibration record. New test outcomes are not used to choose the frozen inputs. Conditional independence of test events is imposed only where stated; integrating one uncertain shared parameter can make those events dependent. A retrospectively chosen split of previously inspected data does not acquire this property merely by being renamed a holdout set.

Write $p_*(d \mid i)$ for the frozen prediction, $p_0(d \mid i)$ for a specified baseline, and $q(d \mid i)$ for the actual test distribution. Here i denotes independently supplied source or instrument inputs. Assume common dominating measures, positive model densities on the support of q, and integrable log density ratios. For the relative-entropy identity, also require both conditional relative entropies to be finite with finite averages over I; otherwise their difference could be the undefined expression $\infty - \infty$. All statements below are conditional on the frozen calibration record.

Proposition 116 (Expected predictive advantage). *The mean test log ratio obeys*

$$\mathbb{E}_q \log \frac{p_*(D \mid I)}{p_0(D \mid I)} = \mathbb{E}_I \left[D(q(\cdot \mid I) \| p_0(\cdot \mid I)) - D(q(\cdot \mid I) \| p_*(\cdot \mid I)) \right]. \tag{1357}$$

If $q = p_*$, this quantity is nonnegative and is strictly positive exactly when the frozen and baseline distributions differ on a set of source inputs of positive probability. For independent identically distributed test pairs with an integrable log ratio, the sample average converges almost surely to this expectation.

Proof. For fixed i, subtract the two integrals $\int q \log(q/p_0)$ and $\int q \log(q/p_*)$. The terms $\log q$ cancel and leave $\int q \log(p_*/p_0)$. Average over I to obtain (1357). Relative entropy is nonnegative, with equality precisely for equal probability

distributions. The convergence statement is the strong law applied to the integrable independent log ratios. □

The same identity explains a negative result: an incorrect frozen prediction can be farther from q than the baseline. Theorem-level mathematical consistency does not fix q. Moreover, a free source nuisance parameter that reproduces the physical response can eliminate observable separation even when the physical coefficients were selected uniquely.

26.9.1. *A finite-sample result with specified detector noise.* An explicit power calculation is possible when each test event has a fixed finite detector vector, an independently fixed positive covariance Σ_e, and two fully specified mean vectors $\mu_{*,e}, \mu_{0,e}$. Assume independent Gaussian noise with this same covariance under both models. Put

$$s_e = \mu_{*,e} - \mu_{0,e}, \qquad v_e = s_e^{\top} \Sigma_e^{-1} s_e, \qquad V = \sum_{e=1}^{n} v_e. \tag{1358}$$

These means include the physical detector map. A field amplitude, a mode frequency or a source catalogue entry alone is not a detector mean vector.

THEOREM 117 (Conditional finite-sample detection power). *For $V > 0$, the summed log likelihood ratio*

$$L = \sum_{e} \left[s_e^{\top} \Sigma_e^{-1} (D_e - \mu_{0,e}) - \tfrac{1}{2} v_e \right]$$

has law $N(V/2, V)$ under the frozen model and $N(-V/2, V)$ under the baseline. A threshold $h_\alpha = -V/2 + \sqrt{V}\, z_{1-\alpha}$ has false-positive probability α and frozen-model power

$$1 - \Phi_{\mathrm{N}}(z_{1-\alpha} - \sqrt{V}). \tag{1359}$$

Here Φ_{N} is the standard normal cumulative distribution function and $z_p = \Phi_{\mathrm{N}}^{-1}(p)$. For $0 < \alpha, \beta < 1/2$, power at least $1 - \beta$ is equivalent to $V \geq (z_{1-\alpha} + z_{1-\beta})^2$.

Proof. Expanding the two Gaussian quadratic forms cancels their common covariance normalization and gives the displayed expression for L. Under the frozen model, $D_e = \mu_{0,e} + s_e + \varepsilon_e$, so the event contribution is $v_e/2 + s_e^{\top} \Sigma_e^{-1} \varepsilon_e$. The random term has mean zero and variance v_e. Under the baseline, the mean is instead $-v_e/2$ and the variance is unchanged. Independence adds means and variances, proving both normal laws. Standardizing the baseline gives the threshold and its false-positive rate. Standardizing the frozen-model distribution gives (1359). Finally $1 - \Phi_{\mathrm{N}}(z_{1-\alpha} - \sqrt{V}) \geq 1 - \beta$ is equivalent to $\sqrt{V} \geq z_{1-\alpha} + z_{1-\beta}$. □

For example, $\alpha = \beta = 0.05$ requires $V \geq 10.822174$. This is a design sensitivity criterion for the specified Gaussian experiment, not an observed significance. If $V = 0$, both distributions are identical and no test based on these vectors can distinguish them. Unknown covariance, fitted nuisance parameters, non-Gaussian noise, selection effects and posterior mixtures change the likelihood calculation; they cannot be absorbed into this fixed-mean theorem without derivation.

26.9.2. *Independent checks across several physical branches.* For independent branch data, log likelihood ratios and their expected advantages add. A joint test must use the same frozen shared physical parameters in every branch, with declared branch-specific source inputs. If the physical parameter is represented by a frozen posterior mixture rather than a single value, its joint predictive density is

$$p_*(D_1, \ldots, D_n) = \int \prod_{e=1}^{n} p(D_e \mid \vartheta, I_e)\, \Pi_{\mathrm{cal}}(d\vartheta).$$

The common parameter is integrated once after multiplying event likelihoods. Multiplying separately mixed event predictions generally corresponds to independent parameters and does not test the shared-coupling model.

These results close the mathematical definition, expectation and sensitivity of a conditional independent test. They do not establish that real GWOSC, NICER, EHT or turbulence observations follow the proposed distribution. That conclusion requires the completed forward map and an actual frozen-data comparison. In particular, the existing retrospective strain calculation retains its recorded unresolved preference and is not upgraded by this theorem.

26.10. *Common physical parameters and propagated prediction errors.* A common dynamical description becomes restrictive when one parameter choice determines several measurable responses. This requires more than using the same symbol in several equations. The physical units, projection, source data, and nuisance parameters must be fixed before a comparison. We give quantitative conditions for this interpretation. The results apply to a specified physical branch; an unevaluated observation map remains an additional input.

26.10.1. *Physical constraints and observable directions.* Let ϑ belong to a gauge-fixed p-dimensional physical chart, and let $C(\vartheta) = 0$ be a set of derived cross-sector constraints. At a regular point where DC has constant rank r, the constant-rank theorem gives a local admissible manifold of dimension $p - r$. Its tangent space is $\ker DC$. This count is local and does not compare disconnected branches. A constraint obtained by fitting the observation being tested does not supply independent predictive information.

Choose a matrix Z whose columns span $\ker DC$. For a differentiable observation map $\mathcal{O}(\vartheta, \eta)$ with nuisance parameter η and a fixed positive observation covariance Σ, put

$$J_\vartheta = \Sigma^{-1/2} D_\vartheta \mathcal{O}\, Z, \qquad J_\eta = \Sigma^{-1/2} D_\eta \mathcal{O}, \qquad P_\eta = J_\eta J_\eta^{+}.$$

The superscript + denotes the Moore–Penrose inverse. The locally profiled information matrix is

$$I_{\mathrm{phys}} = J_\vartheta^T (I - P_\eta) J_\vartheta. \tag{1360}$$

Indeed, minimizing $\|J_\vartheta v + J_\eta w\|^2$ over w removes the orthogonal projection onto the nuisance range and leaves $v^T I_{\mathrm{phys}} v$. Positivity of this matrix means that no nonzero allowed infinitesimal physical change can be absorbed by the declared nuisance parameters. It does not imply global identifiability or internal selection of the physical parameter.

26.10.2. *A quantitative error bound for a conditional selector.* Suppose a fixed-reference reduction gives the quadratic objective $F(\xi) = \frac{1}{2}\xi^T H \xi - h^T \xi + c$, after eliminating nuisance directions. All reference inputs are held fixed. Let $H \succeq \gamma I$, $\gamma > 0$, and suppose the unconstrained minimizer belongs to the interior of the allowed chart.

Proposition 118 (Perturbation of a selected effective coefficient). *Let $\widehat{H} = H + E$ be symmetric, $\|E\| \le e < \gamma$, and $\widehat{h} = h + f$, $\|f\| \le d$. If both minimizers are interior, then*

$$\|\widehat{\xi} - \xi_*\| \le \frac{d + e\|\xi_*\|}{\gamma - e}, \qquad \xi_* = H^{-1} h, \quad \widehat{\xi} = \widehat{H}^{-1} \widehat{h}.$$

For a physical map K with Lipschitz constant L_K on the segment joining these points, the physical-coefficient error is at most L_K times this bound.

Proof. The eigenvalue bound gives $\widehat{H} \succeq (\gamma - e) I$. Subtracting the two normal equations yields $\widehat{H}(\widehat{\xi} - \xi_*) = f - E\xi_*$. Apply the inverse norm bound $(\gamma - e)^{-1}$ and the triangle inequality. The last claim is the defining Lipschitz estimate for K. □

An a posteriori variant is $\|\widehat{\xi} - \xi_*\| \le (d + e\|\widehat{\xi}\|)/\gamma$, obtained by multiplying the difference by H. Statistical and discretization contributions to d, e must be included. A boundary minimizer requires a variational-inequality estimate; the displayed interior formula cannot be used across an active-set change. Neither estimate fixes a fundamental parameter that is still free in the reference law or in K.

26.10.3. *Dimensionful matching across source scales.* On the specified curvature–scalar branch, let M be the geometrized source mass, M_P the Planck normalization, m_φ the physical scalar mass, and λ_3 its curvature coupling. In

units $c = \hbar = 1$, M has length dimension, M_P and m_φ have inverse-length dimension, and λ_3 has length dimension. Define

$$\mu(M) = m_\varphi M, \qquad \epsilon(M) = \frac{\lambda_3}{M_P M^2}, \qquad \zeta(M) = \epsilon(M)^2. \tag{1361}$$

Thus a fixed physical parameter pair gives $\mu(M_2)/\mu(M_1) = M_2/M_1$ and $\zeta(M_2)/\zeta(M_1) = (M_1/M_2)^4$. Fixing the same nonzero μ independently at different masses changes m_φ. For cosmological sources, the mass in μ is the source-frame mass; the product of detector-frame mass and observed frequency equals the corresponding source-frame product under the stated redshift convention.

For the isolated action with linear $\lambda_3\varphi\mathcal{G}$ and a quadratic scalar potential, the transformation $(\lambda_3, \varphi) \mapsto (-\lambda_3, -\varphi)$ leaves the action invariant. Even metric responses therefore cannot identify the sign of λ_3 independently of this field convention. Additional matter couplings may make relative signs measurable, but they must be specified.

Suppose two dimensionless responses on the same source satisfy

$$X = \zeta C + R_X, \qquad Y = \zeta D + R_Y, \qquad |R_X| \le A_X\zeta^2, \quad |R_Y| \le A_Y\zeta^2.$$

Then elimination of the common amplitude gives the exact bound

$$|DX - CY| \le (|D|A_X + |C|A_Y)\zeta^2. \tag{1362}$$

The proof is the identity $DX - CY = DR_X - CR_Y$ and the triangle inequality. This form remains meaningful if C is small or vanishes. For numerical coefficients and responses, their additional errors must also be propagated. The relation becomes a physical prediction only after C, D, their matching, and their remainders have been calculated.

26.10.4. *From field residuals to a detector likelihood.* For a specified linear boundary realization $Ak = s$, an inverse estimate $\|A^{-1}\| \le K_A$ gives $\|k - k_N\| \le K_A\|s - Ak_N\|$. A discretization requires separate consistency and boundary errors. A small matrix residual is not, by itself, a bound for a continuum inverse. The same distinction applies when the observable depends on a derivative of k or on a poorly conditioned resonance.

For a finite detector vector, take one fixed positive covariance Σ and the norm $\|v\|_\Sigma^2 = v^T\Sigma^{-1}v$. Let the exact prediction be h, the computed prediction $h + \delta h$, and the residual $r = d - h$. The Gaussian log likelihood obeys

$$|\log L(h + \delta h) - \log L(h)| \le \|r\|_\Sigma\|\delta h\|_\Sigma + \tfrac{1}{2}\|\delta h\|_\Sigma^2. \tag{1363}$$

To prove this, expand $-\frac{1}{2}(\|r - \delta h\|_\Sigma^2 - \|r\|_\Sigma^2)$ and use Cauchy–Schwarz. The covariance and normalization must be the same in the two likelihoods. Noise-model and parameter-integration errors are additional contributions.

There is also a useful bound for a common frozen calibration posterior Π. Suppose event likelihoods are positive and $|\log \widehat{L}_e(\vartheta) - \log L_e(\vartheta)| \le b_e$ uniformly on its support. Multiplication followed by integration gives

$$e^{-\sum_e b_e} \int \prod_e L_e \, d\Pi \le \int \prod_e \widehat{L}_e \, d\Pi \le e^{\sum_e b_e} \int \prod_e L_e \, d\Pi.$$

Hence the joint predictive log likelihood has error at most $\sum_e b_e$. The posterior is integrated once for the shared parameter. Changing it between test events invalidates this bound for a common-parameter test.

These estimates connect conditional mathematical control to observable accuracy. They neither select the data-generating law nor guarantee a favorable comparison. An independent test requires untouched data, specified source and detector maps, and a predicted separation larger than the relevant numerical and systematic uncertainties.

26.11. *Calibrated parameters and the scope of empirical evidence.* A predictive physical branch may contain constants determined by measurement. Internal selection of every constant is a stronger claim than predictive adequacy. Once an identifiable parameter vector has been calibrated, an effective theory is tested by carrying that vector, its uncertainty and the same observation map to a different measurement. The distinction is between parameters fixed before prediction and parameters adjusted to its outcome. An internally unique coupling is therefore not a prerequisite for a useful test. Conversely, identifying a coupling from data does not prove that the mother model selects it without physical inputs.

Let ϑ denote shared physical parameters and let η_b denote independently specified experimental conditions and nuisance parameters in branch b. A joint prediction has the form

$$p(D_{\mathrm{test}} \mid D_{\mathrm{cal}}) = \int p(D_{\mathrm{test}} \mid \vartheta, \eta_{\mathrm{test}}) p(\vartheta, \eta_{\mathrm{test}} \mid D_{\mathrm{cal}}) \, d\vartheta \, d\eta_{\mathrm{test}}. \tag{1364}$$

Here the distribution of test conditions is specified from the experimental design or independent auxiliary measurements. It is not inferred from the test responses whose prediction is being assessed. In a frequentist implementation the analogous calculation propagates calibration and instrument uncertainty through a fixed forward map. In either approach, changing a common parameter to improve a held-out response invalidates that response as a test of the previously fixed prediction.

A finite stochastic example supplies a precise warning. A projected Ornstein–Uhlenbeck process and its optimal stationary Markov approximation can have exactly the same invariant covariance while having different frequency responses and time correlations. Thus agreement with an equilibrium distribution does not establish agreement with dynamical observations. The

response difference must also exceed the uncertainty of the chosen observation protocol. Independent numerical implementations test an implementation; independent noise realizations test sampling; experimental observations test a physical observation map. These are distinct uses of independence.

For the present family, thermal response and finite-regulator entropy provide accessible branch tests. Neither a successful thermal test nor a downloaded black-hole data set supplies the missing gravitational waveform. A massive rotating calculation still requires the coupled tensor, scalar and constraint sectors, the physical boundary conditions, and a controlled detector response. Likewise, a turbulence test requires the actual nonlinear projected generator, forcing covariance and observation filter. A common parameter establishes a cross-sector prediction only after these maps have been derived and the same dimensionful parameter has been used in each sector.

26.12. *A fixed finite mother process and its stationary law.* A hidden degree of freedom can store information about the earlier state of an observed system. Eliminating that degree of freedom therefore changes more than the equal-time distribution. To examine this effect without introducing an uncontrolled continuum approximation, consider the declared, dimensionless process

$$dX_t = (-AX_t + Gf(t))\,dt + \sqrt{2}\,dW_t,$$

$$A = \begin{pmatrix} 1 & .25 & .15 \\ -.15 & 1.4 & .2 \\ .1 & -.2 & 2 \end{pmatrix}, \qquad G = \begin{pmatrix} 1 \\ 0 \\ 0 \end{pmatrix}. \tag{1365}$$

Here W is a three-dimensional standard Brownian motion, $X = (Y, Z)$, $Y = (X_1, X_2)$, and $P = (I_2\ 0)$ is the observation projection. The entries of A, the noise strength and the time unit are inputs. They are neither measured thermal constants nor curvature couplings. The forcing is deterministic and the unforced stationary law is used as the initial distribution for the response experiment.

The symmetric part of A is

$$A_s = \begin{pmatrix} 1 & .05 & .125 \\ .05 & 1.4 & 0 \\ .125 & 0 & 2 \end{pmatrix}.$$

For a real vector v, the inequality $2|v_i v_j| \le v_i^2 + v_j^2$ gives $v^T A_s v \ge .825|v|^2$. Consequently $\|e^{-At}\|_2 \le e^{-.825t}$. In particular,

$$C = 2\int_0^\infty e^{-At} e^{-A^T t}\,dt, \qquad AC + CA^T = 2I_3 \tag{1366}$$

exists and is positive definite: its quadratic form is the integral of $2|e^{-A^T t}v|^2$, which is strictly positive for $v \neq 0$. Differentiating the integrand proves the

Lyapunov equation. Conversely, the difference H between any two solutions satisfies $e^{-At}He^{-A^Tt} = H$ and must vanish as $t \to \infty$.

The explicit solution with $f = 0$ is $X_t = e^{-At}X_0 + \sqrt{2}\int_0^t e^{-A(t-s)}dW_s$. It proves invariance of $N(0, C)$ and convergence in distribution from every fixed initial point. It also proves uniqueness of the invariant probability without a moment assumption: if ϕ is the characteristic function of an invariant law, then

$$\phi(k) = \phi(e^{-A^Tt}k)\exp\{-\tfrac{1}{2}k^T(C - e^{-At}Ce^{-A^Tt})k\}.$$

Continuity of ϕ at zero and $t \to \infty$ give $\phi(k) = \exp(-k^TCk/2)$. With finite second moments, synchronous coupling also gives a Wasserstein contraction factor $e^{-.825t}$. This is a theorem for the specified finite model, not for every branch of the unified theory.

The computed covariance and stationary Markov drift are

$$C \simeq \begin{pmatrix} 1.010676204 & -.006617615 & -.060145331 \\ -.006617615 & .712178430 & .009787776 \\ -.060145331 & .009787776 & .503986044 \end{pmatrix}, \tag{1367}$$

$$B = A_{yy} + A_{yz}C_{zy}C_{yy}^{-1} \simeq \begin{pmatrix} .991086457 & .251978690 \\ -.161884724 & 1.402638253 \end{pmatrix}. \tag{1368}$$

Indeed, Gaussian conditioning gives $\mathbb{E}[Z \mid Y] = C_{zy}C_{yy}^{-1}Y$. The upper-left block of (1366) implies $BC_{yy} + C_{yy}B^T = 2I_2$. Thus $d\bar{Y} = -B\bar{Y}\,dt + \sqrt{2}\,dW_y$ has the correct stationary covariance. This conditional drift does not make Y an exact Markov process, and its unforced selection does not establish exact driven response.

26.13. *Exact elimination produces memory and colored noise.* Write $a = A_{zz} = 2$ and partition A into observed and hidden blocks. Variation of constants in the hidden equation gives

$$\begin{aligned} Z_t = e^{-at}Z_0 - \int_0^t e^{-a(t-s)}A_{zy}Y_s\,ds + \int_0^t e^{-a(t-s)}G_zf(s)\,ds \\ + \sqrt{2}\int_0^t e^{-a(t-s)}dW_z(s). \end{aligned} \tag{1369}$$

Substitution into the Y equation yields a positive-sign memory term $\int_0^t A_{yz}e^{-a(t-s)}A_{zy}Y_s\,ds$, an initial contribution $-A_{yz}e^{-at}Z_0$, and a colored random force $-\sqrt{2}A_{yz}\int_0^t e^{-a(t-s)}dW_z(s)$, in addition to the direct drift, forcing and white noise. The sign follows from the two minus signs in the original off-diagonal drifts. It must not be replaced by an assumed dissipative sign. Stability follows here from the full matrix estimate, not from the memory kernel alone.

For a stationary realization on the entire time axis, the lower integration limit is $-\infty$. The hidden noise contribution then has covariance

$$\mathbb{E}[\xi_z(t)\xi_z(s)^T] = a^{-1}e^{-a|t-s|}A_{yz}A_{yz}^T. \tag{1370}$$

This follows by the Itô isometry and $2\int_{-\infty}^{\min(t,s)} e^{-a(t+s-2u)}du = a^{-1}e^{-a|t-s|}$. The driving white noises in the two blocks are independent. The hidden initial state in a finite-time stationary experiment is correlated with Y_0 and cannot be replaced by an independent draw without changing transient correlations.

26.14. *Response and fluctuation spectra obey the same elimination.* Use the forcing convention $f(t) = \operatorname{Re} e^{i\omega t}$. The complex susceptibility, defined by the steady mean response per unit forcing amplitude, is

$$\begin{aligned} H(\omega) &= (A + i\omega I_3)^{-1}, \qquad \chi(\omega) = PH(\omega)G, \\ R_z(\omega) &= (a + i\omega)^{-1}, \\ R(\omega) &= [A_{yy} + i\omega I_2 - A_{yz}R_zA_{zy}]^{-1}, \\ \chi(\omega) &= R(\omega)[G_y - A_{yz}R_zG_z]. \end{aligned} \tag{1371}$$

To verify the last identity, solve the hidden row of $(A + i\omega I)x = G$ for $z = R_z(G_z - A_{zy}y)$ and substitute into the observed row. Invertibility follows from stability of A and $a > 0$. This derivation also displays the hidden forcing correction, which happens to vanish for the declared G.

Define the two-sided spectrum by $S_Y(\omega) = \int_{\mathbb{R}} e^{-i\omega t}\mathbb{E}[Y_tY_0^T]dt$, so that $C_{yy} = (2\pi)^{-1}\int S_Y(\omega)d\omega$. The white-noise spectrum is $2I_3$. Fourier transformation gives

$$\begin{aligned} S_Y(\omega) &= PH(\omega)(2I_3)H(\omega)^\dagger P^T \\ &= R(\omega)[2I_2 + 2|R_z(\omega)|^2A_{yz}A_{yz}^T]R(\omega)^\dagger. \end{aligned} \tag{1372}$$

The dagger denotes conjugate transpose. The second equality follows by eliminating the hidden white-noise input with the same block inverse used for the forcing. Retaining the memory correction in R but omitting the colored-noise term changes the fluctuation law. Neither equality is an equilibrium fluctuation–dissipation theorem: the declared matrix includes stationary circulation.

For the selected memoryless model, the corresponding susceptibility is $(B + i\omega I_2)^{-1}G_y$. The two lag covariances are $Pe^{-At}CP^T$ and $e^{-Bt}C_{yy}$ for $t \geq 0$. They agree at $t = 0$ but generally not at positive lags. Thus invariant-law recovery, response recovery and path-law recovery are separate mathematical requirements.

26.15. *Entropy decay and stationary irreversibility are distinct.* For the unforced diffusion, let $\pi = N(0, C)$ and $u(x) = (-A + C^{-1})x$. The stationary probability current is $j_*(x) = u(x)\pi(x)$ and satisfies $\nabla \cdot j_* = 0$ by (1366). If

$p = f\pi$ is a smooth positive density with sufficiently decaying boundary terms, its evolution is

$$\partial_t(f\pi) = -\nabla \cdot (uf\pi) + \nabla \cdot (\pi \nabla f).$$

Multiply by $1+\log f$ and integrate. The circulation contribution is $\int u \cdot \nabla f \, d\pi = 0$ and the diffusion contribution is negative. Hence

$$\frac{d}{dt} \int f \log f \, d\pi = -\int \frac{|\nabla f|^2}{f} \, d\pi \leq 0. \tag{1373}$$

This statement extends to finite relative entropy initial laws by regularization and lower semicontinuity. It does not assert monotonicity of the differential Shannon entropy or positivity on every trajectory.

Assign all three coordinates even parity under time reversal. The stationary reversed drift is $b^R = -b + 2\nabla \log \pi$ with $b = -Ax$. Consequently $b - b^R = 2u$. The stationary path relative entropy per unit time, from the drift change formula at diffusion covariance $2I_3$, is

$$\sigma_{\text{path}} = \frac{1}{4}\mathbb{E}_\pi |b - b^R|^2 = \text{tr}[(-A + C^{-1})^T (-A + C^{-1})C] \simeq 0.1194617975. \tag{1374}$$

The finite-time change-of-measure identity can be justified first for stopped linear diffusions and then by Gaussian integrability and localization. Its stationary rate is finite because C is finite. It vanishes exactly when $A = C^{-1}$, which is detailed balance in this even-parity setting. Different physical reversal parities require a different reversed process. Identification of this information-theoretic rate with reservoir entropy additionally requires a physical energy, reservoir temperatures and local detailed balance. In particular, relative entropy can cease changing at stationarity while the stationary path entropy rate remains positive.

26.16. *Frozen response calculations and their resolving power.* For $X_0 \sim N(0, C)$ and $f(t) = \cos(\omega t)$, direct integration gives

$$m(t) = \text{Re}\{[e^{i\omega t} I_3 - e^{-At}](A + i\omega I_3)^{-1} G\}. \tag{1375}$$

Differentiating this expression verifies $\dot{m} = -Am + G\cos \omega t$ and $m(0) = 0$. Deterministic forcing leaves the covariance equal to C. At step length h, define $F = e^{-Ah}$ and $Q_h = C - FCF^T = 2\int_0^h e^{-As} e^{-A^T s} ds$. The exact update uses independent $N(0, Q_h)$ increments and forcing increment

$$\text{Re}\{e^{i\omega t}(e^{i\omega h} I_3 - F)(A + i\omega I_3)^{-1} G\}.$$

It introduces no Euler time-discretization bias for this linear model.

The calculation used $h = .05$, duration 30, frequencies $.3, 1, 3$, and 8192 independent replicas at each frequency. Inputs and noise seeds were fixed before drawing the trajectories. A separate adaptive ordinary differential equation

solver checked the mean formula. These are synthetic observations generated under declared parameters.

Frequency	Mean ODE discrepancy	Monte Carlo mean RMS error
.3	$1.46\,10^{-12}$	.01033
1	$1.40\,10^{-12}$	.01157
3	$6.96\,10^{-13}$	.01124

The tabulated discrepancies round the computed bounds upwards. Over 160 logarithmically spaced frequencies in $[.03, 30]$, the block-inverse and full-system susceptibilities differed by at most $4.45\,10^{-16}$, and their spectral matrices by $1.78\,10^{-15}$. The largest relative susceptibility difference between the full and memoryless models on that grid was .0041702. This maximum is a grid result, not a certified supremum over frequencies.

At times $2, 5, 10, 20, 30$, the coordinate standard errors are exactly $\sqrt{C_{ii}/8192}$. A Bonferroni simultaneous 95% bound for 30 scalar checks uses $z = 3.14398$ and does not require independence among the checks. All selected snapshot means were within this bound. The shaded envelope in the response plot is calibrated at these snapshots; it is not a simultaneous confidence band for the entire curve.

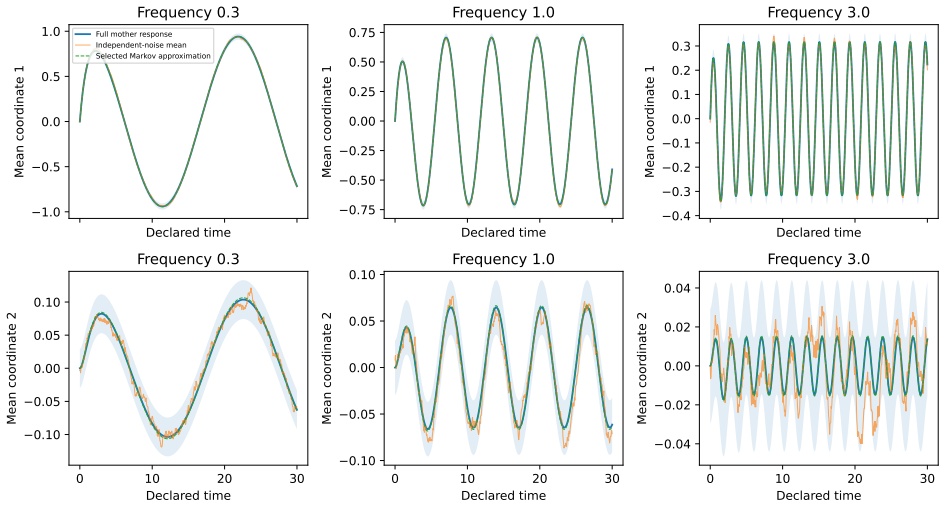


Figure 44. Synthetic mean response at three fixed frequencies. The independent-noise average is compared with the exact mother response and its stationary Markov approximation. The displayed uncertainty envelope is calibrated only for the declared snapshot checks.

The difference between the predicted models is smaller than the observed sampling error. Its detectability can be quantified without treating successive

observations from one trajectory as independent. Stack both coordinates at the five snapshot times. The single-replica covariance is the positive definite block matrix

$$K_{ij} = Pe^{-A(t_i - t_j)}CP^T \quad (t_i \geq t_j), \qquad K_{ji} = K_{ij}^T. \tag{1376}$$

Let $\delta = m_1 - m_0$ be the stacked difference between two prescribed mean responses. In the mean-only comparison with common stipulated covariance K/R, the statistic

$$T = \frac{\delta^T K^{-1}(\bar{Y} - m_0)}{\sqrt{\delta^T K^{-1}\delta / R}}$$

has law $N(0,1)$ under the first mean and $N(\sqrt{Rq}, 1)$ under the second, where $q = \delta^T K^{-1}\delta$. Thus a one-sided test of size α has power $\Phi(\sqrt{Rq} - z_{1-\alpha})$, and power at least $1 - \beta$ requires

$$R \geq (z_{1-\alpha} + z_{1-\beta})^2 / q. \tag{1377}$$

This result follows directly from the mean and variance of a linear Gaussian functional. It is not the likelihood-ratio test between the two full path laws, whose covariance matrices differ.

The computed q values at the three frequencies are $4.39940\,10^{-5}$, $2.72290\,10^{-5}$ and $5.35454\,10^{-6}$. Pooling the independent frequency experiments adds their q values. At 8192 replicas per frequency the resulting power is .19688. For $\alpha = \beta = .05$, the mean-only design requires 141324 replicas per frequency. This is a prospective calculation made after the first simulation, not a predeclared success criterion. It excludes measurement noise and calibration uncertainty, both of which can alter the required sample size. It explains why agreement of the initial synthetic curves cannot establish resolved memory effects.

26.17. *An openly available experimental benchmark.* Liao, Ang, Lai and Jun studied a colloidal Brownian gyrator in a hybrid thermal and active bath [110]. Their model makes the active Ornstein–Uhlenbeck noise an explicit hidden variable. It is therefore directly relevant to the distinction between observed dynamics and complete energetic accounting. The physical mechanism and experimental discovery belong to that work. They are not new predictions of the present framework.

The public workbook [109] contains both theoretical curves and experimental summaries. Figure 9 of the source paper identifies the 10 ms persistence-time experiment and six measured quantities: total work rate, hot-bath heat rate, efficiency, entropy production rate, work diffusion and the thermodynamic uncertainty ratio. The reported uncertainties are bootstrap standard deviations from 17 experimental trajectories, with 10^4 bootstrap samples. The workbook has 12 control settings for each quantity. The summaries do not establish

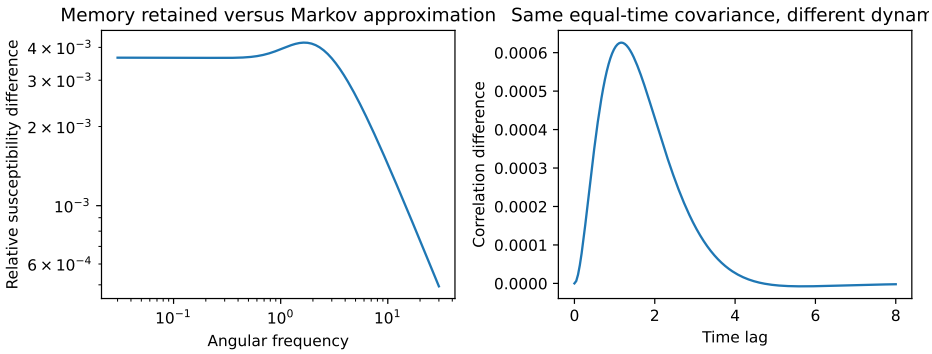


Figure 45. Dynamic differences despite equal stationary covariance. Left: relative susceptibility difference on the evaluated frequency grid. Right: difference in the first-coordinate lag covariance.

statistical independence across quantities or control settings, and 10^4 bootstrap samples are not independent experiments.

We compare the experimental means in columns A–C of the six corresponding sheets with the published 10 ms theoretical curve in columns D and F, without adjusting parameters. Linear interpolation is restricted to the tabulated control interval. At each experimental setting, define the descriptive residual $r_i = (y_i - y_i^{\mathrm{pub}})/s_i$, where s_i is the published bootstrap standard deviation. The first rows and column descriptions were examined before this comparison was chosen. It is a retrospective reanalysis, not a blind calibration–test split.

Observable	Points	RMS of r_i	$\lvert r_i\rvert \le 2$
Total work rate	12	1.338	11
Hot-bath heat rate	12	.707	12
Efficiency	12	1.065	11
Entropy production rate	12	2.351	8
Work diffusion	12	1.592	9
Uncertainty ratio	12	28.949	10

These summaries retain all six panels. The largest residual in the entropy-production panel is 4.940 reported standard deviations. The largest descriptive uncertainty-ratio residual is 100.222 at $\epsilon = 25$ pN/μm, where the published theoretical ratio is approximately 10498.22, while the experimental summary is 40.83 ± 104.34. This is a ratio containing the squared mean work in the denominator, which becomes small near stall. A Gaussian significance interpretation of this residual is unjustified. A different averaging order, finite observation time and uncertainty in the near-zero denominator can matter strongly. No point is removed to improve agreement.

In particular, no global chi-square probability is assigned: the six observables share trajectories and their joint covariance is not provided by these figure summaries. A more stable test near stall uses the primitive current, current variance and entropy-production estimates jointly, rather than assuming a normal distribution for their ratio. The workbook's reported entropy-production means are positive at all twelve settings. That observation is compatible with the source model's thermodynamic accounting; it does not prove a universal entropy theorem from experiments.

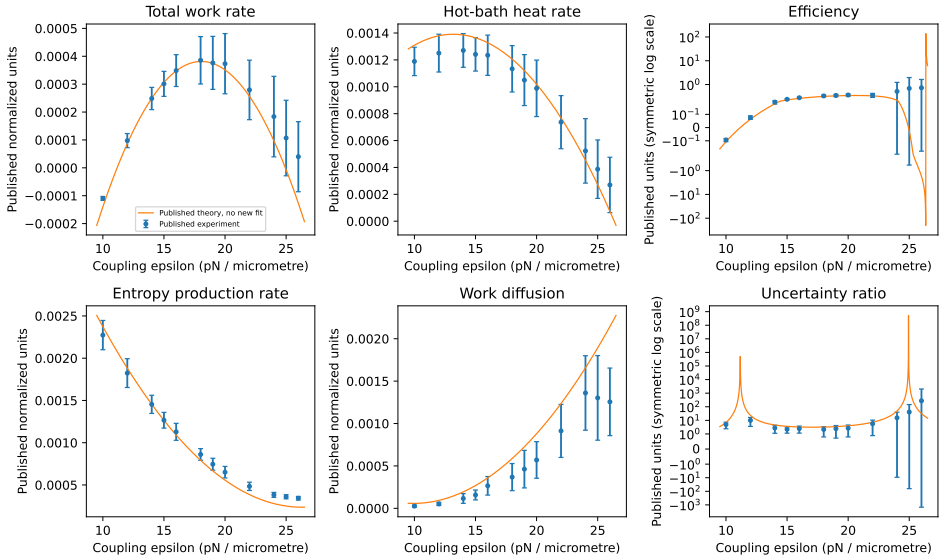


Figure 46. Retrospective reproduction of published experimental summaries and theoretical curves for the 10 ms active-bath experiment [110] and [109]. Error bars are the source's bootstrap standard deviations. The plotted curves are shown on symmetric logarithmic axes for efficiency and the uncertainty ratio to retain their near-pole behavior without hiding other points. The curves are the source's theory, with no new fit. They are not predictions from the three-coordinate example of (1365).

26.18. *From a benchmark to a discriminating physical test.* The dimensionless matrix in (1365) cannot be identified with a colloidal trap by relabelling its coordinates. A physical reduction must specify the force calibration, mobility, thermal reservoirs, active-noise correlation time and readout units. In particular, a generalized Langevin reduction must retain the same memory kernel in its response and the corresponding hidden noise in its fluctuation spectrum.

These requirements produce testable compatibility conditions once the physical mapping is fixed.

For a linear readout with transfer matrix $H_{\mathrm{det}}(\omega)$ and independent stationary detector noise spectrum S_n, the continuous-time measured spectrum is

$$S_{\mathrm{meas}}(\omega) = H_{\mathrm{det}}(\omega) S_Y(\omega) H_{\mathrm{det}}(\omega)^\dagger + S_n(\omega). \tag{1378}$$

The deterministic response uses $H_{\mathrm{det}}\chi$, not χ alone. If observations are sampled at interval h, their discrete spectrum, under the convention $\sum_k \Gamma_k e^{-ik\Omega}$, is

$$S_{\mathrm{sample}}(\Omega) = \frac{1}{h} \sum_{n\in\mathbb{Z}} S_{\mathrm{meas}}\left(\frac{\Omega + 2\pi n}{h}\right), \quad -\pi \le \Omega \le \pi. \tag{1379}$$

This identity follows by substituting the inverse Fourier integral for the covariance at lag kh and applying the Fourier comb identity. It requires an integrable effective continuous spectrum; finite exposure or filtering must precede sampling of ideal white detector noise. Independent discrete readout noise instead contributes its constant discrete spectrum directly.

For a physical test, fit a designated calibration block using this observation model, and preserve its parameter uncertainty. Then freeze the physical parameters, preprocessing and discrepancy statistic before evaluating an independent forcing frequency, bath condition or experiment. Compare a memory-retaining reduction with a specified alternative under the same instrument model. If both descriptions reduce to the same ordinary stochastic thermodynamics in that experiment, agreement supports their shared branch and cannot identify the proposed unification uniquely. An independent cross-sector test needs an additional derived relation between the physical parameters of different sectors; no such relation follows from the numerical entries of A alone.

26.19. *Exact physical projection and the scope of entropy recovery.* To recover a branch from a mother process, specifying its variables is not sufficient. Their future law must also close. This subsection makes that requirement explicit and derives the entropy statement that follows from it. The result applies to a finite regulator; a regulator limit requires its own uniform estimates and identification argument.

Let E, F be standard Borel state spaces, $R : E \to F$ a measurable physical projection, and P_t, Q_t Markov semigroups on bounded measurable functions. Assume the exact intertwining identity

$$P_t(f \circ R) = (Q_t f) \circ R \quad (t \ge 0) \tag{1380}$$

for every bounded measurable f. This is an assumption on the physical projection and the dynamics, not a consequence of writing variables in one vector. It can be established from generator matching on a suitable determining domain, provided the associated martingale problem is well posed and the

domain and integrability conditions permit passage from generators to transition laws.

PROPOSITION 119 (Invariant laws and entropy under an exact projection). *Suppose π is an invariant probability for P_t and* (1380) *holds. Then $\nu = R_{\#}\pi$ is invariant for Q_t, and for any initial law ρ_0, $R_{\#}(P_t^*\rho_0) = Q_t^*(R_{\#}\rho_0)$. For $\rho \ll \pi$,*

$$D(R_{\#}\rho\|\nu) \le D(\rho\|\pi).$$

If the mother entropy satisfies $D(P_t^*\rho\|\pi) \le e^{-\lambda t}D(\rho\|\pi)$ for all finite-entropy initial laws, then

$$D(Q_t^*\sigma\|\nu) \le e^{-\lambda t}D(\sigma\|\nu) \tag{1381}$$

for every $\sigma \ll \nu$ of finite entropy.

Proof. Integrate (1380) against ρ_0; equality against every bounded measurable f proves the equality of projected laws. Setting $\rho_0 = \pi$ proves invariance of ν. If $h = d\rho/d\pi$, disintegration gives the projected density $\bar{h}(Rx) = \mathbb{E}_\pi[h \mid R](x)$. Convexity of $z\log z$ and conditional Jensen give

$$\int_F \bar{h}\log\bar{h}\,d\nu \le \int_E h\log h\,d\pi.$$

The inequality extends to infinite entropy by standard nonnegative relative-entropy approximations. To prove the final assertion, let $g = d\sigma/d\nu$ and choose the particular lift $d\rho_0 = (g\circ R)d\pi$. Then $R_{\#}\rho_0 = \sigma$ and $D(\rho_0\|\pi) = D(\sigma\|\nu)$. Apply projected-law equality, conditional Jensen and mother entropy decay successively. This yields (1381) with no unobserved initial entropy term. □

For a general lift of σ, the microscopic initial entropy can be larger. Substituting the macro initial entropy into that particular trajectory's microscopic bound would therefore require the preceding choice of lift or a separate argument. Exact intertwining makes this choice harmless for the macro law. Without it, different hidden-state preparations can give different macro dynamics and memory cannot be discarded.

For example, in an isothermal finite-dimensional realization with symmetric positive mobility M and invariant density π, let

$$Lf = \frac{\theta}{\pi}\nabla\cdot(\pi\mathsf{M}\nabla f) + c\cdot\nabla f, \qquad \nabla\cdot(\pi c) = 0.$$

Assume sufficient smoothness, finite entropy and the integrability needed below. On a bounded domain impose $\pi\mathsf{M}\nabla h\cdot n = 0$ and $c\cdot n = 0$ for $h = \rho/\pi$; on an unbounded domain require the corresponding boundary terms to vanish in an exhaustion. Then

$$\partial_t h = \frac{\theta}{\pi}\nabla\cdot(\pi\mathsf{M}\nabla h) - c\cdot\nabla h.$$

Multiplication by $(1+\log h)\pi$ and integration by parts give

$$\frac{d}{dt}D(\rho_t\|\pi) = -\theta\int \rho_t\,\nabla\log h_t^T\mathsf{M}\nabla\log h_t\,dx \le 0. \tag{1382}$$

The current term vanishes because it is the integral of $-\pi c\cdot\nabla(h\log h)$. An entropy–dissipation inequality bounding the last integral below by $\lambda D/\theta$ supplies exponential decay. Invariance and this calculation alone do not supply existence of a conservative process, normalizability, or uniqueness among every invariant law. Those hypotheses must be established in the chosen state space. If a finite Galerkin branch satisfies the exact projection identity with matched covariance, the proposition transfers the proved entropy statement to that branch.

26.19.1. *Path reversal is a separate comparison.* Let $\mathbb{P}_T$ be a stationary path law over $[0,T]$, and let $\mathcal{R}_E$ reverse time and apply the prescribed parity to odd variables. Let $\widehat{R}$ act pointwise on paths, and require $\widehat{R}\mathcal{R}_E = \mathcal{R}_F\widehat{R}$. The data-processing inequality, proved by the same conditional Jensen argument on path space, gives

$$D(\widehat{R}_\#\mathbb{P}_T\|\mathcal{R}_{F\#}\widehat{R}_\#\mathbb{P}_T) \le D(\mathbb{P}_T\|\mathcal{R}_{E\#}\mathbb{P}_T).$$

This includes infinite relative entropies in the extended sense. If the mother stationary law is reversible, the right-hand side is zero, so its exact observed stationary path law is reversible as well. This conclusion does not require Markov closure of the observed process. Thus exact observation of a reversible stationary process cannot, by itself, create positive stationary path-reversal entropy. Relaxation from a nonequilibrium preparation, maintained irreversible currents, discarded memory, and an incorrectly specified reversal operation are different mechanisms and must not be conflated. Relative-entropy decay and a physical stationary time arrow remain distinct statements.

For the mother model, the admissible tangent space in the following calculation is formed only from constraints derived from its fixed primitive data. A fitted cross-sector relation cannot be counted again as an independent reduction of parameter freedom. The curvature example uses a specified effective branch, not a selection of the mother inputs.

26.20. *A real-data diagnostic and the boundary of the present test.* The public GWOSC release gives a useful empirical readiness check, but it does not by itself supply a test of the new coupling. We analysed the 4096-Hz, 32-s H1 and L1 strain files for GW170104, whose event time is 1167559936.6 GPS. The two series contain 131072 samples each. After a fixed fourth-order 20–500 Hz band-pass, we computed the maximum absolute normalized cross-correlation in a 0.4-s event window, allowing a lag in $[-15,15]$ ms. The identical statistic was evaluated in four disjoint off-source windows centred at 8, 12, 20, and 24 s

after the file start. The filtering rule, window length, lag range, and event were fixed before calculating the reported statistic.

The event-window statistic is 0.16834 at a lag of −0.244 ms. The four off-source values have mean 0.19181 and sample standard deviation 0.07747, giving the descriptive standardized difference

$$z_{\mathrm{desc}} = (0.16834 - 0.19181)/0.07747 = -0.303.$$

The event-window root-mean-square strains are 5.3203×10^{-19} for H1 and 4.4764×10^{-19} for L1. These numbers describe the released strain data and the stated finite-window statistic; they are not a likelihood ratio, a ringdown fit, or a measurement of $C_{\ell m}$.

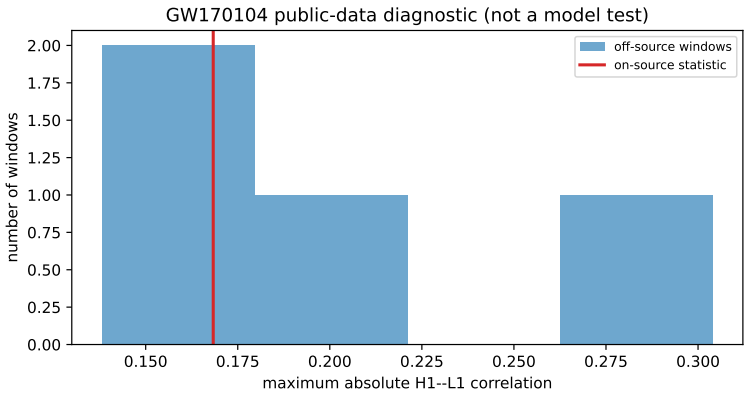


Figure 47. Exploratory GWOSC diagnostic for GW170104. The red line is the event-window H1–L1 statistic and the bars are four disjoint off-source windows after the fixed band-pass. The comparison is a data-quality and resolvability check; it is not evidence for or against the massive Kerr branch.

The result is deliberately non-confirmatory. A physical test would require the frozen coupling and scalar mass, a complete Lorentzian massive Kerr waveform including detector response, a calibrated noise likelihood, and a disjoint calibration–holdout event design. The present mother data do not yet supply that forward map, so the correct empirical status is "real-data diagnostic, physical validation pending."

26.21. *A conditional four-event gravitational likelihood.* The observable map must distinguish parameter selection, source radiation and detector response. Parameter sensitivity is evaluated after nuisance field elimination, as established in Proposition 86. A frozen input is not thereby a physically selected coupling. A stationary scalar solution and a tensor resonance frequency likewise do not specify source excitation or a full waveform.

For a supplied radiation model, the long-wavelength response is

$$\widetilde{h}_I(f) = \sum_{A=+,\times} (D_I : e_A) e^{-2\pi i f \Delta t_I} \widetilde{h}_A(f),$$
$$D_I = \tfrac{1}{2}(u_I \otimes u_I - v_I \otimes v_I), \qquad \Delta t_I = -n \cdot x_I / c.$$

Here the antenna geometry and delays are physical projections; strain calibration does not replace them by identity factors. For fixed off-source noise covariance and Gaussian shared source quadratures, let y be the whitened network data and X its two-column template map. Analytical integration gives

$$\log B_e = \tfrac{1}{2}\left[(X^\top y)^\top (I + X^\top X)^{-1} (X^\top y) - \log\det(I + X^\top X)\right].$$

This finite statistical statement is independent of whether the supplied waveform is a complete physical prediction of the mother theory.

The companion Kerr calculation uses a stated massless polar-led reference, true Hanford/Livingston antenna tensors and delays, and raw off-source Welch covariance. Its Gaussian quadratures are shared across detectors; event-dependent source parameters are integrated under prescribed priors. Catalogue posterior masses and spins are not treated as independent inputs. Three dimensionful coupling scenarios are updated on GW150914 and GW151226 and frozen before GW170104 and GW170814 are evaluated in the current execution. The test events share the same fundamental scenario; their conditional likelihoods are multiplied before integrating over it. The joint predictive log ratio to the zero-coupling reference is approximately 3.30×10^{-5}, with nearly uniform calibration weights. Orientation-integration differences exceed some of these contrasts, so there is no resolved new-physics preference. The split is retrospective and the calculation is limited to one physical sector.

For the retained massive branch, the necessary continuation includes the order-coupling-squared metric background, full angular tensor–scalar blocks, constraint identities, causal massive boundary conditions and source-dependent excitation data. These objects cannot be replaced by a scalar-only solve or a universal mass-dependent tensor frequency factor. The reference calculation therefore supplies a reproducible conditional likelihood, while unique mother-model coupling selection and the full massive rotating waveform remain separate unfinished computations.

26.22. *Stationary action, path cost and physical identification.* The common variational proposal has three mathematically distinct levels. A mechanical action determines stationary trajectories. A stochastic path cost compares probability laws or selects admissible controls. A physical matching rule identifies the coefficients and observables of an effective sector. Conflating these levels would hide precisely the assumptions needed for a common mechanism.

Consider the mechanical oscillator action with fixed endpoint variations,

$$\mathscr{A}[q] = \frac{1}{2}\int_0^T (\dot{q}^2 - \omega_0^2 q^2)dt, \qquad \eta(0) = \eta(T) = 0.$$

Its first variation is $\delta\mathscr{A}[q;\eta] = -\int(\ddot{q} + \omega_0^2 q)\eta\, dt$, so stationary paths satisfy the oscillator equation. Its second variation on $\eta_j(t) = \sin(j\pi t/T)$ is exactly

$$\delta^2\mathscr{A}[q;\eta_j] = \frac{T}{2}\left[(j\pi/T)^2 - \omega_0^2\right]. \tag{1383}$$

For $T > \pi/\omega_0$ the $j = 1$ direction is negative, whereas sufficiently large j gives positive directions. Thus a physically valid stationary trajectory can be a saddle. The framework must recover stationarity rather than require every classical mechanical action to have a global minimum.

For a diffusion with fixed covariance, the minimum-cost statement has a different precise meaning. Let the reference equation be $dX = b_0(X)dt + \sigma(X)dW$, and let an admissible controlled law use drift $b_0 + \sigma u$ and the same initial distribution. Assume uniqueness in law, finite quadratic control cost and a valid Girsanov change of measure. For the equality below also assume that the likelihood is measurable in the canonical state-path filtration, as for a state-path-adapted minimal-range control with the requisite covariance regularity. The controlled path likelihood is

$$\log\frac{d\mathbb{P}^u}{d\mathbb{P}^0} = \int_0^T u_t \cdot dW_t^u + \frac{1}{2}\int_0^T |u_t|^2 dt.$$

Taking its expectation under $\mathbb{P}^u$ gives

$$D(\mathbb{P}^u\|\mathbb{P}^0) = \frac{1}{2}\mathbb{E}^u\int_0^T |u_t|^2 dt. \tag{1384}$$

With redundant noise directions the path law sees only their effective projection; equality uses the minimal-norm control in the range of $\sigma^\top$. Otherwise the right side is an upper bound on path relative entropy, as do unobserved control randomness or a larger driving filtration when the likelihood is not state-path measurable. Initial-law changes add an initial relative-entropy term. This formula is a statement about path laws, not a proof that their typical realizations minimize the mechanical action.

A derived control cost can select a unique feedback for specified inputs without selecting those inputs themselves. The same distinction applies to an invariant Gibbs law: uniqueness of that law for each fixed generator does not identify the generator's fundamental coupling. The earlier parameter-fiber and product-factor calculations remain in force.

26.22.1. *An explicit conditional selector and its scope.* Suppose a physical quotient of parameter equivalences has been identified with a closed convex subset $K \subset \mathbb{R}^r$ after fixing physical units. If an independently specified selection functional F is lower semicontinuous, coercive on K and strictly convex, then it has one minimizer on K. Indeed a minimizing sequence lies in a compact sublevel set; its limit is admissible and minimizes F. Two distinct minimizers would have a strictly lower value at their midpoint, which is impossible. If F is m-strongly convex, a perturbation $\widetilde{F}$ with $\sup_K |\widetilde{F} - F| \le \epsilon$ gives, for its minimizing point,

$$\|\widetilde{\vartheta}_* - \vartheta_*\| \le 2\sqrt{\epsilon/m}.$$

This follows from quadratic growth of F at its constrained minimizer and $F(\widetilde{\vartheta}_*) - F(\vartheta_*) \le 2\epsilon$. The theorem establishes conditional selection and sensitivity; it does not derive F from the mother action. A nonconvex quotient needs a genuine geometric or discrete-gap argument rather than the midpoint proof. An arbitrary regularizer, choice of parameter coordinates or desired coupling cannot serve as a hidden derivation of a new physical principle.

26.22.2. *The meaning of recovery.* For each sector the recovery statement must specify a projection, an admissible family of initial and boundary data, a limiting scale and a topology of convergence. If a projected observable has an evolution defect bounded by ϵ in that topology, its accumulated error must be controlled before the sector is called recovered. Equality of equation symbols is insufficient when covariance, units, constraints or domains differ. The controlled orbital recovery, finite-mode fluid balances and massive response calculations in this family supply distinct examples of these requirements; they are not interchangeable demonstrations of one unproved continuum limit.

26.22.3. *Applications beyond field dynamics.* Learning, market making and network decision models can use the same control and equilibrium methods. This is a common mathematical architecture unless a further identification establishes a common physical mechanism. In market making, a cost-minimizing Nash equilibrium additionally requires market clearing, funding and no-arbitrage conditions to determine a European claim price. A positive state-price kernel may then give $C_0 = \mathbb{E}_{\mathbb{P}}[M_T H]$ without assuming a risk-neutral measure at the outset; an equivalent risk-neutral representation can still exist. For a combinatorial problem, a minimum-energy encoding requires polynomial encoding size, precision and runtime analysis before any claim about NP complexity. For neural dynamics, operationally measured correlations must remain separate from an assertion that a model has derived subjective experience. These applications do not determine the unresolved field couplings or quantum reconstruction data.

26.23. *A coupled positive-coordinate realization with proved convergence.* A logarithmic state penalty and an invariant density answer different questions. The penalty may be integrable along trajectories that reach a boundary. Likewise, an invariant density does not by itself prove attraction. The following finite realization makes the boundary mechanism, invariant law and convergence estimate consequences of one specified generator. Its coordinates are declared positive variables. Their identification with fluid density or internal energy would additionally require the physical projection and covariance matching established elsewhere in this programme.

Let $y \in (0,\infty)^n$, $s_y = \sum_i y_i$, and fix

$$d > 0, \qquad b > 0, \qquad g \geq 0, \qquad k_i \geq 1.$$

The letter b here is a scalar confinement coefficient, not a drift vector. Define the dimensionless potential and density

$$V_+(y) = bs_y + \tfrac{1}{2} g s_y^2, \tag{1385}$$

$$\pi_+(y) = Z_+^{-1} \exp[-V_+(y)] \prod_i y_i^{k_i - 1}, \tag{1386}$$

$$L_+ f = d \sum_i \{ y_i \partial_{ii} f + [k_i - y_i(b + g s_y)] \partial_i f \}. \tag{1387}$$

Thus the mobility is $d\,\mathrm{diag}(y_i)$ and the covariance is twice that matrix. The equation is

$$dY_i = d[k_i - Y_i(b + g s_Y)]\, dt + \sqrt{2dY_i}\, dW_i.$$

All coefficients are model inputs; they are not selected constants of the full field theory. The off-diagonal coupling comes from the common potential through $g s_y$, rather than from a separately appended dissipation term.

Proposition 120 (Positive paths, invariant law and entropy contraction). *For every strictly positive initial point the displayed stochastic equation has a pathwise unique, nonexplosive solution that stays in* $(0,\infty)^n$. *Its unique invariant probability is* (1386). *For initial densities with finite relative entropy, its semigroup satisfies*

$$D(\rho_t \| \pi_+) \leq e^{-dbt} D(\rho_0 \| \pi_+). \tag{1388}$$

The entropy identity and its bound first hold on the regular form domain and extend by approximation. Point-mass initial conditions are allowed in the path statement but are not assigned finite initial relative entropy.

Proof. On any compact subset of the open orthant the coefficients are locally Lipschitz and the covariance is positive definite. Local strong existence

and uniqueness therefore hold up to exit. Consider the sum s_Y:

$$L_+ s_y = d\sum_i k_i - dbs_y - dgs_y^2 \le d\sum_i k_i - dbs_y.$$

The stopped first-moment estimate bounds the probability of an upper exit before any fixed time by a constant divided by the exit level. Hence there is no finite-time explosion once lower boundary exits are excluded.

Stop when s_Y reaches a fixed upper level R. Before that stopping time, the ith drift is bounded below by $d[k_i - (b+gR)Y_i]$. Compare Y_i, with the same Brownian motion, to the one-dimensional square-root diffusion

$$dZ_i = d[k_i - (b+gR)Z_i]dt + \sqrt{2dZ_i}\, dW_i.$$

For this diffusion the scale derivative is, up to a positive constant, $z^{-k_i}e^{(b+gR)z}$. Its integral diverges at zero when $k_i \ge 1$; the lower endpoint is inaccessible from a positive starting point. The one-dimensional comparison theorem for the common square-root coefficient gives $Y_i \ge Z_i$ before the upper stop. Exhausting the upper levels proves absence of lower exits. Local uniqueness then gives global pathwise uniqueness. No discrete projection or cutoff appears in this argument.

Normalizability follows from $b > 0$, $g \ge 0$ and $k_i > 0$. In divergence form,

$$L_+ f = \pi_+^{-1}\sum_i \partial_i(dy_i\pi_+\partial_i f), \qquad \int f L_+ h\, \pi_+ dy = -d\sum_i \int y_i f_i h_i\, \pi_+ dy.$$

The conservative natural-boundary realization of this form agrees with the unique stochastic equation. It follows that π_+ is invariant and reversible. Interior ellipticity and the localized transition kernel give strong Feller regularity and irreducibility on the connected open orthant. Nonexplosion and lower-boundary inaccessibility permit exhaustion by compact interior domains. Consequently there cannot be two invariant probabilities. This uniqueness argument concerns a fixed generator, not a choice of its physical parameters.

To obtain a quantitative bound, put $z_i = 2\sqrt{y_i}$. Itô's formula gives constant covariance $2dI$ and the gradient generator

$$\widetilde{L}_+ = d(\Delta_z - \nabla W_+ \cdot \nabla), \qquad W_+(z) = b\frac{|z|^2}{4} + \frac{g}{2}\left(\frac{|z|^2}{4}\right)^2 - \sum_i (2k_i - 1)\log z_i.$$

The Jacobian $dy = \prod_i (z_i/2)dz$ is included in this transformed density; omitting it would give the wrong logarithmic coefficient. Writing $s_z = |z|^2/4$ gives the explicit Hessian

$$\nabla^2 W_+ = \frac{b}{2}I + g\left(\frac{s_z}{2}I + \frac{zz^\top}{4}\right) + \operatorname{diag}\left(\frac{2k_i - 1}{z_i^2}\right) \succeq \frac{b}{2}I. \tag{1389}$$

The Bakry–Emery logarithmic Sobolev estimate on this convex domain [9] gives

$$D(\rho\|\pi_+) \le \frac{1}{b}\int |\nabla_z \log(\rho/\pi_+)|^2\,\rho\,dz.$$

It can be obtained on convex truncated orthants with reflecting boundaries; their curvature lower bound is independent of the truncation. Passing to the natural form realization gives the displayed estimate. Entropy differentiation in the same coordinates yields

$$\frac{d}{dt}D(\rho_t\|\pi_+) = -d\int |\nabla_z \log(\rho_t/\pi_+)|^2\rho_t\,dz \le -dbD(\rho_t\|\pi_+).$$

Gronwall's inequality proves (1388). □

For a smooth initial law with finite entropy, Pinsker's inequality also gives convergence in total variation with the explicit bound

$$\|\rho_t - \pi_+\|_{\mathrm{TV}} \le \sqrt{D(\rho_0\|\pi_+)/2}\,e^{-dbt/2}.$$

Strict state admissibility, uniqueness of a probability law and convergence have thus been proved separately. The stationary process is reversible: free-energy relaxation of a displaced law does not imply persistent stationary entropy production. A nonreversible extension must specify its additional current, parity and reservoir interpretation.

26.23.1. *An exact microscopic ancestor for half-integer shapes.* For $k_i = n_i/2$ with integers $n_i \ge 2$, the generator above follows from an explicit smooth Euclidean microscopic model. Let $x_i \in \mathbb{R}^{n_i}$, set $y_i = |x_i|^2/4$, and use

$$U(x) = \frac{b}{4}|x|^2 + \frac{g}{32}|x|^4, \qquad dX = -d\nabla U(X)dt + \sqrt{2d}\,dW.$$

The microscopic generator is $d(\Delta_x - \nabla U\cdot\nabla_x)$. For $f(y(x))$, the exact chain rule gives

$$\Delta_{x_i} f = y_i f_{ii} + \frac{n_i}{2} f_i, \qquad \nabla_{x_i} U\cdot\nabla_{x_i} f = y_i(b + gs_y)f_i.$$

It therefore projects exactly to (1387) with $k_i = n_i/2$. The radial Jacobian of Euclidean volume is proportional to $\prod_i y_i^{n_i/2-1}dy$, which gives the same invariant law. Both the normal diffusion and inward drift are thus derived together. In this subclass the threshold $k_i \ge 1$ is the microscopic dimension condition $n_i \ge 2$, not a logarithmic penalty added after projection.

The ancestor also has $\nabla^2 U = (b/2 + g|x|^2/8)I + gxx^\top/4 \succeq bI/2$. Its entropy contraction passes to the radial branch by taking initial densities whose ratio to the microscopic invariant density depends only on the radii. The chain rule above applies to every smooth radial test function, including functions that couple the two blocks. The numerical shapes $(1.2, 1.8)$ used below are not half-integers and are not assigned this particular Euclidean ancestor. This

exact finite microscopic projection is a separate constructive witness; it does not identify these blocks with the unconstructed compressible fluid or Cartan-field continuum.

26.23.2. *Why finite logarithmic costs do not protect a boundary.* Set $g = 0$ and $n = 1$. The stationary distribution is gamma with shape k and rate b. For every $k > 0$,

$$\int |\log y| \pi_+(dy) < \infty, \qquad \mathbb{E}_{\pi_+}[-\log Y] = \log b - \psi_{\mathrm{dg}}(k),$$

where ψ_{dg} is the digamma function. Nevertheless zero is attainable for $0 < k < 1$ in the conservative square-root realization. For a stationary path, Tonelli's theorem gives finite expected integrated absolute logarithmic cost on each finite interval. The same path law can therefore hit the boundary even though this cost is finite. Inaccessibility comes from the drift–normal-covariance threshold $k \geq 1$, not from the integrability of $-\log y$ or from an interior ellipticity statement. This counterexample is also why positivity at discrete sampling times cannot prove that a continuous path has avoided zero between them.

26.23.3. *A compatible stationary arrow with the same invariant law.* Attraction and stationary irreversibility can coexist. In the transformed two-coordinate model let η be a nonconstant smooth compactly supported function inside the positive orthant, and let

$$J = \begin{pmatrix} 0 & 1 \\ -1 & 0 \end{pmatrix}, \qquad Q = e^{W_+} J \nabla \eta.$$

Replace the transformed drift by $-d\nabla W_+ + Q$. Since $\operatorname{div}(e^{-W_+}Q) = \operatorname{div}(J\nabla\eta) = 0$, the same π_+ remains invariant. The current is bounded, supported away from every boundary, and therefore leaves the nonexplosion and boundary arguments intact. Its contribution to relative-entropy differentiation is

$$\int \pi_+ Q \cdot \nabla(\rho/\pi_+)\, dz = 0.$$

Consequently the same contraction estimate holds. On the other hand, with both coordinates declared even under reversal, the reversed stationary drift is $-d\nabla W_+ - Q$. Girsanov's formula with covariance $2dI$ gives

$$\frac{1}{T} D(\mathbb{P}_{[0,T]} \| \mathbb{P}^{\mathrm{rev}}_{[0,T]}) = \frac{1}{d} \int |Q|^2 \pi_+ \, dz > 0. \tag{1390}$$

The initial law is stationary and common to both experiments; bounded Q supplies the finite-time change-of-measure condition. The result proves a stationary statistical arrow for this declared extension. Identification with heat and thermodynamic reservoir entropy needs local detailed balance and work bookkeeping; it is not implied by the path likelihood alone.

This stationary current also has an exact microscopic realization in the two-block subclass $k_i = n_i/2$, $n_i \geq 2$. Write $z_i = |x_i|$ and set

$$v_i(x) = \frac{x_i}{z_i} Q_i(z), \qquad dX = (-d\nabla U + v)dt + \sqrt{2d}\, dW.$$

Extend v by zero wherever a block radius vanishes. The support of Q is a compact subset of the positive radial quadrant, so this extension is smooth and bounded on the Euclidean state space. Let $w(z) = \prod_i z_i^{n_i - 1}$. The radial divergence identity gives

$$\begin{aligned} \operatorname{div}_x(e^{-U} v) &= \frac{1}{w(z)} \sum_i \partial_{z_i}[w(z) e^{-U(z)} Q_i(z)] \\ &= \frac{1}{w(z)} \operatorname{div}_z(e^{-W_+} Q) = 0. \end{aligned}$$

Thus the microscopic invariant law remains proportional to $e^{-U} dx$. For a radial test function $f(z)$, $v \cdot \nabla_x f = Q \cdot \nabla_z f$; the radial projection has precisely the current used above. Since $|v(x)|^2 = \sum_i |Q_i(z)|^2$, the two stationary reversal rates agree:

$$\frac{1}{d} \int |v|^2 \pi_x \, dx = \frac{1}{d} \int |Q|^2 \pi_z \, dz > 0.$$

Here all microscopic coordinates and radial coordinates are declared even, and π_z is the pushforward of π_x. In this constructed branch the radial observation therefore retains the entire stationary reversal cost. With Q replaced by ξQ, the invariant law is unchanged and this rate is multiplied by ξ^2; $\xi \to 0$ recovers the reversible law. This supplies a finite microscopic example of compatible relaxation and a stationary arrow. The current and its amplitude remain specified model data, and their physical origin is not selected by the construction.

For the synthetic parameters $k = (1.2, 1.8)$, $b = 1$, $g = 0.2$, $d = 0.7$, take

$$\eta(z) = 0.05\, h((z_1 - 1.5)/0.6)\, h((z_2 - 2)/0.6), \qquad h(u) = \begin{cases} e^{-1/(1-u^2)}, & |u| < 1, \\ 0, & |u| \geq 1. \end{cases}$$

This specifies the extra current independently of the reversible simulation below. Its entropy-rate integral is evaluated with 96 and 144 Gauss nodes per coordinate. The computed rate is 3.9304128×10^{-5}; refining the quadrature changes it by less than 7.5×10^{-19}. This comparison is a floating-point quadrature check, not an interval-certified error bound. It is not a fitted physical time-arrow parameter, and the synthetic trajectories below retain $Q = 0$.

26.23.4. *A positive splitting calculation.* The generator splits into independent square-root components and the deterministic coupled flow. Both subflows

preserve positive coordinates. For a step h, the independent component has the exact transition

$$Y_i' = c_h\,\chi^{\prime 2}_{2k_i}(\lambda_i), \quad c_h = \frac{1-e^{-dbh}}{2b}, \quad \lambda_i = \frac{Y_i e^{-dbh}}{c_h}.$$

The coupled subflow is exactly $Y_i' = Y_i/(1+dgs_Y h)$. Half a coupled step, a full independent step and half a coupled step define a symmetric splitting without clipping. Exact positivity of the subflows does not establish exact invariance of their composed discrete chain. No uniform weak-order or numerical entropy theorem is inferred from this finite experiment.

For $k = (1.2, 1.8)$, $b = 1$, $g = 0.2$, $d = 0.7$, the invariant density is integrated by separating s_Y and the Dirichlet proportions. Its means are $(0.79913806, 1.19870709)$, and its covariance is

$$\begin{pmatrix} 0.46374871 & -0.05599308 \\ -0.05599308 & 0.66762652 \end{pmatrix}.$$

The exact one-dimensional integral gives $\int L_+ s_Y\, d\pi_+$ and $\int L_+ s_Y^2\, d\pi_+$ with numerical residuals below 3.2×10^{-15}. Starting at $(0.05, 0.10)$, three independently seeded sets of 12,000 synthetic paths are advanced to time 12:

h	mean Y_1	standard error	mean Y_2	standard error
0.100	0.799610	0.006222	1.193806	0.007390
0.050	0.795789	0.006272	1.203903	0.007460
0.025	0.784132	0.006000	1.183319	0.007472

The last realization differs from the invariant means by about 2.50 and 2.06 Monte Carlo standard errors. All runs are reported. The error bars describe sampling uncertainty only; they do not include finite-time bias or splitting error. These samples are not a convergence-order certificate.

The construction provides verifiable sufficient conditions for a finite positive-state branch. Applying it to compressible turbulence would require deriving the distance variables, their Itô drift and their normal covariance from the actual mother projection, while preserving mass and energy exchange. It is not a proof of that presently unspecified fluid identification.

26.24. *One nonzero parameter vector across different source masses.* Dimensionless couplings change when the source mass changes even when the physical theory is unchanged. To distinguish this required scaling from recalibration, keep the common-weight matching relations

$$m_\varphi^2 = q_\sigma + \frac{6A_\varphi}{\ell^2}, \quad K_{\mathrm{curv}} = \frac{\lambda_3^2}{M_{\mathrm{P}}^2} = \frac{A_\varphi \ell^4}{32}, \quad a_m = \frac{\gamma}{2}, \quad \gamma^2 = \frac{2A_\varphi}{M_{\mathrm{P}}^2}. \tag{1391}$$

These identities use the declared constant-vacuum, torsionless, order-reduced Ricci-flat matching branch. They do not suppress additional threshold operators

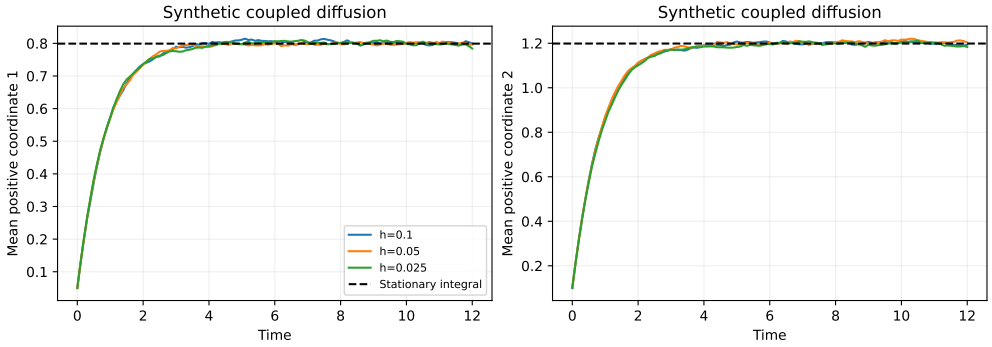


Figure 48. Synthetic moment evolution under positive subflow splitting. The dashed levels are stationary integrals of the continuous generator. The analytic state-boundary and entropy results concern the continuous model, whereas the plotted trajectories use a discrete split law.

in a more general effective theory. With $\bar{\alpha}_3 = -M_{\mathrm{P}}^2\ell^2/8$ and $\lambda_3 = -\bar{\alpha}_3\gamma$, a source of geometrical mass M has

$$\mu = m_\varphi M, \quad \zeta = \frac{A_\varphi \ell^4}{32M^4}, \quad \beta = \frac{a_m\lambda_3}{M^2} = \frac{A_\varphi\ell^2}{8M^2}, \quad \frac{\beta}{\zeta} = \frac{4M^2}{\ell^2}. \tag{1392}$$

In particular, the scalar mass cannot be reset to zero while retaining this nonzero common weight and $q_\sigma \geq 0$.

Use a fixed reference length M_0 and supply, once,

$$A_\varphi = 10^{-5}, \qquad \ell/M_0 = 0.03, \qquad m_\varphi M_0 = 0.3, \qquad M_{\mathrm{P}}M_0 = 1.$$

It follows that $q_\sigma M_0^2 = 0.0233333333 > 0$ and $K_{\mathrm{curv}}/M_0^4 = 2.53125 \times 10^{-13}$. These are illustrative input parameters, not measured constants or the output of a physical selector. They are held fixed for sources $M/M_0 = 1/3, 1, 10/3$, whose scalar masses μ are consequently $0.1, 0.3, 1$.

26.24.1. *A relation between two conditional response channels.* For the stationary massive scalar on the Schwarzschild reference exterior, let $I_0(\mu)$ be its normalized positive energy-form susceptibility. The physical scalar strength is $\mathcal{B}_0 = \zeta I_0(\mu)$. For the declared steady, thin, radiatively efficient, zero-inner-torque test disc, let D_ζ and D_β^R denote the derivatives of the local one-face emitted flux at fixed physical circumferential radius $R/M = 10$ and fixed asymptotic mass and accretion-rate normalization. Combining the shared couplings gives

$$\frac{\delta F_R}{F_{R,0}} = \zeta D_\zeta(\mu) + \beta D_\beta^R(\mu) + \mathcal{R}_F, \tag{1393}$$

$$\frac{\delta F_R/F_{R,0}}{\mathcal{B}_0} = \frac{D_\zeta(\mu) + (4M^2/\ell^2)D^R_\beta(\mu)}{I_0(\mu)} + \frac{\mathcal{R}_F}{\mathcal{B}_0}. \tag{1394}$$

The second identity eliminates the common response amplitude at retained linear order; it does not eliminate the independent length ℓ. The remainder includes unretained metric and matter terms, higher powers of the response, and any operators absent from the declared matched branch. No regulator-independent or complete effective-theory bound on that remainder is supplied by this calculation.

M/M_0	$I_0(\mu)$	$\mathcal{B}_0$	$\delta F_R/F_{R,0}$
1/3	3.93015303	$8.05804\,10^{-11}$	$-1.74670\,10^{-8}$
1	2.45540366	$6.21524\,10^{-13}$	$1.61503\,10^{-9}$
10/3	0.68063025	$1.39550\,10^{-15}$	$2.14104\,10^{-11}$

The susceptibility integrals are recomputed with the algebraic forced far-field tail, then compared with an independent compactified Galerkin solve. Their relative differences are below 3.3×10^{-12}. The local fluxes are evaluated both by the combined derivatives and by directly solving the disc integrals in the supplied truncated metric; their absolute relative-flux differences are below 1.2×10^{-15}. This numerical agreement checks retained-order arithmetic. It does not bound the physical remainder $\mathcal{R}_F$ or observational uncertainties. In particular, dividing by a very small $\mathcal{B}_0$ can amplify an omitted remainder.

The sign change between the first two local flux corrections follows from the computed massive scalar and the physical-radius response. It is a conditional prediction of this supplied parameter vector at these specified radii. It is not an arbitrary-spin claim, a measured luminosity change or a signal at an instrument. All masses and the common parameters remain fixed as prescribed; there is no separate disc amplitude fit.

The elementary unscreened matter convention would also fix the static force correction $A_\varphi(1 + m_\varphi r)e^{-m_\varphi r}$ relative to its tensor reference. Composite-body charges and environmental screening need separate matching. Thus the same parameter registry relates laboratory and black-hole channels conditionally, without replacing the missing physical coupling selector, stellar matching, or detector-forward calculation.

26.25. *A single registry and the map from the master process to physics.* The construction is only predictive after its inputs, quotient identifications, and physical projections have been separated. We therefore use the following registry throughout the eight-paper family. A symbol in the "input" column is fixed before solving an observable problem; a symbol in the "derived" column is computed from the displayed equations.

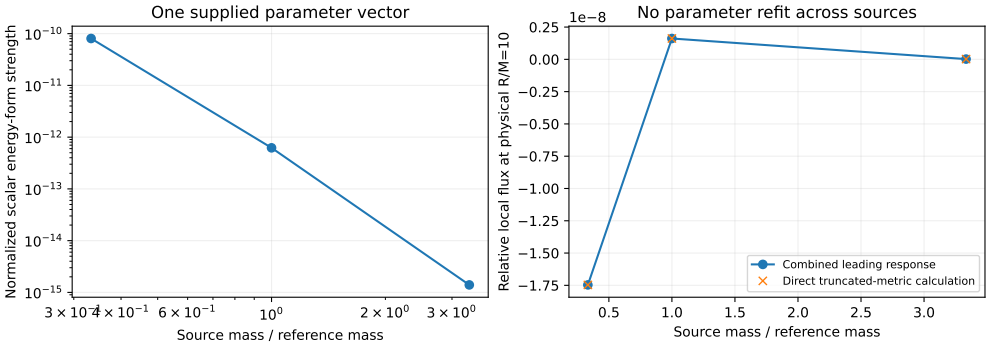


Figure 49. Two retained-order responses with one nonzero supplied parameter vector and three prescribed source masses. The scalar quantity is an energy-form diagnostic; the disc quantity is local emitted flux at fixed physical radius. Agreement with the direct truncated-metric calculation does not establish an observational validation or a complete rotating response.

object	status	convention
$\mathcal{Z} = (g, A, \varphi, \psi, \rho)$	input state	metric, connection, scalar, matter and reference density
$c, \hbar, k_{\mathrm{B}}$	conversion constants	one declared unit convention
M_{P}	physical parameter	fixed or independently calibrated
$\kappa_{\mathrm{cost}}, \kappa_P, \kappa_{\mathrm{trap}}$	branch inputs	cost, curvature and trapping coefficients
$\kappa_H(M, J)$	derived geometry	normalized horizon surface gravity
$\bar{\kappa}$	derived only when specified	a declared common-coupling map
Π_{phys}	input map	projection to a metric, clock, fields and observables
S, m, M, θ	primitive data	action, reference measure, mobility, temperature
$P_t, \mathcal{L}, \pi$	conditional consequences	require a specified realization

In particular, equality of these differently defined quantities is never inferred from notation. A proposed common coupling is a matching relation among independent branch coefficients,

$$(\kappa_{\mathrm{cost}}, \kappa_P, \kappa_{\mathrm{trap}}, \ldots) \longmapsto \bar{\kappa}$$

and is a result only if the map is fixed by a stated selector or by an independent measurement. This convention prevents a change of normalization from being mistaken for a physical prediction.

The dependence of the generator and observations on primitive data is

$$\begin{aligned}(S, m, M, \theta, c_{\mathrm{drift}}, \mathcal{D}(L), \text{boundary data}) &\longmapsto L \longmapsto \mathrm{Law}(\mathcal{Z}),\\ Y_t = \Pi_{\mathrm{phys}}(\mathcal{Z}_t), \qquad y &= \mathcal{R}(Y; \mathcal{I}) + \text{measurement noise}.\end{aligned} \tag{R1}$$

Here $\mathcal{D}(L)$ is the generator domain, and $\mathcal{I}$ denotes instrument and nuisance parameters. An action alone does not determine a stochastic generator: mobility, noise, conservative drift and boundary realization also enter. In particular, (R1) does not apply an action to a sample path as though the result were a generator.

For a Lorentzian projection with signature $(-,+,+,+)$, the operational clock is the proper time

$$d\tau = \frac{1}{c}\sqrt{-g_{\mu\nu}dx^\mu dx^\nu}, \qquad g_{\mu\nu}dx^\mu dx^\nu < 0. \tag{R2}$$

The stochastic parameter t orders the master path. It is identified with τ only after a clock calibration, for example by requiring that a chosen clock functional $C[\mathcal{Z}]$ obey $dC/dt = (d\tau/dt)$ on the calibration trajectories. Thus causality, elapsed proper time and entropy production are three distinct structures.

Projection and conservation under explicit domain hypotheses. A uniquely specified master path law has a uniquely specified measurable image under Π_{phys}. This image need not be Markov. To obtain an autonomous projected generator A, require a separating test class $\mathcal{C}$, $f \circ \Pi_{\mathrm{phys}} \in \mathcal{D}(L)$, and

$$L(f \circ \Pi_{\mathrm{phys}}) = (Af) \circ \Pi_{\mathrm{phys}}, \qquad f \in \mathcal{C}.$$

The boundary terms must satisfy the same identity, the stopped martingales must be integrable, and the martingale problem for A must be well posed in the claimed class. The master martingale identity, conditioned on the smaller filtration of Y, then proves the projected martingale identity; well-posedness identifies its law. Smooth Itô coordinates require C^2 regularity or a separately justified generalized formula. Local Lipschitz regularity of a projection alone supplies neither this closure nor uniqueness for an independently proposed projected equation.

For a charge $Q_\xi \in \mathcal{D}(L)$ with integrable generator and a true stopped martingale, Dynkin's formula gives, in integral form,

$$\mathbb{E}Q_\xi(\mathcal{Z}_t) - \mathbb{E}Q_\xi(\mathcal{Z}_0) = \int_0^t \mathbb{E}(LQ_\xi)(\mathcal{Z}_s)\,\mathrm{d}s.$$

If $LQ_\xi = 0$ and boundary contributions vanish, the mean is constant. Pathwise conservation additionally requires zero martingale coefficient, for example $\sigma^{\mathsf{T}}\nabla Q_\xi = 0$ for a diffusion. A variational symmetry supplies such identities

only through a compatible Noether theorem; the existence of a differentiable symmetry alone is insufficient.

As a unit check, every term in the projected action must have the same dimension. A physical mechanical action has dimensions of $\hbar$; a Gibbs energy and an optimal-control cost need not have those dimensions. With $[x] = L$, $[t] = T$, and the value dimension left as $[V]$, the diffusion term $\frac{1}{2}\operatorname{tr}(a\nabla^2 V)$ has units $[V]/T$, while $b \cdot \nabla V$ has the same units only when $[b] = L/T$ and $[a] = L^2/T$. This check is applied before any numerical matching and is part of the registry, rather than an after-the-fact rescaling.

26.26. *Selector provenance and protection against circularity.* The registry is completed by recording the provenance of a possible coupling selector. Let P_0 be the reference path law obtained from a declared zero-cross-coupling or no-external-drive limit of the same master equation. Let $\mathcal{A} \subset \Theta/\sim$ be the set satisfying dimensional, gauge, positivity, anomaly, boundary and stability constraints. Define

$$F_{\mathrm{sel}}([\vartheta]) = \mathcal{R}([\vartheta]) + \iota_{\mathcal{A}}([\vartheta]), \qquad \mathcal{R}([\vartheta]) = \limsup_{T\to\infty} \frac{\tau_*}{T} D_{\mathrm{KL}}\Big(P_\vartheta^{[0,T]} \Big\| P_0^{[0,T]}\Big)\,. \tag{R3}$$

Here $\tau_* > 0$ is a fixed reference duration, and $\iota_{\mathcal{A}}$ is zero on the admissible class and $+\infty$ elsewhere. Both path laws live on the same measurable path space with the same clock and boundary convention. The reference law, equivalence relation, admissible set and limiting procedure in (R3) must be fixed before the calibration record is opened. The score must also be invariant under the declared equivalences in order to descend to the quotient.

Finiteness of this relative entropy is a substantive restriction. For example, the path laws of $\sigma_1 W_t$ and $\sigma_2 W_t$ on a fixed positive time interval are singular when $\sigma_1^2 \neq \sigma_2^2$, because their quadratic variations are the distinct constants $\sigma_1^2 t$ and $\sigma_2^2 t$. A Girsanov calculation of (R3) therefore requires a common covariance, drift difference in its noise range, compatible boundary laws and appropriate absolute-continuity/integrability conditions. An unrestricted change of diffusion is not covered by a quadratic drift-control formula.

Moreover, an entropy rate can lose finite-time information: an initial-law relative entropy divided by T vanishes as $T \to \infty$ for identical subsequent dynamics. Distinct candidate packages may consequently have the same rate. Strict convexity in the physical quotient and injectivity of any map from a selected path law to a coupling remain separate claims.

The selector-independence condition is

$$F_{\mathrm{sel}},\ P_0,\ \mathcal{A},\ \sim \quad \text{depend only on primitive model data.} \tag{R4}$$

Calibration observations may estimate declared detector nuisance parameters after $[\vartheta_*]$ has been selected, but may not change (R3). If (R3) is not derivable from the master action, it is a new physical axiom and must be labelled a

selection-law hypothesis. Gibbs invariance constrains a stationary law for a fixed generator; it does not identify a normalization or relative weights between independent couplings.

27. Spatial correlation, inverse geometry, and an interacting mode limit

A field describes values at neighboring points, not merely a list of one-point distributions. This distinction matters for fluctuating geometry. A positive determinant at each point does not by itself control an inverse metric uniformly over space. Nor do finite inverse moments at individual lattice sites establish such control as the lattice grows. We therefore construct a spatially correlated example in which these questions can be answered directly. The construction isolates a useful geometric mechanism: summable fluctuations of the logarithm of a coframe give a common bound on its size, its inverse, and their truncation errors.

The reference covariance is specified as part of this model. Its smooth mode tail is retained in the limit; it is not derived from the full gravitational action. Thus the limit below removes a mode truncation of a chosen spatial random field. It does not remove a physical ultraviolet scale from an interacting Lorentzian quantum theory.

27.1. *A correlated logarithmic reference.* Let K be a compact spatial domain with a Borel volume measure m of total mass one. One example is the three-dimensional torus with normalized coordinate volume. Let $F_k : K \to \mathrm{Sym}(4)$ be continuous, $\|F_k\|_{\infty,\mathrm{op}} \le 1$, and let $a_k \ge 0$ satisfy $A = \sum_{k\ge1} a_k \in (0,\infty)$. On a common probability space with independent standard real Gaussian variables ξ_k, define

$$S_N(x) = \sum_{k=1}^{N} a_k \xi_k F_k(x), \qquad M = \sum_{k\ge1} a_k |\xi_k|, \qquad A_{>N} = \sum_{k>N} a_k. \tag{1395}$$

Choose a deterministic continuous $R : K \to SO(4)$ and put $e_N = R \exp S_N$. This is a Euclidean coframe model. The use of $SO(4)$ here does not assert Lorentzian local symmetry. The rotation is fixed, and the matrix exponential acts pointwise.

The matrices represent coframe coefficients in a fixed reference trivialization. For $K = \mathbb{T}^3$, they can be interpreted as four-dimensional coframe data restricted to one slice of $\mathbb{R} \times \mathbb{T}^3$, relative to its product frame. They are not four independent one-forms on a three-dimensional tangent space. The norms and volume measure used below refer to that declared reference.

The elementary Gaussian estimates needed below have constants independent of N. Tonelli's theorem gives $\mathbb{E}M = \sqrt{2/\pi}A < \infty$, so $M < \infty$ almost

surely. For $t \geq 0$ and every real $p \geq 1$, Jensen's inequality with weights a_k/A gives

$$\mathbb{E}e^{tM} \leq 2e^{t^2A^2/2}, \qquad \mathbb{E}M^p \leq A^p\mathbb{E}|\xi_1|^p, \qquad \mathbb{E}M_{>N}^2 \leq A_{>N}^2, \tag{1396}$$

where $M_{>N} = \sum_{k>N} a_k|\xi_k|$. To see the first estimate, use $\mathbb{E}e^{u|\xi_1|} = 2e^{u^2/2}\Phi(u) \leq 2e^{u^2/2}$, where Φ is the standard normal distribution function. For a finite sum the unused weight can be assigned to zero; monotone convergence then justifies the infinite sum. Applying the same argument to its tail gives the last estimate. In particular, $\mathbb{E}M^4 \leq 3A^4$.

27.2. *Uniform nondegeneracy and a nonlinear interacting measure.* The interaction is chosen before the truncation is removed:

$$W_N = g\int_K \|S_N(x)\|_F^4\, dm(x), \qquad Z_N = \mathbb{E}e^{-W_N},$$
$$d\mu_N = Z_N^{-1}e^{-W_N}\, d\mathbb{P}, \qquad g \geq 0. \tag{1397}$$

It couples the Gaussian mode amplitudes through their common spatial field. It is a nonlinear spatial interaction, rather than a product law over sites. All tilted measures are first defined on the same sequence space; their coframe laws are then obtained by evaluating e_N.

THEOREM 121 (A correlated interacting coframe limit). *Under the preceding assumptions, S_N converges almost surely uniformly to a continuous symmetric field S. The coframes e_N and their inverses converge uniformly to $e = R\exp S$ and e^{-1}. Set $W = g\int_K \|S\|_F^4\, dm$, $Z = \mathbb{E}e^{-W}$, and $d\mu = Z^{-1}e^{-W}d\mathbb{P}$. With $z_* = \exp(-48gA^4)$, one has*

$$Z_N, Z \geq z_* > 0, \qquad \|\mu_N - \mu\|_{\mathrm{TV}} \leq \min\{1, 192gz_*^{-1}A^3A_{>N}\}, \tag{1398}$$

$$\mathbb{E}_{\mu_N}\|e_N^{-1}\|_{\infty,\mathrm{op}}^r \leq 2z_*^{-1}e^{r^2A^2/2}, \qquad r \geq 0,$$
$$\mathbb{E}_{\mu}\|e^{-1}\|_{\infty,\mathrm{op}}^r \leq 2z_*^{-1}e^{r^2A^2/2}, \tag{1399}$$
$$\mathbb{E}_{\mu}\sup_{x\in K}(\det e(x))^{-r} \leq 2z_*^{-1}e^{8r^2A^2}. \tag{1400}$$

Almost surely, $\inf_{x\in K}\sigma_{\min}(e(x)) \geq e^{-M} > 0$. *The same inverse-moment and determinant estimates hold for every finite truncation. Total variation in* (1398) *compares the tilted measures on the common sequence space, not coframe laws supported on different finite-dimensional subspaces.*

Proof. The Weierstrass bound $\|S - S_N\|_{\infty,\mathrm{op}} \leq M_{>N} \to 0$ gives uniform convergence and continuity. Symmetry gives real eigenvalues with absolute values at most M. Consequently

$$\|e^{\pm S}\|_{\infty,\mathrm{op}} \leq e^M, \qquad \det e = e^{\operatorname{tr} S} \geq e^{-4M}. \tag{1401}$$

The smallest singular value is at least e^{-M} because R is orthogonal. For any two symmetric matrices B, C, differentiating $e^{(1-t)B}e^{tC}$ and integrating gives

$$\|e^B - e^C\|_{\mathrm{op}} \le \|B - C\|_{\mathrm{op}} e^{\max(\|B\|_{\mathrm{op}}, \|C\|_{\mathrm{op}})}. \tag{1402}$$

This argument requires no commutativity of B and C. Applying it to S_N, S and to $-S_N, -S$ proves uniform convergence of both coframes and inverses, with error at most $e^M M_{>N}$ for each.

For a 4×4 symmetric matrix, $\|S\|_F \le 2\|S\|_{\mathrm{op}}$. It follows that $0 \le W_N, W \le 16gM^4$ and $\mathbb{E}W_N, \mathbb{E}W \le 48gA^4$. Jensen's inequality applied to the convex function e^{-u} yields the common lower bound z_*. The quartic difference obeys

$$|W_N - W| \le 64gM^3 M_{>N}, \qquad \delta_N := \mathbb{E}|W_N - W| \le 192gA^3 A_{>N}. \tag{1403}$$

Indeed $|u^4 - v^4| \le 4\max(u, v)^3|u - v|$, and Hölder's inequality gives

$$\mathbb{E}(M^3 M_{>N}) \le (\mathbb{E}M^4)^{3/4}(\mathbb{E}M_{>N}^4)^{1/4} \le 3A^3 A_{>N}.$$

Since e^{-u} is one-Lipschitz on $[0, \infty)$, $|Z_N - Z| \le \delta_N$. Splitting the difference of normalized densities gives an $L^1(\mathbb{P})$ bound $2\delta_N/z_*$ and hence the stated total-variation bound, with the convention $\|\nu - \rho\|_{\mathrm{TV}} = \frac{1}{2}\int |d\nu - d\rho|$. Finally, multiplication by the tilted density costs at most z_*^{-1}. Combining (1401) with (1396) proves the inverse and determinant moments, uniformly in N. □

Proposition 122 (An observable error bound). *For a functional Ψ of a coframe and its inverse, suppose $|\Psi| \le B_\Psi$ and Ψ is Lipschitz with constant L_Ψ for the maximum of the two uniform operator norms. Then*

$$\left|\mathbb{E}_{\mu_N}\Psi(e_N, e_N^{-1}) - \mathbb{E}_\mu \Psi(e, e^{-1})\right| \le z_*^{-1}\left(\sqrt{2}L_\Psi e^{A^2} + 384gB_\Psi A^3\right) A_{>N}. \tag{1404}$$

Proof. First change the field at fixed measure μ_N, and then change the measure at fixed field (e, e^{-1}). The first error is at most $L_\Psi z_*^{-1}\mathbb{E}(e^M M_{>N})$. Cauchy–Schwarz and (1396) bound this by $\sqrt{2}L_\Psi z_*^{-1} e^{A^2} A_{>N}$. The second error is at most $2B_\Psi\|\mu_N - \mu\|_{\mathrm{TV}}$. □

27.3. *A compatible finite-mode stochastic dynamics.* The interacting reference also admits an explicit finite-mode dynamics. This supplies a useful connection with dissipation, while keeping the choice of an evolution rate visible. Let $z = (\xi_1, \dots, \xi_N)$ and write $W_N(z)$ for the quartic interaction above. Its probability density with respect to Lebesgue measure is

$$q_N(z) = \mathcal{Z}_N^{-1} e^{-V_N(z)}, \qquad V_N(z) = \tfrac{1}{2}|z|^2 + W_N(z), \qquad \mathcal{Z}_N = (2\pi)^{N/2} Z_N. \tag{1405}$$

PROPOSITION 123 (Finite-mode evolution and entropy balance). *For $\gamma > 0$ and square-integrable initial data, the diffusion*

$$dZ_s = -\gamma \nabla V_N(Z_s) ds + \sqrt{2\gamma}\, dB_s \tag{1406}$$

has a unique nonexplosive strong solution. Its invariant density is q_N. For a smooth positive normalized evolving density p_s with finite relative entropy, sufficient decay, and justified differentiation and integration by parts, one has

$$\frac{d}{ds} D(p_s \| q_N) = -\gamma \int_{\mathbb{R}^N} p_s \left| \nabla \log \frac{p_s}{q_N} \right|^2 dz \le 0. \tag{1407}$$

The invariant law is independent of γ; its evolution rate is not.

Proof. The quartic interaction is a nonnegative homogeneous polynomial of degree four in z. Its drift is locally Lipschitz. For the generator $\mathcal{L}_N = \gamma(\Delta - \nabla V_N \cdot \nabla)$, Euler's homogeneity identity gives

$$\mathcal{L}_N |z|^2 = 2\gamma N - 2\gamma |z|^2 - 8\gamma W_N(z) \le 2\gamma N - 2\gamma |z|^2. \tag{1408}$$

The stopped Itô estimate bounds the probability of reaching radius R before time T by $(\mathbb{E}|Z_0|^2 + 2\gamma N T)/R^2$. Letting $R \to \infty$ excludes finite-time explosion; local strong existence and pathwise uniqueness therefore extend globally. The density e^{-V_N} has Gaussian decay and its gradient is a polynomial times that decay. Its current $\nabla q_N + q_N \nabla V_N$ vanishes. Equivalently, the symmetric divergence generator with this finite confining potential preserves its normalized measure, giving invariance.

The Fokker–Planck current for p is $j = -\gamma(\nabla p + p \nabla V_N) = -\gamma p \nabla \log(p/q_N)$. Differentiating relative entropy, using normalization to remove its constant derivative term, and integrating the continuity equation $\partial_s p = -\nabla \cdot j$ by parts gives (1407). The assumed decay removes the boundary term. Multiplying the generator by γ changes time without changing its zero-current density. □

The normalization and geometric estimates above are uniform in the number of modes. In contrast, the Lyapunov bound for the unweighted Gaussian coordinate norm contains N, as it must. The proposition does not assert a dimension-uniform bound for $|Z|^2$ or construct an infinite-dimensional stochastic evolution. Moreover, identifying its relative-entropy loss with physical heat requires a reservoir, energy scale, and time calibration. A chosen reversible generator establishes compatibility with the reference; it does not prove that the mother theory uniquely selects this generator.

If K is a compact smooth domain or manifold and $\sum_k a_k \|F_k\|_{C^j} < \infty$ for an integer $j \ge 1$, the same Weierstrass argument gives $S_N \to S$ almost surely in C^j. When R is also C^j, the coframes and inverses converge in that topology. These are additional regularity assumptions. With $a_k = 2^{-k}$, the uniform tail in (1404) is 2^{-N}. By contrast, $e_\varepsilon = \operatorname{diag}(\varepsilon, \varepsilon^{-1}, 1, 1)$ has determinant one and

inverse norm tending to infinity. The singular-value estimate above supplies precisely the shape control missing from a determinant-only condition.

The construction supplies an infinite-mode, nonlinear spatial random geometry with explicit inverse-observable bounds. It also identifies the remaining physical matching problem. A complete gravitational theory would have to produce a suitable reference or a replacement uniform estimate from its own action, include the independent connection and matter fields, and establish physical-time dynamics and positivity. Neither the chosen summable covariance nor the nonnegative quartic tilt implies the Hamiltonian constraint, reflection positivity, or Lorentzian unitarity.

27.4. *A fixed spatial test with nonlinear mode coupling.* For a reproducible example take $K = \mathbb{T}^3$, $R = I$, $a_k = 2^{-k}$, and $g = 0.02$. Enumerate the nonzero integer wavevectors by increasing squared length and then lexicographic order, keeping the sign for which the first nonzero component is positive. Use $F_k(x) = D_k \cos(n_k \cdot x)$, where D_k cycles through the four diagonal matrix units and the six matrices $E_{ij} + E_{ji}$, ordered lexicographically by $i < j$. Each has operator norm one. Thus $A = 1$, $A_{>N} = 2^{-N}$, and $z_* = e^{-0.96} = 0.38289289$.

The observable is $\Psi = \tanh \max_{x \in G} \|e^{-1}(x) - I\|_{\mathrm{op}}$ on the fixed 9^3-point equally spaced torus grid G. It is bounded by one and has Lipschitz constant one for the norm in Proposition 122. The analytic error bound is therefore 30.097793542^{-N}. The grid defines this observable; it does not replace the continuous supremum in Theorem 121.

Eight independently scrambled Sobol replicates, each with 512 Gaussian samples and dimension 24, estimate the normalized interacting expectations. Within a replicate the same coefficients are used at all truncations. The Gaussian variables are the inverse normal transforms of the Sobol coordinates. The largest component frequency among these 24 modes is two. Consequently the 9^3-point quadrature integrates the quartic interaction exactly in exact arithmetic: its trigonometric degree in each coordinate is at most eight and no nonzero such frequency is a multiple of nine. A comparison with an 11^3 grid for two samples differs by less than $4 \cdot 10^{-19}$ in floating-point arithmetic.

N	Z_N	$\mathbb{E}_{\mu_N} \Psi$	Δ_N	B_N
2	0.99836845	0.46273720	$-1.270 \cdot 10^{-2}$	$7.524 \cdot 10^{0}$
4	0.99830132	0.46821304	$-7.221 \cdot 10^{-3}$	$1.881 \cdot 10^{0}$
8	0.99829261	0.47520098	$-2.329 \cdot 10^{-4}$	$1.176 \cdot 10^{-1}$
12	0.99829258	0.47543203	$-1.836 \cdot 10^{-6}$	$7.348 \cdot 10^{-3}$
16	0.99829258	0.47543387	$7.039 \cdot 10^{-9}$	$4.593 \cdot 10^{-4}$
24	0.99829258	0.47543386	0	$1.794 \cdot 10^{-6}$

Here Δ_N is the signed paired difference from 24 modes and B_N is the analytic bound to the infinite law. The standard error across independent replicate estimates is approximately $2.07 \cdot 10^{-5}$ for Z_{24} and $1.69 \cdot 10^{-4}$ for its normalized

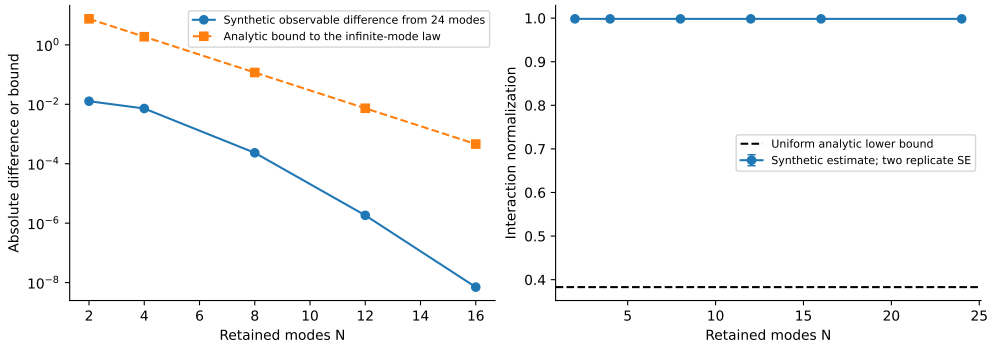


Figure 50. Synthetic convergence for the prescribed correlated coframe model. Left: the absolute paired observable difference from 24 retained modes, together with a conservative analytic bound to the infinite-mode law. Right: estimated interaction normalizations and the common lower bound. Error bars show two standard errors across randomized replicates; they are not rigorous confidence bounds. The data test a specified spatial model and are not observations of quantum gravity.

observable. For the paired difference at $N = 16$ it is $1.03 \cdot 10^{-8}$, exceeding the absolute difference displayed in the table. That small difference is therefore not evidence for a resolved nonzero truncation effect. The analytic bound from 24 modes to the infinite law is $1.794 \cdot 10^{-6}$; it does not remove sampling error. Importance-weight effective sample sizes exceed 511.98 out of 512 within every replicate. This favorable overlap does not make the randomized quadrature an interval certificate.

28. **Physical reduction and quantum constraint tests**

A proposed unification must test the degrees of freedom that remain after constraints are imposed. A degeneracy of the velocity Hessian is the beginning of that reduction, not its conclusion. Similarly, a vanishing constraint expectation can be automatic on a selected space of states. The following finite examples explain why the full reduction and a nontrivial quantum algebra test are both needed.

28.1. *A negative kinetic direction removed by second-class constraints.* Consider three real coordinates (x, y, λ) with

$$L = \tfrac{1}{2}\dot{x}^2 - \tfrac{1}{2}\dot{y}^2 + \lambda y, \qquad H = \tfrac{1}{2}p_x^2 - \tfrac{1}{2}p_y^2 - \lambda y. \tag{1409}$$

The velocity Hessian is $\mathrm{diag}(1, -1, 0)$. The negative y direction is orthogonal, in these coordinates, to its null λ direction. Nevertheless the constraint chain

removes y. With total Hamiltonian $H + up_\lambda$, preservation gives

$$p_\lambda = 0 \implies y = 0 \implies p_y = 0 \implies \lambda = 0 \implies u = 0. \tag{1410}$$

Here $\dot{p}_\lambda = y$, $\dot{y} = -p_y$, and $\dot{p}_y = \lambda$. For the ordered constraints $(p_\lambda, y, p_y, \lambda)$ the Poisson matrix is

$$C = \begin{pmatrix} 0 & 0 & 0 & -1 \\ 0 & 0 & 1 & 0 \\ 0 & -1 & 0 & 0 \\ 1 & 0 & 0 & 0 \end{pmatrix}, \qquad \det C = 1, \qquad H_{\mathrm{red}} = \tfrac{1}{2}p_x^2. \tag{1411}$$

All four constraints are second class. Their reduction leaves the canonical pair (x, p_x) with positive kinetic energy. The example disproves a general rule that a negative kinetic direction must project nontrivially onto the Hessian kernel in order to be removed. More generally, a phase-space mode and a velocity-Hessian null vector need not even belong to the same vector space without additional choices.

For the field theory the appropriate sequence is to derive the complete constraint chain on a stated constant-rank sector, reduce its symplectic structure, and then examine the surviving Hamiltonian and physical propagator. A degree-of-freedom count alone does not establish positive energy, real characteristic frequencies, or a positive quantum inner product. Conversely, a different connection formulation must derive its own reduced spectrum before it can replace a negative-residue metric restriction. This mechanical example proves no such replacement for the gravitational mother action.

28.2. *Why exact-kernel expectations are insufficient.* Let H_N, H_M, C_Z act on a common domain stable under the required products. Define, at fixed $\hbar > 0$,

$$\mathcal{A} = (i\hbar)^{-1}(H_N H_M - H_M H_N) - C_Z. \tag{1412}$$

If all three operators annihilate ψ, then $\mathcal{A}\psi = 0$ by substitution. Thus the expectation on this exact common kernel cannot distinguish a correct off-shell constraint algebra from an incorrect one. Moreover, for

$$P = \begin{pmatrix} 1 & 0 \\ 0 & 0 \end{pmatrix}, \qquad B = \begin{pmatrix} 0 & 1 \\ 1 & 0 \end{pmatrix}, \qquad PBP = 0, \tag{1413}$$

the vector $B(1,0)^T = (0,1)^T$ lies outside the range of P. Vanishing compression does not establish preservation of a proposed physical subspace.

A sufficient regulator target must instead specify a test domain, comparison maps I_h, operator ordering for the structure functions, and a topology, for example

$$\|\mathcal{A}_h[N, M] I_h \psi\|_{-s} \le \epsilon_h(N, M)\|\psi\|_s, \qquad \epsilon_h(N, M) \longrightarrow 0 \quad \text{at fixed } \hbar > 0. \tag{1414}$$

A justified dual-space or rigging-map formulation may provide a different criterion. It must still define a nonzero physical space and represent the intended classical generators. A common constraint kernel in the kinematic Hilbert space can be zero even when distributional physical states exist. Likewise an $O(\hbar)$ discrepancy is not, by itself, an error tending to zero with h at fixed $\hbar$.

28.3. *Spectral continuation and the choice of quantum theory.* Discreteness alone does not remove analytic spectral variables. For a finite self-adjoint matrix K, the resolvent $(zI - K)^{-1}$ is meromorphic in complex z. Continuous time on a spatial lattice also retains a continuous frequency. These facts do not define a prescription for continuation across interacting thresholds, but they rule out an impossibility argument based only on finitely many spatial momenta.

A negative physical residue in an unchanged higher-derivative covariance still has to be addressed. An effective theory uses a declared energy range and controlled operator expansion. A fakeon construction changes the continuation and the physical state prescription. A conventional reflection-positive reconstruction must satisfy its own positivity condition. These are separate routes with different assumptions; a positive transfer operator for one reduced sector does not establish positivity for another sector with a negative reflection form.

29. **Equilibrium, evolution, and the calibration of time**

An equilibrium distribution answers how often a state is occupied. A clock answers how rapidly a transition occurs. These are different measurements. Their distinction is especially useful in a framework that uses an equilibrium reference to organize stochastic and quantum dynamics. We give a finite quantum example in which the ambiguity and its resolution can both be computed, and then explain the corresponding classical time change.

29.1. *What the KMS condition fixes.* Let H be a self-adjoint matrix, $\beta > 0$ an inverse energy, and $\hbar > 0$. Define

$$\rho_\beta = \frac{e^{-\beta H}}{\operatorname{tr} e^{-\beta H}}, \qquad \alpha_t(B) = e^{itH/\hbar} B e^{-itH/\hbar}, \qquad \omega_\beta(B) = \operatorname{tr}(\rho_\beta B). \tag{1415}$$

Here $\beta = (k_B T)^{-1}$ when a physical temperature T has been specified. All matrix observables are entire analytic in t. Direct trace cyclicity gives the Kubo–Martin–Schwinger boundary identity

$$\omega_\beta(\alpha_t(A)B) = \omega_\beta(B\alpha_{t+i\beta\hbar}(A)). \tag{1416}$$

For example, in an energy basis the (i, j) term on the left has weight $e^{-\beta E_i} e^{it(E_i - E_j)/\hbar}$; on the right the same weight is $e^{-\beta E_j} e^{-\beta(E_i - E_j)} e^{it(E_i - E_j)/\hbar}$. This verifies both the sign and the factor $\hbar$. The imaginary-time shift has units of time.

The transformation $H \mapsto aH + E_0 I$, $\beta \mapsto \beta/a$, with $a > 0$, leaves the Gibbs density unchanged. The scalar E_0 cancels from both this density and the Heisenberg evolution, whereas a changes the evolution rate. KMS is a condition on a state together with a specified evolution. It does not determine an absolute rate from the density alone. Failure of KMS may also describe a driven state; it does not by itself invalidate the clock used to observe that state.

29.2. *Removing the scale ambiguity by an independent transition.*

PROPOSITION 124 (Population and frequency calibration). *Let $H = E_0 I + cH_*$, where the finite-dimensional self-adjoint matrix H_* is known and dimensionless, c has units of energy, and $\Delta = \varepsilon_j - \varepsilon_i > 0$ is an ordered gap of H_*. Suppose $c, \beta > 0$, the state is ρ_β, and its populations p_i, p_j are measured in this known eigenbasis. The population ratio determines only*

$$b = -\frac{\log(p_j/p_i)}{\Delta} = \beta c. \tag{1417}$$

If the angular transition frequency ω_{ji} is also measured relative to an independently calibrated time unit, then

$$c = \frac{\hbar\omega_{ji}}{\Delta}, \qquad \beta = \frac{b}{c}. \tag{1418}$$

These measurements do not determine E_0. Suppose estimates obey $|\widehat{b} - b| \le \epsilon_b$ and $|\widehat{\omega} - \omega_{ji}| \le \epsilon_\omega$. If $\epsilon_c = \hbar\epsilon_\omega/\Delta < c$, then

$$|\widehat{c} - c| \le \epsilon_c, \qquad |\widehat{\beta} - \beta| \le \frac{\epsilon_b}{c - \epsilon_c} + \frac{b\epsilon_c}{c(c - \epsilon_c)}, \qquad \widehat{\beta} = \widehat{b}/\widehat{c}. \tag{1419}$$

Proof. The ratio of Gibbs populations is $p_j/p_i = \exp[-\beta c(\varepsilon_j - \varepsilon_i)]$. The same pair of energy levels gives angular frequency $c\Delta/\hbar$. These are two independent relations for b and c. The frequency estimate gives the first bound. Since $\widehat{c} \ge c - \epsilon_c > 0$,

$$\left|\frac{\widehat{b}}{\widehat{c}} - \frac{b}{c}\right| \le \frac{|\widehat{b} - b|}{\widehat{c}} + \frac{b|\widehat{c} - c|}{c\widehat{c}},$$

which proves the second. An additive scalar in H cancels from every displayed observable, proving its nonidentifiability here. □

For example, take $\hbar = 1$, $H_* = \mathrm{diag}(0, 1, 3)$, $c = 1.7$, and $\beta = 0.8$. The three populations are approximately $(0.78519546, 0.20152888, 0.01327567)$, and $b = 1.36$. The pair $c' = 3.4$, $\beta' = 0.4$ gives exactly the same populations. For the first gap the angular frequencies are 1.7 and 3.4, respectively. With $\epsilon_b = 0.002$ and $\epsilon_\omega = 0.001$, the bound in (1419) is approximately 0.00164803. These are synthetic examples in declared units. They illustrate identifiability and are not measurements of a new interaction.

The independent time unit is essential. An unknown apparatus Hamiltonian or an unknown common frequency standard would introduce another scale ambiguity. The proposition therefore supplies an operational matching test, rather than selecting a preferred clock from equilibrium alone.

29.3. *The corresponding stochastic time change.* Let L be a Markov generator with invariant law π. For the time change $dt = r(X_s)ds$, assume r is positive, bounded above and below, and integrable against π. The new generator and invariant law are

$$L_r = r^{-1}L, \qquad d\pi_r = \frac{r\,d\pi}{\int r\,d\pi}. \tag{1420}$$

Indeed integrating $L_r f$ against π_r cancels r and leaves a constant multiple of $\int Lf\,d\pi = 0$. In the constant case $r = r_0$, the invariant law is unchanged, while every decay rate is divided by r_0. For an overdamped harmonic mode $dX_s = -\kappa X_s ds + \sqrt{2\theta\gamma}\,dW_s$ with $\kappa = \gamma k > 0$, the stationary variance is θ/k and the stationary correlation is $(\theta/k)e^{-\kappa|s|}$. In the new time it is $(\theta/k)e^{-\kappa|t|/r_0}$. Thus a variance measurement fixes an equilibrium combination, while a time correlation tests the mobility relative to a clock.

For a normalized density p at a corresponding state and a reversible model, $d\mathcal{F}/dt = r_0^{-1}d\mathcal{F}/ds$. Physical heat and work rates transform in the same way if the bath and energy are held fixed. Their integrated values over the same trajectory segment are unchanged. For a state-dependent r, the occupation law itself changes as in (1420); assigning physical heat then requires the declared reservoir model. An arbitrary change of an occupation potential is not a derivation of a new mechanical energy.

30. **A mother-parameter registry and a no-refit stellar transfer**

The framework contains several distinct maps that are often compressed into the phrase "the common parameter." To make a cross-sector claim testable, one must record which quantities are derived from the mother action, which are fixed by an independent calibration, and which remain nuisance parameters. The registry below is a formal interface between the microscopic branch and the stellar observation map. It does not turn an effective response coefficient into a fundamental constant.

30.1. *Three levels of a registered quantity.* Use the dimensionless scalar coordinate $x = \varphi/(\sqrt{2}M_{\mathrm{P}})$, the common-weight slope $a_0 = \partial_x \log A|_0$, the scalar inverse range $\mu_\varphi = m_\varphi c/\hbar$, and the matching length ℓ. The common-weight

relation used in the stellar calculation gives

$$q^2=\frac{2a_0^2}{1-3a_0^2},\qquad Z_0=\frac{1}{1-3a_0^2},\qquad m_\sigma^2=\frac{\mu_\varphi^2-6a_0^2/\ell^2}{1-3a_0^2},\qquad |a_0|<\frac{1}{\sqrt{3}}. \tag{1421}$$

Here m_σ is also expressed as an inverse length, so every term in its squared-mass formula has inverse-length-squared units. This is a derived algebraic fibre once (a_0,μ_φ,ℓ) have been supplied. It is not a numerical selection of those three inputs. The matter derivatives $d_\Lambda=\partial_x\log\Lambda_3|_0$ and $d_p=\partial_x\log X_p|_0$ require microscopic threshold matching and nuclear or hadronic response data. They cannot be inferred from a background equation of state alone.

For the linear stellar branch define the registered response vector

$$\vartheta=(\vartheta_1,\vartheta_2)^T,\qquad \vartheta_1=a_0+d_\Lambda,\qquad \vartheta_2=d_b, \tag{1422}$$

where d_b denotes one explicitly chosen rest-energy response direction. The response coefficients C_A^{tr} and C_A^b are computed from the same GR background and EOS prescription for each body A:

$$a_A^{\mathrm{lin}}=C_A\vartheta,\qquad C_A=(C_A^{\mathrm{tr}},C_A^b). \tag{1423}$$

The vector ϑ is a two-dimensional effective coordinate for this test. A complete microscopic matching must replace d_b by the relevant set of d_p and enlarge the response matrix accordingly.

Quantity	Meaning	Source of value	Status in this test
a_0	common conformal slope	mother branch	registered input
μ_φ	inverse scalar range	mother branch or calibration	registered input
ℓ	matching length	mother branch or calibration	registered input
d_Λ	QCD scale derivative	threshold matching	independent input
d_b	rest-energy response direction	declared matter basis	effective nuisance
C_A	GR stellar response row	EOS/background calculation	computed per body
a_A^{lin}	effective stellar scalar charge	$C_A\vartheta$	predicted

The table prevents a silent change of level. In particular, a fitted a_A cannot be fed back into a_0 and then described as a prediction. The scalar range also enters the radiative transfer and must be held fixed when the charge map is transferred to another binary.

30.2. *No-refit transfer theorem.* Let $A\in\mathbb{R}^{m\times d}$ contain the response rows of m calibration systems, let $b\in\mathbb{R}^d$ be the target response row, and let

$$y_c=A\vartheta+\epsilon_c,\qquad \widehat{y}_t=b^TA^+y_c, \tag{1424}$$

where A^+ is the Moore–Penrose inverse. The target is not used in forming A^+.

PROPOSITION 125 (Identifiable no-refit transfer). *Assume* $\ker A \subseteq \ker b^T$. *Then*

$$b^T A^+ A = b^T, \qquad \mathbb{E}\widehat{y}_t = b^T\vartheta \quad \text{if } \mathbb{E}\epsilon_c = 0. \tag{1425}$$

If ϵ_c *has covariance* Σ_c, *then*

$$\operatorname{Var}(\widehat{y}_t) = b^T A^+ \Sigma_c (A^+)^T b. \tag{1426}$$

If an independent target measurement has variance σ_t^2, *the variance of its prediction residual is*

$$V_t = \sigma_t^2 + b^T A^+ \Sigma_c (A^+)^T b \tag{1427}$$

when calibration and target errors are uncorrelated. If the kernel condition fails, there is a direction n *with* $An = 0$ *and* $b^T n \neq 0$; *then the same calibration is compatible with* ϑ *and* $\vartheta + tn$ *but predicts different targets.*

Proof. The matrix A^+A is the orthogonal projector onto $(\ker A)^\perp$. The kernel condition says that b is orthogonal to $\ker A$, so $b^T A^+ A = b^T$. Taking expectations in $\widehat{y}_t = b^T A^+ (A\vartheta + \epsilon_c)$ gives the first claim. The variance follows by multiplying the covariance of ϵ_c on the left and right. An independent target error adds σ_t^2. If the kernel condition fails, direct substitution gives $A(\vartheta + tn) = A\vartheta$ but $b^T(\vartheta + tn) = b^T\vartheta + tb^T n$. □

This theorem is deliberately conditional. It proves transfer of the registered response map; it does not prove that the map is the unique output of the complete mother action. It also requires that EOS choices, source masses, range, and transfer normalization be frozen before the target is evaluated. Re-fitting C_A, ϑ, or the target charge after seeing the target would invalidate the no-refit statement.

30.3. *A three-star calculation with one common parameter vector.* For an explicit calculation, use the response rows already obtained from the stated GR backgrounds and EOS prescription:

$$\begin{aligned} &C_1 = (0.643076, 0.777694), \qquad C_2 = (0.336327, 0.600851), \\ &C_3 = (0.493724, 0.691873), \end{aligned} \tag{1428}$$

corresponding respectively to the J1738, J0348, and J2222 benchmark systems in the SLy background calculation. Use systems 1 and 2 only for calibration, and system 3 only for evaluation. The calibration matrix has

$$\begin{aligned} A &= \begin{pmatrix} 0.643076 & 0.777694 \\ 0.336327 & 0.600851 \end{pmatrix}, \\ \det A &= 0.124833367738, \qquad \kappa_2(A) = 11.87164334, \end{aligned} \tag{1429}$$

and its singular values are 1.21736487 and 0.10254392. It is therefore invertible, although not perfectly conditioned.

Take the declared synthetic common vector $\vartheta = (10^{-3}, 2 \times 10^{-4})^T$. The three charges calculated without changing that vector are

$$(a_1^{\mathrm{lin}}, a_2^{\mathrm{lin}}, a_3^{\mathrm{lin}}) = (7.986148, 4.564972, 6.320986) \times 10^{-4}. \tag{1430}$$

Inverting only the first two exact charges returns $\widehat{\vartheta} = (10^{-3}, 2 \times 10^{-4})^T$ and predicts $\widehat{a}_3 = 6.320986 \times 10^{-4}$, equal to the target generated by the same vector. This is a self-consistency calculation, not a measurement of a stellar charge.

For a quantitative error check, assign independent calibration standard uncertainties 10^{-7} to the first two charge summaries and an independent target standard uncertainty 10^{-7}. The transfer row is

$$L = C_3 A^{-1} = (0.51235491, 0.48833681), \tag{1431}$$

so the prediction residual variance is $V_3 = 1.50098039 \times 10^{-14}$ and its standard deviation is 1.225144×10^{-7}. A simultaneous one-standard-error perturbation of both calibration charges changes the predicted target between $6.31998531 \times 10^{-4}$ and $6.32198669 \times 10^{-4}$ over the four sign combinations. The spread is due to the declared calibration noise, not a second fit.

The calculation demonstrates the desired architecture: a single registered vector determines several effective stellar charges, and an unused system is predicted from the first systems. It does not yet meet the stronger claim that the vector (a_0, d_Λ, d_b) is uniquely derived from the full mother action. To make that claim physical, the microscopic threshold and nuclear response coefficients must be replaced by a specified matter calculation or independently measured calibration, and the massive scalar transfer function must be included consistently in every binary.

30.4. *Acceptance conditions for a framework-level prediction.* The result is promoted to an empirical test only after all of the following are recorded: (i) the mother parameters and their units; (ii) the derivation or independent calibration of each matter derivative; (iii) the EOS and stellar background version; (iv) the scalar range and radiative threshold; (v) the calibration/target split and data hashes; (vi) the full covariance, including shared systematic errors; and (vii) a likelihood evaluated without target-dependent parameter changes. Failure of any item changes the result to a conditional transfer or a bound. This registry therefore improves the framework's predictive credibility by making the missing microscopic step explicit rather than silently assuming it.

30.5. *Finite Lean certificates and their exact scope.* The algebraic parts of this interface are checked in the accompanying Lean file `QuantumCriteriaCalibration20261105.lean`. In particular, `two_by_two_calibration_inverse` verifies the displayed inverse of the

nonsingular two-by-two calibration matrix, while `product_and_gap_identify` verifies the elementary identification step used when a nonzero gap fixes a shared coefficient. The same file checks the finite identities used by the reduced dynamics: `quartic_homogeneity_identity` is Euler's identity for the stated two-mode quartic interaction, `quartic_lyapunov_identity` is the corresponding finite-mode generator identity, `scalar_covariance_step_nonnegative` gives the scalar covariance positivity step, and `finite_state_reversible_dissipation_identity` gives the exact two-state sign calculation. Finally, `positive_clock_rate_preserves_order` records the elementary order preservation of a positive clock-rate rescaling; `two_state_mass_conservation` checks cancellation of the two-state exchange currents, and `two_mode_covariance_trace_nonnegative` checks positivity of the propagated two-mode variance trace.

These certificates are kernel-checked finite algebra. They do not formalize the analytic stellar equation of state, the microscopic threshold matching, the infinite-mode Gaussian or interacting measure, the full Lorentzian constraint algebra, or an interacting quantum-gravity continuum limit. Accordingly, the Lean results support the finite transfer and reduced-model identities above; they do not upgrade the conditional registry into a proof of mother-action parameter uniqueness or a complete quantum-gravity theory.

31. **Synthetic comparisons of uncertainty, memory and response**

The preceding estimates answer different parts of one prediction problem. Calibration has uncertainty, an observation can omit memory, and an approximate field solution has a numerical residual. The following examples keep those effects separate so that each comparison has a known reference. All inputs in this section are synthetic and dimensionless, obtained by fixing one consistent unit for each model. No generated value is an experimental or market measurement.

31.1. *Finite calibration and an unused response.* Use $\beta = 1.7$, $\alpha = 0.4$, $\eta = 0.8$ and $\delta = 0.01$ in (507). The target is $(r_*, s_*) = (0.7, 0.6)$, whose response is 2.0861370875485. To make the calculation reproducible, the displayed estimates use the same three log errors $(0.010, -0.008, 0.006)$ at each design. Table 27 compares their actual error with the uniform bound; the latter applies to every error triple in the stated box, not only the displayed one. Increasing the spacings improves these bounds under the same log-error budget, but the experiment must establish that budget at the larger perturbations. For an additional numerical check, 20,000 independent uniform error triples were generated per design with seed 20261117; all target errors stayed within the proved bound.

Table 27. Synthetic finite-response prediction at a fixed unused setting. The last two columns are dimensionless absolute logarithmic errors.

h	r	$\widehat{Q}_*$	Actual error	Bound E_*
0.25	0.2	1.99704834	0.043644	0.128000
1	0.2	2.06281233	0.011244	0.092000
0.25	0.8	2.01060400	0.036879	0.078000
1	0.8	2.07681439	0.004479	0.042000

Table 28. Omitting a stationary hidden force at fixed hidden variance. The final column is the minimum of the analytic upper bounds.

κ	$\Delta_V(1.5)$	Upper bound
0.5	0.179316277	0.224326378
0.8	0.158842448	0.224326378
2	0.106091853	0.131250000
8	0.037130985	0.041761364
32	0.010135715	0.010442536

This sampling checks the implementation and does not replace the proof or establish an instrument error distribution.

31.2. *The observable cost of omitted memory.* In (1889), take $a = 0.8$, $b = 0.7$, $D = 0.4$, $v = 0.6$ and $T = 1.5$. Only the hidden decay rate κ changes. Table 28 evaluates the exact variance defect and the minimum of the three bounds in (1893). The exact endpoint covariance was also computed independently from the matrix Lyapunov equation and used to generate 60,000 Gaussian endpoints per rate. For n independent centered Gaussian samples of variance V, the sample second moment has standard error $V\sqrt{2/n}$; this is the sampling uncertainty in that comparison. Exact endpoint sampling introduces no Euler time-discretization error. The decay in the table relies on holding v fixed. Rescaling it as $v = \kappa q$ leaves the nonzero limiting contribution in (1900).

31.3. *An exterior boundary and a finite frequency band.* Set $R = 1$, $\mu = 0.4$, $\chi = -0.25$ and $f = 1$ in (1293). Then $K = 0.09$, $C_P = 1/2$ and $\gamma_\omega = 1 - (0.09 + \omega^2)/2$. The following frequencies are inside the sufficient band, on both sides of the radiation threshold $\omega = \mu$. Table 29 uses $N = 4$, hence a polynomial of degree eight. Its errors and residual bounds were evaluated with 80-decimal-digit arithmetic. The small errors are reported to three significant

Table 29. Energy-error comparison for the synthetic outgoing scalar problem. The entries evaluate an analytic bound; high arithmetic precision does not constitute interval enclosure of every numerical operation.

ω	γ_ω	$E_0[u-u_N]^{1/2}$	Residual bound
0	0.955	2.26×10^{-14}	6.78×10^{-13}
0.4	0.875	1.48×10^{-12}	4.82×10^{-11}
0.6	0.775	1.67×10^{-11}	6.16×10^{-10}
1.3	0.110	5.50×10^{-9}	1.42×10^{-6}

figures because a long decimal display would add no physical information. At $\omega = 1.3$, the surface error is approximately 3.35438×10^{-17} while the energy error is 5.49754×10^{-9}. Their different sizes follow from (1303); they are not two interchangeable measures of accuracy. As the sufficient margin decreases, the residual bound grows. Refining the approximation reduces its residual but cannot make a lost analytic margin positive.

31.4. *What the comparisons establish.* Figure 51 places these examples alongside the incomplete-market calculation of Section 2.5.1. The financial minimizer selects the call price 6.86109236092030 from the no-arbitrage interval $(100/51, 220/17)$. Its uniqueness is relative to the prescribed reference law. Likewise the physical error bounds are conditional on their prescribed source, branch and calibration. The shared variational organization is useful because it makes these dependencies explicit and allows an unused observable to challenge them.

The quadratic gravitational estimate gives a further scale check. At $\ell|p| = 0.1$, the error of D_1 relative to D_{quad} is 10^{-4}, and its error relative to D_0 is $10^{-4}/1.01 \simeq 9.90099\times10^{-5}$. At $\ell|p| = 0.3$ the corresponding values are 0.0081 and $0.0081/1.09 \simeq 0.00743119$. These are response-expansion errors, not probabilities of correctness or resolutions of the reflection-positivity obstruction.

Together the calculations supply finite quantitative tests of several arrows in the programme: coefficient to response, full state to observed state, and source to field. The next physical comparison must fix the measurement law and all transferred coefficients before its target data are examined. The same rule applies to an economic reference probability chosen from information outside the option price being predicted.

32. **Conclusions and further directions**

The organizing idea is that admissible change, stochastic evolution, selection and observation can be specified together. The representative models

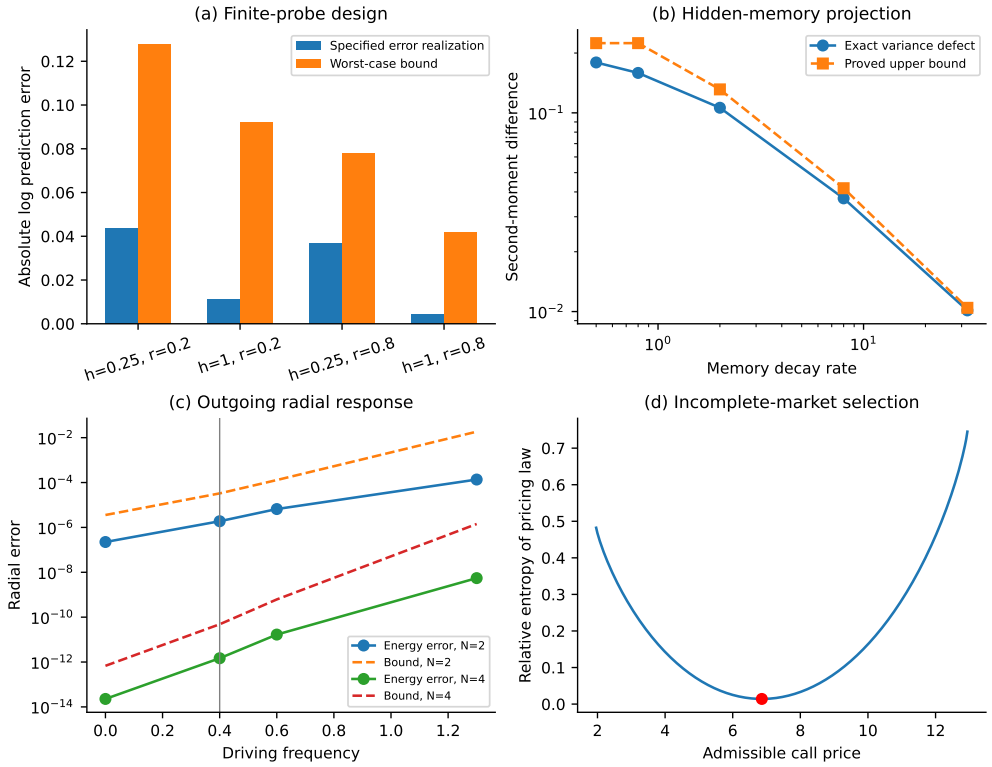


Figure 51. Synthetic comparisons using the stated inputs. (a) Target log errors and worst-case calibration bounds. (b) Exact second-moment defect from omitted memory and the minimum analytic bound. (c) High-precision energy errors and residual bounds for basis orders $N = 2, 4$; the vertical line is the radiation threshold. (d) Relative entropy along the feasible martingale line, with its minimizing price marked. These panels concern different explicit models and do not assert a common empirical fit.

in Section 2 give this idea a calculable form. One transition operator supplies a relaxation geometry, a growth-weighted population equation and an information update. Their different normalization and sampling operations explain why a bath equilibrium, a selected population and a driven history have different stationary fractions. The oscillator supplies the complementary physical link: conservative transport remains when the matched damping and noise are removed, while the same reservoir coupling fixes fluctuations and response when it is retained. These examples identify the common operations that the geometric field construction develops.

The finite geometric extension sharpens the connection between symmetry and probability. Local rotations act on the coframe as well as the links, and the logarithmic reference law gives finite inverse moments. Its interaction-dependent normalization remains visible in the bounds, so a uniform field limit is a further requirement. The temporal calculation likewise removes an explicit row factor without removing the shared inertia. In the retained gauge–scalar dynamics, the leading scalar source oscillates at twice the gauge frequency. The resulting response has a resonant denominator and a proved finite-time error bound. These results provide specific comparison quantities for future measurements: calibrated inertia, observation-scale determinant statistics, and amplitude-dependent response under a specified preparation. Extending them to the mother theory requires deriving the representation and reference law, reducing its full constraint spectrum, and obtaining estimates uniform in the spatial regulator.

Section 15.29 advances the structural uniqueness question at a fixed regulator. The calibrated generator and its domain determine the stochastic path law; a specified positive invariant density, reference volume and fluctuation energy reconstruct the Gibbs energy, mobility and stationary current. Complete affine generator probes give a global compatibility criterion with an explicit singular-value error bound. A positive reduced-action Gram matrix also gives coefficient uniqueness and stability within a fixed physical basis. For the specified square realization, Theorem 94 establishes this condition analytically: $G_\alpha \succeq (2/25)I_6$ for $|\alpha| \leq 1/2$. The resulting drift and probe error bounds quantify recovery of the four group weights, scalar edge coefficient and scalar mass coefficient. Exact rank loss at zero edge weight and under operator duplication identifies two concrete limits of that inverse problem. Theorem 96 extends the calculation to all four-dimensional periodic regulators of side length at least three, with $G_{\alpha,n}/n \succeq (96/53225)I_6$. Other geometries and continuum scalings require their own conditioning and limit estimates. The same analysis constructs exact equilibrium, sampling and hidden-state ambiguities, which explain why these conditional results do not select the entire primitive physical package from a reduced observation record.

The observation extension makes this limitation quantitative. A positive population Gram margin survives a bounded loss of coverage and a calibrated sensor contraction on the feature directions. Finite observations require an additional matrix-error bound; repeating a sensor that annihilates a coefficient direction cannot recover that direction. The contact example likewise replaces an exact rate ratio by a tolerance interval and gives finite-time mean and covariance bounds. Its independent moment calculation separates integration error from the physical contact uncertainty. Applying these estimates to measurements

requires experimentally justified coverage, noise and contact-tolerance bounds, rather than further adjustment to the same target data.

The positive-coordinate realization proves finite-state admissibility and law convergence from the same generator, with an additional specified current showing how attraction can coexist with a stationary statistical arrow. The nonzero mass-scaled example enforces common scalar and matter couplings before computing distinct response channels. Its amplitude-free relation retains an independent length and an explicit physical remainder. Extending these results requires deriving the physical projection, selecting or measuring the remaining common inputs, and controlling the continuum and observation maps; neither finite construction substitutes for those tasks.

The finite coupled realization in Section 14.28 exhibits a nonempty common domain for mechanical stability, stationary statistics, thermal exchange, and projected memory. Its entropy calculation identifies unequal reservoirs as the source of maintained irreversibility, and its conservative limit requires friction and noise to vanish together. These explicit results make simultaneous compatibility testable; the joint physical domain of the field branches still requires their additional matching conditions.

The clock and control-projection calculations impose additional consistency conditions on a common origin. Physical occupation laws transform with the clock rate, while resolved force costs follow from a constrained minimum of the mother cost. Existing two-fluid and GP models can therefore be connected through explicit matching tests. Classical Noether charges are recovered in the matched conservative limit; stochastic expectation conservation and pathwise conservation require different conditions. The remaining Lorentzian, quantum, and observational completions must respect these same clock, covariance, and balance conventions.

The common-cone calculation makes the physical time interface more specific. On the matched two-derivative vacuum branch, the scalar and gauge symbols, the square of the Dirac symbol, and the harmonic Einstein symbol have the same null set. Their group delays can nevertheless differ because masses enter the dispersion relation. A finite-frequency phase bound quantifies one such comparison, while an independently calibrated correlation gives a transport-rate interval and a prediction at a new lag. The next structural step is to derive the admissibility of this shared kinetic branch, including the controlled treatment of higher derivatives and the first-order fermion construction, from the mother data. Neither a shared Gibbs law nor entropy positivity supplies those conditions by itself.

Appendix H compares deterministic metric trembling with the present regulated stochastic construction. Explicit counterexamples separate spatial homogeneity from polarization alignment, mean-zero perturbation averaging from

action stationarity, and causal admissibility from a normalized gravitational response. These distinctions also supply a finite prediction-separation criterion; a shared explanation is not an independently distinguishing observation.

32.1. *Synthesis of the common objective and its physical branches.* The overview paper brings together the field, probability-law, control, and hydrodynamic descriptions without conflating their different mathematical roles. The shared configuration and regulated dynamics are specified in (43) and (893); the joint objective is (922). Their physical interpretation is that the same declared microscopic data constrain the candidate geometry, the equilibrium reference, the cost of changing a drift, and the transport observables. This interpretation becomes a statement about a particular physical branch only after the corresponding matching conditions are verified.

One residual space and one coupled metric. The four entries of (914) are the extended master curvature, an admissible controlled drift displacement, the score relative to the Gibbs reference, and a finite-test hydrodynamic generator defect. Their reference scales make the entries dimensionally commensurate. The operator $\mathbb{B}_{0,a,N}$ denotes the control map, not the field-space metric $\mathbb{G}$; Ψ remains the matter field, while $\mathcal{G}^{\mathrm{term}}_{a,N}$ is the terminal cost. The coordinate densities ρ and π_θ are both relative to $\mathrm{d}x$, as in (888).

With $q = \langle \mathfrak{R}, \mathbb{H}_{a,N}\mathfrak{R}\rangle$, the lower bound in (916) gives

$$\varphi_\kappa(q) \geq \frac{q}{4} \geq \frac{h_-}{4} \sum_{i\in\{\mathrm{F,u,th,NS}\}} \|\mathfrak{R}_i\|^2, \qquad \kappa \geq 0. \tag{1432}$$

The first inequality follows from $e^z \geq 1 + z$ for $z \geq 0$, with equality at $\kappa = 0$. Thus a single running integrand controls every declared channel. Allowed cross blocks generate mixed responses and must satisfy the positivity and representation conditions in (918). At $\kappa = 0$, a block-diagonal metric gives an algebraic sum of channel norms. It does not imply independent dynamics if the entries, diagonal blocks, probability law, terminal cost, or constraints depend on shared variables. Conversely, nonadditivity alone does not establish a unique microscopic model or a new physical law.

The curvature channel is not itself an Euler residual. Its norm is varied to obtain the master field equations; setting the entire curvature vector to zero would impose a separate flatness restriction. The independently established low-energy field branch is summarized in (980). Compatibility with an optimizer of the joint objective requires the additional field, terminal, and induced-law conditions associated with (981). An optimization over u and ρ does not replace a coframe variation.

Full variation and the relative-entropy direction. The state- and law-dependent metric contributes both $D_x\mathbb{H}[\xi]$ and $D_\rho\mathbb{H}[\eta]$ to the pointwise variation (938). At a fixed Eulerian state point, the score variation is $D_\rho\nabla\log(\rho/\pi_\theta)[\eta] = \nabla(\eta/\rho)$

when the reference is fixed. Variation of the reference density or gradient operator requires its additional derivative.

The pointwise differential is not the full variation of the expectation. The Eulerian formula (940) includes the change of density multiplying the running and terminal costs, with η constrained by (939). The alternative strong-path formula (945) includes the state response once under a fixed Wiener realization. A likelihood representation instead includes the canonical-path likelihood score. These are alternative descriptions of the same response where their hypotheses hold; adding a likelihood contribution to a strong-state contribution for the same perturbation can double-count it. Passing to a fixed reference measure changes the representation of the response rather than removing it.

For a comparison with the same initial law and diffusion covariance, put $v_t = \mathbb{B}_{0,a,N}(X_t)u_t$. On the admissible covariance range, the minimal noise lift and the true-martingale, measurability, uniqueness, and finite-energy conditions in (934) give

$$\frac{1}{4}\,\mathbb{E}^{\mathbb{P}^u}\int_0^T v_t^{\mathsf{T}}\mathbb{M}^{\dagger}v_t\,\mathrm{d}t = \theta D_{\mathrm{KL}}(\mathbb{P}^u\|\mathbb{P}^0). \tag{1433}$$

This equality is recovered from the isolated quadratic control channel only when $H_{\mathrm{u}}/\ell_{\mathrm{u}}^2$ is calibrated to $\mathbb{M}^{\dagger}$ on that range. An arbitrary noise lift with an unobservable kernel component need not give equality for state-path entropy. Nor does the complete coupled objective generally equal a pure KL cost. The identity therefore identifies an existing direction of the joint norm; it does not authorize appending a second independent KL penalty. For the conservative finite-regulator implementation used for calibration, the recommended baseline is therefore $\kappa = 0$, together with a sector-preserving positive metric that contains only representation-allowed nonzero cross blocks and the separately declared low-energy matching conditions. This choice requires square integrability rather than the exponential integrability needed for $\kappa > 0$, while retaining genuine bilinear coupling whenever an admissible cross block is present. The $\kappa > 0$ family remains a legitimate nonlinear extension, but it requires the additional exponential bounds in (926) and its Euler–Bellman equations must be interpreted with the factor $\varphi_\kappa'(q) = e^{\kappa q}/4$.

Gibbs calibration and the thermodynamic balance. The dissipative drift must be matched to the chosen reference; operator skewness and positivity alone do not provide this match. In coordinate notation, let $\nu(\mathrm{d}x) = m(x)\mathrm{d}x$, $\theta > 0$, and define

$$\begin{gathered}(\beta_m)_i = m^{-1}\partial_j(m\mathbb{M}_{ij}), \quad b_{\mathrm{th}} = \theta\beta_m + \theta\mathbb{M}\nabla\log(\pi_\theta/m),\\ \nabla\cdot(\pi_\theta b_{\mathrm{rev}}) = 0.\end{gathered} \tag{1434}$$

For the grand reference in (986), the logarithm is

$$\log(\pi_\theta/m) = s - E/\theta - \log Z_\theta, \qquad \mathcal{S}_{\mathrm{M}} = E - \theta s + C_\theta. \tag{1435}$$

The second identity is the additional matching condition for this normalized reference to coincide with the master-action Gibbs law; C_θ is independent of the state and cancels on normalization. Under that identification, $\pi_\theta \propto m\exp(-\mathcal{S}_{\mathrm{M}}/\theta)$ gives $b_{\mathrm{th}} = -\mathbb{M}\nabla\mathcal{S}_{\mathrm{M}} + \theta\beta_m$. The last line is the invariant-density condition on the reversible transport, with the corresponding boundary condition. Under the integration-by-parts hypotheses of (991), put $g_\rho = \log(\rho/\pi_\theta)$, $h = f_{\mathrm{ext}} + \mathbb{B}_{0,a,N}u$, and $\mathcal{F}_\theta = \theta D_{\mathrm{KL}}(\rho\|\pi_\theta)$. Then

$$\begin{aligned} J_{\mathrm{irr}} = -\theta\rho\mathbb{M}\nabla g_\rho, \quad \frac{\mathrm{d}}{\mathrm{d}t}\mathcal{F}_\theta(\rho_t) &= -\theta^2\int \rho_t(\nabla g_{\rho_t})^{\mathsf{T}}\mathbb{M}\nabla g_{\rho_t}\,\mathrm{d}x \\ &\quad +\theta\int \rho_t h\cdot\nabla g_{\rho_t}\,\mathrm{d}x. \end{aligned} \tag{1436}$$

Here J_{irr} denotes the calibrated thermal current, not the whole driven probability current. The first contribution is nonpositive, whereas the drive contribution has no universal sign. The latter is initially a relative-free-energy input, not automatically mechanical work. Physical entropy production requires the reservoir and local-detailed-balance conditions of Section 4.10, together with the time calibration in (1021). In particular, an open subsystem need not have increasing Shannon entropy. Equilibrium attraction also needs a convergence argument beyond Gibbs invariance. A closed GENERIC interpretation imposes the additional Poisson and degeneracy conditions stated in the nonequilibrium section; it is not identical to every canonical Gibbs gradient diffusion.

The controlled hydrodynamic interface. For a hydrodynamic projection $U_t^N = \Pi_{\mathrm{NS}}^{a,N}(X_t)$, reference-generator matching proves an uncontrolled branch only. Let $w = w(t,U)$ be an admissible fluid feedback and define $\mathcal{L}_N^{\mathrm{NS},w}F = \mathcal{L}_N^{\mathrm{NS}}F + \langle G_N w, \nabla F\rangle_H$. The controlled branch additionally requires

$$\mathcal{L}_{a,N}^{u}(F\circ\Pi_{\mathrm{NS}}^{a,N}) = (\mathcal{L}_N^{\mathrm{NS},w}F)\circ\Pi_{\mathrm{NS}}^{a,N} \tag{1437}$$

on a determining core, together with matching initial laws and well-posed martingale problems. In particular, the induced control displacement must descend as $D\Pi_{\mathrm{NS}}^{a,N}\mathbb{B}_{0,a,N}u = G_N w(t,\Pi_{\mathrm{NS}}^{a,N}(x))$, and the noise covariance and Itô projection drift must match. The fluid feedback must be adapted to its declared information filtration. Agreement on finitely many tests is only a finite generator diagnostic.

The target in (906) is the uncontrolled generator $\mathcal{L}_N^{\mathrm{NS}}$, whereas (1437) uses $\mathcal{L}_N^{\mathrm{NS},w}$. Under the latter matching,

$$r_{\mathrm{NS},\alpha}^{a,N;u}(t,x) = \langle G_N w(t,U), \nabla F_\alpha(U)\rangle_H, \qquad U = \Pi_{\mathrm{NS}}^{a,N}(x). \tag{1438}$$

Thus the original joint channel need not vanish on a controlled fluid branch. A diagnostic relative to that controlled target must instead subtract $\mathcal{L}_N^{\mathrm{NS},w}F_\alpha$ in the defect definition. Choosing this target changes the declared residual and

hence the optimization problem; it is not an implicit redefinition of the original joint objective.

Once this interface is established, the finite solenoidal process obeys

$$\mathrm{d}U_t^N = [-\nu_{\mathrm{v}} A_N U_t^N - B_N(U_t^N, U_t^N) + f_N + G_N w_t]\,\mathrm{d}t + \sqrt{2\theta Q_N}\,\mathrm{d}W_t^N. \tag{1439}$$

The cancellation in (1002) and Itô's formula give, with $E_N = \|U^N\|_H^2/2$,

$$\begin{aligned}\mathrm{d}E_N = {} & \big[-\nu_{\mathrm{v}}\|A_N^{1/2}U_t^N\|_H^2 + \langle f_N + G_N w_t, U_t^N\rangle_H + \theta\,\mathrm{Tr}\,Q_N\big]\,\mathrm{d}t \\ & + \sqrt{2\theta}\langle Q_N^{1/2}U_t^N, \mathrm{d}W_t^N\rangle_H.\end{aligned} \tag{1440}$$

For controls satisfying the stated moment and martingale-integrability conditions, noise injects mean resolved energy, viscosity removes it, and convection redistributes it among modes without changing the total. The conditional microscopic–macroscopic bridge is this projection and balance structure, not an identification of classical Wiener noise with quantum fluctuations. The numerical realization in Section 13.7.2 tests the declared finite fluid equation; it does not independently verify a microscopic generator match or an unregulated turbulent cascade.

This synthesis belongs in Paper I because it specifies how the common architecture links the five-paper programme. Paper III develops the thermodynamic and hydrodynamic branch in greater detail, including transport closure, invariant measures, stress selection, and numerical comparisons. The division of material changes neither the hypotheses nor the status of the field, quantum, and continuum completion problems.

32.2. *Logical status of the five-paper programme.* The breadth of the construction makes it important to state the logical status of each implication before comparing different sectors. We use four labels throughout this paper. A *proved theorem* is a consequence of the displayed hypotheses on the stated regulated or finite-dimensional domain. A *conditional theorem* is a theorem whose conclusion follows once an explicitly listed matching, regularity, representation, or scale assumption is imposed. An *explicit regulated realization* is a fully specified lattice, finite-mode, or otherwise cut-off model; its result is exact for that regulator and is not silently promoted to a continuum statement. An *open completion criterion* is a precise additional statement needed for a regulator-independent, quantum-complete, or parameter-free theory; it is not asserted here.

proved theorem | conditional theorem
explicit regulated realization | open completion criterion

(1441)

With this convention, the finite-dimensional variational identities, Girsanov formula under its range and integrability assumptions, the Fokker–Planck and free-energy identities, the coercivity and full first variation of the joint objective in Propositions 50 and 53, and the classical CHSH obstruction are proved results on their stated finite-regulator domains. The definition of the joint objective is exact once its metric, channel maps, and admissible density class have been supplied; existence of an optimizer is not inferred from that definition. The lattice equilibrium and finite Galerkin constructions are explicit regulated realizations. The density-space Bellman equation (978) is conditional on a dynamic programming and differentiability theory. The Einstein–Yang–Mills equations remain the independent matched field branch (980); the joint objective does not derive them. Equation (981) is only a noncontamination condition for the added channels. Joint field stationarity would additionally require the localization or static-embedding and law-adjoint conditions stated after that equation. The Einstein–Yang–Mills recovery in Theorem 9, the restricted family-count statement in Theorem 16, and the Euclidean-to- Lorentzian route are conditional theorems. A regulator-independent four-dimensional Yang–Mills mass gap, a turbulent continuum limit with universal intermittency exponents, a unique group and parameter selection, and a noncommutative quantum completion are open completion criteria. In particular, none of these last statements is changed into a proved result by adding the same symbols to the master action.

32.3. *Completion boundary and conditional solvability.* The four logical labels above determine the strongest claim supported by the present construction. The programme establishes one regulated variational–stochastic architecture and derives its finite-regulator identities. It also supplies conditional interfaces to low-energy gravity, gauge theory, matter, thermodynamics, turbulence, quantum reconstruction, and cosmology. The displayed residual spaces, measures, projections, and hypotheses specify the inputs used by each result. They do not turn every interface into a parameter-free fundamental theory.

The established implication has the form

$$\begin{gathered}\text{declared regulated data and analytic hypotheses}\\ \text{with specified matching and projection assumptions} \Longrightarrow\\ \text{finite-regulator identities and conditional effective branches.}\end{gathered} \tag{1442}$$

The limitation is expressed by the nonimplication

$$\begin{gathered}\text{one master functional} \not\Longrightarrow\\ \text{unique group, all masses, or quantum gravity}\\ \text{and does not by itself imply empirical confirmation.}\end{gathered} \tag{1443}$$

Additional physical and mathematical arguments are needed for each of these conclusions.

Within the present programme, the following can be completed rigorously on the stated domains: the common configuration and joint residual metric; the regulated stochastic law, Gibbs reference, Fokker–Planck equation, free-energy identity, and path-space entropy-production formula; the finite Galerkin injection–transfer–dissipation balance; the classical Bell obstruction; the conditional Einstein–Yang–Mills and matter interfaces; the declared 331 anomaly, flavor, and threshold relations; and the conditional cosmological, dark-sector, fifth-force, and tabletop relations. The associated simulations verify the displayed regulated algorithms and identities, not external observations.

The following conclusions are conditional rather than unconditional: ordinary Einstein and canonical Yang–Mills recovery; inertial–gravitational mass equality in the universally coupled tensor sector; the 331 family mechanism; macroscopic convergence to a Gibbs law; structured-collapse diagnostics; and ultralight-scalar dark matter. Each requires the matching, regularity, representation, boundary, constitutive, or calibration hypotheses stated in the relevant theorem. These assumptions define the physical domain of the result; they are not hidden proofs of uniqueness.

Several completion tasks require genuinely new mathematics, microscopic data, or independent experiments and cannot be obtained merely by adding pages. They include a regulator-independent four-dimensional Yang–Mills mass gap, unique selection of $SU(3)_c$, G_{331}, three families, and all charges, first-principles values of all masses and mixing parameters, a complete quantum-gravity construction, a global continuum theorem for three- dimensional turbulence, black-hole singularity avoidance, and a derivation of the observed cosmological constant or dark-matter identity. These are stated as open completion criteria rather than completed claims.

A conditional result has scientific content when its premises can be specified and investigated independently of its conclusion. Analytic premises include non-explosion, regularity, integrability, and boundary estimates. Physical premises include the field content, universal metric coupling, reservoir identification, observable projection, and conversion from stochastic to physical time. Resolving the former does not establish the latter. In particular, assuming that a projected generator is the Navier–Stokes generator yields a compatibility result, not an independent derivation of Navier–Stokes dynamics. Assuming a desired low-energy action as matching data likewise does not uniquely select that action.

For a completion based on a regulator limit, estimates must be expressed in fixed physical units and shown to survive the prescribed limit. A positive gap at each cutoff does not suffice if the gap tends to zero. Conversely, an

independently established uniform connected-correlation decay bound, together with reconstruction, a unique vacuum, and a dense family of centered observable states, gives the conditional spectral-gap implication in Proposition 47. The uniform decay bound remains a separate nonperturbative task; replacing it by the assertion that the desired continuum gap is positive would only restate the conclusion.

The five-paper series therefore formulates a *computable and falsifiable unified research programme*: one regulated variational architecture supports conditional physical interfaces with independently specified inputs and observable consequences. The distinction between finite-regulator identities, effective physical branches, and continuum completion problems remains essential throughout.

32.4. *Interfaces among the five companion papers.* The material is organized as a five-paper sequence without duplicating logical claims. Paper I contains the master configuration, action, path-space cost, equilibrium theory, and the conditional low-energy Einstein–Yang–Mills projection. Its output to the other papers is the regulated law (893), the equilibrium reference measure (986), and the matching data that are held fixed when a sector is studied in isolation. Paper II contains the chiral 331 realization: global-group and anomaly analyses, the scalar breaking chain, flavor and seesaw maps, and threshold matching. It must treat the group, representations, and Yukawa coefficients as inputs unless the selection problem of Section 6.1 has independently selected them. At a matching scale $\mu \simeq v_\chi$, its color output is passed to the pure-glue sector of Paper I through the effective action

$$\Gamma_{\mathrm{eff}}^{(c)}[A_c;\mu] = \frac{1}{4g_c^2(\mu)} \int F^a_{c\,\mu\nu} F_c^{a\,\mu\nu}\, \mathrm{d}^4x + \sum_i c_i(\mu)\, \mathcal{O}_i[A_c]. \tag{1444}$$

The coefficients in (1444) include the threshold effects of the heavy 331 fields and must be computed in one declared renormalization scheme. This interface does not prove the Yang–Mills mass gap or fix the absolute value of g_c.

Paper III isolates the nonequilibrium extension developed in Section 13.1. It contains the reversible–irreversible decomposition, entropy production, external-work balance, and the finite Galerkin stochastic Navier–Stokes branch. Its finite-regulator identities are exact at fixed (a, N, T). Its two-dimensional periodic, fixed-viscosity, additive trace-class-noise branch additionally proves a stationary Galerkin limit, uniqueness in law for a prescribed initial distribution, and the exact stationary injection–dissipation equality. An explicit small-control cost estimate removes both the drift residual and its mean work when the separate uniform moment bounds hold. This does not establish uniqueness of the invariant law, a three-dimensional regularity theorem, or a universal inviscid cascade; those remain different completion questions.

Paper IV takes the gauge-invariant Euclidean observables and regulated measures of Paper I as input. It is responsible for regulator removal, reflection positivity, Osterwalder–Schrader or direct Lorentzian reconstruction, physical local or relational algebras, Born instruments, entanglement, and Bell observables. Classical filtering and shared noise from Papers I and III are not substitutes for this reconstruction. A fully specified nearest-neighbour free scalar branch provides a positive finite-time-lattice measure, a positive transfer operator, its explicit Hamiltonian spectrum, and the ordinary massive free-field continuum limit. This constructive example demonstrates that a reconstruction route can be completed in a declared branch; it does not establish the same positivity or limit for the coupled interacting master action.

Paper V studies cosmological and dark-sector solutions of the matched effective equations. It must solve the background and perturbation systems, include the vacuum-curvature balance (295), propagate threshold and initial-data uncertainties, and confront independently calibrated predictions with cosmological and laboratory data. Dark matter, dark energy, inflation, and singularity avoidance are not inherited merely from the common action. Its laboratory interface includes whitening and projection away from independently calibrated environmental response directions. The projected scalar covariance amplitude is identifiable precisely when its response has a nonzero component outside that nuisance span. Independent Gaussian segments then yield an exact gamma sampling law, power function, and a conservative threshold for bounded Gaussian calibration leakage. Without the response and sampling assumptions, coherent cross-channel fluctuations do not constitute a scalar detection.

The five interfaces are directional. Paper II supplies matched chiral and color data to Paper I; Paper III supplies a hydrodynamic projection and constitutive tests for its regulated law; Paper IV tests whether the gauge-invariant Euclidean output admits a positive quantum reconstruction; and Paper V receives the renormalized effective equations and states needed for cosmology. Paper I supplies the common action, reference measure, and logical status of each input. A result proved in one regulated sector is not automatically a theorem about another sector or the unregulated unified theory.

32.5. *Conclusion.* The finite uncertainty and response calculations add a common practical lesson. A calibrated law predicts an unused response only through a specified observation map. The fourth-corner relation tests that map without a new fit; the radial residual bounds separate numerical error from a large physical response; and the memory example determines when a discarded variable changes a measurable second moment. In the financial realization, the same discipline separates a unique entropy minimizer from a price uniquely implied by the traded assets. These results give concrete

targets for independent physical and economic comparison while leaving the reference-law and microscopic matching assumptions visible.

The programme connects geometry, probability and variational selection through explicit operations on shared dynamical data. Its finite models show how a common mechanism can produce different effective structures once the state space, growth or observation weights, and constraints are specified. The field results establish conditional recovery and identification statements for a regulated realization. Their physical content lies in relations between observables obtained with the same inputs. Coefficient identification within a fixed action basis is distinct from selecting that basis, its quantum realization and its physical parameters. This distinction also determines which experiments can test the programme without waiting for every open microscopic problem to be resolved.

Appendix S makes the gravitational comparison concrete. It verifies exact Einstein critical points of the constant-weight Cartan sector under independent coframe and connection variations, and computes a sharp quadratic response bound from the actual coefficient ratio. The same ratio exposes a reflection-positivity obstruction to extrapolating the torsionless four-derivative kernel into a quantum completion. A separate construction removes the spatial ultraviolet cutoff in the free two-polarization sector. Propositions 162 and 163 further construct spatially varying initial data satisfying the nonlinear Einstein constraints and a stochastic sampling law that preserves them. The calculated Itô correction shows why tangent noise alone fails. These results establish specific classical and free quantum branches; the full mother constraint algebra, physical evolution of the nonlinear family, and an interacting positive continuum theory remain to be constructed.

The new identifiability calculation makes the empirical boundary equally explicit. The two-source squared-signal map is locally rank two but ill-conditioned for the archived stellar responses, and an admissible common matter derivative changes the unused third prediction while leaving the two calibration charges fixed. The eccentric-orbit calculation sums all open massive-scalar harmonics and supplies an analytic Bessel tail bound. A matched Bianchi-I Einstein–Λ evolution verifies that the displayed homogeneous constraint family has a physical-time realization. These are reproducible conditional results; they do not establish a mother-selected charge, a fifth-force detection, or a full Lorentzian evolution of the independent-connection theory.

Section 5.8 connects this geometric origin to a quantitative comparison with canonical gauge dynamics. Its residual identity retains both the gradient and normalization errors of a variable kinetic coefficient. The finite examples separate resolution error, physical correction and stability, while the limiting argument states the regularity and source convergence it uses. A further

Lorentzian recovery theorem must establish the hyperbolic reduction and constraint propagation needed for its time-dependent energy estimate.

The finite quantum test in Appendix AB turns a prescribed kinetic branch and coherent preparation into a joint spectral–Bell prediction with two frozen calibration inputs. That relation has not been measured. A separate comparison of released Bell runs has a positive predictive-score difference against the calibrated full local polytope, but the quantum benchmark fails a more sensitive absolute-fit diagnostic under its working assumptions. Neither result selects a unique physical mother coupling or validates all sectors of the programme. Appendix AC further resolves the published count conventions and constructs a positive source-and-readout family. Seven parameters account for much of the within-run discrepancy, but their transfer between runs remains unfavorable. This distinguishes an observation-model improvement from independent physical confirmation.

The common-origin bridge in Section X supplies an exact test connecting a master Gibbs energy to its selected stochastic drift. It retains boundary compatibility, separates relaxation from path irreversibility, and quantifies the information and dynamical defects of a physical projection. Together with the Schwarzschild curvature calculation, these relations distinguish a closed regulated realization from a local gravitational or quantum completion. The next step is to derive its remaining coefficients and observation map independently and test an unused observable with those values fixed.

The common architecture has physical content when its shared inputs impose relations that survive independent observation. It does not acquire that content merely by collecting established equations. The score derivatives in Appendix J identify the missing selection data, while the companion transport and laboratory analyses specify how a previously fixed branch can be tested without adjusting its response coefficients to the validation data.

The framework places Cartan geometry, internal gauge fields, matter, order parameters, thermodynamic variables, and a regulated hydrodynamic projection in one variational–stochastic data package. The Einstein and Yang–Mills equations arise as conditional low-energy components of the master Euler system, whereas the Fokker–Planck, entropy-production, HJB, and finite Galerkin Navier–Stokes equations have distinct roles within the same regulated dynamics. The joint residual functional organizes these channels and their permitted cross responses; it does not erase their constraint, projection, or limiting hypotheses.

The common-weight stellar calculation adds a constraint on the same logic of recovery and prediction. Its exact canonical map fixes the conformal slope, while its matter exchange law retains the explicit scalar derivative of the Jordan energy density. A coercive scalar operator gives a residual-to-observable

bound; a nearly neutral mode requires a separate stability analysis. Combining a justified source bound with the minimal mass relation yields the analytic circular-dipole envelope in Proposition 111. For the declared trace responses and common stellar scale caps, even its maximized signal is far below the quoted binary summary errors. This identifies a limitation of that branch and those channels, while leaving a clear task for microscopic matter matching and frequency-dependent response calculations. Within a specified two-source response truncation, Proposition 106 eliminates the common coefficients and gives two possible third-binary signals. An additional density response preserves the first two calibrations while changing the third. The resulting error bound states which microscopic response projections must be controlled before this conditional relation becomes a physical prediction. The laboratory relation in (2069) requires a different set of inputs: coherence, environmental memory and an independently checked observation map. It provides a test of joint records beyond a matched decay envelope. Future work should compare its complete acquisition and calibration costs with attainable instrument precision, freeze its target protocol, and seek independent replication. Such a test would establish the scope of that branch; a distinctive confirmation of the mother construction would require additional shared restrictions across physical sectors.

The orbital calculation in Section 14.39 gives one explicit chain from the Cartan norm to the physical metric and timelike orbit. On the scalar-decoupled, vacuum-matched branch the derived spherical solution produces the standard leading Mercury advance with prescribed solar and orbital inputs. The quadratic curvature term is checked in the field equation rather than removed by hand. Retaining the original cosmological term or the common scalar slope changes the calculation and requires the corresponding matching and source data.

The analysis of time separates deterministic invertibility, kinematic time-reversal covariance, stationary path-law reversibility, and physical entropy production. Neither a vanishing diffusion coefficient nor a vanishing drift determines the arrow. Path-space relative entropy, parity, reservoirs, boundary and initial data, and observation scale do. The data-processing result (152) further shows that an exact filter cannot manufacture irreversibility from a reversible master law.

In the tensor matter branch, the common effective action gives the sequence

$$\begin{aligned} &\Gamma^{(2)}_{\mathrm{phys}} \longrightarrow M_{\mathrm{pole}} \longrightarrow g^{\mu\nu}\partial_\mu S \partial_\nu S + M^2_{\mathrm{pole}} = 0 \\ &\longrightarrow \text{geodesic propagation}, \frac{\delta \Gamma_{\mathrm{m}}}{\delta g^{\mu\nu}} \longrightarrow T_{\mu\nu} \longrightarrow \text{coframe response}. \end{aligned} \tag{1445}$$

This chain explains inertial motion and tensor gravitational charge as two responses of the same selected excitation. It also specifies what remains: the physical mass numbers require a non-circular solution of (279); strong Machian

closure requires (288); and the small observed vacuum curvature requires a radiatively stable solution of (295), not merely minimization of a potential.

The proposed control representation of confinement, the topology-switching QVI, and the information-filtering interface are correspondingly precise research criteria. Confinement still requires a gauge-invariant continuum area law or the appropriate physical-state statement; a QVI does not equate a value-function singularity with a spacetime singularity; and filtering becomes holographic only when a recovery map satisfying (863) exists. Quantum gravity likewise requires a positive physical state space, anomaly-free constraint closure, relational observables, and causal Lorentzian response. These distinctions leave the proved finite-regulator results intact while identifying the exact equations that a fundamental completion must still solve.

Black-hole collapse boundary. The common variational–stochastic structure does not, by itself, imply that a black hole must collapse uniformly, must collapse non-uniformly, or must avoid a singularity. Spherical collapse remains an admissible idealized sector, while nonspherical perturbations, angular momentum, radiation, and horizon boundary conditions require a separate dynamical analysis. A claim that the selected evolution approaches a regular or non-uniform black-hole state would require a constrained perturbation theorem, a causal horizon flux law, and regulator-uniform estimates of the type (869). In their absence, the present paper makes no black-hole collapse prediction; its topology-switching construction is a regulated research extension rather than a solution of gravitational collapse or singularity resolution.

32.6. *Relation to entropic-force proposals.* The framework shares with entropic-force proposals the idea that a macroscopic force may be an effective response of unobserved degrees of freedom, but it does not assume the identity

$$F_{\mathrm{ent}} = T\,\frac{\partial S_{\mathrm{coarse}}}{\partial q} \tag{1446}$$

or holographic equipartition as a microscopic axiom. A coarse-grained force can be defined only after an observable map, a state function, and a thermodynamic coordinate have been declared. In the present notation its candidate reversible response is obtained from the reduced effective potential and the calibrated current, while the irreversible response is the mobility-weighted score in (991). Identifying the two with the right-hand side of (1446) requires a local-equilibrium and thermodynamic-coordinate matching assumption. Consequently, the present programme is a joint minimum-cost stochastic construction, not a derivation of a holographic entropic force; conversely, an entropic-force postulate does not imply the joint residual metric, the HJB control problem, or the finite regulator path identities. This distinction is consistent with the

original entropic-gravity proposal [157] and makes the physical comparison explicit without treating either framework as a completed quantum theory.

32.7. *A regulated diagnostic for structured collapse.* The preceding boundary statement admits a finite perturbation test, but stability, noise-driven fluctuations, and nonlinear collapse must be distinguished. On a declared spherical regulated branch, expand a physically normalized perturbation as

$$\delta\Phi(t,\Omega)=\sum_{\ell,m} a_{\ell m}(t)u_{\ell m}(\Omega), \qquad \ddot{a}_{\ell m}+\gamma_{\ell m}\dot{a}_{\ell m}+\lambda_{\ell m}a_{\ell m}=\sigma_{\ell m}\dot{W}_{\ell m}. \tag{1447}$$

The displayed scalar equations describe a special inertial branch: a positive kinetic form, a compatible damping/noise closure, and an independent modal reduction must be supplied after gauge and constraint reduction. A generic Hessian–mobility diffusion instead gives a first-order system; rotation and shear can couple its modes. The general matrix dynamics and their exact covariance are derived in Appendix I. The amplitude ratio

$$\mathcal{A}(t)=\frac{\max_{\ell\geq 2,m}|a_{\ell m}(t)|}{|a_{00}(t)|+\varepsilon}, \qquad \varepsilon>0. \tag{1448}$$

is a descriptive feature, not a calibrated test: its numerator depends on the angular basis and its denominator can become small. For a complete orthonormal multiplet the rotation-invariant angular power is

$$P_\ell(t)=\sum_{m=-\ell}^{\ell}|a_{\ell m}(t)|^2. \tag{1449}$$

Even when $\lambda_{\ell m},\gamma_{\ell m}>0$, persistent noise gives nonzero stationary power. Positive long-time fluctuation amplitudes therefore do not establish a coherent anisotropic instability. The appropriate test compares P_ℓ, growth rates, and temporal spectra with a declared noise baseline and finite-sample uncertainty; a uniform probability law need not consist of pointwise uniform configurations. Appendix I proves the required finite energy, covariance, rotation, and error-probability statements.

Near-horizon accretion is a distinct, generally nonspherical transport application. Its principal fluid interface belongs to the companion paper on nonequilibrium thermodynamics and turbulence: physical conservation, magnetic constraints, causal constitutive response, and horizon flux must precede comparison with a GRMHD baseline [76] and [133]. The cosmological companion separately treats population formation, radiative response, and selection for early-galaxy observations [37]. Neither interface follows from a modal amplitude ratio. No present finite perturbation calculation proves horizon formation, singularity avoidance, a continuum collapse theorem, improved accretion simulation, or an explanation of the observed early-galaxy population.

Appendix A. Variation of the master curvature

The calculation below fixes the coframe, and hence g and vol_g, while varying only the isotropy-connection components of the Cartan field. The matter fields and the information parameter are also fixed. Let $b : \mathfrak{g} \to \mathfrak{g}^*$ be the symmetric map defined by $b(X)(Y) = h(X, Y)$, and assume in this calculation that the curvature pairing is Hodge-compatible and covariantly constant. The allowed variation is $\delta\mathbb{A} = \iota_{\mathfrak{h}}(\delta a)$, where $\delta a \in \Omega^1(M, \mathrm{ad}\, P_H)$. No variation of the translational coframe is included. Assume either that M is closed or that the boundary conditions eliminate boundary terms. For $\mathfrak{g}$-valued forms α, β, set

$$\langle \alpha, \beta \rangle_{\mathfrak{g},g}\, \mathrm{vol}_g = \langle b(\alpha) \wedge \star\beta \rangle = h_{IJ}\alpha^I \wedge \star\beta^J. \tag{1450}$$

The brackets on the right pair $\mathfrak{g}^*$ with $\mathfrak{g}$; the map b must be retained even if an orthonormal basis later makes its matrix the identity. Define the formal adjoint by the standard sign convention

$$\int_M \langle \alpha, \mathbb{D}\eta \rangle_{\mathfrak{g},g}\, \mathrm{vol}_g = \int_M \langle \mathbb{D}^*\alpha, \eta \rangle_{\mathfrak{g},g}\, \mathrm{vol}_g \tag{1451}$$

for every compactly supported test form η. For two-forms in four Euclidean dimensions, the corresponding local identity is $\mathbb{D}^*\alpha = \star^{-1}\mathbb{D}(\star\alpha)$, with the understanding that b commutes with $\mathbb{D}$ under the stated invariance hypothesis.

For an allowed infinitesimal connection variation, the curvature identity and the first variation of the 1/4-normalized curvature action are

$$\begin{aligned} \delta_a\mathbb{F} = \mathbb{D}\iota_{\mathfrak{h}}(\delta a), \quad \delta_a\mathcal{S}_{\mathrm{curv}} &= \frac{1}{2}\int_M \langle \mathbb{F}, \mathbb{D}\iota_{\mathfrak{h}}(\delta a) \rangle_{\mathfrak{g},g}\, \mathrm{vol}_g \\ &= \int_M \left\langle \frac{1}{2} b(\star\mathbb{F}) \wedge \mathbb{D}\iota_{\mathfrak{h}}(\delta a) \right\rangle . \end{aligned} \tag{1452}$$

Thus the curvature momentum, as a coadjoint-valued two-form, is

$$\mathbb{P}_{\mathrm{curv}} = \frac{1}{2} b(\star\mathbb{F}). \tag{1453}$$

Using (1451), or integrating the final line of (1452) by parts, gives the two equivalent expressions

$$\delta_a\mathcal{S}_{\mathrm{curv}} = \frac{1}{2}\int_M \langle \mathbb{D}^*\mathbb{F}, \iota_{\mathfrak{h}}(\delta a) \rangle_{\mathfrak{g},g}\, \mathrm{vol}_g = -\int_M \langle \mathbb{D}\mathbb{P}_{\mathrm{curv}} \wedge \iota_{\mathfrak{h}}(\delta a) \rangle . \tag{1454}$$

The signs agree because a three-form and a one-form anticommute under the wedge product. In the source-free curvature theory, stationarity therefore implies

$$\iota_{\mathfrak{h}}^* b(\mathbb{D}^*\mathbb{F}) = 0, \qquad \text{equivalently} \qquad \iota_{\mathfrak{h}}^* \mathbb{D}\big(b(\star\mathbb{F})\big) = 0. \tag{1455}$$

The unrestricted equation $\mathbb{D}^*\mathbb{F} = 0$ would require independent variations in every $\mathfrak{g}$ direction while keeping the Hodge operator fixed; varying the

translational Cartan component changes the coframe and does not meet that condition.

In the extended action, covariant derivatives and any other explicit connection dependence add a coadjoint-valued three-form current $\mathbb{J}_{\mathrm{ext}}$, with the sign fixed by (171). A gauge-invariant algebraic potential $\mathfrak{U}_H(\Phi_H, \sigma)$ and a fixed, field-independent information source $\mathfrak{I}(\mu_{\mathrm{info}})$ contribute no such current. The general fixed-coframe connection equation is

$$\iota_{\mathfrak{h}}^*(\mathbb{D}\mathbb{P} - \mathbb{J}_{\mathrm{ext}}) = 0, \qquad \mathbb{P} = \frac{\partial \mathcal{L}_{\mathrm{M}}}{\partial \mathbb{F}}. \tag{1456}$$

Both $\mathbb{D}\mathbb{P}$ and $\mathbb{J}_{\mathrm{ext}}$ are coadjoint-valued three-forms before restriction, so this equation is type-consistent. For the isolated curvature action in (1452), it reads

$$\iota_{\mathfrak{h}}^* \left[\frac{1}{2} \mathbb{D}\big(b(\star\mathbb{F})\big) - \mathbb{J}_{\mathrm{ext}} \right] = 0. \tag{1457}$$

No factor of two has been transferred to the source. Applying $\star^{-1}$ gives the corresponding one-form equation $\iota_{\mathfrak{h}}^*[\frac{1}{2} b(\mathbb{D}^*\mathbb{F}) - \star^{-1}\mathbb{J}_{\mathrm{ext}}] = 0$. The internal Yang–Mills term in (310) has the different normalization $\frac{1}{2}\int \widehat{\kappa}_{AB} F^A \wedge \star F^B$; its curvature momentum is consequently $\widehat{\kappa}_{AB} \star F^B$, exactly as used in Section 5.6. If a reduced curvature pairing is not Hodge-compatible, $\mathbb{P}$ in (1456) remains the fiber derivative of the full local density rather than a multiple of $\star\mathbb{F}$. The independent coframe variation, including changes of $\star_e$ and vol_{g_e}, is treated in Section 5.1; it cannot be supplied by the fixed-coframe equation in this appendix.

Appendix B. Proof of the Gibbs identity

Let ν be the reference measure from Section 4.1, assume $0 < Z < \infty$, and let p be a normalized density with $p \ll p_*$. First suppose that the action and entropy integrals at both p and p_* are finite, so that no subtraction of infinities occurs. Let

$$p_* = Z^{-1} e^{-\mathcal{S}_{\mathrm{M}}/\theta}. \tag{1458}$$

Then

$$\log \frac{p}{p_*} = \log p + \frac{\mathcal{S}_{\mathrm{M}}}{\theta} + \log Z. \tag{1459}$$

Multiplication by θp and integration gives

$$\theta\, \mathrm{KL}(p \| p_*) = \theta \int p \log p \, \nu(\mathrm{d}\mathbb{X}) + \int p \mathcal{S}_{\mathrm{M}} \, \nu(\mathrm{d}\mathbb{X}) + \theta \log Z. \tag{1460}$$

To evaluate the value at equilibrium, insert $\log p_* = -\mathcal{S}_{\mathrm{M}}/\theta - \log Z$ into the entropy integral. The stated integrability permits cancellation of the action

terms:

$$\begin{aligned}\mathcal{F}[p_*] &= \int p_* \mathcal{S}_{\mathrm{M}} \,\mathrm{d}\nu + \theta \int p_* \left(-\frac{\mathcal{S}_{\mathrm{M}}}{\theta} - \log Z\right) \mathrm{d}\nu \\ &= -\theta \log Z \int p_* \,\mathrm{d}\nu = -\theta \log Z.\end{aligned} \tag{1461}$$

we obtain

$$\mathcal{F}[p] - \mathcal{F}[p_*] = \theta \,\mathrm{KL}(p\|p_*). \tag{1462}$$

For general densities, use the extended-real definition

$$\mathcal{F}[p] := \theta \,\mathrm{KL}(p\|p_*) - \theta \log Z. \tag{1463}$$

It agrees with the action-plus-entropy expression wherever those separate integrals are defined. This definition never interprets $+\infty - \infty$ as a number, and it retains uniqueness of the minimizer because $\mathrm{KL}(p\|p_*) = 0$ holds precisely for $p = p_*$. More explicitly, writing $r = p/p_*$ converts the relative entropy into the integral of $r \log r - r + 1$ against the equilibrium probability. This integrand is nonnegative and vanishes only at one, as used in (95). This argument remains valid when the relative entropy is infinite and avoids subtracting two infinite action-plus-entropy values. Thus the finite-integral identity and its extended version have the same minimizer for precisely stated reasons.

Appendix C. Girsanov representation of the cost

Let

$$\mathrm{d}X_t = b(X_t)\mathrm{d}t + \boldsymbol{\sigma}(X_t)\mathrm{d}W_t, \qquad \boldsymbol{\sigma}\boldsymbol{\sigma}^* = 2\theta\widehat{\mathbb{M}}. \tag{1464}$$

Let a controlled process with the same initial law satisfy

$$\mathrm{d}X_t^u = b(X_t^u)\mathrm{d}t + v_t\mathrm{d}t + \boldsymbol{\sigma}(X_t^u)\mathrm{d}W_t^u. \tag{1465}$$

Assume v_t lies in the range of $\boldsymbol{\sigma}$, $\mathbb{E}^u \int_0^T \|\boldsymbol{\sigma}^\dagger v_t\|^2 \mathrm{d}t < \infty$, and, under the reference law, $\mathbb{E}^0 \exp\{\frac{1}{2}\int_0^T \|\boldsymbol{\sigma}^\dagger v_t\|^2 \mathrm{d}t\} < \infty$ (Novikov's condition). Assume also that the realization is finite dimensional, or that $\boldsymbol{\sigma}$ has closed range so that its Moore–Penrose inverse is well defined on the relevant range. Let $\boldsymbol{\sigma}^\dagger$ denote this inverse and choose the minimum-norm control

$$u_t = \boldsymbol{\sigma}^\dagger v_t. \tag{1466}$$

The drift increment v_t is assumed to be a progressively measurable functional of the canonical state path in its own completed filtration under both laws; otherwise the two weak solutions cannot be identified by the displayed Radon–Nikodym density without an additional law-identification argument. Let W denote the Brownian motion under the reference law $\mathbb{P}^0$. Under the tilted law, $W_t^u := W_t - \int_0^t u_s \,\mathrm{d}s$ is Brownian. Girsanov's theorem then gives

$$\frac{\mathrm{d}\mathbb{P}^u}{\mathrm{d}\mathbb{P}^0} = \exp\left(\int_0^T \langle u_t, \mathrm{d}W_t\rangle - \frac{1}{2}\int_0^T \|u_t\|^2 \,\mathrm{d}t\right). \tag{1467}$$

Here W in the stochastic exponential is the reference Brownian motion under $\mathbb{P}^0$. Under the controlled law, $W_t^u = W_t - \int_0^t u_s \, \mathrm{d}s$ is Brownian, so substitution into the logarithm of the preceding density gives

$$\log \frac{\mathrm{d}\mathbb{P}^u}{\mathrm{d}\mathbb{P}^0} = \int_0^T \langle u_t, \mathrm{d}W_t^u \rangle + \frac{1}{2} \int_0^T \|u_t\|^2 \, \mathrm{d}t. \tag{1468}$$

The first term has zero $\mathbb{P}^u$-expectation by square integrability. Consequently,

$$\mathrm{KL}(\mathbb{P}^u \| \mathbb{P}^0) = \frac{1}{2} \mathbb{E}^u \int_0^T \|u_t\|^2 \, \mathrm{d}t. \tag{1469}$$

Since $\boldsymbol{\sigma}\boldsymbol{\sigma}^* = 2\theta\widehat{\mathbb{M}}$,

$$\frac{1}{2} \|u_t\|^2 = \frac{1}{4\theta} \|v_t\|^2_{\widehat{\mathbb{M}}^\dagger}, \tag{1470}$$

where $\widehat{\mathbb{M}}^\dagger$ is the Moore–Penrose inverse on the tangent mobility range and coincides with $\widehat{\mathbb{M}}^{-1}$ in the strictly positive case. This identity uses, on $\operatorname{Ran} \boldsymbol{\sigma}$, the Moore–Penrose relation

$$(\boldsymbol{\sigma}\boldsymbol{\sigma}^*)^\dagger = (\boldsymbol{\sigma}^\dagger)^* \boldsymbol{\sigma}^\dagger, \tag{1471}$$

together with $\boldsymbol{\sigma}\boldsymbol{\sigma}^* = 2\theta\widehat{\mathbb{M}}$. To justify that this is entropy of state-path laws, let $N_t = X_t - X_0 - \int_0^t b(X_s) \, \mathrm{d}s$ be the canonical martingale under the reference law. Put $a = \boldsymbol{\sigma}\boldsymbol{\sigma}^*$. In finite dimension (or under the stated closed-range assumptions), $\widehat{u} = \boldsymbol{\sigma}^* a^\dagger v$, and

$$\int_0^T \langle \widehat{u}_t, \mathrm{d}W_t \rangle = \int_0^T \langle a^\dagger(X_t) v_t, \mathrm{d}N_t \rangle. \tag{1472}$$

The equality follows from $\mathrm{d}N = \boldsymbol{\sigma} \mathrm{d}W$. Both the stochastic integral on the right and its quadratic variation are measurable in the canonical state path. Thus its exponential is a state-path Radon–Nikodym derivative. Uniqueness in law for the controlled martingale problem identifies the tilted law with the stated controlled law, proving (73). With additional unobserved randomization one must instead use the projection inequality (74).

Appendix D. Heat-kernel convention

For a Laplace-type operator

$$L = -(g^{\mu\nu} \nabla_\mu \nabla_\nu + E), \tag{1473}$$

the heat kernel is defined by

$$(\partial_t + L) K(t; x, y) = 0, \qquad K(0; x, y) = \delta(x, y) \, \mathrm{Id}\,. \tag{1474}$$

On a smooth closed four-manifold,

$$\mathrm{Tr}(e^{-tL}) \sim (4\pi t)^{-2} \sum_{k \geq 0} t^k A_{2k}(L), \tag{1475}$$

with

$$A_{2k}(L) = \int_M \operatorname{tr}(a_{2k}(x, L))\,\mathrm{vol}_g\,. \tag{1476}$$

With the convention (341), the first coefficients used in the main text are

$$a_0 = \mathrm{Id}, \tag{1477}$$

$$a_2 = E + \frac{1}{6} R\,\mathrm{Id}, \tag{1478}$$

$$\begin{aligned} a_4 = \frac{1}{360}\Big[&60\nabla^\mu\nabla_\mu E + 60RE + 180E^2 + 30\Omega_{\mu\nu}\Omega^{\mu\nu} \\ &+ \big(12\Box R + 5R^2 - 2R_{\mu\nu}R^{\mu\nu} + 2R_{\mu\nu\rho\sigma}R^{\mu\nu\rho\sigma}\big)\,\mathrm{Id}\Big]. \end{aligned} \tag{1479}$$

Here $\Omega_{\mu\nu} = [\nabla_\mu, \nabla_\nu]$, and the displayed derivatives are local coefficients; their integrals are boundary terms on a closed manifold. The formula is unchanged only after all sign conventions for the Laplacian, curvature, and bundle connection have been fixed. The convention is stated explicitly because sign differences in E, the Riemann tensor, and the Laplacian change the displayed coefficients. A numerical calculation in the master model must use one convention consistently from the operator definition through renormalization.

Appendix E. Dimensions, normalization, and covariance under changes of units

A change of units must preserve the probability law of the physical observables and the ordering of admissible controls. This requirement is stronger than checking that a single sum is well typed: the drift, diffusion, reference density, observation maps, and endpoint costs must all be transformed together. This appendix fixes those transformations on a finite regulator. It makes no identification of regulator time with laboratory time and no assertion about a continuum limit.

E.1. *Action, energy, and the entropy convention.* Write E, T_{s}, and T_{L} for energy, stochastic-time, and Lorentzian-time units, respectively. An action has units $\mathsf{E}\mathsf{T}_{\mathrm{L}}$. The normalization (58) separates three objects:

$$\begin{aligned} [\mathcal{I}_{\mathrm{M}}] = [I_{\mathrm{ref}}] = \mathsf{E}\mathsf{T}_{\mathrm{L}}, \qquad \overline{S}_{\mathrm{M}} = \mathcal{I}_{\mathrm{M}}/I_{\mathrm{ref}}, \\ U_{\mathrm{M}} = E_{\mathrm{ref}}\overline{S}_{\mathrm{M}} \equiv \mathcal{S}_{\mathrm{M}}, \qquad [U_{\mathrm{M}}] = [\theta] = \mathsf{E}. \end{aligned} \tag{1480}$$

The barred action is dimensionless. Throughout the dimensional stochastic formulas, $\mathcal{S}_{\mathrm{M}}$ denotes the energy-normalized version. Consequently $\exp(-U_{\mathrm{M}}/\theta) = \exp(-\overline{S}_{\mathrm{M}}/\overline{\theta})$, where $\overline{\theta} = \theta/E_{\mathrm{ref}}$. A density relative to a dimensional reference volume has the reciprocal volume units; its ratio to another density relative to the same volume is dimensionless. No logarithm of an unspecified dimensional density is used in the KL identities.

The state entropy s is dimensionless. On a calibrated thermal branch, $s = S_{\mathrm{phys}}/k_{\mathrm{B}}$ and $\theta = k_{\mathrm{B}}T_{\mathrm{bath}}$, so that $\theta s = T_{\mathrm{bath}}S_{\mathrm{phys}}$. The matching condition $U_{\mathrm{M}} = E - \theta s + C_\theta$ therefore has energy units in every term. A thermal interpretation of θ is a calibration condition; a change of units does not establish that interpretation.

In natural units $\hbar = c = 1$, let mdim denote mass dimension. Then $\mathrm{mdim}(x^\mu) = -1$, $\mathrm{mdim}(\partial_\mu) = 1$, and $\mathrm{mdim}(\mathrm{d}^4x) = -4$. The physical action has mass dimension zero, while an energy-normalized U_{M} has mass dimension one. Natural units do not identify these two quantities. With dimensionless coframe components $e^a{}_\mu$, the one-form $e^a = e^a{}_\mu \mathrm{d}x^\mu$ has dimension -1, and the reference length ℓ has dimension -1. Thus $\ell^{-1}e^a$ and the connection one-form have dimension zero; curvature components have dimension two. The Einstein coefficient satisfies

$$\mathrm{mdim}(G^{-1}) = 2. \tag{1481}$$

Four-dimensional gauge couplings have mass dimension zero.

Reference scales in the extended curvature are not all physical lengths. For example, before any field rescaling, a canonically normalized scalar Φ_H has mass dimension one, so $D_\mu\Phi_H$ has dimension two, whereas $\partial_\mu\sigma$ has dimension one when σ is dimensionless. To compare both with curvature components of dimension two, the multiplying factors must have dimensions zero and one, respectively. A canonical spinor has dimension $3/2$, so the factor applied to $D_\mu\Psi$ would have dimension $-1/2$ in that particular component normalization. This dimensional observation does not construct a first-order Dirac action from a second-order norm; the separate fermionic requirements stated after (51) remain in force. Equivalently, the conversion factors may be assigned to the blocks of $\mathbf{h}$. A realization must specify one of these equivalent conventions, including all mixed blocks, before identifying its coefficients with physical couplings.

E.2. *Component units of the finite-regulator equation.* Let $[X_i] = \mathsf{Q}_i$; different state components may have different units. With $[E] = [\theta] = \mathsf{E}$ and $[s] = 1$, the coordinate coefficients in the dimensional stochastic equation have the units

$$\begin{aligned} [L_{ij}] = [M_{ij}] &= \frac{\mathsf{Q}_i\mathsf{Q}_j}{\mathsf{E}\mathsf{T}_{\mathrm{s}}}, \quad [\partial_j E] = \frac{\mathsf{E}}{\mathsf{Q}_j}, \\ [b_i] = [f_i] = [(B_0 u)_i] &= \frac{\mathsf{Q}_i}{\mathsf{T}_{\mathrm{s}}}, \qquad [\beta_{m,i}] = \frac{\mathsf{Q}_i}{\mathsf{E}\mathsf{T}_{\mathrm{s}}}, \\ [\Sigma_{i\alpha}] &= \frac{\mathsf{Q}_i}{\sqrt{\mathsf{T}_{\mathrm{s}}}}, \quad [\mathrm{d}W_\alpha] = \sqrt{\mathsf{T}_{\mathrm{s}}}. \end{aligned} \tag{1482}$$

Here M denotes the cotangent-to-tangent coordinate mobility, not an endomorphism obtained without the field-space metric. A factor $\Sigma\Sigma^{\mathsf{T}} = 2\theta M$ is used

for the noise. The notation $\sqrt{2\theta M}$ is understood in normalized coordinates or with the declared metric and noise frame. A Euclidean matrix square root in mixed physical coordinates need not transform as the chosen factor Σ.

For example,

$$[M_{ij}\partial_j U_{\mathrm{M}}\,\mathrm{d}t_{\mathrm{s}}] = \mathsf{Q}_i, \qquad [\Sigma_{i\alpha}\,\mathrm{d}W_\alpha] = \mathsf{Q}_i. \tag{1483}$$

The same calculation applies to $L\nabla E$, $\theta M\nabla s$, and $\theta\beta_m$. Indeed, $\beta_{m,i} = m^{-1}\partial_j(mM_{ij})$ has the units of M_{ij}/X_j; the reference density cancels in this expression. The Gibbs exponent $s - E/\theta$ and the density ratio ρ/π are dimensionless.

E.3. *A complete change of state, energy, and time units.* Fix positive constant scales $x_{i,\mathrm{ref}}$, E_{ref}, and t_{ref}, and put

$$D = \mathrm{diag}(x_{1,\mathrm{ref}}, \dots, x_{d,\mathrm{ref}}), \qquad X = Dy, \qquad t_{\mathrm{s}} = t_{\mathrm{ref}}\tau. \tag{1484}$$

Thus D is constant and invertible. Bars in this subsection distinguish dimensionless objects from their dimensional counterparts. Define

$$\begin{aligned} &\bar{E}(y) = E(Dy)/E_{\mathrm{ref}}, \qquad \bar{s}(y) = s(Dy), \qquad \bar{\theta} = \theta/E_{\mathrm{ref}}, \\ &\bar{m}(y) = (\det D)m(Dy), \quad \bar{\rho}_\tau(y) = (\det D)\rho_{t_{\mathrm{ref}}\tau}(Dy), \quad \bar{\pi}(y) = (\det D)\pi(Dy). \end{aligned} \tag{1485}$$

The transformation of m pushes forward the same reference measure; its overall normalization has no effect on β_m. The required coefficient transformations are

$$\begin{aligned} \bar{M}(y) = t_{\mathrm{ref}}E_{\mathrm{ref}}D^{-1}M(Dy)D^{-\mathsf{T}}, \quad \bar{L}(y) = t_{\mathrm{ref}}E_{\mathrm{ref}}D^{-1}L(Dy)D^{-\mathsf{T}}, \\ \bar{\Sigma}(y) = \sqrt{t_{\mathrm{ref}}}D^{-1}\Sigma(Dy), \quad \bar{f}(y) = t_{\mathrm{ref}}D^{-1}f(Dy). \end{aligned} \tag{1486}$$

If $u = A_{\mathrm{ref}}\bar{u}$ for a positive diagonal control-scale map, put $\bar{B}_0(y) = t_{\mathrm{ref}}D^{-1}B_0(Dy)A_{\mathrm{ref}}$. The controls, their admissible sets and their filtrations are transported by this deterministic state and time change.

Proposition 126 (Covariance under a fixed change of units). *Suppose the finite-regulator Itô equation is well posed on the declared domain, with C^1 mobility and positive C^1 reference density. Use the coefficient conventions above and transform its boundary and initial conditions by* (1484). *Then $Y_\tau = D^{-1}X_{t_{\mathrm{ref}}\tau}$ satisfies the same form of stochastic equation in barred variables. In particular,*

$$\bar{\beta}_{\bar{m}}(y) = t_{\mathrm{ref}}E_{\mathrm{ref}}D^{-1}\beta_m(Dy), \qquad \bar{\Sigma}\bar{\Sigma}^{\mathsf{T}} = 2\bar{\theta}\bar{M}. \tag{1487}$$

For a smooth test F, the corresponding generators obey

$$\bar{\mathcal{L}}^{\bar{u}}_\tau(F \circ D)(y) = t_{\mathrm{ref}}(\mathcal{L}^u_{t_{\mathrm{ref}}\tau}F)(Dy). \tag{1488}$$

Consequently a change of units preserves the physical law of every transformed observable.

Proof. The energy and entropy derivatives transform as $\nabla_y \bar{E} = D^{\mathsf{T}} \nabla_X E / E_{\mathrm{ref}}$ and $\nabla_y \bar{s} = D^{\mathsf{T}} \nabla_X s$. Substitution into (1486) therefore multiplies each deterministic transport term by $t_{\mathrm{ref}} D^{-1}$. In components,

$$\begin{aligned}(\bar{\beta}_{\bar{m}})_i &= \frac{1}{(\det D) m(Dy)} \sum_j \partial_{y_j} \left[\frac{(\det D) t_{\mathrm{ref}} E_{\mathrm{ref}}}{x_{i,\mathrm{ref}} x_{j,\mathrm{ref}}} m(Dy) M_{ij}(Dy) \right] \\ &= \frac{t_{\mathrm{ref}} E_{\mathrm{ref}}}{x_{i,\mathrm{ref}}} (\beta_m)_i(Dy).\end{aligned} \tag{1489}$$

Brownian scaling gives $\bar{W}_\tau = t_{\mathrm{ref}}^{-1/2} W_{t_{\mathrm{ref}}\tau}$, a standard Wiener process. The linear change of state has no Itô Hessian term, so the noise factor is exactly $\bar{\Sigma}$ above. Its covariance identity follows by matrix multiplication. The gradient and Hessian chain rules now give (1488); well-posedness identifies the transformed law. This proof concerns constant unit changes. A nonlinear coordinate transformation requires its own Itô correction. □

Positive semidefiniteness and skewness survive these congruences. If $M \nabla E = 0$ and $L \nabla s = 0$, the corresponding barred identities hold as well. If a Poisson structure is present, a constant coordinate change and constant bracket rescaling preserve its Jacobi identity. The proposition does not infer a Poisson structure from skewness.

E.4. *Path costs, entropy decay, and optimal-control ordering.* The density Jacobians cancel in the likelihood ratio. Hence

$$\bar{g}(y) := \log(\bar{\rho}/\bar{\pi})(y) = g(Dy), \qquad \nabla_y \bar{g} = D^{\mathsf{T}} \nabla_X g, \qquad \mathrm{KL}(\bar{\rho} \| \bar{\pi}) = \mathrm{KL}(\rho \| \pi). \tag{1490}$$

The invertible state and time map on path space also preserves path KL. For positive definite M, writing $\bar{v} = t_{\mathrm{ref}} D^{-1} v$ gives

$$\frac{1}{4\bar{\theta}} \int_0^{T/t_{\mathrm{ref}}} \bar{v}^{\mathsf{T}} \bar{M}^{-1} \bar{v} \, \mathrm{d}\tau = \frac{1}{4\theta} \int_0^T v^{\mathsf{T}} M^{-1} v \, \mathrm{d}t_{\mathrm{s}}. \tag{1491}$$

Indeed, the quadratic form before time integration is multiplied by $t_{\mathrm{ref}}/E_{\mathrm{ref}}$, and $(\bar{\theta}, \mathrm{d}\tau) = (\theta/E_{\mathrm{ref}}, \mathrm{d}t_{\mathrm{s}}/t_{\mathrm{ref}})$. This is a dimensionless cost. The same equality holds after expectation under the corresponding controlled laws. Its identification with path KL uses the separate Girsanov hypotheses, including the common initial law.

For a degenerate mobility, do not replace the ordinary inverse in this proof by an unproved tensor transformation rule for a Moore–Penrose inverse. Instead use the covariance factor. At every accessible drift,

$$\frac{1}{2} \inf_{\Sigma h = v} |h|^2, \qquad \bar{\Sigma} \bar{h} = \bar{v} \iff \Sigma \bar{h} = \sqrt{t_{\mathrm{ref}}} v. \tag{1492}$$

The minimum control energy per unit barred time is t_{ref} times the original value. Its time integral is unchanged. An inaccessible drift remains inaccessible

and has infinite cost. This proof does not assume that the pseudoinverse itself transforms by congruence; that operator identity is generally false.

The weighted Fisher quantity $\mathcal{I}_M(\rho) = \int \rho(\nabla g)^{\mathsf{T}} M \nabla g \, \mathrm{d}X$ has units $(\mathsf{ET}_{\mathrm{s}})^{-1}$. The transformations above give

$$\overline{\mathcal{I}} = t_{\mathrm{ref}} E_{\mathrm{ref}} \mathcal{I}_M, \qquad \overline{\mathcal{F}} = \mathcal{F}/E_{\mathrm{ref}}, \qquad \frac{\mathrm{d}\overline{\mathcal{F}}}{\mathrm{d}\tau} = \frac{t_{\mathrm{ref}}}{E_{\mathrm{ref}}} \frac{\mathrm{d}\mathcal{F}}{\mathrm{d}t_{\mathrm{s}}}. \tag{1493}$$

Thus $\mathrm{d}\mathcal{F}/\mathrm{d}t_{\mathrm{s}} = -\theta^2 \mathcal{I}_M$ has energy-per-time units and transforms to the same barred identity. Its analytic and boundary hypotheses are those of Theorem 57.

Let ℓ_{dim} be an energy rate and G_{dim} an endpoint energy. Then

$$\bar{\ell} = \frac{t_{\mathrm{ref}}}{E_{\mathrm{ref}}} \ell_{\mathrm{dim}}, \qquad \bar{G} = G_{\mathrm{dim}}/E_{\mathrm{ref}}, \qquad \bar{J} = J_{\mathrm{dim}}/E_{\mathrm{ref}}. \tag{1494}$$

Together with path-KL invariance, this proves that the baseline objective and every admissible control comparison transform by the same positive factor. The infimum and every attained minimizer therefore correspond under the change of units. This conclusion does not prove attainment. For an ergodic problem, $\bar{\lambda} = t_{\mathrm{ref}} \lambda / E_{\mathrm{ref}}$, while $\bar{V} = V/E_{\mathrm{ref}}$. In particular, the compatibility equation (1054) contains only energy rates on its right-hand side, and its completed-square selector transforms consistently.

E.5. *Units of the four joint channels.* An unnormalized control displacement has units $\mathsf{Q}_i/\mathsf{T}_{\mathrm{s}}$, a score component has units Q_i^{-1}, and a generator defect for an observable F_α has units $[F_\alpha]/\mathsf{T}_{\mathrm{s}}$. The curvature block has its own field and spatial units. These quantities cannot be added using arbitrary dimensionless cross weights before normalization.

Let r collect these dimensional components, and let C_{ch} be a constant invertible block normalization whose columns carry the corresponding component units. Put

$$R = C_{\mathrm{ch}}^{-1} r, \qquad q = R^{\mathsf{T}} H R = r^{\mathsf{T}} K r, \qquad K = C_{\mathrm{ch}}^{-\mathsf{T}} H C_{\mathrm{ch}}^{-1}. \tag{1495}$$

Here R, H, q are dimensionless. Each entry of K has reciprocal units of the two residual components it pairs. A change of numerical component units $r' = Ar$ must be accompanied by $C'_{\mathrm{ch}} = AC_{\mathrm{ch}}$; then $R' = R$ and $q' = q$, with the state and law arguments of H transported by the same map. Equivalently $K' = A^{-\mathsf{T}} K A^{-1}$. This includes all cross blocks. Changing a channel scale without this corresponding metric change changes the relative physical weighting and is a model modification.

For a dimensional observation scale $F_{\alpha,\mathrm{ref}}$, the dimensionless test is $\bar{F}_\alpha = F_\alpha/F_{\alpha,\mathrm{ref}}$ composed with the state map. Equation (1488) then makes the normalized projection defect

$$\bar{r}_\alpha = \frac{t_{\mathrm{ref}}}{F_{\alpha,\mathrm{ref}}} r_\alpha. \tag{1496}$$

The target generator, target state coordinates, and projection must be transformed in the same manner. A scalar ℓ_{NS} suffices only after the observable components have been made commensurate.

Since q is dimensionless, κ is dimensionless and the exponential in φ_κ is defined. The dimensional restoration (924) supplies a cost rate $C_{\mathrm{ref}}\varphi_\kappa(q)/t_{\mathrm{ref}}$ and a terminal cost $C_{\mathrm{ref}}\mathcal{G}^{\mathrm{term}}$. It therefore preserves the ordering of admissible controls when the normalization, dynamics and horizon are transformed together. The exponential integrability conditions are still required; dimensional consistency does not imply them.

E.6. *An exactly soluble fluctuation–dissipation example.* For a scalar coordinate of unit Q, let $U(x) = kx^2/2$, $[k] = \mathsf{E}/\mathsf{Q}^2$, and $[\mu] = \mathsf{Q}^2/(\mathsf{E}\mathsf{T}_{\mathrm{s}})$. The equation

$$\mathrm{d}X = -\mu k X\,\mathrm{d}t_{\mathrm{s}} + \sqrt{2\theta\mu}\,\mathrm{d}W, \qquad X_0 = x_0, \tag{1497}$$

has mean and variance

$$\mathbb{E}X_T = x_0 e^{-\mu k T}, \qquad \mathrm{Var}(X_T) = \frac{\theta}{k}(1 - e^{-2\mu k T}). \tag{1498}$$

The relaxation time $(\mu k)^{-1}$ has stochastic-time units and the stationary variance θ/k has units Q^2. For $X = x_{\mathrm{ref}}Y$, the normalized parameters are

$$\bar{\mu} = \frac{t_{\mathrm{ref}}E_{\mathrm{ref}}}{x_{\mathrm{ref}}^2}\mu, \quad \bar{k} = \frac{x_{\mathrm{ref}}^2}{E_{\mathrm{ref}}}k, \quad \bar{\theta} = \theta/E_{\mathrm{ref}}. \tag{1499}$$

Consequently $\bar{\mu}\bar{k}(T/t_{\mathrm{ref}}) = \mu k T$ and $x_{\mathrm{ref}}^2\bar{\theta}/\bar{k} = \theta/k$. Both the transient law and the stationary variance agree after restoring units. Itô's formula also gives

$$\frac{\mathrm{d}}{\mathrm{d}t_{\mathrm{s}}}\mathbb{E}U(X_t) = -\mu k^2 \mathbb{E}X_t^2 + \theta\mu k. \tag{1500}$$

Every term has energy-rate units. The second term is the fluctuation injection that balances mean dissipation at equilibrium.

For a numerical illustration, prescribe the synthetic reference-unit values $\mu = 0.4$, $k = 1.7$, $\theta = 0.8$, $x_0 = 0.6$, and $T = 2.3$. Independently integrate the normalized moment equations

$$\frac{\mathrm{d}\bar{m}_1}{\mathrm{d}\tau} = -\bar{\mu}\bar{k}\bar{m}_1, \qquad \frac{\mathrm{d}\bar{v}}{\mathrm{d}\tau} = -2\bar{\mu}\bar{k}\bar{v} + 2\bar{\theta}\bar{\mu}, \tag{1501}$$

with initial mean x_0/x_{ref} and variance zero. An adaptive DOP853 integration uses relative tolerance 10^{-11} and absolute tolerances $10^{-13}/x_{\mathrm{ref}}$ for the mean and $10^{-13}/x_{\mathrm{ref}}^2$ for the variance. After restoring units, compare with (1498) at 101 equally spaced reference times. The resulting maximum sampled absolute differences are shown in Table 30. They are numerical discrepancies, not rigorous interval error bounds. The restored terminal mean is approximately 0.1255783234592, and the terminal variance is approximately 0.4499739668981, in all three cases.

Table 30. One prescribed OU model expressed in three sets of reference units. Errors compare restored moments with the dimensional exact solution.

$(x_{\mathrm{ref}}, t_{\mathrm{ref}}, E_{\mathrm{ref}})$	Mean error	Variance error
$(1, 1, 1)$	8.69×10^{-14}	4.71×10^{-12}
$(10^{-2}, 10^{-3}, 4.2)$	9.28×10^{-14}	4.84×10^{-12}
$(10^{3}, 50, 0.02)$	8.34×10^{-14}	4.53×10^{-12}

The calculation tests the explicit conversion of drift, noise intensity, time, and moments. Its inputs are synthetic; it supplies no empirical calibration of a thermal bath or physical clock. Keeping μ unchanged after rescaling the coordinate or time would describe a different model and would not reproduce this agreement.

Appendix F. Joint metrics, physical projections, and the meaning of unification

F.1. *A joint quadratic form is not coordinate-independent nonadditivity.* The declared residual channels correspond to physically different observations and constraints. Their units are fixed by the reference scales ℓ_i. A positive joint metric supplies one quadratic form on this space, but positivity alone does not prove an irreducible physical coupling. Every finite-dimensional positive matrix can be diagonalized after an arbitrary linear change of coordinates. Such a change may mix a curvature observable with a thermodynamic score or a generator defect and therefore destroy the declared physical channel interpretation.

The relevant separation question is consequently restricted to admissible transformations preserving units, symmetry, observables, and the channel partition. For two normalized channels,

$$q(r_1, r_2) = r_1^2 + 2c r_1 r_2 + r_2^2, \qquad H = \begin{pmatrix} 1 & c \\ c & 1 \end{pmatrix}. \tag{1502}$$

Its eigenvalues are $1-c$ and $1+c$; it is positive definite exactly when $|c| < 1$. The substitution $z_\pm = (r_1 \pm r_2)/\sqrt{2}$ makes it diagonal. That algebraic fact does not make the original observable channels independent. Conversely, merely writing the off-diagonal term does not establish a new physical law. The coupling coefficient must come from a symmetry-compatible microscopic construction or matching, and be tested through physical observables.

For $\kappa = 0$, a necessary obstruction to additive separation in the declared variables is a nonzero mixed derivative:

$$\partial_{r_1}\partial_{r_2}\big(q/4\big) = c/2. \tag{1503}$$

If $c \neq 0$, no representation as $f(r_1) + g(r_2)$ exists on an open product domain. This conclusion concerns the declared variables, not all possible coordinate systems. Even when the running cost separates, the state dynamics, shared law, and admissibility constraints can still couple the optimization problem.

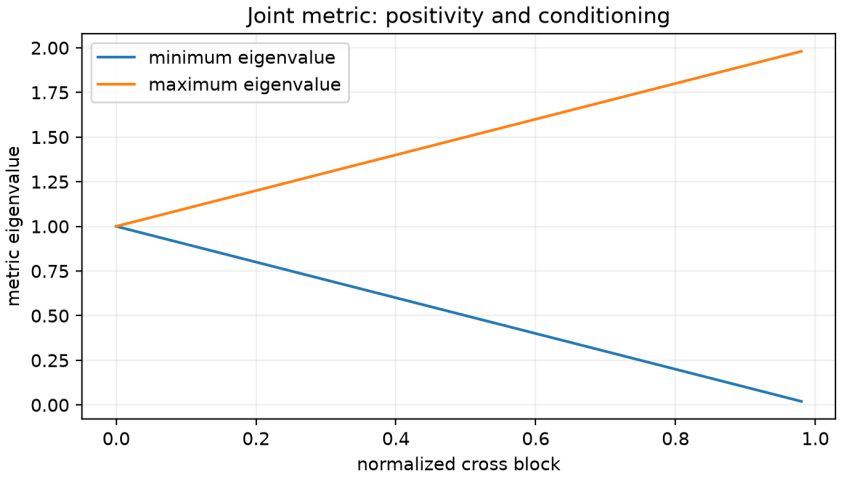


Figure 52. Synthetic two-channel metric. The smallest eigenvalue approaches zero as the normalized cross block approaches its positivity boundary. The example illustrates the Schur-complement requirement and numerical conditioning, not a measured universal coupling.

F.2. *Exponential costs require a genuine exponential moment.* For a centered Gaussian residual R with covariance Σ, and a fixed positive matrix H, write $q = R^{\mathsf{T}}HR$. On the support of Σ, let $K = \Sigma^{1/2}H\Sigma^{1/2}$. Then

$$\mathbb{E}e^{\kappa q} = \det(I - 2\kappa K)^{-1/2} \tag{1504}$$

if $2\kappa\lambda_{\max}(K) < 1$; the expectation is infinite if this condition fails on a positive-variance direction. To prove the formula, write $R = \Sigma^{1/2}Z$, with a standard normal vector Z, and diagonalize K. Orthogonal invariance makes the coordinates independent. Each factor is

$$\frac{1}{\sqrt{2\pi}}\int_{\mathbb{R}} \exp\Big[-\frac{1}{2}(1 - 2\kappa\lambda_j)z^2\Big]\,\mathrm{d}z = (1 - 2\kappa\lambda_j)^{-1/2}. \tag{1505}$$

At zero or negative coefficient of z^2, that integral diverges. Multiplication proves the determinant formula.

Thus even a Gaussian law with every polynomial moment need not admit an arbitrarily large positive κ. This is a concrete reason to retain the quadratic branch when using the established low-energy recovery formulae. It also shows that an exponential transform of a quadratic cost is a different statistical model, not automatically a harmless way to strengthen the same selection principle.

F.3. *Field dependence and the induced statistical measure.* A field-dependent metric has several distinct appearances. In a residual norm its variation contributes $\langle R, (\delta H)R\rangle$. If it is also used to define a configuration-space volume measure, the measure can carry a factor $\sqrt{\det H}$. Its variation is

$$\delta \log \sqrt{\det H} = \frac{1}{2}\operatorname{Tr}(H^{-1}\delta H). \tag{1506}$$

These two terms are not interchangeable. In addition, the probability law changes when the controlled drift changes. The complete weak formulation must vary the density subject to the forward equation, and a path-space formulation must include the change of law under its absolute-continuity conditions. A pointwise residual variation alone is not the total derivative of an expectation under a changing path law.

The mobility, residual metric, and configuration metric need not be the same operator. Identifying them is an additional constitutive choice. Their roles must remain explicit: mobility fixes dissipation and noise, the residual metric weights departures in the objective, and the configuration metric defines geometric derivatives and possibly a reference volume. The notation must not imply an equality that has not been assumed.

F.4. *A generator-matching penalty does not select a unique fluid law.* For a hydrodynamic projection Π, a defect

$$r_F = L(F \circ \Pi) - (L_{\mathrm{NS}}F) \circ \Pi \tag{1507}$$

is a useful compatibility observable once L_{NS} has been declared. Minimizing its square can enforce agreement with that generator on the tested functions. It does not, by itself, derive the Navier–Stokes constitutive law or viscosity from data that contain neither of them. If the target generator is chosen after observing the desired answer, the matching problem has no independent predictive content.

A physical recovery requires the projection, conserved quantities, constitutive coefficients, boundary conditions, and physical clock to be fixed independently of the tested trajectory. Finite test functions verify only their span unless a core or approximation argument extends the identity. This is the interface developed in Paper III. A finite-shell energy transfer identity then follows from the projected generator and incompressibility, but a universal continuum cascade requires additional scale limits and statistical estimates.

F.5. *Equilibrium, the second law, and physical time.* For mobility M, thermal noise covariance $2\theta M$, and an appropriate reference correction, the Gibbs law is invariant. Attraction requires more: irreducibility, confinement, and, for a quantitative rate, a functional inequality or another convergence estimate. A generic feedback drift can destroy detailed balance even when a stationary law still exists. The variational problem must therefore specify which controls preserve equilibrium and which represent external driving.

The path-space relative entropy between a law and its physical reverse is nonnegative. Interpreting it as thermodynamic total entropy requires local detailed balance and reservoir bookkeeping. The system's Shannon entropy can decrease while its total entropy production remains nonnegative. Nonzero reversible Hamiltonian current need not produce entropy; vanishing drift or vanishing diffusion does not independently decide the time arrow. Paper III's parity-aware examples make these distinctions explicit.

Finally, a relaxation time of an auxiliary diffusion is not automatically proper time of the Lorentzian metric. A particle pole mass, a physical Hamiltonian gap, and a stochastic generator decay rate can all have units of inverse time after normalization, but dimensional similarity is not a proof of equality. The observable map and time calibration are part of the physical matching problem.

F.6. *The interfaces among the five physical sectors.* Paper II supplies a specified chiral gauge package and threshold coefficients. These are inputs to the low-energy effective action, not consequences of the norm notation alone. Its Higgs and Yukawa masses require pole matching; its unbroken color sector requires the separate nonperturbative construction. Paper IV supplies the quantum reconstruction conditions and examples of quantum equilibrium states. A normalized classical Gibbs measure is not sufficient for those conditions.

Paper V uses a declared Lorentzian effective branch and follows its cosmological solutions and calibrated laboratory responses. A shared field can constrain different observations through the same coefficients, but does not guarantee a detectable signal, a common temporal spectrum across cosmology and a laboratory, or a unique dark-sector interpretation. The common architecture becomes a physical unification when these interfaces are established by matching and prediction, not merely because all the quantities can be collected into a single residual vector.

Appendix G. Finite-resolution dynamics, calibration, and identifiable predictions

The equilibrium reference specifies the relative statistical weights of configurations. It does not, by itself, specify how rapidly those configurations

are explored. This distinction matters when the same reference is used to discuss field excitations, hydrodynamic transport, and observations made with a physical clock. We first make it explicit in a coupled model with no limiting or closure approximation. We then state what finite observations can determine and what they cannot determine.

G.1. *A coupled equilibrium with an independently variable clock.* Let $x \in \mathbb{R}^d$, let $A = A^T \succ 0$ and $M = M^T \succ 0$, and set

$$E(x) = \tfrac{1}{2} x^T A x, \qquad \pi(x) = Z^{-1} \exp[-E(x)/\theta], \qquad \theta > 0. \tag{1508}$$

For each $c > 0$, consider the Itô diffusion

$$\mathrm{d}X_t = -cMAX_t \,\mathrm{d}t + \sqrt{2c\theta M}\,\mathrm{d}W_t. \tag{1509}$$

Here t is the declared clock. Changing c without changing this clock changes a dynamical input rather than changing the equilibrium reference.

Proposition 127 (Equilibrium does not determine the transport clock). *The diffusion* (1509) *has the unique invariant law* $N(0, C)$*, where* $C = \theta A^{-1}$*, for every* $c > 0$*. Its stationary time correlation and integrated scalar correlation are*

$$C_c(t) = \mathbb{E}[X_t X_0^T] = e^{-cMAt} C, \tag{1510}$$

$$I_c(v) = \int_0^\infty \mathbb{E}[(v^T X_t)(v^T X_0)]\,\mathrm{d}t = \frac{\theta}{c} v^T A^{-1} M^{-1} A^{-1} v. \tag{1511}$$

Thus equal equilibrium statistics do not imply equal correlation times or equal linear-response transport coefficients.

Proof. The matrix MA is similar to the symmetric positive matrix $M^{1/2} A M^{1/2}$, since

$$MA = M^{1/2}(M^{1/2} A M^{1/2}) M^{-1/2}. \tag{1512}$$

Its eigenvalues are positive. Variation of constants gives

$$X_t = e^{-cMAt} X_0 + \int_0^t e^{-cMA(t-s)} \sqrt{2c\theta M}\,\mathrm{d}W_s. \tag{1513}$$

The covariance satisfies the Lyapunov equation

$$\dot{C}_t = -cMAC_t - cC_t AM + 2c\theta M. \tag{1514}$$

Substitution of $C = \theta A^{-1}$ makes the right-hand side zero: both negative terms equal $-c\theta M$. Exponential stability of MA makes the initial mean vanish and the covariance converge to C. The explicit solution also shows convergence in law for deterministic initial data; its transition noise has strictly positive covariance for every positive time. The limiting Gaussian is consequently the unique invariant probability. Multiplying (1513) by X_0^T and averaging

in stationarity gives (1510), because the future stochastic integral has zero covariance with X_0. Finally,

$$\int_0^\infty e^{-cMAt} C \, \mathrm{d}t = (cMA)^{-1}\theta A^{-1} = \frac{\theta}{c} A^{-1} M^{-1} A^{-1}. \tag{1515}$$

Taking its quadratic form proves the assertion. □

The reversible probability current is zero for every c. Indeed, $\nabla\pi = -\theta^{-1}Ax\pi$ cancels the drift current against $-c\theta M\nabla\pi$. This example has fluctuations and relaxation but no stationary irreversible-current entropy production. Starting from a nonstationary density can still decrease relative free energy. These are different statements: a relaxation experiment does not imply a sustained nonequilibrium entropy-production rate at equilibrium.

A Green–Kubo formula uses a physically identified stress or current and a physically calibrated time variable. Equation (1511) therefore describes the clock dependence that such an interface must resolve, not an independently derived viscosity of the complete master field. Neither a Gibbs density nor a Hessian alone identifies a relativistic pole mass. The latter requires the physical kinetic operator, constraints, and the continued two-point function described in the main text.

G.2. *Quantitative local identification and held-out observables.* Choose a finite parameter vector $p \in \mathbb{R}^d$ only after fixing the regulator, units, reference normalization, observable projection, and clock convention. Let $F : U \subset \mathbb{R}^d \to \mathbb{R}^m$ map it to independently calibrated observables. Both parameter and observable norms below use declared dimensionless scales; otherwise the singular values depend on arbitrary choices of units.

Proposition 128 (A finite local identification bound). *Let $\overline{B}(p_0, r) \subset U$ be a convex ball, let F be continuously differentiable there, and suppose that $m \geq d$ and $DF(p_0)$ has full column rank. Define its minimum gain using all parameter directions, and assume that*

$$\|DF(p) - DF(p')\| \leq L\|p - p'\|, \qquad \sigma_0 = \inf_{\|v\|=1} \|DF(p_0)v\| > 0, \qquad Lr \leq \sigma_0/2. \tag{1516}$$

Then for any p, p' in that ball,

$$\|F(p) - F(p')\| \geq \tfrac{1}{2}\sigma_0 \|p - p'\|. \tag{1517}$$

In particular, F is injective there. If $\|F(\widehat{p}) - F(p_*)\| \leq \varepsilon$, then $\|\widehat{p} - p_*\| \leq 2\varepsilon/\sigma_0$.

Proof. Write $J_0 = DF(p_0)$ and let $J_0^\dagger$ be its left pseudoinverse. Full column rank gives $J_0^\dagger J_0 = I$ and $\|J_0^\dagger\| = 1/\sigma_0$. With $h = p - p'$, the segment joining

the two points stays in the ball, and the fundamental theorem of calculus gives

$$F(p) - F(p') = J_0 h + \int_0^1 [DF(p' + sh) - J_0]h \, \mathrm{d}s. \tag{1518}$$

Every point on the segment is at distance at most r from p_0. Multiplication by $J_0^\dagger$ and the triangle inequality give

$$\|h\| \le \frac{\|F(p) - F(p')\|}{\sigma_0} + \frac{Lr}{\sigma_0}\|h\|. \tag{1519}$$

Moving the last term to the left proves the claim. No cancellation estimate for the vector integral is assumed. □

The minimum-gain definition includes null parameter directions. It is not the smallest entry of a reduced rectangular SVD that omits those directions. An underdetermined map, such as $F(p_1, p_2) = p_1$, does not satisfy the assumption even though its one listed singular value is one.

If measured data y satisfy $\|y - F(p_*)\| \le \varepsilon$ and a fit satisfies $\|F(\widehat{p}) - y\| \le \varepsilon$, the appropriate bound is $4\varepsilon/\sigma_0$, not $2\varepsilon/\sigma_0$. For a held-out observable Q with Lipschitz constant L_Q, and a separately bounded theoretical remainder δ_Q, this yields

$$|Q(\widehat{p}) - Q_{\mathrm{physical}}(p_*)| \le \frac{4L_Q\varepsilon}{\sigma_0} + \delta_Q. \tag{1520}$$

The calibration outputs and the held-out output must be distinguished before fitting. Fitting Q itself and then reporting it as a new prediction does not supply an independent test.

If DF instead has constant rank $k < d$ in a neighborhood, the constant-rank theorem gives local level sets of dimension $d - k$. Observationally indistinguishable parameter directions then remain. Even full local rank does not exclude distinct solutions far outside the ball. Identification from observations is also not a derivation of the parameters from a microscopic selection principle.

G.3. *A finite candidate certificate and its physical scope.* Let a candidate class be fixed without using the held-out observation. Suppose each candidate $j \in \{1, \dots, n\}$ has a rigorously enclosed score $s_j \in [\underline{s}_j, \overline{s}_j]$. If

$$\overline{s}_{j_*} < \min_{j \ne j_*} \underline{s}_j, \tag{1521}$$

then j_* is the unique score minimizer in this declared finite class. The proof is the direct chain $s_{j_*} \le \overline{s}_{j_*} < \underline{s}_j \le s_j$ for every competitor. An enclosure must include numerical discretization and optimization errors, not only statistical sampling errors. If intervals overlap, this certificate is inconclusive rather than evidence of a tie. The result does not prove that the candidate class includes nature, nor that it exhausts all physically inequivalent groups or representations.

G.4. *Why the vacuum constant needs a separate physical condition.* On a fixed background with fixed volume V_M, replacing the potential by $V(\phi) + b$ replaces the action by $S + bV_M$. Normalization gives

$$\frac{e^{-(S+bV_M)/\theta}}{\int e^{-(S+bV_M)/\theta}\,\mathrm{d}\nu} = \frac{e^{-S/\theta}}{\int e^{-S/\theta}\,\mathrm{d}\nu}. \tag{1522}$$

The fixed-background normalized Gibbs law, and scalar equations based on V', cannot identify b. For the Lorentzian convention $S_b = -\int \sqrt{-g}\, b\, \mathrm{d}^4x$ and $T_{\mu\nu} = -2(\sqrt{-g})^{-1}\delta S_b/\delta g^{\mu\nu}$,

$$T^{(b)}_{\mu\nu} = -b g_{\mu\nu}, \qquad \Lambda_{\mathrm{eff}} = \Lambda_{\mathrm{bare}} + 8\pi G b. \tag{1523}$$

If geometry is itself integrated over, the volume is generally configuration dependent, and $bV_M[g]$ is not a common additive constant. The cancellation in (1522) then does not apply. Neither case supplies the missing absolute renormalization condition or radiative protection mechanism by itself.

G.5. *Reproducible finite checks and cross-sector consequences.* For a numerical illustration, choose dimensionless data

$$A = \begin{pmatrix} 2 & 0.45 \\ 0.45 & 1.3 \end{pmatrix}, \quad M = \begin{pmatrix} 0.7 & 0.08 \\ 0.08 & 1.1 \end{pmatrix}, \quad \theta = 0.6. \tag{1524}$$

Both matrices are positive definite. The nonzero off-diagonal entry of A produces an equilibrium correlation, while the off-diagonal entry of M also couples dynamical responses. The stationary Pearson coefficient is

$$\mathrm{Corr}(X_1, X_2) = -\frac{0.45}{\sqrt{2(1.3)}}. \tag{1525}$$

The numerical experiment uses exact Gaussian transition pairs, with transition matrix $P_c(t) = e^{-cMAt}$ and innovation covariance

$$Q_c(t) = C - P_c(t) C P_c(t)^T. \tag{1526}$$

The pairs sampled at each declared time are independent replicates; uncertainty bars are the standard errors of their product estimator. There is no Euler time-discretization bias. All samples in this illustration are synthetic and are not measurements of a field, fluid, or cosmological background.

Three physical consequences follow within their stated scope. First, a measured equilibrium cross-correlation can test a declared Hessian but cannot alone identify transport. Second, at independently calibrated clock and temperature, equilibrium and correlation-time measurements jointly constrain mobility. Third, changing a mobility normalization while keeping equilibrium fixed changes dynamic predictions and must not be absorbed into an unreported time recalibration.

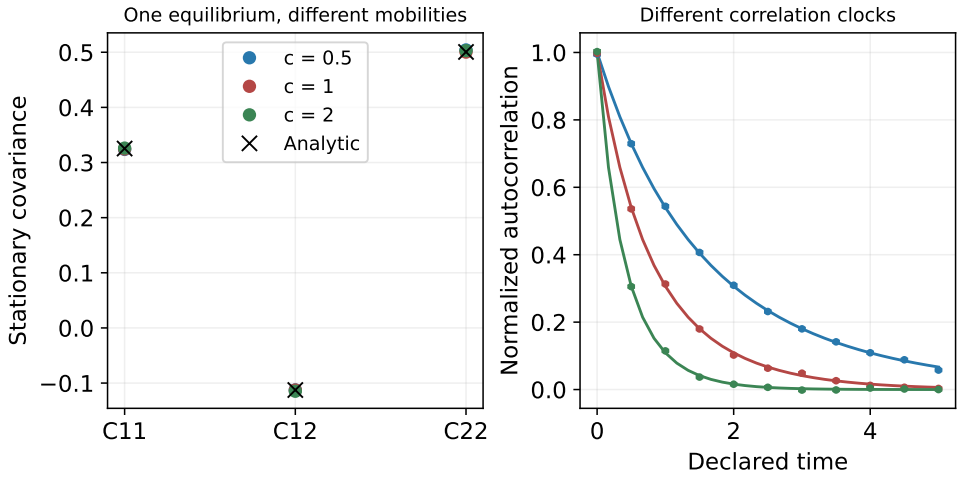


Figure 53. Exact finite coupled-equilibrium benchmark. Left: the stationary covariance is unchanged when the mobility is multiplied by c. Right: correlation decays at different speeds in the same declared clock. Curves are analytic; points with standard errors are independent synthetic Gaussian transition-pair estimates. Equal equilibrium laws therefore do not identify a dynamical clock.

The nonlinear finite bath reduction in Paper III derives damping and noise together for a specified projected momentum model; it supplies a substantive finite realization of part of the transport interface, not an identification of the complete Cartan–matter stress. Paper IV constructs a positive interacting semigroup in its auxiliary time and distinguishes that time from relativistic time. Paper V compares a declared scalar response with an independently published equivalence-principle result. These statements are compatible with (1509): they use a common equilibrium idea but require separate, explicit physical matching data. The present finite-resolution conclusions do not require three-dimensional global smoothness, an inviscid turbulent limit, or universal intermittency exponents. Those results are needed only for stronger claims that invoke them.

Appendix H. Geometric response and independently distinguishing tests

A common microscopic description can explain several responses without making those responses identical. To compare proposed explanations, one must specify the variables, the evolution law, the normalization, and the observations that distinguish the proposals. This appendix gives finite tests

for three potentially misleading shortcuts: replacing a tensor contraction by the product of its magnitudes, inferring action stationarity from zero-mean perturbations, and inferring mass equivalence from causal admissibility alone. The calculations do not introduce a new physical postulate. They specify which additional information an explanation needs.

H.1. *Deterministic trembling geometry and the present programme.* Declercq's trembling-spacetime proposal writes a Lorentzian metric as a smooth background plus a bounded deterministic deformation and interprets inertia as an overlap with a long-wavelength background [56]. This shares the aim of relating local response to global geometry. It differs from the present construction in both its primitive objects and its evolution law. Here the Cartan connection, internal connection, matter, reference measure, and mobility are specified on a regulated configuration space. The resulting stochastic parameter is not automatically Lorentzian proper time. The exact clock nonidentifiability in Proposition 127 makes this distinction operational rather than terminological.

The two quantum routes also differ. Section 10.7 of [56] allows the hidden-variable law to depend on the measurement settings. The classical Bell statement of this paper retains measurement independence; a quantum extension instead needs observables and states not supplied by classical conditioning. Furthermore, Appendix J.2 of [56] does not vary the complete metric to obtain Einstein field equations. Its worldline reduction is therefore a different claim from the matched coframe and connection variation considered here. Neither a shared geometric motivation nor a worldline limit establishes equivalence of the two microscopic programmes.

H.2. *Tensor alignment is independent of spatial homogeneity.* Let V be a finite-dimensional real inner-product space of physical polarizations, after constraints and gauge reduction. For tensor sources $J_1, J_2 : \Sigma \to V$, define

$$B(J_1, J_2) = \int_\Sigma \langle J_1(x), J_2(x)\rangle \, \mathrm{d}\mu(x), \qquad B_{\mathrm{mag}} = \int_\Sigma \|J_1(x)\|\|J_2(x)\| \, \mathrm{d}\mu(x). \tag{1527}$$

Assume the sources are measurable and both integrals are finite. Define $\widehat{J}_i = J_i/\|J_i\|$ where $J_i \neq 0$, and set $\widehat{J}_i = 0$ at its zeros. Where both sources are nonzero, put $c = \langle \widehat{J}_1, \widehat{J}_2\rangle$; the weight vanishes elsewhere.

Proposition 129 (The independent polarization error). *The exact discrepancy is*

$$B_{\mathrm{mag}} - B = \frac{1}{2}\int_\Sigma \|J_1\|\|J_2\|\|\widehat{J}_1 - \widehat{J}_2\|^2 \, \mathrm{d}\mu. \tag{1528}$$

If the unit-polarization difference is at most ε on the weighted support, then

$$0 \le B_{\mathrm{mag}} - B \le \tfrac{1}{2}\varepsilon^2 B_{\mathrm{mag}}. \tag{1529}$$

Spatial homogeneity of J_2 alone supplies no such estimate, even if both tensors are symmetric and tracefree.

Proof. For unit vectors, $\|\widehat{J}_1 - \widehat{J}_2\|^2 = 2 - 2c$. Multiplication by the nonnegative weight and integration gives the identity and bound. For the last assertion, use the Frobenius inner product and the constant tracefree symmetric matrices

$$A = \operatorname{diag}(1, -1, 0), \qquad B = \operatorname{diag}(1, 1, -2), \qquad A : B = 0, \quad \|A\|\|B\| = \sqrt{12}. \tag{1530}$$

Take $\Sigma = \mathbb{R}^3$ with Lebesgue measure, $J_1 = fA$ and $J_2 = B$, where $f \in C_c(\mathbb{R}^3)$ is nonnegative and not identically zero. Continuity makes f positive on a set of positive measure, so $B_{\mathrm{mag}} = \sqrt{12} \int f > 0$, whereas $B(J_1, J_2) = 0$. The background is exactly homogeneous. There is no spatial gradient that can bound this difference. □

Consequently, a scalar-envelope reduction of a tensor interaction must retain polarization or prove an alignment mechanism separately. A norm product is also not a bilinear functional on an unrestricted vector space: changing the sign of one argument changes B but not B_{mag}. This distinction applies to any geometric overlap proposal, including the reduction discussed in Section 2.5 of [56]. The joint residual construction of this paper retains the complete declared channels. If a reduced channel discards polarization, its error budget must include (1528) in addition to spatial-gradient and curvature remainders.

H.3. *Mean-zero variations do not establish a stationary action.* For a differentiable functional S, the first variation is a linear functional $DS[x](v)$ of a prescribed admissible perturbation v. Hamilton stationarity requires $DS[x](v) = 0$ for every such perturbation. This differs from averaging over a symmetric distribution of perturbations.

Proposition 130 (A zero-mean averaging obstruction). *Let v be any admissible variation and let η take values $+1$ and -1 with equal probability. Then $\mathbb{E}DS[x](\eta v) = 0$ for every x, including nonstationary paths. In particular, this averaged identity cannot imply an Euler equation.*

Proof. Linearity gives $DS[x](\eta v) = \eta DS[x](v)$, whose expectation is zero. An endpoint-fixed example with dimensionless units is

$$S[x] = \tfrac{1}{2} \int_0^1 \dot{x}(t)^2 \, \mathrm{d}t, \quad x_a(t) = t^2 + at(1-t), \quad v(t) = t(1-t). \tag{1531}$$

Direct integration, without an equation-of-motion assumption, gives

$$S[x_a] = \frac{a^2 - 2a + 4}{6}, \qquad DS[x_a](v) = \frac{a-1}{3}, \tag{1532}$$

$$\mathbb{E}S[x_a + \epsilon\eta v] - S[x_a] = \frac{\epsilon^2}{6}, \qquad \mathbb{E}DS[x_a](\eta v) = 0. \tag{1533}$$

Only $a = 1$ is stationary, yet the averaged first variation vanishes for every a. The positive second-order term is not a stationarity condition on x_a. □

A valid averaging theorem instead starts from independently established microscopic equations, specifies the averaging map, and estimates the effective equation and its remainder. Alternatively, a control problem starts from a stated admissible dynamics and cost; dynamic programming then characterizes the optimizer. It does not establish that an arbitrary worldline action is stationary because its unresolved perturbations have zero mean. Moreover, stationary mechanical action need not be a minimum. Its relation to a nonnegative stochastic cost requires a stated matching argument rather than a change of vocabulary.

H.4. *Action normalization, rest energy, and mass equivalence.* Rest energy has units of energy, whereas action has units of energy times time. In a matched local Lorentz frame, a stable massive excitation has

$$E^2 = c^2|\mathbf{p}|^2 + m^2c^4, \qquad E_0 = mc^2. \tag{1534}$$

The corresponding point-particle action, when its matching hypotheses hold, is

$$S_{\mathrm{pp}} = -mc^2 \int \mathrm{d}\tau. \tag{1535}$$

The stationary value of S_{pp} is not E_0. Energy is obtained from the time-translation response or the corresponding Hamiltonian; the action coefficient has to be fixed by the physical propagator and stress response. In particular, an unspecified dimensional normalization cannot yield a numerical rest mass merely by identifying it with c^2.

For a weak potential and slow speed,

$$\frac{\mathrm{d}\tau}{\mathrm{d}t} = 1 + \frac{\Phi_N}{c^2} - \frac{|\mathbf{v}|^2}{2c^2} + O\big((|\Phi_N|/c^2 + |\mathbf{v}|^2/c^2)^2\big). \tag{1536}$$

Substitution in (1535) gives $L = -mc^2 + \frac{1}{2}m|\mathbf{v}|^2 - m\Phi_N$ to this order. Thus the same coefficient multiplies kinetic response and tensor gravitational response *once the universal worldline matching is established.* The main text obtains this matching conditionally from the physical pole, stress Ward identity, and universal coupling. It does not infer it from causality alone.

To see the extra input in a susceptibility explanation, take $\alpha > 0$ and $c > 0$ on the massive branch, and let

$$I = \int_\Sigma \Xi_1\Xi_2 \,\mathrm{d}\mu > 0, \qquad m_i = \frac{\alpha I}{c^2}, \qquad \delta\Xi_2 = \chi\Phi_N\Xi_2 + O(\Phi_N^2). \tag{1537}$$

If its gravitational response is defined by $\delta E = C\int \Xi_1 \delta\Xi_2 \,\mathrm{d}\mu = m_g\Phi_N + O(\Phi_N^2)$, then algebra gives

$$m_g = C\chi I, \qquad \frac{m_g}{m_i} = \frac{c^2 C\chi}{\alpha}. \tag{1538}$$

The equality of the masses requires $C\chi = \alpha/c^2$; positivity of I or bounded causal evolution does not determine this response coefficient. Section 2.6 of [56] imposes the corresponding calibration. In this programme the equivalent requirement is exposed as universal physical coupling and stress normalization, not hidden in an overlap notation. This comparison does not exclude an independently derived susceptibility mechanism; it identifies the coefficient that such a derivation must determine. Scalar charges, composition dependence, finite size, and self-gravity still require their own response analysis.

H.5. *What independently distinguishes a selected physical branch.* A candidate branch must fix its response coefficients before the observation used to test them. Suppose two fully specified candidates predict $f_1(p_1)$ and $f_2(p_2)$ in the same finite-dimensional observable space. Their independent calibrations restrict p_i to K_i and their theory remainder is bounded by δ_i. Define

$$\mathcal{Y}_i = \{f_i(p) + r : p \in K_i,\ \|r\| \le \delta_i\}. \tag{1539}$$

An observation y with a justified error bound ε is compatible with candidate i only if $\operatorname{dist}(y, \mathcal{Y}_i) \le \varepsilon$. If

$$\operatorname{dist}(\mathcal{Y}_1, \mathcal{Y}_2) > 2\varepsilon, \tag{1540}$$

it cannot be compatible with both. Indeed, two compatible predictions would be at distance at most 2ε by the triangle inequality. For probabilistic errors, the same conclusion applies on the declared coverage event; it is not an absolute exclusion outside that event.

This elementary criterion distinguishes a new physical prediction from a reformulation of an existing relation. Shared covariance, geodesic motion, or $E_0 = mc^2$ can verify consistency without satisfying (1540). A useful experimental programme therefore seeks an independently calibrated response, a bounded remainder, and an observable separating viable alternatives. The numerical examples below test the finite algebra, not the actual existence of trembling geometry or a new interaction.

The calculations use 401 polarization angles, 401 path coefficients, and 401 response normalizations. Independent adaptive quadrature evaluates the kinetic action and first variation on the path family. Equal-weight positive and negative perturbations give the expectation exactly, so no sampling uncertainty is attached to that cancellation. The data retain both the unsaturated contraction and the magnitude product, and both the directed and averaged variations. This preserves precisely the information that the incorrect reductions would discard.

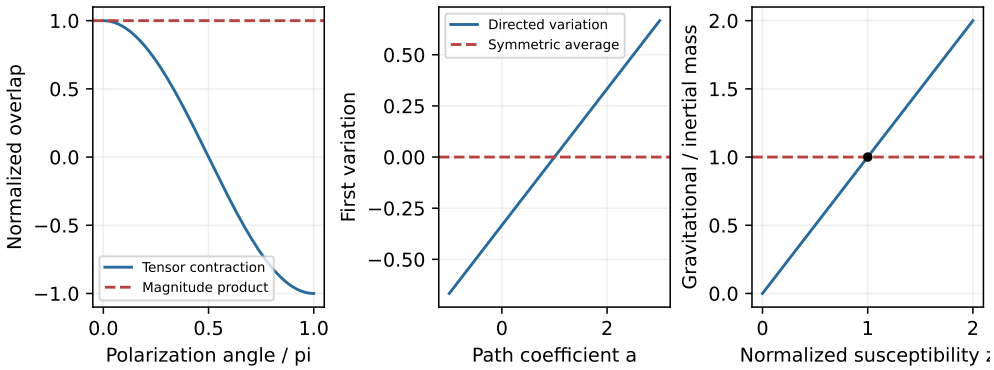


Figure 54. Analytic finite counterexamples, with independent quadrature checks. Left: the normalized contraction of two trace-free tensor polarizations depends on their angle; a homogeneous background does not fix that angle. Centre: endpoint-fixed paths have nonzero first variation except at $a = 1$, whereas symmetric perturbation averaging gives zero for all a. Right: the overlap response yields $m_g/m_i = z$ for $z = c^2 C\chi/\alpha$; mass equality occurs only at the independently fixed normalization $z = 1$. All curves are constructed examples, not measurements.

Appendix I. Physical perturbations, angular power, and noise-calibrated tests

I.1. *From a common configuration to physical mode coordinates.* A perturbation can be small without being physically observable. Gauge directions can change coordinate components while leaving a density, curvature invariant, or measured flux unchanged. A perturbation diagnostic must therefore begin with the physical quotient and an observable, not with the largest component of the master configuration.

Fix a finite regulator, a selected background, and a smooth local chart $\Phi = \phi(q)$ of the constraint surface after removal of gauge directions. Here $q \in \mathbb{R}^d$, all field components have declared reference scales, and the chosen observable is differentiable on this chart. Define

$$E_{\mathrm{red}}(q) = E(\phi(q)), \qquad K = D^2 E_{\mathrm{red}}(0), \qquad \delta O = D(O \circ \phi)(0)q + O(|q|^2). \tag{1541}$$

At a constrained critical point, K is the constrained Hessian, not in general the unrestricted Hessian restricted to arbitrary coordinate components. For a nonlinear chart the second derivative contains the curvature of the constraint surface. Equivalently, when independent constraints have Lagrange multipliers,

their second derivatives enter the Hessian of the constrained Lagrangian. These terms must not be omitted.

An energy Hessian specifies a restoring response. It does not specify an inertial kinetic form or a physical clock. The overdamped model

$$\mathrm{d}q = -\mathcal{M}Kq\,\mathrm{d}t + \sqrt{2\Theta\mathcal{M}}\,\mathrm{d}W_t, \qquad \mathcal{M} = \mathcal{M}^T \succ 0, \tag{1542}$$

is first order. An inertial branch instead requires a kinetic matrix M, a damping closure C, and a force-noise matrix B. These data must be derived or independently calibrated in the physical branch. They are not supplied by renaming the overdamped mobility as a particle inertia.

We use M for the finite kinetic matrix only in this appendix; it is not the spacetime manifold or the master field-space mobility. For constant coefficients, consider

$$\begin{aligned} \mathrm{d}q &= v\,\mathrm{d}t, \\ M\,\mathrm{d}v &= (-Kq - Cv + f(t))\,\mathrm{d}t + B\,\mathrm{d}W_t, \qquad M = M^T \succ 0, \quad K = K^T, \end{aligned} \tag{1543}$$

where $C = C^T \succeq 0$, $B \in \mathbb{R}^{d\times r}$, and W is an r-dimensional standard Brownian motion. A quadratic conservative action with kinetic form M supplies the undamped part. The damping and noise are additional open-system constitutive data. Thus the Hamiltonian variational sector and the stochastic dissipative sector have distinct, compatible roles.

For one physically normalized coordinate, the unit-inertia convention is $\ddot{q} + \gamma\dot{q} + \lambda q = \sigma\dot{W}$. If q has amplitude units Q and t has time units T, then $[\gamma] = T^{-1}$, $[\lambda] = T^{-2}$, and $[\sigma] = QT^{-3/2}$. Any numerical illustration below is nondimensionalized; no astronomical mass, temperature, or damping time is inferred from its dimensionless numbers.

I.2. *The exact finite kinetic energy balance.* Define the quadratic perturbation energy

$$E_2(q, v) = \tfrac{1}{2}q^T Kq + \tfrac{1}{2}v^T Mv. \tag{1544}$$

It is positive definite only if $K \succ 0$. Negative Hessian directions are permitted in a local instability calculation, but then E_2 is not a positive norm.

Proposition 131 (Kinetic Itô balance). *For* (1543),

$$\mathrm{d}E_2 = \left[-v^T Cv + v^T f + frac12\,\mathrm{tr}(M^{-1}BB^T)\right]\mathrm{d}t + v^T B\,\mathrm{d}W_t. \tag{1545}$$

On a finite interval with integrable force and second moments, expectation removes the stochastic integral. In a stationary unforced branch, mean dissipation equals noise injection.

Proof. The q equation has finite variation, so $\mathrm{d}(q^T Kq/2) = q^T Kv\,\mathrm{d}t$. The gradient and velocity Hessian of the kinetic term are Mv and M. Substitution

into Itô's formula gives

$$\mathrm{d}(v^T M v/2) = v^T(-Kq - Cv + f)\,\mathrm{d}t + v^T B\,\mathrm{d}W_t + \tfrac{1}{2}\operatorname{tr}(MM^{-1}BB^TM^{-1})\,\mathrm{d}t. \tag{1546}$$

Symmetry of K cancels $q^TKv - v^TKq$; cyclicity of the trace gives (1545). Finite linear SDE moment bounds, or stopping followed by the stated integrability, justify expectation of the martingale. Stationarity sets the expected energy derivative to zero. □

For $f = B = 0$ and $K \succ 0$, total E_2 cannot grow. Growth of one coordinate or of an unweighted coordinate norm need not be growth of physical energy. Conversely, an open shearing background can transfer energy to perturbations; its production term cannot be discarded and the resulting full drift need not have the closed form (1543). If $M(t)$ and $K(t)$ vary, the same calculation adds $v^T\dot{M}v/2 + q^T\dot{K}q/2$ to the right-hand side when the velocity equation is written with the displayed $M(t)\mathrm{d}v$ convention. A physical time-dependent kinetic action also contributes $\dot{M}v$ to its Euler equation. These background-work terms are part of the reduction, not a stationary energy identity.

I.3. *Coupled modes and their full Gaussian evolution.* For constant coefficients set $X = (q, v)^T$ and define

$$A = \begin{pmatrix} 0 & I \\ -M^{-1}K & -M^{-1}C \end{pmatrix}, \qquad L = \begin{pmatrix} 0 \\ M^{-1}B \end{pmatrix}, \qquad g(t) = \begin{pmatrix} 0 \\ M^{-1}f(t) \end{pmatrix}. \tag{1547}$$

The diffusion in phase space is L, not B. Independent scalar oscillators are justified only when the kinetic, restoring, damping, and noise data admit the required simultaneous modal reduction. In particular, spherical geometry alone does not diagonalize an anisotropic forcing covariance.

THEOREM 132 (Finite Gaussian evolution). *Let $A(t), L(t)$ and $g(t)$ be deterministic continuous finite matrices and vectors on $[0, T]$, and let X_0 be Gaussian and independent of W. Write $U(t, s)$ for the fundamental matrix of $A(t)$. Then*

$$\mu_t = U(t,0)\mu_0 + \int_0^t U(t,s)g(s)\,\mathrm{d}s, \tag{1548}$$

$$\Sigma_t = U(t,0)\Sigma_0 U(t,0)^T + \int_0^t U(t,s)L(s)L(s)^T U(t,s)^T\,\mathrm{d}s. \tag{1549}$$

Equivalently, $\dot{\mu} = A\mu + g$ and $\dot{\Sigma} = A\Sigma + \Sigma A^T + LL^T$.

Proof. Variation of constants gives

$$X_t = U(t,0)X_0 + \int_0^t U(t,s)g(s)\,\mathrm{d}s + \int_0^t U(t,s)L(s)\,\mathrm{d}W_s. \tag{1550}$$

The last integral is a centered Gaussian vector because its integrand is deterministic. Its covariance is the integral in (1549) by Itô isometry. Independence from X_0 removes the mixed covariance. Differentiating the deterministic formulas gives the two differential equations. □

For the unique attracting stationary construction below, assume that A is Hurwitz: every eigenvalue has negative real part. If $M, K, C \succ 0$ this holds. Indeed, an eigenvalue $z = \alpha + i\beta$ satisfies, for some complex nonzero u, $z^2 u^* M u + z u^* C u + u^* K u = 0$. If $\beta \neq 0$, its imaginary part implies $\alpha = -u^* C u/(2u^* M u) < 0$. If $\beta = 0$, no real $\alpha \geq 0$ satisfies that equality. Semidefinite C alone is insufficient: an undamped mode can remain on the imaginary axis.

Proposition 133 (Stationary covariance). *For a constant Hurwitz A and $g = 0$, the unique stationary Gaussian law has zero mean and covariance*

$$\Sigma_* = \int_0^\infty e^{As} L L^T e^{A^T s} \, \mathrm{d}s, \qquad A\Sigma_* + \Sigma_* A^T + L L^T = 0. \tag{1551}$$

This covariance may be singular. It is positive definite if and only if the controllability matrix $[L, AL, \ldots, A^{n-1}L]$ has rank $n = \dim X$.

Proof. Exponential decay of e^{As} makes the integral finite. Integrating the derivative of its integrand proves the Lyapunov equation. The difference of two solutions obeys $AD + DA^T = 0$, hence $e^{At} D e^{A^T t} = D$; decay forces $D = 0$. Formula (1549) shows convergence to Σ_* and gives the invariant Gaussian law. The convolution with its Gaussian noise, together with the vanishing initial term, also implies uniqueness among invariant probability laws by their characteristic functions. Finally, $z^T \Sigma_* z = \int_0^\infty |L^T e^{A^T s} z|^2 \mathrm{d}s$ vanishes exactly when z is orthogonal to every column of $A^j L$. Analyticity and Cayley–Hamilton reduce this condition to $j = 0, \ldots, n-1$. □

At sampling interval $h > 0$, exact transitions are

$$\begin{aligned} X_{k+1} &= F_h X_k + \eta_k, \qquad F_h = e^{Ah}, \\ Q_h &= \int_0^h e^{As} L L^T e^{A^T s} \, \mathrm{d}s = \Sigma_* - F_h \Sigma_* F_h^T. \end{aligned} \tag{1552}$$

Here the independent increments η_k have law $N(0, Q_h)$. Stationary pairs generated with this formula avoid numerical drift discretization error. Roundoff must not be confused with a physical negative noise variance; numerical covariance factorization uses its symmetric part and a tolerance bounded separately in the supplied finite calculation.

I.4. *Thermal balance and physical-time calibration.* If a declared bath obeys fluctuation–dissipation at energy scale $\Theta > 0$,

$$BB^T = 2\Theta C, \tag{1553}$$

and $M, K, C \succ 0$, the covariance is

$$\Sigma_* = \Theta \begin{pmatrix} K^{-1} & 0 \\ 0 & M^{-1} \end{pmatrix}. \tag{1554}$$

Substitution into the Lyapunov equation cancels the off-diagonal blocks; the velocity block is $-2\Theta M^{-1}CM^{-1} + M^{-1}BB^TM^{-1} = 0$. Uniqueness then proves the formula. The invariant density relative to $\mathrm{d}q\,\mathrm{d}v$ is proportional to $\exp[-E_2/\Theta]$. This is a derived consequence of (1553), not a consequence of arbitrary additive noise. Identifying Θ with k_BT requires a physical reservoir and the thermodynamic matching described in the main text.

Equilibrium covariance does not fix a clock. If an auxiliary time is $t_s = c_t t_{\mathrm{phys}}$, $c_t > 0$, Brownian scaling gives

$$A_{\mathrm{phys}} = c_t A_s, \qquad L_{\mathrm{phys}} = \sqrt{c_t} L_s, \qquad \Sigma_{*,\mathrm{phys}} = \Sigma_{*,s}. \tag{1555}$$

These formulas keep the state coordinates fixed. Position covariance is unchanged while every temporal relaxation scale changes. If the kinetic coordinate is redefined as the physical velocity $v_{\mathrm{phys}} = dq/dt_{\mathrm{phys}} = c_t v_s$, set $\mathsf{T}_c = \mathrm{diag}(I, c_t I)$. The correct coordinate transformation is then

$$A_{\mathrm{phys}} = \mathsf{T}_c (c_t A_s) \mathsf{T}_c^{-1}, \qquad L_{\mathrm{phys}} = \sqrt{c_t}\mathsf{T}_c L_s, \qquad \Sigma_{*,\mathrm{phys}} = \mathsf{T}_c \Sigma_{*,s} \mathsf{T}_c^T. \tag{1556}$$

Physical velocity covariance scales by c_t^2; its kinetic normalization must also be transformed consistently. The invariant position distribution still does not fix c_t. The independent calibration requirement of Appendix G therefore applies also to perturbation spectra. A relativistic application must specify the observer's proper time or an asymptotic coordinate time; a common rescaling does not replace lapse, redshift, or detector transfer calculations.

I.5. *Rotations and the distinction between symmetry and fluctuations.* Choose a complete real orthonormal spherical multiplet of degree ℓ, after physical normalization of the observable. Its coefficient vector $a_\ell \in \mathbb{R}^{2\ell+1}$ transforms under a rotation R as $a_\ell \mapsto D_\ell(R) a_\ell$, where $D_\ell(R)$ is orthogonal. It follows exactly that

$$P_\ell = a_\ell^T a_\ell, \qquad P_\ell(D_\ell(R)a_\ell) = P_\ell(a_\ell). \tag{1557}$$

In contrast, $\max_m |a_{\ell m}|$ is not invariant under this mixing. Truncating a multiplet to selected m values destroys the stated invariance.

For $\ell = 2$, this can be seen without angular coordinates. Represent the quadrupole by a real symmetric tracefree tensor $Q = \sum_{j=1}^{5} a_j T_j$, where

$\mathrm{tr}(T_iT_j) = \delta_{ij}$. Under $Q \mapsto RQR^T$,

$$P_2 = \mathrm{tr}(Q^2) = \sum_{j=1}^{5} a_j^2. \tag{1558}$$

This equality supplies both the observable normalization and the rotation test used in the numerical illustration.

If the Gaussian law has zero mean and isotropic covariance $\nu_\ell I$, it is invariant under rotations while typical realizations have $P_\ell > 0$. Rotational invariance of the probability law is therefore not pointwise spherical symmetry of every realization. Spherical geometry does not alone imply isotropic forcing; the drift, diffusion and initial law must have the relevant symmetry. For a Gaussian law on an irreducible real multiplet, isotropic covariance is the explicit sufficient condition used here. Anisotropic forcing can create anisotropic covariance without a gravitational instability.

PROPOSITION 134 (A stable fluctuation counterexample). *For a real scalar mode with $\lambda, \gamma, \sigma > 0$,*

$$\mathrm{Var}(v) = \frac{\sigma^2}{2\gamma}, \qquad \mathrm{Cov}(q, v) = 0, \qquad \mathrm{Var}(q) = \frac{\sigma^2}{2\gamma\lambda}. \tag{1559}$$

Consequently, five independent, equally forced quadrupole coordinates remain nonzero in stationary angular power even though all deterministic modes decay and their joint law is rotationally invariant.

Proof. Stationarity of q^2 gives $\mathbb{E}[qv] = 0$. Stationarity of qv gives $\mathbb{E}[v^2] = \lambda\mathbb{E}[q^2]$. Stationarity of v^2 gives $2\gamma\mathbb{E}[v^2] = \sigma^2$. The Hurwitz property proved above supplies the invariant law. These three equations determine its covariance and prove (1559). Taking the product of five identical copies gives covariance νI_5, where $\nu = \sigma^2/(2\gamma\lambda)$. □

This counterexample rules out interpreting a positive long-time amplitude limsup as evidence of a coherent collapsing shape. It also avoids an unstable denominator: angular power may be reported in a fixed independently calibrated amplitude scale, whereas division by a random monopole requires its joint distribution. The parameter ε in (1448) does not supply that distribution.

I.6. *Finite-time thresholds and their error probabilities.*

PROPOSITION 135 (An isotropic instantaneous null). *If $a_\ell \sim N(0, \nu_\ell I_{2\ell+1})$ with known $\nu_\ell > 0$, then*

$$P_\ell/\nu_\ell \sim \chi^2_{2\ell+1}. \tag{1560}$$

The threshold $\nu_\ell \chi^2_{2\ell+1,1-\alpha}$ has instantaneous false-alarm probability α. If the mean is m_ℓ, the law is noncentral $\chi^2_{2\ell+1}(|m_\ell|^2/\nu_\ell)$, and its survival function gives the exact power against that specified mean.

Proof. Divide every coordinate by $\sqrt{\nu_\ell}$. The coordinates are independent unit Gaussians because their joint covariance is the identity. Their squared sum is the defining central or noncentral chi-square random variable. Continuity of this distribution gives the threshold probability. □

General covariance requires its eigenvalues, not an isotropic substitution. Let $Z \sim N(0, \Sigma)$, $W = W^T \succeq 0$, and $S = W^{1/2}\Sigma W^{1/2}$. Put $Q = Z^T W Z$.

PROPOSITION 136 (A Gaussian quadratic upper bound). *For every $x > 0$,*

$$\mathbb{P}\left\{Q > \operatorname{tr} S + 2\sqrt{\operatorname{tr}(S^2)x} + 2\|S\|x\right\} \le e^{-x}. \tag{1561}$$

The same bound with S replaced by a known $\overline{S} \succeq S$ is conservative.

Proof. Diagonalization represents Q as $\sum_j s_j G_j^2$ with independent unit Gaussians and eigenvalues $s_j \ge 0$. For $0 < t < (2\max_j s_j)^{-1}$,

$$\log \mathbb{E}e^{t(Q-\operatorname{tr} S)} = \sum_j [-ts_j - \tfrac{1}{2}\log(1-2ts_j)] \le \frac{t^2 \sum_j s_j^2}{1 - 2t\max_j s_j}. \tag{1562}$$

The inequality follows by expanding $-\log(1-z) - z$ and bounding the terms of degree at least two by $z^2/[2(1-z)]$. Chernoff's inequality with $t = \sqrt{x}/(\sqrt{\sum_j s_j^2} + 2\max_j s_j\sqrt{x})$ yields (1561). If $S = 0$, $Q = 0$ almost surely and the assertion is immediate. Loewner order implies ordered eigenvalue inequalities; therefore $\operatorname{tr} S$, $\operatorname{tr}(S^2)$ and $\|S\|$ are bounded by their counterparts for $\overline{S}$. □

For observations at J predetermined times, use $x = \log(J/\alpha)$ in the respective time-dependent covariance bounds. The union bound then gives probability at most α of one or more false alarms. Temporal independence is not required. This result does not control crossings between the sampled times or the supremum over continuous time.

An independent calibration can be incorporated without pretending its covariance is exactly known. Suppose, with probability at least $1 - \delta_{\mathrm{cal}}$, the calibration supplies valid bounds $S_j \preceq \overline{S}_j$ and $\|W^{1/2}m_j\| \le b_j$ for every declared test time. Define

$$H_j = \left[b_j + \sqrt{\operatorname{tr}\overline{S}_j + 2\sqrt{\operatorname{tr}(\overline{S}_j^2)x} + 2\|\overline{S}_j\|x}\right]^2. \tag{1563}$$

For calibration outcomes on the valid-bounds event, the triangle inequality for $\|W^{1/2}(m_j + Z_j)\|$ and Proposition 136 give familywise error at most α; unconditionally it is at most $\alpha + \delta_{\mathrm{cal}}$. A separately controlled nonlinear observation remainder of weighted norm r_j enlarges b_j by r_j on its validity event, with that event's failure probability added. No such remainder estimate is supplied by the Gaussian null itself.

These are finite tests of a specified reference model. Rejection can result from an incorrect forcing law, an incorrect observation map, an unmodelled background, or a genuine mode instability. It does not identify the cause without independent physical controls.

I.7. *Deterministic instability and open-system transient growth.* For the scalar deterministic branch with $\lambda < 0$ and $\gamma > 0$, the local characteristic exponent

$$r_+ = \frac{-\gamma + \sqrt{\gamma^2 - 4\lambda}}{2} > 0 \tag{1564}$$

predicts initial exponential amplification. This is a statement about the linearization during its validity interval. It does not determine nonlinear fragmentation, trapping surfaces, or the end state of a collapsing object.

Eigenvalue stability is also insufficient for a general open transport matrix. An exact finite example is

$$A_s = \begin{pmatrix} -1 & s \\ 0 & -1 \end{pmatrix}, \qquad e^{A_s t} = e^{-t} \begin{pmatrix} 1 & st \\ 0 & 1 \end{pmatrix}, \qquad G_s(t) = e^{-t} \frac{\sqrt{s^2 t^2 + 4} + |s| t}{2}. \tag{1565}$$

The last expression is the Euclidean operator norm of the propagator, obtained from the larger singular value of the triangular matrix. Both eigenvalues are -1. Nevertheless, $G_{10}(1) = 3.715221655\ldots$. For $|s| > 2$, differentiating $\log G_s$ gives $-1 + |s|/\sqrt{s^2 t^2 + 4}$, so the largest amplification occurs at $t_* = \sqrt{1 - 4/s^2}$; for $|s| \le 2$, the maximum is $G_s(0) = 1$.

This model is an open shearing reduction, not an instance of a closed positive-energy oscillator with strictly dissipative C. Its Euclidean energy obeys

$$\frac{\mathrm{d}}{\mathrm{d}t} \frac{x^T x}{2} = -x_1^2 - x_2^2 + s x_1 x_2. \tag{1566}$$

The last term represents the declared background exchange. The distinction prevents a component amplification from being called a violation of the closed energy law. In a rotating or shearing fluid, one must derive the corresponding physical energy norm and production term from the fluid model.

I.8. *Temporal spectra, detectors, and exact sampling.* Let A be Hurwitz and define a linear physical observable $Y = DX$. We use the two-sided angular-frequency convention $C_Y(\tau) = (2\pi)^{-1} \int e^{i\omega\tau} S_Y(\omega) \mathrm{d}\omega$. The stationary stochastic convolution gives

$$S_Y(\omega) = D(i\omega I - A)^{-1} L L^T (-i\omega I - A^T)^{-1} D^T. \tag{1567}$$

Indeed the impulse kernel is $De^{At}L\,1_{t\geq 0}$; its Fourier transform is $D(i\omega I-A)^{-1}L$. Multiplying that transform by its adjoint proves the formula. For one unit-inertia scalar position,

$$S_q(\omega)=\frac{\sigma^2}{(\lambda-\omega^2)^2+\gamma^2\omega^2}. \tag{1568}$$

Integration reproduces (1559). The nonzero spectral peak is at $\sqrt{\lambda-\gamma^2/2}$ when $\gamma^2<2\lambda$; otherwise its maximum is at zero. This peak is not the undamped frequency $\sqrt{\lambda}$, nor the underdamped pole frequency $\sqrt{\lambda-\gamma^2/4}$.

A detector with an integrable causal impulse response h_O measures $Y_O=h_O*Y+\epsilon_O$. If detector noise is independent and has an integrable spectral density S_{ϵ_O},

$$S_{Y_O}(\omega)=\widehat{h}_O(\omega)S_Y(\omega)\widehat{h}_O(\omega)^*+S_{\epsilon_O}(\omega). \tag{1569}$$

An ideal continuous white detector noise is a generalized process, not a finite-variance instantaneous reading. A band-limited response or a sampled measurement model must therefore be specified.

For sampled readings $Y_k=DX_{kh}+\epsilon_k$, with independent $\epsilon_k\sim N(0,R_O)$, the discrete spectrum on $[-\pi,\pi]$ is

$$S_Y^{(h)}(\nu)=D(I-F_he^{-i\nu})^{-1}Q_h(I-F_h^Te^{i\nu})^{-1}D^T+R_O. \tag{1570}$$

The discrete covariance convention integrates this spectrum with $\mathrm{d}\nu/(2\pi)$. The state-only part also equals $h^{-1}\sum_{k\in\mathbb{Z}}S_Y((\nu+2\pi k)/h)$ whenever the alias sum is convergent. Thus a coarse sample cadence can hide a dynamical feature; the detector and cadence must enter a proposed observational test.

I.9. *Finite illustrations and the astrophysical interfaces.* The supplied numerical illustration uses independently seeded synthetic Gaussian draws, exact sampled transitions, and deterministic matrix identities. A stationary quadrupole with $\gamma=\lambda=1$ and $\sigma=0.1$ has $\nu=0.005$, mean power 0.025, and instantaneous one-percent threshold $0.0754313623\ldots$. Its nonzero ordinary power is not an instability. A specified nonzero quadrupole mean is compared with the exact noncentral law, and a finite collection of sampled times is tested with the conservative union-bound threshold.

Physical rotations are implemented as $Q\mapsto RQR^T$ in a trace-orthonormal five-tensor basis. They preserve P_2 but change the largest coordinate. For a separate positive kinetic matrix example, an independently solved Lyapunov equation checks the energy injection/dissipation identity. Quadrature of the scalar spectrum checks the covariance normalization; exact transition sampling separately checks temporal covariance. Figure 55 displays these declared examples. No curve is a black-hole solution or a JWST measurement.

The mathematical tests above can be completed at fixed resolution without an unregulated Navier–Stokes theorem. Applying them to near-horizon

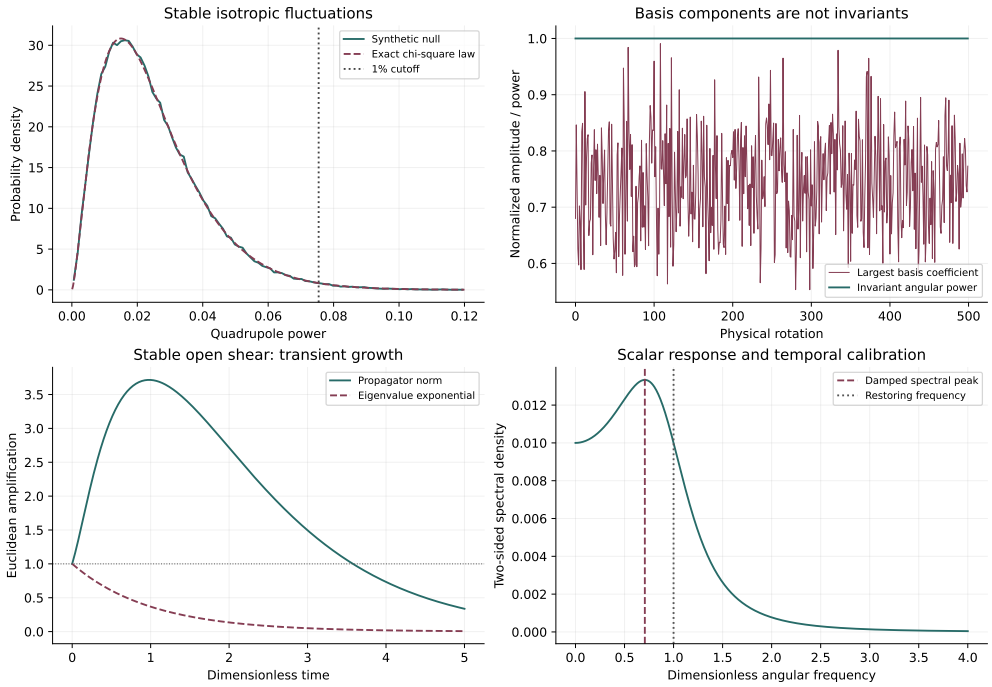


Figure 55. Finite synthetic mode diagnostics. The angular-power law contains ordinary nonzero fluctuations under a stable isotropic null. Rotations preserve trace-normalized quadrupole power but change the largest basis coefficient. A stable open shear matrix transiently amplifies a coordinate norm, unlike a closed positive-energy dissipative oscillator. The scalar spectrum distinguishes the restoring frequency from its damped spectral peak. Parameters and normalizations are declared in the text; the figure does not depict an astronomical simulation or observation.

accretion requires a separate constrained GRMHD reduction and radiative observation map. Their primary fluid treatment belongs to the turbulence companion, where a Kerr background, magnetic constraints, energy flux and causal transport are declared before reduced-mode comparisons [76] and [133]. A phenomenological finite shear model can illustrate these tests; it cannot establish an improvement over those GRMHD simulations.

An early-galaxy application requires a population formation law, cosmological volume and time, gas physics, stellar and nuclear emission, and a selection operator. A larger brightness or inferred stellar mass is not a direct measurement of a collapse-mode amplitude. The stellar-light and AGN issues in [37] motivate the separate population-forward treatment in the cosmological

companion. Neither a mode power nor a Gaussian significance calculation resolves those astrophysical inputs.

A new physical prediction would fix the kinetic, damping, noise and observable response from independent microscopic or calibration data before testing them. It would then predict a spectrum or mode relation different from a fully specified alternative, with theoretical and observational errors included. The oscillator identities proved here are reference calculations, not new laws of gravitation. Their role is to make a proposed departure quantitatively falsifiable without equating fluctuations with collapse or an observation fit with a first-principles derivation.

Appendix J. Selection, matching, and independent physical tests

A common variational structure is a statement about how sectors depend on shared data. A prediction is a statement about an observable after those data have been fixed. To connect the two, three operations must be kept distinct. Selection compares admissible microscopic packages. Matching translates a selected package into physically normalized effective coefficients. Validation compares the resulting observables with data that were not used to choose those coefficients. The order matters: fitting a coefficient during the last operation does not derive it during the first.

J.1. *Differentiating the equilibrium score with its reference measure.* Fix a regulator, a common configuration domain D, and a temperature $\theta > 0$. Let p vary in an open subset of $\mathbb{R}^m$. In one declared coordinate chart, write the reference measure as $w_p(x)\,\mathrm{d}x$, where $w_p > 0$, and define

$$\begin{aligned} Z(p) &= \int_D e^{-S_p(x)/\theta} w_p(x)\,\mathrm{d}x, \quad \mathcal{F}(p) = -\theta \log Z(p), \\ \pi_p(x) &= Z(p)^{-1} e^{-S_p(x)/\theta} w_p(x). \end{aligned} \tag{1571}$$

Here S_p includes all parameter dependence of the chosen joint action, including its permitted field-dependent metric. The following calculation holds at a fixed regulator; it does not exchange a parameter derivative with a continuum limit.

Proposition 137 (The reference-dependent selection derivatives). *Suppose $0 < Z(p) < \infty$, S_p and $\log w_p$ are twice continuously differentiable in p, and differentiation under the integral is justified locally by an integrable majorant for the integrand and its first two derivatives. Set*

$$U_i = \partial_i S_p - \theta \partial_i \log w_p, \qquad U_{ij} = \partial_{ij} S_p - \theta \partial_{ij} \log w_p. \tag{1572}$$

Then

$$\partial_i \mathcal{F} = \mathbb{E}_{\pi_p} U_i, \tag{1573}$$

$$\partial_{ij}\mathcal{F} = \mathbb{E}_{\pi_p} U_{ij} - \theta^{-1} \operatorname{Cov}_{\pi_p}(U_i, U_j). \tag{1574}$$

Proof. Differentiate the unnormalized integrand. Its logarithmic derivative is $-U_i/\theta$, so

$$\partial_i Z = -\theta^{-1} Z \mathbb{E}_{\pi_p} U_i. \tag{1575}$$

Using $\partial_i \mathcal{F} = -\theta(\partial_i Z)/Z$ proves (1573). The normalized density therefore satisfies

$$\partial_j \pi_p = -\theta^{-1} \pi_p (U_j - \mathbb{E}_{\pi_p} U_j). \tag{1576}$$

For any differentiable integrable observable f_p, apply the product rule to $\int f_p \pi_p \, \mathrm{d}x$. The result is

$$\partial_j \mathbb{E}_{\pi_p} f_p = \mathbb{E}_{\pi_p} \partial_j f_p - \theta^{-1} \operatorname{Cov}_{\pi_p}(f_p, U_j). \tag{1577}$$

Taking $f_p = U_i$ yields (1574). □

The negative covariance contribution is essential. Positive curvature of S_p with respect to configurations does not imply a positive Hessian of $\mathcal{F}$ with respect to parameters. Likewise, a field-dependent reference measure cannot be held constant in this derivative unless that restriction is part of the model. A parameter-dependent domain requires additional boundary terms; the proposition assumes a fixed common domain and hence does not suppress such terms.

J.2. *An exact example separating inner stability from outer convexity.* Take one dimension, $p > 0$, $w_p = 1$, and $S_p(x) = px^2/2$. Gaussian integration gives

$$Z(p) = \sqrt{\frac{2\pi\theta}{p}}, \quad \mathcal{F}(p) = \frac{\theta}{2} \log \frac{p}{2\pi\theta}, \quad \mathbb{E}_{\pi_p} x^2 = \frac{\theta}{p}. \tag{1578}$$

Every inner equilibrium is stable: its configuration Hessian is $p > 0$. Nevertheless,

$$\mathcal{F}'(p) = \frac{\theta}{2p}, \qquad \mathcal{F}''(p) = -\frac{\theta}{2p^2} < 0. \tag{1579}$$

For a direct check, $U = x^2/2$, $U_{pp} = 0$, and the Gaussian fourth moment is $\mathbb{E}x^4 = 3\theta^2/p^2$. Thus

$$\operatorname{Var}(U) = \tfrac{1}{4}(3\theta^2/p^2 - \theta^2/p^2) = \frac{\theta^2}{2p^2}, \tag{1580}$$

which reproduces (1579). On the open half-line the score has no minimizer and tends to $-\infty$ as $p \downarrow 0$. Restricting p to a closed interval bounded away from zero restores attainment, but selects its lower endpoint. That endpoint is an imposed admissibility boundary, not a predicted physical constant.

More generally, let $S_p = a(p)x^2/2 + c(p)$ and let the coordinate weight be a positive scalar $w(p)$. Then

$$\mathcal{F}(p) = c(p) - \theta \log w(p) + \frac{\theta}{2} \log \frac{a(p)}{2\pi\theta}. \tag{1581}$$

Both $c(p)$ and $w(p)$ change the comparison score while canceling from the normalized Gaussian law. Consequently, candidate-independent action zero, units, and reference normalization are physical comparison conventions, not optional simplifications.

J.3. *What a conditional uniqueness theorem would require.* Let K be a nonempty compact convex parameter set contained in the admissible domain. Suppose $\mathcal{F}$ extends continuously to K and is twice differentiable in a neighborhood. A sufficient condition for a unique minimizer is

$$v^T \left(\mathbb{E}_{\pi_p} U_{ij} - \theta^{-1} \operatorname{Cov}_{\pi_p}(U_i, U_j) \right)_{ij} v \geq \mu |v|^2, \qquad \mu > 0, \tag{1582}$$

for all $p \in K$ and all v. Indeed, continuity and compactness give attainment. Integrating the second derivative along any segment gives strict convexity, which excludes two distinct minimizers. At an interior minimizer, (1573) additionally gives $\mathbb{E}_{\pi_p} U_i = 0$. At a boundary minimizer these equations are replaced by the appropriate one-sided or constrained optimality conditions.

This is a genuine conditional theorem only after (1582) has been verified for the proposed package. Positivity of the joint residual metric does not verify it. Nor does uniqueness in K establish that nature belongs to the declared candidate class. Discrete group selection uses the finite score-separation criterion in Appendix G, rather than this continuous convexity argument.

J.4. *From selected parameters to a falsifiable relation.* Write the effective matching map as $c = \mathcal{M}(p)$ and a predicted observable as $Q = \mathcal{O}(c)$. If both maps are differentiable, then

$$D_p Q = D_c \mathcal{O}\, D_p \mathcal{M}. \tag{1583}$$

Thresholds, field normalizations, and the physical clock belong to $\mathcal{M}$; they cannot be varied without changing the prediction. The local identification bound of Appendix G controls calibration uncertainty, while a separately bounded matching remainder controls the difference between the regulated and physical observables.

The five papers implement different parts of this chain. Paper II supplies representation constraints and heavy-field matching, and examines how renormalization-group relations can reduce coupling data without fixing all scales. Paper III calculates a bath response and its fluctuation spectrum for independently declared momentum modes. Paper IV shows why classical equilibrium weights alone do not determine quantum phases or measurement

statistics. Paper V compares fixed response directions and states when environmental noise or spatial decoherence removes the test. These interfaces supplement, rather than replace, the common field equations.

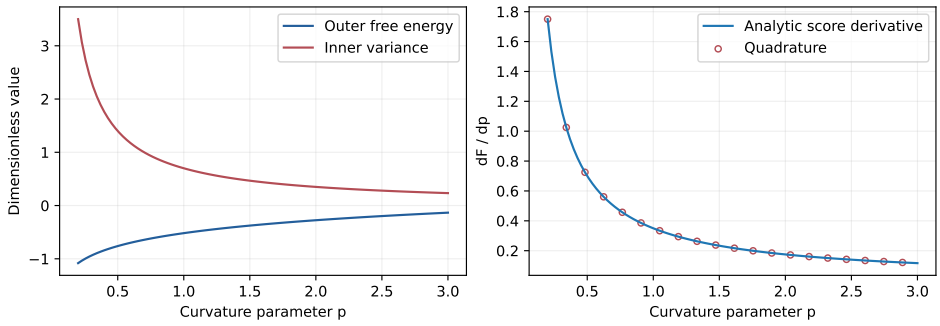


Figure 56. Exact dimensionless Gaussian selection example at $\theta = 0.7$. The inner variance decreases as $1/p$, whereas the outer free energy is increasing and concave. Independent quadrature reproduces its derivative. The figure illustrates the distinction between configuration stability and parameter selection; it contains no measured coupling or experimental fit.

Appendix K. Common-weight selection, radiative matching, and material observables

The observable relations of Section 11.11 depend on more than the existence of a positive master norm. They depend on a common curvature weight, on a specified propagating scalar, and on the matching of its couplings to physical matter. This appendix gives a sufficient algebraic condition for the common weight, follows its linear response through renormalization and thresholds, and derives a source-driven clock/force relation. Natural units are used until the laboratory formulas, where c_{light} denotes the speed of light. The dimensionless scalar coordinate is always

$$s := \frac{\varphi}{M_{\mathrm{P}}}, \qquad \partial_s = M_{\mathrm{P}}\partial_\varphi, \qquad M_{\mathrm{P}}^{-2} = 8\pi G_*. \tag{1584}$$

The Planck normalization and renormalization reference scales in these derivatives are held fixed on the selected Einstein-frame branch.

K.1. *A sufficient algebraic condition and its scope.* Let $\mathfrak{g}$ be a compact real simple Lie algebra, and let h_0 be a fixed positive invariant form on it. The following result concerns the Euclidean curvature pairing before symmetry breaking. It does not establish the existence of a physically admissible simple master algebra containing the required Cartan and matter data.

PROPOSITION 138 (Conditional selection of one curvature weight). *Suppose a scalar singlet σ changes a positive symmetric pairing h_σ on one copy of the adjoint representation of $\mathfrak{g}$. Suppose h_σ remains invariant under the full master group at every σ, with no additional tensor spurions. Then there is a positive scalar function $w(\sigma)$ such that*

$$h_\sigma(X,Y) = w(\sigma)h_0(X,Y). \tag{1585}$$

Fix embeddings $\iota_a : \mathfrak{g}_a \hookrightarrow \mathfrak{g}$, normalizations h_a, representation traces, and all reference-scale factors. For simple residual factors their restriction indices $I_a > 0$ obey

$$h_0(\iota_a X, \iota_a Y) = I_a h_a(X,Y), \qquad g_a^{-2}(\sigma) = \frac{I_a}{g_{\mathrm{M}}^2} w(\sigma), \qquad B_a(\sigma) = \frac{w(\sigma)}{w(\sigma_*)}. \tag{1586}$$

Here g_{M} is a fixed master normalization, and B_a is the kinetic coefficient after canonical normalization at the vacuum.

Proof. Write $h_\sigma(X,Y) = h_0(T_\sigma X, Y)$. Symmetry makes T_σ self-adjoint, and invariance makes it commute with every adjoint map. Each eigenspace of T_σ is therefore an invariant ideal. Simplicity leaves one eigenvalue, giving (1585); positivity makes it positive. This is the self-adjoint form of the adjoint Schur argument. Restricting the fixed form gives the first equality in (1586). The fixed trace and kinetic conventions give the second, and division by the vacuum coefficient gives the third. □

With conventional root normalizations, the I_a's are Dynkin embedding indices. For an Abelian factor the inherited norm is fixed only after the generator and its embedding have been fixed. Changing a representation trace changes a known normalization factor; it does not select that representation. Likewise, obtaining a gravitational coefficient from a restricted Cartan curvature requires the fixed coframe scale, expansion convention, and continuation already used in the main text. The proposition does not imply equality of the canonically normalized gauge couplings. It also leaves the function w, its vacuum value, its derivative, and the scalar stabilization mechanism undetermined. Algebraic uniqueness of an invariant form is not a vacuum-selection theorem.

The hypotheses concerning multiplicity and singlet dependence matter. For m copies of the adjoint, the pairing can contain a positive matrix on the multiplicity space, rather than one scalar weight. For a compact semisimple algebra it has independent weights on the simple ideals. The present product Cartan/internal candidate consequently admits, for example,

$$h_\sigma = w_{\mathrm{C}}(\sigma)h_{\mathrm{C}} \oplus \bigoplus_a w_a(\sigma)h_a, \qquad w_{\mathrm{C}} > 0, \quad w_a > 0. \tag{1587}$$

Neither positivity nor invariance equates these functions. A shared scalar can couple their dynamics even when the functions differ. Minimization over the fields of a fixed action solves field equations for the supplied pairing; it does not minimize over, or select, the functions defining that pairing. Equation (226) is therefore explicit data of the present product candidate. An independent derivation by Proposition 138 would require a different, fully specified master-algebra and representation selection problem.

The same freedom is visible in a joint positive channel metric. With $\mathbf{1} = (1,1,1,1)^\top$, the family

$$\begin{gathered} H_E = 0.9 I_4 + 0.1 \mathbf{1}\mathbf{1}^\top + E, \qquad E = E^\top, \quad \|E\|_F < \frac{1}{40}, \\ 0.875 I_4 \prec H_E \prec 1.325 I_4. \end{gathered} \tag{1588}$$

has every off-diagonal entry between 0.075 and 0.125, while ten independent symmetric entries vary on an open set. Nonzero cross blocks and uniform positivity alone do not fix their ratios or a physical gauge/matter dictionary. The physical dictionary must be supplied by the identified fields and their matching.

K.2. *The signed scalar lock and a counterfamily.* Consider a metric scalar–tensor branch with one Jordan scalar ϕ, a locally matched flat vacuum, and constant elementary Jordan masses. A positive common functional can allow different scalar weights:

$$\begin{gathered} S_J = \int \sqrt{-g_J}\, \mathrm{d}^4x \left[\frac{M_{\mathrm{P}}^2}{2} F_G(\phi) R_J - \frac{1}{2}(\partial\phi)_J^2 \right. \\ \left. - V_J(\phi) - \frac{1}{4} B_\gamma(\phi) \mathcal{F}_{\mu\nu}\mathcal{F}^{\mu\nu} \right] + S_{\mathrm{m}}, \quad F_G = e^{-c_G\phi}, \qquad B_\gamma = e^{-c_\gamma \phi}, \\ V_J(0) = V_J'(0) = 0, \qquad V_J''(0) > 0. \end{gathered} \tag{1589}$$

Both functions are positive. For nonzero c_G, c_γ, one shared scalar couples gravity, electromagnetism, and matter. This family shows why sharing a scalar and a functional does not select the equal-weight choice.

Let φ be the local canonical Einstein scalar and let $A = F_G^{-1/2}$ multiply the point-particle Einstein-frame mass. Define the signed, dimensionful slopes

$$Z_* = 1 + \frac{3}{2} c_G^2 M_{\mathrm{P}}^2, \qquad \gamma_a := -\,\partial_\varphi \log B_a|_0\,, \qquad a_{\mathrm{m}} := \partial_\varphi \log A|_0\,. \tag{1590}$$

For (1589), these are $\gamma_\gamma = c_\gamma/\sqrt{Z_*}$ and $a_{\mathrm{m}} = c_G/(2\sqrt{Z_*})$. Constant Jordan masses are essential for identifying a_{m} with an elementary mass slope; explicit Jordan mass dependence adds its own derivative.

PROPOSITION 139 (Signed common-weight relation). *Under the common-weight hypothesis $B_a = F_G$, with the metric diagonalization and elementary-mass assumptions just stated,*

$$\gamma_a - 2a_{\mathrm{m}} = 0. \tag{1591}$$

For unscreened elementary point masses and a direct tree-level photon vertex, this implies

$$\alpha_\varphi = 2M_{\mathrm{P}}^2 a_{\mathrm{m}}^2, \qquad \Gamma_{\gamma\gamma} = \frac{\gamma_\gamma^2 m_\varphi^3}{64\pi}, \qquad \alpha_\varphi = 32\pi M_{\mathrm{P}}^2 \frac{\Gamma_{\gamma\gamma}}{m_\varphi^3}. \tag{1592}$$

Proof. The identity $A = F_G^{-1/2}$ gives $2\partial_\varphi \log A = -\partial_\varphi \log F_G$. With $B_a = F_G$, this is (1591). The scalar charge of an elementary mass is $a_{\mathrm{m}} m$. Dividing its canonical exchange potential by the tensor Newton potential gives the first equality in (1592). The vertex $\gamma_\gamma \varphi \mathcal{F}^2/4$, including the identical photon phase-space factor, gives the second. Eliminating the slope gives the last equality. □

The signed relation contains more information than a comparison of two squares. An opposite sign between γ_γ and a_{m} can satisfy the width/force equality while violating (1591). In the independent-weight family one gets

$$\frac{\alpha_\varphi}{32\pi M_{\mathrm{P}}^2 \Gamma_{\gamma\gamma}/m_\varphi^3} = \frac{c_G^2}{c_\gamma^2}, \qquad c_\gamma \neq 0. \tag{1593}$$

The right-hand side can be any positive number without changing the positivity of either weight.

Common dilatonic functions and their possible stabilization have a long history, including the least-coupling mechanism of [52]. Composition-dependent light-dilaton charges are developed in [50]. A scalar–tensor effective theory with the same F_G, B_a, V_J, kinetic term, and matter functions reproduces the present branch. The derivation above gives a conditional consistency relation and a way to falsify that branch; it does not make the relation exclusive to this master construction.

K.3. *Differentiated running and threshold matching.* Distinguish the normalized kinetic function $B_a(s)$ from the inverse coupling $\mathcal{B}_a(\mu, s) := g_a^{-2}(\mu, s)$. At a fixed renormalization scale define

$$d_a(\mu) := \partial_s \log g_a^2(\mu, s)\big|_0 = -g_a^2(\mu, 0)\, \partial_s \mathcal{B}_a(\mu, s)\big|_0 . \tag{1594}$$

At the tree matching scale, a common normalized weight gives $d_a(M) = M_{\mathrm{P}} \gamma_a$. At lower scales the coefficients must be evolved in the broken theory. The definition concerns a background scalar sufficiently slowly varying for local matching; momenta, scalar gradients, and curvature must lie within the retained effective expansion.

Choose the beta-function convention $\mathrm{d}g_a/\mathrm{d}\log\mu = -b_a g_a^3/(16\pi^2) + \cdots$. In an interval with fixed active particle content and no moving thresholds, one-loop running at fixed M, μ is

$$\mathcal{B}_a(\mu, s) = \mathcal{B}_a(M, s) + \frac{b_a}{8\pi^2}\log\frac{\mu}{M}, \qquad d_a(\mu) = \frac{g_a^2(\mu, 0)}{g_a^2(M, 0)} d_a(M). \tag{1595}$$

The second equality follows by differentiating the first. Even equal $d_a(M)$'s need not remain equal when the factors have different beta functions. This is a calculable effect once the spectrum and scheme have been specified. If the scale is instead tied to a scalar-dependent mass or to Jordan-frame units, its derivative must also be included; it cannot be silently held fixed in one frame and varied in another.

For a heavy mass $m_h(s)$ between two fixed scales $M > m_h > \mu$, let b_H, b_L be the one-loop coefficients above and below the threshold. In a mass-independent scheme, including a finite local matching function $\Delta_{\mathrm{fin}}(s)$, write

$$\begin{aligned} \mathcal{B}_L(\mu, s) &= \mathcal{B}_H(M, s) + \frac{b_H}{8\pi^2}\log\frac{m_h(s)}{M} + \frac{b_L}{8\pi^2}\log\frac{\mu}{m_h(s)} + \Delta_{\mathrm{fin}}(s), \\ \partial_s\mathcal{B}_L|_0 &= \partial_s\mathcal{B}_H|_0 + \frac{b_H - b_L}{8\pi^2}\kappa_h + \partial_s\Delta_{\mathrm{fin}}|_0\,, \qquad \kappa_h := \partial_s \log m_h|_0\,. \end{aligned} \tag{1596}$$

The coefficient of κ_h is a difference, because the threshold appears in the numerator of the first logarithm and in the denominator of the second. Equivalently,

$$d_L(\mu) = g_L^2(\mu, 0)\left[\frac{d_H(M)}{g_H^2(M, 0)} - \frac{b_H - b_L}{8\pi^2}\kappa_h - \partial_s\Delta_{\mathrm{fin}}|_0\right]. \tag{1597}$$

These formulas require that the background variation does not cross an endpoint threshold or change the active representations. They also require the heavy masses' scalar derivatives, which are not determined by the positivity of the master pairing.

A multiscale calculation must evolve a vector λ containing all relevant couplings, masses, Wilson coefficients, and field normalizations, including those controlling matter. Let $v = \partial_s\lambda|_0$. Within one effective theory, its tangent running and a general threshold map satisfy

$$\begin{gathered} \frac{\mathrm{d}\lambda}{\mathrm{d}t} = \boldsymbol{\beta}_{\mathrm{RG}}(\lambda, s), \qquad t = \log\mu, \quad \frac{\mathrm{d}v}{\mathrm{d}t} = D_\lambda\boldsymbol{\beta}_{\mathrm{RG}}\, v + \partial_s\boldsymbol{\beta}_{\mathrm{RG}}, \\ \lambda_L = \mathcal{T}_h(\lambda_H, \ell_h, s), \qquad \ell_h = \log\frac{\mu_h}{m_h(s)}, \\ v_L = D_\lambda\mathcal{T}_h\, v_H - \partial_{\ell_h}\mathcal{T}_h\,\kappa_h + \partial_s\mathcal{T}_h. \end{gathered} \tag{1598}$$

The threshold scale μ_h is fixed in this display. The explicit s derivative of $\mathcal{T}_h$ is taken at fixed λ_H and ℓ_h, so mass dependence must not be counted twice. Successive maps give the full chain of Jacobians and inhomogeneous terms. Finite counterterms, operator mixing, tadpole matching, and changes

of canonical fields belong in these maps. For a physical observable the final derivative is

$$\partial_s \mathcal{O}|_0 = D_\lambda \mathcal{O}\, v_{\mathrm{IR}} + \partial_s \mathcal{O}|_{\lambda,0}\,. \tag{1599}$$

Equations (1598)–(1599) are an all-orders organizational framework. Evaluating them at a given order requires the corresponding beta functions, threshold amplitudes, finite terms, and spectrum. They do not constitute a computation of every correction. In particular, an on-shell photon width may include charged-particle loop amplitudes and mixing that are absent from the direct tree vertex in (1592).

K.4. *Composite charges and independent material data.* For a stable neutral atom with fixed proton and neutron numbers Z, N, write its rest energy in natural units as

$$m_A(s) = Z m_p(s) + N m_n(s) + Z m_e(s) - B_A(s), \qquad \beta_A := \partial_s \log m_A|_0\,. \tag{1600}$$

Here B_A includes nuclear and electronic binding in a specified state. Differentiating gives the exact identity

$$m_A \beta_A = Z m_p \beta_p + N m_n \beta_n + Z m_e \beta_e - \partial_s B_A|_0\,. \tag{1601}$$

Every mass on the right is evaluated at the vacuum. This identity extends to molecules and solids by including their constituent rest energies and all binding contributions in the declared state. It does not replace the calculation of the binding derivative.

Proposition 140 (Bound-state scalar derivative). *At a fixed regulator, suppose $\mathcal{H}_A(s)$ is a differentiable self-adjoint family on a common domain with an isolated differentiable normalized eigenstate $|A(s)\rangle$. If its eigenvalue is the rest energy $m_A(s)$, then*

$$\partial_s m_A|_0 = \langle A(0)|\, \partial_s \mathcal{H}_A|_0\, |A(0)\rangle. \tag{1602}$$

Proof. Differentiate $\mathcal{H}_A|A\rangle = m_A|A\rangle$, multiply by $\langle A|$, and use self-adjointness. The terms containing $\partial_s|A\rangle$ cancel because $\langle A|\mathcal{H}_A = m_A\langle A|$. Normalization gives (1602). □

The operator derivative contains quark-mass, gluonic, electromagnetic, and other matched operators. Their nucleon and nuclear matrix elements, electromagnetic binding energies, and atomic responses are independent material information. An isolated-state hypothesis must be reconsidered for degeneracy, resonances, finite-temperature ensembles, or macroscopic material preparation. Light-dilaton phenomenology uses precisely this distinction between fundamental couplings and composite charges [50].

It is useful to separate a universal mass scale from dimensionless ratios. Choose a reference mass $m_{\rm ref}(s)$, and a sufficient set of independent dimensionless parameters $X_p(s)$, such that

$$\begin{aligned} m_A(s) &= m_{\rm ref}(s)\mathcal{M}_A(X(s)), \\ d_0 &= \partial_s \log m_{\rm ref}|_0\,, \qquad d_p = \partial_s \log X_p|_0\,, \\ \beta_A &= d_0 + \sum_p Q_A^p d_p, \qquad Q_A^p = \left.\frac{\partial \log \mathcal{M}_A}{\partial \log X_p}\right|_0, \\ \beta_A - \beta_B &= \sum_p (Q_A^p - Q_B^p) d_p. \end{aligned} \tag{1603}$$

For a reference mass constant in the Jordan frame, the conformal part of d_0 is $M_{\rm P} a_{\rm m}$; explicit mass dependence contributes as well. Changing the reference mass changes the decomposition, not the total Einstein-frame charge. Examples of the X_p's are the fine-structure constant and fermion-mass ratios to a hadronic scale. Gauge coupling slopes at a running scale must first be matched onto this dimensionless low-energy basis.

An equilibrium or nonequilibrium stochastic density is not by itself the isolated quantum eigenstate in Proposition 140. In particular, for a normalized stationary density p_s and a fixed reference measure,

$$\partial_s \int E(s,x) p_s(x)\,\mathrm{d}x = \int (\partial_s E) p_s\,\mathrm{d}x + \int E\,\partial_s p_s\,\mathrm{d}x. \tag{1604}$$

The second term generally survives in a nonequilibrium steady state and requires its own response calculation. Thus identifying the common stochastic scalar with a measured material mass derivative requires additional state preparation and quantum/material matching.

K.5. *A source-driven clock/force relation without a second fit.* Use colocated clock ratios to eliminate a common choice of time or mass unit. For two standards i, j, define independently calibrated dimensionless sensitivities and the scalar response by

$$\begin{aligned} K_{ij}^p &:= \left.\frac{\partial \log(\nu_i/\nu_j)}{\partial \log X_p}\right|_0, \qquad \Delta D_{ij} := \sum_p K_{ij}^p d_p, \\ y_{ij}(x) &:= \delta \log \frac{\nu_i(x)}{\nu_j(x)} = \Delta D_{ij} s(x) + O(s^2), \quad \Delta\beta_{AB} := \beta_A - \beta_B. \end{aligned} \tag{1605}$$

The universal conformal mass term cancels from both the clock ratio and the test-body charge difference. Atomic sensitivities K_{ij}^p and material coefficients Q_A^p must be supplied independently; precision frequency comparisons and their systematic corrections are discussed in [142]. A single rank-one clock cross spectrum cannot determine the absolute scalar normalization or the source charges by itself.

THEOREM 141 (Static clock/force comparison for one scalar). *Assume a single canonical scalar of mass m_φ, linear responses, unscreened sources and test bodies, negligible scalar backreaction, and a static field in the relevant laboratory region. Let r increase radially outward from a point source of mass m_S and charge β_S. Define a_A to be the positive* inward *acceleration, and let $\delta a_{AB;S}$ be its scalar-induced difference between test bodies A, B. Let $y_{ij;S}$ denote the source-induced clock-ratio change relative to its source-free or asymptotic value. With $\lambda_\varphi = \hbar/(m_\varphi c_{\rm light})$,*

$$\begin{aligned} s_S(r) &= -\frac{2\beta_S G_* m_S}{r c_{\rm light}^2} e^{-r/\lambda_\varphi}, \quad y_{ij;S}(r) = \Delta D_{ij} s_S(r), \\ \delta a_{AB;S}(r) &= \Delta\beta_{AB} c_{\rm light}^2 \partial_r s_S(r) = \frac{2\beta_S \Delta\beta_{AB} G_* m_S}{r^2}\left(1+\frac{r}{\lambda_\varphi}\right) e^{-r/\lambda_\varphi} \end{aligned} \tag{1606}$$

at the retained linear-field and leading weak-force order. In particular, without dividing by a possibly vanishing charge,

$$\boxed{\Delta\beta_{AB}\left(1+\frac{r}{\lambda_\varphi}\right) y_{ij;S}(r) + \Delta D_{ij}\frac{r\,\delta a_{AB;S}(r)}{c_{\rm light}^2} = 0.} \tag{1607}$$

When the displayed denominator is nonzero, the equivalent ratio is

$$\frac{y_{ij;S}(r)}{r\,\delta a_{AB;S}(r)/c_{\rm light}^2} = -\frac{\Delta D_{ij}}{\Delta\beta_{AB}}\frac{1}{1+r/\lambda_\varphi}. \tag{1608}$$

Proof. The point-particle coupling is $-\beta_S m_S\varphi/M_{\rm P}$. The static Green function of $\Delta - m_\varphi^2$, with vanishing asymptotic source field, gives $s_S = -\beta_S m_S e^{-m_\varphi r}/(4\pi M_{\rm P}^2 r)$ in natural units. Equation (1584) and restoration of laboratory units give the first line of (1606). The scalar potential energy per unit test mass is $\beta_A c_{\rm light}^2 s_S$, so its positive inward acceleration is $\beta_A c_{\rm light}^2 \partial_r s_S$. Taking the difference gives the second line. Finally $\partial_r s_S = -(1+r/\lambda_\varphi)s_S/r$; elimination of the source field proves both comparison formulas. □

The point-source amplitude relation has a useful local extension. For an extended unscreened source, the field is the linear Yukawa integral over its scalar charge density. If clock and force channels probe the same field and spatial derivative, the inward component still satisfies

$$\boxed{\Delta D_{ij}\,\delta a_{AB;S} - \Delta\beta_{AB} c_{\rm light}^2 \partial_r y_{ij;S} = 0.} \tag{1609}$$

For general geometry, ∂_r denotes the specified outward measurement direction, with inward acceleration defined oppositely. For finite spatial sampling or different instrument kernels, the same source integral must be evaluated with each known kernel before applying a comparison. Replacing an extended source by a point mass without a justified geometric approximation is insufficient.

Once the scalar mass, coupling functions, threshold matching, and material sensitivities have been fixed independently, these identities predict the second measurement without a new source coupling fit. Even when those charges are not known, two sources S, T interrogated with the same test pair and clock pair obey the charge-independent consequence

$$\delta a_{AB;S}\,\partial_r y_{ij;T} - \delta a_{AB;T}\,\partial_r y_{ij;S} = 0 \tag{1610}$$

at the stated order and after the sampling corrections. This cross-multiplied form remains meaningful when one response vanishes. For weak scalar forces, if $\eta^{\mathrm{sgn}}_{AB;S} = 2(a_A - a_B)/(a_A + a_B)$ and g_S is the independently calibrated tensor inward acceleration ($g_S = G_* m_S/r^2$ for a point source), then $\eta^{\mathrm{sgn}}_{AB;S} g_S = \delta a_{AB;S}$ at leading order. Thus the cross-source identity can also be tested with signed equivalence-principle measurements and spatial clock-ratio profiles. Screening, extra scalar modes, environment-dependent charges, or unmatched instrumental common modes change the premises.

K.6. *Signal ranges and remaining free parameters.* The preceding identities eliminate a source amplitude, but do not predict a strictly positive laboratory signal interval. A common weight may be constant: $w(\sigma) = w_*$ is positive and gives $c = \gamma_a = a_{\mathrm{m}} = 0$. Even when this point is excluded, the equal-weight family $c_n \to 0$, with a fixed positive matched scalar mass, stays within the same local low-energy branch and has

$$\begin{aligned} &Z_n = 1 + \frac{3}{2} c_n^2 M_{\mathrm{P}}^2, \qquad \alpha_n = \frac{c_n^2 M_{\mathrm{P}}^2}{2 Z_n} \longrightarrow 0, \quad \frac{\Gamma_{\gamma\gamma,n}}{m_\varphi^3} = \frac{c_n^2}{64\pi Z_n} \longrightarrow 0, \\ &d_p = O(c_n M_{\mathrm{P}}), \qquad \beta_A = O(c_n M_{\mathrm{P}}), \quad y_{ij;S},\ \delta a_{AB;S} = O(c_n^2 M_{\mathrm{P}}^2). \end{aligned} \tag{1611}$$

The last line assumes a smooth matched family with no independent scalar matter couplings that survive $c_n \to 0$, and fixed source mass and geometry. It supplies an explicit counterexample to a strictly positive minimum source-driven signal. The mass can be held fixed by varying the positive local quadratic matching coefficient continuously; no lower bound on c follows from the displayed vacuum conditions.

A stochastic or coherent ambient scalar signal has the additional free field amplitude or power spectrum, which can also vanish. A short Compton wavelength suppresses finite-distance source signals, while $\Delta D_{ij} = 0$ or $\Delta\beta_{AB} = 0$ removes the corresponding channel. An independently selected nonzero coupling and mass, actual source geometry, renormalized matter matching, and calibrated clock/material sensitivities are therefore needed for an absolute signal forecast. Upper bounds from experiments or from a controlled hierarchy can restrict this parameter space; they do not establish a nonzero lower endpoint.

The source comparisons above are conditional falsifiable relations across measured channels, with the same physical scope as other matched single-dilaton theories.

Appendix L. Microscopic inputs, effective restrictions, and identifiable predictions

A common functional becomes predictive only when its coefficients and its physical interpretation are fixed. It is useful to distinguish three questions. Which quantities follow from a specified microscopic package? Which effective theories are excluded by the resulting relations? Which unmeasured observable is already determined by an independent calibration? The last question can sometimes be answered without identifying every microscopic parameter. This appendix gives exact finite criteria for all three questions, without changing the master configuration or adding an independent force term.

L.1. *Inputs and consequences of the declared package.* At fixed regulator, let p label a microscopic package. The package includes the action and residual pairing, the reference measure, mobility, admissible controls, boundary and initial conditions, and the map to physical observables. Fixing such a package means assigning these data before the target observations are used. It does not mean that the variational equations have derived the data themselves. For instance, varying a field-dependent pairing produces its field derivative; it does not select that pairing from all positive forms.

Table 31 does not introduce separate sectorwise dynamics. It identifies the shared data on which the joint dynamics depend. In particular, an invariant density does not fix a mobility or a physical clock. The explicit response reconstruction in Paper III uses time-lagged data to supply that missing information. An independently specified outer selection problem could determine some of these inputs, but the derivatives and comparison normalization of Appendix J must then be included.

L.2. *A strict restriction inside an effective theory.* Use the signed slopes of (1590) and introduce dimensionless coefficients $u = M_{\mathrm{P}} a_{\mathrm{m}}$ and $v_I = M_{\mathrm{P}} \gamma_I$. On the common-weight branch with constant Jordan elementary masses, the local restriction is

$$\mathcal{C} = \{(u, v_1, \dots, v_k) : v_I = 2u \text{ for every } I\}. \tag{1612}$$

The ambient coefficient space allows these $k+1$ slopes to vary independently; $\mathcal{C}$ has dimension one and codimension k. Positive scalar-dependent weights do not impose (1612): exponentials with different slopes give admissible nearby counterexamples. For one photon channel, the choices $(u, v) = (u, 2u)$ and $(u, 4u)$ with $u \neq 0$ have the same leading scalar force strength and different

Table 31. Dependence of physical quantities on the regulated package. "Derived" always refers to the fixed premises in the same row.

Quantity	Consequence available	Input or selection still required
Group and matter content	Covariance and anomaly constraints	Candidate algebra, representations and comparison class
Curvature weights	Relative restrictions for the simple-algebra hypothesis of Appendix K	Present product-factor weights and their scalar dependence
Residual metric	Coupled Euler derivatives and positivity tests	Allowed cross blocks and their coefficient functions
Equilibrium law	Normalized Gibbs law when integrable	Action, reference measure, noise scale and boundary domain
Stochastic dynamics	Generator and selected feedback under well-posedness and control hypotheses	Mobility, reversible drift, controls and physical time calibration
Nonlinear cost	Feedback equations for the chosen κ	Value and units of κ, and the implemented control mechanism
Particle couplings	Running and threshold-matched responses	Spectrum, renormalized boundary data, scalar vacuum and normalization
Material charges	Mass derivatives including binding	Composition, nuclear response and thermodynamic state
Fluid observables	Projected coefficients if generator closure holds	Observation map, scale separation and constitutive identification
Quantum observables	Conditional reconstruction and detector response	Physical correlations, state and measurement operations
Signal amplitude	Forward prediction after the preceding matching	Source or ambient population, geometry and calibrated detector response

direct photon widths. In fact,

$$\alpha_{\varphi} = 2u^2, \qquad \frac{32\pi M_{\mathrm{P}}^2 \Gamma_{\gamma\gamma}}{\alpha_{\varphi} m_{\varphi}^3} = \frac{v^2}{4u^2}. \tag{1613}$$

The two choices give one and four, respectively. Thus the common-weight branch excludes part of the ambient effective theory. The effective theory still contains the branch: no impossibility of effective-theory representation follows. Moreover, a squared width does not distinguish $v = 2u$ from $v = -2u$; testing the signed relation requires a signed interference or response observable.

This restriction is conditional on the common weight. The current product-algebra model has not independently selected it. The stronger claim of a restriction of the entire mother-model family would require showing that every selected physical package belongs to this branch.

PROPOSITION 142 (Transport of an effective constraint). *Let $\mathcal{C} = \{p : R(p) = 0\}$ be a regular codimension-k submanifold, so that DR has rank k on $\mathcal{C}$. If the matching map T is a local diffeomorphism on the parameter neighborhood under consideration, then its image obeys the codimension-k constraint*

$$\widetilde{R}(c) = R(T^{-1}(c)) = 0, \qquad D\widetilde{R} = DR\,[DT]^{-1}. \tag{1614}$$

Proof. Composition gives the zero set exactly on the selected local branch. Multiplication on the right by an invertible matrix preserves row rank. The implicit function theorem gives the stated codimension. □

A smooth renormalization-group flow over a finite interval is locally invertible when the forward and backward solutions exist uniquely on that interval. A threshold map need not be invertible after heavy data have been discarded. In that case the admissible low-energy set is the image $T(\mathcal{C})$, and its restriction must be computed anew. For example, observing only u maps both the line $v = 2u$ and the full (u, v) plane onto the same real line. A microscopic restriction can therefore be real but invisible to a particular experiment.

L.3. *Predicting an observable without identifying every parameter.* Let K be the admissible parameter set, let $F : K \to \mathcal{Y}$ be the independently calibrated observable map, and let $Q : K \to \mathcal{Z}$ be the target. Parameters that give the same calibration lie in the same fiber $F^{-1}(y)$. These are physical degeneracies of the chosen measurement, not failures of numerical optimization.

PROPOSITION 143 (Prediction on calibration fibers). *There is a single-valued prediction $q : F(K) \to \mathcal{Z}$ satisfying $Q = q \circ F$ if and only if*

$$F(p) = F(p') \quad \Longrightarrow \quad Q(p) = Q(p') \quad (p, p' \in K). \tag{1615}$$

For a scalar target and any nonempty calibration fiber with bounded target values, every point prediction based only on that calibration has worst-case absolute error at least

$$\frac{1}{2}\left[\sup_{p \in F^{-1}(y)} Q(p) - \inf_{p \in F^{-1}(y)} Q(p)\right]. \tag{1616}$$

Proof. If the factorization exists, equal values of F give equal values of Q. Conversely define $q(y) = Q(p)$ for any p with $F(p) = y$; (1615) makes this independent of the choice. For two target values a, b on the fiber and any reported value z, $|a - b| \le |a - z| + |b - z|$. Taking suprema gives the lower bound, including when the endpoints are approached but not attained. □

This set-theoretic factorization alone does not guarantee continuity or robustness. In a constant-rank coordinate neighborhood, smoothness gives a useful local criterion. By the constant-rank theorem, F is equivalent to projection onto coordinates x with unobserved coordinates z. If

$$\ker DF(p) \subseteq \ker DQ(p) \tag{1617}$$

throughout that neighborhood, then $\partial_z Q = 0$ and $Q = q(x)$ there. Conversely a differentiable factorization implies the kernel inclusion by the chain rule. For a global statement, disconnected fiber components must also give the same value; the differential criterion alone cannot compare them. For example, $F(p) = p^2$ and $Q(p) = p$ have a sign ambiguity away from zero even though DF is locally invertible.

The common-weight example is immediate. Calibration of u fixes the prediction $v = 2u$ on $\mathcal{C}$. In the unrestricted effective theory the same calibration leaves v arbitrary. If only a squared force measures u^2, a signed target still has a sign ambiguity. This is why the type of calibration matters as much as its precision.

L.4. *Finite uncertainty and a sufficient measurement design.* For observed calibration y, define a nonempty compatibility set

$$K_y = \{p \in K : \|F(p) - y\|_{\mathrm{cal}} \le \epsilon_{\mathrm{cal}}\}. \tag{1618}$$

If K_y is compact, Q is continuous, and the physical matching error is bounded by a continuous $r(p) \ge 0$, a conservative target interval is

$$I_Q(y) = \left[\min_{p \in K_y}(Q(p) - r(p)), \quad \max_{p \in K_y}(Q(p) + r(p))\right]. \tag{1619}$$

It has the calibration coverage conditional on the asserted model-error bound. Disjointness from a separately constructed observational interval rejects at least one premise. Agreement does not establish uniqueness of the microscopic explanation.

In an exactly linear finite model, $F(p) = Ap$ and $Q(p) = Bp$ for unrestricted $p \in \mathbb{R}^d$, the fiber condition becomes

$$\ker A \subseteq \ker B \quad \Longleftrightarrow \quad B = LA \text{ for some } L. \tag{1620}$$

Here A^+ denotes the Moore–Penrose inverse. To verify the equivalence, take the orthogonal decomposition into $\ker A$ and its complement. The condition gives $B = BA^+A$, so $L = BA^+$ works; the reverse implication is immediate. If a vector n satisfies $An = 0$ but $Bn \neq 0$, then $p + tn$ gives the same calibration and different predictions. If instead $Bn = 0$ for all such vectors, the target can be known even though p is not. Additional calibration channels need only remove the null directions visible to B.

The calibration and validation covariance calculation in Paper V implements this criterion with independent data. Paper III supplies a finite example in which a covariance and one physical lag identify the entire reversible drift and mobility. Paper II follows constraints through thresholds. Paper IV distinguishes observable completeness from classical equilibrium information. These are different applications of the same requirement: fix the shared data relevant to the target, then propagate them without selecting new target-dependent coefficients.

Appendix M. Dynamic programming and adjoint selection for the common cost

The variational proposal has two distinct tasks. It specifies a physical package, and it selects a controlled evolution within that package. A selection theorem addresses the second task; it determines the first only when a separate, normalized comparison of packages is supplied. This appendix connects dynamic programming to the stochastic maximum principle for one fixed regulated model. It also identifies the extra state required by the density-dependent score in the joint residual.

Dynamic programming assigns a value to every possible current state and remaining time. The maximum principle describes variations around an optimal trajectory through a backward adjoint equation. Both methods refer to the same objective and admissible controls. Their agreement is a consistency requirement, not two independent physical postulates. The underlying control results are classical [68], [127], and [168]; the role here is to specify their application to the common residual, rather than to claim their invention.

M.1. *State, information, and admissibility.* Fix the regulator, a constraint-compatible coordinate chart, and physical units. Write $X \in \mathbb{R}^d$ for the resulting state and $u \in U$ for the control. In the first part, U is a fixed compact subset of $\mathbb{R}^m$. The filtration is the completed Brownian filtration, possibly augmented by an independent initial state. Controls are progressively measurable. In particular, a control cannot use a future noise realization. Consider

$$dX_s = b(s, X_s, u_s)\, ds + \Sigma(s, X_s)\, dW_s,$$
$$J(t, x; u) = \mathbb{E}_{t,x}\left[\int_t^T \ell(s, X_s, u_s)\, ds + g(X_T)\right], \qquad V(t, x) = \inf_u J(t, x; u). \tag{1621}$$

The diffusion is initially control independent. Assume continuous coefficients, uniform Lipschitz bounds in the state, linear growth of the state coefficients, and sufficient moment bounds for the stated costs and derivatives. These assumptions give a unique nonexplosive strong state process and permit the

expectations below. Smoothness of V is an additional assumption when classical differentiation is used.

The admissible family is closed under restriction and pasting at the deterministic times used below. Assume measurable, arbitrarily nearly optimal continuation policies can be selected as a function of the state; standard measurable-selection versions of dynamic programming provide this step under their stated hypotheses [68]. Unbounded controls, stopping, partial observation and random environments require the corresponding admissibility, boundary or state augmentation. They are not included merely by retaining the same symbols.

M.2. *The common residual and its derivatives.* For a prescribed external density curve, or a declared finite Markov augmentation containing all required statistics, let

$$q = R(t,x,u)^T H(t,x,u) R(t,x,u), \qquad \ell = \varphi_\kappa(q), \qquad H = H^T \succ 0. \quad (1622)$$

Here R denotes the dimensionally normalized joint residual in the chosen realization. This includes its allowed cross blocks. For any state or control coordinate ζ,

$$\partial_\zeta \ell = \frac{e^{\kappa q}}{4}\left(2(\partial_\zeta R)^T H R + R^T(\partial_\zeta H)R\right). \quad (1623)$$

The expression remains valid at $\kappa = 0$. Thus the adjoint uses the metric derivative as well as the residual derivative. A positive residual metric does not by itself make ℓ convex in the state. If H is control independent and $R = r + Bu$, then q is convex in u and φ_κ is increasing and convex for $\kappa \geq 0$; in that particular slice their composition is convex. Nonlinear residuals and control-dependent metrics require a fresh Hessian calculation.

Finiteness of the regulator does not guarantee integrability of an exponential cost. If Z is a centered Gaussian with variance $s^2 > 0$, direct completion of the Gaussian exponent gives

$$\mathbb{E}e^{\kappa Z^2} = (1 - 2\kappa s^2)^{-1/2} \quad \text{if } 2\kappa s^2 < 1; \qquad \mathbb{E}e^{\kappa Z^2} = \infty \quad \text{otherwise.} \quad (1624)$$

Also $\mathbb{E}e^{\kappa Z^4} = \infty$ for every $\kappa > 0$, because the positive quartic exponent dominates the Gaussian quadratic decay. An exponential branch therefore needs bounded residuals on an invariant domain, or an independently proved exponential-moment estimate. The exact quadratic construction in Paper III uses $\kappa = 0$. Exponentiating an instantaneous residual and then taking an expectation is different from exponentiating the accumulated path cost. Only the latter, logarithmic risk-sensitive criterion produces its usual extra quadratic value-gradient term after transformation.

M.3. *Dynamic programming and verification.* For $t < s < T$, conditioning at s and using the Markov state gives

$$V(t,x) = \inf_u \mathbb{E}_{t,x}\left[\int_t^s \ell(r, X_r, u_r)\, dr + V(s, X_s)\right]. \tag{1625}$$

Indeed, every continuation costs at least $V(s, X_s)$, which proves one inequality after taking the initial infimum. Conversely paste an ϵ-optimal measurable continuation onto an arbitrary initial control. Its conditional excess is at most ϵ; take the initial infimum and let $\epsilon \downarrow 0$. Closure under pasting and the measurable continuation assumption are the substantive information conditions in this argument.

Define the dynamic-programming Hamiltonian by

$$h(t,x,u,p,P) = \ell(t,x,u) + b(t,x,u)\cdot p + \tfrac{1}{2}\operatorname{tr}(\Sigma\Sigma^T(t,x)P). \tag{1626}$$

For a classical value, the short-time form of (1625) and Itô's formula give

$$V_t + \inf_{u\in U} h(t,x,u,DV,D^2V) = 0, \qquad V(T,x) = g(x). \tag{1627}$$

This step uses continuity and local moment control to pass from the short-time expected generator to its value at (t,x). When derivatives are absent, a viscosity formulation replaces this classical equation; the differentiations below are then not asserted.

Proposition 144 (Verification and a quantitative policy bound). *Let $W \in C^{1,2}$ have the growth and integrability needed for Itô's formula under every admissible control being compared. Suppose throughout the domain*

$$|W(T,x) - g(x)| \le \epsilon_T, \qquad \left|W_t + \inf_u h(t,x,u,DW,D^2W)\right| \le \epsilon. \tag{1628}$$

Suppose an admissible feedback $\widehat{u}$ has Hamiltonian excess at most $\delta \ge 0$ over that infimum. Then

$$\begin{aligned} W - \epsilon_T - (T-t)\epsilon \le V \le J(\widehat{u}) \le W + \epsilon_T + (T-t)(\epsilon+\delta),\\ 0 \le J(\widehat{u}) - V \le 2\epsilon_T + (T-t)(2\epsilon+\delta). \end{aligned} \tag{1629}$$

All values in the first line start at (t,x).

Proof. Writing $\mathcal{L}^u$ for the controlled generator, integration of Itô's formula gives the exact identity

$$\begin{aligned} J(t,x;u) - W(t,x) = \mathbb{E}_{t,x}[g(X_T) - W(T,X_T)]\\ + \mathbb{E}_{t,x}\int_t^T (W_t + \mathcal{L}^u W + \ell)(s, X_s)\, ds. \end{aligned} \tag{1630}$$

The stochastic integral has zero mean under the stated integrability assumption. For every control the integrand is at least $-\epsilon$. For $\widehat{u}$ it is at most $\epsilon + \delta$. Apply the terminal bound and take the infimum for the first inequality. Subtracting

the lower bound for V from the upper bound for $J(\widehat{u})$ gives the second line. Exact zero residual, terminal error and selection error prove optimality without assuming joint convexity of the state problem. □

A residual measured only on a mesh is not the uniform bound in (1628). It needs an interpolation estimate or an independent enclosure between nodes. A stopped computation also needs its boundary discrepancy and exit contribution in (1630). A small mean residual alone gives no such certificate.

M.4. *First variation and the stochastic adjoint.* Assume now a convex U, differentiable data with square-integrable linearizations, and an optimal control u_*. For an admissible comparison v, set $u^\varepsilon = u_* + \varepsilon(v - u_*)$. The state derivative $\xi = \partial_\varepsilon X^\varepsilon|_0$ satisfies

$$d\xi = (b_x\xi + b_u(v - u_*))\,dt + \sum_{k=1}^{r} \Sigma_x^k \xi\, dW^k, \qquad \xi_t = 0. \tag{1631}$$

Coefficients are evaluated on (X_*, u_*), and Σ^k is the kth diffusion column. Define the minimization-convention adjoint Hamiltonian

$$\mathscr{H}(t, x, u, p, Z) = \ell(t, x, u) + p \cdot b(t, x, u) + \sum_{k=1}^{r} Z^k \cdot \Sigma^k(t, x). \tag{1632}$$

For a well-posed square-integrable backward equation, take

$$dp = -\left(\ell_x + b_x^T p + \sum_k (\Sigma_x^k)^T Z^k\right) dt + Z\, dW, \qquad p_T = Dg(X_T). \tag{1633}$$

This is called a maximum principle historically, although our Hamiltonian uses minimization signs throughout.

Proposition 145 (Variational identity and conditional sufficiency). *Under the preceding differentiability and integrability assumptions,*

$$DJ(u_*)[v - u_*] = \mathbb{E}\int_t^T (\ell_u + b_u^T p) \cdot (v - u_*)\, ds \geq 0. \tag{1634}$$

If, in addition, g is convex, $\mathscr{H}(s, \cdot, \cdot, p_s, Z_s)$ is jointly convex in (x, u) almost everywhere, and the candidate satisfies the pointwise control variational inequality, it is globally optimal.

Proof. Differentiation under expectation gives $DJ = \mathbb{E}[Dg(X_T)\cdot\xi_T + \int(\ell_x \cdot \xi + \ell_u \cdot (v - u_*))ds]$. The product rule for $p \cdot \xi$ gives drift

$$-\ell_x \cdot \xi + p \cdot b_u(v - u_*). \tag{1635}$$

The terms containing b_x cancel. The quadratic covariation $\sum_k Z^k \cdot \Sigma_x^k \xi$ cancels the corresponding adjoint drift. Integrating and substituting gives (1634).

Localized adapted choices of v give the pointwise normal-cone condition when admissible variations allow them.

For sufficiency compare any admissible (X,u) with the candidate and write $\Delta X = X - X_*$. Convexity of the terminal cost gives $g(X_T) - g(X_{*,T}) \geq p_T \cdot \Delta X_T$. Apply the same product rule without linearizing the state difference. Then

$$\begin{aligned} J(u) - J(u_*) &\geq \mathbb{E}\int_t^T \big[\mathscr{H}(X,u,p,Z) - \mathscr{H}(X_*,u_*,p,Z) \\ &\qquad - \mathscr{H}_x(X_*,u_*,p,Z)\cdot\Delta X\big]\,ds \qquad (1636) \\ &\geq \mathbb{E}\int_t^T \mathscr{H}_u(X_*,u_*,p,Z)\cdot(u-u_*)\,ds \geq 0. \end{aligned}$$

The second inequality uses joint convexity, not merely control convexity. □

M.5. *How the two Hamiltonian methods agree.* Suppose $V \in C^{1,3}$, the optimal selector is smooth and interior, and the required derivatives, Itô formula and adjoint uniqueness hold. At an optimal trajectory define

$$p_s = DV(s,X_s), \qquad Z_s = D^2V(s,X_s)\Sigma(s,X_s). \qquad (1637)$$

Differentiate (1627) in x. The derivative of the selector vanishes by its first-order minimizing condition. Componentwise,

$$\frac{1}{2}\partial_{x_i}\operatorname{tr}(\Sigma\Sigma^T D^2V) = \frac{1}{2}\operatorname{tr}(\Sigma\Sigma^T\partial_{x_i}D^2V) + \sum_k(\partial_{x_i}\Sigma^k)^T D^2V\Sigma^k. \qquad (1638)$$

Itô's formula for $DV(s,X_s)$ now yields precisely (1633), including the state-dependent diffusion term. The terminal condition follows from $V(T) = g$. Uniqueness identifies the two adjoints. A value martingale has coefficient $\Sigma^T DV$, which is an r-vector; the adjoint martingale has coefficient $D^2V\Sigma$, which is a $d \times r$ matrix. They are distinct objects.

Substitution of (1637) does not make h and $\mathscr{H}$ identical: the trace contribution to $\mathscr{H}$ is $\operatorname{tr}(\Sigma\Sigma^T D^2V)$, while that of h has a factor $1/2$. For control-independent diffusion these terms do not affect their common control minimizer. Adjoint differentiation holds p, Z fixed; it must not differentiate the substituted identity as if Z were an independent state function inside $\mathscr{H}_x$.

M.6. *A control-dependent noise counterexample.* If Σ depends on the control, first-order convex variations add $\sum_k(\Sigma_u^k)^T Z^k$ to (1634). For nonconvex control sets, spike variations also require a second adjoint [127]. The following scalar example shows why this matters. Let $X_0 = 0$, $dX = u\,dW$, $U = \{0,1\}$, terminal cost $X_T^2/2$, and running cost $-cu^2$, where $0 < c < 1/2$. Itô isometry gives

$$J(u) = (1/2 - c)\mathbb{E}\int_0^T u_s^2\,ds \geq 0. \qquad (1639)$$

The optimum is $u_* = 0$. On that trajectory $p = Z = 0$, so the first-adjoint Hamiltonian is $-cu^2$, whose global minimizer is instead $u = 1$. The missing second-adjoint correction is $\frac{1}{2}u^2$; its addition recovers the positive coefficient $1/2 - c$. Equivalently the HJB trace already contains this term. Thus globally minimizing only the first adjoint Hamiltonian would select the wrong control.

Changing diffusion can also change quadratic variation and make path laws singular. The drift-only Girsanov relative-entropy formula cannot be extended to arbitrary diffusion controls without a separate equivalence argument. The cost-mobility example in Paper III keeps its diffusion fixed.

M.7. *Self-consistent laws and the missing density derivative.* The joint score depends on the actual law. Replacing that law by an external curve changes the optimization problem. An exact finite alternative uses a controlled n-state Markov chain with population law p, row generator $Q(p, u)$ and forward velocity

$$\dot{p} = F(p, u) := Q(p, u)^T p, \qquad L(p, u) = \sum_{i=1}^{n} p_i \ell_i(p, u). \tag{1640}$$

Here u denotes the complete vector of transition controls, selected as a function of time and the population law. Off-diagonal rates are nonnegative, row sums vanish, and exit rates are bounded by Λ. For positive initial probabilities, $\dot{p}_i \geq -\Lambda p_i$ implies $p_i(t) \geq p_i(0)e^{-\Lambda t}$. Thus logarithmic scores and their derivatives remain defined on each finite horizon.

With terminal law cost $G(p)$, the value $\mathcal{W}(t, p)$ obeys, under the corresponding deterministic dynamic-programming hypotheses,

$$\mathcal{W}_t + \inf_u \{L(p, u) + D_p \mathcal{W} \cdot F(p, u)\} = 0, \qquad \mathcal{W}(T, p) = G(p). \tag{1641}$$

The simplex has only $n-1$ independent coordinates. Ambient derivatives below mean a smooth extension; adding a multiple of the all-ones vector to a covector has no effect on a tangent velocity. Define $\mathscr{K} = L + \lambda \cdot F$. The adjoint equation and control condition are

$$\dot{\lambda} = -L_p - (D_p F)^T \lambda, \quad \lambda_T = D_p G, \quad \mathscr{K}_u \cdot (v - u_*) \geq 0. \tag{1642}$$

The full cost derivative is

$$\partial_{p_j} L = \ell_j + \sum_i p_i \partial_{p_j} \ell_i, \qquad D_p F[\eta] = Q^T \eta + (D_p Q[\eta])^T p. \tag{1643}$$

The second term in $\partial_{p_j} L$ includes the score derivative, the metric derivative and every declared density-dependent cross block. It is absent in an optimization for a single agent against a frozen population. Omitting it therefore changes the objective's first variation.

The deterministic product rule for $\lambda \cdot \delta p$ proves (1642) exactly as above, without a martingale term because this population law has no common noise. A

smooth interior minimizer gives $\lambda = D_p \mathcal{W}$ by differentiating (1641). Convexity of the joint Hamiltonian and terminal cost supplies a sufficient condition; in its absence these adjoint conditions are necessary only. A Bellman residual bound supplies the alternative verification route. Common noise would make the conditional law stochastic and require a different lifted generator.

M.8. *A nonlinear population calculation with the full score.* Take three cyclically indexed states, $p(0) = (.25, .35, .40)$, $\pi = (.2, .3, .5)$, $T = 1.2$, and $|u_i| \le .4$. Set the forward and backward cyclic rates to $1 + .1p_i + .2u_i$ and .6, respectively, and choose the diagonal rates so that each row sums to zero. The largest exit rate is at most 1.78. Use

$$\begin{aligned} s_i &= \log(p_i/\pi_i) - \log(p_{i-1}/\pi_{i-1}), \quad R_i = (.3(i-2), u_i, s_i)^T, \\ H_i &= \begin{pmatrix} 1 + .2p_i & .05 & .1 \\ .05 & 1.5 & .08 \\ .1 & .08 & 1 + .1p_i \end{pmatrix}, \quad L = \sum_i p_i \varphi_{.12}(R_i^T H_i R_i), \\ G(p) &= .1 \sum_i p_i \log(p_i/\pi_i). \end{aligned} \tag{1644}$$

Strict diagonal dominance with positive diagonal entries proves $H_i \succ 0$. Positivity of the law on the finite horizon bounds the logarithms, and the compact control box then bounds the exponential cost. All coefficients and data are dimensionless synthetic inputs.

The numerical control class has six equal time intervals and three constant controls on each interval. Forward probability integration and backward adjoint integration give the exact derivative of this 18-parameter continuous-time objective, up to ODE error. Eight centered directional finite differences agree with the adjoint gradient to 1.02×10^{-11} absolute error. At the initial law and zero control, the directional derivative in direction $(1, -1, 0)$ is 0.16412989; retaining only the outer probability weights gives 0.06785744. The difference is the density response of the running cost.

A bounded quasi-Newton iteration lowers the cost from 0.11503781 at zero control to 0.11286338. Its projected-gradient infinity norm is 3.40×10^{-10}. Normalization error on 121 retained times is 4.45×10^{-16}, and the smallest retained probability is .25. These facts identify a stationary numerical candidate in the stated piecewise-constant class. They do not prove a global minimum of this nonlinear law-control problem or of the larger adapted-control class.

M.9. *Continuous symmetries and a stochastic Noether identity.* A continuous symmetry compares nearby states without changing the running dynamics or its cost. In deterministic mechanics its associated charge may be constant along a trajectory. In a stochastic control problem the corresponding statement is generally a local-martingale identity. This distinction is established in the

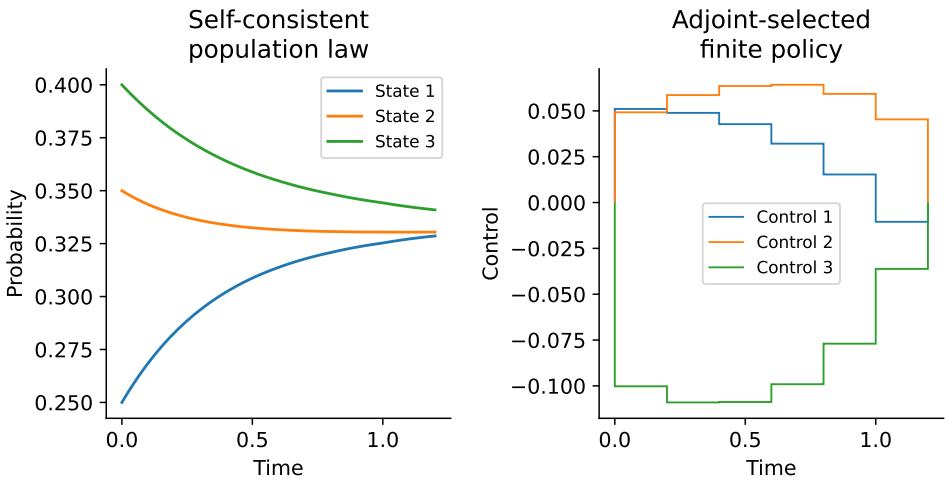


Figure 57. A dimensionless self-consistent three-state calculation. The probability law evolves with the selected transition controls, while its logarithmic score enters the same running cost. The plotted policy is a stationary candidate in a finite control class; the independent quadratic construction in Paper III supplies the global verification example.

stochastic Noether literature; contact symmetries of the Bellman equation provide a broader formulation [58]. The following direct calculation is a restricted version adapted to the common residual and its adjoint.

Let $\mathsf{A}, \mathsf{B}, \mathsf{R}$ be constant skew-symmetric matrices acting respectively on state, control and Brownian coordinates. Assume that $e^{\varepsilon \mathsf{B}} U = U$ and that the state domain, admissible variations and noise law respect the stated transformations. The diffusion remains control independent. At each time require

$$\begin{aligned} b(t, e^{\varepsilon \mathsf{A}} x, e^{\varepsilon \mathsf{B}} u) = e^{\varepsilon \mathsf{A}} b(t, x, u), \quad \Sigma(t, e^{\varepsilon \mathsf{A}} x) = e^{\varepsilon \mathsf{A}} \Sigma(t, x) e^{-\varepsilon \mathsf{R}}, \\ \ell(t, e^{\varepsilon \mathsf{A}} x, e^{\varepsilon \mathsf{B}} u) = \ell(t, x, u). \end{aligned} \tag{1645}$$

The Brownian rotation is essential for an isotropic additive diffusion: the coefficient matrix need not be unchanged with its noise columns held fixed, although the diffusion law is rotation covariant.

Theorem 146 (Adjoint symmetry balance). *Suppose the differentiability and adjoint assumptions above hold. Suppose the optimal control satisfies first-order stationarity along every admissible two-sided symmetry orbit. Assume either* $\mathsf{R} = 0$, *or the smooth Bellman identification* $Z = D^2 V \Sigma$ *holds. Then*

$$\mathcal{C}_t = p_t^T \mathsf{A} X_t, \qquad d\mathcal{C}_t = \mathcal{N}_t \cdot dW_t, \qquad \mathcal{N}_t = Z_t^T \mathsf{A} X_t + \Sigma_t^T \mathsf{A}^T p_t. \tag{1646}$$

Thus $\mathcal{C}$ is a local martingale. If $\mathbb{E}|\mathcal{C}_0| < \infty$ and $\mathbb{E}\int_0^T |\mathcal{N}_t|^2 dt < \infty$, it is a true martingale and $\mathbb{E}\mathcal{C}_t = \mathbb{E}\mathcal{C}_0$. If $\mathcal{C}_0$ is also square integrable, then

$$\mathbb{E}(\mathcal{C}_t - \mathcal{C}_0)^2 = \mathbb{E}\int_0^t |\mathcal{N}_s|^2 ds. \tag{1647}$$

Proof. Differentiating (1645) at zero gives

$$b_x \mathsf{A}x + b_u \mathsf{B}u = \mathsf{A}b, \qquad \Sigma_x[\mathsf{A}x] = \mathsf{A}\Sigma - \Sigma\mathsf{R}, \qquad \ell_x \cdot \mathsf{A}x + \ell_u \cdot \mathsf{B}u = 0. \tag{1648}$$

Use the Itô product rule on $p^T \mathsf{A}X$. In addition to the two drift terms it contains the quadratic covariation $\mathrm{tr}(Z^T \mathsf{A}\Sigma)dt$. Substitution of the adjoint gives the drift

$$\begin{aligned} p \cdot (\mathsf{A}b - b_x \mathsf{A}x) + \mathrm{tr}\{Z^T(\mathsf{A}\Sigma - \Sigma_x[\mathsf{A}x])\} - \ell_x \cdot \mathsf{A}x \\ = \mathscr{H}_u \cdot \mathsf{B}u + \mathrm{tr}(Z^T \Sigma \mathsf{R}). \end{aligned} \tag{1649}$$

The first term vanishes by stationarity along the two-sided orbit; this needs only feasible orbit variations, not an unconstrained control. The second vanishes if $\mathsf{R} = 0$. Otherwise $Z^T\Sigma = \Sigma^T D^2 V \Sigma$ is symmetric and R is skew-symmetric, so their trace product is zero. The remaining stochastic coefficient is $\mathcal{N}$. Localization proves the local-martingale statement, and the stated integrability removes the localization. Itô isometry proves (1647). □

The balance also identifies what breaks the symmetry. Without imposing (1645), define

$$\begin{aligned} &\delta b = \mathsf{A}b - b_x \mathsf{A}x - b_u \mathsf{B}u, \quad \delta\Sigma = \mathsf{A}\Sigma - \Sigma_x[\mathsf{A}x] - \Sigma\mathsf{R}, \\ &\delta\ell = \ell_x \cdot \mathsf{A}x + \ell_u \cdot \mathsf{B}u, \quad \mathcal{B} = p \cdot \delta b + \mathrm{tr}(Z^T \delta\Sigma) - \delta\ell. \end{aligned} \tag{1650}$$

When the orbit stationarity and trace cancellation still apply, the same calculation gives

$$d\mathcal{C}_t = \mathcal{B}_t dt + \mathcal{N}_t \cdot dW_t, \qquad \mathbb{E}\mathcal{C}_t - \mathbb{E}\mathcal{C}_0 = \mathbb{E}\int_0^t \mathcal{B}_s ds. \tag{1651}$$

The expectation formula assumes integrable drift and a true martingale. Without Bellman identification the additional trace in (1649) must be retained.

For the common residual, let $\mathcal{D}$ denote differentiation along $(\mathsf{A}x, \mathsf{B}u)$ at fixed time. Then, including the metric response,

$$\delta\ell = \frac{e^{\kappa q}}{4}\{2(\mathcal{D}R)^T H R + R^T(\mathcal{D}H)R\}. \tag{1652}$$

Here R is the residual vector, distinct from the Brownian generator R. A sufficient exact symmetry is an invertible residual representation T_ε with $R(e^{\varepsilon\mathsf{A}}x, e^{\varepsilon\mathsf{B}}u) = T_\varepsilon R(x,u)$ and $H(e^{\varepsilon\mathsf{A}}x, e^{\varepsilon\mathsf{B}}u) = T_\varepsilon^{-T} H(x,u) T_\varepsilon^{-1}$. Thus an exponential outer cost preserves every exact symmetry of q. A nonzero κ does not alone produce symmetry breaking, radiation, or a time arrow. For a law-dependent cost, the probability law and reference data must transform as

well; freezing them can explicitly break the purported symmetry. The theorem applies directly to a genuine finite Markov augmentation, not to a state equation that has silently omitted its law dependence.

M.10. *What symmetry can actually fix about common weights.* The symmetry requirement can constrain a residual metric, but only when the physical representation of the symmetry is independently specified. For a constant quadratic metric and a linear residual generator S, invariance of $q = R^T H R$ for every residual is equivalent to

$$\mathsf{S}^T H + H\mathsf{S} = 0. \tag{1653}$$

Indeed differentiation gives $\mathcal{D}q = R^T(\mathsf{S}^T H + H\mathsf{S})R$; the symmetric matrix in parentheses is zero if and only if its quadratic form vanishes for every R. For two dimensionally normalized residual coordinates with a prescribed rotation $\mathsf{S} = \left(\begin{smallmatrix} 0 & -1 \\ 1 & 0 \end{smallmatrix}\right)$, write $H = \left(\begin{smallmatrix} a & c \\ c & b \end{smallmatrix}\right)$. Then

$$\mathsf{S}^T H + H\mathsf{S} = \begin{pmatrix} 2c & b-a \\ b-a & -2c \end{pmatrix}. \tag{1654}$$

The symmetry therefore requires $c = 0$ and $a = b > 0$. It fixes the ratio of the two weights, but leaves their common normalization free. For a field-dependent metric the corresponding condition includes $\mathcal{D}H$; the constant-matrix calculation applies also at a symmetry-fixed background with the stated linear residual representation.

More generally invariant quadratic forms can retain independent coefficients on inequivalent representation sectors. Repeated equivalent representations can admit cross terms in their multiplicity space. It would therefore be circular to declare an unmotivated rotation mixing gravity and gauge residuals solely to force their coefficients to agree. One must first derive or independently specify that symmetry of the mother data, with compatible units, constraints, observable maps and reference measure.

This calculation identifies a concrete route to reducing assumptions: an independently established residual symmetry restricts metric coefficients; the common optimal dynamics then propagates that restriction to responses. It also identifies the remaining obstacle: symmetry of an assigned cost is not evidence that the physical configurations possess the assigned symmetry. The free normalization and all invariant coefficients not fixed by the representation still need selection or independent calibration.

M.11. *When a symmetry charge is nontrivial.* The adjoint p is a cost gradient. It becomes mechanical momentum only after an independent physical identification of the action, units, kinematics and observable map. In addition,

an invariant terminal cost can make the preceding charge trivial. If the terminal cost, boundary data and full admissible family are invariant under the state symmetry, transforming every admissible policy in both directions gives $V(t, e^{\varepsilon \mathsf{A}}x) = V(t, x)$. Consequently

$$DV(t, x) \cdot \mathsf{A}x = 0. \tag{1655}$$

In the smooth Bellman branch $\mathcal{C}$ then vanishes identically. This is a substantive distinction from assigning arbitrary independent mechanical initial momenta. A running symmetry with a terminal target that breaks it can instead have a nonzero martingale charge.

For an explicit example let $d = 2$, $H_0 = hI$, $M = mI$, $Q = q_0 I$, and $\Sigma = \sqrt{2\theta m}I$ in the quadratic realization of Paper III. Use $\mathsf{A} = \mathsf{B} = \mathsf{R} = \left(\begin{smallmatrix} 0 & -1 \\ 1 & 0 \end{smallmatrix}\right)$. Let the terminal Hessian F_T be symmetric and anisotropic. The optimal adjoint is $p = P(t)X$, with

$$\dot{P} = -q_0 I + 2mhP + mP^2, \qquad \mathcal{C} = X^T P \mathsf{A} X, \qquad \mathcal{N} = \sqrt{2\theta m}(P\mathsf{A} - \mathsf{A}P)X. \tag{1656}$$

Writing $S = \mathbb{E}(XX^T)$,

$$\dot{S} = -m(hI + P)S - S\, m(hI + P) + 2\theta m I, \qquad \mathbb{E}\mathcal{C} = \operatorname{tr}(P\mathsf{A}S). \tag{1657}$$

Differentiate the last trace and use both equations. The h terms cancel; the P^2 terms reduce to the trace of $P\mathsf{A}P$ against the symmetric S; the remaining terms contain A times a symmetric matrix. Each trace vanishes because A is skew. This verifies mean conservation independently of the adjoint product rule. For isotropic F_T, P is scalar and the charge and its noise coefficient both vanish.

Finally the Bellman equation gives a different martingale:

$$V(t, X_t) + \int_0^t \ell(s, X_s, u_{*,s})ds = V(0, X_0) + \int_0^t (\Sigma^T DV)(s, X_s) \cdot dW_s. \tag{1658}$$

For other admissible policies the left side is a submartingale under the verification assumptions. In a stationary ergodic problem, replace V by the value corrector and ℓ by $\ell - \lambda$. This is a conditional cost balance, not an identification of cost with physical energy. Autonomous data do not by themselves impose time-reversal symmetry or conservation of the subsystem's energy.

M.12. *The zero-diffusion limit and classical Noether conservation.* Classical conservation is recovered in two logically separate steps: first the martingale fluctuations must vanish, and then the deterministic control problem must be identified with a classical variational problem. Neither step follows solely from writing a small diffusion coefficient.

For a family $\Sigma_\varepsilon = \sqrt{\varepsilon}\Sigma_0$, suppose the symmetry hypotheses hold for each $\varepsilon > 0$. The symmetry charge satisfies $\mathcal{C}_t^\varepsilon - \mathcal{C}_0^\varepsilon = \int_0^t \mathcal{N}_s^\varepsilon \cdot dW_s$. If

$$\mathbb{E}\int_0^T |\mathcal{N}_s^\varepsilon|^2 ds \longrightarrow 0, \tag{1659}$$

Doob's inequality gives the quantitative statement

$$\mathbb{E}\sup_{t\le T} |\mathcal{C}_t^\varepsilon - \mathcal{C}_0^\varepsilon|^2 \le 4\mathbb{E}\int_0^T |\mathcal{N}_s^\varepsilon|^2 ds \longrightarrow 0. \tag{1660}$$

Suppose also that the charges and initial charges converge to those of a well-defined deterministic limiting extremal. Its charge is then constant in time. In a smooth Bellman family,

$$\mathcal{N}^\varepsilon = \sqrt{\varepsilon}\,\Sigma_0^T\{D^2 V_\varepsilon\, \mathsf{A}X^\varepsilon + \mathsf{A}^T DV_\varepsilon\}. \tag{1661}$$

A uniform bound on the expected time integral of the squared expression after $\sqrt{\varepsilon}$ proves an $O(\varepsilon)$ bound in (1660). If value derivatives develop boundary layers or shocks, this uniform estimate must be established rather than assumed. Small noise alone is not a bound on a value Hessian.

To identify the classical mechanical limit, choose deterministic kinematics $\dot q = u$ and running cost $L(q,u,t)$. Assume a smooth unconstrained minimizing extremal with a regular velocity Legendre map; strict convexity and appropriate growth of L in u are sufficient local conditions for the minimizing selector. The control Hamiltonian, stationarity and adjoint equation become

$$\mathscr{H} = L(q,u,t) + p\cdot u, \qquad L_u + p = 0, \qquad \dot p = -L_q. \tag{1662}$$

Consequently

$$P_{\mathrm{mech}} = L_u = -p, \qquad \frac{d}{dt}L_u = L_q. \tag{1663}$$

This is the Euler–Lagrange equation. The minus sign between mechanical momentum and the minimization-convention costate is essential. For a spatial symmetry $\delta q = \mathsf{A}q$, $\delta u = \mathsf{A}u$, invariance gives $L_q \cdot \mathsf{A}q + L_u \cdot \mathsf{A}u = 0$. Direct differentiation yields

$$\frac{d}{dt}(P_{\mathrm{mech}} \cdot \mathsf{A}q) = L_q \cdot \mathsf{A}q + L_u \cdot \mathsf{A}u = 0. \tag{1664}$$

The classical charge is the negative of the costate charge above. The same product rule treats translations, whose infinitesimal generator is constant rather than $\mathsf{A}q$.

Time translation is a separate symmetry. Along a regular extremal define $E = P_{\mathrm{mech}}\cdot u - L$. Then

$$\dot E = (\dot P_{\mathrm{mech}} - L_q)\cdot u - \partial_t L = -\partial_t L. \tag{1665}$$

For an autonomous mechanical Lagrangian, E is conserved. This derivation recovers classical Noether energy conservation on the identified mechanical

branch; the finite-horizon value-cost martingale is not itself that energy. A minimum-action control formulation describes minimizing extremals in its admissible class. General stationary classical actions may also have saddle extremals and require their own variational treatment.

There is a simple counterexample to the unrestricted implication. For $dX^\varepsilon = -\gamma X^\varepsilon dt + \sqrt{2\varepsilon}\, dW$, the zero-noise limit is $\dot{x} = -\gamma x$. Its natural quadratic energy obeys $d(x^2/2)/dt = -\gamma x^2$. Friction survives when the diffusion vanishes. Thus this framework contains a classical Noether branch under the stated mechanical identification and limiting estimates, while also containing deterministic dissipative branches.

M.13. *The physical content of a common selection mechanism.* These constructions make control selection precise. They do not assign unprovided curvature weights, choose a gauge group, or identify a fluid projection. Nor does adding an equation residual to a loss independently derive that equation. Low-energy field recovery still uses the matched action and compatibility conditions already stated in the main text.

A useful finite realization must instead fix the same coefficients before computing feedback, invariant statistics and responses. Paper III supplies such a coupled quadratic example: its Bellman and adjoint equations select one feedback, and that feedback determines one effective Hessian, invariant Gaussian law and relaxation generator. A restricted common weight then relates two independently defined observation channels. Paper II differentiates the optimized cost with respect to genuine package inputs; Paper IV treats supplied quantum measurement dynamics; Paper V propagates calibration and control errors without refitting the target. Their shared role is to turn the physical selection proposal into explicit consequences of a declared model, with the remaining physical inputs visible.

Appendix N. Smooth stochastic symmetries and constrained physical realization

A symmetry statement becomes useful only after the state, the random forcing, the admissible controls and the measured quantity have been specified. This appendix extends the linear calculation in Theorem 146 to smooth changes of state. It also makes explicit the conditions needed to interpret the resulting balance in a physical model. Stochastic Noether results associated with Bellman equations predate the present programme [154] and [58]. The results below give direct adjoint calculations for the regulated common cost; they do not assert priority for the general correspondence between symmetry and martingales.

N.1. *From an assigned energy to a compatible generator.* Fix a finite-dimensional coordinate domain, a strictly positive reference density w, a smooth

energy E, a temperature parameter $\theta > 0$, and a symmetric positive mobility M. Assume the following integrals exist and that boundary terms vanish, for example on a compact manifold without boundary in compatible coordinate charts. With respect to coordinate volume dx, set

$$\begin{aligned} \pi(x) &= Z^{-1} w(x) e^{-E(x)/\theta}, \qquad Z = \int w e^{-E/\theta}\, dx, \\ Lf &= \theta \pi^{-1} \partial_i (\pi M_{ij} \partial_j f) + j \cdot \nabla f, \qquad \nabla \cdot (\pi j) = 0. \end{aligned} \tag{1666}$$

Repeated coordinate indices are summed. Expanding the derivative gives diffusion covariance $2\theta M$ and drift

$$b = -M \nabla E + \theta \operatorname{div} M + \theta M \nabla \log w + j. \tag{1667}$$

Integration by parts proves $\int Lf\, \pi dx = 0$. The symmetric part satisfies $\int f L_{\mathrm{sym}} g\, \pi dx = -\theta \int \nabla f^T M \nabla g\, \pi dx$. Consequently, for a sufficiently regular density ρ solving $\partial_t \rho = L^* \rho$,

$$\frac{d}{dt} \left[\theta \int \rho \log(\rho/\pi) dx \right] = -\theta^2 \int \rho\, \nabla \log(\rho/\pi)^T M \nabla \log(\rho/\pi) dx. \tag{1668}$$

For the j term, write $\rho = f\pi$ and integrate $\pi j \cdot \nabla f$; it vanishes by the displayed divergence condition. This constructs a compatible dynamics once E, M, w, j are supplied. It does not select M or j uniquely from E. In particular, a stationary circulation can coexist with zero free-energy derivative. Its path irreversibility requires the separately specified time reversal.

For a drift perturbation $v = Gu$ in the range of M, identical initial laws and an applicable Girsanov theorem give

$$D_{\mathrm{KL}}(\mathbb{P}^u \| \mathbb{P}^0) = \frac{1}{4\theta} \mathbb{E}^u \int_0^T v^T M^\dagger v\, dt. \tag{1669}$$

Indeed the minimal noise shift has squared norm $v^T (2\theta M)^\dagger v$, and the logarithmic likelihood has mean one half its time integral. This requires an actual martingale density, absolute continuity and finite expected energy; different initial laws add their relative entropy. A joint residual cost with other channels or nonlinear outer penalty is not, in general, this KL divergence.

N.2. *Units, physical time and constraint preservation.* Let $X = D\bar{X}$, $t = \tau \bar{t}$, where D is an invertible diagonal matrix of state units and $\tau > 0$ a measured time unit. Brownian scaling gives

$$d\bar{X} = \tau D^{-1} b(D\bar{X}, u)\, d\bar{t} + \sqrt{\tau} D^{-1} \Sigma(D\bar{X})\, d\bar{W}. \tag{1670}$$

Both drift and noise must be calibrated. A rate per unit auxiliary simulation time is divided by τ to become a physical rate. If ℓ has units of cost per time, $p = DV$ has units of cost per state; a momentum interpretation needs a separate action and kinematic map.

Suppose constraints define a regular embedded manifold $\mathcal{M} = \{x : C_a(x) = 0\}$. For a locally well-posed Itô equation with smooth coefficients, its invariance requires

$$DC_a\Sigma = 0, \qquad DC_a b + \tfrac{1}{2}\operatorname{tr}(\Sigma\Sigma^T D^2 C_a) = 0 \quad \text{on } \mathcal{M}. \tag{1671}$$

These are sufficient locally under the regular-manifold hypotheses. To see this, write the equation in Stratonovich form. The noise vectors are tangent. Differentiating $DC_a\Sigma_k = 0$ along Σ_k shows that the second condition is exactly tangency of the Stratonovich drift. Local uniqueness then preserves the manifold, up to explosion or chart exit. A nonexplosion argument extends this conclusion globally.

For example, on the unit sphere in $\mathbb{R}^d$ let $P_x = I - xx^T$ on the sphere and choose

$$dX = -\theta(d-1)X\,dt + \sqrt{2\theta}P_X\,dW. \tag{1672}$$

For $C = |x|^2 - 1$, the noise in dC is zero and its drift is $-2\theta(d-1) + 2\theta \operatorname{tr} P_x = 0$. Omitting the inward drift would violate the constraint. This is a finite example of why projecting noise alone is insufficient.

N.3. *A smooth adjoint symmetry theorem.* Consider $dX = b(t, X, u)dt + \Sigma(t, X)dW$ with running cost ℓ, terminal cost g, and control-independent noise. Use the same minimization adjoint as in Appendix M:

$$\mathscr{H} = \ell + p \cdot b + \operatorname{tr}(Z^T\Sigma), \qquad dp = -\mathscr{H}_x dt + Z\,dW, \qquad p_T = Dg(X_T). \tag{1673}$$

All coefficients in the following identities are evaluated along the extremal. Assume local differentiability sufficient for these equations, a field $\xi \in C^{1,2}$, and the integrability needed after localization. More explicitly, b and ℓ have continuous first state and control derivatives, Σ has continuous first state derivatives, the state and adjoint are well-defined continuous semimartingales up to the chosen horizon, and all product-rule coefficients are locally integrable. For d state and m noise coordinates, $p \in \mathbb{R}^d$ and $Z \in \mathbb{R}^{d\times m}$. In $\mathscr{H}_x$ the adjoint variables are held fixed. These hypotheses permit localization of every calculation; the later moment conditions specify when localization can be removed. Write $a = \Sigma\Sigma^T$. A control-orbit generator is denoted by $\zeta(t, x, u)$ and a constant skew Brownian generator by Ω. Define the defects

$$\begin{gathered}\Delta b = \partial_t\xi + D\xi b + \tfrac{1}{2}a : D^2\xi - b_x\xi - b_u\zeta, \quad \Delta\Sigma = D\xi\Sigma - \Sigma_x[\xi] - \Sigma\Omega, \\ \Delta\ell = \ell_x \cdot \xi + \ell_u \cdot \zeta.\end{gathered} \tag{1674}$$

The contraction $a : D^2\xi$ is componentwise. The $a : D^2\xi/2$ term is necessary even for a deterministic change of stochastic state coordinates.

THEOREM 147 (Smooth adjoint symmetry balance). *Under the preceding hypotheses, let $Q = p \cdot \xi(t, X)$. Then*

$$\begin{aligned} dQ &= \{\mathscr{H}_u \cdot \zeta + \operatorname{tr}(Z^T \Sigma \Omega) + B\}\, dt + N \cdot dW, \\ B &= p \cdot \Delta b + \operatorname{tr}(Z^T \Delta\Sigma) - \Delta\ell, \quad N = Z^T \xi + \Sigma^T (D\xi)^T p. \end{aligned} \tag{1675}$$

If the control orbit is two-sided feasible and stationary, its first term vanishes. If also $\Omega = 0$ or $Z = D^2 V \Sigma$ for a smooth Bellman value, the trace term vanishes. Under both cancellations and exact symmetry $B = 0$, Q is a local martingale. If Q_0 is integrable and $\mathbb{E}\int_0^T |N|^2 dt < \infty$, it is a true martingale.

Proof. Itô's formula first yields

$$d\xi = (\partial_t \xi + D\xi b + \tfrac{1}{2} a : D^2 \xi) dt + D\xi \Sigma dW. \tag{1676}$$

In $d(p \cdot \xi)$ the covariation is $\operatorname{tr}(Z^T D\xi \Sigma) dt$. Substituting the adjoint, the drift is therefore

$$p \cdot (\partial_t \xi + D\xi b + \tfrac{1}{2} a : D^2 \xi - b_x \xi) + \operatorname{tr}\{Z^T (D\xi \Sigma - \Sigma_x[\xi])\} - \ell_x \cdot \xi. \tag{1677}$$

Insert the three defect definitions. The control terms combine to $(\ell_u + b_u^T p) \cdot \zeta = \mathscr{H}_u \cdot \zeta$. The two stochastic product terms give N. Feasible orbit stationarity removes the first drift. For Bellman identification, $Z^T \Sigma = \Sigma^T D^2 V \Sigma$ is symmetric, and its trace against Ω is zero. Square integrability of the stochastic integral then upgrades the localized identity to the asserted martingale identity. □

The exact infinitesimal conditions arise from genuine Itô symmetries. If $T_\varepsilon(t, x)$ is the state transformation, S_ε the control transformation and $O_\varepsilon = e^{\varepsilon \Omega}$, the drift transformation must read

$$b(t, T_\varepsilon, S_\varepsilon u) = \partial_t T_\varepsilon + DT_\varepsilon b + \tfrac{1}{2} a : D^2 T_\varepsilon, \qquad \Sigma(t, T_\varepsilon) = DT_\varepsilon \Sigma O_\varepsilon^{-1}. \tag{1678}$$

Differentiate at zero and impose cost invariance to obtain zero defects. The transformed domain, boundary and admissible information must also be compatible. These are state symmetries at fixed physical time; a theorem for time transformations or spacetime diffeomorphisms requires its own extended-state and boundary construction.

N.4. *Fluctuations, leakage and several charges.* For charges Q^r satisfying the canceled balance, put $M_t^r = Q_t^r - Q_0^r - \int_0^t B_s^r ds$. If their noises are square integrable, Itô isometry gives

$$\mathbb{E}[M_t^r M_t^s] = \mathbb{E} \int_0^t N_v^r \cdot N_v^s \, dv. \tag{1679}$$

This is the covariance of the compensated increments, not the variance of an uncompensated charge with a random drift. Moreover,

$$|\mathbb{E}(Q_t - Q_0)| \le \sqrt{t}\left(\mathbb{E}\int_0^t |B_s|^2 ds\right)^{1/2}. \tag{1680}$$

For a bounded stopping time, the same true-martingale assumptions permit optional stopping of M. Local martingales without uniform integrability need not conserve their means.

For $q = R^T H R$ and $\ell = \varphi_\kappa(q)$, the cost defect is

$$\Delta\ell = \frac{e^{\kappa q}}{4}\{2(\mathcal{D}R)^T H R + R^T(\mathcal{D}H)R\}, \qquad \mathcal{D} = \xi\cdot\partial_x + \zeta\cdot\partial_u. \tag{1681}$$

If $\mathcal{D}R = SR$, exact invariance for all residuals requires $\mathcal{D}H + S^T H + HS = 0$. This includes field-dependent cross blocks. The probability law must be transformed too whenever it enters R or H. An assigned sector-mixing representation restricts weights only after that representation has been justified physically. Multiplying an invariant metric by a positive constant preserves this equation.

N.5. *An explicit nonlinear coordinate example.* Let $dX = u\,dt + \sigma dW$, $\ell = u^2/2$, $g(x) = \beta x$, with finite horizon and square-integrable controls. Completing the square gives $u_* = -\beta$ and $V(t,x) = \beta x - \beta^2(T-t)/2$. Choose $h(x) = x + cx^3$, $c > 0$, and $Y = h(X)$. This is a global smooth change of coordinates. In the y coordinate, with $x = h^{-1}(y)$ and $k = 1 + 3cx^2$,

$$b_y = ku + 3c\sigma^2 x, \quad \Sigma_y = \sigma k, \quad \xi(y) = k, \quad p_y = \beta/k, \quad Z_y = -6c\beta\sigma x/k^2. \tag{1682}$$

Here b_y names the drift in the new coordinate, not its derivative. The transformed translation is $T_\varepsilon(y) = h(x+\varepsilon)$. Its generator has

$$\xi' = 6cx/k, \qquad \xi'' = 6c(1-3cx^2)/k^3. \tag{1683}$$

Substitution in (1674), with $\zeta = \Omega = 0$, gives $\Delta b = \Delta\Sigma = \Delta\ell = 0$. Thus $Q = p_y\xi = \beta$ and $N = Z_y\xi + \Sigma_y\xi' p_y = 0$. This nonzero charge tests coordinate invariance. The anisotropic-terminal quadratic example in (1656) separately tests a charge with nonzero fluctuations. Neither example identifies a new mechanical conservation law without an observable dictionary.

N.6. *Nonsmooth boundaries, stopping and jumps.* Smoothness cannot be dropped silently at a stopping interface. In one dimension, if F is continuous, piecewise C^2 with one-sided derivatives at zero, generalized Itô's formula contains

$$dF(X) = F'(X)dX + \tfrac{1}{2}F''(X)d[X] + \tfrac{1}{2}\{F'(0+) - F'(0-)\}\,dL^0(X). \tag{1684}$$

This convention uses symmetric semimartingale local time; the ordinary second derivative is used off the interface and the derivative at the interface is the average of its one-sided values. One may impose a nondegenerate diffusion near zero, which spends zero Lebesgue time there, to avoid any interface drift convention. For $F(x) = |x|$, the last term is dL^0. Thus even zero bulk drift does not imply a martingale charge when an interface contribution remains. Smooth fit removes this term in this example; a viscosity solution alone does not establish it.

For a hybrid Markov model with compensated jump measure $\widetilde{\mu}(dt, dz) = \mu(dt, dz) - \nu_t(dz)dt$, suppose the complete charge calculation yields

$$dQ = Bdt + N \cdot dW + \int K(t, z)\widetilde{\mu}(dt, dz). \tag{1685}$$

If all terms are square integrable and Brownian and jump martingales are orthogonal, the compensated-increment variance is $\mathbb{E}\int(|N|^2 + \int K^2\nu_t(dz))dt$. One must include jump compensators in B when deriving this form. For a killed diffusion, L becomes $L - \lambda$ on live states. A charge set to zero at killing acquires drift $-\lambda Q$; if a terminal payment h is accumulated at killing, the contribution is $\lambda(h - Q)$. A stopping intensity therefore does not automatically preserve a pre-stopping symmetry or define a black-hole horizon.

N.7. *Local field symmetries and their additional requirements.* A regulated state-space symmetry is not yet a local gauge-current theorem. For a local classical action with variation $\delta\mathcal{L} = E_a\delta\phi^a + \partial_\mu\Theta^\mu$ and symmetry variation $\delta\mathcal{L} = \partial_\mu K^\mu$, its current satisfies the identity

$$\partial_\mu(\Theta^\mu - K^\mu) = -E_a\delta\phi^a. \tag{1686}$$

This follows by subtracting the two variations before imposing the equations of motion. Boundary fluxes remain when integrated over a region. Gauge redundancy additionally produces constraint identities; it does not necessarily give an independent observable charge for every gauge parameter. In a regulated functional integral, a change of variables also differentiates the reference measure. A nonzero Jacobian or regulator defect is a further contribution to the Ward identity. The finite theorem above does not prove cancellation of such quantum anomalies.

N.8. *Which analytical limits are actually available.* Finite dimension alone does not give finite exponential cost. A useful sufficient condition is a positive Lyapunov function W satisfying $L^u W \le a - be^{\kappa q}$ uniformly over the admissible controls, with $b > 0$. Stopped Itô expectation and Fatou's lemma give

$$\mathbb{E}\int_0^T e^{\kappa q(X_t, u_t)}dt \le \{W(X_0) + aT\}/b. \tag{1687}$$

This proves a running-cost bound, not the exponential of accumulated cost. Alternatively a compact invariant state and bounded controls bound q directly. The unconstrained Gaussian quadratic example has its familiar finite threshold for $\mathbb{E}e^{\kappa q}$; a quartic positive residual can fail for every $\kappa > 0$.

Normalizability of gravity-related Gibbs factors is a separate issue. An attractive pair potential $E(r) = -a/r$ gives

$$\int_0^\epsilon r^2 e^{a/(\theta r)} dr = \left(\frac{a}{\theta}\right)^3 \int_{a/(\theta\epsilon)}^\infty e^s s^{-4} ds = \infty. \tag{1688}$$

A finite number of coordinates has not prevented collapse. A core regularization on a bounded domain makes the finite partition function well defined; uniform removal of that core is an additional assertion. Likewise, small noise restores a deterministic charge only if the integrated charge-noise variance tends to zero, as in (1660), and the extremals converge. Friction can survive that limit.

Finally, a law-dependent cost uses the law as part of the state, as in the finite-simplex construction above. Under partial observation, the information state is the conditional law given the observations. With common noise that conditional law is itself stochastic. These models need their respective Bellman and adjoint equations; the single-state theorem applies only after an actual Markov realization has been specified. For control-dependent diffusion and nonconvex controls, the second-adjoint qualification in the preceding appendix continues to apply.

Appendix O. Coefficient restrictions and physically identified stochastic balances

A common functional has physical consequences when it restricts quantities that could otherwise be chosen independently. The first question is therefore which coefficients are fixed by the actual symmetry, rather than by an additional identification of sectors. The second is how a stochastic charge is related to a measured quantity. This appendix answers both questions in finite dimensions. It gives an explicit coefficient calculation and a mechanical realization in which one relaxation measurement determines a second relaxation rate and a matrix of compensated momentum fluctuations. The realization illustrates the required inference; its Langevin and martingale ingredients are established constructions, not new universal laws.

O.1. *Invariant curvature metrics on the declared product branch.* Fix the contraction of spacetime indices and consider the algebra part of a regulated curvature residual. On a compact product branch let

$$\mathfrak{g} = \mathfrak{g}_1 \oplus \cdots \oplus \mathfrak{g}_s \oplus \mathfrak{z}, \qquad \mathfrak{z} \simeq \mathbb{R}^r, \tag{1689}$$

where the $\mathfrak{g}_i$ are compact simple ideals. Each factor acts by its own adjoint action. For each simple ideal choose once and for all a positive multiple K_i of minus its Killing form. These normalizations must be fixed before a coefficient is interpreted as an inverse squared gauge coupling.

PROPOSITION 148 (Independent product-factor weights). *Every symmetric positive adjoint-invariant bilinear form on* (1689) *has the form*

$$H = \operatorname{diag}(h_1 K_1, \dots, h_s K_s, H_{\mathfrak{z}}), \qquad h_i > 0, \quad H_{\mathfrak{z}} \succ 0. \tag{1690}$$

There is no invariant cross pairing between two distinct simple ideals, including isomorphic ideals acted on independently, or between a simple ideal and the center. The coefficients h_i remain independent.

Proof. Write the bilinear form as B. Invariance says

$$B([z,x],y) + B(x,[z,y]) = 0. \tag{1691}$$

If $z, x \in \mathfrak{g}_i$ and y belongs to a different ideal or the center, then $[z,y] = 0$. Since $[\mathfrak{g}_i, \mathfrak{g}_i] = \mathfrak{g}_i$, the resulting identity $B([z,x],y) = 0$ makes the entire cross block zero. On one simple ideal, write $B(x,y) = K_i(Tx,y)$ with T self-adjoint relative to K_i. Invariance makes T commute with every adjoint map. Its real eigenspaces are consequently ideals. Simplicity allows just one eigenvalue, so $T = h_i I$. Positivity is equivalent to $h_i > 0$. The center carries the trivial adjoint representation, so its symmetric block is unrestricted apart from positivity. This proves every assertion. □

For example, on the compact regulated product $SO(5) \times SU(3)_c \times SU(3)_L \times U(1)_X$, orthonormal algebra bases give

$$H_{\mathrm{curv}} = \operatorname{diag}(h_{\mathrm{G}} I_{10}, h_c I_8, h_L I_8, h_X). \tag{1692}$$

This is a four-parameter positive cone, not a uniquely normalized metric. The finite central quotient of the internal group does not change the adjoint calculation. If a gauge-singlet scalar ϕ enters the metric, each h_i may independently be a positive function of ϕ. Thus the gauge symmetry permits both $h_i(\phi) = c_i f(\phi)$ and unrelated functions $h_i(\phi)$. It does not select a common exponential slope.

The compact assumption is substantive. A noncompact Lorentz algebra does not admit a positive definite adjoint-invariant inner product of this kind: such an inner product would make every adjoint generator skew, whereas a noncompact simple algebra contains adjoint generators with real nonzero eigenvalues. A positive regulated residual metric must therefore refer to the declared compact or Euclidean realization, a gauge-fixed construction with its own transformation rule, or another explicit positive space. It is not the indefinite Lorentzian curvature contraction.

Allowed cross terms can nevertheless occur elsewhere in the extended residual. For m copies of the same orthogonal irreducible representation V whose real commutant is $\mathbb{R}I$, all invariant symmetric metrics on $\mathbb{R}^m \otimes V$ are

$$H = A \otimes I_V, \qquad A = A^T \succ 0. \tag{1693}$$

Indeed each block commutes with the representation and is therefore a scalar identity; symmetry and positivity reduce to those of A. Complex or quaternionic commutants require the corresponding Hermitian commutant calculation. All gauge singlets are copies of the trivial representation and can mix through a positive symmetric block after their units have been normalized. A matter-dependent covariant intertwiner can allow further field-dependent terms, but then its own transformation enters $\mathcal{D}H$. These possibilities do not license a constant cross pairing between independently acted-on simple ideals.

O.2. *A finite coefficient test, including normalization.* Consider a prescribed family of symmetric residual metrics

$$H_c(x) = \sum_{\alpha=1}^{m} c_\alpha H_\alpha(x). \tag{1694}$$

The H_α are fixed, linearly independent matrix-valued functions, and c consists of constant parameters. For each specified infinitesimal symmetry j, let $\mathcal{D}_j$ differentiate the state and control dependence, and let S_j be its residual representation. Exact invariance requires

$$\sum_\alpha c_\alpha \{\mathcal{D}_j H_\alpha + S_j^T H_\alpha + H_\alpha S_j\} = 0 \quad \text{for every } j, x. \tag{1695}$$

When these matrix functions have a known finite basis, coefficient comparison produces a real linear system $\mathcal{A}c = 0$. Otherwise (1695) is the defining linear map into a function space. Checking a few state points cannot replace the identity on the whole physical domain.

Choose a bounded physical coordinate domain with compact closure K, continuous H_α, and a linear normalization $n^T c = 1$. Define

$$\mathcal{C} = \{c : \mathcal{A}c = 0,\ H_c(x) \succ 0\ (x \in K)\}, \qquad \mathcal{C}_1 = \mathcal{C} \cap \{n^T c = 1\}. \tag{1696}$$

The normalization fixes an overall cost scale and must have a physical or conventional meaning independent of the desired answer.

Proposition 149 (When symmetry fixes the normalized metric). *Suppose $\mathcal{C}_1$ is nonempty. Under the preceding compactness and continuity assumptions it is a singleton if and only if* $\dim\ker\mathcal{A} = 1$. *More generally, near every point of $\mathcal{C}_1$ it has dimension* $\dim\ker\mathcal{A} - 1$.

Proof. At $c_0 \in \mathcal{C}_1$, continuity and compactness give $\inf_{x\in K} \lambda_{\min} H_{c_0}(x) > 0$. The finitely many H_α are bounded on K, so small coefficient perturbations

preserve positivity uniformly. Consequently $\mathcal{C}$ is relatively open in $\ker \mathcal{A}$ near c_0. Since $n^T c_0 = 1$, the functional n^T is not zero on that kernel. Its normalized affine slice has dimension $\dim \ker \mathcal{A} - 1$, and positivity contains a neighborhood within that slice. If the kernel is one-dimensional, normalization leaves exactly one point. If its dimension exceeds one, a nonzero vector $v \in \ker \mathcal{A} \cap \ker n^T$ gives distinct feasible points $c_0 \pm \epsilon v$ for sufficiently small ϵ. □

Additional measured conditions may reduce this dimension. Positive semidefinite boundary metrics and noncompact domains without a uniform positive lower bound require separate analysis. If the coefficients are unknown functions of a transforming scalar, invariance is a differential equation for those functions rather than the constant-coefficient test above.

For one genuine planar rotation, the calculation is explicit:

$$S = \begin{pmatrix} 0 & -1 \\ 1 & 0 \end{pmatrix}, \quad H = \begin{pmatrix} a & c \\ c & b \end{pmatrix}, \quad S^T H + HS = \begin{pmatrix} 2c & b-a \\ b-a & -2c \end{pmatrix}. \tag{1697}$$

The rank is two in three parameters, so $c = 0$, $a = b$. The condition $\operatorname{tr} H = 2$ selects $H = I_2$. If the only symmetry is instead an independent rotation on each of two three-dimensional vector spaces, the generators are $\operatorname{diag}(J_j, 0)$ and $\operatorname{diag}(0, J_j)$, where the J_j generate $SO(3)$. Solving their equations gives

$$H = \operatorname{diag}(aI_3, bI_3), \qquad a, b > 0. \tag{1698}$$

The rank is nineteen in twenty-one symmetric parameters. Normalization $\operatorname{tr} H = 6$ leaves $a + b = 2$ and $0 < a < 2$. A symmetry that rotates one space into the other would remove this freedom, but that is an additional physical premise. Well-posedness of a control problem does not supply that premise.

O.3. *Physical observables and adjoint charges.* For $dX = b\,dt + \Sigma\,dW$, write $L_t = b \cdot \nabla + \frac{1}{2}\Sigma\Sigma^T : D^2$. A specified observable $A^r(t, x)$ has drift and noise

$$a^r = (\partial_t + L_t)A^r, \qquad n^r = \Sigma^T \nabla A^r, \qquad dA^r = a^r\,dt + n^r \cdot dW. \tag{1699}$$

Assume $A^r \in C^{1,2}$ and the displayed coefficients are integrable, with square-integrable stochastic integrands. Then

$$M_t^r = A^r(t, X_t) - A^r(0, X_0) - \int_0^t a_s^r\,ds, \quad \mathbb{E}[M_t^r M_t^s] = \mathbb{E}\int_0^t n_v^r \cdot n_v^s\,dv. \tag{1700}$$

These are the generator martingale and Itô isometry. Their measurable content depends on fixing the observable map, physical time, drift and noise before examining the target data.

The adjoint charge in Theorem 147 is $Q = p \cdot \xi$. It becomes a physical observable only after an identity such as $Q = c_A A(t, X) + h(t)$ has been derived from the mechanical realization, including units and boundary conditions.

Without that identification, p is a derivative of the control value, and a symmetry of the control problem is not a proof of physical momentum conservation. Even spatial translation covariance of an open Langevin system permits drag on a particle: the compensating momentum belongs to its reservoir.

If two observed sectors exchange a quantity internally, impose the actual balance conditions

$$a^1 + a^2 = j_{\mathrm{ext}}, \qquad n^1 + n^2 = n_{\mathrm{ext}}. \tag{1701}$$

For a closed exchange, both right-hand sides vanish. Then the sum is constant pathwise, while the separate fluctuations need not vanish. Covariances must include their anticorrelation. A chosen independent noise in each sector generally violates the closed balance.

O.4. *An explicit shared-coefficient mechanical restriction.* Consider three equal calibrated masses $m > 0$ moving along one axis, with momenta $p = (p_1, p_2, p_3)^T$ and kinetic energy $|p|^2/(2m)$. Let the two contact residuals be the relative velocities of adjacent masses. Their incidence matrix and graph Laplacian are

$$B = \begin{pmatrix} 1 & 0 \\ -1 & 1 \\ 0 & -1 \end{pmatrix}, \qquad L = BB^T = \begin{pmatrix} 1 & -1 & 0 \\ -1 & 2 & -1 \\ 0 & -1 & 1 \end{pmatrix}. \tag{1702}$$

Assume local contact friction, identical contacts under endpoint reflection, and a common calibrated reservoir energy $\theta > 0$. The contact metric is then γI_2, $\gamma > 0$. These assumptions are physical inputs: locality excludes an off-diagonal contact mobility, and reflection equates the two remaining weights. The Gibbs-compatible momentum equation is

$$dp = -\frac{\gamma}{m} Lp\, dt + f(t)\, dt + \sqrt{2\theta\gamma}\, B\, dW. \tag{1703}$$

The force f is a declared deterministic probe. Its time integral and the known damping are included when forming compensated increments. Since $\mathbf{1}^T B = 0$, total momentum satisfies

$$d(p_1 + p_2 + p_3) = \mathbf{1}^T f(t)\, dt. \tag{1704}$$

The exchange noise therefore preserves momentum exactly.

The two normalized relative modes are

$$v_- = (1, 0, -1)^T/\sqrt{2}, \qquad v_+ = (1, -2, 1)^T/\sqrt{6}, \qquad Lv_- = v_-, \quad Lv_+ = 3v_+. \tag{1705}$$

Let $y_\pm = v_\pm^T p$. Their noises are independent after an orthogonal Brownian change of coordinates, since $v_-^T L v_+ = 0$. In the absence of the probe they obey

$$dy_\pm = -\lambda_\pm y_\pm\, dt + \sqrt{2\theta m \lambda_\pm}\, dW_\pm, \qquad \lambda_- = \frac{\gamma}{m}, \quad \lambda_+ = \frac{3\gamma}{m}. \tag{1706}$$

Consequently their invariant variances are both $m\theta$, and their conditional means decay at the two displayed rates. On each fixed-total- momentum plane the invariant density is the normalized restriction of $\exp[-|p|^2/(2m\theta)]$. There is no normalizable equilibrium for the free center-of-mass position on the entire real line; this does not affect the momentum calculation.

Proposition 150 (Prediction after one relaxation calibration). *Under the stated contact, reservoir and observation assumptions, determine λ_- from one mean-relaxation experiment while m and θ are calibrated independently. The other mode and the compensated momenta then satisfy, without another fitted coefficient,*

$$\begin{aligned} &\lambda_+ = 3\lambda_-, \qquad \mathbb{E}[M_t M_t^T] = 2\theta m \lambda_- t L, \\ &M_t = p_t - p_0 + \frac{\gamma}{m}\int_0^t L p_s \, ds - \int_0^t f(s)\, ds. \end{aligned} \tag{1707}$$

For each t, the predicted covariance has zero row sums and negative adjacent-sector entries $-2\theta m\lambda_- t$.

Proof. The eigenvalue calculation gives the rate relation. Substituting (1703) into M_t gives $M_t = \sqrt{2\theta\gamma}\, BW_t$. Hence its covariance is $2\theta\gamma t B B^T$, and $\gamma = m\lambda_-$ eliminates the fitted contact coefficient. This also proves the row-sum and sign assertions. □

The restrictions have identifiable failure mechanisms. For unequal local contacts $a, b > 0$, replace γL by $B\,\mathrm{diag}(a, b)B^T$. Its nonzero relaxation rates are

$$\lambda_\pm = \frac{a + b \pm \sqrt{a^2 - ab + b^2}}{m}, \qquad \frac{\lambda_+}{\lambda_-} \geq 3, \tag{1708}$$

with equality only for $a = b$. Indeed the square root is at least $(a+b)/2$, because the difference of the squared quantities is $3(a-b)^2/4$. Conversely, reflection alone permits the positive contact metric

$$A = \begin{pmatrix} a & c \\ c & a \end{pmatrix}, \quad |c| < a, \qquad \lambda_- = \frac{a+c}{m}, \quad \lambda_+ = \frac{3(a-c)}{m}. \tag{1709}$$

Thus an allowed nonlocal cross contact destroys the fixed ratio. The subscripts here label the fixed eigenvectors, not their ordering for every c. Independent contact-noise strengths likewise preserve total momentum while violating the covariance prediction unless their covariance is $2\theta A$.

For an explicit alternative, $a = 1$, $b = 2$, $m = 1$ gives rates $3 - \sqrt{3}$ and $3 + \sqrt{3}$, whose ratio is $2 + \sqrt{3}$. Both models conserve total momentum and can have the same Gibbs momentum distribution, yet their temporal response differs. If the observation system, finite projection and force calibration have certified errors, those errors must be propagated before this difference is interpreted experimentally. Neither a good fit nor rejection of one contact model alone

establishes the full geometric programme. The example identifies the additional content required of a common origin: fixed physical maps, restricted coefficients and a prediction in an uncalibrated channel.

For a reproducible finite-sample calculation, use $m = 2$, $\theta = 0.6$, $\gamma = 0.7$, and initial amplitude 3 in the mode being probed. Generate 120000 independent exact Ornstein–Uhlenbeck observations of y_- at $t = 1.2$. On the admissible event $\widehat{\mu}_- > 0$, estimate from their sample mean $\widehat{\mu}_-$ and then freeze

$$\widehat{\lambda}_- = -\frac{1}{1.2}\log\frac{\widehat{\mu}_-}{3}, \qquad \widehat{\mu}_+(0.8) = 3e^{-3\widehat{\lambda}_-(0.8)}. \tag{1710}$$

A nonpositive sample mean does not define this logarithmic estimator and must be reported as an inadmissible calibration rather than clipped. The reported sample satisfies the condition. The target experiment uses 160000 new independent observations of y_+ at $t = 0.8$. A fixed generated sample gives $\widehat{\lambda}_- = 0.34902864$, with delta-method standard error 0.00100542, compared with the generating value 0.35. The predicted target mean is 1.29815439 and the independent sample mean is 1.28879587. Their difference is -2.34736 times the combined standard error 0.00398682, which includes uncertainty in the frozen calibration. This particular sample lies outside the nominal two-sided 95% interval; a single such event is possible under the specified Gaussian experiment and should not be removed by choosing another seed. No experimental observations enter this calculation.

Independent compensated-increment samples give a maximum absolute covariance-entry difference 0.00681504 from the generating matrix

$$2\theta\gamma(0.8)L = \begin{pmatrix} 0.672 & -0.672 & 0 \\ -0.672 & 1.344 & -0.672 \\ 0 & -0.672 & 0.672 \end{pmatrix}. \tag{1711}$$

Their momentum-sum residual is below 9×10^{-16}. These samples test exact finite-dimensional distributions and arithmetic. They do not assess time-discretization error or validate a physical reservoir model.

O.4.1. *Robustness to unequal and weakly coupled contacts.* Exact equality of two physical contacts is an idealization. A useful prediction must allow independently bounded deviations from that equality. Keep the calibrated mass m, temperature scale θ, incidence matrix B and total-momentum constraint fixed. Replace γI_2 by a constant symmetric positive definite contact matrix A and write

$$dp = -K_A p\,dt + \sqrt{2\theta}\,BA^{1/2}\,dW, \qquad K_A = m^{-1}BAB^{\mathsf{T}}. \tag{1712}$$

No external force is applied in this relaxation calculation. A nonzero known force can be removed from the mean and compensated increments. Let $P = I - \mathbf{1}\mathbf{1}^{\mathsf{T}}/3$ be the orthogonal projection onto the relative-momentum plane. On that plane,

K_A is positive definite. Its two ordered eigenvalues are denoted $r_1 \le r_2$; unlike the subscripts in (1709), these are ordered rates.

PROPOSITION 151 (A contact-tolerance prediction). *Suppose an independently specified tolerance* $0 \le \delta < 1$ *satisfies*

$$\gamma(1-\delta)I_2 \preceq A \preceq \gamma(1+\delta)I_2. \tag{1713}$$

Then

$$\frac{\gamma}{m}(1-\delta) \le r_1 \le \frac{\gamma}{m}(1+\delta),$$
$$\frac{3\gamma}{m}(1-\delta) \le r_2 \le \frac{3\gamma}{m}(1+\delta), \tag{1714}$$
$$\max\left\{1, \frac{3(1-\delta)}{1+\delta}\right\} \le \frac{r_2}{r_1} \le \frac{3(1+\delta)}{1-\delta}. \tag{1715}$$

For the correctly compensated increment $M_t = p_t - p_0 + \int_0^t K_A p_s\, ds$, *the covariance obeys*

$$2\theta\gamma(1-\delta)tL \preceq \mathbb{E}[M_t M_t^{\mathsf{T}}] \preceq 2\theta\gamma(1+\delta)tL. \tag{1716}$$

The inequalities hold as quadratic forms on all of $\mathbb{R}^3$, *with the common zero direction* $\mathbf{1}$.

Proof. For $v \in \mathbb{R}^3$, the tolerance gives

$$\gamma(1-\delta)|B^{\mathsf{T}}v|^2 \le v^{\mathsf{T}}BAB^{\mathsf{T}}v \le \gamma(1+\delta)|B^{\mathsf{T}}v|^2.$$

Thus $\gamma(1-\delta)L/m \preceq K_A \preceq \gamma(1+\delta)L/m$. The min–max characterization of the two eigenvalues on $P\mathbb{R}^3$, where L has eigenvalues $1, 3$, proves (1714). Division uses $r_1 > 0$; the extra lower bound one uses their ordering. Finally, $M_t = \sqrt{2\theta}BA^{1/2}W_t$, so its covariance is exactly $2\theta tBAB^{\mathsf{T}}$. The same quadratic-form inequalities give (1716). □

At $\delta = 0.05$, the ratio interval is $[19/7, 63/19] = [2.714285\ldots, 3.315789\ldots]$. The unequal-contact example $a : b = 1 : 2$ has ratio $2 + \sqrt{3} = 3.732050\ldots$ and lies outside this interval. This comparison distinguishes two specified model classes only after the five-percent tolerance is established independently; selecting it after observing the target ratio would invalidate that interpretation.

The tolerance also propagates to finite-time predictions. Put $K_0 = \gamma L/m$ and $\Delta K = K_A - K_0$. Then $\|\Delta K\|_{\mathrm{op}} \le 3\gamma\delta/m$, since $\|B\|_{\mathrm{op}}^2 = 3$. Duhamel's identity on the relative plane gives

$$e^{-K_A t} - e^{-K_0 t} = -\int_0^t e^{-K_A(t-s)}\Delta K e^{-K_0 s}\, ds.$$

Both symmetric semigroups are contractions there, with rates at least $\gamma(1-\delta)/m$ and γ/m. Therefore

$$\left|(e^{-K_A t} - e^{-K_0 t})Pp_0\right| \le \frac{3\gamma\delta}{m}\, te^{-\gamma(1-\delta)t/m}|Pp_0|. \tag{1717}$$

The factor t is essential: a pointwise drift tolerance does not directly equal a trajectory error.

For deterministic initial momentum, the centered covariance is

$$C_A(t) = m\theta\left(P - e^{-2K_A t}P\right). \tag{1718}$$

Indeed $\dot{C}_A = -K_A C_A - C_A K_A + 2m\theta K_A$ and $C_A(0) = 0$. Here $K_A P = PK_A = K_A$, so the displayed expression satisfies both the equation and its initial condition. In particular, all these fluctuation–dissipation-compatible contact matrices have the same limiting covariance $m\theta P$. Their relaxation rates and transient cross-covariances can differ even when their equilibrium distributions agree. Applying the preceding semigroup estimate at time $2t$ yields

$$\|C_A(t) - C_0(t)\|_{\mathrm{op}} \le 6\theta\gamma\delta\, te^{-2\gamma(1-\delta)t/m}. \tag{1719}$$

No claim about a nonlinear reservoir or state-dependent A follows from these constant-coefficient formulas.

The compensation convention matters for an experiment. If only the nominal drift K_0 is known, the recorded increment is $\widetilde{M}_t = M_t - R_t$, where $R_t = \int_0^t \Delta K p_s\, ds$. It is generally not a martingale. For the deterministic initial condition used here, (1718) and contraction of the mean give $\mathbb{E}|Pp_s|^2 \le |Pp_0|^2 + 2m\theta$. Cauchy–Schwarz in time therefore gives

$$\left(\mathbb{E}|R_t|^2\right)^{1/2} \le b_t := \frac{3\gamma\delta}{m}\, t\sqrt{|Pp_0|^2 + 2m\theta}. \tag{1720}$$

Moreover $\mathbb{E}|M_t|^2 \le 8\theta\gamma(1+\delta)t$. Expanding the centered covariance of $M_t - R_t$ and bounding the two cross terms by Cauchy–Schwarz gives

$$\|\operatorname{Cov}(\widetilde{M}_t) - \operatorname{Cov}(M_t)\|_{\mathrm{op}} \le 2\sqrt{8\theta\gamma(1+\delta)t}\, b_t + b_t^2.$$

Thus the exact covariance prediction cannot be applied to nominally compensated observations while omitting drift-calibration error.

O.4.2. *Independent moment evolution and time-step comparison.* The following synthetic calculation tests time integration and transient prediction separately from the exact Gaussian sampling described above. Use $m = 2$, $\theta = 0.6$, $\gamma = 0.7$, $p_0 = 3v_- + 2v_+$, and $C(0) = 0$. Compare identical contacts $A = \gamma I_2$ with the unequal-contact alternative $A = \gamma\,\mathrm{diag}(1, 2)$. On $0 \le t \le 4$, integrate the three mean equations and all nine covariance entries,

$$\dot{\mu} = -K_A\mu, \qquad \dot{C} = -K_A C - CK_A + 2\theta BAB^{\mathsf{T}}, \tag{1721}$$

using classical fourth-order Runge–Kutta. Compare this twelve-variable calculation with the independent two-mode matrix-exponential solution. The mean error is the maximum Euclidean error at the computed time nodes; the covariance error is the maximum Frobenius error there. They are numerical errors in these declared units, not experimental uncertainties or interval bounds between the nodes.

Time step	Mean error	Covariance error
0.200	5.626×10^{-5}	1.184×10^{-3}
0.100	3.060×10^{-6}	5.843×10^{-5}
0.050	1.785×10^{-7}	3.179×10^{-6}
0.025	1.078×10^{-8}	1.854×10^{-7}

Table 32. Maximum node errors for the synthetic contact moment equations. The unequal-contact case is included in each maximum. Halving the time step approaches the fourth-order rate of the numerical method.

O.5. *A projected fluid coefficient restriction.* There is also a useful fluid example in which the coefficient restriction comes directly from a specified projection. For a periodic velocity field independent of its third coordinate, retain the planar Fourier vorticity triad with wavevectors $(1,0)$, $(1,1)$ and $(2,1)$. In normalized energy coordinates $X = (X_1, X_2, X_3)$, the quadratic drift has the form

$$b(X) = (a_1 X_2 X_3, a_2 X_1 X_3, a_3 X_1 X_2), \qquad E = \frac{|X|^2}{2}, \quad Z = \frac{X_1^2 + 2X_2^2 + 5X_3^2}{2}. \tag{1722}$$

Energy and enstrophy preservation for all X require, respectively,

$$a_1 + a_2 + a_3 = 0, \qquad a_1 + 2a_2 + 5a_3 = 0, \qquad (a_1, a_2, a_3) = c_0(-3, 4, -1). \tag{1723}$$

Indeed $\nabla E \cdot b$ and $\nabla Z \cdot b$ are the two left-hand linear forms multiplied by $X_1 X_2 X_3$. Subtracting the first linear equation from the second gives $a_2 = -4a_3$, and the first then gives $a_1 = 3a_3$. Thus two physical conservation laws leave one overall scale; the Fourier normalization and physical time fix that scale through the explicit Galerkin integral. The two conservation laws alone do not determine its numerical value. The restrictions are consequences of the planar Euler projection. A controlled dissipative realization must retain their conservative part and state the force, dissipation and noise contributions to each balance. Enstrophy conservation is not imposed on a general three-dimensional Euler flow. This example shows how an explicitly identified projection can

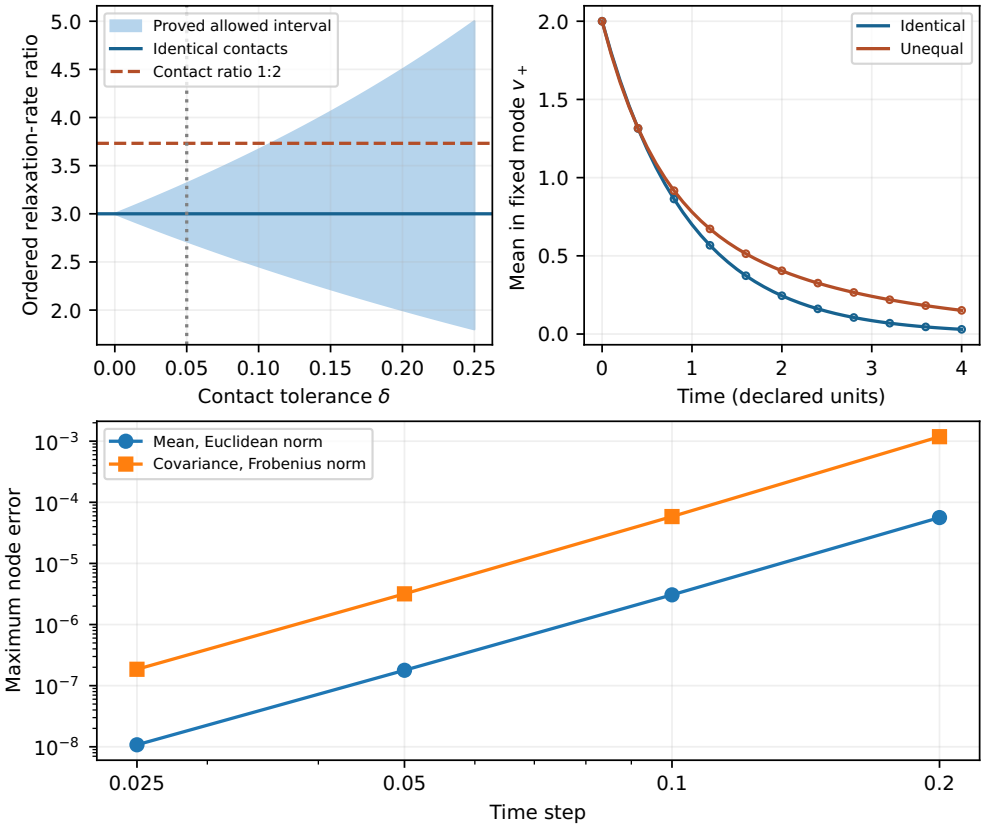


Figure 58. Synthetic contact comparison. Upper left: the proved tolerance interval for the ordered rate ratio, the identical-contact ratio, and an unequal-contact alternative. Upper right: mean relaxation observed in the fixed mode v_+; markers are a separate integration of the moment equations. Lower panel: time-step errors against the two-mode solution. Shared stationary covariance does not imply shared transient response.

yield coefficient restrictions without postulating a fictitious symmetry between unrelated gauge factors.

Appendix P. Irreversible dynamics, convergence, and boundary symmetries

The physical proposal starts with a stochastic law for the regulated configuration and asks which reversible equations, stable distributions, and effective field responses it permits. This changes the direction of construction: randomness need not first be explained as ignorance of a specified deterministic

trajectory. It does not make every stochastic process irreversible. A fundamental stochastic interpretation and a nonzero time-reversal defect are distinct physical premises. An equilibrium diffusion can fluctuate indefinitely while its stationary path law is exactly reversible.

P.1. *Physical premises and mathematical consequences.* A concrete realization supplies a regulated configuration, an energy or action with its units, a reference measure, mobility, admissible information and controls, and an observation map. Interpreting the noise as fundamental is a physical hypothesis; choosing time-reversal parity is part of the physical identification. Neither choice follows from positivity of a residual metric. The time arrow is then measured by comparing forward and physically reversed path laws.

An irreversible-first realization means that a specified physical branch has a nonzero reversal defect before a limiting approximation is taken. A reversible branch can arise through an exact symmetry, removal of a drive, or a suitable limit. Vanishing noise is neither necessary nor sufficient. A limit must specify the drift, parity, initial law and observation scale. A common construction can contain both types of branch.

Equilibrium has two connected meanings. An invariant law is a stationary statistical state; attraction describes the evolution toward that law from other distributions. The latter requires normalizability, recurrence and mixing estimates. Macroscopic stability can be studied with the same law-based description after a physical projection is supplied. It does not follow that every cosmological solution converges or that an attracting regulated law prevents an unregulated gravitational singularity.

P.2. *Path cost, likelihood and units.* In finite-dimensional coordinates, write

$$dX_t = (b_0 + v_t)(X_t)dt + \Sigma(X_t)dW_t, \quad \Sigma\Sigma^T = 2\theta M, \quad v_t = G(X_t)u_t. \tag{1724}$$

Here θ has energy units. For a length coordinate, mobility has units $\text{length}^2/(\text{energy}\,\text{time})$. For $v \in \operatorname{Ran}\Sigma$, the minimum-norm Brownian shift is $z = \Sigma^\dagger v$. In a square-root realization with $M > 0$,

$$z = (2\theta)^{-1/2} M^{-1/2} v, \qquad |z|^2 = (2\theta)^{-1} v^T M^{-1} v. \tag{1725}$$

Thus z has units $\text{time}^{-1/2}$ and the exponential likelihood has a dimensionless exponent.

Assume equal initial laws, well-posed martingale problems, a genuine Girsanov martingale, and finite expected shift energy under the controlled law. Novikov's sufficient condition is

$$\mathbb{E}^0 \exp\left(\frac{1}{2}\int_0^T |z_t|^2 dt\right) < \infty. \tag{1726}$$

For bounded v and $M \succeq m_0 I$, its left side is bounded by $\exp(T\|v\|_\infty^2/(4\theta m_0))$. Finite expected quadratic energy alone is not exponential integrability. For example, let an initial random variable Y, independent of W, have a Student distribution with three degrees of freedom, and set $z_t = Y$. Then $\mathbb{E}Y^2 < \infty$ but $\mathbb{E}e^{TY^2/2} = \infty$. Conditional expectation still makes the exponential a true martingale in this example. Novikov is sufficient, not necessary; alternative martingale criteria must be verified in their own form.

With $W^u = W^0 - \int z dt$, the likelihood satisfies

$$\log \frac{d\mathbb{P}^u}{d\mathbb{P}^0} = \int_0^T z_t \cdot dW_t^0 - \frac{1}{2}\int_0^T |z_t|^2 dt = \int_0^T z_t \cdot dW_t^u + \frac{1}{2}\int_0^T |z_t|^2 dt. \quad (1727)$$

It is the integral against W^u, not that against W^0, that has zero controlled expectation. If the control is a state-path functional and the minimum-norm likelihood is measurable on the state path, this gives

$$\theta D_{\mathrm{KL}}(\mathbb{P}^u \| \mathbb{P}^0) = \frac{1}{4}\mathbb{E}^u \int_0^T v_t^T M^\dagger v_t \, dt. \quad (1728)$$

On a larger information space the identity holds there first; projection to the state path can reduce relative entropy. Different initial laws add their initial relative entropy.

For dimensionless joint residuals fix state units, a time unit τ_0 and an energy unit E_0. A consistent convention is

$$\mathfrak{J} = \mathbb{E}^u \left[\frac{E_0}{\tau_0} \int_0^T \varphi_\kappa(q_t) dt + g_T \right], \qquad q = R^T H R, \quad (1729)$$

where q, κ are dimensionless and g_T has energy units. Dimensionless formulas set these declared units to one. The isolated control channel at $\kappa = 0$ is exactly (1728) when its scaled quadratic form is $(\tau_0/E_0)v^T M^\dagger v$. This cost has energy units; mechanical action has energy times time. Their identification requires the additional kinematics and unit conversion of the classical branch in Appendix M.

An exponential penalty on an instantaneous residual is different from an exponential of accumulated random cost:

$$\mathbb{E}\int_0^T e^{\kappa q_t} dt \neq \mathbb{E}\exp\left(\kappa \int_0^T q_t dt\right) \quad \text{in general.} \quad (1730)$$

The first has an additive Bellman running cost with nonlinear penalty; the second is a different risk-sensitive optimization problem. Neither supplies a radiation channel without a physical detector and an energy-transfer law.

P.3. *The complete density variation.* Assume here deterministic Markov feedback $u = u(t,x)$, a positive smooth density, and differentiability and integrable bounds justifying the displayed derivatives. History-dependent policies require an augmented Markov state or a state–control occupation law before this representation is used. At fixed coordinates let $\ell = (E_0/\tau_0)\varphi_\kappa(q)$ and $J = \int_0^T \int \rho\ell\, dxdt + \int \rho_T g_T\, dx$. For $h = \delta\rho$, $\int h dx = 0$, and $v = \delta u$, differentiation gives

$$\begin{aligned} DJ[h,v] = &\int_0^T \int \left[h\ell + \rho \frac{E_0 e^{\kappa q}}{4\tau_0} \{2\langle \delta R, HR\rangle + \langle R, \delta H R\rangle\} \right] dxdt \\ &+ \int \{h_T g_T + \rho_T \delta g_T\} dx. \end{aligned} \tag{1731}$$

All dependencies present in the selected model enter δR and δH. For fixed reference π, $\delta\nabla\log(\rho/\pi) = \nabla(h/\rho)$; a varying reference adds $-\nabla\delta\log\pi$. If $\eta = \delta\rho/\rho$ is used instead, the first integrand is $\rho\eta\ell$, not $\eta\ell$. Moving coordinates require their Jacobian or a fixed-reference formulation.

For a density-independent controlled generator, admissible variations obey

$$\partial_t h = (L^u)^* h + (\delta L^u)^* \rho, \qquad h_0 = 0. \tag{1732}$$

A law-dependent generator has its additional density derivative. A multiplier for this constraint, or the law-state Bellman and adjoint equations in Appendix M, connects optimization to the forward law. Unconstrained static density differentiation does not produce Fokker–Planck dynamics. Stationarity of a first variation is necessary at an interior minimum, but requires convexity or verification to establish global optimality.

P.4. *Free-energy decay and stationary path irreversibility.* Let $\pi = Z^{-1}e^{-A/\theta}$ be positive and normalized, M smooth and symmetric, and $\nabla\cdot(\pi j) = 0$. Assume vanishing boundary terms and sufficient regularity for the following integrations. Set

$$b_{\mathrm{th}} = \theta\,\mathrm{div}\, M + \theta M\nabla\log\pi, \qquad b = b_{\mathrm{th}} + j + h. \tag{1733}$$

The current is $J = \rho j + \rho h - \theta\rho M\nabla\log(\rho/\pi)$. Writing $s = \nabla\log(\rho/\pi)$, integration by parts gives

$$\begin{aligned} \frac{d}{dt} D_{\mathrm{KL}}(\rho\|\pi) &= -\theta \int \rho s^T M s\, dx + \int \rho h\cdot s\, dx, \\ \frac{d}{dt}\{\theta D_{\mathrm{KL}}(\rho\|\pi)\} &= -\theta^2 \int \rho s^T M s\, dx + \theta \int \rho h\cdot s\, dx. \end{aligned} \tag{1734}$$

The j term is $\int \pi j\cdot\nabla(\rho/\pi)dx = 0$. There is no pointwise negative-sign rule for $b_{\mathrm{th}}\cdot\nabla\log\pi$: constant M and $A = |x|^2/2$ give $x^T Mx/\theta \geq 0$. Dissipation is the integrated law above. The condition $h = 0$ specifies an undriven isothermal model, not an isolated system free of a heat bath.

Suppose $h = 0$, $M \succeq m_0 I$, and

$$\mathrm{Ent}_\pi(f^2) \le 2C_{\mathrm{LS}} \int |\nabla f|^2 d\pi. \tag{1735}$$

For $f = \sqrt{\rho/\pi}$ the gradient integral is one quarter of $\int \rho |s|^2 dx$. Substitution in the entropy balance and Gronwall's inequality yield

$$D_{\mathrm{KL}}(\rho_t \| \pi) \le e^{-2\theta m_0 t / C_{\mathrm{LS}}} D_{\mathrm{KL}}(\rho_0 \| \pi). \tag{1736}$$

For $dX = -\gamma X dt + \sqrt{2D}\, dW$, $D = \theta m_0$, the Gaussian constant is $C_{\mathrm{LS}} = D/\gamma$ and a shifted invariant Gaussian attains rate 2γ. Decay fitted for a single initial distribution does not identify the optimal log-Sobolev constant. Uniformity across regulators requires a separate estimate.

For stationary all-even variables the reverse drift is

$$b^{\leftarrow} = -b + 2\theta \,\mathrm{div}\, M + 2\theta M \nabla \log \pi. \tag{1737}$$

In a nonstationary problem use the time-$T - t$ density; for odd variables apply the declared parity and reverse time-odd external parameters. Under stationarity and the path-space absolute-continuity hypotheses,

$$\frac{1}{T} D_{\mathrm{KL}}(\mathbb{P}_{[0,T]} \| \mathbb{P}^{\leftarrow}_{[0,T]}) = \frac{1}{\theta} \int \frac{J_\pi^T M^\dagger J_\pi}{\pi}\, dx. \tag{1738}$$

This stationary representation and the importance of its noise-range conditions are developed in [49]. The parity-aware formulation uses the irreversible current in Section 4.11. This entropy rate is different from the control entropy in (1728).

For a circle of circumference L, take

$$dX = v dt + \sqrt{2D}\, dW \pmod L, \qquad X_0 \sim \mathrm{Uniform}[0, L). \tag{1739}$$

Every marginal is uniform. The lifted continuous displacement Y_T has mean vT and variance $2DT$. Path reversal entropy $\Sigma_T = (v/D) Y_T$ therefore gives

$$\mathbb{E}\Sigma_T = v^2 T/D, D_{\mathrm{KL}}(\mathbb{P}^v \| \mathbb{P}^0) = v^2 T/(4D), \qquad D_{\mathrm{KL}}(\rho_t \| \rho_{T-t}) = 0. \tag{1740}$$

The lifted record includes winding; a wrapped endpoint loses information. Pure diffusion is reversible in this example. Adding an unrestricted drift makes the rate unbounded, so pure diffusion is not a universal maximum of irreversibility. Marginal comparison is not a controlled approximation to path entropy without further information. A stationary drive can also preserve the undriven Gibbs density, as it does here.

More generally, let Q be the reversed-protocol law on forward path space and suppose P, Q are equivalent. The definition $\Sigma = \log(dP/dQ)$ implies

$$\mathbb{E}_P e^{-\Sigma} = 1, \qquad \mathbb{E}_P \Sigma = D(P\|Q) \ge 0. \tag{1741}$$

The first identity follows by integrating dQ. Lost support can change it when equivalence fails. A detailed forward/backward fluctuation relation also uses

the reversal involution and protocol identification. The work formula $\Sigma = \beta(W-\Delta F)$ needs equilibrium preparation and the appropriate reservoir balance; it is not a generic difference of squared control costs. Relative entropy is generally lower semicontinuous, not continuous under arbitrary weak convergence.

P.5. *Boundary terms in stochastic Noether theory.* The minimization costate p is defined by its backward equation. A Brownian trajectory has no ordinary velocity from which to define it. The canonical mechanical one-form is $p_i\,dq^i$, whereas contraction of the Hamiltonian vector field with $\omega = \sum_i dq^i \wedge dp_i$ gives dH. These are distinct objects. Likewise an antisymmetric matrix is a Poisson tensor only if the associated bracket satisfies the Jacobi identity. Divergence-free flow need not preserve a specified symplectic form in dimension greater than two.

Use Theorem 147, with control-independent noise, $\Omega = 0$, and a two-sided feasible stationary control orbit. Let $\mathcal{A}^u = \partial_t + L^u$ and $F \in C^{1,2}$. Write

$$\Delta\ell = \mathcal{A}^u F + \epsilon_\ell, \qquad B_F = p\cdot\Delta b + \operatorname{tr}(Z^T\Delta\Sigma) - \epsilon_\ell. \tag{1742}$$

The boundary function F describes a change of running cost. Domain, information and terminal data must transform compatibly when this is used as a symmetry of the whole optimization problem.

Proposition 152 (Quasi-invariance and compensated charge). *Under the regularity of Theorem 147,*

$$\begin{aligned} \widetilde{Q} &= p\cdot\xi + F(t,X), \\ d\widetilde{Q} &= B_F dt + \{Z^T\xi + \Sigma^T(D\xi)^T p + \Sigma^T\nabla F\}\cdot dW. \end{aligned} \tag{1743}$$

If the displayed noise is square integrable in mean and $\widetilde{Q}_0$ is integrable, subtracting $\int B_F dt$ gives a true martingale. Exact infinitesimal quasi-symmetry sets $B_F = 0$.

Proof. The product-rule drift of $p\cdot\xi$ is $p\cdot\Delta b + \operatorname{tr}(Z^T\Delta\Sigma) - \Delta\ell$ after orbit stationarity. Itô differentiation of $F(t,X)$ adds $\mathcal{A}^u F dt + \Sigma^T\nabla F\cdot dW$. The boundary drift cancels. Square integrability makes the stochastic integral a true martingale. □

The plus sign before F follows from the minimization convention. On the mechanical branch $p = -P_{\mathrm{mech}}$, the physical charge $P_{\mathrm{mech}}\cdot\xi - F$ is its negative. Charge leakage is determined by the first-order infinitesimal defect; a second-order group-parameter term alone does not supply a first-order leakage.

For a direct check let $dX = u\,dt + \sigma dW$, $\ell = u^2/2 + \lambda x u$, and $g(x) = \beta x - \lambda x^2/2$, with square-integrable adapted controls on a finite horizon. Itô

integration and completion of the square give

$$\begin{aligned} V(t,x) &= \beta x - \lambda x^2/2 - (\beta^2 + \lambda\sigma^2)(T-t)/2, \qquad u_* = -\beta, \\ p &= \beta - \lambda X, \quad Z = -\lambda\sigma, \quad \xi = 1, \quad F = \lambda x. \end{aligned} \tag{1744}$$

Thus $\Delta\ell = \lambda u = \mathcal{A}^u F$ and $\widetilde{Q} = \beta$; both noise and drift vanish. Fully invariant terminal data with $\delta g = -F(T,\cdot)$ can instead give zero terminal corrected charge. A true martingale with zero terminal value is identically zero. Nontrivial observable charges therefore require attention to terminal data as well as local symmetry equations.

Unconditional mean conservation alone does not imply a martingale. The process $Q_t = tW_t$ has zero mean for every t, but $\mathbb{E}[Q_t \mid \mathcal{F}_s] = tW_s \neq sW_s$. This is why adapted drift cancellation is needed, not only an expected endpoint variation. Autonomous coefficients likewise do not conserve physical energy: for the Ornstein–Uhlenbeck process,

$$d(X^2/2) = (-\gamma X^2 + D)dt + \sqrt{2D}X\, dW. \tag{1745}$$

Even under its stationary law, energy is not generally a martingale. Reflection of an even potential is discrete and has no infinitesimal translation generator. A driven double well instead has the exact moment balance $d\mathbb{E}X/dt = -\mathbb{E}U'(X) + A\cos(\omega t)$.

P.6. *Limits, numerical projection and field recovery.* A reversible deterministic limit needs $b(\Theta x) = -D\Theta(x)b(x)$ and a compatible ensemble. Hamiltonian form gives this for an appropriate anti-symplectic involution and parity-invariant Hamiltonian, with external odd parameters included. Smooth finite-dimensional ODE paths and their smooth projections have zero quadratic variation. They cannot reproduce a nondegenerate Itô diffusion exactly. A deterministic shift on a random infinite path space is a different representation, not a finite hidden mechanical model.

There is no universal noncommutation of noise and mobility limits. For $dX = AX dt + \sqrt{2\theta m}\, dW$ with fixed A, either iterated limit $\theta \downarrow 0$, $m \downarrow 0$ gives $e^{At}X_0$ in mean square on a finite horizon. Any noncommutation claim must specify the coefficients and observation times; an infinite-time limit is a separate operation.

A reversible nearest-neighbor numerical approximation to $dX = -U'(X)dt + \sqrt{2\theta}\, dW$ can use

$$k_{i,i+1} = \frac{\theta}{h^2} e^{-(U_{i+1}-U_i)/(2\theta)}, \qquad \pi_i = \frac{e^{-U_i/\theta}}{\sum_j e^{-U_j/\theta}}. \tag{1746}$$

The reverse rate has the opposite energy difference. Multiplication gives $\pi_i k_{i,i+1} = \pi_{i+1} k_{i+1,i}$. Taylor expansion in the interior gives drift $-U'$ and diffusion coefficient θ. Using the full energy difference instead selects $e^{-2U_i/\theta}$

and limiting drift $-2U'$. The chain is a constructed approximation; binning a diffusion path does not generally yield a Markov chain. A spectral gap determines a Poincare constant under its stated convention, not generally a log-Sobolev constant.

The curvature channel must originate in primitive master geometry. Squaring a prescribed target field equation does not independently derive it. For a nonlinear residual, stationarity of $\|R(x)\|^2/4$ gives $DR(x)^*R(x) = 0$, not necessarily $R = 0$; $R = x^2 + 1$ at $x = 0$ is a counterexample. Positive weights and refinement alone do not prove vanishing residuals. Section 5 instead uses a matched action expansion, boundary conditions and quantified remainder. Masses require kinetic normalization and pole identification; stress requires variation of the volume factor and all coupled fields.

P.7. *Finite numerical illustrations.* Figure 59 uses exact Gaussian transitions and finite matrix calculations. The ring has $v = 0.6$, $D = 0.4$, $T = 2$ and 200000 independently generated paths of lifted increments. The Ornstein–Uhlenbeck process has $\gamma = 0.7$, $D = 0.4$, initial mean one and invariant initial variance D/γ. Its exact entropy is $\gamma e^{-2\gamma t}/(2D)$. No time discretization is used for these Gaussian samples. The grid comparison uses $U(x) = (x^2 - 1)^2/4$, $\theta = 0.4$, $h = 0.1$ on $[-2, 2]$ with reflecting endpoints. Raw synthetic samples and symbolic boundary-charge checks accompany the calculation. These are checks of the finite formulas, not independent experimental confirmation of the mother model. At $T = 2$, the ring estimates are 1.80028 (standard error 0.00425) and 0.45014 (standard error 0.00212), against exact values 1.8 and 0.45. The exponential fluctuation estimate is 1.01497 with standard error 0.01382, against exact value one; rare weighted paths make this estimator less precise. The final Gaussian entropy is 0.05305 (delta-method standard error 0.00073), against 0.05321.

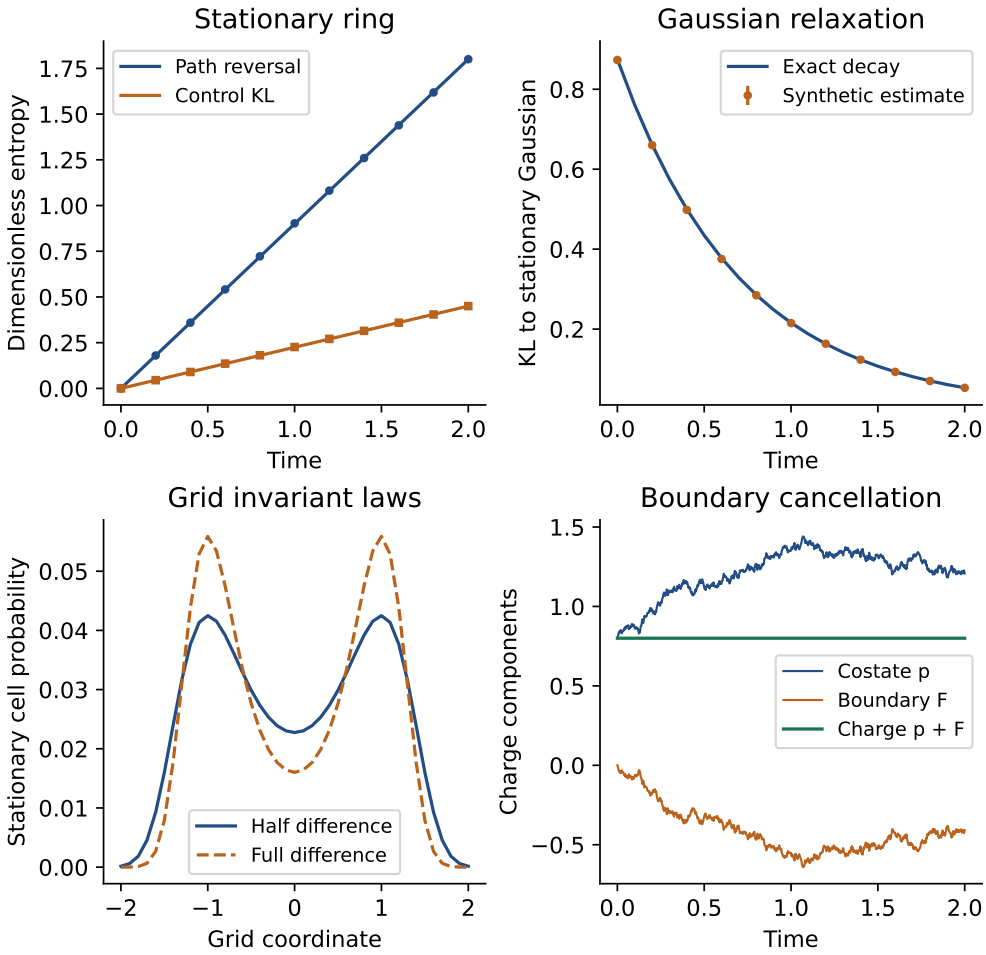


Figure 59. Synthetic foundational comparisons. Top left: ring path-reversal entropy and control entropy differ by four despite identical marginals. Top right: shifted Gaussian entropy decays at rate 2γ. Bottom left: full-difference grid rates select the wrong Gibbs temperature. Bottom right: the boundary-corrected adjoint charge is constant although its two terms fluctuate. Error bars are pointwise 95% Monte Carlo intervals, not experimental errors.

Appendix Q. What a fixed stochastic model determines

The proposal starts from a stochastic physical description and treats reversible behavior as a branch that must be identified within it. This choice does not remove the need to specify the stochastic law. Two questions are especially important. Does the optimal policy determine the cost and its physical coupling constants? Does the probability law determine a quantum Hamiltonian and the measurements that it describes? The following results separate these questions. They concern finite regulated models, so neither conclusion depends on an unresolved continuum existence problem.

Q.1. *Optimal behavior and the inverse determination of a cost.* Let an admissible control u drive a nonexplosive diffusion with backward generator L^u. For a fixed initial state x at time t write

$$J_{t,x}(u) = \mathbb{E}^u_{t,x}\left[\int_t^T \ell(s, X_s, u_s)\, ds + g(X_T)\right], \qquad V(t,x) = \inf_u J_{t,x}(u). \tag{1747}$$

Here L^u is fixed before solving the inverse problem. Assume that the expectations below are finite and that Itô's formula for $F \in C^{1,2}$ has an integrable zero-mean martingale term for every admissible control. Fix $a > 0$ and a deterministic integrable function c. Define

$$\widetilde{\ell} = a\ell + (\partial_t + L^u)F + c(t), \qquad \widetilde{g} = ag - F(T, \cdot). \tag{1748}$$

Proposition 153 (A boundary and scale freedom in inverse control). *The transformed problem has exactly the same optimal controls whenever the infimum is attained. Its costs and value satisfy*

$$\begin{aligned} \widetilde{J}_{t,x}(u) &= aJ_{t,x}(u) - F(t,x) + \int_t^T c(s)\, ds, \\ \widetilde{V}(t,x) &= aV(t,x) - F(t,x) + \int_t^T c(s)\, ds. \end{aligned} \tag{1749}$$

For smooth values the two Bellman equations are equivalent under this change of variables.

Proof. Itô's formula and the zero-mean hypothesis give

$$\mathbb{E}^u_{t,x}\int_t^T (\partial_s + L^{u_s})F(s, X_s)\, ds = \mathbb{E}^u_{t,x}F(T, X_T) - F(t,x).$$

The terminal expectation cancels the added terminal term. This proves the cost identity for each control. Multiplication by a positive constant and addition of a control-independent number preserve the order of all admissible costs and therefore their minimizers. Taking the infimum proves the value formula, even if no optimizer exists. For the classical Bellman equation, $-\partial_t V = \inf_u\{\ell + L^u V\}$,

substitution yields

$$\inf_u\{\widetilde{\ell} + L^u\widetilde{V}\} = -a\partial_t V + \partial_t F + c(t) = -\partial_t\widetilde{V},$$

because a generator annihilates spatial constants. The terminal values also agree, completing the proof. □

This freedom is not an argument that different measured gauge couplings are physically equivalent. It is an obstruction to identifying a running cost from optimal behavior alone. Some transformations in (1748) leave a specified positive residual ansatz, so that ansatz must be checked separately. A concrete example shows that the ambiguity can survive even strict positivity.

Take $dX_s = u_s\,ds + \sqrt{2D}\,dW_s$, $D > 0$, with square-integrable adapted controls, and

$$\ell(x,u) = \tfrac{1}{2}(x^2+u^2), \quad g(x) = \tfrac{1}{2}x^2, \quad V(t,x) = \tfrac{1}{2}x^2 + D(T-t), \quad u^*(t,x) = -x. \tag{1750}$$

Indeed $-\partial_t V = D$, while $\inf_u\{\frac{1}{2}(x^2+u^2) + ux + D\} = D$. Completion of the square, with Itô's formula for V, proves global optimality and uniqueness up to equality almost everywhere under the state-control occupation measure. Choose $F(x) = fx^2/2$, $0 < f < a$, and $c = 0$. Then

$$\begin{gathered}\widetilde{\ell}(x,u) = \tfrac{a}{2}(x^2+u^2) + fxu + Df, \quad \widetilde{g}(x) = \tfrac{a-f}{2}x^2, \\ \widetilde{V}(t,x) = \tfrac{a-f}{2}x^2 + aD(T-t).\end{gathered} \tag{1751}$$

The quadratic running matrix has eigenvalues $a - f$ and $a + f$, both positive. The terminal quadratic is positive and the constant Df is positive. Nevertheless

$$\partial_u\{\widetilde{\ell} + u\partial_x\widetilde{V}\} = au + fx + (a-f)x = a(u+x), \tag{1752}$$

so every member has the identical feedback $u^* = -x$. Its full controlled path law is also identical for the same D and initial law. Equivalently, at $u = -x$ the transformed running cost is $(a-f)x^2 + Df$, the transport term is $-(a-f)x^2$, and the diffusion term is $D(a-f)$. Their sum is aD, exactly $-\partial_t\widetilde{V}$. This is a continuous family of well-posed positive quadratic problems, not a failed Bellman problem excluded by positivity.

Q.2. *Why a stochastic Noether identity does not remove this freedom.* Suppose a smooth spatial symmetry with generator ξ transforms the state and control covariantly and leaves the time coordinate unchanged. Denote its derivative on scalar functions by δ_ξ. Covariance of the generator means

$$\delta_\xi[(\partial_t + L^u)F] = (\partial_t + L^u)(\delta_\xi F)$$

when both the state and the control are transformed. Suppose the original running cost is quasi-invariant, $\delta_\xi\ell = (\partial_t + L^u)B$, and the hypotheses of

the smooth quasi-Noether theorem in Appendix P hold. Under (1748), the boundary function and costate become

$$\widetilde{B} = aB + \delta_\xi F, \qquad \widetilde{p} = ap - \nabla F. \tag{1753}$$

Consequently the minimization-convention charge obeys

$$\widetilde{p} \cdot \xi + \widetilde{B} = a(p \cdot \xi + B), \qquad \delta_\xi F = \nabla F \cdot \xi. \tag{1754}$$

The boundary terms cancel. Thus the local-martingale balance, and the true-martingale balance when its integrability conditions hold, are preserved. A Noether identity is a restriction on symmetry-compatible data; it is not an independent mechanism for selecting one representative of an equivalence class of costs.

Even after removing such conventional freedoms, independently acted-on simple gauge ideals retain the positive coefficients proved in Proposition 148. To select physical couplings one must specify the candidate class modulo the declared equivalences, fix algebra and field normalizations, derive the selection functional from the chosen mother data, and solve its global comparison problem. A strictly convex prescribed selector can give a unique minimizer; strict convexity does not establish that nature uses that selector. The companion particle analysis supplies a conditional selection construction and its sensitivity, keeping this distinction explicit.

Q.3. *Quantum reconstruction and stationary probability currents.* A precise finite comparison is possible without identifying auxiliary stochastic time with physical time. Let Q be an irreducible continuous-time Markov generator on a finite configuration set, with rows summing to zero and invariant probabilities $\pi_i > 0$. Set $D_\pi = \mathrm{diag}(\pi_i)$ and choose an action scale $\hbar_{\mathrm{aux}} > 0$. The direct ground-state transform is

$$H_Q = -\hbar_{\mathrm{aux}} D_\pi^{1/2} Q D_\pi^{-1/2}, \qquad \Omega = (\sqrt{\pi_i})_i, \qquad H_Q \Omega = 0. \tag{1755}$$

For this particular transform, self-adjointness is equivalent to detailed balance:

$$H_Q = H_Q^\dagger \quad \Longleftrightarrow \quad \pi_i Q_{ij} = \pi_j Q_{ji} \quad \text{for all } i, j. \tag{1756}$$

To see this, multiply the matrix identity by the appropriate factors of $D_\pi^{1/2}$. It becomes $D_\pi Q = Q^T D_\pi$. When it holds, the quadratic form is

$$\langle D_\pi^{1/2} f, H_Q D_\pi^{1/2} f \rangle = \frac{\hbar_{\mathrm{aux}}}{2} \sum_{i,j} \pi_i Q_{ij} |f_j - f_i|^2 \geq 0. \tag{1757}$$

It follows by expanding the square and using both stationarity and the generator row sums. Connectedness gives a one-dimensional null space, since equality forces f to be constant on every edge.

Define the stationary edge current by $J_{ij} = \pi_i Q_{ij} - \pi_j Q_{ji}$. The exact defect of Hermiticity is

$$(H_Q - H_Q^\dagger)_{ij} = -\hbar_{\mathrm{aux}} \frac{J_{ij}}{\sqrt{\pi_i \pi_j}}. \tag{1758}$$

In particular, stationary circulating probability cannot be retained unchanged by this direct transform and at the same time produce a self-adjoint closed-system Hamiltonian. Replacing Q by its reversible part changes the dynamics, although it preserves π. The companion quantum analysis gives a quantitative error estimate for that replacement and an inverse characterization of the finite Hamiltonians obtainable in this way.

This statement uses ordinary configuration reversal, with all state labels even. Odd variables, reversed external fields and an explicit involution require the corresponding generalized balance calculation. Nor does (1756) forbid a dissipative quantum completion with a bath. Such a completion has different data: for example, a completely positive quantum dynamical semigroup rather than the unchanged matrix in (1755). A classical jump chain can be embedded into a Lindblad evolution [112] using operators $\sqrt{Q_{ij}}\,|j\rangle\langle i|$ for $i \neq j$, but additional dephasing and Hamiltonian terms can leave its diagonal probabilities unchanged. This elementary nonuniqueness explains why classical transition probabilities do not by themselves fix all off-diagonal quantum evolution.

For example, fix two classical rates $r_{12}, r_{21} > 0$ and choose the quantum jumps $\sqrt{r_{12}}|2\rangle\langle 1|$ and $\sqrt{r_{21}}|1\rangle\langle 2|$. Add $H_\omega = \hbar_{\mathrm{aux}}\omega Z/2$ and the dephasing operator $\sqrt{\gamma/2}\,Z$, where $Z = \mathrm{diag}(1,-1)$, $\omega \in \mathbb{R}$ and $\gamma \geq 0$. In the Lindblad equation each choice gives exactly

$$\dot\rho_{11} = -r_{12}\rho_{11} + r_{21}\rho_{22}, \qquad \dot\rho_{12} = -\left[\tfrac{1}{2}(r_{12}+r_{21}) + \gamma + i\omega\right]\rho_{12}. \tag{1759}$$

The first identity follows from the two gain–loss terms. Their anticommutators contribute half the total exit rate to the second, the Z jump contributes $-\gamma\rho_{12}$, and the Hamiltonian commutator contributes $-i\omega\rho_{12}$. Thus all diagonal preparations and observations have the same classical dynamics for every (γ, ω), whereas a coherent preparation has $\rho_{12}(t) = \rho_{12}(0)\exp[-\{(r_{12}+r_{21})/2 + \gamma + i\omega\}t]$. The ambiguity remains even among completely positive, trace-preserving evolutions.

Finally, a Hamiltonian matrix, a physical interpretation and a measurement theory are distinct pieces of information. The finite transform fixes a Hamiltonian after Q, π and $\hbar_{\mathrm{aux}}$ have been supplied. The physical clock and the relation of this action scale to the measured Planck constant remain to be derived or calibrated. A tensor-product structure, local observables and quantum instruments must also be identified. A four-dimensional interacting field reconstruction further requires the appropriate physical Euclidean correlations and their continuum properties. These requirements locate the next

model-specific calculations. They preserve the stochastic starting point without equating an auxiliary reversible construction with a completed quantum theory of the mother fields.

Appendix R. Geometric control, quantum reconstruction, and the gravitational limit

An optimal-control equation can select a stochastic law without selecting the geometry on which that law is defined. To connect this selection to gravity, one must distinguish a frame at a spacetime point, an entire field configuration, and a physical history. This section establishes a control–spectral correspondence on a fixed regulated configuration space, constructs dynamics that preserve regular constraints, and gives quantitative conditions for a separate gravitational matching step. The final part treats reflection positivity in the time variable used for reconstruction. These distinctions make it possible to develop the proposal without identifying different variational problems.

R.1. *Fields, frames, and the state space.* For a spin manifold with a specified internal principal bundle, write $P = P_{\mathrm{Spin}} \times_M P_{\mathrm{YM}}$. A point of P specifies a point of M and frames in its two fibres. A connection is a Lie-algebra-valued one-form on a bundle; it is not an additional coordinate of a frame point. A tetrad is a field, and a matter configuration is a section of an associated bundle. Consequently the physical variables (e, ω, A, Φ) belong to a space of fields, denoted here by $\mathcal{C}$, rather than to the finite-dimensional manifold P. The derivative of a scalar function along a horizontal lift of a spacetime direction is not the functional derivative of a functional on $\mathcal{C}$.

After a regulator has been chosen, let Q_N be a specified bosonic configuration manifold. Its variables may include finitely many tetrad components, connection links and matter coefficients. A lattice internal gauge group acts on these variables. The choice of Q_N, its metric, reference measure and boundary conditions is part of the model. A compact regular realization can be obtained only with explicit cutoffs or compact variables; an unrestricted tetrad or scalar field is not compact. Fermionic variables require a Grassmann or operator treatment. Integrating them out gives an ordinary positive density only when the resulting determinant or Pfaffian has the required sign.

An ordinary diffusion uses a positive covariance. Its Euclidean frame group is Spin(4), whereas the Lorentzian spin group covers $\mathrm{SO}^+(1,3)$. A general Lorentzian geometry does not come with a canonical global Wick rotation. A Euclidean regulator and its possible Lorentzian reconstruction must therefore be specified separately. For basic scalar functions, a suitably defined horizontal Laplacian on a Riemannian frame bundle projects to the base Laplace–Beltrami

operator. The term "horizontal" does not turn that operator into a Laplacian on the space of field configurations.

Both Itô and Stratonovich formulations are covariant when their transformation rules and connection corrections are retained. Stratonovich notation makes the ordinary chain rule explicit; it does not justify dropping the correction needed to realize a chosen Laplace–Beltrami generator [148].

R.2. *A constraint-preserving regulated diffusion.* The following construction applies to regular finite constraints. It does not assume that a discretization of the gravitational constraints is regular or that its algebra closes.

PROPOSITION 154 (Diffusion on a regular constraint manifold). *Let* $C : \mathcal{U} \subset \mathbb{R}^d \to \mathbb{R}^r$ *be smooth, with full row rank on the nonempty compact connected set* $\mathcal{S} = C^{-1}(0)$*, which has no boundary. Put*

$$P = I - DC^T(DC\,DC^T)^{-1}DC, \qquad V_i(x) = P(x)e_i \quad (1 \le i \le d).$$

For $\varepsilon > 0$ *and smooth* u *on* $\mathcal{S}$*, the Stratonovich equation*

$$dX_t = -\nabla_{\mathcal{S}} u(X_t)\,dt + \sqrt{2\varepsilon}\sum_{i=1}^{d} V_i(X_t) \circ dW_t^i \tag{1760}$$

preserves $C(X_t) = 0$ *and has backward generator* $\varepsilon\Delta_{\mathcal{S}} - \nabla_{\mathcal{S}} u \cdot \nabla_{\mathcal{S}}$*. Its invariant probability has density proportional to* $e^{-u/\varepsilon}$ *relative to induced volume.*

Proof. The rank condition makes P the smooth orthogonal projection onto $\ker DC = T\mathcal{S}$. Both drift and noise fields are tangent; the Stratonovich chain rule gives $dC(X_t) = 0$. Smoothness and compactness give a global diffusion. For an extension $\widetilde{f}$ of a smooth function on $\mathcal{S}$, the extrinsic formula is

$$\sum_i V_i V_i f = \operatorname{tr}(PD^2\widetilde{f}) + \left(\sum_i D_{Pe_i}(Pe_i)\right) \cdot D\widetilde{f} = \Delta_{\mathcal{S}} f.$$

The middle vector is the mean-curvature vector with this Laplacian convention. This proves the generator formula, including its first-order geometric correction. The adjoint equation is $\partial_t \rho = \varepsilon\Delta_{\mathcal{S}}\rho + \operatorname{div}_{\mathcal{S}}(\rho\nabla_{\mathcal{S}} u)$. For $\rho = Z^{-1}e^{-u/\varepsilon}$, the current $-\rho\nabla u - \varepsilon\nabla\rho$ vanishes. Compactness makes Z finite. Ellipticity on the connected manifold gives uniqueness of the invariant probability. □

For a compact internal gauge group acting isometrically, an invariant cost and invariant diffusion preserve the algebra of gauge-invariant observables. This formulation remains meaningful without treating the whole quotient as a smooth manifold. A smooth quotient can instead be used on a free, proper, regular stratum, with its induced metric and volume factors retained. Singular orbits require a separate analysis. The gravitational Hamiltonian and spatial-diffeomorphism constraints are additional constraints: quotienting by internal

frame rotations does not impose them. A regulator must either preserve their algebra or bound its violation and prove its disappearance in the limit.

R.3. *The exact quadratic control–spectral correspondence.* Work on a fixed compact connected Riemannian manifold Q without boundary. The Laplacian has convention $\int f\Delta f\, dm = -\int |\nabla f|^2\, dm$, where dm is Riemannian volume. All quantities in this subsection are nondimensionalized. Let $V \in C^\infty(Q)$, and let an adapted drift $a_t \in T_{X_t}Q$ have finite expected squared norm on each finite time interval. Its generator and long-run cost are

$$L^a f = \varepsilon\Delta f + a\cdot\nabla f, \qquad J(a) = \liminf_{T\to\infty} \frac{1}{T}\mathbb{E}\int_0^T \left(V(X_t) + \tfrac{1}{2}|a_t|^2\right) dt. \quad (1761)$$

The drift penalty belongs in the running cost. The gradient power in the Bellman equation is its convex dual, not an additional cost imposed after the optimization. A local Euclidean realization has noise amplitude $\sqrt{2\varepsilon}$; amplitude σ would give $\varepsilon = \sigma^2/2$.

Theorem 155 (Optimal feedback and the positive ground state). *The self-adjoint operator $\mathsf{H}_\varepsilon = -2\varepsilon^2\Delta + V$ has a simple lowest eigenvalue λ_ε with a strictly positive smooth eigenfunction h_ε, normalized by $\int h_\varepsilon^2 dm = 1$. Set $u_\varepsilon = -2\varepsilon\log h_\varepsilon$. Then*

$$-\varepsilon\Delta u_\varepsilon + \tfrac{1}{2}|\nabla u_\varepsilon|^2 = V - \lambda_\varepsilon. \quad (1762)$$

The feedback $a^* = -\nabla u_\varepsilon$ attains $\inf_a J(a) = \lambda_\varepsilon$, and its unique invariant law is $d\pi_\varepsilon = h_\varepsilon^2 dm$. Writing $L^* = \varepsilon\Delta - \nabla u_\varepsilon\cdot\nabla$,

$$\mathsf{H}_\varepsilon - \lambda_\varepsilon = -2\varepsilon\, U L^* U^{-1}, \qquad Uf = h_\varepsilon f : L^2(\pi_\varepsilon) \longrightarrow L^2(m). \quad (1763)$$

Here the star on L^* denotes the optimal policy, not the adjoint.

Proof. The Rayleigh quotient is

$$\lambda_\varepsilon = inf_{\|h\|_2=1}\left(2\varepsilon^2\int |\nabla h|^2 dm + \int V h^2 dm\right). \quad (1764)$$

Compactness of $H^1(Q) \hookrightarrow L^2(Q)$ and weak lower semicontinuity give a minimizer. Replacing it by its absolute value does not increase the form. Elliptic regularity and the strong maximum principle give a smooth strictly positive minimizer. Integration by parts with $v = hf$ and $\mathsf{H}_\varepsilon h = \lambda h$ gives

$$\langle v, (\mathsf{H}_\varepsilon - \lambda)v\rangle = 2\varepsilon^2\int h^2|\nabla f|^2 dm.$$

Every lowest eigenfunction is therefore a multiple of h, since Q is connected. The logarithmic substitution gives

$$\Delta u = -2\varepsilon\left(\frac{\Delta h}{h} - \frac{|\nabla h|^2}{h^2}\right), \qquad -\varepsilon\Delta u + \tfrac{1}{2}|\nabla u|^2 = 2\varepsilon^2\frac{\Delta h}{h} = V - \lambda.$$

Completing the square, for every admissible drift,

$$V + \tfrac{1}{2}|a|^2 + L^a u = \lambda + \tfrac{1}{2}|a + \nabla u|^2. \tag{1765}$$

Itô's formula has zero expected martingale term under the stated integrability conditions. Integrating the identity gives

$$\frac{1}{T}\mathbb{E}\int_0^T (V + \tfrac{1}{2}|a_t|^2)dt = \lambda + \frac{1}{2T}\mathbb{E}\int_0^T |a_t + \nabla u|^2 dt - \frac{\mathbb{E}u(X_T) - u(X_0)}{T}.$$

The final term tends to zero because u is bounded. This proves the lower bound and attainment for a^*. The stationary equation is $\varepsilon\Delta\rho + \operatorname{div}(\rho\nabla u) = 0$, with a plus sign in the drift-divergence term; $\rho = h^2$ has zero current. Finally, expand $(\mathsf{H}_\varepsilon - \lambda)(hf)$ and cancel the terms proportional to f. The remaining terms are $-2\varepsilon^2 h\Delta f - 4\varepsilon^2\nabla h \cdot \nabla f$, which prove (1763). □

The theorem is a fixed-model verification result in the sense of [68]. The second-order term belongs to the diffusion generator; the control Hamiltonian is a function of the state and costate, not of Δu. A constant shift $V \mapsto V + b$ changes $\lambda_\varepsilon \mapsto \lambda_\varepsilon + b$ but leaves h, the feedback and the path law unchanged. Thus the ergodic value cannot by itself identify a gravitational cosmological constant. With dimensional coordinates, ε and u have units length squared per time, while V and λ have units length squared per time squared for this cost normalization. A scalar curvature has units inverse length squared. Their matching requires a dimensional coefficient and a physical clock; neither $\hbar$ nor Λ is fixed by a relabelling.

R.4. *A controlled zero-noise limit and its limitation.*

Proposition 156 (The selected first-order equation). *For the preceding fixed compact model, $\lambda_\varepsilon \to \min_Q V$ as $\varepsilon \downarrow 0$. If $u_\varepsilon - u_\varepsilon(q_0)$ are uniformly bounded and equicontinuous, every locally uniform subsequential limit u_0 is a viscosity solution of*

$$\tfrac{1}{2}|\nabla u_0|^2 = V - \min_Q V. \tag{1766}$$

Proof. The Rayleigh quotient gives $\lambda_\varepsilon \geq \min V$. A normalized smooth bump supported within distance δ of a minimum has gradient energy at most $C\delta^{-2}$ and potential energy at most $\min V + \omega_V(\delta)$, with fixed local geometry constants. Therefore $\lambda_\varepsilon \leq \min V + 2C\varepsilon^2\delta^{-2} + \omega_V(\delta)$. Taking $\delta = \sqrt{\varepsilon}$ proves the limit. Arzelà–Ascoli gives the subsequential limit of normalized values. If a smooth test function φ touches u_0 strictly from above at q, nearby maxima of $u_\varepsilon - \varphi$ satisfy $-\varepsilon\Delta\varphi + \frac{1}{2}|\nabla\varphi|^2 - V + \lambda_\varepsilon \leq 0$. Passing to the limit gives the viscosity subsolution inequality. Touching from below gives the reverse inequality. A small strictifying perturbation treats non-strict contacts. □

This result neither proves smoothness of u_0 nor supplies a global power-series expansion. If smooth expansions are justified separately, write both $u_\varepsilon = u_0 + \varepsilon u_1 + \cdots$ and $\lambda_\varepsilon = \lambda_0 + \varepsilon\lambda_1 + \cdots$. The first correction obeys $-\Delta u_0 + \nabla u_0 \cdot \nabla u_1 = -\lambda_1$. Omitting the eigenvalue correction is generally incorrect. A deterministic gradient feedback is not, by itself, a derivation of a constrained Hamiltonian theory on gravitational phase space.

A simple geometry shows why a curvature running cost is insufficient. On $M = S^2(r_1) \times S^2(r_2)$, use the product Riemannian metric, trivial matter and internal fields, and $V = R$. The scalar curvature is the constant $2/r_1^2 + 2/r_2^2$. For every ε, $u = 0$ and $\lambda = R$ solve (1762) on the base and on its basic horizontal lift. Yet the Ricci endomorphism has eigenvalues $1/r_1^2$ and $1/r_2^2$. If $r_1 \neq r_2$, the geometry is not Einstein for any cosmological constant. The quadratic control Legendre map is still invertible. An assumption that the characteristics already correspond to Palatini critical fields would supply precisely the missing conclusion.

R.5. *An independent gravitational matching theorem.* In units $c = 1$, the normalized Lorentzian action to recover is

$$S[g, \Phi] = \frac{1}{16\pi G} \int (R - 2\Lambda)\sqrt{-g}\, d^4x + S_{\mathrm{m}}[g, \Phi]. \tag{1767}$$

For admissible variations with the boundary terms treated, its metric equation is $G_{\mu\nu} + \Lambda g_{\mu\nu} = 8\pi G T_{\mu\nu}$, where $T_{\mu\nu} = -2(-g)^{-1/2}\delta S_{\mathrm{m}}/\delta g^{\mu\nu}$. An integrand $R - \lambda$ instead gives the coefficient $\lambda/2$ in the metric equation. In a first-order Palatini description, the torsion-free conclusion additionally needs an invertible tetrad, the stated connection class, and absence of a spin source or other connection terms. Fermionic spin can source torsion.

The required connection to the mother model is convergence of the derived action and its variations, with controlled boundaries and constraints. Convergence of scalar values alone is insufficient: $r_N(x) = N^{-1}\sin(N^2 x)$ converges uniformly to zero while $r_N'(0) = N$. The following local estimate states a useful sufficient condition without assuming the limiting field equation as a consequence of HJB.

Proposition 157 (Local stability of a matched Einstein branch). *Let X, Y be Banach spaces of perturbations and equations after a specified gauge and boundary realization. Suppose the reduced Einstein Euler map near a solution is $F(h) = Lh + N(h)$, where $L : X \to Y$ is a bounded linear isomorphism with bounded inverse. Let $K, M, \eta \geq 0$, $\|L^{-1}\| \leq K$, $N(0) = 0$, and*

$$\|N(h)\| \leq M\|h\|^2, \qquad \|N(h) - N(k)\| \leq 2Mr\|h - k\| \quad (\|h\|, \|k\| \leq r).$$

Suppose an independently derived regulated Euler map is $F_N(h) = F(h) + r_N(h)$, with $\sup_{\|h\| \leq r} \|r_N(h)\| \leq \delta$ and Lipschitz constant at most η. If $\delta > 0$, $r = 2K\delta$,

$KMr \le 1/4$ and $K\eta \le 1/4$, then F_N has a unique zero in the closed radius-r ball, and $\|h_N\| \le 2K\delta$.

Proof. Use $T(h) = -L^{-1}(N(h)+r_N(h))$. Its norm is at most $KMr^2+K\delta \le r/4 + r/2 = 3r/4$, so it maps the ball into itself. Its Lipschitz constant is at most $2KMr+K\eta \le 3/4$. The contraction theorem gives the unique fixed point, which is exactly a zero of F_N. □

The proposition applies only after invertibility, gauge consistency and the variation bounds have been established for an actual branch. It is suited to nondegenerate Euclidean boundary problems; Lorentzian initial-value problems instead require hyperbolic energy estimates and constraint propagation. If gauge fixing introduces auxiliary equations, their vanishing must be proved before a reduced solution is called a solution of the ungauged field equations. The matched Palatini branch in the main text supplies a candidate action to which such estimates may be applied. A positive control cost cannot simply be substituted for that action: Einstein stationary fields can be saddles, whereas the ground-state small-noise problem selects minima of its specified cost.

R.6. *What reflection positivity does and does not supply.* The stationary reversible process in Theorem 155 is reflection positive in its auxiliary time. For a bounded future cylinder function F, reversibility and conditional independence of past and future given X_0 imply

$$\mathbb{E}[\overline{F(\vartheta X)}F(X)] = \int \big|\mathbb{E}[F \mid X_0 = q]\big|^2 d\pi_\varepsilon(q) \ge 0, \tag{1768}$$

where $(\vartheta X)_t = X_{-t}$. The associated semigroup is unitarily equivalent to $\exp[-t(\mathsf{H}_\varepsilon - \lambda_\varepsilon)/(2\varepsilon)]$. This is a quantum-mechanical reconstruction in the chosen time, not a four-dimensional gravitational reconstruction. A commutative Euclidean probability law can support such a reconstruction: multiplication observables and their Hamiltonian time translates need not commute. Thus a noncommutative stochastic differential equation is a possible additional construction, not a necessary replacement for every classical Euclidean route to quantum theory.

For a physical Euclidean time reflection, the crossing interaction must have the appropriate sign structure. The following finite construction gives a direct sufficient condition.

Proposition 158 (A positive crossing kernel). *Let ν be a finite positive measure on configurations in the positive half, let S_+ be real, and identify the negative half by reflection. Suppose*

$$K(x,y) = \sum_\alpha c_\alpha f_\alpha(x)\overline{f_\alpha(y)}, \qquad c_\alpha \ge 0,$$

is real and nonnegative, and $Z^{-1}e^{-S_+(x)-S_+(y)}K(x,y)\nu(dx)\nu(dy)$ *is a probability measure. Assume absolute convergence permitting the displayed integrals and sum. Then its reflection form is nonnegative for every bounded positive-half observable* F*.*

Proof. Insert the expansion of K into the reflection form. It equals

$$Z^{-1}\sum_{\alpha} c_\alpha \left| \int F(x) f_\alpha(x) e^{-S_+(x)} \nu(dx) \right|^2 \geq 0.$$

The nonnegative kernel hypothesis ensures an ordinary probability law; the sum-of-squares representation supplies the additional reflection property. □

For example, $e^{\beta\cos(x-y)}$, $\beta \geq 0$, has Fourier coefficients $I_n(\beta) = \sum_{k\geq 0}(\beta/2)^{2k+|n|}/[k!(k+|n|)!] \geq 0$. It gives a compact $U(1)$ crossing kernel. A scalar coupling e^{Jxy} with $J \geq 0$ has the analogous power-series representation whenever the confining half-actions make it integrable. These examples identify a design condition for a matter–gauge regulator. They do not establish that a fluctuating-tetrad gravitational action has this representation.

Ordinary covariance positivity is weaker. The stationary Gaussian covariance $C(t) = e^{-t^2}$ is positive definite, since its Fourier transform is nonnegative. For reflection times $1, 2$, however,

$$\det \begin{pmatrix} C(2) & C(3) \\ C(3) & C(4) \end{pmatrix} = e^{-20} - e^{-18} < 0. \tag{1769}$$

It fails reflection positivity. A positive covariance or a bounded conformal Hessian therefore cannot replace this test. Convergence of all needed cylinder moments preserves each finite reflection inequality; tightness alone does not ensure convergence of unbounded moments. Full relativistic reconstruction requires the remaining regularity, Euclidean symmetry, permutation and growth hypotheses of the selected Osterwalder–Schrader theorem, with the physical observable algebra and constraint realization [124] and [125]. Clustering adds the corresponding vacuum uniqueness property.

R.7. *Fluctuations, nonlinear penalties, and horizons.* A single measure on frame points cannot define joint field values at two distinct spacetime points. On a genuine regulated field law, let $\xi = q - \bar{q}$ and suppose the localized value is exactly quadratic, $u = u(\bar{q}) + \frac{1}{2}\xi^T K \xi$, $K > 0$. Then $\mathrm{Cov}(\xi) = \varepsilon K^{-1}$. For a nonlinear value, this is only a Laplace approximation, requiring concentration, nondegeneracy and bounds on higher derivatives. For the metric map, the first-order term is $\delta g_{\mu\nu} = \eta_{ab}(\bar{e}^a_\mu \delta e^b_\nu + \delta e^a_\mu \bar{e}^b_\nu)$; the exact expression also contains $\eta_{ab}\delta e^a_\mu \delta e^b_\nu$. Thus the leading covariance is $J\varepsilon K^{-1}J^T$, with the field-to-metric derivative J, rather than a factorization of arbitrary four-point expectations.

Already for $g = (e_0 + \xi)^2$ and $\xi \sim N(0, s^2)$, $\mathrm{Var}(g) = 4e_0^2 s^2 + 2s^4$. Gauge zero modes and indefinite conformal modes must be treated before taking an inverse.

For a Hamiltonian power $\gamma > 1$, the running drift penalty is $|a|^q/q$, with $q = \gamma/(\gamma - 1)$. Convex duality gives

$$\inf_a \{\tfrac{1}{q}|a|^q + a \cdot \nabla u\} = -\tfrac{1}{\gamma}|\nabla u|^\gamma, \qquad a^* = -|\nabla u|^{\gamma-2}\nabla u.$$

The noise is still linear diffusion. With the feedback fixed, its Fokker–Planck equation is linear in the density. The drift need not be an ordinary gradient, but $\gamma = 2$ is not its only gradient case: for $u(x) = x^2/2$ on the line it is the negative derivative of $|x|^\gamma/\gamma$. In two dimensions, $u = (x^2 + 2y^2)/2$ and $\gamma = 4$ give the vector field $b = (x^2 + 4y^2)(x, 2y)$, with $\partial_x b_y - \partial_y b_x = -4xy$; it is not a gradient in general. No universal Gibbs formula in u follows in that case.

A uniformly elliptic diffusion on a connected compact configuration space communicates between open sets. A Lorentzian event horizon is a causal boundary of physical spacetime, not an automatically absorbing set of this auxiliary diffusion. Killing, reflection or degeneracy changes its generator and invariant-law problem. Nor is relative entropy alone an area law. If $\pi(A) = p > 0$, then $D(\pi(\cdot \mid A)\|\pi) = \log(1/p)$, which depends on the probability weight. A probability supported on a hypersurface is singular relative to a smooth volume law and has infinite relative entropy. At equilibrium $D(\pi\|\pi) = 0$. None of these quantities equals the nonzero black-hole entropy $k_B c^3 \,\mathrm{Area}\,/(4G\hbar)$ without additional physical structure [158].

R.8. *A finite gauge model and the next construction.* Take four oriented $U(1)$ links around one plaquette, with angles θ_e, and gauge-invariant holonomy $\phi = \sum_{e=1}^4 \theta_e \pmod{2\pi}$. A vertex rotation adds its angle to an outgoing link and subtracts it from an incoming link. Therefore ϕ and any function of it satisfy the infinitesimal Gauss constraints. With $V(\phi) = 1 - 0.6\cos\phi$, the invariant ground-state problem is

$$[-8\varepsilon^2\partial_\phi^2 + V(\phi)]h = \lambda h, \quad u = -2\varepsilon \log h, \quad -4\varepsilon u'' + 2(u')^2 = V - \lambda. \quad (1770)$$

The factor four comes from $\sum_e \partial_{\theta_e}^2 f(\phi) = 4f''(\phi)$. This is an actual compact gauge-link model; it is not a tetrad or graviton model. Its numerical comparison below uses synthetic inputs.

For a larger regulator, compact internal gauge invariance can be proved before solving the spectral problem: the operator commutes with the group action, and uniqueness of its normalized positive ground state forces that state to be invariant. The remaining gravitational work is to construct the tetrad–connection constraint realization, derive a common effective action with first-variation bounds, and verify a physical-time reflection-positive family with a controlled continuum limit. Appendix S carries out the independent coframe–connection variation on an exact Einstein branch and the constraint

Table 33. Synthetic plaquette spectral calculation at 512 periodic points. Residuals compare the numerical value with the continuum HJB equation; the convergence order uses the last two meshes, not a certified error enclosure.

ε	λ	HJB residual	observed order
0.2	0.687136818	9.80×10^{-5}	1.999
0.4	0.870700110	1.56×10^{-5}	2.000
0.8	0.965051911	2.96×10^{-6}	2.000

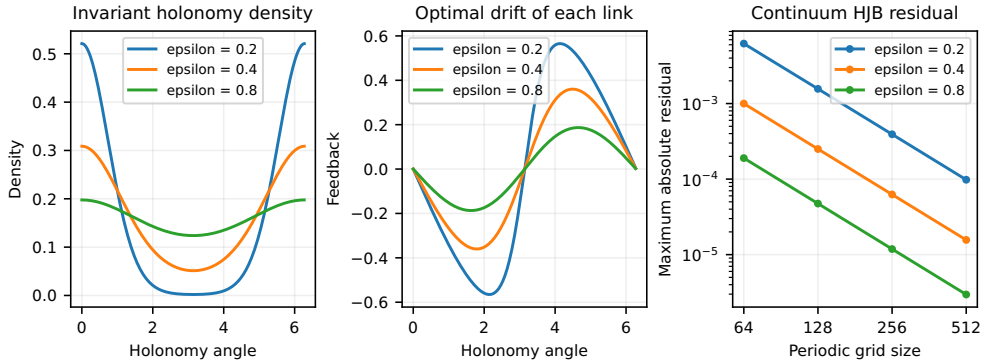


Figure 60. Synthetic periodic-plaquette calculation. The same specified potential fixes the positive ground state, optimal feedback and invariant density at each noise scale. Mesh refinement tests the continuum Bellman residual. This residual converges with discretization error; a finite-difference chain rule is not treated as an exact continuum identity. These are numerical consistency tests, not gravitational data.

reduction and ultraviolet construction in the free sector. It also gives an explicit obstruction for a different, four-derivative quantum candidate. None of these results selects a unique interacting quantum-gravity theory or determines all its physical constants.

Appendix S. Einstein branches, a quantitative response bound, and a free gravitational limit

A controlled gravitational construction must specify the field variables, the equations that constrain them, and the limit in which quantum states are defined. These are different requirements. This appendix treats the constant-weight geometric sector of the explicit Cartan action (217). It first verifies a family of exact Einstein critical points with an independent connection. It then computes the response error and a quantum obstruction for its torsionless quadratic

restriction. An exact nonlinear initial-data family then makes the curvature correction for constraint-preserving stochastic sampling explicit. Finally, it removes the spatial ultraviolet cutoff in the two-derivative free physical sector. The last construction describes free gravitational waves, not the interacting mother theory.

S.1. *Exact Einstein critical points of the independent-connection sector.* The variables here are a nondegenerate solder form e and an independent $SO(4)$ connection ω on the orthonormal frame bundle of an oriented four-dimensional Euclidean manifold. Local sections give the coframes used in the formulas; a global coframe on the base is not required. Let $S_g = w_* S_{\mathrm{c}}$, where $w_* > 0$ is held fixed. Matter fields and any scalar that would make w_* vary are absent from this sector. Variations have compact support, or the manifold is closed.

Proposition 159 (An exact Einstein branch of the Cartan sector). *Every smooth Einstein metric with* $\mathrm{Ric}(g) = 3\ell^{-2} g$*, equipped with its solder form and Levi–Civita connection, is a critical point of* S_g *under independent variations of both* e *and* ω*. The coframe and connection equation residuals vanish identically.*

Proof. The torsion vanishes. Decompose the curvature as

$$R^{ab} = C^{ab} + \ell^{-2} e^a \wedge e^b, \qquad F_{\mathrm{c}}^{ab} = C^{ab}, \qquad F_{\mathrm{c}}^{a5} = 0, \tag{1771}$$

where C is the Weyl tensor. With the coframe fixed, an independent connection variation gives $\delta F^{ab} = D_\omega \delta\omega^{ab}$. Terms involving δF^{a5} have zero first variation because $F^{a5} = 0$. Integration by parts reduces the connection equation to $D_\omega \star C^{ab} = 0$. The contracted differential Bianchi identity gives $\nabla^\mu R_{\mu\nu\rho\sigma} = \nabla_\rho R_{\nu\sigma} - \nabla_\sigma R_{\nu\rho} = 0$; the constant-curvature part is parallel. This proves that equation.

For a coframe variation at fixed ω, the explicit curvature variation is $\delta F^{ab} = -\ell^{-2}(\delta e^a \wedge e^b + e^a \wedge \delta e^b)$. Its contraction with C^{ab} vanishes by the trace-free property of the Weyl tensor. It remains essential to vary the Hodge operator. Its contribution is proportional to the Yang–Mills stress tensor of C, which vanishes by the four-dimensional algebraic identity

$$C_{\mu\alpha\beta\gamma} C_\nu{}^{\alpha\beta\gamma} = \tfrac{1}{4} g_{\mu\nu} C_{\alpha\beta\gamma\delta} C^{\alpha\beta\gamma\delta}. \tag{1772}$$

One way to see the identity is to split the curvature operator on two-forms into its self-dual and anti-self-dual blocks. The Weyl operator preserves these orthogonal blocks. In an orthonormal internal basis, each corresponding two-form is self-dual or anti-self-dual, and satisfies $F_{\mu\rho} F_\nu{}^\rho = g_{\mu\nu} F_{\rho\sigma} F^{\rho\sigma}/4$. Summing these identities proves (1772); the pair symmetry of C identifies the internal and spacetime contractions. The torsion term again has zero first variation. Both independent Euler equations therefore vanish. □

This family contains more than the flat Cartan connection on the round four-sphere. The product $S^2(r) \times S^2(r)$, with $r = \ell/\sqrt{3}$, has nonzero Weyl curvature and satisfies

$$|C|^2 = 48\ell^{-4}, \qquad \mathrm{Vol} = 16\pi^2\ell^4/9, \qquad S_g = \frac{32\pi^2 w_*}{3g_{\mathrm{c}}^2}. \tag{1773}$$

Indeed, each surface has sectional curvature $3\ell^{-2}$, so that $|\,\mathrm{Rm}\,|^2 = 72\ell^{-4}$, whereas the constant-curvature Einstein component has squared norm $24\ell^{-4}$. This is an exact critical point, with zero Einstein-equation residual and positive action. The round sphere has zero action on a different topology; that comparison does not decide local minimality on the product manifold. The calculation does not bound the distance of a generic Cartan solution from the Einstein branch, or prove stability of that branch. If the weight is a dynamical scalar function, its equation contains $w'(\sigma)|C|^2$; it must be satisfied separately. Nor does a family of exact solutions determine the full Hamiltonian constraint algebra of the independent-connection theory.

S.2. *The actual coefficient and the linear Einstein response error.* Now restrict to the torsionless metric theory and freeze the common weight. A flat expansion additionally requires a declared cancellation of the vacuum energy. The original Cartan branch has $\Lambda_E = 3\ell^{-2}$, so flatness is not a consequence of that unmodified action. In this vacuum-matched restriction, the coefficients in (237) give

$$M_{\mathrm{P}}^2 := \frac{1}{8\pi G} = \frac{w_*}{g_{\mathrm{c}}^2\ell^2}, \qquad \alpha_3 = \frac{w_*}{8g_{\mathrm{c}}^2}, \qquad \frac{8\alpha_3}{M_{\mathrm{P}}^2} = \ell^2. \tag{1774}$$

Thus a change of the common weight alone cannot suppress the relative four-derivative term. With a dimensionless metric perturbation $\gamma_{\mu\nu} = 2h_{\mu\nu}/M_{\mathrm{P}}$, the positive Euclidean quadratic form on a transverse, traceless polarization is

$$S_{2,\ell}[h] = \tfrac{1}{2}\int h(-p)K_\ell(p)h(p)\,\mathrm{d}p, \qquad K_\ell(p) = p^2(1+\ell^2p^2). \tag{1775}$$

Here p is a Euclidean four-momentum and $c = 1$. The normalization follows by substituting $\gamma = 2h/M_{\mathrm{P}}$ into (790) and using the Euclidean sign with a positive p^4 term. This sign is fixed for the following calculation; it is not an assertion about every Lorentzian continuation.

Proposition 160 (A sharp response bound and a reflection obstruction). *Let a Euclidean transverse, traceless source J have Fourier support in $0 < p_{\min} \le |p| \le P$, and put $h_\ell = K_\ell^{-1}J$, $h_0 = (p^2)^{-1}J$. For any common positive spectral weight defining an L^2 norm,*

$$\|h_\ell - h_0\| \le \frac{\ell^2P^2}{1+\ell^2P^2}\,\|h_0\|. \tag{1776}$$

The multiplier bound is sharp. Nevertheless, for every $\ell > 0$, the Gaussian covariance $\hbar K_\ell^{-1}$ on unrestricted Euclidean time fails reflection positivity even in a single nonzero spatial transverse, traceless mode.

Proof. Pointwise in Fourier space, $h_\ell - h_0 = -[\ell^2 p^2/(1+\ell^2 p^2)]h_0$. The bracketed multiplier increases with p^2; multiplication, squaring and integration prove (1776). A mode at $|p| = P$ gives equality on a discrete spectrum, and wave packets concentrating there approach equality on a continuous spectrum.

To test reflection, use the full time-frequency covariance, without the band restriction imposed on the comparison source. Partial fractions give

$$\frac{\hbar}{p^2(1+\ell^2 p^2)} = \frac{\hbar}{p^2} - \frac{\hbar}{p^2+\ell^{-2}}. \tag{1777}$$

At fixed spatial frequency $a = |k| > 0$, let $b = (a^2+\ell^{-2})^{1/2} > a$. Fourier inversion in Euclidean time gives $C_\ell(t,k) = \hbar e^{-a|t|}/(2a) - \hbar e^{-b|t|}/(2b)$. For $0 < t_1 < t_2$, choose $c_1 = e^{-at_2}$, $c_2 = -e^{-at_1}$. Then

$$\mathcal{Q}_\ell := \sum_{i,j=1}^{2} c_i c_j C_\ell(t_i + t_j, k) = -\frac{\hbar}{2b}\big(e^{-at_2-bt_1} - e^{-at_1-bt_2}\big)^2 < 0. \tag{1778}$$

The positive massless contribution cancels exactly, and the remaining square is nonzero since $(b-a)(t_2-t_1) > 0$. Smooth time tests concentrated at the two positive times preserve the strict inequality, by continuity. Thus the failure is not an artifact of using point evaluations. A positive covariance in the usual probabilistic sense is insufficient for positive quantum reconstruction. □

For example, $P\ell = 0.1, 0.3, 1$ give the exact relative bounds $1/101, 9/109, 1/2$, respectively. They are linear Euclidean source-response errors, not nonlinear Lorentzian evolution errors. With $a = \ell = \hbar = 1$ and $(t_1, t_2) = (1, 2)$, the negative reflection form is approximately -4.40215496×10^{-5}. Figure 61 displays these specified calculations. Reversing the sign of the p^4 term instead makes the quadratic form negative for $p^2 > \ell^{-2}$. Neither extrapolation of this local metric truncation is a positive ultraviolet quantum completion. The negative-residue issue is a standard difficulty of higher-derivative gravity [147]; here its coefficient and a strict reflection test are obtained for the specified Cartan restriction. The obstruction does not exclude a different independent-connection, nonlocal, or enlarged-field completion, whose physical covariance would have to be derived afresh. Keeping the term only as a low-energy expansion also makes no claim about that completion.

S.2.1. *The response that remains controlled at low momentum.* The reflection test concerns the full frequency dependence of the displayed higher-derivative covariance. A separate question is how accurately its linear response can be approximated in a prescribed low-momentum band. This distinction

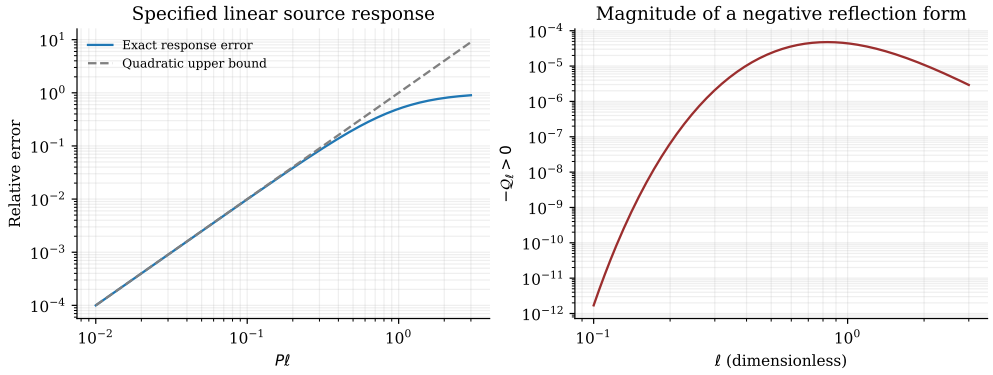


Figure 61. Specified quadratic gravitational sector, with synthetic dimensionless inputs. Left: the exact maximum relative source-response error and its quadratic upper bound. Right: the magnitude of a strictly negative reflection form, with $a = \hbar = 1$ and reflection times $1, 2$. The curves are evaluations of (1776) and (1778); they are not observational measurements.

allows one to quantify the effective response while retaining the positivity obstruction.

For a nonzero Euclidean momentum, write $x = \ell^2 p^2 \geq 0$ and let $D_0(p) > 0$ be the Einstein transverse-traceless covariance with the same normalization. The quadratic branch and its first expansion are

$$D_{\rm quad}(p) = \frac{D_0(p)}{1+x}, \qquad D_1(p) = D_0(p)(1-x), \qquad \frac{D_{\rm quad}(p) - D_1(p)}{D_0(p)} = \frac{x^2}{1+x}. \tag{1779}$$

The identity follows by multiplying by $1+x$: $1-(1-x)(1+x) = x^2$. Therefore, on $\ell|p| \leq \varepsilon$,

$$0 \leq \frac{D_{\rm quad} - D_1}{D_0} \leq \varepsilon^4, \qquad \frac{|D_{\rm quad} - D_1|}{D_{\rm quad}} = x^2 \leq \varepsilon^4. \tag{1780}$$

For $\varepsilon < 1$, the approximate multiplier $1 - x$ is positive throughout that band. This is a pointwise multiplier statement; it is not time-reflection positivity of a complete covariance. The error is relative to the specified quadratic branch, so loop corrections, other operators, changing backgrounds and nonlinear backreaction are not included in it. In particular this estimate does not repair the negative reflection form or construct an interacting quantum Hilbert space.

S.3. *Linear gravitational constraints on field configurations.* The two-derivative physical sector can nevertheless be completed as a free theory. Take a flat spatial torus of side 2π, use its normalized volume measure, and fix the homogeneous modes. Fixing them removes zero-frequency oscillators, which

would have no normalizable stationary Gaussian law. The spatial metric and its canonical momentum are genuine tensor fields, rather than a single point of a frame bundle. To first order the vacuum constraints, up to nonzero fixed normalizations, are

$$C_H^{(1)} = \partial_i \partial_j h_{ij} - \Delta h_{ii} = 0, \qquad C_i^{(1)} = \partial_j \pi_{ij} = 0. \tag{1781}$$

For a nonzero spatial Fourier vector k, define

$$P_{ij}(k) = \delta_{ij} - \frac{k_i k_j}{|k|^2}, \qquad \mathcal{P}_{ij,kl}(k) = \tfrac{1}{2}(P_{ik}P_{jl} + P_{il}P_{jk} - P_{ij}P_{kl}). \tag{1782}$$

The symbol $\mathcal{P}$ here is a tensor projector, not the frame bundle or the momentum cutoff P in the preceding bound.

Proposition 161 (Constraint-preserving free field dynamics). *On symmetric spatial tensors $\mathcal{P}(k)$ is an orthogonal rank-two projector onto the transverse, traceless subspace. Restricting both h and π to this subspace satisfies all constraints* (1781). *The linearized constraint brackets vanish. After gauge reduction the two-derivative Einstein action is a collection of canonical oscillators with frequencies $\omega_a = |k_a|$. For any finite spatial cutoff their Euclidean vacuum law is the invariant law of*

$$\mathrm{d}q_a = -\omega_a q_a \,\mathrm{d}\tau + \sqrt{\hbar}\,\mathrm{d}W_a, \qquad \mathrm{Var}(q_a) = \frac{\hbar}{2\omega_a}. \tag{1783}$$

Both the free Hamiltonian motion and this stochastic motion remain in the linear constraint surface.

Proof. Since $P^2 = P = P^T$, $Pk = 0$ and $\operatorname{tr} P = 2$, $\mathcal{P}$ is self-adjoint, removes the transverse trace, and annihilates longitudinal tensors. Its image consists of symmetric trace-free tensors on a two-dimensional plane, a space of dimension two. It acts as the identity there, proving idempotence and the rank claim. The constraints then vanish mode by mode. The Hamiltonian constraint is linear in h, while the momentum constraints are linear in π; brackets within either family vanish. Their mixed bracket is zero because the scalar symbol annihilates a spatial gauge variation:

$$(k_i k_j - |k|^2 \delta_{ij})(k_i \xi_j + k_j \xi_i) = 0. \tag{1784}$$

These are the linearized brackets, not the nonlinear hypersurface deformation algebra.

Orthonormal real Fourier functions and polarizations, together with $\gamma = 2h/M_{\mathrm{P}}$, reduce the Lorentzian action to $\frac{1}{2}\sum_a \int (\dot{q}_a^2 - \omega_a^2 q_a^2)\,\mathrm{d}t$. The Hamiltonian is $\frac{1}{2}\sum_a (p_a^2 + \omega_a^2 q_a^2)$; its motion preserves this reduced space. Put $\varepsilon = \hbar/2$,

$u_K = \frac{1}{2}\sum_a \omega_a q_a^2$ and $V_K = \frac{1}{2}\sum_a \omega_a^2 q_a^2$. Direct differentiation gives

$$-\frac{\hbar}{2}\Delta u_K + \frac{1}{2}|\nabla u_K|^2 = V_K - \lambda_K, \qquad \lambda_K = \frac{\hbar}{2}\sum_a \omega_a. \tag{1785}$$

The associated Schrödinger ground state is proportional to $\exp[-\sum_a \omega_a q_a^2/(2\hbar)]$. Its square is the invariant Gaussian density of (1783), as follows either from the Fokker–Planck equation or from $\frac{\mathrm{d}}{\mathrm{d}\tau}\mathbb{E}q_a^2 = -2\omega_a \mathbb{E}q_a^2 + \hbar$. All field increments are transverse and traceless. The constraints are linear, so their Itô second-derivative correction is zero. □

Euclidean time has a physical interpretation here because the specified quadratic Lorentzian action fixes the frequencies and its Wick rotation has this same covariance. This identification is additional to the abstract control construction. The original process does not uniquely select a physical clock. Moreover, transverse and traceless noise alone does not preserve nonlinear gravitational constraints: their quadratic terms and their Itô Hessian terms are generally nonzero. For example, take an exactly flat spatial metric and its ADM canonical momentum density $\Pi^{11} = A\cos z$, $\Pi^{22} = -A\cos z$, with all other components zero. This density is conjugate to the full spatial metric, before the constant canonical rescaling used for h. The momentum constraint and every linear constraint vanish, but the exact vacuum ADM Hamiltonian density is

$$\mathcal{H} = 16\pi G(\Pi^{ij}\Pi_{ij} - \tfrac{1}{2}(\operatorname{tr}\Pi)^2) = 32\pi G A^2 \cos^2 z, \tag{1786}$$

which is not identically zero for $A \neq 0$, although it vanishes at the nodes of $\cos z$. Here the determinant of the spatial metric is one and its scalar curvature is zero. Higher-order corrections to the geometry and the global constraints are therefore indispensable; linear constraint preservation does not establish nonlinear linearization stability on this compact background.

S.4. *An exact nonlinear constraint family and its stochastic sampling.* The preceding counterexample leaves a constructive question: can the trace of the extrinsic curvature compensate its shear while preserving the momentum constraint? For a spatially varying polarization with constant norm, the answer is explicit. The construction below concerns the Lorentzian two-derivative Einstein sector with a specified positive cosmological constant. It does not identify its initial-data space with that of the independent-connection mother action.

Fix a length L_0, set $c = 1$, and use dimensionless coordinates on $\mathbb{T}^3 = (\mathbb{R}/2\pi\mathbb{Z})^3$. The physical spatial metric is $L_0^2\delta_{ij}$. In the dimensionless equations below, $\gamma_{ij} = \delta_{ij}$, K_{ij} denotes L_0 times the physical orthonormal components of the extrinsic curvature, and $\Lambda = L_0^2\Lambda_E > 0$. Thus the original Cartan value can be retained as $\Lambda = 3(L_0/\ell)^2$; no flat-spacetime vacuum subtraction is used here.

A flat spatial slice need not have a flat spacetime development. With either consistent overall sign convention for K, the vacuum initial constraints are

$$\mathcal{C} := \mathrm{Scal}(\gamma) + (\mathrm{tr}_\gamma K)^2 - |K|^2_\gamma - 2\Lambda = 0, \qquad \mathcal{M}_i := \nabla^j (K_{ij} - \gamma_{ij}\,\mathrm{tr}_\gamma K) = 0. \tag{1787}$$

These are nonlinear constraints of Einstein gravity. They are not the additional connection or matter constraints of the unreduced theory.

Proposition 162 (Exact spatially varying nonlinear initial data). *Let $a \in \mathbb{R}$, $k \in \mathbb{Z}$, and let ψ be any smooth 2π-periodic real function. Put $z = x^3$, $\vartheta(z) = kz + \psi(z)$, and define*

$$Q(\vartheta) = \begin{pmatrix} \cos\vartheta & \sin\vartheta & 0 \\ \sin\vartheta & -\cos\vartheta & 0 \\ 0 & 0 & 0 \end{pmatrix}, \qquad \tau(a) = \sqrt{3(a^2+\Lambda)}, \qquad K = aQ + \tfrac{1}{3}\tau(a) I. \tag{1788}$$

Then (γ, K) satisfies every equation in (1787) *pointwise. The parameter τ is the mean curvature, not a time coordinate.*

Proof. The entries of Q are periodic even when ϑ has winding number k. Direct multiplication gives $\mathrm{tr}\, Q = 0$, $Q_{i3} = 0$, and $|Q|^2 = 2$. Only z varies, so $\partial^j Q_{ij} = \partial_z Q_{i3} = 0$. Since a and τ are spatial constants, the momentum constraint vanishes. The metric is flat, and

$$\mathrm{tr}\, K = \tau, \qquad |K|^2 = 2a^2 + \tfrac{1}{3}\tau^2, \qquad \mathcal{C} = \tfrac{2}{3}\tau^2 - 2a^2 - 2\Lambda = 0. \tag{1789}$$

The last equality uses the stated choice of τ. No expansion in a or derivatives of ψ is involved. □

The norm of the shear is fixed on each slice, while its orientation may vary freely with z. This is why its divergence and the scalar constraint can be satisfied simultaneously. The family is infinite dimensional through ψ, but has a fixed flat spatial metric and special shear. It is not an open set of general gravitational initial data. Replacing the rotating pair by a lone cosine would make its norm spatially variable and would invalidate (1789) with a constant mean curvature.

We next allow the amplitude and the phase profile to fluctuate. This tests the compatibility between a stochastic law and the nonlinear constraints. The parameter s below is an auxiliary sampling parameter. No identification with proper time, lapse evolution or a Lorentzian Einstein trajectory is made. Choose smooth periodic functions e_j, independent Brownian motions $B_0, \ldots, B_m$, and positive rates β_j. Set $\vartheta_s(z) = kz + \sum_{j=1}^m x_j(s) e_j(z)$. For fixed real noise amplitudes σ_j, let

$$\mathrm{d}a = -\beta_0 a\,\mathrm{d}s + \sigma_0\,\mathrm{d}B_0, \qquad \mathrm{d}x_j = -\beta_j x_j\,\mathrm{d}s + \sigma_j\,\mathrm{d}B_j. \tag{1790}$$

Write $b_a = -\beta_0 a$, $b_\vartheta(z) = -\sum_j \beta_j x_j e_j(z)$, and $v(z) = \sum_j \sigma_j^2 e_j(z)^2$. Let $R = \partial_\vartheta Q$, so that $\partial_\vartheta^2 Q = -Q$, $Q : R = 0$, and $|R|^2 = 2$.

PROPOSITION 163 (A stochastic law on the nonlinear family). *For every finite m, reconstructing K_s by* (1788) *from* (1790) *gives smooth spatial initial data satisfying* (1787) *at all sampling times, almost surely. Its Itô differential is*

$$\begin{aligned} \mathrm{d}K &= \left[b_a K_a + a b_\vartheta R + \frac{\sigma_0^2 \tau''}{6} I - \frac{av}{2} Q\right] \mathrm{d}s + \sigma_0 K_a \,\mathrm{d}B_0 + aR \sum_{j=1}^{m} \sigma_j e_j \,\mathrm{d}B_j, \\ K_a &= Q + \tfrac{1}{3}\tau' I, \qquad \tau' = \frac{3a}{\tau}, \qquad \tau'' = \frac{9\Lambda}{\tau^3}. \end{aligned} \tag{1791}$$

If both curvature-drift terms $\sigma_0^2 \tau'' I/6 - avQ/2$ are omitted, the remaining drift and noise are tangent to the scalar constraint at the family, but their Itô generator satisfies

$$(\mathcal{L}_{\mathrm{omit}} \mathcal{C})(a, z) = -\frac{2\sigma_0^2 \Lambda}{a^2 + \Lambda} - 2a^2 v(z). \tag{1792}$$

The complete generator instead has $\mathcal{L}\mathcal{C} = 0$ there. In particular, nonzero amplitude noise makes the omitted-drift defect strictly negative for every a.

Proof. For $\Lambda > 0$ the map from $(a, x_1, \dots, x_m)$ to K is smooth everywhere. The parameter processes are global continuous Ornstein–Uhlenbeck processes. Proposition 162 therefore proves the pathwise constraint assertion simultaneously for all z and s. The multivariable Itô formula gives (1791); independence removes the mixed quadratic variations between amplitude and phase.

For a symmetric increment H, the first and second derivatives of the scalar constraint at the fixed metric are

$$D\mathcal{C}_K[H] = 2\tau \operatorname{tr} H - 2K : H, \qquad \tfrac{1}{2} D^2 \mathcal{C}_K[H, H] = (\operatorname{tr} H)^2 - |H|^2. \tag{1793}$$

Both K_a and aR are tangent: substitution of $\tau\tau' = 3a$ gives $D\mathcal{C}_K[K_a] = 0$, while $\operatorname{tr} R = Q : R = 0$ gives $D\mathcal{C}_K[aR] = 0$. For the independent amplitude and phase noise, the total half-Hessian contribution is

$$\sigma_0^2 \left(\tfrac{2}{3}(\tau')^2 - 2\right) - 2a^2 v = -\frac{2\sigma_0^2 \Lambda}{a^2 + \Lambda} - 2a^2 v. \tag{1794}$$

The omitted drift has zero first-derivative contribution, proving (1792). The two added drift terms contribute exactly

$$D\mathcal{C}_K\left[\frac{\sigma_0^2 \tau''}{6} I - \frac{av}{2} Q\right] = \frac{2\sigma_0^2 \Lambda}{a^2 + \Lambda} + 2a^2 v. \tag{1795}$$

This cancels (1794). The momentum constraint also remains zero: the off-diagonal entries in the third column vanish, and its remaining entry after trace

subtraction is independent of z. This argument applies to the reconstructed paths directly, without assuming that the parameterization is injective. □

The strict positivity of Λ is used for smooth sampling at $a = 0$. Indeed, $\sup_a \tau''(a) = \sqrt{3/\Lambda}$, so there is no uniform second-derivative bound as $\Lambda \downarrow 0$. At exactly $\Lambda = 0$, the positive root is $\sqrt{3}|a|$, and the ordinary smooth Itô formula does not apply through zero. Choosing the different, signed branch $\tau = \sqrt{3}a$ gives a smooth constraint family; retaining the absolute-value branch requires its local-time term. Neither change may be silently substituted into the positive-Λ proposition.

For a dimensionless synthetic calculation, take $\Lambda = 3/4$, $k = 1$, $e_1(z) = \cos z$, $e_2(z) = \sin 2z$, $(\beta_0, \beta_1, \beta_2) = (0.7, 1.1, 1.7)$, and $(\sigma_0, \sigma_1, \sigma_2) = (0.4, 0.3, 0.2)$. From $(a, x_1, x_2) = (0.6, 0.2, -0.15)$, exact Gaussian transitions of the three parameter processes with step $1/128$ give 513 states over $0 \le s \le 4$. On 257 equally spaced spatial points, the largest directly evaluated $|\mathcal{C}|$ is 2.23×10^{-15}, rounded upward. A separate Fourier differentiation of the momentum tensor gives a largest residual below 1.33×10^{-13}. These floating-point diagnostics illustrate the identities; they are not bounds on an uncomputed spacetime evolution.

At the specified initial state and $z = 0.8$, $v = 0.0836519170123371$ and $\mathcal{L}_{\mathrm{omit}}\mathcal{C} = -0.276445596465099$. An independent three-node Gaussian quadrature in each of the three noise directions evaluates one ambient Euler step. At steps 10^{-2} and 10^{-4}, respectively, $\mathbb{E}\mathcal{C}/h$ equals approximately $-0.27890373, -0.27647018$ when the correction is omitted, and $-0.00333055, -0.00003331$ when it is included. The latter nonzero values are the finite-step error of an ambient Euler method. Reconstructing the data from updated parameters instead satisfies the nonlinear constraints at each step up to roundoff. Figure 62 shows the sampled amplitudes and the distinct generator limits.

This construction supplies exact nonlinear initial data and a stochastic law that stays on their restricted family. It does not determine a physical stochastic law from the mother functional. In particular, it neither computes the full independent-connection Dirac algebra nor proves that the frozen-weight Einstein family is invariant when the remaining mother fields are evolved. The next result concerns a different limit: the ultraviolet completion of the specified free physical sector, for which both the covariance and the Hilbert space can be constructed explicitly.

S.5. *Removal of the free spatial ultraviolet cutoff.* Let the cutoff be $\|k\|_\infty \le K$ and couple all finite models using the same countable family of independent stationary processes (1783). For each representative of a pair $\{k, -k\}$, use two normalized real trigonometric functions and two polarizations. This gives

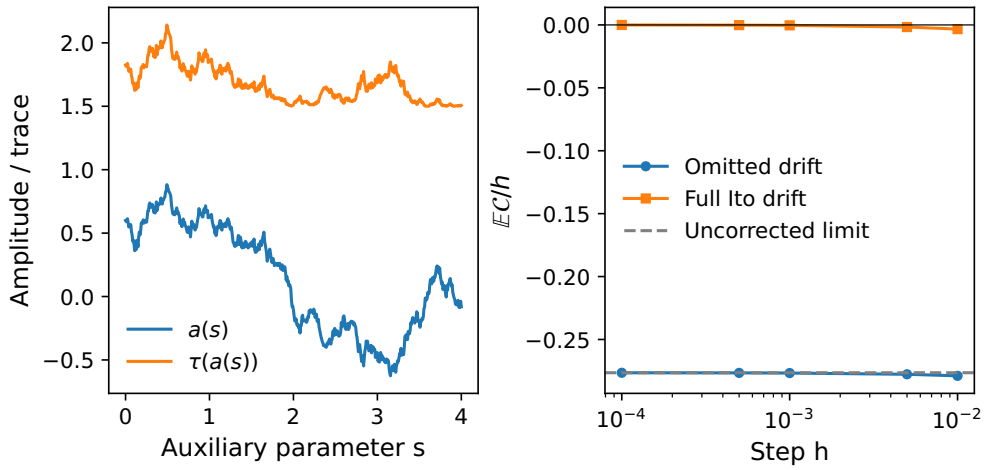


Figure 62. Nonlinear constraint sampling with the synthetic parameters stated in the text. Left: amplitude and mean curvature from exact parameter transitions. Right: Gaussian quadrature of an ambient Euler step, with and without the two Itô curvature-drift terms. The corrected continuous generator vanishes; the uncorrected one approaches a nonzero negative value. The sampling parameter is not physical time.

$2[(2K+1)^3-1]$ real oscillators. Define the tensor Sobolev norm by its Fourier weight $(1+|k|^2)^{-s}$.

Proposition 164 (A free physical ultraviolet limit). *For $s>1$, the cutoff fields converge at each time in $L^2(\Omega;H^{-s}(\mathbb{T}^3))$ to a Gaussian transverse, traceless field h, with the explicit bound*

$$\mathbb{E}\|h(\tau)-h_K(\tau)\|_{H^{-s}}^2 \le \frac{28\hbar}{2s-2}K^{2-2s}, \qquad K\ge 1. \tag{1796}$$

Its finite-time joint laws have covariance $\hbar e^{-|k||\tau-\sigma|}/(2|k|)$ in each real polarization. The Gaussian law is reflection positive in Euclidean time and represents the vacuum correlations of the positive free two-polarization Fock Hamiltonian on this fixed spatial torus.

Proof. The real-mode convention above gives exactly the same trace of the covariance as summing over all signed nonzero lattice vectors with two polarizations. Therefore the mean squared tail is

$$\hbar \sum_{\|k\|_\infty>K} \frac{(1+|k|^2)^{-s}}{|k|}. \tag{1797}$$

The shell $\|k\|_\infty = m$ contains $(2m+1)^3 - (2m-1)^3 = 24m^2 + 2 \le 28m^2$ lattice points. Since $|k| \ge m$, its contribution is at most $28\hbar m^{1-2s}$. The integral comparison $\sum_{m>K} m^{1-2s} \le \int_K^\infty r^{1-2s}\,\mathrm{d}r$ proves (1796). Completeness gives the asserted random distribution. The same construction at finitely many times gives their joint Gaussian law, with the covariance obtained from the stationary Ornstein–Uhlenbeck equation.

For a smooth, positive-time, spatially smeared test with oscillator components f_a, its covariance reflection form is

$$\sum_a \frac{\hbar}{2\omega_a} \left| \int_0^\infty e^{-\omega_a \tau} f_a(\tau)\,\mathrm{d}\tau \right|^2 \ge 0. \tag{1798}$$

Smooth spatial smearing makes the sum convergent. To pass from linear tests to the Gaussian algebra, take exponentials of smeared fields. Their reflection matrix is, up to positive diagonal factors, the entrywise exponential of the covariance reflection matrix. The latter is positive semidefinite by (1798); its entrywise powers are positive semidefinite by the Schur product theorem, so their exponential sum is positive semidefinite. Linear combinations and closure give reflection positivity of the Gaussian theory.

Finally, on the one-particle space with these two polarizations, the positive multiplication operator ω_a defines $\widehat{H} = \mathrm{d}\Gamma(\hbar\omega)$ on bosonic Fock space. The vacuum matrix elements of Euclidean translates by $e^{-\tau \widehat{H}/\hbar}$ have the same displayed covariance; Wick's rule gives the same higher Gaussian correlations. This explicitly constructs a positive free quantum theory for this reduced sector. □

This result removes the spatial ultraviolet cutoff at fixed volume. It does not assert pathwise convergence in a continuous-time Sobolev topology, removal of the infrared regulator, or a local covariant metric field satisfying all interacting gravitational constraints. The transverse projector itself is spatially nonlocal. The vacuum constants λ_K diverge with the cutoff; passing to the displayed Fock Hamiltonian subtracts them and does not determine a cosmological constant.

The free limit and the higher-derivative obstruction concern different operators. At fixed $\ell > 0$, sending K to infinity cannot preserve the low-energy condition $\ell K \ll 1$. Recovering the free operator through a joint limit would require $\ell K \to 0$, a consistent matching of the vacuum energy, and control of the other couplings. These conditions have not been derived from a selected mother phase. The results above establish an exact classical branch, an actual quadratic response bound, and a complete free ultraviolet construction. They also identify why the resummed four-derivative metric branch does not supply the required positive interacting quantum continuum theory.

S.6. *A closed nonlinear Einstein–Yang–Mills branch.* The preceding recovery statements concern a selected two-derivative branch. Here we make one genuinely nonlinear constrained sector explicit. This calculation is useful because it tests the joint gravitational–gauge Hamiltonian rather than either field in isolation. It is also deliberately scoped: a symmetry-reduced solution cannot establish the hyperbolicity or constraint algebra of the unrestricted mother theory.

We use units $c = \hbar = 1$ and a unit comoving spatial volume. On a flat isotropic background and an isotropic $SU(2)$ gauge configuration, take

$$ds^2 = -N(t)^2\,dt^2 + a(t)^2\delta_{ij}\,dx^i dx^j, \qquad A^a_0 = 0, \qquad A^a_i = \psi(t)\,\delta_i{}^a. \tag{1799}$$

The structure constants are $\epsilon^a{}_{bc}$, and the gauge coupling is $g > 0$. We use the canonical convention $F = dA + gA\wedge A$ and gauge Lagrangian $-F^a_{\mu\nu}F_a^{\mu\nu}/4$. The full benchmark in (1815) instead places the coupling in the kinetic coefficient; its connection and curvature are $\widetilde{A} = gA$ and $\widetilde{F} = gF$, with $g_{\mathrm{YM}} = g$. Thus $-\widetilde{F}^2/(4g^2_{\mathrm{YM}}) = -F^2/4$ for the constant coupling used here. The nonzero curvature components are

$$F^a_{0i} = \dot\psi\,\delta_i{}^a, \qquad F^a_{ij} = g\psi^2\epsilon^a{}_{ij}. \tag{1800}$$

Substitution into the Einstein–Yang–Mills action, followed by the usual integration by parts in the Einstein term, gives the reduced Lagrangian

$$L(a,\psi,\dot a,\dot\psi;N) = -\frac{3M_{\mathrm{P}}^2 a\dot a^2}{N} + \frac{3a\dot\psi^2}{2N} - \frac{3Ng^2\psi^4}{2a}. \tag{1801}$$

The lapse has no time derivative and therefore imposes a constraint. The canonical momenta and the Hamiltonian are

$$p_a = -\frac{6M_{\mathrm{P}}^2 a\dot a}{N}, \qquad p_\psi = \frac{3a\dot\psi}{N}, \qquad H = N\,\mathcal{H}, \tag{1802}$$

$$\mathcal{H} = -\frac{p_a^2}{12M_{\mathrm{P}}^2 a} + \frac{p_\psi^2}{6a} + \frac{3g^2\psi^4}{2a} = 0. \tag{1803}$$

The first term is the familiar negative gravitational kinetic term in the minisuperspace constraint; the other two terms are respectively the electric and magnetic Yang–Mills contributions. Equation (1803) is not an imposed numerical normalization: it is the Euler equation for the lapse.

For $N = 1$, Hamilton's equations are

$$\dot a = -\frac{p_a}{6M_{\mathrm{P}}^2 a}, \qquad \dot\psi = \frac{p_\psi}{3a}, \tag{1804}$$

$$\dot p_a = -\frac{p_a^2}{12M_{\mathrm{P}}^2 a^2} + \frac{p_\psi^2}{6a^2} + \frac{3g^2\psi^4}{2a^2}, \qquad \dot p_\psi = -\frac{6g^2\psi^3}{a}. \tag{1805}$$

The nonlinear coupling is visible in both the $a^{-1}\psi^4$ potential and the a^{-1} factors in the kinetic terms. It cannot be reproduced by adding two independent free trajectories.

PROPOSITION 165 (Exact constraint propagation on the reduced branch). *For every smooth solution of* (1804)– (1805) *with* $a > 0$*, the Hamiltonian constraint is preserved. More precisely,*

$$\frac{d}{dt}\mathcal{H} = \{\mathcal{H}, \mathcal{H}\} = 0. \tag{1806}$$

Consequently, initial data satisfying (1803) *remain on the nonlinear constraint surface for the whole interval on which the solution exists.*

Proof. The reduced Hamiltonian has no explicit time dependence. With canonical coordinates (a, ψ, p_a, p_ψ), Hamilton's equations give $\dot{z} = \{z, N\mathcal{H}\}$ for each coordinate z. Hence $\dot{\mathcal{H}} = \{\mathcal{H}, N\mathcal{H}\} = N\{\mathcal{H}, \mathcal{H}\} = 0$, because the Poisson bracket is antisymmetric. This is an exact identity, independent of the value of g; it is the finite-dimensional analogue of constraint propagation. It does not establish propagation of the full ADM Hamiltonian, momentum, and Yang–Mills Gauss constraints, which require the unreduced spatial fields and a specified gauge. □

As an independent numerical check, we integrated (1804)–(1805) with DOP853 at $M_{\mathrm{P}} = g = 1$, $a(0) = 1$, $\psi(0) = 0.2$, $p_\psi(0) = 0.3$, and

$$p_a(0) = -\sqrt{2p_\psi(0)^2 + 18g^2\psi(0)^4} = -0.4569463863518345, \tag{1807}$$

which solves the constraint exactly in the stated units. The integration uses relative tolerance 10^{-12}, absolute tolerance 10^{-14}, and maximum step 5×10^{-3} on $0 \le t \le 1.5$. The resulting dimensionless checks are

$$\begin{aligned} \max_t |\mathcal{H}(t)| &\le 3.13 \times 10^{-17}, \\ \max_{\Delta t>0} \left| \frac{\mathcal{H}(t_{n+1}) - \mathcal{H}(t_n)}{\Delta t} \right| &\le 2.09 \times 10^{-15}, \\ \min_t a(t) &= 1. \end{aligned} \tag{1808}$$

At $t = 1.5$, the state is

$$(a, \psi, p_a, p_\psi) = (1.1083650992,\ 0.3118760731,\ -0.4569463864,\ 0.1387541999). \tag{1809}$$

The trajectory and residual are generated from the same equations and are shown in Fig. 63; the data and executable verification record are archived with the supplementary computational material. These are synthetic dimensionless values, not observations or a fit to a cosmological data set.

This result closes one concrete nonlinear branch: the metric and gauge variables are coupled, the lapse constraint is derived rather than assumed, and

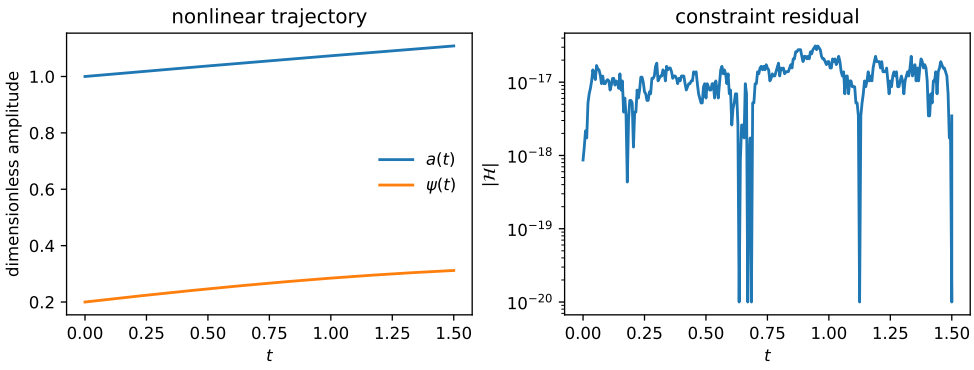


Figure 63. Nonlinear Einstein–Yang–Mills minisuperspace branch with the synthetic initial data stated in the text. The left panel shows the scale factor and isotropic $SU(2)$ amplitude; the right panel shows the absolute Hamiltonian-constraint residual on a logarithmic scale. The calculation verifies the reduced constraint propagation and does not represent a full inhomogeneous evolution.

its preservation is both analytically and numerically checked. It does not close the unrestricted mother dynamics. The remaining requirements are the full spatial ADM–Yang–Mills constraint algebra, a gauge-fixed strongly hyperbolic reduction with a uniform energy estimate, and control of the higher-curvature and stochastic terms. Recent analyses of Einstein–Yang– Mills well-posedness likewise obtain local results only after such a gauge choice [113], [119], [77], and [120].

S.7. *A gauge-fixed principal-symbol certificate.* The nonlinear minisuperspace calculation above does not address local well-posedness of inhomogeneous fields. We therefore record the principal symbol of a second, explicitly declared branch. Linearize the matched two-derivative Einstein–Yang–Mills equations around Minkowski space, impose harmonic gauge on the metric perturbation and Lorenz gauge on the Yang–Mills potential, and write $\bar{h}_{\mu\nu}$ for the trace-reversed metric perturbation. The principal parts are then wave operators,

$$\Box \bar{h}_{\mu\nu} = \text{lower-order terms}, \quad \Box A^a_\mu = \text{lower-order terms},$$
$$\Box = -\partial_t^2 + \sum_{j=1}^{3} \partial_j^2. \tag{1810}$$

There are ten independent components of the symmetric metric perturbation and $4 \dim SU(2) = 12$ gauge-potential components, hence 22 wave blocks. For one scalar wave component introduce the first-order variables

$U = (u, \pi, v_1, v_2, v_3)$, with $\pi = \partial_t u$ and $v_j = \partial_j u$. The spatial principal matrix in a unit direction $n \in \mathbb{R}^3$ is

$$A(n) = \begin{pmatrix} 0 & 0 & 0 & 0 & 0 \\ 0 & 0 & -n_1 & -n_2 & -n_3 \\ 0 & -n_1 & 0 & 0 & 0 \\ 0 & -n_2 & 0 & 0 & 0 \\ 0 & -n_3 & 0 & 0 & 0 \end{pmatrix}. \tag{1811}$$

It is symmetric, and for $|n| = 1$ its eigenvalues are

$$\operatorname{spec} A(n) = \{-1, 0, 0, 0, 1\}. \tag{1812}$$

The full first-order principal matrix is the direct sum of 22 copies of (1811). For arbitrary spatial covector k, direct expansion gives

$$\det\big(\lambda I_5 - A(k)\big) = \lambda^3(\lambda^2 - |k|^2), \qquad \det\big(\lambda I_{110} - A_{\text{full}}(k)\big) = \lambda^{66}(\lambda^2 - |k|^2)^{22}. \tag{1813}$$

The factor λ^{66} records three zero-speed reduction variables per wave component: u itself and the two components of v transverse to k. They are not additional propagating physical polarizations. For $k \neq 0$, the nonzero eigenvalues are $\pm|k|$, and the corresponding normalized propagation speeds are ± 1. The determinant of the original *second-order* wave symbol is instead $q(\omega, k)^{22}$, where $q(\omega, k) = -\omega^2 + |k|^2$. Distinguishing these two systems retains the zero-speed factors in the first-order reduction. All characteristic speeds are real and bounded by one on this branch. The identity matrix is a positive symmetrizer for the first-order principal part. Lower-order terms are controlled on a compact time interval by the usual energy estimate

$$E(t) \le E(0) \exp\left(\int_0^t C(s)\, \mathrm{d}s \right), \qquad E = \frac{1}{2} \int \big(|u|^2 + |\pi|^2 + |v|^2 \big)\, \mathrm{d}x, \tag{1814}$$

provided their coefficient bound C is finite. Equation (1814) is a branch-specific linear estimate; it does not supply the coefficient bound for the full mother action.

The accompanying computation evaluates (1811) for five independent unit directions. The largest eigenvalue error relative to (1812) is 1.11×10^{-16}, every matrix is symmetric to machine precision, and the positive symmetrizer has minimum eigenvalue one. These values are algebraic checks with no fitted physical data. They establish a transparent hyperbolic certificate for the declared linear branch, while the nonlinear mother problem still requires a uniform symmetrizer, constraint propagation, and estimates for all retained higher-curvature and stochastic terms.

Appendix T. A complete four-dimensional classical interaction benchmark

The reduced calculations above establish nonlinear and hyperbolic subbranches. We now state one full four-dimensional classical interaction model in a form that makes every constraint visible. This benchmark is the ordinary two-derivative Einstein–Yang–Mills theory on a globally hyperbolic spacetime. Its purpose is to separate a completed classical reference model from the still open claim that the finite-regulator mother functional selects that model uniquely.

Let $M = I \times \Sigma$, where Σ is a smooth oriented three-manifold, and let G be a compact matrix Lie group with positive invariant form κ_{ab}. The benchmark action is

$$\begin{aligned} S_{\mathrm{EYM}}[g, A] &= \int_M \sqrt{-g}\, \left[\frac{M_{\mathrm{P}}^2}{2}(R - 2\Lambda) - \frac{1}{4g_{\mathrm{YM}}^2} \kappa_{ab} F^a_{\mu\nu} F^{b\,\mu\nu} \right] \mathrm{d}^4 x, \\ F^a &= \mathrm{d}A^a + \frac{1}{2} f^a{}_{bc} A^b \wedge A^c. \end{aligned} \tag{1815}$$

The parameters M_{P}, g_{YM}, and Λ are kept explicit. The action is a concrete model; writing it as a branch of the mother action is an additional matching assumption that must be tested by the coefficient and remainder conditions in Section 5.8.

Variation with respect to g and A gives the full nonlinear Lorentzian field equations of this benchmark:

$$M_{\mathrm{P}}^2 (G_{\mu\nu} + \Lambda g_{\mu\nu}) = T^{\mathrm{YM}}_{\mu\nu}, \tag{1816}$$

$$D_\mu F^{a\,\mu\nu} = 0, \tag{1817}$$

where

$$T^{\mathrm{YM}}_{\mu\nu} = \frac{1}{g_{\mathrm{YM}}^2} \kappa_{ab} \left(F^a_{\mu\rho} F^{b\,\rho}_{\nu} - \frac{1}{4} g_{\mu\nu} F^a_{\rho\sigma} F^{b\,\rho\sigma} \right). \tag{1818}$$

The identity $D_{[\mu} F_{\nu\rho]} = 0$ and the contracted Bianchi identity $\nabla^\mu G_{\mu\nu} = 0$ give the corresponding differential compatibility conditions. They are necessary for constraint propagation, but the canonical calculation below also displays the constraints and their Poisson brackets explicitly.

T.1. *ADM variables and all classical constraints.* Write

$$ds^2 = -N^2 dt^2 + h_{ij}(dx^i + N^i dt)(dx^j + N^j dt), \qquad K_{ij} = \frac{1}{2N}(\dot{h}_{ij} - D_i N_j - D_j N_i). \tag{1819}$$

The canonical variables are (h_{ij}, π^{ij}) and (A^a_i, E^i_a). With E^i_a a density of weight one, the canonical action is

$$\begin{aligned} S &= \int dt \int_\Sigma \mathrm{d}^3 x\, \left(\pi^{ij} \dot{h}_{ij} + E^i_a \dot{A}^a_i - N \mathcal{H}_\perp - N^i \mathcal{C}_i - A^a_0 \mathcal{G}_a \right), \\ \mathcal{C}_i &:= -2 h_{ik} D_j \pi^{jk} + F^a_{ij} E^j_a. \end{aligned} \tag{1820}$$

The three secondary constraints are

$$\mathcal{H}_\perp = \frac{2}{M_{\rm P}^2\sqrt{h}}\left(\pi^{ij}\pi_{ij} - \frac{1}{2}\pi^2\right) - \frac{M_{\rm P}^2\sqrt{h}}{2}\left({}^{(3)}R - 2\Lambda\right) + \frac{g_{\rm YM}^2}{2\sqrt{h}}\kappa^{ab}h_{ij}E_a^iE_b^j + \frac{\sqrt{h}}{4g_{\rm YM}^2}\kappa_{ab}h^{ik}h^{jl}F_{ij}^aF_{kl}^b, \tag{1821}$$

$$\mathcal{C}_i = -2h_{ik}D_j\pi^{jk} + F_{ij}^aE_a^j, \tag{1822}$$

$$\mathcal{G}_a = -D_iE_a^i = -\partial_iE_a^i - f_{ab}{}^cA_i^bE_c^i. \tag{1823}$$

The lapse, shift, and A_0^a are multipliers. Their variations give, respectively, the Hamiltonian, momentum, and Gauss constraints. The signs in (1822) correspond to the extrinsic-curvature convention (1819); changing that convention changes the displayed canonical signs together, not the constraint content. The conjugate momenta of N, N^i, and A_0^a are primary constraints; preservation of these primary constraints gives the three secondary families above.

T.2. *Constraint algebra and propagation.* For smearing fields N, M, vector fields X, Y, and Lie-algebra functions λ, μ, use $[\lambda,\mu]^a = f^a{}_{bc}\lambda^b\mu^c$ and define $H[N] = \int_\Sigma N\mathcal{H}_\perp$, $C[X] = \int_\Sigma X^i\mathcal{C}_i$, $V[X] = \int_\Sigma X^i\mathcal{V}_i$, $G[\lambda] = \int_\Sigma \lambda^a\mathcal{G}_a$. Here

$$\mathcal{V}_i := \mathcal{C}_i + A_i^a\mathcal{G}_a. \tag{1824}$$

The generator $V[X]$ acts by the ordinary spatial Lie derivative on the connection; C_i alone generates the gauge-covariant Lie derivative. In the equivalent canonical action one replaces $N^iC_i + A_0^aG_a$ by $N^iV_i + (A_0^a - N^iA_i^a)G_a$. The canonical Poisson brackets give the first-class algebra

$$\{G[\lambda], G[\mu]\} = -G[[\lambda,\mu]], \tag{1825}$$

$$\{V[X], G[\lambda]\} = G[\mathcal{L}_X\lambda], \tag{1826}$$

$$\{V[X], V[Y]\} = V[[X,Y]], \tag{1827}$$

$$\{H[N], G[\lambda]\} = 0, \tag{1828}$$

$$\{H[N], V[X]\} = -H[\mathcal{L}_XN], \tag{1829}$$

$$\{H[N], H[M]\} = C[Z] = V[Z] - G[Z^iA_i], \qquad Z^i = h^{ij}(N\partial_jM - M\partial_jN). \tag{1830}$$

The minus sign in (1825) follows from the declared choice $\mathcal{G} = -DE$: it generates $\{A_i, G[\lambda]\} = D_i\lambda$ and $\{E^i, G[\lambda]\} = [E^i, \lambda]$. The finite-link moment-map convention in Proposition 30 uses the opposite generator sign; comparison of the two conventions therefore includes $G \mapsto -G$. The two momentum presentations are related by the displayed change of first-class constraint basis. In particular, the Gauss term in (1830) is present off the Gauss surface when the ordinary diffeomorphism generator V is used. In the C_i basis, other brackets

acquire curvature-dependent Gauss terms. These are basis effects within the same first-class system.

PROPOSITION 166 (Classical closure of the benchmark constraints). *On a compact* Σ*, or for boundary conditions that remove the surface terms, the constraints* (1821)– (1823) *form a first-class system with algebra* (1825)–(1830)*. Consequently, the total Hamiltonian preserves the constraint surface:*

$$\dot{C} = \{C, H[N] + V[N^i] + G[A_0 - N^i A_i]\} \in \mathrm{span}\{\mathcal{H}_\perp, \mathcal{V}_i, \mathcal{G}_a\} \tag{1831}$$

for each smeared constraint C*.*

Proof. Use the canonical bracket $\{A_i^a(x), E_b^j(y)\} = \delta_i^j \delta_b^a \delta(x-y)$ and assume the surface terms vanish. The transformation laws just stated give $\delta_\mu \mathcal{G} = [\mathcal{G}, \mu]$; invariance of the Lie-algebra pairing then yields $\{G[\lambda], G[\mu]\} = -G[[\lambda, \mu]]$. Integration by parts gives $V_{\mathrm{YM}}[X] = \int E_a^j \mathcal{L}_X A_j^a$, which proves the ordinary Lie-derivative action and the spatial brackets.

For completeness, put $F_a^{ij} = \kappa_{ab} h^{ik} h^{jl} F_{kl}^b$. The Yang–Mills Hamiltonian has the functional derivatives

$$\frac{\delta H_{\mathrm{YM}}[N]}{\delta E_a^j} = \frac{N g_{\mathrm{YM}}^2}{\sqrt{h}} \kappa^{ab} h_{jk} E_b^k, \qquad \frac{\delta H_{\mathrm{YM}}[N]}{\delta A_j^a} = -D_i \left(\frac{N\sqrt{h}}{g_{\mathrm{YM}}^2} F_a^{ij} \right). \tag{1832}$$

In the antisymmetrized bracket the terms proportional to NM cancel. The remaining lapse derivatives give

$$\{H_{\mathrm{YM}}[N], H_{\mathrm{YM}}[M]\} = \int_\Sigma h^{ij} (N \partial_j M - M \partial_j N) F_{ik}^a E_a^k = C_{\mathrm{YM}}[Z]. \tag{1833}$$

The pure gravitational bracket is the hypersurface-deformation identity [8] and [33]. The mixed gravitational–Yang–Mills brackets cancel under $N \leftrightarrow M$, since the matter Hamiltonian depends algebraically on h and not on π. Adding the two momentum contributions gives $C[Z]$, and substituting $C_i = V_i - A_i^a \mathcal{G}_a$ proves (1830). Gauge invariance and the scalar-density transformation law give the remaining brackets. Substitution into the total Hamiltonian bracket proves (1831). This is a classical canonical theorem for the explicitly specified benchmark action; it is not a derivation of the same algebra for the higher-curvature, stochastic mother functional. □

T.3. *Local existence and uniqueness after gauge fixing.* The first-class algebra alone is not a Cauchy theorem. Select harmonic coordinates for g and Lorenz gauge for A. To state a sufficient Sobolev setting, take a smooth compact three-manifold Σ without boundary, fix a smooth background metric and bundle charts, and prescribe

$$(h, A_i) \in H^s(\Sigma), \qquad (K, E^i) \in H^{s-1}(\Sigma), \qquad s > \frac{5}{2}. \tag{1834}$$

Here K is the second fundamental form and E^i is the canonical Yang–Mills electric density. Require a uniform positive lower bound for h relative to the background metric, the Hamiltonian, momentum and Gauss constraints, and initial lapse, shift and temporal gauge data compatible with the harmonic and Lorenz conditions and their constraint propagation equations. The reduced fields have wave principal part; their coefficients are smooth functions of the fields and the inverse metric, with terms at most quadratic in first derivatives on this branch. The standard local Einstein–Yang–Mills Cauchy theory then gives $(g, A) \in C([0,T]; H^s) \cap C^1([0,T]; H^{s-1})$ in the chosen charts for some $T > 0$, uniqueness in the chosen gauge, and continuous dependence in the corresponding Sobolev topology. Gauge-related solutions are identified by residual transformations. On a noncompact Σ, one must instead specify bounded geometry or suitable weighted spaces, asymptotic conditions, and uniform coefficient and metric bounds; the compact statement does not supply these hypotheses. The principal-symbol calculation in Section S.7 checks the corresponding flat-background block directly, while the local well-posedness results of Liu–Wang and Mondal establish the required gauge-fixed framework [113] and [119].

This theorem closes the classical benchmark only. It does not imply local existence for the unrestricted mother action, where higher derivatives, additional fields, and stochastic forcing change both the principal symbol and the constraint propagation equations.

T.4. *What the benchmark does and does not prove.* The benchmark is already a regulator-free classical continuum model: no Fourier or lattice cutoff appears in (1815). Therefore there is no regulator to remove in this benchmark. This fact cannot be reinterpreted as a proof that the finite-regulator mother theory converges to it. The latter would require uniform estimates for the regulated equations, compactness modulo gauge, identification of the limiting nonlinear terms, and convergence of the constraints. Only the free physical sector has such a cutoff-removal result in this manuscript.

Likewise, the free two-polarization sector has a positive Fock/Hilbert construction, but no positive reflection-positive construction of the full interacting four-dimensional Einstein–Yang–Mills quantum theory is supplied here. Canonical quantization of the constraints, renormalization, and a nonperturbative interacting continuum limit remain open.

The parameters in (1815) are not all selected by the mother functional. M_{P} and the low-energy gauge couplings can be matched to independent measurements; Λ, the group, and the remaining matter-sector parameters require additional input. Finally, the benchmark by itself predicts the ordinary Einstein–Yang–Mills limit, not a new deviation from GR or the Standard Model. A

no-refit new signal would require a separately derived higher-curvature or scalar coefficient, its full response function, and an observable held out from calibration. Until those conditions are met, the manuscript must call such signals conditional predictions rather than detections.

T.5. *A finite-regulator energy certificate and a controlled tail diagnostic.* The preceding Einstein–Yang–Mills benchmark fixes the classical field content and the constraint convention. We next record a smaller result that can be proved without silently assuming a continuum limit. It is useful for checking whether a proposed finite regulator is dissipative, but it is not a replacement for the missing interacting field-theory estimate.

For $N \in \mathbb{N}$, consider the diagonal Galerkin system

$$\dot{x}_k^{(N)} + \nu k^2 x_k^{(N)} = f_k, \qquad 1 \le k \le N, \qquad \nu > 0, \tag{1835}$$

with energy $E_N(t) = \frac{1}{2}\sum_{k=1}^{N} |x_k^{(N)}(t)|^2$. This is a finite-dimensional dissipative comparison problem. It is deliberately separated from the mother action: no claim is made that the coefficients (ν, f_k) are uniquely selected by that action.

Proposition 167 (Uniform finite-mode energy inequality). *Assume that $x^{(N)}$ is a classical solution of* (1835)*, that $x^{(N)}(0) \in \mathbb{R}^N$, and that $f \in \mathbb{R}^N$. Then, for every $t \ge 0$,*

$$E_N(t) + \frac{\nu}{2}\int_0^t \sum_{k=1}^{N} k^2 |x_k^{(N)}(s)|^2 \,\mathrm{d}s \le E_N(0) + \frac{t}{2\nu}\sum_{k=1}^{N} \frac{|f_k|^2}{k^2}. \tag{1836}$$

The constant in the right-hand side is independent of the dimension N whenever the two displayed sums are bounded uniformly in N.

Proof. Multiply the kth equation by $x_k^{(N)}$ and sum over k. The exact identity is

$$\frac{\mathrm{d}}{\mathrm{d}t} E_N(t) + \nu \sum_{k=1}^{N} k^2 |x_k^{(N)}(t)|^2 = \sum_{k=1}^{N} f_k x_k^{(N)}(t). \tag{1837}$$

For $a > 0$, the elementary square $(ax - f)^2 \ge 0$ gives

$$fx \le \frac{ax^2}{2} + \frac{f^2}{2a}. \tag{1838}$$

Taking $a = \nu k^2$ and integrating yields (1836). The algebraic inequality is also checked in Lean by the declarations `weighted_young` and `mode_dissipation_term`; the recorded axiom report contains only the standard foundations `propext`, `Classical.choice`, and `Quot.sound`. □

The estimate has a precise scope. It provides dimension-uniform control for the declared diagonal family when $\sup_N \sum_{k\le N} |x_k^{(N)}(0)|^2 < \infty$ and $\sup_N \sum_{k\le N} |f_k|^2/k^2 < \infty$. It does not identify a limiting probability law, prove

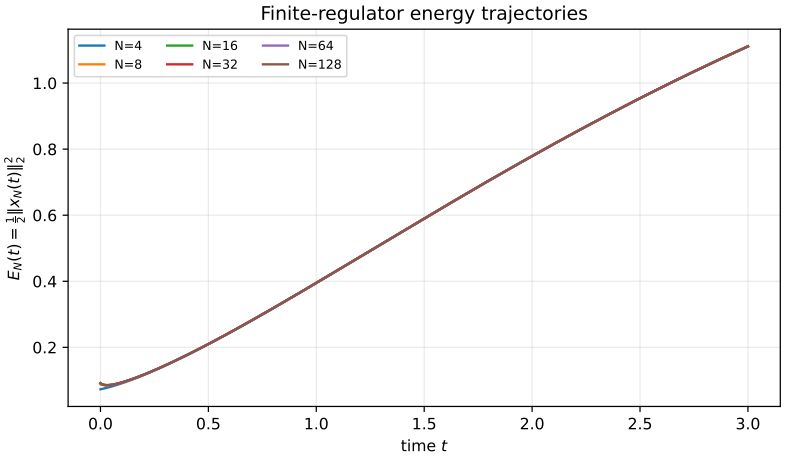


Figure 64. Exact trajectories of the finite diagonal comparison system (1835) for increasing mode dimension. The plot illustrates the stated finite-mode estimate and truncation diagnostic; it is not evidence for a continuum limit of the full mother theory.

compactness for a non-diagonal interacting operator, or show that constraints and gauge symmetries survive as $N \to \infty$. Those are additional hypotheses, as required by the continuum-limit ledger in Section AG.

For a reproducible numerical diagnostic we used

$$x_k(0) = 0.3e^{-k/5}, \qquad f_k = e^{-k/4}, \qquad \nu = 0.4, \qquad 0 \le t \le 3, \tag{1839}$$

and the exact mode solution

$$x_k(t) = x_k(0)e^{-\nu k^2 t} + \frac{f_k}{\nu k^2}\left(1 - e^{-\nu k^2 t}\right). \tag{1840}$$

The largest defect of the left side of (1836) minus its right side was negative for every tested dimension. The maximum L^2 difference from the $N = 256$ reference after zero-padding the lower-dimensional vector decreased from 1.9221×10^{-1} at $N = 4$ to 7.1077×10^{-4} at $N = 32$ and 1.1810×10^{-6} at $N = 64$. The calculation and the input/output hash are stored in the supplementary verification directory; all numbers are synthetic and serve only as a finite-mode consistency check.

T.6. *Non-diagonal coercive regulators.* The diagonal example above is useful but overly special. The same finite-mode argument extends to a non-diagonal symmetric operator, provided that its coercivity constant is controlled uniformly. Let $A_N \colon \mathbb{R}^N \to \mathbb{R}^N$ be symmetric and suppose that

$$\langle A_N v, v\rangle \ge \alpha \|v\|_2^2, \qquad \alpha > 0, \qquad v \in \mathbb{R}^N, \tag{1841}$$

where the same α is used for every member of the regulator family. For the forced system

$$\dot{x}_N + A_N x_N = f_N(t), \qquad x_N(0) = x_{N,0}, \tag{1842}$$

testing by x_N gives the exact identity

$$\frac{\mathrm{d}}{\mathrm{d}t}\frac{1}{2}\|x_N\|_2^2 + \langle A_N x_N, x_N\rangle = \langle f_N, x_N\rangle. \tag{1843}$$

The Cauchy–Young inequality and (1841) then imply the following finite-dimensional certificate:

Proposition 168 (Coercive non-diagonal energy estimate). *If $f_N \in L^2(0,T;\mathbb{R}^N)$ and (1841) holds, then*

$$\begin{aligned}\frac{1}{2}\|x_N(t)\|_2^2 + \frac{1}{2}\int_0^t \langle A_N x_N(s), x_N(s)\rangle\,\mathrm{d}s \\ \le \frac{1}{2}\|x_{N,0}\|_2^2 + \frac{1}{2\alpha}\int_0^t \|f_N(s)\|_2^2\,\mathrm{d}s, \qquad 0 \le t \le T.\end{aligned} \tag{1844}$$

Consequently, the right side is independent of N whenever the initial energies and forcing norms are uniformly bounded and the same coercivity constant α applies.

Proof. For each time, use

$$\langle f_N, x_N\rangle \le \frac{\alpha}{2}\|x_N\|_2^2 + \frac{1}{2\alpha}\|f_N\|_2^2 \le \frac{1}{2}\langle A_N x_N, x_N\rangle + \frac{1}{2\alpha}\|f_N\|_2^2. \tag{1845}$$

Substitution into the exact energy identity and integration from 0 to t give (1844). The scalar algebraic step is checked in Lean by `coercive_forcing_bound` and `coercive_quadratic_step`. The Lean file records the standard foundational axioms and does not encode the matrix or continuum argument. □

To test the genuinely non-diagonal case, we used the symmetric tridiagonal family

$$A_N = 1.2 I_N + 0.25(T_N + T_N^{\mathsf{T}}), \tag{1846}$$

where T_N has ones on the first superdiagonal. Its smallest eigenvalue is strictly larger than 0.7 for every tested N, so $\alpha = 0.7$ is a uniform coercivity constant. With

$$x_{N,0,k} = 0.3e^{-k/5}, \qquad f_{N,k}(t) = e^{-k/4}e^{-0.2t}, \qquad 0 \le t \le 3, \tag{1847}$$

we evaluated the matrix solution by diagonalizing A_N. The minimum eigenvalues for $N = 4, 8, 16, 32, 64$ were

$$0.79549, \quad 0.73015, \quad 0.70851, \quad 0.70226, \quad 0.70058,$$

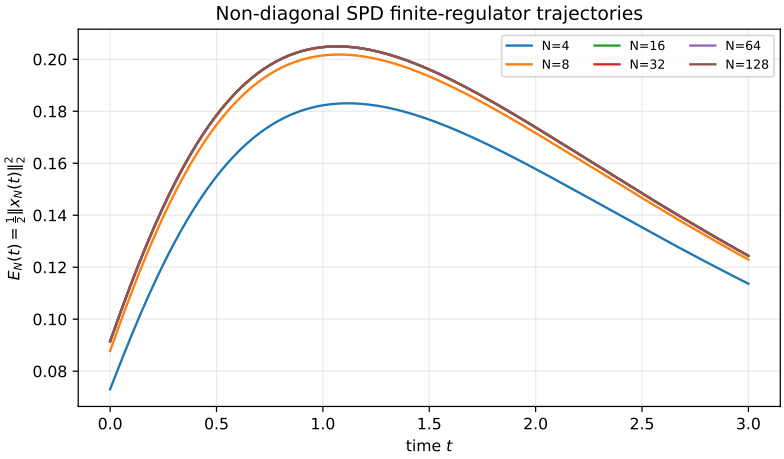


Figure 65. Energy trajectories for the non-diagonal symmetric positive-definite regulator family. The common coercivity constant is $\alpha = 0.7$; the curves and the truncation diagnostic are synthetic finite-mode calculations.

and the zero-padded L^2 differences from the $N = 128$ reference were

$$2.2982\times10^{-1}, \quad 9.0086\times10^{-2}, \quad 1.7437\times10^{-2}, \quad 7.1077\times10^{-4}, \quad 1.1810\times10^{-6}.$$

The largest computed energy inequality defect was non-positive to machine precision. These values are a finite-dimensional numerical certificate for the declared SPD family; they do not establish compactness, gauge-constraint preservation, stochastic martingale convergence, or a regulator-independent continuum theory.

Appendix U. Exact nonlinear feedback and a cross-channel response restriction

A joint cost has more content than a collection of separately fitted response laws when it relates their nonlinear coefficients. The present appendix identifies such a relation in a finite branch that can be solved completely. First, the joint residual is reduced without discarding its cross blocks. Second, the Bellman minimizer is obtained exactly. Third, the same minimizer is realized by a state equation whose mean displacement is an observable. This last step matters: a derivative of a cost is not yet a measured response. The calculation uses the dynamic-programming and adjoint conventions of Appendix M; those methods are established stochastic-control tools [68].

U.1. *A finite branch with the cross blocks retained.* Fix physical units for the state, control, residual and time. At this stage the coefficients are constant,

the control is unconstrained, and the residual has the affine form

$$r(u) = r_0 + Du, \qquad q(u) = r(u)^T H r(u), \qquad H = H^T \succ 0, \quad \operatorname{rank} D = m. \tag{1848}$$

Here r_0 can contain the non-control channels evaluated on the declared branch; D describes how the control enters the joint residual. It is not the drift map, which will be denoted by G. In particular, all permitted cross blocks of H enter $D^T H r_0$ and $D^T H D$. Define

$$R = D^T H D, \qquad v = -R^{-1} D^T H r_0, \qquad q_\perp = r_0^T H r_0 - v^T R v. \tag{1849}$$

Then $R \succ 0$ and

$$q(u) = q_\perp + (u - v)^T R (u - v), \qquad q_\perp \geq 0. \tag{1850}$$

For the first identity, expand both sides and use $Rv = -D^T H r_0$. For the second, let $\mathcal{P} = H^{1/2} D (D^T H D)^{-1} D^T H^{1/2}$. This is the Euclidean orthogonal projector onto the range of $H^{1/2} D$, so $q_\perp = \|(I - \mathcal{P}) H^{1/2} r_0\|^2$. Thus the residual outside the controllable range remains in the cost; it has not been set to zero by choosing a convenient control.

The assumptions in (1848) specify a restricted branch of the joint functional. If the thermodynamic score, the projection residual, H, or D varies with the state, density or control, the corresponding derivatives must be included. Completing the square at a fixed point remains useful, but does not eliminate those derivatives from the full variational problem. Singular R, bounded controls and state-dependent diffusion also require their own optimization conditions.

U.2. *Exact Bellman minimization.* For a fixed drift costate p put $g = G^T p$. The control-dependent Hamiltonian is

$$h_\kappa(g, u) = g^T u + \varphi_\kappa\big(q_\perp + (u - v)^T R (u - v)\big). \tag{1851}$$

The exponent κq is dimensionless. The running cost is $\varphi_\kappa(q) = (e^{\kappa q} - 1)/(4\kappa)$ for $\kappa > 0$, with $\varphi_0(q) = q/4$. This is the local running penalty already defined in the master objective. It is not the logarithm of an exponential expectation of an accumulated path cost.

For $x \geq 0$, write $W(x)$ for the unique nonnegative solution of $W(x) e^{W(x)} = x$. Existence and uniqueness follow because $z \mapsto z e^z$ is continuous, strictly increasing on $[0, \infty)$, and unbounded.

THEOREM 169 (Unique nonlinear feedback). *Under* (1848)*, set* $s = g^T R^{-1} g$*. For* $\kappa > 0$*, the unique global minimizer is*

$$z = \frac{W(8\kappa e^{-2\kappa q_\perp} s)}{2\kappa}, \qquad a = 2e^{-\kappa(q_\perp + z)}, \qquad u_*(g) = v - a R^{-1} g. \tag{1852}$$

For $\kappa = 0$*, it is* $u_*(g) = v - 2R^{-1} g$*. The quantity* z *is exactly* $(u_* - v)^T R (u_* - v)$*.*

Proof. Let $w = u - v$. Differentiation gives

$$\begin{aligned} D_u h_\kappa &= g + \tfrac{1}{2} e^{\kappa(q_\perp + w^T R w)} R w, \\ D_u^2 h_\kappa &= e^{\kappa(q_\perp + w^T R w)} \{ \tfrac{1}{2} R + \kappa (Rw)(Rw)^T \} \succ 0. \end{aligned} \tag{1853}$$

For $\kappa = 0$ the Hessian is $R/2$. The positive quadratic lower bound for the penalty dominates the linear term as $\|u\| \to \infty$, so a minimum exists. Strict convexity then makes any stationary point the unique global minimum. Stationarity gives $w = -2e^{-\kappa(q_\perp + z)} R^{-1} g$. Taking its squared R norm yields

$$z = 4e^{-2\kappa(q_\perp + z)} s, \qquad (2\kappa z) e^{2\kappa z} = 8\kappa e^{-2\kappa q_\perp} s. \tag{1854}$$

The definition of W proves (1852). If $s = 0$, positive definiteness implies $g = 0$, and the same formula gives $z = 0$ and $u_* = v$. The limit $\kappa \downarrow 0$ follows from $W(x)/x \to 1$ at zero and agrees with direct quadratic minimization. □

For fixed g, increasing $q_\perp$ reduces the feedback amplitude. This is a consequence of the specified local cost, rather than a new force law. Comparing optimized dynamical solutions at different κ generally changes $p = \nabla V_\kappa$ as well; the next realization fixes that costate by an explicit endpoint condition.

U.3. *Anisotropic susceptibility and a cubic tensor identity.* The complete derivative of the feedback, including its scalar amplitude, is

$$D_g u_* = -aR^{-1} + \frac{2\kappa a^3}{1 + 2\kappa z} (R^{-1} g)(R^{-1} g)^T. \tag{1855}$$

Indeed, differentiating (1854) gives $dz/ds = a^2/(1+2\kappa z)$ and $da/ds = -\kappa a^3/(1+2\kappa z)$. Since $D_g s = 2R^{-1} g$, the chain rule proves (1855). In normalized coordinates $\widehat{g} = R^{-1/2} g$ and $\widehat{u} = R^{1/2}(u_* - v)$, the derivative has one radial eigenvalue and $m - 1$ transverse eigenvalues:

$$\lambda_{\text{radial}} = -\frac{a}{1 + 2\kappa z}, \qquad \lambda_{\text{transverse}} = -a. \tag{1856}$$

At $g = 0$ all are $-a_0$, where $a_0 = 2e^{-\kappa q_\perp}$. Thus the radial response is more strongly suppressed than the transverse response at a nonzero probe. This anisotropy is relative to the probe and the calibrated residual metric, not an assumed preferred spacetime direction.

PROPOSITION 170 (Cross-channel third-order restriction). *Let $K = R^{-1}$ and $s = g^T K g$. Then*

$$u_*(g) = v - a_0 K g + \kappa a_0^3 s K g + \mathcal{E}(g), \qquad \|R^{1/2} \mathcal{E}(g)\| \le \tfrac{5}{2} \kappa^2 a_0^5 s^{5/2}. \tag{1857}$$

The expansion extends to $\kappa = 0$ with zero remainder. If $\mathcal{C} = -D_g u_*(0) = a_0 K$, its third derivative obeys

$$\partial_{g_j} \partial_{g_k} \partial_{g_l} u_{*,i}(0) = 2\kappa a_0 \{ \mathcal{C}_{ij} \mathcal{C}_{kl} + \mathcal{C}_{ik} \mathcal{C}_{jl} + \mathcal{C}_{il} \mathcal{C}_{jk} \}. \tag{1858}$$

The linear and mixed cubic responses therefore cannot be chosen independently within this branch.

Proof. Put $t = \kappa a_0^2 s$ and $r = a/a_0$. The scalar equation becomes $re^{tr^2} = 1$, so $0 < r \le 1$. Implicit differentiation gives

$$r' = -\frac{r^3}{1+2tr^2}, \qquad r'' = \frac{r^5(5+6tr^2)}{(1+2tr^2)^3}. \tag{1859}$$

For $x \ge 0$, $(5+6x)/(1+2x)^3 \le 5$; subtraction after clearing the positive denominator proves this inequality. Consequently $0 \le r'' \le 5$ and, by Taylor's integral remainder, $0 \le r - 1 + t \le 5t^2/2$. Substitute $u_* - v = -a_0 rKg$ and use $\|R^{1/2}Kg\| = \sqrt{s}$ to obtain the stated error bound. The cubic term is $\kappa a_0^3 K_{ij} g_j K_{kl} g_k g_l$. Three derivatives give $2\kappa a_0^3 (K_{ij}K_{kl} + K_{ik}K_{jl} + K_{il}K_{jk})$. Replacing K by $\mathcal{C}/a_0$ proves (1858). □

An explicit comparison makes the restriction observable in principle. With $R = I_2$, $q_\perp = 0$ and $v = 0$, the joint cost predicts

$$u_{*,1} = -2g_1 + 8\kappa(g_1^2 + g_2^2)g_1 + O(\|g\|^5). \tag{1860}$$

The separable alternative $\varphi_\kappa(u_1^2) + \varphi_\kappa(u_2^2) + g^T u$ has the same linear response, and exactly the same response on either coordinate axis, but $u_{*,1} = -2g_1 + 8\kappa g_1^3 + O(g_1^5)$. Its mixed derivative $\partial_{g_1}\partial_{g_2}^2 u_{*,1}(0)$ is zero, whereas the joint value is 16κ. Thus one-channel tests alone cannot distinguish these two costs; a simultaneous two-channel probe can. An effective model supplied with the same mixed response can reproduce this relation. The result restricts alternatives; it does not establish that the relation lies outside all effective descriptions.

U.4. *A complete dynamic-programming and adjoint realization.* Consider the declared finite state process

$$dX_t = (b_0 + Gu_t)\,dt + \Sigma\,dW_t, \qquad X_0 = x, \tag{1861}$$

with constant coefficients and objective

$$J_\eta(u) = \mathbb{E}\left[\int_0^T \varphi_\kappa(q(u_t))\,dt + \eta^T X_T\right]. \tag{1862}$$

Take progressively measurable controls with finite running cost and $\mathbb{E}\int_0^T \|u_t\|^2 dt < \infty$. The constant control from Theorem 169 belongs to this class. The endpoint coefficient η is a calibrated terminal probe; it is not a new gravitational or electromagnetic coupling.

Proposition 171 (Global selected law and measured mean). *Set $g = G^T\eta$ and let $c_\kappa = \min_u h_\kappa(g,u)$. The unique optimum is the constant $u_*(g)$, up to $dt \otimes d\mathbb{P}$ null sets. The Bellman value and adjoint are*

$$V(t,x) = \eta^T x + (T-t)(\eta^T b_0 + c_\kappa), \qquad p_t = \eta, \quad Z_t = 0. \tag{1863}$$

For any fixed observation matrix P,

$$\mathbb{E}[PX_T] = P\{x + T(b_0 + Gu_*(G^T\eta))\}, \qquad \mathrm{Cov}(PX_T) = TP\Sigma\Sigma^T P^T. \tag{1864}$$

Proof. The stochastic integral has mean zero. Integrating the state equation therefore expresses the objective as $\eta^T x + T\eta^T b_0 + \mathbb{E}\int_0^T h_\kappa(G^T\eta, u_t)\,dt$. The pointwise minimum gives a lower bound attained by the displayed constant control. Strict convexity implies equality only for this control almost everywhere. The stated value has $\nabla V = \eta$ and $D^2V = 0$, so its time derivative and the minimized generator satisfy the Bellman equation, with terminal value $\eta^T x$. The adjoint equation has zero state derivative and terminal condition $p_T = \eta$, giving $p = \eta$ and $Z = 0$; its stationarity condition is exactly (1853). Finally, $X_T = x + T(b_0 + Gu_*) + \Sigma W_T$, which proves both observable formulas. The argument includes the control-dependent path law directly through the state equation, rather than varying an expectation while incorrectly keeping that law fixed. □

This realization converts the cubic identity into derivatives of a measured endpoint mean:

$$D_\eta \mathbb{E}[PX_T] = TPG(D_g u_*)G^T. \tag{1865}$$

Higher derivatives use the same fixed maps P and G. There is no refitting of either map when the probe changes. The diffusion contributes sampling variance but, for this affine endpoint branch, does not enter the selected constant control. This example therefore gives a nonlinear controlled response, not a derivation of quantum radiation from classical noise.

U.5. *Symmetry, stochastic charges and the nonlinear penalty.* The adjoint symmetry balance of Theorem 147 applies to the same running cost. Its general cost defect is multiplied by the marginal factor $e^{\kappa q}/4$ [58]. If the drift and covariance symmetry defects vanish, the control orbit is two-sided feasible and stationary, and the Brownian rotation term cancels as in that theorem, then for a residual symmetry generator $\mathcal{D}$,

$$dQ_t = -\tfrac{1}{4}e^{\kappa q_t}\mathcal{D}q_t\,dt + N_t \cdot dW_t. \tag{1866}$$

In particular, $\mathcal{D}q = 0$ preserves the local-martingale charge for every $\kappa \geq 0$. Exact symmetry alone does not select κ, a positive overall metric scale, or the physical residual representation. Conversely, a small symmetry defect may have a large effect at a large residual.

For a quantitative statement, stop before q_t exceeds a prescribed $Q_{\max}$ and suppose $|\mathcal{D}q_t| \leq \epsilon$ there. If Q_0 is integrable and $\mathbb{E}\int_0^{T\wedge\tau}\|N_t\|^2 dt \leq V_N$, the

compensated charge increment is a square-integrable martingale and

$$|\mathbb{E}(Q_{T\wedge\tau}-Q_0)|\le \tfrac{1}{4}Te^{\kappa Q_{\max}}\epsilon,$$
$$\mathbb{P}\left(\sup_{t\le T}\left|Q_{t\wedge\tau}-Q_0+\tfrac{1}{4}\int_0^{t\wedge\tau}e^{\kappa q_s}\mathcal{D}q_s\,ds\right|\ge b\right)\le V_N/b^2. \tag{1867}$$

The first bound integrates the drift in (1866); the second is the martingale maximal inequality applied to its square. Both require the displayed integrability, not merely formal invariance.

For (1861), a constant translation generator ξ has $Q=\eta^T\xi$, which is constant pathwise because $p=\eta$. It is an adjoint charge. Identifying it with mechanical momentum would require a separate mechanical state and a proved observable dictionary. The endpoint displacement in (1864) already has such a dictionary and is the observable used below. This distinction prevents an optimization symmetry from being mistaken for an additional physical conservation law.

U.6. *A frozen-calibration numerical calculation.* The following calculation uses exact endpoint laws, so there is no time discretization error. All observations are synthetic. Set $r_0=0$, $b_0=x=0$ and, in declared model units,

$$R=\begin{pmatrix}1.6 & 0.28\\ 0.28 & 0.95\end{pmatrix},\quad G=\begin{pmatrix}1 & 0.2\\ -0.1 & 0.85\end{pmatrix},$$
$$\Sigma=\operatorname{diag}(0.25,0.18),\quad T=1.1,\qquad \kappa_{\mathrm{gen}}=0.7. \tag{1868}$$

R, G, Σ and the physical clock are frozen before nonlinear calibration. Use $\eta_c=f_ce_1$, $f_c=0.35$, and let $d=G^Te_1$, $v_c=GR^{-1}d$ and $s_c=f_c^2d^TR^{-1}d$. For a calibration sample mean $\overline{X}_c$, the amplitude estimator and its inversion are

$$\widehat{a}=-\frac{v_c^T\overline{X}_c}{Tf_c\|v_c\|^2},\qquad \widehat{\kappa}=\frac{\log(2/\widehat{a})}{\widehat{a}^2s_c},\quad 0<\widehat{a}<2. \tag{1869}$$

The generating identity is $a=2e^{-\kappa a^2s_c}$. An estimate outside this interval is inadmissible for this positive branch; it is neither clipped nor replaced by another sample. For n_c independent observations,

$$\operatorname{Var}(\widehat{a})=\frac{v_c^T(T\Sigma\Sigma^T)v_c}{n_c(Tf_c\|v_c\|^2)^2},\qquad \frac{d\kappa}{da}=-\frac{1+2\log(2/a)}{a^3s_c}. \tag{1870}$$

The first formula is exact; propagating it to $\widehat{\kappa}$ by the second is a delta-method approximation.

With $n_c=200000$, the fixed sample gives $\widehat{a}=1.71173662$ and $\widehat{\kappa}=0.69302041$, with propagated standard error 0.00827892. Freeze this estimate and predict new probes $\eta_A=(0,-0.8)^T$ and $\eta_B=(0.4,0.6)^T$. Each target uses 160000 independent new observations. The predicted means are $(-0.04006069,0.87721337)^T$ and $(-0.32156366,-0.69278139)^T$.

The corresponding sample means are $(-0.04033130, 0.87530399)^T$ and $(-0.32043192, -0.69058551)^T$. These are unchanged after the target data are examined.

For uncertainty propagation at $q_\perp = 0$,

$$\partial_\kappa u_* = \frac{az}{1+2\kappa z} R^{-1} g, \qquad \partial_\kappa \mu = TG\, \partial_\kappa u_*. \tag{1871}$$

Stacking both target means gives a four-dimensional prediction. Its covariance includes $\mathrm{Var}(\widehat{\kappa})(\partial_\kappa \mu)(\partial_\kappa \mu)^T$, including the nonzero cross covariance of the targets, plus their independent endpoint-sampling covariance. The resulting quadratic discrepancy is 3.31691; its asymptotic χ^2_4 tail probability is 0.50626. There is no subtraction of a target-fitted parameter. The nonlinear calibration makes this a large-sample test, not an exact finite-sample χ^2 pivot. An independent Monte Carlo calculation with 12000 repetitions gives a rejection fraction 0.05033 at the nominal 0.05 threshold, with binomial standard error about 0.00199 and no inadmissible calibrations.

Direct numerical minimization of the strictly convex Hamiltonian over 75 parameter/probe combinations gives a maximum control difference 1.32×10^{-8} from (1852). The exact feedback's stationarity residual is below 7.6×10^{-15}, and a central-difference check of (1855) has maximum error 1.71×10^{-9}. For the normalized two-channel example, the mixed cubic coefficient converges to $8\kappa = 5.6$; Richardson extrapolation gives 5.59999374. The full residual calculation also verifies the positive orthogonal remainder rather than suppressing it.

The restriction in (1858) is a concrete consequence of one specified joint cost. Its use as a physical test requires the same residual scales, source map, state observable, clock and admissible branch in calibration and validation. In a field application these quantities must be matched to geometry, matter or transport before the response is interpreted in that sector. The present calculation supplies the exact finite relation and an independent synthetic test; it leaves that microscopic matching to the corresponding physical realization.

Appendix V. Generator conditions for the time arrow, attraction, and physical validation

A stochastic variational principle selects a law after its state, noise, controls, and coefficients have been specified. Brownian noise alone does not determine time-reversal properties. A normalizable Gibbs density does not establish attraction, and attraction of a regulated law does not establish geodesic completeness. We give distinct conditions for these statements. All coordinates in the first calculation are even under reversal; the drive is held fixed. Odd coordinates require the parity-aware criterion in the main text.

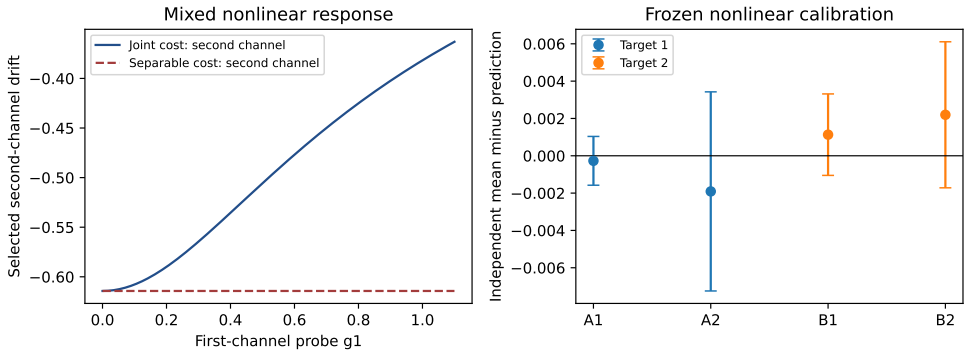


Figure 66. Nonlinear response of the declared finite affine branch. Left: with the second probe fixed, the joint cost changes the second-channel drift when the first probe increases; the separable alternative does not. Right: independent endpoint means minus the frozen predictions, with pointwise 95% intervals including calibration uncertainty. The plotted data are synthetic, and simultaneous inference uses the full joint covariance rather than these individual intervals.

V.1. *One potential with independently specified circulation.* Use a finite-dimensional physical coordinate domain with periodic boundary conditions or sufficient decay for the integrations below. Let $S(x)$ be a regulated energy, $\theta > 0$ the noise-energy scale, and $M(x) = M(x)^T \succ 0$ a smooth mobility. Assume well-posedness, nonexplosion, and a finite partition function. Define

$$\begin{aligned} \pi &= Z^{-1} \exp[-S/\theta], \\ b &= -M\nabla S + \theta \operatorname{div} M + c, \qquad a = \Sigma\Sigma^T = 2\theta M, \\ \mathcal{L}f &= b \cdot \nabla f + \theta M : D^2 f, \qquad \operatorname{div}(\pi c) = 0. \end{aligned} \tag{1872}$$

Here $(\operatorname{div} M)_i = \partial_j M_{ij}$. The circulation c must come from specified mother dynamics, maintained forcing, or selected feedback. The energy alone does not determine it. The probability density p is distinct from physical mass density. With $h = p/\pi$, the Itô current is

$$j_p = bp - \theta \operatorname{div}(Mp) = pc - \theta p M \nabla \log h, \qquad j_\pi = \pi c. \tag{1873}$$

The $\operatorname{div} M$ terms cancel, and $\nabla \log \pi = -\nabla S/\theta$. Thus π is invariant for every permitted c; invariance cannot by itself select c.

Proposition 172 (Contraction and irreversible circulation). *Suppose $p > 0$, the displayed integrals are finite, and all time derivatives and integrations*

by parts are justified. Then

$$H(p \mid \pi) = \int p \log(p/\pi)\,\mathrm{d}x,$$
$$\frac{\mathrm{d}}{\mathrm{d}t} H(p_t \mid \pi) = -\theta I_M(p_t \mid \pi), \qquad I_M(p \mid \pi) = \int p\, \nabla \log h^T M \nabla \log h\,\mathrm{d}x. \tag{1874}$$

The quadratic even-reversal current expression decomposes as

$$\int \frac{j_p^T M^{-1} j_p}{\theta p}\,\mathrm{d}x = \theta I_M(p \mid \pi) + \frac{1}{\theta}\int p\, c^T M^{-1} c\,\mathrm{d}x. \tag{1875}$$

At stationarity, assuming equivalent forward and reversed path laws and the required Girsanov integrability, their relative-entropy rate is

$$\sigma_\pi = \frac{1}{\theta}\int \pi c^T M^{-1} c\,\mathrm{d}x. \tag{1876}$$

It is positive exactly when $c \neq 0$ on a set of positive π-measure. The choice $c = 0$ gives a reversible stationary diffusion even with nonzero noise.

Proof. Mass conservation and the Fokker–Planck equation give

$$H' = \int \nabla \log h \cdot j_p = \int \pi c \cdot \nabla h - \theta I_M = -\theta I_M.$$

The first integral vanishes by $\operatorname{div}(\pi c) = 0$. The cross term in the current square is this integral times -2. The stationary reversed drift is

$$b^{\mathrm{R}} = -b + 2\theta \operatorname{div}(M\pi)/\pi = -M\nabla S + \theta \operatorname{div} M - c.$$

The difference is $2c$, so the entropy rate equals $\frac{1}{2}\int \pi (2c)^T (2\theta M)^{-1}(2c) = \sigma_\pi$. Strict positivity follows from $M \succ 0$. Nonstationary reversal also contains evolving-density and endpoint data. □

For semidefinite M, use its pseudoinverse and require c in the noise range for a finite rate; transverse drift can make the path laws singular. Conserved functions $C_j(X)$ require

$$DC_j \Sigma = 0, \qquad DC_j b + \tfrac{1}{2} a : D^2 C_j = 0. \tag{1877}$$

A lower-dimensional constrained law needs an intrinsic measure, rather than an assumed smooth ambient density.

V.2. *Quantitative attraction and persistent dissipation.* A sufficient convergence condition is the weighted logarithmic Sobolev inequality

$$H(p \mid \pi) \leq I_M(p \mid \pi)/(2\lambda), \qquad \lambda > 0. \tag{1878}$$

Gronwall's and Pinsker's inequalities give

$$H(p_t \mid \pi) \leq e^{-2\theta\lambda t} H(p_0 \mid \pi), \quad \|p_t - \pi\|_{\mathrm{TV}} \leq \sqrt{H(p_0 \mid \pi)/2}\, e^{-\theta\lambda t}. \tag{1879}$$

Here $\|p-\pi\|_{\mathrm{TV}} = \frac{1}{2}\int |p-\pi|$. Existence of λ must be checked for the potential, mobility, boundary, and regulated measure [85]. For degenerate noise, a hypocoercive or Harris argument is separate, with its own conditions [89].

Positive σ_π and attraction coexist. With $c \neq 0$, the Gibbs-shaped invariant law is a maintained stationary state rather than thermal equilibrium under the fixed-drive reversal. Relaxation dissipates transient free-energy excess; circulation can continue to dissipate at stationarity. With local detailed balance, $\theta = k_B T$, and thermal mobility M, the nonconservative force $F_{\mathrm{nc}} = M^{-1}c$ has stationary power

$$\dot{W}_{\mathrm{nc}} = \int F_{\mathrm{nc}} \cdot j_\pi \,\mathrm{d}x = \theta\sigma_\pi. \tag{1880}$$

Without a reservoir map, a path rate is not automatically a heat rate.

V.3. *A stable irreversible finite branch.* Take two even coordinates with a fixed rotational drive:

$$S = \tfrac{1}{2}h|x|^2, \quad M = \mu I, \quad c = \omega J x, \quad J = \begin{pmatrix} 0 & -1 \\ 1 & 0 \end{pmatrix}, \qquad \gamma = \mu h > 0. \tag{1881}$$

Its invariant covariance is $C_\pi = (\theta/h)I$. Since $x \cdot Jx = 0$ and $\operatorname{tr} J = 0$, $\operatorname{div}(\pi c) = 0$. Eigenvalues $-\gamma \pm i\omega$ are stable, and

$$\sigma_\pi = 2\omega^2/\gamma, \qquad \mathbb{E}|X_t|^2 = e^{-2\gamma t}\mathbb{E}|X_0|^2 + (2\theta/h)(1 - e^{-2\gamma t}). \tag{1882}$$

For an initial Gaussian with covariance C_π and mean m_0,

$$m_t = e^{-\gamma t}e^{\omega J t}m_0, \qquad H(p_t \mid \pi) = \frac{h|m_0|^2}{2\theta}e^{-2\gamma t}. \tag{1883}$$

Setting $\omega = 0$ leaves attraction and noise intact but makes the stationary arrow vanish. Changing ω changes the arrow without changing the invariant law. These branches separate relaxation and path irreversibility within one generator family.

V.4. *A finite-state escape theorem.*

Proposition 173 (Coercive stochastic stability). *Suppose the state has a unique local continuous solution. Let $W \in C^2$, $W \geq 1$, with sublevels compact inside its domain. Assume continuation until exit from every compact sublevel, and*

$$\mathcal{L}W \leq A - BW, \qquad A \geq 0, \quad B > 0 \tag{1884}$$

for the selected feedback. For $R > W(X_0)$ and $\tau_R = \inf\{t : W(X_t) \geq R\}$,

$$\mathbb{P}(\tau_R \leq T) \leq [W(X_0) + AT]/R. \tag{1885}$$

The solution is nonexplosive, and

$$\mathbb{E}W(X_t) \leq e^{-Bt}W(X_0) + (A/B)(1 - e^{-Bt}). \tag{1886}$$

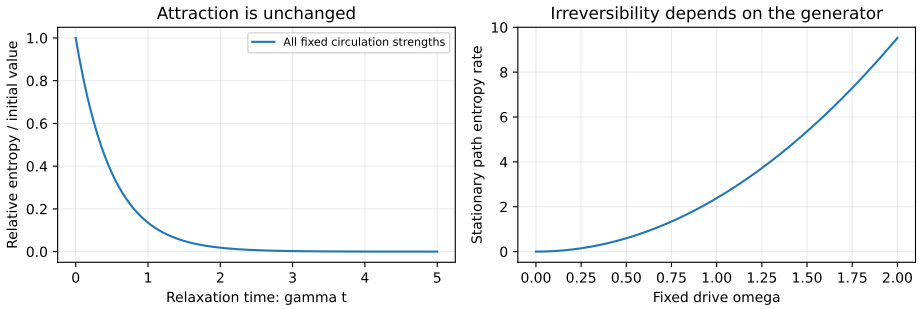


Figure 67. Exact Gaussian diagnostics. Relative entropy of a displaced initial law decays independently of circulation; stationary path entropy varies quadratically with the drive. These finite-model calculations are neither experimental nor cosmological observations.

Proof. Stopped Itô integration and martingale localization give $\mathbb{E}W(X_{T\wedge\tau_R}) \le W(X_0) + AT$. Continuity gives $W(X_{\tau_R}) = R$ on exit. Nonnegativity on the complement proves the probability bound. Let $R \to \infty$ and use continuation for nonexplosion. Itô integration of $e^{Bt}W(X_t)$, localization, and Fatou's lemma give the moment bound. □

For the Gaussian branch, $W = 1 + |x|^2$ has $\mathcal{L}W = -2\gamma|x|^2 + 4\theta\mu$. Explicit choices are $B = 2\gamma$, $A = 2\gamma + 4\theta\mu$. A positive residual metric alone does not imply this drift inequality.

The theorem concerns configuration paths. A curvature probability bound additionally needs a derived metric map with, for example, $\mathcal{K}[g(X)] \le C_{\mathcal{K}}W(X)$ in a regular chart. Only then does the escape bound imply

$$\mathbb{P}(\sup_{t\le T} \mathcal{K}[g(X_t)] \ge C_{\mathcal{K}}R) \le [W(X_0) + AT]/R.$$

Geodesic completeness further needs a global Lorentzian solution and extension criteria. A compact regulator supplies neither result.

V.5. *Observable errors and independent physical tests.* Let $Y_t = \Pi(X_t)$, and let $\mathcal{L}_{\mathrm{f}}$ be a proposed finite fluid generator with the same projected initial condition. Assume nonexplosion and a smooth bounded backward solution $v(t,y) = P^{\mathrm{f}}_{T-t}F(y)$, with justified Itô expectation. It satisfies $v_t + \mathcal{L}_{\mathrm{f}}v = 0$. Put

$$r_v(t,x) = \mathcal{L}(v(t,\cdot)\circ\Pi)(x) - \mathcal{L}_{\mathrm{f}}v(t,\Pi x). \tag{1887}$$

Itô's formula gives the exact identity

$$\mathbb{E}F(\Pi X_T) - \mathbb{E}\Big[P^{\mathrm{f}}_T F(\Pi X_0)\Big] = \mathbb{E}\int_0^T r_v(t,X_t)\,\mathrm{d}t. \tag{1888}$$

The initial semigroup value is averaged over the projected initial law; for a deterministic initial state this expectation reduces to evaluation at that state. A uniform bound $|r_v(t,x)| \le \varepsilon(t)$ gives an observable error at most $\int_0^T \varepsilon(t)\,\mathrm{d}t$. Few fixed test functions do not establish this for every backward observable. Boundaries, memory, and sampling must enter if present. Autonomy of the projection was not assumed; it is tested by the mismatch.

If independent calibration identifies a parameter set $\mathcal{C} = \{\vartheta : f(\vartheta) = d_{\mathrm{cal}}\}$, a unique target $g(\vartheta)$ requires g to be constant on $\mathcal{C}$. Otherwise the prediction is the set $g(\mathcal{C})$. A block-diagonal generator $\mathcal{L} = \mathcal{L}_{\mathrm{f}} + \mathcal{L}_{\mathrm{g}}$ preserves fluid trajectories while an unobserved gravitational block varies. Fluid agreement alone cannot constrain that freedom. A shared cost changes this only when its independently fixed data remove the free direction. The same requirement applies to quantum observations.

V.6. *An explicit observable error caused by an omitted memory variable.* A resolved variable need not be Markovian even when the full state is. To quantify the resulting error, consider a hidden fluctuation with a known correlation time. Its amplitude and correlation time are independent model inputs. This distinction is essential when taking a short-memory limit.

Fix $a, \kappa, v > 0$, $D \ge 0$, and $b \in \mathbb{R}$. Let W^1, W^2 be independent standard Brownian motions, let $X_0 = Y_0 = 0$, and let $Z_0 \sim N(0, v)$ be independent of their future increments. Define

$$\begin{aligned} \mathrm{d}X_t &= (-aX_t + bZ_t)\mathrm{d}t + \sqrt{2D}\,\mathrm{d}W_t^1, \\ \mathrm{d}Z_t &= -\kappa Z_t \mathrm{d}t + \sqrt{2\kappa v}\,\mathrm{d}W_t^2, \\ \mathrm{d}Y_t &= -aY_t \mathrm{d}t + \sqrt{2D}\,\mathrm{d}W_t^1. \end{aligned} \tag{1889}$$

Here $1/a$ is the resolved relaxation time, $1/\kappa$ is the hidden correlation time, v is the stationary hidden variance, and b converts the hidden coordinate into a resolved force. The process Y is the proposed approximation that omits this force. The two-dimensional system is a finite benchmark for the generator comparison, not an asserted projection of the full gravitational action.

Proposition 174 (Exact memory contribution to a resolved second moment). *For the processes in* (1889)*, put* $\Delta_V(T) = \mathbb{E}X_T^2 - \mathbb{E}Y_T^2$*. Then*

$$\Delta_V(T) = b^2 v \int_0^T \int_0^T e^{-a(2T-s-t)} e^{-\kappa|s-t|}\,\mathrm{d}s\,\mathrm{d}t \ge 0. \tag{1890}$$

For $\kappa \ne a$ *this is*

$$\Delta_V(T) = \frac{2b^2 v}{a+\kappa}\left\{\frac{1-e^{-2aT}}{2a} - \frac{e^{-(a+\kappa)T} - e^{-2aT}}{a-\kappa}\right\}. \tag{1891}$$

At $\kappa = a$ the continuous extension is

$$\Delta_V(T) = \frac{b^2 v}{2a^2}\left[1 - (1 + 2aT)e^{-2aT}\right]. \tag{1892}$$

For every $T \geq 0$,

$$\Delta_V(T) \leq \min\left\{\frac{b^2 v(1 - e^{-aT})^2}{a^2},\ \frac{b^2 v(1 - e^{-2aT})}{a\kappa},\ \frac{b^2 v}{a(a + \kappa)}\right\}. \tag{1893}$$

The last bound is attained in the limit $T \to \infty$.

Proof. The stationary hidden covariance is $\mathbb{E}[Z_s Z_t] = v e^{-\kappa|s-t|}$. Variation of constants gives

$$X_T = Y_T + b\int_0^T e^{-a(T-s)} Z_s \,\mathrm{d}s, \qquad \mathbb{E}Y_T^2 = \frac{D}{a}(1 - e^{-2aT}). \tag{1894}$$

The added integral is independent of Y_T and has zero mean. Its variance therefore equals the second-moment difference, which proves (1890). Fubini is justified because the integrand is continuous and bounded on the compact square.

An equivalent derivation exposes the moment closure. Set $c(t) = \mathbb{E}[X_t Z_t]$. The cross quadratic variation is zero, and Itô's product rule gives

$$c' = -(a + \kappa)c + bv, \qquad c(0) = 0, \qquad c(t) = \frac{bv}{a + \kappa}(1 - e^{-(a+\kappa)t}). \tag{1895}$$

Subtracting the two resolved second-moment equations gives

$$\Delta_V' + 2a\Delta_V = 2bc(t), \qquad \Delta_V(0) = 0. \tag{1896}$$

Multiplying by e^{2at} and integrating yields

$$\Delta_V(T) = \frac{2b^2 v}{a + \kappa}\int_0^T e^{-2a(T-t)}(1 - e^{-(a+\kappa)t})\,\mathrm{d}t.$$

The first exponential integrates to $(1 - e^{-2aT})/(2a)$. The second integrates to $(e^{-(a+\kappa)T} - e^{-2aT})/(a - \kappa)$ when $a \neq \kappa$, and to Te^{-2aT} when $a = \kappa$. This proves both exact formulas.

For the first bound in (1893), replace $e^{-\kappa|s-t|}$ by one. For the second, extend $f_T(s) = e^{-a(T-s)}\mathbf{1}_{[0,T]}(s)$ by zero to $\mathbb{R}$ and write $k_\kappa(s) = e^{-\kappa|s|}$. Cauchy–Schwarz and the L^1–L^2 convolution inequality give

$$\langle f_T, k_\kappa * f_T\rangle \leq \|k_\kappa\|_{L^1}\|f_T\|_{L^2}^2 = \frac{2}{\kappa}\frac{1 - e^{-2aT}}{2a}.$$

For the final bound substitute $r = T - s$ and $q = T - t$ in the double integral. Its nonnegative integrand becomes $e^{-a(r+q)}e^{-\kappa|r-q|}$ on the increasing square $[0, T]^2$. The integral is increasing in T and converges to its integral on $[0, \infty)^2$. Either direct integration or the exact formulas give $b^2 v/[a(a + \kappa)]$ for that limit. □

Evaluation of the generator residual. For $F(y) = y^2$, the reduced backward solution is

$$u(t, y) = e^{-2a(T-t)}y^2 + \frac{D}{a}(1 - e^{-2a(T-t)}). \tag{1897}$$

The full generator acting on a function of x differs from the reduced generator only through $bz\partial_x$. Thus its actual residual is

$$r_u(t, x, z) = 2be^{-2a(T-t)}xz. \tag{1898}$$

It is unbounded on the state space. A uniform statewise residual estimate would therefore be inappropriate here. Instead, all Gaussian moments are finite on finite time intervals, so localization and uniform integrability justify the expected identity

$$\mathbb{E}\int_0^T r_u(t, X_t, Z_t)\,\mathrm{d}t = 2b\int_0^T e^{-2a(T-t)}c(t)\,\mathrm{d}t = \Delta_V(T). \tag{1899}$$

This supplies an explicit constant for a particular observable, rather than assuming that the projected variable has an autonomous law.

What is held fixed in the limit. At fixed a, b, v, D, (1893) gives the uniform-in-time estimate $\Delta_V(T) \le b^2v/(a\kappa)$. The omitted force then makes a vanishing contribution as its correlation time tends to zero. Its integrated covariance is $2b^2v/\kappa$, which also tends to zero. If instead $v = \kappa q$ with $q > 0$ fixed, then

$$\lim_{\kappa\to\infty} \Delta_V(T) = \frac{b^2q}{a}(1 - e^{-2aT}). \tag{1900}$$

This equals the variance contribution of an additional independent white noise of amplitude $\sqrt{2b^2q}$. The approximation Y omits that finite contribution. Equation (1900) is a second-moment limit; a path-law convergence statement requires its own tightness and identification argument.

A positive stationary energy and the role of circulation. Assume now $D > 0$. Define $\xi = (x, z)^{\mathsf{T}}$ and

$$\begin{aligned} B &= \begin{pmatrix} -a & b \\ 0 & -\kappa \end{pmatrix}, \qquad Q = \begin{pmatrix} D & 0 \\ 0 & \kappa v \end{pmatrix}, \\ C &= \begin{pmatrix} D/a + b^2v/[a(a+\kappa)] & bv/(a+\kappa) \\ bv/(a+\kappa) & v \end{pmatrix}. \end{aligned} \tag{1901}$$

Its determinant is

$$\det C = \frac{Dv}{a} + \frac{b^2v^2\kappa}{a(a+\kappa)^2} > 0.$$

Hence C is positive definite. Direct multiplication gives $BC + CB^{\mathsf{T}} + 2Q = 0$, so $N(0, C)$ is the stationary law. For any fixed $\theta > 0$, set

$$S(\xi) = \frac{\theta}{2}\xi^{\mathsf{T}}C^{-1}\xi, \quad M = Q/\theta, \quad J = \frac{BC + Q}{\theta} = \frac{b\kappa v}{\theta(a+\kappa)}\begin{pmatrix} 0 & 1 \\ -1 & 0 \end{pmatrix}. \tag{1902}$$

Then $B\xi = (J - M)\nabla S(\xi)$ and $2\theta M = 2Q$. The Gibbs density proportional to $e^{-S/\theta}$ is therefore the same stationary Gaussian. The circulation $J\nabla S$ preserves that density: its divergence is zero because J is constant and skew, and its scalar product with ∇S vanishes.

For $b \neq 0$, $J \neq 0$. Thus this construction is not reversible under ordinary reversal with both coordinates even. Indeed detailed balance for this stationary Ornstein–Uhlenbeck diffusion would require $BC = -Q$, which the displayed nonzero skew part excludes. This example fits a positive quadratic energy with separately specified circulation; it does not show that the energy alone determines that circulation or that the model is a reversible Hamiltonian heat-bath elimination.

Appendix W. Stochastic Noether balances: physical charges and Bellman contact symmetries

A charge may be constant along each sample path, may be a martingale, or may have only a constant unconditional mean. These statements differ. González Lezcano and Cabo Montes de Oca [82] study mean mechanical charges under random external forces. De Vecchi, Mastrogiacomo, Turra, and Ugolini [58] relate contact symmetries of a Bellman equation to local martingales along an optimal state. The latter is the more direct foundation for the present control problem. Neither result identifies an adjoint charge with physical energy without an additional map.

W.1. *The complete randomly forced mechanical balance.* For a mechanical Lagrangian $L_0(q, \dot{q})$, let $\xi(q)$ generate a symmetry, $\delta_\xi L_0 = 0$, and set $J_0 = \partial_{\dot{q}} L_0 \cdot \xi$. The forced equation implies

$$\frac{\mathrm{d}}{\mathrm{d}t}\partial_{\dot{q}} L_0 - \partial_q L_0 = Q, \qquad \frac{\mathrm{d}J_0}{\mathrm{d}t} = Q \cdot \xi, \qquad \frac{\mathrm{d}}{\mathrm{d}t}\mathbb{E}J_0 = \mathbb{E}(Q \cdot \xi). \tag{1903}$$

The expectation identity requires integrability and interchange of time differentiation and averaging. Crucially the force is evaluated on its driven trajectory. A zero mean random field at a prescribed point does not establish a zero mean force on a correlated path. For example, $\mathbb{E}Z = 0$ for an equiprobable sign Z, while $\mathbb{E}[ZZ] = 1$.

Suppose a random Lagrangian $L_{\mathrm{r}}(t, q, \dot{q}, \zeta)$ supplies $\pi_{\mathrm{r}} = \partial_{\dot{q}} L_{\mathrm{r}}$ and $Q = \partial_q L_{\mathrm{r}} - \mathrm{d}\pi_{\mathrm{r}}/\mathrm{d}t$. On differentiable paths the complete variation is

$$\delta_\xi L_{\mathrm{r}} = Q \cdot \xi + \frac{\mathrm{d}}{\mathrm{d}t}(\pi_{\mathrm{r}} \cdot \xi). \tag{1904}$$

For compactly supported deterministic $k(t)$,

$$\int k\, \delta_\xi L_{\mathrm{r}}\, \mathrm{d}t = \int kQ \cdot \xi\, \mathrm{d}t - \int \dot{k}\, \pi_{\mathrm{r}} \cdot \xi\, \mathrm{d}t. \tag{1905}$$

Compact support removes the boundary term, not the $\dot{k}$ term. If the characteristic functional $\mathcal{C}[k;q] = \mathbb{E}\exp(i\int kL_{\mathrm{r}}\,\mathrm{d}t)$ is invariant, and differentiation at $k=0$ is justified under the stated ensemble, its first-moment consequence is

$$\mathbb{E}(Q\cdot\xi) = -\frac{\mathrm{d}}{\mathrm{d}t}\mathbb{E}(\pi_{\mathrm{r}}\cdot\xi). \tag{1906}$$

Thus the conserved mean is that of $J_0+\pi_{\mathrm{r}}\cdot\xi$. Bare-charge mean conservation additionally requires $\mathrm{d}\mathbb{E}(\pi_{\mathrm{r}}\cdot\xi)/\mathrm{d}t = 0$. A position-only random potential has $\pi_{\mathrm{r}}=0$; a velocity-dependent interaction need not. The characteristic-functional argument in [82] must retain this term or justify an assumption eliminating it. Prescribed-path and noise-driven-path ensembles must not be silently interchanged.

An exact example is

$$L_0 = \tfrac{1}{2}m\dot{q}^2, \quad L_{\mathrm{r}} = \tfrac{1}{2}\varepsilon Zt\dot{q}^2, \quad Z=\pm1, \quad \dot{q}(0)=v_0, \quad |\varepsilon t|<m. \tag{1907}$$

Both terms are translation invariant on every realization. The total momentum equals mv_0, but

$$(m+\varepsilon Zt)\dot{q} = mv_0, \qquad \mathbb{E}J_0(t) = \frac{mv_0}{1-(\varepsilon t/m)^2}. \tag{1908}$$

The random kinetic term carries the compensating mean. This illustrative random-inertia model demonstrates the bookkeeping issue; it is not a particle-mass prediction.

W.2. *Itô mechanical charges and reservoir energy.* Brownian velocities do not permit the preceding ordinary path derivatives. Instead specify

$$\mathrm{d}q = P\,\mathrm{d}t/m, \qquad \mathrm{d}P = (-\nabla U - \Gamma P + f)\,\mathrm{d}t + \Sigma\,\mathrm{d}W. \tag{1909}$$

For $\xi(q) = Aq+d$, $A^T=-A$, and $\nabla U\cdot\xi = 0$, direct Itô calculation gives

$$J = P\cdot\xi(q), \qquad \mathrm{d}J = \xi\cdot(-\Gamma P+f)\,\mathrm{d}t + \xi^T\Sigma\,\mathrm{d}W. \tag{1910}$$

Here q has finite variation, so $[q,P]=0$, and $P^TAP/m=0$. The charge with its explicit drift integral removed is a local martingale. Integrability promotes it to a true martingale. Isotropic noise does not eliminate the friction contribution.

For $E_{\mathrm{mech}} = |P|^2/(2m) + U(q)$,

$$\mathrm{d}E_{\mathrm{mech}} = \left(-\frac{P^T\Gamma P}{m} + \frac{P\cdot f}{m} + \frac{\mathrm{tr}(\Sigma\Sigma^T)}{2m}\right)\mathrm{d}t + \frac{P^T\Sigma}{m}\,\mathrm{d}W. \tag{1911}$$

With $\Gamma=\gamma I$ and $\Sigma\Sigma^T = 2\gamma m\theta I$, the mean balance is

$$(\mathbb{E}E_{\mathrm{mech}})' = -\gamma\mathbb{E}|P|^2/m + d\gamma\theta + \mathbb{E}(P\cdot f)/m.$$

At an unforced Gibbs state $\mathbb{E}|P|^2 = dm\theta$. Injection balances friction, while fluctuating trajectories continue. This equilibrium model is reversible under the odd momentum parity $P\mapsto -P$. Mean charge conservation and energy exchange therefore do not determine the path arrow.

W.3. *The contact-symmetry theorem in the minimization convention.* For $a = \Sigma\Sigma^T$, use

$$V_t + \mathcal{H}(t, x, DV, D^2V) = 0, \qquad \mathcal{H}(t, x, p, Q) = \inf_{\alpha \in U} \{\ell + b \cdot p + \tfrac{1}{2} a : Q\}. \tag{1912}$$

The arXiv version of [58] uses reward maximization. Negating reward and value consistently gives this minimization convention. We refer to Theorem 4.3 using the numbering of that version.

Assume $\mathcal{H}$ is smooth on the visited jet domain, a measurable minimizing selector exists, and the envelope identities $\mathcal{H}_p = b^*$, $\mathcal{H}_Q = a^*/2$ hold. For the following direct proof require continuous third spatial derivatives and continuous $\partial_t DV$, in addition to the usual Bellman derivatives. Sufficient classical regularity is $C^{1,3}$ with those mixed derivatives. A $C^{1,2}$ statement alone does not justify applying the classical Itô formula to DV. We use stronger explicit assumptions rather than silently invoking a nonsmooth extension.

Let $\Omega(t, x, v, p)$ be a smooth evolutionary characteristic of a contact symmetry that leaves time fixed. Its total derivative is

$$D_i\Omega = \Omega_{x_i} + p_i\Omega_v + \sum_j Q_{ij}\Omega_{p_j}.$$

The next total derivative includes the third-derivative jet. In this convention the determining identity is

$$\Omega_t - \mathcal{H}\Omega_v + b^* \cdot D_x\Omega + \tfrac{1}{2} a^* : D_x^2\Omega - (D_x\mathcal{H}) \cdot \Omega_p = 0. \tag{1913}$$

It is an identity on the Bellman solution jet.

Proposition 175 (Contact charge along the optimal law). *Under the regularity, envelope, selector, and well-posedness assumptions above, set*

$$O_t = \Omega(t, X_t, V(t, X_t), DV(t, X_t)), \qquad \mathcal{N}_t = \Sigma^{*T} D_x\Omega|_V(t, X_t). \tag{1914}$$

If (1913) *holds, then* $\mathrm{d}O_t = \mathcal{N}_t \cdot \mathrm{d}W_t$. *With* $\mathbb{E}|O_0| < \infty$ *and* $\mathbb{E}\int_0^T |\mathcal{N}_s|^2 \,\mathrm{d}s < \infty$, *it is a true martingale. If* $O_0 \in L^2$,

$$\mathbb{E}O_t = \mathbb{E}O_0, \qquad \mathbb{E}(O_t - O_0)^2 = \mathbb{E}\int_0^t |\mathcal{N}_s|^2 \,\mathrm{d}s. \tag{1915}$$

Proof. Put $\phi(t, x) = \Omega(t, x, V(t, x), DV(t, x))$. Then $D_x\phi = D_x\Omega|_V$, $D_x^2\phi = D_x^2\Omega|_V$, and

$$\phi_t = \Omega_t + \Omega_v V_t + \Omega_p \cdot \partial_t DV = \Omega_t - \Omega_v\mathcal{H} - \Omega_p \cdot D_x\mathcal{H}.$$

Itô's formula along the optimal state has exactly the drift in (1913). Localization proves the first statement. Square-integrable stochastic integration and Itô isometry prove the remaining claims. This composition proof retains every mixed second-derivative contribution with its full coefficient. □

For a point-symmetry characteristic $\Omega = p \cdot \xi(x)$, $O = DV \cdot \xi$ agrees with the adjoint charge under smooth Bellman–adjoint identification. Mechanical momentum additionally requires a physical Legendre and units map. For example, $V_t + DV_{xx} = 0$ and $V = e^{-Dk^2(T-t)} \sin(kx)$ give the translation charge

$$\begin{aligned} \mathrm{d}X &= \sqrt{2D}\,\mathrm{d}W, \qquad O_t = ke^{-Dk^2(T-t)} \cos(kX_t), \\ \mathrm{d}O_t &= -\sqrt{2D}\,k^2 e^{-Dk^2(T-t)} \sin(kX_t)\,\mathrm{d}W_t. \end{aligned} \tag{1916}$$

Its mean is constant, but its sample values fluctuate. There is no massive-particle momentum in this heat-equation example.

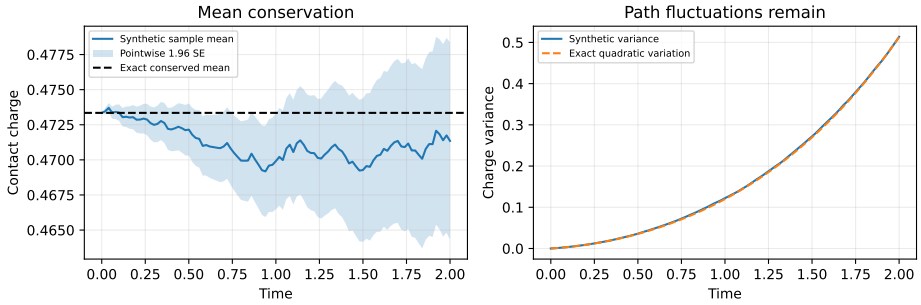


Figure 68. Exact Brownian sampling of the heat-equation contact charge, using 40000 independent paths. The conserved ensemble mean coexists with increasing charge variance. Shading gives pointwise 1.96-standard-error bands; it is not a simultaneous confidence band. The dashed variance is the exact integrated quadratic variation.

For an approximate value $\widehat{V}$, define $r = \widehat{V}_t + \mathcal{H}(t, x, D\widehat{V}, D^2\widehat{V})$ and let d_Ω be the determining-expression defect. The charge drift along its minimizing selector is

$$d_\Omega + \Omega_v r + \Omega_p \cdot D_x r. \tag{1917}$$

A different policy adds $(b^\alpha - b^*) \cdot D_x\phi + \frac{1}{2}(a^\alpha - a^*) : D_x^2\phi$. Value error alone therefore cannot bound the symmetry error; the gradient of the Bellman residual matters. Integrating absolute expected defects bounds the mean-charge error. More explicitly, for the minimizing approximate policy, suppose the stochastic integral is a true martingale and the two derivatives of Ω below are bounded on the visited jets. Then

$$\begin{aligned} |\mathbb{E}O_T - \mathbb{E}O_0| \le \int_0^T \mathbb{E}|d_\Omega(t, X_t)|\,dt \\ + \|\Omega_v\|_\infty \int_0^T \mathbb{E}|r(t, X_t)|\,dt \end{aligned}$$

$$+ \|\Omega_p\|_\infty \int_0^T \mathbb{E}|D_x r(t, X_t)|\, dt.$$

Here O_t is formed from $\widehat{V}$, and all defects are evaluated on its jet. The estimate follows by integrating (1917), taking expectation, and applying the triangle inequality. A policy mismatch adds the integral of the absolute expected policy defect displayed above. For Galerkin approximations, convergence of this bound requires these integrals to vanish with the cutoff. Convergence of the value function alone does not supply that requirement.

A random-field Bellman equation $\mathrm{d}V_t(x) = -\mathcal{H}^{\mathrm{s}}\mathrm{d}t + \Psi_t(x) \cdot \mathrm{d}W_t$ requires Itô–Wentzell and its cross term $\sum_\ell \Sigma_\ell \cdot D_x \Psi_\ell$. Theorem 4.8 of that version uses a compensated charge. Corollary 4.9 permits an uncompensated charge only for its restricted Lie-point form and diffusion-commutator conditions. Endogenous-law costs also need law-space derivatives or a genuine Markov augmentation. The fixed-state theorem does not erase these terms.

W.4. *Physical interpretation and the quantum boundary.* The theorem gives a consequence of a specified symmetry, not a selection of that symmetry or of all coupling weights. Its charge is not automatically the physical metric or mechanical energy. Time-changing transformations have their own conditions; the article separates them in Remarks 4.1 and 4.4. Classical mechanical Noether conservation is recovered only with a regular mechanical Legendre branch and convergence of its extremals, in addition to vanishing noise.

Finally mean two-particle momentum conservation is weaker than pairwise conservation. For independent Brownian motions,

$$P_1 = p_0 + \sigma W_1(t), \qquad P_2 = -p_0 + \sigma W_2(t),$$
$$\mathbb{E}(P_1 + P_2) = 0, \qquad \mathrm{Var}(P_1 + P_2) = 2\sigma^2 t.$$

The zero mean does not allow exact remote inference. Shared classical noise creates ordinary correlations, but a Bell-local, measurement-independent model still obeys CHSH. The EPR discussion in [82] does not replace the quantum reconstruction and measurement conditions of Paper IV.

Appendix X. A common variational origin with a closed stochastic realization

X.1. *What must be shared before a claim of unification is meaningful.* An action determines stationary field configurations; a stochastic generator determines a law of evolving configurations. These are different mathematical objects. To connect them, fix a finite regulator, a gauge treatment, and local coordinates z on the admissible configuration space. Let $S(z)$ be the regulated master energy, $\theta > 0$ the energy scale of fluctuations, and $M(z) = M(z)^T$ a positive mobility. Positivity refers to the physical reduced directions, not to the

indefinite gravitational DeWitt form. The reference volume is declared before a probability density is written. In this section it is coordinate Lebesgue volume; a volume weight is included below.

For a joint residual $R(z,u)$, a single running cost may be defined by

$$q(z,u) = R(z,u)^T H(z) R(z,u), \qquad \ell_0(z,u) = \frac{1}{4} q(z,u), \qquad H = H^T \succ 0. \tag{1918}$$

The components of R must first be divided by their physical scales so that q has consistent units. Cross blocks are permitted only between compatible representations. For $H = \left(\begin{smallmatrix} H_1 & C \\ C^T & H_2 \end{smallmatrix}\right)$ with positive diagonal blocks, completing the square gives

$$\begin{aligned} r^T H r = {} & \big(r_2 + H_2^{-1} C^T r_1\big)^T H_2 \big(r_2 + H_2^{-1} C^T r_1\big) \\ & + r_1^T \big(H_1 - C H_2^{-1} C^T\big) r_1. \end{aligned} \tag{1919}$$

Thus positivity is equivalent to a positive Schur complement. Eliminating the second residual changes the first sector's stiffness. This is a real cross-sector restriction after H has been fixed; it does not determine H from a symmetry that leaves several invariant metrics possible.

For the direct product of two distinct simple gauge algebras, a bilinear invariant pairing between their adjoint representations vanishes: invariance under the first factor forces every cross-functional to annihilate its commutators, and a simple algebra equals its commutator algebra. Shared scalars, spacetime geometry, matter representations, and the reduced mobility can couple the sectors without violating this restriction.

X.2. *An exact compatibility theorem for cost, drift, and Gibbs law.* The following construction supplies a precise version of the statement that one cost can produce dynamics and statistical equilibrium. Its strength is an exact calculation; its restriction is that the cost and generator must satisfy the displayed compatibility relation. Work on a compact torus, or on a smooth bounded domain with reflecting conditions. All coefficients are smooth, M is uniformly positive. Reflection is conormal, with backward boundary condition $n \cdot M \nabla f = 0$, and the candidate value S satisfies this condition. On the torus there is no boundary. Assume

$$\pi = Z^{-1} e^{-S/\theta}, \qquad \nabla \cdot (\pi c) = 0, \qquad c \cdot n = 0 \tag{1920}$$

at a reflecting boundary. An admissible gradient must also satisfy the boundary condition of the value equation.

Proposition 176 (Cost–generator compatibility). *Consider the controlled generator*

$$L^u f = (c + \theta \nabla \cdot M + u) \cdot \nabla f + \theta M : D^2 f \tag{1921}$$

and the cost $\ell = W + \frac{1}{2}u^T M^{-1}u$. *If*

$$W = \lambda + \frac{1}{2}\nabla S^T M \nabla S - c \cdot \nabla S - \theta \nabla \cdot (M \nabla S), \tag{1922}$$

then $V = S$ *solves the ergodic HJB equation* $\lambda = \inf_u\{\ell + L^u V\}$, *and the minimizing feedback is* $u_* = -M\nabla S$. *Subject to the usual verification integrability, transversality, and boundary conditions, this is optimal. Its invariant law is* π, *and its density current is*

$$j_p = pc - \theta p M \nabla \log(p/\pi). \tag{1923}$$

Proof. Substitution of $V = S$ gives

$$\ell + L^u S - \lambda = \frac{1}{2}(u + M\nabla S)^T M^{-1}(u + M\nabla S). \tag{1924}$$

The unique minimizer follows from positive definiteness. Applying Itô's formula and taking expectations makes the integrated right side the excess cost, up to the endpoint term $-\mathbb{E}[S(Z_T) - S(Z_0)]$. On a compact space that endpoint divided by T tends to zero; on a noncompact space it is a separate transversality condition. The noise covariance is $2\theta M$. Its forward current is $bp - \theta\nabla \cdot (Mp)$, which simplifies to (1923). At $p = \pi$ this is πc, whose divergence vanishes by (1920). □

The potential W in this proposition is constructed, not independently derived from a microscopic field theory. Therefore the result closes a specified realization and gives a test for any proposed independently derived cost. It cannot prove that arbitrary residual costs automatically generate the same Gibbs law. In particular, the master energy, running cost, value function, and mechanical Hamiltonian may coincide only through an explicit relation. At a reflecting endpoint this distinction is essential: for the half-line potential $\Phi(M) = M$, the candidate $V = \Phi$ fails the Neumann condition $V'(0) = 0$. Its Gibbs diffusion is well defined, but the displayed reflected HJB verification cannot use that candidate. A compatible value must obey the boundary condition, or the cost must include the appropriate boundary-local-time term. Boundary data are part of the common-origin test.

If the reference volume is $w(z)\,dz$, replace the coordinate energy in this calculation by $U = S - \theta \log w$. The probability density relative to dz is then $Z^{-1}we^{-S/\theta}$. Equivalently one can formulate the generator in weighted divergence form. This correction prevents a change of coordinates from being mistaken for a change of physical equilibrium.

X.3. *Free-energy loss and maintained irreversibility.* Let $f = p/\pi$, let $\mathcal{D}(p\|\pi) = \int p \log f\, dz$, and assume positive smooth densities with finite weighted

Fisher information. A direct integration by parts yields

$$\frac{d}{dt}\mathcal{D}(p_t\|\pi) = \int j_p \cdot \nabla \log f \, dz$$
$$= -\theta \int p \, \nabla \log f^T M \nabla \log f \, dz. \tag{1925}$$

Indeed, the circulation contribution is $\int \pi c \cdot \nabla f = -\int f \nabla \cdot (\pi c) = 0$. Expanding the current square gives a second, distinct identity:

$$\frac{1}{\theta}\int \frac{j_p^T M^{-1} j_p}{p}\, dz = \frac{1}{\theta}\int p \, c^T M^{-1} c \, dz$$
$$+ \theta \int p \, \nabla \log f^T M \nabla \log f \, dz. \tag{1926}$$

The two terms measure maintained circulation and relaxation, respectively. The excess free energy is $\theta\mathcal{D}(p\|\pi)$; it decreases even when the limiting law carries a nonzero circulation. At stationarity its derivative is zero while the first term may remain positive.

For even state variables, a stationary law and a fixed-drive reversal, assume the forward and reverse path laws are mutually absolutely continuous and the Girsanov energy is finite. The reversed drift differs by $2c$. Consequently the path relative-entropy rate is

$$\lim_{T\to\infty} \frac{1}{T}\mathcal{D}(P_{[0,T]}\|P^R_{[0,T]}) = \frac{1}{\theta}\int \pi c^T M^{-1} c \, dz. \tag{1927}$$

The factor follows from $\frac{1}{2}(2c)^T(2\theta M)^{-1}(2c) = c^T M^{-1} c/\theta$. For odd variables or reversed external parameters, the reverse generator must first be conjugated by the declared parity map; c alone is no universal irreversible current. Singular noise limits may destroy absolute continuity.

If a logarithmic Sobolev inequality has the convention $\mathcal{D}(p\|\pi) \le C_{\mathrm{LS}} I_M(p\|\pi)/2$, (1925) implies decay at rate $2\theta/C_{\mathrm{LS}}$. Gibbs invariance, attraction of laws, nonzero stationary path asymmetry, and regularity of individual spacetime geometries remain separate claims. This separation permits an irreversible realization without incorrectly declaring every equilibrium diffusion irreversible.

X.4. *Two nonlinear objectives that must not be confused.* For a dimensionless residual square, the nonlinear running penalty

$$\varphi_\kappa(q) = \frac{e^{\kappa q} - 1}{4\kappa}, \qquad \varphi_0(q) = \frac{q}{4} \tag{1928}$$

has derivative $e^{\kappa q}/4$. Its ordinary expected-integral objective therefore changes both the feedback and the variational field equations. In particular,

$$\delta \int \varphi_\kappa(q) = \frac{1}{4}\int e^{\kappa q}\, \delta q, \tag{1929}$$

with variations of the measure and state dependence of H added where present. The factor cannot be silently omitted in a low-energy recovery. For bounded $0 \le q \le Q$, the expansion $\varphi_\kappa(q) = q/4 + \kappa q^2/8 + O(\kappa^2 Q^3 e^{\kappa Q})$ specifies a controlled weak-nonlinearity regime.

By contrast, for $\kappa > 0$ the entropic risk objective

$$V_\kappa(t,z) = \frac{1}{\kappa} \log \inf_u \mathbb{E}_{t,z} \exp\left[\kappa\left(\int_t^T \ell\, ds + G(Z_T)\right)\right] \tag{1930}$$

has, when finite and smooth, the equation

$$0 = \partial_t V_\kappa + \inf_u \left\{\ell + b^u \cdot \nabla V_\kappa + \tfrac{1}{2} a : D^2 V_\kappa + \tfrac{\kappa}{2} \nabla V_\kappa^T a \nabla V_\kappa\right\}. \tag{1931}$$

The extra gradient square comes from differentiating $e^{\kappa V}$, not from putting $e^{\kappa q}$ in the running cost. These models may be studied together, but they are not equivalent. Neither entails a new radiated particle species or a Hawking-spectrum correction without a field equation, a quantized state, and a detector observable. For $\kappa < 0$, minimization of $\kappa^{-1} \log \mathbb{E} e^{\kappa C^u}$ corresponds to a *supremum* of the exponential expectations before applying the decreasing logarithmic transform. The displayed infimum definition is therefore restricted to positive κ. Its zero limit is the expected-cost problem under the required integrability assumptions.

If a residual contains $\nabla \log p_t$, it depends on the evolving law. A conventional state-space HJB can then be used only with a frozen declared law, followed by a consistency problem, or within an explicitly derived mean-field control system on probability measures. The variation through p_t is part of that system. Treating a score-dependent cost as a law-independent cost would omit a functional derivative.

X.5. *Independent projection and observable restrictions.* Let $\mathcal{O}$ be a measurable observation of a path and suppose it commutes with the specified reversal. On standard Borel path spaces, disintegration gives the exact chain rule

$$\begin{aligned}\mathcal{D}(P\|P^R) = \mathcal{D}(\mathcal{O}_* P \| \mathcal{O}_* P^R) \\ + \int \mathcal{D}\big(P(\cdot \mid y) \| P^R(\cdot \mid y)\big)\, (\mathcal{O}_* P)(dy).\end{aligned} \tag{1932}$$

Finite entropy and the corresponding conditional absolute continuity are assumed. The nonnegative conditional term is hidden irreversibility. An observed fluid current therefore supplies a lower bound on the mother path entropy, not an equality unless conditional sufficiency is proved. This result does not identify information filtering with gravitational holography: no area entropy bound or bulk–boundary algebra follows from disintegration.

PROPOSITION 177 (A conditional bound on hidden relative entropy). *Let P, Q be equivalent probability laws on a standard Borel space, let Y be a measurable observation, and assume $D(P\|Q) < \infty$. Write $\Lambda = \log(dP/dQ)$. Suppose that, for Q_Y-almost every y, the conditional essential range of Λ under $Q(\cdot \mid y)$ lies in an interval $[a(y), b(y)]$, with measurable finite endpoints. If $\mathbb{E}_P[(b(Y) - a(Y))^2] < \infty$, then*

$$0 \le D(P\|Q) - D(P_Y\|Q_Y) \le \frac{1}{8}\mathbb{E}_P[(b(Y) - a(Y))^2]. \tag{1933}$$

The statement does not require the observed process to be Markovian.

Proof. Disintegrate Q and define, conditionally on $Y = y$,

$$K_y(t) = \log \int e^{t\Lambda}\, Q(d\omega \mid y), \qquad 0 \le t \le 1.$$

The conditional bound makes this function twice differentiable. At $t = 1$, $e^{K_y(1)} = dP_Y/dQ_Y(y)$, and the tilted conditional law $e^{\Lambda - K_y(1)}Q(d\omega \mid y)$ is $P(d\omega \mid y)$. Thus its relative entropy is $K_y'(1) - K_y(1)$, since $K_y(0) = 0$. For the intermediate tilt $Q_{y,t}$, differentiation gives

$$K_y'(t) = \mathbb{E}_{Q_{y,t}}\Lambda, \qquad K_y''(t) = \mathrm{Var}_{Q_{y,t}}\,\Lambda.$$

Every probability law supported in $[a, b]$ has variance at most $(b-a)^2/4$. To verify this bound, average $(X - a)(b - X) \ge 0$, subtract the square of the mean, and maximize $(\mathbb{E}X - a)(b - \mathbb{E}X)$ over the interval. Integration by parts consequently gives

$$K_y'(1) - K_y(1) = \int_0^1 tK_y''(t)\, dt \le \frac{(b(y) - a(y))^2}{8}.$$

The relative-entropy chain rule and integration with respect to P_Y prove the assertion. Nonnegativity follows from the conditional relative entropy, rather than from a sign assumption on Λ. □

In a time-reversal application Q is the specified reversed experiment, and the observation must commute with the declared reversal. The result quantifies approximate sufficiency of an observation: little variation of the full log likelihood among hidden states with the same observation implies little hidden entropy. It does not establish that variation bound from a small error in a one-time density or a fitted drift. Gaussian path likelihoods often have unbounded conditional range, so the proposition is not asserted to apply to every diffusion.

If $\Lambda = g(Y) + r$ and $|r| \le \varepsilon$, the bound becomes $\varepsilon^2/2$. This is a finite-time statement. A rate conclusion requires a bound on $\mathbb{E}_P[(b_T - a_T)^2]/T$; dividing a bound that grows as T^2 by T does not give uniform long-time control.

For a finite check, let Q be uniform on $(y,z) \in \{-1,1\}^2$ and let $P(y,z) \propto \exp(\gamma y + \varepsilon z)Q(y,z)$. Observation of y alone gives

$$D(P\|Q) - D(P_Y\|Q_Y) = \varepsilon \tanh \varepsilon - \log\cosh \varepsilon \le \varepsilon^2/2.$$

Summing the four probabilities proves the equality directly. Its expansion is $\varepsilon^2/2 - \varepsilon^4/4 + O(\varepsilon^6)$, so the leading quadratic coefficient in the general bound cannot be improved. This finite likelihood example checks the information estimate; it is not an experimental measurement of thermodynamic entropy production.

A second bridge concerns evolution. If P_N is a field projection, L the mother generator, and L_N a proposed reduced generator, define

$$\mathfrak{d}_N\phi = L(\phi \circ P_N) - (L_N\phi) \circ P_N. \tag{1934}$$

For $v(s,y) = e^{(T-s)L_N}\phi(y)$, Dynkin's formula gives

$$\mathbb{E}\phi(P_N Z_T) - \mathbb{E}\phi(Y_T) = \int_0^T \mathbb{E}\big[\mathfrak{d}_N v(s,\cdot)(Z_s)\big]\,ds, \tag{1935}$$

for matching projected initial data and adequate domain and martingale conditions. A uniform bound δ_N on the integrand gives $T\delta_N$. Independent microscopic derivation means controlling this defect with coefficients fixed from the mother model. A fitted fluid closure is a different, useful, task.

X.6. *Dynamic programming, the maximum principle, and stochastic symmetry.* For a finite-horizon cost $\mathbb{E}[\int \ell\,dt + G]$, the HJB equation is $V_t + \inf_u\{\ell + b\cdot V_z + \frac{1}{2}a : D^2V\} = 0$. On a domain without reflecting boundaries, with a convex control set, control-independent diffusion, and the required differentiability, integrability and optimality assumptions, the first-order maximum principle uses the same ℓ, b, σ, with Hamiltonian $H_{\mathrm{SMP}} = \ell + p^T b + \mathrm{tr}(q^T\sigma)$, and

$$dp = -\partial_z H_{\mathrm{SMP}}\,dt + q\,dW, \qquad p_T = \nabla G(Z_T). \tag{1936}$$

For a sufficiently smooth value function, $p_t = \nabla V(t, Z_t)$ and $q_t = D^2V(t,Z_t)\sigma(Z_t)$. Reflection requires additional finite-variation adjoint terms and boundary conditions. The displayed backward equation is an interior identity and is not asserted as the maximum principle for a reflected process. The stochastic symmetry formulation has a prior Bellman/contact-symmetry theory [58]. These identities require a third spatial derivative in a classical Itô proof. They do not identify the adjoint with physical momentum.

For example, suppose a constant translation direction η leaves the drift, covariance, running cost, and admissible controls invariant on a domain without boundary. Differentiate the HJB equation along η; the envelope condition cancels derivatives of the optimizing control. Then

$$(\partial_t + L^{u_*})(\eta\cdot\nabla V) = 0. \tag{1937}$$

Itô's formula makes $\eta \cdot \nabla V(t, Z_t)$ a local martingale. Square integrability makes it a true martingale. Reflection adds its normal derivative times the boundary regulator; a vanishing value-function normal derivative does not by itself eliminate the derivative of this charge. Hence a symmetry charge may have an explicit boundary balance.

The deterministic limit gives the corresponding control symmetry statement. It recovers the usual mechanical Noether charge only after the control problem is shown equivalent to a regular mechanical Lagrangian problem with its physical time and boundary data. The existence of this stochastic symmetry theorem cannot uniquely select a common scalar coupling: many distinct symmetry-invariant positive costs satisfy the same regularity conditions.

X.7. *From local consistency to a physical completion.* On a low-energy covariant branch, gauge invariance gives the appropriate current identities and diffeomorphism invariance gives the matter conservation identity on the coupled field equations. With external driving, the reservoir stress or work flux must be included. A path-cost minimizer, by itself, is not a solution of the gravitational constraints. These constraints must either be imposed on the admissible state space or propagated by the proposed generator. If $C(z) = 0$ defines a smooth constraint and the noise vector fields are σ_α, Itô invariance requires

$$DC\,\sigma_\alpha = 0, \qquad DC\,b + \tfrac{1}{2}a : D^2C = 0 \quad \text{on } \{C = 0\}. \tag{1938}$$

The first relation prevents Brownian escape; the second includes the noise-induced drift of a curved constraint surface.

The completion problem consequently has a definite order. Specify a single action and its allowed residual couplings; derive or match a tangent positive generator; prove its invariant law and coercivity; control the physical projection; and determine which measurements identify the remaining inputs. A classical probability model may satisfy all these steps while retaining the Bell-local CHSH bound. Complex quantum amplitudes, noncommuting observables, physical states, and a four-dimensional interacting limit require additional construction. Likewise, convergence of a probability law on Schwarzschild or Kerr parameters does not change the curvature of a sample geometry.

For a bounded stopping rate $0 \le h \le h_*$ up to a finite geometric endpoint τ, conditional survival is $\exp[-\int_0^\tau h(Z_s)ds] \ge e^{-h_*\tau} > 0$. Thus killing a controlled path cannot supply a regular interior extension. An extension needs local field equations, a regular metric, matching data, and an extendibility or geodesic-completeness argument. This is a structural requirement, not a matter of choosing a larger penalty.

Appendix Y. Endpoint measures, fluctuation identities, and three distinct arrows

Y.1. *The reverse experiment is part of the observable.* A statement about the direction of time requires two specified experiments. Let P be the forward law on a finite interval $[0,T]$, let $\widetilde{P}$ be a declared reverse experiment, and set $Q = \mathcal{R}_{\#}\widetilde{P}$, where $(\mathcal{R}\omega)_t = \Theta\omega_{T-t}$ and Θ changes the sign of odd variables. The reversed driving protocol, initial law, and parity of external fields belong to this definition. Comparing two unspecified "directions" has no invariant thermodynamic meaning.

PROPOSITION 178 (Path likelihood and absolute irreversibility). *Suppose P and Q are equivalent probability measures and put $\Sigma = \log(dP/dQ)$. Then*

$$\mathbb{E}_P e^{-\Sigma} = 1, \qquad \mathbb{E}_P\Sigma = D(P\|Q) \geq 0, \qquad P(\Sigma \leq -s) \leq e^{-s} \quad (s \geq 0). \tag{1939}$$

The mean may be infinite; equality of the finite mean to zero holds exactly when $P = Q$. More generally let $Q = Q_{\mathrm{ac}} + Q_{\mathrm{s}}$ be the Lebesgue decomposition with respect to P, write $q = dQ_{\mathrm{ac}}/dP$, and let $\lambda = Q_{\mathrm{s}}(\Omega)$. With $\Sigma = -\log q$, including $+\infty$ on $\{q = 0\}$,

$$\mathbb{E}_P e^{-\Sigma} = 1 - \lambda. \tag{1940}$$

When $P \ll Q$, this Σ is $\log(dP/dQ)$, P-almost surely. Its negative part is integrable, so its mean is well defined with values in $(-\infty, +\infty]$. If $\lambda < 1$, $\mathbb{E}_P\Sigma \geq -\log(1-\lambda)$. For arbitrary $0 \leq \lambda \leq 1$, the sharper tail bound is $P(\Sigma \leq -s) \leq (1-\lambda)e^{-s}$, $s \geq 0$.

Proof. For equivalent laws, integrating dQ/dP gives the fluctuation identity, while the definition of relative entropy gives $\mathbb{E}_P\Sigma = D(P\|Q)$, including the infinite case. Gibbs' inequality gives nonnegativity and the stated equality condition.

In the general case, $\int q\, dP = Q_{\mathrm{ac}}(\Omega) = 1 - \lambda$. Write $\Sigma^- := \max\{-\Sigma, 0\}$. Since $\Sigma^- = \max\{\log q, 0\} \leq q$, its integral is finite. Thus $\mathbb{E}_P\Sigma = \mathbb{E}_P\Sigma^+ - \mathbb{E}_P\Sigma^-$ is well defined and can equal $+\infty$; no subtraction of two infinite integrals occurs. If $P(q = 0) > 0$, the mean is $+\infty$. For $a = 1 - \lambda > 0$, the claimed lower bound is immediate when the positive part has infinite integral. In the remaining case $q > 0$ almost surely and $-\log q$ is integrable. The pointwise inequality $\log(q/a) \leq q/a - 1$, after integration, yields $\mathbb{E}_P[-\log q] \geq -\log a$. Finally, $e^{-\Sigma} = q$, with $e^{-\infty} = 0$, so Markov's inequality gives $P(\Sigma \leq -s) \leq e^{-s}\mathbb{E}_P q = (1-\lambda)e^{-s}$. This also covers $\lambda = 1$, for which $q = 0$ almost surely. Setting $\lambda = 0$ recovers the equivalent-law bound. □

Nonnegative mean production permits negative production on individual finite histories. Identifying $k_B\Sigma$ with physical total entropy requires local

detailed balance and a specified reservoir; the measure identity alone does not supply a thermometer, a heat variable, or a microscopic bath.

Y.2. *A reference-density correction in the heat formula.* To display every endpoint term, use even variables on a torus, a constant positive diffusion matrix D, a smooth time-independent drift b, and the equation $dX = b(X)dt + \sqrt{2D}\,dW$. Let p_0, p_T denote positive densities relative to coordinate volume. The reverse experiment uses the same drift and starts from p_T. Under the finite-window absolute-continuity assumptions, the path ratio is

$$\Sigma = \log \frac{p_0(X_0)}{p_T(X_T)} + \int_0^T (D^{-1}b)(X_t) \circ dX_t. \tag{1941}$$

One way to verify the sign is to compare midpoint transition weights. The difference of the two quadratic actions for increments dX and $-dX$ is $b^T D^{-1} \circ dX$; their divergence terms cancel. Multiplication by the initial densities gives the two endpoint terms. Equivalently, the diffusion time-reversal theorem and Girsanov's formula give the same expression. In a thermal realization $b = DF/\theta$, $\theta = k_B T_{\mathrm{bath}}$, the integral is Q_{bath}/θ, with $Q_{\mathrm{bath}} = \int F \circ dX$.

Now introduce a Gibbs reference $\pi = Z^{-1}e^{-U/\theta}$ and write $p_t = f_t\pi$. Merely changing the reference density gives

$$\log \frac{p_0(X_0)}{p_T(X_T)} = \log \frac{f_0(X_0)}{f_T(X_T)} + \frac{U(X_T) - U(X_0)}{\theta},$$
$$\Sigma = \log \frac{f_0(X_0)}{f_T(X_T)} + \frac{\Delta U + Q_{\mathrm{bath}}}{\theta}. \tag{1942}$$

Consequently a Gibbs-relative endpoint logarithm cannot simply be added to the full bath heat. For a conservative undriven force $F = -\nabla U$, $Q_{\mathrm{bath}} = -\Delta U$ and those energy terms cancel. With work $W = \Delta U + Q_{\mathrm{bath}}$, the last term is W/θ. Time-dependent reference potentials also require their partition-function change and the prescribed protocol reversal; they are not covered by the fixed-reference simplification above.

Y.3. *Relaxation, stationary circulation, and information loss.*

Proposition 179 (Endpoint-matched relaxation identity). *Let a Markov diffusion have invariant probability π and be reversible under the declared measurable parity involution Θ, with $\Theta_{\#}\pi = \pi$. Write $R = P_\pi$ for its stationary path law, so $\mathcal{R}_{\#}R = R$. Let $p_T = (X_T)_{\#}P_{p_0}$ and set $Q = \mathcal{R}_{\#}P_{\Theta_{\#}p_T}$. Assume $p_0 = f_0\pi$ and $p_T = f_T\pi$, where f_0, f_T are measurable, finite and positive π-almost everywhere, and $\int |\log f_i|\, dp_i < \infty$ for $i = 0, T$. Then the path laws are*

equivalent, all three relative entropies below are finite, and

$$\log \frac{dP_{p_0}}{dQ} = \log f_0(X_0) - \log f_T(X_T), \qquad D(P_{p_0}\|Q) = D(p_0\|\pi) - D(p_T\|\pi). \tag{1943}$$

Proof. Let K_x denote the conditional path law started at x. It is concentrated on $\{X_0 = x\}$, and $P_p = \int K_x\, p(dx)$. For every nonnegative measurable path function g,

$$\int g\, dP_{p_0} = \int f_0(x) \Big(\int g\, dK_x \Big)\, \pi(dx) = \int g\, f_0(X_0)\, dR.$$

Thus the initial-density change is derived from the path kernel. Parity invariance gives $d(\Theta_{\#} p_T)/d\pi = f_T \circ \Theta$. Reversing this path law and using $\Theta X_0 = X_T \circ \mathcal{R}$ and $\mathcal{R}_{\#} R = R$ gives $dQ/dR = f_T(X_T)$. Both densities are positive R-almost everywhere because the two stationary endpoint marginals are π. Their Radon–Nikodym ratio therefore gives the first identity. The prescribed endpoint logarithmic moments make both terms integrable under P_{p_0}, since its endpoint laws are exactly p_0, p_T. Integrating their difference proves the second identity with finite terms; no subtraction of two infinite entropies is used. □

Thus stationary equilibrium has zero path production while relaxation from a nonequilibrium law can have positive endpoint-matched path production. There is no contradiction between reversible equilibrium dynamics and a strictly decreasing nonequilibrium free energy.

For a complementary maintained process, retain even variables and set

$$b = D\nabla \log \pi + c, \qquad \nabla \cdot (\pi c) = 0, \qquad f = p/\pi, \qquad J = pc - Dp\nabla \log f. \tag{1944}$$

Integration by parts, with periodic conditions or vanishing boundary terms, gives

$$\begin{aligned} -\frac{d}{dt} D(p\|\pi) &= \int p\, \nabla \log f^T D \nabla \log f =: \mathcal{I}_D(p), \\ \int \frac{J^T D^{-1} J}{p} &= \mathcal{I}_D(p) + \int p\, c^T D^{-1} c. \end{aligned} \tag{1945}$$

Indeed the transport contribution is $\int \pi c \cdot \nabla f = 0$; the same expression removes the cross term in the second line. The first formula expresses free-energy decay since $F(p) - F(\pi) = \theta D(p\|\pi)$. Under the thermal interpretation of (1941), the second formula is the expected rate of total entropy production in units of k_B: the mean medium rate is $\int J \cdot D^{-1} b$, and the Shannon entropy rate is $-\int J \cdot \nabla \log p$.

At $p = \pi$, the state KL is constant and the stationary path rate is $\int \pi c^T D^{-1} c$. Directly, the reversed stationary drift is $b^R = -b + 2D\nabla \log \pi$; Girsanov's quadratic cost is $\frac{1}{2}(2c)^T (2D)^{-1} (2c) = c^T D^{-1} c$. This calculation

requires the stated all-even fixed-drive reversal. An odd Hamiltonian transport current must not be counted as dissipative by this formula without its parity decomposition and noise-range test.

Finally, suppose a Markov evolution K_t preserves π and strictly decreases $D(p\|\pi)$ for a particular nonequilibrium p. There is no positive Markov kernel R_t preserving π with $R_tK_tp = p$: data processing would give

$$D(p\|\pi) = D(R_tK_tp\|R_t\pi) \le D(K_tp\|\pi) < D(p\|\pi). \tag{1946}$$

This is an information-recovery obstruction, not a prohibition on defining a reverse diffusion. Exponential decay, if needed, requires a functional inequality such as $\mathcal{I}_D(p) \ge \lambda D(p\|\pi)$. Invariance alone does not give that inequality or cosmic convergence.

Y.4. *What can be inferred across physical sectors.* The common origin supplies a testable statement only after the energy, mobility, noise, physical time, and observation map have been fixed. For an observation $Y = P(X)$ on standard Borel path spaces, disintegration gives the following decomposition when $P_X \ll Q_X$ and $D(P_X\|Q_X) < \infty$:

$$D(P_X\|Q_X) = D(P_Y\|Q_Y) + \int D(P_X(\cdot \mid y)\|Q_X(\cdot \mid y))P_Y(dy). \tag{1947}$$

An observed arrow is therefore bounded by the full arrow. Under these finite-entropy hypotheses, the deficit is the integral of nonnegative conditional relative entropies. It vanishes if and only if $P_X(\cdot \mid y) = Q_X(\cdot \mid y)$ for P_Y-almost every y, because relative entropy is zero exactly for identical probability laws. Data processing remains valid with extended values, but an equality $+\infty = +\infty$ does not imply equality of hidden conditional laws. Small simulation error does not establish this equality criterion. Convergence of a regulated probability law likewise does not establish bounded spacetime curvature, preservation of a physical constraint, or regularity after removal of the regulator. Those statements need their own dynamical estimates. The distinction makes the proposed common origin falsifiable without assigning the same evidential meaning to every sector.

Appendix Z. Scale consistency of the common variational architecture

Projection is an exact starting point for comparing regulators, but a closed flow of a few coefficients is an additional result. The Mori–Zwanzig construction [121] and [169] generally produces memory and colored forcing. Its instantaneous projected term need not be reversible. For an autonomous finite block system with retained variable x,

$$\dot{x} = Ax + By, \qquad \dot{y} = Cx + Dy, \qquad K(t) = Be^{tD}C, \tag{1948}$$

eliminating y gives $\dot{x} = Ax + K * x + Be^{tD}y_0$. The exact retained resolvent is

$$\left[zI - A - B(zI - D)^{-1}C\right]^{-1}. \tag{1949}$$

Successive elimination of coupled blocks preserves this resolvent when all intermediate inverses exist. A local-in-time approximation need not preserve it. This is a concrete consistency criterion connecting microscopic projection, effective response, and the cost used to select a closure.

For differentiable blocks on fixed spaces and logarithmic wave-number scale $s = \log(\Lambda/\Lambda_0)$, direct differentiation gives

$$\begin{aligned}\partial_s K_s(t) =&(\partial_s B_s)e^{tD_s}C_s + B_s e^{tD_s}(\partial_s C_s)\\ &+ B_s \int_0^t e^{(t-r)D_s}(\partial_s D_s)e^{rD_s}dr\, C_s.\end{aligned} \tag{1950}$$

The derivative of the matrix exponential follows by variation of constants. This formula contains information about the unresolved blocks; it is not a universal beta function of the kernel alone. Sharp finite projections have rank jumps, whereas smooth filters need not be idempotent. A continuous renormalization calculation must specify which of these constructions it uses. Wave-number refinement, box-size growth, and a small-noise limit are different limiting operations.

There is an explicit constructive case. A thermal bath with skew exchange and positive relaxation rates generates a friction kernel

$$\Gamma_n(t) = \sum_j g_j^2 e^{-\lambda_j t}, \qquad \mathbb{E}F_n(t)F_n(r) = \theta\Gamma_n(|t-r|), \quad \lambda_j > 0. \tag{1951}$$

The reduced force is $-\Gamma_n * x$; the fluctuation–dissipation sign refers to this positive friction convention and a stationary thermal preparation. Positive spectral quadratures can converge to $\Gamma(t) = t^{-\beta}$, $0 < \beta < 1$. For a lower rate cutoff δ and upper cutoff Λ,

$$\|\Gamma - \Gamma_{\delta,\Lambda}\|_{L^1(0,T)} \le \frac{T\delta^\beta}{\beta\Gamma_{\mathrm{E}}(\beta)} + \frac{\Lambda^{\beta-1}}{(1-\beta)\Gamma_{\mathrm{E}}(\beta)}. \tag{1952}$$

The fluid branch supplies the quadrature and Volterra-response error bounds. This is a continuous spectral memory limit in a specified linear thermal class. The spectral exponent is an input there; it is not a derived Kolmogorov or intermittency exponent.

Scale reduction also has exact entropy and symmetry constraints. For path laws P, Q, let $\Sigma = \log(dP/dQ)$ and observe a path variable Y. Conditional expectation gives

$$\Sigma_Y = -\log \mathbb{E}_P[e^{-\Sigma} \mid Y], \qquad D(P_Y\|Q_Y) \le D(P\|Q). \tag{1953}$$

Thus the observed fluctuation identity survives when its comparison law is projected consistently, while hidden entropy can be lost. A true stochastic

Noether martingale remains a martingale after optional projection onto the observed filtration; its projected expression may depend on history. A state-only closure must control the memory it omits.

Functional renormalization provides another, distinct route [164] and [23]. Its effective action is defined by a generating functional and a modified Legendre transform, not by the trace of a projected generator. In a dynamic formulation, memory belongs to the retarded response vertex and is coupled to noise and higher vertices. Likewise, projecting a nonlinear control cost need not preserve its algebraic form or commute with optimization. Uniform cost convergence on the same admissible class bounds the change of the optimum; restricting the observation filtration can increase it.

These statements strengthen the common architecture by imposing compatibility tests across scales. They do not identify a nonlinear fluid flux or prove that all regulators converge to the same physical theory. That further claim requires the nonlinear interaction, admissible controls, reference measure, time calibration, and observables to satisfy uniform estimates together.

Appendix AA. Quantum states, physical projections, and measurement selection

AA.1. *The data fixed by a mother realization.* A quantum prediction requires a state, a collection of measurable operators, and a rule connecting these operators to apparatus records. These objects have different dependencies. A stationary classical probability is not itself an assignment of probabilities to all noncommuting measurements. We make the dependencies explicit in a finite branch, where operator domains and normalization can be checked without a continuum limit.

Fix a connected finite configuration set with $d \geq 2$ states, its configuration basis, and an irreducible backward generator Q. Its entries are $\mathsf{Q}_{ij} = q_{ij} \geq 0$ for $i \neq j$ and $\mathsf{Q}_{ii} = -r_i$, where $r_i = \sum_{j \neq i} q_{ij}$. The stationary column vector π satisfies $\mathsf{Q}^T \pi = 0$, $\pi_i > 0$, and $\sum_i \pi_i = 1$. The generator, rather than its invariant density alone, is the input to the transfer reconstruction. A physical realization must additionally identify which configurations, perturbations, and time intervals its coordinates describe.

AA.2. *Transfer reconstruction and conditional state selection.* Suppose $\pi_i q_{ij} = \pi_j q_{ji}$ and write $D_g = \operatorname{diag}(\sqrt{\pi_i})$. The standard positive transfer construction [93] gives

$$\mathsf{H} = -D_g \mathsf{Q} D_g^{-1}, \qquad \mathsf{H} g = 0, \qquad e^{-\tau \mathsf{H}} = D_g e^{\tau \mathsf{Q}} D_g^{-1}. \tag{1954}$$

Object	Fixed mathematical consequence	Additional physical premise
Stationary law π	Unique for the specified irreducible Q	Action, mobility, reference measure, and regulator are fixed
Positive transfer state	$g_i = \sqrt{\pi_i}$ and $\mathsf{H} = -D_g \mathsf{Q} D_g^{-1}$	Detailed balance and the stated representation
Physical ground preparation	Unique ground density of the identified Hamiltonian	Physical clock, energy conversion, and ground preparation
Gauge-invariant projection	Haar projection onto a specified invariant subspace	Gauge action, representation, and inner product
Outcome probabilities	Unique trace representation of an affine effect probability	Full quantum effect space and operational affinity
Postmeasurement state	Fixed by a complete instrument; rank-one sharp repeatability gives uniqueness	Apparatus coupling or explicit instrument assumptions

Table 34. Dependencies within a fixed realization. Uniqueness after specifying a representation or apparatus does not select that representation or apparatus from classical equilibrium data.

Detailed balance makes H self-adjoint. For $f \in \mathbb{C}^d$,

$$-\langle f, \mathsf{Q} f \rangle_\pi = \frac{1}{2} \sum_{i,j} \pi_i q_{ij} |f_j - f_i|^2 \geq 0. \tag{1955}$$

Connectedness makes its null space the constants, so H has a simple zero eigenvalue and unique positive normalized ground vector g. This fixes both the amplitude and auxiliary Hamiltonian for the declared representation; no phase is left free within that positive transform.

If $t_{\mathrm{E}} = \xi\tau$ with specified $\xi > 0$, the Hamiltonian in energy units is $H_{\mathrm{ph}} = (\hbar/\xi)\mathsf{H}$. Neither ξ nor $\hbar$ is determined by normalization of π. Changing all rates by $c > 0$ preserves π and multiplies every transfer energy by c. A physical clock or a mother prediction of those rates is therefore required to obtain absolute frequencies.

PROPOSITION 180 (State selection after physical identification). *If H_{ph} is the physical Hamiltonian and preparation minimizes $\mathrm{Tr}(\rho H_{\mathrm{ph}})$ over density matrices, then the unique minimizing state is $\rho_0 = |g\rangle\langle g|$. For a separately fixed*

physical temperature $T_{\mathrm{Q}} > 0$, the unique minimizer of

$$F_{\mathrm{Q}}(\rho) = \operatorname{Tr}(\rho H_{\mathrm{ph}}) + k_{\mathrm{B}} T_{\mathrm{Q}} \operatorname{Tr}(\rho \log \rho) \tag{1956}$$

is $\rho_{T_{\mathrm{Q}}} = Z_{\mathrm{Q}}^{-1} e^{-H_{\mathrm{ph}}/(k_{\mathrm{B}} T_{\mathrm{Q}})}$.

Proof. The least energy is zero. If a density matrix attains it, then

$$0 = \operatorname{Tr}(\rho H_{\mathrm{ph}}) = \| H_{\mathrm{ph}}^{1/2} \rho^{1/2} \|_{\mathrm{HS}}^2.$$

Its support lies in the one-dimensional ground eigenspace, proving the first assertion. At positive temperature,

$$F_{\mathrm{Q}}(\rho) - F_{\mathrm{Q}}(\rho_{T_{\mathrm{Q}}}) = k_{\mathrm{B}} T_{\mathrm{Q}} D(\rho \| \rho_{T_{\mathrm{Q}}}) \geq 0.$$

For completeness, finite-dimensional nonnegativity follows from Klein's inequality. One direct proof uses a spectral basis of ρ: concavity of the logarithm gives $\langle v_i, \log \sigma \, v_i \rangle \leq \log \langle v_i, \sigma v_i \rangle$ for positive σ. The resulting classical relative entropy is nonnegative. Equality, for full-rank $\sigma = \rho_{T_{\mathrm{Q}}}$, requires $\rho = \sigma$. This proves uniqueness, including density matrices with a kernel by continuous approximation. □

The proposition derives the state from a specified physical Hamiltonian and preparation principle. The preparation principle and physical-time identification remain premises. The classical noise temperature θ in $\pi \propto e^{-S/\theta}$ is not thereby identified with $k_{\mathrm{B}} T_{\mathrm{Q}}$. A classical Gibbs density generally gives neither the quantum thermal density nor its energy populations.

AA.3. *A physical projection fixed by declared gauge constraints.* Let a compact group G have normalized Haar measure and a unitary representation U on the chosen Hilbert space. Its invariant-space projection is

$$P_G = \int_G U(a) \, \mathrm{d}a. \tag{1957}$$

The integral is understood strongly for a strongly continuous representation. Haar invariance gives $U(b) P_G = P_G$, $P_G^* = P_G$, and $P_G^2 = \int_G \int_G U(ab) \, \mathrm{d}a \, \mathrm{d}b = P_G$. Conversely, an invariant vector v satisfies $P_G v = v$. Thus P_G is exactly, and uniquely, the orthogonal projector onto the declared invariant subspace. If a self-adjoint Hamiltonian commutes with this group action at the resolvent level, its dynamics preserves the range of P_G.

This construction applies directly to the regulated gauge–neutral-scalar branch with configuration space $K^{\mathcal{E}} \times \mathbb{R}^{\mathcal{V}}$. The local group $G = K^{\mathcal{V}}$ acts on a link by $U_{ij} \mapsto a_i U_{ij} a_j^{-1}$ and leaves neutral scalars fixed. Plaquette traces, the scalar energy, product Haar measure, and the declared bi-invariant link metric are invariant. Pullback by this action is unitary on both $L^2(\pi \, \mathrm{d}\nu)$ and $L^2(\mathrm{d}\nu)$. The weighted Dirichlet form satisfies $\mathcal{E}(U(a) f, U(a) h) = \mathcal{E}(f, h)$, and its closed domain is invariant. Uniqueness of the weak resolvent solution then

implies that the resolvent commutes with $U(a)$; the amplitude Hamiltonian and its semigroup consequently commute with P_G. Since $g = \sqrt{\pi}$ is invariant, $P_G g = g$.

This proves an actual constrained auxiliary projection for that bosonic regulator. It excludes integrated coframes, charged fermions, and unresolved gravitational constraints. Choosing G, its action, and the physical inner product is prior information. Symmetry alone does not decide which transformations are gauge redundancies and which label physically distinct states. Nor does it fix a tensor decomposition into separated detector regions. Covariance of an open quantum channel under G is also weaker than preservation of the support of P_G; the latter requires a separate invariant-subspace condition.

AA.4. *Exact quantum lifts with the same classical records.* The configuration process can be retained exactly in an open quantum extension without choosing its coherence dynamics. This is a different construction from (1954): the transfer formula reproduces auxiliary Euclidean correlations, whereas the following channel reproduces population evolution in its declared real time.

Set $P_i = |i\rangle\langle i|$, $K_{ji} = \sqrt{q_{ij}}|j\rangle\langle i|$ for $i \neq j$, and let $H_\epsilon = \sum_i \epsilon_i P_i$ with real ϵ_i. For an independently chosen $\lambda_{\mathrm{d}} \geq 0$, define

$$\mathcal{G}_{\lambda_{\mathrm{d}},\epsilon}(\rho) = -\frac{\mathrm{i}}{\hbar}[H_\epsilon, \rho] + \sum_{i\neq j}\left(K_{ji}\rho K_{ji}^* - \frac{1}{2}\{K_{ji}^* K_{ji}, \rho\}\right) + \lambda_{\mathrm{d}} \sum_i \left(P_i \rho P_i - \frac{1}{2}\{P_i, \rho\}\right). \tag{1958}$$

This is a Lindblad generator [112]; the finite-dimensional semigroup is completely positive and trace preserving. In particular, a short-time map with Kraus operators $I - t(\mathrm{i}H_\epsilon/\hbar + \frac{1}{2}\sum A_k^* A_k)$ and $\sqrt{t}A_k$ agrees to first order with this generator. Taking the first Kraus operator as $e^{-\mathrm{i}tH_\epsilon/\hbar}(I - t\sum A_k^* A_k)^{1/2}$ gives a trace-preserving completely positive step for sufficiently small t. Products of these steps converge to $e^{t\mathcal{G}}$, establishing the claimed channel property.

Proposition 181 (Population closure without coherence uniqueness). *Every generator in* (1958) *gives*

$$\dot{\rho}_{ii} = \sum_{j\neq i} q_{ji}\rho_{jj} - r_i \rho_{ii}, \tag{1959}$$

$$\dot{\rho}_{ij} = -\left[\frac{r_i + r_j}{2} + \lambda_{\mathrm{d}} + \frac{\mathrm{i}(\epsilon_i - \epsilon_j)}{\hbar}\right]\rho_{ij}, \qquad i \neq j. \tag{1960}$$

Its unique stationary density is $\rho_{\mathrm{st}} = \operatorname{diag}\pi$*, and every initial density converges to it in finite dimension. Nevertheless, its coherence lifetimes and phases vary with* λ_{d} *and the relative* ϵ_i*. All sequential projective configuration records*

have the same Markov transition probabilities $e^{t\mathsf{Q}}$, independently of these extra coefficients.

Proof. The gain term $K_{ji}\rho K_{ji}^*$ is $q_{ij}\rho_{ii}P_j$, while $\sum_{j\neq i} K_{ji}^*K_{ji} = r_iP_i$. The diagonal and off-diagonal entries give the two displayed equations. The diagonal Hamiltonian changes no population. The last dissipator is $\lambda_{\mathrm{d}}(\sum_i P_i\rho P_i - \rho)$, so it changes no population and damps each off-diagonal entry at rate λ_{d}. Irreducibility of the finite chain makes π unique and gives population convergence. Since $d \geq 2$ and the chain is irreducible, each $r_i > 0$; every coherence decays by (1960). This proves uniqueness and convergence of the full density. A sharp configuration outcome i prepares P_i. Its next configuration probabilities are the ith row of $e^{t\mathsf{Q}}$. Iterating proves equality of all such joint records. □

Thus even the entire fixed configuration dynamics does not select a unique extension to noncommuting observables. A choice of the displayed lift is an extra representation of that dynamics. Additional microscopic information may specify a different open-system completion. This result does not assume that the coherent transfer model and the dissipative lift have identical real-time quantum laws; they do not.

AA.5. *Probability representation under an operational axiom.* Let $\mathfrak{E}_d = \{E \in M_d(\mathbb{C}) : 0 \leq E \leq I\}$ be the full quantum effect space. An effect represents a possible measurement event. Assume its probability $p(E)$ is noncontextual on this space, takes values in $[0,1]$, satisfies $p(0) = 0$, $p(I) = 1$, and is affine:

$$p(tE + (1-t)F) = tp(E) + (1-t)p(F), \qquad 0 \leq t \leq 1. \tag{1961}$$

Operationally, this says that randomizing between two implementations with fixed probabilities gives the same randomized event probability. It presupposes which implementations represent the same quantum effect.

Proposition 182 (Conditional Born representation). *Under these assumptions, in every finite dimension there is a unique density matrix ρ such that*

$$p(E) = \mathrm{Tr}(\rho E), \qquad E \in \mathfrak{E}_d. \tag{1962}$$

Knowing this functional only on diagonal effects determines the diagonal entries ρ_{ii} but does not, in general, determine ρ.

Proof. Affinity with $F = 0$ gives $p(tE) = tp(E)$. If $E + F \leq I$, affinity and this homogeneity give $p(E+F) = p(E) + p(F)$ by evaluating $p((E+F)/2)$ in two ways. For a positive matrix A, set $\ell(A) = ap(A/a)$ for any $a \geq \|A\|$, $a > 0$. Homogeneity proves independence of a. Scaling $A + B$ into the effect interval proves additivity on positive matrices. Extending by $\ell(A-B) = \ell(A) - \ell(B)$ is well defined: if $A-B = C-D$, positive-cone additivity applied to $A+D = C+B$

gives the same result. The extension is real linear on Hermitian matrices. The finite trace pairing therefore represents it uniquely as $\ell(A) = \operatorname{Tr}(\rho A)$ with Hermitian ρ. Since $\ell(|v\rangle\langle v|) \geq 0$ for every v, $\rho \geq 0$, and $\ell(I) = 1$ gives $\operatorname{Tr}\rho = 1$. For the final assertion, the two density matrices

$$\rho_+ = \frac{1}{2}\begin{pmatrix} 1 & 1 \\ 1 & 1 \end{pmatrix}, \qquad \rho_- = \frac{1}{2}\begin{pmatrix} 1 & -1 \\ -1 & 1 \end{pmatrix}$$

are distinct positive rank-one matrices of trace one and give the same probability for every diagonal effect. Thus diagonal observations need not determine the state. The qualification is necessary: probabilities $(1, 0, \ldots, 0)$ determine the corresponding basis state, since positivity implies $|\rho_{ij}|^2 \leq \rho_{ii}\rho_{jj}$ and forces all other entries to vanish. □

This is the finite effect-space form of an established generalized Gleason argument [22]. It does not derive the quantum effect space or operational affinity from a classical path cost. If the state has already been selected by Proposition 180, its positive functional is $p(E) = \langle g, Eg\rangle$ under the trace-state identification. That identification is a quantum operational premise. It must not be replaced by the assertion that classical Gibbs positivity alone has derived the Born rule.

AA.6. *When probabilities do and do not determine an instrument.* For outcome a, a quantum instrument is a completely positive map $\mathcal{I}_a$. Its effect is $E_a = \mathcal{I}_a^*(I)$; completeness requires $\sum_a E_a = I$. The event probability and conditioned state are

$$p_a = \operatorname{Tr}(\rho E_a), \qquad \rho_a = \mathcal{I}_a(\rho)/p_a \quad (p_a > 0). \tag{1963}$$

The effects determine the probabilities, but generally not ρ_a.

For $E_+ = (I + \eta Z)/2$, $E_- = (I - \eta Z)/2$, $0 < \eta < 1$, both $\mathcal{I}_\pm(\rho) = \sqrt{E_\pm}\rho\sqrt{E_\pm}$ and $\widetilde{\mathcal{I}}_\pm(\rho) = X\sqrt{E_\pm}\rho\sqrt{E_\pm}X$ have the same effects. On input $|+\rangle\langle+|$, both give $p_+ = 1/2$. Their conditioned + states have Z expectations η and $-\eta$, respectively. A fixed Born probability consequently leaves a measurable instrument ambiguity.

Proposition 183 (Rank-one sharp repeatability). *Let P_a be mutually orthogonal rank-one projectors summing to I. If a completely positive instrument has effects P_a and, for every input, its outcome-a output is supported in the range of P_a, then its unique form is*

$$\mathcal{I}_a(\rho) = P_a\rho P_a. \tag{1964}$$

For degenerate projectors, repeatability alone does not give uniqueness.

Proof. Write $\mathcal{I}_a(\rho) = \sum_\mu L_{a\mu}\rho L_{a\mu}^*$. The effect condition gives $\sum_\mu L_{a\mu}^* L_{a\mu} = P_a$. If $v \perp \operatorname{ran} P_a$, the sum of $\|L_{a\mu}v\|^2$ is zero, so each

$L_{a\mu} = L_{a\mu}P_a$. For a vector in the range of P_a, positivity of the output and its support condition imply that every $L_{a\mu}$ maps it into that same range. Hence $L_{a\mu} = P_a L_{a\mu} P_a = c_\mu P_a$. The effect condition becomes $\sum_\mu |c_\mu|^2 = 1$, proving (1964). For a higher-rank projector, any unitary V_a acting inside its range gives another repeatable map $V_a P_a \rho P_a V_a^*$ with the same effect. These maps need not preserve coherence within that range. □

For example, take $P_0 = |0\rangle\langle 0| \otimes I$ and $P_1 = |1\rangle\langle 1| \otimes I$. The two instruments $P_a \rho P_a$ and $(I \otimes Z)P_a \rho P_a (I \otimes Z)$ are both repeatable. Input $|0+\rangle$ gives outcome 0 with certainty, but the second-spin X expectation after the measurement is $+1$ or -1. Selecting the ordinary projection update for such a degenerate measurement requires a stronger assumption about its disturbance or an actual apparatus model.

AA.7. *A finite interacting example with explicit dependencies.* Use the fixed two-spin heat-bath branch

$$\begin{aligned} \pi_{s,t} &= \frac{e^{\beta st}}{4\cosh\beta}, & s,t \in \{-1,1\}, \\ q_{(s,t),(-s,t)} &= q_{(s,t),(s,-t)} = \frac{\gamma}{2}(1 - st\tanh\beta). \end{aligned} \tag{1965}$$

Here $\beta \in \mathbb{R}$ and $\gamma > 0$ are fixed mother-branch inputs. The positive transfer gives

$$\mathsf{H} = \gamma\left[I - \tanh\beta\, Z_1 Z_2 - \frac{\operatorname{sech}\beta}{2}(X_1 + X_2)\right], \tag{1966}$$

$$|g_\beta\rangle = \frac{1}{\sqrt{4\cosh\beta}} \sum_{s,t} e^{\beta st/2} |s,t\rangle, \tag{1967}$$

$$\operatorname{spec}\mathsf{H} = \{0, \gamma(1-\tanh\beta), \gamma(1+\tanh\beta), 2\gamma\}. \tag{1968}$$

After specifying the displayed tensor structure, ground preparation, and local Pauli instruments, the concurrence and optimized CHSH value are $|\tanh\beta|$ and $2\sqrt{1+\tanh^2\beta}$. The diagonal preparation $\operatorname{diag}\pi$ has identical configuration probabilities and is separable. It is also the unique stationary state of every lift in (1958). Its optimized CHSH value for traceless local Pauli directions is $2|\tanh\beta|$. Allowing constant dichotomic observables can attain the classical value 2, without a violation.

At $\beta = 0.8$, $\gamma = 1.3$, the coherent ground branch has concurrence 0.66403677 and CHSH value 2.40078723. These are conditional matrix predictions, not experimental observations. For the dissipative lifts with $H_\epsilon = 0$, at the declared time $t = 1$ the coherence between $|++\rangle$ and $|--\rangle$, starting from the uniform positive pure state, is

$$\rho_{++,--}(1) = \frac{1}{4} e^{-\gamma(1-\tanh\beta)-\lambda_{\mathrm{d}}}. \tag{1969}$$

Changing λ_{d} from 0 to 0.7 changes this coherence while preserving every configuration record. Direct superoperator exponentiation checks the population law, the coherence formula, stationary-state uniqueness, channel positivity, and trace preservation.

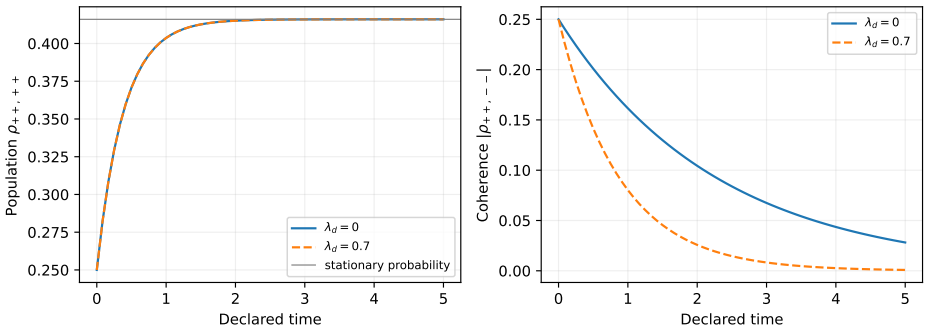


Figure 69. Two conditional Lindblad lifts of one fixed interacting configuration generator. Population predictions coincide while the unobserved additional dephasing changes the coherence. Both channels converge to the same diagonal stationary density. The curves are exact finite-matrix calculations and do not represent measured quantum data.

AA.8. *Apparatus completion and the remaining physical decision.* A supplied quantum apparatus converts a Hamiltonian interaction into an instrument. Let the apparatus start in $|0\rangle_A$, let $W = e^{-\mathrm{i}tH_{SA}/\hbar}$ be the specified joint unitary, and let $\{|a,\mu\rangle_A\}$ describe a pointer decomposition. Then

$$L_{a\mu} = {}_A\langle a,\mu|W|0\rangle_A, \qquad \mathcal{I}_a(\rho) = \sum_{\mu} L_{a\mu}\rho L_{a\mu}^*, \qquad \sum_{a,\mu} L_{a\mu}^* L_{a\mu} = I. \quad (1970)$$

The last identity follows from unitarity and completeness of the pointer basis. The formula predicts the instrument if the joint quantum Hamiltonian, ready state, interaction duration, and readout have been determined. It presupposes a quantum tensor product and the joint probability interpretation; it is not an independent derivation of these objects from classical randomness.

For the present mother construction, the most precise finite closure is therefore conditional. The fixed reversible branch determines its auxiliary transfer Hamiltonian and positive ground vector. Declared gauge constraints determine an invariant-space projector. A physical time identification and ground or thermal preparation select a quantum state. The effect-space probability axiom determines its trace representation, while rank-one sharp repeatability or a specified apparatus determines an instrument. Physical locality, detector access,

charged and gravitational constraints, and regulator-independent reconstruction require their own matching arguments.

None of these conditional uniqueness statements selects the entire quantum operational structure from an arbitrary classical generator. The explicit family (1958) shows why such a universal selection claim would need additional premises. Conversely, once those premises are physically fixed, the displayed formulas yield definite states, response frequencies, measurement probabilities, and updates that can be compared with independent observations.

Appendix AB. Frozen quantum predictions and a spectral thought experiment

AB.1. *A fixed two-spin branch and its physical premises.* A useful quantum test must distinguish a calibrated consequence from an assumption about the quantum realization. We first construct a finite example in which two calibration quantities determine two unmeasured responses. We then analyse two public Bell-test runs with a separate, explicitly specified quantum benchmark. The public runs do not measure the spectral quantities in the finite example. These are therefore two different tests, with different conclusions.

Let the configurations be $(s,t) \in \{-1,1\}^2$, with equilibrium law

$$\pi_{st} = \frac{e^{\beta st}}{4\cosh\beta}, \qquad m = \sum_{s,t} st\pi_{st} = \tanh\beta, \qquad 0 < m < 1. \tag{1971}$$

Here β is a dimensionless equilibrium parameter. It is not identified with an independently measured inverse quantum temperature. Specify single-spin transition rates

$$q_{(s,t),(-s,t)} = q_{(s,t),(s,-t)} = \frac{\Gamma}{2}(1 - mst), \qquad \Gamma > 0. \tag{1972}$$

The diagonal entries of the backward generator Q_0 are $-\Gamma(1-mst)$. Its rows sum to zero, its off-diagonal entries are positive, and its transition graph is connected. Since $e^{2\beta st} = (1+mst)/(1-mst)$, each edge satisfies $\pi_i q_{ij} = \pi_j q_{ji}$. Thus π is its unique invariant law. Equation (1972), rather than equilibrium alone, fixes the kinetic branch.

Write $g_{st} = \sqrt{\pi_{st}}$ and $D_g = \mathrm{diag}(g_{st})$. The positive transfer construction [93] gives $\mathsf{H}_0 = -D_g \mathsf{Q}_0 D_g^{-1}$. We explicitly assume that the physical Hilbert space is $\mathbb{C}^2 \otimes \mathbb{C}^2$, that these are its configuration coordinates, that physical energy is $H_0 = \hbar \mathsf{H}_0$, and that the system is prepared in its ground state $\rho_0 = |g\rangle\langle g|$. This choice includes the physical clock conversion in Γ. Pauli measurements and the trace probability rule are also specified. None of these physical identifications follows from the normalization of π alone.

Let X_i, Y_i, Z_i denote Pauli operators on factor i. In the ordered configuration basis $(++, +-, -+, --)$,

$$H_0 = \hbar\Gamma \left[I - mZ_1Z_2 - \frac{\sqrt{1-m^2}}{2}(X_1 + X_2) \right]. \tag{1973}$$

To check the off-diagonal coefficient directly, the ratio of ground amplitudes across a flip is $e^{\beta st}$; hence $q_{ij}g_i/g_j = \Gamma\sqrt{1-m^2}/2$. The diagonal entry is $\Gamma(1-mst)$. These two calculations reproduce (1973) without fitting a quantum spectrum.

AB.2. *Spectral predictions from two calibration quantities.* Introduce the symmetric and antisymmetric observables

$$O_s = \frac{Z_1 + Z_2}{\sqrt{2}}, \qquad O_a = \frac{Z_1 - Z_2}{\sqrt{2}}. \tag{1974}$$

Their ground-state means vanish, and $\|O_s g\|^2 = 1 + m$, $\|O_a g\|^2 = 1 - m$. The normalized vectors are

$$v_s = \frac{|++\rangle - |--\rangle}{\sqrt{2}}, \qquad v_a = \frac{|+-\rangle - |-+\rangle}{\sqrt{2}}.$$

The transverse term in (1973) annihilates both vectors. The longitudinal term therefore gives

$$H_0 v_s = \hbar\Omega_s v_s, \quad H_0 v_a = \hbar\Omega_a v_a, \qquad \Omega_s = \Gamma(1-m), \quad \Omega_a = \Gamma(1+m). \tag{1975}$$

For completeness, on the even Bell-vector subspace spanned by $\Phi_+ = (|++\rangle + |--\rangle)/\sqrt{2}$ and $\Psi_+ = (|+-\rangle + |-+\rangle)/\sqrt{2}$, the matrix of $H_0/(\hbar\Gamma)$ is

$$\begin{pmatrix} 1-m & -\sqrt{1-m^2} \\ -\sqrt{1-m^2} & 1+m \end{pmatrix}.$$

It has determinant zero and trace two. Thus the complete spectrum is $0, \hbar\Gamma(1-m), \hbar\Gamma(1+m), 2\hbar\Gamma$, with a simple ground eigenvalue. The ground vector is

$$g = \sqrt{\frac{1+m}{2}}\Phi_+ + \sqrt{\frac{1-m}{2}}\Psi_+. \tag{1976}$$

The ordered ground correlations are consequently

$$\langle O_s(t)O_s(0)\rangle_0 = (1+m)e^{-i\Omega_s t}, \qquad \langle O_a(t)O_a(0)\rangle_0 = (1-m)e^{-i\Omega_a t}. \tag{1977}$$

These equations give both line positions and relative weights. Their real parts give the symmetrized correlations. Preparation and detector matching must specify which correlation an instrument measures.

Calibrate only the longitudinal correlation m and symmetric line Ω_s. Then freeze

$$\widehat{\beta} = \operatorname{atanh}(\widehat{m}), \qquad \widehat{\Gamma} = \frac{\widehat{\Omega}_s}{1-\widehat{m}}. \tag{1978}$$

Under the declared branch, the unmeasured antisymmetric line is predicted as

$$\widehat{\Omega}_a = \widehat{\Omega}_s \frac{1+\widehat{m}}{1-\widehat{m}}. \tag{1979}$$

No antisymmetric line or Bell outcome is used in this calibration. The restriction $m < 1$ matters: near $m = 1$ the symmetric spectral weight remains finite but its frequency tends to zero, making the inverse calibration sensitive to clock and frequency errors.

AB.3. *Bell response and the joint spectral relation.* For the coherent ground state, direct Pauli multiplication gives

$$\langle X_i\rangle_0 = \sqrt{1-m^2}, \quad \langle Z_i\rangle_0 = 0, \quad T = \mathrm{diag}(1,-m,m), \tag{1980}$$

where $T_{uv} = \langle \sigma_u \otimes \sigma_v\rangle_0$ and its off-diagonal entries vanish. The nonzero local X means are essential when constructing the full outcome table.

Choose, after calibration and before Bell outcomes are collected,

$$A_0 = X_1, \quad A_1 = Z_1, \qquad B_0 = \frac{X_2 + mZ_2}{\sqrt{1+m^2}}, \quad B_1 = \frac{X_2 - mZ_2}{\sqrt{1+m^2}}. \tag{1981}$$

These observables square to the identity. For the CHSH combination

$$S = \langle A_0B_0\rangle + \langle A_0B_1\rangle + \langle A_1B_0\rangle - \langle A_1B_1\rangle, \tag{1982}$$

the four correlations are $1/\sqrt{1+m^2}, 1/\sqrt{1+m^2}, m^2/\sqrt{1+m^2}, -m^2/\sqrt{1+m^2}$, respectively. Hence

$$S = 2\sqrt{1+m^2}, \qquad R := \frac{\Omega_a - \Omega_s}{\Omega_a + \Omega_s} = m, \qquad \left(\frac{S}{2}\right)^2 - 1 - R^2 = 0. \tag{1983}$$

This is a joint prediction of the single-flip kinetic branch and the specified coherent quantum preparation. Its experimental interest lies in using the same frozen parameters in spectral and correlation channels. Standard quantum mechanics for (1973) gives the same relation; it does not independently establish the microscopic origin of that Hamiltonian.

For outcomes $a, b \in \{-1, 1\}$ and projectors $P_a^x = (I + aA_x)/2$, $P_b^y = (I + bB_y)/2$, the complete probabilities are

$$p(a,b \mid x,y) = \mathrm{Tr}(\rho_0 P_a^x P_b^y) = \frac{1 + a\langle A_x\rangle_0 + b\langle B_y\rangle_0 + ab\langle A_xB_y\rangle_0}{4}. \tag{1984}$$

Summing over b removes both terms containing b, so the Alice marginal is independent of y, and similarly for Bob. This proves no-signalling for the specified local measurements. It does not assert Bell-local factorization. Replacing (1984) by a zero-marginal formula would give incorrect joint predictions for this ground state.

AB.4. *An explicit conditional preparation of the singlet.* The coherent transfer ground need not already be the singlet. Its preparation and conversion can nevertheless be written as a complete finite quantum protocol. Let $W = (X + Z)/\sqrt{2}$ be the Hadamard unitary. Using (1976),

$$(W \otimes W)g = \sqrt{\lambda_+}|00\rangle + \sqrt{\lambda_-}|11\rangle, \qquad \lambda_\pm = \frac{1 \pm \sqrt{1 - m^2}}{2}. \tag{1985}$$

Both Schmidt weights are positive for $m > 0$. Their inequality for $m < 1$ explains why a local unitary alone cannot turn this state into a maximally entangled singlet.

Specify the successful local filter on Alice's Schmidt coordinate as

$$F = \operatorname{diag}\left(\sqrt{\lambda_-/\lambda_+}, 1\right), \qquad F_{\text{fail}} = (I - F^\dagger F)^{1/2}. \tag{1986}$$

Then $F^\dagger F + F_{\text{fail}}^\dagger F_{\text{fail}} = I$, so the two outcomes define a complete local quantum instrument. Successful filtering gives $\sqrt{\lambda_-}(|00\rangle + |11\rangle)$. Applying $U = XZ = -iY$ to Bob converts its normalization to the singlet. Thus the successful joint operation is

$$K_{\text{succ}} = (FW) \otimes (UW), \qquad K_{\text{succ}} g = \sqrt{2\lambda_-}|\Psi^-\rangle, \qquad |\Psi^-\rangle = \frac{|01\rangle - |10\rangle}{\sqrt{2}}. \tag{1987}$$

The ideal success probability is

$$P_{\text{succ}} = 2\lambda_- = 1 - \sqrt{1 - m^2} = 1 - \sqrt{1 - R^2}. \tag{1988}$$

This is the standard local filtering mechanism for concentrating a partly entangled pure state [15], here connected to the calibrated finite generator. It supplies a further conditional yield prediction. Detector efficiencies, imperfect filtering and herald losses need independent matching before comparison with measured yield.

Heralding must occur and become available to the two sites before the Bell settings are chosen. No trial is discarded on the basis of a subsequent Bell outcome or setting. Communicating the herald uses an ordinary causal channel. The success-conditioned ensemble then has the single state in (1987), independent of the future settings. Without this event-ready ordering, a selected sample can create a setting-dependent eligibility bias.

The singlet projector has the exact Pauli expansion

$$\rho_- = \frac{1}{4}\left(I \otimes I - \sum_{u=x,y,z} \sigma_u \otimes \sigma_u\right). \tag{1989}$$

It is a pure nonseparable state: its two reduced densities are $I/2$, whereas a pure product has pure reduced densities. Nonfactorization of an arbitrary

mixed joint density alone would not prove entanglement. For unit directions $\mathbf{a}, \mathbf{b}$, use the effects $[I + a(\mathbf{a} \cdot \boldsymbol{\sigma})]/2$ and $[I + b(\mathbf{b} \cdot \boldsymbol{\sigma})]/2$. Pauli traces give

$$p_-(a, b \mid \mathbf{a}, \mathbf{b}) = \frac{1 - ab\,\mathbf{a} \cdot \mathbf{b}}{4}, \qquad E(\mathbf{a}, \mathbf{b}) = -\mathbf{a} \cdot \mathbf{b}. \tag{1990}$$

Each local outcome has probability $1/2$ for every remote direction. The singlet's correlation cannot therefore be used to control the remote outcome distribution or send a superluminal message.

Taking $\mathbf{a}_0 = \mathbf{e}_z$, $\mathbf{a}_1 = \mathbf{e}_x$, $\mathbf{b}_0 = (\mathbf{e}_z + \mathbf{e}_x)/\sqrt{2}$ and $\mathbf{b}_1 = (\mathbf{e}_z - \mathbf{e}_x)/\sqrt{2}$ gives $S = -2\sqrt{2}$. This saturates the quantum bound: for commuting opposite-site observables and dichotomic local observables, the CHSH operator obeys $\mathcal{C}^2 = 4I - [A_0, A_1] \otimes [B_0, B_1]$ and hence $\|\mathcal{C}\|^2 \leq 8$. In contrast, measurement-independent Bell-local responses obey $|S| \leq 2$. The latter statement includes stochastic answers: conditioned on a hidden variable, each response mean lies in $[-1, 1]$, and $|B_0 + B_1| + |B_0 - B_1| \leq 2$. Integrating this pointwise bound proves the classical inequality. The violation excludes that combination of premises, rather than all deterministic or all hidden-variable accounts.

For a singlet of linear polarization modes, an analyser at angle α measures $M_\alpha = \cos(2\alpha)Z + \sin(2\alpha)X$. Consequently,

$$E(\alpha, \beta) = -\cos[2(\alpha - \beta)]. \tag{1991}$$

The doubled angle follows from the polarization projector, not a different signalling mechanism. Preparing such photon modes is an additional physical realization; the spin protocol does not by itself construct a photon source.

Calibration errors also affect filtering. If the filter ratio is $\widehat{r} = \sqrt{\lambda_-(\widehat{m})/\lambda_+(\widehat{m})}$ but the prepared ground has parameter m, the yield and the normalized concurrence of the successful state are

$$P = \widehat{r}^{\,2}\lambda_+(m) + \lambda_-(m), \qquad \mathcal{C}_{\mathrm{ent}} = \frac{\widehat{r}m}{P}. \tag{1992}$$

Its correlation tensor after U is $\mathrm{diag}(-\mathcal{C}_{\mathrm{ent}}, -\mathcal{C}_{\mathrm{ent}}, -1)$. At the fixed ideal singlet directions above, the result is $S = -\sqrt{2}(1 + \mathcal{C}_{\mathrm{ent}})$, rather than automatically $-2\sqrt{2}$. These formulas follow by normalizing the two surviving Schmidt amplitudes; they make imperfect calibration explicit.

The completed conditional chain is therefore

$$\begin{aligned} &\text{fixed physical realization of } \mathsf{Q}_0 \longrightarrow (H_0, g) \\ &\longrightarrow \text{specified ground preparation and local filter} \longrightarrow \rho_- \\ &\longrightarrow \text{specified Pauli or polarization effects and Born rule} \longrightarrow (E, S, P_{\mathrm{succ}}). \end{aligned} \tag{1993}$$

Every arrow is calculated above, with its physical premises stated. This is a conditional recovery and preparation result. It is not an unconditional

derivation of Bell violation from classical noise; that would conflict with the classical inequality while its premises hold.

AB.5. *Two alternatives that the calibration does not exclude.* An equilibrium distribution cannot select the kinetic operator. To exhibit the remaining freedom, let $\delta \geq 0$ have units of frequency and consider

$$H_\delta = H_0 + \hbar\delta|v_a\rangle\langle v_a|. \tag{1994}$$

The added operator annihilates g and v_s. It therefore preserves the ground state, its longitudinal correlation, and Ω_s. It changes the antisymmetric line to $\Omega_a + \delta$. The inverse transform $\mathsf{Q}_\delta = -D_g^{-1}(H_\delta/\hbar)D_g$ adds $\delta/2$ to both exchange rates between $(+,-)$ and $(-,+)$, and subtracts $\delta/2$ from their diagonal entries. Their equilibrium weights are equal. The resulting generator is conservative, irreducible, and reversible with the same π.

Thus this alternative respects detailed balance and both calibration quantities, but its ratio

$$R_\delta = \frac{2\Gamma m + \delta}{2\Gamma + \delta} \tag{1995}$$

satisfies $R_\delta > m$ for $\delta > 0$. The residual in (1983) becomes $m^2 - R_\delta^2 < 0$. The thought experiment tests the absence of this exchange operator; it cannot derive that absence from equilibrium. The two generators have the same selected calibration data, not the same complete path law.

A second alternative is preparation with $\rho_{\mathrm{diag}} = \mathrm{diag}(\pi)$ instead of ρ_0. It retains every instantaneous configuration probability. Its only nonzero Pauli correlation is $T_{zz} = m$. At the settings in (1981), it gives

$$S_{\mathrm{diag}} = \frac{2m^2}{\sqrt{1+m^2}}, \tag{1996}$$

whereas the coherent state gives $2\sqrt{1+m^2}$. These are values at the prescribed settings, not a claim about the optimized Bell value of all separable states or all measurement classes. The diagonal state is not stationary under H_0 in general. A comparison using it therefore requires immediate measurement or a specified preparation/dephasing channel, rather than quietly treating it as the same physical ground state.

For example, $\beta = 0.8$ and $\Gamma = 1.3$ give $m = 0.66403677$, $\Omega_s = 0.43675220$, $\Omega_a = 2.16324780$ and $S = 2.40078723$. At $\delta = 0.4$ the antisymmetric line becomes 2.56324780, while the ground Bell value and calibration remain unchanged. Direct four-dimensional calculations at four distinct values of m reproduce the eigenvector, inverse-generator, probability and joint-relation identities with maximum absolute error 8.89×10^{-16}. These computations check the finite formulas; they supply no measured evidence for this proposed physical realization.

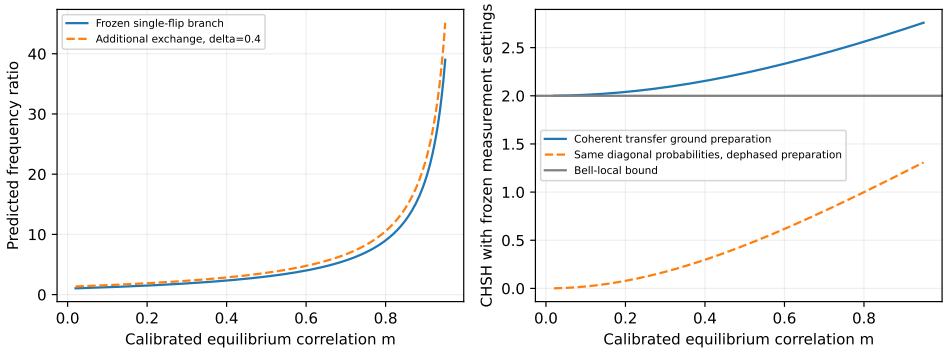


Figure 70. Calculated predictions of the finite thought experiment. Left: frequency ratios for the specified single-flip branch and a reversible branch with an additional exchange rate, using $\Gamma = 1.3$ and $\delta = 0.4$ in one fixed time unit. Right: CHSH values at calibration-fixed settings for coherent and dephased preparations with the same diagonal law. These curves are mathematical calculations, not laboratory observations.

AB.6. *A prospective test with finite calibration and apparatus errors.* The ideal relation must be accompanied by an uncertainty rule. If $\widehat{m}$ is used to set Bob's apparatus but the true ground parameter is m, keeping the apparatus fixed gives

$$S(m;\widehat{m}) = \frac{2(1+m\widehat{m})}{\sqrt{1+\widehat{m}^2}}. \tag{1997}$$

It is generally incorrect to substitute the true, subsequently estimated m into the measurement angles after outcomes have been exposed. For $m \in [m_-, m_+] \subset (0,1)$ and $\Omega_s \in [\omega_-, \omega_+] \subset (0,\infty)$, monotonicity gives the conservative frozen prediction interval

$$\Omega_a \in \left[\omega_- \frac{1+m_-}{1-m_-},\ \omega_+ \frac{1+m_+}{1-m_+}\right]. \tag{1998}$$

The interval must include clock-conversion error when frequencies are not measured against the same physical reference.

Suppose the trace distance between actual and prescribed states is at most η, and the operator norm errors of the implemented observables are ϵ_{A_x} and ϵ_{B_y}. All actual and target observables are assumed contractions. For each correlation the state error is at most 2η, and the apparatus error is at most $\epsilon_{A_x} + \epsilon_{B_y}$, by expansion of the tensor product. Summing the four CHSH terms

gives the deterministic bound

$$|S_{\mathrm{actual}} - S(m;\widehat{m})| \le 8\eta + 2\sum_{x=0}^{1}\epsilon_{A_x} + 2\sum_{y=0}^{1}\epsilon_{B_y}. \tag{1999}$$

For independent outcomes with fixed setting counts $n_{xy} > 0$, the empirical correlations additionally obey, with probability at least $1-\alpha$,

$$|\widehat{S} - S_{\mathrm{actual}}| \le \sum_{x,y}\sqrt{\frac{2\log(8/\alpha)}{n_{xy}}}. \tag{2000}$$

This follows from Hoeffding's inequality for four variables in $[-1,1]$ and a union bound. A sequential or dependent design needs a corresponding martingale or dependence bound instead.

A prospective experiment would first identify the physical kinetic branch and preparation, calibrate m and Ω_s, freeze the apparatus and error bounds, and collect new spectral and Bell outcomes. The frequency and Bell predictions should both be tested, together with their joint residual. A joint identity alone can have compensating errors in its two channels. No experiment completing this protocol is reported here.

AB.7. *Public Bell data and the calibration–test split.* For a separate experimental benchmark we use the released pair records associated with Rosenfeld et al. [138], preserved in the public archive [139]. The archive identifies runs beginning on 15 April and 14 June 2016. The preservation record was published on 24 September 2026; that date is not the measurement date. Repository checksums were verified before analysis. Every released pair row is retained, with no additional time cut or outcome exclusion.

The April run supplies 10,201 calibration pairs: 5,147 with herald label Ψ^+ and 5,054 with label Ψ^-. The June run supplies 10,202 test pairs: 5,082 and 5,120, respectively. Setting and outcome labels are read from the calibration codebook and retained unchanged. The eligibility of a released pair was already determined by the original experiment. We do not reconstruct its heralding criterion, re-establish its experimental loophole closure, or reproduce its complete published analysis.

The comparison model, eligibility rule, split and success criterion were recorded locally before this analysis read the calibration outcomes. Calibration parameters were then saved before the test outcomes were analysed, and both records are preserved with cryptographic hashes. The underlying experimental outcomes had already been made public. This is a locally frozen reanalysis, not an externally registered, blinded, or newly performed laboratory experiment. The runs share an apparatus; independence and stationarity of their conditional outcome laws are working assumptions, not consequences of different run dates.

AB.8. *Quantum benchmark, full local competitor, and scoring.* For each herald label h we fit the specified isotropic two-qubit benchmark at ideal CHSH geometry,

$$p_Q(a,b \mid x,y,h) = \frac{1 + ab\, c_{xy,h} t_h}{4}, \qquad t_h = \frac{v_h}{\sqrt{2}}, \quad 0 \le v_h \le 1, \quad \prod_{x,y} c_{xy,h} = -1. \tag{2001}$$

Its local means are zero. This benchmark is different from the coherent ground state in (1976). The visibility and one of eight CHSH sign frames are selected by maximum likelihood on April alone. Let $n^{\mathrm{cal}}_{xyab,h}$ denote its cell counts and N^{cal}_h their sum. For a fixed sign frame define $U_h = \sum_{xyab} n^{\mathrm{cal}}_{xyab,h} ab\, c_{xy,h}$. The log likelihood depends on t_h through

$$\frac{N^{\mathrm{cal}}_h + U_h}{2} \log(1 + t_h) + \frac{N^{\mathrm{cal}}_h - U_h}{2} \log(1 - t_h) - N^{\mathrm{cal}}_h \log 4.$$

Differentiation gives its constrained optimum $\widehat{t}_h = \min(1/\sqrt{2}, \max(0, U_h / N^{\mathrm{cal}}_h))$. The sign frame with largest calibration likelihood is then frozen.

The competitor is the entire Bell-local conditional probability polytope, with its 16 deterministic assignments $(A_0, A_1, B_0, B_1) \in \{-1,1\}^4$. Its probabilities are

$$p_L(a,b \mid x,y,h) = \sum_{j=1}^{16} w_{j,h} \mathbf{1}_{\{a = A_x^{(j)},\, b = B_y^{(j)}\}}, \qquad w_{j,h} \ge 0, \quad \sum_j w_{j,h} = 1. \tag{2002}$$

Its weights are maximum-likelihood calibrated separately for each herald label, using a probability floor 10^{-12} for numerical evaluation. The minimized negative log likelihood is convex in these weights; the computed active-weight optimality residuals are below 8×10^{-7}. This is a fitted full local competitor, rather than an artificially restricted one-parameter local model.

The frozen test score is the natural-log predictive difference

$$\Delta\ell_h = \sum_{xyab} n^{\mathrm{test}}_{xyab,h} \log \frac{p_Q(a,b \mid x,y,h)}{p_L(a,b \mid x,y,h)}. \tag{2003}$$

No June outcome is used to adjust either model. Conditional on each test setting count $n_{xy,h}$, let $\widehat{p}$ be its empirical outcome probabilities, $z_{ab} = \log(p_Q / p_L)$ and $\overline{z} = \sum_{ab} \widehat{p}_{ab} z_{ab}$. The variance estimate is

$$\widehat{V}_h = \sum_{xy} \frac{n^2_{xy,h}}{n_{xy,h} - 1} \sum_{ab} \widehat{p}_{ab} (z_{ab} - \overline{z})^2.$$

The pooled normal-approximation lower bound is $\Delta\ell - 1.96\sqrt{\sum_h \widehat{V}_h}$. This is conditional on the frozen fits and an independent conditional-sampling

approximation. It is neither a Bayes factor nor a posterior probability for unification.

The locally specified comparative rule additionally requires nonempty April quantum confidence sets and no test cell outside their enlarged bounds. For $H = 2$ herald labels and each setting count n, the cell error is $\sqrt{\log(32H/\alpha)/(2n)}$, with $\alpha = 0.025$ separately for calibration and test. Calibration-compatible parameter intervals and sign frames are retained; their predicted cell intervals are then enlarged by the test errors. This conservative compatibility condition is distinct from a sensitive absolute-fit test.

AB.9. *Experimental results and an additional absolute-fit diagnostic.* April calibration gives $v_+ = 0.7762100862$ and $v_- = 0.7935713619$, with sign frames $(-,-,-,+)$ and $(-,-,+,-)$ in setting order $(00, 01, 10, 11)$. The June predictions and observations are summarized in Table 35. The pooled score improvement is 116.365255, its estimated conditional standard error is 10.341780, and its approximate 95 percent lower bound is 96.095367. Both herald-specific score differences are positive, both calibration confidence sets are nonempty, and no test cell fails the conservative enlarged intervals. The specified comparative rule is therefore satisfied.

Herald	Test pairs	Predicted S	Observed S	$\Delta\ell_h$
Ψ^+	5,082	2.195454	2.048801	46.531927
Ψ^-	5,120	2.244559	2.141695	69.833329

Table 35. June outcomes evaluated against April-frozen predictions. The observed CHSH values use the sign frames fixed in April.

This comparative result does not establish adequate absolute prediction. The simultaneous conservative errors on the two observed CHSH values are 0.381246 and 0.379863. Their corresponding lower bounds are below two. This particular conservative calculation does not independently certify a Bell violation, despite both point estimates exceeding two; the original experiment's statistical conclusions use its own analysis.

To test absolute agreement, independently parse the released cell counts and calculate deviance against the saturated conditional outcome model:

$$G_Q = 2 \sum_{h,xy,ab} n^{\mathrm{test}}_{xyab,h} \log \frac{\widehat{p}^{\,\mathrm{test}}_{xyab,h}}{p_Q(a, b \mid x, y, h)}. \tag{2004}$$

Terms with zero count are defined by continuity. The quantum deviances are 48.373021 and 92.335534, totaling 140.708555. The local deviances are

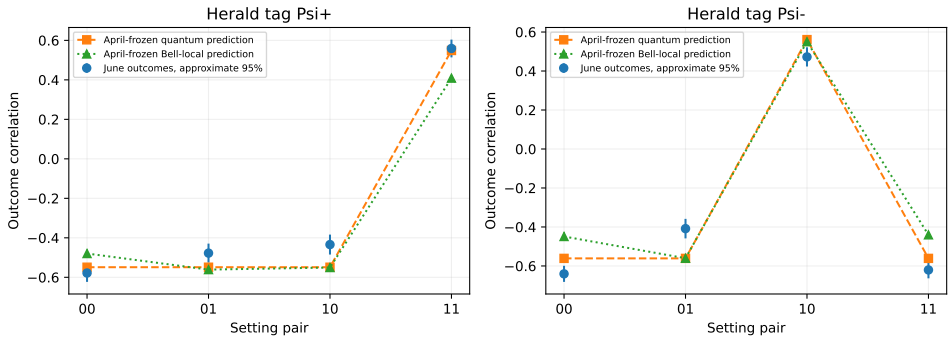


Figure 71. Real June outcome correlations with April-frozen quantum and full Bell-local predictions. Error bars are approximate conditional 95 percent intervals for individual correlations, not simultaneous Bell-certification bounds. Setting dependence remains visible even though the quantum benchmark predicts a common correlation magnitude.

141.436874 and 232.002191. Their difference verifies independently that $(G_L - G_Q)/2 = \Delta\ell$.

An additional plug-in predictive bootstrap assesses the absolute quantum discrepancy. For each of 20,000 replicas, generate synthetic April and June conditional multinomial tables using the frozen quantum probabilities and the actual setting counts. Recalibrate the visibility and sign frame on the synthetic April sample only, then evaluate the synthetic June deviance with those recalibrated synthetic parameters. This procedure includes calibration sampling error while keeping the real June outcomes outside fitting. The two herald deviances are summed in each replica.

The simulated median, 95th, 99th and 99.9th percentiles are 25.224676, 40.177392, 47.995422 and 56.914852. None of the 20,000 replicas reaches the observed 140.708555. The add-one Monte Carlo tail estimate is $1/20001 \simeq 5.00 \times 10^{-5}$. This estimate has finite simulation resolution; it is not an exact tail probability or a distribution-free guarantee. It is also an additional diagnostic introduced after the original comparative analysis, not a replacement predeclared success criterion.

Under the independent, stationary isotropic benchmark, these calculations give strong evidence of inadequate absolute fit. Thus two conclusions must be retained together: the frozen quantum benchmark predicts these outcomes better than the calibrated full local competitor, and its restricted probability model is nevertheless inadequate. Possible sources include unequal setting correlations, nonzero local means, apparatus drift, and dependent outcomes.

Identifying their cause requires further analysis and a new test sample; none is selected here by refitting the already exposed test run.

The benchmark uses an established quantum state family and specified measurement geometry. It does not measure (1983), determine a unique mother coupling, or validate the entire unification programme. Its value is a reproducible frozen comparison and an explicit unfavorable absolute-fit result, while the spectral thought experiment supplies a separate concrete target for a genuinely new physical test.

AB.10. *Further finite thought experiments for the common framework.* Thought experiments can test the relations between the programme's branches without assuming that a finite auxiliary model is already a physical field theory. Three examples isolate clock, reservoir and geometric premises.

A change of clock at unchanged equilibrium. Consider $\mathrm{d}X = -aX\mathrm{d}\tau + \sqrt{2D}\mathrm{d}W_\tau$, with $a, D > 0$. Under $t = \xi_t\tau$, $\xi_t > 0$, its physical-time coefficients become a/ξ_t and D/ξ_t. The stationary variance remains D/a, but

$$\langle X(t)X(0)\rangle_{\mathrm{st}} = (D/a)e^{-a|t|/\xi_t}.$$

Thus equal equilibrium statistics do not fix a physical clock or relaxation frequency. Both processes satisfy detailed balance and have zero stationary path-reversal entropy production. Nonzero motion and decaying correlations alone therefore do not prove a thermodynamic arrow. A future physical realization must match its clock before comparing spectral predictions across departments.

A resolved bath and a projected memory response. Let one energy be $U(x, y) = (k_x x^2 + k_y y^2 + 2c_0 xy)/2$, with $k_x, k_y > 0$ and $c_0^2 < k_x k_y$. For positive mobilities μ_x, μ_y and one reservoir energy scale θ, specify

$$\begin{aligned}\mathrm{d}x &= -\mu_x(k_x x + c_0 y)\mathrm{d}t + \sqrt{2\mu_x\theta}\mathrm{d}W_x,\\ \mathrm{d}y &= -\mu_y(k_y y + c_0 x)\mathrm{d}t + \sqrt{2\mu_y\theta}\mathrm{d}W_y.\end{aligned}$$

Its stationary covariance is θK^{-1}, where $K = \begin{pmatrix} k_x & c_0 \\ c_0 & k_y \end{pmatrix}$. Eliminating y exactly and integrating its exponential convolution by parts gives

$$\begin{aligned}\frac{\dot{x}(t)}{\mu_x} &= -\left(k_x - \frac{c_0^2}{k_y}\right)x(t)\\ &\quad - \int_0^t \mathcal{K}(t-s)\dot{x}(s)\mathrm{d}s + \xi_w(t) + \xi_c(t), \qquad (2005)\\ \mathcal{K}(t) &= \frac{c_0^2}{k_y}e^{-\mu_y k_y t}.\end{aligned}$$

The derivatives and white noise are interpreted distributionally or through the integrated equation. If the initial bath is sampled conditionally from the common Gibbs law, then $\eta_0 = y(0) + c_0 x(0)/k_y$ has variance θ/k_y and is independent of $x(0)$ and the future Wiener increments. The colored force is

$$\xi_c(t) = -c_0 e^{-\lambda t}\eta_0 - c_0\sqrt{2\mu_y\theta}\int_0^t e^{-\lambda(t-u)}\mathrm{d}W_y(u), \qquad \lambda = \mu_y k_y.$$

Direct covariance integration then gives

$$\langle \xi_c(t)\xi_c(s)\rangle = \theta\mathcal{K}(|t-s|), \qquad \langle \xi_w(t)\xi_w(s)\rangle = \frac{2\theta}{\mu_x}\delta(t-s). \tag{2006}$$

The colored covariance follows from

$$\frac{\theta c_0^2}{k_y}e^{-\lambda(t+s)} + 2\mu_y\theta c_0^2\int_0^{\min(t,s)} e^{-\lambda(t+s-2u)}\mathrm{d}u = \frac{\theta c_0^2}{k_y}e^{-\lambda|t-s|}.$$

Thus the projected memory and fluctuations cannot be varied independently while retaining this mother realization. After its equilibrium and bath parameters are fixed, a delayed-response and noise experiment tests the same parameter set. These are exact finite fluctuation–dissipation relations, not a new continuum turbulence theorem or an exclusive prediction of unification.
Stationary black-hole labels versus interior geometry. A stationary label law cannot establish a nonsingular interior. As a diagnostic, choose a probability on positive masses supported on $M \geq M_{\min} > 0$ and assign each label the Schwarzschild metric. Its curvature invariant is

$$R_{abcd}R^{abcd} = \frac{48G^2M^2}{c^4r^6}.$$

The label distribution can be normalizable and dynamically stationary, yet the expected invariant is bounded below by $48G^2M_{\min}^2/(c^4r^6)$ and still diverges at $r = 0$. This is a logical test of what stationarity proves, not a proposed regular-core solution. A stable-interior claim must instead supply a physical metric, local stresses, constraints and curvature control. Observable consequences of such a completed geometry would then need a separate frozen forward calculation.

Appendix AC. Physical observation models and transfer between Bell runs

AC.1. *Data definitions and independent source checks.* The unfavorable absolute fit of the frozen isotropic benchmark motivates a physically constrained analysis of preparation and measurement imperfections. We use the same released April and June records [138] and [139]. Both samples have already been examined. The following fits and temporal comparisons are exploratory;

they do not constitute a new independent test of the spectral relation or the mother model.

Tables VIII and X of the original Supplemental Material specify the same nominal spin-space angles for both runs:

$$\alpha_0 = 0, \quad \alpha_1 = \pi/2, \qquad \beta_0 = -\pi/4, \quad \beta_1 = \pi/4.$$

The published tables retain the first 5000 events for each heralded state, whereas the complete downloadable archives contain 10201 April pairs and 10202 June pairs. Reconstructing the first 5000 events per label reproduces every published outcome count exactly. Archive result one corresponds to the published up outcome. The corresponding CHSH values are $2.203917, 2.239913$ in April and $2.057091, 2.133688$ in June, in the order Ψ^+, Ψ^-. The earlier frozen comparison used all released pairs; its slightly different summary values are therefore consistent with the original publication.

For every released pair, its pointers to the two local records reproduce both settings and outcomes, the herald label and the recorded eligibility. The maximum computer-clock difference is 79 milliseconds, within the archive's stated 100 millisecond matching window. These computer times are not the precision timing used to establish spacelike separation. The June local logs also record 318 detector-shutdown exclusions on each side. The original Supplemental Material specifies maintenance and failure rules before the run. Those excluded records are not reintroduced or used to change the released-pair eligibility here. These checks establish consistency of the records being analysed; they do not independently re-establish closure of all experimental loopholes.

AC.2. *A positive state and measurement family.* Let $h \in \{+, -\}$ denote the herald label and $v_h \in [0, 1]$ a visibility. Consider the states

$$\rho_h = (I \otimes U_y(\phi)) \left[v_h |\Psi^h\rangle\langle\Psi^h| + (1 - v_h)\frac{I_4}{4} \right] (I \otimes U_y(\phi))^\dagger, \qquad U_y(\phi) = e^{-i\phi Y/2}. \tag{2007}$$

The common angle ϕ represents an effective relative rotation. It may describe a source phase or an analyser mismatch; these possibilities are not identifiable separately from the present outcomes.

Use $A_0 = Z, A_1 = X$ and $B_0 = (Z - X)/\sqrt{2}, B_1 = (Z + X)/\sqrt{2}$. Model readout biases by

$$\begin{aligned} E_{+|x} &= \frac{(1 + b_{Ax})I + \nu_{Ax} A_x}{2}, & E_{-|x} &= I - E_{+|x}, \\ F_{+|y} &= \frac{(1 + b_{By})I + \nu_{By} B_y}{2}, & F_{-|y} &= I - F_{+|y}, \\ \nu_{Ax} &= 1 - |b_{Ax}|, & \nu_{By} &= 1 - |b_{By}|. \end{aligned} \tag{2008}$$

The maximal-contrast choice for each bias is a restricted factorization, not a detector calibration inferred uniquely from the mother model. The eigenvalues of E_+ are $(1 + b_A \pm (1 - |b_A|))/2$, which lie in $[0, 1]$ for $|b_A| \le 1$; the same argument applies to F_+. The state eigenvalues are $(1 + 3v_h)/4$ and $(1 - v_h)/4$, the latter with multiplicity three. Thus the state and all effects are positive.

Write $a, b \in \{-1, 1\}$ for the outcomes and let $c_{xy,h}(\phi)$ be the ideal correlation of the rotated Bell state. Since its local Bloch vectors vanish, direct expansion of the trace gives

$$p_h(a, b|x, y) = \frac{1}{4}\big[1 + ab_{Ax} + bb_{By} + ab\{b_{Ax}b_{By} + v_h\nu_{Ax}\nu_{By}c_{xy,h}(\phi)\}\big]. \quad (2009)$$

This is normalized and has local marginals independent of the remote setting. Positivity follows from $\mathrm{Tr}[\rho_h(E_{a|x} \otimes F_{b|y})] \ge 0$. For explicit computation in the x, z plane, set

$$\mathbf{a}_0 = (0, 1)^T, \qquad \mathbf{a}_1 = (1, 0)^T, \qquad \mathbf{b}_{0,1} = (\mp 1, 1)^T/\sqrt{2},$$
$$T_+ = \mathrm{diag}(1, -1), \qquad T_- = -I_2.$$

Then

$$c_{xy,h}(\phi) = \mathbf{a}_x^T T_h R_y(\phi)^T \mathbf{b}_y, \qquad R_y(\phi) = \begin{pmatrix} \cos\phi & \sin\phi \\ -\sin\phi & \cos\phi \end{pmatrix}.$$

The seven parameters are two visibilities, four readout biases and one common angle. The explored domain is $|b| \le 0.30$ and $|\phi| \le \pi/4$. All reported optima lie within that domain. Variants omit biases or rotation, or allow one angle per herald. These are observation models within standard quantum mechanics, not new physical couplings selected by the mother construction.

AC.3. *Exploratory fits and mathematical consistency.* For conditional counts n_{hxyab}, maximize $\sum n_{hxyab} \log p_h(a, b|x, y)$. We report the deviance from the saturated conditional table. The isotropic two-visibility optimum has a closed form; nonlinear variants use seven initializations. Agreement among their optima is a numerical check, not a proof of global uniqueness. Direct density-matrix evaluation reproduces the compact probability formula to within 2.3×10^{-16} in all reported full-run fits.

Family	Parameters	April fit	June fit	April to June
Visibility	2	82.612	127.355	140.709
Visibility, common angle	3	42.517	44.227	300.071
Visibility, separate angles	4	42.484	39.904	299.191
Visibility, biases	6	55.063	104.086	208.508
Visibility, biases, common angle	7	15.891	21.405	365.130
Visibility, biases, separate angles	8	15.862	17.461	364.271

The common-angle biased family reduces the June fitted deviance from 127.354990 to 21.404734, using seven parameters rather than the sixteen observable parameters of an unrestricted quantum-compatible table. With 17 residual degrees of freedom, the conditional independent multinomial approximation gives a tail probability about 0.209; the April value is about 0.532. These are exploratory diagnostics under the model's sampling and regularity assumptions. They are not probabilities that the model is true and do not account for selecting the family after observing the data.

For the June fit, $v_+ = 0.749758$, $v_- = 0.796367$, and

$$(b_{A0}, b_{A1}, b_{B0}, b_{B1}) = (-0.004034,\ 0.001208,\ -0.005890,\ -0.052294).$$

The two density matrices have minimum eigenvalues 0.062561 and 0.050908. Thus the improvement is achieved with explicit positive quantum states and effects, without assigning an arbitrary probability to every cell.

AC.4. *Transfer, time variation and the meaning of an effective angle.* The fitted common angle is $+5.285^\circ$ in April and -8.287° in June. The nominal angles in the source tables agree, so these effective values cannot be attributed to a documented nominal setting change. They describe the outcome tables within the chosen factorization. Independent source or analyser measurements are needed to identify their physical cause.

Keeping all seven April parameters fixed gives June deviance 365.130, which is worse than the original isotropic prediction. A good fit within each run therefore does not establish parameter transfer. In particular, it would be incorrect to change the June angle after seeing its Bell outcomes and report the resulting improvement as a frozen prediction.

A chronological diagnostic fits each run's first half and scores its second half. In April, the two-visibility and seven-parameter deviances are 64.833 and 36.174, respectively; in June they are 124.238 and 59.389. These reductions support further development of a time-dependent observation model, but do not establish its adequacy. Both samples had already been exposed before this split was selected, so these calculations are developmental comparisons, not new untouched holdouts.

AC.5. *Independent calibration and subsequent physical predictions.* A new run should measure source preparation, analyser orientation and readout response through auxiliary calibration observations before its Bell outcomes are used. Those measurements must identify, or bound, the nuisance directions that are degenerate in (2009). In particular, a product of source visibility and detector contrast cannot be separated by merely giving its factors different names.

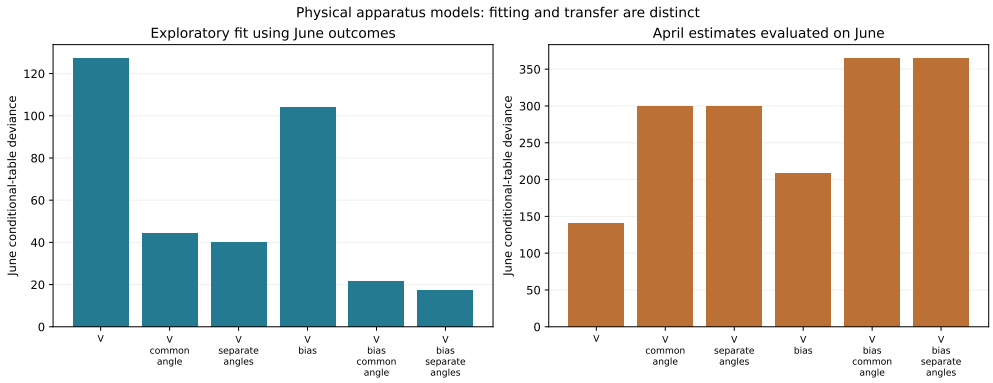


Figure 72. Exploratory physical observation models. Left: each model is estimated using June outcomes. Right: April estimates are evaluated on June outcomes without adjustment. Lower within-run deviance does not imply successful transfer of source and apparatus parameters.

Freeze the rule for incorporating auxiliary calibration, the shared physical parameters, the observation likelihood and the uncertainty propagation. Predict complete outcome tables and assess both absolute agreement and comparative score against a calibrated standard quantum model. If temporal dependence is present, use a justified dependent-data analysis rather than treating every event as independent.

The spectral, $Y \otimes Y$, and preparation-yield relations provide additional targets only in an apparatus physically matched to their finite mother branch. The present Bell archive contains no corresponding spectroscopic calibration. The seven-parameter fit supplies a concrete candidate observation model and exposes failure of parameter constancy within that family. It does not establish a unique microscopic coupling or an independently confirmed unified theory.

Appendix AD. **Operational joint predictions and public coherence data**

AD.1. *The physical target and the meaning of a joint test.* A joint prediction uses one calibrated physical model in several measurements whose outcomes were not used to determine its parameters. Its force comes from a restriction between the measurements. A better description of one data set, by itself, does not establish that restriction. We consider a two-spin example and then a different, experimentally accessible noise branch. Their measured frequencies have different physical meanings and must be kept separate.

For the positive transfer construction [93], specify the physical Hamiltonian

$$H_0/\hbar = \Gamma\left[I - mZ_1Z_2 - \frac{\sqrt{1-m^2}}{2}(X_1+X_2)\right], \qquad 0<m<1, \quad \Gamma>0. \tag{2010}$$

Its normalized ground vector in the configuration basis is

$$|g_m\rangle = \tfrac{1}{2}\left(\sqrt{1+m}, \sqrt{1-m}, \sqrt{1-m}, \sqrt{1+m}\right)^T.$$

The transfer-to-energy conversion, tensor-product identification, ground preparation, local effects and trace probability rule are physical premises. They are not consequences of Gibbs normalization alone. The ground correlation tensor is $\mathrm{diag}(1,-m,m)$, with local X mean $\sqrt{1-m^2}$. The symmetric and antisymmetric excitation frequencies are

$$\Omega_s = \Gamma(1-m), \qquad \Omega_a = \Gamma(1+m), \qquad R = \frac{\Omega_a-\Omega_s}{\Omega_a+\Omega_s} = m. \tag{2011}$$

These are excitation frequencies of (2010), measured relative to its ground energy.

After calibrating $\widehat{m}$ and $\widehat{\Omega}_s$, freeze the clock scale $\widehat{\Gamma} = \widehat{\Omega}_s/(1-\widehat{m})$ and the measurement settings

$$A_0 = X_1, \quad A_1 = Z_1, \qquad B_{0,1} = \frac{X_2 \pm \widehat{m}Z_2}{\sqrt{1+\widehat{m}^2}}.$$

For the actual ideal ground g_m, the fixed-setting CHSH value is

$$S_0(m,\widehat{m}) = \frac{2(1+m\widehat{m})}{\sqrt{1+\widehat{m}^2}}. \tag{2012}$$

Thus a calibration error in m need not be absorbed into a new choice of the Bell settings. The joint residual to test is

$$\mathcal{R}_B = \frac{\sqrt{1+\widehat{m}^2}}{2}S - 1 - \widehat{m}R. \tag{2013}$$

It vanishes for every actual m in the ideal branch, even when $m \neq \widehat{m}$. The expression $(S/2)^2 - 1 - R^2$ instead assumes settings optimized at the actual m.

The calibrated local filter supplies a third observable [15]. Define

$$\lambda_\pm(m) = \frac{1 \pm \sqrt{1-m^2}}{2}, \qquad r_f^2 = \frac{\lambda_-(\widehat{m})}{\lambda_+(\widehat{m})}.$$

With $W = (X+Z)/\sqrt{2}$, $U = XZ$ and $K_f = (\mathrm{diag}(r_f,1)W)\otimes(UW)$, its success probability on the actual ideal ground is

$$q_f(m,\widehat{m}) = r_f^2\lambda_+(m) + \lambda_-(m). \tag{2014}$$

When $m = \widehat{m}$, this becomes $1-\sqrt{1-m^2}$ and the normalized successful state is the singlet. For unequal parameters, (2014) is the prediction to use.

All preparation attempts, including failed filters, must enter the success-rate denominator.

AD.2. *Quantitative stability of the spectral and Bell relation.* Finite precision and imperfect state preparation should lead to a specified tolerance, rather than to a free change in the prediction. Let $D(\rho,\rho_0)=\frac{1}{2}\|\rho-\rho_0\|_1$ be trace distance and assume $D(\rho,|g_m\rangle\langle g_m|)\le d_\rho$. Let measured excitation frequencies be $\widetilde{\Omega}_j=\Omega_j+\Delta_j$, with $|\Delta_j|\le e_j$, $j=s,a$. If $e_a+e_s<2\Gamma$, direct subtraction of the two ratios gives

$$|\widetilde{R}-m|\le\eta_R,\qquad \eta_R=\frac{(1-m)e_a+(1+m)e_s}{2\Gamma-e_a-e_s}. \tag{2015}$$

Indeed,

$$\widetilde{R}-m=\frac{(1-m)\Delta_a-(1+m)\Delta_s}{2\Gamma+\Delta_a+\Delta_s}.$$

This calculation retains the common denominator error. Treating the two line errors as unrelated errors of R would miss this dependence. For an operational bound, suppose independent calibration gives $m\in[m_{\mathrm{lo}},m_{\mathrm{hi}}]$ and $\Gamma\ge\Gamma_{\min}$. The numerator in (2015) is affine in m. Replace it by the larger of its two endpoint values, and replace the denominator by $2\Gamma_{\min}-e_a-e_s$, provided this is positive. The resulting tolerance contains only calibrated bounds. If the physical energy operator is H_0+V with V Hermitian, Weyl's eigenvalue inequality bounds each energy eigenvalue error by $\|V\|$. The corresponding ground-to-excited frequency error is at most $2\|V\|/\hbar$. Excitation labels must be maintained by parity identification or by a separately verified noncrossing condition.

Let actual local observables be Hermitian contractions $\widetilde{A}_x,\widetilde{B}_y$. Suppose their deviations from the frozen ideal settings have operator norms at most a_x and b_y. Define

$$e_{\mathrm{inst}}=2(a_0+a_1+b_0+b_1).$$

The CHSH operator for the ideal settings has norm at most $2\sqrt{2}$. Trace duality therefore bounds the state contribution to its expectation error by $4\sqrt{2}\,d_\rho$. For an individual product,

$$\|\widetilde{A}_x\otimes\widetilde{B}_y-A_x\otimes B_y\|\le a_x+b_y.$$

Summing the four CHSH terms yields the following result.

Proposition 184 (Operational joint tolerance). *Under the state, spectral and instrument assumptions above,*

$$|\mathcal{R}_B|\le\frac{\sqrt{1+\widehat{m}^2}}{2}(4\sqrt{2}\,d_\rho+e_{\mathrm{inst}})+\widehat{m}\,\eta_R. \tag{2016}$$

If a Y_1Y_2 measurement has additional operator-norm error e_Y, then

$$\left|\widetilde{\langle Y_1Y_2\rangle_\rho} + \widetilde{R}\right| \le 2d_\rho + e_Y + \eta_R.$$

Proof. The first bound follows by inserting (2012) into (2013), using (2015), and adding the state and apparatus expectation errors just derived. For the second, the ideal expectation is $-m$ and $\|Y_1Y_2\| = 1$. Trace duality gives $2d_\rho$, while the measurement replacement contributes e_Y. □

Independent calibration supplies bounds on d_ρ, e_j, a_x, b_y; target outcomes must not be used to enlarge them until the residual passes. Their statistical confidence statements require a common error budget. If separate confidence events fail with probabilities α_i, a union bound gives joint coverage at least $1 - \sum_i \alpha_i$, without requiring independence.

The relation also distinguishes a concrete kinetic alternative. Adding equal-rate exchange between the two anti-aligned configurations preserves the Gibbs ground and Ω_s, while shifting Ω_a by a frequency $\delta \ge 0$. Then

$$R_\delta = \frac{2\Gamma m + \delta}{2\Gamma + \delta}, \qquad \mathcal{R}_{B,\delta} = -\frac{\widehat{m}\,\delta(1-m)}{2\Gamma + \delta}. \tag{2017}$$

The filtering probability and the coherent ground correlations stay unchanged. Detectability requires this residual to exceed the specified systematic tolerance and statistical uncertainty. The measurement discriminates two kinetic realizations; standard quantum mechanics with the respective Hamiltonians gives the same alternatives.

AD.3. *Herald calibration and the effect of conditioning.* An observed herald is not automatically a successful ideal filter. Let its independently calibrated sensitivity be η and its false-positive probability be d_h, with $\eta > d_h$. In the elementary binary observation model,

$$P_h = d_h + (\eta - d_h)q, \qquad q_{\mathrm{corr}} = \frac{P_h - d_h}{\eta - d_h}. \tag{2018}$$

The factor $\eta - d_h$ determines how measurement error is amplified by correction. The herald must be recorded before the later Bell settings and outcomes. Background-dependent or setting-dependent eligibility requires a fuller instrument model.

On $0 \le u \le m_{\max} < 1$, the derivative of (2014) satisfies

$$\left|\frac{\partial q_f(u,\widehat{m})}{\partial u}\right| = \frac{(1-r_f^2)u}{2\sqrt{1-u^2}} \le L_f := \frac{(1-r_f^2)m_{\max}}{2\sqrt{1-m_{\max}^2}}.$$

If both m and $\widetilde{R}$ lie in this interval, an ideal physical filter on a state at trace distance at most d_ρ satisfies

$$|q - q_f(\widetilde{R},\widehat{m})| \le d_\rho + L_f\eta_R. \tag{2019}$$

An independently bounded error of the filter effect contributes its operator norm to the right-hand side. A corrected herald error e_h contributes $e_h/(\eta - d_h)$ when the calibrated sensitivity and false-positive rate are exact; their own uncertainties must also be propagated through (2018). The state term is d_ρ, because a success effect lies between zero and the identity. An arbitrary norm-one observable would instead give the less sharp $2d_\rho$ bound.

Conditioning can magnify a small preparation error. For a fixed trace-nonincreasing completely positive success map $\mathcal{K}$, put $\sigma = \mathcal{K}(\rho)$, $\tau = \mathcal{K}(\rho_0)$ and $p = \operatorname{Tr}\sigma$, $q = \operatorname{Tr}\tau$. If $p, q > 0$, then

$$D(\sigma/p, \tau/q) \le \frac{D(\rho, \rho_0)}{p}. \tag{2020}$$

To prove this, complete the map with a failure branch and retain its classical flag. Trace-norm contraction gives $\|\sigma - \tau\|_1 + |p - q| \le 2D(\rho, \rho_0)$. Adding and subtracting τ/p gives

$$\|\sigma/p - \tau/q\|_1 \le \frac{\|\sigma - \tau\|_1 + |p - q|}{p},$$

which proves (2020). For a matched ideal filter, τ/q is the singlet. Its Bell error after filtering can therefore be bounded using d_ρ/p. Near zero success probability this guarantee becomes weak, even if the unconditioned state error is small. This is why a preparation rate and a successful-state correlation are separate measurements.

AD.4. *A controlled Gaussian phase branch.* Public spin-qubit records permit a different test: whether the same noise description transfers between two independently recorded Bell coherence measurements [20] and [21]. Its stochastic variable represents environmental shifts of the single-qubit resonance frequencies, expressed in hertz. It is not the excitation ratio R of (2011).

For a specific finite stochastic branch, let

$$d\xi = -\tau_c^{-1}\xi\, dt + \sqrt{2\Sigma/\tau_c}\, dW_t, \qquad \Sigma > 0, \quad \tau_c > 0. \tag{2021}$$

Its generator is $\mathcal{L}_\xi f = -\tau_c^{-1}\xi \cdot \nabla f + \tau_c^{-1}\Sigma : \nabla^2 f$. The explicit solution is

$$\xi_t = e^{-t/\tau_c}\xi_0 + \sqrt{2\Sigma/\tau_c}\int_0^t e^{-(t-u)/\tau_c}\, dW_u.$$

The invariant probability is $N(0, \Sigma)$: if ξ_0 has that law, the covariance at time t is $e^{-2t/\tau_c}\Sigma + (1 - e^{-2t/\tau_c})\Sigma = \Sigma$. For any deterministic initial condition, the mean decays to zero and the covariance tends to Σ. Uniqueness among invariant probabilities follows from characteristic functions: invariance at time t gives

$$\varphi(k) = \varphi(e^{-t/\tau_c}k)\exp[-\tfrac{1}{2}(1 - e^{-2t/\tau_c})k^T\Sigma k],$$

and letting t tend to infinity gives the Gaussian characteristic function. This proves existence, uniqueness and convergence for this declared environmental branch. It does not prove uniqueness for an unrestricted quantum-field state.

Assume a matched quantum coupling $H_z(t)/\hbar = \pi \sum_i (\nu_i + \xi_i(t)) Z_i$ and local quantum preparation and readout. For each path this is unitary evolution; averaging paths gives a completely positive, trace-preserving random unitary channel. In stationarity, $\mathrm{Cov}(\xi_t, \xi_0) = e^{-|t|/\tau_c}\Sigma$. Put $u_\pm = (1, \pm 1)^T$ and $\sigma_\pm^2 = u_\pm^T \Sigma u_\pm$. The corresponding Bell coherence envelope is exactly

$$W_\pm(t) = \exp\left\{-4\pi^2\sigma_\pm^2[\tau_c t - \tau_c^2(1 - e^{-t/\tau_c})]\right\}. \tag{2022}$$

Indeed, the accumulated frequency integral has variance $2\sigma_\pm^2[\tau_c t - \tau_c^2(1 - e^{-t/\tau_c})]$, and the Gaussian characteristic function of its 2π phase yields (2022).

The quasi-static approximation follows with a controlled error. Writing the bracket as $\int_0^t (t-u)e^{-u/\tau_c}\, du$ gives

$$0 \le \frac{t^2}{2} - [\tau_c t - \tau_c^2(1 - e^{-t/\tau_c})] \le \frac{t^3}{6\tau_c}.$$

Consequently $W_\pm(t) \to \exp[-2\pi^2\sigma_\pm^2 t^2]$ as $\tau_c \to \infty$ for fixed t. The error in the logarithmic envelope is at most $2\pi^2\sigma_\pm^2 t^3/(3\tau_c)$. The colored-noise branch and its limit use specified environmental couplings and quantum measurement structure. They are conventional physical ingredients within a conditional stochastic realization. The environmental Ornstein–Uhlenbeck process is reversible at stationarity. Its existence does not establish a positive steady thermodynamic entropy production. Echo reversal of accumulated quasi-static phase is also compatible with this model.

Write $\Sigma_{11} = \sigma_1^2$, $\Sigma_{22} = \sigma_2^2$ and $\Sigma_{12} = \rho_c\sigma_1\sigma_2$. In the Gaussian limit, inverse squared coherence times obey

$$\begin{gathered} A_+ := T_\Phi^{-2} = 2\pi^2(\sigma_1^2 + \sigma_2^2 + 2\rho_c\sigma_1\sigma_2), \\ A_- := T_\Psi^{-2} = 2\pi^2(\sigma_1^2 + \sigma_2^2 - 2\rho_c\sigma_1\sigma_2), \quad A_+ + A_- = 2(T_1^{-2} + T_2^{-2}). \end{gathered} \tag{2023}$$

The last identity is independent of the cross-correlation coefficient. Changing only ρ_c cannot repair a failure of this sum. Moreover

$$\rho_c = \frac{A_+ - A_-}{8\pi^2\sigma_1\sigma_2}, \qquad \rho_c \ge \frac{A_+ - A_-}{A_+ + A_-} \quad \text{if } A_+ \ge A_-. \tag{2024}$$

The inequality follows from $2\sigma_1\sigma_2 \le \sigma_1^2 + \sigma_2^2$. Two Bell coherence times determine the noise sum and cross covariance, but not the two individual variances. An independently measured single-qubit noise amplitude is therefore a substantive extra test.

The sum constraint has a stronger form that does not require a quasi-static approximation. For jointly Gaussian accumulated phases ϕ_i with any finite covariance, remove deterministic carrier phases and define the positive

envelopes $W_i = \mathbb{E}e^{-i(\phi_i - \mathbb{E}\phi_i)}$ and $W_\pm = \mathbb{E}e^{-i[(\phi_1 - \mathbb{E}\phi_1) \pm (\phi_2 - \mathbb{E}\phi_2)]}$. The Gaussian characteristic function gives

$$W_+(t)W_-(t) = [W_1(t)W_2(t)]^2. \tag{2025}$$

This follows because the cross covariance cancels when $\mathrm{Var}(\phi_1 + \phi_2)$ and $\mathrm{Var}(\phi_1 - \phi_2)$ are added. The phases must be generated under matched control filters and noise conditions. A different fit window or a changed bath can change an extracted Gaussian time without violating this waveform identity. Thus introducing a finite τ_c cannot arbitrarily remove a failure of (2025) for matched waveforms. Same-session single-qubit envelope measurements would test this stronger relation; they are not present in the inspected Bell archive.

AD.5. *Public measurements and frozen estimation.* The silicon experiment of Boter and collaborators [20] and [21] measures return probabilities after preparing parallel and anti-parallel Bell states, allowing their phases to accumulate, and reversing the preparation circuit. Its two Ramsey batches are separated by approximately 50 hours. The first contains five acquisitions of each Bell family. The second contains three anti-parallel and four parallel acquisitions. The released arrays include binary single-shot outcomes, sweep values, and reference settings. Their 17 acquisitions contain 4 794 000 two-spin readouts over all settings. The physical fitting window used here contains 4 080 000 readouts: 2 400 000 in calibration and 1 680 000 in the held-out batch. Reference and excluded setup settings account for the remainder.

The supporting files for a programmable silicon processor [159] were also inspected. They include instrument normalization and state-tomography methods, but do not establish preparation of (2010) with its simultaneous excitation and filtering measurements. Calibration values from one acquisition must not be assigned to another without a transfer justification.

For the Ramsey data, four measured outcome proportions $\widehat{p} = (p_{00}, p_{01}, p_{10}, p_{11})^T$ are corrected using the reference-setting rule of the original analysis. For each spin, let $F_\downarrow$ and $F_\uparrow$ be the reference-derived readout fidelities. The forward confusion matrix is

$$F_i = \begin{pmatrix} F_{\downarrow,i} & 1 - F_{\uparrow,i} \\ 1 - F_{\downarrow,i} & F_{\uparrow,i} \end{pmatrix}, \qquad F = F_1 \otimes F_2.$$

The supplied reference preparation factors 0.985 and 0.966 enter the up-state normalization. They remain inputs. Reference calibration does not by itself separate every preparation error from a readout error. Matrix inversion is used to extract the returned-population observable, not to assert positivity of every corrected empirical state.

As a separate exposed-data diagnostic, the 34 reference-setting tables have maximum absolute binary correlation 0.03796. The largest ratio to its

whole-block bootstrap standard error is 2.54. These reference checks do not certify product readout, especially when reference preparation is imperfect. They are not used to adjust the frozen prediction or its uncertainty.

If c^T is the first row of F^{-1} and there are n readouts at a sweep point, the corrected estimate and conditional variance are

$$\widehat{q}_{00} = c^T \widehat{p}, \qquad \mathrm{Var}(\widehat{q}_{00} \mid F) = \frac{\sum_j c_j^2 p_j - (c^T p)^2}{n}. \tag{2026}$$

The formula follows from multinomial covariance $[\mathrm{diag}(p) - pp^T]/n$. Reference-setting uncertainty is incorporated by resampling full acquisition blocks together with their reference measurements.

Each returned-population curve is represented by

$$q_{00}(t) = e + v \min(e, 1-e) e^{-(t/T)^2} \sin(2\pi f t + \phi), \quad 0 < v < 1, \quad 0 < e < 1. \tag{2027}$$

This parametrization keeps the fitted returned population between zero and one. Time is expressed in microseconds and f in megahertz. Here f is the carrier of the controlled Ramsey phase, rather than an excitation frequency of (2010). The zero-delay point and the setup/reference settings are excluded according to the published physical fitting window; no outcome-based event cut is introduced.

Weighted nonlinear least squares uses (2026). A block bootstrap with 256 replicates resamples the last acquisition axis, retaining all sweep values and first-axis repetitions within each selected block. The four curve nuisance quantities e, v, f, ϕ are fitted when extracting the held-out observable T. They do not update its predicted value. This is therefore a prediction of extracted coherence times, not a frozen prediction of all raw return counts. The data split, observation rule, model comparisons and bootstrap rule were fixed before extracting the target curves. The original article and its reported averages had already been read; this is a retrospective archival calculation, not external preregistration or a new experiment.

Let v_j be the bootstrap variance of calibration acquisition j. For each family h, the frozen prediction is its equal-weight calibration mean $\overline{T}_h$, with variance $s_h^2 = \sum_{j \in h} v_j / 25$. The common-time comparator uses the mean of all ten calibration acquisitions. The third model fixes the independent single-qubit amplitudes at the published values $T_1 = 0.97 \pm 0.02\,\mu$s, $T_2 = 0.59 \pm 0.02\,\mu$s and calibrates only

$$d_A = \tfrac{1}{2}(\overline{T}_\Phi^{-2} - \overline{T}_\Psi^{-2}).$$

It predicts

$$T_{\Psi,\mathrm{ind}} = (s_A - d_A)^{-1/2}, \quad T_{\Phi,\mathrm{ind}} = (s_A + d_A)^{-1/2}, \qquad s_A = T_1^{-2} + T_2^{-2}. \tag{2028}$$

No additional noise rescaling or fitted drift variance is introduced.

For the seven target times, put $r = T_{\mathrm{obs}} - T_{\mathrm{pred}}$. Prediction covariance includes measurement variances and the common calibration error shared by every target in a family:

$$V_{ij} = \delta_{ij} v_i + s_h^2 \mathbf{1}_{i,j \in h}, \qquad Q = r^T V^{-1} r. \tag{2029}$$

The independent-amplitude model also propagates the two published single-qubit errors by the delta method. Assuming independent calibration errors, the full Gaussian score is $Q + \log\det V + 7\log(2\pi)$ in fixed microsecond units. The approximation $Q \sim \chi^2_7$ is diagnostic: nonlinear observable extraction, temporal drift and unknown cross-acquisition correlations limit its accuracy. Neither a fitted extra dispersion nor target deletion is used to improve agreement.

AD.6. *The transfer result and its limits.* The first batch freezes $\overline{T}_\Psi = 0.51703\,\mu$s and $\overline{T}_\Phi = 0.37298\,\mu$s. The calibration covariance lower bound (2024) is 0.31544. This is a lower bound under the Gaussian model, not a uniquely identified microscopic noise mechanism. The common-time prediction is $0.44501\,\mu$s. Keeping the independent single-qubit amplitudes fixed instead predicts $0.67240\,\mu$s and $0.42036\,\mu$s for the anti-parallel and parallel channels.

Table 36. Held-out coherence-time estimates and block-bootstrap standard errors. Each predicted family time was frozen using only the first batch. All seven acquisitions are retained.

Family	Acquisition	Observed T (ns)	Standard error (ns)
Anti-parallel	1	534.75	29.85
Anti-parallel	2	476.25	33.41
Anti-parallel	3	508.02	29.91
Parallel	1	333.64	44.85
Parallel	2	387.60	39.25
Parallel	3	468.68	24.74
Parallel	4	423.79	29.68

Table 37. Frozen transfer diagnostics for seven extracted times. Tail probabilities use the stated Gaussian approximation. The last column includes prediction-covariance normalization.

Model	Q	Tail probability	Gaussian score
Separate Bell channels	15.941	0.02566	−18.078
Common-time comparator	23.221	0.001560	−11.334
Fixed single-qubit amplitudes	18.389	0.01033	−13.921

The two-channel prediction improves the Gaussian score by 6.744 relative to the common-time comparator. This supports retaining a difference between the two Bell coherence channels. Absolute agreement remains unfavorable under the declared uncertainty approximation. In particular, the third parallel acquisition has a substantial positive residual. Its removal is not part of the test. Fixing the independent single-qubit amplitudes also leaves a discrepancy; changing only the cross covariance cannot enforce the sum identity in (2023). The original article already notes a related need to increase its effective noise amplitudes when matching Bell and single-qubit times. That adjustment is a different model assumption and cannot be counted as an independent amplitude prediction.

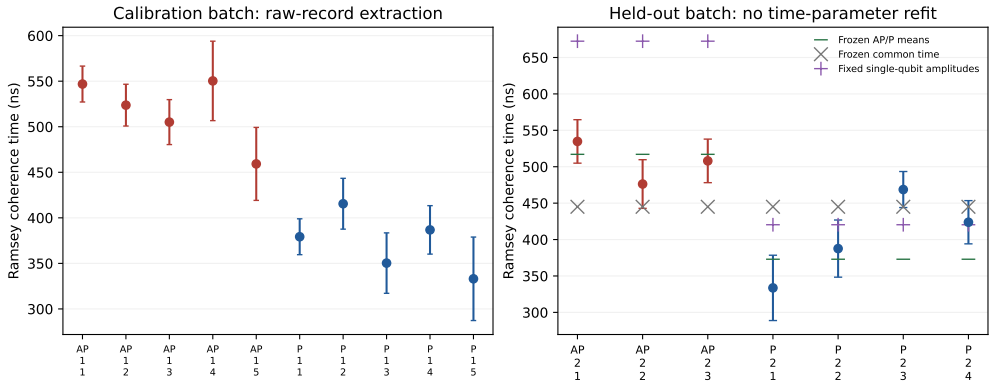


Figure 73. Calibration acquisitions and the independent second batch. Error bars show whole-block bootstrap uncertainties. The marks in the second panel are frozen predictions from the three declared models. Fitted target nuisance quantities extract the times; they do not change the predicted times.

Finite-matrix calculations additionally check (2010)–(2019) on 1000 algebraic state and perturbation cases. The largest spectral formula discrepancy is 7.99×10^{-15} in the chosen numerical units, and the stated inequalities have no positive violation beyond numerical precision. These calculations supplement the explicit proofs; they are not laboratory data. They also exhibit strong amplification under low-probability conditioning, as anticipated by (2020). Across both batches, the independently reconstructed mean times are 513.02 ns and 386.51 ns, consistent with the original rounded reported values 513 ns and 387 ns. These all-data averages are a reconstruction check and never enter the frozen calibration.

AD.7. *Data coverage and a complete prospective measurement.* The noise archive contains same-acquisition reference settings and single-shot Bell coherence records. It does not contain the two ground-relative excitations of (2010), its specified partially entangled ground, and a complete local-filter trial count in one matched realization. The inspected silicon processor archive contains tomography and calibration material, while an inspected multi-ion correlation spectroscopy deposit provides resonance and phase-correlation data. Neither establishes this exact three-channel match. This statement describes the inspected sources; it is not a proof that no suitable experiment exists elsewhere.

A complete measurement must first identify the physical Hamiltonian, its clock scale and excitation parity, and independently bound state-preparation and apparatus errors. It then determines $\widehat{m}, \widehat{\Omega}_s$ from a calibration sample and fixes $\widehat{\Gamma}$, all Bell settings, the filter and the observation model. A disjoint target sample measures Ω_a, the four Bell correlations, $\langle Y_1 Y_2 \rangle$ and both filter outcomes. Reference calibrations may be taken during the target run only under the previously fixed procedure; target outcomes cannot reselect the physics or its tolerance.

The residuals (2013) and (2019) retain their shared calibration covariance. Their joint statistic must include that covariance rather than multiplying three nominally independent agreement probabilities. Comparison with the exchange alternative (2017), and with specified preparation and detector alternatives, tests the particular kinetic relation. Recovering the same formulas from an engineered transverse-Ising Hamiltonian is a test of the matched realization. Establishing its origin in a universal mother dynamics still requires a derived physical projection and independently constrained couplings. The public coherence calculation supplies a completed conditional transfer test and a measured limitation of a simple noise description. The exact spectral–Bell–filter relation remains an unmeasured joint prediction in the inspected records.

Appendix AE. **Frequency-dependent phase noise and transfer between control sequences**

AE.1. *Gaussian phases and the restriction imposed by one temporal kernel.* Two Bell coherences sample different combinations of the same local frequency fluctuations. A parallel coherence samples their sum, whereas an anti-parallel coherence samples their difference. A control pulse can reverse the sign with which a fluctuation contributes to accumulated phase. It therefore changes the temporal part of the measurement, without changing the sum or difference that identifies the Bell family. This distinction makes a transfer between Ramsey and echo sequences a useful test of the environmental model [20] and [21].

Let $\xi = (\xi_1, \xi_2)^T$ be a centered stationary Gaussian frequency process, measured in cycles per unit physical time, with covariance $C(u) = \mathbb{E}[\xi(s+u)\xi(s)^T]$. The tensor factors, physical clock, spin observables, prepared quantum state and trace probability rule are specified inputs. For the same real control function y on both spins, put

$$\phi_y = 2\pi \int_0^t y(s)\xi(s)\, ds, \qquad K_y = 4\pi^2 \int_0^t \int_0^t y(s)y(u)C(s-u)\, ds\, du. \quad (2030)$$

The matrix K_y is a covariance and is therefore positive semidefinite, even if y changes sign. Write $v_+ = (1,1)^T$ and $v_- = (1,-1)^T$. The centered coherence envelopes are

$$W_\pm^y = \mathbb{E}\exp(iv_\pm^T\phi_y) = \exp\left(-\tfrac{1}{2}v_\pm^T K_y v_\pm\right). \quad (2031)$$

The last equality is the characteristic function of a centered Gaussian vector. It concerns the magnitude of a coherence after removing its deterministic carrier phase.

PROPOSITION 185 (Restriction of a separable temporal covariance). *Suppose $C(u) = \Sigma k(u)$, with a fixed covariance matrix Σ and a scalar kernel that defines the specified stationary process. If $v_-^T\Sigma v_- > 0$, then every matched control obeys*

$$-\log W_+^y = r(-\log W_-^y), \qquad r = \frac{v_+^T\Sigma v_+}{v_-^T\Sigma v_-}. \quad (2032)$$

Changing the scalar memory kernel alone cannot change this ratio.

Proof. Substituting the covariance into (2030) gives $K_y = a_y\Sigma$, where

$$a_y = 4\pi^2 \int_0^t \int_0^t y(s)y(u)k(s-u)\, ds\, du \geq 0.$$

Taking logarithms in (2031) cancels a_y. The equality includes controls for which $a_y = 0$, when both sides vanish. □

If Ramsey envelopes are Gaussian, $W_\pm^R = \exp[-(t/T_\pm^R)^2]$, then $r = (T_-^R/T_+^R)^2$. If echo envelopes are exponential, (2032) requires

$$T_+^E = T_-^E/r. \quad (2033)$$

The inference from fitted times assumes that these envelope forms and matched controls describe the measurement. The exact claim is the waveform identity (2032); fitted times are a more restricted observable.

There is a second restriction that survives arbitrary temporal memory. For the matched local envelopes $W_i^y = \exp[-(K_y)_{ii}/2]$,

$$W_+^y W_-^y = (W_1^y W_2^y)^2. \quad (2034)$$

Indeed, the sum of the two quadratic forms in (2031) is $2\,\mathrm{tr}\, K_y$. An additional jointly Gaussian component can relax temporal separability, but cannot remove

(2034) for the same unconditional Gaussian law. In particular, changing only cross covariance does not repair a failed local–Bell sum within that law. An acquisition mixture of different conditional Gaussian laws need not remain Gaussian; the unconditional identity is then not applicable without a new derivation.

AE.2. *A constructive slow and fast phase-noise branch.* A simple model that permits different spatial correlations at different time scales has two independent ingredients. A slow Gaussian frequency process follows

$$d\xi = -\xi\, dt/\tau_s + \sqrt{2\Sigma_s/\tau_s}\, dW_t, \qquad \tau_s > 0, \quad \Sigma_s > 0. \tag{2035}$$

Independent fast phase increments obey $d\phi_i^{\mathrm{f}} = \sqrt{2d_i}\, dB_i$, with $d_i > 0$. The Brownian motions B_1, B_2 and W are independent. Set $\gamma = d_1 + d_2$ and $\sigma_{\pm,s}^2 = v_\pm^T \Sigma_s v_\pm$. In the toggling frame of ideal instantaneous pulses, the complete envelopes are

$$W_\pm^R(t) = \exp[-4\pi^2 \sigma_{\pm,s}^2 G_R(t) - \gamma t], \tag{2036}$$

$$W_\pm^E(t) = \exp[-4\pi^2 \sigma_{\pm,s}^2 G_E(t) - \gamma t], \tag{2037}$$

$$G_R(t) = \tau_s t - \tau_s^2(1 - e^{-t/\tau_s}),$$

$$G_E(t) = \tau_s t - \tau_s^2(3 - 4e^{-t/(2\tau_s)} + e^{-t/\tau_s}).$$

Ramsey uses $y = 1$. Hahn echo uses $y = 1$ in the first half and $y = -1$ in the second. To calculate G_E, the two same-half integrals contribute $2[\tau_s t - 2\tau_s^2(1 - e^{-t/(2\tau_s)})]$ to the full double integral. The two opposite-half integrals subtract $2\tau_s^2(1 - e^{-t/(2\tau_s)})^2$. Dividing their difference by two gives the stated expression. Fast independent increments give the same γt in both Bell families, because $y^2 = 1$ almost everywhere and each coefficient in $v_\pm$ has squared magnitude one.

Proposition 186 (Controlled echo cancellation). *For the specified stationary branch and $t \geq 0$,*

$$0 \leq G_E(t) \leq \frac{t^3}{12\tau_s}, \qquad \left|\log W_\pm^E(t) + \gamma t\right| \leq \frac{\pi^2 \sigma_{\pm,s}^2 t^3}{3\tau_s}. \tag{2038}$$

Moreover,

$$\left|\log \frac{W_+^E(t)}{W_-^E(t)}\right| \leq \frac{\pi^2 |\sigma_{+,s}^2 - \sigma_{-,s}^2| t^3}{3\tau_s}. \tag{2039}$$

Consequently, with Σ_s and d_i fixed, both echo envelopes converge uniformly on every bounded time interval to $e^{-\gamma t}$ as $\tau_s \to \infty$.

Proof. Direct differentiation yields $G_E'(t) = \tau_s(1 - e^{-t/(2\tau_s)})^2$ and $G_E(0) = 0$. The inequality $0 \leq 1 - e^{-x} \leq x$ gives $0 \leq G_E'(t) \leq t^2/(4\tau_s)$. Integration proves the first bound. Substitution into (2037) proves the logarithmic bounds.

Finally, $|W_{\pm}^{E} - e^{-\gamma t}| \le 4\pi^2 \sigma_{\pm,s}^2 G_E$, since $1 - e^{-z} \le z$ for $z \ge 0$. The right-hand side is uniformly bounded by its value at the end of any fixed time interval and tends to zero. □

The slow process is effectively static during a sufficiently short Ramsey evolution: $G_R(t) = t^2/2 + O(t^3/\tau_s)$. It can therefore produce unequal Ramsey envelopes while ideal echo removes its leading contribution. This is a physical assumption about two noise time scales, with a quantitative approximation error. It is not a selection of Σ_s, τ_s or d_i by the mother model. A finite-error application of (2038) requires independent bounds on these quantities; the equal-echo-time comparison below tests the limiting restriction, without asserting that such bounds were measured.

For a phase path, the spin propagator is a tensor product of local unitaries. Its average defines

$$\mathcal{E}_t(\rho) = \mathbb{E}[U_1 \otimes U_2 \, \rho \, U_1^{\dagger} \otimes U_2^{\dagger}].$$

This map is completely positive and trace preserving. Taking a partial trace removes U_2 and leaves a local mixture of U_1 conjugations; a remote choice cannot change this marginal when the local coupling and preparation are fixed. A convex mixture of product unitaries also maps every separable input state to a separable state. Thus the classical noise does not prepare the Bell state whose subsequent dephasing is being measured.

AE.3. *Existence, uniqueness and convergence of the specified bath.* The bath can be represented as an autonomous finite-dimensional diffusion by retaining the phase variables modulo 2π:

$$d\Phi = 2\pi\xi \, dt + \sqrt{2D} \, dB_t \pmod{2\pi}, \qquad D = \operatorname{diag}(d_1, d_2). \tag{2040}$$

This representation distinguishes a stationary noise environment from a prepared spin state.

Proposition 187 (Unique invariant bath and two convergence statements). *Under $\Sigma_s > 0$, $\tau_s > 0$ and $d_1, d_2 > 0$, the joint diffusion* (2035)–(2040) *on $\mathbb{R}^2 \times \mathbb{T}^2$ is nonexplosive and has the unique invariant probability*

$$\pi_b(d\xi, d\Phi) = N(0, \Sigma_s)(d\xi) \frac{d\Phi_1 \, d\Phi_2}{(2\pi)^2}. \tag{2041}$$

Its law converges weakly to π_b from every initial probability. For an initial relative density $g_0 \in L^2(\pi_b)$,

$$\|g_t - 1\|_{L^2(\pi_b)} \le e^{-\lambda_b t} \|g_0 - 1\|_{L^2(\pi_b)}, \qquad \lambda_b = \min\{\tau_s^{-1}, d_1, d_2\}. \tag{2042}$$

Proof. The explicit solution of the linear frequency equation is

$$\xi_t = e^{-t/\tau_s} \xi_0 + \sqrt{2\Sigma_s/\tau_s} \int_0^t e^{-(t-u)/\tau_s} \, dW_u.$$

The stochastic integral has covariance $(1-e^{-2t/\tau_s})\Sigma_s$. Together with the time integral in (2040), it defines finite paths at every finite time. Thus there is no explosion.

A stationary Gaussian initial frequency remains stationary. An independent uniform initial phase remains uniform and independent of the entire frequency path after addition of any path-dependent translation and independent Brownian increments. This proves invariance of (2041).

For uniqueness and weak convergence, let $u \in \mathbb{R}^2$ and $k \in \mathbb{Z}^2$. Independence of B gives

$$\begin{aligned}&\mathbb{E}e^{iu^T\xi_t+ik^T\Phi_t}\\&\quad= e^{-tk^TDk}\,\mathbb{E}\exp\left(iu^T\xi_t+ik^T\Phi_0+2\pi ik^T\int_0^t\xi_s\,ds\right).\end{aligned}$$

For $k\neq 0$, its absolute value is bounded by $e^{-tk^TDk}\to 0$. For $k=0$, the explicit frequency solution and bounded convergence give the limit $e^{-u^T\Sigma_s u/2}$ for every initial law. The frequency marginals are tight as $t\to\infty$ and the torus is compact. Every subsequential limit is therefore determined by these mixed Fourier transforms and equals (2041). An invariant initial probability must equal this limit, proving uniqueness.

The generator on smooth functions is

$$\mathcal{G}_b=\tau_s^{-1}(\Sigma_s:\nabla_\xi^2-\xi\cdot\nabla_\xi)+2\pi\xi\cdot\nabla_\Phi+\sum_i d_i\partial_{\Phi_i}^2.$$

The phase transport term is skew-adjoint in $L^2(\pi_b)$. Integration by parts for the relative-density equation gives

$$\frac{d}{dt}\|g_t-1\|_2^2=-2\int\left[\tau_s^{-1}(\nabla_\xi g_t)^T\Sigma_s\nabla_\xi g_t+\sum_i d_i|\partial_{\Phi_i}g_t|^2\right]d\pi_b.$$

The Gaussian Poincaré inequality with covariance Σ_s and the Poincaré inequality on the 2π-periodic torus tensorize to bound $\|g_t-1\|_2^2$ by the same integral with all three coefficients replaced by one. Gronwall's inequality proves (2042). The argument extends from smooth densities by the closed Dirichlet form and semigroup approximation. □

This theorem fixes the bath parameters before proving uniqueness. It does not choose those parameters. It also does not imply a unique quantum equilibrium: the dephasing channel preserves all computational basis populations, and every diagonal spin density matrix is fixed. Existence of a unique stationary bath, uniqueness of a physical coupling and uniqueness of a quantum stationary state are distinct questions.

AE.4. *Released counts and the primary frozen comparison.* The released silicon archive contains sixteen echo acquisitions, four for each of the anti-parallel and parallel Bell families with XX and XY pulses [20] and [21]. The two pulse axes both reverse Z_i in the ideal instantaneous-pulse model; they can change the fitted carrier phase. The archive provides 4,042,000 spin-pair readouts over all settings, of which 3,440,000 belong to the declared eighty-point physical fitting windows. Its sixteen arrays include reference settings for readout correction. The original article and its echo summaries were known before this analysis. This is a retrospective archival comparison.

The previously declared product-confusion correction is applied to each acquisition, with the supplied up-reference preparation factors 0.985 and 0.966. For the first row c^T of the inverse confusion matrix and empirical four-outcome probabilities p,

$$\widehat{q}_{00} = c^T p, \qquad \operatorname{Var}(\widehat{q}_{00} \mid c) = \frac{\sum_j c_j^2 p_j - (c^T p)^2}{n}.$$

The physical fitting window excludes the first delay point, consistently with the released analysis convention. The extraction curve is

$$q_{00}(t) = e + v \min(e, 1-e) e^{-t/T} \sin(2\pi f t + \varphi), \quad 0 < e < 1, \quad 0 < v < 1. \tag{2043}$$

This parameterization keeps the model probability in $[0, 1]$. Whole last-axis acquisition blocks are resampled 256 times, retaining reference settings, sweep points and first-axis repetitions together. The physical time predictions are frozen before extracting the twelve target times. Target visibility, carrier, phase and offset are nuisance quantities in observable extraction. They do not provide a fully frozen waveform or a raw-count likelihood prediction.

Four anti-parallel XX acquisitions calibrate

$$\widehat{T}_E = 2.04120 \ \mu\text{s}, \qquad s_E = 0.11732 \ \mu\text{s}. \tag{2044}$$

The equal-weight mean is used, with variance equal to the sum of four block variances divided by sixteen. The earlier frozen Ramsey calibration supplies $r = 1.92158$, with standard error 0.18072. The fast-independent-echo branch predicts $T = \widehat{T}_E$ in every target. The separable-covariance branch predicts the same time for anti-parallel XY targets and $T = \widehat{T}_E / r = 1.06225 \ \mu$s for all parallel targets. Neither prediction is recalibrated on target decay times.

Let V_{meas} be the diagonal matrix of target block variances. The fast-model predictive covariance is $V_f = V_{\text{meas}} + s_E^2 \mathbf{1}\mathbf{1}^T$. For the separable model, set $a_i = 1$ in anti-parallel targets and $a_i = 1/r$ in parallel targets, and $b_i = 0$ or $-\widehat{T}_E / r^2$, respectively. Its covariance is

$$V_s = V_{\text{meas}} + s_E^2 a a^T + s_r^2 b b^T. \tag{2045}$$

Table 38. Target echo times extracted from released spin-pair measurements. Errors are whole-block standard errors, in microseconds. All twelve targets enter both model comparisons.

Target family and pulses	1	2	3	4
Anti-parallel XY	2.378 ± 0.413	2.236 ± 0.247	2.003 ± 0.185	1.796 ± 0.173
Parallel XX	2.064 ± 0.157	2.200 ± 0.249	2.393 ± 0.228	1.733 ± 0.139
Parallel XY	2.727 ± 0.425	2.032 ± 0.163	1.718 ± 0.139	1.496 ± 0.094

This retains uncertainty shared by predictions that use the same calibration. With $z = T_{\mathrm{obs}} - T_{\mathrm{pred}}$, report

$$Q = z^T V^{-1} z, \qquad J = Q + \log\det V + 12\log(2\pi), \tag{2046}$$

using microseconds consistently in all scores.

Table 39. Primary frozen time predictions. The tail probabilities use an approximate χ^2_{12} reference. Lower J gives the better Gaussian predictive score in the stated common unit.

Model	Q	Approximate tail	J
Fast independent echo noise	37.9817	1.55×10^{-4}	23.1177
Separable temporal covariance	71.7690	1.49×10^{-10}	57.3577

The fast-noise model improves the full score by 34.2400, yet its absolute diagnostic remains unfavorable. Thus separating the noise time scales improves the relative description but does not make one common echo time adequate for every acquisition. Six central visibility estimates reach the declared upper bound; the highest bootstrap upper-bound fraction is 0.9258. Non-Gaussian fitted-observable errors, unrecorded between-acquisition dependence and preparation uncertainty limit the tail-probability approximation. No additional drift variance is fitted to improve either primary result.

AE.5. *A duration-conditioned development analysis.* The original acquisitions have four averaging-duration classes, approximately 47, 66, 100 and 148 minutes. The primary comparison ignores variation between these classes. After its target outcomes were known, a secondary model was formulated: use the corresponding anti-parallel XX time as calibration for each duration class. This is a post-exposure development analysis. The acquisition classes do not establish simultaneous measurements, equal bath realizations or a causal law relating averaging duration to dephasing rate.

The four registered calibration values are

$$\widehat{t} = (2.12687,\ 2.25623,\ 2.03848,\ 1.74324)^T\ \mu\mathrm{s}. \tag{2047}$$

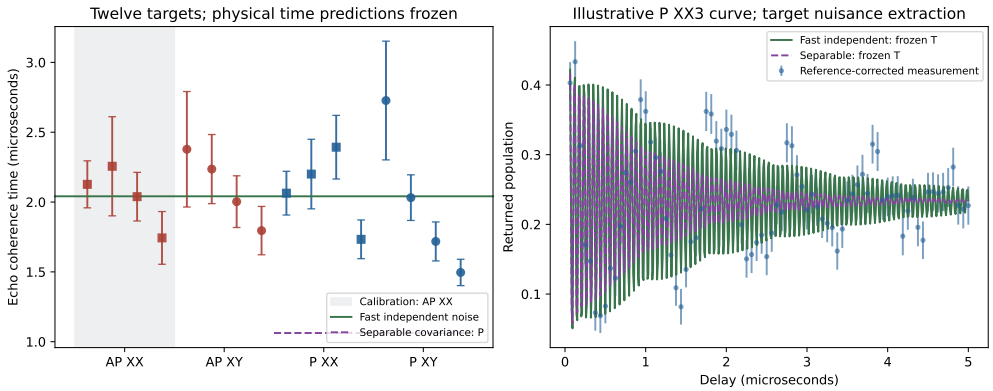


Figure 74. Frozen physical time predictions and all twelve target measurements. The shaded group supplies the four calibration times. The right panel illustrates one target curve using target-extracted carrier and visibility nuisance quantities; it is not a frozen raw-count waveform prediction.

They are measured environment-specific inputs. No target time is used to determine them. For the twelve targets, let $A_{ij} = 1$ if target i belongs to duration class j, and zero otherwise. Each row of A has exactly one nonzero entry. The fast-noise prediction and covariance become

$$T_f = A\widehat{t}, \qquad V_f = V_{\mathrm{meas}} + A\,\mathrm{diag}(s_j^2)A^T. \tag{2048}$$

The competing separable model uses exactly the same four calibration inputs, with the parallel times divided by the frozen Ramsey ratio. Its calibration Jacobian with respect to $\widehat{t}$ is $\mathrm{diag}(a)A$, and its ratio derivative is $b_i = -(A\widehat{t})_i/r^2$ in parallel targets and zero otherwise. This specifies its covariance without adding a target-fitted variance.

Table 40. Post-exposure duration-conditioned comparison. The target set is unchanged, but this model choice was made after seeing primary results and is not an independent confirmation.

Model	Q	Approximate tail	J
Duration-conditioned fast noise	13.9344	0.3049	3.8248
Duration-conditioned separable noise	59.6138	2.65×10^{-8}	48.1793

The fast model's score improves by 44.3545 relative to the equally conditioned separable model. A centered marginal block-bootstrap null calculation, with 20,000 draws and shared calibration errors, gives a tail probability of 0.2874 with Monte Carlo standard error 0.0032. It checks sensitivity to the

normal approximation; it does not correct model selection after exposure or unknown cross-run dependence. The result is compatible with a common fast-noise sensitivity within the registered duration classes under the stated error approximation. It does not certify the noise time scales or establish duration as the physical cause of heterogeneity.

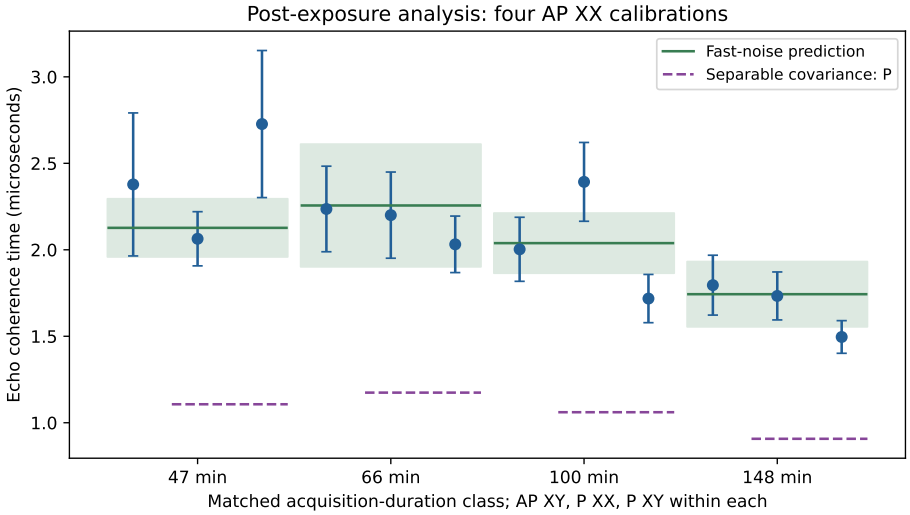


Figure 75. Secondary duration-conditioned predictions. Each green line and band use one anti-parallel XX calibration and its block error; blue points are anti-parallel XY, parallel XX and parallel XY targets. Dashed lines show the separable-covariance parallel prediction.

The pooled reconstructions, using all sixteen acquisitions only as a descriptive check, are 2.072 ± 0.090 μs for the anti-parallel family and 2.045 ± 0.078 μs for the parallel family. They are close to the article's reported 2.03 ± 0.09 and 1.98 ± 0.09 μs. The present probability constraints and whole-block uncertainty method differ from the original extraction, so exact numerical agreement is not assumed. These pooled values do not enter either prediction calibration.

AE.6. *What the comparison establishes and what a new test requires.* The calculations show why one spatial covariance multiplied by one temporal kernel is a substantive restriction. A classical two-scale Gaussian bath can relax it while retaining completely positive spin evolution, the local–Bell waveform identity and a unique invariant bath law. The archival comparison favors this relaxation. The duration-conditioned analysis is a development description: its absolute agreement depends on how dependence between acquisition blocks is treated. Neither regrouping acquisitions nor propagating their instrument

errors establishes independent predictive agreement. The primary discrepancy is retained.

The construction does not repair the earlier mismatch between Bell and separately measured single-qubit amplitudes. It does not identify a unique physical mother coupling or measure the distinct ground excitation–Bell–filter-yield relation. Conventional quantum dynamics with the same Hamiltonian and noise assumptions makes the same predictions. Physical credibility of a distinctive mother-model constraint therefore requires an additional matched measurement.

For a prospective noise test, fix the control pulses, analysis window, duration classes, readout-reference model, preparation-error bounds and dependence assumptions before exposing new outcomes. Independently calibrate the bath rates and slow-memory bounds in each registered environment. Freeze them and measure both local envelopes and both Bell envelopes in interleaved, matched runs. Test (2034) at the waveform level, together with (2038) and the uncertainty propagated from the instrument references. Data from a different device cannot supply the missing calibration numerically. A failure must remain visible; changing the bath after seeing it creates another development model.

Appendix AF. Cosmological fate: local equilibration and global non-extinction

The equilibrium construction developed above is a statement about a probability law on a declared state space. It does not, by itself, determine the scale factor of an expanding universe or its asymptotic thermodynamic fate. This section makes the missing cosmological interface explicit. In particular, it distinguishes three notions that are often conflated: equilibration in a bounded laboratory region, disappearance of usable free energy in every bounded region, and extinction of all macroscopic free-energy density in an infinite or expanding universe. The distinction is essential for the claim that local systems may approach equilibrium while the global universe need not become thermodynamically empty.

AF.1. *Operational definitions and order of limits.* Let t denote cosmological proper time in a chosen FLRW chart and let t_{s} denote the stochastic parameter used by the finite-regulator construction. No identification $t = t_{\mathrm{s}}$ is made here. A physical clock calibration is an additional map, as required in Section 4.1; in a relativistic realization it must agree with the proper-time relation $d\tau^2 = -g_{\mu\nu}dx^\mu dx^\nu$ (with $c = 1$).

For a bounded comoving region R with physical volume $V_R(t) = a(t)^3 V_R(0)$, write $\mathcal{F}_R(t)$ for its nonequilibrium available free energy relative to the selected local equilibrium reference. The reference subtracts the equilibrium vacuum contribution. Thus a constant cosmological vacuum density is not counted as usable free energy. A convenient definition is

$$\mathcal{F}_R(t) = \int_{R(t)} \big[\rho - Ts - \sum_j \mu_j n_j\big]_{\mathrm{av}}\, dV, \qquad \mathcal{F}_R(t) \geq 0, \tag{2049}$$

where the subscript av means that the equilibrium reference has been subtracted and that the same coarse-graining convention is used at all times. We call R locally equilibrated if

$$\mathcal{F}_R(t) \longrightarrow 0, \qquad \int_{R(t)} \sigma(x,t)\, dV \longrightarrow 0 \quad (t \to \infty), \tag{2050}$$

where $\sigma \geq 0$ is the physical entropy-production density after reservoir and boundary terms have been included. Equation (2050) does not state that microscopic motion ceases; an invariant Gibbs law generally has nonzero fluctuations.

For an increasing family of comoving regions R_L, define the spatially averaged available free-energy density by

$$\overline{f}_L(t) = \frac{1}{V_{R_L}(t)} \mathcal{F}_{R_L}(t). \tag{2051}$$

The global heat-death statement is an assertion about a specified order of limits. One infinite-volume-first version is $\lim_{t\to\infty}\lim_{L\to\infty}\overline{f}_L(t)=0$, whereas an infinite-volume or expanding-universe non-extinction statement requires a positive lower limit or a nonvanishing limsup in the same declared observable. The limits $t\to\infty$ and $L\to\infty$ need not commute. Consequently, local equilibration alone neither proves nor disproves global heat death.

AF.2. *The cosmological interface of the master model.* Take the homogeneous and isotropic ansatz

$$ds^2=-N(t)^2dt^2+a(t)^2\gamma_{ij}dx^idx^j,\qquad {}^{(3)}R[\gamma]=6k,\quad k\in\{-1,0,1\}. \tag{2052}$$

The lapse N is retained until the field equation has been varied. To identify the source without counting the gravitational term twice, split the selected effective master action before variation:

$$\mathcal{S}_{\rm M}^{\rm eff}=\frac{1}{2}\int\sqrt{-g}\,M^2(R-2\Lambda_L)\,d^4x+\mathcal{S}_{\rm src}+\mathcal{S}_{\rm corr},\qquad M^2=(8\pi G_{\rm eff})^{-1}>0. \tag{2053}$$

Here Λ_L is the Lorentzian cosmological constant with dimensions of inverse length squared. The corresponding vacuum-energy density is $\rho_{\rm vac}=M^2\Lambda_L$; on the same continued branch it is the quantity denoted $\Lambda_{\rm eff}$ in (188), so $\Lambda_L=8\pi G_{\rm eff}\Lambda_{\rm eff}$. Keeping these quantities distinct is necessary both in the action and in the Friedmann equation. All three terms must come from the same matched action and selected state law. The source action contains the retained matter and other source fields; the correction action contains the higher-curvature and other terms whose metric variations are placed in the remainders. If M^2 or Λ_L depends on scalar fields, vary its covariant field dependence before imposing homogeneity. The source stress is

$$T^{\rm eff}_{\mu\nu}:=-\frac{2}{\sqrt{-g}}\frac{\delta\mathcal{S}_{\rm src}}{\delta g^{\mu\nu}},\qquad \rho_{\rm eff}=T^{\rm eff}_{\mu\nu}u^\mu u^\nu,\qquad p_{\rm eff}=\frac{1}{3}T^{\rm eff}_{\mu\nu}h^{\mu\nu}, \tag{2054}$$

where u^μ is the comoving unit vector and $h^{\mu\nu}=g^{\mu\nu}+u^\mu u^\nu$. Varying the *full* action in this definition would instead include $-M^2(G_{\mu\nu}+\Lambda_L g_{\mu\nu})$ in the putative source, and that full Euler derivative vanishes on a solution. It therefore cannot serve as the source in an Einstein equation with that same gravitational term already on the left.

For a scalar-dependent M^2, the metric variation of (2053) gives

$$G_{\mu\nu}+\Lambda_L g_{\mu\nu}=M^{-2}T^{\rm eff}_{\mu\nu}+\Delta_{\mu\nu}, \tag{2055}$$

$$\Delta_{\mu\nu}:=-M^{-2}\left[(g_{\mu\nu}\Box-\nabla_\mu\nabla_\nu)M^2+\frac{2}{\sqrt{-g}}\frac{\delta\mathcal{S}_{\rm corr}}{\delta g^{\mu\nu}}\right].$$

Here M^{-2} means $1/M^2 = 8\pi G_{\text{eff}}$. With cosmic proper time $N = 1$, put $\Delta_{00} = \Delta_{\mu\nu}u^\mu u^\nu$ and $\Delta_s = h^{\mu\nu}\Delta_{\mu\nu}/3$. The action-derived remainders are

$$\mathcal{R}_H = \frac{\Delta_{00}}{3}, \qquad \mathcal{R}_{\dot{H}} = -\frac{\Delta_{00} + \Delta_s}{2}. \tag{2056}$$

Any additional regulator, state-law or coarse-graining residual must be matched and added to these projections. In particular, if only the field dependence of M^2 is retained, writing $z(t) = M^2(t)$ gives $\mathcal{R}_H = -H\dot{z}/z$ and $\mathcal{R}_{\dot{H}} = (H\dot{z} - \ddot{z})/(2z)$. Thus a varying Newton coefficient cannot be inserted while silently discarding its metric-variation terms. The reduced equations have the form

$$H^2 = \frac{8\pi G_{\text{eff}}}{3}\rho_{\text{eff}} - \frac{k}{a^2} + \frac{\Lambda_L}{3} + \mathcal{R}_H, \tag{2057}$$

$$\dot{H} = -4\pi G_{\text{eff}}(\rho_{\text{eff}} + p_{\text{eff}}) + \frac{k}{a^2} + \mathcal{R}_{\dot{H}}, \tag{2058}$$

with $H = \dot{a}/a$ after setting $N = 1$. The Bianchi identity gives the compatibility equation

$$\dot{\rho}_{\text{eff}} + 3H(\rho_{\text{eff}} + p_{\text{eff}}) = Q_{\text{eff}}, \tag{2059}$$

where Q_{eff} is the exchange with the remaining variables. These equations constrain that exchange. For differentiable coefficients with $G_{\text{eff}} > 0$, differentiating (2057) and substituting (2058) gives

$$Q_{\text{eff}} = -\frac{\dot{G}_{\text{eff}}}{G_{\text{eff}}}\rho_{\text{eff}} - \frac{\dot{\Lambda}_L}{8\pi G_{\text{eff}}} + \frac{3}{8\pi G_{\text{eff}}}(2H\mathcal{R}_{\dot{H}} - \dot{\mathcal{R}}_H). \tag{2060}$$

No division by H is used, so the identity also applies at a turnaround. A separately conserved sector has $Q_{\text{eff}} = 0$, which requires the right side to vanish; the coupling, vacuum term and two remainders cannot be chosen independently. A cosmological prediction therefore requires these quantities and their error bounds to be matched to the same action and state law.

The thermodynamic interface is an entropy balance, not an identification of entropy with the scale factor:

$$\frac{dS_R}{dt} = \int_{R(t)} \sigma\, dV - \int_{\partial R(t)} J_s \cdot n\, dA, \qquad \sigma \geq 0. \tag{2061}$$

For a globally closed system the boundary flux is absent only after a global boundary condition has been stated. In an expanding spacetime, the physical boundary of an observational region and the causal horizon are distinct, so one must specify which of them enters (2061).

AF.3. *Conditional local equilibration theorem.* The next result states the physical-clock and dissipation conditions needed to transfer a finite-regulator entropy estimate to a comoving region. An invariant probability law alone does not identify relative-entropy loss with total physical entropy production.

THEOREM 188 (Local asymptotic equilibration). *Fix a bounded comoving region R and $[t_0,\infty)$. Assume that the projected Markov evolution has a fixed invariant law π_R. For a fixed $\theta>0$, let $\mathcal{F}_R(t)=\theta\,\mathrm{KL}(\mu_t\|\pi_R)$ be finite initially and locally absolutely continuous in physical time. Suppose the matched energy balance and entropy coercivity estimate are*

$$\mathcal{F}_R'(t)=-\mathcal{D}_R(t),\qquad \mathcal{D}_R(t)\ge\lambda_R\mathcal{F}_R(t)\ge 0\quad \textit{for almost every } t,\qquad \lambda_R>0.$$

Boundary and driving terms must be absent or already included in this balance. Then

$$\mathcal{F}_R(t)\le\mathcal{F}_R(t_0)e^{-\lambda_R(t-t_0)},\qquad \int_{t_0}^{\infty}\mathcal{D}_R(t)\,dt\le\mathcal{F}_R(t_0). \tag{2062}$$

If, in addition, $\mathcal{D}_R$ has a nonnegative uniformly continuous representative on $[t_0,\infty)$, and the physical entropy-production rate obeys

$$0\le\Sigma_R(t):=\int_{R(t)}\sigma\,dV\le C_R\mathcal{D}_R(t),\qquad 0<C_R<\infty,$$

then $\mathcal{D}_R(t)\to 0$, $\Sigma_R(t)\to 0$, and (2050) holds.

Proof. The energy balance and coercivity give $\mathcal{F}_R'\le-\lambda_R\mathcal{F}_R$. Gronwall's inequality proves the exponential bound. Integration of the balance and nonnegativity of $\mathcal{F}_R$ prove the integral bound. For the additional conclusion, suppose $\mathcal{D}_R(t_n)\ge\varepsilon>0$ along $t_n\to\infty$. Uniform continuity supplies one $h>0$ such that $\mathcal{D}_R(t)\ge\varepsilon/2$ whenever $|t-t_n|\le h$. Choose a subsequence with disjoint intervals of this fixed length. Their integrals have an infinite sum, contradicting (2062). Thus $\mathcal{D}_R\to 0$; the stated comparison then gives $\Sigma_R\to 0$. □

The entropy estimate above may follow from an appropriate logarithmic Sobolev inequality [85] and [9]. A Poincaré inequality alone controls a quadratic deviation and does not give this relative-entropy estimate for arbitrary initial densities. The comparison with Σ_R is also substantive: an invariant nonequilibrium law can have zero relative-free-energy loss and positive stationary physical entropy production. A reversible isothermal realization with correctly included reservoirs can supply the required comparison.

For example, on a circle of length L, the driven diffusion $dX_t=v\,dt+\sqrt{2\kappa}\,dW_t \pmod L$, with $\kappa>0$ and constant $v\neq 0$, preserves $\pi=1/L$. Starting at π gives $\mathcal{F}=\mathcal{D}=0$, while its stationary current $j=v/L$ yields the path entropy rate $\int_0^L j^2/(\kappa\pi)\,dx=v^2/\kappa>0$. Under local detailed balance, the corresponding physical entropy rate is k_Bv^2/κ. Thus even at stationarity the comparison with $\mathcal{D}$ fails for a driven realization; it is not a consequence of Gibbs invariance [49].

Continuity without uniform continuity does not suffice for the final limit. For an explicit scalar example on $t\ge 0$, put

$$a_n=\tfrac14 e^{-2n},\qquad b_n(t)=\max\{1-|t-n|/a_n,0\},$$

$$D(t) = e^{-t} + \sum_{n\geq 1} b_n(t), \qquad F(t) = \int_t^\infty D(s)\, ds.$$

The sum is locally finite. Each triangular pulse has area a_n, so D is continuous and integrable, $F' = -D$, and $F \to 0$. For a pulse contributing to the tail, $t \leq n + a_n \leq n + 1$, hence $e^t \int_t^\infty b_n \leq e^{1-n}/4$. Summing gives $F(t) \leq [1 + e/(4(e-1))]e^{-t} < 2e^{-t}$, and therefore $D \geq F/2$. Nevertheless $D(n) = 1 + e^{-n}$, so D does not tend to zero. Figure 76 displays this failure of the inference from integrability to a pointwise limit.

The theorem is local. The constant λ_R may depend on the region, the expansion history, and the regulator. A uniform lower bound in R is an additional thermodynamic-limit hypothesis and is generally unavailable for long-wavelength modes.

AF.4. *Global non-extinction criterion.* Let $f_{\mathrm{av}}(t)$ denote a homogeneous available free-energy density after the equilibrium vacuum term has been removed. The entropy balance alone does not determine this density: the energy balance, temperature, reference state and mechanical work must also be specified. Suppose that this thermodynamic matching yields the volume balance

$$\frac{d}{dt}\big(a(t)^3 f_{\mathrm{av}}(t)\big) = a(t)^3\big(q_{\mathrm{av}}(t) - \chi_{\mathrm{av}}(t)\big), \qquad q_{\mathrm{av}}, \chi_{\mathrm{av}} \geq 0, \tag{2063}$$

where q_{av} is the positive part of the matched supply, including transport and work, and χ_{av} contains irreversible loss and any negative part of that supply. Temperature and reference-state changes, if present, also enter the supply. In particular, χ_{av} cannot be identified with temperature times entropy production without an additional isothermal matching argument. The symbols in (2063) are not free parameters: a closed model must calculate them from the master action, the state law, and the cosmological solution.

Theorem 189 (Conditional global non-extinction). *Suppose $a > 0$ and $a^3 f_{\mathrm{av}} \geq 0$ are locally absolutely continuous, $a^3(q_{\mathrm{av}} - \chi_{\mathrm{av}})$ is locally integrable, and* (2063) *holds almost everywhere. If*

$$\limsup_{t\to\infty} \frac{1}{a(t)^3}\left[a(t_0)^3 f_{\mathrm{av}}(t_0) + \int_{t_0}^t a(s)^3\big(q_{\mathrm{av}}(s) - \chi_{\mathrm{av}}(s)\big)\, ds\right] > 0, \tag{2064}$$

then the global spatially averaged available free energy does not converge to zero. Writing $B(t)$ for the bracket, heat death in this observable is equivalent to $B(t)/a(t)^3 \to 0$. In particular, $B(t) \to 0$ is sufficient if $\inf_{t\geq t_0} a(t) > 0$. This lower bound holds on a noncontracting branch with $a(t_0) > 0$.

Proof. Integration of (2063) gives exactly $f_{\mathrm{av}}(t) = B(t)/a(t)^3$. The limsup condition therefore proves the non-extinction assertion, and the normalized limit

proves the heat-death assertion. If $a(t) \geq a_* > 0$, then $0 \leq f_{\mathrm{av}}(t) \leq B(t)/a_*^3$, which proves the stated sufficient condition. Without a lower bound on volume, it is false: $a(t) = e^{-t}$, $B(t) = e^{-3t}$ and $f_{\mathrm{av}}(t) = 1$ satisfy the balance with $q_{\mathrm{av}} = 0$, $\chi_{\mathrm{av}} = 3$. The total available energy tends to zero but its density stays constant. □

The criterion is the integrated balance expressed in terms of the observable density. It does not derive the required source or loss from the mother dynamics, nor does it construct a cosmology in which local equilibration and global non-extinction coexist. Such a construction must also justify the spatial limit and the order of limits.

The criterion is conditional rather than a new axiom. For an isolated system of fixed physical volume satisfying the local decay hypotheses of Theorem 188, $q_{\mathrm{av}} = 0$ after the initial preparation and the theorem reduces to ordinary asymptotic heat death. For an infinite-volume system, a cosmologically expanding background, or a nonequilibrium steady state sustained by a derived flux, the source term may remain nontrivial. This possibility must be demonstrated by (2057)–(2059) and (2063); it cannot be inferred from the words "equilibrium" or "minimum action" alone.

AF.5. *Why finite-time extinction is not the generic prediction.* Assume on a bounded interval that the local free-energy balance satisfies $|d\mathcal{F}_R/dt| \leq C\mathcal{F}_R$

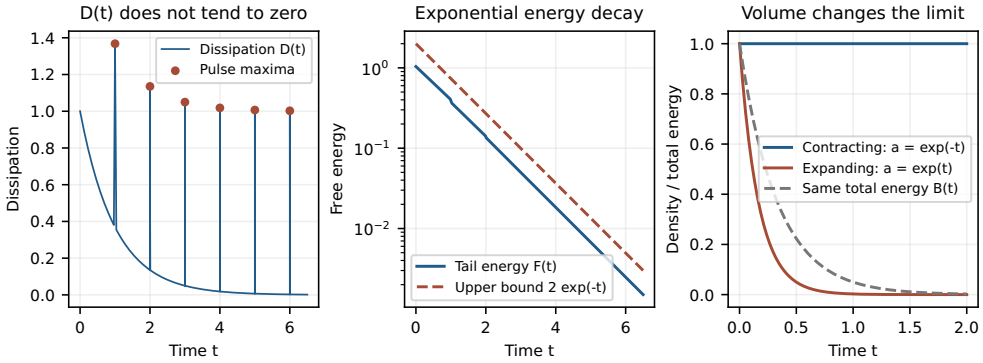


Figure 76. Analytic counterexamples evaluated numerically in dimensionless units. Left: the continuous integrable dissipation D retains pulses of height greater than one. Middle: its tail F still obeys an exponential bound and $F' = -D$. Right: the same total energy $B = e^{-3t}$ gives density e^{-6t} for $a = e^t$, but constant density for $a = e^{-t}$. These are tests of limiting arguments, not observations or solutions of a matched cosmological field theory.

with finite C. Gronwall's inequality gives

$$\mathcal{F}_R(t) \geq \mathcal{F}_R(t_0)e^{-C(t-t_0)} > 0 \quad \text{whenever } \mathcal{F}_R(t_0) > 0. \tag{2065}$$

Thus exact extinction can occur only asymptotically under this regularity condition. This mathematical statement does not imply that an observer has access to unlimited time or volume; causal horizons and finite experimental resolution must be included in any operational claim.

AF.6. *Relation to the observed expanding universe.* The currently standard observational comparison is the ΛCDM branch, in which a positive late-time vacuum term gives asymptotically positive H and no recollapse for the usual parameter range [131]. This is an empirical benchmark, not a consequence of the present master model. A claimed departure must be tested through a frozen forward map

$$\vartheta \longmapsto \{H(z), D_A(z), D_L(z), f\sigma_8(z), \text{CMB distance and growth summaries}\}, \tag{2066}$$

with parameters calibrated on one declared data set and evaluated without refitting on an independent set. The likelihood, nuisance parameters, selection cuts, and covariance matrix must be frozen before the holdout is opened. A successful fit of $H(z)$ alone would not establish the global non-extinction condition (2064); the latter also requires a thermodynamic observable or a derived free-energy proxy.

For the same reason, the present paper does not claim that the universe is proven to avoid heat death. The mathematically supported statement is the following conditional implication:

$$\begin{aligned} &\text{local spectral-gap equilibration} \\ &\quad + \ \text{derived expanding-volume source satisfying(2064)} \\ &\qquad \Longrightarrow \quad \text{local equilibrium with global non-extinction} \\ &\qquad\qquad\qquad\qquad \text{in the declared observable.} \end{aligned} \tag{2067}$$

The converse is false: local equilibration by itself supplies no information about the global limit. Closing this interface is therefore a concrete, falsifiable cosmological extension of the programme rather than a retrospective interpretation of the finite-regulator results.

AF.7. *Reproducible cosmological calculation protocol.* For a numerical implementation, one first derives the dimensionless system $a' = aH$, $\rho_i' = -3H(\rho_i + p_i) + Q_i$, and the free-energy balance (2063) on a fixed redshift or time interval. The following checks are required before a physical conclusion is reported:

(i) vary the time step and integration tolerance until H, ρ_i, a, and f_{av} change below a predeclared threshold;

(ii) verify the Friedmann constraint and the continuity residual at every saved time;
(iii) propagate an ensemble of initial laws and check positivity of all densities and of f_{av};
(iv) repeat the calculation for increasing spatial boxes and report the order of limits in t and L;
(v) compare the frozen prediction with held-out expansion and growth data, while reporting the ΛCDM likelihood and a posterior-predictive check as a control model.

No cosmological numerical value is inserted in this section without a declared action, parameter registry, calibration set, and public data provenance. The existing finite-regulator turbulence and response calculations therefore remain evidence for their stated sectors only; they are not silently promoted to a measurement of the cosmic fate.

Appendix AG. Assumptions connecting the finite and continuum branches

The finite construction, its physical applications, and a continuum limit require different data. Let $\mathsf{C}_{\mathrm{core}}$ denote the finite-regulator data used in the main construction: the declared state space and gauge quotient, master action, mobility, noise covariance, reference measure, boundary conditions, and the finite-dimensional or Galerkin generator. Let $\mathsf{A}_{\mathrm{app}}$ denote optional physical applications, such as the complete massive Kerr response or a cosmological forward map. Finally, let $\mathsf{M}_{\mathrm{cont}}$ denote the additional compactness, tightness, renormalization, and martingale-problem hypotheses required for a regulator-independent continuum statement.

The dependency structure is

$$\mathsf{C}_{\mathrm{core}} \longrightarrow \begin{cases} \text{finite-regulator variational identities,} \\ \text{finite-regulator invariant-law and entropy results,} \\ \text{conditional effective-sector and Galerkin results,} \end{cases} \qquad (2068)$$

$\mathsf{A}_{\mathrm{app}}$ and $\mathsf{M}_{\mathrm{cont}}$ are additional branches.

Remark 190 (Dependencies of the finite construction). *The finite-regulator variational identities, Gibbs and entropy balances, and finite Galerkin energy identities use their stated action, generator, integrability, and boundary hypotheses. They do not use a massive Kerr calculation or a cosmological data fit. If a physical application supplies a coefficient, boundary condition, or reference measure used in one of these identities, that input becomes part of its hypotheses. Such a dependency must be retained when the identity is applied.*

The complete massive nonzero-spin Kerr response and a cosmological expansion-data analysis require additional forward models. Each must specify its action, boundary conditions, shared parameters, numerical errors, and independent comparison data before it supplies a quantitative test of the common physical parameters.

Remark 191 (Continuum limits require a specified family). *The passage from a regulator indexed by N to a continuum law is a separate mathematical assertion. It requires, for example,*

$$\pi_N \Rightarrow \pi, \qquad P_t^{(N)} \Rightarrow P_t,$$

uniform energy and moment estimates, tightness, identification of the limiting generator or martingale problem, and preservation of the relevant constraint and entropy inequalities. The topology of semigroup convergence and the identification maps between state spaces must also be specified. Section 10.18 gives sufficient compactness and martingale-identification hypotheses. The explicit nonlinear scalar realization separately constructs its continuous-space law, invariant measure, and convergent spectral approximations. That example fixes the background geometry and smoothing powers; it does not provide these limits for the full geometric, gauge, and matter system.

For the full field system, the remaining mathematical problem is to prove uniform estimates for its actual coefficients and then identify the limiting generator, constraints, and observables. The physical problem is to determine whether the resulting shared parameters predict observations outside the calibration set. Neither problem is resolved by the finite-dimensional identities alone.

Appendix AH. **Detailed connections with the sector constructions**

The following reading guide collects the connections between the common principles and the specialized results. It complements the representative models in Section 2 and records the conditions used in each field, stochastic and observation branch.

AH.1. *Reconstruction and coefficient identification.* Reconstruction of the underlying model is therefore a separate inverse problem. At a fixed regulator, Section 15.29 shows how a calibrated generator determines drift and covariance, and how specified Gibbs data determine energy, mobility and stationary current. Within an independently fixed reduced-action basis, Proposition 93 proves coefficient uniqueness through a positive Gram matrix and gives a quantitative stability estimate. Exact equilibrium, sampling and hidden-state examples identify information that these conditional results cannot supply. This provides

a constructive criterion for model identification without presuming a new physical selection principle.

Section 15.30 implements that criterion on a square plaquette of the existing compact-group lattice model. Haar orthogonality and Gaussian integration give its six-by-six coefficient Gram matrix exactly. A uniform lower bound for the declared scalar-exponent interval yields an explicit inverse-error estimate. Vanishing edge weights and a duplicated operator show how identification can fail outside the stated hypotheses. This supplies a concrete link between the finite-regulator existence theorem and coefficient recovery, with applications to calibrated inverse problems and regulator design. For a four-dimensional periodic family, the normalized Gram matrix is independent of lattice volume, and Theorem 96 gives one coefficient-recovery bound for every side length at least three. Volume uniformity here does not assume the distinct continuum limit. The added joint-recovery certificate makes the reduction explicit: a generator defect gives a Dynkin error bound, the common diffusion gives cross-covariances through the carré du champ, and a strongly convex Legendre map gives quantitative action-to-Hamiltonian remainder bounds. For a generally covariant branch, the ADM lapse and shift generate first-class constraints whose stochastic preservation is required separately. These are finite-regulator conditional statements, not an unconditional mother-model uniqueness theorem.

AH.2. *Physical branches and their observation requirements.* Time enters this problem through causal order, duration measured by physical clocks, and asymmetry of path statistics. A Lorentzian metric specifies the first two; a stochastic law and its physical reversal specify the third. Sections 14.17, 14.11 and 14.21 give these definitions and their conditional connections. Section 14.28 then provides a complete finite realization in which one set of couplings fixes mechanical motion, stationary statistics, heat transport and a projected memory kernel. This example establishes simultaneous compatibility for those branches without identifying its coordinates with the unconstructed continuum field theory.

Appendix AB gives a concrete finite quantum test. Two calibration quantities in a declared single-flip branch determine an unmeasured excitation and Bell response; explicit alternative operators show which kinetic premise this relation tests. A separate frozen comparison on two public Bell runs improves predictive score over a full Bell-local competitor but has poor absolute fit. These different outcomes distinguish a derived prospective relation from a completed, limited experimental benchmark.

Appendix AD supplies explicit apparatus and state tolerances for the joint spectral–Bell–filter prediction. It also calculates a separate frozen transfer of public silicon Bell coherence times. Distinct channels improve agreement

over a common-time comparator, while absolute agreement and fixed single-qubit noise amplitudes remain unfavorable under the declared uncertainty model. The data constrain a conditional noise branch; they do not measure the excitation–Bell–filter relation.

AH.3. *Recovery, additional predictions, and experimental choice.* Recovering an established equation is a necessary consistency test. An additional prediction must constrain an observable that was not used to choose the relevant inputs. A further question is whether another theory imposes the same constraint. These three questions have different answers: a correct limit can be shared by many theories, and a successful prediction of one effective model need not determine its microscopic origin. We use this distinction to choose between the observational routes developed below.

The stellar scalar calculation illustrates a limitation of the current matter specification. A background equation of state $\varepsilon_0(n)$ does not determine the derivative of $\varepsilon_J(n,x) = \varepsilon_0(n) + xh(n)$ at $x = 0$. The added term leaves the background energy and pressure unchanged but changes the scalar source by $h(n)$. Section 21 propagates this freedom to the stellar response. In the two-source truncation, Proposition 106 gives a cross-binary prediction, including its sign ambiguity. An additional common density response changes the target while preserving two calibrations. Microscopic matching must therefore determine or bound the unresolved response. More accurate integration of the same background equations does not provide that missing information.

This obstruction concerns a particular interface; it does not prevent every conditional test of the framework. The phase-noise construction in Appendix AE, for example, predicts coherence under several control sequences once the same bath and observation parameters are fixed. A single spatial covariance times one temporal kernel imposes a control-independent logarithmic Bell-envelope ratio. A slow–fast bath relaxes that restriction in a specified way. Both statements can be tested without determining a nuclear scalar charge. They test an environmental model within the stated quantum measurement rules, not a derived violation of quantum mechanics or an objective-collapse law.

A related single-qubit measurement makes the role of temporal memory particularly explicit. Consider an autonomous stationary two-state environment with switching generator Q, total switching rate $s > 0$, stationary row law w^T, and positive phase-decay rates $R = \operatorname{diag}(r_1, r_2)$. Put $K_d = e^{(Q-R)d}$ and $W(d) = w^T K_d \mathbf{1}$. The spin is prepared afresh for each shot, while readout and preparation do not change the environment. Phase increments and outcome randomness are independent between shots conditional on the environment path. For phase-aligned binary outcomes X_1, X_2, shot duration d, and end-to-start

gap g, these assumptions give

$$\mathrm{Cov}(X_1, X_2) = \frac{W(2d) - W(d)^2}{4} e^{-sg}. \tag{2069}$$

To see this, write $\Pi = \mathbf{1}w^T$, so that $e^{Qg} = \Pi + e^{-sg}(I - \Pi)$, and use the outcome map $B_1 = (e^{Qd} + K_d)/2$. Stationarity cancels the terms containing e^{Qd} in the covariance, leaving $e^{-sg} w^T K_d (I - \Pi) K_d \mathbf{1}/4$. The semigroup identity $K_d^2 = K_{2d}$ proves (2069). Independent readout errors multiply its right side by the squared readout visibility. Correlated detector errors do not obey this rule. The test concerns the stated relation between marginal and joint observations; repeated readout itself is an established method of studying environmental fluctuations [67] and [166].

This route has a useful comparator. A suitable static mixture can reproduce the whole single-shot envelope W, yet predicts a gap-independent covariance when its label is retained within a pair. Calibrating the envelope and one rate, then predicting unused gaps, therefore tests more than goodness of fit to a decay curve. The preparation of labels across different pairs, instrument calibration and the complete chronological record law must also be specified. Agreement would support this effective environmental description; other mechanisms with the same record law would remain indistinguishable.

Two further routes concern different observations. For several clocks or cavities sampling one coherent scalar amplitude, independently matched linear responses give a rank-one signal cross-spectrum and fixed complex response ratios. Shared instrumental noise can mimic rank one, so the field interpretation requires additional controls. Within the declared 331 representation class, one nonuniversal family projector gives relations between neutral-current couplings. These constrain that particle model but do not select the representation class or its mass scale. Cosmological histories similarly become predictions after a potential, matter coupling and initial-data distribution are specified. An oscillating quadratic scalar has a matter-like averaged pressure; this familiar limit does not identify the observed dark matter without parameter and data matching.

The practical ordering is consequently determined by identifiable inputs and achievable errors. A laboratory noise experiment can first calibrate its observation map and test a frozen joint law. A stellar test additionally needs composite-matter matching and consistent massive propagation. A cosmological or particle test must retain its own source, vacuum, threshold and nuisance parameters. The common framework is supported more strongly only when independently fixed shared inputs restrict several such tests simultaneously.

Methodological logic: contradiction, recovery, and extension. The methodological model is the use of thought experiments to expose an incompatibility between otherwise successful principles and then to search for a structure in

which the incompatibility disappears. A thought experiment is not a substitute for a physical premise: its force comes from applying the declared principles to an idealized situation and deriving their unavoidable consequences. The same distinction is essential here. The proposed variational–stochastic architecture is first required to be internally consistent, to preserve the declared constraints, and to recover established theories in controlled limits. Only its additional consequences—for example, a regulated equilibrium sector or a correlated near-horizon response— constitute new physical hypotheses. Thus the mathematical implication is understood in the precise form

$$\text{fixed assumptions and mother equation} \Longrightarrow$$
$$\text{mathematically necessary consequences}$$

whereas the claim that the extended theory describes nature requires that its non-classical consequences survive independent physical tests. This separation identifies which part of the argument is a logical reconstruction and which part is an empirical hypothesis.

Section X connects this common-origin question to the autonomous isothermal second law and the geometry of stationary black-hole exteriors [100] and [101]. An exact cost–generator compatibility identity gives one class in which dynamic programming selects the same drift that preserves the master Gibbs law. It separates free-energy relaxation from maintained path irreversibility, controls the observation defect, and specifies the constraint-tangency conditions needed by a stochastic field realization. The Schwarzschild and rotating Kerr examples then show why statistical convergence cannot be used in place of a local gravitational completion.

Appendix AA makes the quantum dependencies constructive. The fixed reversible generator determines an auxiliary transfer state; declared gauge constraints determine an invariant-space projection. Ground or thermal preparation then selects a state after physical-time identification. An affine probability assignment on the full quantum effect space has a unique trace representation, but its operational premises are additional. A family of completely positive lifts gives identical configuration records with different coherences, and a sharp repeatability theorem identifies when measurement updates are unique. These results separate the consequences of one specified realization from selection of its physical quantum interface. Section Z adds a scale-consistency test: exact block elimination preserves a frequency-dependent response, while its memory, noise, projected entropy, and observed symmetry charges must be reduced together. A constructive continuous-bath example has explicit kernel and response errors; the associated spectral exponent remains a declared input.

The selection mechanism is made explicit in Appendix M. Dynamic programming and the stochastic maximum principle act on the same regulated

objective, including its state and density derivatives. A symmetry calculation gives a local-martingale analogue of a Noether charge, its symmetry-breaking balance, and conditions for recovering classical conservation at zero diffusion. The companion quadratic realization connects one selected feedback to equilibrium, relaxation and independently calibrated response channels; the input weights are kept distinct from the quantities selected by optimization.

Appendix N extends this balance to smooth state transformations with the required Itô correction. It derives charge covariances and symmetry-defect bounds, treats stopping and jump contributions, and specifies constraint preservation and physical-time calibration. This use of stochastic Noether theory builds on its existing Bellman formulation; the physical content lies in the stated residual structure and observable identification.

A stochastic starting point and its reversible branches. The physical interpretation takes a regulated stochastic path law as the starting description and asks how reversible mechanics and stable macroscopic laws can arise within it. Irreversibility is characterized by the law's physical time-reversal defect, while attraction to equilibrium is a separate dynamical property. The noise may be interpreted as fundamental, but that interpretation does not make every noisy law irreversible. Appendix P develops this distinction, the density variation with consistent units, and a boundary-term extension of the stochastic Noether identity. The conceptual proposal is assessed through its physical implications, independently of whether the tools used to derive those implications are new.

Shared structure and predictive restrictions. The physical question is whether coefficients that could otherwise be chosen independently become linked by the specified mother data. Appendix O answers this question at the level of invariant residual metrics. It computes the freedom left by product symmetries, gives a normalized rank criterion for coefficient identification, and distinguishes an adjoint charge from a measured conserved quantity. A common scalar dependence is an additional premise unless those equations determine it. This distinction makes the proposed unification testable: a relation between observables must follow from fixed shared inputs before the target measurements are used.

Section 16.2 distinguishes full parameter identification from identification of a target observable. In an affine calibration model, the target is determined precisely when it is constant on calibration fibres. The resulting factorization includes nuisance cancellation and gives a prediction-error bound with design uncertainty and nonlinear remainders. A synthetic example shows both an unresolved parameter direction that leaves the target unchanged and the loss of prediction after a necessary calibration channel is removed. This provides an explicit criterion for choosing an informative cross-branch observation.

Two quantitative extensions address imperfect measurements and imperfect physical symmetry. Proposition 95 transfers a complete-field identification bound to a specified sampling and observation system, provided both coverage and sensor sensitivity are controlled. Equation (1179) then propagates errors in the estimated Gram matrix and measured probes. In the three-mass realization, Proposition 151 bounds relaxation-rate ratios and exchange covariance when the contacts differ within a prescribed tolerance. Separate moment integration tests the predicted transient response and its time-step error. These results supply finite-dimensional inverse and experimental-design tools; their use with physical data requires independent calibration of the observation map and tolerances.

Appendices V and W give generator-level conditions for the arrow and attraction, an escape bound, and a contact-symmetry proof with explicit physical-charge and reservoir balances. These conditions distinguish finite-state stability from black-hole singularity avoidance.

The companion papers develop successive parts of that test. The revised programme also treats the relative coupling as a falsifiable selection-law hypothesis. The physical quotient, admissible class, reference path law, and selector are fixed before calibration; strict convexity is a conditional mathematical route to uniqueness, while independent held-out observations are required before the selected coupling can be regarded as a law of nature. Paper II transports a conditional common boundary relation through explicit one-loop running. Paper III tests a specified finite nonlinear projection with coefficients fixed before changes of forcing. Paper IV identifies quantum observables that remain undetermined by a calibration algebra, and Paper V tests joint predictions with sampling and matching errors. These roles do not require every microscopic parameter to be identifiable. They require the target observable to be constant over the parameter choices still allowed by independent calibration.

Appendix U develops a further consequence of the joint cost: its nonlinear feedback imposes a tensor relation between linear and mixed cubic responses. An exactly solved affine stochastic branch connects that relation to endpoint observations using the same Bellman and adjoint equations. The companion calculations then address symmetry restrictions on relative weights, physical fluctuation–response relations, an external fluid reference, finite quantum spectral observables, and an independently tilted equilibrium response. In each case the source and observation maps are fixed before validation.

Throughout, “finite regulator” means that the displayed state space and operators have been reduced to a finite-dimensional or finite Galerkin realization, with labels such as a and N. The limits $a \downarrow 0$, $N \to \infty$, and infinite-volume limits are separate completion problems; finite-regulator identities are not, by themselves, regulator-independent quantum-field-theory results. In particular,

the expression

$$S_{\mathrm{tot}} = S_{\mathrm{grav}} + S_{\mathrm{strong}} + S_{\mathrm{weak}} + S_{\mathrm{em}} \tag{2070}$$

does not specify whether the sectors share fields, constraints, or independently fixed coupling data. Additive actions can describe interacting systems; for example, a gauge action built from the gravitational metric couples to that metric through its stress tensor. Dynamical independence follows only when the configurations, action, and stochastic covariance factor into independent blocks.

The central distinction is whether the sectors are determined by shared microscopic data. Writing separately specified costs in one expression does not establish that dependence. Here a common geometric configuration is varied, and its geometry, stable phases, and matched effective limits organize the low-energy sectors. Consequently, a physical prediction requires more than a common notation: independently inserted relative normalizations, couplings, representations, and groups remain inputs. Describing them as components of one master object does not alone change that status. They become outputs only after a previously fixed candidate class, a selection rule, and a matching prescription determine them.

The shared scalar offers a concrete physical interpretation of coupling in this setting. It changes the energetic cost of both Cartan and internal curvature, so a scalar fluctuation can affect gravitational and gauge responses simultaneously. At a fixed scalar value the curvature pairing may still be block diagonal. Correlation is then a question about the coupled equilibrium Hessian and the observable map, rather than about the number of symbols used for the noise. The explicit covariance calculation and heavy-field matching below give two ways to make this distinction quantitative.

For physical perturbations, persistent stochastic amplitudes must be distinguished from an unstable coherent deformation. The finite-mode construction in Appendix I supplies rotation-invariant angular power, exact covariance evolution, and calibrated finite-time error bounds. It explicitly includes the kinetic and observation data missing from a Hessian-only argument. Relativistic accretion and early-galaxy observations require additional fluid and population interfaces, respectively, rather than an interpretation of every nonzero fluctuation as gravitational collapse.

That covariance mechanism remains classical. Shared noise, a common filtration, or a nonfactorizing Gibbs density can correlate two sectors, but none of them supplies incompatible observables or a nonseparable quantum state. Section 12.1 proves the resulting classical CHSH bound, identifies precisely which Bell-local assumptions a violation excludes, and gives the operator-algebraic, no-signalling, and Osterwalder–Schrader conditions that a genuine quantum completion would have to satisfy. Those conditions are requirements

on a future completion of the same microscopic package, not consequences of the classical stochastic equilibrium already constructed here.

The mathematical language combines three ingredients. First, a master connection $\mathbb{A}$ collects the geometric and internal degrees of freedom on a principal bundle. Second, a master action $\mathcal{S}_{\mathrm{M}}$ uses one invariant curvature pairing and a covariant matter–order-parameter–information state. Third, a stochastic process $\mathbb{X}_t$ has drift determined by the action, mobility and reference measure, with fluctuations determined by the same mobility. The drift includes the reference-measure correction required by the specified invariant law. Its path objective uses one joint residual metric. The isolated quadratic drift-control restriction recovers the Girsanov cost; the full construction also includes the declared geometric, thermodynamic and projection residuals, and the nonlinear penalty when $\kappa > 0$.

This viewpoint has precedents in several areas of mathematical physics without being identical to any one of them. Geometric unification based on a larger connection has a long history, including the MacDowell–Mansouri construction of gravity from a gauge-geometric curvature [116]. Spectral-action methods have shown how gravitational and Standard-Model-type terms can arise from a common spectral functional [26], [27], [42], [43], and [29]. Heat-kernel methods provide a systematic expansion of one-loop effective actions in terms of geometric invariants [156]. Stochastic quantization relates equilibrium distributions of stochastic processes to Euclidean field-theoretic structures [126] and [170]. None of these precedents, however, by itself establishes the particular minimum-cost plus equilibrium architecture proposed below.

AH.4. *Common recovery and contributions.* The common recovery statement is formulated through an explicit mother-equation interface. A single regulated diffusion, with its master energy, mobility, circulation drift, covariance, boundary conditions, and calibrated clock fixed in advance, yields the Gibbs invariant law and the relative-free-energy dissipation identity. A second map from the same generator to a declared divergence-free Galerkin space recovers the stochastic Navier–Stokes drift and covariance when the two generator-matching identities hold. The resulting energy balance contains forcing, conservative modal transfer, stochastic injection, and viscous dissipation. This is a common-origin theorem at finite regulator, not a claim that arbitrary Navier–Stokes equations or an unconditional continuum limit follow from notation alone. The hypotheses and the exact defect bound are stated in Section 14.

Contributions and architecture. Appendix G makes the distinction between equilibrium and physical calibration quantitative. A coupled finite diffusion has the same Gibbs law at different mobility scales but different correlation times. A local inverse bound then specifies what independent measurements

can determine, with explicit parameter and held-out prediction errors. This supplements the common variational architecture with tests of its dynamical and observational interpretation. Appendix J then differentiates the outer equilibrium score with its reference measure included. The resulting covariance term explains why positivity of the inner action does not imply convexity or uniqueness of parameter selection. Together these calculations separate microscopic selection, physical matching, and an independent test. Appendix K supplies a sufficient invariant-pairing condition for common curvature weights and shows why the present direct-product branch does not enforce it. Differentiated threshold matching and composite-mass response then connect the selected scalar branch to a source-eliminated clock/force relation, without asserting a nonzero signal before its physical parameters are fixed. Appendix L then identifies which inputs remain free, which effective responses the common-weight branch excludes, and when an unmeasured observable is fixed despite residual parameter degeneracy. These conditions specify how to test the same package across different physical sectors without introducing a new target-dependent fit. Appendix Q makes the remaining inverse questions explicit. Positive, well-posed costs can generate the same optimal path law, and a stochastic Noether identity respects the corresponding boundary freedom. For finite Markov models, a stationary probability current is also an exact obstruction to the direct self-adjoint ground-state transform. A complementary quantum jump example shows why classical populations do not determine coherent response. These results identify which additional mother-model data must be fixed before uniqueness can be claimed.

The paper makes five connected contributions. First, it specifies one master configuration, one invariant curvature pairing, and one stochastic covariance, so that gravity, internal gauge fields, matter, order parameters, and the information coordinate are varied in a common state space. Second, under the displayed range, boundary, and integrability hypotheses, it derives the finite-regulator Fokker–Planck, Gibbs, relative-free-energy, and Girsanov identities. Third, it establishes a conditional low-energy projection onto Einstein–higher-curvature and Yang–Mills constitutive equations and gives a conditional (331) realization, while retaining the distinction between a chosen candidate and a group selected by a solved comparison problem. Within the same matched branch and its weak-field hypotheses it derives the chain from a physical two-point-function pole to WKB propagation, worldline stress, and Newtonian tensor-mass equivalence. It also gives a Schur-complement criterion for strong Machian closure and an additive-vacuum-shift test that prevents ordinary equilibrium minimization from being misidentified as a solution of the cosmological-constant problem. Fourth, it constructs a state- and law-dependent joint residual objective, derives

its finite-regulator first variation under the stated differentiability and integrability assumptions, and then constructs a finite Galerkin stochastic Navier–Stokes branch with energy injection, dissipation, and shell-flux identities. This branch supplies a conditional mathematical bridge between microscopic random forcing and macroscopic transport: it retains finite-mode fluctuations while exposing nonlinear energy transfer and positive viscous dissipation, provided the generator-matching, constitutive fluctuation–dissipation, and physical-time calibration conditions stated below are satisfied. Fifth, under measurement-independence and Bell-local response assumptions, it proves the classical Bell obstruction and states the reflection-positivity, local-algebra, Born-rule, and no-signalling conditions required for a genuine quantum completion. The main development proceeds through foundations; master configuration and cost; equilibrium and limits; geometric and gauge recovery; group selection and the (331) phase; well-posedness and parameter matching; equilibrium observables; quantum completion; nonequilibrium thermodynamics and regulated turbulence; and the joint recovery and observation bounds; and conclusions. The appendices retain the variational, Gibbs, Girsanov, heat-kernel, and dimensional calculations.

The kinetic interface separates collision conservation from the constitutive assumptions needed for transport. A finite-source scalar calculation then links clock and differential-acceleration responses through the same couplings, with a range-identification bound and a third-radius prediction. These relations distinguish an explicit additional interaction from a numerical cutoff, a static boundary response, or entropy production alone. Section 19 applies the same canonical scalar normalization to two published binary-pulsar timing summaries. It derives the radiative threshold and conditional charge bounds while distinguishing effective stellar charges from common fundamental coefficients. Section 20 computes these charges for a fixed conditional matter coupling and transfers them to a third binary. It also derives a necessary mass–coupling condition for relating that calculation to the original common-weight scalar branch and incorporates the newer J0348 timing result without reusing a decay-derived mass. Section 21 identifies the additional matter derivatives needed for that matching, computes their linear stellar response map, and quantifies the separation of the conditional benchmark predictions from GR under an explicit summary error model. Section 22 then keeps the nonlinear canonical normalization and the explicit matter derivative in the massive-fluid equations. A coercive radial estimate supplies a conditional field-to-readout error bound, with exact rational examples. The same section derives a source-conditioned circular-radiation envelope. It shows why increasing the coupling can close the radiation channel, and why the previous massless benchmark cannot stand in for the unaltered minimal common-weight branch. These results support source

matching and experiment selection; they do not provide the missing nuclear sensitivities or a new signal. Section 26 then separates relativistic clock rates from stochastic time changes and distinguishes vanishing direct scalar coupling from the absence of scalar gravitational stress.

Status of the results. The logical status is kept explicit throughout. Finite-regulator identities and finite-dimensional energy balances are proved under their listed analytic assumptions. Low-energy Einstein–Yang–Mills equations, matter mass relations, the 331 phase, and the stochastic Navier–Stokes bridge are conditional results on specified matching, projection, constitutive, and calibration hypotheses. The regulated constructions provide benchmark calculations and falsifiable parameter relations, not regulator-independent experimental confirmations. A regulator-independent interacting quantum field theory, a unique group and matter selection, parameter-free numerical values, a nonperturbative Yang–Mills mass gap, and the unregularized turbulent continuum are open completion criteria rather than claims of the present work.

Why the stochastic fluid branch is a bridge. The phrase "microscopic" is used here in a controlled mathematical sense: the finite-dimensional modes retain random forcing and covariance information that are absent from a purely deterministic macroscopic closure. The phrase "macroscopic" refers to the projected velocity field, its quadratic kinetic energy, and the shell-wise balance observed after many stochastic relaxation times. The proposed bridge is the map $\Pi_{\mathrm{NS}}^{a,N}$, together with the generator identity (1019), the constitutive relations (1004)–(1008), and the physical-time calibration (1021). At fixed a and N, the noise injects energy at specified modes, the skew convection term redistributes energy without creating it, and viscosity removes energy. The stationary identity therefore has the form

$$\text{mean injection} + \text{mean noise input} = \text{mean viscous dissipation},$$

with the exact coefficients given in (1034). The same regulated package gives a nonnegative irreversible entropy-production term in the undriven Fokker–Planck equation. Subject to the displayed matching and calibration hypotheses, thermodynamic irreversibility and fluid energy transfer can therefore be compared as two projections of one stochastic law. The bridge does not assert that every nonzero drift and diffusion is turbulent: turbulence requires nonlinear transfer, sustained forcing, dissipation, and a scale range. Nor does it assert that the limit $N \to \infty$ exists; that is recorded as an open completion criterion.

What is unified about the arrow of time. Randomness and irreversibility are not synonyms. A deterministic equation may be dissipative, while a diffusion in its invariant state may satisfy detailed balance. We therefore distinguish three questions that are often conflated: whether an ordinary differential equation has an invertible flow, whether the law of a stationary path is invariant under

the parity-corrected reversal of the path, and whether the forward path can be statistically distinguished from the reversed path at a positive relative-entropy rate. The last rate is the entropy production. Section 4.9 proves the corresponding finite-regulator criterion and applies it to the two scale limits of Section 4.6. In particular, collective averaging makes the noise vanish but does not remove a dissipative gradient drift, whereas a microscopic tangent scaling makes the drift negligible but can still yield a reversible equilibrium diffusion. A reversible macroscopic limit follows only from a matched fluctuation–dissipation scaling that also removes the dissipative drift and leaves a parity-reversible conservative vector field.

Section 4.11 adds four complementary descriptions: parity-aware generator balance, the obstruction to positive Markov recovery after strict information contraction, attraction and nonrecurrence of nonequilibrium laws, and forward–reverse path distinguishability. These descriptions separate stationary reversibility from irreversible relaxation and from maintained driven dissipation.

The abstract selection problem therefore allows the residual internal group to vary. The later worked candidate explicitly includes $SU(3)_c \times SU(2)_L \times U(1)_Y$ as input. It demonstrates a coupled realization with that group; deriving the group requires an independently specified candidate class and a solved comparison problem.

The construction has five components. First, it defines a single master cost functional. Second, it establishes the relation between minimum cost, the master drift, and the equilibrium state. Third, it formulates a non-circular group-selection problem. Fourth, it proves a controlled effective-sector recovery theorem for the standard low-energy curvature equations. Fifth, under the stated reductions, closure assumptions, and scalings, it identifies macroscopic motion without stochastic forcing and microscopic fluctuation limits, thereby specifying a mathematical meaning for the proposed scale-dependent transition.

The central correspondence claim is stated in set-theoretic form only after the target class and the reduction maps have been declared. If $\mathfrak{T}_{\mathrm{cl}}^{(r)}$ denotes the specified finite-regulator classical mechanical, Einstein, Yang–Mills, and Galerkin-fluid generators and $\mathfrak{T}_{\mathrm{un}}^{(r)}$ denotes their images under the mother generator, then the theorem to be checked is

$$\mathfrak{T}_{\mathrm{cl}}^{(r)} \subseteq \mathfrak{T}_{\mathrm{un}}^{(r)}.$$

In the unregulated problem the corresponding statement is a closure relation, not a formal identity:

$$\mathfrak{T}_{\mathrm{cl}} \subseteq \overline{\bigcup_{r} \mathfrak{T}_{\mathrm{un}}^{(r)}}.$$

The first inclusion is established by exact generator and constraint matching; the second requires uniform remainder, compactness, and time-calibration estimates. Thus classical mechanics is recovered by the zero-noise, zero-dissipation Hamiltonian scaling, Einstein and Yang–Mills dynamics by their controlled low-energy projections, and the finite fluid equation by the drift-and-covariance identity. The inclusion is a theorem only on the declared class; it does not silently include arbitrary continuum equations or arbitrary quantum theories.

These components have different logical status. The master algebra, bundle, pairing, representations, and information map are microscopic data of a candidate realization; they are not silently replaced by the observed Standard-Model data. The path-space and equilibrium identities are mathematical consequences once a finite-dimensional or rigorously regularized realization and the hypotheses stated below have been fixed. The residual gauge group, chiral matter content, numerical coupling constants, and a fully selected physical Lorentzian completion are outputs only if the subsequent selection and matching problems have solutions. The effective Einstein and Yang–Mills equations nevertheless follow on the matched sector specified in Theorem 9. Thus the displayed candidate $SU(3)_c \times SU(2)_L \times U(1)_Y$ is not derived by notation alone; a derivation consists of solving the selection and matching problems.

The geometric part includes one explicit joint candidate. Section 5.4 fixes a four-dimensional Cartan quotient, places the Cartan and Standard Model connections in one master field, and uses a shared order parameter in the single norm and stochastic mobility. The residual Standard Model group and the one-generation representation used in that candidate are prescribed inputs of this existence witness; they have not been selected by the variational problem. Thus "one model" below means one well-typed coupled action and one stochastic law, not a completed parameter-free derivation of the observed particle theory. Section 5.3 expands a positive Cartan curvature norm, fixes the coefficients of its specified torsionless curvature-invariant expansion, and gives an exact Euclidean Einstein vacuum. Sections 11.7 and 11.8 derive the equilibrium correlation criterion and response identities of a coupled quadratic model. Section 11.10 computes the effective operator coefficients generated by one heavy scalar and the resulting rank restriction. Each calculation fixes its algebraic and analytic data explicitly. Section 11.9 compares the coupled quadratic formulas with simulations using the exact discrete-time transition. Section 12.1 then separates those classical correlations from quantum entanglement, applies the standard Bell-local CHSH argument to this framework, records and proves the quantum Tsirelson bound for completeness, and states the additional reconstruction, gauge-reduction, measurement, and locality requirements for a unified quantum theory. The joint candidate is an algebraic realization of coupled sectors; its unique selection and global stochastic or

nonperturbative continuum completion remain separate mathematical conditions. Section 6.1 formulates those conditions on a quotient of candidate packages and proves the corresponding direct-method existence and uniqueness criteria. The conditional Galerkin theorem in Section 10.18 gives the precise compactness and martingale-problem hypotheses needed for a continuum limit, while Section 7.3 separates renormalized matching, threshold corrections, fitted inputs, and genuine parameter-free relations. Section 10.19 then gives a separate conditional Krylov–Bogoliubov criterion for existence of an invariant probability measure and a Wasserstein-contraction criterion for its uniqueness. These stochastic-continuum conclusions apply only after the gauge quotient, well-posedness, Lyapunov compactness, and coupling hypotheses stated there have been verified for the chosen realization. The additional hypotheses connect the finite-dimensional calculations to possible continuum realizations. In the joint candidate the common scalar also requires confinement: Section 5.4.1 derives its Euler equation, exhibits a divergent constant-mode integral, and gives an explicit stabilizing extension. These analytic requirements are separate from the proved conditional variational recovery of the effective field equations.

Several of these construction problems admit explicit solutions once the background and regulator are specified. Theorem 11 proves existence, smoothness, and uniqueness of the stabilized scalar vacuum, with a quantitative maximum bound. Theorem 19 constructs the reversible finite gauge–scalar diffusion and proves uniqueness of its invariant probability among all probability laws. Theorem 39 gives a nonlinear infinite-dimensional realization retaining the exponential coupling, with global dynamics, convergent spectral approximations, and a unique Gibbs invariant law. Its stronger Gaussian smoothing is part of that realization and is not inferred from the original two-derivative scalar action.

Selection requires a different argument. Theorem 15 proves that a freely variable positive coefficient of a nonnegative action term makes the minimized free energy strictly increasing in that coefficient. Thus the unrestricted class has no minimizing positive coefficient. The scalar–plaquette calculation in Section 6.5 illustrates this obstruction without changing the reference normalization. Finally, Section 11.11 derives conditional decay-width and force relations after vacuum matching and diagonalization of scalar–metric mixing. The higher-curvature scale restricts the regime in which these observables can be computed from the truncated action. Section 11.11.5 then isolates the most accessible low-energy prediction program of this branch: a single equilibrium scalar mode gives a rank-one correlated drift pattern in dissimilar clocks or optical cavities and a composition-dependent Yukawa force whose signed material pattern is governed by the same scalar-charge vector. The equilibrium

theorems, the selection obstruction, and the effective predictions therefore address different steps of the same construction.

Section 6.6 adds a separate intermediate-scale 331 candidate class. Within its declared representations and threshold assumptions, it derives a conditional family-number relation, a vacuum-aligned flavor realization, and heavy-mass ratios. It also gives an explicit generalized-color counterexample and records the flavor, global-group, and scale data that remain to be selected. This construction does not replace the prescribed G_{SM} joint candidate or solve the abstract selection problem.

The curvature variation, Gibbs identity, Girsanov calculation, heat-kernel convention, and dimensional checks are derived in Appendices A, B, C, D, and E, respectively. Their use presupposes the regularity, absolute-continuity, and finite-dimensional or regularized hypotheses stated below.

AH.5. *Reading the common structure and its conditional branches.* Physical clocks and existing matter branches. The interpretation of stochastic evolution also requires a physical clock. Causal order, duration measured by a material clock, and statistical time-reversal asymmetry are distinct structures. A positive state-dependent clock reweights the invariant law, so clock calibration belongs to the projection problem itself. The finite-temperature two-fluid and coherent GP companion models provide concrete matter interfaces; their force metrics are inherited only when the projected mother cost agrees with their specified effective costs. These questions lead to the explicit clock and cost identities below, with their relativistic and conservation conditions retained.

The common structure is a specification of data, not a shortcut past the matching problems. Figure 77 separates the field variation, stochastic-law, and hydrodynamic-projection branches. Table 41 records the hypotheses that connect their results. A shared configuration makes such comparisons meaningful, but does not by itself make the projections dynamically equivalent. The concluding synthesis in Section 32.1 collects the common objective, its full variation, and the thermodynamic–hydrodynamic interface in the overview paper.

Candidate data Γ: configuration, representations, pairing, reference measure, mobility, and regulator

⇓ Explicit realization of the master action and path cost

Field variation	Stochastic law	Observable projection
Matching, torsion and low-curvature assumptions	Range, boundary, stationarity and parity conditions	Generator matching, constitutive relations and time calibration
⇓	⇓	⇓
Einstein–Yang–Mills branch and covariant matter response	Gibbs law, relative free energy and path entropy	Finite Galerkin fluid law and energy transfer

Quantum and continuum completion: additional positivity, locality, tightness, identification, and renormalization conditions

Figure 77. Conditional branches of the common regulated data. Each downward step includes the displayed hypotheses; arrows do not assert that optimizing the path cost alone derives every field or constitutive equation. Quantum reconstruction and removal of the regulator are separate requirements.

Table 41. Assumptions and results on their stated domains. The middle column summarizes, but does not replace, the hypotheses in the cited statements.

Result	Required interface or analytic assumptions	Precise location
Path-space cost and entropy	Same initial law; canonical-path adapted drift in the noise range; true Girsanov martingale; finite shift energy and uniqueness in law	(71) and Appendix C
Gibbs law and relative-free-energy decay	Finite partition function; reference-measure drift correction; specified boundary domain and integrability; uniqueness requires a separate irreducibility argument	(92), (87), Theorem 19
Time-reversal and entropy rate	Stationary positive density; specified parity and covariance; compatible reverse path law and finite relative-entropy energy	Proposition 6 and Proposition 7
Einstein–Yang–Mills recovery	Matched low-energy action; coframe variation; torsion and kinetic assumptions; curvature and derivative control	Theorem 9, (213)
Tensor monopole-mass equality	Isolated physical pole; anomaly-free stress Ward identity; universal coupling; neutral constant-mass, weak-field point-particle limit	(275), (278)
Machian and vacuum response	Reduced Hessian and specified boundary data; Schur invertibility; a simple curvature root for implicit response	(286), (301)
Fluid energy and entropy balances	Finite solenoidal projection; skew convection; trace-defined noise; reservoir bookkeeping and physical-time matching for thermodynamic interpretation	(1019), (1023), (1021)
Classical Bell bound; quantum completion	Measurement independence and Bell locality for the classical bound; physical Euclidean correlations and the full reconstruction conditions for a quantum theory	Theorem 44, (858), Section 12.1
Parameter and continuum conclusions	Declared renormalization scheme and identifiability; uniform tightness, limit identification and well-posedness; not implied by a finite calculation	Section 7.3, hypotheses G1–G3

Table 42. Core notation and distinctions. Regulator-dependent objects retain their (a, N) labels when the distinction matters.

Symbol	Meaning and restriction
M, $\mathfrak{X}_\Gamma$	Spacetime and field-configuration space, respectively; stochastic differentiation is on the latter.
e, ω, A	Coframe, geometric connection and internal connection; the coframe induces the metric on the selected nondegenerate branch.
$\Phi, \mathbb{X}$	Typed master fields and their realization as state coordinates, as specified in (43) and (889).
$\Phi_H, \chi, \Psi, \sigma$	Order-parameter, information-state, matter and shared-scalar coordinates; the scalar σ is not the noise operator $\boldsymbol{\sigma}$.
ρ_t, π_θ, m	Coordinate law density, equilibrium coordinate density and reference-density factor, respectively; none is a coframe or a matter field.
$\mathbb{G}, \mathbb{M}, \mathbb{H}_{a,N}$	Field-space metric, mobility, and joint residual metric; their domains, positivity and symmetry constraints are different.
$\theta, t, \Delta t$	Noise energy scale, stochastic time and numerical step; $\theta = k_{\mathrm{B}}T$ and identification of t with physical time require a reservoir and calibration.
$\Pi_{\mathrm{NS}}^{a,N}$	Declared map to solenoidal fluid modes; Markov generator matching is an extra property of the map.

AH.6. *Variational structure and the meaning of unification.*

AH.7. *Shared data and variational dependence.* Let $\mathcal{X}_1, \dots, \mathcal{X}_4$ denote four fields and suppose one writes

$$\mathcal{J}_{\mathrm{agg}} = \mathcal{J}_1[\mathcal{X}_1] + \cdots + \mathcal{J}_4[\mathcal{X}_4]. \tag{2071}$$

This expression has one symbol but four independent variational mechanisms. The Euler–Lagrange equation for $\mathcal{X}_i$ depends only on $\mathcal{J}_i$ unless explicit cross-couplings are inserted. The number of fundamental principles has therefore not been reduced.

A stronger requirement is that there exists a single configuration $\mathbb{X}$ and a single scalar functional $\mathcal{S}_{\mathrm{M}}[\mathbb{X}]$ such that

$$\delta\mathcal{S}_{\mathrm{M}}[\mathbb{X}] = 0 \tag{2072}$$

produces the complete microscopic Euler–Lagrange system. This stationarity condition describes critical configurations. It should be distinguished from the zero-cost stochastic-time equation introduced below: the latter is a gradient-flow trajectory and approaches a critical configuration only under additional compactness and convergence assumptions. For example, when $\mathcal{S}_{\mathrm{M}}(x) = x^2/2$

and the mobility is one, stationarity gives $x = 0$, whereas the zero-cost equation admits every trajectory $x(t) = x_0 e^{-t}$. The low-energy sectors must be obtained by restricting the same solution space to stable strata, rather than by separately postulating their equations.

The same criterion is imposed on the stochastic theory. There must be one process

$$\mathrm{d}\mathbb{X}_t = \mathbb{B}(\mathbb{X}_t)\,\mathrm{d}t + \boldsymbol{\sigma}(\mathbb{X}_t)\,\mathrm{d}W_t, \tag{2073}$$

where $\mathbb{B}$ is generated by $\mathcal{S}_{\mathrm{M}}$, and one path cost

$$\mathcal{J}_T[x] = \frac{1}{4\theta}\int_0^T \|\dot{x}_t - \mathbb{B}(x_t)\|^2_{\widehat{\mathbb{M}}(x_t)^{-1}}\,\mathrm{d}t, \qquad x \in AC([0,T];\mathfrak{X}). \tag{2074}$$

There is no second term representing another physical sector. The same object is used for all sectors.

AH.8. *The hierarchy of the construction.* The complete architecture is

$$\boxed{\begin{array}{l}\text{master algebra} \longrightarrow \text{master connection} \longrightarrow \text{master curvature}\\ \longrightarrow \text{master action} \longrightarrow \text{master stochastic drift} \longrightarrow \text{one path cost}\\ \longrightarrow \text{one equilibrium} \longrightarrow \text{low-energy sectors.}\end{array}} \tag{2075}$$

Each arrow specifies a mathematical construction required by the framework. The constructions of equilibrium, unique selection, and physical matching are conditional on the hypotheses stated in the corresponding sections.

In a realization that satisfies the selection and effective-limit hypotheses, the intended emergence of low-energy interactions is summarized schematically by

$$\begin{aligned}\mathbb{F} &\xrightarrow{\text{symmetry breaking}} (\mathbb{F}_{\mathrm{grav}}, \mathbb{F}_3, \mathbb{F}_2, \mathbb{F}_1)\\ &\xrightarrow{\text{effective limit}} (G_{\mathrm{eff}}, SU(3)_c, SU(2)_L, U(1)_Y).\end{aligned} \tag{2076}$$

with electromagnetism arising after electroweak symmetry breaking. The displayed coupling and groups describe the target effective structure. For the explicit candidate in Section 5.4, the internal group is prescribed; proving its unique selection is a separate problem.

The following concrete realizations sharpen the common-mechanism question. Section 26.22 separates mechanical stationarity from relative-entropy control and conditional parameter selection. Section 26.23 constructs one finite coupled generator with strictly positive paths, a unique equilibrium law and an explicit entropy contraction estimate; a compact stationary current adds path irreversibility without changing that law. Section 26.24 holds a nonzero matched parameter vector fixed across three source masses and computes scalar and local-disc responses. These results supply explicit sufficient conditions and

response relations, while the field projections and continuum identifications retain their separately stated hypotheses.

References

[1] R. Abbott et al., Open data from the first and second observing runs of Advanced LIGO and Advanced Virgo, *SoftwareX* **13** (2021), 100658. DOI: 10.1016/j.softx.2021.100658.

[2] E. G. Adelberger, B. R. Heckel, and A. E. Nelson, Tests of the gravitational inverse-square law, *Annu. Rev. Nucl. Part. Sci.* **53** (2003), 77–121. https://doi.org/10.1146/annurev.nucl.53.041002.110503.

[3] D. Anselmi, Fakeons and Lee–Wick models, *Journal of High Energy Physics* **02** (2018), 141. https://doi.org/10.1007/JHEP02(2018)141.

[4] D. Anselmi and M. Piva, Quantum gravity, fakeons and microcausality, *Journal of High Energy Physics* **11** (2018), 021. https://doi.org/10.1007/JHEP11(2018)021.

[5] J. Antoniadis, P. C. C. Freire, N. Wex, et al., A massive pulsar in a compact relativistic binary, *Science* **340** (2013), 1233232. https://doi.org/10.1126/science.1233232.

[6] J. Armstrong, D. Brigo, and E. Ferrucci, Projections of SDEs onto submanifolds, *Information Geometry* **7**, Suppl. 1 (2024), S397–S427. https://doi.org/10.1007/s41884-022-00093-7.

[7] V. I. Arnold, *Mathematical Methods of Classical Mechanics*, 2nd ed., Springer, New York, 1989. https://doi.org/10.1007/978-1-4757-2063-1.

[8] R. Arnowitt, S. Deser, and C. W. Misner, The dynamics of general relativity, in *Gravitation: An Introduction to Current Research*, ed. L. Witten, Wiley, New York, 1962, 227–265.

[9] D. Bakry, I. Gentil, and M. Ledoux, *Analysis and Geometry of Markov Diffusion Operators*, Springer, 2014. DOI: 10.1007/978-3-319-00227-9.

[10] J. W. Barrett, Lorentzian version of the noncommutative geometry of the standard model of particle physics, *J. Math. Phys.* **48** (2007), 012303. https://doi.org/10.1063/1.2408400.

[11] A. Batrakov, H. Hu, N. Wex, et al., A new pulsar timing model for scalar-tensor gravity with applications to PSR J2222-0137 and pulsar-black hole binaries, *Astron. Astrophys.* **686** (2024), A101. https://doi.org/10.1051/0004-6361/202245246.

[12] C. Becchi, A. Rouet, and R. Stora, Renormalization of gauge theories, *Ann. Physics* **98** (1976), 287–321. https://doi.org/10.1016/0003-4916(76)90156-1.

[13] J. S. Bell, On the Einstein Podolsky Rosen paradox, *Physics Physique Fizika* **1** (1964), 195–200. https://doi.org/10.1103/PhysicsPhysiqueFizika.1.195.

[14] J. Bellorin, C. Bórquez, and B. Droguett, Batalin–Fradkin–Vilkovisky quantization of quadratic gravity, *Physical Review D* **113** (2026), 106006. https://doi.org/10.1103/c22r-2v5h.

[15] C. H. Bennett, H. J. Bernstein, S. Popescu, and B. Schumacher, Concentrating partial entanglement by local operations, *Phys. Rev. A* **53** (1996), 2046–2052. https://doi.org/10.1103/PhysRevA.53.2046.

[16] B. Bertotti, L. Iess and P. Tortora, A test of general relativity using radio links with the Cassini spacecraft, *Nature* **425** (2003), 374–376. https://doi.org/10.1038/nature01997.

[17] N. D. Birrell and P. C. W. Davies, *Quantum Fields in Curved Space*, Cambridge University Press, Cambridge, 1982. https://doi.org/10.1017/CBO9780511622632.

[18] R. Bluhm and V. A. Kostelecký, Spontaneous Lorentz violation, Nambu–Goldstone modes, and gravity, *Physical Review D* **71** (2005), 065008. https://doi.org/10.1103/PhysRevD.71.065008.

[19] V. I. Bogachev, *Measure Theory*, Vols. I–II, Springer, Berlin, 2007. https://doi.org/10.1007/978-3-540-34514-5.

[20] J. M. Boter, X. Xue, T. Krähenmann, T. F. Watson, V. N. Premakumar, D. R. Ward, D. E. Savage, M. G. Lagally, M. Friesen, S. N. Coppersmith, M. A. Eriksson, R. Joynt, and L. M. K. Vandersypen, Spatial noise correlations in a Si/SiGe two-qubit device from Bell state coherences, *Phys. Rev. B* **101** (2020), 235133. https://doi.org/10.1103/PhysRevB.101.235133.

[21] J. M. Boter et al., Supporting data for Spatial Noise Correlations in a Si/SiGe Two-Qubit Device from Bell State Coherences, version 3, Zenodo, 20 May 2020. https://doi.org/10.5281/zenodo.3835990.

[22] P. Busch, Quantum states and generalized observables: A simple proof of Gleason's theorem, *Phys. Rev. Lett.* **91** (2003), 120403. https://doi.org/10.1103/PhysRevLett.91.120403.

[23] L. Canet, B. Delamotte, and N. Wschebor, Fully developed isotropic turbulence: Nonperturbative renormalization group formalism and fixed-point solution, *Phys. Rev. E* **93** (2016), 063101. DOI: 10.1103/PhysRevE.93.063101.

[24] H. Casini, M. Huerta, and J. A. Rosabal, Remarks on entanglement entropy for gauge fields, *Phys. Rev. D* **89** (2014), 085012. https://doi.org/10.1103/PhysRevD.89.085012.

[25] C. Cercignani, R. Illner, and M. Pulvirenti, *The Mathematical Theory of Dilute Gases*, Springer, New York, 1994. https://doi.org/10.1007/978-1-4419-8524-8.

[26] A. H. Chamseddine and A. Connes, Universal formula for noncommutative geometry actions: unification of gravity and the standard model, *Phys. Rev. Lett.* **77** (1996), 4868–4871. https://doi.org/10.1103/PhysRevLett.77.4868.

[27] A. H. Chamseddine and A. Connes, The spectral action principle, *Commun. Math. Phys.* **186** (1997), 731–750. https://doi.org/10.1007/s002200050126.

[28] A. H. Chamseddine and A. Connes, The uncanny precision of the spectral action, *Commun. Math. Phys.* **293** (2010), 867–897. https://doi.org/10.1007/s00220-009-0949-3.

[29] A. H. Chamseddine, A. Connes, and M. Marcolli, Gravity and the standard model with neutrino mixing, *Adv. Theor. Math. Phys.* **11** (2007), 991–1089. https://doi.org/10.4310/ATMP.2007.v11.n6.a3.

[30] A. H. Chamseddine, A. Connes, and W. D. van Suijlekom, Entropy and the spectral action, *Commun. Math. Phys.* **373** (2020), 457–471. https://doi.org/10.1007/s00220-019-03297-8.

[31] R. Chetrite and K. Gawedzki, Fluctuation relations for diffusion processes, *Commun. Math. Phys.* **282** (2008), 469–518. https://doi.org/10.1007/s00220-008-0502-9.

[32] R. Chetrite and H. Touchette, Nonequilibrium Markov processes conditioned on large deviations, *Ann. Henri Poincaré* **16** (2015), 2005–2057. https://doi.org/10.1007/s00023-014-0375-8.

[33] Y. Choquet-Bruhat, *General Relativity and the Einstein Equations*, Oxford University Press, Oxford, 2009.

[34] T. Christodoulakis and J. Zanelli, Operator ordering in quantum mechanics and quantum gravity, *Nuovo Cimento B* **93** (1986), 1–21. https://doi.org/10.1007/BF02728299.

[35] T. Christodoulakis and J. Zanelli, Consistent algebra for the constraints of quantum gravity, *Nuovo Cimento B* **93** (1986), 22–35. https://doi.org/10.1007/BF02728300.

[36] A. K.-W. Chung and N. Yunes, Quasinormal mode frequencies and gravitational perturbations of black holes with any subextremal spin in modified gravity through METRICS: The scalar-Gauss-Bonnet gravity case, *Phys. Rev. D* **110** (2024), 064019. DOI: 10.1103/PhysRevD.110.064019.

[37] K. Chworowsky, S. L. Finkelstein, M. Boylan-Kolchin, et al., Evidence for a shallow evolution in the volume densities of massive galaxies at $z = 4$–8 from CEERS, *Astron. J.* **168** (2024), article 113. https://doi.org/10.3847/1538-3881/ad57c1.

[38] B. S. Cirel'son, Quantum generalizations of Bell's inequality, *Lett. Math. Phys.* **4** (1980), 93–100. https://doi.org/10.1007/BF00417500.

[39] J. F. Clauser, M. A. Horne, A. Shimony, and R. A. Holt, Proposed experiment to test local hidden-variable theories, *Phys. Rev. Lett.* **23** (1969), 880–884. https://doi.org/10.1103/PhysRevLett.23.880.

[40] R. Clifton and H. Halvorson, Entanglement and open systems in algebraic quantum field theory, *Stud. Hist. Philos. Mod. Phys.* **32** (2001), 1–31. https://doi.org/10.1016/S1355-2198(00)00033-2.

[41] S. Coleman and J. Mandula, All possible symmetries of the S matrix, *Phys. Rev.* **159** (1967), 1251–1256. https://doi.org/10.1103/PhysRev.159.1251.

[42] A. Connes, *Noncommutative Geometry*, Academic Press, San Diego, 1994.

[43] A. Connes, Gravity coupled with matter and the foundation of non-commutative geometry, *Commun. Math. Phys.* **182** (1996), 155–176. https://doi.org/10.1007/BF02506388.

[44] A. Connes, Noncommutative geometry and the standard model with neutrino mixing, *J. High Energy Phys.* 11 (2006), article 081. https://doi.org/10.1088/1126-6708/2006/11/081.

[45] A. Connes and J. Lott, Particle models and noncommutative geometry, *Nucl. Phys. B Proc. Suppl.* **18** (1991), 29–47. https://doi.org/10.1016/0920-5632(91)90120-4.

[46] A. Connes and M. Marcolli, *Noncommutative Geometry, Quantum Fields and Motives*, American Mathematical Society, Providence, 2008. https://doi.org/10.1090/coll/055.

[47] G. E. Crooks, Entropy production fluctuation theorem and the nonequilibrium work relation for free energy differences, *Phys. Rev. E* **60** (1999), 2721–2726. https://doi.org/10.1103/PhysRevE.60.2721.

[48] I. Csiszár, I-divergence geometry of probability distributions and minimization problems, *Ann. Probab.* **3** (1975), 146–158. https://doi.org/10.1214/aop/1176996454.

[49] L. Da Costa and G. A. Pavliotis, The entropy production of stationary diffusions, *J. Phys. A: Math. Theor.* **56** (2023), no. 36, 365001. https://doi.org/10.1088/1751-8121/acdf98.

[50] T. Damour and J. F. Donoghue, Equivalence principle violations and couplings of a light dilaton, *Phys. Rev. D* **82** (2010), 084033. https://doi.org/10.1103/PhysRevD.82.084033.

[51] T. Damour and G. Esposito-Farèse, Tensor-scalar gravity and binary-pulsar experiments, *Phys. Rev. D* **54** (1996), 1474–1491. https://doi.org/10.1103/PhysRevD.54.1474.

[52] T. Damour and A. M. Polyakov, The string dilaton and a least coupling principle, *Nucl. Phys. B* **423** (1994), 532–558. https://doi.org/10.1016/0550-3213(94)90143-0.

[53] G. Da Prato and J. Zabczyk, *Stochastic Equations in Infinite Dimensions*, Cambridge University Press, Cambridge, 1992. https://doi.org/10.1017/CBO9780511666223.

[54] G. Da Prato and J. Zabczyk, *Ergodicity for Infinite Dimensional Systems*, Cambridge University Press, Cambridge, 1996. https://doi.org/10.1017/CBO9780511662829.

[55] J. Davighi, B. Gripaios, and N. Lohitsiri, Global anomalies in the Standard Model(s) and beyond, *J. High Energy Phys.* (2020), no. 7, 232. https://doi.org/10.1007/JHEP07(2020)232.

[56] N. F. Declercq, Derived dynamics in trembling spacetime relativity: a unified geometric basis for the principles of inertia, equivalence, action, and energy–mass relations, preprint (2025). https://doi.org/10.5281/zenodo.18050230.

[57] A. Derevianko and M. Pospelov, Hunting for topological dark matter with atomic clocks, *Nat. Phys.* **10** (2014), 933–936. https://doi.org/10.1038/nphys3137.

[58] F. C. De Vecchi, E. Mastrogiacomo, M. Turra, and S. Ugolini, Noether theorem in stochastic optimal control problems via contact symmetries, *Mathematics* **9** (2021), no. 9, 953. https://doi.org/10.3390/math9090953.

[59] B. S. DeWitt, *Dynamical Theory of Groups and Fields*, Gordon and Breach, New York, 1965.

[60] H. Ding, A. T. Deller, P. Freire, et al., Very long baseline astrometry of PSR J1012+5307 and its implications on alternative theories of gravity, *Astrophys. J.* **896** (2020), 85. https://doi.org/10.3847/1538-4357/ab8f27.

[61] W. Donnelly and S. B. Giddings, Observables, gravitational dressing, and obstructions to locality and subsystems, *Phys. Rev. D* **94** (2016), 104038. https://doi.org/10.1103/PhysRevD.94.104038.

[62] S. Doplicher and R. Longo, Standard and split inclusions of von Neumann algebras, *Invent. Math.* **75** (1984), 493–536. https://doi.org/10.1007/BF01388641.

[63] A. Einstein, Die Grundlage der allgemeinen Relativitätstheorie, *Ann. Phys.* **354** (1916), 769–822. https://doi.org/10.1002/andp.19163540702.

[64] S. Elitzur, Impossibility of spontaneously breaking local symmetries, *Phys. Rev. D* **12** (1975), 3978–3982. https://doi.org/10.1103/PhysRevD.12.3978.

[65] F. Englert and R. Brout, Broken symmetry and the mass of gauge vector mesons, *Phys. Rev. Lett.* **13** (1964), 321–323. https://doi.org/10.1103/PhysRevLett.13.321.

[66] A. Fine, Hidden variables, joint probability, and the Bell inequalities, *Phys. Rev. Lett.* **48** (1982), 291–295. https://doi.org/10.1103/PhysRevLett.48.291.

[67] T. Fink and H. Bluhm, Noise spectroscopy using correlations of single-shot qubit readout, *Phys. Rev. Lett.* **110** (2013), 010403. https://doi.org/10.1103/PhysRevLett.110.010403.

[68] W. H. Fleming and H. M. Soner, *Controlled Markov Processes and Viscosity Solutions*, second ed., Springer, New York, 2006. https://doi.org/10.1007/0-387-31071-1.

[69] R. Foot, H. N. Long, and T. A. Tran, $SU(3)_L \otimes U(1)_N$ and $SU(4)_L \otimes U(1)_N$ gauge models with right-handed neutrinos, *Phys. Rev. D* **50** (1994), R34–R38. https://doi.org/10.1103/PhysRevD.50.R34.

[70] P. H. Frampton, Chiral dilepton model and the flavor question, *Phys. Rev. Lett.* **69** (1992), 2889–2891. https://doi.org/10.1103/PhysRevLett.69.2889.

[71] D. S. Freed and K. K. Uhlenbeck, *Instantons and Four-Manifolds*, Springer, New York, 1984. https://doi.org/10.1007/978-1-4684-0258-2.

[72] M. I. Freidlin and A. D. Wentzell, *Random Perturbations of Dynamical Systems*, 3rd ed., Springer, Berlin, 2012. https://doi.org/10.1007/978-3-642-25847-3.

[73] P. C. C. Freire, N. Wex, G. Esposito-Farèse, et al., The relativistic pulsar-white dwarf binary PSR J1738+0333 – II. The most stringent test of scalar-tensor gravity, *Mon. Not. R. Astron. Soc.* **423** (2012), 3328–3343. https://doi.org/10.1111/j.1365-2966.2012.21253.x.

[74] C. D. Froggatt and H. B. Nielsen, Hierarchy of quark masses, Cabibbo angles and CP violation, *Nucl. Phys. B* **147** (1979), 277–298. https://doi.org/10.1016/0550-3213(79)90316-X.

[75] M. Fukushima, Y. Oshima, and M. Takeda, *Dirichlet Forms and Symmetric Markov Processes*, second revised and extended edition, de Gruyter, Berlin, 2011. https://doi.org/10.1515/9783110218091.

[76] C. F. Gammie, J. C. McKinney, and G. Tóth, HARM: a numerical scheme for general relativistic magnetohydrodynamics, *Astrophys. J.* **589** (2003), 444–457. https://doi.org/10.1086/374594.

[77] S. Ghanem, Exterior stability of the $(1 + 3)$-dimensional Minkowski space-time solution to the Einstein–Yang–Mills equations, arXiv:2310.08196 [gr-qc] (2023). https://arxiv.org/abs/2310.08196.

[78] P. B. Gilkey, *Invariance Theory, the Heat Equation, and the Atiyah–Singer Index Theorem*, 2nd ed., CRC Press, Boca Raton, 1995.

[79] I. V. Girsanov, On transforming a certain class of stochastic processes by absolutely continuous substitution of measures, *Theory of Probability and Its Applications* **5** (1960), 285–301. doi:10.1137/1105027.

[80] D. Giulini and D. Marolf, A uniqueness theorem for constraint quantization, *Class. Quantum Grav.* **16** (1999), 2489–2505. https://doi.org/10.1088/0264-9381/16/7/322.

[81] S. L. Glashow, Partial-symmetries of weak interactions, *Nucl. Phys.* **22** (1961), 579–588. https://doi.org/10.1016/0029-5582(61)90469-2.

[82] A. González Lezcano and A. Cabo Montes de Oca, A stochastic version of the Noether theorem, *Found. Phys.* **48** (2018), no. 6, 726–746. https://doi.org/10.1007/s10701-018-0174-z.

[83] J. M. Gracia-Bondía, J. C. Várilly, and H. Figueroa, *Elements of Noncommutative Geometry*, Birkhäuser, Boston, 2001. https://doi.org/10.1007/978-1-4612-0005-5.

[84] M. Grmela and H. C. Oettinger, Dynamics and thermodynamics of complex fluids. I. Development of a general formalism, *Phys. Rev. E* **56** (1997), 6620–6632. https://doi.org/10.1103/PhysRevE.56.6620.

[85] L. Gross, Logarithmic Sobolev inequalities, *Amer. J. Math.* **97** (1975), no. 4, 1061–1083. https://doi.org/10.2307/2373688.

[86] Y. J. Guo, P. C. C. Freire, L. Guillemot, et al., PSR J2222–0137. I. Improved physical parameters for the system, *Astron. Astrophys.* **654** (2021), A16. https://doi.org/10.1051/0004-6361/202141450.

[87] R. Haag, *Local Quantum Physics: Fields, Particles, Algebras*, 2nd rev. ed., Springer, Berlin, 1996. https://doi.org/10.1007/978-3-642-61458-3.

[88] R. Haag, J. T. Lopuszanski, and M. Sohnius, All possible generators of supersymmetries of the S-matrix, *Nucl. Phys. B* **88** (1975), 257–274. https://doi.org/10.1016/0550-3213(75)90279-5.

[89] M. Hairer and J. C. Mattingly, Yet another look at Harris' ergodic theorem for Markov chains, in *Seminar on Stochastic Analysis, Random Fields and Applications VI*, Springer, Basel, 2011, 109–117. https://doi.org/10.1007/978-3-0348-0021-1_7.

[90] M. Harper, Information geometry and evolutionary game theory, arXiv:0911.1383 (2009). https://arxiv.org/abs/0911.1383.

[91] J. M. Harrison and S. R. Pliska, Martingales and stochastic integrals in the theory of continuous trading, *Stochastic Process. Appl.* **11** (1981), 215–260. https://doi.org/10.1016/0304-4149(81)90026-0.

[92] A. Hatcher, *Algebraic Topology*, Cambridge University Press, Cambridge, 2002.

[93] C. L. Henley, From classical to quantum dynamics at Rokhsar–Kivelson points, *J. Phys.: Condens. Matter* **16** (2004), S891–S898. https://doi.org/10.1088/0953-8984/16/11/045.

[94] M. Henneaux and C. Teitelboim, *Quantization of Gauge Systems*, Princeton University Press, Princeton, 1992.

[95] P. W. Higgs, Broken symmetries and the masses of gauge bosons, *Phys. Rev. Lett.* **13** (1964), 508–509. https://doi.org/10.1103/PhysRevLett.13.508.

[96] J. Hofbauer and K. Sigmund, *Evolutionary Games and Population Dynamics*, Cambridge University Press, Cambridge, 1998. https://doi.org/10.1017/CBO9781139173179.

[97] P. A. Höhn, A. R. H. Smith, and M. P. E. Lock, Trinity of relational quantum dynamics, *Phys. Rev. D* **104** (2021), 066001. https://doi.org/10.1103/PhysRevD.104.066001.

[98] S. Hu, *Variational Selection of Coupled Subgrid Stresses and Mutual-Friction Defects in Finite-Resolution Superfluid Turbulence*, unpublished manuscript, 2026.

[99] S. Hu, *Particle Transfer and Energy-Constrained Closure in Gross–Pitaevskii Quantum-Vortex Dynamics*, unpublished manuscript, 2026.

[100] S. Hu, *A Stochastic-Dynamical Reconstruction of the Autonomous Isothermal Second Law: Onsager–Rayleigh Currents, Relative-Entropy Contraction, Convergence in Law, and Time-Reversal Asymmetry*, unpublished manuscript, version 5.2, revised October 25, 2026.

[101] S. Hu, *Stationary Action and Effective Equilibrium on the Moduli Space of Static Schwarzschild Exteriors: Singularity Diagnostics and Identification Limits*, unpublished manuscript, revised October 25, 2026.

[102] W. Israel and J. M. Stewart, Transient relativistic thermodynamics and kinetic theory, *Ann. Phys.* **118** (1979), 341–372. https://doi.org/10.1016/0003-4916(79)90130-1.

[103] C. Jarzynski, Nonequilibrium equality for free energy differences, *Phys. Rev. Lett.* **78** (1997), 2690–2693. https://doi.org/10.1103/PhysRevLett.78.2690.

[104] R. E. Kalman and R. S. Bucy, New results in linear filtering and prediction theory, *Journal of Basic Engineering* **83** (1961), 95–108. doi:10.1115/1.3658902.

[105] I. Karatzas and S. E. Shreve, *Brownian Motion and Stochastic Calculus*, 2nd ed., Springer, New York, 1991. https://doi.org/10.1007/978-1-4612-0949-2.

[106] R. Kubo, Statistical-mechanical theory of irreversible processes. I. General theory and simple applications to magnetic and conduction problems, *J. Phys. Soc. Japan* **12** (1957), 570–586. https://doi.org/10.1143/JPSJ.12.570.

[107] K. Kuwae and T. Shioya, Convergence of spectral structures: a functional analytic theory and its applications to spectral geometry, *Communications in Analysis and Geometry* **11** (2003), 599–673. https://doi.org/10.4310/CAG.2003.v11.n4.a1.

[108] D. Langlois and K. Noui, Hamiltonian analysis of higher derivative scalar-tensor theories, *Journal of Cosmology and Astroparticle Physics* **07** (2016), 016. https://doi.org/10.1088/1475-7516/2016/07/016.

[109] Y.-H. Liao, Second Law-abiding account of heat engines in active bath, Zenodo data release (2025). DOI: 10.5281/zenodo.17681574.

[110] Y.-H. Liao, J. V. Ang, P.-Y. Lai, and Y. Jun, Second law-abiding-account of heat engines in active bath, *Physical Review Research* **8** (2026), 023136. DOI: 10.1103/2yzz-mq4r.

[111] D. Liberzon, *Calculus of Variations and Optimal Control Theory: A Concise Introduction*, Princeton University Press, Princeton, 2012. https://doi.org/10.1515/9781400842643.

[112] G. Lindblad, On the generators of quantum dynamical semigroups, *Commun. Math. Phys.* **48** (1976), 119–130. https://doi.org/10.1007/BF01608499.

[113] C. Liu and J. Wang, A new symmetric hyperbolic formulation and the local Cauchy problem for the Einstein–Yang–Mills system in the temporal gauge, arXiv:2111.04540 [gr-qc] (2021). https://arxiv.org/abs/2111.04540.

[114] R. Loll, On the diffeomorphism commutators of lattice quantum gravity, *Classical and Quantum Gravity* **15** (1998), 799–809. https://doi.org/10.1088/0264-9381/15/4/008.

[115] J. Louko and A. Molgado, Group averaging in the (p, q) oscillator representation of $\mathrm{SL}(2, \mathbb{R})$, *Journal of Mathematical Physics* **45** (2004), 1919–1943. https://doi.org/10.1063/1.1689001.

[116] S. W. MacDowell and F. Mansouri, Unified geometric theory of gravity and supergravity, *Phys. Rev. Lett.* **38** (1977), 739–742. https://doi.org/10.1103/PhysRevLett.38.739.

[117] J. W. Maluf, The teleparallel equivalent of general relativity, *Annalen der Physik* **525** (2013), 339–357. https://doi.org/10.1002/andp.201200272.

[118] F. Mansouri, Superunified theories based on the geometry of local (super-) gauge invariance, *Phys. Rev. D* **16** (1977), 2456–2467. https://doi.org/10.1103/PhysRevD.16.2456.

[119] P. Mondal, Local well-posedness of the Einstein–Yang–Mills system in CMCSHGC gauge, arXiv:2112.14273 [gr-qc] (2021). https://arxiv.org/abs/2112.14273.

[120] P. Mondal and S.-T. Yau, Global exterior stability of the Minkowski space: coupled Einstein–Yang–Mills perturbations, arXiv:2211.03167 [gr-qc] (2022). https://arxiv.org/abs/2211.03167.

[121] H. Mori, Transport, collective motion, and Brownian motion, *Prog. Theor. Phys.* **33** (1965), 423–455. https://doi.org/10.1143/PTP.33.423.

[122] M. Nakahara, *Geometry, Topology and Physics*, 2nd ed., Taylor & Francis, Boca Raton, 2003. https://doi.org/10.1201/9781420056945.

[123] F. W. J. Olver, D. W. Lozier, R. F. Boisvert, and C. W. Clark (eds.), *NIST Handbook of Mathematical Functions*, Cambridge University Press, Cambridge, 2010. Online companion: *NIST Digital Library of Mathematical Functions*, Sections 10.32 and 10.40. https://dlmf.nist.gov/10.40.

[124] K. Osterwalder and R. Schrader, Axioms for Euclidean Green's functions, *Commun. Math. Phys.* **31** (1973), 83–112. https://doi.org/10.1007/BF01645738.

[125] K. Osterwalder and R. Schrader, Axioms for Euclidean Green's functions II, *Commun. Math. Phys.* **42** (1975), 281–305. https://doi.org/10.1007/BF01608978.

[126] G. Parisi and Y.-S. Wu, Perturbation theory without gauge fixing, *Sci. Sin.* **24** (1981), 483–496.

[127] S. Peng, A general stochastic maximum principle for optimal control problems, *SIAM J. Control Optim.* **28** (1990), no. 4, 966–979. https://doi.org/10.1137/0328054.

[128] M. E. Peskin and D. V. Schroeder, *An Introduction to Quantum Field Theory*, Addison–Wesley, Reading, MA, 1995.

[129] D. Petz, Sufficient subalgebras and the relative entropy of states of a von Neumann algebra, *Commun. Math. Phys.* **105** (1986), 123–131. https://doi.org/10.1007/BF01212345.

[130] F. Pisano and V. Pleitez, $SU(3) \otimes U(1)$ model for electroweak interactions, *Phys. Rev. D* **46** (1992), 410–417. https://doi.org/10.1103/PhysRevD.46.410.

[131] Planck Collaboration, N. Aghanim et al., Planck 2018 results. VI. Cosmological parameters, *Astron. Astrophys.* **641** (2020), A6. https://doi.org/10.1051/0004-6361/201833910.

[132] J. Polchinski, *String Theory*, Vol. I: *An Introduction to the Bosonic String*, Cambridge University Press, Cambridge, 1998. https://doi.org/10.1017/CBO9780511816079.

[133] O. Porth, K. Chatterjee, R. Narayan, et al., The Event Horizon general relativistic magnetohydrodynamic code comparison project, *Astrophys. J. Suppl. Ser.* **243** (2019), article 26. https://doi.org/10.3847/1538-4365/ab29fd.

[134] K. Prabhu and L. C. Stein, Black hole scalar charge from a topological horizon integral in Einstein-dilaton-Gauss-Bonnet gravity, *Phys. Rev. D* **98** (2018), 021503. https://doi.org/10.1103/PhysRevD.98.021503.

[135] J. S. Read, B. D. Lackey, B. J. Owen, and J. L. Friedman, Constraints on a phenomenologically parametrized neutron-star equation of state, *Phys. Rev. D* **79** (2009), 124032. https://doi.org/10.1103/PhysRevD.79.124032.

[136] M. Reuter, Nonperturbative evolution equation for quantum gravity, *Phys. Rev. D* **57** (1998), 971–985. https://doi.org/10.1103/PhysRevD.57.971.

[137] H. Risken, *The Fokker–Planck Equation: Methods of Solution and Applications*, 2nd ed. (1989), corrected reprint, Springer, Berlin, 1996. https://doi.org/10.1007/978-3-642-61544-3.

[138] W. Rosenfeld, D. Burchardt, R. Garthoff, K. Redeker, N. Ortegel, M. Rau, and H. Weinfurter, Event-ready Bell test using entangled atoms simultaneously closing detection and locality loopholes, *Phys. Rev. Lett.* **119** (2017), 010402. https://doi.org/10.1103/PhysRevLett.119.010402.

[139] W. Rosenfeld, D. Burchardt, R. Garthoff, K. Redeker, N. Ortegel, M. Rau, and H. Weinfurter, Experimental data and archived website material for "Event-Ready Bell Test Using Entangled Atoms Simultaneously Closing Detection and Locality Loopholes", Zenodo, 24 September 2026. https://doi.org/10.5281/zenodo.22936124.

[140] C. Rovelli, *Quantum Gravity*, Cambridge University Press, Cambridge, 2004. https://doi.org/10.1017/CBO9780511755804.

[141] A. Saffer, E. Fonseca, S. Ransom, et al., A lower mass estimate for PSR J0348+0432 based on CHIME/Pulsar precision timing, *Astrophys. J. Lett.* **983** (2025), L20. https://doi.org/10.3847/2041-8213/adc25e.

[142] M. S. Safronova, D. Budker, D. DeMille, D. F. Jackson Kimball, A. Derevianko, and C. W. Clark, Search for new physics with atoms and molecules, *Rev. Mod. Phys.* **90** (2018), 025008. https://doi.org/10.1103/RevModPhys.90.025008.

[143] A. Salam, Weak and electromagnetic interactions, in *Elementary Particle Theory: Relativistic Groups and Analyticity* (N. Svartholm, ed.), Almqvist & Wiksell, Stockholm, 1968, pp. 367–377.

[144] U. Seifert, Stochastic thermodynamics, fluctuation theorems and molecular machines, *Rep. Prog. Phys.* **75** (2012), 126001. https://doi.org/10.1088/0034-4885/75/12/126001.

[145] R. W. Sharpe, *Differential Geometry: Cartan's Generalization of Klein's Erlangen Program*, Springer, New York, 1997.

[146] R. E. Spinney and I. J. Ford, Entropy production in full phase space for continuous stochastic dynamics, *Phys. Rev. E* **85** (2012), 051113. https://doi.org/10.1103/PhysRevE.85.051113.

[147] K. S. Stelle, Renormalization of higher-derivative quantum gravity, *Phys. Rev. D* **16** (1977), 953–969. https://doi.org/10.1103/PhysRevD.16.953.

[148] D. W. Stroock and S. R. S. Varadhan, *Multidimensional Diffusion Processes*, Springer, Berlin, 1979.

[149] S. J. Summers and R. Werner, The vacuum violates Bell's inequalities, *Phys. Lett. A* **110** (1985), 257–259. https://doi.org/10.1016/0375-9601(85)90093-3.

[150] S. J. Summers and R. Werner, Maximal violation of Bell's inequalities is generic in quantum field theory, *Commun. Math. Phys.* **110** (1987), 247–259. https://doi.org/10.1007/BF01207366.

[151] H. F. Trotter, On the product of semi-groups of operators, *Proceedings of the American Mathematical Society* **10** (1959), 545–551. https://doi.org/10.1090/S0002-9939-1959-0108732-6.

[152] R. Utiyama, Invariant theoretical interpretation of interaction, *Phys. Rev.* **101** (1956), 1597–1607. https://doi.org/10.1103/PhysRev.101.1597.

[153] J.-P. Uzan, The fundamental constants and their variation: observational and theoretical status, *Rev. Mod. Phys.* **75** (2003), 403–455. https://doi.org/10.1103/RevModPhys.75.403.

[154] J. A. van Casteren, The Hamilton–Jacobi–Bellman equation and the stochastic Noether theorem, in *Evolution Equations: Applications to Physics, Industry, Life Sciences and Economics*, Birkhäuser, 2003, pp. 375–401. https://doi.org/10.1007/978-3-0348-8085-5_27.

[155] W. D. van Suijlekom, *Noncommutative Geometry and Particle Physics*, Springer, Dordrecht, 2015. https://doi.org/10.1007/978-94-017-9162-5.

[156] D. V. Vassilevich, Heat kernel expansion: user's manual, *Phys. Rep.* **388** (2003), 279–360. https://doi.org/10.1016/j.physrep.2003.09.002.

[157] E. P. Verlinde, On the origin of gravity and the laws of Newton, *JHEP* **04** (2011), 029. https://doi.org/10.1007/JHEP04(2011)029.

[158] R. M. Wald, *Quantum Field Theory in Curved Spacetime and Black Hole Thermodynamics*, University of Chicago Press, Chicago, 1994.

[159] T. F. Watson, S. G. J. Philips, E. Kawakami, D. R. Ward, P. Scarlino, M. Veldhorst, D. E. Savage, M. G. Lagally, M. Friesen, S. N. Coppersmith, M. A.

Eriksson, and L. M. K. Vandersypen, A programmable two-qubit quantum processor in silicon, *Nature* **555** (2018), 633–637. https://doi.org/10.1038/nature25766. Supporting data: https://doi.org/10.5281/zenodo.1135014.

[160] S. Weinberg, A model of leptons, *Phys. Rev. Lett.* **19** (1967), 1264–1266. https://doi.org/10.1103/PhysRevLett.19.1264.

[161] S. Weinberg, *The Quantum Theory of Fields*, Vol. I: *Foundations*, Cambridge University Press, Cambridge, 1995. https://doi.org/10.1017/CBO9781139644167.

[162] S. Weinberg, *The Quantum Theory of Fields*, Vol. II: *Modern Applications*, Cambridge University Press, Cambridge, 1996. https://doi.org/10.1017/CBO9781139644174.

[163] R. F. Werner, Quantum states with Einstein–Podolsky–Rosen correlations admitting a hidden-variable model, *Phys. Rev. A* **40** (1989), 4277–4281. https://doi.org/10.1103/PhysRevA.40.4277.

[164] C. Wetterich, Exact evolution equation for the effective potential, *Phys. Lett. B* **301** (1993), 90–94. DOI: 10.1016/0370-2693(93)90726-X.

[165] K. G. Wilson, Confinement of quarks, *Phys. Rev. D* **10** (1974), 2445–2459. https://doi.org/10.1103/PhysRevD.10.2445.

[166] F. Wudarski, Y. Zhang, and M. I. Dykman, Nonergodic measurements of qubit frequency noise, *Phys. Rev. Lett.* **131** (2023), 230201. https://doi.org/10.1103/PhysRevLett.131.230201.

[167] C. N. Yang and R. L. Mills, Conservation of isotopic spin and isotopic gauge invariance, *Phys. Rev.* **96** (1954), 191–195. https://doi.org/10.1103/PhysRev.96.191.

[168] J. Yong and X. Y. Zhou, *Stochastic Controls: Hamiltonian Systems and HJB Equations*, Springer, New York, 1999. https://doi.org/10.1007/978-1-4612-1466-3.

[169] R. Zwanzig, Memory effects in irreversible thermodynamics, *Phys. Rev.* **124** (1961), 983–992. https://doi.org/10.1103/PhysRev.124.983.

[170] D. Zwanziger, Covariant quantization of gauge fields without Gribov ambiguity, *Nucl. Phys. B* **192** (1981), 259–269. https://doi.org/10.1016/0550-3213(81)90202-9.

Shipei Hu
College of Finance and Mathematics, West Anhui University, Lu'an, Anhui 237012, China
E-mail: hushipei@126.com